

**Ongoing Face Recognition
Vendor Test (FRVT)**
Part 1: Verification

Patrick Grother
Mei Ngan
Kayee Hanaoka
Joyce C. Yang
Austin Hom

*Information Access Division
Information Technology Laboratory*

This publication is available free of charge from:
<https://www.nist.gov/programs-projects/face-recognition-vendor-test-frvt-ongoing>

2022/11/07



ACKNOWLEDGMENTS

The authors are grateful for the long-standing support and collaboration of the the Department of Homeland Security's Science & Technology Directorate (S&T) and the Office of Biometric Identity Management (OBIM).

Additionally, the authors are grateful to staff in the NIST Biometrics Research Laboratory for infrastructure supporting rapid evaluation of algorithms.

DISCLAIMER

Specific hardware and software products identified in this report were used in order to perform the evaluations described in this document. In no case does identification of any commercial product, trade name, or vendor, imply recommendation or endorsement by the National Institute of Standards and Technology, nor does it imply that the products and equipment identified are necessarily the best available for the purpose.

INSTITUTIONAL REVIEW BOARD

The National Institute of Standards and Technology's Research Protections Office reviewed the protocol for this project and determined it is not human subjects research as defined in Department of Commerce Regulations, 15 CFR 27, also known as the Common Rule for the Protection of Human Subjects (45 CFR 46, Subpart A).

FRVT STATUS

This report is a draft NIST Interagency Report, and is open for comment. It is the thirty sixth edition of the report since the first was published in June 2017. Prior editions of this report are maintained on the FRVT [website](#), and may contain useful information about older algorithms and datasets no longer used in FRVT.

FRVT remains open: All [four tracks](#) of the FRVT are open to new algorithm submissions.

2022-11-06 changes since 2022-09-26:

- ▷ We have added results for first algorithms from six developers: AFR Engine, CMC Institute of Science and Technology, Saga Densan Center, Turkcell Technology, UXLabs, and Wise AI SDN BHD.
- ▷ We have added results for new algorithms from 14 returning developers: Coretech Knowledge, Cloudwalk - Moontime, Cloudmatrix, Deepglint, Guangzhou Pixel Solutions, Hangzhou Allu Network Information Technology, NEO Systems, One More Security, Palit Microsystems, Panasonic R+D Center Singapore, Samsung S1, Seventh Sense Artificial Intelligence, Touchless ID, and Veridas Digital Authentication Solutions S.L.
- ▷ We have retired results for 10 algorithms per our policy to only list results for two algorithms per developer. Results for retired algorithms appear in prior versions of this report in the [archive](#).

2022-09-26 changes since 2022-08-30:

- ▷ We have added results for first algorithms from three developers: Codeline, First Credit Bureau Kazakhstan, and InfoCert.
- ▷ We have added results for new algorithms from 14 returning developers: Advancegroup, Armatura LLC, Beijing Hisign Technology, Cybercore, Cyberlink Corp, Herta Security, ICM Airport Technics, InsightFace AI, Metsakuur, NSENSE Corp, Samsung-SDS, Videmo Intelligente Videoanalyse, Vietnam Posts and Telecommunications Group, and Vision Intelligence Center of Meituan.
- ▷ We have retired results for 11 algorithms per our policy to only list results for two algorithms per developer. Results for retired algorithms appear in prior versions of this report in the [archive](#).

2022-08-30 changes since 2022-07-29:

- ▷ We have added results for first algorithms from two developers: Aximetria, Intellibrain Technological Projects
- ▷ We have added results for new algorithms from twelve returning developers: Alchera Inc, Dermalog, Idemia, Incode Technologies Inc, Intellivision, Kasikorn Labs, Megvii/Face++, Techsign, TuringTech.vip, Universidade de Coimbra, Verijelais, Vixvizon
- ▷ We have retired results for six algorithms per our policy to only list results for two algorithms per developer. Results for retired algorithms appear in prior versions of this report in the [archive](#).

2022-07-29 changes since 2022-06-27:

- ▷ We have added results for first algorithms from seven developers: FRP LLC (Hawaii), IMDS Software, Inspur (Beijing) Electronic Information Industry, Intema - LGL Group, PAPAGO, Qaz Biometric Systems, and VIDA-Digital Identity

- ▷ We have added results for new algorithms from nine returning developers: Cyberextruder, Glory, Maxvision Technology, Rank One Computing, Securif AI, Suprema AI, Suprema ID, Toshiba, and Yuan High-Tech Development.
- ▷ We have retired results for nine algorithms per our policy to only list results for two algorithms per developer. Results for retired algorithms appear in prior versions of this report in the [archive](#).

2022-07-29 changes since 2022-06-27:

- ▷ We have added results for first algorithms from seven developers: FRP LLC (Hawaii), IMDS Software, Inspur (Beijing) Electronic Information Industry, Intema - LGL Group, PAPAGO, Qaz Biometric Systems, and VIDA-Digital Identity
- ▷ We have added results for new algorithms from nine returning developers: Cyberextruder, Glory, Maxvision Technology, Rank One Computing, Securif AI, Suprema AI, Suprema ID, Toshiba, and Yuan High-Tech Development.
- ▷ We have retired results for nine algorithms per our policy to only list results for two algorithms per developer. Results for retired algorithms appear in prior versions of this report in the [archive](#).

2022-06-27 changes since 2022-06-03:

- ▷ We have added results for first algorithms from two developers: Krungthai Bank, and Smartbiometrik.
- ▷ We have added results for new algorithms from thirteen returning developers: Aiseemu, Corsight, Digidata, Griaule, Guangzhou Pixel Solutions, Hangzhuo AI Network Information Technology, Neurotechnology, Real Networks, Samsung S1, SenseTime Group, Smart Engines, Verihubs Inteligensia, and VinBigData.
- ▷ We have retired results for eight algorithms per our policy to only list results for two algorithms per developer. Results for retired algorithms appear in prior versions of this report in the [archive](#).

2022-06-03 changes since 2022-05-05:

- ▷ We have added results for first algorithms from seven developers: Jaak IT, Metsakuur, Palit Microsystems, Smarvist Teknoloji, and Touchless ID.
- ▷ We have added results for new algorithms from sixteen returning developers: Cyberlink, FaceOnLive, Kakao Enterprise, Line Corporation (Line Clova), Multi-Modality Intelligence, NEO Systems, and Unissey
- ▷ We have retired results for four algorithms per our policy to only list results for two algorithms per developer. Results for retired algorithms appear in prior versions of this report in the [archive](#).
- ▷ We have moved the results for the twenty human-difficult pairs used in the May 2018 paper [*Face recognition accuracy of forensic examiners, superrecognizers, and face recognition algorithms*](#) by Phillips et al. [1]. to the algorithm-specific report cards (example: [PDF](#)).
- ▷ Likewise, we have added figures showing impostor distribution shifts across demographics to the report card.

2022-05-05 changes since 2022-03-18:

- ▷ We have added results for first algorithms from seven developers: Accurascan, DICIO, FacePhi, Pangiam, University of Surrey-CVSSP, and Veridium.
- ▷ We have added results for new algorithms from sixteen returning developers: ACI Software, Canon Inc, Cloudwalk - Moontime Smart Technology, Cybercore,

2022-05-05 changes since 2022-03-18:

- ▷ We have added results for first algorithms from seven developers: Accurascan, DICIO, FacePhi, Pangiam, University of Surrey-CVSSP, and Veridium.
- ▷ We have added results for new algorithms from sixteen returning developers: ACI Software, Canon Inc, Cloudwalk - Moontime Smart Technology, Cybercore, Cyberextruder, Gemalto Cogent, HyperVerge Inc, KuKe3D Technology, Megvii/Face++, Mobbeel Solutions, Panasonic R+D Center Singapore, Qnap Security, Samsung-SDS, Vietnam Posts and Telecommunications Group, Viettel Group, and Vision Intelligence Center of Meituan.
- ▷ We have retired results for 12 algorithms per our policy to only list results for two algorithms per developer. Results for retired algorithms appear in prior versions of this report in the [archive](#).

2022-03-18 changes since 2022-02-23:

- ▷ We have added support for the detection of multiple people in a single image (see Section 1.2). Specifically the API allows an algorithm to extract features from one or more faces it detects in an image. NIST scores such cases as a correct match when any detected face matches the reference photo, and as a false positive when either face matches a non-mated reference photo. The expected effect of doing this will be to improve reported false non-match rates, and to minimally elevate false match rates. This technique was only applied to images of type "border" and "kiosk".
- ▷ We have added results for first algorithms from four developers: IntelliVIX, Kasikorn Labs, Lebentech Biometrics, and Wicket.
- ▷ We have added results for new algorithms from 10 returning developers: Chunghwa Telecom, Cloudmatrix, Beijing DeepSense Technologies, FarBar Inc, Imagus Technology Pty, Intellivision, Maxvision Technology, NHN Corp, Seventh Sense Artificial Intelligence, and Verigram.
- ▷ We have retired results for 4 algorithms per our policy to only list results for two algorithms per developer. Results for retired algorithms appear in prior versions of this report in the [archive](#).

2022-02-23 changes since 2022-01-24:

- ▷ We have added results for first algorithms from four developers: AFIS and Biometrics Consulting, Digidata, Graymatics, Hangzhuo Allu Network Information Technology, KnowUTech LLC, Sukshi Technology Innovation, T4iSB, and TuringTech.vip
- ▷ We have added results for new algorithms from 18 returning developers: Cognitec Systems GmbH, GeoVision Inc, Glory, Herta Security, Intel Research Group, InsightFace AI, Kakao Enterprise, N-Tech Lab, Omnidarde Ltd, Papilon Savunma, Paravision, Reveal Networks Inc, Reveal Media Ltd, Shenzhen Inst Adv Integrated Tech CAS, Suprema AI Inc, Toshiba, Universidade de Coimbra, and Yuan High-Tech Development
- ▷ We have retired results for 14 algorithms per our policy to only list results for two algorithms per developer. Results for retired algorithms appear in prior versions of this report in the [archive](#).

2022-01-24 changes since 2022-01-20:

- ▷ We have added results for new algorithms from one returning developer: Vocord.

2022-01-20 changes since 2021-12-18:

- ▷ We have added results for first algorithms from four developers: Armatura, Beyne.AI, One More Security, and VinBigData
- ▷ We have added results for new algorithms from 19 returning developers: AuthenMetric, BOE Technology Group, Cybercore, Cyberlink, Dahua Technology, FaceTag Co, Innovatrics, Megvii, Mobbeel Solutions, Neurotechnology, Oz Forensics, Rank One Computing, Regula Forensics, Samsung S1, Securif AI, Sensetime Group, TigerIT Americas, Videmo Intelligent Videoanalyse, and YooniK.
- ▷ We have retired results for 14 algorithms per our policy to only list results for two algorithms per developer. Results for retired algorithms appear in prior versions of this report in the [archive](#).

: 2021-12-16 changes since 2021-11-22:

- ▷ We have added results for first algorithms from five developers: Alfabeto, Cloudmatrix, Euronovate SA, FaceOnLive Inc, and Mobiclip Technology.
- ▷ We have added results for new algorithms from ten returning developers: ACI Software, ITMO University, NEO Systems, Guangzhou Pixel Solutions, Panasonic R+D Center Singapore, Qnap Security, Scanovate, Tevian, Unissey, and Vietnam Posts and Telecommunications Group.
- ▷ We have retired results for eight algorithms per our policy to only list results for two algorithms per developer. Results for retired algorithms appear in prior versions of this report in the [archive](#).
- ▷ We have revamped the figure showing performance on 20 pairs of open-source images. It now color-codes false negatives and positives against a default threshold value.

2021-11-22 changes since 2021-10-28:

- ▷ We have added results to the [website](#) for kiosk-collected images where the design and geometry configuration mean that many images have considerable downward pitch angle. In some images, the face is partially cropped. Some images have other background faces.
- ▷ We have stopped using child exploitation images in FRVT, as we lost access to the imagery. All results for that set have been removed from the [website](#), and will be removed from future PDF reports.
- ▷ We have added results for first algorithms from seven new developers: CUDO Communication, Daon, KuKe3D Technology, Mantra Softtech India, Maxvision Technology, Multi-Modality Intelligence, and Samsung-SDS.
- ▷ We have added results for new algorithms from seven returning developers: Acer Incorporated, Cloudwalk-Moontime Smart Technology, Gorilla Technology, ID3 Technology, Incode Technologies, NSENSE Corp., and SQIssoft.
- ▷ We have retired results for six algorithms per our policy to only list results for two algorithms per developer. Results for retired algorithms appear in prior versions of this report in the [archive](#).

2021-10-28 changes since 2021-09-08:

- ▷ We have substantially revised the algorithm-specific report cards that are linked from the [FRVT results page](#). (Example: [HTML](#)).
- ▷ We have added results for first algorithms from eight new developers: Beijing Mendaxia Technology, Beijing Hisign Technology, Biocube Matrics, Clearview AI, Reveal Media, Toppan ID Gate, Verigram, and Viettel High Technology.
- ▷ We have added results for new algorithms from thirty returning developers: 20Face, 3divi, Canon Inc Chunghwa Telecom, Corsight, Decatur Industries, Deepglint, Dermalog, FaceTag, Fiberhome Telecommunication Technologies, GeoVision, ICM Airport Technics, Imagus Technology, InsightFace AI, Kakao Enterprise, Kookmin University, Line Corporation, N-Tech Lab, NotionTag Technologies, Realnetworks, Suprema ID, Taiwan-Certificate Authority, Toshiba, Tripleize, Trueface.ai, Veridas Digital Authentication, Visidon, VisionLabs, YooniK, and Yuan High-Tech Development.
- ▷ We have retired results for twenty algorithms per our policy to only list results for two algorithms per developer. Results for retired algorithms appear in prior versions of this report in the [archive](#).

2021-09-08 changes since 2021-08-02:

- ▷ We have added results for first algorithms from seven new developers: Griaule, SQISoft, Qnap Security, Techsign, Smart Engines, Verihubs, and Wuhan Tianyu Information Industry.
- ▷ We have added results for new algorithms from sixteen returning developers: ADVANCE.AI, AuthenMetric, CloudSmart Consulting, Code Everest Pvt, Cognitec Systems, Thales Gemalto Cogent, Intel Research Group, Omnidarde, Oz Forensics, Rank One Computing, Samsung S1 Corp, Securif AI, Tevian, TigerIT Americas, Universidade de Coimbra, and Vigilant Solutions
- ▷ We have retired results for eleven algorithms per our policy to only list results for two algorithms per developer. Results for retired algorithms appear in prior versions of this report in the [archive](#).

2021-08-02 changes since 2021-06-25:

- ▷ We have added results for first algorithms from eight new developers: Bee the Data, Closeli Inc, Coretech Knowledge Inc, Deepsense (France), ioNetworks Inc, Kakao Pay Corp, Seventh Sense Artificial Intelligence, and SK Telecom.
- ▷ We have added results for new algorithms from fifteen returning developers: Alchera Inc, Adera Global PTE, Aware, Bresee Technology, Cyberlink Corp, Expasoft LLC, Fujitsu Research and Development Center, Gorilla Technology, Idemia, Neurotechnology, NEO Systems, NHN Corp, Paravision, Panasonic R+D Center Singapore, and Shenzhen University-Macau University of Science and Technology.
- ▷ We have retired results for twelve algorithms per our policy to only list results for two algorithms per developer. Results for retired algorithms appear in prior versions of this report in the [archive](#).

2021-06-25 changes since 2021-05-21:

- ▷ We have added results for first algorithms from six new developers: Alice Biometrics, BOE Technology Group, Fincore, Neosecu, Sodec App, and Yuntu Data and Technology.

- ▷ We have added results for new algorithms from seven returning developers: Incode Technologies, HyperVerge, Mobbeel Solutions, Guangzhou Pixel Solutions, Remark Holdings, Sensetime, and Vietnam Posts and Telecommunications Group.
- ▷ We have retired results for four algorithms per our policy to only list results for two algorithms per developer. Results for retired algorithms appear in prior versions of this report in the [archive](#).

2021-05-21 changes since 2021-04-26:

- ▷ We have added results for first algorithms from five new developers: Ekin Smart City Technologies, Suprema ID, Tripleize, Taiwan-Certificate Authority, and Vision Intelligence Center of Meituan.
- ▷ We have added results for new algorithms from eight returning developers: ID3 Technology, Imagus Technology, Momentum Digital, N-Tech Lab, NSENSE, Shanghai Jiao Tong University, Vision-Box, and Yuan High-Tech Development
- ▷ We have retired results for seven algorithms per our policy to only list results for two algorithms per developer. Results for retired algorithms appear in prior versions of this report in the [archive](#).

2021-04-26 changes since 2021-04-16:

- ▷ We have added results for first algorithms from three new developers: Quantasoft, Rendip, and NEO Systems.
- ▷ We have added results for new algorithms from four returning developers: 3Divi, Realnetworks, Veridas Digital Authentication Solutions, and Universidade de Coimbra.
- ▷ We have retired results for three algorithms per our policy to only list results for two algorithms per developer. Results for retired algorithms appear in prior versions of this report in the [archive](#).

2021-04-16 changes since 2021-03-19:

- ▷ We have added results for first algorithms from six new developers: 20Face, Beijing DeepSense Technologies, BitCenter UK, Enface, FaceTag, InsightFace AI, Line Corporation, Lema Labs, Nanjing Kiwi Network Technology, Omnidarde, Regula Forensics, and Suprema.
- ▷ We have added results for new algorithms from ten returning developers: CloudSmart Consulting, Dermalog, GeoVision, Neurotechnology, Panasonic R+D Center Singapore, Samsung S1, Securif AI, Trueface.ai, Vigilant Solutions, and Visidon.
- ▷ We have retired results for ten algorithms per our policy to only list results for two algorithms per developer. Results for retired algorithms appear in prior versions of this report in the [archive](#).

2021-03-19 changes since 2021-03-05:

- ▷ We have added results for first algorithms from six new developers: Ajou University, AuthenMetric, Code Everest, Corsight, Papilon Savunma, and NHN Corp
- ▷ We have added results for new algorithms from seven returning developers: Alchera, Deepglint, Fiber-home Telecommunication Technologies, Kakao Enterprise, Kookmin University, Megvii/Face++, and NotionTag Technologies.

- ▷ We have updated many of the hyperlinked HTML report-cards to include seven figures on demographic dependence. Figures of this kind first appeared, and are documented in, the December 2019 document, [NIST Interagency Report 8280](#) on demographic differentials in face recognition. The figures quantify false negative dependence on demographics using “visa-border” comparisons, and false positive dependence using comparisons of “application” photos that uniformly of quality and similar to visa photos.

2021-03-05 changes since 2021-01-19:

- ▷ We have added results for first algorithms from three new developers: IVA Cognitive, Mobbeel, and MoreDian Technology.
- ▷ We have added results for new algorithms from returning developers: Ability Enterprise - Andro Video, ACI Software, Adera Global, AnyVision, BioID Technologies, China Electronics Import-Export, Cognitec Systems, Fujitsu Research and Development Center, Glory, Guangzhou Pixel Solutions, Hengrui AI Technology, Incode Technologies, Intel Research, iQIYI, Mobai, Oz Forensics, Paravision, VisionLabs, and Xforward AI Technology.
- ▷ We have added a new “resources” tab to the main [webpage](#). It includes sortable columns for data related to speed, model size, storage, and memory consumption.
- ▷ We have retired results for 13 algorithms per our policy to only list results for two algorithms per developer. Results for retired algorithms appear in prior versions of this report in the [archive](#).

2021-01-19 changes since 2020-12-18:

- ▷ This report adds results for first algorithms from four developers: Herta Security, Irex AI, Shenzhen University-Macau University of Science and Technology, and Vietnam Posts and Telecommunications Group. See Table 7 for more information.
- ▷ The report also includes results for thirteen developers who have previously submitted algorithms: Bresee Technology, Canon (previously Canon Information Technology (Beijing)), Cyberlink, CSA IntelliCloud Technology, Dahua Technology, ID3 Technology, Imagus Technology (Vixvizon), Moontime Smart Technology, N-Tech Lab, Thales Cogent, Veridas Digital Authentication Solutions, Vocord, and Yuan High-Tech Development.
- ▷ We have retired results for ten algorithms per our policy to only list results for two algorithms per developer. Results for retired algorithms appear in prior versions of this report in the [archive](#).

2020-12-18 changes since 2020-10-09:

- ▷ This report adds results for first algorithms from ten developers: BitCenter UK, CloudSmart Consulting, Cubox, Institute of Computing Technology, Naver Corp, Minivision, NSENSE Corp, Viettel Group, Visage Technologies, and Xiamen University. See Table 7 for more information.
- ▷ The report also includes results for eighteen developers who have previously submitted algorithms: ADVANCE.AI, Awidit Systems, Chosun University, Dermalog, GeoVision, ICM Airport Technics, Idemia, Institute of Information Technologies, Kakao Enterprise, Neurotechnology, Panasonic R+D Center Singapore, Rank One Computing, SenseTime Group, Shanghai Jiao Tong University, TigerIT Americas LLC, Vigilant Solutions, Winsense, and YooniK

- ▷ We have retired results for twelve algorithms per our policy to only list results for two algorithms per developer. Results for retired algorithms appear in prior versions of this report in the [archive](#).

Changes since September 18, 2020:

- ▷ This report adds results for first algorithms from five developers: Aigen, Cortica, Kookmin University, Securif AI and Vinai.
- ▷ The report also includes results for three developers who have previously submitted algorithms: Fujitsu Laboratories, Hengrui AI, and X-Forward AI.
- ▷ In the per-algorithm report-cards linked from tables and the main webpage, we have added a chart to showing reduction in error rates over the course of FRVT i.e. from 2017 onwards for all algorithms supplied by that developer. Similarly we have added a chart showing error rate reductions for our test of protective face mask verification.
- ▷ We plan to continue evaluating algorithms on various mask datasets. We hold that algorithms should be capable of detecting masks and verifying identity of all combinations of masked and unmasked faces. We have accordingly increased the amount of time allowed to extract those features from 1.0 to 1.5 seconds.

Changes since August 25, 2020:

- ▷ This report adds results for first algorithms from eight new developers. Akurat Satu Indonesia, Cybercore, Decatur Industries, Innef Labs, Satellite Innovation/Eocortex, Expasoft, and Mobai.
- ▷ The report includes results for seven developers who have previously submitted algorithms: 3Divi, BioID Technologies, Incode Technologies, Innovatrics, iSAP Solution, Synology, and Tevian.
- ▷ We have retired results for five algorithms per our policy to only list results for two algorithms per developer. Results for retired algorithms appear in prior versions of this report in the [archive](#).

Changes since July 27, 2020:

- ▷ We have introduced per-algorithm report sheets. These are HTML documents linked from the accuracy tables in this report (i.e. Table 29) and on the FRVT 1:1 [homepage](#). The sheets contain interactive graphics allowing, for example, mouseover exploration of FNMR(T) and FMR(T). Some of their content had previously appeared in this document.
- ▷ This report adds results for algorithms from six new developers. ACI Software, Bresee Technology, Fiberhome Telecommunication Technologies, Imageware Systems, Oz Forensics, and Pensees.
- ▷ The report includes results for thirteen developers who have previously submitted algorithms: Canon Information Technology (Beijing), Cyberlink, Dahua Technology, Gorilla Technology, ID3 Technology, Intel Research Group, iQIYI Inc, Momentum Digital, Netbridge Technology, Tech5 SA, Shenzhen AiMall Tech, Vigilant Solutions, and VisionLabs.
- ▷ We have retired results for nine algorithms per our policy to only list results for two algorithms per developer. Results for retired algorithms appear in prior versions of this report in the [archive](#).

Changes since May 18, 2020:

- ▷ The report is the first FRVT update since the pandemic closed it from March to June 2020.

- ▷ This report includes results for algorithms from nine new developers: GeoVision Inc, Su Zhou NaZhi-TianDi Intelligent Technology, YooniK, AYF Technology, PXL Vision AG, Yuan High-Tech Development, Beihang University-ERCACAT, ICM Airport Technics, and Staqu Technologies
- ▷ This report includes results for algorithms from 15 returning developers Acer Incorporated, Antheus Technologia, Chosun University, Chunghwa Telecom, Idemia, Moontime Smart Technology, Neurotechnology, Guangzhou Pixel Solutions, Panasonic R+D Center Singapore, Rank One Computing, Scanovate, Shanghai University - Shanghai Film Academy, Synesis, Trueface.ai, and Veridas Digital Authentication Solutions
- ▷ We have retired results for ten algorithms per our policy to only list results for two algorithms per developer. Results for retired algorithms appear in prior versions of this report in the [archive](#).
- ▷ We separated timing and other resource consumption from the main participation table. The new Table 18 includes template generation durations for four kinds of images, not just mugshots.
- ▷ We have published a separate report, [NIST Interagency Report 8311](#) on accuracy of pre-pandemic algorithms on subjects wearing face masks. We plan to track improvements in accuracy on masked images going forward. In particular, we invite submission of algorithms that can detect whether a person is wearing a mask, extract features from the full face or the exposed periocular region, and do appropriate comparison. We do not intend to evaluate algorithms that assume 100% of images will be of masked individuals.

Changes since March 25, 2020:

- ▷ The report is a maintenance release - it does not add any new algorithms, and FRVT has been closed to new algorithms since mid March 2020.
- ▷ We modified the primary accuracy summary, Table 29, as follows:
 - ▷▷ For visa images, the column for FNMR at FMR = 0.0001 has been removed. The visa images are so highly controlled that the error rates for the most accurate algorithms are dominated by false rejection of very young children and by the presence of a few noisy greyscale images. For now, two visa columns remain: FNMR at $FMR = 10^{-6}$ and, for matched covariates, FNMR at $FMR = 10^{-4}$.
 - ▷▷ We have inserted a new column labelled "BORDER" giving accuracy for comparison of moderately poor webcam border-crossing photos that exhibit pose variations, poor compression, and low contrast due to strong background illumination. The accuracies are the worst from all cooperative image datasets used in FRVT.
- ▷ Accordingly, we updated the failure-to-template rates in Table 37.
- ▷ We withdrew a figure showing how false matches are concentrated in certain visa images used in cross-comparison, because it didn't attempt to include demographic information.

Changes since February 27, 2020:

- ▷ The report adds results algorithms from two new developers: Beijing Alleyes Technology, and the Chinese University of Hong Kong. Results for newly submitted algorithms from two other developers will appear in the next report.
- ▷ The report adds results for algorithms from thirteen returning developers: ASUSTek Computer, Aware, Cyberlink Corp, Gorilla Technology, Innovative Technology, Kakao Enterprise, Lomonosov Moscow State University, Panasonic R+D Center Singapore, Shenzhen AiMall Technology, Shenzhen Intellifusion Technologies, Synology, Tech5 SA, and Via Technologies.

- ▷ Per policy to only list results for two algorithms per developer, we have dropped results for algorithms from Aware, Cyberlink, Gorilla Technology, Kakao Enterprise, Lomonosov Moscow State University, Panasonic R+D Center Singapore, and Tech5 SA.

Changes since January 20, 2020:

- ▷ The report adds results for five new developers: Ability Enterprise (Andro Video), Chosun University, Fujitsu Research and Development Center, University of Coimbra, and Xforward AI Technology.
- ▷ The report adds results for algorithms from six returning developers: AlphaSSTG, Incode Technologies, Kneron, Shanghai Jiao Tong University, Vocord, and X-Laboratory.
- ▷ We have corrected template comparison timing numbers for algorithms submitted September 2019 to January 2020. The values reported previously were slower due to a software bug.
- ▷ We have dropped results for algorithms from Vocord and Incode per policy to only list results for two algorithms per developer.
- ▷ The [FRVT 1:1 homepage](#) has been updated with latest accuracy results.
- ▷ The [FRVT 1:N homepage](#) now includes an update to the September 2019 NIST Interagency Report 8271. The new report adds results for one-to-many search algorithms submitted to NIST from June 2019 to January 2020.

Changes since January 6, 2020:

- ▷ Section 2 has been updated to better describe the Visa and Border images. The caption for Table 29 has been updated to better relate the accuracy values to particular image comparisons.
- ▷ The report adds results for five new developers: Acer, Advance.AI, Expasoft, Netbridge Technology, and Videmo Intelligent Videoanalyse.
- ▷ The report adds results for algorithms from 7 returning developers: China Electronics Import-Export Corp, Intel Research Group, ITMO University, Neurotechnology, N-Tech Lab, Rokid, and VisionLabs.
- ▷ We have dropped results from this edition of the report per policy to only list results for two algorithms per developer: N-Tech Lab, Neurotechnology, ITMO, Visionlabs, and CEIEC.
- ▷ The [FRVT homepage](#) has been updated with latest accuracy results.

Changes since November 11, 2019:

- ▷ Table 18 has been updated to include runtime memory usage. This is the first time such a quantity has been reported. The value is the peak size of the resident set size logged during enrollment of single images.
- ▷ We have migrated summary results table to a new platform that supports sortable tables:
<https://pages.nist.gov/frvt/html/frvt11.html>
- ▷ The report adds results for four new developers: Antheus Technologia, BioID Technologies SA, Canon Information Tech. (Beijing), Samsung S1 (listed in the tables as S1), and Taiwan AI Labs.
- ▷ The report adds results for algorithms from 13 returning developers: Anke Investments, Chunghwa Telecom, Deepglint, Institute of Information Technologies, iQIYI, Kneron, Ping An Technology, Paravision, KanKan Ai, Rokid Corporation, Shanghai Universiy - Shanghai Film Academy, Veridas Digital Authentication Solutions, and Videonetics Technology.

- ▷ We have dropped results from this edition of the report per policy to only list results for two algorithms per developer: remarkai-000, veridas-001, sensetime-001, iit-000, anke-003, and everai-002. Results for these are available in prior editions of this report linked from the FRVT page.
- ▷ We issued [NIST Interagency Report 8280: FRVT Part 3: Demographics](#) on 2019-12-19. It includes results for many of the algorithms covered by this report.

Changes since October 16, 2019:

- ▷ The report adds results for ten new developers: Ai-Union Technology, ASUSTek Computer, DiDi ChuXing Technology, Innovative Technology, Luxand, MVision, Pyramid Cyber Security + Forensic, Scanovate, Shenzhen AiMall Tech, and TUPU Technology.
- ▷ The report adds results for 12 returning developers: CTBC Bank Glory Gorilla Technology Guangzhou Pixel Solutions Imagus Technology Incode Technologies Lomonosov Moscow State University Rank One Computing Samtech InfoNet Shanghai Ulucu Electronics Technology Synesis, and Winsense.
- ▷ We have dropped results from this edition of the report per policy to only list results for two algorithms per developer: glory-000, gorilla-002, incode-003, rankone-006, and synesis-004.
- ▷ Results for five recently submitted algorithms will appear in the next report.

Changes since September 11, 2019:

- ▷ The report adds results for five new participants: Awidit Systems (Awiros), Momenmtum Digital (Sertis), Trueface AI, Shanghai Jiao Tong University, and X-Laboratory.
- ▷ The reports adds results for five new algorithms from returning developers: Cyberlink, Hengrui AI Technology, Idemia, Panasonic R+D Singapore, and Tevian. This causes three algorithm, to be de-listed from the report per policy to list results for two algorithms per developer.

Changes since July 31 2019:

- ▷ The HTML table on the [FRVT 1:1 homepage](#) has been updated to include a column for cross-domain Visa-Border verification. Results for this new dataset appeared in the July 29 report under the name "CrossEV" - these are now renamed "Visa-Border".
- ▷ The [FRVT 1:1 homepage](#) lists algorithms according to lowest mean rank accuracy:

$$\begin{aligned} & \text{Rank(FNMR}_{\text{VISA}} \text{ at FMR = 0.000001}) + \\ & \text{Rank(FNMR}_{\text{VISA-BORDER}} \text{ at FMR = 0.000001}) + \\ & \text{Rank(FNMR}_{\text{MUGSHOT}} \text{ at FMR = 0.00001 after 14 years}) + \\ & \text{Rank(FNMR}_{\text{WILD}} \text{ at FMR = 0.00001}) \end{aligned}$$

This ordering rewards high accuracy across all datasets.
- ▷ The main results in Table 29 is now in landscape format to accomodate extra columns for the Visa-Border set, and mugshot comparisons after at least 12 years.
- ▷ The report adds results for nine new participants: Alpha SSTG, Intel Research, ULSee, Chungwa Telecon, iSAP Solution, Rokid, Shenzhen EI Networks, CSA Intellicloud, Shenzhen Intellifusion Technologies.
- ▷ The reports adds results for six new algorithms from returning developers: Innovatrics, Dahua Technology, Tech5 SA, Intellivision, Nodeflux and Imperial College, London. One algorithm, from Imperial has been retired, per policy to list results for two algorithms per developer.
- ▷ The cross-country false match rate heatmaps have been replotted to reveal more structure by listing countries by region instead of alphabetically.

- ▷ The next version of this report will be posted around October 18, 2019.

Changes since July 3 2019:

- ▷ The HTML table on the [FRVT 1:1 homepage](#) has been updated to list the 20 most accurate developers rather than algorithms, choosing the most accurate algorithm from each developer based on visa and mugshot results. Also, the algorithms are ordered in terms of lowest mean rank across mugshot, visa and wild datasets, rewarding broad accuracy over a good result on one particular dataset.
- ▷ This report includes results for a new dataset - see the column labelled "visa-border" in Table 5. It compares a new set of high quality visa-like portraits with a set webcam border-crossing photos that exhibit moderately poor pose variations and background illumination. The two new sets are described in sections [2.2](#) and [2.3](#). The comparisons are "cross-domain" in that the algorithm must compare "visa" and "wild" images. Results for other algorithms will be added in future reports as they become available.
- ▷ This report adds results for algorithms from 9 developers submitted in early July 2019. These are from 3DiVi, Camvi, EverAI-Paravision, Facesoft, Farbar (F8), Institute of Information Technologies, Shanghai U. Film Academy, Via Technologies, and Ulucu Electronics Tech. Six of these are new participants.
- ▷ Several other algorithms have been submitted and are being evaluated. Results will be released in the next report, scheduled for September 5. That report will include results for new datasets.
- ▷ Older algorithms from Everai, Camvi and 3DiVi, have been retired, per the policy to list only two algorithms per developer.

Changes since June 20 2019:

- ▷ This report adds results for algorithms from 18 developers submitted in early June 2019. These are from CTBC Bank, Deep Glint, Thales Cogent, Ever AI Paravision, Gorilla Technology, Imagus, Incode, Kneron, N-Tech Lab, Neurotechnology, Notiontag Technologies, Star Hybrid, Videonetics, Vigilant Solutions, Winsense, Anke Investments, CEIEC, and DSK. Nine of these are new participants.
- ▷ Several other algorithms have been submitted and are being evaluated. Results will be released in the next report, scheduled for August 1.
- ▷ Older algorithms from Everai, Thales Cogent, Gorilla Technology, Incode, Neurotechnology, N-Tech Lab and Vigilant Solutions have been retired, per the policy to list only two algorithms per developer.

Changes since April 2019:

- ▷ This report adds results for nine algorithms from nine developers submitted in early June 2019. These are from Tencent Deepsea, Hengrui, Kedacom, Moontime, Guangzhou Pixel, Rank One Computing, Synesis, Sensetime and Vocord.
- ▷ Another 23 algorithms have been submitted and are being evaluated. Results will be released in the next report, scheduled for July 3.
- ▷ Older algorithms for Rank One, Synesis, and Vocord have been retired, per the policy to list only two algorithms per developer.

Changes since February 2019:

- ▷ This report adds results for 49 algorithms from 42 developers submitted in early March 2019.
- ▷ This report omits results for algorithms that we retired. We retired for three reasons: 1. The developer submitted a new algorithm, and we only list two. 2. The algorithm needs a GPU, and we no longer allow GPU-based algorithms. 3. Inoperable algorithms.
- ▷ Previous results for retired algorithms are available in older editions of this report linked [here](#).
- ▷ The mugshot database used from February 2017 to January 2019 has been replaced with an extract of the mugshot database documented in NIST Interagency Report 8238, November 2018. The new mugshot set is described in section [2.4](#) and is adopted because:

- ▷▷ It has much better identity label integrity, so that false non-match rates are substantially lower than those reported in FRVT 1:1 reports to date - see Figure 110.
- ▷▷ It includes images collected over a 17 year period such that ageing can be much better characterized - - see Figure 355.
- ▷ Using the new mugshot database, Figure 355 shows accuracy for four demographic groups identified in the biographic metadata that accompanies the data: black females, black males, white females and white males.
- ▷ The report added a figure (now moved to web) with results for the twenty human-difficult pairs used in the May 2018 paper *Face recognition accuracy of forensic examiners, superrecognizers, and face recognition algorithms* by Phillips et al. [1].
- ▷ The report uses an update to the wild image database that corrects some ground truth labels.
- ▷ Some results for the child exploitation database are not complete. They are typically updated less frequently than for other image sets.

Contents

ACKNOWLEDGMENTS	1
DISCLAIMER	1
INSTITUTIONAL REVIEW BOARD	1
1 METRICS	55
1.1 CORE ACCURACY	55
1.2 MULTI-TEMPLATE SCORING METHODOLOGY	55
2 DATASETS	56
2.1 VISA IMAGES	56
2.2 APPLICATION IMAGES	56
2.3 BORDER CROSSING IMAGES	56
2.4 MUGSHOT IMAGES	57
2.5 KIOSK IMAGES	57
2.6 WILD IMAGES	57
3 RESULTS	58
3.1 TEST GOALS	58
3.2 TEST DESIGN	58
3.3 FAILURE TO ENROLL	61
3.4 RECOGNITION ACCURACY	70
3.5 GENUINE DISTRIBUTION STABILITY	355
3.5.1 EFFECT OF BIRTH PLACE ON THE GENUINE DISTRIBUTION	355
3.5.2 EFFECT OF AGEING	395
3.5.3 EFFECT OF AGE ON GENUINE SUBJECTS	425
3.6 IMPOSTOR DISTRIBUTION STABILITY	466
3.6.1 EFFECT OF BIRTH PLACE ON THE IMPOSTOR DISTRIBUTION	466
3.6.2 EFFECT OF AGE ON IMPOSTORS	469

List of Tables

1 PARTICIPANT INFORMATION	24
2 PARTICIPANT INFORMATION	25
3 PARTICIPANT INFORMATION	26
4 PARTICIPANT INFORMATION	27
5 PARTICIPANT INFORMATION	28
6 PARTICIPANT INFORMATION	29
7 PARTICIPANT INFORMATION	30
8 ALGORITHM SUMMARY	31
9 ALGORITHM SUMMARY	32
10 ALGORITHM SUMMARY	33
11 ALGORITHM SUMMARY	34
12 ALGORITHM SUMMARY	35
13 ALGORITHM SUMMARY	36
14 ALGORITHM SUMMARY	37
15 ALGORITHM SUMMARY	38
16 ALGORITHM SUMMARY	39
17 ALGORITHM SUMMARY	40
18 ALGORITHM SUMMARY	41
19 FALSE NON-MATCH RATE	42

20	FALSE NON-MATCH RATE	43
21	FALSE NON-MATCH RATE	44
22	FALSE NON-MATCH RATE	45
23	FALSE NON-MATCH RATE	46
24	FALSE NON-MATCH RATE	47
25	FALSE NON-MATCH RATE	48
26	FALSE NON-MATCH RATE	49
27	FALSE NON-MATCH RATE	50
28	FALSE NON-MATCH RATE	51
29	FALSE NON-MATCH RATE	52
30	FAILURE TO ENROL RATES	62
31	FAILURE TO ENROL RATES	63
32	FAILURE TO ENROL RATES	64
33	FAILURE TO ENROL RATES	65
34	FAILURE TO ENROL RATES	66
35	FAILURE TO ENROL RATES	67
36	FAILURE TO ENROL RATES	68
37	FAILURE TO ENROL RATES	69

List of Figures

1	PERFORMANCE SUMMARY: FNMR VS. TEMPLATE SIZE TRADEOFF	53
2	PERFORMANCE SUMMARY: FNMR VS. TEMPLATE TIME TRADEOFF	54
3	EXAMPLE IMAGES	58
(A)	VISA	58
(B)	MUGSHOT	58
(C)	WILD	58
(D)	BORDER	58
4	PERFORMANCE ON 20 HUMAN-DIFFICULT PAIRS	71
5	PERFORMANCE ON 20 HUMAN-DIFFICULT PAIRS	72
6	PERFORMANCE ON 20 HUMAN-DIFFICULT PAIRS	73
7	PERFORMANCE ON 20 HUMAN-DIFFICULT PAIRS	74
8	PERFORMANCE ON 20 HUMAN-DIFFICULT PAIRS	75
9	PERFORMANCE ON 20 HUMAN-DIFFICULT PAIRS	76
10	PERFORMANCE ON 20 HUMAN-DIFFICULT PAIRS	77
11	PERFORMANCE ON 20 HUMAN-DIFFICULT PAIRS	78
12	PERFORMANCE ON 20 HUMAN-DIFFICULT PAIRS	79
13	PERFORMANCE ON 20 HUMAN-DIFFICULT PAIRS	80
14	PERFORMANCE ON 20 HUMAN-DIFFICULT PAIRS	81
15	PERFORMANCE ON 20 HUMAN-DIFFICULT PAIRS	82
16	PERFORMANCE ON 20 HUMAN-DIFFICULT PAIRS	83
17	PERFORMANCE ON 20 HUMAN-DIFFICULT PAIRS	84
18	PERFORMANCE ON 20 HUMAN-DIFFICULT PAIRS	85
19	PERFORMANCE ON 20 HUMAN-DIFFICULT PAIRS	86
20	PERFORMANCE ON 20 HUMAN-DIFFICULT PAIRS	87
21	PERFORMANCE ON 20 HUMAN-DIFFICULT PAIRS	88
22	PERFORMANCE ON 20 HUMAN-DIFFICULT PAIRS	89
23	PERFORMANCE ON 20 HUMAN-DIFFICULT PAIRS	90
24	PERFORMANCE ON 20 HUMAN-DIFFICULT PAIRS	91
25	PERFORMANCE ON 20 HUMAN-DIFFICULT PAIRS	92
26	PERFORMANCE ON 20 HUMAN-DIFFICULT PAIRS	93
27	PERFORMANCE ON 20 HUMAN-DIFFICULT PAIRS	94
28	PERFORMANCE ON 20 HUMAN-DIFFICULT PAIRS	95
29	PERFORMANCE ON 20 HUMAN-DIFFICULT PAIRS	96
30	PERFORMANCE ON 20 HUMAN-DIFFICULT PAIRS	97

31	PERFORMANCE ON 20 HUMAN-DIFFICULT PAIRS	98
32	PERFORMANCE ON 20 HUMAN-DIFFICULT PAIRS	99
33	PERFORMANCE ON 20 HUMAN-DIFFICULT PAIRS	100
34	PERFORMANCE ON 20 HUMAN-DIFFICULT PAIRS	101
35	PERFORMANCE ON 20 HUMAN-DIFFICULT PAIRS	102
36	PERFORMANCE ON 20 HUMAN-DIFFICULT PAIRS	103
37	PERFORMANCE ON 20 HUMAN-DIFFICULT PAIRS	104
38	PERFORMANCE ON 20 HUMAN-DIFFICULT PAIRS	105
39	PERFORMANCE ON 20 HUMAN-DIFFICULT PAIRS	106
40	ERROR TRADEOFF CHARACTERISTIC: VISA IMAGES	107
41	ERROR TRADEOFF CHARACTERISTIC: VISA IMAGES	108
42	ERROR TRADEOFF CHARACTERISTIC: VISA IMAGES	109
43	ERROR TRADEOFF CHARACTERISTIC: VISA IMAGES	110
44	ERROR TRADEOFF CHARACTERISTIC: VISA IMAGES	111
45	ERROR TRADEOFF CHARACTERISTIC: VISA IMAGES	112
46	ERROR TRADEOFF CHARACTERISTIC: VISA IMAGES	113
47	ERROR TRADEOFF CHARACTERISTIC: VISA IMAGES	114
48	ERROR TRADEOFF CHARACTERISTIC: VISA IMAGES	115
49	ERROR TRADEOFF CHARACTERISTIC: VISA IMAGES	116
50	ERROR TRADEOFF CHARACTERISTIC: VISA IMAGES	117
51	ERROR TRADEOFF CHARACTERISTIC: VISA IMAGES	118
52	ERROR TRADEOFF CHARACTERISTIC: VISA IMAGES	119
53	ERROR TRADEOFF CHARACTERISTIC: VISA IMAGES	120
54	ERROR TRADEOFF CHARACTERISTIC: VISA IMAGES	121
55	ERROR TRADEOFF CHARACTERISTIC: VISA IMAGES	122
56	ERROR TRADEOFF CHARACTERISTIC: VISA IMAGES	123
57	ERROR TRADEOFF CHARACTERISTIC: VISA IMAGES	124
58	ERROR TRADEOFF CHARACTERISTIC: VISA IMAGES	125
59	ERROR TRADEOFF CHARACTERISTIC: VISA IMAGES	126
60	ERROR TRADEOFF CHARACTERISTIC: VISA IMAGES	127
61	ERROR TRADEOFF CHARACTERISTIC: VISA IMAGES	128
62	ERROR TRADEOFF CHARACTERISTIC: VISA IMAGES	129
63	ERROR TRADEOFF CHARACTERISTIC: VISA IMAGES	130
64	ERROR TRADEOFF CHARACTERISTIC: VISA IMAGES	131
65	ERROR TRADEOFF CHARACTERISTIC: VISA IMAGES	132
66	ERROR TRADEOFF CHARACTERISTIC: VISA IMAGES	133
67	ERROR TRADEOFF CHARACTERISTIC: VISA IMAGES	134
68	ERROR TRADEOFF CHARACTERISTIC: VISA IMAGES	135
69	ERROR TRADEOFF CHARACTERISTIC: VISA IMAGES	136
70	ERROR TRADEOFF CHARACTERISTIC: VISA IMAGES	137
71	ERROR TRADEOFF CHARACTERISTIC: VISA IMAGES	138
72	ERROR TRADEOFF CHARACTERISTIC: VISA IMAGES	139
73	ERROR TRADEOFF CHARACTERISTIC: VISA IMAGES	140
74	ERROR TRADEOFF CHARACTERISTIC: VISA IMAGES	141
75	ERROR TRADEOFF CHARACTERISTIC: VISA IMAGES	142
76	ERROR TRADEOFF CHARACTERISTIC: VISA IMAGES	143
77	ERROR TRADEOFF CHARACTERISTIC: VISA IMAGES	144
78	ERROR TRADEOFF CHARACTERISTIC: VISA IMAGES	145
79	ERROR TRADEOFF CHARACTERISTIC: VISA IMAGES	146
80	ERROR TRADEOFF CHARACTERISTIC: VISA IMAGES	147
81	ERROR TRADEOFF CHARACTERISTIC: VISA IMAGES	148
82	ERROR TRADEOFF CHARACTERISTIC: VISA IMAGES	149
83	ERROR TRADEOFF CHARACTERISTIC: VISA IMAGES	150
84	ERROR TRADEOFF CHARACTERISTIC: VISA IMAGES	151
85	ERROR TRADEOFF CHARACTERISTIC: VISA IMAGES	152
86	ERROR TRADEOFF CHARACTERISTIC: VISA IMAGES	153

87	ERROR TRADEOFF CHARACTERISTIC: MUGSHOT IMAGES	154
88	ERROR TRADEOFF CHARACTERISTIC: MUGSHOT IMAGES	155
89	ERROR TRADEOFF CHARACTERISTIC: MUGSHOT IMAGES	156
90	ERROR TRADEOFF CHARACTERISTIC: MUGSHOT IMAGES	157
91	ERROR TRADEOFF CHARACTERISTIC: MUGSHOT IMAGES	158
92	ERROR TRADEOFF CHARACTERISTIC: MUGSHOT IMAGES	159
93	ERROR TRADEOFF CHARACTERISTIC: MUGSHOT IMAGES	160
94	ERROR TRADEOFF CHARACTERISTIC: MUGSHOT IMAGES	161
95	ERROR TRADEOFF CHARACTERISTIC: MUGSHOT IMAGES	162
96	ERROR TRADEOFF CHARACTERISTIC: MUGSHOT IMAGES	163
97	ERROR TRADEOFF CHARACTERISTIC: MUGSHOT IMAGES	164
98	ERROR TRADEOFF CHARACTERISTIC: MUGSHOT IMAGES	165
99	ERROR TRADEOFF CHARACTERISTIC: MUGSHOT IMAGES	166
100	ERROR TRADEOFF CHARACTERISTIC: MUGSHOT IMAGES	167
101	ERROR TRADEOFF CHARACTERISTIC: MUGSHOT IMAGES	168
102	ERROR TRADEOFF CHARACTERISTIC: MUGSHOT IMAGES	169
103	ERROR TRADEOFF CHARACTERISTIC: MUGSHOT IMAGES	170
104	ERROR TRADEOFF CHARACTERISTIC: MUGSHOT IMAGES	171
105	ERROR TRADEOFF CHARACTERISTIC: MUGSHOT IMAGES	172
106	ERROR TRADEOFF CHARACTERISTIC: MUGSHOT IMAGES	173
107	ERROR TRADEOFF CHARACTERISTIC: MUGSHOT IMAGES	174
108	ERROR TRADEOFF CHARACTERISTIC: MUGSHOT IMAGES	175
109	ERROR TRADEOFF CHARACTERISTIC: MUGSHOT IMAGES	176
110	ERROR TRADEOFF CHARACTERISTIC: MUGSHOT IMAGES	177
111	ERROR TRADEOFF CHARACTERISTIC: WILD IMAGES	178
112	ERROR TRADEOFF CHARACTERISTIC: WILD IMAGES	179
113	ERROR TRADEOFF CHARACTERISTIC: WILD IMAGES	180
114	ERROR TRADEOFF CHARACTERISTIC: WILD IMAGES	181
115	ERROR TRADEOFF CHARACTERISTIC: WILD IMAGES	182
116	ERROR TRADEOFF CHARACTERISTIC: WILD IMAGES	183
117	ERROR TRADEOFF CHARACTERISTIC: WILD IMAGES	184
118	ERROR TRADEOFF CHARACTERISTIC: WILD IMAGES	185
119	ERROR TRADEOFF CHARACTERISTIC: WILD IMAGES	186
120	ERROR TRADEOFF CHARACTERISTIC: WILD IMAGES	187
121	ERROR TRADEOFF CHARACTERISTIC: WILD IMAGES	188
122	ERROR TRADEOFF CHARACTERISTIC: WILD IMAGES	189
123	ERROR TRADEOFF CHARACTERISTIC: WILD IMAGES	190
124	ERROR TRADEOFF CHARACTERISTIC: WILD IMAGES	191
125	ERROR TRADEOFF CHARACTERISTIC: WILD IMAGES	192
126	ERROR TRADEOFF CHARACTERISTIC: WILD IMAGES	193
127	ERROR TRADEOFF CHARACTERISTIC: WILD IMAGES	194
128	ERROR TRADEOFF CHARACTERISTIC: WILD IMAGES	195
129	ERROR TRADEOFF CHARACTERISTIC: WILD IMAGES	196
130	ERROR TRADEOFF CHARACTERISTIC: WILD IMAGES	197
131	FALSE MATCH RATES WITHIN AND ACROSS DEMOGRAPHIC GROUPS	198
132	FALSE MATCH RATES WITHIN AND ACROSS DEMOGRAPHIC GROUPS	199
133	FALSE MATCH RATES WITHIN AND ACROSS DEMOGRAPHIC GROUPS	200
134	FALSE MATCH RATES WITHIN AND ACROSS DEMOGRAPHIC GROUPS	201
135	FALSE MATCH RATES WITHIN AND ACROSS DEMOGRAPHIC GROUPS	202
136	FALSE MATCH RATES WITHIN AND ACROSS DEMOGRAPHIC GROUPS	203
137	FALSE MATCH RATES WITHIN AND ACROSS DEMOGRAPHIC GROUPS	204
138	FALSE MATCH RATES WITHIN AND ACROSS DEMOGRAPHIC GROUPS	205
139	FALSE MATCH RATES WITHIN AND ACROSS DEMOGRAPHIC GROUPS	206
140	FALSE MATCH RATES WITHIN AND ACROSS DEMOGRAPHIC GROUPS	207
141	FALSE MATCH RATES WITHIN AND ACROSS DEMOGRAPHIC GROUPS	208
142	FALSE MATCH RATES WITHIN AND ACROSS DEMOGRAPHIC GROUPS	209
143	FALSE MATCH RATES WITHIN AND ACROSS DEMOGRAPHIC GROUPS	210

144	FALSE MATCH RATES WITHIN AND ACROSS DEMOGRAPHIC GROUPS	211
145	FALSE MATCH RATES WITHIN AND ACROSS DEMOGRAPHIC GROUPS	212
146	FALSE MATCH RATES WITHIN AND ACROSS DEMOGRAPHIC GROUPS	213
147	FALSE MATCH RATES WITHIN AND ACROSS DEMOGRAPHIC GROUPS	214
148	FALSE MATCH RATES WITHIN AND ACROSS DEMOGRAPHIC GROUPS	215
149	FALSE MATCH RATES WITHIN AND ACROSS DEMOGRAPHIC GROUPS	216
150	FALSE MATCH RATES WITHIN AND ACROSS DEMOGRAPHIC GROUPS	217
151	FALSE MATCH RATES WITHIN AND ACROSS DEMOGRAPHIC GROUPS	218
152	FALSE MATCH RATES WITHIN AND ACROSS DEMOGRAPHIC GROUPS	219
153	SEX AND RACE EFFECTS: MUGSHOT IMAGES	220
154	SEX AND RACE EFFECTS: MUGSHOT IMAGES	221
155	SEX AND RACE EFFECTS: MUGSHOT IMAGES	222
156	SEX AND RACE EFFECTS: MUGSHOT IMAGES	223
157	SEX AND RACE EFFECTS: MUGSHOT IMAGES	224
158	SEX AND RACE EFFECTS: MUGSHOT IMAGES	225
159	SEX AND RACE EFFECTS: MUGSHOT IMAGES	226
160	SEX AND RACE EFFECTS: MUGSHOT IMAGES	227
161	SEX AND RACE EFFECTS: MUGSHOT IMAGES	228
162	SEX AND RACE EFFECTS: MUGSHOT IMAGES	229
163	SEX AND RACE EFFECTS: MUGSHOT IMAGES	230
164	SEX AND RACE EFFECTS: MUGSHOT IMAGES	231
165	SEX AND RACE EFFECTS: MUGSHOT IMAGES	232
166	SEX AND RACE EFFECTS: MUGSHOT IMAGES	233
167	SEX AND RACE EFFECTS: MUGSHOT IMAGES	234
168	SEX AND RACE EFFECTS: MUGSHOT IMAGES	235
169	SEX AND RACE EFFECTS: MUGSHOT IMAGES	236
170	SEX AND RACE EFFECTS: MUGSHOT IMAGES	237
171	SEX AND RACE EFFECTS: MUGSHOT IMAGES	238
172	SEX AND RACE EFFECTS: MUGSHOT IMAGES	239
173	SEX AND RACE EFFECTS: MUGSHOT IMAGES	240
174	SEX AND RACE EFFECTS: MUGSHOT IMAGES	241
175	SEX AND RACE EFFECTS: MUGSHOT IMAGES	242
176	SEX AND RACE EFFECTS: MUGSHOT IMAGES	243
177	SEX EFFECTS: VISA IMAGES	244
178	SEX EFFECTS: VISA IMAGES	245
179	SEX EFFECTS: VISA IMAGES	246
180	SEX EFFECTS: VISA IMAGES	247
181	SEX EFFECTS: VISA IMAGES	248
182	SEX EFFECTS: VISA IMAGES	249
183	SEX EFFECTS: VISA IMAGES	250
184	SEX EFFECTS: VISA IMAGES	251
185	SEX EFFECTS: VISA IMAGES	252
186	SEX EFFECTS: VISA IMAGES	253
187	SEX EFFECTS: VISA IMAGES	254
188	SEX EFFECTS: VISA IMAGES	255
189	SEX EFFECTS: VISA IMAGES	256
190	SEX EFFECTS: VISA IMAGES	257
191	SEX EFFECTS: VISA IMAGES	258
192	SEX EFFECTS: VISA IMAGES	259
193	SEX EFFECTS: VISA IMAGES	260
194	SEX EFFECTS: VISA IMAGES	261
195	SEX EFFECTS: VISA IMAGES	262
196	SEX EFFECTS: VISA IMAGES	263
197	SEX EFFECTS: VISA IMAGES	264
198	SEX EFFECTS: VISA IMAGES	265
199	SEX EFFECTS: VISA IMAGES	266
200	SEX EFFECTS: VISA IMAGES	267

201	SEX EFFECTS: VISA IMAGES	268
202	SEX EFFECTS: VISA IMAGES	269
203	SEX EFFECTS: VISA IMAGES	270
204	SEX EFFECTS: VISA IMAGES	271
205	SEX EFFECTS: VISA IMAGES	272
206	SEX EFFECTS: VISA IMAGES	273
207	SEX EFFECTS: VISA IMAGES	274
208	SEX EFFECTS: VISA IMAGES	275
209	SEX EFFECTS: VISA IMAGES	276
210	SEX EFFECTS: VISA IMAGES	277
211	SEX EFFECTS: VISA IMAGES	278
212	SEX EFFECTS: VISA IMAGES	279
213	SEX EFFECTS: VISA IMAGES	280
214	SEX EFFECTS: VISA IMAGES	281
215	SEX EFFECTS: VISA IMAGES	282
216	FALSE MATCH RATE CALIBRATION: MUGSHOT IMAGES	283
217	FALSE MATCH RATE CALIBRATION: MUGSHOT IMAGES	284
218	FALSE MATCH RATE CALIBRATION: MUGSHOT IMAGES	285
219	FALSE MATCH RATE CALIBRATION: MUGSHOT IMAGES	286
220	FALSE MATCH RATE CALIBRATION: MUGSHOT IMAGES	287
221	FALSE MATCH RATE CALIBRATION: MUGSHOT IMAGES	288
222	FALSE MATCH RATE CALIBRATION: MUGSHOT IMAGES	289
223	FALSE MATCH RATE CALIBRATION: MUGSHOT IMAGES	290
224	FALSE MATCH RATE CALIBRATION: MUGSHOT IMAGES	291
225	FALSE MATCH RATE CALIBRATION: MUGSHOT IMAGES	292
226	FALSE MATCH RATE CALIBRATION: MUGSHOT IMAGES	293
227	FALSE MATCH RATE CALIBRATION: MUGSHOT IMAGES	294
228	FALSE MATCH RATE CALIBRATION: MUGSHOT IMAGES	295
229	FALSE MATCH RATE CALIBRATION: MUGSHOT IMAGES	296
230	FALSE MATCH RATE CALIBRATION: MUGSHOT IMAGES	297
231	FALSE MATCH RATE CALIBRATION: MUGSHOT IMAGES	298
232	FALSE MATCH RATE CALIBRATION: MUGSHOT IMAGES	299
233	FALSE MATCH RATE CALIBRATION: MUGSHOT IMAGES	300
234	FALSE MATCH RATE CALIBRATION: MUGSHOT IMAGES	301
235	FALSE MATCH RATE CALIBRATION: MUGSHOT IMAGES	302
236	FALSE MATCH RATE CALIBRATION: MUGSHOT IMAGES	303
237	FALSE MATCH RATE CALIBRATION: MUGSHOT IMAGES	304
238	FALSE MATCH RATE CALIBRATION: MUGSHOT IMAGES	305
239	FALSE MATCH RATE CALIBRATION: MUGSHOT IMAGES	306
240	FALSE MATCH RATE CALIBRATION: VISA IMAGES	307
241	FALSE MATCH RATE CALIBRATION: VISA IMAGES	308
242	FALSE MATCH RATE CALIBRATION: VISA IMAGES	309
243	FALSE MATCH RATE CALIBRATION: VISA IMAGES	310
244	FALSE MATCH RATE CALIBRATION: VISA IMAGES	311
245	FALSE MATCH RATE CALIBRATION: VISA IMAGES	312
246	FALSE MATCH RATE CALIBRATION: VISA IMAGES	313
247	FALSE MATCH RATE CALIBRATION: VISA IMAGES	314
248	FALSE MATCH RATE CALIBRATION: VISA IMAGES	315
249	FALSE MATCH RATE CALIBRATION: VISA IMAGES	316
250	FALSE MATCH RATE CALIBRATION: VISA IMAGES	317
251	FALSE MATCH RATE CALIBRATION: VISA IMAGES	318
252	FALSE MATCH RATE CALIBRATION: VISA IMAGES	319
253	FALSE MATCH RATE CALIBRATION: VISA IMAGES	320
254	FALSE MATCH RATE CALIBRATION: VISA IMAGES	321
255	FALSE MATCH RATE CALIBRATION: VISA IMAGES	322
256	FALSE MATCH RATE CALIBRATION: VISA IMAGES	323
257	FALSE MATCH RATE CALIBRATION: VISA IMAGES	324

258	FALSE MATCH RATE CALIBRATION: VISA IMAGES	325
259	FALSE MATCH RATE CALIBRATION: VISA IMAGES	326
260	FALSE MATCH RATE CALIBRATION: VISA IMAGES	327
261	FALSE MATCH RATE CALIBRATION: VISA IMAGES	328
262	FALSE MATCH RATE CALIBRATION: VISA IMAGES	329
263	FALSE MATCH RATE CALIBRATION: VISA IMAGES	330
264	FALSE MATCH RATE CALIBRATION: VISA IMAGES	331
265	FALSE MATCH RATE CALIBRATION: VISA IMAGES	332
266	FALSE MATCH RATE CALIBRATION: VISA IMAGES	333
267	FALSE MATCH RATE CALIBRATION: VISA IMAGES	334
268	FALSE MATCH RATE CALIBRATION: VISA IMAGES	335
269	FALSE MATCH RATE CALIBRATION: VISA IMAGES	336
270	FALSE MATCH RATE CALIBRATION: VISA IMAGES	337
271	FALSE MATCH RATE CALIBRATION: VISA IMAGES	338
272	FALSE MATCH RATE CALIBRATION: VISA IMAGES	339
273	FALSE MATCH RATE CALIBRATION: VISA IMAGES	340
274	FALSE MATCH RATE CALIBRATION: VISA IMAGES	341
275	FALSE MATCH RATE CALIBRATION: VISA IMAGES	342
276	FALSE MATCH RATE CALIBRATION: VISA IMAGES	343
277	FALSE MATCH RATE CALIBRATION: VISA IMAGES	344
278	FALSE MATCH RATE CALIBRATION: VISA IMAGES	345
279	FALSE MATCH RATE CALIBRATION: VISA IMAGES	346
280	FALSE MATCH RATE CALIBRATION: VISA IMAGES	347
281	FALSE MATCH RATE CALIBRATION: VISA IMAGES	348
282	FALSE MATCH RATE CALIBRATION: VISA IMAGES	349
283	FALSE MATCH RATE CALIBRATION: VISA IMAGES	350
284	FALSE MATCH RATE CALIBRATION: VISA IMAGES	351
285	FALSE MATCH RATE CALIBRATION: VISA IMAGES	352
286	FALSE MATCH RATE CALIBRATION: VISA IMAGES	353
287	FALSE MATCH RATE CALIBRATION: VISA IMAGES	354
288	EFFECT OF COUNTRY OF BIRTH ON FNMR	356
289	EFFECT OF COUNTRY OF BIRTH ON FNMR	357
290	EFFECT OF COUNTRY OF BIRTH ON FNMR	358
291	EFFECT OF COUNTRY OF BIRTH ON FNMR	359
292	EFFECT OF COUNTRY OF BIRTH ON FNMR	360
293	EFFECT OF COUNTRY OF BIRTH ON FNMR	361
294	EFFECT OF COUNTRY OF BIRTH ON FNMR	362
295	EFFECT OF COUNTRY OF BIRTH ON FNMR	363
296	EFFECT OF COUNTRY OF BIRTH ON FNMR	364
297	EFFECT OF COUNTRY OF BIRTH ON FNMR	365
298	EFFECT OF COUNTRY OF BIRTH ON FNMR	366
299	EFFECT OF COUNTRY OF BIRTH ON FNMR	367
300	EFFECT OF COUNTRY OF BIRTH ON FNMR	368
301	EFFECT OF COUNTRY OF BIRTH ON FNMR	369
302	EFFECT OF COUNTRY OF BIRTH ON FNMR	370
303	EFFECT OF COUNTRY OF BIRTH ON FNMR	371
304	EFFECT OF COUNTRY OF BIRTH ON FNMR	372
305	EFFECT OF COUNTRY OF BIRTH ON FNMR	373
306	EFFECT OF COUNTRY OF BIRTH ON FNMR	374
307	EFFECT OF COUNTRY OF BIRTH ON FNMR	375
308	EFFECT OF COUNTRY OF BIRTH ON FNMR	376
309	EFFECT OF COUNTRY OF BIRTH ON FNMR	377
310	EFFECT OF COUNTRY OF BIRTH ON FNMR	378
311	EFFECT OF COUNTRY OF BIRTH ON FNMR	379
312	EFFECT OF COUNTRY OF BIRTH ON FNMR	380
313	EFFECT OF COUNTRY OF BIRTH ON FNMR	381
314	EFFECT OF COUNTRY OF BIRTH ON FNMR	382

315	EFFECT OF COUNTRY OF BIRTH ON FNMR	383
316	EFFECT OF COUNTRY OF BIRTH ON FNMR	384
317	EFFECT OF COUNTRY OF BIRTH ON FNMR	385
318	EFFECT OF COUNTRY OF BIRTH ON FNMR	386
319	EFFECT OF COUNTRY OF BIRTH ON FNMR	387
320	EFFECT OF COUNTRY OF BIRTH ON FNMR	388
321	EFFECT OF COUNTRY OF BIRTH ON FNMR	389
322	EFFECT OF COUNTRY OF BIRTH ON FNMR	390
323	EFFECT OF COUNTRY OF BIRTH ON FNMR	391
324	EFFECT OF COUNTRY OF BIRTH ON FNMR	392
325	EFFECT OF COUNTRY OF BIRTH ON FNMR	393
326	EFFECT OF COUNTRY OF BIRTH ON FNMR	394
327	ERROR TRADEOFF CHARACTERISTIC: MUGSHOT IMAGES	396
328	ERROR TRADEOFF CHARACTERISTIC: MUGSHOT IMAGES	397
329	ERROR TRADEOFF CHARACTERISTIC: MUGSHOT IMAGES	398
330	ERROR TRADEOFF CHARACTERISTIC: MUGSHOT IMAGES	399
331	ERROR TRADEOFF CHARACTERISTIC: MUGSHOT IMAGES	400
332	ERROR TRADEOFF CHARACTERISTIC: MUGSHOT IMAGES	401
333	ERROR TRADEOFF CHARACTERISTIC: MUGSHOT IMAGES	402
334	ERROR TRADEOFF CHARACTERISTIC: MUGSHOT IMAGES	403
335	ERROR TRADEOFF CHARACTERISTIC: MUGSHOT IMAGES	404
336	ERROR TRADEOFF CHARACTERISTIC: MUGSHOT IMAGES	405
337	ERROR TRADEOFF CHARACTERISTIC: MUGSHOT IMAGES	406
338	ERROR TRADEOFF CHARACTERISTIC: MUGSHOT IMAGES	407
339	ERROR TRADEOFF CHARACTERISTIC: MUGSHOT IMAGES	408
340	ERROR TRADEOFF CHARACTERISTIC: MUGSHOT IMAGES	409
341	ERROR TRADEOFF CHARACTERISTIC: MUGSHOT IMAGES	410
342	ERROR TRADEOFF CHARACTERISTIC: MUGSHOT IMAGES	411
343	ERROR TRADEOFF CHARACTERISTIC: MUGSHOT IMAGES	412
344	ERROR TRADEOFF CHARACTERISTIC: MUGSHOT IMAGES	413
345	ERROR TRADEOFF CHARACTERISTIC: MUGSHOT IMAGES	414
346	ERROR TRADEOFF CHARACTERISTIC: MUGSHOT IMAGES	415
347	ERROR TRADEOFF CHARACTERISTIC: MUGSHOT IMAGES	416
348	ERROR TRADEOFF CHARACTERISTIC: MUGSHOT IMAGES	417
349	ERROR TRADEOFF CHARACTERISTIC: MUGSHOT IMAGES	418
350	ERROR TRADEOFF CHARACTERISTIC: MUGSHOT IMAGES	419
351	ERROR TRADEOFF CHARACTERISTIC: MUGSHOT IMAGES	420
352	ERROR TRADEOFF CHARACTERISTIC: MUGSHOT IMAGES	421
353	ERROR TRADEOFF CHARACTERISTIC: MUGSHOT IMAGES	422
354	ERROR TRADEOFF CHARACTERISTIC: MUGSHOT IMAGES	423
355	ERROR TRADEOFF CHARACTERISTIC: MUGSHOT IMAGES	424
356	EFFECT OF SUBJECT AGE ON FNMR	426
357	EFFECT OF SUBJECT AGE ON FNMR	427
358	EFFECT OF SUBJECT AGE ON FNMR	428
359	EFFECT OF SUBJECT AGE ON FNMR	429
360	EFFECT OF SUBJECT AGE ON FNMR	430
361	EFFECT OF SUBJECT AGE ON FNMR	431
362	EFFECT OF SUBJECT AGE ON FNMR	432
363	EFFECT OF SUBJECT AGE ON FNMR	433
364	EFFECT OF SUBJECT AGE ON FNMR	434
365	EFFECT OF SUBJECT AGE ON FNMR	435
366	EFFECT OF SUBJECT AGE ON FNMR	436
367	EFFECT OF SUBJECT AGE ON FNMR	437
368	EFFECT OF SUBJECT AGE ON FNMR	438
369	EFFECT OF SUBJECT AGE ON FNMR	439

370	EFFECT OF SUBJECT AGE ON FNMR	440
371	EFFECT OF SUBJECT AGE ON FNMR	441
372	EFFECT OF SUBJECT AGE ON FNMR	442
373	EFFECT OF SUBJECT AGE ON FNMR	443
374	EFFECT OF SUBJECT AGE ON FNMR	444
375	EFFECT OF SUBJECT AGE ON FNMR	445
376	EFFECT OF SUBJECT AGE ON FNMR	446
377	EFFECT OF SUBJECT AGE ON FNMR	447
378	EFFECT OF SUBJECT AGE ON FNMR	448
379	EFFECT OF SUBJECT AGE ON FNMR	449
380	EFFECT OF SUBJECT AGE ON FNMR	450
381	EFFECT OF SUBJECT AGE ON FNMR	451
382	EFFECT OF SUBJECT AGE ON FNMR	452
383	EFFECT OF SUBJECT AGE ON FNMR	453
384	EFFECT OF SUBJECT AGE ON FNMR	454
385	EFFECT OF SUBJECT AGE ON FNMR	455
386	EFFECT OF SUBJECT AGE ON FNMR	456
387	EFFECT OF SUBJECT AGE ON FNMR	457
388	EFFECT OF SUBJECT AGE ON FNMR	458
389	EFFECT OF SUBJECT AGE ON FNMR	459
390	EFFECT OF SUBJECT AGE ON FNMR	460
391	EFFECT OF SUBJECT AGE ON FNMR	461
392	EFFECT OF SUBJECT AGE ON FNMR	462
393	EFFECT OF SUBJECT AGE ON FNMR	463
394	EFFECT OF SUBJECT AGE ON FNMR	464
395	IMPOSTOR COUNTS FOR CROSS COUNTRY FMR CALCULATIONS	468

	Location	Developer Name	Short Name	Seq. Num.	Validation Date
1	NL	20Face	20face-000	000	2021-04-12
2	NL	20Face	20face-001	001	2021-09-29
3	US	3Divi	3divi-006	006	2021-04-14
4	US	3Divi	3divi-007	007	2021-09-27
5	TH	ACI Software	acisw-007	007	2021-11-15
6	TH	ACI Software	acisw-008	008	2022-03-22
7	US	AFIS and Biometrics Consulting	afisbiometrics-000	000	2022-01-27
8	US	AFR Engine	afrengine-000	000	2022-09-29
9	TW	ASUSTek Computer Inc	asusaics-000	000	2019-10-24
10	TW	ASUSTek Computer Inc	asusaics-001	001	2020-02-25
11	CN	AYF Technology	ayftech-001	001	2020-07-06
12	TW	Ability Enterprise - Andro Video	androvideo-000	000	2021-01-25
13	TW	Acer Incorporated	acer-001	001	2020-06-30
14	TW	Acer Incorporated	acer-002	002	2021-11-10
15	SG	Adera Global PTE	ader-002	002	2021-02-16
16	SG	Adera Global PTE	ader-003	003	2021-07-12
17	SG	Advancegroup	advance-003	003	2021-08-05
18	SG	Advancegroup	advance-004	004	2022-09-06
19	TH	Ai First	aifirst-001	001	2019-11-21
20	TW	AiUnion Technology	aiunionface-000	000	2019-10-22
21	TH	Aigen	aigen-001	001	2020-10-06
22	TH	Aigen	aigen-002	002	2021-03-15
23	CN	Aiseemu Technology	aiseemu-001	001	2022-06-16
24	KR	Ajou University	ajou-001	001	2021-03-08
25	ID	Akurat Satu Indonesia	ptakuratsatu-000	000	2020-09-11
26	KR	Alchera Inc	alchera-003	003	2021-07-13
27	KR	Alchera Inc	alchera-004	004	2022-08-12
28	ID	Alfabeta	alfabeta-001	001	2021-12-02
29	ES	Alice Biometrics	alice-000	000	2021-06-15
30	RU	Alivia / Innovation Sys	isystems-001	001	2018-06-12
31	RU	Alivia / Innovation Sys	isystems-002	002	2018-10-18
32	IN	AllGoVision	allgovision-000	000	2019-03-01
33	CN	AlphaSSTG	alphaface-001	001	2019-09-03
34	CN	AlphaSSTG	alphaface-002	002	2020-02-20
35	GB	Amplified Group	amplifiedgroup-001	001	2019-03-01
36	CN	Anke Investments	anke-004	004	2019-06-27
37	CN	Anke Investments	anke-005	005	2019-11-21
38	BR	Antheus Technologia	antheus-000	000	2019-12-05
39	BR	Antheus Technologia	antheus-001	001	2020-06-25
40	GB	AnyVision	anyvision-004	004	2018-06-15
41	GB	AnyVision	anyvision-005	005	2021-02-03
42	US	Armatura LLC	armatura-001	001	2022-01-04
43	US	Armatura LLC	armatura-002	002	2022-09-16
44	CN	AuthenMetric	authenmetric-003	003	2021-08-09
45	CN	AuthenMetric	authenmetric-004	004	2022-01-03
46	US	Aware	aware-005	005	2020-02-27
47	US	Aware	aware-006	006	2021-07-03
48	IN	Awidit Systems	awidit-001	001	2019-09-23
49	IN	Awidit Systems	awidit-002	002	2020-10-28
50	CH	Aximetria	aximetria-001	001	2022-08-10
51	JP	Ayonix	ayonix-000	000	2017-06-22
52	CN	BOE Technology Group	boetech-001	001	2021-06-22
53	CN	BOE Technology Group	boetech-002	002	2021-12-21
54	ES	Bee the Data	beethedata-000	000	2021-07-26
55	CN	Beihang University-ERCACAT	ercacat-001	001	2020-07-06
56	CN	Beijing Alleyes Technology	alleyes-000	000	2020-03-09
57	CN	Beijing DeepSense Technologies	deepsense-000	000	2021-03-19
58	CN	Beijing DeepSense Technologies	deepsense-001	001	2022-03-11
59	CN	Beijing Hisign Technology	hisign-001	001	2021-09-24
60	CN	Beijing Hisign Technology	hisign-002	002	2022-09-09
61	CN	Beijing Mendaxia Technology	mendaxiatech-000	000	2021-09-15
62	CN	Beijing Vion Technology Inc	vion-000	000	2018-10-19
63	KZ	Beyne.AI	beyneai-000	000	2022-01-03
64	CH	BioID Technologies SA	bioidechswiss-001	001	2020-08-28
65	CH	BioID Technologies SA	bioidechswiss-002	002	2021-02-17
66	IN	Biocube Matrics	biocube-001	001	2021-09-08
67	UK	BitCenter UK	farfaces-001	001	2021-04-09
68	CN	Bitmain	bm-001	001	2018-10-17
69	CN	Bresee Technology	bresee-001	001	2020-12-30
70	CN	Bresee Technology	bresee-002	002	2021-06-30

Table 1: Summary of participant information included in this report.

	Location	Developer Name	Short Name	Seq. Num.	Validation Date
71	VN	CMC Institute of Science and Technology	cist-001	001	2022-10-20
72	CN	CSA IntelliCloud Technology	intellicloudai-001	001	2019-08-13
73	CN	CSA IntelliCloud Technology	intellicloudai-002	002	2020-12-17
74	TW	CTBC Bank	ctbcbank-000	000	2019-06-28
75	TW	CTBC Bank	ctbcbank-001	001	2019-10-28
76	KR	CUDO Communication	cudocommunication-001	001	2021-10-20
77	US	Camvi Technologies	camvi-002	002	2018-10-19
78	US	Camvi Technologies	camvi-004	004	2019-07-12
79	JP	Canon Inc	canon-003	003	2021-09-15
80	JP	Canon Inc	canon-004	004	2022-04-25
81	CN	China Electronics Import-Export Corp	ceiec-003	003	2020-01-06
82	CN	China Electronics Import-Export Corp	ceiec-004	004	2021-01-18
83	CN	China University of Petroleum	upc-001	001	2019-06-05
84	CN	Chinese University of Hong Kong	cuhkee-001	001	2020-03-18
85	KR	Chosun University	chosun-001	001	2020-07-01
86	KR	Chosun University	chosun-002	002	2020-11-25
87	TW	Chunghwa Telecom	chtface-004	004	2021-10-08
88	TW	Chunghwa Telecom	chtface-005	005	2022-03-09
89	US	Clearview AI Inc	clearviewai-000	000	2021-09-22
90	CN	Closeli Inc	closeli-001	001	2021-07-15
91	US	CloudSmart Consulting LLC	csc-002	002	2021-03-24
92	US	CloudSmart Consulting LLC	csc-003	003	2021-08-26
93	TW	Cloudmatrix	cloudmatrix-001	001	2022-02-16
94	TW	Cloudmatrix	cloudmatrix-002	002	2022-10-17
95	CN	Cloudwalk - Hengrui AI Technology	cloudwalk-hr-003	003	2020-09-25
96	CN	Cloudwalk - Hengrui AI Technology	cloudwalk-hr-004	004	2021-02-10
97	CN	Cloudwalk - Moontime Smart Technology	cloudwalk-mt-005	005	2022-03-29
98	CN	Cloudwalk - Moontime Smart Technology	cloudwalk-mt-006	006	2022-10-20
99	IN	Code Everest Pvt	facex-001	001	2021-03-08
100	IN	Code Everest Pvt	facex-002	002	2021-08-24
101	KR	Codeline	codeline-000	000	2022-09-13
102	DE	Cognitec Systems GmbH	cognitec-003	003	2021-07-30
103	DE	Cognitec Systems GmbH	cognitec-004	004	2022-02-10
104	TW	Coretech Knowledge Inc	coretech-000	000	2021-07-12
105	TW	Coretech Knowledge Inc	coretech-001	001	2022-09-29
106	IL	Corsight	corsight-002	002	2021-09-01
107	IL	Corsight	corsight-003	003	2022-06-09
108	IL	Cortica	cor-001	001	2020-09-24
109	KR	Cubox	cubox-001	001	2020-12-07
110	KR	Cubox	cubox-002	002	2021-08-24
111	JP	Cybercore	cybercore-002	002	2022-04-25
112	JP	Cybercore	cybercore-003	003	2022-08-31
113	US	Cyberextruder	cyberextruder-003	003	2022-03-16
114	US	Cyberextruder	cyberextruder-004	004	2022-07-20
115	TW	Cyberlink Corp	cyberlink-009	009	2022-05-12
116	TW	Cyberlink Corp	cyberlink-010	010	2022-09-16
117	MX	DICIO	dicio-001	001	2022-03-22
118	CN	DSK	dsk-000	000	2019-06-28
119	CN	Dahua Technology	dahua-006	006	2020-12-30
120	CN	Dahua Technology	dahua-007	007	2021-12-20
121	IE	Daon	daon-000	000	2021-11-03
122	US	Decatur Industries Inc	decatur-000	000	2020-08-18
123	US	Decatur Industries Inc	decatur-001	001	2021-09-27
124	CN	Deepglint	deepglint-004	004	2021-09-17
125	CN	Deepglint	deepglint-005	005	2022-10-17
126	FR	Deepsense	dps-000	000	2021-07-16
127	DE	Dermalog	dermalog-009	009	2021-10-06
128	DE	Dermalog	dermalog-010	010	2022-07-25
129	CN	DiDi ChuXing Technology	didiglobalface-001	001	2019-10-23
130	IN	Digidata	digidata-000	000	2022-01-27
131	IN	Digidata	digidata-001	001	2022-06-10
132	GB	Digital Barriers	digitalbarriers-002	002	2019-03-01
133	TR	Ekin Smart City Technologies	ekin-002	002	2021-05-04
134	RU	Enface	enface-000	000	2021-04-09
135	RU	Enface	enface-001	001	2021-12-17
136	CH	Euronovate SA	euronovate-001	001	2021-11-15
137	RU	Expasoft LLC	expasoft-001	001	2020-09-03
138	RU	Expasoft LLC	expasoft-002	002	2021-07-26
139	US	FRP LLC	frpkauai-001	001	2022-07-18
140	DE	FaceOnLive Inc	faceonlive-001	001	2021-11-23

Table 2: Summary of participant information included in this report.

	Location	Developer Name	Short Name	Seq. Num.	Validation Date
141	DE	FaceOnLive Inc	faceonlive-002	002	2022-04-11
142	ES	FacePhi	facephi-000	000	2022-04-06
143	GB	FaceSoft	facesoft-000	000	2019-07-10
144	KR	FaceTag Co	facetag-000	000	2021-03-22
145	KR	FaceTag Co	facetag-002	002	2022-01-06
146	TW	FarBar Inc	f8-001	001	2019-07-11
147	TW	FarBar Inc	f8-002	002	2022-03-02
148	CN	Fiberhome Telecommunication Technologies	fiberhome-nanjing-003	003	2021-03-12
149	CN	Fiberhome Telecommunication Technologies	fiberhome-nanjing-004	004	2021-09-14
150	UK	Fincore Ltd	fincore-000	000	2021-06-07
151	KZ	First Credit Bureau Kazakhstan	firstcreditKZ-001	001	2022-08-22
152	CN	Fujitsu Research and Development Center	fujitsulab-002	002	2021-02-24
153	CN	Fujitsu Research and Development Center	fujitsulab-003	003	2021-07-12
154	US	Gemalto Cogent	cogent-006	006	2021-07-28
155	US	Gemalto Cogent	cogent-007	007	2022-04-11
156	TW	GeoVision Inc	geo-002	002	2021-04-01
157	TW	GeoVision Inc	geo-004	004	2022-02-10
158	JP	Glory	glory-004	004	2022-02-08
159	JP	Glory	glory-005	005	2022-07-08
160	TW	Gorilla Technology	gorilla-007	007	2021-06-28
161	TW	Gorilla Technology	gorilla-008	008	2021-11-08
162	US	Graymatics	graymatics-001	001	2022-01-13
163	US	Griaule	griaule-000	000	2021-08-20
164	US	Griaule	griaule-001	001	2022-05-31
165	CN	Guangzhou Pixel Solutions	pixelall-008	008	2022-06-16
166	CN	Guangzhou Pixel Solutions	pixelall-009	009	2022-10-26
167	CN	Hangzhuo Allu Network Information Technology	hzailu-002	002	2022-06-02
168	CN	Hangzhuo Allu Network Information Technology	hzailu-003	003	2022-10-11
169	ES	Herta Security	hertasecurity-001	001	2022-01-18
170	ES	Herta Security	hertasecurity-002	002	2022-09-02
171	CN	Hikvision Research Institute	hik-001	001	2019-03-01
172	IN	HyperVerge Inc	hyperverge-002	002	2021-05-27
173	IN	HyperVerge Inc	hyperverge-003	003	2022-04-11
174	AU	ICM Airport Technics	icm-003	003	2021-09-06
175	AU	ICM Airport Technics	icm-004	004	2022-09-07
176	FR	ID3 Technology	id3-006	006	2020-12-17
177	FR	ID3 Technology	id3-008	008	2021-11-10
178	CA	IMDS Software	imds-software-001	001	2022-07-06
179	RU	ITMO University	itmo-007	007	2020-01-06
180	RU	ITMO University	itmo-008	008	2021-11-19
181	RU	IVA Cognitive	ivacognitive-001	001	2021-01-29
182	FR	Idemia	idemia-008	008	2021-07-07
183	FR	Idemia	idemia-009	009	2022-07-27
184	US	Imageware Systems	iws-000	000	2020-08-12
185	GB	Imperial College London	imperial-000	000	2019-03-01
186	GB	Imperial College London	imperial-002	002	2019-08-28
187	US	Incode Technologies Inc	incode-010	010	2021-10-22
188	US	Incode Technologies Inc	incode-011	011	2022-08-10
189	IT	InfoCert	infocert-001	001	2022-09-08
190	IN	Innef Labs	innefulabs-000	000	2020-09-04
191	GB	Innovative Technology	innovativetechnologyltd-001	001	2019-10-22
192	GB	Innovative Technology	innovativetechnologyltd-002	002	2020-02-26
193	SK	Innovatrics	innovatrics-007	007	2020-08-19
194	SK	Innovatrics	innovatrics-008	008	2021-12-15
195	CN	InsightFace AI	insightface-001	001	2021-09-27
196	CN	InsightFace AI	insightface-003	003	2022-08-23
197	CN	Inspur (Beijing) Electronic Information Industry Co	inspur-000	000	2022-07-19
198	CN	Institute of Computing Technology	icthtc-000	000	2020-11-29
199	RU	Institute of Information Technologies	iit-002	002	2019-12-04
200	RU	Institute of Information Technologies	iit-003	003	2020-12-01
201	IS	Intel Research Group	intelresearch-004	004	2021-08-24
202	IS	Intel Research Group	intelresearch-005	005	2022-02-13
203	KR	IntelliVIX	intellivix-001	001	2022-02-25
204	KR	IntelliVIX	intellivix-002	002	2022-07-14
205	AE	Intellibrain Technological Projects	g42-intellibrain-001	001	2022-07-27
206	US	Intellivision	intellivision-003	003	2022-03-07
207	US	Intellivision	intellivision-004	004	2022-07-28
208	LU	Intema-LGL Group	intema-000	000	2022-07-15
209	US	IrexAI	irex-000	000	2020-12-17
210	IL	Is It You	isityou-000	000	2017-06-26

Table 3: Summary of participant information included in this report.

	Location	Developer Name	Short Name	Seq. Num.	Validation Date
211	MX	Jaak IT	jaakit-001	001	2022-05-20
212	KR	Kakao Enterprise	kakao-007	007	2022-01-12
213	KR	Kakao Enterprise	kakao-008	008	2022-05-12
214	KR	Kakao Pay Corp	kakaopay-001	001	2021-07-06
215	TH	Kasikorn Labs	kasikornlabs-000	000	2022-03-02
216	TH	Kasikorn Labs	kasikornlabs-001	001	2022-07-26
217	SG	Kedacom International Pte	kedacom-000	000	2019-06-03
218	US	Kneron Inc	kneron-003	003	2019-07-01
219	US	Kneron Inc	kneron-005	005	2020-02-21
220	US	KnowUTech LLC	knowutech-000	000	2022-02-13
221	KR	Kookmin University	kookmin-002	002	2021-03-05
222	TH	Krungthai	krungthai-002	002	2022-06-21
223	CN	KuKe3D Technology	kuke3d-001	001	2021-10-28
224	CN	KuKe3D Technology	kuke3d-002	002	2022-04-14
225	MX	Lebentech Biometrics	lebentech-000	000	2022-02-16
226	IN	Lema Labs	lemalabs-001	001	2021-04-13
227	JP	Line Corporation	lineclova-001	001	2021-09-26
228	JP	Line Corporation	lineclova-002	002	2022-05-18
229	RU	Lomonosov Moscow State University	intsysmsu-001	001	2019-10-22
230	RU	Lomonosov Moscow State University	intsysmsu-002	002	2020-03-12
231	IN	Lookman Electroplast Industries	lookman-002	002	2018-06-13
232	IN	Lookman Electroplast Industries	lookman-004	004	2019-06-03
233	US	Luxand Inc	luxand-000	000	2019-11-07
234	RU	MVision	mvision-001	001	2019-11-12
235	IN	Mantra Softech India	mantra-000	000	2021-10-28
236	CN	Maxvision Technology	maxvision-001	001	2022-03-03
237	CN	Maxvision Technology	maxvision-002	002	2022-07-12
238	CN	Megvii/Face++	megvii-005	005	2022-03-28
239	CN	Megvii/Face++	megvii-006	006	2022-08-08
240	KR	Metsakuur	metsakuurcompany-001	001	2022-05-12
241	KR	Metsakuur	metsakuurcompany-002	002	2022-09-14
242	GB	MicroFocus	microfocus-001	001	2018-06-13
243	GB	MicroFocus	microfocus-002	002	2018-10-17
244	CN	Minivision	minivision-000	000	2020-10-28
245	NO	Mobai	mobai-000	000	2020-08-26
246	NO	Mobai	mobai-001	001	2021-02-17
247	ES	Mobbeel Solutions	mobbl-001	001	2021-06-16
248	ES	Mobbeel Solutions	mobbl-003	003	2022-04-19
249	KR	Mobipin Technology	mobilpintech-000	000	2021-11-23
250	TH	Momentum Digital	sertis-000	000	2019-10-07
251	TH	Momentum Digital	sertis-002	002	2021-05-13
252	CN	MoreDian Technology	moreidian-000	000	2021-02-24
253	US	Mukh Technologies	mukh-001	001	2022-03-22
254	CN	Multi-Modality Intelligence	multimodality-000	000	2021-10-19
255	CN	Multi-Modality Intelligence	multimodality-001	001	2022-05-16
256	RU	N-Tech Lab	ntechlab-011	011	2021-09-13
257	RU	N-Tech Lab	ntechlab-012	012	2022-01-20
258	CA	NEO Systems	neosystems-004	004	2022-05-02
260	KR	NHN Corp	nhn-002	002	2021-07-15
261	KR	NHN Corp	nhn-003	003	2022-02-22
262	KR	NSENSE Corp	nsensecorp-003	003	2021-10-29
263	KR	NSENSE Corp	nsensecorp-004	004	2022-09-08
264	CN	Nanjing Kiwi Network Technology	kiwitech-000	000	2021-03-19
265	KR	Neosecu Co	openface-001	001	2021-06-15
266	TW	Netbridge Technology Incoporation	netbridgetech-001	001	2020-01-08
267	TW	Netbridge Technology Incoporation	netbridgetech-002	002	2020-08-11
268	LT	Neurotechnology	neurotechnology-013	013	2022-01-07
269	LT	Neurotechnology	neurotechnology-015	015	2022-06-07
270	ID	Nodeflux	nodeflux-002	002	2019-08-13
271	IN	NotionTag Technologies Private Limited	notiontag-001	001	2021-03-04
272	IN	NotionTag Technologies Private Limited	notiontag-002	002	2021-09-17
273	US	Omnigarde Ltd	omnigarde-001	001	2021-08-23
274	US	Omnigarde Ltd	omnigarde-002	002	2022-01-19
275	KR	One More Security	omface-000	000	2021-12-15
276	KR	One More Security	omface-001	001	2022-10-21
277	RU	Oz Forensics LLC	oz-003	003	2021-08-09
278	RU	Oz Forensics LLC	oz-004	004	2021-12-13
279	TW	PAPAGO Inc	papago-001	001	2022-07-19
280	CH	PXL Vision AG	pxl-001	001	2020-06-30

Table 4: Summary of participant information included in this report.

	Location	Developer Name	Short Name	Seq. Num.	Validation Date
281	TW	Palit Microsystems	palit-000	000	2022-05-16
282	TW	Palit Microsystems	palit-001	001	2022-09-26
283	SG	Panasonic R+D Center Singapore	psl-010	010	2022-04-19
284	SG	Panasonic R+D Center Singapore	psl-011	011	2022-10-06
285	US	Pangiam	pangiam-000	000	2022-04-04
286	TR	Papilon Savunma	papsav1923-001	001	2021-03-10
287	TR	Papilon Savunma	papsav1923-002	002	2022-01-20
288	US	Paravision	paravision-008	008	2021-06-30
289	US	Paravision (EverAI)	paravision-010	010	2022-02-02
290	SG	Pensees Pte	pensees-001	001	2020-08-17
291	IN	Pyramid Cyber Security + Forensic (P)	pyramid-000	000	2019-11-04
292	KZ	Qaz Biometric Systems	qazbs-000	000	2022-06-22
293	TW	Qnap Security	qnap-001	001	2021-12-09
294	TW	Qnap Security	qnap-002	002	2022-04-15
295	CZ	Quantasoft	quantasoft-003	003	2021-04-19
296	US	Rank One Computing	rankone-012	012	2021-12-27
297	US	Rank One Computing	rankone-013	013	2022-07-09
298	US	Realnetworks Inc	realnetworks-006	006	2022-02-09
299	US	Realnetworks Inc	realnetworks-007	007	2022-06-14
300	US	Regula Forensics	regula-000	000	2021-04-13
301	US	Regula Forensics	regula-001	001	2021-12-14
302	CN	Remark Holdings	remarkai-001	001	2019-03-01
303	CN	Remark Holdings	remarkai-003	003	2021-06-22
304	SG	Rendip	rendip-000	000	2021-04-19
305	UK	Reveal Media Ltd	revealmedia-005	005	2021-09-24
306	UK	Reveal Media Ltd	revealmedia-006	006	2022-01-26
307	CN	Rokid Corporation	rokid-000	000	2019-08-01
308	CN	Rokid Corporation	rokid-001	001	2019-12-13
309	KR	SK Telecom	sktelecom-000	000	2021-07-09
310	KR	SQIsoft	sqisoft-001	001	2021-07-27
311	KR	SQIsoft	sqisoft-002	002	2021-11-03
312	DE	Saffe	saffe-001	001	2018-10-19
313	DE	Saffe	saffe-002	002	2019-03-01
314	JP	Saga Densan Center Co Ltd	sdc-000	000	2022-10-18
315	KR	Samsung S1 Corp	s1-005	005	2022-06-17
316	KR	Samsung S1 Corp	s1-006	006	2022-10-17
317	KR	Samsung-SDS	samsungsds-001	001	2022-04-18
318	KR	Samsung-SDS	samsungsds-002	002	2022-09-16
319	IN	Samtech InfoNet Limited	samtech-001	001	2019-10-15
320	RU	Satellite Innovation/Eocortex	eocortex-000	000	2020-08-26
321	IL	Scanovate	scanovate-002	002	2020-06-26
322	IL	Scanovate	scanovate-003	003	2021-11-15
323	RO	Securif AI	securifai-004	004	2021-12-21
324	RO	Securif AI	securifai-005	005	2022-05-16
325	CN	Sensemte Group	sensemte-006	006	2021-12-28
326	CN	Sensemte Group	sensemte-007	007	2022-06-17
327	SG	Seventh Sense Artificial Intelligence	seventhsense-001	001	2022-03-04
328	SG	Seventh Sense Artificial Intelligence	seventhsense-002	002	2022-10-17
329	US	Shaman Software	shaman-000	000	2017-12-05
330	US	Shaman Software	shaman-001	001	2018-01-13
331	CN	Shanghai Jiao Tong University	sjtu-003	003	2020-11-02
332	CN	Shanghai Jiao Tong University	sjtu-004	004	2021-05-13
333	CN	Shanghai Ulucu Electronics Technology	uluface-002	002	2019-07-10
334	CN	Shanghai Ulucu Electronics Technology	uluface-003	003	2019-11-12
335	CN	Shanghai University - Shanghai Film Academy	shu-002	002	2019-12-10
336	CN	Shanghai University - Shanghai Film Academy	shu-003	003	2020-06-24
337	CN	Shanghai Yitu Technology	yitu-003	003	2019-03-01
338	CN	Shenzhen AiMall Tech	aimall-002	002	2020-03-12
339	CN	Shenzhen AiMall Tech	aimall-003	003	2020-08-12
340	CN	Shenzhen EI Networks	einetworks-000	000	2019-08-13
341	CN	Shenzhen Inst Adv Integrated Tech CAS	siat-002	002	2018-06-13
342	CN	Shenzhen Inst Adv Integrated Tech CAS	siat-005	005	2022-02-08
343	CN	Shenzhen Intellifusion Technologies	intellifusion-001	001	2019-08-22
344	CN	Shenzhen Intellifusion Technologies	intellifusion-002	002	2020-03-18
345	CN	Shenzhen University-Macau University of Science and Technology	sztu-000	000	2020-12-17
346	CN	Shenzhen University-Macau University of Science and Technology	sztu-001	001	2021-07-13
347	RU	Smart Engines	smartengines-000	000	2021-08-25
348	RU	Smart Engines	smartengines-001	001	2022-05-31
349	ES	Smartbiometrik	smartbiometrik-001	001	2022-05-16
350	TR	Smarvist Teknoloji	smartvist-000	000	2022-05-10

Table 5: Summary of participant information included in this report.

	Location	Developer Name	Short Name	Seq. Num.	Validation Date
351	DE	Smilart	smilart-002	002	2018-02-06
352	DE	Smilart	smilart-003	003	2019-03-01
353	TR	Sodec App Inc	sodec-000	000	2021-06-02
354	IN	StaQu Technologies	staqu-000	000	2020-07-15
355	CN	Star Hybrid Limited	starhybrid-001	001	2019-06-19
356	CN	Su Zhou NaZhiTianDi intelligent technology	nazhai-000	000	2020-06-25
357	IN	Sukshi Technology Innovation	sukshi-000	000	2022-02-13
358	KR	Suprema AI Inc	suprema-002	002	2022-02-11
359	KR	Suprema AI Inc	suprema-003	003	2022-07-20
360	KR	Suprema ID Inc	supremaid-001	001	2021-05-04
361	KR	Suprema ID Inc	supremaid-002	002	2022-06-24
362	RU	Synesis	synesis-006	006	2019-10-10
363	RU	Synesis	synesis-007	007	2020-06-24
364	TW	Synology Inc	synology-000	000	2019-10-23
365	TW	Synology Inc	synology-002	002	2020-08-20
366	BR	T4iSB	t4isb-000	000	2022-01-28
367	CN	TUPU Technology	tuputech-000	000	2019-10-11
368	TW	Taiwan AI Labs	ailabs-001	001	2019-12-18
369	TW	Taiwan-Certificate Authority Incorporation	twface-000	000	2021-05-14
370	TW	Taiwan-Certificate Authority Incorporation	twface-001	001	2021-09-14
371	CH	Tech5 SA	tech5-004	004	2020-03-09
372	CH	Tech5 SA	tech5-005	005	2020-07-24
373	TR	Techsign	techsign-000	000	2021-08-25
374	TR	Techsign	techsign-001	001	2022-07-01
375	CN	Tencent Deepsea Lab	deepsea-001	001	2019-06-03
376	RU	Tevian	tevian-007	007	2021-08-06
377	RU	Tevian	tevian-008	008	2021-12-06
378	US	TigerIT Americas LLC	tiger-005	005	2021-07-29
379	US	TigerIT Americas LLC	tiger-006	006	2021-12-13
380	RU	Tinkoff Bank	tinkoff-001	001	2021-05-13
381	CN	TongYi Transportation Technology	tongyi-005	005	2019-06-12
382	TW	Toppan ID Gate	toppanidgate-000	000	2021-09-28
383	JP	Toshiba	toshiba-004	004	2021-09-27
384	JP	Toshiba	toshiba-006	006	2022-06-29
385	ES	Touchless ID	touchlessid-000	000	2022-05-02
386	ES	Touchless ID	touchlessid-001	001	2022-09-21
387	JP	Tripleize	aize-001	001	2021-04-23
388	JP	Tripleize	aize-002	002	2021-10-08
389	US	Trueface.ai	trueface-002	002	2021-03-29
390	US	Trueface.ai	trueface-003	003	2021-09-30
391	CN	TuringTech.vip	turingtechvip-001	001	2022-02-03
392	CN	TuringTech.vip	turingtechvip-002	002	2022-07-27
393	TR	Turkcell Technology	turkcell-000	000	2022-10-11
394	CN	ULSee Inc	ulsee-001	001	2019-07-31
395	TW	UXLabs	uxlabs-001	001	2022-09-19
396	FR	Unissey	unissey-001	001	2021-11-29
397	FR	Unissey	unissey-002	002	2022-04-29
398	PT	Universidade de Coimbra	visteam-003	003	2022-01-31
399	PT	Universidade de Coimbra	visteam-004	004	2022-08-01
400	UK	University of Surrey-CVSSP	surrey-cvssp-000	000	2022-03-25
401	UK	University of Surrey-CVSSP	surrey-cvssp-001	001	2022-09-22
402	US	VCognition	vcog-002	002	2017-06-12
403	ES	Veridas Digital Authentication Solutions S.L.	veridas-007	007	2021-09-02
404	ES	Veridas Digital Authentication Solutions S.L.	veridas-008	008	2022-10-17
405	UK	Veridium	veridium-000	000	2022-03-28
406	KZ	Verigram	verigram-000	000	2021-09-06
407	KZ	Verigram	verigram-001	001	2022-03-09
408	ID	Verihubs	verihubs-inteligensia-000	000	2021-07-27
409	ID	Verihubs	verihubs-inteligensia-001	001	2022-06-16
410	ID	Verijelas	verijelas-000	000	2022-08-01
411	TW	Via Technologies Inc	via-000	000	2019-07-08
412	TW	Via Technologies Inc	via-001	001	2020-01-08
413	DE	Videmo Intelligent Videoanalyse	videmo-001	001	2021-12-22
414	DE	Videmo Intelligent Videoanalyse	videmo-002	002	2022-08-31
415	IN	Videonetics Technology Pvt	videonetics-001	001	2019-06-19
416	IN	Videonetics Technology Pvt	videonetics-002	002	2019-11-21
417	VN	Vietnam Posts and Telecommunications Group	vnpt-004	004	2022-04-15
418	VN	Vietnam Posts and Telecommunications Group	vnpt-005	005	2022-08-24
419	VN	Viettel Group	vts-000	000	2020-11-04
420	VN	Viettel Group	vts-001	001	2022-04-20

Table 6: Summary of participant information included in this report.

	Location	Developer Name	Short Name	Seq. Num.	Validation Date
421	VN	Viettel High Technology	viettelhightech-000	000	2021-08-04
422	US	Vigilant Solutions	vigilantsolutions-010	010	2021-04-07
423	US	Vigilant Solutions	vigilantsolutions-011	011	2021-08-07
424	VN	VinAI Research VietNam	vinai-000	000	2020-09-24
425	VN	VinBigData	vinbigdata-001	001	2022-01-06
426	VN	VinBigData	vinbigdata-002	002	2022-06-07
427	SE	Visage Technologies	visage-000	000	2020-12-09
428	FI	Visidon	vd-002	002	2021-04-12
429	FI	Visidon	vd-003	003	2021-10-12
430	CN	Vision Intelligence Center of Meituan	meituan-001	001	2022-03-25
431	CN	Vision Intelligence Center of Meituan	meituan-002	002	2022-09-14
432	PT	Vision-Box	visionbox-001	001	2019-03-01
433	PT	Vision-Box	visionbox-002	002	2021-04-29
434	RU	VisionLabs	visionlabs-010	010	2021-01-25
435	RU	VisionLabs	visionlabs-011	011	2021-10-13
436	AU	Vixvizon	vixvizon-005	005	2022-03-03
437	AU	Vixvizon	vixvizon-006	006	2022-08-11
438	RU	Vocord	vocord-009	009	2020-12-28
439	RU	Vocord	vocord-010	010	2021-12-20
440	US	Wicket	wicket-000	000	2022-02-14
441	CN	Winsense	winsense-001	001	2019-10-16
442	CN	Winsense	winsense-002	002	2020-11-20
443	MY	Wise AI SDN BHD	wiseai-001	001	2022-10-25
444	CN	Wuhan Tianyu Information Industry	wuhantianyu-001	001	2021-08-05
445	CN	X-Laboratory	x-laboratory-000	000	2019-09-03
446	CN	X-Laboratory	x-laboratory-001	001	2020-01-21
447	CN	Xforward AI Technology	xforwardai-001	001	2020-09-25
448	CN	Xforward AI Technology	xforwardai-002	002	2021-02-10
449	CN	Xiamen Meiya Pico Information	meiya-001	001	2019-03-01
450	CN	Xiamen University	xm-000	000	2020-10-19
451	PT	YooniK	yoonik-002	002	2021-09-06
452	PT	YooniK	yoonik-003	003	2022-01-06
453	TW	Yuan High-Tech Development	yuan-004	004	2022-01-14
454	TW	Yuan High-Tech Development	yuan-005	005	2022-06-22
455	CN	Yuntu Data and Technology	ytu-000	000	2021-06-16
456	CN	Zhuhai Yisheng Electronics Technology	yisheng-004	004	2018-06-12
457	CN	iQIYI Inc	iqface-000	000	2019-06-04
458	CN	iQIYI Inc	iqface-003	003	2021-02-23
459	TW	iSAP Solution Corporation	isap-001	001	2019-08-07
460	TW	iSAP Solution Corporation	isap-002	002	2020-09-01
461	TW	ioNetworks Inc	ionetworks-000	000	2021-07-20

Table 7: Summary of participant information included in this report.

	ALGORITHM	CONFIG	LIBRARY	TEMPLATE								COMPARISON ⁴		
				NAME	DATA	DATA	MEMORY	SIZE	GENERATION TIME (ms) ⁴				TIME (ns) ⁵	
									(KB) ¹	(KB) ²	(MB) ³	(B)	MUGSHOT	480x720
1	20face-000	117155	324083	²⁰⁹ 905	²⁵¹ 2048 ± 0	⁴⁰ 232 ± 1	²⁹ 223 ± 1	²⁵ 226 ± 4	²¹ 222 ± 1	¹⁵ 224 ± 1	⁴³⁶ 44880 ± 134	⁴³⁵ 44462 ± 163		
2	20face-001	226824	324119	³⁶⁴ 1940	⁴¹¹ 4096 ± 0	⁵¹ 279 ± 2	³⁵ 266 ± 1	²⁷ 266 ± 1	²⁶ 267 ± 1	²¹ 267 ± 0	³³⁹ 5553 ± 54	³³⁷ 5541 ± 65		
3	3divi-006	273866	52656	⁸⁵ 472	²³³ 2048 ± 0	²⁰⁹ 654 ± 1	¹⁷³ 651 ± 0	¹⁵⁴ 660 ± 1	¹³⁷ 678 ± 2	¹³⁷ 759 ± 13	¹¹¹ 775 ± 19	¹¹⁰ 770 ± 22		
4	3divi-007	483115	24723	²⁸⁶ 1285	²⁸⁸ 2048 ± 0	¹⁹⁰ 615 ± 1	¹⁶⁰ 616 ± 1	¹⁴¹ 623 ± 1	¹²⁸ 644 ± 1	¹²⁷ 727 ± 5	⁹⁶ 707 ± 31	⁹⁷ 712 ± 25		
5	acer-001	36650	66086	⁷⁰ 417	³⁸ 512 ± 0	³⁶ 199 ± 0	³¹ 237 ± 28	²⁶ 229 ± 26	²⁵ 242 ± 37	¹⁹ 259 ± 21	²⁵⁵ 2453 ± 44	²⁵⁶ 2461 ± 62		
6	acer-002	43922	624858	³⁷ 187	²⁹⁴ 2048 ± 0	³⁰ 184 ± 0	²³ 184 ± 0	¹⁶ 185 ± 0	¹³ 185 ± 0	¹² 186 ± 0	²⁹⁵ 3370 ± 47	²⁹⁵ 3350 ± 54		
7	acisw-007	267619	36111	⁵¹ 286	²⁰⁴ 2048 ± 0	⁵⁶ 283 ± 0	⁴⁵ 293 ± 3	⁶¹ 414 ± 0	⁵³ 404 ± 0	⁵⁵ 484 ± 1	¹⁶⁷ 1316 ± 22	¹⁶⁷ 1297 ± 23		
8	acisw-008	171703	39359	²⁵² 1101	¹³⁶ 2048 ± 0	⁹³ 400 ± 1	⁶⁴ 362 ± 28	⁴⁸ 369 ± 9	³¹ 300 ± 2	²⁶ 336 ± 5	¹⁶⁸ 1327 ± 19	¹⁷⁰ 1337 ± 32		
9	ader-a-002	0	749797	²¹⁵ 921	⁴⁴⁵ 5120 ± 0	⁴³⁸ 1394 ± 11	³⁹⁹ 1381 ± 1	³⁹⁵ 1393 ± 1	³⁷⁵ 1403 ± 1	³²³ 1464 ± 2	²⁴¹ 2163 ± 32	²⁴³ 2158 ± 28		
10	ader-a-003	0	749778	²¹³ 917	⁴⁴⁶ 5120 ± 0	⁴³⁰ 1381 ± 12	⁴⁰⁰ 1385 ± 1	³⁹⁸ 1394 ± 1	³⁷² 1401 ± 1	³²⁴ 1469 ± 1	²⁴⁰ 2148 ± 34	²⁴⁰ 2130 ± 32		
11	advance-003	258867	78699	¹⁰⁰ 518	¹³⁸ 2048 ± 0	¹⁷³ 586 ± 0	¹⁴⁶ 584 ± 0	¹²⁵ 583 ± 0	¹⁰³ 588 ± 0	⁸³ 591 ± 1	²¹⁵ 1813 ± 17	²¹⁰ 1788 ± 26		
12	advance-004	803133	954494	¹⁴³ 679	¹⁰³ 2048 ± 0	³⁶¹ 1099 ± 20	³²⁷ 1107 ± 15	³⁰⁶ 1093 ± 21	²⁷³ 1103 ± 21	²³³ 1138 ± 21	²²⁷ 1935 ± 35	²²⁹ 1936 ± 32		
13	afisbiometrics-000	545886	32882	²⁴⁹ 1088	³⁹ 512 ± 0	³⁹¹ 1219 ± 1	³³⁴ 1135 ± 1	³¹⁹ 1137 ± 2	²⁸⁴ 1137 ± 1	²³⁴ 1147 ± 1	¹⁷⁴ 1400 ± 29	¹⁷¹ 1357 ± 32		
14	affengine-000	151875	382842	³⁶ 177	⁴⁰⁹ 4096 ± 0	¹⁸ 107 ± 0	¹² 112 ± 0	³ 284 ± 2	¹⁴⁸ 697 ± 2	³⁹⁶ 3299 ± 17	⁴⁴² 54329 ± 140	⁴⁴² 56195 ± 256		
15	aifirst-001	224157	808777	⁸⁷ 485	²³⁵ 2048 ± 0	¹⁷⁶ 587 ± 2	¹³⁸ 568 ± 2	¹²⁶ 584 ± 3	¹¹⁰ 601 ± 6	¹³⁵ 755 ± 5	¹⁴⁸ 1099 ± 14	¹⁵⁰ 1087 ± 45		
16	aigen-001	256958	595227	²⁶⁰ 1136	¹¹⁹ 2048 ± 0	⁴⁴⁹ 1448 ± 9	⁴¹⁹ 1451 ± 8	⁴²⁶ 1759 ± 6	⁴²² 2594 ± 4	⁴⁰⁸ 5691 ± 44	³¹⁰ 3772 ± 57	³⁰⁹ 3736 ± 56		
17	aigen-002	205300	1316138	²⁰³ 874	²⁸⁹ 2048 ± 0	¹⁷⁴ 586 ± 24	¹⁴⁵ 582 ± 4	²³⁷ 920 ± 4	⁴⁰⁶ 1758 ± 5	⁴⁰⁷ 5427 ± 17	³⁰⁶ 3678 ± 44	³⁰⁵ 3646 ± 48		
18	ailabs-001	1054663	338989	²⁷⁸ 1252	²⁵⁵ 2048 ± 0	²¹⁵ 664 ± 4	²¹² 774 ± 50	³²³ 1145 ± 12	⁴¹² 1972 ± 74	⁴⁰⁴ 5205 ± 272	⁴⁵⁴ 104034 ± 661	⁴⁵⁴ 103415 ± 7722		
19	aimall-002	370156	25210	³²⁶ 1576	¹⁶² 2048 ± 0	²⁵² 776 ± 27	²⁷¹ 927 ± 27	²⁴⁶ 940 ± 21	²²⁸ 955 ± 34	¹⁹⁶ 1003 ± 75	⁴⁵¹ 72811 ± 7399	⁴⁵⁰ 71216 ± 6286		
20	aimall-003	504324	171935	³⁶⁰ 1913	⁷⁶ 1024 ± 0	²¹² 662 ± 1	²⁰² 740 ± 51	¹⁸⁵ 752 ± 62	¹⁶² 741 ± 46	¹⁴⁶ 807 ± 47	⁴²⁹ 34565 ± 93	⁴³⁰ 34598 ± 118		
21	aiseemu-001	0	1005354	³⁹⁶ 2697	⁴²⁰ 4096 ± 0	³⁴¹ 1001 ± 1	³⁰³ 1017 ± 0	²⁸³ 1014 ± 5	²⁵³ 1022 ± 2	²¹² 1059 ± 4	³²⁷ 4864 ± 25	³²⁷ 4855 ± 32		
22	aiunionface-000	241642	840295	⁶⁷ 402	¹⁸⁵ 2048 ± 0	²⁰¹ 637 ± 13	²⁰⁷ 754 ± 41	²⁸⁵ 1025 ± 28	²⁹⁸ 1179 ± 29	³⁵¹ 1639 ± 47	¹⁴² 1072 ± 19	¹⁴⁸ 1080 ± 47		
23	aize-001	268456	168970	³¹⁰ 1436	²²⁷ 2048 ± 0	¹¹¹ 437 ± 10	⁹⁰ 440 ± 8	¹⁰⁹ 542 ± 17	¹⁶⁵ 756 ± 27	³⁴⁵ 1583 ± 53	²²⁹ 1937 ± 22	²²³ 1919 ± 23		
24	aize-002	257106	182517	¹²⁰ 586	²¹⁴ 2048 ± 0	¹²³ 467 ± 1	¹⁰² 479 ± 1	¹⁸⁶ 756 ± 1	³⁹² 1477 ± 1	⁴⁰¹ 4617 ± 41	⁶¹ 597 ± 16	⁶⁷ 598 ± 14		
25	ajou-001	363257	31734	⁷⁸ 442	¹⁰⁵ 2048 ± 0	¹⁴⁶ 530 ± 0	¹²⁴ 536 ± 0	¹⁰⁷ 535 ± 0	⁹³ 549 ± 0	⁸⁰ 577 ± 0	⁶⁰ 597 ± 19	⁶⁵ 596 ± 13		
26	alchera-003	487718	24613	²⁹⁸ 1376	¹⁵³ 2048 ± 0	²⁸⁵ 854 ± 3	²⁴¹ 862 ± 2	²¹⁷ 870 ± 1	²⁰² 882 ± 2	¹⁷⁶ 918 ± 1	²⁹⁸ 3426 ± 57	²⁹⁶ 3383 ± 53		
27	alchera-004	1001019	388616	²⁸² 1270	¹⁶¹ 2048 ± 0	³³¹ 975 ± 0	²⁸⁰ 955 ± 0	²⁵⁷ 960 ± 0	²⁴⁰ 989 ± 0	²³⁵ 1152 ± 1	³⁰¹ 3529 ± 54	³⁰¹ 3530 ± 63		
28	alfabeta-001	128232	21780	⁸⁷ 3	⁴¹ 512 ± 0	⁴⁷ 271 ± 0	⁴⁰ 276 ± 2	⁷⁷ 459 ± 2	²⁰⁴ 886 ± 2	³⁸² 2547 ± 9	⁴² 470 ± 25	⁴⁴ 458 ± 20		
29	alice-000	1741293	19355	³⁴⁶ 1732	³⁹⁷ 4096 ± 0	³²¹ 950 ± 2	²⁷³ 933 ± 1	²⁵¹ 949 ± 1	²⁵² 1011 ± 3	²⁶³ 1264 ± 8	³⁹⁷ 14975 ± 201	³⁹⁷ 14890 ± 229		
30	alleyes-000	507636	997090	²⁰⁰ 857	¹²⁸ 2048 ± 0	²⁵⁷ 784 ± 1	²⁸⁶ 970 ± 61	²⁶¹ 974 ± 62	²²⁴ 943 ± 69	²¹⁰ 1057 ± 23	¹⁶⁶ 1298 ± 34	¹⁶⁸ 1303 ± 51		
31	allgovision-000	172509	155862	¹¹² 561	²⁶⁵ 2048 ± 0	⁸⁹ 384 ± 8	⁷² 395 ± 17	⁶⁰ 413 ± 14	⁷⁰ 471 ± 14	¹²² 710 ± 21	⁴²⁰ 29903 ± 406	⁴²¹ 29735 ± 194		
32	alphaface-001	259849	81636	¹⁰³ 527	²⁵⁶ 2048 ± 0	¹⁸⁶ 612 ± 1	¹⁵⁵ 613 ± 3	¹³⁷ 612 ± 1	¹¹⁵ 619 ± 1	¹⁰³ 640 ± 2	¹³³ 1008 ± 10	¹³³ 1002 ± 19		
33	alphaface-002	768995	70692	³⁰⁹ 1434	¹²⁶ 2048 ± 0	¹⁹⁶ 628 ± 2	²⁰⁴ 746 ± 19	¹⁸⁴ 751 ± 18	¹⁶⁹ 779 ± 22	¹⁵¹ 828 ± 40	¹²⁸ 945 ± 25	¹²⁶ 935 ± 17		
34	amplifiedgroup-001	0	47053	¹² 81	⁶² 866 ± 2	¹² 93 ± 0	-	-	-	-	⁴⁴⁴ 57803 ± 4210	⁴⁴³ 56365 ± 1196		
35	androvideo-000	174847	585063	⁶⁸ 403	¹³¹ 2048 ± 0	⁴⁹ 277 ± 0	⁴³ 285 ± 0	³⁶ 314 ± 0	⁴² 372 ± 1	⁹³ 620 ± 0	²⁷⁴ 2860 ± 28	²⁷³ 2847 ± 22		
36	anke-004	349388	410776	¹⁵⁵ 706	³⁶² 2056 ± 0	¹⁹³ 625 ± 1	¹⁶³ 627 ± 2	¹⁴⁸ 635 ± 3	¹³⁰ 653 ± 2	¹⁹¹ 982 ± 8	⁸⁰ 633 ± 22	⁸⁰ 632 ± 34		
37	anke-005	328553	429160	²⁵⁸ 1134	³⁷⁰ 2056 ± 0	¹⁷⁷ 590 ± 2	¹⁵¹ 594 ± 5	¹³⁴ 601 ± 3	¹²⁴ 638 ± 4	¹⁵⁰ 821 ± 24	⁹⁰ 685 ± 19	⁹³ 687 ± 26		
38	antheus-000	119453	41994	²⁰ 116	⁵¹ 520 ± 0	¹⁶ 109 ± 1	²⁴ 187 ± 1	¹⁸ 189 ± 1	¹⁴ 195 ± 1	¹⁷ 236 ± 2	³⁵⁷ 6901 ± 268	³⁵⁷ 6936 ± 103		
39	antheus-001	119453	41962	²¹ 118	⁴⁹ 520 ± 0	¹⁹ 120 ± 1	³⁴ 265 ± 13	⁸³ 468 ± 22	³¹³ 1223 ± 27	³⁸³ 2660 ± 87	³⁵² 6218 ± 47	³⁵¹ 6216 ± 45		
40	anyvision-004	401001	630797	²⁵³ 1102	⁷¹ 1024 ± 0	⁷⁸ 355 ± 1	-	-	-	-	²²⁴ 1891 ± 51	²¹⁵ 1829 ± 85		
41	anyvision-005	190979	116595	²²² 963	⁷³ 1024 ± 0	³³⁶ 985 ± 1	²⁹⁴ 997 ± 1	²⁷⁹ 1004 ± 1	²⁴² 995 ± 1	¹⁹⁴ 995 ± 1	¹⁰⁴ 733 ± 14	¹⁰⁴ 733 ± 16		
42	armatura-001	0	374608	²⁶⁴ 1151	¹⁶⁴ 2048 ± 0	²²⁵ 688 ± 1	¹⁸⁷ 689 ± 1	¹⁶⁹ 693 ± 1	¹⁵¹ 708 ± 3	¹³⁶ 756 ± 13	¹⁹ 270 ± 17	²¹ 268 ± 11		
43	armatura-002	0	1258644	²⁷⁵ 1222	⁴⁴⁸ 6144 ± 0	⁴⁵⁶ 1476 ± 3	⁴²² 1458 ± 5	³⁹⁵ 1505 ± 12	³⁴⁷ 1605 ± 26	¹⁹¹ 1605 ± 26	¹⁹¹ 1589 ± 25			
44	asusaics-000	257418	245320	¹²⁷ 605	²⁴⁰ 2048 ± 0	¹³³ 484 ± 13	¹¹⁸ 506 ± 21	²¹² 850 ± 26	⁴⁰⁸ 1789 ± 61	⁴¹⁰ 6305 ± 188	³³⁷ 5455 ± 78	³³⁶ 5422 ± 112		

Notes

- 1 The configuration size does not capture static data included in libraries.
- 2 The library size is the combined total of all files provided in the submission lib folder. These libraries e.g. OpenCV may or may not be installed on any end user's platform natively and would not need to be installed with the algorithm. Some developers put neural network models in their libraries.
- 3 The memory usage is the peak resident set size reported by the ps system call during template generation.
- 4 The median template creation times are measured on Intel®Xeon®CPU E5-2630 v4 @ 2.20GHz processors.
- 5 The comparison durations, in nanoseconds, are estimated using std::chrono::high_resolution_clock which on the machine in (2) counts 1ns clock ticks. Precision is somewhat worse than that however. The ± value is the median absolute deviation times 1.48 for Normal consistency.

	ALGORITHM	CONFIG	LIBRARY	TEMPLATE								COMPARISON ⁴									
				NAME	DATA	DATA	MEMORY	SIZE	GENERATION TIME (ms) ⁴				TIME (ns) ⁵								
									(KB) ¹	(KB) ²	(MB) ³	(B)	MUGSHOT	480x720	960x1440	1600x2400	3000x4500	GENUINE	IMPOSTOR		
45	asusaics-001	257418	245330	124	595	423	4096 ± 0	281	842 ± 17	301	1008 ± 20	390	1377 ± 28	421	2423 ± 90	415	7284 ± 277	367	8618 ± 42	367	8638 ± 136
46	authenmetric-003	293599	39492	226	982	134	2048 ± 0	339	992 ± 1	299	1006 ± 1	277	1003 ± 2	247	1002 ± 1	203	1036 ± 1	205	1757 ± 19	205	1755 ± 19
47	authenmetric-004	381165	39492	272	1214	283	2048 ± 0	306	910 ± 1	266	909 ± 1	234	915 ± 1	216	921 ± 2	184	950 ± 1	200	1724 ± 14	198	1691 ± 29
48	aware-005	300017	26320	280	1265	98	1572 ± 0	303	886 ± 23	311	1038 ± 21	313	1121 ± 22	348	1337 ± 58	368	2195 ± 144	184	1475 ± 63	180	1427 ± 115
49	aware-006	298543	14124	219	943	14	352 ± 0	375	1148 ± 3	339	1146 ± 2	337	1190 ± 2	335	1306 ± 20	360	1754 ± 84	263	2598 ± 42	263	2559 ± 60
50	awiros-001	15499	87480	14	88	42	512 ± 0	12	97 ± 6	10	98 ± 4	11	138 ± 6	22	225 ± 7	76	556 ± 8	145	1079 ± 44	142	1050 ± 45
51	awiros-002	289016	203723	113	562	218	2048 ± 0	129	479 ± 0	112	500 ± 0	106	534 ± 0	114	618 ± 0	182	946 ± 1	230	1966 ± 31	231	1957 ± 25
52	aximetria-001	408902	487912	142	674	171	2048 ± 0	346	1013 ± 1	304	1023 ± 21	288	1029 ± 5	245	999 ± 2	222	1091 ± 5	320	4401 ± 94	319	4490 ± 80
53	ayftech-001	195423	43580	164	731	35	512 ± 0	100	408 ± 23	100	476 ± 52	199	814 ± 108	410	1827 ± 384	406	5412 ± 1029	71	615 ± 16	122	885 ± 44
54	ayonix-000	58505	5252	6	69	83	1036 ± 0	2	18 ± 2	-	-	-	-	-	-	-	-	74	621 ± 23	77	620 ± 26
55	beethedata-000	227849	1087592	111	555	129	2048 ± 0	121	465 ± 0	99	467 ± 0	81	468 ± 0	68	467 ± 0	52	467 ± 0	237	2121 ± 34	238	2110 ± 38
56	beyneai-000	256958	591433	256	1124	179	2048 ± 0	114	451 ± 8	92	449 ± 1	188	767 ± 7	402	1603 ± 25	402	4669 ± 124	308	3730 ± 57	306	3668 ± 54
57	biocube-001	25030	6192987	82	458	403	4096 ± 0	54	282 ± 22	44	292 ± 24	104	521 ± 57	138	684 ± 59	270	1282 ± 68	411	21787 ± 96	411	21812 ± 109
58	bioittechswiss-001	1178769	120811	312	1455	15	512 ± 0	329	966 ± 4	371	1270 ± 270	362	1294 ± 96	376	1409 ± 157	363	1793 ± 79	264	2610 ± 25	264	2624 ± 32
59	bioittechswiss-002	744786	114842	231	993	25	512 ± 0	311	917 ± 2	272	930 ± 2	252	952 ± 2	226	947 ± 3	211	1058 ± 11	244	2177 ± 29	245	2170 ± 31
60	bm-001	287734	38076	27	148	1	64 ± 0	112	444 ± 88	-	-	-	-	-	-	-	223	1887 ± 31	221	1877 ± 26	
61	boetech-001	261376	88710	301	1384	121	2048 ± 0	46	271 ± 1	36	268 ± 1	28	273 ± 0	29	286 ± 1	23	318 ± 1	448	68519 ± 1921	448	67648 ± 822
62	boetech-002	294347	88710	317	1489	295	2048 ± 0	62	305 ± 4	47	296 ± 1	32	302 ± 1	32	313 ± 1	28	348 ± 2	449	68921 ± 2137	449	69473 ± 2104
63	bresee-001	287880	23227	273	1214	307	2048 ± 0	393	1223 ± 3	356	1216 ± 1	374	1331 ± 1	316	1227 ± 1	292	1360 ± 1	431	37240 ± 655	432	37167 ± 584
64	bresee-002	313627	30902	366	1956	228	2048 ± 0	243	743 ± 4	337	1143 ± 2	324	1146 ± 2	286	1148 ± 2	247	1176 ± 2	208	1778 ± 22	208	1775 ± 23
65	camvi-002	236278	225285	165	737	69	1024 ± 0	220	677 ± 7	201	726 ± 36	216	869 ± 28	278	1129 ± 43	388	2785 ± 113	70	612 ± 26	70	603 ± 20
66	camvi-004	280733	615819	214	919	157	2048 ± 0	246	759 ± 10	240	861 ± 17	269	986 ± 34	331	1279 ± 51	390	2891 ± 158	126	948 ± 40	127	963 ± 31
67	canon-003	2550850	101378	444	5472	449	6180 ± 0	403	1263 ± 3	369	1263 ± 1	359	1283 ± 1	343	1320 ± 1	328	1482 ± 2	325	4783 ± 17	322	4780 ± 19
68	canon-004	2399160	114188	446	5956	430	6200 ± 0	320	948 ± 4	279	955 ± 3	256	959 ± 3	233	977 ± 3	217	1064 ± 2	363	7172 ± 63	362	7169 ± 51
69	ceiec-003	260371	88707	74	430	249	2048 ± 0	269	817 ± 4	255	883 ± 57	227	897 ± 60	210	899 ± 72	180	944 ± 72	250	2256 ± 38	250	2241 ± 54
70	ceiec-004	263476	67011	69	408	151	2048 ± 0	348	1024 ± 1	307	1027 ± 1	287	1027 ± 1	255	1030 ± 1	207	1055 ± 1	217	1844 ± 26	216	1836 ± 20
71	chosun-001	765615	707	91	491	124	2048 ± 0	256	783 ± 2	228	826 ± 4	425	1662 ± 13	427	3679 ± 67	423	11694 ± 243	130	998 ± 25	140	1035 ± 11
72	chosun-002	234001	31875	79	450	304	2048 ± 0	42	248 ± 3	37	273 ± 3	419	1495 ± 14	428	7920 ± 90	424	80302 ± 1349	75	623 ± 17	83	634 ± 13
73	chtface-004	409656	311027	316	1487	132	2048 ± 0	70	332 ± 0	53	323 ± 1	40	329 ± 1	36	335 ± 1	32	377 ± 1	201	1727 ± 17	200	1720 ± 16
74	chtface-005	408364	311100	305	1412	170	2048 ± 0	67	322 ± 0	51	316 ± 1	38	325 ± 2	34	324 ± 1	40	411 ± 2	225	1907 ± 19	222	1898 ± 23
75	cist-001	0	300551	117	583	184	2048 ± 0	330	972 ± 0	288	977 ± 1	263	981 ± 0	236	983 ± 0	214	1061 ± 0	279	2947 ± 20	278	2940 ± 22
76	clearviewai-000	342491	211852	403	2750	302	2048 ± 0	441	1402 ± 1	410	1403 ± 1	406	1412 ± 1	379	1420 ± 1	310	1418 ± 1	190	1592 ± 37	188	1561 ± 37
77	cloesli-001	420342	9851	173	773	427	4096 ± 0	280	839 ± 1	234	843 ± 1	210	841 ± 1	190	845 ± 1	163	865 ± 1	336	5404 ± 17	335	5400 ± 25
78	cloudmatrix-001	10390	542121	44	249	110	2048 ± 0	18	114 ± 1	13	117 ± 0	10	118 ± 0	9	123 ± 1	10	169 ± 1	439	50263 ± 212	439	50243 ± 237
79	cloudmatrix-002	256635	693318	235	1030	163	2048 ± 0	91	395 ± 1	73	398 ± 1	56	399 ± 1	51	402 ± 1	47	437 ± 20	438	49578 ± 120	438	49602 ± 180
80	cloudwalk-hr-003	383739	144263	229	984	371	2057 ± 0	183	606 ± 0	148	588 ± 0	130	594 ± 0	113	612 ± 1	-	-	359	6982 ± 80	358	6972 ± 84
81	cloudwalk-hr-004	502916	520169	304	1394	325	2049 ± 0	295	873 ± 1	251	877 ± 1	222	876 ± 1	201	879 ± 1	172	902 ± 3	382	11652 ± 127	382	11608 ± 123
82	cloudwalk-mt-005	846026	573253	411	2928	213	2048 ± 0	380	1179 ± 3	353	1200 ± 3	342	1209 ± 3	314	1226 ± 5	259	1229 ± 3	389	12525 ± 225	388	12394 ± 152
83	cloudwalk-mt-006	563322	480071	406	2836	120	2048 ± 0	433	1385 ± 0	404	1392 ± 1	399	1398 ± 1	371	1397 ± 4	318	1444 ± 2	294	3364 ± 96	293	3324 ± 83
84	codeline-000	361659	138388	270	1188	108	2048 ± 0	451	1453 ± 0	421	1456 ± 2	415	1456 ± 0	383	1457 ± 0	329	1483 ± 1	242	2171 ± 69	246	2194 ± 84
85	cogent-006	1078167	58108	323	1547	86	1062 ± 0	250	768 ± 0	216	789 ± 1	206	831 ± 2	218	930 ± 1	189	971 ± 1	211	1802 ± 17	211	1797 ± 23
86	cogent-007	621565	72316	359	1884	59	550 ± 0	422	1329 ± 2	391	1333 ± 5	377	1337 ± 4	352	1353 ± 5	302	1390 ± 4	31	355 ± 8	34	367 ± 14
87	cognitec-003	471458	62502	188	817	339	2052 ± 0	83	366 ± 9	77	403 ± 9	58	408 ± 9	57	424 ± 9	58	509 ± 13	297	3417 ± 51	299	3433 ± 53
88	cognitec-004	705645	62678	119	585	340	2052 ± 0	118	463 ± 9	110	497 ± 9	95	504 ± 10	84	521 ± 10	94	631 ± 12	285	3028 ± 197	286	3059 ± 238

Notes

1 The configuration size does not capture static data included in libraries.

2 The library size is the combined total of all files provided in the submission lib folder. These libraries e.g. OpenCV may or may not be installed on any end user's platform natively and would not need to be installed with the algorithm. Some developers put neural network models in their libraries.

3 The memory usage is the peak resident set size reported by the ps system call during template generation.

4 The median template creation times are measured on Intel®Xeon®CPU E5-2630 v4 @ 2.20GHz processors.

5 The comparison durations, in nanoseconds, are estimated using std::chrono::high_resolution_clock which on the machine in (2) counts 1ns clock ticks. Precision is somewhat worse than that however. The \pm value is the median absolute deviation times 1.48 for Normal consistency.

	ALGORITHM	CONFIG	LIBRARY	TEMPLATE								COMPARISON ⁴		
				NAME	DATA	DATA	MEMORY	SIZE	GENERATION TIME (ms) ⁴				TIME (ns) ⁵	
									(KB) ¹	(KB) ²	(MB) ³	(B)	MUGSHOT	480x720
89	cor-001	1194948	11240	²⁷⁷ 1249	³⁷³ 2060 ± 0	²³⁵ 699 ± 3	²⁴² 863 ± 76	²¹⁴ 865 ± 80	¹⁹⁷ 872 ± 89	¹⁸⁵ 952 ± 39	⁴⁵⁷ 270145 ± 2259	⁴⁵⁷ 282686 ± 11788		
90	coretech-000	186423	43964	⁶⁶ 393	³⁴ 512 ± 0	¹⁸² 602 ± 15	¹⁷⁴ 659 ± 12	³²⁰ 1139 ± 24	²⁸⁷ 1149 ± 25	²⁴¹ 1165 ± 23	²⁶ 333 ± 14	²⁷ 321 ± 13		
91	coretech-001	235361	305490	³²¹ 1524	²⁴¹ 2048 ± 0	²²⁷ 688 ± 7	¹⁹⁰ 695 ± 7	²¹⁸ 870 ± 17	²⁰⁰ 879 ± 15	¹⁶⁵ 877 ± 15	⁷⁶ 625 ± 25	⁸⁵ 641 ± 25		
92	corsight-002	1474921	32093	³⁷¹ 2061	³⁷⁸ 2080 ± 0	⁴¹¹ 1290 ± 1	³⁷⁶ 1287 ± 1	³⁶⁰ 1290 ± 1	³³⁷ 1307 ± 2	³⁰¹ 1388 ± 4	⁴¹⁵ 24953 ± 637	⁴¹⁴ 24263 ± 578		
93	corsight-003	1413063	32198	³³⁴ 1637	³⁷⁷ 2080 ± 0	³⁸⁸ 1202 ± 2	³⁵² 1190 ± 5	³⁴⁰ 1199 ± 3	³¹⁷ 1236 ± 3	²⁸⁸ 1349 ± 7	⁴¹⁹ 28754 ± 434	⁴²⁰ 28279 ± 446		
94	csc-002	0	519768	²⁹⁹ 1376	⁵⁵ 544 ± 0	¹²⁵ 473 ± 0	¹⁰⁸ 494 ± 0	⁸⁶ 481 ± 1	⁷⁴ 490 ± 1	⁶² 514 ± 5	³⁴ 367 ± 11	³⁵ 371 ± 10		
95	csc-003	0	400435	³³² 1609	⁵⁶ 544 ± 0	¹³⁸ 499 ± 0	¹¹⁴ 500 ± 1	⁹⁴ 502 ± 0	⁸¹ 508 ± 1	⁶⁸ 535 ± 4	³⁷ 393 ± 8	³⁸ 397 ± 7		
96	ctcbcank-000	257208	599238	¹¹⁵ 570	²¹⁶ 2048 ± 0	¹⁶⁴ 568 ± 43	¹⁶⁸ 606 ± 38	¹⁵² 690 ± 53	¹⁵² 711 ± 50	¹⁵² 831 ± 51	³⁰² 3551 ± 87	³²⁴ 4805 ± 209		
97	ctcbcank-001	275511	599238	¹²⁵ 603	¹⁵⁹ 2048 ± 0	²⁰⁶ 652 ± 35	²¹⁴ 781 ± 30	²²¹ 875 ± 43	²⁰⁹ 898 ± 51	²⁰² 1030 ± 47	³¹¹ 3926 ± 45	³¹⁰ 3924 ± 56		
98	cubox-001	369627	75427	¹³⁵ 649	²⁵⁴ 2048 ± 0	³⁰⁴ 907 ± 1	²⁶³ 902 ± 1	²³¹ 903 ± 0	²¹⁴ 917 ± 0	¹⁷⁷ 931 ± 0	¹⁷⁰ 1379 ± 37	¹⁷⁷ 1417 ± 38		
99	cubox-002	542254	90975	³⁶⁷ 1964	²⁷⁰ 2048 ± 0	³¹² 921 ± 1	²⁶⁸ 921 ± 1	²⁴⁰ 922 ± 1	²²⁰ 933 ± 1	¹⁹⁷ 1003 ± 1	²³³ 2008 ± 72	²³³ 1969 ± 57		
100	cudocommunication-001	385258	341277	²⁴⁶ 1077	²³¹ 2048 ± 0	³¹⁴ 925 ± 1	²⁶⁹ 923 ± 1	²⁴⁵ 928 ± 1	²¹⁹ 932 ± 0	¹⁸⁶ 964 ± 1	²⁵⁹ 2534 ± 20	²⁶¹ 2537 ± 20		
101	cuhkee-001	787853	74917	³⁸⁹ 2515	³³⁴ 2052 ± 0	³³³ 977 ± 31	-	-	-	-	²⁶⁶ 2719 ± 60	²⁷⁰ 2783 ± 56		
102	cybercore-002	166096	7374	³⁹² 2564	¹¹⁶ 2048 ± 0	¹³⁶ 489 ± 1	¹¹³ 500 ± 4	⁹³ 500 ± 1	⁷⁹ 499 ± 2	⁶⁷ 528 ± 1	³⁸⁷ 12389 ± 123	³⁸⁷ 12352 ± 112		
103	cybercore-003	289176	7969	⁴³³ 4310	³⁹⁸ 4096 ± 0	²⁸² 844 ± 2	²³⁸ 855 ± 4	²¹³ 864 ± 4	¹⁹⁵ 862 ± 4	¹⁶⁶ 878 ± 2	³⁴³ 5744 ± 41	³⁴⁵ 5737 ± 31		
104	cyberextruder-003	253300	12354	⁷⁶ 437	³¹ 512 ± 0	⁹⁰ 390 ± 1	⁷¹ 388 ± 1	⁵⁵ 393 ± 1	⁴⁹ 399 ± 1	⁴⁶ 435 ± 1	¹⁰ 198 ± 4	¹¹ 189 ± 8		
105	cyberextruder-004	169301	12354	⁶¹ 349	² 128 ± 0	³⁷ 206 ± 0	²⁷ 208 ± 0	²² 209 ± 0	²³ 229 ± 0	¹⁸ 249 ± 1	⁵ 145 ± 14	⁶ 155 ± 14		
106	cyberlink-009	588443	102201	³³⁹ 1704	⁴³⁸ 4164 ± 0	⁴³¹ 1384 ± 2	⁴⁰⁷ 1395 ± 2	⁴⁰⁰ 1398 ± 2	³⁷³ 1401 ± 2	³²¹ 1456 ± 2	²³ 299 ± 17	²⁵ 304 ± 16		
107	cyberlink-010	1590818	102180	⁴²² 3672	⁴⁵⁶ 8260 ± 0	⁴⁰⁴ 1265 ± 2	³⁸³ 1314 ± 5	³⁶⁴ 1294 ± 2	³²⁹ 1273 ± 2	²⁷⁸ 1305 ± 2	⁴³ 476 ± 23	⁴⁶ 472 ± 14		
108	dahua-006	831641	119261	⁴⁴⁰ 5068	¹⁵⁴ 2048 ± 0	⁴³⁹ 1398 ± 2	⁴⁰⁹ 1397 ± 1	⁴⁰³ 1404 ± 1	³⁷⁴ 1402 ± 1	³⁰⁶ 1402 ± 1	¹⁸ 249 ± 13	²⁰ 250 ± 11		
109	dahua-007	1578737	119418	⁴⁵¹ 7237	³⁹⁶ 4096 ± 0	⁴³⁷ 1393 ± 2	³⁹⁸ 1373 ± 1	³⁹¹ 1378 ± 1	³⁶² 1378 ± 1	²⁹⁷ 1379 ± 2	³⁵ 367 ± 102	³⁹ 434 ± 108		
110	daon-000	280726	2307	³⁷⁰ 2013	³⁷⁵ 2065 ± 0	¹⁵⁹ 562 ± 3	¹⁴⁴ 581 ± 5	¹⁹¹ 791 ± 9	¹⁸⁷ 838 ± 15	²⁰⁸ 1055 ± 32	⁴⁰⁰ 16052 ± 88	⁴⁰⁰ 16041 ± 85		
111	decatur-000	350495	171271	²¹⁰ 907	⁴³⁰ 4100 ± 0	³⁴⁹ 1024 ± 2	-	-	-	-	³⁸⁰ 11439 ± 80	³⁸¹ 11418 ± 112		
112	decatur-001	342866	253734	³¹⁸ 1507	³⁴⁴ 2052 ± 0	³⁶² 1103 ± 2	³¹⁶ 1064 ± 2	³⁰⁰ 1063 ± 2	²⁶⁵ 1067 ± 2	²¹⁹ 1084 ± 2	⁶⁹ 610 ± 19	⁶⁹ 602 ± 8		
113	deepglint-004	1073382	261571	⁴¹⁴ 3084	¹⁴¹ 2048 ± 0	⁴⁵³ 1470 ± 1	⁴²⁵ 1474 ± 1	⁴¹⁸ 1485 ± 1	³⁹¹ 1474 ± 1	³³¹ 1492 ± 2	³⁴⁸ 5961 ± 34	³⁴⁹ 5955 ± 29		
114	deepglint-005	960326	213877	⁴¹³ 2947	¹⁷⁴ 2048 ± 0	⁴⁴⁴ 1408 ± 1	⁴¹⁶ 1431 ± 2	⁴⁰⁸ 1424 ± 3	³⁸¹ 1424 ± 3	³¹⁹ 1446 ± 2	³⁵⁵ 6765 ± 38	³⁵⁴ 6765 ± 40		
115	deepsea-001	147497	336250	⁶³ 358	⁷⁷ 1024 ± 0	¹⁹⁷ 630 ± 7	²⁰⁶ 752 ± 37	¹⁸³ 746 ± 30	¹⁵⁷ 727 ± 32	¹⁴⁹ 820 ± 32	¹⁷⁵ 1401 ± 37	¹⁸² 1467 ± 50		
116	deeepsense-000	357113	936618	⁴⁵² 7618	²⁴⁸ 2048 ± 0	²¹⁶ 664 ± 3	¹⁷² 645 ± 1	¹⁵⁵ 660 ± 2	¹⁴⁰ 687 ± 2	¹⁴⁷ 808 ± 3	⁴⁴ 480 ± 22	⁴⁵ 459 ± 34		
117	deeepsense-001	73173	1288355	⁴⁴¹ 5314	⁴⁰ 512 ± 0	³⁷³ 1142 ± 2	³⁴² 1164 ± 3	³³⁶ 1183 ± 3	³⁰⁹ 1201 ± 3	²⁸³ 1323 ± 2	²⁵³ 2356 ± 35	²⁵³ 2354 ± 42		
118	dermalog-009	0	319363	¹³⁸ 664	³⁷ 512 ± 0	⁷⁶ 349 ± 0	⁶⁰ 351 ± 0	⁴⁴ 352 ± 0	³⁹ 357 ± 0	³⁶ 389 ± 0	⁴⁶ 487 ± 34	³⁷ 385 ± 29		
119	dermalog-010	0	525908	²³⁴ 1023	³² 512 ± 0	²⁰⁰ 635 ± 0	¹⁷⁰ 640 ± 1	¹⁴⁹ 639 ± 4	¹²⁶ 647 ± 3	¹¹⁵ 691 ± 5	³⁹ 444 ± 13	³¹ 341 ± 26		
120	dicio-001	61751	119517	¹¹ 77	⁵² 520 ± 0	¹⁵¹ 538 ± 0	¹³⁷ 563 ± 10	²³⁵ 915 ± 3	⁴⁰⁹ 1800 ± 7	⁴⁰⁵ 5286 ± 30	²⁷⁰ 2818 ± 20	²⁷¹ 2807 ± 31		
121	digiglobalface-001	259849	70680	¹⁰² 527	¹⁴⁴ 2048 ± 0	¹⁸⁴ 612 ± 1	¹⁶⁷ 633 ± 3	¹⁴⁶ 634 ± 3	¹²⁸ 650 ± 15	¹⁰⁹ 666 ± 4	¹²⁸ 973 ± 20	¹²⁸ 988 ± 20		
122	digidata-000	133370	30249	⁴⁷ 257	¹⁴⁰ 2048 ± 0	⁸² 361 ± 0	⁶² 360 ± 0	⁴⁶ 361 ± 0	⁴⁰ 363 ± 0	³⁴ 380 ± 0	²³⁶ 2084 ± 37	²³⁵ 2039 ± 42		
123	digidata-001	254564	33036	⁶⁴ 367	¹⁷⁶ 2048 ± 0	¹⁵⁸ 559 ± 1	¹³⁵ 561 ± 1	¹¹⁷ 562 ± 1	⁹⁵ 564 ± 1	⁸⁸ 602 ± 1	³⁷⁷ 10308 ± 102	³⁷⁷ 10301 ± 121		
124	digitalbarriers-002	83002	598577	³⁶² 1930	³⁶¹ 2056 ± 0	³⁸ 209 ± 11	³² 250 ± 19	⁵⁹ 411 ± 37	¹⁷⁶ 808 ± 72	³⁷⁰ 2236 ± 123	³⁹⁰ 13409 ± 228	³⁹⁰ 13267 ± 206		
125	dps-000	0	2211812	²⁴⁰ 1058	⁴⁰² 4096 ± 0	²⁸⁷ 868 ± 2	²⁶⁰ 893 ± 6	⁴¹² 1445 ± 9	⁴²⁴ 2910 ± 38	⁴¹⁷ 9345 ± 17	¹⁸³ 1473 ± 37	¹⁸⁴ 1479 ± 37		
126	dsk-000	11967	782905	⁴⁶ 252	²³ 512 ± 0	⁶¹ 304 ± 47	⁵² 317 ± 33	²⁷⁶ 1001 ± 96	⁴²³ 2660 ± 170	⁴²¹ 10451 ± 832	³⁶² 7152 ± 115	³⁶⁰ 7134 ± 111		
127	einetworks-000	372608	219883	²⁰⁶ 880	³⁶⁷ 2056 ± 0	²⁰⁴ 645 ± 3	-	-	-	-	³²⁸ 4876 ± 66	³³⁰ 5156 ± 77		
128	ekin-002	51434	278	²⁴ 139	³⁸⁵ 3072 ± 0	³⁸⁵ 1186 ± 13	³⁴⁹ 1180 ± 12	³³³ 1181 ± 11	³⁰⁶ 1191 ± 11	²⁵⁴ 1207 ± 8	³¹⁸ 4294 ± 80	³³⁹ 5569 ± 112		
129	enface-000	369598	153781	¹³⁷ 662	⁶⁵ 1024 ± 0	¹⁵⁷ 555 ± 4	¹³⁴ 558 ± 4	¹⁵⁹ 669 ± 6	²³⁹ 987 ± 15	³⁷³ 2349 ± 54	³⁶⁰ 7059 ± 62	³⁵⁹ 6980 ± 65		
130	enface-001	370710	173609	¹⁴¹ 670	⁷⁰ 1024 ± 0	¹⁵⁵ 550 ± 4	¹³³ 555 ± 3	¹⁵⁸ 668 ± 7	²³⁴ 981 ± 15	³⁷⁸ 2416 ± 59	³⁵⁴ 6734 ± 68	³⁵⁵ 6766 ± 69		
131	eocortex-000	255937	59432	⁴² 224	²⁹⁷ 2048 ± 0	⁶³ 305 ± 22	⁵⁷ 341 ± 25	⁷³ 440 ± 47	⁶⁶ 464 ± 45	⁵⁹ 513 ± 44	¹²⁴ 923 ± 11	¹²⁵ 918 ± 11		
132	ercacat-001	811623	58012	⁴⁰⁵ 2816	³⁴⁶ 2052 ± 0	³⁵⁶ 1052 ± 3	-	-	-	-	²⁶¹ 2551 ± 62	²⁵⁸ 2501 ± 81		

Notes

- 1 The configuration size does not capture static data included in libraries.
- 2 The library size is the combined total of all files provided in the submission lib folder. These libraries e.g. OpenCV may or may not be installed on any end user's platform natively and would not need to be installed with the algorithm. Some developers put neural network models in their libraries.
- 3 The memory usage is the peak resident set size reported by the ps system call during template generation.
- 4 The median template creation times are measured on Intel®Xeon®CPU E5-2630 v4 @ 2.20GHz processors.
- 5 The comparison durations, in nanoseconds, are estimated using std::chrono::high_resolution_clock which on the machine in (2) counts 1ns clock ticks. Precision is somewhat worse than that however. The ± value is the median absolute deviation times 1.48 for Normal consistency.

Table 10: Summary of algorithms and properties included in this report. The red superscripts give ranking for the quantity in that column.

ALGORITHM				CONFIG	LIBRARY	TEMPLATE						COMPARISON ⁴									
NAME		DATA	DATA	MEMORY	SIZE	GENERATION TIME (ms) ⁴						TIME (ns) ⁵									
		(KB) ¹	(KB) ²	(MB) ³	(B)	MUGSHOT	480x720	960x1440	1600x2400	3000x4500	GENUINE	IMPOSTOR									
133	euronovate-001	0	1774966	291	1308	89	1177 ± 0	351	1034 ± 2	343	1165 ± 3	328	1160 ± 3	297	1177 ± 3	245	1172 ± 2	453	81294 ± 591	453	81631 ± 931
134	expasoft-001	39057	983064	25	142	258	2048 ± 0	8	70 ± 0	674 ± 0	677 ± 0	573 ± 0	474 ± 0	194	1660 ± 35	195	1676 ± 48				
135	expasoft-002	38760	59825	32	168	263	2048 ± 0	5	34 ± 0	34 ± 0	34 ± 0	234 ± 0	234 ± 0	234 ± 0	369	8870 ± 78	369	8838 ± 77			
136	f8-001	272977	19668	283	1276	205	2048 ± 0	274	822 ± 39	-	-	-	-	-	399	15262 ± 139	399	15277 ± 212			
137	f8-002	28278	215616	13	83	115	2048 ± 0	6	39 ± 0	441 ± 0	575 ± 0	17	197 ± 1	118	702 ± 1	396	14765 ± 131	396	14790 ± 133		
138	faceonline-001	0	71529	5	302	368	2056 ± 0	27	179 ± 0	19	179 ± 0	20	190 ± 0	20	217 ± 0	27	343 ± 1	141	1064 ± 37	139	1033 ± 35
139	faceonline-002	155220	141019	232	995	122	2048 ± 0	255	783 ± 1	220	797 ± 2	192	794 ± 2	177	809 ± 3	170	901 ± 2	391	13798 ± 197	391	13743 ± 127
140	facephi-000	148904	5219	455	11481	269	2048 ± 0	290	871 ± 2	253	881 ± 3	224	880 ± 4	206	888 ± 4	183	949 ± 12	316	4067 ± 53	315	4047 ± 53
141	facesoft-000	370120	10612	178	796	206	2048 ± 0	218	675 ± 18	178	669 ± 3	165	686 ± 3	135	675 ± 5	112	687 ± 2	249	2239 ± 28	252	2277 ± 96
142	facetag-000	1232331	4022	224	965	62	2048 ± 0	77	355 ± 17	65	369 ± 8	271	989 ± 33	420	2408 ± 91	416	7930 ± 316	450	72003 ± 625	451	71912 ± 612
143	facetag-002	819806	4021	160	726	296	2048 ± 0	152	544 ± 1	128	544 ± 0	111	542 ± 0	92	545 ± 0	74	554 ± 0	202	1730 ± 25	202	1733 ± 25
144	facex-001	305074	930372	412	2931	225	2048 ± 0	105	422 ± 4	88	434 ± 4	103	520 ± 7	161	737 ± 13	353	1670 ± 27	220	1871 ± 23	218	1846 ± 29
145	facex-002	305074	928334	415	3095	130	2048 ± 0	106	426 ± 5	80	429 ± 4	101	516 ± 8	159	730 ± 12	359	1738 ± 36	79	631 ± 25	75	614 ± 19
146	farfaces-001	346494	44581	48	261	30	512 ± 0	381	1179 ± 1	350	1180 ± 1	332	1180 ± 0	302	1185 ± 1	255	1209 ± 2	120	855 ± 25	119	860 ± 31
147	fiberhome-nanjing-003	352895	1482309	196	845	146	2048 ± 0	369	1136 ± 7	333	1134 ± 4	318	1132 ± 3	285	1139 ± 3	236	1154 ± 5	147	1097 ± 38	149	1083 ± 42
148	fiberhome-nanjing-004	443779	1482313	238	1048	400	4096 ± 0	419	1321 ± 5	380	1304 ± 3	368	1307 ± 2	338	1308 ± 3	285	1326 ± 5	165	1276 ± 40	165	1265 ± 38
149	fincore-000	256615	19409	107	535	257	2048 ± 0	142	508 ± 3	117	505 ± 0	97	508 ± 1	83	513 ± 2	69	535 ± 1	206	1765 ± 31	206	1763 ± 22
150	firstcreditKZ-001	553811	24803	255	1112	229	2048 ± 0	264	808 ± 0	293	997 ± 0	299	1061 ± 1	295	1174 ± 1	362	1774 ± 54	122	904 ± 20	123	903 ± 23
151	frpkauai-001	507771	24807	245	1076	112	2048 ± 0	228	689 ± 1	189	691 ± 0	171	697 ± 2	154	714 ± 6	141	775 ± 31	107	752 ± 29	109	764 ± 23
152	fujitsulab-002	0	1088887	333	1613	436	4104 ± 0	396	1237 ± 2	359	1222 ± 2	345	1236 ± 1	320	1251 ± 2	286	1327 ± 2	271	2836 ± 25	272	2809 ± 44
153	fujitsulab-003	662263	318209	450	6907	437	4104 ± 0	323	951 ± 20	275	941 ± 19	253	952 ± 19	232	971 ± 20	205	1045 ± 21	273	2855 ± 16	274	2849 ± 19
154	g42-intelbrain-001	1031335	235521	460	25628	8	269 ± 0	332	976 ± 6	287	975 ± 1	275	997 ± 2	266	1068 ± 3	294	1362 ± 8	340	5878 ± 96	348	5865 ± 71
155	geo-002	369903	98667	233	1018	315	2048 ± 0	259	791 ± 1	218	793 ± 0	193	794 ± 0	172	795 ± 1	144	803 ± 1	296	3407 ± 45	298	3422 ± 65
156	geo-004	168980	107714	285	1280	310	2048 ± 0	405	1268 ± 1	374	1279 ± 1	336	1274 ± 0	324	1259 ± 1	275	1296 ± 1	137	1023 ± 20	138	1028 ± 22
157	glory-004	0	999639	378	2181	441	4182 ± 0	226	688 ± 0	208	759 ± 1	248	941 ± 1	415	2134 ± 4	418	9360 ± 47	330	4982 ± 66	328	4990 ± 63
158	glory-005	0	999999	384	2428	440	4182 ± 0	236	703 ± 1	217	789 ± 0	259	972 ± 1	417	2200 ± 25	419	9679 ± 22	333	5224 ± 93	332	5176 ± 81
159	gorilla-007	441058	708166	337	1691	451	6288 ± 0	179	592 ± 1	150	592 ± 1	135	603 ± 1	120	625 ± 2	125	722 ± 9	307	3686 ± 37	308	3709 ± 36
160	gorilla-008	450175	707000	352	1789	457	8338 ± 0	181	595 ± 1	149	590 ± 0	130	600 ± 1	118	621 ± 2	124	720 ± 9	322	4530 ± 44	320	4524 ± 38
161	graymatrics-001	13095	70406	22	127	424	4096 ± 0	32	191 ± 1	25	203 ± 1	129	592 ± 5	404	1698 ± 9	414	7150 ± 34	433	39874 ± 309	433	39762 ± 295
162	griaule-000	0	598214	239	1054	337	2052 ± 0	102	416 ± 6	84	425 ± 7	189	770 ± 14	405	1749 ± 43	412	6406 ± 189	314	3987 ± 42	311	3938 ± 38
163	griaule-001	0	412061	281	1269	343	2052 ± 0	378	1164 ± 1	325	1096 ± 5	308	1099 ± 4	282	1136 ± 2	333	1509 ± 2	313	3948 ± 23	313	3957 ± 32
164	hertasecurity-001	0	944427	269	1183	24	512 ± 0	75	346 ± 0	58	345 ± 0	43	349 ± 0	38	354 ± 0	35	388 ± 0	207	1770 ± 45	201	1726 ± 48
165	hertasecurity-002	0	944582	268	1177	29	512 ± 0	134	484 ± 7	101	478 ± 3	85	480 ± 3	78	495 ± 3	65	520 ± 3	252	2289 ± 40	251	2267 ± 48
166	hik-001	667866	9290	448	6597	93	1408 ± 0	205	651 ± 0	177	667 ± 8	162	677 ± 16	139	686 ± 13	130	737 ± 12	47	488 ± 19	47	477 ± 22
167	hisign-001	732412	167488	324	1553	379	2080 ± 0	414	1306 ± 1	384	1320 ± 1	369	1315 ± 1	341	1312 ± 1	284	1325 ± 1	13	201 ± 10	9	185 ± 13
168	hisign-002	1014906	102652	375	2123	376	2080 ± 0	261	797 ± 0	221	800 ± 5	195	800 ± 0	173	801 ± 0	143	803 ± 1	17	232 ± 11	13	207 ± 11
169	hyperverge-002	2951900	198832	368	1975	72	1024 ± 0	316	938 ± 1	274	939 ± 1	247	941 ± 1	225	945 ± 1	190	975 ± 1	350	6023 ± 37	350	5966 ± 40
170	hyperverge-003	1167779	281256	402	2748	66	1024 ± 0	457	1477 ± 2	426	1503 ± 3	421	1520 ± 3	397	1525 ± 4	343	1565 ± 3	54	566 ± 11	55	561 ± 8
171	hzailu-002	1515880	74047	437	4715	355	2056 ± 0	377	1150 ± 5	332	1127 ± 6	315	1129 ± 7	283	1137 ± 7	243	1172 ± 3	144	1079 ± 53	145	1070 ± 31
172	hzailu-003	1923030	222185	438	4817	388	3080 ± 0	435	1389 ± 5	389	1331 ± 7	376	1334 ± 2	351	1349 ± 6	313	1424 ± 8	185	1483 ± 35	181	1464 ± 31
173	icm-003	1513988	940	93	500	183	2048 ± 0	221	681 ± 6	180	672 ± 4	178	714 ± 11	185	837 ± 41	298	1381 ± 131	414	24351 ± 161	413	24227 ± 146
174	icm-004	2012129	1089	237	1040	299	2048 ± 0	104	419 ± 6	78	407 ± 6	76	454 ± 15	111	603 ± 51	338	1527 ± 235	395	14730 ± 154	395	14521 ± 152
175	ichttc-000	172459	1471004	353	1805	292	2048 ± 0	73	338 ± 11	56	338 ± 9	70	437 ± 16	148	705 ± 24	357	1719 ± 44	335	5284 ± 63	334	5290 ± 54
176	id3-006	210116	7706	227	982	50	520 ± 0	223	683 ± 0	319	1088 ± 1	338	1192 ± 1	311	1209 ± 1	267	1270 ± 1	338	5547 ± 34	338	5563 ± 34

Notes

- 1 The configuration size does not capture static data included in libraries.
- 2 The library size is the combined total of all files provided in the submission lib folder. These libraries e.g. OpenCV may or may not be installed on any end user's platform natively and would not need to be installed with the algorithm. Some developers put neural network models in their libraries.
- 3 The memory usage is the peak resident set size reported by the ps system call during template generation.
- 4 The median template creation times are measured on Intel®Xeon®CPU E5-2630 v4 @ 2.20GHz processors.
- 5 The comparison durations, in nanoseconds, are estimated using std::chrono::high_resolution_clock which on the machine in (2) counts 1ns clock ticks. Precision is somewhat worse than that however. The ± value is the median absolute deviation times 1.48 for Normal consistency.

Table 11: Summary of algorithms and properties included in this report. The red superscripts give ranking for the quantity in that column.

ALGORITHM	CONFIG	LIBRARY	TEMPLATE								COMPARISON ⁴											
			NAME	DATA		MEMORY	SIZE	GENERATION TIME (ms) ⁴				TIME (ns) ⁵										
				(KB) ¹	(KB) ²			(B)	MUGSHOT	480x720	960x1440	1600x2400	3000x4500	GENUINE	IMPOSTOR							
177	id3-008		242416	8151	243	1068	7264 ± 0	270	819 ± 0	354	1209 ± 2	366	1297 ± 2	346	1329 ± 1	316	1433 ± 1	341	5658 ± 44	342	5624 ± 40	
178	idemia-008		374017	69922	271	1194	13	348 ± 0	116	457 ± 1	96	461 ± 0	80	466 ± 1	71	476 ± 2	60	513 ± 10	288	3080 ± 41	284	3046 ± 56
179	idemia-009		1066728	70572	397	2702	61	636 ± 0	389	1207 ± 1	357	1218 ± 1	343	1222 ± 2	312	1222 ± 3	268	1280 ± 10	342	5664 ± 84	341	5597 ± 90
180	iit-002		259579	52070	162	731	207	2048 ± 0	143	514 ± 1	120	531 ± 2	114	547 ± 1	101	583 ± 1	128	733 ± 2	130	1023 ± 7	134	1011 ± 66
181	iit-003		261288	53791	189	817	223	2048 ± 0	131	482 ± 0	107	493 ± 0	98	509 ± 0	90	541 ± 0	107	661 ± 0	25	324 ± 17	25	326 ± 8
182	imds-software-001		373399	352623	172	772	194	2048 ± 0	120	465 ± 1	283	958 ± 6	317	1131 ± 5	280	1134 ± 2	228	1119 ± 10	384	11885 ± 120	383	11779 ± 174
183	imperial-000		370120	10623	179	796	217	2048 ± 0	217	669 ± 1	181	675 ± 3	164	683 ± 17	136	676 ± 2	113	689 ± 2	238	2130 ± 32	236	2052 ± 100
184	imperial-002		472327	16134	354	1826	240	2048 ± 0	166	569 ± 1	142	581 ± 15	122	575 ± 5	98	576 ± 2	82	588 ± 3	251	2278 ± 90	241	2131 ± 44
185	incode-010		627808	21014	394	2628	199	2048 ± 0	382	1180 ± 2	347	1178 ± 1	334	1182 ± 1	299	1184 ± 1	256	1221 ± 1	158	1164 ± 32	157	1144 ± 32
186	incode-011		477280	21781	342	1708	314	2048 ± 0	292	872 ± 0	249	875 ± 0	225	881 ± 1	208	892 ± 1	178	939 ± 0	151	1117 ± 31	152	1109 ± 37
187	infocert-001		1204340	38972	315	1483	308	2048 ± 0	296	874 ± 1	257	891 ± 1	295	1050 ± 5	390	1473 ± 2	394	3174 ± 8	331	5055 ± 108	329	5008 ± 100
188	innefulabs-000		370588	162172	77	439	188	2048 ± 0	343	1006 ± 3	305	1025 ± 3	289	1030 ± 4	258	1041 ± 2	231	1135 ± 3	344	5782 ± 41	340	5741 ± 45
189	innovativetechnologyltd-001		177232	335757	59	341	311	2048 ± 0	109	433 ± 7	91	446 ± 8	72	439 ± 4	62	452 ± 4	56	485 ± 7	222	1877 ± 42	226	1924 ± 97
190	innovativetechnologyltd-002		173939	372324	211	912	266	2048 ± 0	211	661 ± 2	200	726 ± 4	260	981 ± 27	243	997 ± 40	139	766 ± 3	216	1841 ± 50	220	1857 ± 59
191	innovatricks-007	0	493269	363	1937	87	1064 ± 0	460	1485 ± 7	429	1785 ± 184	428	2078 ± 24	414	2123 ± 15	369	2210 ± 42	349	5978 ± 88	344	5690 ± 102	
192	innovatricks-008		307323	59842	307	1424	53	538 ± 0	254	778 ± 6	210	767 ± 3	190	770 ± 3	175	803 ± 3	158	853 ± 10	283	3021 ± 66	266	2673 ± 88
193	insightface-001		776777	16606	424	3852	243	2048 ± 0	425	1366 ± 2	396	1368 ± 3	387	1372 ± 3	361	1375 ± 5	300	1386 ± 4	152	1119 ± 29	151	1108 ± 34
194	insightface-003		1016917	26668	319	1515	148	2048 ± 0	358	1073 ± 0	320	1092 ± 2	303	1070 ± 1	269	1082 ± 1	223	1101 ± 1	59	597 ± 16	64	595 ± 17
195	inspur-000		364844	91926	183	808	392	4096 ± 0	426	1367 ± 1	390	1331 ± 2	382	1368 ± 2	389	1465 ± 1	365	1861 ± 3	375	9831 ± 37	374	9860 ± 40
196	intellicloudai-001		220831	868246	136	655	117	2048 ± 0	124	468 ± 2	94	456 ± 1	79	466 ± 3	76	492 ± 1	95	632 ± 2	139	1056 ± 4	143	1051 ± 72
197	intellicloudai-002		259047	58559	420	3584	431	4100 ± 0	283	847 ± 1	235	847 ± 2	211	849 ± 1	192	853 ± 1	167	878 ± 4	117	822 ± 28	116	818 ± 23
198	intellifusion-001		271872	289387	169	762	143	2048 ± 0	247	764 ± 38	213	774 ± 39	194	797 ± 42	174	803 ± 34	145	805 ± 33	150	1112 ± 28	154	1128 ± 41
199	intellifusion-002		762731	385841	218	941	390	4096 ± 0	322	950 ± 2	326	1096 ± 42	305	1088 ± 33	293	1168 ± 31	242	1171 ± 10	199	1713 ± 57	194	1665 ± 87
200	intellivision-003		64023	133748	181	799	369	2056 ± 0	96	407 ± 3	74	398 ± 2	64	418 ± 2	61	450 ± 1	84	591 ± 4	378	11069 ± 56	375	11066 ± 75
201	intellivision-004		117727	131310	99	515	359	2056 ± 0	69	330 ± 0	55	330 ± 0	42	347 ± 0	44	382 ± 0	61	514 ± 0	379	11197 ± 63	379	11165 ± 72
202	intellivision-001		256654	111858	194	842	303	2048 ± 0	86	378 ± 1	66	379 ± 1	50	381 ± 1	46	384 ± 1	43	421 ± 3	149	1100 ± 16	153	1109 ± 22
203	intellivix-002		361566	116162	267	1172	215	2048 ± 0	326	956 ± 0	278	947 ± 6	263	976 ± 0	237	984 ± 4	221	1089 ± 1	421	30096 ± 128	423	31287 ± 140
204	intelresearch-004		646918	85290	357	1856	308	2048 ± 0	418	1319 ± 2	389	1322 ± 3	372	1330 ± 3	350	1345 ± 3	309	1411 ± 5	323	4696 ± 63	321	4692 ± 66
205	intelresearch-005		398137	85290	265	1158	320	2048 ± 0	421	1328 ± 1	392	1334 ± 2	379	1344 ± 2	353	1356 ± 2	311	1423 ± 4	321	4524 ± 87	318	4461 ± 74
206	intemta-000		1532392	19488	251	1097	45	513 ± 0	345	1010 ± 0	295	1001 ± 4	273	994 ± 0	241	993 ± 5	209	1056 ± 1	123	910 ± 29	124	906 ± 32
207	intsysmsu-001		384409	172480	177	789	187	2048 ± 0	187	614 ± 2	159	615 ± 2	152	642 ± 2	163	750 ± 3	239	1159 ± 4	73	621 ± 8	73	611 ± 31
208	intsysmsu-002		765921	172298	176	786	68	1024 ± 0	180	593 ± 1	219	793 ± 2	203	827 ± 1	198	875 ± 104	274	1293 ± 3	50	549 ± 25	53	548 ± 29
209	ionetworks-000		287609	51236	62	351	242	2048 ± 0	108	430 ± 0	89	435 ± 0	69	433 ± 0	49	444 ± 0	358	6913 ± 102	361	7150 ± 160		
210	iqface-000		268819	596337	154	704	443	4750 ± 32	150	538 ± 26	109	494 ± 2	112	543 ± 3	160	734 ± 4	304	1393 ± 4	460	636433 ± 38446	460	632654 ± 85615
211	iqface-003		370803	963398	187	817	444	4763 ± 37	145	529 ± 1	122	532 ± 2	132	599 ± 8	191	850 ± 2	354	1694 ± 2	459	575924 ± 2601	459	576653 ± 2051
212	irex-000		741899	47419	373	2086	386	3080 ± 0	284	852 ± 2	237	850 ± 1	220	874 ± 2	222	939 ± 1	261	1249 ± 5	12	201 ± 11	15	208 ± 8
213	isap-001		99049	204201	1	18	412	4096 ± 0	1	0 ± 0	-	-	-	-	-	-	-	-	40	459 ± 17	43	456 ± 11
214	isap-002		256765	49931	53	288	239	2048 ± 0	251	769 ± 3	306	1027 ± 2	223	877 ± 2	168	761 ± 1	173	912 ± 2	286	3045 ± 94	280	2973 ± 66
215	isityou-000		48010	36621	17	110	458	19200 ± 0	17	113 ± 5	-	-	-	-	-	-	-	456	237517 ± 1318	456	237374 ± 1279	
216	isystems-001		274621	639268	250	1091	101	2048 ± 0	57	291 ± 9	-	-	-	-	-	-	-	52	557 ± 16	56	564 ± 22	
217	isystems-002		358984	803389	330	1595	238	2048 ± 0	275	822 ± 8	-	-	-	-	-	-	-	106	749 ± 31	82	632 ± 28	
218	itmo-007		415979	245376	381	2199	208	2048 ± 0	242	741 ± 2	-	-	-	-	-	-	-	260	2551 ± 50	260	2529 ± 80	
219	itmo-008		726866	318238	300	1377	399	4096 ± 0	357	1060 ± 1	315	1058 ± 1	298	1059 ± 1	267	1072 ± 4	225	1104 ± 1	304	3578 ± 25	304	3580 ± 28
220	ivacognitive-001		256958	62791	221	947	200	2048 ± 0	412	1292 ± 3	377	1289 ± 4	361	1292 ± 4	334	1292 ± 3	281	1321 ± 4	317	4228 ± 41	316	4226 ± 41

Notes

- 1 The configuration size does not capture static data included in libraries.
- 2 The library size is the combined total of all files provided in the submission lib folder. These libraries e.g. OpenCV may or may not be installed on any end user's platform natively and would not need to be installed with the algorithm. Some developers put neural network models in their libraries.
- 3 The memory usage is the peak resident set size reported by the ps system call during template generation.
- 4 The median template creation times are measured on Intel®Xeon®CPU E5-2630 v4 @ 2.20GHz processors.
- 5 The comparison durations, in nanoseconds, are estimated using std::chrono::high_resolution_clock which on the machine in (2) counts 1ns clock ticks. Precision is somewhat worse than that however. The ± value is the median absolute deviation times 1.48 for Normal consistency.

Table 12: Summary of algorithms and properties included in this report. The red superscripts give ranking for the quantity in that column.

	ALGORITHM	CONFIG	LIBRARY	TEMPLATE								COMPARISON ⁴			
				NAME		DATA		MEMORY		SIZE		GENERATION TIME (ms) ⁴			
				(KB) ¹	(KB) ²	(MB) ³	(B)	MUGSHOT	480x720	960x1440	1600x2400	3000x4500	GENUINE	IMPOSTOR	
221	iws-000	30875	3063	10 ⁷⁷	33 ^{512 ± 0}	50 ^{277 ± 5}	42 ^{283 ± 1}	92 ^{494 ± 3}	238 ^{984 ± 3}	391 ^{2987 ± 39}	131 ^{999 ± 40}	130 ^{992 ± 22}			
222	jaakit-001	99024	24754	45 ²⁵¹	16 ^{512 ± 0}	9 ^{76 ± 0}	7 ^{77 ± 0}	79 ^{79 ± 0}	6 ^{81 ± 0}	6 ^{93 ± 0}	256 ^{2466 ± 57}	257 ^{2465 ± 66}			
223	kakao-007	526993	129545	431 ³⁹⁵³	147 ^{2048 ± 0}	329 ^{952 ± 1}	284 ^{961 ± 1}	258 ^{958 ± 1}	230 ^{962 ± 1}	188 ^{968 ± 1}	138 ^{1056 ± 16}	141 ^{1047 ± 28}			
224	kakao-008	734583	104820	426 ³⁸⁷⁶	316 ^{2048 ± 0}	368 ^{1135 ± 3}	340 ^{1148 ± 3}	325 ^{1150 ± 3}	289 ^{1156 ± 1}	246 ^{1175 ± 1}	105 ^{736 ± 23}	101 ^{727 ± 22}			
225	kakaopay-001	397864	179869	146 ⁶⁸⁴	421 ^{4096 ± 0}	113 ^{448 ± 0}	127 ^{542 ± 0}	110 ^{542 ± 0}	91 ^{542 ± 0}	72 ^{553 ± 0}	81 ^{633 ± 22}	79 ^{630 ± 22}			
226	kasikornlabs-000	256471	61000	150 ⁶⁹³	309 ^{2048 ± 0}	305 ^{908 ± 36}	252 ^{878 ± 22}	258 ^{969 ± 39}	300 ^{1184 ± 54}	375 ^{2382 ± 145}	423 ^{31669 ± 188}	424 ^{31714 ± 182}			
227	kasikornlabs-001	256471	61037	144 ⁶⁸¹	272 ^{2048 ± 0}	308 ^{912 ± 38}	245 ^{868 ± 10}	280 ^{1005 ± 50}	296 ^{1176 ± 44}	376 ^{2387 ± 147}	422 ^{30759 ± 198}	422 ^{30867 ± 174}			
228	kedacom-000	245292	37401	459 ²³⁵⁷⁴	11 ^{292 ± 0}	140 ^{506 ± 3}	131 ^{547 ± 10}	139 ^{614 ± 9}	105 ^{588 ± 10}	108 ^{605 ± 24}	89 ^{684 ± 14}	91 ^{682 ± 16}			
229	kiwitech-000	369711	21375	184 ⁸⁰⁸	160 ^{2048 ± 0}	178 ^{591 ± 0}	152 ^{594 ± 0}	131 ^{595 ± 1}	109 ^{596 ± 0}	90 ^{609 ± 0}	204 ^{1755 ± 20}	203 ^{1734 ± 16}			
230	kneron-003	58366	1747	38 ¹⁸⁸	197 ^{2048 ± 0}	52 ^{281 ± 3}	41 ^{280 ± 1}	37 ^{315 ± 13}	41 ^{365 ± 7}	258 ^{1224 ± 30}	334 ^{5237 ± 63}	333 ^{5274 ± 99}			
231	kneron-005	375374	13633	81 ⁴⁵⁷	111 ^{2048 ± 0}	144 ^{518 ± 2}	119 ^{522 ± 4}	116 ^{556 ± 5}	166 ^{757 ± 19}	361 ^{1760 ± 25}	226 ^{1922 ± 11}	227 ^{1926 ± 20}			
232	knowutech-000	808045	32886	290 ¹³⁰³	95 ^{1536 ± 0}	445 ^{1419 ± 2}	397 ^{1372 ± 1}	389 ^{1377 ± 1}	363 ^{1382 ± 2}	299 ^{1386 ± 2}	309 ^{3743 ± 31}	307 ^{3693 ± 38}			
233	kookmin-002	371771	30734	190 ⁸²⁷	230 ^{2048 ± 0}	353 ^{1038 ± 2}	313 ^{1047 ± 1}	293 ^{1045 ± 1}	263 ^{1061 ± 1}	226 ^{1116 ± 1}	83 ^{638 ± 19}	84 ^{636 ± 20}			
234	krungthai-002	2360957	15033	266 ¹¹⁷¹	180 ^{2048 ± 0}	64 ^{308 ± 0}	50 ^{314 ± 5}	33 ^{309 ± 0}	31 ^{319 ± 0}	31 ^{362 ± 0}	282 ^{3014 ± 20}	281 ^{2980 ± 22}			
235	kuke3d-001	403462	68786	105 ⁵³⁰	418 ^{4096 ± 0}	267 ^{814 ± 2}	223 ^{811 ± 2}	200 ^{814 ± 2}	178 ^{814 ± 1}	156 ^{834 ± 1}	353 ^{6412 ± 57}	353 ^{6413 ± 51}			
236	kuke3d-002	270544	1227855	185 ⁸⁰⁹	156 ^{2048 ± 0}	139 ^{504 ± 3}	116 ^{504 ± 1}	99 ^{511 ± 1}	86 ^{523 ± 2}	81 ^{585 ± 1}	278 ^{2943 ± 22}	279 ^{2966 ± 38}			
237	lebtech-000	0	10360	18 ¹¹⁰	27 ^{512 ± 0}	32 ^{22 ± 0}	12 ^{22 ± 0}	12 ^{22 ± 0}	13 ^{23 ± 0}	13 ^{23 ± 0}	115 ^{801 ± 42}	117 ^{825 ± 51}			
238	lemalabs-001	748400	198794	401 ²⁷³⁸	262 ^{2048 ± 0}	269 ^{810 ± 0}	224 ^{812 ± 0}	198 ^{813 ± 0}	180 ^{819 ± 0}	157 ^{844 ± 1}	385 ^{11930 ± 35}	385 ^{11913 ± 37}			
239	lineclova-001	944355	407058	383 ²³⁷³	158 ^{2048 ± 0}	278 ^{833 ± 10}	231 ^{830 ± 3}	208 ^{828 ± 4}	186 ^{838 ± 8}	154 ^{833 ± 4}	265 ^{2696 ± 23}	267 ^{2677 ± 35}			
240	lineclova-002	475779	406756	294 ¹³⁵³	271 ^{2048 ± 0}	408 ^{1284 ± 1}	373 ^{1275 ± 2}	357 ^{1275 ± 1}	328 ^{1273 ± 2}	269 ^{1281 ± 2}	269 ^{2765 ± 10}	269 ^{2767 ± 31}			
241	lookman-002	138200	25410	457 ¹⁶⁵¹⁸	58 ^{548 ± 0}	25 ^{173 ± 1}	-	-	-	-	68 ^{610 ± 19}	74 ^{612 ± 22}			
242	lookman-004	244775	37401	458 ²³⁵⁴⁸	57 ^{548 ± 0}	141 ^{507 ± 5}	129 ^{545 ± 12}	138 ^{613 ± 12}	106 ^{590 ± 11}	104 ^{656 ± 16}	121 ^{871 ± 29}	121 ^{878 ± 29}			
243	luxand-000	0	57908	297 ¹³⁶⁶	84 ^{1040 ± 0}	97 ^{407 ± 23}	87 ^{433 ± 11}	74 ^{444 ± 14}	67 ^{464 ± 14}	77 ^{562 ± 25}	118 ^{828 ± 28}	118 ^{828 ± 32}			
244	mantra-000	471458	62566	16 ⁷⁴⁹	332 ^{2052 ± 0}	101 ^{413 ± 18}	106 ^{487 ± 19}	91 ^{494 ± 18}	82 ^{511 ± 18}	86 ^{598 ± 19}	290 ^{3151 ± 51}	289 ^{3127 ± 63}			
245	maxvision-001	256146	61793	409 ²⁸⁸⁰	279 ^{2048 ± 0}	48 ^{275 ± 3}	39 ^{274 ± 2}	29 ^{277 ± 4}	28 ^{280 ± 4}	24 ^{325 ± 3}	97 ^{714 ± 13}	99 ^{717 ± 13}			
246	maxvision-002	171894	60623	358 ¹⁸⁶³	125 ^{2048 ± 0}	24 ^{172 ± 0}	18 ^{171 ± 0}	15 ^{172 ± 0}	12 ^{174 ± 0}	14 ^{221 ± 0}	100 ^{725 ± 5}	100 ^{725 ± 5}			
247	megvii-005	1378009	44038	433 ⁴⁰³⁶	326 ^{2049 ± 0}	417 ^{1319 ± 5}	365 ^{1247 ± 6}	347 ^{1240 ± 2}	319 ^{1245 ± 2}	276 ^{1298 ± 3}	427 ^{32025 ± 121}	428 ^{32008 ± 114}			
248	megvii-006	1554938	44038	436 ⁴³⁵⁴	324 ^{2049 ± 0}	410 ^{1287 ± 3}	375 ^{1286 ± 0}	396 ^{1393 ± 5}	342 ^{1319 ± 1}	293 ^{1360 ± 1}	423 ^{31845 ± 100}	426 ^{31872 ± 118}			
249	meituan-001	615387	333249	254 ¹¹⁰⁶	260 ^{2048 ± 0}	347 ^{1017 ± 4}	300 ^{1008 ± 3}	282 ^{1010 ± 2}	251 ^{1010 ± 3}	198 ^{1011 ± 4}	85 ^{654 ± 10}	88 ^{658 ± 14}			
250	meituan-002	686111	244091	379 ²¹⁹¹	391 ^{4096 ± 0}	355 ^{1052 ± 0}	318 ^{1086 ± 1}	301 ^{1064 ± 2}	262 ^{1060 ± 5}	216 ^{1063 ± 1}	140 ^{1064 ± 10}	144 ^{1070 ± 16}			
251	meiya-001	280055	264913	95 ⁵⁰⁷	323 ^{2049 ± 0}	192 ^{622 ± 12}	-	-	-	-	365 ^{8356 ± 615}	365 ^{8134 ± 97}			
252	mendaxiatech-000	1941475	45484	418 ³¹⁹⁵	429 ^{4097 ± 0}	398 ^{1243 ± 2}	367 ^{1255 ± 1}	388 ^{1373 ± 2}	401 ^{1598 ± 3}	384 ^{2689 ± 8}	437 ^{46906 ± 275}	437 ^{46872 ± 217}			
253	metsakuurcompany-001	445177	1091558	325 ¹⁵⁷²	353 ^{2056 ± 0}	168 ^{578 ± 1}	147 ^{587 ± 3}	127 ^{590 ± 1}	131 ^{659 ± 1}	159 ^{854 ± 1}	366 ^{8600 ± 192}	366 ^{8155 ± 298}			
254	metsakuurcompany-002	0	957558	228 ⁹⁸³	360 ^{2056 ± 0}	334 ^{980 ± 1}	289 ^{978 ± 1}	262 ^{976 ± 2}	248 ^{1005 ± 1}	224 ^{1103 ± 2}	368 ^{8766 ± 326}	368 ^{8786 ± 324}			
255	microfocus-001	104524	27242	39 ¹⁹⁰	3 ^{256 ± 0}	45 ^{264 ± 18}	-	-	-	-	16 ^{215 ± 8}	17 ^{217 ± 10}			
256	microfocus-002	96288	27362	35 ¹⁷⁶	4 ^{256 ± 0}	43 ^{259 ± 18}	-	-	-	-	27 ^{337 ± 34}	18 ^{230 ± 25}			
257	minivision-000	836697	16597	432 ⁴⁰¹³	413 ^{4096 ± 0}	352 ^{1035 ± 1}	309 ^{1033 ± 2}	291 ^{1035 ± 1}	256 ^{1037 ± 1}	213 ^{1059 ± 2}	257 ^{2466 ± 26}	255 ^{2460 ± 25}			
258	mobai-000	365451	80573	175 ⁷⁸⁶	447 ^{6144 ± 0}	248 ^{766 ± 8}	240 ^{869 ± 6}	341 ^{1205 ± 31}	411 ^{1867 ± 45}	399 ^{3549 ± 190}	401 ^{16458 ± 333}	401 ^{16423 ± 1473}			
259	mobai-001	265297	60164	106 ⁵³⁴	319 ^{2048 ± 0}	185 ^{612 ± 3}	157 ^{614 ± 3}	167 ^{687 ± 9}	205 ^{886 ± 31}	356 ^{1707 ± 103}	171 ^{1386 ± 25}	177 ^{1377 ± 26}			
260	mobb1l-001	231160	58706	41 ²²³	261 ^{2048 ± 0}	29 ^{183 ± 32}	22 ^{184 ± 25}	45 ^{354 ± 76}	182 ^{823 ± 396}	387 ^{2781 ± 1166}	383 ^{11832 ± 109}	384 ^{11851 ± 88}			
261	mobb1l-003	172248	60960	50 ²⁷⁰	267 ^{2048 ± 0}	214 ^{664 ± 6}	175 ^{661 ± 5}	157 ^{663 ± 5}	134 ^{665 ± 6}	114 ^{691 ± 5}	388 ^{12506 ± 111}	389 ^{12509 ± 100}			
262	mobilpintech-000	370514	303291	257 ¹¹³⁰	102 ^{2048 ± 0}	399 ^{1245 ± 1}	360 ^{1234 ± 1}	353 ^{1264 ± 1}	357 ^{1360 ± 1}	355 ^{1707 ± 1}	394 ^{14506 ± 214}	394 ^{14433 ± 197}			
263	moreidian-000	525259	21374	217 ⁹³²	211 ^{2048 ± 0}	232 ^{694 ± 0}	191 ^{698 ± 0}	173 ^{699 ± 0}	146 ^{700 ± 0}	123 ^{713 ± 1}	212 ^{1803 ± 11}	209 ^{1779 ± 23}			
264	mukh-001	866223	451194	335 ¹⁶³⁷	78 ^{1024 ± 0}	427 ^{1375 ± 17}	402 ^{1390 ± 12}	404 ^{1406 ± 8}	368 ^{1394 ± 10}	291 ^{1360 ± 11}	38 ^{433 ± 14}	40 ^{435 ± 14}			

Notes

- The configuration size does not capture static data included in libraries.
- The library size is the combined total of all files provided in the submission lib folder. These libraries e.g. OpenCV may or may not be installed on any end user's platform natively and would not need to be installed with the algorithm. Some developers put neural network models in their libraries.
- The memory usage is the peak resident set size reported by the ps system call during template generation.
- The median template creation times are measured on Intel®Xeon®CPU E5-2630 v4 @ 2.20GHz processors.
- The comparison durations, in nanoseconds, are estimated using std::chrono::high_resolution_clock which on the machine in (2) counts 1ns clock ticks. Precision is somewhat worse than that however. The \pm value is the median absolute deviation times 1.48 for Normal consistency.

Table 13: Summary of algorithms and properties included in this report. The red superscripts give ranking for the quantity in that column.

	ALGORITHM	CONFIG	LIBRARY	TEMPLATE								COMPARISON ⁴			
				NAME		DATA		MEMORY		SIZE		GENERATION TIME (ms) ⁴			
				(KB) ¹	(KB) ²	(MB) ³	(B)	MUGSHOT	480x720	960x1440	1600x2400	3000x4500	GENUINE	IMPOSTOR	
265	multimodality-000	0	503924	³⁰⁶ 1417	¹⁶⁹ 2048 ± 0	¹⁰³ 416 ± 0	⁸³ 420 ± 0	⁶⁵ 423 ± 0	⁵⁸ 427 ± 0	⁵¹ 463 ± 0	¹¹⁹ 848 ± 25	¹¹⁴ 800 ± 28			
266	multimodality-001	185719	545045	³⁰² 1388	⁴⁰¹ 4096 ± 0	³⁸⁷ 1190 ± 2	³⁴⁴ 1169 ± 2	³²⁹ 1165 ± 2	²⁹² 1167 ± 2	²⁴⁸ 1177 ± 2	¹⁷⁸ 1424 ± 35	¹⁷⁴ 1384 ± 42			
267	mvision-001	227502	149531	¹⁵⁹ 723	²¹ 512 ± 0	²³⁰ 691 ± 21	¹⁹³ 702 ± 19	¹⁷² 697 ± 24	¹⁶⁰ 708 ± 29	¹²¹ 710 ± 27	¹⁵³ 1123 ± 40	¹⁵⁹ 1154 ± 38			
268	nazhiai-000	547484	16141	³⁹⁸ 2716	²⁰² 2048 ± 0	²²² 683 ± 3	¹⁸⁶ 687 ± 2	²⁰⁸ 835 ± 27	¹⁸⁹ 840 ± 31	¹⁵⁵ 834 ± 34	²⁴⁸ 2230 ± 34	²⁴² 2133 ± 81			
269	neosystems-004	243546	352623	¹⁰⁴ 529	²⁷⁵ 2048 ± 0	⁶⁸ 324 ± 0	¹⁹⁰ 711 ± 3	²⁰² 827 ± 7	¹⁹³ 854 ± 2	¹⁷⁴ 916 ± 2	³⁹³ 14437 ± 176	³⁹³ 14355 ± 173			
271	netbridge-tech-001	133108	205875	⁹⁶ 508	⁴²⁶ 4096 ± 0	¹¹ 85 ± 1	⁸ 83 ± 0	⁸ 84 ± 0	⁸ 92 ± 0	⁸ 113 ± 4	³⁷⁰ 9280 ± 74	³⁷⁰ 9446 ± 512			
272	netbridge-tech-002	257687	49931	⁵⁴ 299	²⁵³ 2048 ± 0	²⁷⁹ 838 ± 6	²³³ 838 ± 2	²⁰⁹ 839 ± 1	¹⁸⁸ 839 ± 3	¹⁶⁰ 859 ± 3	²⁷⁶ 2893 ± 65	²⁸⁵ 3050 ± 123			
273	neurotechnology-013	474749	85552	⁴¹⁰ 2894	⁴⁶ 514 ± 0	³⁴⁰ 1000 ± 1	²⁹⁸ 1006 ± 2	²⁸⁴ 1022 ± 2	²⁶¹ 1053 ± 2	²⁴⁹ 1195 ± 8	² 109 ± 4	¹ 110 ± 4			
274	neurotechnology-015	474782	86045	³⁹¹ 2564	⁴⁷ 515 ± 0	³⁵⁰ 1028 ± 3	³¹⁰ 1033 ± 3	²⁹⁷ 1055 ± 4	²⁷⁰ 1097 ± 4	²⁷⁷ 1304 ± 18	⁴ 130 ± 2	⁴ 130 ± 4			
275	nhn-002	363471	817674	¹⁴⁰ 667	³⁹⁵ 4096 ± 0	³⁷² 1141 ± 3	³³⁵ 1138 ± 2	³²¹ 1141 ± 2	²⁸⁸ 1151 ± 6	²⁵¹ 1203 ± 2	⁴⁴³ 56608 ± 579	⁴⁴⁴ 56549 ± 606			
276	nhn-003	933665	432730	³¹³ 1464	⁴¹² 4096 ± 0	³⁹⁴ 1229 ± 2	³⁶⁸ 1261 ± 1	³⁵² 1263 ± 3	³³² 1279 ± 2	²⁹⁶ 1375 ± 3	⁴⁴⁰ 50560 ± 105	⁴⁴⁰ 50592 ± 142			
277	nodeflux-002	774668	690213	⁸⁴ 466	¹⁶⁸ 2048 ± 0	²³⁸ 708 ± 4	¹⁹⁵ 709 ± 4	¹⁷⁹ 716 ± 5	¹⁵⁶ 716 ± 7	¹²⁹ 736 ± 3	³⁰⁰ 3475 ± 62	²⁹⁷ 3408 ± 143			
278	notiontag-001	92753	427967	¹¹⁴ 566	⁶⁰ 584 ± 0	³¹⁵ 929 ± 35	³²¹ 1092 ± 39	⁴²⁹ 3709 ± 81	⁴²⁹ 10233 ± 180	-	⁴³⁴ 43636 ± 286	⁴³⁴ 43724 ± 330			
279	notiontag-002	271987	967207	⁴⁰⁷ 2840	³⁸² 2120 ± 0	¹¹² 453 ± 2	⁹³ 453 ± 3	⁷³ 453 ± 3	⁶³ 458 ± 2	⁵³ 471 ± 3	⁴⁰⁹ 20278 ± 194	⁴⁰⁹ 20195 ± 186			
280	nsensemcorp-003	199895	117041	¹⁵⁷ 710	¹⁶⁷ 2048 ± 0	²¹⁰ 661 ± 0	¹⁷⁶ 664 ± 0	¹⁵⁶ 662 ± 1	¹³² 659 ± 1	¹⁰⁵ 659 ± 0	⁴³⁵ 44658 ± 51	⁴³⁶ 44654 ± 72			
281	nsensemcorp-004	513276	139178	³³⁶ 1663	³²² 2048 ± 0	⁴⁴⁷ 1433 ± 0	⁴¹⁷ 1445 ± 7	⁴¹³ 1450 ± 3	³⁹⁴ 1487 ± 5	-	²⁵⁴ 2388 ± 42	²⁵⁴ 2385 ± 63			
282	ntechlab-011	786933	209458	⁴⁴⁹ 6867	⁹¹ 1280 ± 0	³⁷⁶ 1148 ± 2	³³⁶ 1142 ± 1	³²⁷ 1159 ± 1	³⁰³ 1185 ± 1	²⁷² 1290 ± 3	⁷ 179 ± 11	⁸ 173 ± 11			
283	ntechlab-012	570796	212350	⁴⁴³ 5451	³⁸³ 2560 ± 0	⁴¹⁶ 1309 ± 1	³⁸⁸ 1323 ± 1	³⁷³ 1331 ± 1	³⁵⁸ 1360 ± 1	³²² 1460 ± 3	¹⁵ 211 ± 8	¹⁶ 211 ± 7			
284	omface-000	45945	844976	²⁹ 150	⁷⁴ 1024 ± 0	³¹ 185 ± 1	²⁶ 206 ± 2	²⁷ 203 ± 1	¹⁵ 195 ± 1	¹³ 193 ± 1	⁴⁵ 481 ± 42	⁴² 456 ± 20			
285	omface-001	146370	1799745	²⁶ 145	⁷⁵ 1024 ± 0	³³ 194 ± 2	²⁸ 222 ± 2	²³ 209 ± 0	¹⁸ 216 ± 1	¹⁶ 233 ± 1	⁴⁰³ 18369 ± 19	⁴⁰³ 18366 ± 32			
286	omnigarde-001	200523	32882	⁸³ 464	¹⁹ 512 ± 0	³¹⁷ 941 ± 0	²⁵⁶ 883 ± 1	²²⁶ 886 ± 1	²⁰⁷ 891 ± 1	¹⁶⁸ 898 ± 0	¹⁷⁶ 1405 ± 31	¹⁷³ 1379 ± 26			
287	omnigarde-002	368860	32882	¹⁶⁸ 757	⁶⁴ 1024 ± 0	⁴¹³ 1303 ± 1	³⁶⁴ 1246 ± 1	³⁵⁰ 1249 ± 1	³²¹ 1253 ± 1	²⁶⁴ 1261 ± 1	²⁶⁸ 2727 ± 34	²⁶⁸ 2686 ± 32			
288	openface-001	0	40111	¹⁶ 100	²⁰⁹ 2048 ± 0	²¹ 148 ± 1	¹⁵ 154 ± 0	⁴⁷ 365 ± 3	⁵⁵ 409 ± 9	⁹² 616 ± 31	⁶⁷ 608 ± 14	⁷¹ 604 ± 13			
289	oz-003	484147	519652	⁴⁵⁶ 11949	³⁴⁸ 2053 ± 0	⁴²⁸ 1375 ± 12	⁴⁰¹ 1388 ± 3	⁴²⁷ 1773 ± 16	⁴¹³ 2039 ± 6	³⁹⁵ 3209 ± 5	⁴⁵² 73905 ± 456	⁴⁵² 73892 ± 444			
290	oz-004	373982	1075452	⁴⁵³ 8071	³⁴⁷ 2053 ± 0	²⁷⁷ 832 ± 7	²⁴⁷ 871 ± 6	²²⁸ 899 ± 10	²⁶⁸ 1078 ± 12	³⁴⁸ 1608 ± 10	⁴⁴⁶ 61654 ± 418	⁴⁴⁶ 61749 ± 450			
291	palit-000	428754	144958	²⁹⁶ 1355	⁴⁰⁷ 4096 ± 0	¹⁶⁷ 570 ± 1	¹⁴¹ 578 ± 1	¹²³ 576 ± 3	¹⁰⁰ 583 ± 1	⁹¹ 614 ± 1	²⁴⁷ 2227 ± 16	²⁴⁹ 2226 ± 16			
292	palit-001	173886	145564	¹¹⁸ 583	¹⁷⁵ 2048 ± 0	³⁹ 227 ± 0	³⁰ 224 ± 1	²⁴ 224 ± 1	²⁴ 229 ± 3	²⁰ 262 ± 2	¹⁵⁴ 1150 ± 16	¹⁵⁵ 1135 ± 23			
293	pangiam-000	464252	24512	⁴³⁰ 3919	¹⁵⁰ 2048 ± 0	¹⁹⁷ 627 ± 5	¹⁶¹ 618 ± 4	¹⁴⁰ 615 ± 3	¹¹⁶ 620 ± 3	¹⁰² 639 ± 3	³ 118 ± 7	³ 113 ± 7			
294	papago-001	669274	528217	³⁸² 2341	²³⁷ 2048 ± 0	⁴⁰⁷ 1272 ± 6	³⁷⁹ 1296 ± 7	³⁶⁵ 1295 ± 6	³³³ 1281 ± 3	²⁸⁷ 1345 ± 3	³⁹⁸ 15236 ± 169	³⁹⁸ 15184 ± 142			
295	papsav1923-001	279210	52652	⁸⁶ 473	¹⁷² 2048 ± 0	¹⁹⁴ 626 ± 1	¹⁶⁴ 628 ± 1	¹⁴³ 630 ± 1	¹²⁷ 648 ± 2	¹³³ 744 ± 3	¹⁰¹ 725 ± 25	¹⁰² 731 ± 28			
296	papsav1923-002	491185	24727	²⁵⁹ 1136	³³⁵ 2052 ± 0	²⁶⁰ 792 ± 1	²⁹⁰ 978 ± 1	²⁹² 1042 ± 1	²⁹⁰ 1158 ± 1	³⁵² 1641 ± 19	¹⁶⁰ 1209 ± 29	¹⁶² 1206 ± 38			
297	paravision-008	542190	204400	³¹¹ 1448	⁴²² 4096 ± 0	²³⁴ 699 ± 0	¹⁹² 700 ± 0	¹⁷⁴ 701 ± 0	¹⁴⁷ 702 ± 1	¹¹⁹ 702 ± 0	²⁸ 337 ± 17	³⁰ 330 ± 13			
298	paravision-010	688291	205854	³⁷⁶ 2150	⁴³³ 4100 ± 0	¹⁹⁹ 634 ± 0	¹⁶⁹ 635 ± 0	¹⁴⁷ 635 ± 0	¹²² 635 ± 0	⁹⁹ 635 ± 1	¹⁸⁹ 1577 ± 35	¹⁸⁹ 1571 ± 32			
299	pensees-001	1619431	408932	³⁶¹ 1922	⁴⁵⁴ 8200 ± 0	³⁶⁴ 1108 ± 3	⁴¹⁸ 1448 ± 17	⁴⁰⁹ 1439 ± 10	³⁸⁸ 1464 ± 5	³⁴² 1546 ± 9	²⁹¹ 3151 ± 34	²⁹⁰ 3143 ± 25			
300	pixelall-008	0	992249	³⁴⁹ 1741	⁴⁵³ 8192 ± 0	⁴⁵⁴ 1471 ± 3	⁴¹² 1405 ± 4	⁴⁰⁵ 1409 ± 4	³⁷⁸ 1413 ± 3	³¹⁵ 1426 ± 4	²¹⁰ 1799 ± 50	²¹⁴ 1807 ± 48			
301	pixelall-009	0	1009114	³⁴⁵ 1731	⁴⁵² 8192 ± 0	⁴⁵⁹ 1484 ± 3	⁴⁰⁸ 1395 ± 3	⁴⁰¹ 1400 ± 4	³⁶⁶ 1391 ± 3	³¹⁷ 1433 ± 3	²¹⁸ 1848 ± 13	²¹⁷ 1842 ± 19			
302	psl-010	411027	591157	⁴⁴² 5361	⁴³⁹ 4168 ± 0	⁴⁴² 1403 ± 9	⁴⁰⁵ 1393 ± 3	³⁹⁴ 1392 ± 3	³⁶⁹ 1395 ± 3	³⁰⁵ 354 ± 53	²⁹ 329 ± 29				
303	psl-011	814579	606050	⁴³⁹ 4984	⁴⁵⁵ 8248 ± 0	⁴²⁰ 1324 ± 2	³⁸⁷ 1323 ± 8	³⁷¹ 1326 ± 8	³⁴⁵ 1324 ± 8	²⁸² 1322 ± 4	¹⁹⁶ 1680 ± 37	¹⁹⁷ 1688 ± 40			
304	ptakuratsatu-000	0	585434	²⁹³ 1347	⁵⁴ 538 ± 0	²⁹⁷ 875 ± 3	²⁴³ 863 ± 48	²⁴⁴ 928 ± 9	²²⁹ 958 ± 17	²¹⁸ 1066 ± 26	³⁴⁷ 5900 ± 103	³⁴³ 5687 ± 167			
305	pxl-001	110116	78231	³¹ 168	³⁶ 512 ± 0	¹⁴ 101 ± 5	¹¹ 104 ± 5	¹⁹ 189 ± 12	⁵⁴ 408 ± 27	³²⁵ 1470 ± 144	³⁴⁰ 5598 ± 45	³⁴⁰ 5590 ± 68			
306	pyramid-000	372608	219883	¹⁸¹ 804	³⁵¹ 2056 ± 0	¹⁷¹ 583 ± 2	-	-	-	-	³⁶¹ 7147 ± 59	³⁶³ 7586 ± 425			
307	qazbs-000	362015	805258	¹⁹⁹ 856	¹⁶⁶ 2048 ± 0	⁴¹⁵ 1307 ± 1	³⁶³ 1243 ± 0	³⁴⁹ 1248 ± 9	³²² 1253 ± 1	²⁶⁶ 1270 ± 0	³³² 5181 ± 62	³³¹ 5167 ± 93			
308	qnap-001	196210	13399	⁵² 286	¹²⁷ 2048 ± 0	¹⁸⁸ 614 ± 1	¹⁵⁸ 615 ± 1	¹⁴² 627 ± 1	¹¹⁹ 623 ± 1	⁹⁶ 634 ± 2	⁸⁴ 649 ± 11	⁸⁶ 648 ± 14			

Notes

- 1 The configuration size does not capture static data included in libraries.
- 2 The library size is the combined total of all files provided in the submission lib folder. These libraries e.g. OpenCV may or may not be installed on any end user's platform natively and would not need to be installed with the algorithm. Some developers put neural network models in their libraries.
- 3 The memory usage is the peak resident set size reported by the ps system call during template generation.
- 4 The median template creation times are measured on Intel®Xeon®CPU E5-2630 v4 @ 2.20GHz processors.
- 5 The comparison durations, in nanoseconds, are estimated using std::chrono::high_resolution_clock which on the machine in (2) counts 1ns clock ticks. Precision is somewhat worse than that however. The ± value is the median absolute deviation times 1.48 for Normal consistency.

Table 14: Summary of algorithms and properties included in this report. The red superscripts give ranking for the quantity in that column.

	ALGORITHM	CONFIG	LIBRARY	TEMPLATE								COMPARISON ⁴		
	NAME	DATA	DATA	MEMORY	SIZE	MUGSHOT	480x720	960x1440	1600x2400	3000x4500	Genuine	Impostor	Time (ns) ⁵	
		(KB) ¹	(KB) ²	(MB) ³	(B)	MUGSHOT	480x720	960x1440	1600x2400	3000x4500	Genuine	Impostor	Time (ns) ⁵	
309	qnap-002	346963	33284	152 ⁷⁰⁰	210 ^{2048 ± 0}	272 ^{821 ± 1}	227 ^{824 ± 1}	202 ^{824 ± 1}	184 ^{826 ± 1}	153 ^{832 ± 1}	21 ^{293 ± 13}	22 ^{287 ± 17}		
310	quantasoft-003	370518	211354	241 ¹⁰⁵⁸	232 ^{2048 ± 0}	198 ^{632 ± 2}	168 ^{634 ± 0}	145 ^{632 ± 0}	121 ^{631 ± 1}	98 ^{634 ± 0}	11 ^{201 ± 7}	12 ^{203 ± 8}		
311	rankone-012	0	264182	23 ¹³⁴	6 ^{261 ± 0}	161 ^{564 ± 3}	132 ^{554 ± 1}	118 ^{564 ± 1}	102 ^{586 ± 1}	116 ^{695 ± 1}	20 ^{273 ± 17}	19 ^{231 ± 14}		
312	rankone-013	0	228729	28 ¹⁴⁹	5 ^{261 ± 0}	229 ^{690 ± 5}	179 ^{672 ± 1}	177 ^{712 ± 1}	171 ^{780 ± 1}	227 ^{1118 ± 3}	32 ^{356 ± 23}	24 ^{304 ± 23}		
313	realnetworks-006	466225	56771	328 ¹⁵⁸⁸	349 ^{2056 ± 0}	202 ^{638 ± 4}	165 ^{630 ± 3}	160 ^{672 ± 5}	149 ^{706 ± 5}	140 ^{774 ± 5}	41 ^{469 ± 19}	48 ^{478 ± 25}		
314	realnetworks-007	570797	101527	416 ³¹³⁷	358 ^{2056 ± 0}	423 ^{1348 ± 2}	395 ^{1358 ± 11}	384 ^{1363 ± 10}	364 ^{1386 ± 9}	335 ^{1517 ± 6}	53 ^{559 ± 31}	52 ^{539 ± 35}		
315	regula-000	262444	29384	129 ⁶¹⁰	300 ^{2048 ± 0}	386 ^{1187 ± 1}	331 ^{1126 ± 1}	316 ^{1129 ± 0}	279 ^{1132 ± 1}	240 ^{1159 ± 1}	49 ^{491 ± 16}	50 ^{500 ± 22}		
316	regula-001	256075	25980	225 ⁹⁷⁶	247 ^{2048 ± 0}	409 ^{1284 ± 1}	358 ^{1220 ± 1}	344 ^{1222 ± 1}	315 ^{1226 ± 1}	262 ^{1255 ± 1}	33 ^{361 ± 10}	32 ^{342 ± 25}		
317	remarkai-001	241857	868314	161 ⁷³⁰	345 ^{2052 ± 0}	276 ^{831 ± 6}	236 ^{849 ± 18}	296 ^{1055 ± 25}	307 ^{1198 ± 34}	330 ^{1519 ± 38}	163 ^{1229 ± 20}	115 ^{805 ± 56}		
318	remarkai-003	280516	58559	428 ³⁸⁹⁶	432 ^{4100 ± 0}	337 ^{986 ± 1}	292 ^{993 ± 1}	272 ^{992 ± 1}	244 ^{999 ± 3}	199 ^{1019 ± 2}	113 ^{787 ± 20}	112 ^{793 ± 22}		
319	rendip-000	0	437653	145 ⁶⁸²	203 ^{2048 ± 0}	119 ^{464 ± 2}	95 ^{458 ± 0}	84 ^{473 ± 0}	72 ^{483 ± 1}	75 ^{556 ± 4}	55 ^{576 ± 13}	57 ^{573 ± 11}		
320	revealmedia-005	293933	202465	171 ⁷⁶³	434 ^{4100 ± 0}	107 ^{428 ± 0}	85 ^{428 ± 0}	68 ^{430 ± 0}	60 ^{433 ± 0}	48 ^{442 ± 0}	234 ^{2023 ± 38}	234 ^{2009 ± 26}		
321	revealmedia-006	293933	200912	166 ⁷⁴¹	328 ^{2052 ± 0}	87 ^{381 ± 0}	68 ^{381 ± 0}	51 ^{382 ± 0}	45 ^{384 ± 0}	38 ^{394 ± 0}	77 ^{626 ± 35}	68 ^{600 ± 2}		
322	rokid-000	258612	396624	274 ¹²¹⁸	363 ^{2056 ± 0}	153 ^{546 ± 3}	126 ^{542 ± 2}	113 ^{545 ± 1}	85 ^{522 ± 3}	78 ^{563 ± 4}	299 ^{3457 ± 62}	300 ^{3463 ± 77}		
323	rokid-001	641223	413733	244 ¹⁰⁷¹	374 ^{2060 ± 0}	307 ^{911 ± 2}	262 ^{901 ± 5}	229 ^{899 ± 2}	211 ^{900 ± 3}	171 ^{901 ± 3}	293 ^{3345 ± 50}	294 ^{3346 ± 149}		
324	s1-005	482369	95685	262 ¹¹³⁷	226 ^{2048 ± 0}	342 ^{1001 ± 0}	297 ^{1002 ± 0}	278 ^{1004 ± 0}	249 ^{1008 ± 0}	201 ^{1029 ± 2}	78 ^{626 ± 74}	59 ^{589 ± 14}		
325	s1-006	482372	95681	261 ¹¹³⁷	259 ^{2048 ± 0}	324 ^{951 ± 0}	281 ^{956 ± 0}	254 ^{957 ± 0}	231 ^{962 ± 0}	193 ^{983 ± 0}	92 ^{696 ± 23}	95 ^{696 ± 29}		
326	saffe-001	85973	62488	33 ¹⁶⁸	92 ^{1280 ± 0}	53 ^{281 ± 1}	-	-	-	-	164 ^{1274 ± 19}	166 ^{1277 ± 26}		
327	saffe-002	260622	28285	198 ⁸⁵⁵	264 ^{2048 ± 0}	268 ^{817 ± 11}	222 ^{805 ± 15}	197 ^{809 ± 19}	179 ^{815 ± 29}	148 ^{813 ± 23}	98 ^{717 ± 7}	98 ^{714 ± 29}		
328	samsungsds-001	1189592	147444	427 ³⁸⁹³	416 ^{4096 ± 0}	370 ^{1140 ± 3}	338 ^{1145 ± 4}	378 ^{1344 ± 5}	359 ^{1366 ± 5}	334 ^{1514 ± 7}	441 ^{51559 ± 773}	441 ^{51721 ± 1003}		
329	samsungsds-002	1040732	147475	385 ²⁴³¹	352 ^{2056 ± 0}	367 ^{1118 ± 1}	345 ^{1175 ± 12}	386 ^{1372 ± 6}	344 ^{1324 ± 2}	330 ^{1489 ± 4}	430 ^{35803 ± 266}	431 ^{36181 ± 674}		
330	samtech-001	288082	219883	126 ⁶⁰⁵	350 ^{2056 ± 0}	58 ^{294 ± 3}	-	-	-	-	364 ^{7694 ± 59}	364 ^{7678 ± 91}		
331	scanovate-002	256986	457227	197 ⁸⁵⁰	273 ^{2048 ± 0}	233 ^{696 ± 32}	197 ^{713 ± 33}	182 ^{738 ± 28}	170 ^{779 ± 32}	244 ^{1172 ± 53}	284 ^{3021 ± 38}	288 ^{3120 ± 163}		
332	scanovate-003	135585	89469	182 ⁸⁰⁸	173 ^{2048 ± 0}	172 ^{585 ± 1}	156 ^{613 ± 12}	128 ^{591 ± 1}	112 ^{610 ± 2}	111 ^{684 ± 1}	277 ^{2926 ± 22}	277 ^{2925 ± 20}		
333	sdc-000	256814	481583	174 ⁷⁸⁶	133 ^{2048 ± 0}	309 ^{913 ± 14}	265 ^{906 ± 9}	322 ^{1142 ± 19}	407 ^{1774 ± 45}	403 ^{4719 ± 222}	428 ^{32645 ± 93}	429 ^{32653 ± 112}		
334	securifai-004	282177	12027	133 ⁶³⁶	181 ^{2048 ± 0}	288 ^{869 ± 1}	244 ^{867 ± 1}	215 ^{867 ± 1}	196 ^{867 ± 1}	162 ^{865 ± 1}	198 ^{1711 ± 19}	199 ^{1705 ± 29}		
335	securifai-005	252532	81777	101 ⁵²⁵	193 ^{2048 ± 0}	429 ^{1377 ± 2}	394 ^{1355 ± 1}	382 ^{1353 ± 0}	355 ^{1357 ± 0}	290 ^{1356 ± 0}	221 ^{1873 ± 25}	219 ^{1847 ± 35}		
336	sensetime-006	765353	37673	447 ⁵⁹⁹⁴	79 ^{1028 ± 0}	424 ^{1352 ± 17}	382 ^{1311 ± 1}	370 ^{1323 ± 1}	354 ^{1357 ± 1}	337 ^{1523 ± 2}	159 ^{1179 ± 28}	160 ^{1157 ± 29}		
337	sensetime-007	765353	37533	445 ⁵⁶⁹⁹	80 ^{1028 ± 0}	434 ^{1386 ± 41}	386 ^{1323 ± 2}	380 ^{1347 ± 2}	360 ^{1366 ± 2}	346 ^{1593 ± 8}	180 ^{1460 ± 29}	179 ^{1425 ± 26}		
338	sertis-000	265572	68770	72 ⁴²⁷	133 ^{2048 ± 0}	245 ^{754 ± 0}	209 ^{759 ± 0}	187 ^{764 ± 0}	167 ^{760 ± 0}	138 ^{763 ± 0}	186 ^{1497 ± 29}	190 ^{1582 ± 38}		
339	sertis-002	460790	68929	303 ¹³⁹¹	219 ^{2048 ± 0}	384 ^{1181 ± 1}	346 ^{1178 ± 0}	335 ^{1183 ± 0}	305 ^{1187 ± 0}	257 ^{1221 ± 0}	146 ^{1086 ± 32}	146 ^{1076 ± 31}		
340	seventhssense-001	369850	3183365	186 ⁸¹¹	330 ^{2052 ± 0}	402 ^{1255 ± 2}	378 ^{1294 ± 15}	358 ^{1277 ± 3}	330 ^{1275 ± 2}	271 ^{1288 ± 3}	228 ^{1936 ± 26}	230 ^{1943 ± 34}		
341	seventhssense-002	452197	1567903	220 ⁹⁴⁴	338 ^{2052 ± 0}	401 ^{1252 ± 1}	372 ^{1271 ± 1}	355 ^{1269 ± 1}	326 ^{1272 ± 1}	273 ^{1290 ± 1}	239 ^{2131 ± 45}	239 ^{2123 ± 45}		
342	shaman-000	0	120033	94 ⁵⁰⁷	406 ^{4096 ± 0}	207 ^{653 ± 16}	-	-	-	-	36 ^{380 ± 25}	36 ^{379 ± 31}		
343	shaman-001	0	174446	98 ⁵¹¹	414 ^{4096 ± 0}	59 ^{294 ± 2}	-	-	-	-	82 ^{635 ± 19}	41 ^{441 ± 25}		
344	shu-002	731250	148309	207 ⁸⁹⁰	394 ^{4096 ± 0}	244 ^{751 ± 2}	211 ^{769 ± 4}	239 ^{922 ± 4}	383 ^{1431 ± 9}	398 ^{3489 ± 47}	461 ^{2930763 ± 47355}	461 ^{2929759 ± 39149}		
345	shu-003	428774	146940	97 ⁵¹¹	271 ^{2048 ± 0}	271 ^{820 ± 6}	229 ^{828 ± 3}	249 ^{941 ± 9}	339 ^{1308 ± 15}	392 ^{3045 ± 44}	258 ^{2506 ± 26}	259 ^{2512 ± 38}		
346	siat-002	486842	7738	386 ²⁴³⁴	327 ^{2052 ± 0}	169 ^{579 ± 0}	-	-	-	-	110 ^{769 ± 13}	107 ^{750 ± 13}		
347	siat-005	380936	16935	289 ¹²⁹⁸	268 ^{2048 ± 0}	95 ^{403 ± 0}	76 ^{400 ± 0}	57 ^{401 ± 0}	52 ^{403 ± 1}	45 ^{422 ± 7}	56 ^{577 ± 13}	58 ^{580 ± 17}		
348	sjtu-003	480795	148243	109 ⁵³⁸	250 ^{2048 ± 0}	273 ^{821 ± 2}	225 ^{820 ± 2}	241 ^{923 ± 3}	308 ^{1201 ± 3}	374 ^{2373 ± 9}	188 ^{1560 ± 20}	187 ^{1560 ± 14}		
349	sjtu-004	1953267	241108	399 ²⁷²⁷	442 ^{4608 ± 0}	395 ^{1236 ± 2}	355 ^{1209 ± 2}	363 ^{1294 ± 4}	399 ^{1554 ± 5}	386 ^{2738 ± 8}	287 ^{3057 ± 14}	287 ^{3070 ± 20}		
350	sktelecom-000	527132	298496	292 ¹³¹¹	94 ^{1536 ± 0}	365 ^{1110 ± 1}	328 ^{1113 ± 1}	311 ^{1114 ± 1}	274 ^{1120 ± 1}	237 ^{1155 ± 1}	418 ^{26583 ± 128}	417 ^{26508 ± 126}		
351	smartbiometrik-001	30875	92620	7 ⁷¹	26 ^{512 ± 0}	191 ^{620 ± 7}	162 ^{625 ± 7}	151 ^{640 ± 4}	158 ^{728 ± 6}	206 ^{1047 ± 8}	94 ^{703 ± 31}	96 ^{710 ± 40}		
352	smartengines-000	1711	3025	4 ⁵⁰	10 ^{288 ± 0}	23 ^{168 ± 7}	20 ^{180 ± 1}	17 ^{188 ± 3}	19 ^{217 ± 3}	22 ^{275 ± 1}	9 ^{197 ± 5}	7 ^{167 ± 11}		

Notes

ALGORITHM	CONFIG	LIBRARY	TEMPLATE									COMPARISON ⁴					
			NAME	DATA	DATA	MEMORY	SIZE	GENERATION TIME (ms) ⁴					TIME (ns) ⁵				
								(KB) ¹	(KB) ²	(MB) ³	(B)	MUGSHOT	480x720	960x1440	1600x2400	3000x4500	GENUINE
353	smartengines-001	7095	4601	346	9288 ± 0	71	333 ± 89	79	408 ± 1	67	423 ± 1	64	460 ± 2	73	553 ± 5	6153 ± 11	5143 ± 13
354	smartvist-000	5959	134084	30165	17512 ± 0	75	59 ± 0	56	56 ± 0	456	56 ± 0	458	58 ± 0	590	90 ± 1	1791435 ± 31	1781422 ± 48
355	smilart-002	111826	87805	49263	671024 ± 0	26	176 ± 16	-	-	-	-	-	-	404	18784 ± 136	40518795 ± 151	
356	smilart-003	67339	91670	40192	28512 ± 0	28	180 ± 12	21	181 ± 10	35	313 ± 22	133	665 ± 49	371	2299 ± 196	1721395 ± 74	1371027 ± 66
357	sodec-000	836592	13142	4173186	4104096 ± 0	354	1041 ± 2	308	1032 ± 1	290	1035 ± 1	257	1037 ± 2	215	1061 ± 2	2091794 ± 37	2071775 ± 23
358	sqisoft-001	278968	386291	148688	3572056 ± 0	126	477 ± 5	393	1348 ± 18	381	1353 ± 26	349	1340 ± 14	303	1393 ± 28	114797 ± 22	111788 ± 22
359	sqisoft-002	278039	386291	139666	3562056 ± 0	122	466 ± 8	98	466 ± 2	82	468 ± 11	65	461 ± 6	54	472 ± 4	108758 ± 11	108760 ± 23
360	stachu-000	879661	624676	2421064	4044096 ± 0	266	813 ± 25	-	-	-	-	-	-	280	2979 ± 31	2833007 ± 75	
361	starhybrid-001	100509	289356	195845	1892048 ± 0	80	358 ± 82	61	355 ± 49	49	379 ± 58	50	401 ± 79	37	393 ± 67	1431075 ± 51	1471078 ± 53
362	sukshi-000	94035	688738	65372	46032768 ± 0	98	407 ± 11	80	413 ± 8	96	504 ± 8	141	689 ± 11	344	1574 ± 28	3749817 ± 50	3739787 ± 62
363	suprema-002	373808	41473	3441731	1982048 ± 0	258	787 ± 3	232	833 ± 3	242	924 ± 4	301	1185 ± 6	381	2479 ± 3	2923255 ± 17	2923253 ± 14
364	suprema-003	498231	116054	2761239	2362048 ± 0	450	1448 ± 1	414	1417 ± 4	407	1418 ± 3	380	1421 ± 4	320	1451 ± 5	2452201 ± 10	2472198 ± 13
365	supremaid-001	258193	23479	110541	2122048 ± 0	127	479 ± 1	104	481 ± 0	87	481 ± 0	75	490 ± 0	66	522 ± 0	95704 ± 19	87652 ± 19
366	supremaid-002	256273	23899	58335	1552048 ± 0	132	483 ± 0	115	501 ± 0	90	488 ± 0	80	503 ± 0	79	565 ± 0	2321990 ± 19	2251923 ± 29
367	surrey-cvssp-000	158030	70795	205879	1772048 ± 0	371	1141 ± 3	341	1157 ± 3	326	1158 ± 4	291	1163 ± 3	260	1245 ± 3	372955 ± 143	3719602 ± 186
368	surrey-cvssp-001	900280	76392	3411707	1522048 ± 0	392	1221 ± 1	361	1238 ± 2	346	1240 ± 0	318	1243 ± 0	263	1257 ± 0	40618970 ± 161	40618999 ± 176
369	synesis-006	731941	21817	3141472	4354104 ± 0	154	549 ± 1	130	546 ± 1	115	552 ± 1	94	558 ± 2	101	639 ± 28	93697 ± 32	94688 ± 31
370	synesis-007	1442961	24145	3872443	3873080 ± 0	390	1215 ± 5	370	1268 ± 30	367	1306 ± 67	340	1311 ± 58	312	1423 ± 52	88684 ± 32	92686 ± 25
371	synology-000	221021	25809	80453	2452048 ± 0	99	407 ± 14	81	415 ± 14	170	694 ± 31	370	1396 ± 58	400	4568 ± 211	40819720 ± 203	40719767 ± 379
372	synology-002	256713	25943	89488	2912048 ± 0	302	886 ± 4	259	892 ± 3	238	920 ± 2	246	1000 ± 5	279	1317 ± 12	1821466 ± 32	1851496 ± 45
373	sztu-000	338637	15871	2871298	3012048 ± 0	148	531 ± 0	121	532 ± 0	105	533 ± 0	87	537 ± 0	70	548 ± 0	57585 ± 11	63592 ± 13
374	sztu-001	338650	15871	2881298	1372048 ± 0	149	535 ± 0	125	537 ± 0	108	538 ± 0	89	540 ± 0	71	553 ± 0	63599 ± 10	66598 ± 10
375	t4isb-000	234227	115237	60343	1062048 ± 0	344	1006 ± 5	296	1001 ± 1	281	1006 ± 1	250	1009 ± 1	200	1022 ± 2	3053586 ± 34	3023534 ± 34
376	tech5-004	2410272	118858	4002733	12321 ± 0	293	872 ± 2	329	1117 ± 164	312	1114 ± 182	281	1134 ± 179	195	999 ± 44	62597 ± 13	61592 ± 16
377	tech5-005	1178769	120517	3081426	22512 ± 0	406	1272 ± 109	312	1038 ± 63	294	1046 ± 39	275	1124 ± 38	289	1351 ± 44	2622573 ± 37	2622545 ± 32
378	techsign-000	0	1101622	3691955	2212048 ± 0	84	366 ± 1	73	398 ± 1	330	1172 ± 3	426	3065 ± 18	422	10460 ± 65	3234758 ± 112	3234789 ± 93
379	techsign-001	0	586983	3481741	2772048 ± 0	252	772 ± 35	215	788 ± 23	196	802 ± 42	227	949 ± 10	308	1409 ± 26	58592 ± 11	62592 ± 13
380	tevian-007	779934	19523	3431714	821032 ± 0	170	583 ± 1	142	579 ± 0	124	580 ± 0	104	588 ± 1	100	636 ± 0	3294894 ± 65	3264841 ± 83
381	tevian-008	847177	19519	4193490	811032 ± 0	301	884 ± 2	264	903 ± 1	230	903 ± 1	213	911 ± 1	181	946 ± 1	3264828 ± 40	3254811 ± 41
382	tiger-005	342866	325734	3221531	3332052 ± 0	359	1097 ± 2	317	1065 ± 2	302	1066 ± 2	220	1088 ± 3	72	620 ± 19	76615 ± 16	
383	tiger-006	421186	394688	156707	3362052 ± 0	436	1392 ± 16	413	1411 ± 10	411	1444 ± 10	398	1531 ± 11	364	1848 ± 10	2141810 ± 20	2131801 ± 13
384	tinkoff-001	274660	389272	123592	2842048 ± 0	379	1176 ± 3	348	1179 ± 3	331	1178 ± 3	294	1169 ± 2	252	1203 ± 3	3194361 ± 74	3174364 ± 75
385	tongyi-005	1140701	138919	3742121	3812089 ± 0	22	165 ± 1	-	-	-	-	-	-	405	18924 ± 65	40820158 ± 103	
386	toppanidgate-000	671181	711850	3511786	4084096 ± 0	310	915 ± 1	267	916 ± 1	236	916 ± 1	215	917 ± 1	175	917 ± 1	41625262 ± 84	41525264 ± 97
387	toshiba-004	599297	27880	3311595	3642056 ± 0	448	1447 ± 3	420	1453 ± 2	416	1457 ± 9	386	1457 ± 3	327	1479 ± 4	1341020 ± 25	131998 ± 32
388	toshiba-006	599566	44078	3291588	3662056 ± 0	458	1481 ± 16	427	1515 ± 7	420	1506 ± 6	396	1521 ± 2	341	1546 ± 30	1351022 ± 17	1361022 ± 23
389	touchlessid-000	92561	64467	158716	2012048 ± 0	65	309 ± 5	48	305 ± 2	34	312 ± 5	27	277 ± 4	29	349 ± 17	42031935 ± 292	42731958 ± 243
390	touchlessid-001	255274	14355	108537	2762048 ± 0	74	344 ± 1	59	347 ± 1	62	414 ± 3	108	595 ± 10	358	1732 ± 61	2131806 ± 35	2121800 ± 35
391	trueface-002	253947	123116	88486	1002000 ± 0	81	360 ± 0	63	361 ± 0	66	423 ± 0	107	590 ± 1	-	8192 ± 14	10186 ± 19	
392	trueface-003	346530	24308	4293915	2802048 ± 0	363	1107 ± 22	183	677 ± 3	181	732 ± 7	212	905 ± 5	-	10103 ± 11	2112112 ± 29	
393	putepatch-000	11476	17185	233	1232048 ± 0	20	122 ± 4	14	120 ± 1	12	142 ± 2	16	196 ± 5	41	411 ± 14	41323893 ± 406	41625279 ± 406
394	turingtechvip-001	399874	54535	131617	2852048 ± 0	432	1384 ± 4	403	1391 ± 1	397	1393 ± 1	377	1411 ± 1	326	1476 ± 2	2031733 ± 19	2041734 ± 20
395	turingtechvip-002	167556	140995	204876	1782048 ± 0	461	1493 ± 2	381	1306 ± 1	392	1382 ± 1	347	1337 ± 1	314	1426 ± 3	39213819 ± 103	39213807 ± 137
396	turkcell-000	271083	133553	134637	3212048 ± 0	366	1110 ± 1	323	1094 ± 0	309	1103 ± 0	277	1126 ± 1	250	1201 ± 1	2752866 ± 23	2762873 ± 40

Notes

- 1 The configuration size does not capture static data included in libraries.
 - 2 The library size is the combined total of all files provided in the submission lib folder. These libraries e.g. OpenCV may or may not be installed on any end user's platform natively and would not need to be installed with the algorithm. Some developers put neural network models in their libraries.
 - 3 The memory usage is the peak resident set size reported by the ps system call during template generation.
 - 4 The median template creation times are measured on Intel®Xeon®CPU E5-2630 v4 @ 2.20GHz processors.
 - 5 The comparison durations, in nanoseconds, are estimated using std::chrono::high_resolution_clock which on the machine in (2) counts 1ns clock ticks. Precision is somewhat worse than that however. The \pm value is the median absolute deviation times 1.48 for Normal consistency.

ALGORITHM			CONFIG	LIBRARY	TEMPLATE						COMPARISON ⁴		
NAME		DATA	DATA	MEMORY	SIZE	GENERATION TIME (ms) ⁴				TIME (ns) ⁵			
		(KB) ¹	(KB) ²	(MB) ³	(B)	MUGSHOT	480x720	960x1440	1600x2400	3000x4500	GENUINE	IMPOSTOR	
397	twface-000	661735	11782	393 2610	313	2048 ± 0	289 871 ± 1	248 873 ± 1	219 873 ± 2	199 876 ± 2	169 898 ± 1	187 1504 ± 29	186 1510 ± 34
398	twface-001	671511	11782	408 2855	223	2048 ± 0	313 923 ± 1	270 925 ± 2	243 926 ± 1	217 929 ± 2	179 940 ± 2	173 1400 ± 32	175 1402 ± 37
399	ulsee-001	370519	57261	-	290	2048 ± 0	208 654 ± 2	-	-	-	-	351 6065 ± 94	352 6228 ± 77
400	uluface-002	0	480761	248 1088	182	2048 ± 0	294 873 ± 42	239 855 ± 9	264 978 ± 24	325 1271 ± 40	372 2333 ± 68	407 19207 ± 1114	404 18501 ± 274
401	uluface-003	97357	529422	279 1264	384	3072 ± 0	328 965 ± 11	285 968 ± 10	304 1087 ± 20	365 1387 ± 36	380 2469 ± 86	417 26057 ± 195	419 26865 ± 566
402	unissey-001	0	1956593	327 1584	417	4096 ± 0	300 880 ± 3	258 892 ± 3	414 1452 ± 8	425 3048 ± 12	420 10017 ± 387	181 1463 ± 35	183 1471 ± 34
403	unissey-002	0	1443765	170 763	420	4096 ± 0	241 736 ± 1	205 752 ± 1	274 994 ± 1	382 1426 ± 1	397 3331 ± 2	386 12308 ± 91	386 12302 ± 137
404	upc-001	0	89914	247 1077	89	1052 ± 0	156 551 ± 15	194 703 ± 56	180 724 ± 51	164 751 ± 49	161 863 ± 33	289 3114 ± 44	291 3165 ± 97
405	uxlabs-001	291127	39378	153 700	419	4096 ± 0	92 395 ± 0	70 387 ± 0	53 388 ± 0	47 390 ± 0	39 396 ± 0	219 1863 ± 31	224 1921 ± 45
406	vcoog-002	3229434	118946	421 3666	461	61504 ± 5	79 357 ± 25	-	-	-	-	458 296154 ± 3077	458 296436 ± 4183
407	vd-002	254498	34389	149 688	48	516 ± 0	224 684 ± 5	184 679 ± 4	161 676 ± 5	143 693 ± 5	134 754 ± 5	24 300 ± 14	26 319 ± 32
408	vd-003	254505	44051	151 696	329	2052 ± 0	231 691 ± 5	188 690 ± 5	163 683 ± 4	142 691 ± 5	126 722 ± 5	132 1003 ± 11	132 1001 ± 7
409	veridas-007	355105	891492	390 2527	118	2048 ± 0	291 872 ± 9	250 875 ± 8	351 1261 ± 18	418 2238 ± 38	411 6374 ± 147	86 655 ± 16	89 660 ± 19
410	veridas-008	1100495	1190915	454 8932	191	2048 ± 0	318 944 ± 12	277 945 ± 11	375 1334 ± 27	419 2382 ± 48	413 6959 ± 172	99 723 ± 14	103 731 ± 16
411	veridium-000	0	47198	15 98	459	29399 ± 2045	10 79 ± 0	8 80 ± 0	9 89 ± 0	7 90 ± 0	7 111 ± 0	447 64880 ± 171	447 64697 ± 247
412	verigram-000	256209	7798	355 1842	139	2048 ± 0	262 807 ± 1	226 821 ± 1	260 972 ± 2	356 1358 ± 3	389 2848 ± 13	162 1222 ± 17	163 1219 ± 17
413	verigram-001	282155	11773	395 2638	281	2048 ± 0	213 664 ± 2	182 675 ± 2	207 833 ± 4	310 1202 ± 7	385 2733 ± 32	195 1664 ± 60	193 1648 ± 56
414	verihubs-inteligensia-000	209562	51877	73 427	278	2048 ± 0	163 567 ± 0	428 1558 ± 8	424 1560 ± 8	400 1568 ± 8	349 1621 ± 8	412 22351 ± 91	412 22371 ± 81
415	verihubs-inteligensia-001	216524	51916	75 437	192	2048 ± 0	160 564 ± 0	136 562 ± 0	119 566 ± 1	96 566 ± 0	87 600 ± 0	410 21770 ± 84	410 21735 ± 102
416	verijelas-000	254540	10322	347 1736	196	2048 ± 0	66 321 ± 0	54 325 ± 1	41 329 ± 0	37 335 ± 5	30 360 ± 0	376 10267 ± 143	376 10218 ± 109
417	via-000	124422	11151	223 964	142	2048 ± 0	237 707 ± 8	203 740 ± 5	232 906 ± 41	223 941 ± 40	204 1040 ± 5	127 966 ± 28	135 1021 ± 44
418	via-001	370255	11151	338 1697	286	2048 ± 0	327 964 ± 3	302 1011 ± 3	286 1026 ± 4	259 1045 ± 3	232 1137 ± 28	129 983 ± 31	129 989 ± 40
419	videmo-001	212051	95063	56 304	113	2048 ± 0	34 199 ± 0	16 164 ± 0	13 164 ± 0	10 164 ± 0	9 165 ± 0	22 296 ± 17	23 288 ± 16
420	videmo-002	212053	32963	51 332	318	2048 ± 0	35 199 ± 0	17 169 ± 0	14 169 ± 0	11 170 ± 0	11 170 ± 0	14 209 ± 7	14 208 ± 8
421	videonetics-001	30875	5963	5 61	20	512 ± 0	44 262 ± 3	38 273 ± 1	71 439 ± 3	181 820 ± 3	377 2393 ± 43	155 1153 ± 38	156 1142 ± 65
422	videonetics-002	121981	6289	19 115	331	2052 ± 0	55 282 ± 5	46 295 ± 1	100 513 ± 4	254 1029 ± 3	393 3151 ± 46	161 1219 ± 57	164 1262 ± 56
423	vettelhightech-000	259471	215557	71 419	114	2048 ± 0	117 461 ± 1	97 461 ± 2	78 461 ± 1	69 467 ± 2	57 494 ± 0	64 599 ± 11	60 591 ± 13
424	vigilantsolutions-010	348798	49973	193 840	98	1548 ± 0	189 615 ± 0	166 631 ± 0	142 632 ± 0	123 636 ± 0	106 659 ± 0	48 490 ± 13	49 488 ± 11
425	vigilantsolutions-011	255661	49973	122 591	97	1548 ± 0	94 402 ± 0	82 418 ± 0	63 418 ± 0	56 422 ± 0	50 445 ± 0	29 339 ± 20	33 366 ± 37
426	vinaai-000	402391	866522	236 1032	195	2048 ± 0	360 1099 ± 1	324 1095 ± 1	307 1093 ± 1	272 1099 ± 1	229 1126 ± 1	281 2996 ± 20	282 2993 ± 26
427	vinbigdata-001	271405	44746	121 589	186	2048 ± 0	440 1400 ± 5	406 1393 ± 2	393 1391 ± 2	367 1393 ± 1	307 1404 ± 1	169 1351 ± 50	169 1310 ± 38
428	vinbigdata-002	256322	138864	128 606	190	2048 ± 0	165 569 ± 2	140 572 ± 1	120 571 ± 1	97 572 ± 1	85 596 ± 1	243 2175 ± 44	244 2160 ± 53
429	vion-000	228219	7533	92 498	341	2052 ± 0	72 333 ± 1	-	-	-	-	432 39839 ± 3561	418 26830 ± 2241
430	visage-000	49218	70150	9 73	18	512 ± 0	427 ± 0	227 ± 0	2 31 ± 0	3 38 ± 0	3 63 ± 0	246 2220 ± 14	248 2218 ± 14
431	visionbox-001	256869	190645	116 579	145	2048 ± 0	335 983 ± 7	322 1093 ± 46	383 1360 ± 68	416 2181 ± 105	409 5955 ± 281	157 1161 ± 22	158 1154 ± 20
432	visionbox-002	259063	135281	130 612	372	2059 ± 0	130 482 ± 1	105 482 ± 0	89 484 ± 1	77 492 ± 1	63 517 ± 3	231 1969 ± 44	228 1931 ± 42
433	visionlabs-010	1067280	19357	208 902	43	513 ± 0	239 730 ± 0	199 717 ± 1	175 709 ± 0	153 713 ± 1	131 739 ± 0	65 600 ± 41	78 626 ± 35
434	visionlabs-011	1067280	19353	201 862	44	513 ± 0	240 731 ± 1	198 717 ± 1	176 710 ± 1	155 714 ± 1	132 741 ± 1	51 556 ± 26	54 559 ± 25
435	visteam-003	215359	33730	90 489	428	4096 ± 0	400 1249 ± 4	366 1251 ± 4	354 1266 ± 5	327 1272 ± 5	295 1370 ± 9	356 6816 ± 111	356 6816 ± 105
436	visteam-004	61594	35369	34 168	220	2048 ± 0	60 303 ± 5	49 313 ± 6	30 278 ± 4	30 288 ± 4	33 377 ± 7	312 3936 ± 72	312 3938 ± 79
437	vixvizacion-005	38886	534579	163 731	222	2048 ± 0	110 433 ± 4	67 381 ± 3	52 383 ± 3	43 373 ± 1	42 411 ± 1	103 731 ± 63	81 632 ± 32
438	vixvizacion-006	594053	396294	212 914	165	2048 ± 0	298 876 ± 9	230 828 ± 3	201 817 ± 1	183 825 ± 2	164 871 ± 1	66 600 ± 23	72 611 ± 25
439	vnpt-004	370110	240841	230 988	107	2048 ± 0	397 1238 ± 1	362 1241 ± 1	348 1242 ± 2	336 1307 ± 2	332 1505 ± 2	312 4047 ± 48	314 4008 ± 108
440	vnpt-005	560630	240888	263 1141	244	2048 ± 0	443 1403 ± 0	411 1404 ± 6	402 1403 ± 6	384 1456 ± 0	350 1630 ± 10	303 3562 ± 23	303 3554 ± 29

Notes

- 1 The configuration size does not capture static data included in libraries.
- 2 The library size is the combined total of all files provided in the submission lib folder. These libraries e.g. OpenCV may or may not be installed on any end user's platform natively and would not need to be installed with the algorithm. Some developers put neural network models in their libraries.
- 3 The memory usage is the peak resident set size reported by the ps system call during template generation.
- 4 The median template creation times are measured on Intel®Xeon®CPU E5-2630 v4 @ 2.20GHz processors.
- 5 The comparison durations, in nanoseconds, are estimated using std::chrono::high_resolution_clock which on the machine in (2) counts 1ns clock ticks. Precision is somewhat worse than that however. The ± value is the median absolute deviation times 1.48 for Normal consistency.

Table 17: Summary of algorithms and properties included in this report. The red superscripts give ranking for the quantity in that column.

	ALGORITHM	CONFIG	LIBRARY	TEMPLATE								COMPARISON ⁴									
				NAME	DATA	DATA	MEMORY	SIZE	GENERATION TIME (ms) ⁴				TIME (ns) ⁵								
									(KB) ¹	(KB) ²	(MB) ³	(B)	MUGSHOT	480x720	960x1440	1600x2400	3000x4500	GENUINE	IMPOSTOR		
441	vocord-009	1380132	201560	434	4162	99	1920 ± 0	455	1472 ± 2	424	1472 ± 1	423	1549 ± 1	403	1667 ± 2	367	2064 ± 2	235	2052 ± 50	237	2056 ± 39
442	vocord-010	902552	206873	425	3858	88	1088 ± 0	452	1459 ± 2	423	1459 ± 1	417	1463 ± 2	393	1484 ± 1	339	1535 ± 3	267	2724 ± 31	265	2653 ± 45
443	vts-000	256589	169760	340	1704	293	2048 ± 0	135	486 ± 1	103	481 ± 0	88	484 ± 0	73	485 ± 1	64	517 ± 0	455	124209 ± 352	455	123652 ± 358
444	vts-001	293000	475743	132	618	298	2048 ± 0	219	676 ± 1	185	683 ± 6	166	687 ± 3	144	695 ± 2	120	709 ± 2	373	9620 ± 44	372	9618 ± 54
445	wicket-000	826392	641802	372	2071	149	2048 ± 0	446	1419 ± 2	415	1429 ± 3	410	1444 ± 4	387	1460 ± 3	340	1537 ± 6	445	60976 ± 232	445	61096 ± 323
446	winsense-001	264428	32035	216	922	90	1280 ± 0	249	766 ± 7	314	1058 ± 47	267	983 ± 97	260	1053 ± 119	280	1320 ± 84	192	1631 ± 28	232	1964 ± 171
447	winsense-002	281379	25780	350	1781	274	2048 ± 0	137	494 ± 2	111	498 ± 1	102	519 ± 1	88	537 ± 1	97	634 ± 1	197	1683 ± 8	196	1685 ± 7
448	wiseai-001	189467	60781	43	245	252	2048 ± 0	41	240 ± 0	33	251 ± 0	39	328 ± 1	35	327 ± 0	25	332 ± 0	272	2850 ± 29	275	2852 ± 31
449	wuhantianyu-001	465118	66457	202	866	234	2048 ± 0	203	642 ± 1	171	642 ± 1	153	644 ± 0	129	652 ± 0	117	697 ± 0	371	9502 ± 151	375	9920 ± 253
450	x-laboratory-000	520020	197310	320	1524	354	2056 ± 0	263	808 ± 7	261	897 ± 113	233	907 ± 103	203	886 ± 103	110	673 ± 39	102	725 ± 19	106	749 ± 34
451	x-laboratory-001	625140	398792	356	1844	365	2056 ± 0	175	586 ± 2	153	596 ± 5	136	603 ± 6	117	620 ± 7	142	793 ± 14	116	813 ± 28	120	872 ± 32
452	xforwardai-001	340100	51163	377	2173	252	2048 ± 0	383	1180 ± 2	351	1182 ± 1	339	1194 ± 1	304	1186 ± 2	253	1203 ± 1	112	779 ± 17	113	797 ± 13
453	xforwardai-002	707715	51163	369	1989	393	4096 ± 0	319	944 ± 1	276	942 ± 1	250	943 ± 4	221	935 ± 1	187	967 ± 1	177	1406 ± 8	176	1405 ± 13
454	xm-000	578041	148920	147	688	342	2052 ± 0	299	878 ± 2	254	882 ± 1	270	988 ± 2	323	1258 ± 3	379	2434 ± 7	193	1634 ± 17	192	1632 ± 20
455	yisheng-004	486351	38653	284	1279	389	3704 ± 0	85	378 ± 12	-	-	-	-	-	-	91	693 ± 137	51	526 ± 34		
456	yitu-003	1525719	138919	423	3737	380	2082 ± 0	286	860 ± 0	-	-	-	-	-	-	402	18305 ± 71	402	18286 ± 62		
457	yoonik-002	453720	265415	404	2755	287	2048 ± 0	374	1145 ± 4	330	1123 ± 2	314	1124 ± 2	276	1125 ± 2	230	1126 ± 3	109	761 ± 32	105	736 ± 32
458	yoonik-003	346691	265415	380	2196	312	2048 ± 0	338	991 ± 3	291	980 ± 1	268	984 ± 4	235	982 ± 1	192	983 ± 1	87	684 ± 45	90	678 ± 41
459	ytu-000	1477360	44032	388	2484	104	2048 ± 0	147	530 ± 0	123	533 ± 0	150	640 ± 0	194	861 ± 2	366	1949 ± 8	424	31797 ± 131	425	31794 ± 133
460	yuan-004	428665	50011	295	1353	405	4096 ± 0	162	567 ± 0	139	569 ± 0	121	573 ± 0	99	579 ± 0	89	607 ± 0	345	5816 ± 35	347	5800 ± 31
461	yuan-005	258312	145564	192	839	306	2048 ± 0	88	381 ± 0	69	386 ± 0	53	387 ± 2	48	390 ± 4	44	421 ± 3	156	1156 ± 8	161	1196 ± 26

Notes

- 1 The configuration size does not capture static data included in libraries.
- 2 The library size is the combined total of all files provided in the submission lib folder. These libraries e.g. OpenCV may or may not be installed on any end user's platform natively and would not need to be installed with the algorithm. Some developers put neural network models in their libraries.
- 3 The memory usage is the peak resident set size reported by the ps system call during template generation.
- 4 The median template creation times are measured on Intel® Xeon® CPU E5-2630 v4 @ 2.20GHz processors.
- 5 The comparison durations, in nanoseconds, are estimated using std::chrono::high_resolution_clock which on the machine in (2) counts 1ns clock ticks. Precision is somewhat worse than that however. The ± value is the median absolute deviation times 1.48 for Normal consistency.

Table 18: Summary of algorithms and properties included in this report. The red superscripts give ranking for the quantity in that column.

	Algorithm	FALSE NON-MATCH RATE (FNMR)										LESS CONSTRAINED, NON-COOP.					
		CONSTRAINED, COOPERATIVE								WILD							
		Name	VISAMC	VISA	MUGSHOT	MUGSHOT12+YRS	VISABORDER	BORDER	BORDER	1E-05							
	FMR	0.0001	1E-06	1E-05	1E-05	1E-06	1E-06	1E-06	1E-05	0.0001							
1	20face-000	0.1268	404	0.1828	398	0.1748	405	0.2768	405	0.1765	390	0.1864	300	0.0927	334	0.0405	283
2	20face-001	0.0521	380	0.0732	380	0.1414	403	0.2549	404	0.0769	366	0.1354	291	0.0419	292	0.0295	172
3	3divi-006	0.0064	191	0.0094	189	0.0047	170	0.0066	174	0.0091	179	0.0191	156	0.0113	151	0.0289	147
4	3divi-007	0.0024	56	0.0038	62	0.0028	63	0.0034	59	0.0046	92	0.0101	81	0.0082	97	0.0300	187
5	acer-001	0.0294	360	0.0504	362	0.0240	354	0.0463	356	0.0436	346	0.0622	259	0.0360	286	0.0307	201
6	acer-002	0.0169	328	0.0262	328	0.0103	288	0.0167	299	0.0182	280	0.0281	197	0.0159	206	0.0297	179
7	acisw-007	0.4276	431	0.5493	433	0.8425	446	0.9185	446	0.8424	430	0.9976	418	0.9930	435	0.4963	430
8	acisw-008	0.0100	258	0.0147	252	0.0094	284	0.0126	253	0.1740	389	0.6651	358	0.4545	387	0.0925	365
9	ader-a-002	0.0052	147	0.0071	144	0.0047	167	0.0064	168	0.0087	170	0.0159	132	0.0136	179	0.0990	368
10	ader-a-003	0.0043	124	0.0059	123	0.0036	121	0.0043	103	0.0076	149	0.0151	121	0.0128	171	0.0989	367
11	advance-003	0.0060	184	0.0087	178	0.0052	187	0.0067	175	0.0389	339	0.4914	340	0.1291	340	0.0508	314
12	advance-004	0.0083	235	0.0101	206	0.0037	128	0.0054	137	0.0051	105	0.3555	328	0.1088	338	0.1635	387
13	afisbiometrics-000	0.0051	144	0.0073	149	0.0030	82	0.0050	126	0.0044	86	0.0077	47	0.0057	42	0.0282	95
14	afrengine-000	0.6244	451	0.7336	450	0.8318	445	0.9083	444	0.8122	427	0.9980	420	0.9895	433	0.6480	437
15	aifirst-001	0.0119	283	0.0170	274	0.0084	263	0.0127	259	0.0131	237	0.0212	167	0.0138	182	0.0432	298
16	aigen-001	0.0124	291	0.0219	305	0.0143	325	0.0217	322	0.0236	307	0.8960	387	0.3255	373	0.0681	340
17	aigen-002	0.0192	340	0.0343	344	0.0256	355	0.0402	350	0.0389	338	0.9196	391	0.3876	381	0.1096	373
18	ailabs-001	0.0158	321	0.0276	333	0.0192	341	0.0317	342	0.0352	333	0.0608	256	0.0434	295	0.0338	245
19	aimall-002	0.0119	282	0.0167	272	0.0224	349	0.0411	352	0.0233	304	0.0373	230	0.0235	256	0.0327	232
20	aimall-003	0.0033	91	0.0041	67	0.0033	107	0.0035	70	0.0056	117	0.0109	88	0.0087	110	0.0312	211
21	aiseemu-001	0.0021	43	0.0029	40	0.0027	50	0.0033	54	0.0038	65	0.0339	219	0.0057	43	0.0282	86
22	aiunionface-000	0.0104	263	0.0154	262	0.0082	260	0.0122	248	0.0141	244	0.0243	180	0.0169	212	0.0306	199
23	aize-001	0.0223	347	0.0344	345	0.0199	342	0.0313	341	0.0367	335	0.0522	250	0.0359	285	0.0446	303
24	aize-002	0.0210	345	0.0327	341	0.0280	358	0.0489	359	0.0504	352	0.0692	263	0.0434	294	0.0854	360
25	ajou-001	0.0093	248	0.0147	253	0.0071	237	0.0126	254	0.0173	277	0.0274	192	0.0186	230	0.0348	252
26	alchera-003	0.0044	126	0.0055	116	0.0031	88	0.0039	87	0.0042	82	0.0077	49	0.0065	60	0.0339	246
27	alchera-004	0.0035	100	0.0052	110	0.0028	69	0.0039	88	0.0029	25	0.0075	43	0.0044	14	0.0304	194
28	alfabeta-001	0.4867	438	0.5831	436	0.6855	431	0.8156	433	0.8253	429	0.7765	374	0.6416	401	0.3427	419
29	alice-000	0.0119	285	0.0192	292	0.0106	295	0.0170	300	0.0167	268	0.0265	188	0.0150	200	0.0288	135
30	alleyes-000	0.0058	173	0.0090	185	0.0055	197	0.0087	217	0.0068	137	0.0105	86	0.0076	85	0.0282	93
31	allgovision-000	0.0346	370	0.0527	366	0.0232	351	0.0339	343	0.0372	337	0.0620	258	0.0443	299	0.0607	330
32	alphaface-001	0.0065	193	0.0097	198	0.0039	134	0.0063	167	0.0083	163	-	-	-	-	0.0280	76
33	alphaface-002	0.0052	149	0.0075	154	0.0030	75	0.0044	108	1.0000	452	0.0115	97	0.0084	103	0.0279	64
34	amplifiedgroup-001	0.5034	440	0.5848	437	0.6973	434	0.8316	434	0.7807	424	0.7724	372	0.6354	398	0.4250	425
35	androvideo-000	0.0243	350	0.0438	357	0.0239	353	0.0365	347	0.0483	351	0.1870	301	0.0635	318	0.1163	376
36	anke-004	0.0080	227	0.0154	261	0.0073	239	0.0112	240	0.0102	205	0.0178	150	0.0118	160	0.0288	138
37	anke-005	0.0070	201	0.0109	218	0.0059	208	0.0094	223	0.0105	207	0.0142	112	0.0102	132	0.0289	145
38	antheus-000	0.2564	416	0.3776	419	0.7240	435	0.8699	439	0.8899	437	0.9872	409	0.9483	425	0.7668	441
39	antheus-001	0.1311	405	0.2306	406	0.5113	423	0.6797	425	0.8748	436	0.9908	413	0.9649	429	0.7586	440
40	anyvision-004	0.0267	355	0.0385	353	0.0258	356	0.0487	358	0.0234	306	0.0301	203	0.0191	234	0.0470	307
41	anyvision-005	0.0023	55	0.0037	59	0.0027	60	0.0035	66	0.0049	100	0.0084	59	0.0069	71	0.0285	111
42	armatura-001	0.0033	88	0.0042	77	0.0031	86	0.0037	77	0.0056	116	0.0110	89	0.0092	118	0.0815	357
43	armatura-002	0.0041	122	0.0052	109	0.0034	112	0.0044	105	0.0040	71	0.8502	385	0.0275	269	0.0753	348
44	asusaics-000	0.0125	294	0.0209	300	0.0085	265	0.0134	267	0.0143	248	0.7189	362	0.0285	270	0.0295	171

Table 19: FNMR is the proportion of mated comparisons below a threshold set to achieve the FMR given in the header on the fourth row. FMR is the proportion of impostor comparisons at or above that threshold. The light grey values give rank over all algorithms in that column. The pink columns use only same-sex impostors; others are selected regardless of demographics. The exception, in the green column, uses “matched-covariates” i.e. impostors of the same sex, age group, and country of birth. The second pink column includes effects of extended ageing. Missing entries for border, visa, mugshot and wild images generally mean the algorithm did not run to completion. The VISA columns compare images described in section 2.1. The MUGSHOT columns compare images described in section 2.4. The VISA-BORDER column compare images described in section 2.2 with those of section 2.3. The BORDER column compares images described in section 2.3. The WILD columns compare images described in section 2.6.

	Algorithm	FALSE NON-MATCH RATE (FNMR)										LESS CONSTRAINED, NON-COOP.					
		CONSTRAINED, COOPERATIVE								WILD							
		Name	VISAMC	VISA	MUGSHOT	MUGSHOT12+YRS	VISA BORDER	BORDER	BORDER	WILD							
	FMR	0.0001	1E-06	1E-05	1E-05	1E-06	1E-06	1E-06	1E-05	0.0001							
45	asusaics-001	0.0125	293	0.0210	301	0.0085	267	0.0134	268	0.0143	249	0.7437	366	0.0289	272	0.0295	170
46	authenmetric-003	0.0036	108	0.0053	113	0.0039	140	0.0051	128	0.0095	192	0.9930	414	0.5932	395	0.0290	148
47	authenmetric-004	0.0027	67	0.0042	78	0.0033	103	0.0036	74	0.0083	166	0.9879	410	0.4058	383	0.0290	154
48	aware-005	0.0457	377	0.0643	375	0.0603	385	0.1094	387	0.0613	358	0.1075	283	0.0491	302	0.0314	216
49	aware-006	0.0487	378	0.0819	383	0.0529	379	0.1090	385	0.1011	378	0.1058	280	0.0502	305	0.0317	222
50	awiros-001	0.4044	429	0.4622	425	0.5530	425	0.6518	422	0.2008	394	0.1994	304	0.1386	345	0.5584	433
51	awiros-002	0.1990	410	0.2561	408	0.3319	412	0.4411	412	0.3821	410	0.9938	415	0.2634	364	0.0997	369
52	aximetria-001	0.0111	273	0.0186	287	0.0110	301	0.0148	284	0.0170	272	0.3928	331	0.2090	357	0.0409	288
53	ayftech-001	0.0946	397	0.1941	400	0.2438	408	0.3625	408	0.1558	386	0.1589	295	0.0936	335	0.0785	350
54	ayonix-000	0.4351	433	0.4872	427	0.6150	430	0.7510	430	0.6557	419	0.6361	354	0.4981	388	0.3635	421
55	beethedata-000	0.0127	298	0.0195	293	0.0092	278	0.0157	290	0.0171	274	0.0306	205	0.0204	243	0.0285	114
56	beyneai-000	0.0071	210	0.0107	215	0.0104	292	0.0131	265	0.0170	273	0.9837	407	0.6171	397	0.0597	329
57	biocube-001	0.5596	446	0.6834	445	0.7700	442	0.8712	440	0.8446	431	0.9661	403	0.7922	412	0.2377	403
58	bioidtechswiss-001	0.0054	157	0.0072	145	0.0069	230	0.0124	251	0.0060	124	0.0094	73	0.0065	63	0.0313	215
59	bioidtechswiss-002	0.0049	135	0.0067	139	0.0064	216	0.0116	243	0.0067	136	0.0117	99	0.0086	107	0.0279	55
60	bm-001	0.7431	455	0.9494	456	0.9586	451	0.9843	450	0.9049	439	0.9021	390	0.8395	418	0.9935	451
61	boetech-001	0.0662	389	0.0802	382	0.0493	377	0.0791	376	0.0682	363	0.1074	282	0.0758	325	0.1719	389
62	boetech-002	0.0535	383	0.0565	371	0.0114	309	0.0136	270	0.0403	340	0.0650	260	0.0606	316	0.1697	388
63	bresee-001	0.0085	236	0.0143	249	0.0086	270	0.0153	288	0.0108	211	0.0168	140	0.0115	156	0.0355	265
64	bresee-002	0.0079	225	0.0101	204	0.0065	220	0.0079	201	0.0129	232	0.0263	187	0.0224	253	0.0327	233
65	camvi-002	0.0125	295	0.0221	307	0.0089	275	0.0145	282	0.0142	246	0.2650	316	0.0166	211	0.0288	133
66	camvi-004	0.0171	333	0.0316	340	0.0042	150	0.0049	124	0.0097	198	0.6636	357	0.0141	187	0.0284	103
67	canon-003	0.0041	123	0.0059	122	0.0030	74	0.0040	91	0.0040	70	0.0073	40	0.0059	47	0.0274	21
68	canon-004	0.0052	150	0.0091	187	0.0033	106	0.0058	152	0.0037	60	0.0770	267	0.0494	303	0.0267	3
69	ceiec-003	0.0071	207	0.0107	213	0.0061	213	0.0079	204	0.0160	260	0.0316	208	0.0260	264	0.0308	207
70	ceiec-004	0.0038	114	0.0051	104	0.0045	163	0.0053	132	0.0062	131	0.3939	332	0.0104	138	0.0325	229
71	chosun-001	0.0525	381	0.0936	385	0.0742	390	0.1263	393	0.0978	377	1.0000	444	0.9354	423	0.4446	427
72	chosun-002	0.0390	372	0.0646	376	0.0339	369	0.0576	368	0.0455	350	0.6904	360	0.1746	354	0.0696	342
73	chtface-004	0.0046	130	0.0062	130	0.0052	186	0.0080	205	0.0088	175	0.0152	122	0.0106	141	0.0306	200
74	chtface-005	0.0033	90	0.0049	99	0.0029	71	0.0041	95	0.0044	85	0.0317	209	0.0066	66	0.0306	198
75	cist-001	0.0046	129	0.0065	136	0.0042	151	0.0063	165	0.9675	446	0.9997	430	0.9994	443	0.0407	285
76	clearviewai-000	0.0010	6	0.0019	14	0.0024	16	0.0028	29	0.0030	28	0.0058	19	0.0050	21	0.0271	7
77	closemi-001	0.0136	302	0.0163	266	0.0039	137	0.0054	136	0.0072	143	1.0000	438	0.0094	122	0.0318	223
78	cloudmatrix-001	0.0668	390	0.1141	389	0.0539	380	0.0905	380	0.3509	407	0.9819	406	0.9010	421	0.0636	333
79	cloudmatrix-002	0.0075	219	0.0113	224	0.0084	264	0.0120	245	0.9248	442	0.9997	429	0.9985	442	0.0358	267
80	cloudwalk-hr-003	0.0026	63	0.0041	70	0.0040	144	0.0058	151	0.0060	128	0.9992	422	0.0094	120	0.7206	439
81	cloudwalk-hr-004	0.0009	5	0.0018	10	0.0034	110	0.0028	34	0.0052	107	0.9992	423	0.0093	119	0.1625	386
82	cloudwalk-mt-005	0.0006	3	0.0009	2	0.0025	30	0.0022	7	0.0017	2	0.9286	395	0.5956	396	0.0287	128
83	cloudwalk-mt-006	0.0006	1	0.0006	1	0.0023	10	0.0019	1	0.0016	1	0.0032	1	0.0030	2	0.0290	151
84	codeline-000	0.0057	165	0.0079	167	0.0037	125	0.0053	135	0.2721	401	1.0000	439	0.9763	430	0.0273	15
85	cogent-006	0.0046	131	0.0059	125	0.0036	117	0.0047	115	0.0058	121	0.0113	94	0.0091	115	0.0343	248
86	cogent-007	0.0022	51	0.0038	60	0.0028	67	0.0031	45	0.0040	73	0.0082	56	0.0067	67	0.0438	301
87	cognitec-003	0.0038	112	0.0052	107	0.0054	195	0.0057	148	0.0225	299	0.0416	236	0.0388	289	0.0348	253
88	cognitec-004	0.0036	103	0.0053	112	0.0053	188	0.0056	145	0.0098	199	0.0202	165	0.0154	202	0.0352	263

Table 20: FNMR is the proportion of mated comparisons below a threshold set to achieve the FMR given in the header on the fourth row. FMR is the proportion of impostor comparisons at or above that threshold. The light grey values give rank over all algorithms in that column. The pink columns use only same-sex impostors; others are selected regardless of demographics. The exception, in the green column, uses “matched-covariates” i.e. impostors of the same sex, age group, and country of birth. The second pink column includes effects of extended ageing. Missing entries for border, visa, mugshot and wild images generally mean the algorithm did not run to completion. The VISA columns compare images described in section 2.1. The MUGSHOT columns compare images described in section 2.4. The VISA-BORDER column compare images described in section 2.2 with those of section 2.3. The BORDER column compares images described in section 2.3. The WILD columns compare images described in section 2.6.

Algorithm	FALSE NON-MATCH RATE (FNMR)												
	CONSTRAINED, COOPERATIVE								LESS CONSTRAINED, NON-COOP.				
	Name	VISAMC	VISA	MUGSHOT	MUGSHOT12+YRS	VISABORDER	BORDER	BORDER	WILD				
FMR	0.0001	1E-06	1E-05	1E-05	1E-06	1E-06	1E-06	1E-05	0.0001	0.0002	117	0.0277	
89	cor-001	0.0075	218	0.0113	222	0.0055	199	0.0084	209	0.0091	181	0.0148	117
90	coretech-000	0.7699	457	1.0000	460	1.0000	458	-	1.0000	455	1.0000	456	1.0000
91	coretech-001	0.0052	148	0.0067	140	0.0083	262	0.0092	220	0.0346	332	0.1363	292
92	corsight-002	0.0053	152	0.0068	142	0.0030	79	0.0041	96	0.0039	68	0.0079	51
93	corsight-003	0.0026	64	0.0040	65	0.0028	64	0.0045	110	0.0035	56	0.0059	21
94	csc-002	0.0099	257	0.0132	239	0.0077	246	0.0142	279	0.0126	231	0.0195	158
95	csc-003	0.0053	153	0.0065	134	0.0037	126	0.0047	116	0.0074	145	0.0124	105
96	ctbcbank-000	0.0168	326	0.0250	321	0.0146	327	0.0224	324	0.0211	296	0.8964	388
97	ctbcbank-001	0.0155	319	0.0235	316	0.0148	332	0.0243	329	0.0207	293	0.9279	394
98	cubox-001	0.0064	190	0.0080	168	0.0037	123	0.0055	140	0.0060	125	0.0111	91
99	cubox-002	0.0034	98	0.0041	71	0.0025	27	0.0025	20	0.0033	44	0.0064	27
100	cudocommunication-001	0.4777	436	1.0000	463	0.4373	418	0.5360	415	1.0000	458	1.0000	454
101	cukee-001	0.0036	106	0.0045	88	0.0031	92	0.0046	113	0.0051	106	0.0095	76
102	cybercore-002	0.0092	246	0.0119	227	0.0049	175	0.0072	182	0.9105	441	1.0000	443
103	cybercore-003	0.0155	318	0.0164	269	0.0032	99	0.0033	58	0.0024	10	0.9719	404
104	cyberextruder-003	0.0109	270	0.0169	273	0.0071	235	0.0112	241	0.0165	266	0.0410	235
105	cyberextruder-004	0.0118	281	0.0181	283	0.0081	257	0.0133	266	0.0191	288	0.0329	212
106	cyberlink-009	0.0018	36	0.0027	36	0.0047	166	0.0046	111	0.0040	76	0.0086	65
107	cyberlink-010	0.0011	11	0.0019	15	0.0041	146	0.0041	92	0.0039	66	0.1829	299
108	dahua-006	0.0027	65	0.0039	63	0.0031	90	0.0039	89	0.0039	67	0.0067	32
109	dahua-007	0.0017	31	0.0023	20	0.0026	42	0.0032	50	0.0033	41	0.0060	22
110	daon-000	0.0095	253	0.0117	226	0.0068	225	0.0077	196	0.0092	185	0.0174	146
111	decatur-000	0.0714	391	0.1115	388	0.0608	386	0.1106	388	0.0866	370	1.0000	441
112	decatur-001	0.0424	374	0.0711	378	0.0237	352	0.0458	355	0.0447	348	1.0000	435
113	deepglint-004	0.0025	61	0.0034	50	0.0039	138	0.0061	162	0.0050	102	0.0091	69
114	deepglint-005	0.0052	146	0.0059	127	0.0030	76	0.0031	46	0.0033	46	0.7620	371
115	deepsea-001	0.0136	303	0.0215	304	0.0142	324	0.0214	321	0.0163	264	0.0250	183
116	deepsense-000	0.0145	310	0.0265	329	0.0113	307	0.0196	314	0.0151	253	0.0215	170
117	deepsense-001	0.0013	19	0.0019	12	0.0024	21	0.0025	18	0.0027	21	0.0115	98
118	dermalog-009	0.0067	197	0.0094	190	0.0051	184	0.0069	177	0.0116	223	0.0312	206
119	dermalog-010	0.0030	77	0.0041	69	0.0034	113	0.0037	79	0.0075	146	0.5181	344
120	dicio-001	0.5486	445	0.6442	440	0.7516	438	0.8607	436	0.8678	435	0.8268	381
121	didiglobalface-001	0.0055	161	0.0092	188	0.0030	78	0.0045	109	0.0088	173	0.0119	102
122	digitida-000	0.0967	398	0.1410	394	0.2596	409	0.3462	407	0.0293	324	0.0363	226
123	digitida-001	0.0224	348	0.0352	347	0.0330	367	0.0570	367	0.0109	213	0.0481	245
124	digitalbarriers-002	0.3360	425	0.3690	417	0.0877	394	0.1557	394	0.0971	376	0.0951	276
125	dps-000	0.0115	277	0.0176	279	0.0149	334	0.0185	309	0.0173	276	0.0275	194
126	dsk-000	0.1526	407	0.2169	405	0.3787	414	0.5426	417	0.3115	403	0.3089	321
127	einetworks-000	0.0099	256	0.0180	282	0.0088	274	0.0140	276	0.0130	233	0.0225	175
128	ekin-002	0.1168	401	0.2042	402	0.1530	404	0.2524	403	0.1777	391	0.2773	318
129	enface-000	0.0028	71	0.0049	100	0.0043	153	0.0072	180	0.0058	122	0.0150	119
130	enface-001	0.0072	214	0.0107	212	0.0071	232	0.0138	272	0.0068	138	0.0151	248
131	eocortex-000	0.3485	426	0.6943	446	0.1122	396	0.1574	395	0.2155	398	0.2257	311
132	ercacat-001	0.0036	104	0.0044	84	0.0033	102	0.0047	117	0.0106	208	0.0202	164

Table 21: FNMR is the proportion of mated comparisons below a threshold set to achieve the FMR given in the header on the fourth row. FMR is the proportion of impostor comparisons at or above that threshold. The light grey values give rank over all algorithms in that column. The pink columns use only same-sex impostors; others are selected regardless of demographics. The exception, in the green column, uses “matched-covariates” i.e. impostors of the same sex, age group, and country of birth. The second pink column includes effects of extended ageing. Missing entries for border, visa, mugshot and wild images generally mean the algorithm did not run to completion. The VISA columns compare images described in section 2.1. The MUGSHOT columns compare images described in section 2.4. The VISA-BORDER column compare images described in section 2.2 with those of section 2.3. The BORDER column compares images described in section 2.3. The WILD columns compare images described in section 2.6.

Algorithm	FALSE NON-MATCH RATE (FNMR)									
	CONSTRAINED, COOPERATIVE								LESS CONSTRAINED, NON-COOP.	
	Name	VISAMC	VISA	MUGSHOT	MUGSHOT12+YRS	VISABORDER	BORDER	BORDER	WILD	
FMR	0.0001	1E-06	1E-05	1E-05	1E-06	1E-06	1E-06	1E-05	0.0001	
133	euronovate-001	0.2786	419	0.3608	416	0.4489	420	0.6105	421	0.5010
134	expasoft-001	0.0328	367	0.0488	359	0.0211	346	0.0342	345	0.0629
135	expasoft-002	0.0170	330	0.0274	331	0.0787	393	0.0768	375	0.1629
136	f8-001	0.0249	352	0.0336	342	0.0178	339	0.0232	325	0.0303
137	f8-002	0.0340	369	0.0591	374	0.0213	348	0.0374	348	0.0452
138	faceonline-001	0.0269	356	0.0359	349	0.0387	372	0.0721	374	0.0246
139	faceonline-002	0.0121	286	0.0135	243	0.0033	104	0.0041	94	0.0037
140	facephi-000	0.0044	127	0.0059	124	0.0047	168	0.0057	149	0.0088
141	facesoft-000	0.0085	237	0.0112	221	0.0064	218	0.0107	236	0.0091
142	facetag-000	0.2836	420	0.4081	422	0.2933	411	0.4303	411	0.3448
143	facetag-002	0.0098	255	0.0147	254	0.0064	219	0.0110	238	0.0116
144	facex-001	1.0000	461	1.0000	461	1.0000	456	-	1.0000	454
145	facex-002	0.0803	393	0.1404	393	0.1283	399	0.1979	400	0.1440
146	farfaces-001	0.4890	439	0.5860	438	0.5650	426	0.7268	428	0.8015
147	fiberhome-nanjing-003	0.0090	240	0.0139	246	0.0082	259	0.0144	280	0.0110
148	fiberhome-nanjing-004	0.0037	110	0.0056	120	0.0031	87	0.0043	102	0.0043
149	fincore-000	0.0309	365	0.0502	361	0.0281	359	0.0510	362	0.0521
150	firstcreditKZ-001	0.0024	57	0.0034	47	0.0024	25	0.0024	14	0.0034
151	frpkauai-001	0.0023	54	0.0035	55	0.0026	36	0.0030	42	0.0040
152	fujitsulab-002	0.0091	245	0.0124	234	0.0105	293	0.0156	289	0.0169
153	fujitsulab-003	0.0045	128	0.0065	135	0.0057	204	0.0083	207	0.0080
154	g42-intelibrain-001	0.0006	2	0.0009	3	0.0037	124	0.0044	106	0.0030
155	geo-002	0.0171	332	0.0187	288	0.0035	116	0.0051	130	0.0064
156	geo-004	0.0030	76	0.0041	66	0.0025	33	0.0030	39	0.0035
157	glory-004	0.0077	222	0.0123	231	0.0074	243	0.0098	230	0.0122
158	glory-005	0.0056	162	0.0076	155	0.0054	196	0.0072	183	0.0075
159	gorilla-007	0.0074	216	0.0111	220	0.0065	221	0.0126	255	0.0100
160	gorilla-008	0.0058	170	0.0091	186	0.0049	174	0.0079	203	0.0079
161	graymatics-001	0.1039	399	0.1620	397	0.1344	401	0.1917	398	0.1648
162	griaule-000	0.0071	208	0.0099	201	0.0050	178	0.0072	179	0.0160
163	griaule-001	0.0057	164	0.0078	162	0.0045	162	0.0065	172	0.0070
164	hertasecurity-001	0.0249	351	0.0309	338	0.0105	294	0.0161	292	0.0245
165	hertasecurity-002	0.0206	344	0.0315	339	0.0060	210	0.0078	199	0.0253
166	hik-001	0.0096	254	0.0125	235	0.0093	283	0.0164	297	0.0108
167	hisign-001	0.0036	107	0.0050	102	0.0034	108	0.0046	112	0.0079
168	hisign-002	0.0029	72	0.0044	85	0.0027	57	0.0032	52	0.0028
169	hyperverge-002	0.0050	138	0.0066	137	0.0035	115	0.0051	127	0.0062
170	hyperverge-003	0.0019	39	0.0030	41	0.0025	28	0.0029	37	0.0027
171	hzailiu-002	0.0051	142	0.0072	147	0.0038	133	0.0055	142	0.0040
172	hzailiu-003	0.0178	335	0.0291	336	0.0031	93	0.0042	100	0.0035
173	icm-003	0.0138	305	0.0222	309	0.0149	333	0.0282	336	0.0227
174	icm-004	0.0079	226	0.0120	228	0.0074	241	0.0107	235	0.0091
175	ichttc-000	0.0260	354	0.0396	354	0.0207	345	0.0339	344	0.0291
176	id3-006	0.0072	212	0.0103	207	0.0049	176	0.0074	188	0.0095

Table 22: FNMR is the proportion of mated comparisons below a threshold set to achieve the FMR given in the header on the fourth row. FMR is the proportion of impostor comparisons at or above that threshold. The light grey values give rank over all algorithms in that column. The pink columns use only same-sex impostors; others are selected regardless of demographics. The exception, in the green column, uses “matched-covariates” i.e. impostors of the same sex, age group, and country of birth. The second pink column includes effects of extended ageing. Missing entries for border, visa, mugshot and wild images generally mean the algorithm did not run to completion. The VISA columns compare images described in section 2.1. The MUGSHOT columns compare images described in section 2.4. The VISA-BORDER column compare images described in section 2.2 with those of section 2.3. The BORDER column compares images described in section 2.3. The WILD columns compare images described in section 2.6.

Algorithm	Name	FALSE NON-MATCH RATE (FNMR)										LESS CONSTRAINED, NON-COOP.					
		CONSTRAINED, COOPERATIVE								WILD							
		VISAMC	VISA	MUGSHOT	MUGSHOT12+YRS	VISA BORDER	BORDER	BORDER	1E-06	1E-05	0.0001						
FMR		0.0001	1E-06	1E-05	1E-05	1E-06			1E-06	1E-05	0.0001						
177	id3-008	0.0039	115	0.0055	117	0.0032	97	0.0042	98	0.0081	160	0.0155	128	0.0134	176	0.8856	443
178	idemia-008	0.0023	53	0.0032	44	0.0023	12	0.0028	28	0.0034	49	0.0067	31	0.0056	40	0.0290	153
179	idemia-009	0.0022	49	0.0030	42	0.0022	5	0.0023	12	0.0023	9	0.0046	6	0.0039	8	0.0285	112
180	iit-002	0.0111	274	0.0177	281	0.0085	266	0.0140	275	0.0193	289	0.0332	215	0.0260	263	0.1373	379
181	iit-003	0.0082	233	0.0151	259	0.0053	190	0.0084	210	0.0122	227	0.0199	162	0.0137	180	0.0407	286
182	imds-software-001	0.0126	297	0.0228	310	0.0130	320	0.0221	323	0.0231	302	0.0469	243	0.0199	242	0.0365	271
183	imperial-000	0.0067	196	0.0108	217	0.0080	254	0.0134	269	0.0087	171	0.0581	252	0.0102	133	0.0281	80
184	imperial-002	0.0058	175	0.0081	170	0.0055	198	0.0085	213	0.0083	164	0.0157	129	0.0103	134	0.0273	17
185	incode-010	0.0041	121	0.0063	132	0.0028	68	0.0043	101	0.0047	96	0.0077	48	0.0061	53	0.0296	178
186	incode-011	0.0032	83	0.0044	83	0.0026	44	0.0034	63	0.0032	38	0.0359	224	0.0140	185	0.0295	173
187	infocert-001	0.0105	265	0.0172	275	0.0078	249	0.0125	252	0.0159	257	0.1573	294	0.0565	312	0.0307	203
188	innefulabs-000	0.0122	288	0.0199	295	0.0112	306	0.0197	315	0.0222	298	0.0372	229	0.0271	267	0.0348	254
189	innovativetechnologyltd-001	0.0578	386	0.0938	386	0.0501	378	0.0981	381	0.0592	357	0.0779	268	0.0422	293	0.0449	305
190	innovativetechnologyltd-002	0.0451	376	0.0716	379	0.0541	381	0.1009	383	0.0506	353	0.0682	261	0.0371	287	0.0804	355
191	innovatrics-007	0.0040	119	0.0054	114	0.0057	203	0.0078	197	0.0079	152	0.0123	103	0.0088	111	0.0282	94
192	innovatrics-008	0.0047	132	0.0064	133	0.0038	131	0.0052	131	0.0053	109	0.0088	66	0.0069	72	0.0287	126
193	insightface-001	0.0009	4	0.0014	4	0.0027	49	0.0024	13	0.0035	54	0.0070	35	0.0065	61	0.0279	61
194	insightface-003	0.0015	24	0.0021	17	0.0045	161	0.0034	64	0.1298	380	1.0000	455	0.9407	424	0.0277	39
195	inspur-000	0.0060	182	0.0078	160	0.7415	437	0.9093	445	0.2838	402	0.9996	426	0.9976	440	0.0283	99
196	intellicloudai-001	0.0142	308	0.0234	314	0.0092	280	0.0145	281	0.0162	262	0.0371	228	0.0171	215	0.0409	289
197	intellicloudai-002	0.0059	178	0.0085	175	0.0060	211	0.0069	178	0.0108	210	0.2477	315	0.0171	214	0.0303	193
198	intellifusion-001	0.0072	211	0.0094	192	0.0056	202	0.0085	214	0.0111	217	0.0212	168	0.0143	190	0.0289	143
199	intellifusion-002	0.0059	176	0.0077	157	0.0040	143	0.0074	187	0.0085	168	0.5352	345	0.0104	139	0.0305	197
200	intellivision-003	0.1177	402	0.2006	401	0.0760	391	0.1244	392	0.1069	379	0.1431	293	0.0839	328	0.0829	359
201	intellivision-004	0.0271	357	0.0559	370	0.0294	364	0.0503	361	0.0327	331	0.0461	241	0.0293	275	0.0645	335
202	intellivix-001	0.0064	192	0.0087	179	0.0046	164	0.0063	166	0.0072	142	0.9233	392	0.7856	411	0.0340	247
203	intellivix-002	0.0062	187	0.0085	176	0.0039	136	0.0056	144	0.0060	127	0.3464	325	0.0857	331	0.0289	144
204	intelresearch-004	0.0025	62	0.0035	52	0.0032	95	0.0038	83	0.0049	101	0.0094	72	0.0072	75	0.0290	155
205	intelresearch-005	0.0016	27	0.0023	21	0.0028	61	0.0034	61	0.0042	83	0.0084	58	0.0066	65	0.0290	152
206	intema-000	0.0012	12	0.0017	8	0.0023	6	0.0022	8	0.0022	8	0.0172	143	0.0061	52	0.0279	60
207	intsysmsu-001	0.9543	460	0.9888	458	0.9923	452	-	0.9977	447	0.9955	416	0.9892	432	0.7871	443	
208	intsysmsu-002	0.0130	299	0.0254	323	0.0137	322	0.0267	334	0.0160	259	0.0267	190	0.0145	193	0.0289	146
209	ionetworks-000	0.0060	183	0.0087	177	0.0044	155	0.0058	154	0.0080	159	0.0144	115	0.0112	148	0.0319	224
210	iqface-000	0.0091	244	0.0143	247	0.0075	244	0.0110	239	0.0171	275	0.2234	309	0.0359	283	0.0381	276
211	iqface-003	0.0058	174	0.0079	165	0.0051	183	0.0058	155	0.0104	206	0.0200	163	0.0193	236	0.0402	281
212	irex-000	0.0052	145	0.0099	202	0.0056	201	0.0083	208	0.0137	242	0.0163	136	0.0078	87	0.0285	115
213	isap-001	0.5092	441	0.6588	442	0.6899	433	0.7978	431	0.7200	420	0.7253	363	0.5373	391	0.1931	394
214	isap-002	0.0114	276	0.0186	286	0.0087	272	0.0151	287	0.0156	256	0.5134	342	0.0333	276	0.0354	264
215	isityou-000	0.5682	447	0.7033	448	1.0000	459	-	1.0000	457	1.0000	460	1.0000	453	1.0000	456	
216	isystems-001	0.0149	315	0.0245	319	0.0138	323	0.0210	319	0.0209	295	0.0332	214	0.0223	252	0.0524	321
217	isystems-002	0.0118	279	0.0182	284	0.0111	303	0.0162	295	0.0166	267	0.0284	200	0.0195	238	0.0516	315
218	itmo-007	0.0080	228	0.0125	236	0.0107	296	0.0185	307	0.0167	269	0.0222	173	0.0144	192	0.0300	186
219	itmo-008	0.0090	241	0.0150	257	0.0058	206	0.0059	157	0.0187	284	0.0355	223	0.0339	277	0.1498	382
220	ivacognitive-001	0.0189	338	0.0351	346	0.0123	316	0.0235	326	0.0198	291	0.0274	193	0.0155	203	0.0296	175

Table 23: FNMR is the proportion of mated comparisons below a threshold set to achieve the FMR given in the header on the fourth row. FMR is the proportion of impostor comparisons at or above that threshold. The light grey values give rank over all algorithms in that column. The pink columns use only same-sex impostors; others are selected regardless of demographics. The exception, in the green column, uses “matched-covariates” i.e. impostors of the same sex, age group, and country of birth. The second pink column includes effects of extended ageing. Missing entries for border, visa, mugshot and wild images generally mean the algorithm did not run to completion. The VISA columns compare images described in section 2.1. The MUGSHOT columns compare images described in section 2.4. The VISA-BORDER column compare images described in section 2.2 with those of section 2.3. The BORDER column compares images described in section 2.3. The WILD columns compare images described in section 2.6.

	Algorithm	FALSE NON-MATCH RATE (FNMR)										WILD							
		CONSTRAINED, COOPERATIVE								LESS CONSTRAINED, NON-COOP.									
		Name	VISAMC	VISA	MUGSHOT	MUGSHOT12+YRS	VISABORDER	BORDER	BORDER										
	FMR	0.0001	1E-06	1E-05	1E-05	1E-05	1E-06	1E-06	1E-05		0.0001								
221	iws-000	0.4824	437	0.5801	435	0.6859	432	0.8155	432	0.8251	428	0.7756	373	0.6400	400	0.3251	418		
222	jaakit-001	0.5830	448	0.7146	449	0.8173	444	0.8893	442	0.8950	438	0.8387	384	0.7091	406	0.5849	435		
223	kakao-007	0.0019	41	0.0028	37	0.0024	15	0.0026	22	0.0033	43	0.0061	23	0.0053	31	0.0427	295		
224	kakao-008	0.0011	10	0.0018	11	0.0023	7	0.0023	10	0.0021	7	0.0041	4	0.0035	3	0.0427	296		
225	kakaopay-001	0.0152	317	0.0252	322	0.0145	326	0.0270	335	0.0232	303	0.0344	220	0.0194	237	0.0416	292		
226	kasikornlabs-000	0.0112	275	0.0184	285	0.0086	268	0.0137	271	0.0130	235	0.0225	174	0.0148	198	0.0674	337		
227	kasikornlabs-001	0.0138	306	0.0206	297	0.0087	271	0.0139	274	0.0142	245	0.0236	178	0.0171	213	0.0729	346		
228	kedacom-000	0.0055	159	0.0081	171	0.0111	305	0.0120	246	0.0415	342	0.0966	278	0.0686	320	0.2511	407		
229	kiwitech-000	0.0076	220	0.0105	210	0.0081	258	0.0128	261	0.0096	194	0.0163	135	0.0101	130	0.0279	63		
230	kneron-003	0.0542	385	0.0902	384	0.0346	370	0.0562	365	0.0919	373	0.1251	288	0.0973	336	0.3053	415		
231	kneron-005	0.0157	320	0.0259	325	0.0126	319	0.0212	320	0.0406	341	0.0693	264	0.0542	310	0.0471	308		
232	knowutech-000	0.0039	116	0.0055	118	0.0028	70	0.0042	97	0.0042	80	0.0077	46	0.0059	49	0.0271	9		
233	kookmin-002	0.0054	156	0.0077	159	0.0043	152	0.0065	171	0.0123	229	0.7591	370	0.0198	241	0.0285	117		
234	krungthai-002	0.0105	267	0.0161	264	0.0091	277	0.0141	277	0.7350	422	0.9889	411	0.9605	427	0.0620	331		
235	kuke3d-001	0.0058	169	0.0104	208	0.0083	261	0.0093	222	0.0270	319	0.9901	412	0.8341	417	0.0404	282		
236	kuke3d-002	0.0077	223	0.0135	242	0.0069	229	0.0098	229	0.0111	216	1.0000	445	1.0000	451	0.0316	220		
237	lebentech-000	0.5940	449	0.7032	447	0.8854	448	0.9511	447	0.9089	440	0.9970	417	0.9861	431	0.6250	436		
238	lemalabs-001	0.0111	272	0.0175	278	0.0088	273	0.0142	278	0.0143	247	0.0228	176	0.0140	184	0.0281	77		
239	lineclova-001	0.0025	60	0.0040	64	0.0026	48	0.0034	65	0.0045	90	0.4127	334	0.0080	93	0.0283	101		
240	lineclova-002	0.0021	44	0.0035	54	0.0025	26	0.0027	26	0.0041	77	0.0086	62	0.0072	76	0.0279	53		
241	lookman-002	0.0297	362	0.0547	369	0.0339	368	0.0562	364	0.0614	359	0.0960	277	0.0790	326	0.2640	412		
242	lookman-004	0.0074	217	0.0099	200	0.0124	318	0.0149	285	0.0430	345	0.0866	271	0.0694	321	0.2516	408		
243	luxand-000	0.2056	411	0.2814	410	0.4053	416	0.5365	416	0.3497	406	0.3743	329	0.2605	362	0.2222	401		
244	mantra-000	0.0037	109	0.0052	111	0.0054	193	0.0056	146	0.0097	197	0.0181	151	0.0151	201	0.0350	257		
245	maxvision-001	0.0305	364	0.0528	367	0.1028	395	0.1921	399	0.0650	362	0.3001	320	0.1553	351	0.0539	322		
246	maxvision-002	0.0070	203	0.0107	214	0.0061	212	0.0093	221	0.0080	156	0.5726	348	0.2943	369	0.0372	273		
247	megvii-005	0.0010	7	0.0015	5	0.0026	41	0.0031	49	0.0019	4	0.0500	247	0.0057	41	0.0292	161		
248	megvii-006	0.0011	8	0.0016	6	0.0026	45	0.0033	57	0.0025	14	0.0050	10	0.0048	20	0.0296	176		
249	meituau-001	0.0164	325	0.1886	399	0.0025	29	0.0026	21	0.0030	31	0.0074	41	0.0051	23	0.1157	375		
250	meituau-002	0.0017	32	0.0025	26	0.0024	18	0.0023	9	0.0024	13	0.0067	33	0.0044	16	0.0312	214		
251	meiya-001	0.0171	331	0.0275	332	0.0159	336	0.0261	333	0.0311	328	0.2250	310	0.0245	259	0.0363	270		
252	mendaxiatech-000	0.0027	66	0.0036	56	0.0029	72	0.0036	75	0.0031	36	0.0057	18	0.0051	24	0.0275	25		
253	metsakuurcompany-001	0.0068	199	0.0087	181	0.0068	227	0.0078	198	0.0095	191	0.8972	389	0.5635	392	0.0351	259		
254	metsakuurcompany-002	0.0048	134	0.0071	143	0.0030	81	0.0043	104	0.0032	40	0.2059	307	0.0665	319	0.0408	287		
255	microfocus-001	0.4482	434	0.5524	434	0.7256	436	0.8416	435	0.7301	421	0.6926	361	0.5180	390	0.2567	411		
256	microfocus-002	0.3605	427	0.5057	429	0.5783	428	0.7223	427	0.5909	416	0.5963	351	0.4160	384	0.1582	384		
257	minivision-000	0.0033	87	0.0048	97	0.0038	130	0.0049	121	0.0055	113	0.0094	75	0.0079	91	0.0273	14		
258	mobai-000	0.0360	371	0.0439	358	0.0372	371	0.0700	372	0.0367	336	0.0939	274	0.0795	327	0.2640	413		
259	mobai-001	0.0199	343	0.0219	306	0.0047	169	0.0061	159	0.0093	188	0.0174	145	0.0138	183	0.1045	370		
260	mobbl-001	0.3208	421	0.4375	423	0.5680	427	0.7193	426	0.6282	417	0.5783	349	0.3984	382	0.1866	393		
261	mobbl-003	0.0087	238	0.0134	241	0.0062	214	0.0087	216	0.0099	200	0.0197	159	0.0122	167	0.0312	212		
262	mobilipintech-000	0.0090	242	0.0149	255	0.0039	142	0.0057	147	0.0115	221	0.0465	242	0.0182	225	0.0315	219		
263	moreedian-000	0.3874	428	0.4912	428	0.9988	454	-				0.9990	449	0.9999	432	0.9998	445	0.4788	428
264	mukh-001	0.0170	329	0.0285	334	0.0225	350	0.0405	351	0.0272	320	0.0950	275	0.0291	274	0.0301	188		

Table 24: FNMR is the proportion of mated comparisons below a threshold set to achieve the FMR given in the header on the fourth row. FMR is the proportion of impostor comparisons at or above that threshold. The light grey values give rank over all algorithms in that column. The pink columns use only same-sex impostors; others are selected regardless of demographics. The exception, in the green column, uses “matched-covariates” i.e. impostors of the same sex, age group, and country of birth. The second pink column includes effects of extended ageing. Missing entries for border, visa, mugshot and wild images generally mean the algorithm did not run to completion. The VISA columns compare images described in section 2.1. The MUGSHOT columns compare images described in section 2.4. The VISA-BORDER column compare images described in section 2.2 with those of section 2.3. The BORDER column compares images described in section 2.3. The WILD columns compare images described in section 2.6.

	Algorithm	FALSE NON-MATCH RATE (FNMR)										LESS CONSTRAINED, NON-COOP.					
		CONSTRAINED, COOPERATIVE															
		Name	VISAMC	VISA	MUGSHOT	MUGSHOT12+YRS	VISABORDER	BORDER	BORDER	WILD							
	FMR	0.0001	1E-06	1E-05	1E-05	1E-06	1E-06	1E-06	1E-05	0.0001							
265	multimodality-000	0.0034	96	0.0047	94	0.0036	122	0.0044	107	0.0077	150	0.9976	419	0.4456	386	0.0287	127
266	multimodality-001	0.0029	74	0.0042	75	0.0031	85	0.0035	67	0.0038	63	0.0071	37	0.0059	48	0.0281	79
267	mvision-001	0.0191	339	0.0233	312	0.0204	344	0.0356	346	0.0198	292	0.0337	217	0.0242	258	0.0431	297
268	nazhai-000	0.0040	117	0.0059	126	0.0036	118	0.0048	119	0.0057	118	0.0125	106	0.0083	100	0.0275	28
269	neosystems-004	0.0279	359	0.0495	360	0.0289	361	0.0585	369	0.0439	347	0.9621	401	0.1296	341	0.0333	240
271	netbridge-tech-001	0.4749	435	0.6599	443	0.4438	419	0.5676	418	0.4491	412	1.0000	437	0.9541	426	0.1098	374
272	netbridge-tech-002	0.0101	260	0.0166	271	0.0077	247	0.0127	258	0.0133	238	0.8215	379	0.0523	308	0.0351	260
273	neurotechnology-013	0.0032	86	0.0045	89	0.0026	47	0.0036	71	0.0037	61	0.0068	34	0.0052	29	0.0278	47
274	neurotechnology-015	0.0022	50	0.0036	57	0.0024	14	0.0028	31	0.0030	29	0.0052	12	0.0041	11	0.0276	33
275	nhn-002	0.0068	200	0.0096	195	0.0057	205	0.0087	218	0.0136	241	0.0253	185	0.0186	232	0.0302	190
276	nhn-003	0.0033	89	0.0048	98	0.0027	54	0.0038	82	0.0036	59	0.0198	160	0.0071	74	0.0285	120
277	nodeflux-002	0.0186	337	0.0340	343	0.0261	357	0.0451	354	0.0548	355	1.0000	442	1.0000	449	0.0299	182
278	notiontag-001	0.6846	453	0.8006	453	0.3955	415	0.5247	414	0.8669	433	0.8313	383	0.6362	399	0.2221	400
279	notiontag-002	0.0066	195	0.0089	183	0.0045	159	0.0061	160	0.0077	151	0.0137	111	0.0104	137	0.0299	181
280	nsensecorp-003	0.0251	353	0.0295	337	0.0212	347	0.0305	339	0.0131	236	0.2139	308	0.0141	188	0.0872	362
281	nsensecorp-004	0.1370	406	0.1397	392	0.0066	223	0.0094	224	1.0000	456	1.0000	459	1.0000	458	0.0805	356
282	ntechlab-011	0.0012	14	0.0019	13	0.0024	19	0.0028	35	0.0029	27	0.0055	14	0.0047	19	0.0288	136
283	ntechlab-012	0.0011	9	0.0016	7	0.0023	13	0.0030	40	0.0026	16	0.0050	11	0.0043	13	0.0280	73
284	omface-000	0.2573	417	0.3835	420	0.3590	413	0.4903	413	0.3956	411	0.5003	341	0.2595	361	0.2400	404
285	omface-001	0.0137	304	0.0212	302	0.0114	311	0.0187	310	0.0174	278	1.0000	450	0.0214	249	0.0789	352
286	omnigarde-001	0.0168	327	0.0260	326	0.0203	343	0.0402	349	0.0243	311	0.0327	211	0.0177	218	0.0288	134
287	omnigarde-002	0.0033	94	0.0046	91	0.0027	59	0.0039	85	0.0041	78	0.0076	44	0.0059	51	0.0278	51
288	openface-001	0.1804	408	0.2921	411	0.2878	410	0.3906	410	0.2054	396	0.2338	313	0.1549	350	0.2445	405
289	oz-003	0.0095	252	0.0143	248	0.0054	194	0.0077	195	0.0096	195	0.0175	148	0.0118	161	0.0288	139
290	oz-004	0.0033	95	0.0049	101	0.0038	132	0.0055	139	0.0081	161	0.0163	137	0.0142	189	0.0329	235
291	palit-000	0.0062	186	0.0084	174	0.0039	135	0.0055	138	0.0055	114	0.4610	338	0.2468	359	0.0280	71
292	palit-001	0.0050	137	0.0068	141	0.0032	100	0.0047	118	0.0045	89	0.0110	90	0.0058	46	0.0287	129
293	pangiam-000	0.0031	80	0.0043	81	0.0026	37	0.0030	44	0.0038	64	0.0071	38	0.0061	56	0.0424	294
294	papago-001	0.0067	198	0.0096	197	0.0051	185	0.0077	194	0.0071	140	0.0126	107	0.0086	108	0.0816	358
295	papsav1923-001	0.0078	224	0.0130	238	0.0068	226	0.0105	234	0.0119	224	0.0221	172	0.0136	178	0.0293	164
296	papsav1923-002	0.0021	47	0.0034	49	0.0026	38	0.0030	43	0.0048	97	0.0093	71	0.0086	106	0.0312	213
297	paravision-008	0.0018	37	0.0025	28	0.0024	17	0.0025	17	0.0036	58	0.0070	36	0.0063	59	0.0279	58
298	paravision-010	0.0012	17	0.0021	16	0.0022	4	0.0021	5	0.0027	20	0.0055	15	0.0050	22	0.0288	140
299	pensees-001	0.0087	239	0.0133	240	0.0071	234	0.0122	250	0.0145	250	0.0252	184	0.0195	239	0.0283	98
300	pixelall-008	0.0015	22	0.0023	23	0.0034	114	0.0049	120	0.0031	35	0.0057	17	0.0052	25	0.0278	44
301	pixelall-009	0.0018	35	0.0025	29	0.0024	22	0.0026	23	0.0031	37	0.3475	326	0.0053	32	0.0276	31
302	psl-010	0.0017	34	0.0035	51	0.0023	8	0.0025	15	0.0035	53	0.0104	82	0.0052	28	0.0282	84
303	psl-011	0.0013	18	0.0026	33	0.0021	1	0.0021	4	0.0024	11	0.0047	7	0.0035	4	0.0285	116
304	ptakuratsatu-000	0.0060	181	0.0089	184	0.0070	231	0.0104	233	0.0096	196	0.0152	124	0.0100	127	0.0284	104
305	pxl-001	0.0488	379	0.0752	381	0.0586	384	0.1087	384	0.0946	374	0.1065	281	0.0625	317	0.1088	372
306	pyramid-000	0.0136	301	0.0233	313	0.0117	313	0.0192	312	0.0185	283	0.0322	210	0.0206	245	0.0304	196
307	qazbs-000	0.0058	167	0.0083	172	0.0046	165	0.0072	181	0.0130	234	0.0244	181	0.0196	240	0.0297	180
308	qnap-001	0.0148	312	0.0215	303	0.0103	289	0.0162	294	0.0183	282	0.0301	202	0.0186	231	0.0360	269

Table 25: FNMR is the proportion of mated comparisons below a threshold set to achieve the FMR given in the header on the fourth row. FMR is the proportion of impostor comparisons at or above that threshold. The light grey values give rank over all algorithms in that column. The pink columns use only same-sex impostors; others are selected regardless of demographics. The exception, in the green column, uses “matched-covariates” i.e. impostors of the same sex, age group, and country of birth. The second pink column includes effects of extended ageing. Missing entries for border, visa, mugshot and wild images generally mean the algorithm did not run to completion. The VISA columns compare images described in section 2.1. The MUGSHOT columns compare images described in section 2.4. The VISA-BORDER column compare images described in section 2.2 with those of section 2.3. The BORDER column compares images described in section 2.3. The WILD columns compare images described in section 2.6.

Algorithm	FALSE NON-MATCH RATE (FNMR)																
	CONSTRAINED, COOPERATIVE								LESS CONSTRAINED, NON-COOP.								
	Name	VISAMC	VISA	MUGSHOT	MUGSHOT12+YRS	VISABORDER	BORDER	BORDER	WILD								
FMR	0.0001	1E-06	1E-05	1E-05	1E-06	1E-06	1E-05	1E-05	0.0001								
309	qnap-002	0.0122	287	0.0191	290	0.0075	245	0.0095	227	0.0146	251	0.0281	199	0.0184	227	0.0352	262
310	quantasoft-003	0.0081	231	0.0113	223	0.0056	200	0.0076	191	0.0091	183	0.0161	134	0.0107	144	0.0414	291
311	rankone-012	0.0043	125	0.0058	121	0.0031	94	0.0038	81	0.0047	94	0.0081	54	0.0065	62	0.0358	266
312	rankone-013	0.0028	68	0.0041	68	0.0026	39	0.0033	55	0.0028	24	0.0055	16	0.0040	9	0.0291	159
313	realnetworks-006	0.0040	118	0.0056	119	0.8657	447	-		0.0059	123	0.0112	92	0.0085	104	0.1790	392
314	realnetworks-007	0.0031	81	0.0051	106	0.0028	66	0.0035	68	0.0048	98	0.0091	68	0.0074	82	0.0279	54
315	regula-000	0.0184	336	0.0376	352	0.0103	290	0.0185	306	0.0120	225	0.9983	421	0.0231	254	0.0273	16
316	regula-001	0.0072	213	0.0107	216	0.0102	287	0.0179	304	0.0123	230	0.0333	216	0.0174	216	0.0295	168
317	remarkai-001	0.0144	309	0.0256	324	0.0102	286	0.0159	291	0.0162	263	0.0582	253	0.0185	229	0.0308	206
318	remarkai-003	0.0047	133	0.0063	131	0.0033	105	0.0049	122	0.0054	110	0.0100	80	0.0072	78	0.0275	29
319	rendip-000	0.0055	160	0.0077	158	0.0048	172	0.0060	158	0.0080	157	0.0142	114	0.0110	147	0.0433	299
320	revealmedia-005	0.0050	141	0.0074	153	0.0050	179	0.0068	176	0.0075	148	0.0124	104	0.0104	140	0.3960	423
321	revealmedia-006	0.0040	120	0.0067	138	0.0041	148	0.0056	143	0.0056	115	0.0085	61	0.0068	69	0.0278	50
322	rokid-000	0.0093	249	0.0145	250	0.0073	240	0.0102	232	0.0164	265	0.0280	196	0.0214	248	0.0857	361
323	rokid-001	0.0105	266	0.0162	265	0.0094	285	0.0163	296	0.0181	279	0.0276	195	0.0165	210	0.0325	230
324	s1-005	0.0024	59	0.0036	58	0.0025	35	0.0029	38	0.0026	17	0.0048	8	0.0038	7	0.0359	268
325	s1-006	0.0029	73	0.0044	82	0.0028	62	0.0033	53	0.0035	51	0.0073	39	0.0044	15	0.0367	272
326	saffe-001	0.4339	432	0.5261	431	0.7539	440	0.8736	441	0.7977	425	0.9810	405	0.7435	409	0.3887	422
327	saffe-002	0.0119	284	0.0206	296	0.0107	299	0.0177	302	0.0244	312	0.9998	431	0.2785	366	0.0308	205
328	samsungsds-001	0.0015	26	0.0026	31	0.0023	11	0.0023	11	0.0024	12	0.1660	296	0.0536	309	0.0282	83
329	samsungsds-002	0.0017	33	0.0027	34	0.0023	9	0.0022	6	0.0021	6	0.0043	5	0.0036	6	0.0283	96
330	samttech-001	0.0197	341	0.0365	350	0.0146	330	0.0241	328	0.0238	310	0.0394	232	0.0251	260	0.0337	241
331	scanovate-002	0.0175	334	0.0355	348	0.0146	328	0.0286	337	0.0269	318	0.0301	201	0.0178	221	0.0301	189
332	scanovate-003	0.0054	155	0.0080	169	0.0054	191	0.0072	185	0.0312	329	0.0599	254	0.0568	313	0.0283	97
333	sdc-000	0.0303	363	0.0526	365	0.0572	383	0.1094	386	0.0867	371	0.6230	352	0.3682	378	0.1201	378
334	securifai-004	0.0136	300	0.0192	291	0.0064	217	0.0099	231	0.0115	220	0.0272	191	0.0127	170	0.0347	250
335	securifai-005	0.0125	292	0.0190	289	0.0080	255	0.0126	256	0.0134	239	0.9861	408	0.9205	422	0.0329	234
336	sensetime-006	0.0014	20	0.0024	25	0.0021	2	0.0020	2	0.0021	5	0.0040	3	0.0036	5	0.0272	12
337	sensetime-007	0.0012	16	0.0022	18	0.0021	3	0.0020	3	0.0018	3	0.0034	2	0.0029	1	0.0280	66
338	sertis-000	0.0118	280	0.0208	299	0.0080	252	0.0127	257	0.0110	215	0.0176	149	0.0114	153	0.0285	118
339	sertis-002	0.0049	136	0.0061	128	0.0039	141	0.0061	163	0.0055	112	0.0099	79	0.0070	73	0.0281	78
340	seventhsense-001	0.0034	99	0.0047	95	0.0025	34	0.0031	48	0.0029	26	0.0338	218	0.0109	146	0.0279	56
341	seventhsense-002	0.0036	105	0.0050	103	0.0028	65	0.0036	72	0.0035	52	0.0811	269	0.0183	226	0.0278	48
342	shaman-000	0.9297	459	0.9774	457	0.9990	455	-		0.9999	450	1.0000	440	0.9999	447	0.9575	449
343	shaman-001	0.3346	424	0.4616	424	0.2368	407	0.3723	409	0.3574	408	0.3527	327	0.2304	358	0.1498	383
344	shu-002	-	0.0079	166	0.0146	329	0.0308	340	1.0000	451	0.0183	152	0.0115	155	0.0284	105	
345	shu-003	0.0028	69	0.0041	73	0.0050	177	0.0088	219	0.0081	162	0.0133	110	0.0094	121	0.0283	102
346	siat-002	0.0091	243	0.0126	237	0.0109	300	0.0190	311	0.0276	321	0.0516	249	0.0464	301	0.0520	317
347	siat-005	0.0021	45	0.0038	61	0.0059	207	0.0049	123	0.0742	364	0.9623	402	0.6801	402	0.0279	57
348	sjtu-003	0.0017	29	0.0033	46	0.0030	80	0.0037	78	0.0058	119	0.0104	83	0.0081	95	0.0284	110
349	sjtu-004	0.0014	21	0.0025	27	0.0027	51	0.0028	36	0.0046	91	0.0086	64	0.0073	80	0.0272	10
350	sktelecom-000	0.0038	113	0.0054	115	0.0031	83	0.0051	129	0.0042	79	0.3418	323	0.0061	55	0.0293	165
351	smartbiometrik-001	0.5485	444	0.6442	439	0.7550	441	0.8611	438	0.8677	434	0.8270	382	0.7030	404	0.3144	417
352	smartengines-000	0.6240	450	0.7562	451	0.9552	450	0.9784	449	0.9515	445	0.9288	397	0.8200	415	0.8037	444

Table 26: FNMR is the proportion of mated comparisons below a threshold set to achieve the FMR given in the header on the fourth row. FMR is the proportion of impostor comparisons at or above that threshold. The light grey values give rank over all algorithms in that column. The pink columns use only same-sex impostors; others are selected regardless of demographics. The exception, in the green column, uses “matched-covariates” i.e. impostors of the same sex, age group, and country of birth. The second pink column includes effects of extended ageing. Missing entries for border, visa, mugshot and wild images generally mean the algorithm did not run to completion. The VISA columns compare images described in section 2.1. The MUGSHOT columns compare images described in section 2.4. The VISA-BORDER column compare images described in section 2.2 with those of section 2.3. The BORDER column compares images described in section 2.3. The WILD columns compare images described in section 2.6.

	Algorithm	FALSE NON-MATCH RATE (FNMR)										LESS CONSTRAINED, NON-COOP.					
		CONSTRAINED, COOPERATIVE								WILD							
		Name	VISAMC	VISA	MUGSHOT	MUGSHOT12+YRS	VISA BORDER	BORDER	BORDER								
	FMR	0.0001	1E-06	1E-05	1E-05	1E-06	1E-06	1E-06	1E-05	0.0001							
353	smartengines-001	0.6434	452	0.7666	452	0.9446	449	0.9750	448	0.9387	444	0.9556	400	0.8647	420	0.7748	442
354	smartvist-000	0.0912	395	0.1587	396	0.1163	398	0.1841	396	0.1397	383	0.9372	398	0.7107	407	0.0779	349
355	smilart-002	0.2440	413	0.3532	415	-	-	-	0.3785	409	0.4145	335	0.2611	363	-	-	
356	smilart-003	0.6944	454	0.8836	454	0.0695	389	0.1193	390	0.0894	372	0.1221	287	0.0737	324	0.1190	377
357	sodec-000	0.0033	93	0.0044	87	0.0040	145	0.0053	134	0.0054	111	0.0096	77	0.0080	92	0.0274	19
358	sqisoft-001	0.1220	403	0.2088	403	0.1978	406	0.3386	406	0.2111	397	0.2798	319	0.1474	348	0.0519	316
359	sqisoft-002	0.0082	234	0.0124	233	0.0051	182	0.0086	215	0.0102	204	0.0183	153	0.0122	166	0.0287	130
360	staqu-000	0.0139	307	0.0208	298	0.0104	291	0.0145	283	0.0156	255	0.8063	377	0.1408	346	0.0332	238
361	starhybrid-001	0.0108	268	0.0138	244	0.0081	256	0.0113	242	0.0152	254	0.0265	189	0.0189	233	0.0350	258
362	sukshi-000	0.5409	442	0.6612	444	0.4556	421	0.6567	423	0.9296	443	0.8898	386	0.7384	408	0.6892	438
363	suprema-002	0.0030	78	0.0041	72	0.0034	111	0.0040	90	0.0045	87	0.0085	60	0.0072	79	0.0295	169
364	suprema-003	0.0028	70	0.0041	74	0.0034	109	0.0039	86	0.0030	32	0.3095	322	0.0580	315	0.0284	106
365	supremaid-001	0.0053	154	0.0073	151	0.0045	158	0.0066	173	0.0099	202	0.0186	154	0.0148	197	0.0352	261
366	supremaid-002	0.0063	189	0.0094	191	0.0044	154	0.0062	164	0.0072	144	0.0229	177	0.0095	124	0.0345	249
367	surrey-cvssp-000	0.9084	458	0.9909	459	0.9923	453	0.9950	451	0.9981	448	0.9994	424	0.9979	441	0.9389	446
368	surrey-cvssp-001	1.0000	462	1.0000	462	0.0077	248	0.0079	202	0.0266	317	0.3822	330	0.0551	311	1.0000	458
369	synesis-006	0.0070	205	0.0096	194	0.0107	297	0.0166	298	-	0.0128	109	0.0089	112	0.0292	160	
370	synesis-007	0.0050	140	0.0073	152	0.0062	215	0.0076	190	-	0.0105	84	0.0080	94	0.0288	132	
371	synology-000	0.0149	314	0.0238	317	0.0148	331	0.0261	331	0.0221	297	0.0331	213	0.0209	246	0.0330	236
372	synology-002	0.0104	264	0.0153	260	0.0107	298	0.0184	305	0.0189	286	0.2032	305	0.0180	222	0.0312	210
373	sztu-000	0.0092	247	0.0139	245	0.0091	276	0.0201	317	0.0136	240	0.0685	262	0.0118	162	0.0270	5
374	sztu-001	0.0031	79	0.0043	80	0.0025	31	0.0028	33	0.0051	103	0.0113	95	0.0089	113	0.0275	22
375	t4isb-000	0.0058	166	0.0087	182	0.0041	149	0.0064	170	0.0083	165	0.0157	130	0.0103	135	0.0282	89
376	tech5-004	0.0123	289	0.0234	315	0.0086	269	0.0162	293	0.0065	135	0.0112	93	0.0082	98	0.0281	82
377	tech5-005	0.0054	158	0.0072	146	0.0069	228	0.0122	249	0.0060	126	0.0094	74	0.0066	64	0.0349	256
378	techsign-000	0.0325	366	0.0511	363	0.0435	375	0.0710	373	0.0746	365	0.1104	284	0.0841	329	0.0639	334
379	techsign-001	0.0110	271	0.0196	294	0.0067	224	0.0120	247	0.0087	172	0.2475	314	0.0883	333	0.0299	183
380	tevian-007	0.0019	40	0.0027	35	0.0032	98	0.0041	93	0.0045	88	0.0086	63	0.0078	88	0.0310	209
381	tevian-008	0.0012	13	0.0017	9	0.0033	101	0.0042	99	0.0042	81	0.0081	53	0.0068	70	0.0290	150
382	tiger-005	0.0624	387	0.2450	407	0.0292	363	0.0556	363	0.0430	344	1.0000	434	0.9964	437	0.0278	45
383	tiger-006	0.0066	194	0.0101	205	0.0050	181	0.0075	189	0.0089	177	0.0158	131	0.0117	159	0.0290	158
384	tinkoff-001	0.0145	311	0.0244	318	0.0318	366	0.0636	371	0.0236	308	1.0000	461	0.0339	278	0.0563	327
385	tongyi-005	0.0073	215	0.0146	251	0.0187	340	0.0421	353	0.0161	261	0.0215	169	0.0149	199	0.0399	280
386	toppanidgate-000	0.0021	46	0.0033	45	0.0026	40	0.0028	30	0.0039	69	0.0075	42	0.0068	68	0.0376	275
387	toshiba-004	0.0030	75	0.0042	76	0.0025	32	0.0027	27	0.0034	48	0.0063	26	0.0053	35	0.0278	43
388	toshiba-006	0.0022	48	0.0035	53	0.0024	23	0.0025	19	0.0027	19	0.7425	365	0.3070	371	0.0275	27
389	touchlessid-000	0.3296	423	0.4804	426	0.4111	417	0.6026	420	0.5324	415	0.9996	427	0.9964	438	0.2521	409
390	touchlessid-001	0.0076	221	0.0104	209	0.0680	388	0.0842	378	0.1358	381	1.0000	436	0.9995	444	0.0499	312
391	trueface-002	0.0060	179	0.0096	196	0.0048	171	0.0061	161	0.0112	218	0.0198	161	0.0155	204	0.0793	354
392	trueface-003	0.0070	202	0.0094	193	0.0053	189	0.0081	206	0.0122	226	0.0217	171	0.0159	207	0.0785	351
393	tuputech-000	0.3218	422	0.3696	418	-	-	-	0.3237	404	0.4304	336	0.2973	370	0.9415	447	
394	turingtechchip-001	0.0330	368	0.0540	368	0.0458	376	0.1007	382	0.4715	413	0.9286	396	0.8448	419	0.4035	424
395	turingtechchip-002	0.0126	296	0.0163	267	0.0092	281	0.0118	244	0.2264	399	1.0000	447	0.9925	434	0.2144	398
396	turkcell-000	0.1134	400	0.1288	391	0.0770	392	0.1112	389	0.2570	400	1.0000	433	0.9999	446	0.9556	448

Table 27: FNMR is the proportion of mated comparisons below a threshold set to achieve the FMR given in the header on the fourth row. FMR is the proportion of impostor comparisons at or above that threshold. The light grey values give rank over all algorithms in that column. The pink columns use only same-sex impostors; others are selected regardless of demographics. The exception, in the green column, uses “matched-covariates” i.e. impostors of the same sex, age group, and country of birth. The second pink column includes effects of extended ageing. Missing entries for border, visa, mugshot and wild images generally mean the algorithm did not run to completion. The VISA columns compare images described in section 2.1. The MUGSHOT columns compare images described in section 2.4. The VISA-BORDER column compare images described in section 2.2 with those of section 2.3. The BORDER column compares images described in section 2.3. The WILD columns compare images described in section 2.6.

	Algorithm	FALSE NON-MATCH RATE (FNMR)												LESS CONSTRAINED, NON-COOP.			
		CONSTRAINED, COOPERATIVE								WILD							
		Name	VISAMC	VISA	MUGSHOT	MUGSHOT12+YRS	VISABORDER	BORDER	BORDER	1E-06	1E-05	0.0001	0.0001				
	FMR	0.0001	1E-06	1E-05	1E-05	1E-05	1E-06	1E-06	1E-05								
397	twface-000	0.0051	143	0.0072	148	0.0041	147	0.0058	150	0.0071	141	0.0153	125	0.0100	126	0.0276	32
398	twface-001	0.0036	101	0.0051	105	0.0031	91	0.0038	80	0.0049	99	0.0091	70	0.0075	84	0.0277	37
399	ulsee-001	0.0151	316	0.0246	320	0.0113	308	0.0185	308	0.0187	285	0.6766	359	0.0181	224	0.0316	221
400	ultinous-000	0.2343	412	0.3484	414	-	-	-	-	-	-	-	-	-	-		
401	ultinous-001	0.2485	414	0.4003	421	-	-	-	-	-	-	-	-	-	-		
402	uluface-002	0.0081	229	0.0123	230	0.0071	233	0.0095	228	0.0107	209	1.0000	453	0.0140	186	0.0444	302
403	uluface-003	0.0100	259	0.0150	256	0.0079	250	0.0128	260	-	-	-	-	-	-	0.0635	332
404	unissey-001	0.0095	251	0.0160	263	0.0134	321	0.0150	286	0.0147	252	0.0253	186	0.0163	208	0.0946	366
405	unissey-002	0.0094	250	0.0151	258	0.0079	251	0.0110	237	0.0114	219	0.4424	337	0.1914	355	0.0420	293
406	upc-001	0.0234	349	0.0519	364	0.0291	362	0.0490	360	0.0294	325	0.2316	312	0.0389	290	0.0314	217
407	uxlabs-001	0.0534	382	0.0570	372	0.0118	314	0.0131	264	0.0237	309	0.0399	233	0.0288	271	0.0876	363
408	vcog-002	0.7522	456	0.9033	455	-	-	-	-	-	-	-	-	-	-		
409	vd-002	0.0429	375	0.0704	377	0.0569	382	0.0844	379	0.0801	367	0.0937	272	0.0577	314	0.0556	326
410	vd-003	0.0199	342	0.0222	308	0.0115	312	0.0130	263	0.0138	243	0.0239	179	0.0177	219	0.0389	277
411	veridas-007	0.0063	188	0.0083	173	0.0044	156	0.0058	153	0.0080	158	0.0152	123	0.0120	165	0.0284	107
412	veridas-008	0.0032	85	0.0045	90	0.0030	77	0.0033	56	0.0085	169	0.0206	166	0.0143	191	0.0288	137
413	veridium-000	0.0726	392	0.1248	390	0.5226	424	0.6652	424	0.6425	418	0.8150	378	0.7989	414	0.4988	431
414	verigram-000	0.0032	82	0.0043	79	0.0031	84	0.0034	60	0.0093	187	0.0175	147	0.0164	209	0.0276	30
415	verigram-001	0.0032	84	0.0044	86	0.0027	52	0.0032	51	0.0030	30	0.9995	425	0.9953	436	0.0276	35
416	verihubs-inteligensia-000	0.0070	204	0.0098	199	0.0048	173	0.0076	193	0.0092	184	0.0160	133	0.0117	157	0.0283	100
417	verihubs-inteligensia-001	0.0071	206	0.0114	225	0.0050	180	0.0076	192	0.0096	193	0.0165	139	0.0114	154	0.0282	87
418	verijelas-000	0.2488	415	0.3431	413	0.4861	422	0.6004	419	0.0811	368	0.1148	285	0.0440	296	0.0524	320
419	via-000	0.0216	346	0.0365	351	0.0177	338	0.0287	338	0.0296	326	0.0572	251	0.0290	273	0.0349	255
420	via-001	0.0149	313	0.0229	311	0.0114	310	0.0177	303	0.0183	281	0.4056	333	0.0176	217	0.0373	274
421	videmo-001	0.0295	361	0.0417	355	0.0164	337	0.0261	332	0.0355	334	0.0603	255	0.0442	298	0.1473	380
422	videmo-002	0.0158	322	0.0288	335	0.0149	335	0.0249	330	0.0230	301	0.3429	324	0.1468	347	0.0294	167
423	videonetics-001	0.5483	443	0.6446	441	0.7517	439	0.8607	437	0.8664	432	0.8255	380	0.6956	403	0.2986	414
424	videonetics-002	0.4274	430	0.5329	432	0.6081	429	0.7438	429	0.7775	423	0.7297	364	0.5756	393	0.1976	396
425	viettelhightech-000	0.0117	278	0.0166	270	0.0110	302	0.0198	316	0.0167	270	0.0249	182	0.0158	205	0.0409	290
426	vigilantsolutions-010	0.0109	269	0.0164	268	0.0074	242	0.0095	226	0.0209	294	0.0365	227	0.0233	255	0.0277	38
427	vigilantsolutions-011	0.0124	290	0.0176	280	0.0073	238	0.0095	225	0.0196	290	0.0360	225	0.0221	251	0.0274	18
428	vinai-000	0.0081	230	0.0124	232	0.0045	157	0.0072	184	0.0089	176	0.1814	298	0.0112	149	0.0274	20
429	vinbigdata-001	0.2576	418	0.2763	409	0.1404	402	0.1988	401	0.1407	384	0.1150	286	0.0703	322	0.9767	450
430	vinbigdata-002	0.0102	261	0.0175	277	0.0071	236	0.0084	211	0.0090	178	0.8017	376	0.3134	372	0.0304	195
431	vion-000	0.0419	373	0.0590	373	0.0422	374	0.0478	357	0.0581	356	0.0968	279	0.0847	330	0.2479	406
432	visage-000	0.0933	396	0.1441	395	0.1316	400	0.2416	402	0.1395	382	0.1920	302	0.1001	337	0.0500	313
433	visionbox-001	0.0159	323	0.0270	330	0.0111	304	0.0173	301	0.0190	287	0.0315	207	0.0205	244	0.0389	278
434	visionbox-002	0.0058	168	0.0079	164	0.0060	209	0.0074	186	0.0084	167	0.0149	118	0.0113	152	0.0447	304
435	visionlabs-010	0.0017	30	0.0024	24	0.0026	43	0.0030	41	0.0033	45	0.0061	24	0.0052	27	0.0282	91
436	visionlabs-011	0.0012	15	0.0022	19	0.0024	24	0.0026	24	0.0028	22	0.0053	13	0.0046	18	0.0280	70
437	visteam-003	0.0804	394	0.2166	404	0.0613	387	0.1204	391	0.0963	375	0.1269	289	0.0441	297	0.0296	177
438	visteam-004	0.0541	384	0.5202	430	0.0406	373	0.0827	377	0.1879	392	0.1795	297	0.0347	281	0.0289	142
439	vixvizion-005	0.0276	358	0.0420	356	0.0302	365	0.0629	370	0.0288	322	0.0447	238	0.0235	257	0.0265	2
440	vixvizion-006	0.0082	232	0.0122	229	0.0093	282	0.0194	313	0.0099	201	0.0169	141	0.0108	145	0.0268	4

Table 28: FNMR is the proportion of mated comparisons below a threshold set to achieve the FMR given in the header on the fourth row. FMR is the proportion of impostor comparisons at or above that threshold. The light grey values give rank over all algorithms in that column. The pink columns use only same-sex impostors; others are selected regardless of demographics. The exception, in the green column, uses “matched-covariates” i.e. impostors of the same sex, age group, and country of birth. The second pink column includes effects of extended ageing. Missing entries for border, visa, mugshot and wild images generally mean the algorithm did not run to completion. The VISA columns compare images described in section 2.1. The MUGSHOT columns compare images described in section 2.4. The VISA-BORDER column compare images described in section 2.2 with those of section 2.3. The BORDER column compares images described in section 2.3. The WILD columns compare images described in section 2.6.

	Algorithm	FALSE NON-MATCH RATE (FNMR)										LESS CONSTRAINED, NON-COOP.					
		CONSTRAINED, COOPERATIVE								WILD							
		Name	VISAMC	VISA	MUGSHOT	MUGSHOT12+YRS	VISABORDER	BORDER	BORDER								
	FMR	0.0001	1E-06	1E-05	1E-05	1E-05	1E-06	1E-06	1E-05			0.0001					
441	vnpt-004	0.0058	171	0.0078	163	0.0037	127	0.0053	133	0.0051	104	0.4640	339	0.1384	344	0.0275	26
442	vnpt-005	0.0036	102	0.0052	108	0.0027	53	0.0031	47	0.0036	57	0.0066	30	0.0056	39	0.0286	123
443	vocord-009	0.0022	52	0.0029	39	0.0036	119	0.0046	114	0.0052	108	0.0098	78	0.0086	109	0.0284	109
444	vocord-010	0.0024	58	0.0031	43	0.0036	120	0.0049	125	0.0025	15	0.0065	28	0.0040	10	0.0280	67
445	vts-000	0.0103	262	0.0174	276	0.0080	253	0.0129	262	0.0250	315	0.0450	240	0.0372	288	0.0596	328
446	vts-001	0.0033	92	0.0048	96	0.0027	55	0.0036	73	0.0032	39	0.6519	356	0.3563	377	0.0338	244
447	wicket-000	0.0018	38	0.0028	38	0.0024	20	0.0027	25	0.0031	34	0.7968	375	0.4340	385	0.0323	227
448	winsense-001	0.0062	185	0.0099	203	0.0092	279	0.0210	318	0.0093	186	0.0144	116	0.0098	125	0.0320	225
449	winsense-002	0.0050	139	0.0073	150	0.0038	129	0.0059	156	0.0064	133	0.0118	101	0.0084	102	0.0307	202
450	wiseai-001	0.0658	388	0.0964	387	0.7743	443	0.8956	443	0.1967	393	0.7526	369	0.3419	374	0.5780	434
451	wuhanianyu-001	0.0163	324	0.0262	327	0.0281	360	0.0569	366	0.0316	330	0.0486	246	0.0344	279	0.0324	228
452	x-laboratory-000	0.0071	209	0.0106	211	0.0123	317	0.0138	273	0.0419	343	0.5629	347	0.2852	368	0.0295	174
453	x-laboratory-001	0.0059	177	0.0110	219	0.0054	192	0.0078	200	0.0094	189	0.0142	113	0.0100	128	0.0294	166
454	xforwardai-001	0.0021	42	0.0034	48	0.0027	56	0.0028	32	0.0046	93	0.0088	67	0.0079	90	0.0281	81
455	xforwardai-002	0.0016	28	0.0023	22	0.0026	46	0.0025	16	0.0040	74	0.0081	55	0.0074	81	0.0282	85
456	xm-000	0.0015	23	0.0026	32	0.0031	89	0.0038	84	0.0058	120	0.0105	85	0.0082	99	0.0282	90
457	yisheng-004	0.1988	409	0.3329	412	0.1147	397	0.1849	397	0.2044	395	-	-	-	-	0.0908	364
458	yitu-003	0.0015	25	0.0026	30	0.0066	222	0.0085	212	0.0064	134	0.0114	96	0.0103	136	0.0325	231
459	yoonik-002	0.0052	151	0.0062	129	0.0029	73	0.0034	62	0.0615	360	0.1279	290	0.1166	339	0.0549	324
460	yoonik-003	0.0034	97	0.0047	93	0.0032	96	0.0037	76	0.0816	369	0.2033	306	0.1601	352	0.0699	343
461	ytu-000	0.0057	163	0.0087	180	0.0121	315	0.0238	327	0.0047	95	0.0078	50	0.0059	50	0.0286	124
462	yuan-004	0.0058	172	0.0078	161	0.0039	139	0.0055	141	0.0234	305	0.0442	237	0.0353	282	0.0299	184
463	yuan-005	0.0037	111	0.0046	92	0.0027	58	0.0035	69	0.0033	42	0.2706	317	0.0876	332	0.0288	141

Table 29: FNMR is the proportion of mated comparisons below a threshold set to achieve the FMR given in the header on the fourth row. FMR is the proportion of impostor comparisons at or above that threshold. The light grey values give rank over all algorithms in that column. The pink columns use only same-sex impostors; others are selected regardless of demographics. The exception, in the green column, uses “matched-covariates” i.e. impostors of the same sex, age group, and country of birth. The second pink column includes effects of extended ageing. Missing entries for border, visa, mugshot and wild images generally mean the algorithm did not run to completion. The VISA columns compare images described in section 2.1. The MUGSHOT columns compare images described in section 2.4. The VISA-BORDER column compare images described in section 2.2 with those of section 2.3. The BORDER column compares images described in section 2.3. The WILD columns compare images described in section 2.6.

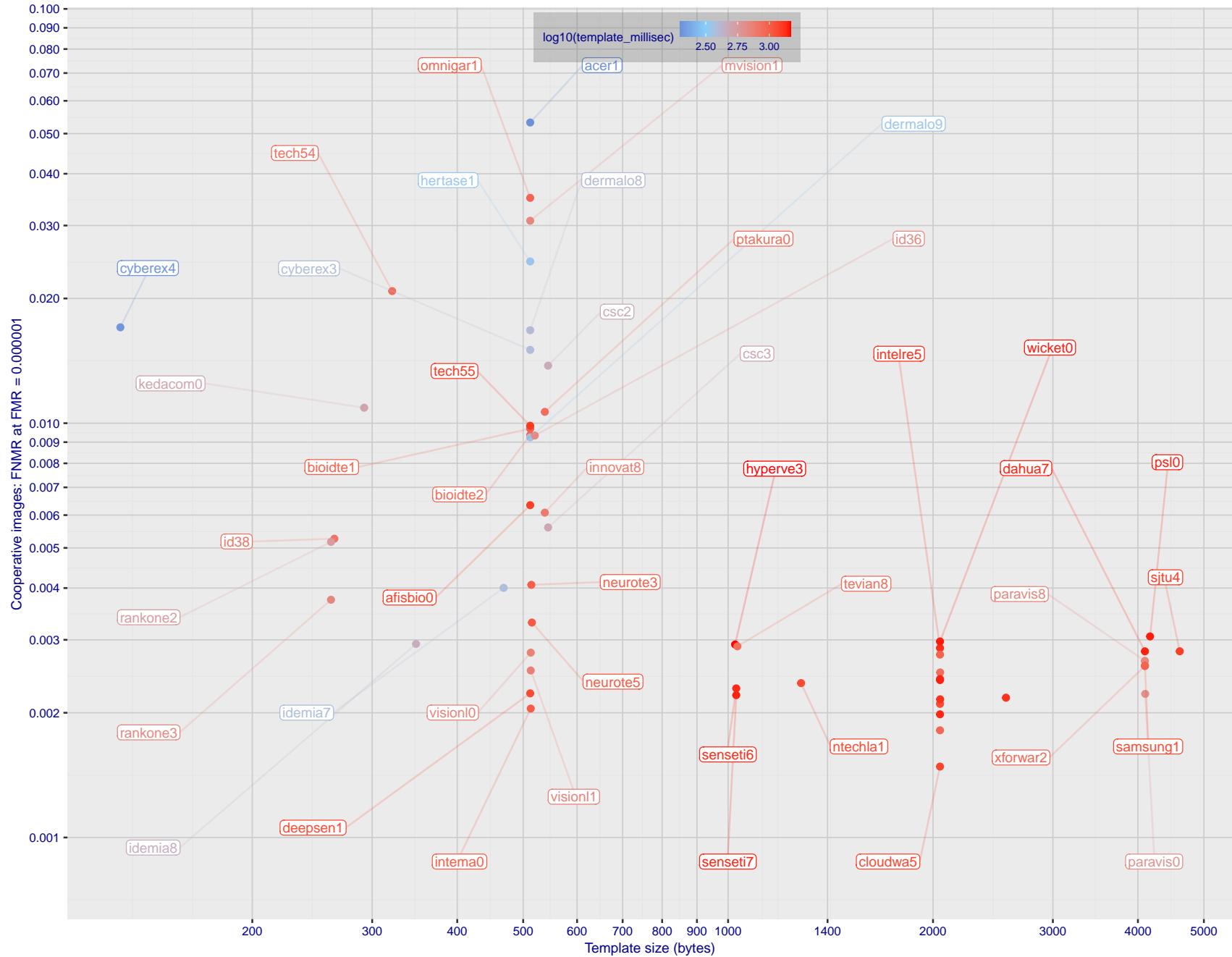


Figure 1: The points show false non-match rates (FNMR) versus the size of the encoded template. FNMR is the geometric mean of FNMR values for visa and mugshot images (from Figs. 86 and 110) at the false match rate (FMR) given in the y-axis label. The color of the points encodes template generation time - which spans at least one order of magnitude. Durations are measured on a single core of a c. 2016 Intel Xeon CPU E5-2630 v4 running at 2.20GHz. Algorithms with poor FNMR are omitted.

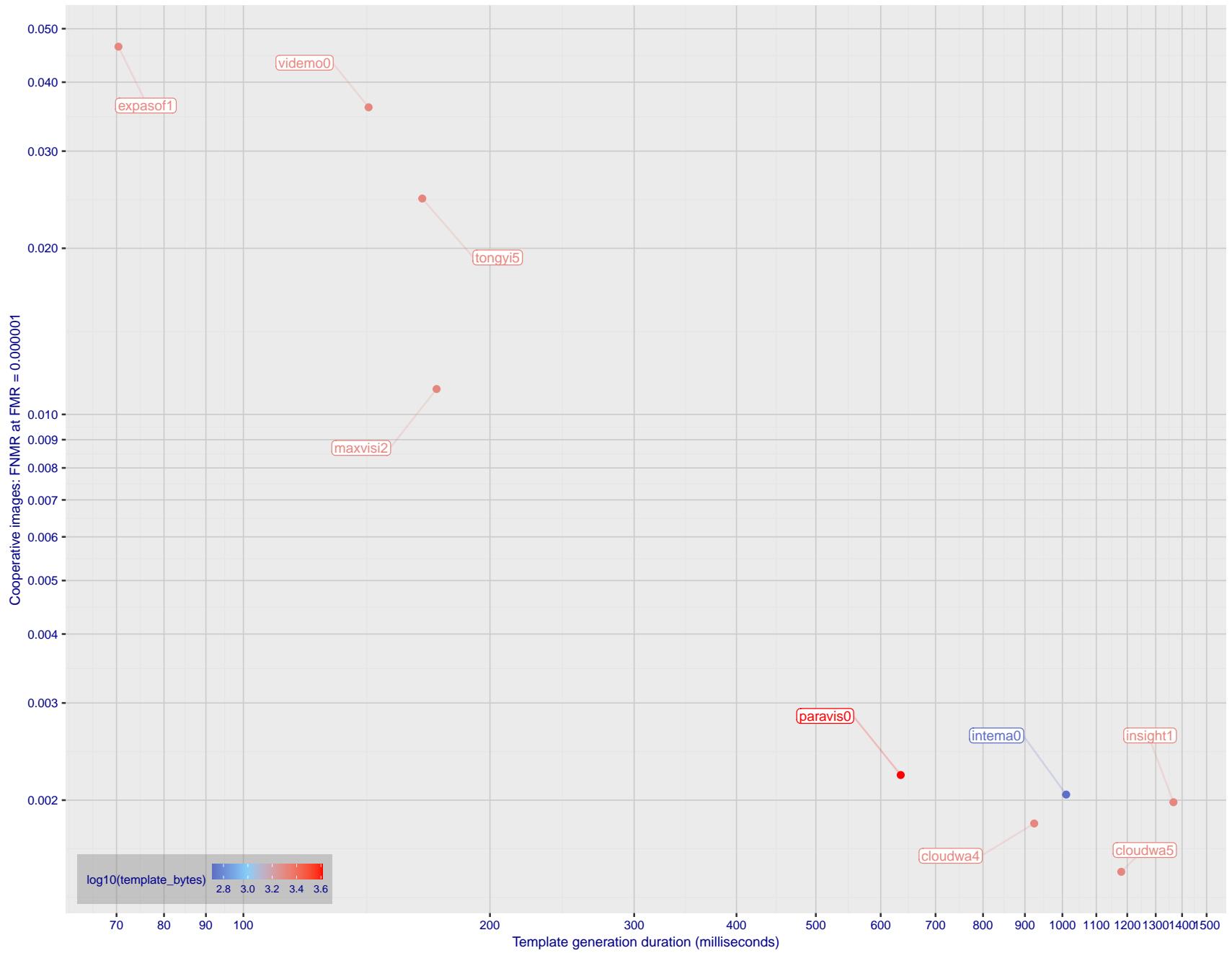


Figure 2: The points show false non-match rates (FNMR) versus the duration of the template generation operation. FNMR is the geometric mean of FNMR values for visa and mugshot images (from Figs. 86 and 110) at a false match rate (FMR) given in the y-axis label. Template generation time is a median estimated over 640 x 480 pixel portraits. It is measured on a single core of a c. 2016 Intel Xeon CPU E5-2630 v4 running at 2.20GHz. The color of the points encodes template size - which span two orders of magnitude. Algorithms with poor FNMR are omitted.

1 Metrics

1.1 Core accuracy

Given a vector of N genuine scores, u , the false non-match rate (FNMR) is computed as the proportion below some threshold, T:

$$\text{FNMR}(T) = 1 - \frac{1}{N} \sum_{i=1}^N H(u_i - T) \quad (1)$$

where $H(x)$ is the unit step function, and $H(0)$ taken to be 1.

Similarly, given a vector of N impostor scores, v , the false match rate (FMR) is computed as the proportion above T:

$$\text{FMR}(T) = \frac{1}{N} \sum_{i=1}^N H(v_i - T) \quad (2)$$

The threshold, T, can take on any value. We typically generate a set of thresholds from quantiles of the observed impostor scores, v , as follows. Given some interesting false match rate range, $[\text{FMR}_L, \text{FMR}_U]$, we form a vector of K thresholds corresponding to FMR measurements evenly spaced on a logarithmic scale

$$T_k = Q_v(1 - \text{FMR}_k) \quad (3)$$

where Q is the quantile function, and FMR_k comes from

$$\log_{10} \text{FMR}_k = \log_{10} \text{FMR}_L + \frac{k}{K} [\log_{10} \text{FMR}_U - \log_{10} \text{FMR}_L] \quad (4)$$

Error tradeoff characteristics are plots of FNMR(T) vs. FMR(T). These are plotted with $\text{FMR}_U \rightarrow 1$ and FMR_L as low as is sustained by the number of impostor comparisons, N. This is somewhat higher than the “rule of three” limit $3/N$ because samples are not independent, due to re-use of images.

1.2 Multi-template scoring methodology

There are some scenarios when one or more people exist and are detected in an image, and some of the proposed test images include $K > 1$ persons for some images and situations where the subject of interest may or may not be the foreground face (largest face in the image). The NIST FRVT 1:1 API supports this by allowing generation of multiple templates representing each person detected in an image. When this occurs, NIST will match all templates generated from the enrollment image with all templates generated from the verification image and use the **maximum** similarity score across all template comparisons. This scoring approach will be used in our calculation of FMR and FNMR (this applies to both genuine and imposter comparisons).

2 Datasets

2.1 Visa images

- ▷ The number of images is on the order of 10^5 .
- ▷ The number of subjects is on the order of 10^5 .
- ▷ The number of subjects with two images is on the order of 10^4 .
- ▷ The images have geometry in reasonable conformance with the ISO/IEC 19794-5 Full Frontal image type. Pose is generally excellent.
- ▷ The images are of size 252x300 pixels. The mean interocular distance (IOD) is 69 pixels.
- ▷ The images are of subjects from greater than 100 countries, with significant imbalance due to visa issuance patterns.
- ▷ The images are of subjects of all ages, including children, again with imbalance due to visa issuance demand.
- ▷ Many of the images are live capture. A substantial number of the images are photographs of paper photographs.
- ▷ When these images are input to the algorithm, they are labelled as being of type "ISO" - see Table 4 of the FRVT API.

2.2 Application images

- ▷ The number of images is on the order of 10^6 .
- ▷ The number of subjects is on the order of 10^6 .
- ▷ The number of subjects with two images is on the order of 10^6 .
- ▷ The images have geometry in good conformance with the ISO/IEC 19794-5 Full Frontal image type. Pose is generally excellent.
- ▷ The images are of size 300x300 pixels. The mean interocular distance (IOD) is 61 pixels.
- ▷ The images are of subjects from greater than 100 countries, with significant imbalance due to population and immigration patterns.
- ▷ The images are of subjects of adults with imbalance due to population and immigration patterns and demand.
- ▷ All of the images are live capture.
- ▷ When these images are input to the algorithm, they are labelled as being of type "ISO" - see Table 4 of the FRVT API.

2.3 Border crossing images

- ▷ The number of images is on the order of 10^6 .
- ▷ The number of subjects is on the order of 10^6 .
- ▷ The number of subjects with two images is on the order of 10^6 .
- ▷ The images are taken with a camera oriented by an attendant toward a cooperating subject. This is done under time constraints so there are roll, pitch and yaw angle variations. Also background illumination is sometimes strong, so the face is under-exposed. There is some perspective distortion due to close range images. Some faces are partially cropped.
- ▷ The images have mean IOD of 38 pixels.
- ▷ The images are of subjects of adults and children aged 12 or above.

- ▷ The images are of subjects from greater than 100 countries, with significant imbalance due to population and immigration patterns.
- ▷ The images are all live capture.
- ▷ When these images are input to the algorithm, they are labelled as being of type "WILD" - see Table 4 of the FRVT API.

2.4 Mugshot images

- ▷ The number of images is on the order of 10^6 .
- ▷ The number of subjects is on the order of 10^6 .
- ▷ The number of subjects with two images is on the order of 10^6 .
- ▷ The images have geometry in reasonable conformance with the ISO/IEC 19794-5 Full Frontal image type.
- ▷ The images are of variable sizes. The median IOD is 105 pixels. The mean IOD is 113 pixels. The 1-st, 5-th, 10-th, 25-th, 75-th, 90-th and 99-th percentiles are 34, 58, 70, 87, 121, 161 and 297 pixels.
- ▷ The images are of subjects from the United States.
- ▷ The images are of adults.
- ▷ The images are all live capture.
- ▷ When these images are input to the algorithm, they are labelled as being of type "mugshot" - see Table 4 of the FRVT API.

2.5 Kiosk images

- ▷ The number of images is on the order of 10^6 .
- ▷ The number of subjects is on the order of 10^5 .
- ▷ The number of subjects with multiple images is the order of 10^5 .
- ▷ The images are taken at kiosk equipped with a camera intended to capture a centered face. However the images have specific quality defects arising from the camera triggering before the subject looks at it. These are downward pitch of the face relative to the optical axis; cropping of the forehead; and cropping of left or right part of the face. Partial cropping affects perhaps 10% of the images. Resolution does not vary widely.
- ▷ The images are of adults.
- ▷ The images have mean IOD of 44 pixels, with maximum below 75, and minimum when both eyes are present above 25 pixels.
- ▷ All of the images are live capture, none are scanned.
- ▷ When these images are input to the algorithm, they are labelled as being of type "WILD" - see Table 4 of the FRVT API.

2.6 Wild images

- ▷ The number of images is on the order of 10^5 .
- ▷ The number of subjects is on the order of 10^4 .
- ▷ The number of subjects with two images on the order of 10^4 .
- ▷ The images include many photojournalism-style images. Images are given to the algorithm using a variable but generally tight crop of the head. Resolution varies very widely. The images are very unconstrained, with wide yaw and pitch pose variation. Faces can be occluded, including hair and hands.

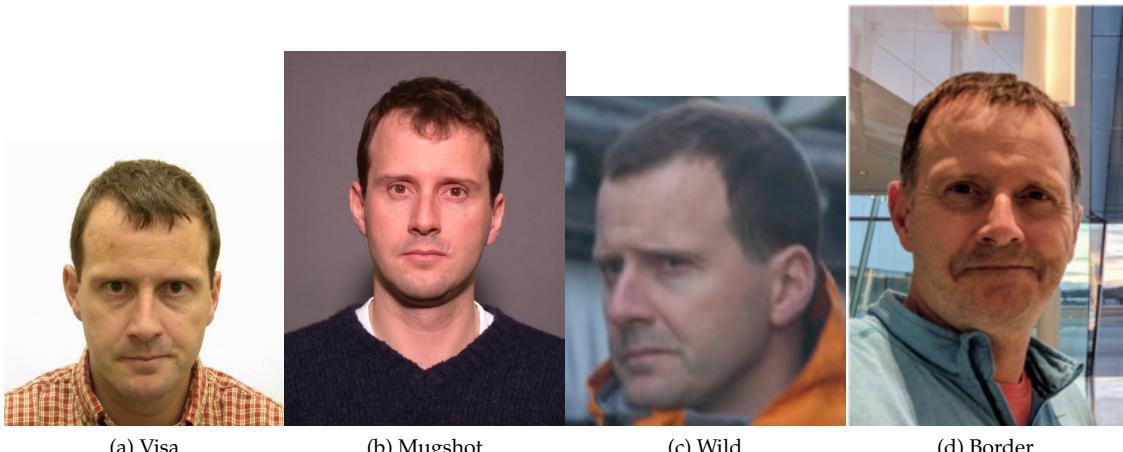


Figure 3: The figure gives simulated samples of image types used in this report.

- ▷ The images are of adults.
 - ▷ All of the images are live capture, none are scanned.
 - ▷ When these images are input to the algorithm, they are labelled as being of type "WILD" - see Table 4 of the FRVT API.

3 Results

3.1 Test goals

- ▷ To state absolute accuracy for different kinds of images, including those with and without subject cooperation.
 - ▷ To state comparative accuracy, across algorithms.

3.2 Test design

Method: For visa images:

- ▷ The comparisons are of visa photos against visa photos.
 - ▷ The number of genuine comparisons is on the order of 10^4 .
 - ▷ The number of impostor comparisons is on the order of 10^{10} .
 - ▷ The comparisons are fully zero-effort, meaning impostors are paired without attention to sex, age or other covariates. However, later analysis is conducted on subsets.
 - ▷ The number of persons is on the order of 10^5 .
 - ▷ The number of images used to make 1 template is 1.
 - ▷ The number of templates used to make each comparison score is two corresponding to simple one-to-one verification.

Method: For mugshot images:

- ▷ The comparisons are of mugshot photos against mugshot photos.

- ▷ The number of genuine comparisons is on the order of 10^6 .
- ▷ The number of impostor comparisons is on the order of 10^8 .
- ▷ The impostors are paired by sex, but not by age or other covariates.
- ▷ The number of persons is on the order of 10^6 .
- ▷ The number of images used to make 1 template is 1.
- ▷ The number of templates used to make each comparison score is two corresponding to simple one-to-one verification.

Method: For visa-border comparisons:

- ▷ The comparisons are of visa-like frontals against border crossing webcam photos.
- ▷ The number of genuine comparisons is on the order of 10^6 .
- ▷ The number of impostor comparisons is on the order of 10^8 .
- ▷ The impostors are paired by sex, but not by age or other covariates.
- ▷ The number of persons is on the order of 10^6 .
- ▷ The number of images used to make 1 template is 1.
- ▷ The number of templates used to make each comparison score is two corresponding to simple one-to-one verification.

Method: For kiosk-border comparisons:

- ▷ The comparisons are of visa-like frontals against kiosk-style photos.
- ▷ The number of genuine comparisons is on the order of 10^6 .
- ▷ The number of impostor comparisons is on the order of 10^8 .
- ▷ The impostors are paired by sex, but not by age or other covariates.
- ▷ The number of persons is on the order of 10^5 .
- ▷ The number of images used to make 1 template is 1.
- ▷ The number of templates used to make each comparison score is two corresponding to simple one-to-one verification.

Method: For border-border comparisons:

- ▷ The comparisons are of border crossing webcam photos.
- ▷ The number of genuine comparisons is on the order of 10^6 .
- ▷ The number of impostor comparisons is on the order of 10^8 .
- ▷ The impostors are paired by sex, but not by age or other covariates.
- ▷ The number of persons is on the order of 10^6 .
- ▷ The number of images used to make 1 template is 1.
- ▷ The number of templates used to make each comparison score is two corresponding to simple one-to-one verification.

Method: For wild images:

- ▷ The comparisons are of wild photos against wild photos.

- ▷ The number of genuine comparisons is on the order of 10^6 .
- ▷ The number of impostor comparisons is on the order of 10^8 .
- ▷ The comparisons are fully zero-effort, meaning impostors are paired without attention to sex, age or other covariates.
- ▷ The number of persons is on the order of 10^4 .
- ▷ The number of images used to make 1 template is 1.
- ▷ The number of templates used to make each comparison score is two corresponding to simple one-to-one verification.

Method: For child exploitation images:

- ▷ The comparisons are of unconstrained child exploitation photos against others of the same type.
- ▷ The number of genuine comparisons is on the order of 10^4 .
- ▷ The number of impostor comparisons is on the order of 10^7 .
- ▷ The comparisons are fully zero-effort, meaning impostors are paired without attention to sex, age or other covariates.
- ▷ The number of persons is on the order of 10^3 .
- ▷ The number of images used to make 1 template is 1.
- ▷ The number of templates used to make each comparison score is two corresponding to simple one-to-one verification.
- ▷ We produce two performance statements. First, is a DET as used for visa and mugshot images. The second is a cumulative match characteristic (CMC) summarizing a simulated one-to-many search process. This is done as follows.
 - We regard M enrollment templates as items in a gallery.
 - These M templates come from $M > N$ individuals, because multiple images of a subject are present in the gallery under separate identifiers.
 - We regard the verification templates as search templates.
 - For each search we compute the rank of the highest scoring mate.
 - This process should properly be conducted with a 1:N algorithm, such as those tested in NIST IR 8009. We use the 1:1 algorithms in a simulated 1:N mode here to a) better reflect what a child exploitation analyst does, and b) to show algorithm efficacy is better than that revealed in the verification DETs.

3.3 Failure to enroll

	Algorithm	Failure to Enrol Rate ¹									
		APPLICATION		BORDER		KIOSK		MUGSHOT		VISA	
Name	SEC. 2.2	SEC. 2.3	SEC. 2.5	SEC. 2.4	SEC. 2.1	SEC. 2.6					
1	20face-000	0.0000	260	0.0008	237	0.0217	171	0.0000	137	0.0004	261
2	20face-001	0.0000	278	0.0008	236	0.0000	26	0.0000	133	0.0004	262
3	3divi-006	0.0000	218	0.0007	205	0.0214	169	0.0001	245	0.0002	141
4	3divi-007	0.0000	225	0.0007	207	0.0214	168	0.0001	243	0.0002	140
5	acer-001	0.0000	214	0.0011	293	-	411	0.0001	215	0.0004	278
6	acer-002	0.0000	377	0.0008	229	0.0191	148	0.0003	333	0.0004	277
7	acisw-007	0.0000	111	0.0000	60	0.0000	41	0.0000	98	0.0000	59
8	acisw-008	0.0000	239	0.0009	258	0.0173	133	0.0004	358	0.0004	199
9	adera-002	0.0000	360	0.0034	381	-	413	0.0003	340	0.0005	373
10	adera-003	0.0000	362	0.0034	380	0.0403	237	0.0003	339	0.0005	376
11	advance-003	0.0000	347	0.0012	303	0.0247	186	0.0001	270	0.0004	327
12	advance-004	0.0001	410	0.0010	284	0.0157	124	0.0008	405	0.0006	389
13	afisbiometrics-000	0.0000	231	0.0008	220	0.0213	166	0.0000	136	0.0004	280
14	afrengine-000	0.0000	256	0.0015	320	0.0254	194	0.0008	404	0.0004	222
15	aifirst-001	0.0000	120	0.0000	42	-	338	0.0000	29	0.0000	82
16	aigen-001	0.0000	150	0.0000	38	-	347	0.0000	1	0.0000	83
17	aigen-002	0.0000	138	0.0000	28	0.0000	30	0.0000	12	0.0000	97
18	ailabs-001	0.0000	285	0.0090	421	-	303	0.0007	398	0.0005	350
19	aimall-002	0.0000	363	0.0043	398	-	432	0.0012	416	0.0005	367
20	aimall-003	0.0000	343	0.0012	308	-	358	0.0004	353	0.0005	345
21	aiseemu-001	0.0000	170	0.0000	19	0.0000	1	0.0000	51	0.0000	106
22	aiunionface-000	0.0000	168	0.0000	21	-	292	0.0000	49	0.0000	102
23	aise-001	0.0001	411	0.0040	393	0.0652	254	0.0026	437	0.0022	440
24	aise-002	0.0000	190	0.0014	317	0.0230	180	0.0005	381	0.0004	264
25	ajou-001	0.0000	226	0.0020	342	-	447	0.0001	248	0.0004	331
26	alchera-003	0.0001	423	0.0013	313	0.0317	212	0.0002	313	0.0004	289
27	alchera-004	0.0000	262	0.0009	256	0.0228	178	0.0001	277	0.0004	221
28	alfabeta-001	0.0005	434	0.0650	456	0.2142	283	0.0024	433	0.0018	435
29	alice-000	0.0000	142	0.0006	177	0.0133	108	0.0000	151	0.0004	216
30	alleyes-000	0.0000	220	0.0010	275	-	452	0.0002	287	0.0004	303
31	allgvision-000	0.0007	439	0.0062	415	-	430	0.0026	436	0.0052	452
32	alphaface-001	0.0000	210	0.0012	298	-	426	0.0000	200	0.0004	302
33	alphaface-002	0.0000	236	0.0012	297	-	385	0.0000	201	0.0004	305
34	amplifiedgroup-001	0.0114	455	0.1023	458	-	374	0.0189	457	0.0279	460
35	androvideo-000	0.0000	15	0.0000	113	-	418	0.0000	72	0.0000	1
36	anke-004	0.0000	286	0.0011	289	-	301	0.0001	259	0.0004	317
37	anke-005	0.0000	232	0.0012	300	-	434	0.0001	273	0.0004	323
38	antheus-000	0.0000	177	0.0000	5	-	323	0.0000	40	0.0000	117
39	antheus-001	0.0000	156	0.0000	34	-	343	0.0000	6	0.0000	92
40	anyvision-004	0.0000	351	0.0017	332	-	294	0.0001	272	0.0004	274
41	anyvision-005	0.0000	243	0.0013	309	-	368	0.0000	170	0.0004	212
42	armatura-001	0.0000	370	0.0021	348	0.0257	197	0.0005	374	0.0005	354
43	armatura-002	0.0000	352	0.0018	333	0.0206	158	0.0003	348	0.0004	329
44	asusaics-000	0.0000	103	0.0000	64	-	400	0.0000	93	0.0000	55
45	asusaics-001	0.0000	22	0.0000	110	-	420	0.0000	75	0.0000	2
46	authenmetric-003	0.0000	155	0.0000	33	0.0000	22	0.0000	7	0.0000	91
47	authenmetric-004	0.0000	191	0.0000	12	0.0000	13	0.0000	33	0.0000	112
48	aware-005	0.0000	311	0.0020	340	-	414	0.0001	286	0.0004	311
49	aware-006	0.0000	219	0.0009	253	0.0249	188	0.0000	173	0.0004	269
50	awiros-001	0.0039	443	0.0369	448	-	335	0.0386	458	0.0872	463
51	awiros-002	0.0000	379	0.0038	391	-	370	0.0007	397	0.0012	425
52	aximetria-001	0.0000	314	0.0010	286	0.0217	172	0.0001	285	0.0004	259
53	ayftech-001	0.0002	426	0.0046	402	-	417	0.0043	446	0.0011	411
54	ayonix-000	0.0053	447	0.0341	445	-	302	0.0113	455	0.0137	457
55	beethedata-000	0.0005	433	0.0042	397	0.0366	228	0.0002	297	0.0010	406
56	beyneai-000	0.0000	133	0.0000	47	0.0000	17	0.0000	24	0.0000	75
57	biocube-001	0.0006	437	0.0391	449	0.1207	275	0.0015	421	0.0020	438
58	boidtechswiss-001	0.0000	234	0.0007	201	-	440	0.0000	160	0.0004	293

Table 30: FTE is the proportion of failed template generation attempts. Failures can occur because the software throws an exception, or because the software electively refuses to process the input image. This would typically occur if a face is not detected. FTE is measured as the number of function calls that give EITHER a non-zero error code OR that give a “small” template. This is defined as one whose size is less than 0.3 times the median template size for that algorithm. This second rule is needed because some algorithms incorrectly fail to return a non-zero error code when template generation fails.

A hyphen “-” indicates the dataset was not produced.¹ The effects of FTE are included in the accuracy results of this report by regarding any template comparison involving a failed template to produce a low similarity score. Thus higher FTE results in higher FNMR and lower FMR.

	Algorithm	Failure to Enrol Rate ¹											
		APPLICATION	BORDER	KIOSK	MUGSHOT	VISA	WILD	SEC. 2.2	SEC. 2.3	SEC. 2.5	SEC. 2.4	SEC. 2.1	SEC. 2.6
59	bioditechswiss-002	0.0000	289	0.0007	204	-	305	0.0000	162	0.0004	291	0.0005	263
60	bm-001	0.0000	148	0.0000	39	-	348	0.0000	122	0.0000	84	0.0000	18
61	boetech-001	0.0087	451	0.0272	440	0.2117	281	0.0032	443	0.0160	458	0.0946	440
62	boetech-002	0.0087	452	0.0272	439	0.2117	280	0.0032	442	0.0160	459	0.0946	439
63	bresee-001	0.0000	264	0.0010	280	-	392	0.0002	298	0.0003	170	0.0003	138
64	bresee-002	0.0000	353	0.0020	346	0.0219	173	0.0008	399	0.0004	248	0.0031	341
65	camvi-002	0.0000	88	0.0000	59	-	404	0.0000	99	0.0000	61	0.0000	103
66	camvi-004	0.0000	49	0.0000	120	-	450	0.0000	60	0.0000	21	0.0000	65
67	canon-003	0.0000	259	0.0008	219	0.0234	183	0.0000	195	0.0004	282	0.0003	182
68	canon-004	0.0000	212	0.0008	221	0.0234	184	0.0000	194	0.0004	276	0.0003	180
69	ceiec-003	0.0000	83	0.0013	316	-	367	0.0001	226	0.0004	294	0.0004	197
70	ceiec-004	0.0000	16	0.0008	234	-	416	0.0000	168	0.0004	217	0.0004	233
71	chosun-001	0.0000	91	0.0000	58	-	408	0.0000	100	0.0000	62	0.0000	101
72	chosun-002	0.0000	99	0.0000	68	-	396	0.0000	90	0.0000	53	0.0000	96
73	chtface-004	0.0000	109	0.0017	329	0.0320	214	0.0000	182	0.0004	306	0.0020	328
74	chtface-005	0.0000	136	0.0017	328	0.0320	213	0.0000	180	0.0004	308	0.0020	327
75	cist-001	0.0000	114	0.0005	171	0.0087	91	0.0000	27	0.0000	78	0.0000	10
76	clearviewai-000	0.0000	258	0.0003	137	0.0081	88	0.0000	185	0.0003	157	0.0003	139
77	closeli-001	0.0000	189	0.0000	13	0.0000	10	0.0000	32	0.0000	110	0.0001	124
78	cloudmatrix-001	0.0000	331	0.0028	360	0.0225	175	0.0001	218	0.0004	209	0.0004	219
79	cloudmatrix-002	0.0000	328	0.0028	359	0.0225	176	0.0001	219	0.0004	210	0.0004	220
80	cloudwalk-hr-003	0.0000	275	0.0008	238	-	328	0.0001	229	0.0004	214	0.0113	380
81	cloudwalk-hr-004	0.0000	296	0.0011	296	-	295	0.0004	355	0.0003	190	0.0129	384
82	cloudwalk-mt-005	0.0000	276	0.0005	163	0.0130	107	0.0003	329	0.0004	314	0.0004	207
83	cloudwalk-mt-006	0.0000	216	0.0006	179	0.0158	125	0.0002	309	0.0004	310	0.0004	200
84	codeline-000	0.0000	42	0.0000	87	0.0000	57	0.0000	69	0.0000	31	0.0000	76
85	cogent-006	0.0000	154	0.0000	35	0.0000	24	0.0000	5	0.0000	87	0.0000	15
86	cogent-007	0.0000	358	0.0000	116	0.0000	60	0.0000	169	0.0000	127	0.0001	119
87	cognitec-003	0.0001	402	0.0194	434	0.0820	269	0.0003	345	0.0005	356	0.0039	346
88	cognitec-004	0.0001	403	0.0037	390	0.0580	248	0.0003	346	0.0005	353	0.0035	342
89	cor-001	0.0000	249	0.0006	183	-	365	0.0002	324	0.0004	270	0.0004	247
90	coretech-000	0.0000	33	0.0000	91	0.0000	58	0.0000	65	0.0000	27	0.0000	74
91	coretech-001	0.0000	397	0.0033	377	0.0677	259	0.0005	378	0.0011	418	0.0027	336
92	corsight-002	0.0000	248	0.0005	174	0.0152	120	0.0001	262	0.0004	251	0.0003	181
93	corsight-003	0.0000	238	0.0006	190	0.0175	134	0.0001	253	0.0004	260	0.0003	190
94	csc-002	0.0015	442	0.0033	374	-	461	0.0006	390	0.0006	393	0.0968	442
95	csc-003	0.0015	441	0.0033	375	0.0445	243	0.0006	391	0.0006	392	0.0968	441
96	ctbcbank-000	0.0001	406	0.0051	408	-	425	0.0011	414	0.0019	436	0.0868	435
97	ctbcbank-001	0.0000	380	0.0036	389	-	391	0.0005	375	0.0010	404	0.0844	432
98	cubox-001	0.0000	4	0.0000	105	-	433	0.0000	83	0.0000	12	0.0000	56
99	cubox-002	0.0000	319	0.0006	186	0.0159	127	0.0002	323	0.0005	372	0.0016	319
100	cudocommunication-001	0.0000	74	0.0000	85	0.0000	34	0.0000	106	0.0000	34	0.0000	110
101	cuhkee-001	0.0000	274	0.0011	295	-	329	0.0000	134	0.0004	254	0.1278	450
102	cybercore-002	0.0000	368	0.0001	126	0.0014	67	0.0002	291	0.0002	135	0.0018	323
103	cybercore-003	0.0000	205	0.0003	140	0.0060	76	0.0005	380	0.0003	158	0.0192	399
104	cyberextruder-003	0.0000	366	0.0077	420	0.0887	272	0.0001	281	0.0006	387	0.0009	296
105	cyberextruder-004	0.0000	361	0.0097	422	0.1025	274	0.0001	276	0.0007	394	0.0213	401
106	cyberlink-009	0.0000	143	0.0004	157	0.0106	99	0.0000	128	0.0003	171	0.0002	135
107	cyberlink-010	0.0000	175	0.0004	156	0.0106	98	0.0000	130	0.0003	172	0.0002	136
108	dahua-006	0.0000	17	0.0000	115	-	415	0.0000	190	0.0003	186	0.0000	50
109	dahua-007	0.0000	116	0.0000	114	0.0000	61	0.0000	186	0.0003	189	0.0000	7
110	daon-000	0.0000	386	0.0028	363	0.0577	247	0.0014	420	0.0015	429	0.0030	340
111	decatur-000	0.0000	317	0.0020	339	-	369	0.0004	362	0.0005	344	0.0236	405
112	decatur-001	0.0000	246	0.0009	261	0.0194	149	0.0001	233	0.0004	242	0.0004	240
113	deepglint-004	0.0000	305	0.0005	160	0.0130	106	0.0002	322	0.0004	227	0.0003	161
114	deepglint-005	0.0000	335	0.0019	336	0.0438	242	0.0006	387	0.0006	390	0.0028	339
115	deepsea-001	0.0000	126	0.0000	51	-	330	0.0000	20	0.0000	69	0.0000	3
116	deepsense-000	0.0000	56	0.0006	191	-	443	0.0000	147	0.0004	192	0.0003	165

Table 31: FTE is the proportion of failed template generation attempts. Failures can occur because the software throws an exception, or because the software electively refuses to process the input image. This would typically occur if a face is not detected. FTE is measured as the number of function calls that give EITHER a non-zero error code OR that give a “small” template. This is defined as one whose size is less than 0.3 times the median template size for that algorithm. This second rule is needed because some algorithms incorrectly fail to return a non-zero error code when template generation fails.

A hyphen “-” indicates the dataset was not produced.¹ The effects of FTE are included in the accuracy results of this report by regarding any template comparison involving a failed template to produce a low similarity score. Thus higher FTE results in higher FNMR and lower FMR.

	Algorithm	Failure to Enrol Rate ¹							
		APPLICATION	BORDER	KIOSK	MUGSHOT	VISA	WILD		
	Name	SEC. 2.2	SEC. 2.3	SEC. 2.5	SEC. 2.4	SEC. 2.1	SEC. 2.6		
117	deepsense-001	0.0000	72	0.0006	193	0.0191	147	0.0000	155
118	dermalog-009	0.0000	376	0.0031	370	0.0148	117	0.0006	383
119	dermalog-010	0.0000	374	0.0031	371	0.0148	116	0.0006	384
120	dicio-001	0.0005	436	0.0649	453	0.2136	282	0.0024	431
121	didiglobalface-001	0.0000	213	0.0012	299	-	419	0.0000	199
122	digidata-000	0.0000	282	0.0023	351	0.0375	232	0.0004	365
123	digidata-001	0.0000	294	0.0023	350	0.0375	231	0.0004	366
124	digitalbarriers-002	0.0001	414	0.0045	400	-	460	0.0028	439
125	dps-000	0.0000	3	0.0000	104	0.0000	53	0.0000	82
126	dsk-000	0.0000	65	0.0000	72	-	375	0.0000	118
127	einetworks-000	0.0000	381	0.0017	330	-	344	0.0002	310
128	ekin-002	0.0000	185	0.0000	118	0.0004	66	0.0000	129
129	enface-000	0.0000	174	0.0012	306	0.0305	210	0.0000	179
130	enface-001	0.0000	117	0.0012	305	0.0304	209	0.0000	158
131	eocortex-000	0.0095	453	0.0602	452	-	357	0.0094	453
132	ercacat-001	0.0000	141	0.0005	165	-	354	0.0000	177
133	euronovate-001	0.0255	459	0.0102	424	0.0517	245	0.0021	428
134	expasoft-001	0.0000	53	0.0000	94	-	436	0.0000	62
135	expasoft-002	0.0000	182	0.0000	4	0.0000	15	0.0000	43
136	f8-001	0.0003	427	0.0059	413	-	399	0.0035	444
137	f8-002	0.0000	400	0.0150	432	0.0685	263	0.0005	370
138	faceonlive-001	0.0000	392	0.0029	367	0.0481	244	0.0013	418
139	faceonlive-002	0.0002	424	0.0009	264	0.0075	82	0.0008	401
140	facephi-000	0.0000	27	0.0004	144	0.0090	92	0.0001	261
141	facesoft-000	0.0000	68	0.0000	71	-	379	0.0000	119
142	facetag-000	0.0000	7	0.0000	103	0.0000	52	0.0000	84
143	facetag-002	0.0000	24	0.0000	109	0.0000	46	0.0000	76
144	facex-001	0.0001	422	0.0360	446	-	363	0.0047	448
145	facex-002	0.0001	421	0.0360	447	0.2663	285	0.0047	449
146	farfaces-001	0.0000	378	0.0007	203	0.0061	77	0.0003	343
147	fiberhome-nanjing-003	0.0000	25	0.0004	151	-	409	0.0000	78
148	fiberhome-nanjing-004	0.0000	178	0.0004	150	-	322	0.0000	41
149	fimcore-000	0.0000	304	0.0008	239	0.0185	142	0.0001	209
150	firstcreditKZ-001	0.0000	337	0.0019	338	0.0321	215	0.0000	197
151	frpkauai-001	0.0000	341	0.0024	354	0.0360	226	0.0001	220
152	fujitsulab-002	0.0000	184	0.0009	249	-	319	0.0001	269
153	fujitsulab-003	0.0000	129	0.0008	227	0.0166	131	0.0001	257
154	g42-intellibrain-001	0.0000	29	0.0000	107	0.0000	47	0.0000	80
155	geo-002	0.0000	271	0.0015	319	0.0332	219	0.0001	204
156	geo-004	0.0000	284	0.0005	173	0.0138	111	0.0001	242
157	glory-004	0.0000	329	0.0020	344	0.0345	221	0.0001	264
158	glory-005	0.0000	325	0.0020	345	0.0345	222	0.0001	263
159	gorilla-007	0.0000	209	0.0009	268	0.0252	192	0.0001	232
160	gorilla-008	0.0000	267	0.0009	267	0.0259	198	0.0001	230
161	graymatics-001	0.0000	94	0.0010	269	0.0210	161	0.0001	280
162	griaule-000	0.0000	389	0.0026	358	0.0531	246	0.0004	368
163	griaule-001	0.0000	80	0.0012	307	0.0366	229	0.0000	149
164	hertasecurity-001	0.0000	77	0.0000	121	0.0000	63	0.0000	142
165	hertasecurity-002	0.0000	75	0.0000	84	0.0000	36	0.0000	141
166	hik-001	0.0000	123	0.0000	123	-	334	0.0000	17
167	hisign-001	0.0000	161	0.0000	17	0.0000	5	0.0000	54
168	hisign-002	0.0000	315	0.0006	187	0.0150	118	0.0001	267
169	hyperverge-002	0.0000	118	0.0008	226	0.0210	163	0.0002	325
170	hyperverge-003	0.0000	199	0.0008	224	0.0210	162	0.0002	326
171	hzailou-002	0.0000	371	0.0015	322	0.0424	238	0.0003	347
172	hzailou-003	0.0000	288	0.0004	145	0.0081	89	0.0002	292
173	icm-003	0.0000	172	0.0001	125	0.0023	68	0.0000	53
174	icm-004	0.0000	387	0.0033	379	0.0698	264	0.0006	389
								0.0010	410
								0.0026	335

Table 32: FTE is the proportion of failed template generation attempts. Failures can occur because the software throws an exception, or because the software electively refuses to process the input image. This would typically occur if a face is not detected. FTE is measured as the number of function calls that give EITHER a non-zero error code OR that give a “small” template. This is defined as one whose size is less than 0.3 times the median template size for that algorithm. This second rule is needed because some algorithms incorrectly fail to return a non-zero error code when template generation fails.

A hyphen “-” indicates the dataset was not produced.¹ The effects of FTE are included in the accuracy results of this report by regarding any template comparison involving a failed template to produce a low similarity score. Thus higher FTE results in higher FNMR and lower FMR.

	Algorithm	Failure to Enrol Rate ¹											
		APPLICATION	BORDER	KIOSK	MUGSHOT	VISA	WILD	SEC. 2.2	SEC. 2.3	SEC. 2.5	SEC. 2.4	SEC. 2.1	SEC. 2.6
175	icthtc-000	0.0001	420	0.0047	405	-	339	0.0028	440	0.0029	447	0.0086	371
176	id3-006	0.0000	336	0.0009	266	-	421	0.0004	357	0.0005	362	0.0008	292
177	id3-008	0.0000	145	0.0006	189	0.0184	139	0.0001	279	0.0004	200	0.0003	141
178	idemria-008	0.0000	70	0.0004	158	0.0078	87	0.0000	144	0.0003	176	0.0003	154
179	idemria-009	0.0000	195	0.0004	154	0.0077	84	0.0000	138	0.0003	179	0.0003	159
180	iit-002	0.0000	385	0.0021	347	-	376	0.0009	410	0.0005	374	0.0443	421
181	iit-003	0.0000	221	0.0008	240	-	455	0.0000	167	0.0004	207	0.0069	363
182	imds-software-001	0.0000	2	0.0000	106	0.0000	54	0.0000	81	0.0000	13	0.0000	55
183	imperial-000	0.0000	158	0.0000	32	-	342	0.0000	8	0.0000	90	0.0000	22
184	imperial-002	0.0000	30	0.0000	92	-	459	0.0000	64	0.0000	28	0.0000	73
185	incode-010	0.0000	316	0.0009	255	0.0255	195	0.0002	299	0.0004	231	0.0007	286
186	incode-011	0.0000	312	0.0009	254	0.0255	196	0.0002	300	0.0004	233	0.0007	287
187	infocert-001	0.0000	348	0.0059	414	0.0424	239	0.0001	236	0.0006	379	0.0018	324
188	innneflabs-000	0.0000	270	0.0024	353	-	336	0.0003	342	0.0005	359	0.0004	218
189	innovativetechnologyltd-001	0.0001	418	0.0050	407	-	448	0.0024	435	0.0025	443	0.0055	356
190	innovativetechnologyltd-002	0.0000	345	0.0046	401	-	291	0.0057	452	0.0005	360	0.0247	409
191	innovatrics-007	0.0000	207	0.0007	214	-	427	0.0001	206	0.0003	163	0.0003	160
192	innovatrics-008	0.0000	290	0.0009	259	0.0204	154	0.0000	175	0.0004	196	0.0003	184
193	insightface-001	0.0000	167	0.0000	22	0.0000	2	0.0000	48	0.0000	101	0.0000	30
194	insightface-003	0.0000	163	0.0000	14	0.0000	6	0.0000	56	0.0000	108	0.0000	33
195	inspur-000	0.0000	85	0.0000	78	0.0000	33	0.0000	112	0.0000	40	0.0000	82
196	intellicloudai-001	0.0000	95	0.0000	56	-	403	0.0000	102	0.0000	65	0.0001	120
197	intellicloudai-002	0.0000	45	0.0008	230	-	457	0.0000	166	0.0004	197	0.0012	310
198	intellifusion-001	0.0000	253	0.0005	169	-	407	0.0001	228	0.0003	184	0.0005	258
199	intellifusion-002	0.0000	97	0.0000	119	-	402	0.0000	126	0.0000	64	0.0001	121
200	intellivision-003	0.0000	254	0.0012	302	0.0308	211	0.0003	336	0.0004	341	0.0185	397
201	intellivision-004	0.0000	252	0.0011	290	0.0266	202	0.0002	327	0.0004	337	0.0179	395
202	intellivix-001	0.0000	149	0.0000	37	0.0000	23	0.0000	2	0.0000	85	0.0000	17
203	intellivix-002	0.0000	181	0.0009	265	0.0184	140	0.0000	42	0.0000	120	0.0000	44
204	intelresearch-004	0.0000	269	0.0006	181	-	333	0.0000	152	0.0004	223	0.0003	163
205	intelresearch-005	0.0000	240	0.0006	182	0.0144	114	0.0000	156	0.0004	219	0.0003	166
206	intema-000	0.0000	38	0.0005	161	0.0126	104	0.0000	189	0.0004	206	0.0003	153
207	intsysmsu-001	0.0000	128	0.0010	276	-	326	0.0001	247	0.0004	271	0.0004	228
208	intsysmsu-002	0.0000	52	0.0010	279	-	437	0.0001	249	0.0004	268	0.0004	231
209	ionetworks-000	0.0000	180	0.0016	326	0.0387	234	0.0004	351	0.0005	351	0.0004	238
210	iqface-000	0.0000	108	0.0000	61	-	389	0.0000	96	0.0000	57	0.0000	100
211	iqface-003	0.0000	382	0.0076	419	-	382	0.0006	385	0.0005	377	0.0069	362
212	irex-000	0.0000	350	0.0009	263	-	299	0.0000	184	0.0005	346	0.0003	179
213	isap-001	0.0000	132	0.0000	48	-	327	0.0000	23	0.0000	74	0.0000	4
214	isap-002	0.0000	196	0.0000	9	-	308	0.0000	36	0.0000	114	0.0000	40
215	isityou-000	0.0068	450	0.0316	443	-	324	0.0023	430	0.0010	408	0.0663	429
216	isystems-001	0.0000	391	0.0035	385	-	315	0.0010	412	0.0007	396	0.0128	383
217	isystems-002	0.0000	390	0.0035	386	-	361	0.0010	411	0.0007	395	0.0128	382
218	itm0-007	0.0000	20	0.0009	248	-	422	0.0003	349	0.0000	3	0.0004	208
219	itm0-008	0.0000	147	0.0135	429	0.1239	276	0.0024	434	0.0000	86	0.0836	431
220	ivacognitive-001	0.0000	320	0.0011	292	-	406	0.0001	222	0.0004	324	0.0011	302
221	iws-000	0.0005	435	0.0650	455	-	351	0.0024	432	0.0012	421	0.0936	438
222	jaakit-001	0.0008	440	0.0858	457	0.2713	286	0.0042	445	0.0021	439	0.1062	443
223	kakao-007	0.0000	166	0.0007	194	0.0165	130	0.0001	241	0.0004	225	0.0097	377
224	kakao-008	0.0000	176	0.0009	251	0.0209	160	0.0001	239	0.0004	228	0.0097	378
225	kakaipay-001	0.0000	308	0.0013	314	0.0322	216	0.0001	225	0.0004	326	0.0078	368
226	kasikornlabs-000	0.0000	395	0.0035	384	0.0713	265	0.0004	363	0.0012	424	0.0270	412
227	kasikornlabs-001	0.0001	419	0.0050	406	0.0885	271	0.0006	392	0.0035	451	0.0305	413
228	kedacom-000	0.0000	76	0.0000	83	-	372	0.0000	107	0.0000	37	0.0000	78
229	kiwitech-000	0.0000	306	0.0009	246	-	313	0.0004	359	0.0005	348	0.0004	241
230	kneron-003	0.0239	457	0.0306	441	-	297	0.0044	447	0.0016	433	0.1823	454
231	kneron-005	0.0000	394	0.0226	435	-	320	0.0006	382	0.0005	358	0.0097	376
232	knowutech-000	0.0000	203	0.0008	222	0.0215	170	0.0000	172	0.0004	279	0.0003	187

Table 33: FTE is the proportion of failed template generation attempts. Failures can occur because the software throws an exception, or because the software electively refuses to process the input image. This would typically occur if a face is not detected. FTE is measured as the number of function calls that give EITHER a non-zero error code OR that give a “small” template. This is defined as one whose size is less than 0.3 times the median template size for that algorithm. This second rule is needed because some algorithms incorrectly fail to return a non-zero error code when template generation fails.

A hyphen “-” indicates the dataset was not produced.¹ The effects of FTE are included in the accuracy results of this report by regarding any template comparison involving a failed template to produce a low similarity score. Thus higher FTE results in higher FNMR and lower FMR.

	Algorithm	Failure to Enrol Rate ¹							
		Name	APPLICATION	BORDER	KIOSK	MUGSHOT	VISA	WILD	
			SEC. 2.2	SEC. 2.3	SEC. 2.5	SEC. 2.4	SEC. 2.1	SEC. 2.6	
233	kookmin-002	0.0000	186	0.0000	1	-	318	0.0000	45
234	krungthai-002	0.0000	230	0.0005	164	0.0111	101	0.0002	312
235	kuke3d-001	0.0000	90	0.0000	57	0.0000	45	0.0000	101
236	kuke3d-002	0.0000	119	0.0000	44	0.0000	20	0.0000	28
237	lebentech-000	0.0042	444	0.0029	369	0.0252	191	0.0051	451
238	lemalabs-001	0.0000	54	0.0005	172	0.0141	112	0.0002	308
239	lineclova-001	0.0000	107	0.0000	62	0.0000	40	0.0000	95
240	lineclova-002	0.0000	152	0.0007	195	0.0181	137	0.0000	4
241	lookman-002	0.0000	61	0.0000	75	-	388	0.0000	115
242	lookman-004	0.0000	201	0.0000	6	-	310	0.0000	39
243	luxand-000	0.0000	169	0.0000	20	-	296	0.0000	50
244	mantra-000	0.0001	404	0.0041	396	0.0680	262	0.0003	341
245	maxvision-001	0.0000	59	0.0000	77	0.0000	37	0.0000	113
246	maxvision-002	0.0000	303	0.0009	244	0.0229	179	0.0002	289
247	megvii-005	0.0000	299	0.0010	270	0.0206	156	0.0002	318
248	megvii-006	0.0000	245	0.0010	272	0.0206	157	0.0002	319
249	meituan-001	0.0000	227	0.0014	318	0.0295	208	0.0001	252
250	meituan-002	0.0000	241	0.0013	312	0.0251	190	0.0001	254
251	meiya-001	0.0000	388	0.0028	364	-	456	0.0004	364
252	mendaxiatech-000	0.0000	266	0.0010	271	0.0206	155	0.0002	321
253	metsakuurcompany-001	0.0000	66	0.0011	288	0.0208	159	0.0002	317
254	metsakuurcompany-002	0.0000	121	0.0000	43	0.0000	19	0.0000	30
255	microfocus-001	0.0001	416	0.0053	411	-	304	0.0008	403
256	microfocus-002	0.0001	417	0.0053	410	-	312	0.0008	402
257	minivision-000	0.0000	41	0.0000	88	-	453	0.0000	68
258	mobai-000	0.0000	359	0.0114	426	-	309	0.0003	344
259	mobai-001	0.0000	332	0.0040	392	-	314	0.0001	260
260	mobabl-001	0.0000	383	0.0052	409	0.0678	260	0.0002	294
261	mobabl-003	0.0000	393	0.0029	368	0.0633	253	0.0002	314
262	mobipintech-000	0.0000	73	0.0000	86	0.0000	35	0.0000	105
263	moreidian-000	0.0000	307	0.0009	245	-	311	0.0004	360
264	mukh-001	0.0000	40	0.0010	277	0.0154	122	0.0001	258
265	multimodality-000	0.0000	46	0.0000	99	0.0000	55	0.0000	57
266	multimodality-001	0.0000	8	0.0009	243	0.0259	199	0.0000	86
267	mvision-001	0.0000	57	0.0000	93	-	441	0.0000	63
268	nazhiai-000	0.0000	71	0.0000	69	-	377	0.0000	121
269	neosystems-004	0.0000	139	0.0000	27	0.0000	29	0.0000	13
271	netbridge-tech-001	0.0000	113	0.0000	46	-	340	0.0000	25
272	netbridge-tech-002	0.0000	78	0.0000	82	-	371	0.0000	108
273	neurotechnology-013	0.0000	160	0.0008	241	0.0185	141	0.0000	132
274	neurotechnology-015	0.0000	43	0.0004	146	0.0082	90	0.0000	70
275	nhn-002	0.0000	35	0.0004	159	0.0091	93	0.0000	163
276	nhn-003	0.0000	344	0.0000	16	0.0000	4	0.0001	284
277	nodeflux-002	0.0000	301	0.0261	438	-	316	0.0008	400
278	notiontag-001	0.0000	102	0.0000	65	-	401	0.0027	438
279	notiontag-002	0.0000	28	0.0000	108	0.0000	48	0.0000	79
280	nsensecorp-003	0.0000	106	0.0000	124	0.0002	64	0.0000	154
281	nsensecorp-004	0.0406	460	0.0035	383	0.0181	136	0.0016	423
282	ntechlab-011	0.0000	173	0.0003	130	0.0057	73	0.0000	188
283	ntechlab-012	0.0000	12	0.0003	131	0.0057	74	0.0000	191
284	omface-000	0.0000	144	0.0000	25	0.0000	28	0.0000	15
285	omface-001	0.0000	44	0.0000	117	0.0000	62	0.0000	71
286	omnigarde-001	0.0000	206	0.0008	218	0.0213	165	0.0000	161
287	omnigarde-002	0.0000	281	0.0008	217	0.0213	164	0.0000	157
288	openface-001	0.0000	367	0.0104	425	0.0668	255	0.0004	356
289	oz-003	0.0000	153	0.0002	128	0.0042	70	0.0000	127
290	oz-004	0.0000	372	0.0003	135	0.0041	69	0.0000	135

Table 34: FTE is the proportion of failed template generation attempts. Failures can occur because the software throws an exception, or because the software electively refuses to process the input image. This would typically occur if a face is not detected. FTE is measured as the number of function calls that give EITHER a non-zero error code OR that give a “small” template. This is defined as one whose size is less than 0.3 times the median template size for that algorithm. This second rule is needed because some algorithms incorrectly fail to return a non-zero error code when template generation fails.

A hyphen “-” indicates the dataset was not produced. ¹The effects of FTE are included in the accuracy results of this report by regarding any template comparison involving a failed template to produce a low similarity score. Thus higher FTE results in higher FNMR and lower FMR.

	Algorithm	Failure to Enrol Rate ¹											
		APPLICATION		BORDER		KIOSK		MUGSHOT		VISA			
Name	SEC. 2.2	SEC. 2.3	SEC. 2.5	SEC. 2.4	SEC. 2.1	SEC. 2.6				WILD			
291	palit-000	0.0000	247	0.0005	167	0.0134	110	0.0002	304	0.0004	218	0.0004	232
292	palit-001	0.0000	298	0.0007	216	0.0201	153	0.0002	303	0.0004	226	0.0004	230
293	pangiam-000	0.0000	87	0.0021	349	0.0364	227	0.0001	207	0.0005	347	0.0095	375
294	papago-001	0.0000	333	0.0008	225	0.0159	128	0.0002	328	0.0004	249	0.0190	398
295	papsav1923-001	0.0000	228	0.0007	206	-	446	0.0001	244	0.0002	139	0.0005	251
296	papsav1923-002	0.0000	295	0.0018	335	0.0268	203	0.0000	178	0.0004	284	0.0004	217
297	paravision-008	0.0000	188	0.0010	274	0.0201	152	0.0001	234	0.0004	201	0.0003	185
298	paravision-010	0.0000	200	0.0010	273	0.0201	151	0.0001	235	0.0004	202	0.0003	186
299	pensees-001	0.0000	237	0.0000	76	-	381	0.0000	114	0.0000	43	0.0000	89
300	pixelall-008	0.0000	11	0.0008	233	0.0247	187	0.0000	88	0.0000	16	0.0000	63
301	pixelall-009	0.0000	198	0.0000	7	0.0000	9	0.0000	38	0.0000	116	0.0000	38
302	psl-010	0.0000	272	0.0004	149	0.0095	94	0.0000	123	0.0004	194	0.0003	155
303	psl-011	0.0000	257	0.0003	132	0.0063	79	0.0000	125	0.0003	177	0.0003	152
304	ptakuratsatu-000	0.0000	268	0.0007	213	-	341	0.0001	205	0.0003	166	0.0003	156
305	pxl-001	0.0000	401	0.0044	399	-	398	0.0005	373	0.0022	441	0.0323	416
306	pyramid-000	0.0001	413	0.0041	395	-	424	0.0005	372	0.0007	397	0.0015	318
307	qazbs-000	0.0000	58	0.0009	252	0.0265	201	0.0000	150	0.0004	244	0.0003	191
308	qnap-001	0.0000	255	0.0000	122	0.0002	65	0.0000	183	0.0001	130	0.0001	123
309	qnap-002	0.0000	384	0.0033	373	0.0761	267	0.0004	354	0.0002	132	0.0017	321
310	quantasoft-003	0.0000	355	0.0015	323	0.0355	224	0.0005	371	0.0006	386	0.0088	373
311	rankone-012	0.0000	192	0.0000	11	0.0000	11	0.0000	34	0.0000	111	0.0000	36
312	rankone-013	0.0000	21	0.0005	162	0.0126	105	0.0000	145	0.0003	146	0.0003	145
313	realnetworks-006	0.0000	291	0.0002	129	0.0045	71	0.0000	124	0.0002	142	0.0003	151
314	realnetworks-007	0.0000	261	0.0013	315	0.0425	240	0.0000	131	0.0004	253	0.0004	235
315	regula-000	0.0000	151	0.0000	36	0.0000	25	0.0000	3	0.0000	88	0.0000	14
316	regula-001	0.0000	82	0.0000	80	0.0000	31	0.0000	110	0.0000	38	0.0000	84
317	remarkai-001	0.0000	47	0.0000	98	-	445	0.0000	58	0.0000	19	0.0000	113
318	remarkai-003	0.0000	223	0.0007	202	0.0187	143	0.0000	181	0.0004	211	0.0004	222
319	rendip-000	0.0000	340	0.0016	325	0.0293	207	0.0002	301	0.0004	338	0.0013	316
320	revealmedia-005	0.0000	349	0.0007	209	0.0189	145	0.0009	409	0.0004	343	0.0076	367
321	revealmedia-006	0.0000	89	0.0009	260	0.0238	185	0.0001	255	0.0004	295	0.0004	246
322	rokid-000	0.0000	179	0.0072	417	-	321	0.0001	240	0.0005	357	0.0354	419
323	rokid-001	0.0000	110	0.0013	311	-	393	0.0000	97	0.0000	60	0.0007	284
324	s1-005	0.0000	93	0.0004	152	0.0120	103	0.0001	221	0.0002	134	0.0050	354
325	s1-006	0.0000	164	0.0003	133	0.0074	81	0.0001	214	0.0002	136	0.0050	355
326	saffe-001	0.0000	134	0.0000	30	-	359	0.0000	10	0.0000	94	0.0000	25
327	saffe-002	0.0000	122	0.0000	41	-	337	0.0000	31	0.0000	79	0.0000	13
328	samsungsds-001	0.0000	92	0.0005	168	0.0146	115	0.0001	238	0.0003	185	0.0003	192
329	samsungsds-002	0.0000	105	0.0004	153	0.0119	102	0.0001	237	0.0003	173	0.0003	173
330	samtech-001	0.0001	412	0.0032	372	-	289	0.0004	361	0.0008	399	0.0013	314
331	scanovate-002	0.0000	326	0.0018	334	-	346	0.0000	198	0.0004	334	0.0008	291
332	scanovate-003	0.0000	324	0.0233	436	0.3371	288	0.0006	386	0.0004	342	0.0007	285
333	sdc-000	0.0000	399	0.0035	382	0.0678	261	0.0005	379	0.0011	417	0.0028	338
334	securifai-004	0.0000	162	0.0000	15	0.0000	7	0.0000	55	0.0000	109	0.0000	32
335	securifai-005	0.0000	62	0.0000	74	0.0000	39	0.0000	116	0.0000	46	0.0000	86
336	sensetime-006	0.0000	86	0.0004	147	0.0106	97	0.0000	165	0.0003	165	0.0002	134
337	sensetime-007	0.0000	112	0.0004	148	0.0106	96	0.0000	164	0.0003	164	0.0002	133
338	sertis-000	0.0000	55	0.0007	208	-	435	0.0000	203	0.0004	230	0.0004	210
339	sertis-002	0.0000	32	0.0007	198	0.0152	119	0.0000	196	0.0004	232	0.0004	204
340	seventhSense-001	0.0000	208	0.0006	192	0.0184	138	0.0001	210	0.0004	266	0.0003	168
341	seventhSense-002	0.0000	130	0.0003	143	0.0076	83	0.0000	202	0.0004	193	0.0003	150
342	shaman-000	0.0000	84	0.0000	79	-	366	0.0000	111	0.0000	41	0.0000	81
343	shaman-001	0.0000	171	0.0000	18	-	290	0.0000	52	0.0000	105	0.0000	108
344	shu-002	0.0000	327	0.0010	281	-	307	0.0005	369	0.0004	322	0.0007	282
345	shu-003	0.0000	34	0.0007	196	-	458	0.0001	211	0.0003	162	0.0004	244
346	siat-002	0.0000	233	0.0012	304	-	442	0.0000	176	0.0004	250	0.0048	352
347	siat-005	0.0000	19	0.0000	111	0.0000	59	0.0000	74	0.0000	4	0.0000	48
348	sjtu-003	0.0000	60	0.0005	175	-	383	0.0000	192	0.0003	156	0.0003	171

Table 35: FTE is the proportion of failed template generation attempts. Failures can occur because the software throws an exception, or because the software electively refuses to process the input image. This would typically occur if a face is not detected. FTE is measured as the number of function calls that give EITHER a non-zero error code OR that give a “small” template. This is defined as one whose size is less than 0.3 times the median template size for that algorithm. This second rule is needed because some algorithms incorrectly fail to return a non-zero error code when template generation fails.

A hyphen “-” indicates the dataset was not produced.¹ The effects of FTE are included in the accuracy results of this report by regarding any template comparison involving a failed template to produce a low similarity score. Thus higher FTE results in higher FNMR and lower FMR.

	Algorithm	Failure to Enrol Rate ¹											
		APPLICATION	BORDER	KIOSK	MUGSHOT	VISA	WILD	SEC. 2.2	SEC. 2.3	SEC. 2.5	SEC. 2.4	SEC. 2.1	SEC. 2.6
349	sjtu-004	0.0000	193	0.0000	10	0.0000	12	0.0000	35	0.0003	154	0.0000	37
350	sktelecom-000	0.0000	293	0.0008	232	0.0190	146	0.0000	187	0.0004	283	0.0013	313
351	smartbiometrik-001	0.0005	432	0.0649	454	0.2147	284	0.0017	424	0.0008	400	0.0123	381
352	smartengines-000	0.0066	449	0.0150	431	0.1656	277	0.0022	429	0.0013	426	0.0826	430
353	smartengines-001	0.0003	429	0.0073	418	0.0714	266	0.0007	394	0.0005	363	0.0169	393
354	smartvist-000	0.0000	36	0.0026	357	0.0357	225	0.0002	288	0.0011	415	0.0152	388
355	smilart-002	0.0000	396	0.0036	387	-	353	-	459	0.0011	414	-	460
356	smilart-003	0.0003	428	0.0100	423	-	298	0.0014	419	0.0013	428	0.0555	427
357	sodec-000	0.0000	10	0.0000	101	0.0000	49	0.0000	87	0.0000	17	0.0000	62
358	sqisoft-001	0.0000	79	0.0003	141	0.0078	85	0.0000	143	0.0003	182	0.0003	149
359	sqisoft-002	0.0000	1	0.0003	138	0.0078	86	0.0000	146	0.0003	187	0.0003	148
360	stachu-000	0.0000	37	0.0000	90	-	463	0.0000	66	0.0000	30	0.0000	71
361	starhybrid-001	0.0001	415	0.0033	378	-	444	0.0009	408	0.0023	442	0.0044	347
362	sukshi-000	0.0000	14	0.0000	100	0.0000	50	0.0000	89	0.0000	18	0.0000	61
363	suprema-002	0.0000	334	0.0010	285	0.0271	205	0.0002	296	0.0004	238	0.0005	256
364	suprema-003	0.0000	222	0.0008	235	0.0231	181	0.0000	139	0.0004	234	0.0003	175
365	supremaid-001	0.0000	215	0.0020	343	0.0330	218	0.0001	250	0.0004	330	0.0045	348
366	supremaid-002	0.0000	242	0.0020	341	0.0330	217	0.0001	251	0.0004	333	0.0045	350
367	surrey-cvssp-000	0.0000	96	0.0000	55	0.0000	43	0.0000	103	0.0000	66	0.0000	105
368	surrey-cvssp-001	0.0173	456	0.0007	199	0.0179	135	0.0011	415	0.0015	430	0.0038	345
369	synesis-006	0.0000	64	0.0003	142	-	387	0.0000	193	0.0003	147	0.0002	132
370	synesis-007	0.0000	287	0.0013	310	-	306	0.0002	316	0.0004	256	0.0005	249
371	synology-000	0.0000	39	0.0000	89	-	462	0.0000	67	0.0000	29	0.0000	72
372	synology-002	0.0000	100	0.0000	67	-	395	0.0000	91	0.0000	52	0.0000	97
373	sztu-000	0.0000	51	0.0000	95	-	438	0.0000	61	0.0000	25	0.0000	69
374	sztu-001	0.0000	104	0.0000	63	0.0000	42	0.0000	94	0.0000	54	0.0000	95
375	t4isb-000	0.0000	98	0.0000	54	0.0000	44	0.0000	104	0.0000	67	0.0000	104
376	tech5-004	0.0000	263	0.0008	223	-	390	0.0003	335	0.0004	328	0.0006	269
377	tech5-005	0.0000	300	0.0007	215	-	325	0.0000	159	0.0004	299	0.0049	353
378	techsign-000	0.0007	438	0.0334	444	0.2093	279	0.0020	427	0.0011	413	0.0170	394
379	techsign-001	0.0000	224	0.0008	242	0.0253	193	0.0002	306	0.0004	258	0.0004	225
380	tevian-007	0.0000	302	0.0015	324	0.0429	241	0.0002	311	0.0004	285	0.0008	290
381	tevian-008	0.0000	229	0.0006	178	0.0109	100	0.0000	153	0.0003	161	0.0004	226
382	tiger-005	0.0000	217	0.0009	262	0.0194	150	0.0001	231	0.0004	241	0.0004	239
383	tiger-006	0.0000	318	0.0011	294	0.0396	235	0.0001	278	0.0004	340	0.0009	295
384	tinkoff-001	0.0000	309	0.0008	231	0.0171	132	0.0001	271	0.0004	240	0.0014	317
385	tongyi-005	0.0000	101	0.0000	66	-	394	0.0000	92	0.0000	51	0.0000	98
386	toppanidgate-000	0.0000	279	0.0008	228	0.0232	182	0.0004	352	0.0004	273	0.0005	262
387	toshiba-004	0.0000	140	0.0000	26	0.0000	27	0.0000	14	0.0000	98	0.0000	27
388	toshiba-006	0.0000	211	0.0004	155	0.0050	72	0.0001	274	0.0003	159	0.0003	146
389	touchlessid-000	0.0042	445	0.0133	428	0.2009	278	0.0018	426	0.0032	450	0.0457	422
390	touchlessid-001	0.0000	23	0.0036	388	0.0923	273	0.0000	77	0.0000	7	0.0000	54
391	trueface-002	0.0000	321	0.0046	404	-	397	0.0003	331	0.0005	369	0.0330	417
392	trueface-003	0.0000	322	0.0046	403	0.0397	236	0.0003	332	0.0005	370	0.0330	418
393	tuputech-000	0.0003	430	0.0116	427	-	451	-	461	0.0081	456	0.6383	458
394	turingtechvip-001	0.0001	408	0.0007	210	0.0061	78	0.0007	393	0.0006	381	0.0057	358
395	turingtechvip-002	0.0001	407	0.0017	331	0.0097	95	0.0007	395	0.0006	380	0.0057	357
396	turkcell-000	0.0110	454	0.0234	437	0.0350	223	0.0103	454	0.0306	461	0.7213	459
397	twface-000	0.0000	131	0.0000	49	0.0000	16	0.0000	22	0.0000	73	0.0000	6
398	twface-001	0.0000	127	0.0000	50	0.0000	18	0.0000	21	0.0000	72	0.0000	1
399	ulsee-001	0.0000	125	0.0000	52	-	331	0.0000	19	0.0000	68	0.0001	114
400	ultinous-000	-	462	-	461	-	380	-	463	0.0003	169	-	463
401	ultinous-001	-	461	-	463	-	439	-	462	0.0003	168	-	462
402	uluface-002	0.0000	159	0.0000	31	-	345	0.0000	9	0.0000	93	0.0000	20
403	uluface-003	0.0000	9	0.0001	127	-	429	0.0002	290	0.0002	137	0.0244	408
404	unissey-001	0.0000	48	0.0000	97	0.0000	56	0.0000	59	0.0000	22	0.0000	64
405	unissey-002	0.0000	197	0.0000	8	0.0000	8	0.0000	37	0.0000	113	0.0000	41
406	upc-001	0.0000	369	0.0003	136	-	384	0.0003	334	0.0003	175	0.0011	300

Table 36: FTE is the proportion of failed template generation attempts. Failures can occur because the software throws an exception, or because the software electively refuses to process the input image. This would typically occur if a face is not detected. FTE is measured as the number of function calls that give EITHER a non-zero error code OR that give a “small” template. This is defined as one whose size is less than 0.3 times the median template size for that algorithm. This second rule is needed because some algorithms incorrectly fail to return a non-zero error code when template generation fails.

A hyphen “-” indicates the dataset was not produced.¹ The effects of FTE are included in the accuracy results of this report by regarding any template comparison involving a failed template to produce a low similarity score. Thus higher FTE results in higher FNMR and lower FMR.

	Algorithm	Failure to Enrol Rate ¹							
		APPLICATION	BORDER	KIOSK	MUGSHOT	VISA	WILD	SEC. 2.1	SEC. 2.6
	Name	SEC. 2.2	SEC. 2.3	SEC. 2.5	SEC. 2.4	SEC. 2.1	SEC. 2.6	SEC. 2.1	SEC. 2.6
407	uxlabs-001	0.0000	115	0.0000	45	0.0000	21	0.0000	26
408	vcog-002	-	463	-	460	-	300	-	460
409	vd-002	0.0000	18	0.0000	112	1.0000	423	0.0000	73
410	vd-003	0.0001	409	0.0041	394	0.0676	258	0.0030	441
411	veridas-007	0.0000	364	0.0026	356	0.0595	250	0.0001	265
412	veridas-008	0.0000	365	0.0026	355	0.0595	249	0.0001	266
413	veridium-000	0.0061	448	0.5956	459	0.2889	287	0.0050	450
414	verigram-000	0.0000	339	0.0068	416	0.0822	270	0.0003	350
415	verigram-001	0.0000	310	0.0003	139	0.0060	75	0.0002	315
416	verihubs-inteligensia-000	0.0000	297	0.0029	365	0.0669	256	0.0001	217
417	verihubs-inteligensia-001	0.0000	283	0.0029	366	0.0669	257	0.0001	216
418	verijelas-000	0.0000	250	0.0023	352	0.0375	233	0.0004	367
419	via-000	0.0000	124	0.0000	53	-	332	0.0000	18
420	via-001	0.0000	137	0.0000	29	-	364	0.0000	11
421	videmo-001	0.0000	357	0.0170	433	0.0332	220	0.0010	413
422	videmo-002	0.0000	67	0.0006	188	0.0189	144	0.0001	246
423	videonetics-001	0.0004	431	0.0309	442	-	410	0.0015	422
424	videonetics-002	0.0000	342	0.0459	451	-	362	0.0006	388
425	viettelhightech-000	0.0000	373	0.0019	337	0.0368	230	0.0007	396
426	vigilantsolutions-010	0.0000	354	0.0028	362	0.0609	252	0.0001	224
427	vigilantsolutions-011	0.0000	356	0.0028	361	0.0609	251	0.0001	223
428	vinai-000	0.0000	146	0.0000	24	-	356	0.0000	16
429	vinbigdata-001	0.0000	81	0.0000	81	0.0000	32	0.0000	109
430	vinbigdata-002	0.0000	31	0.0015	321	0.0250	189	0.0000	171
431	vion-000	0.0050	446	0.0392	450	-	428	0.0130	456
432	visage-000	0.0000	375	0.0054	412	-	360	0.0009	406
433	visionbox-001	0.0000	398	0.0033	376	-	349	0.0005	377
434	visionbox-002	0.0000	26	0.0017	327	0.0270	204	0.0000	174
435	visionlabs-010	0.0000	346	0.0009	250	-	412	0.0001	275
436	visionlabs-011	0.0000	135	0.0006	185	0.0156	123	0.0001	227
437	visteam-003	0.0000	202	0.0010	283	0.0225	177	0.0001	212
438	visteam-004	0.0000	273	0.0010	282	0.0225	174	0.0001	256
439	vixvizion-005	0.0000	63	0.0000	73	0.0000	38	0.0000	117
440	vixvizion-006	0.0000	165	0.0000	23	0.0000	3	0.0000	47
441	vnpt-004	0.0000	235	0.0006	180	0.0160	129	0.0002	295
442	vnpt-005	0.0000	157	0.0006	176	0.0154	121	0.0002	305
443	vocord-009	0.0000	251	0.0006	184	-	405	0.0001	282
444	vocord-010	0.0000	323	0.0005	170	0.0141	113	0.0002	307
445	vts-000	0.0000	338	0.0011	291	-	386	0.0001	283
446	vts-001	0.0000	13	0.0003	134	0.0073	80	0.0000	140
447	wicket-000	0.0000	204	0.0009	247	0.0260	200	0.0000	148
448	winsense-001	0.0000	69	0.0000	70	-	378	0.0000	120
449	winsense-002	0.0000	187	0.0000	2	-	317	0.0000	46
450	wiseai-001	0.0001	405	0.0137	430	0.0768	268	0.0018	425
451	wuhantianyu-001	0.0000	194	0.0007	200	0.0159	126	0.0001	208
452	x-laboratory-000	0.0247	458	0.0000	40	-	350	0.0005	376
453	x-laboratory-001	0.0000	244	0.0012	301	-	373	0.0001	268
454	xforwardai-001	0.0000	292	0.0007	211	-	293	0.0003	338
455	xforwardai-002	0.0000	277	0.0007	212	-	355	0.0003	337
456	xm-000	0.0000	5	0.0007	197	-	431	0.0001	213
457	yisheng-004	0.0002	425	-	462	-	454	0.0013	417
458	yitu-003	0.0000	50	0.0000	96	-	449	0.0009	407
459	yoonik-002	0.0000	313	0.0010	278	0.0284	206	0.0003	330
460	yoonik-003	0.0000	330	0.0009	257	0.0214	167	0.0002	293
461	ytu-000	0.0000	280	0.0010	287	-	352	0.0002	320
462	yuan-004	0.0000	6	0.0000	102	0.0000	51	0.0000	85
463	yuan-005	0.0000	265	0.0005	166	0.0134	109	0.0002	302

Table 37: FTE is the proportion of failed template generation attempts. Failures can occur because the software throws an exception, or because the software electively refuses to process the input image. This would typically occur if a face is not detected. FTE is measured as the number of function calls that give EITHER a non-zero error code OR that give a “small” template. This is defined as one whose size is less than 0.3 times the median template size for that algorithm. This second rule is needed because some algorithms incorrectly fail to return a non-zero error code when template generation fails.

A hyphen “-” indicates the dataset was not produced.¹ The effects of FTE are included in the accuracy results of this report by regarding any template comparison involving a failed template to produce a low similarity score. Thus higher FTE results in higher FNMR and lower FMR.

3.4 Recognition accuracy

Core algorithm accuracy is stated via:

▷ **Cooperative subjects**

- The summary table of Figure 29;
- The visa image DETs of Figure 86;
- The mugshot DETs of Figure 110;
- The mugshot ageing profiles of Figure 355;
- The human-difficult pairs of Figure 39

▷ **Non-cooperative subjects**

- The photojournalism DET of Figure 130

Figure 287 shows dependence of false match rate on algorithm score threshold. This allows a deployer to set a threshold to target a particular false match rate appropriate to the security objectives of the application.

Figure 239 likewise shows FMR(T) but for mugshots, and specially four subsets of the population.

Note that in both the mugshot and visa sets false match rates vary with the ethnicity, age, and sex, of the enrollee and impostor. For example figure 152 summarizes FMR for impostors paired from four groups black females, black males, white females, white males.

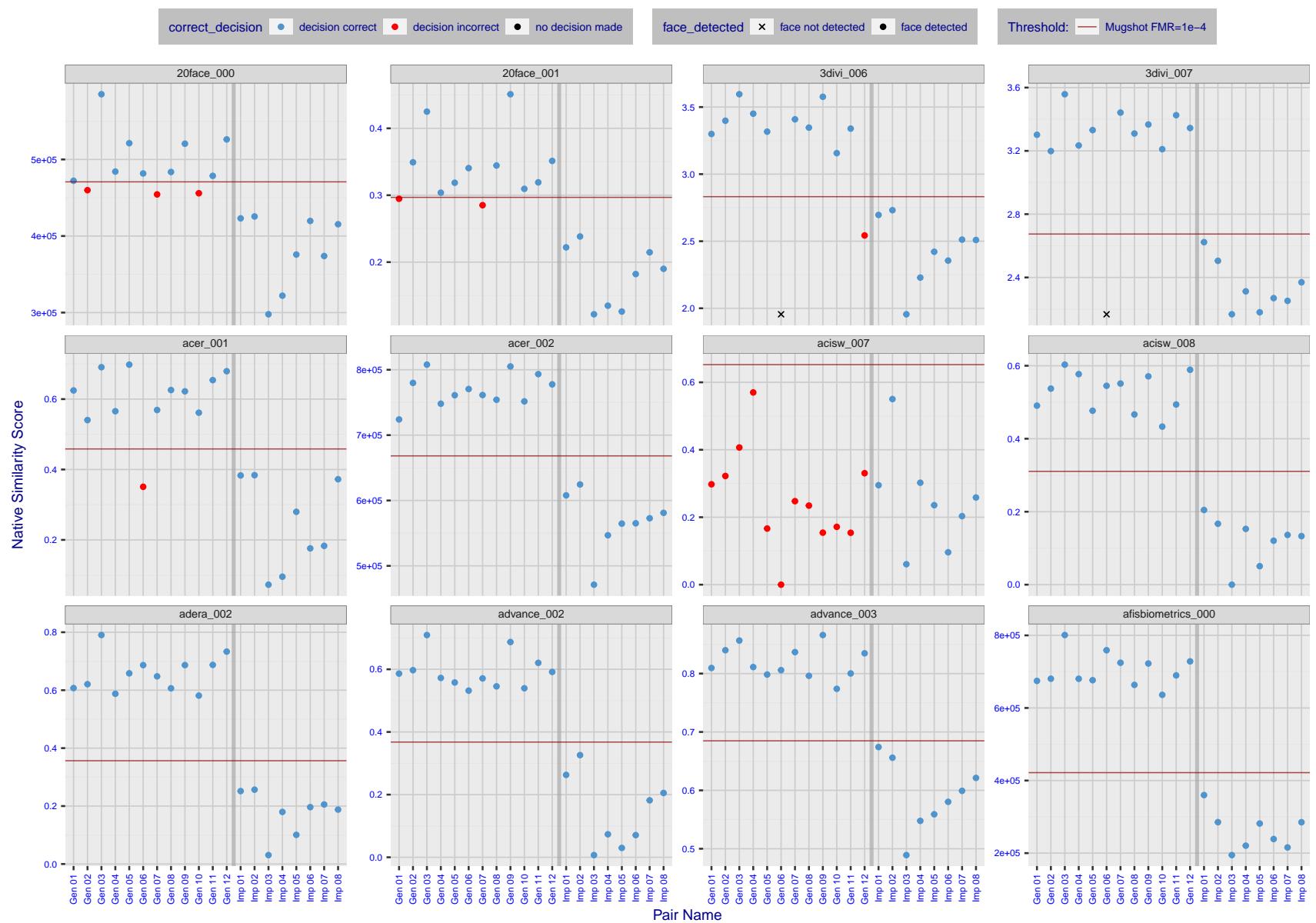


Figure 4: The figure shows algorithms' similarity scores for 12 genuine and 8 impostor image pairs used in a May 2018 paper by Phillips et al. ([1]). The threshold (red horizontal line) is a value calibrated to give $FMR = 0.0001$ on mugshot images. Points above the threshold correspond to pairs determined to be genuine, and points below the threshold correspond to pairs determined to be impostors. If the determined class (genuine or impostor) matches the real class, points will be blue; if not, red. An X represents face detection failure in either of the images in the pair. Note that the sample size ($n=20$) is small, and the figure may change substantially if larger or different sets are used. The images can be viewed on p. 13 of the [Appendix](#), where Gen 01 corresponds to Same-Identity Pair 1, Gen 02 corresponds to Same-Identity Pair 2, and so on.

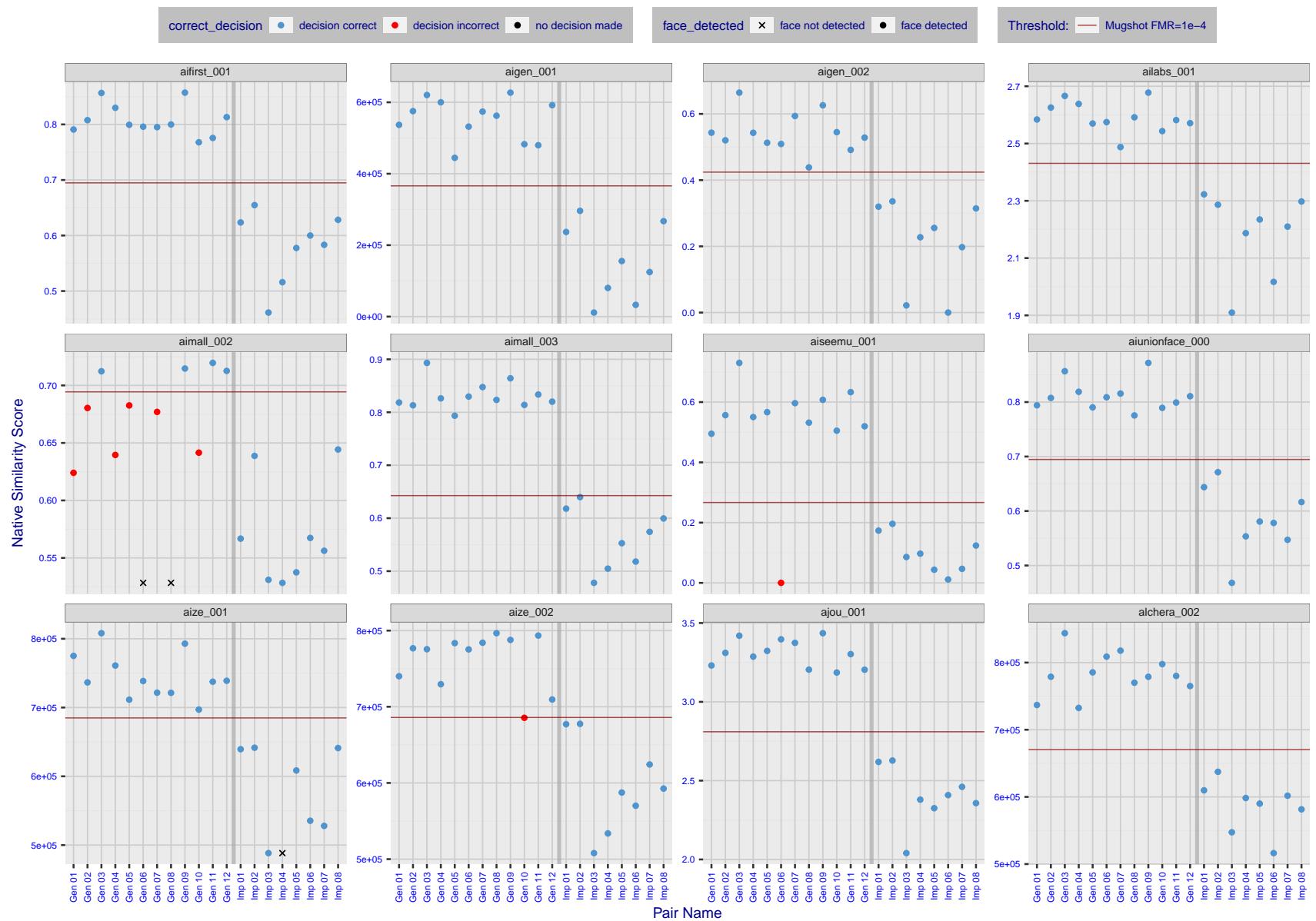


Figure 5: The figure shows algorithms' similarity scores for 12 genuine and 8 impostor image pairs used in a May 2018 paper by Phillips et al. ([1]). The threshold (red horizontal line) is a value calibrated to give $FMR = 0.0001$ on mugshot images. Points above the threshold correspond to pairs determined to be genuine, and points below the threshold correspond to pairs determined to be impostors. If the determined class (genuine or impostor) matches the real class, points will be blue; if not, red. An X represents face detection failure in either of the images in the pair. Note that the sample size ($n=20$) is small, and the figure may change substantially if larger or different sets are used. The images can be viewed on p. 13 of the Appendix, where Gen 01 corresponds to Same-Identity Pair 1, Gen 02 corresponds to Same-Identity Pair 2, and so on.

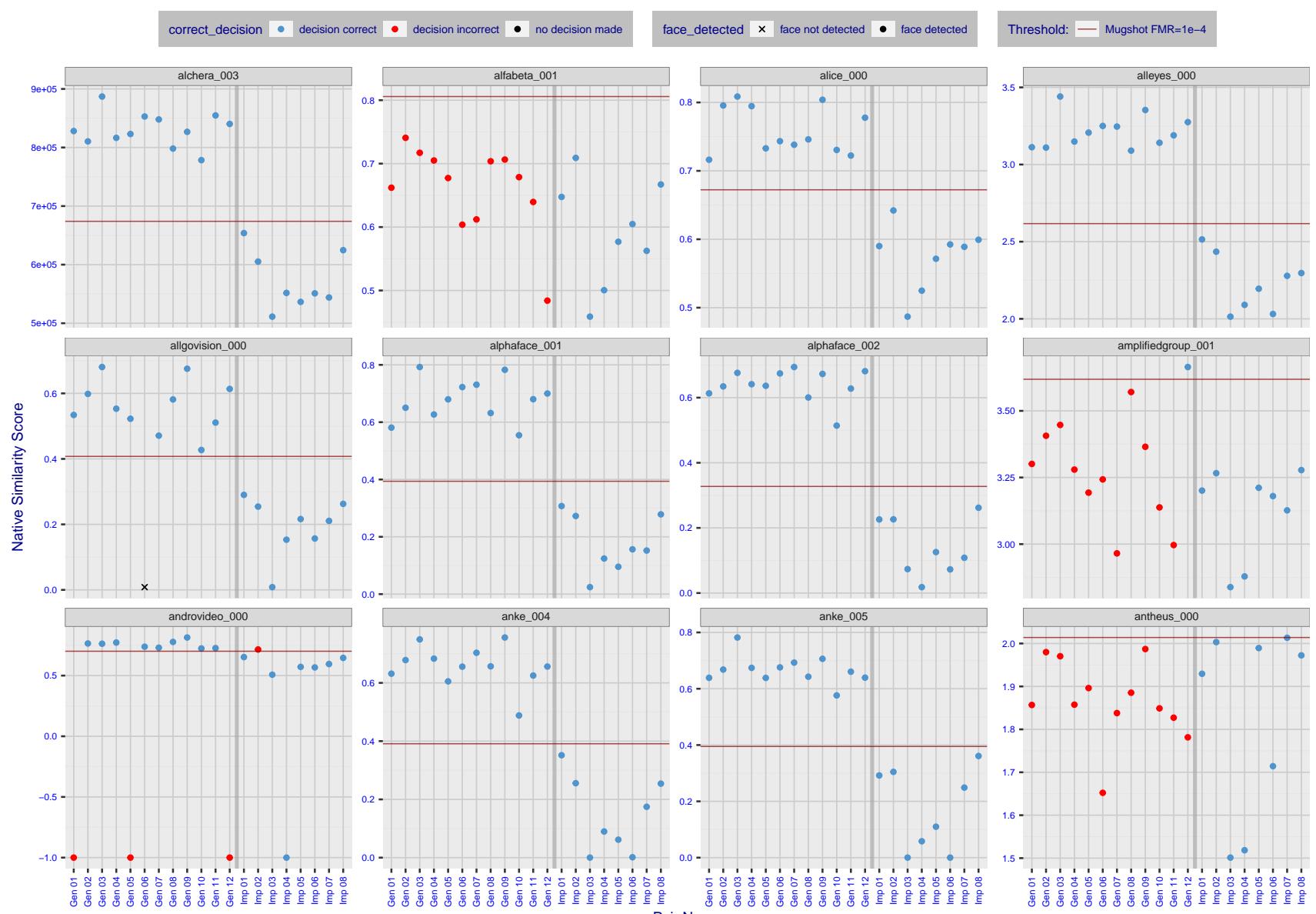


Figure 6: The figure shows algorithms' similarity scores for 12 genuine and 8 impostor image pairs used in a May 2018 paper by Phillips et al. ([1]). The threshold (red horizontal line) is a value calibrated to give $FMR = 0.0001$ on mugshot images. Points above the threshold correspond to pairs determined to be genuine, and points below the threshold correspond to pairs determined to be impostors. If the determined class (genuine or impostor) matches the real class, points will be blue; if not, red. An X represents face detection failure in either of the images in the pair. Note that the sample size ($n=20$) is small, and the figure may change substantially if larger or different sets are used. The images can be viewed on p. 13 of the Appendix, where Gen 01 corresponds to Same-Identity Pair 1, Gen 02 corresponds to Same-Identity Pair 2, and so on.

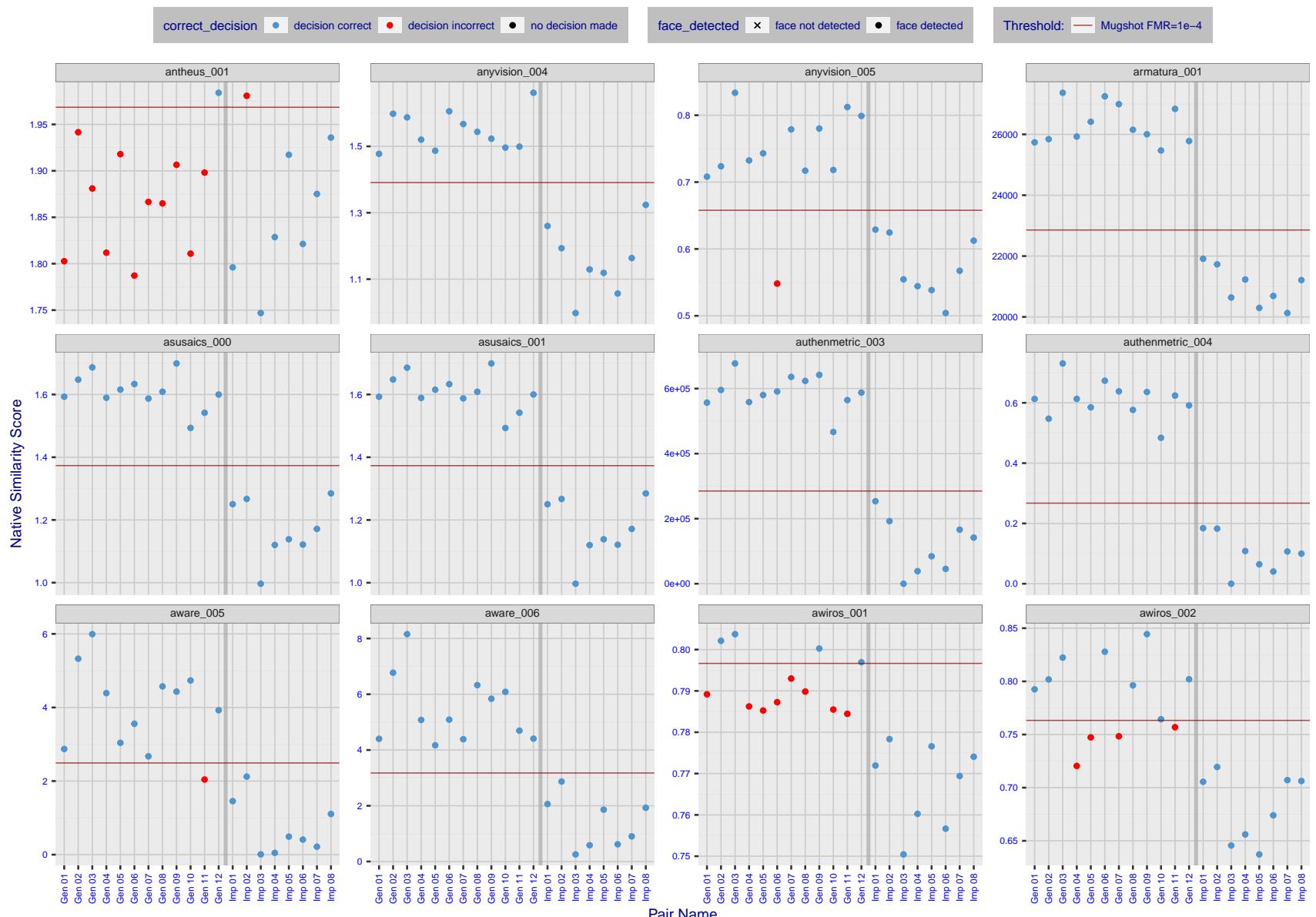


Figure 7: The figure shows algorithms' similarity scores for 12 genuine and 8 impostor image pairs used in a May 2018 paper by Phillips et al. ([1]). The threshold (red horizontal line) is a value calibrated to give $FMR = 0.0001$ on mugshot images. Points above the threshold correspond to pairs determined to be genuine, and points below the threshold correspond to pairs determined to be impostors. If the determined class (genuine or impostor) matches the real class, points will be blue; if not, red. An X represents face detection failure in either of the images in the pair. Note that the sample size ($n=20$) is small, and the figure may change substantially if larger or different sets are used. The images can be viewed on p. 13 of the Appendix, where Gen 01 corresponds to Same-Identity Pair 1, Gen 02 corresponds to Same-Identity Pair 2, and so on.

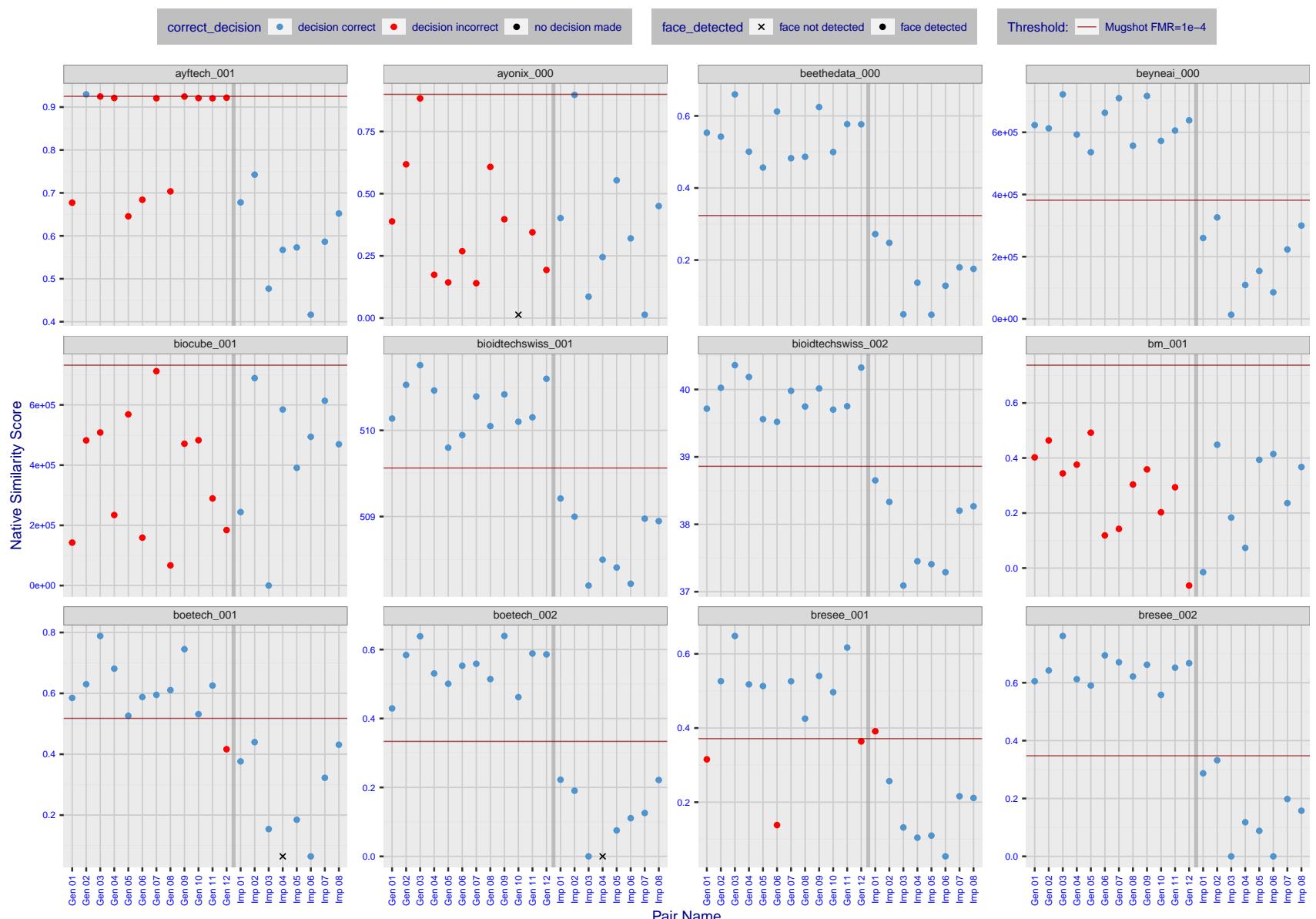


Figure 8: The figure shows algorithms' similarity scores for 12 genuine and 8 impostor image pairs used in a May 2018 paper by Phillips et al. ([1]). The threshold (red horizontal line) is a value calibrated to give $FMR = 0.0001$ on mugshot images. Points above the threshold correspond to pairs determined to be genuine, and points below the threshold correspond to pairs determined to be impostors. If the determined class (genuine or impostor) matches the real class, points will be blue; if not, red. An X represents face detection failure in either of the images in the pair. Note that the sample size ($n=20$) is small, and the figure may change substantially if larger or different sets are used. The images can be viewed on p. 13 of the Appendix, where Gen 01 corresponds to Same-Identity Pair 1, Gen 02 corresponds to Same-Identity Pair 2, and so on.

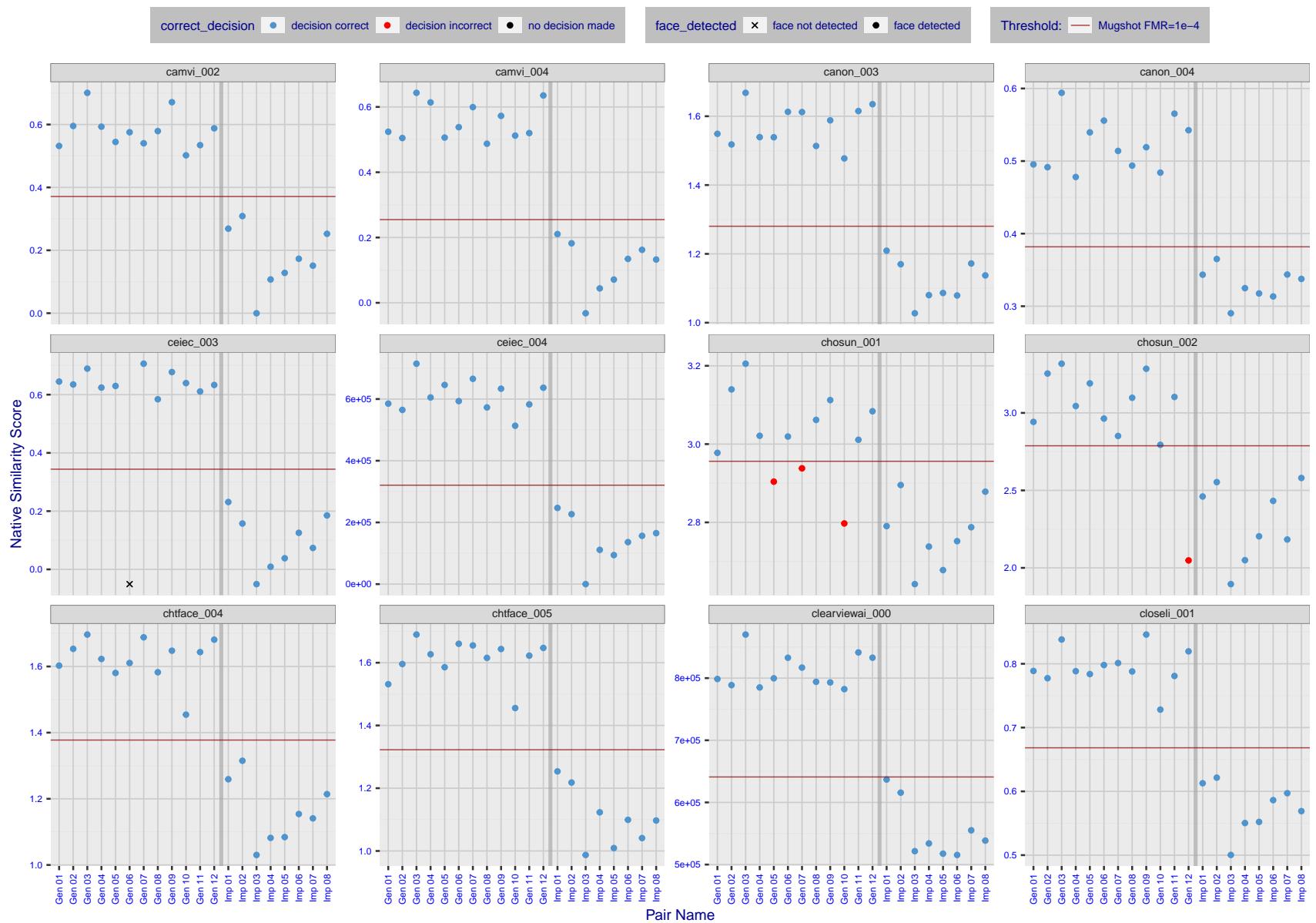


Figure 9: The figure shows algorithms' similarity scores for 12 genuine and 8 impostor image pairs used in a May 2018 paper by Phillips et al. ([1]). The threshold (red horizontal line) is a value calibrated to give $FMR = 0.0001$ on mugshot images. Points above the threshold correspond to pairs determined to be genuine, and points below the threshold correspond to pairs determined to be impostors. If the determined class (genuine or impostor) matches the real class, points will be blue; if not, red. An X represents face detection failure in either of the images in the pair. Note that the sample size ($n=20$) is small, and the figure may change substantially if larger or different sets are used. The images can be viewed on p. 13 of the Appendix, where Gen 01 corresponds to Same-Identity Pair 1, Gen 02 corresponds to Same-Identity Pair 2, and so on.

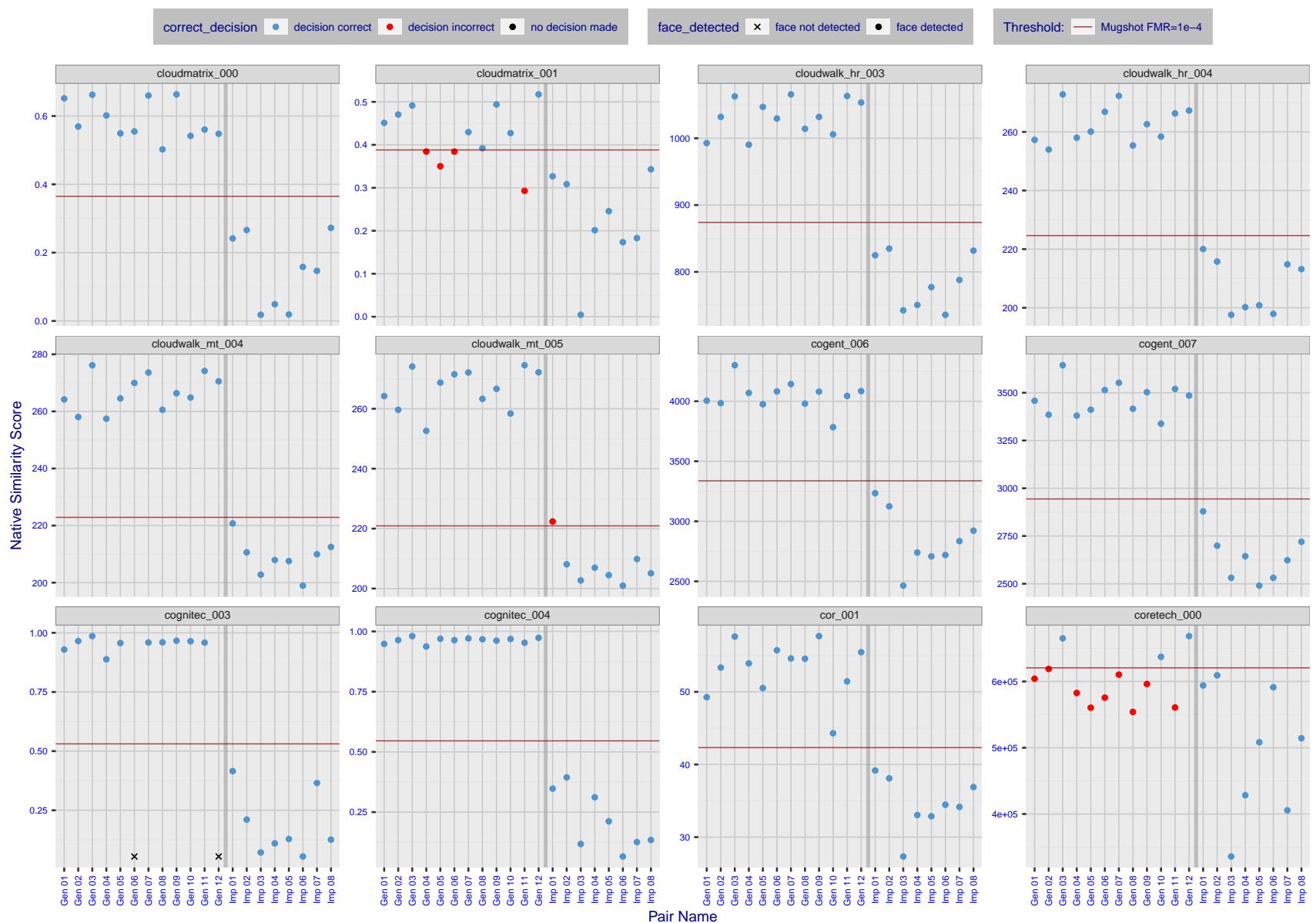


Figure 10: The figure shows algorithms' similarity scores for 12 genuine and 8 impostor image pairs used in a May 2018 paper by Phillips et al. ([1]). The threshold (red horizontal line) is a value calibrated to give $FMR = 0.0001$ on mugshot images. Points above the threshold correspond to pairs determined to be genuine, and points below the threshold correspond to pairs determined to be impostors. If the determined class (genuine or impostor) matches the real class, points will be blue; if not, red. An X represents face detection failure in either of the images in the pair. Note that the sample size ($n=20$) is small, and the figure may change substantially if larger or different sets are used. The images can be viewed on p. 13 of the Appendix, where Gen 01 corresponds to Same-Identity Pair 1, Gen 02 corresponds to Same-Identity Pair 2, and so on.

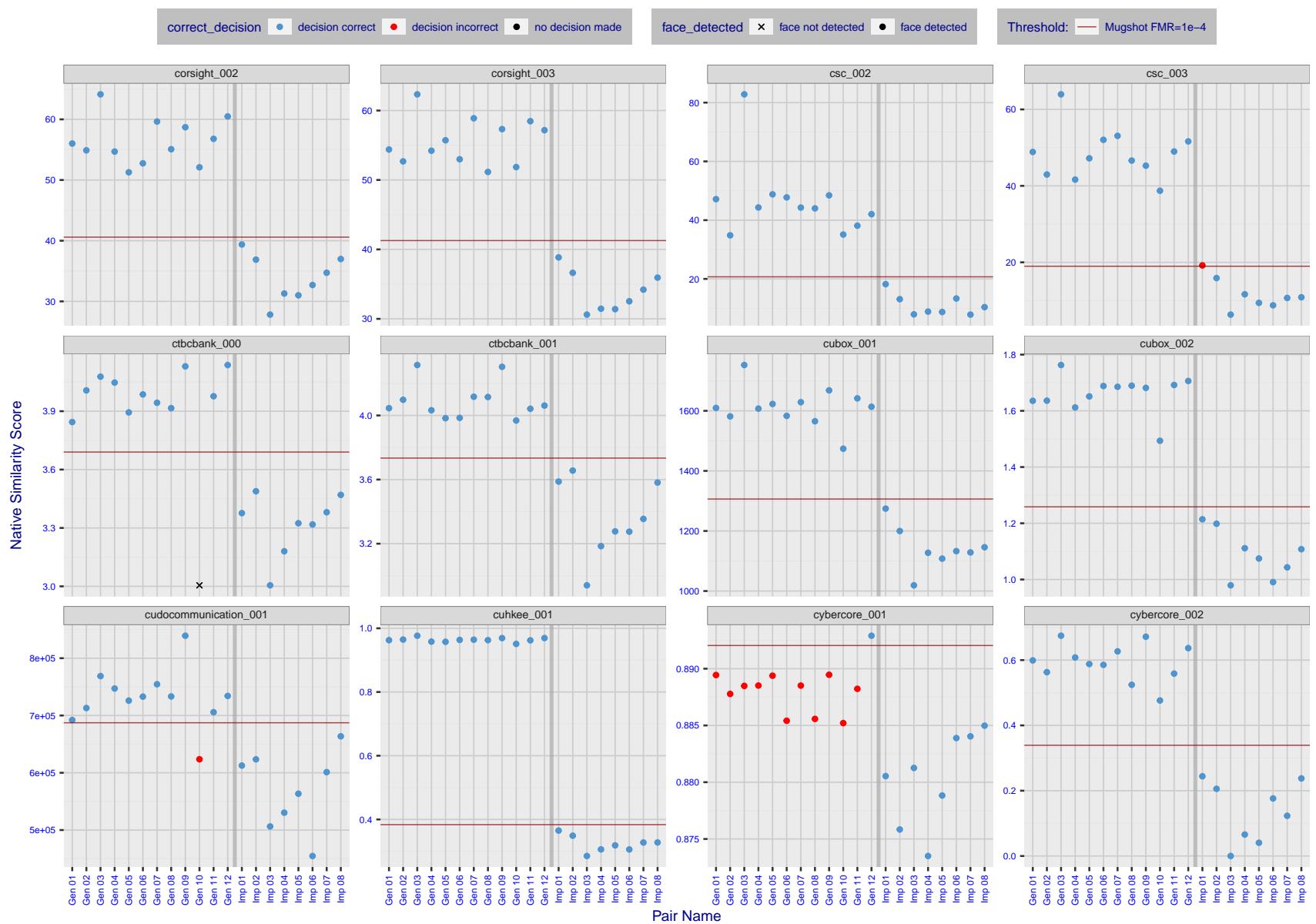


Figure 11: The figure shows algorithms' similarity scores for 12 genuine and 8 impostor image pairs used in a May 2018 paper by Phillips et al. ([1]). The threshold (red horizontal line) is a value calibrated to give $FMR = 0.0001$ on mugshot images. Points above the threshold correspond to pairs determined to be genuine, and points below the threshold correspond to pairs determined to be impostors. If the determined class (genuine or impostor) matches the real class, points will be blue; if not, red. An X represents face detection failure in either of the images in the pair. Note that the sample size ($n=20$) is small, and the figure may change substantially if larger or different sets are used. The images can be viewed on p. 13 of the Appendix, where Gen 01 corresponds to Same-Identity Pair 1, Gen 02 corresponds to Same-Identity Pair 2, and so on.

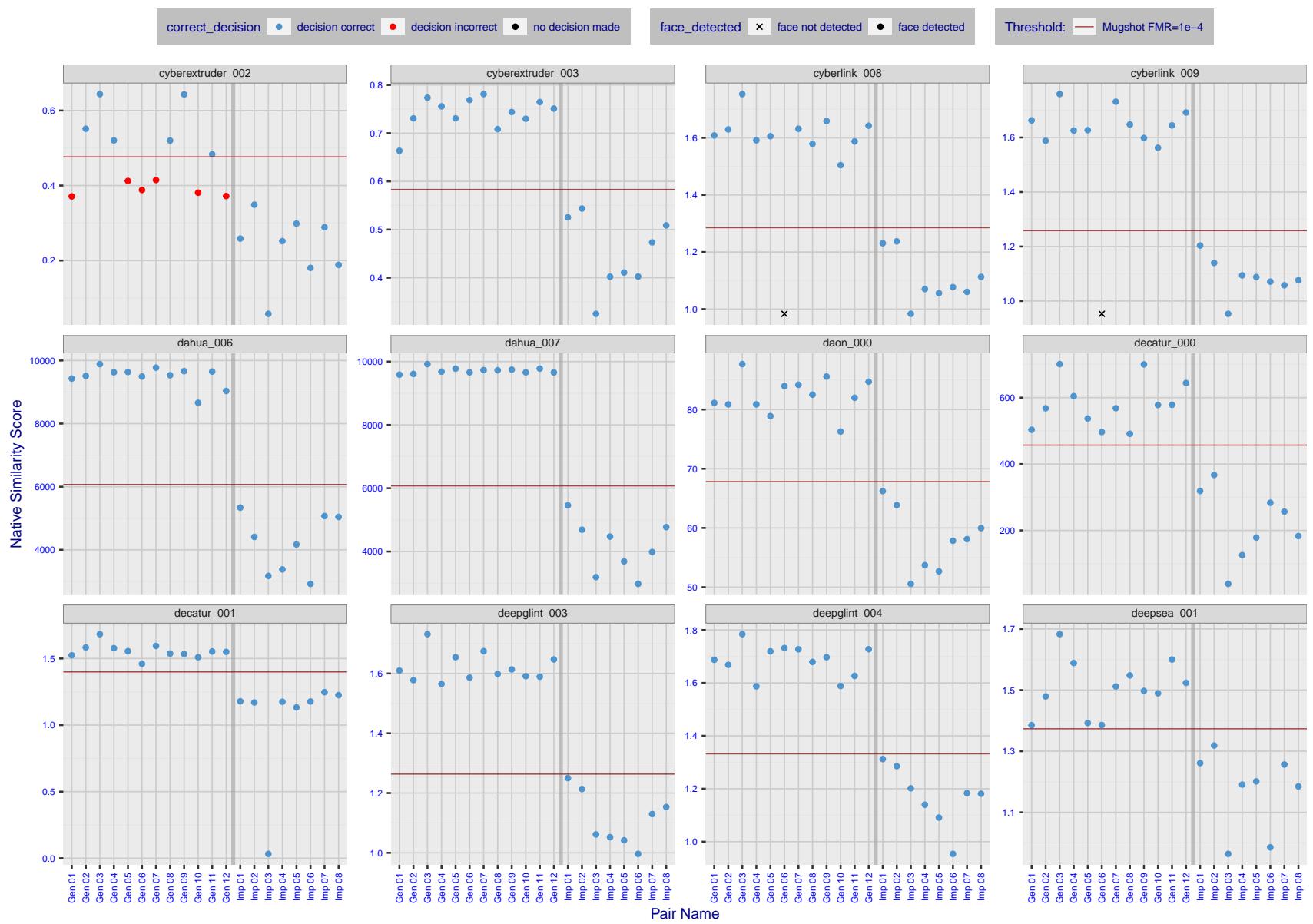


Figure 12: The figure shows algorithms' similarity scores for 12 genuine and 8 impostor image pairs used in a May 2018 paper by Phillips et al. ([1]). The threshold (red horizontal line) is a value calibrated to give $FMR = 0.0001$ on mugshot images. Points above the threshold correspond to pairs determined to be genuine, and points below the threshold correspond to pairs determined to be impostors. If the determined class (genuine or impostor) matches the real class, points will be blue; if not, red. An X represents face detection failure in either of the images in the pair. Note that the sample size ($n=20$) is small, and the figure may change substantially if larger or different sets are used. The images can be viewed on p. 13 of the Appendix, where Gen 01 corresponds to Same-Identity Pair 1, Gen 02 corresponds to Same-Identity Pair 2, and so on.

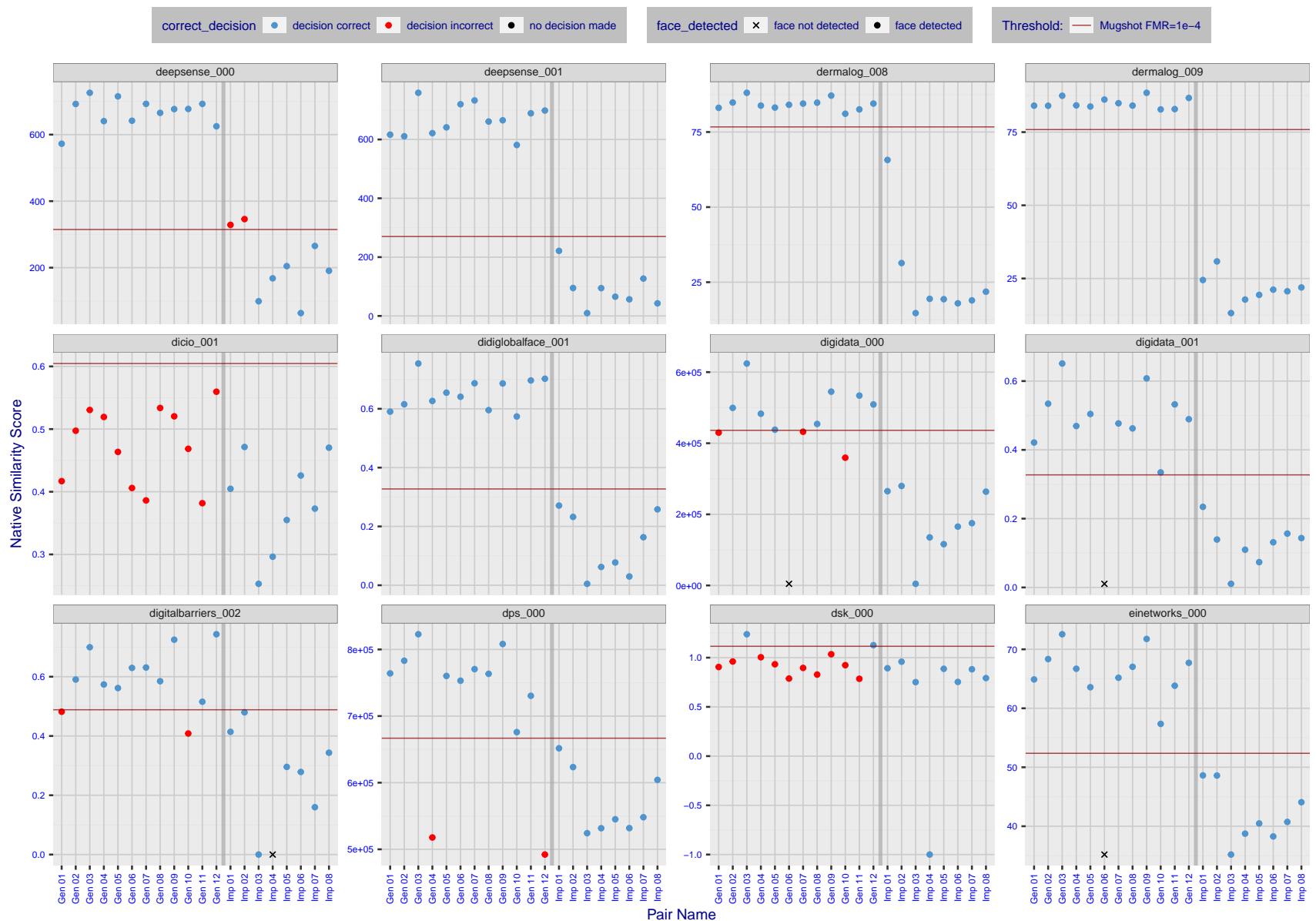


Figure 13: The figure shows algorithms' similarity scores for 12 genuine and 8 impostor image pairs used in a May 2018 paper by Phillips et al. ([1]). The threshold (red horizontal line) is a value calibrated to give $FMR = 0.0001$ on mugshot images. Points above the threshold correspond to pairs determined to be genuine, and points below the threshold correspond to pairs determined to be impostors. If the determined class (genuine or impostor) matches the real class, points will be blue; if not, red. An X represents face detection failure in either of the images in the pair. Note that the sample size ($n=20$) is small, and the figure may change substantially if larger or different sets are used. The images can be viewed on p. 13 of the Appendix, where Gen 01 corresponds to Same-Identity Pair 1, Gen 02 corresponds to Same-Identity Pair 2, and so on.

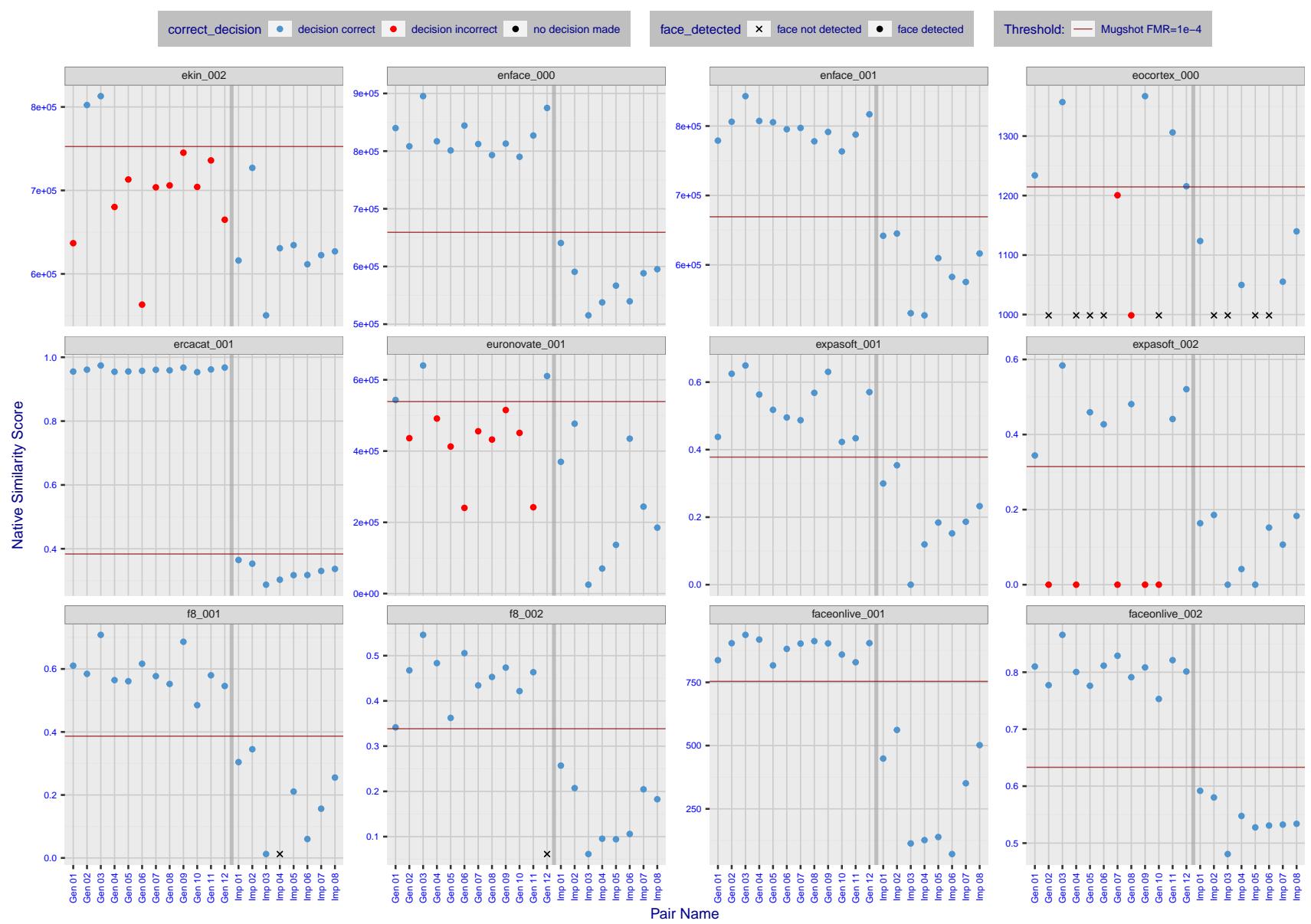


Figure 14: The figure shows algorithms' similarity scores for 12 genuine and 8 impostor image pairs used in a May 2018 paper by Phillips et al. ([1]). The threshold (red horizontal line) is a value calibrated to give $FMR = 0.0001$ on mugshot images. Points above the threshold correspond to pairs determined to be genuine, and points below the threshold correspond to pairs determined to be impostors. If the determined class (genuine or impostor) matches the real class, points will be blue; if not, red. An X represents face detection failure in either of the images in the pair. Note that the sample size ($n=20$) is small, and the figure may change substantially if larger or different sets are used. The images can be viewed on p. 13 of the Appendix, where Gen 01 corresponds to Same-Identity Pair 1, Gen 02 corresponds to Same-Identity Pair 2, and so on.

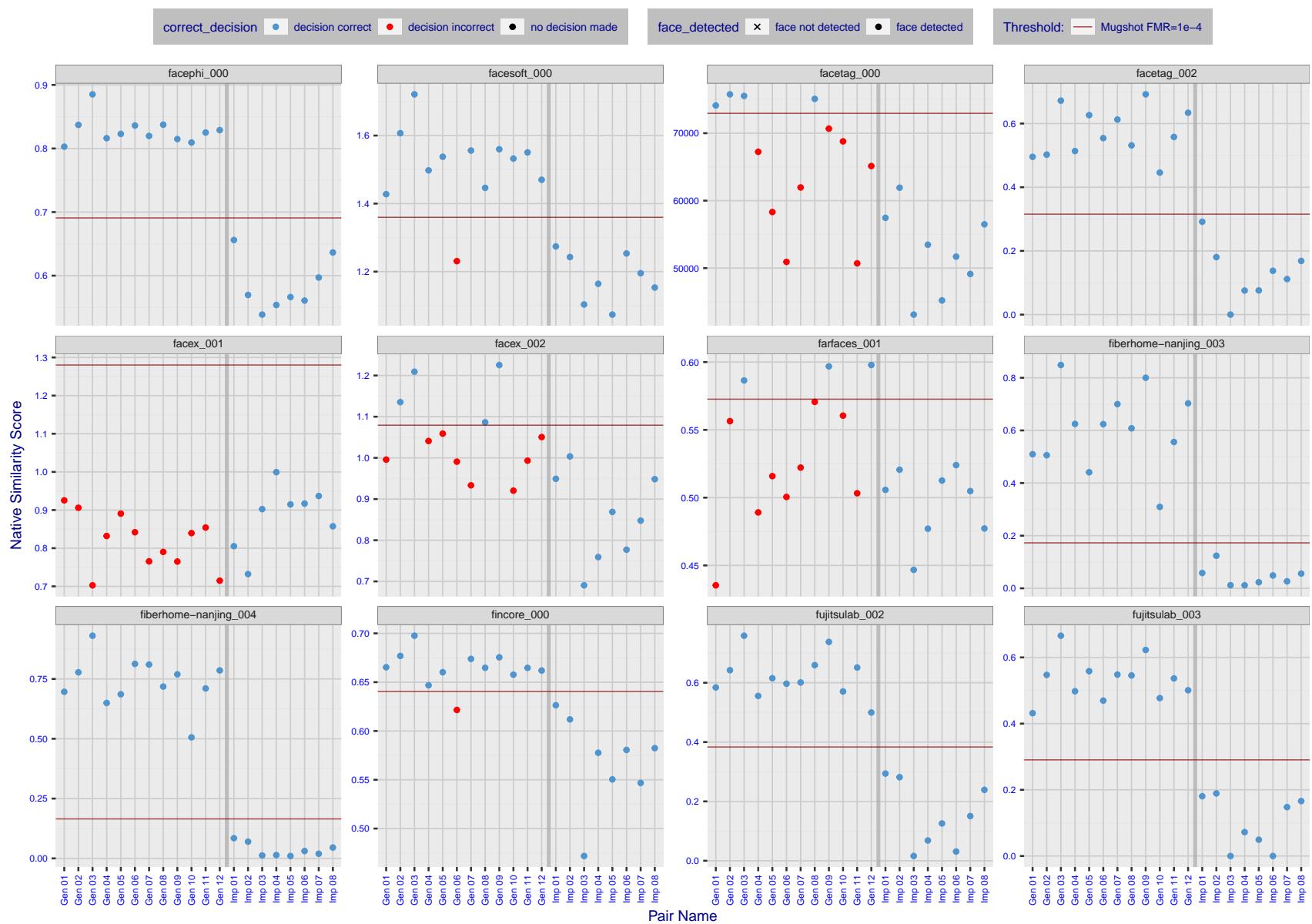


Figure 15: The figure shows algorithms' similarity scores for 12 genuine and 8 impostor image pairs used in a May 2018 paper by Phillips et al. ([1]). The threshold (red horizontal line) is a value calibrated to give $FMR = 0.0001$ on mugshot images. Points above the threshold correspond to pairs determined to be genuine, and points below the threshold correspond to pairs determined to be impostors. If the determined class (genuine or impostor) matches the real class, points will be blue; if not, red. An X represents face detection failure in either of the images in the pair. Note that the sample size ($n=20$) is small, and the figure may change substantially if larger or different sets are used. The images can be viewed on p. 13 of the Appendix, where Gen 01 corresponds to Same-Identity Pair 1, Gen 02 corresponds to Same-Identity Pair 2, and so on.

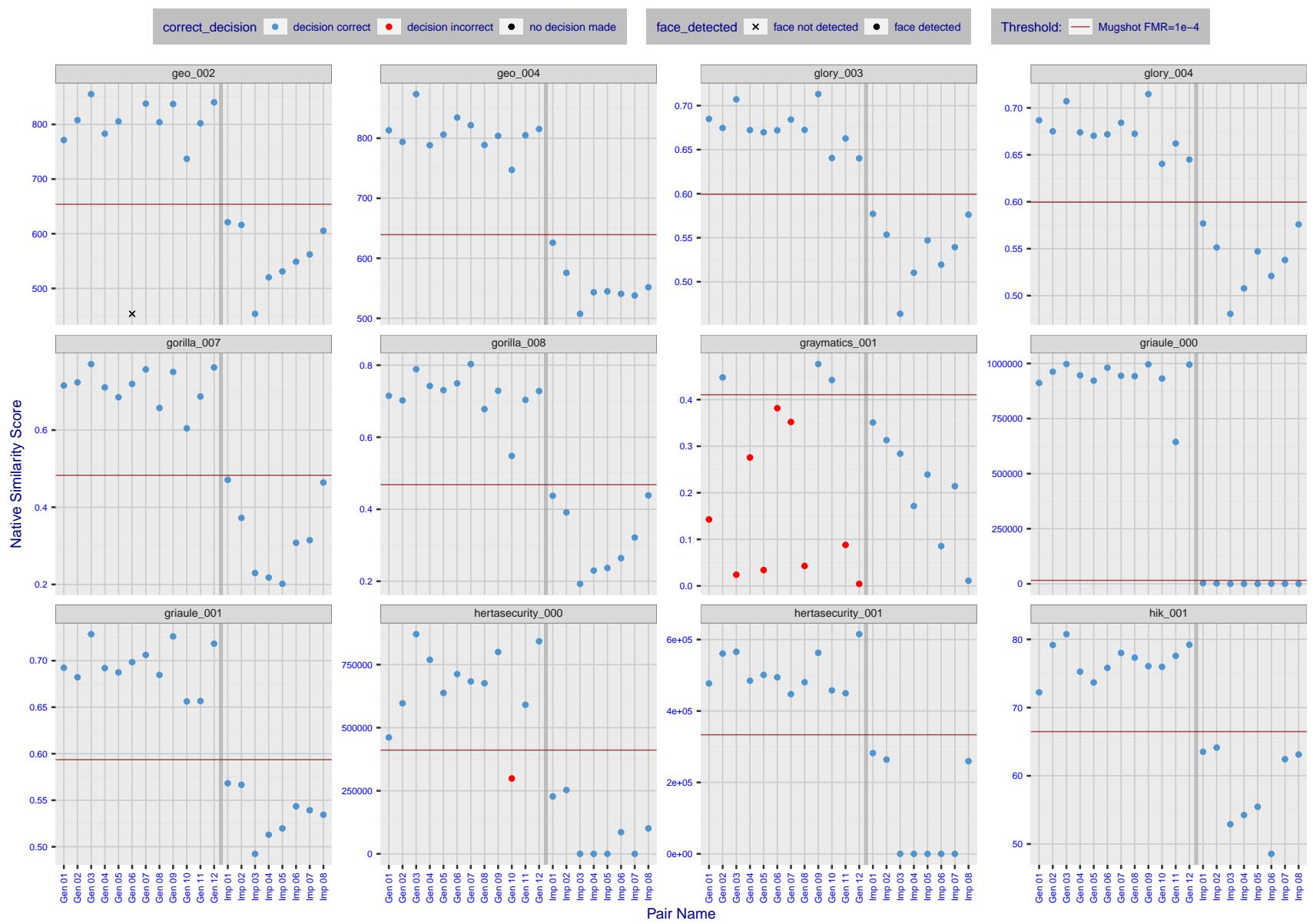


Figure 16: The figure shows algorithms' similarity scores for 12 genuine and 8 impostor image pairs used in a May 2018 paper by Phillips et al. ([1]). The threshold (red horizontal line) is a value calibrated to give $FMR = 0.0001$ on mugshot images. Points above the threshold correspond to pairs determined to be genuine, and points below the threshold correspond to pairs determined to be impostors. If the determined class (genuine or impostor) matches the real class, points will be blue; if not, red. An X represents face detection failure in either of the images in the pair. Note that the sample size ($n=20$) is small, and the figure may change substantially if larger or different sets are used. The images can be viewed on p. 13 of the Appendix, where Gen 01 corresponds to Same-Identity Pair 1, Gen 02 corresponds to Same-Identity Pair 2, and so on.

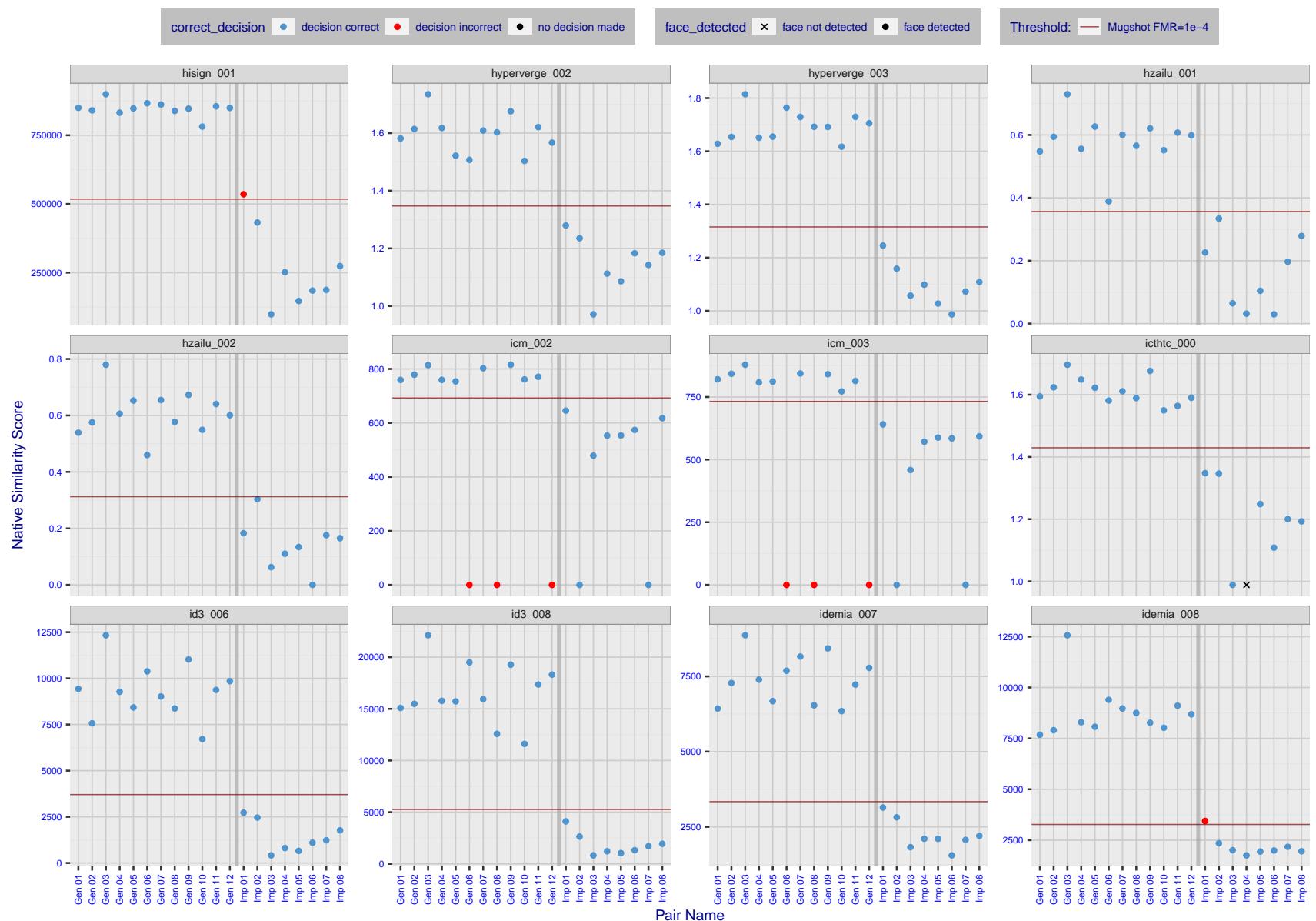


Figure 17: The figure shows algorithms' similarity scores for 12 genuine and 8 impostor image pairs used in a May 2018 paper by Phillips et al. ([1]). The threshold (red horizontal line) is a value calibrated to give $FMR = 0.0001$ on mugshot images. Points above the threshold correspond to pairs determined to be genuine, and points below the threshold correspond to pairs determined to be impostors. If the determined class (genuine or impostor) matches the real class, points will be blue; if not, red. An X represents face detection failure in either of the images in the pair. Note that the sample size ($n=20$) is small, and the figure may change substantially if larger or different sets are used. The images can be viewed on p. 13 of the Appendix, where Gen 01 corresponds to Same-Identity Pair 1, Gen 02 corresponds to Same-Identity Pair 2, and so on.

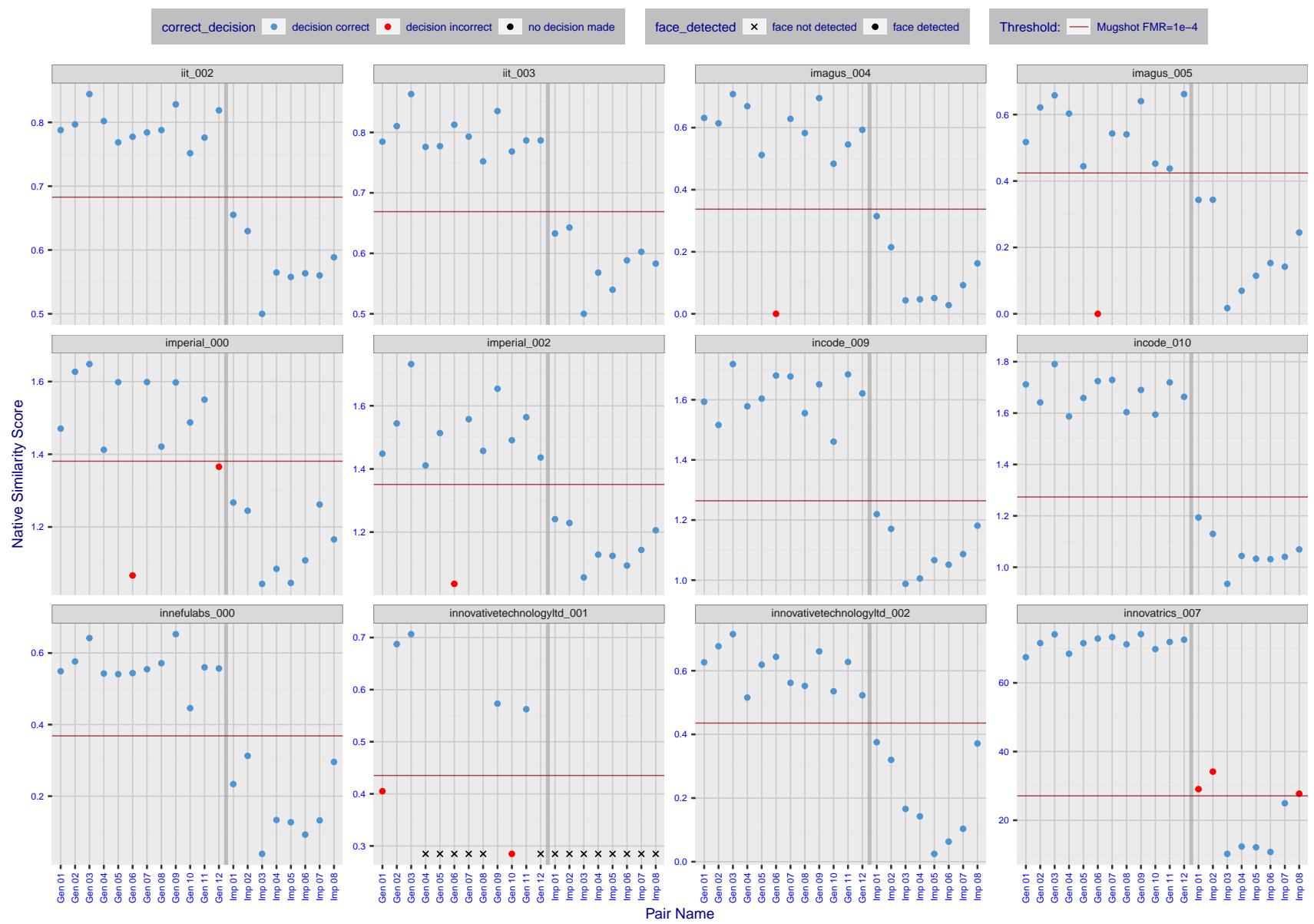


Figure 18: The figure shows algorithms' similarity scores for 12 genuine and 8 impostor image pairs used in a May 2018 paper by Phillips et al. ([1]). The threshold (red horizontal line) is a value calibrated to give $FMR = 0.0001$ on mugshot images. Points above the threshold correspond to pairs determined to be genuine, and points below the threshold correspond to pairs determined to be impostors. If the determined class (genuine or impostor) matches the real class, points will be blue; if not, red. An X represents face detection failure in either of the images in the pair. Note that the sample size ($n=20$) is small, and the figure may change substantially if larger or different sets are used. The images can be viewed on p. 13 of the Appendix, where Gen 01 corresponds to Same-Identity Pair 1, Gen 02 corresponds to Same-Identity Pair 2, and so on.

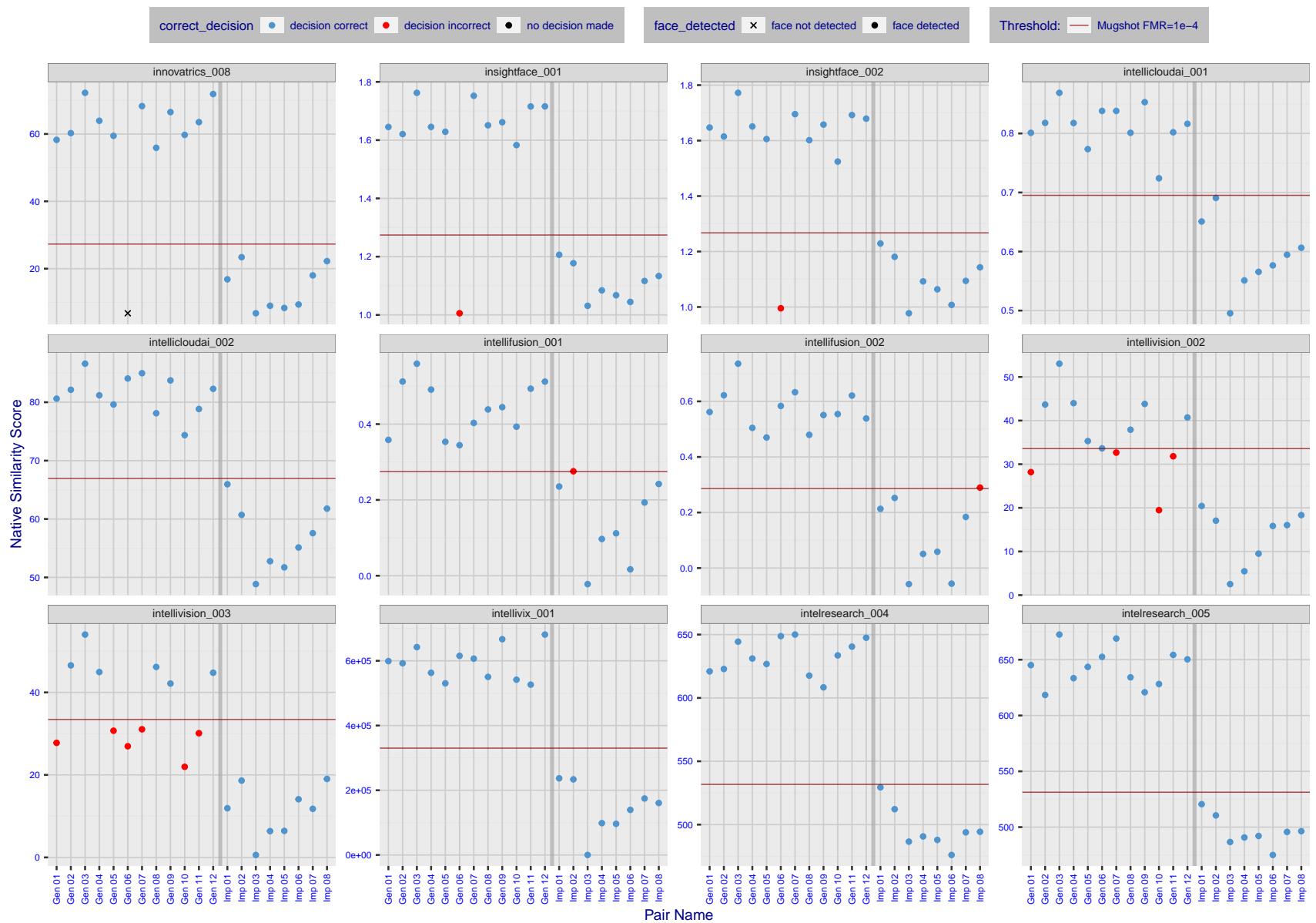


Figure 19: The figure shows algorithms' similarity scores for 12 genuine and 8 impostor image pairs used in a May 2018 paper by Phillips et al. ([1]). The threshold (red horizontal line) is a value calibrated to give $FMR = 0.0001$ on mugshot images. Points above the threshold correspond to pairs determined to be genuine, and points below the threshold correspond to pairs determined to be impostors. If the determined class (genuine or impostor) matches the real class, points will be blue; if not, red. An X represents face detection failure in either of the images in the pair. Note that the sample size ($n=20$) is small, and the figure may change substantially if larger or different sets are used. The images can be viewed on p. 13 of the Appendix, where Gen 01 corresponds to Same-Identity Pair 1, Gen 02 corresponds to Same-Identity Pair 2, and so on.

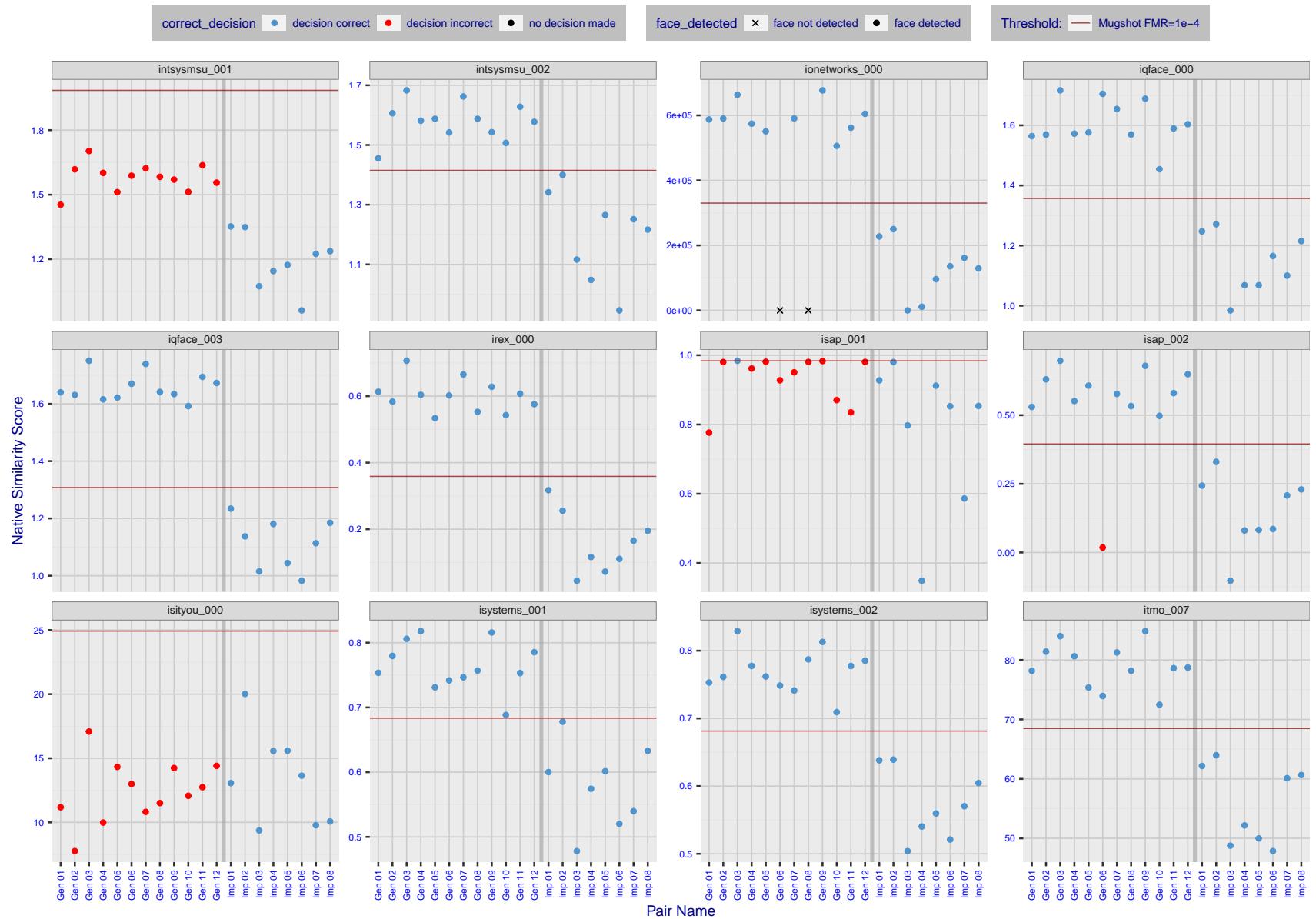


Figure 20: The figure shows algorithms' similarity scores for 12 genuine and 8 impostor image pairs used in a May 2018 paper by Phillips et al. ([1]). The threshold (red horizontal line) is a value calibrated to give $FMR = 0.0001$ on mugshot images. Points above the threshold correspond to pairs determined to be genuine, and points below the threshold correspond to pairs determined to be impostors. If the determined class (genuine or impostor) matches the real class, points will be blue; if not, red. An X represents face detection failure in either of the images in the pair. Note that the sample size ($n=20$) is small, and the figure may change substantially if larger or different sets are used. The images can be viewed on p. 13 of the Appendix, where Gen 01 corresponds to Same-Identity Pair 1, Gen 02 corresponds to Same-Identity Pair 2, and so on.

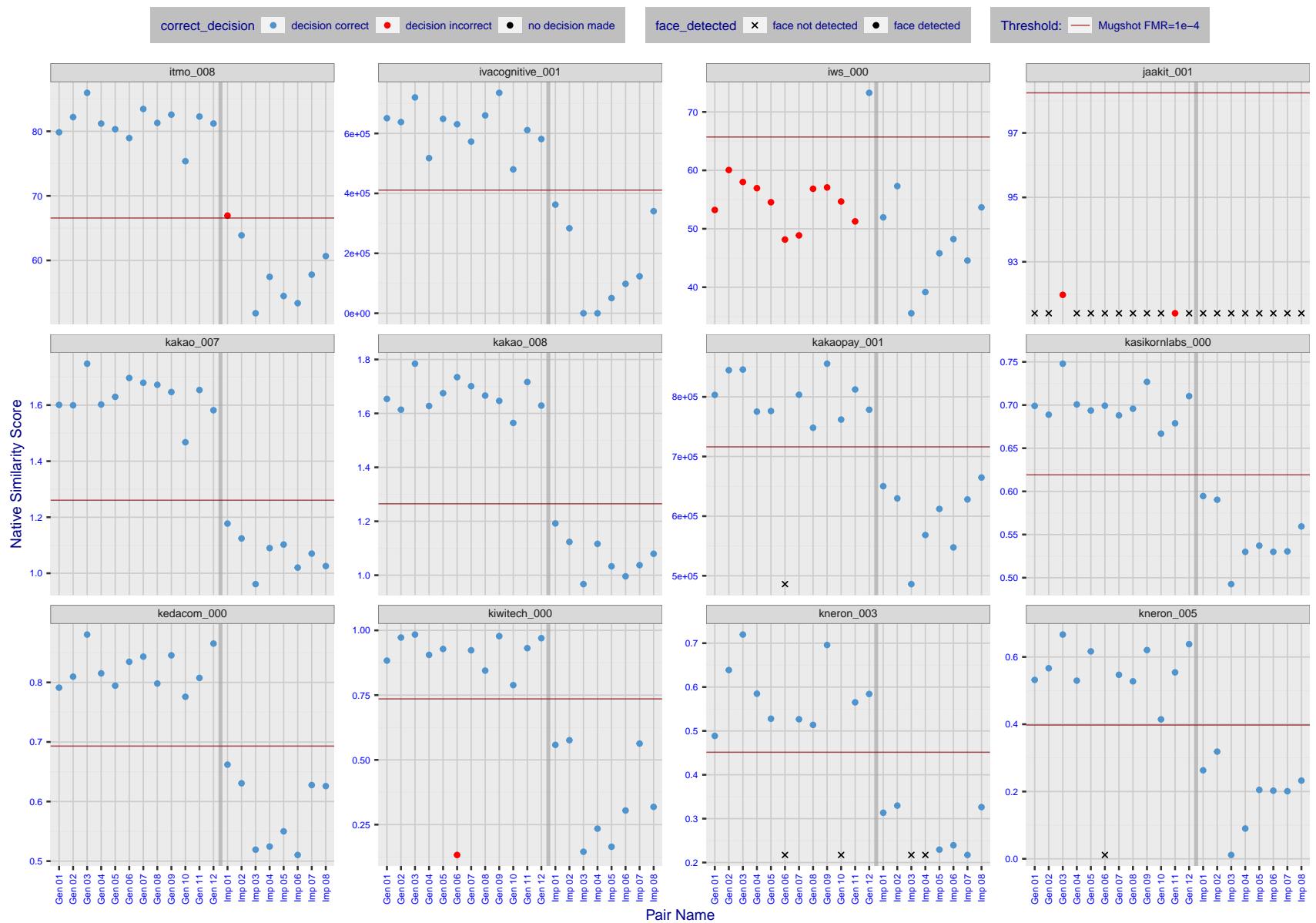


Figure 21: The figure shows algorithms' similarity scores for 12 genuine and 8 impostor image pairs used in a May 2018 paper by Phillips et al. ([1]). The threshold (red horizontal line) is a value calibrated to give $FMR = 0.0001$ on mugshot images. Points above the threshold correspond to pairs determined to be genuine, and points below the threshold correspond to pairs determined to be impostors. If the determined class (genuine or impostor) matches the real class, points will be blue; if not, red. An X represents face detection failure in either of the images in the pair. Note that the sample size ($n=20$) is small, and the figure may change substantially if larger or different sets are used. The images can be viewed on p. 13 of the Appendix, where Gen 01 corresponds to Same-Identity Pair 1, Gen 02 corresponds to Same-Identity Pair 2, and so on.

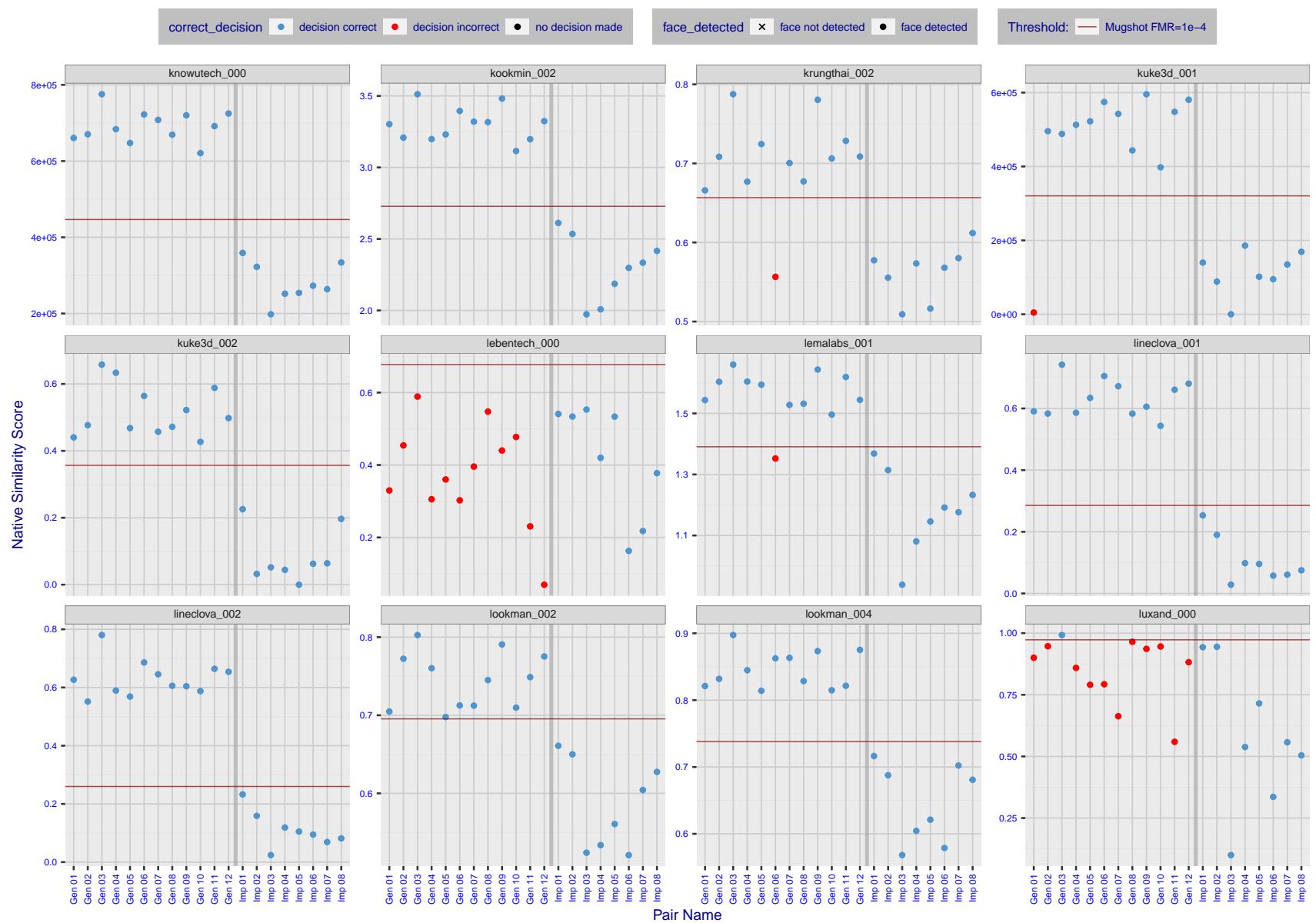


Figure 22: The figure shows algorithms' similarity scores for 12 genuine and 8 impostor image pairs used in a May 2018 paper by Phillips et al. ([1]). The threshold (red horizontal line) is a value calibrated to give $FMR = 0.0001$ on mugshot images. Points above the threshold correspond to pairs determined to be genuine, and points below the threshold correspond to pairs determined to be impostors. If the determined class (genuine or impostor) matches the real class, points will be blue; if not, red. An X represents face detection failure in either of the images in the pair. Note that the sample size ($n=20$) is small, and the figure may change substantially if larger or different sets are used. The images can be viewed on p. 13 of the Appendix, where Gen 01 corresponds to Same-Identity Pair 1, Gen 02 corresponds to Same-Identity Pair 2, and so on.

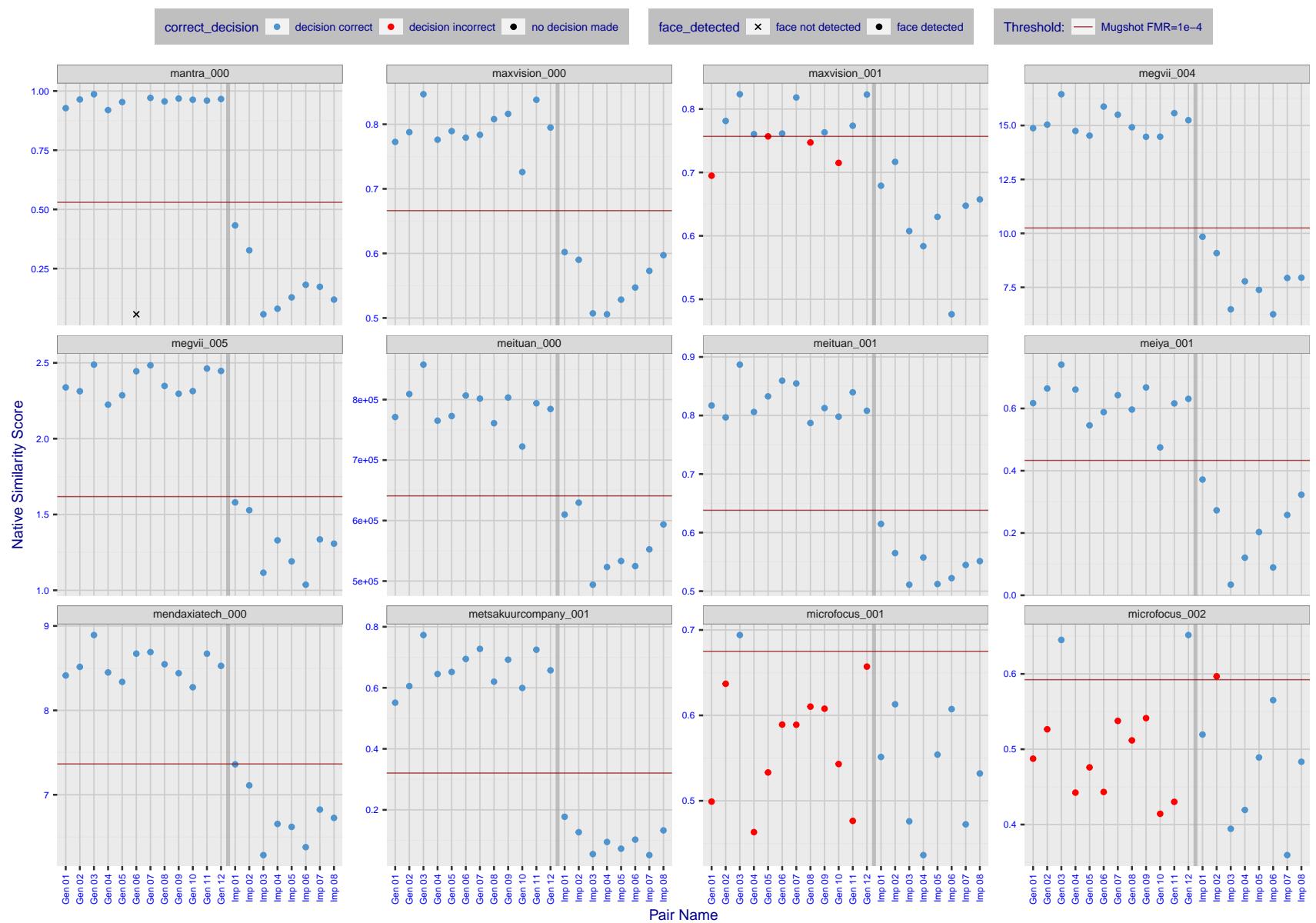


Figure 23: The figure shows algorithms' similarity scores for 12 genuine and 8 impostor image pairs used in a May 2018 paper by Phillips et al. ([1]). The threshold (red horizontal line) is a value calibrated to give $FMR = 0.0001$ on mugshot images. Points above the threshold correspond to pairs determined to be genuine, and points below the threshold correspond to pairs determined to be impostors. If the determined class (genuine or impostor) matches the real class, points will be blue; if not, red. An X represents face detection failure in either of the images in the pair. Note that the sample size ($n=20$) is small, and the figure may change substantially if larger or different sets are used. The images can be viewed on p. 13 of the Appendix, where Gen 01 corresponds to Same-Identity Pair 1, Gen 02 corresponds to Same-Identity Pair 2, and so on.

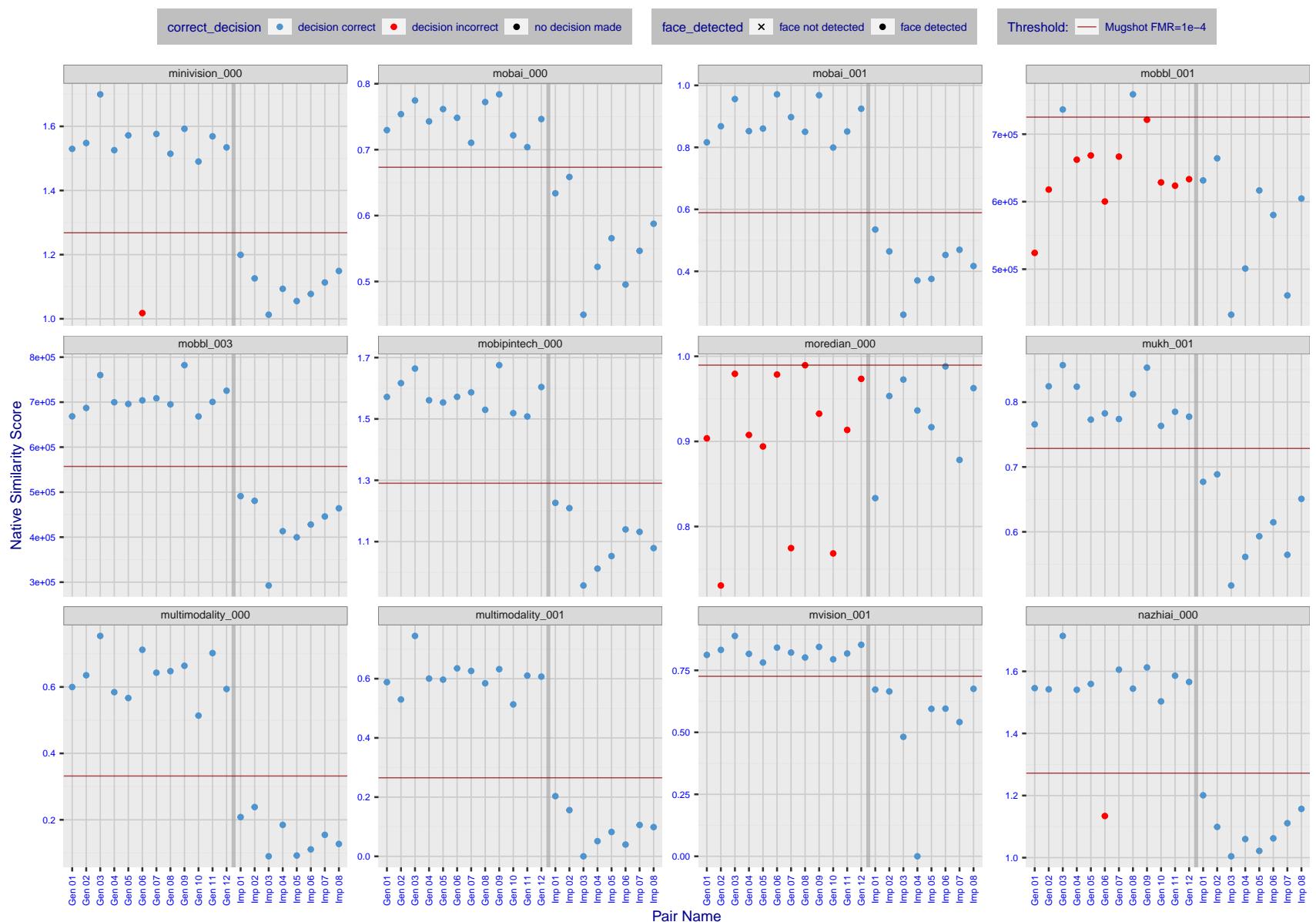


Figure 24: The figure shows algorithms' similarity scores for 12 genuine and 8 impostor image pairs used in a May 2018 paper by Phillips et al. ([1]). The threshold (red horizontal line) is a value calibrated to give $FMR = 0.0001$ on mugshot images. Points above the threshold correspond to pairs determined to be genuine, and points below the threshold correspond to pairs determined to be impostors. If the determined class (genuine or impostor) matches the real class, points will be blue; if not, red. An X represents face detection failure in either of the images in the pair. Note that the sample size ($n=20$) is small, and the figure may change substantially if larger or different sets are used. The images can be viewed on p. 13 of the Appendix, where Gen 01 corresponds to Same-Identity Pair 1, Gen 02 corresponds to Same-Identity Pair 2, and so on.

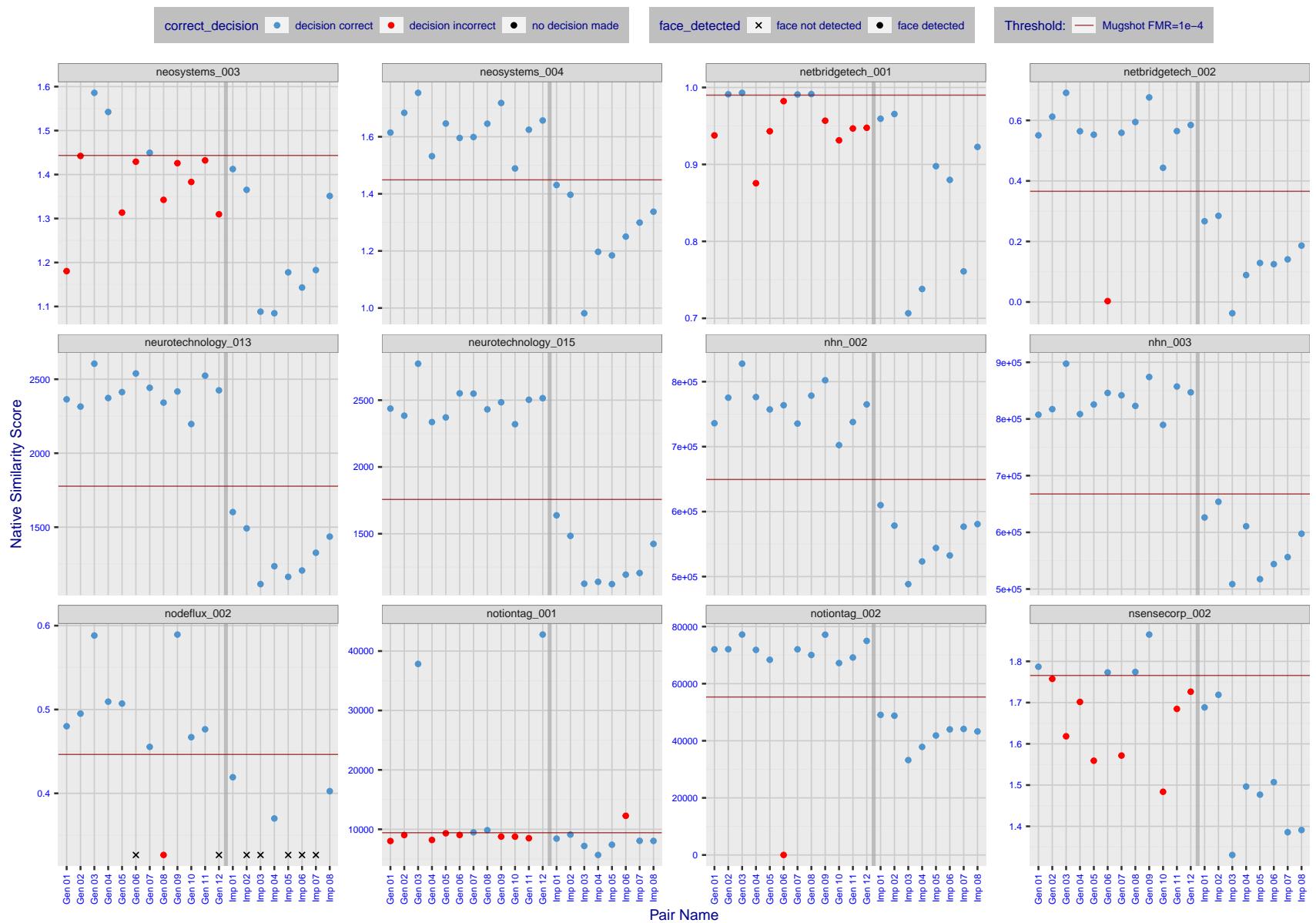


Figure 25: The figure shows algorithms' similarity scores for 12 genuine and 8 impostor image pairs used in a May 2018 paper by Phillips et al. ([1]). The threshold (red horizontal line) is a value calibrated to give $FMR = 0.0001$ on mugshot images. Points above the threshold correspond to pairs determined to be genuine, and points below the threshold correspond to pairs determined to be impostors. If the determined class (genuine or impostor) matches the real class, points will be blue; if not, red. An X represents face detection failure in either of the images in the pair. Note that the sample size ($n=20$) is small, and the figure may change substantially if larger or different sets are used. The images can be viewed on p. 13 of the Appendix, where Gen 01 corresponds to Same-Identity Pair 1, Gen 02 corresponds to Same-Identity Pair 2, and so on.

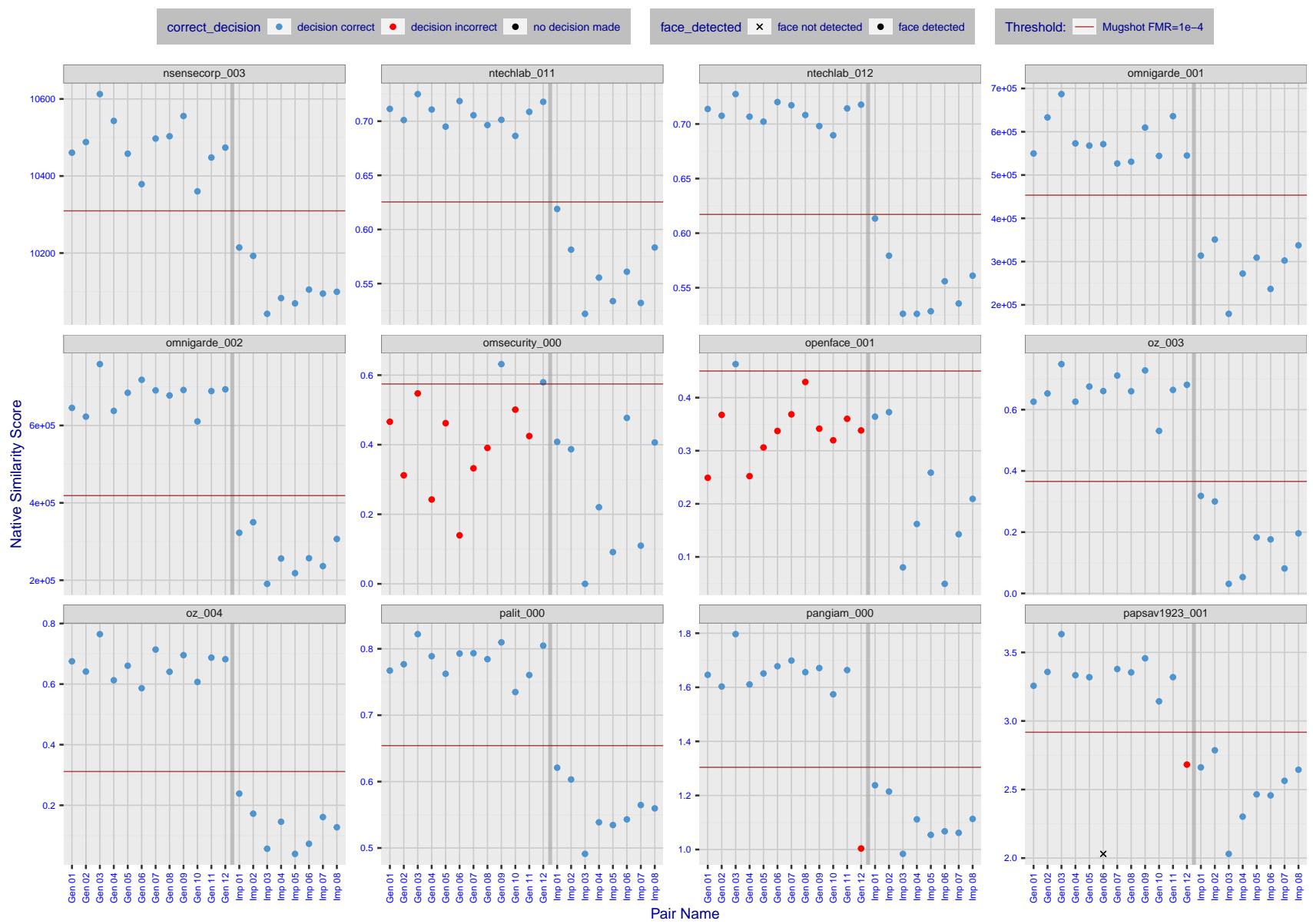


Figure 26: The figure shows algorithms' similarity scores for 12 genuine and 8 impostor image pairs used in a May 2018 paper by Phillips et al. ([1]). The threshold (red horizontal line) is a value calibrated to give $FMR = 0.0001$ on mugshot images. Points above the threshold correspond to pairs determined to be genuine, and points below the threshold correspond to pairs determined to be impostors. If the determined class (genuine or impostor) matches the real class, points will be blue; if not, red. An X represents face detection failure in either of the images in the pair. Note that the sample size ($n=20$) is small, and the figure may change substantially if larger or different sets are used. The images can be viewed on p. 13 of the Appendix, where Gen 01 corresponds to Same-Identity Pair 1, Gen 02 corresponds to Same-Identity Pair 2, and so on.

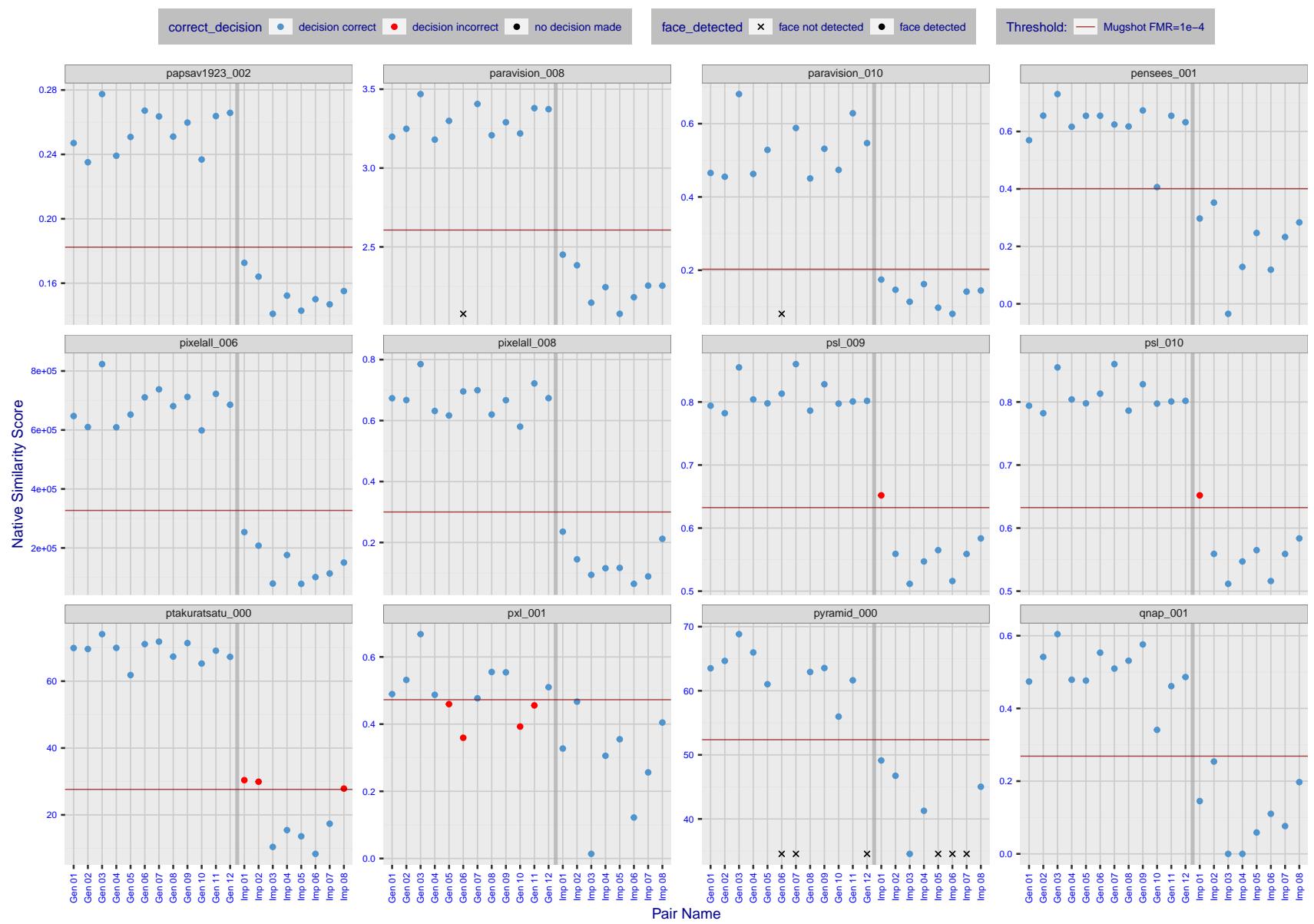


Figure 27: The figure shows algorithms' similarity scores for 12 genuine and 8 impostor image pairs used in a May 2018 paper by Phillips et al. ([1]). The threshold (red horizontal line) is a value calibrated to give $FMR = 0.0001$ on mugshot images. Points above the threshold correspond to pairs determined to be genuine, and points below the threshold correspond to pairs determined to be impostors. If the determined class (genuine or impostor) matches the real class, points will be blue; if not, red. An X represents face detection failure in either of the images in the pair. Note that the sample size ($n=20$) is small, and the figure may change substantially if larger or different sets are used. The images can be viewed on p. 13 of the Appendix, where Gen 01 corresponds to Same-Identity Pair 1, Gen 02 corresponds to Same-Identity Pair 2, and so on.

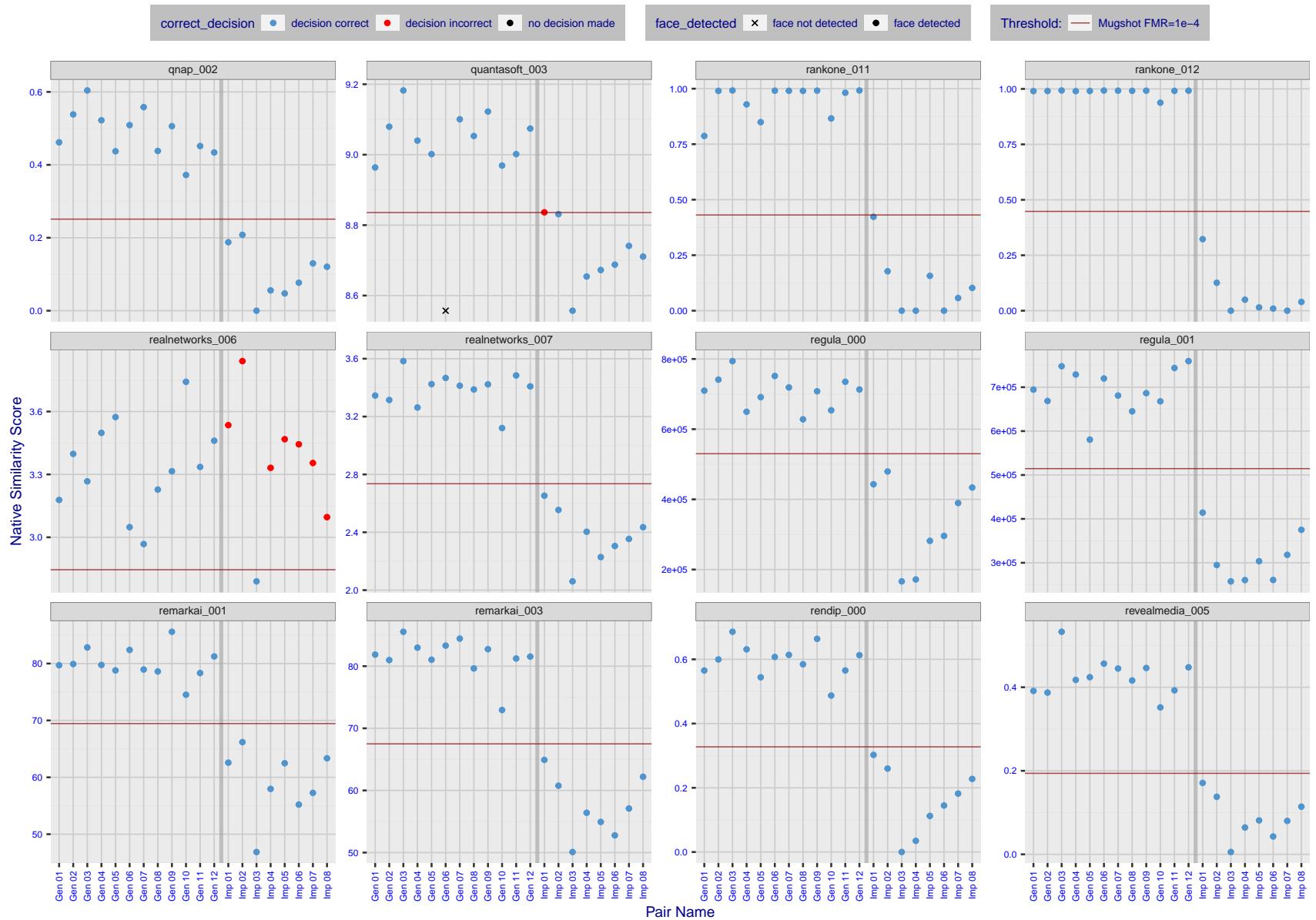


Figure 28: The figure shows algorithms' similarity scores for 12 genuine and 8 impostor image pairs used in a May 2018 paper by Phillips et al. ([1]). The threshold (red horizontal line) is a value calibrated to give $FMR = 0.0001$ on mugshot images. Points above the threshold correspond to pairs determined to be genuine, and points below the threshold correspond to pairs determined to be impostors. If the determined class (genuine or impostor) matches the real class, points will be blue; if not, red. An X represents face detection failure in either of the images in the pair. Note that the sample size ($n=20$) is small, and the figure may change substantially if larger or different sets are used. The images can be viewed on p. 13 of the Appendix, where Gen 01 corresponds to Same-Identity Pair 1, Gen 02 corresponds to Same-Identity Pair 2, and so on.

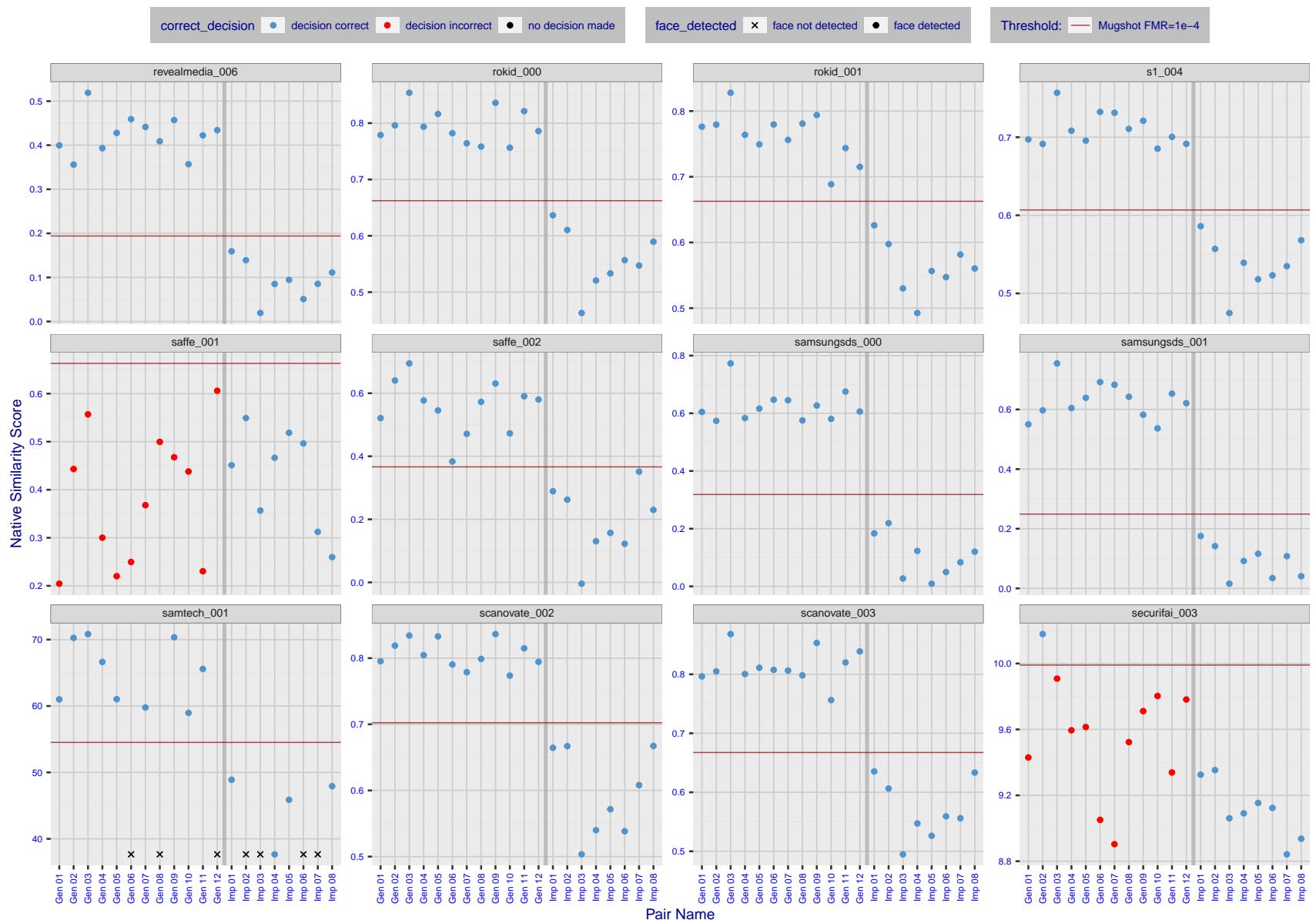


Figure 29: The figure shows algorithms' similarity scores for 12 genuine and 8 impostor image pairs used in a May 2018 paper by Phillips et al. ([1]). The threshold (red horizontal line) is a value calibrated to give $FMR = 0.0001$ on mugshot images. Points above the threshold correspond to pairs determined to be genuine, and points below the threshold correspond to pairs determined to be impostors. If the determined class (genuine or impostor) matches the real class, points will be blue; if not, red. An X represents face detection failure in either of the images in the pair. Note that the sample size ($n=20$) is small, and the figure may change substantially if larger or different sets are used. The images can be viewed on p. 13 of the Appendix, where Gen 01 corresponds to Same-Identity Pair 1, Gen 02 corresponds to Same-Identity Pair 2, and so on.

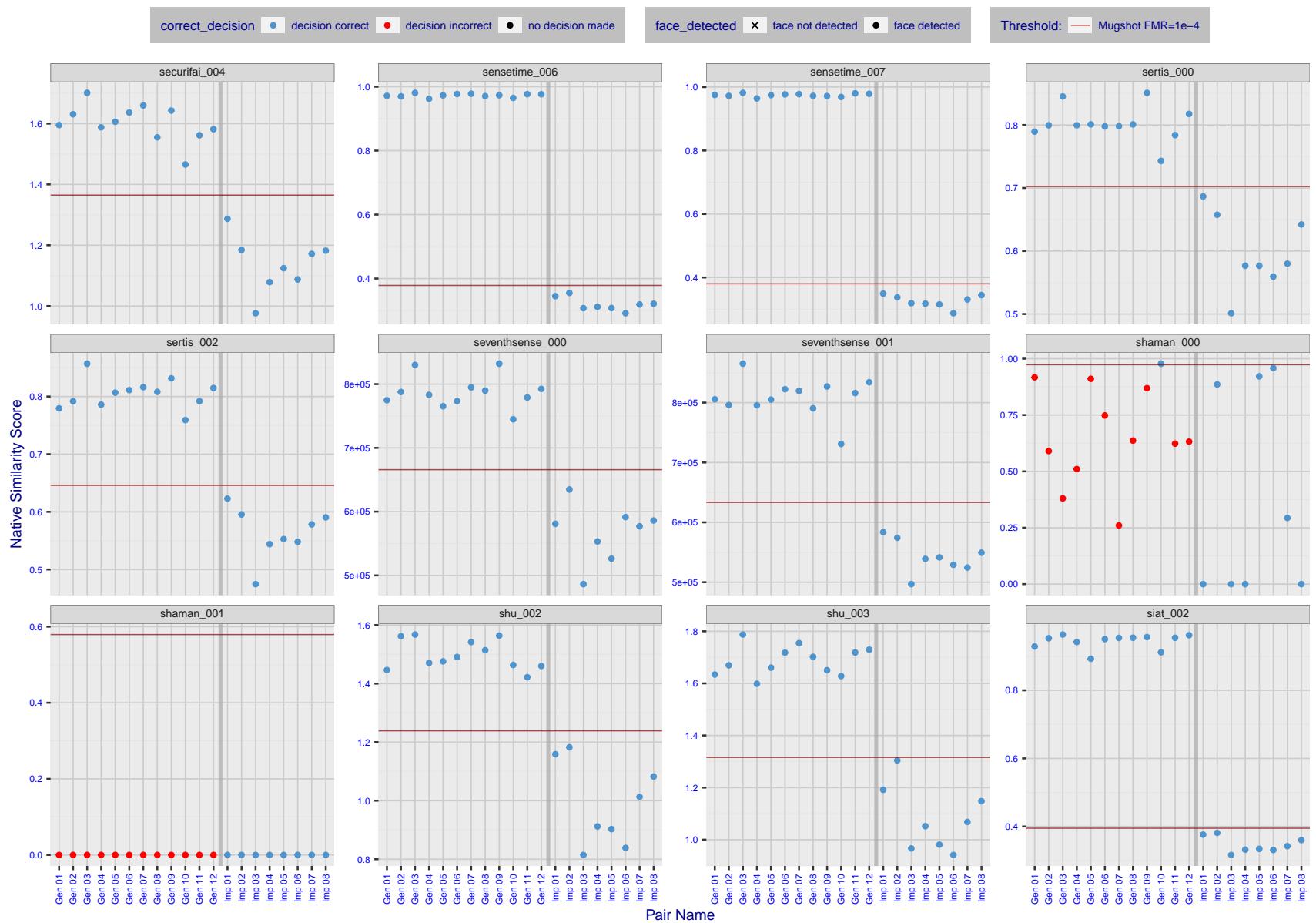


Figure 30: The figure shows algorithms' similarity scores for 12 genuine and 8 impostor image pairs used in a May 2018 paper by Phillips et al. ([1]). The threshold (red horizontal line) is a value calibrated to give $FMR = 0.0001$ on mugshot images. Points above the threshold correspond to pairs determined to be genuine, and points below the threshold correspond to pairs determined to be impostors. If the determined class (genuine or impostor) matches the real class, points will be blue; if not, red. An X represents face detection failure in either of the images in the pair. Note that the sample size ($n=20$) is small, and the figure may change substantially if larger or different sets are used. The images can be viewed on p. 13 of the Appendix, where Gen 01 corresponds to Same-Identity Pair 1, Gen 02 corresponds to Same-Identity Pair 2, and so on.

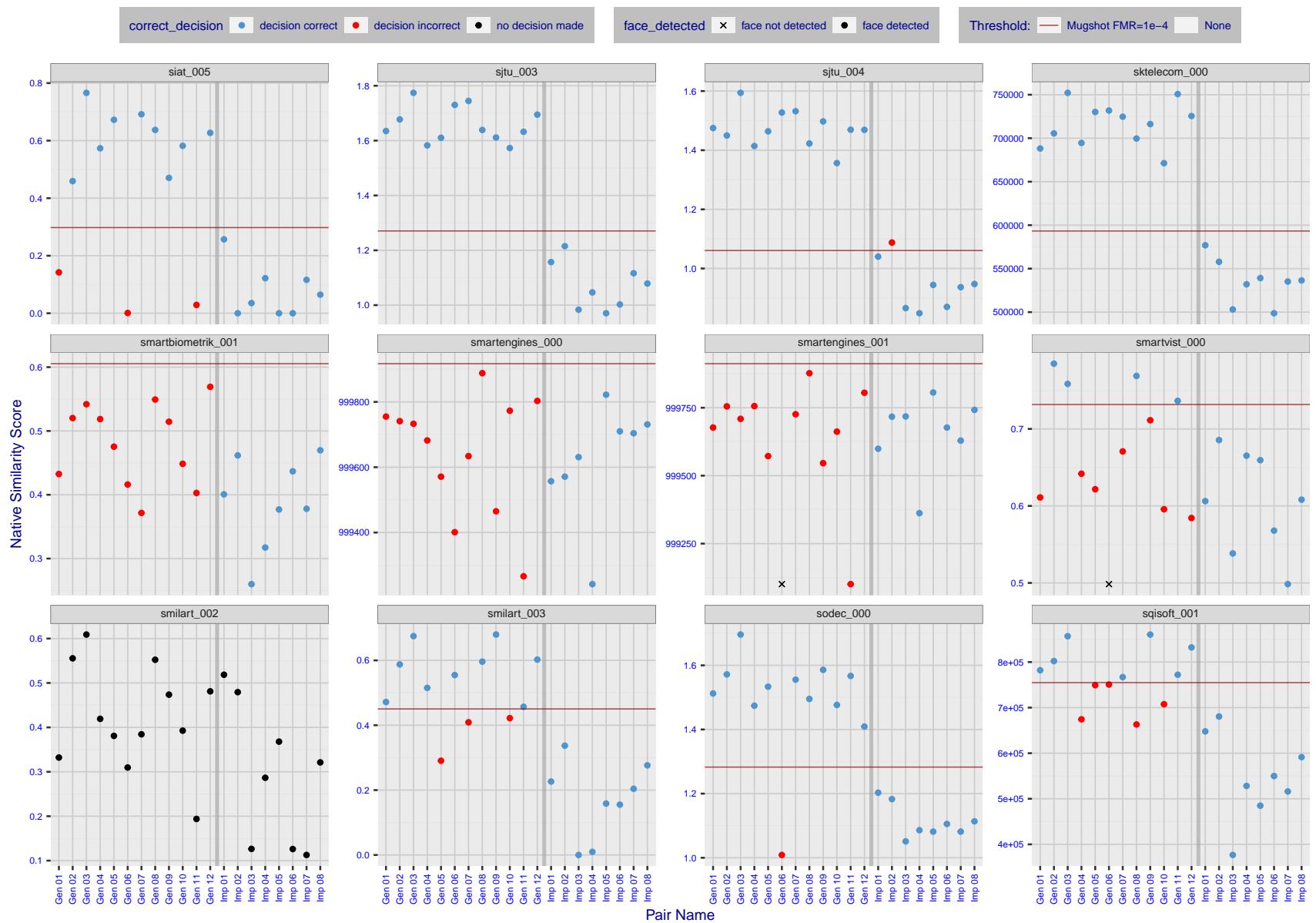


Figure 31: The figure shows algorithms' similarity scores for 12 genuine and 8 impostor image pairs used in a May 2018 paper by Phillips et al. ([1]). The threshold (red horizontal line) is a value calibrated to give $FMR = 0.0001$ on mugshot images. Points above the threshold correspond to pairs determined to be genuine, and points below the threshold correspond to pairs determined to be impostors. If the determined class (genuine or impostor) matches the real class, points will be blue; if not, red. An X represents face detection failure in either of the images in the pair. Note that the sample size ($n=20$) is small, and the figure may change substantially if larger or different sets are used. The images can be viewed on p. 13 of the Appendix, where Gen 01 corresponds to Same-Identity Pair 1, Gen 02 corresponds to Same-Identity Pair 2, and so on.

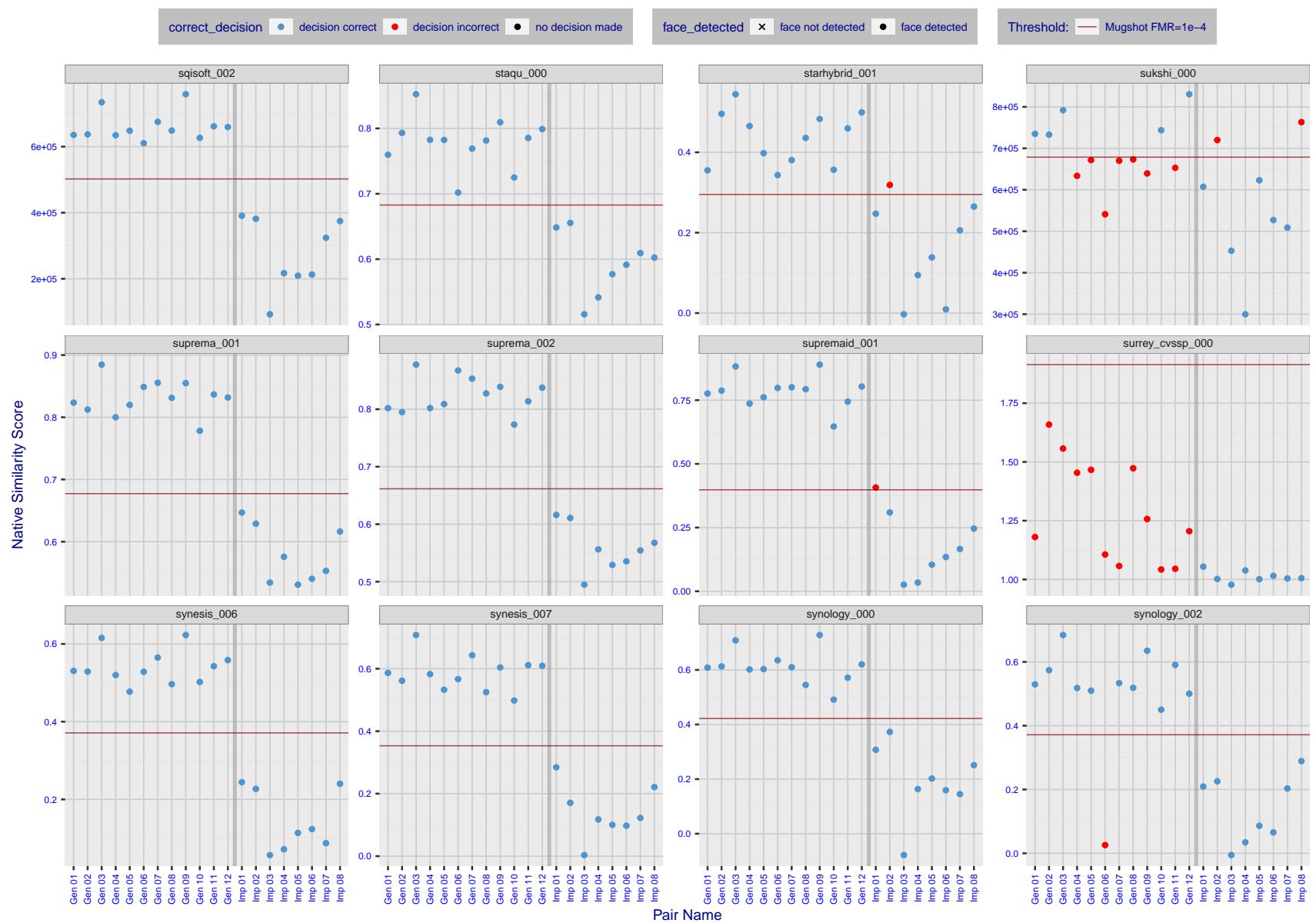


Figure 32: The figure shows algorithms' similarity scores for 12 genuine and 8 impostor image pairs used in a May 2018 paper by Phillips et al. ([1]). The threshold (red horizontal line) is a value calibrated to give $FMR = 0.0001$ on mugshot images. Points above the threshold correspond to pairs determined to be genuine, and points below the threshold correspond to pairs determined to be impostors. If the determined class (genuine or impostor) matches the real class, points will be blue; if not, red. An X represents face detection failure in either of the images in the pair. Note that the sample size ($n=20$) is small, and the figure may change substantially if larger or different sets are used. The images can be viewed on p. 13 of the Appendix, where Gen 01 corresponds to Same-Identity Pair 1, Gen 02 corresponds to Same-Identity Pair 2, and so on.

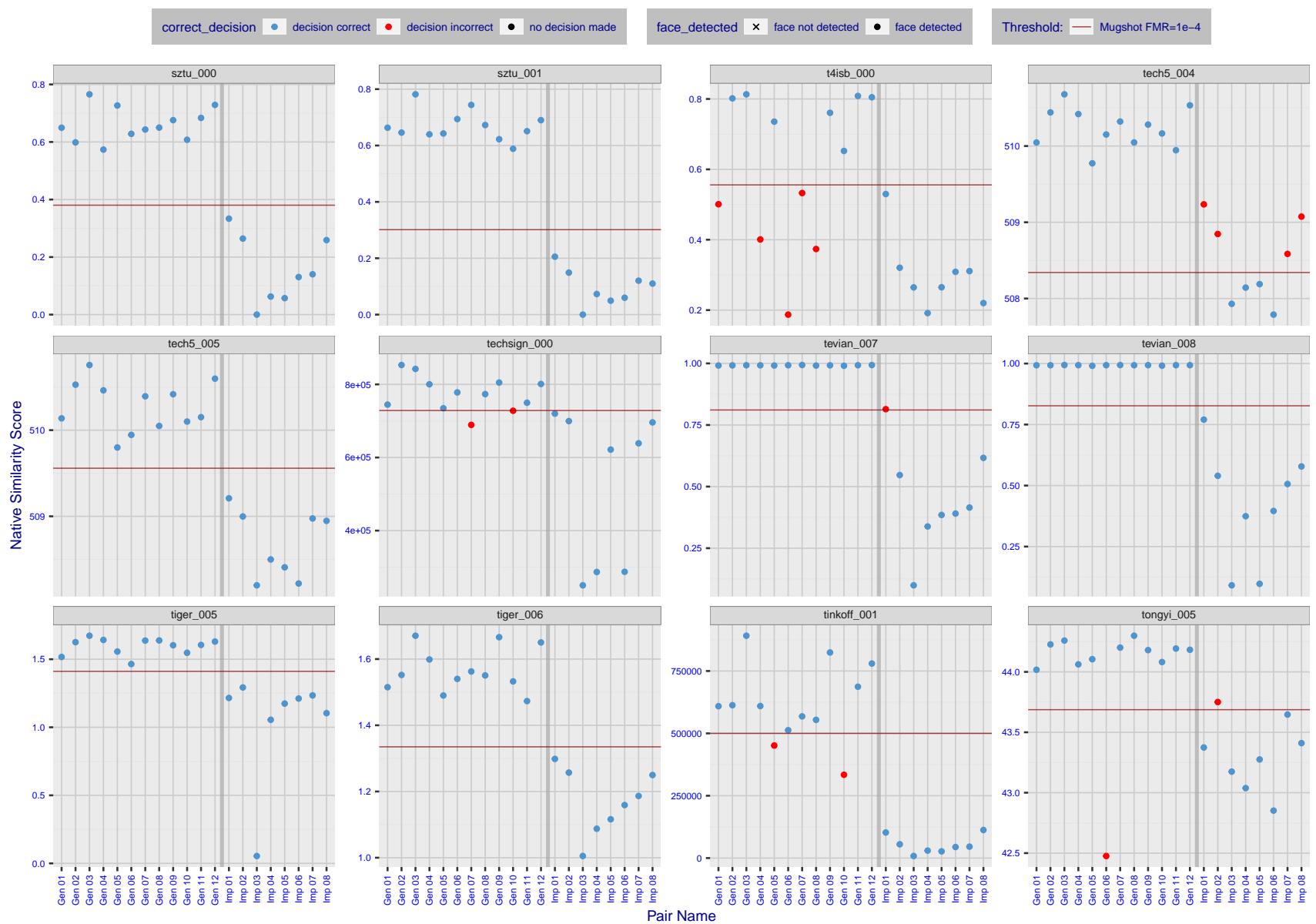


Figure 33: The figure shows algorithms' similarity scores for 12 genuine and 8 impostor image pairs used in a May 2018 paper by Phillips et al. ([1]). The threshold (red horizontal line) is a value calibrated to give $FMR = 0.0001$ on mugshot images. Points above the threshold correspond to pairs determined to be genuine, and points below the threshold correspond to pairs determined to be impostors. If the determined class (genuine or impostor) matches the real class, points will be blue; if not, red. An X represents face detection failure in either of the images in the pair. Note that the sample size ($n=20$) is small, and the figure may change substantially if larger or different sets are used. The images can be viewed on p. 13 of the Appendix, where Gen 01 corresponds to Same-Identity Pair 1, Gen 02 corresponds to Same-Identity Pair 2, and so on.

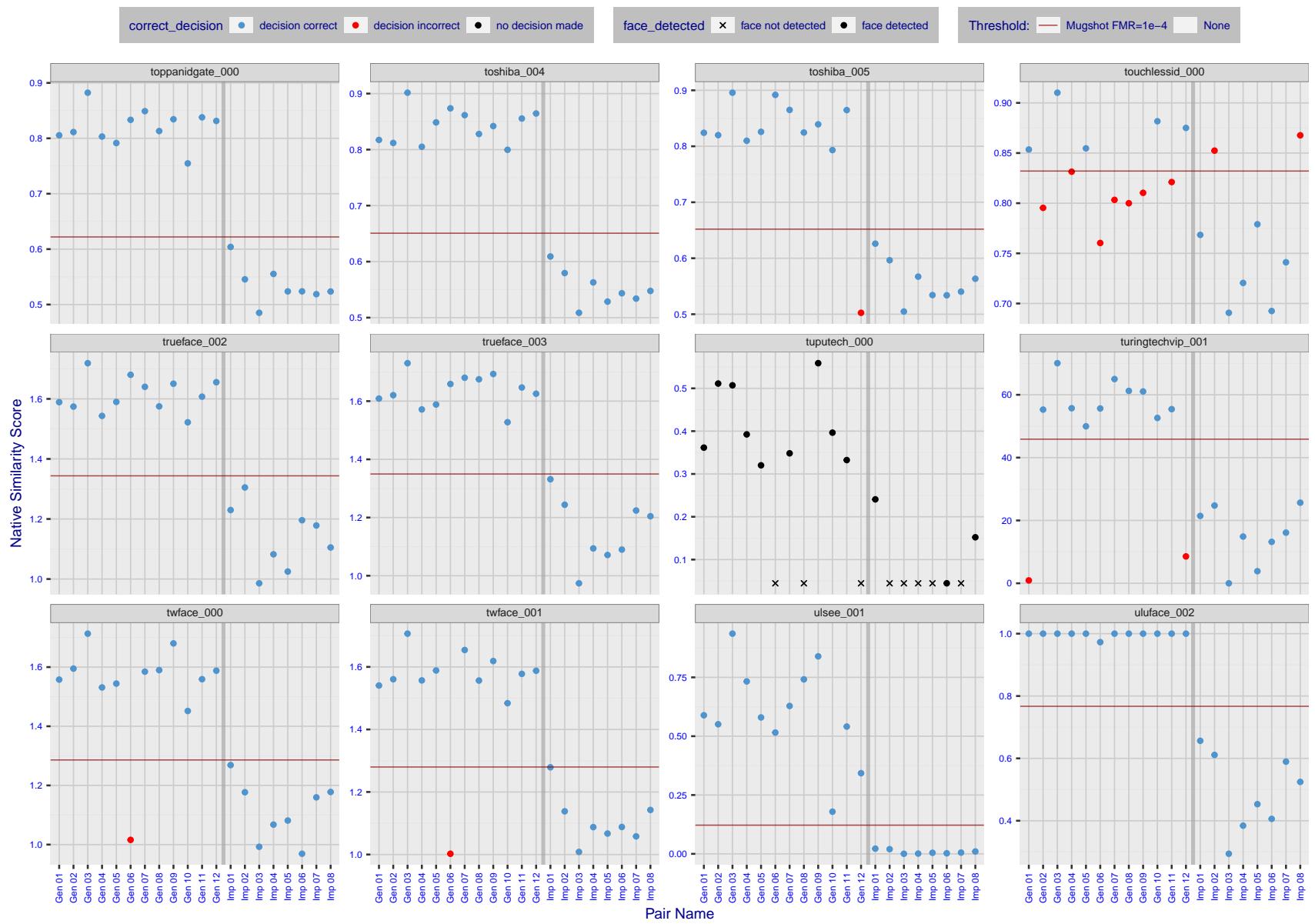


Figure 34: The figure shows algorithms' similarity scores for 12 genuine and 8 impostor image pairs used in a May 2018 paper by Phillips et al. ([1]). The threshold (red horizontal line) is a value calibrated to give $FMR = 0.0001$ on mugshot images. Points above the threshold correspond to pairs determined to be genuine, and points below the threshold correspond to pairs determined to be impostors. If the determined class (genuine or impostor) matches the real class, points will be blue; if not, red. An X represents face detection failure in either of the images in the pair. Note that the sample size ($n=20$) is small, and the figure may change substantially if larger or different sets are used. The images can be viewed on p. 13 of the Appendix, where Gen 01 corresponds to Same-Identity Pair 1, Gen 02 corresponds to Same-Identity Pair 2, and so on.

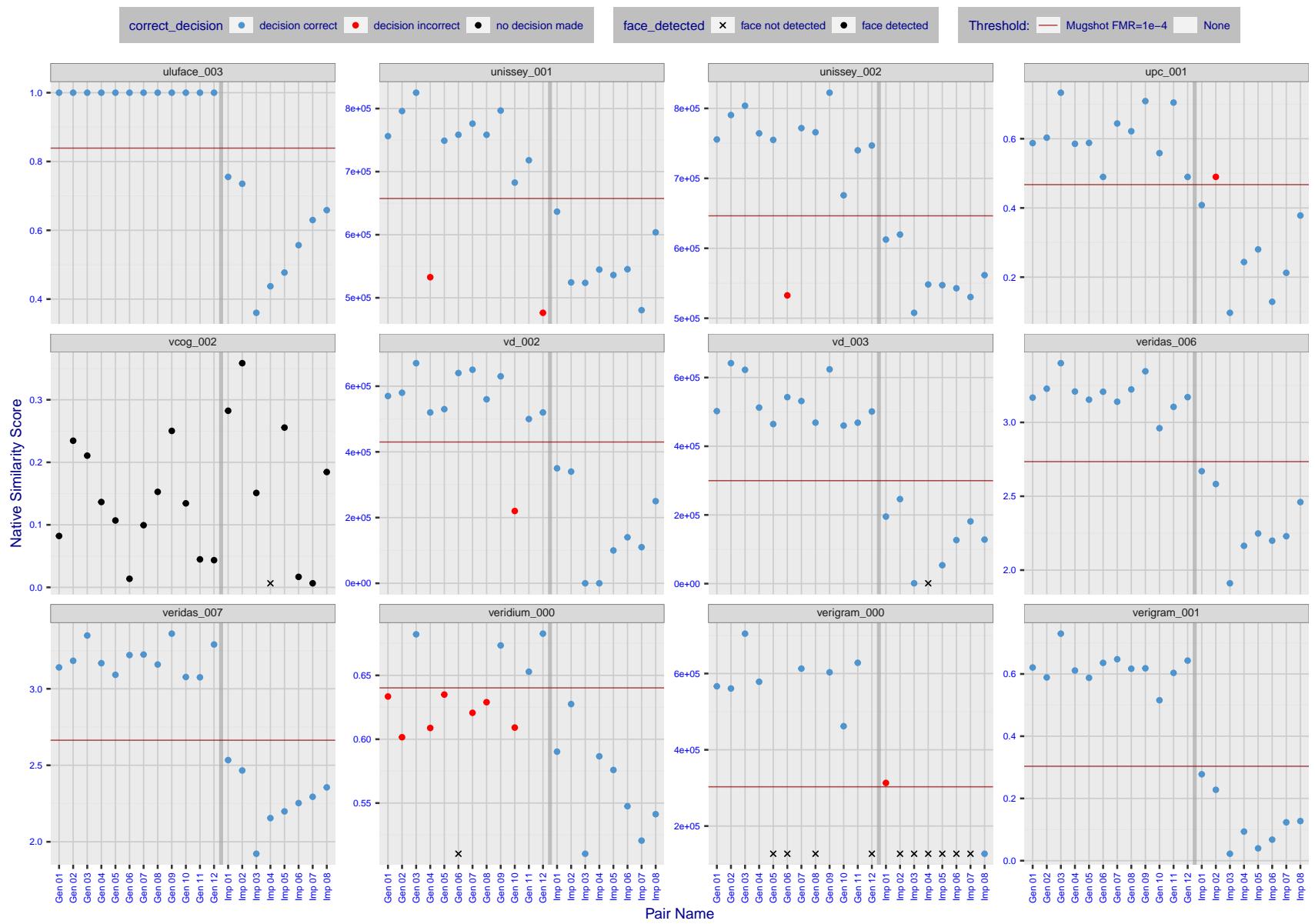


Figure 35: The figure shows algorithms' similarity scores for 12 genuine and 8 impostor image pairs used in a May 2018 paper by Phillips et al. ([1]). The threshold (red horizontal line) is a value calibrated to give $FMR = 0.0001$ on mugshot images. Points above the threshold correspond to pairs determined to be genuine, and points below the threshold correspond to pairs determined to be impostors. If the determined class (genuine or impostor) matches the real class, points will be blue; if not, red. An X represents face detection failure in either of the images in the pair. Note that the sample size ($n=20$) is small, and the figure may change substantially if larger or different sets are used. The images can be viewed on p. 13 of the Appendix, where Gen 01 corresponds to Same-Identity Pair 1, Gen 02 corresponds to Same-Identity Pair 2, and so on.

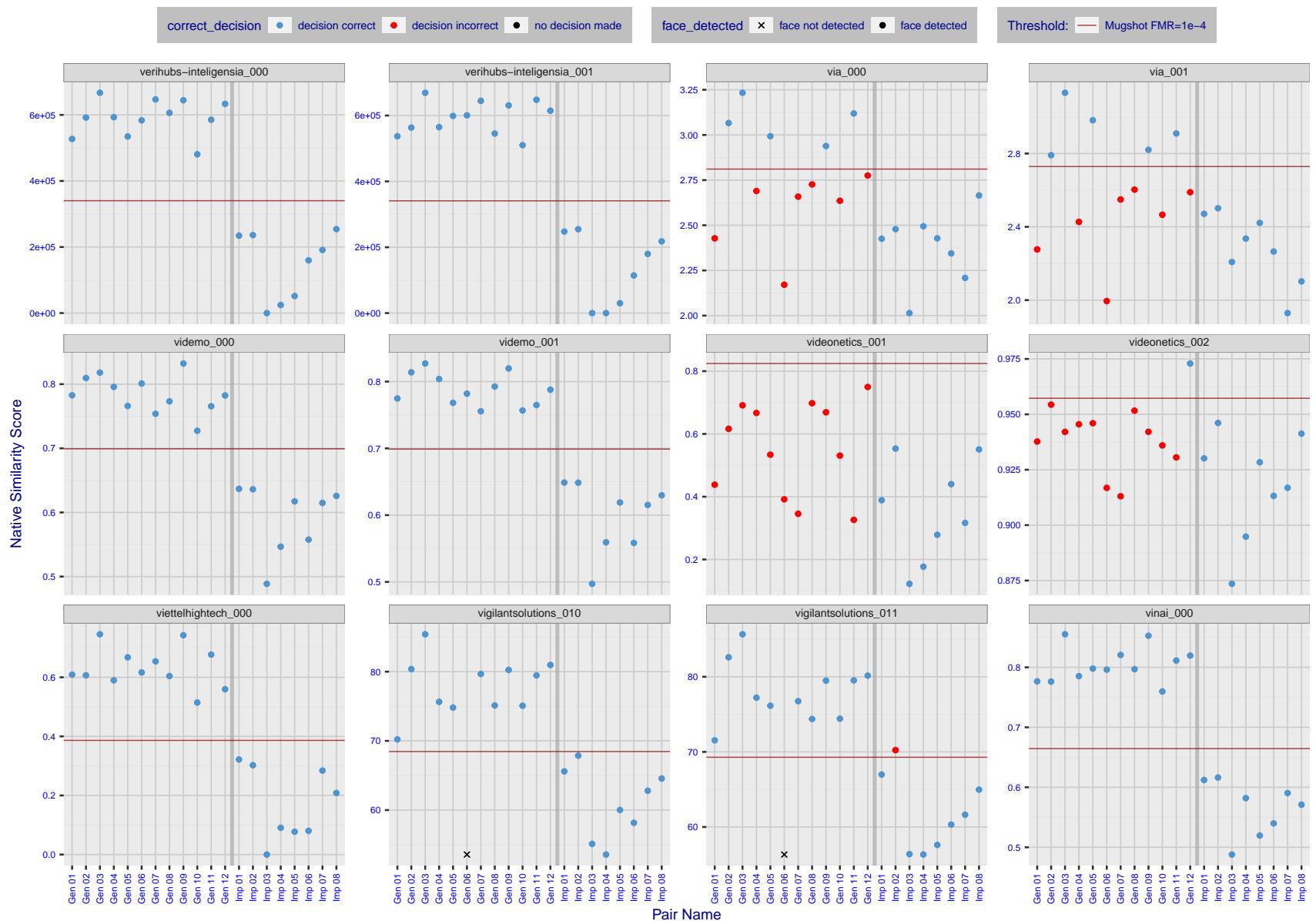


Figure 36: The figure shows algorithms' similarity scores for 12 genuine and 8 impostor image pairs used in a May 2018 paper by Phillips et al. ([1]). The threshold (red horizontal line) is a value calibrated to give $FMR = 0.0001$ on mugshot images. Points above the threshold correspond to pairs determined to be genuine, and points below the threshold correspond to pairs determined to be impostors. If the determined class (genuine or impostor) matches the real class, points will be blue; if not, red. An X represents face detection failure in either of the images in the pair. Note that the sample size ($n=20$) is small, and the figure may change substantially if larger or different sets are used. The images can be viewed on p. 13 of the Appendix, where Gen 01 corresponds to Same-Identity Pair 1, Gen 02 corresponds to Same-Identity Pair 2, and so on.

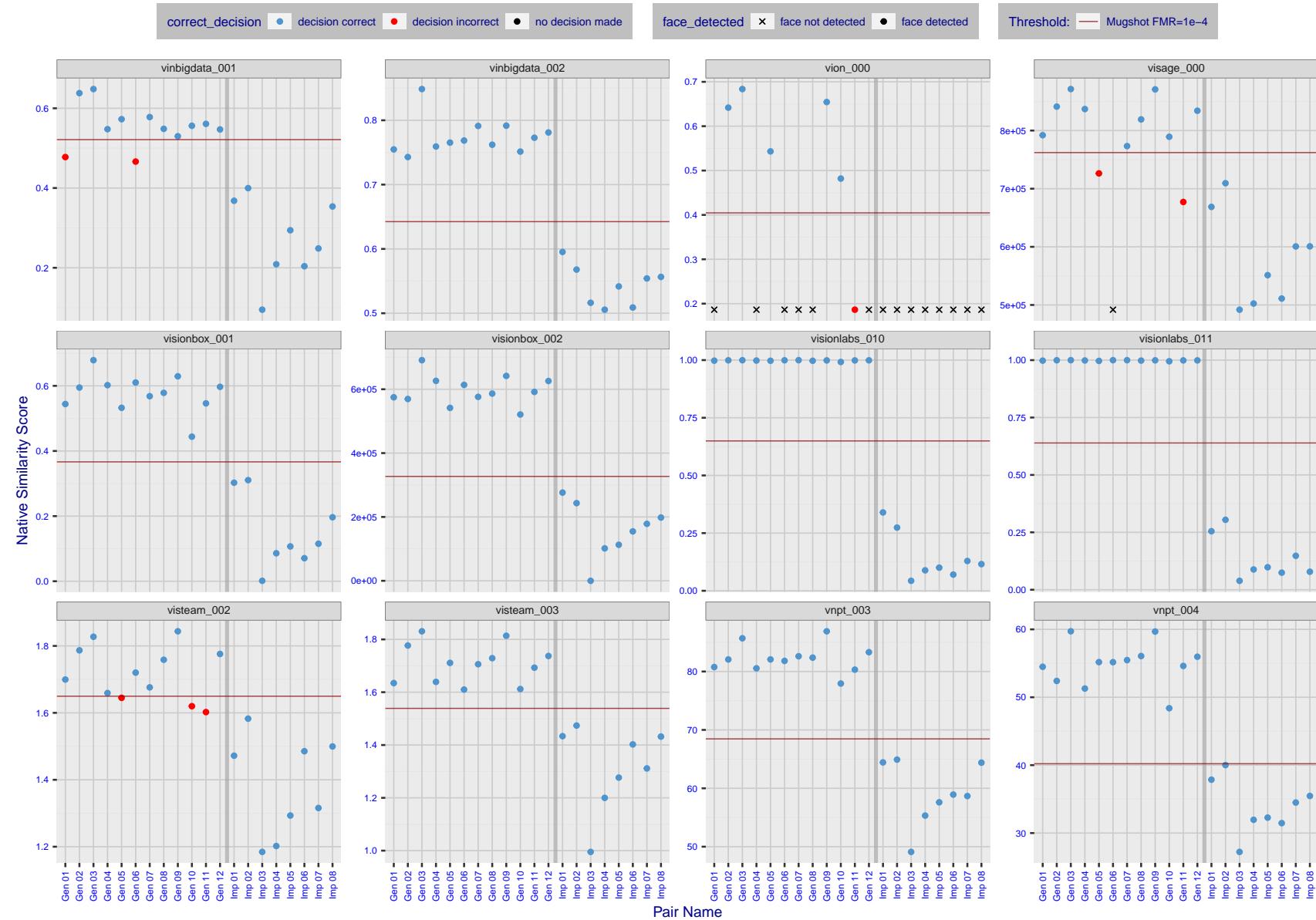


Figure 37: The figure shows algorithms' similarity scores for 12 genuine and 8 impostor image pairs used in a May 2018 paper by Phillips et al. ([1]). The threshold (red horizontal line) is a value calibrated to give $FMR = 0.0001$ on mugshot images. Points above the threshold correspond to pairs determined to be genuine, and points below the threshold correspond to pairs determined to be impostors. If the determined class (genuine or impostor) matches the real class, points will be blue; if not, red. An X represents face detection failure in either of the images in the pair. Note that the sample size ($n=20$) is small, and the figure may change substantially if larger or different sets are used. The images can be viewed on p. 13 of the Appendix, where Gen 01 corresponds to Same-Identity Pair 1, Gen 02 corresponds to Same-Identity Pair 2, and so on.

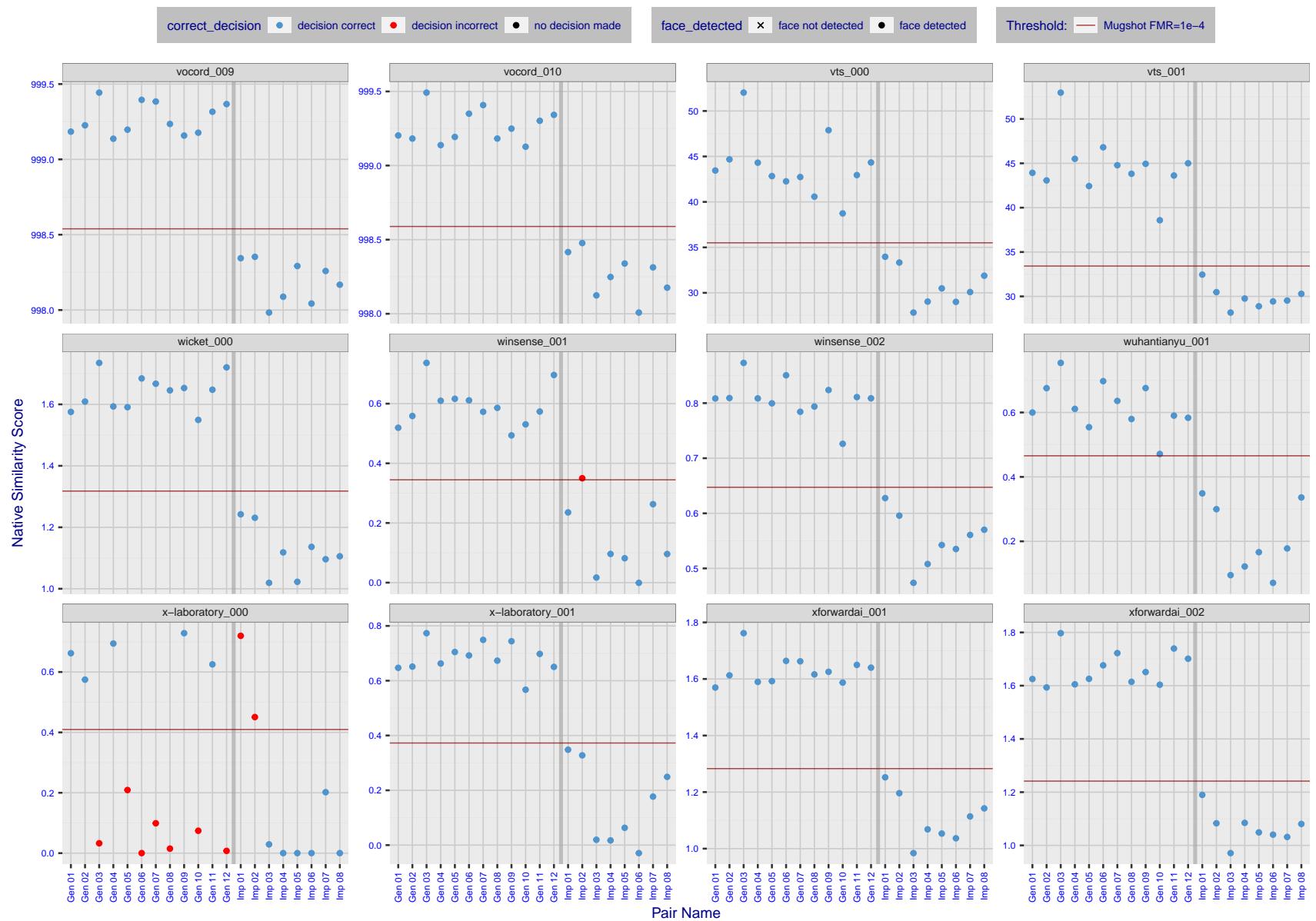


Figure 38: The figure shows algorithms' similarity scores for 12 genuine and 8 impostor image pairs used in a May 2018 paper by Phillips et al. ([1]). The threshold (red horizontal line) is a value calibrated to give $FMR = 0.0001$ on mugshot images. Points above the threshold correspond to pairs determined to be genuine, and points below the threshold correspond to pairs determined to be impostors. If the determined class (genuine or impostor) matches the real class, points will be blue; if not, red. An X represents face detection failure in either of the images in the pair. Note that the sample size ($n=20$) is small, and the figure may change substantially if larger or different sets are used. The images can be viewed on p. 13 of the Appendix, where Gen 01 corresponds to Same-Identity Pair 1, Gen 02 corresponds to Same-Identity Pair 2, and so on.

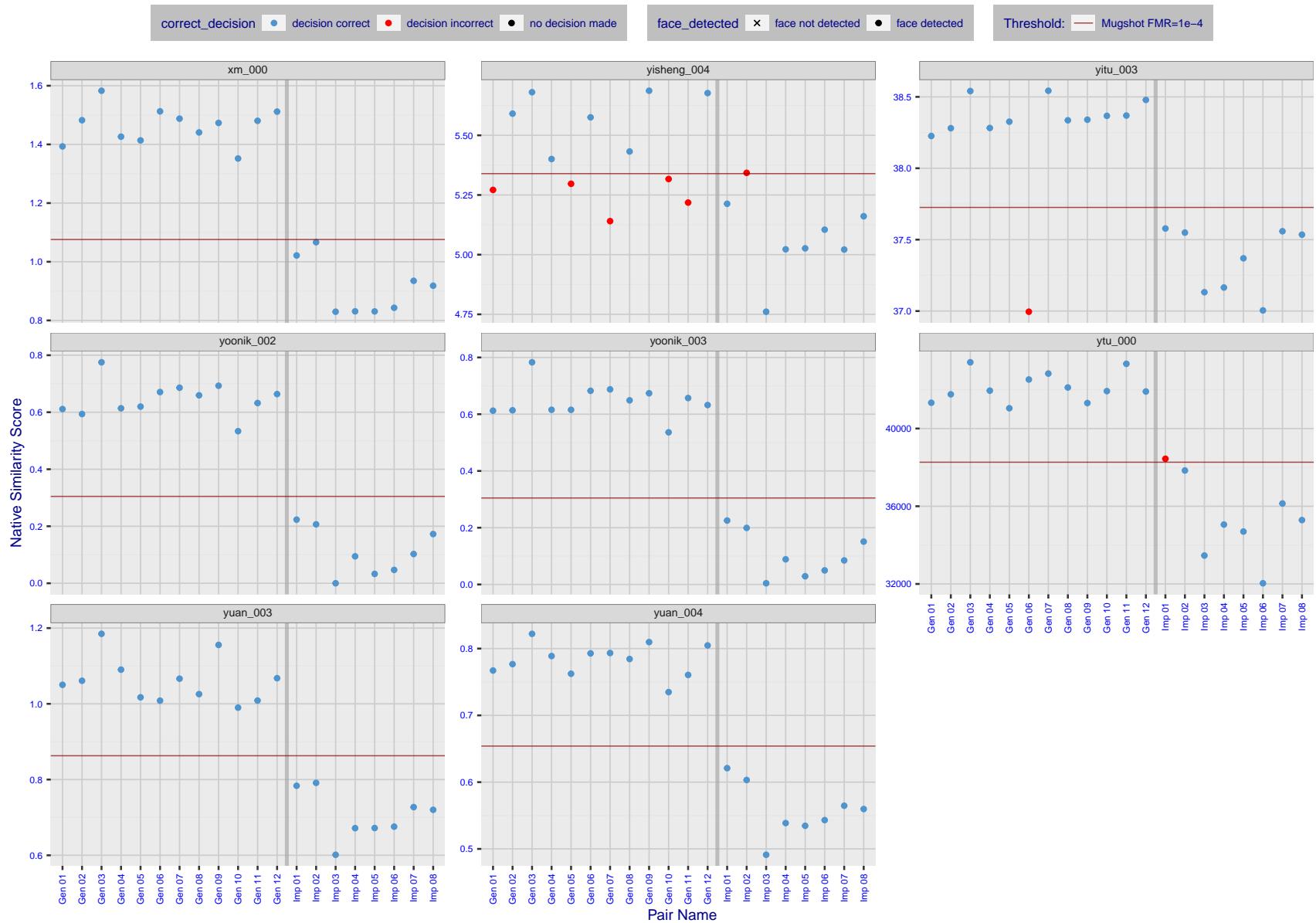


Figure 39: The figure shows algorithms' similarity scores for 12 genuine and 8 impostor image pairs used in a May 2018 paper by Phillips et al. ([1]). The threshold (red horizontal line) is a value calibrated to give $FMR = 0.0001$ on mugshot images. Points above the threshold correspond to pairs determined to be genuine, and points below the threshold correspond to pairs determined to be impostors. If the determined class (genuine or impostor) matches the real class, points will be blue; if not, red. An X represents face detection failure in either of the images in the pair. Note that the sample size ($n=20$) is small, and the figure may change substantially if larger or different sets are used. The images can be viewed on p. 13 of the Appendix, where Gen 01 corresponds to Same-Identity Pair 1, Gen 02 corresponds to Same-Identity Pair 2, and so on.

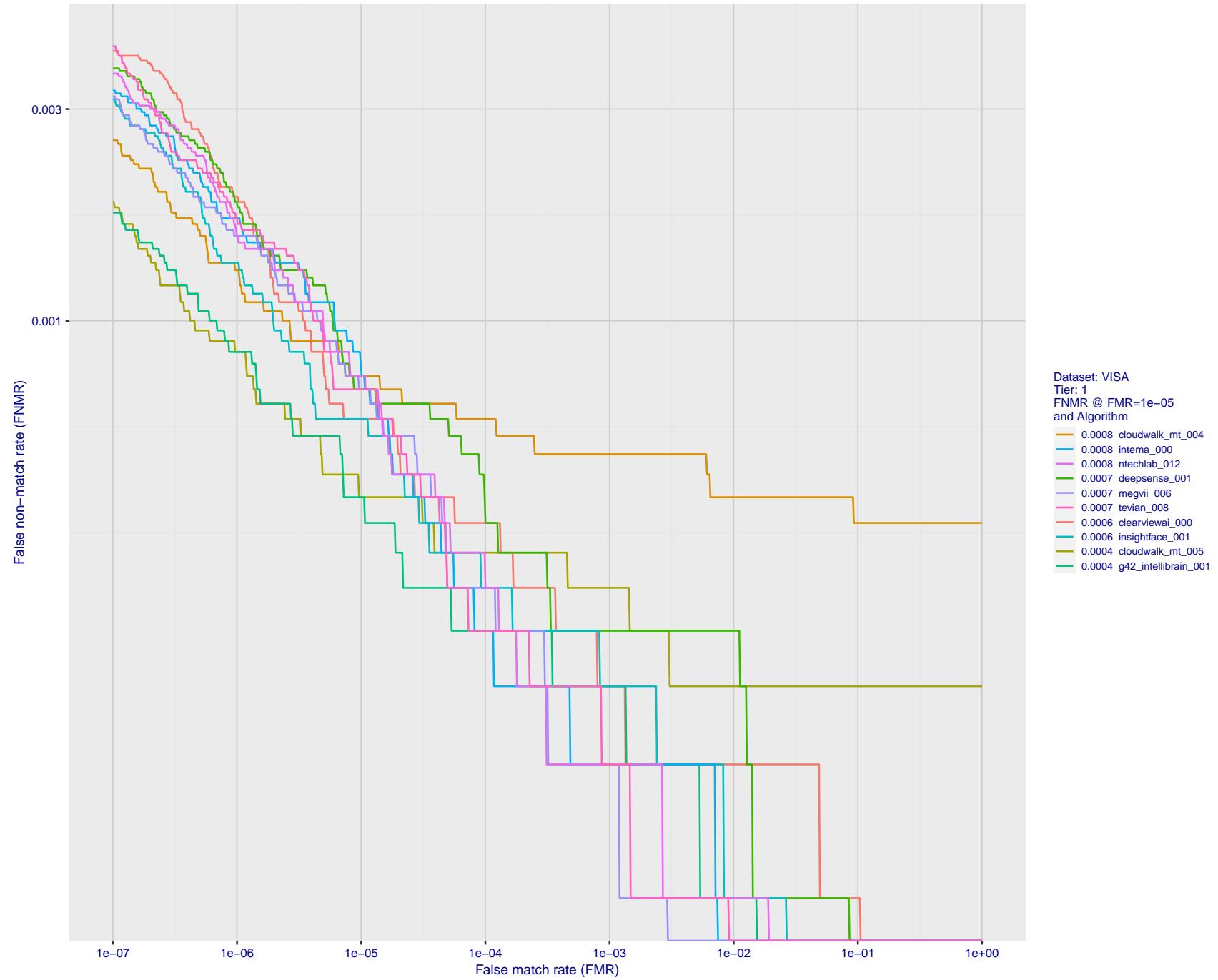


Figure 40: For the visa images, detection error tradeoff (DET) characteristics showing false non-match rate vs. false match rate plotted parametrically on threshold, T . The scales are logarithmic in order to show many decades of FMR.

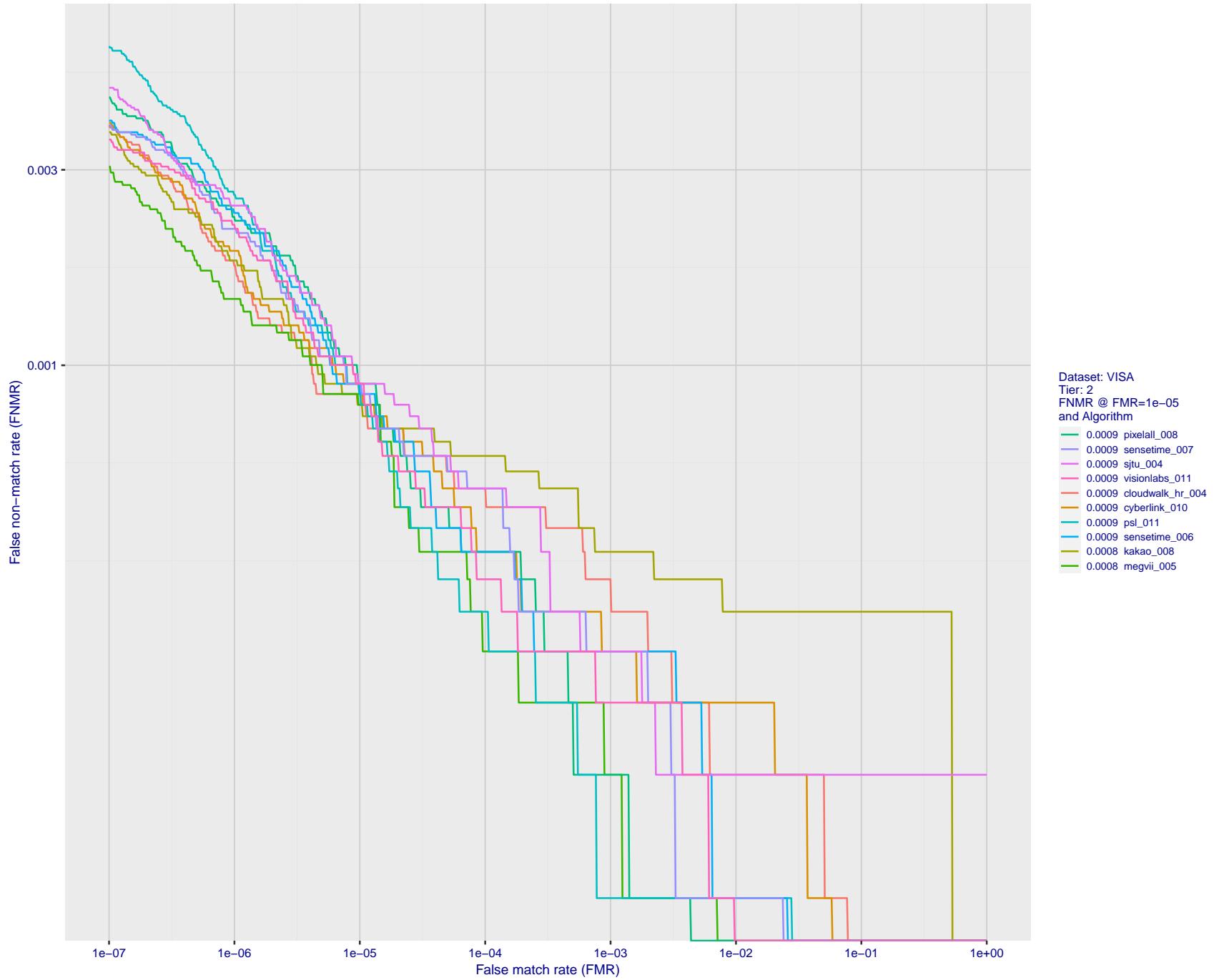


Figure 41: For the visa images, detection error tradeoff (DET) characteristics showing false non-match rate vs. false match rate plotted parametrically on threshold, T . The scales are logarithmic in order to show many decades of FMR.

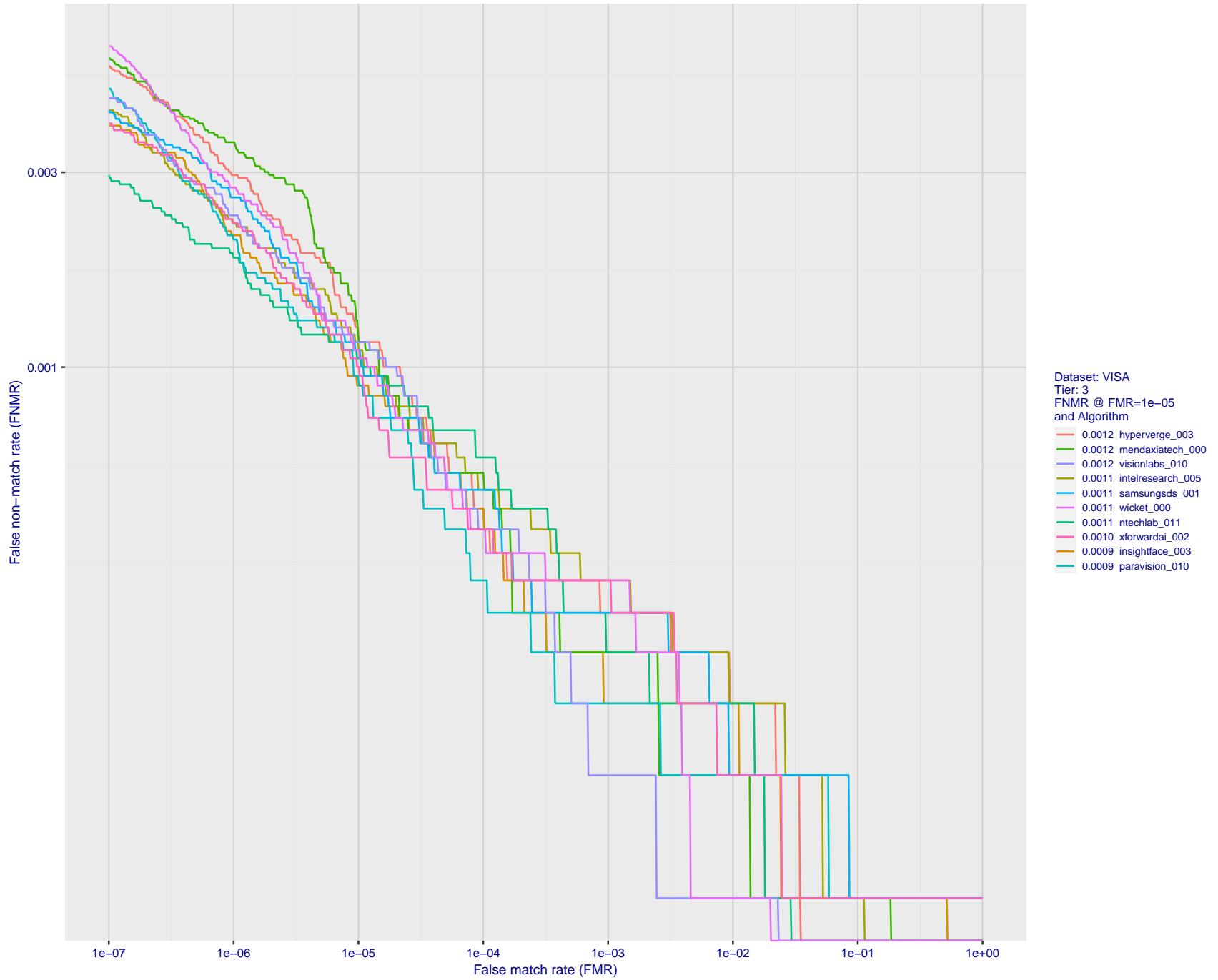


Figure 42: For the visa images, detection error tradeoff (DET) characteristics showing false non-match rate vs. false match rate plotted parametrically on threshold, T . The scales are logarithmic in order to show many decades of FMR.

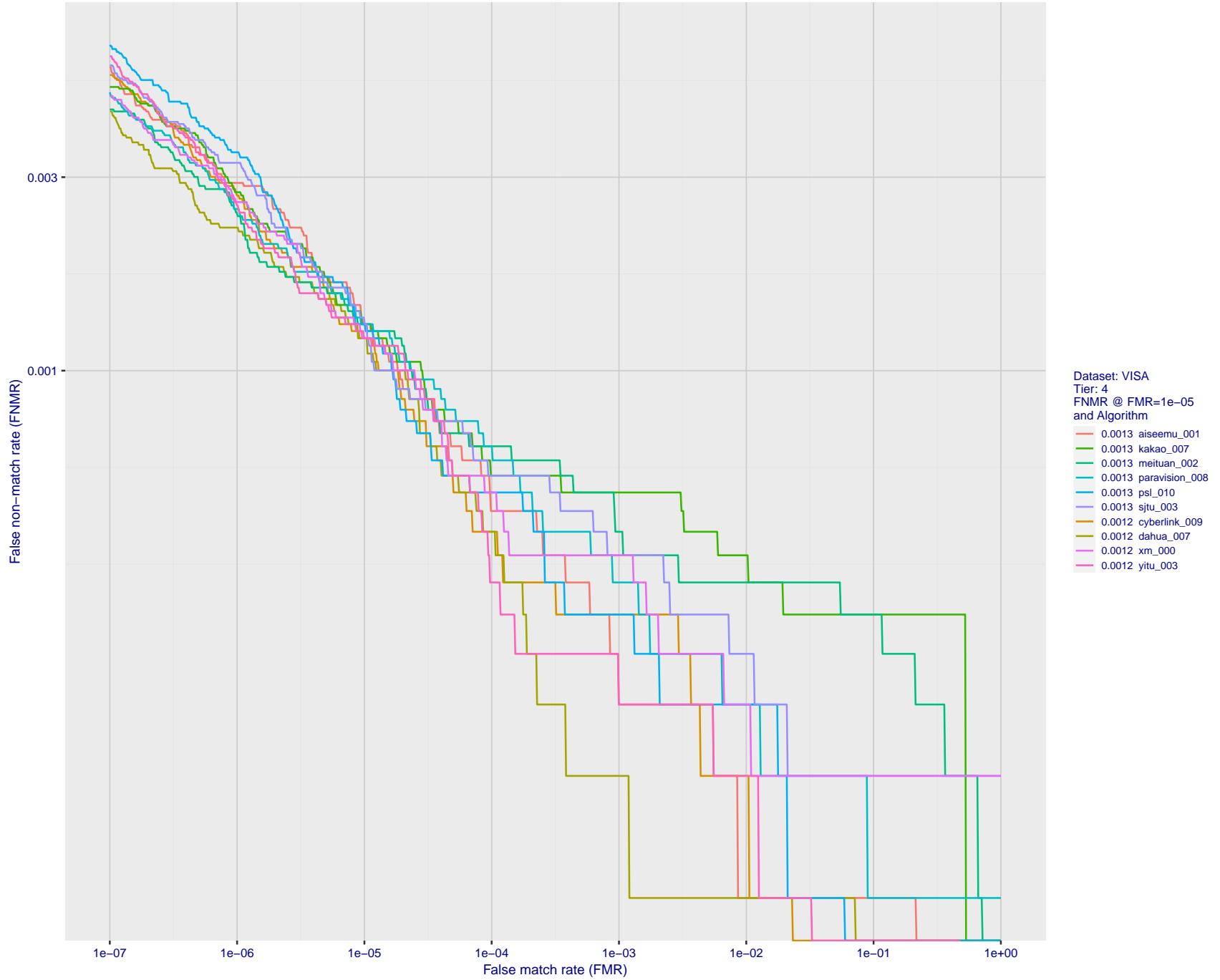


Figure 43: For the visa images, detection error tradeoff (DET) characteristics showing false non-match rate vs. false match rate plotted parametrically on threshold, T . The scales are logarithmic in order to show many decades of FMR.

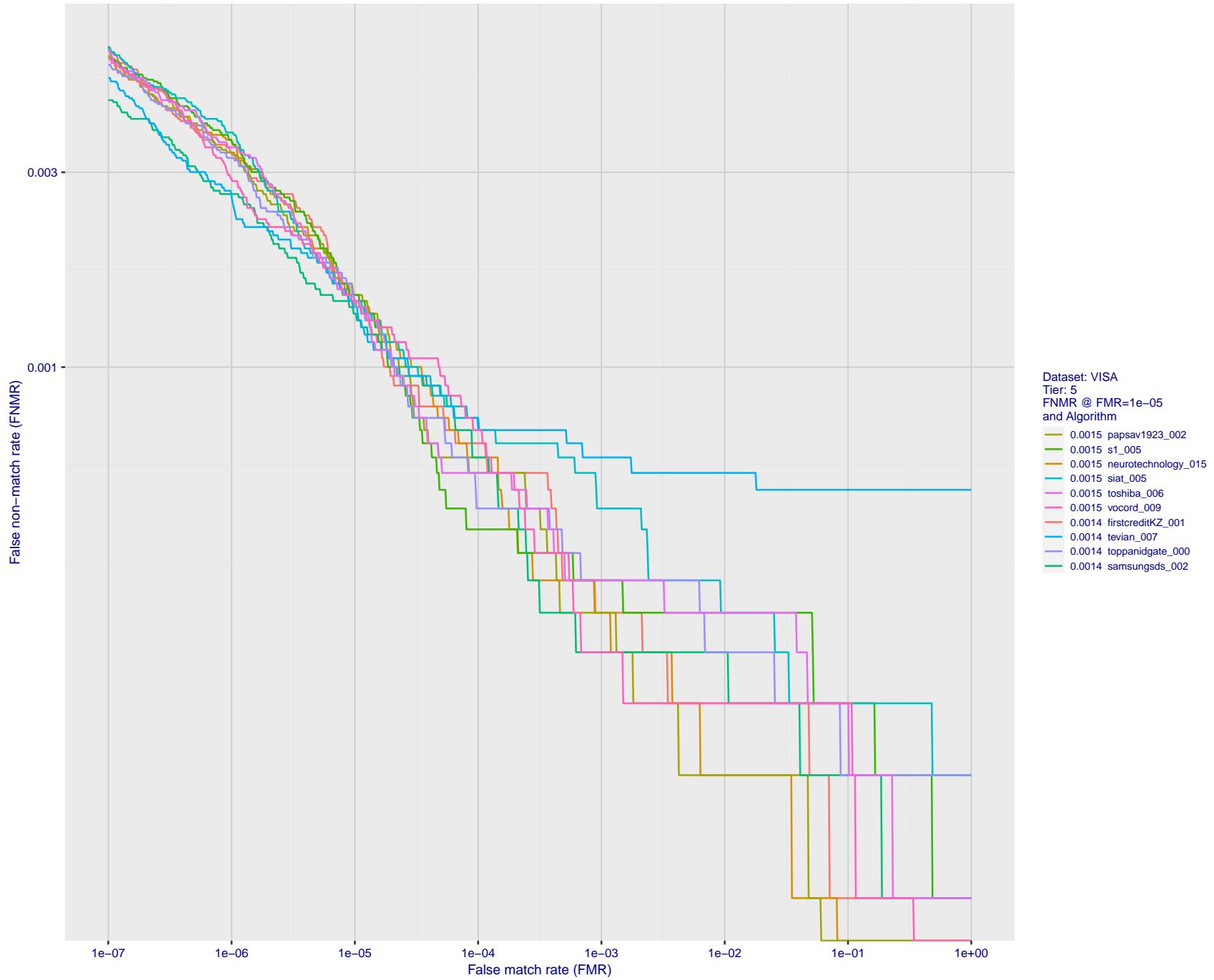


Figure 44: For the visa images, detection error tradeoff (DET) characteristics showing false non-match rate vs. false match rate plotted parametrically on threshold, T . The scales are logarithmic in order to show many decades of FMR.

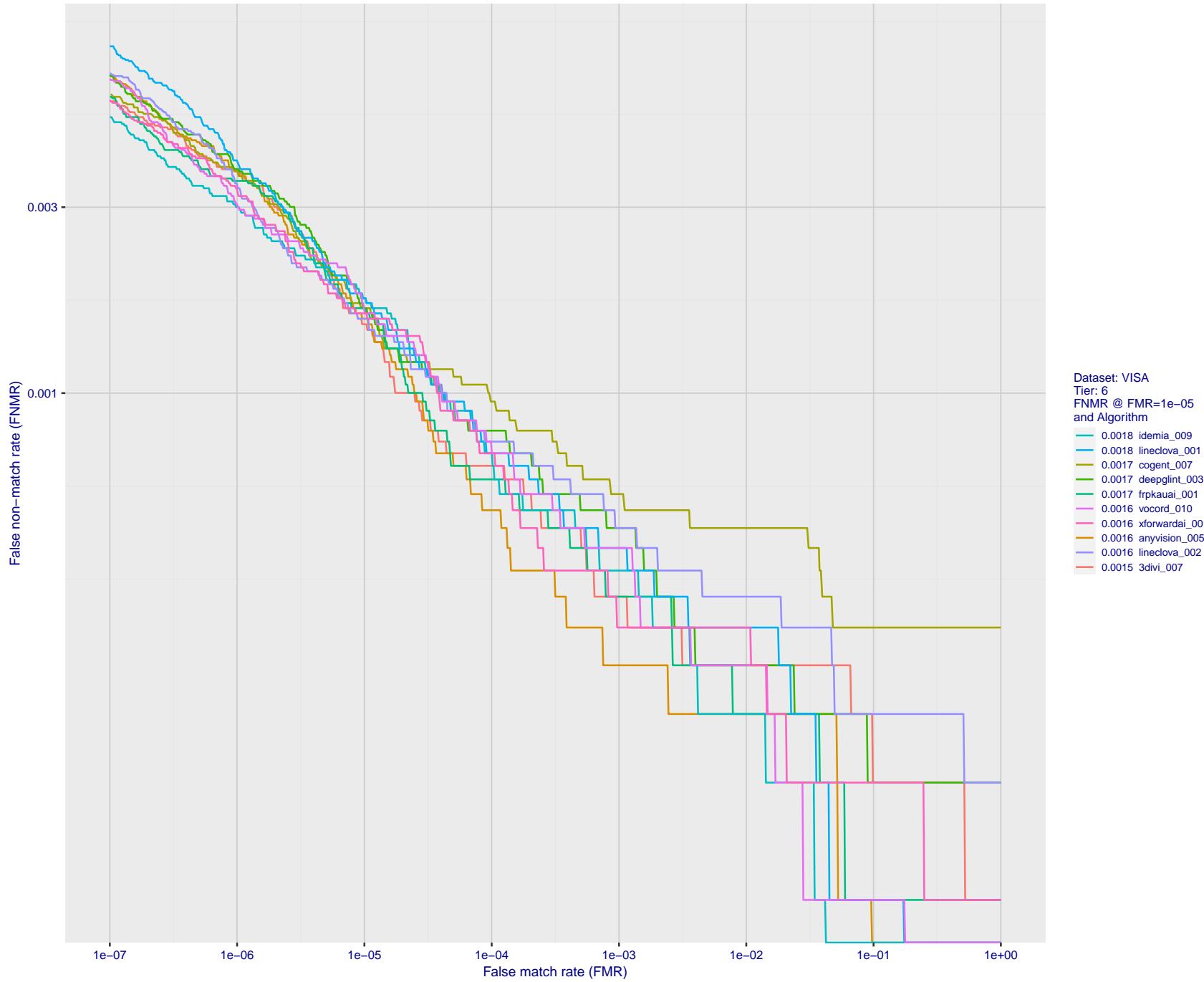


Figure 45: For the visa images, detection error tradeoff (DET) characteristics showing false non-match rate vs. false match rate plotted parametrically on threshold, T . The scales are logarithmic in order to show many decades of FMR.

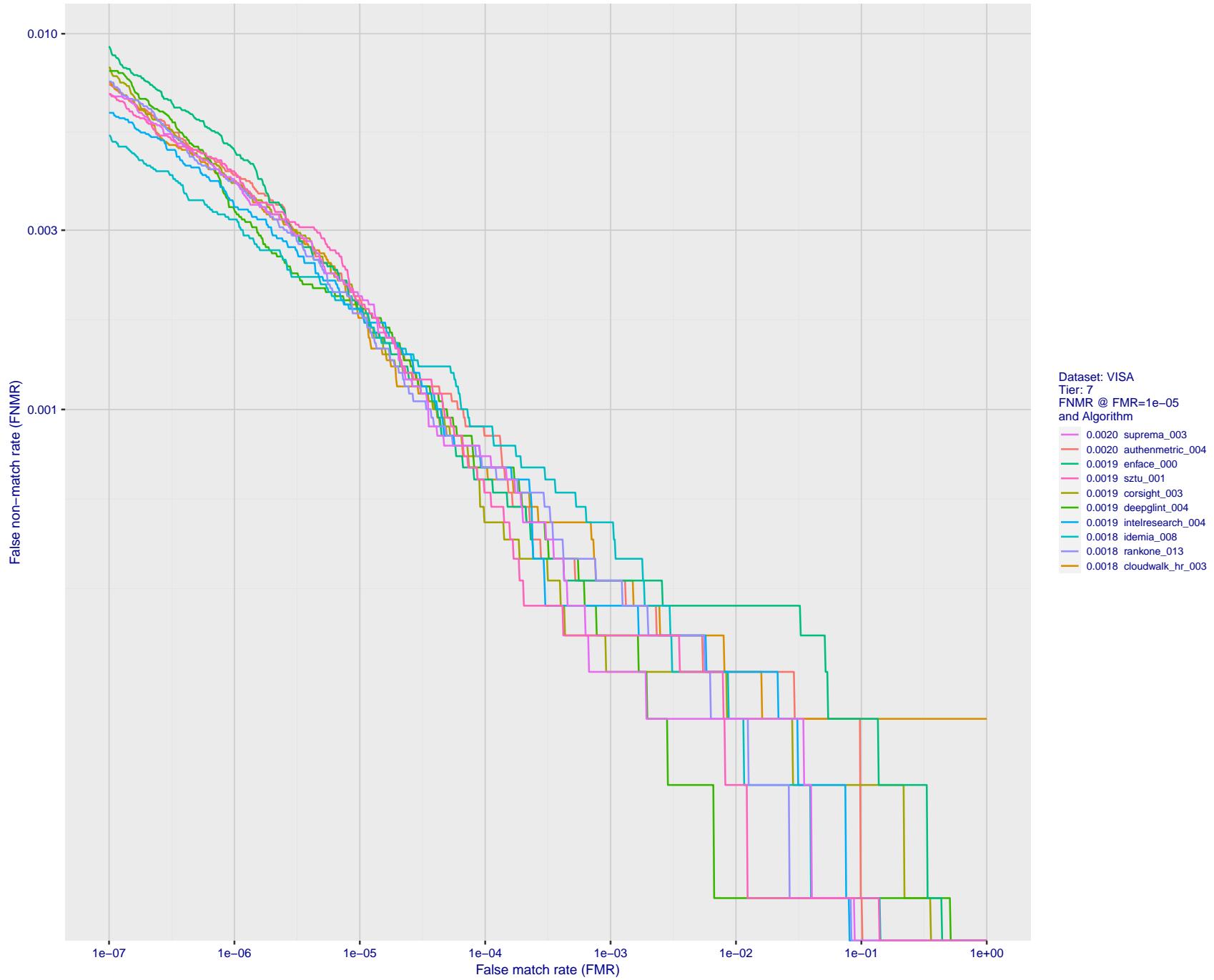


Figure 46: For the visa images, detection error tradeoff (DET) characteristics showing false non-match rate vs. false match rate plotted parametrically on threshold, T . The scales are logarithmic in order to show many decades of FMR.

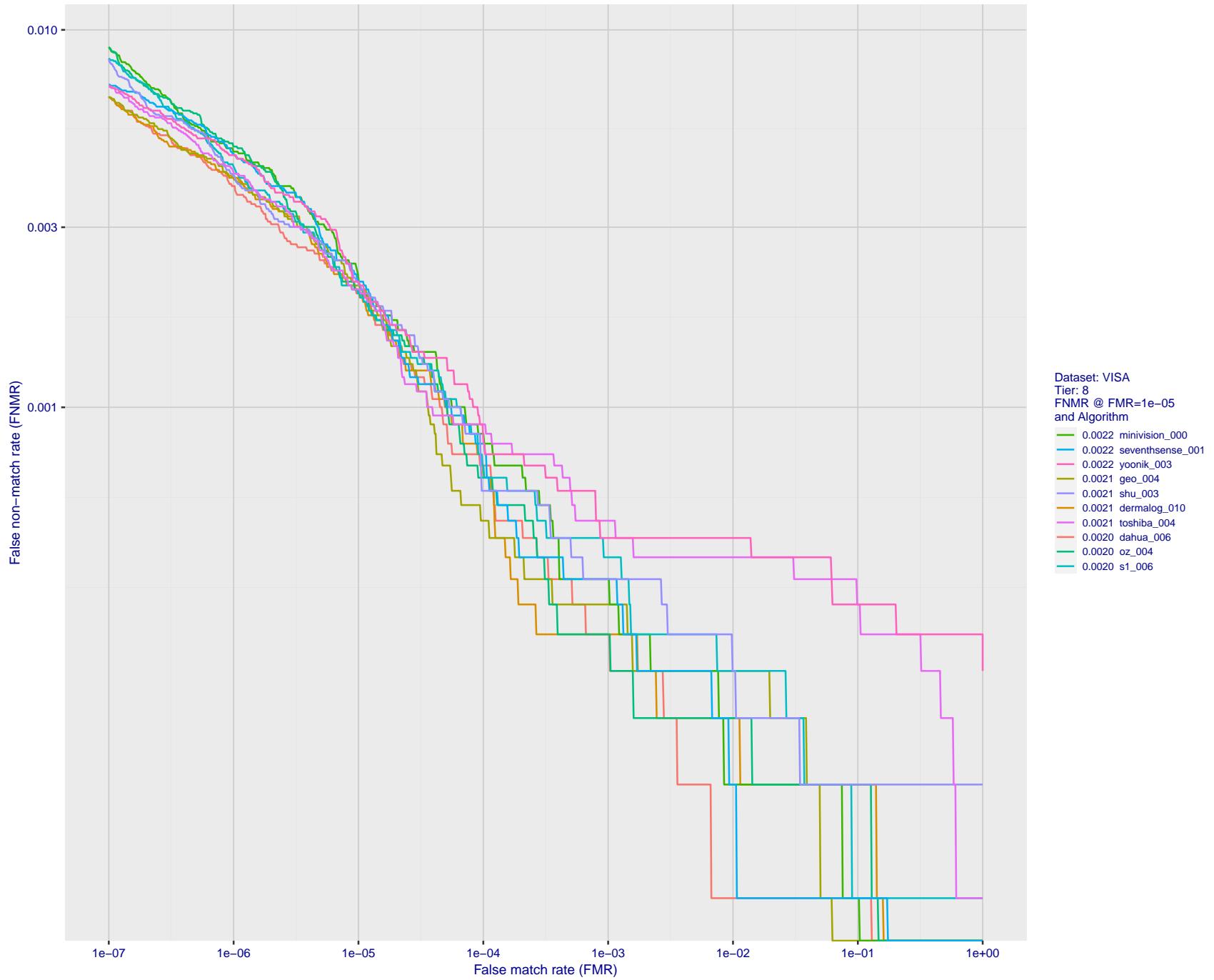


Figure 47: For the visa images, detection error tradeoff (DET) characteristics showing false non-match rate vs. false match rate plotted parametrically on threshold, T . The scales are logarithmic in order to show many decades of FMR.

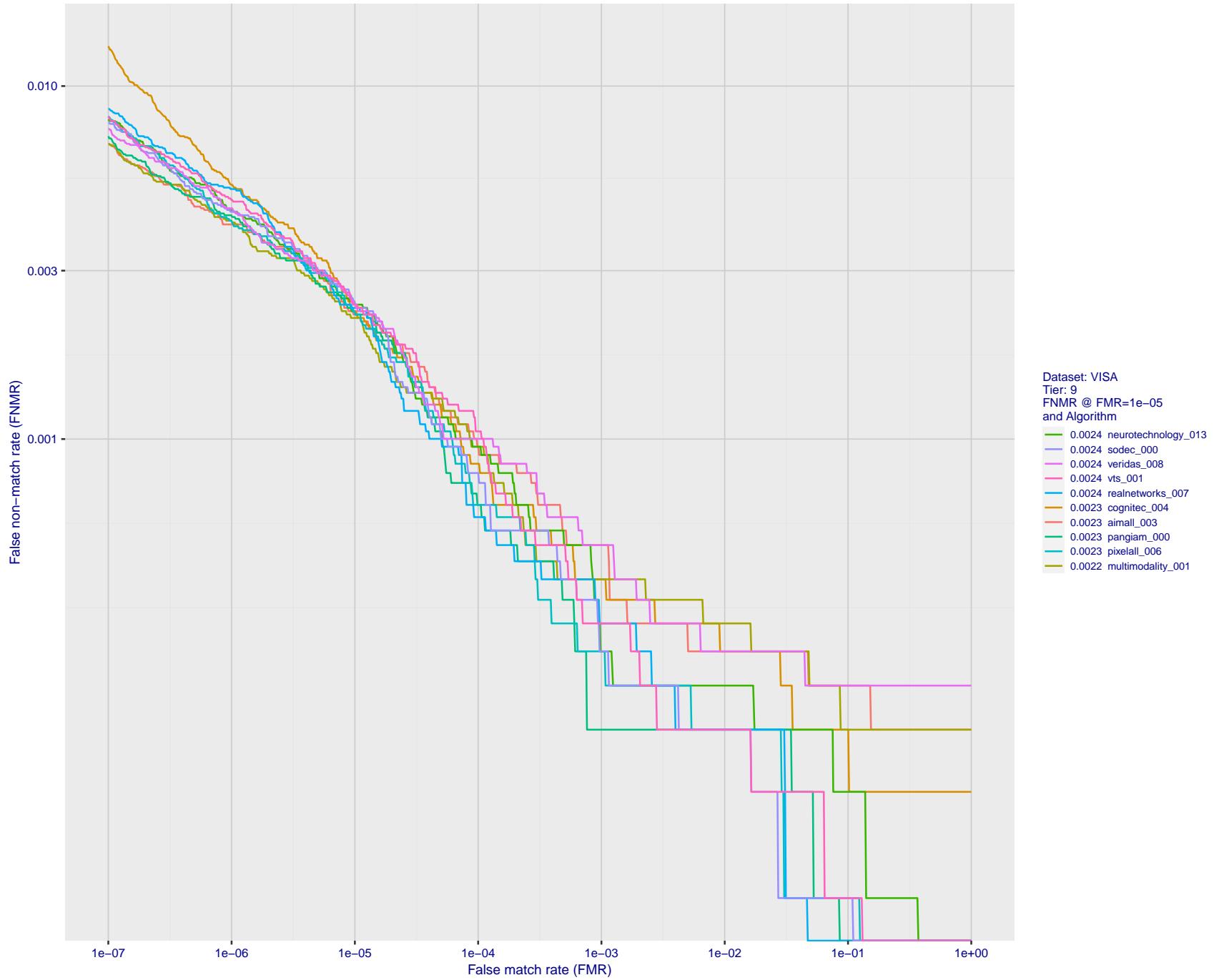


Figure 48: For the visa images, detection error tradeoff (DET) characteristics showing false non-match rate vs. false match rate plotted parametrically on threshold, T . The scales are logarithmic in order to show many decades of FMR.

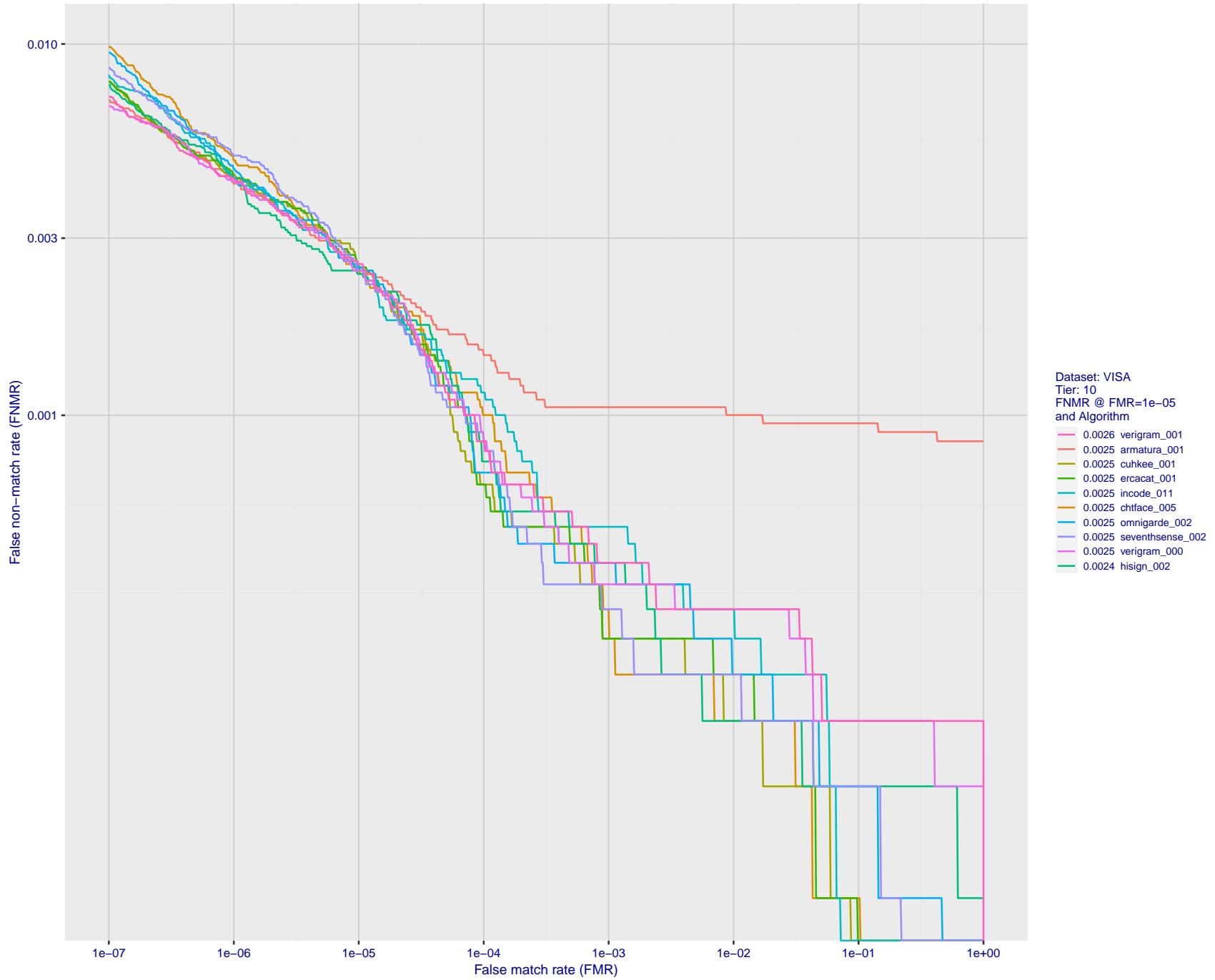


Figure 49: For the visa images, detection error tradeoff (DET) characteristics showing false non-match rate vs. false match rate plotted parametrically on threshold, T . The scales are logarithmic in order to show many decades of FMR.

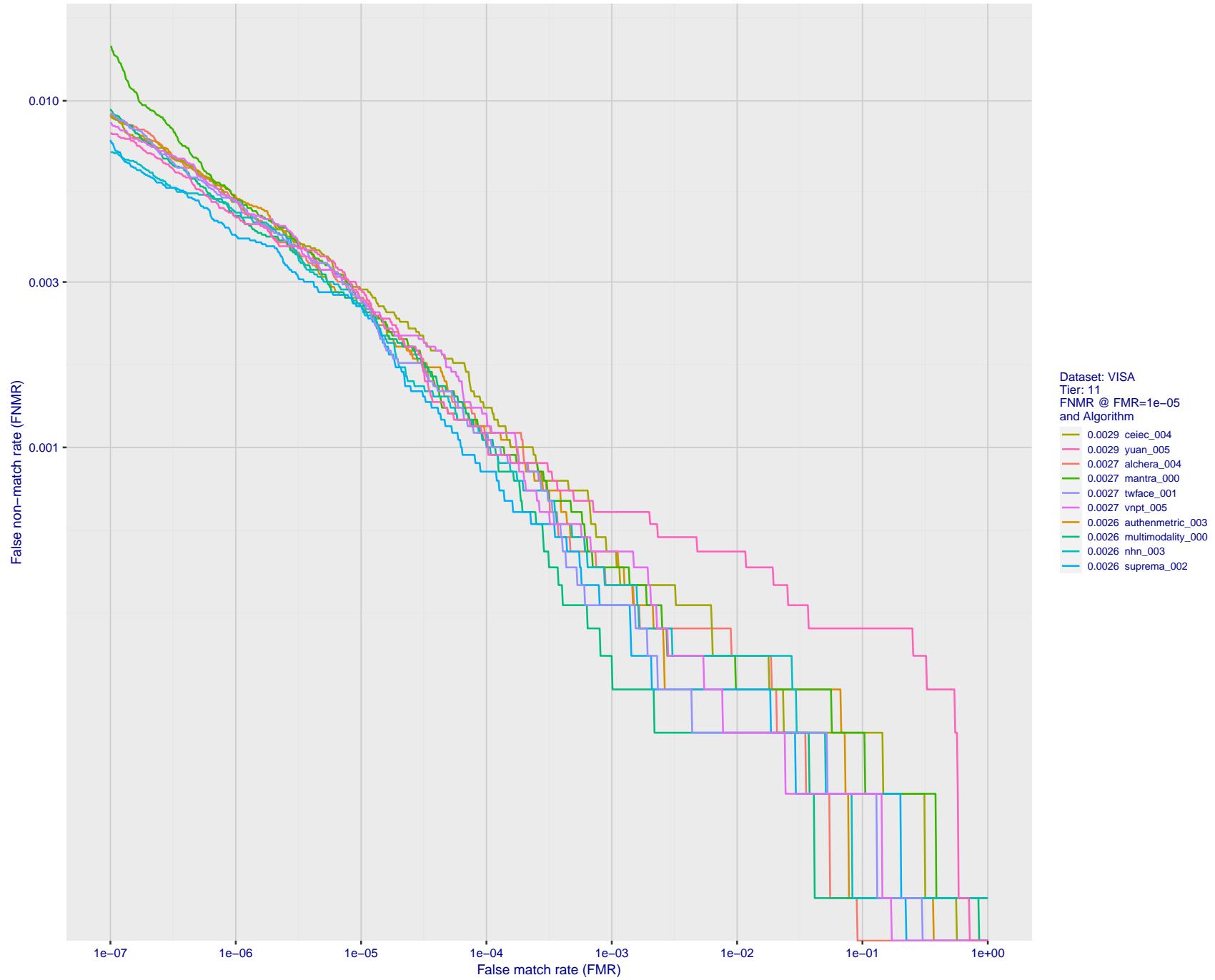


Figure 50: For the visa images, detection error tradeoff (DET) characteristics showing false non-match rate vs. false match rate plotted parametrically on threshold, T . The scales are logarithmic in order to show many decades of FMR.

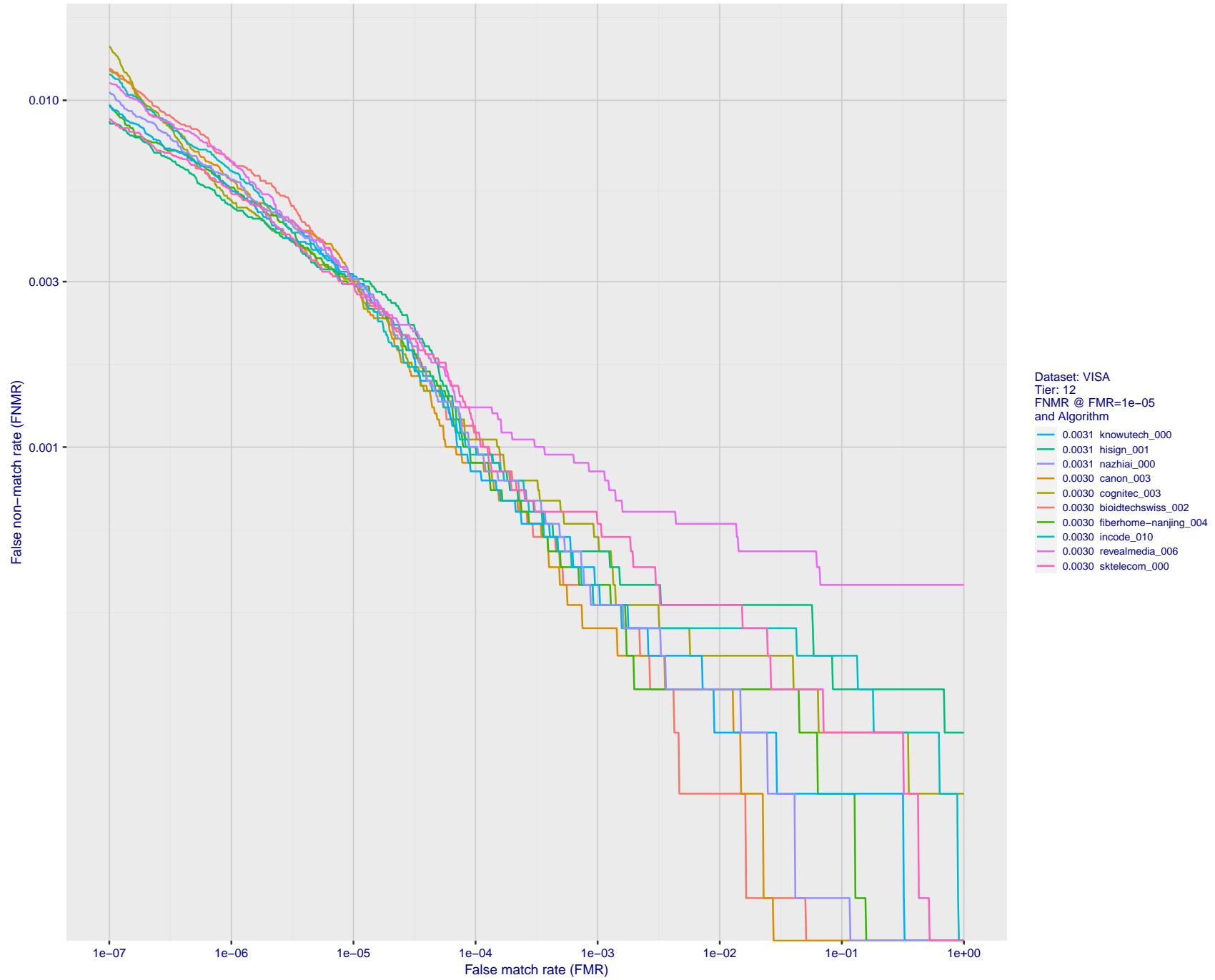


Figure 51: For the visa images, detection error tradeoff (DET) characteristics showing false non-match rate vs. false match rate plotted parametrically on threshold, T . The scales are logarithmic in order to show many decades of FMR.

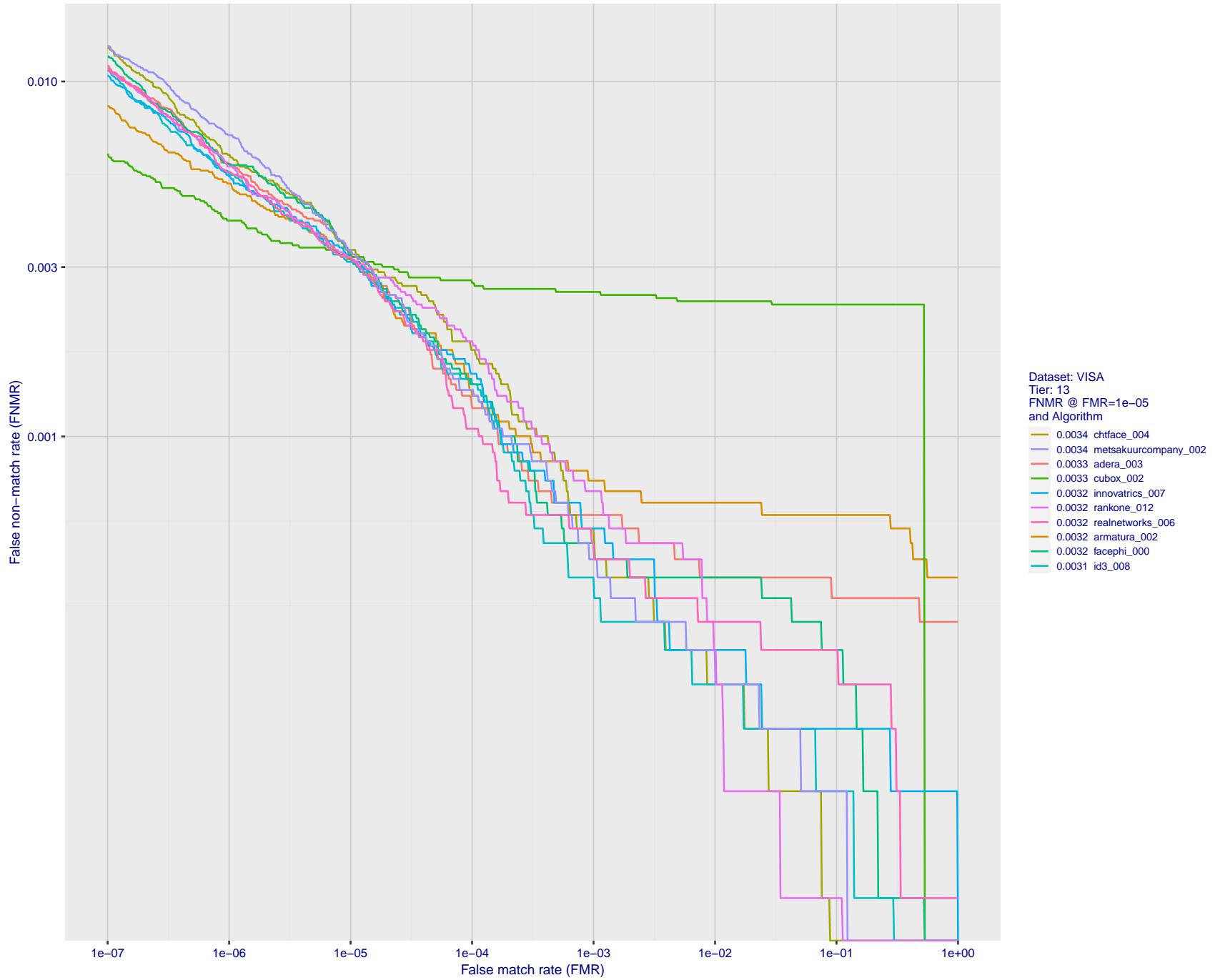


Figure 52: For the visa images, detection error tradeoff (DET) characteristics showing false non-match rate vs. false match rate plotted parametrically on threshold, T . The scales are logarithmic in order to show many decades of FMR.

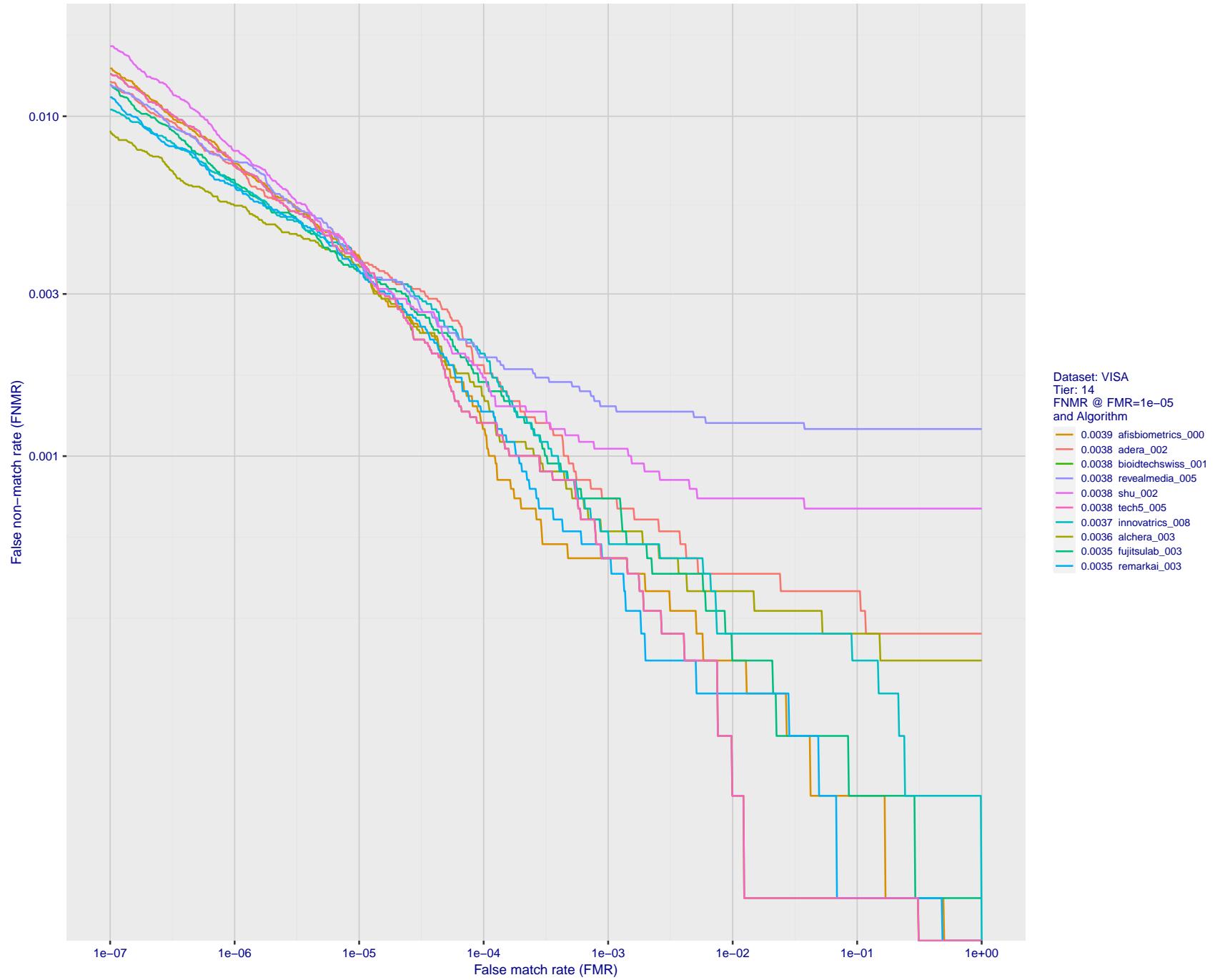


Figure 53: For the visa images, detection error tradeoff (DET) characteristics showing false non-match rate vs. false match rate plotted parametrically on threshold, T . The scales are logarithmic in order to show many decades of FMR.

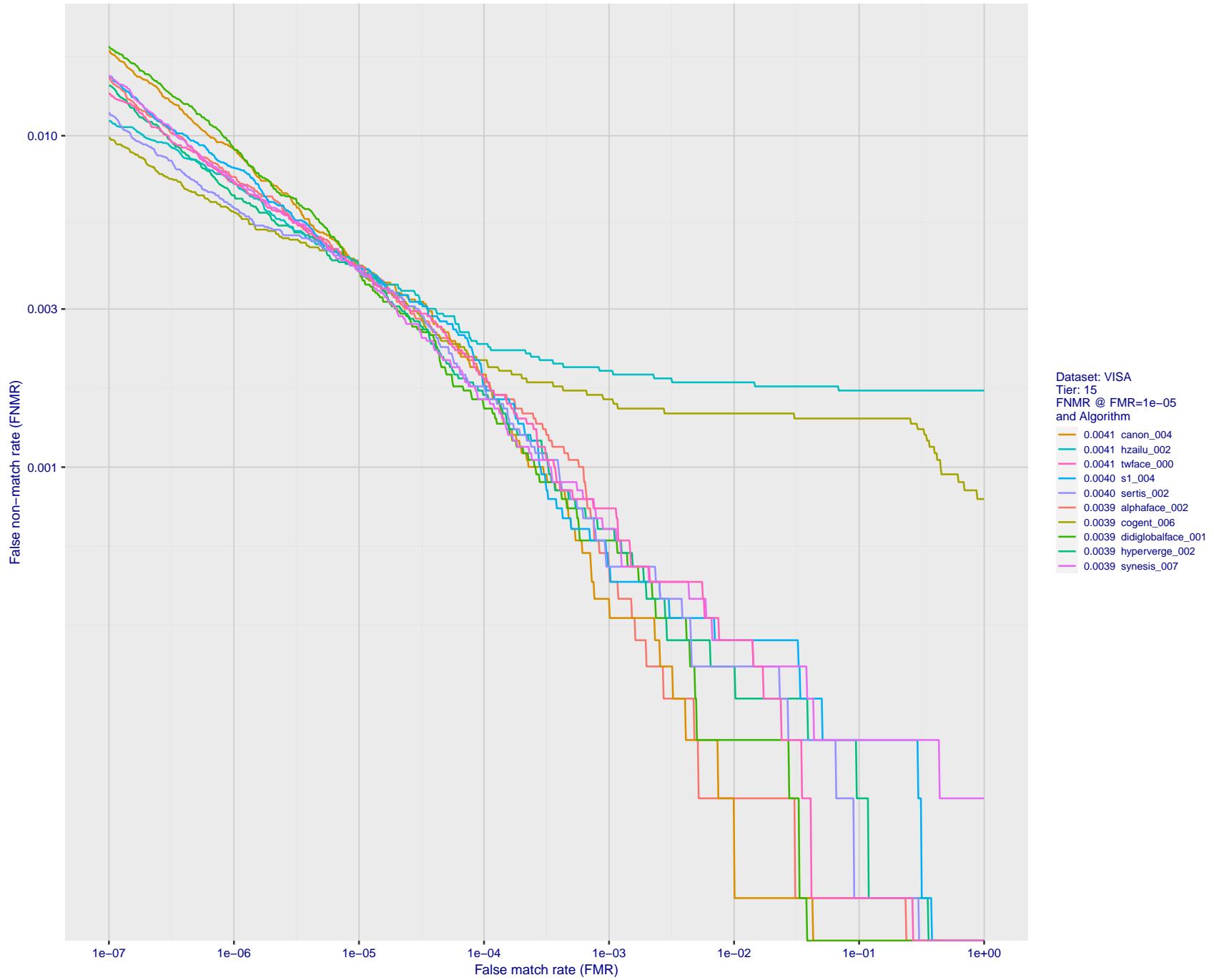


Figure 54: For the visa images, detection error tradeoff (DET) characteristics showing false non-match rate vs. false match rate plotted parametrically on threshold, T . The scales are logarithmic in order to show many decades of FMR.

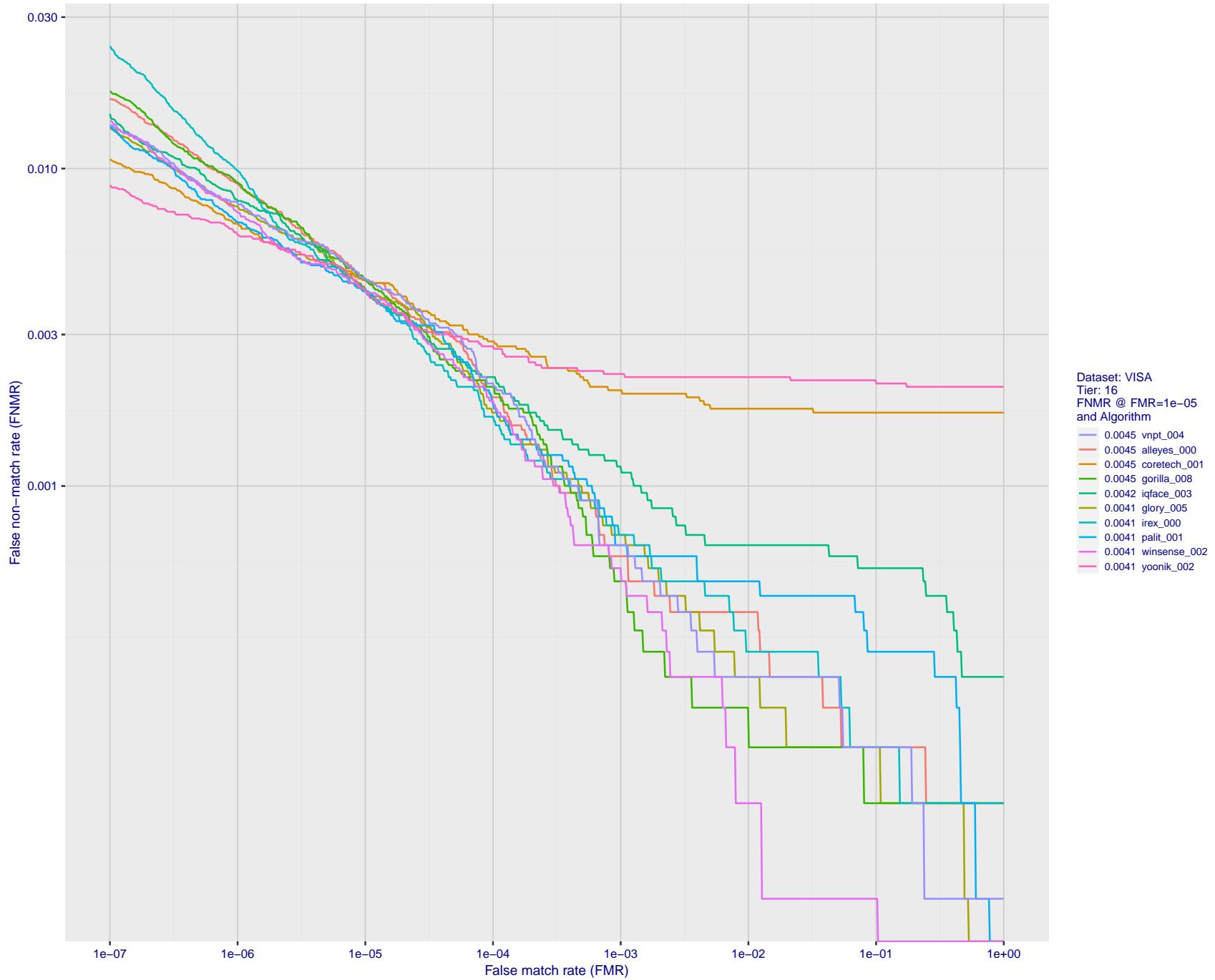


Figure 55: For the visa images, detection error tradeoff (DET) characteristics showing false non-match rate vs. false match rate plotted parametrically on threshold, T . The scales are logarithmic in order to show many decades of FMR.

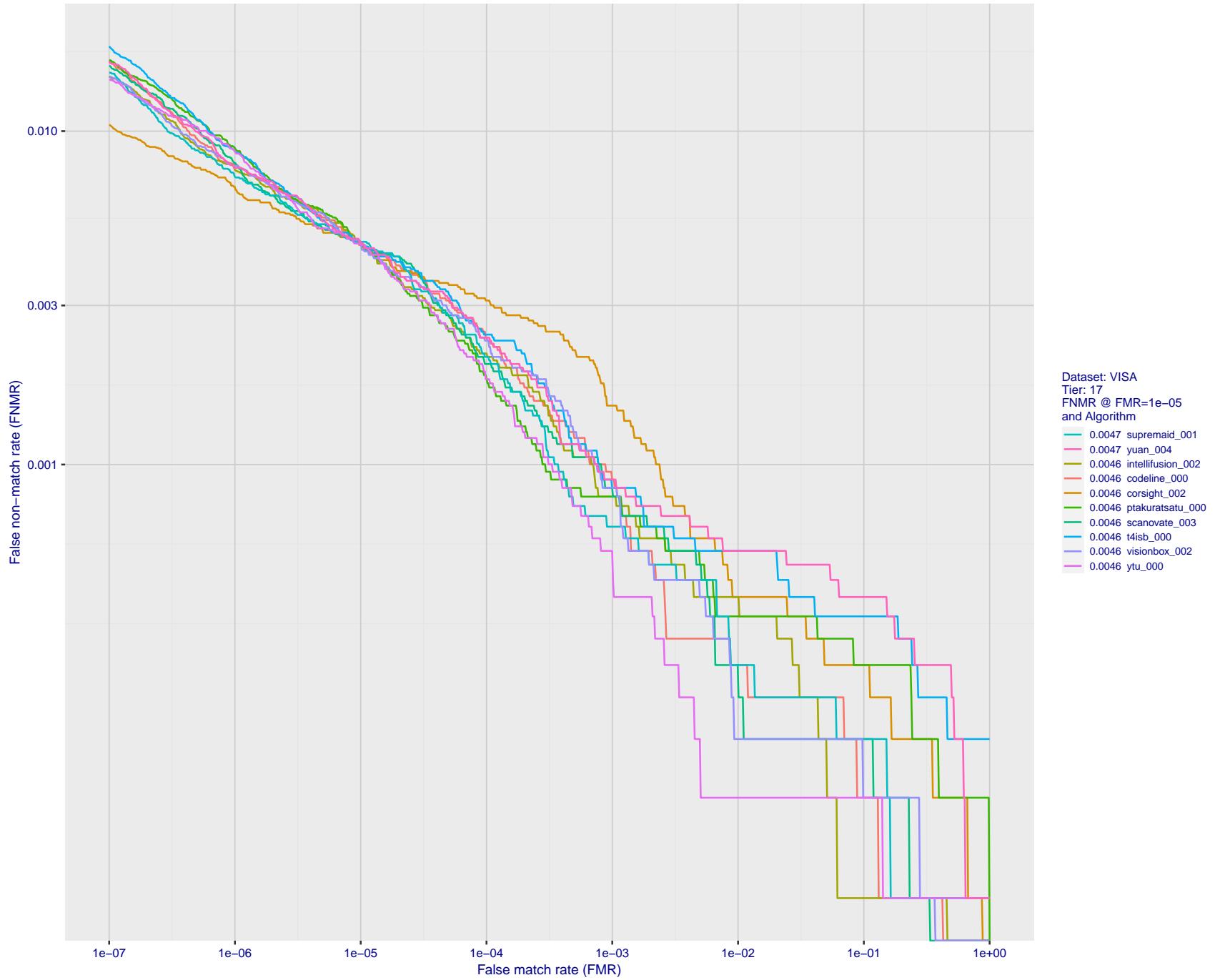


Figure 56: For the visa images, detection error tradeoff (DET) characteristics showing false non-match rate vs. false match rate plotted parametrically on threshold, T . The scales are logarithmic in order to show many decades of FMR.

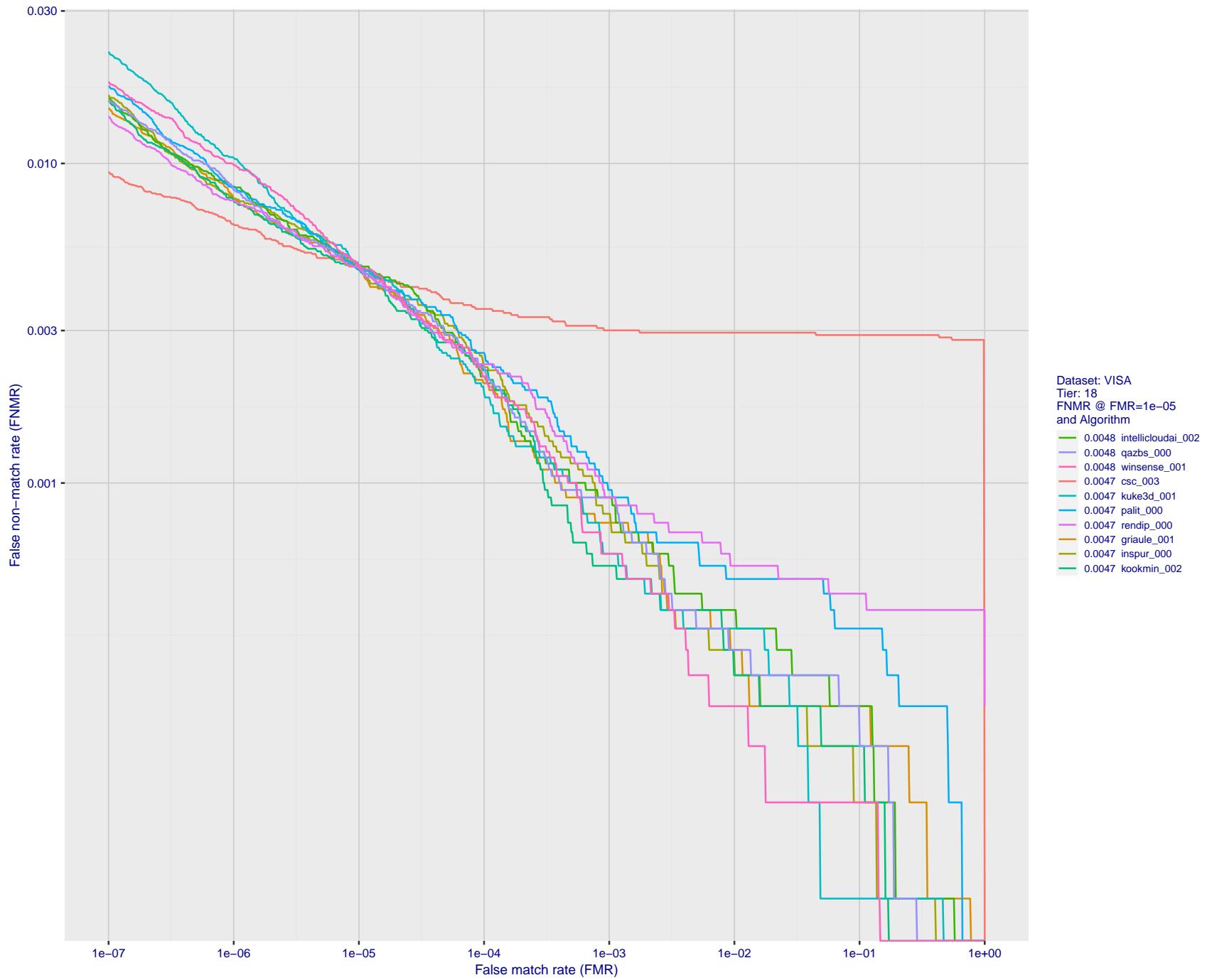


Figure 57: For the visa images, detection error tradeoff (DET) characteristics showing false non-match rate vs. false match rate plotted parametrically on threshold, T . The scales are logarithmic in order to show many decades of FMR.

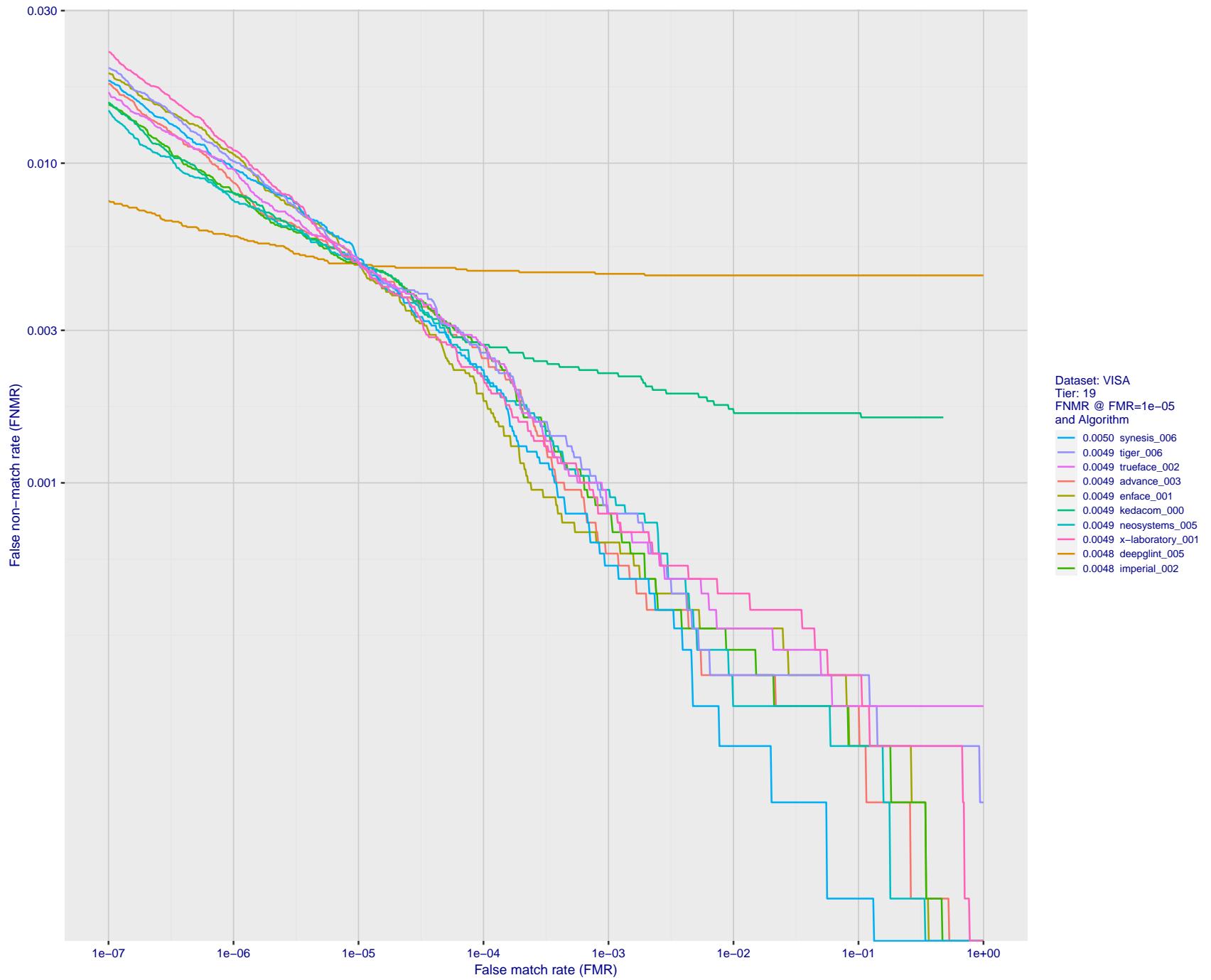


Figure 58: For the visa images, detection error tradeoff (DET) characteristics showing false non-match rate vs. false match rate plotted parametrically on threshold, T . The scales are logarithmic in order to show many decades of FMR.

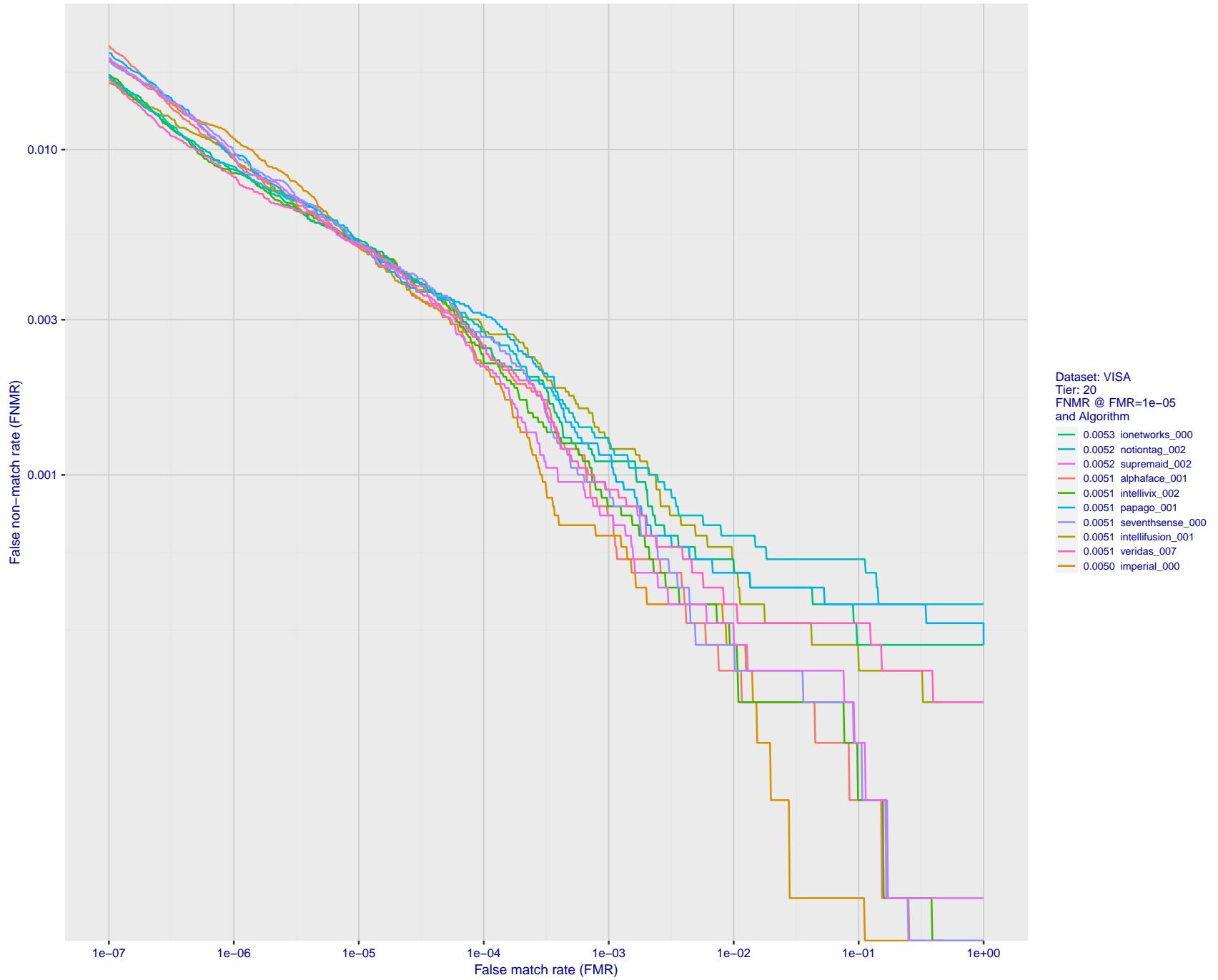


Figure 59: For the visa images, detection error tradeoff (DET) characteristics showing false non-match rate vs. false match rate plotted parametrically on threshold, T . The scales are logarithmic in order to show many decades of FMR.

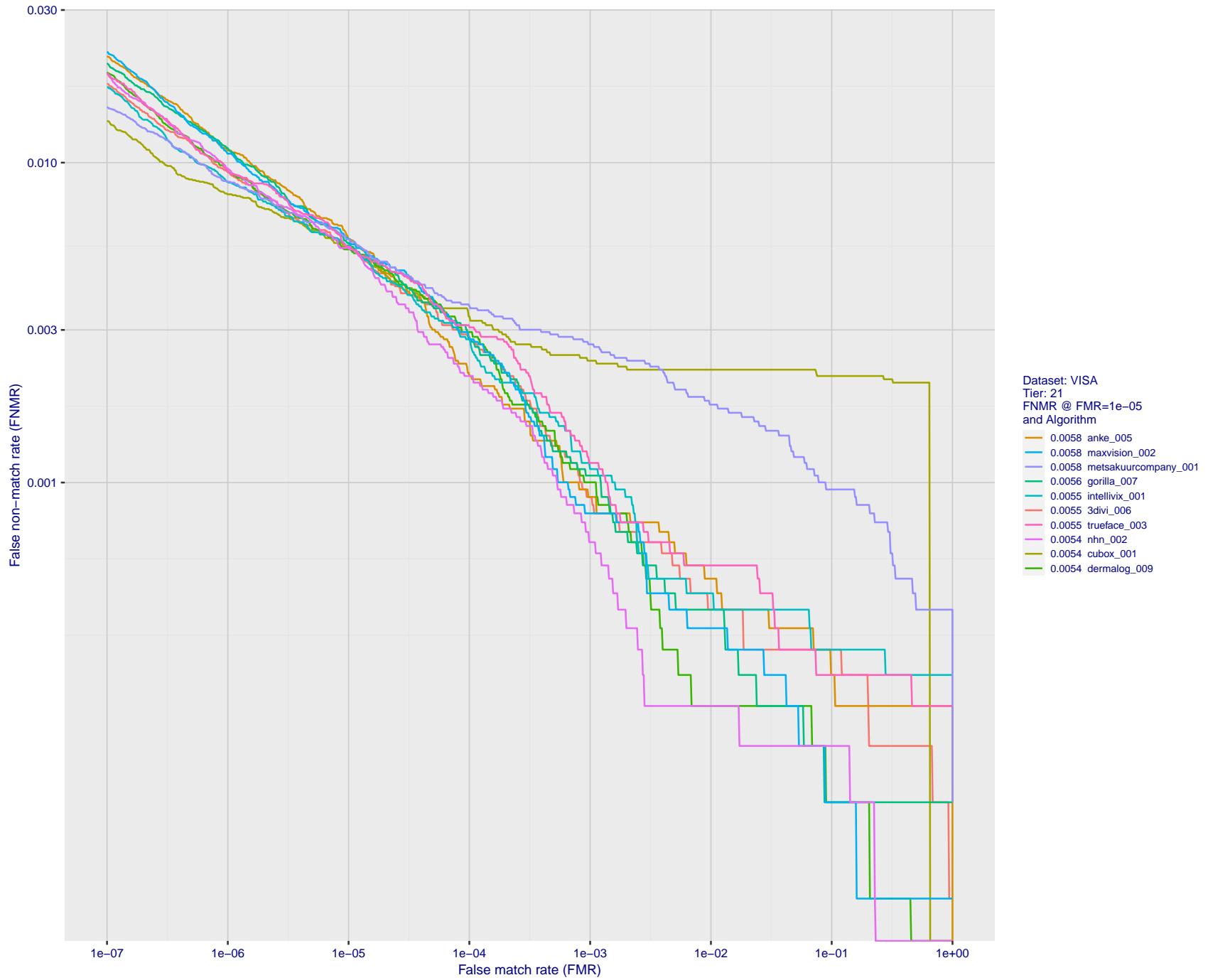


Figure 60: For the visa images, detection error tradeoff (DET) characteristics showing false non-match rate vs. false match rate plotted parametrically on threshold, T . The scales are logarithmic in order to show many decades of FMR.

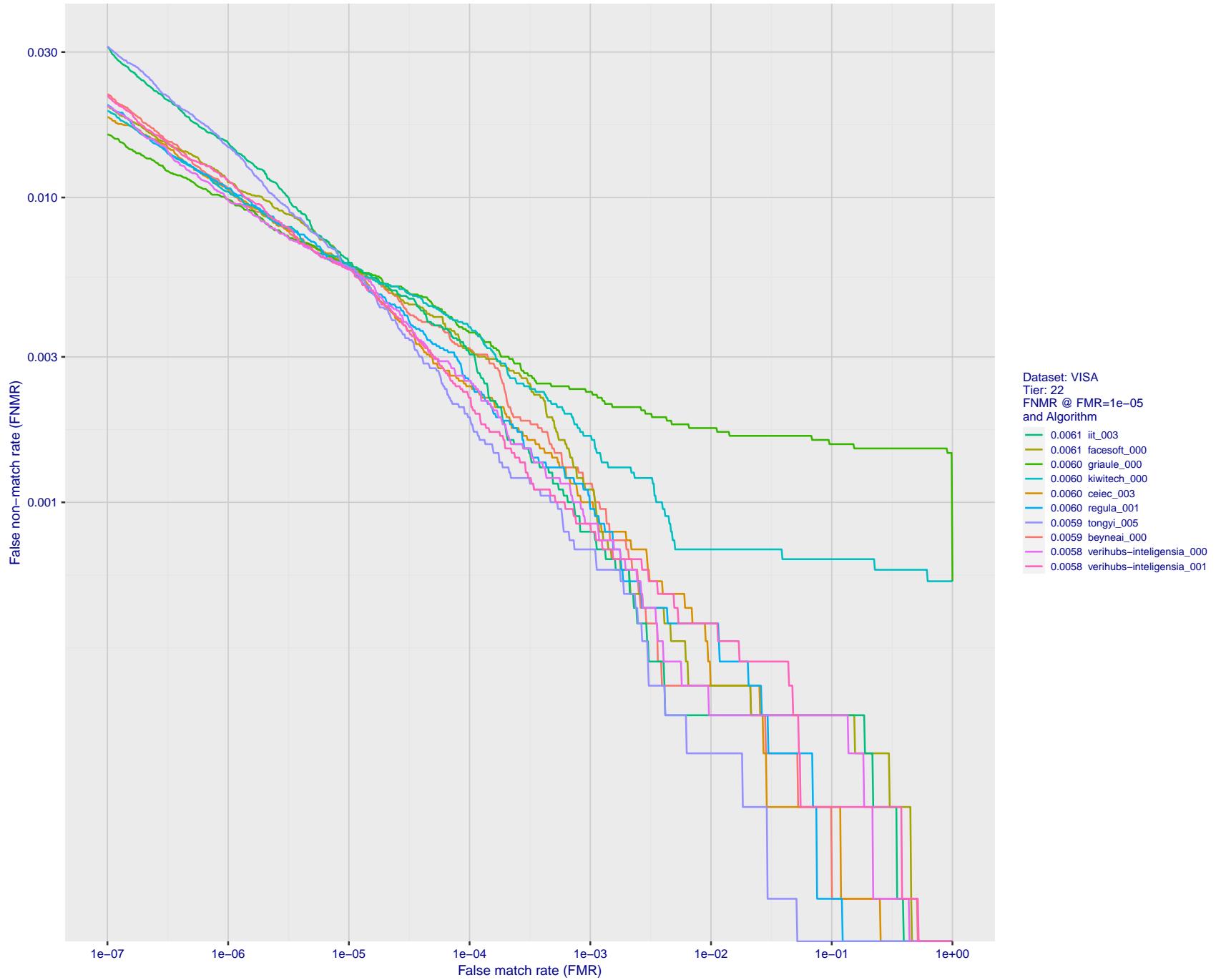


Figure 61: For the visa images, detection error tradeoff (DET) characteristics showing false non-match rate vs. false match rate plotted parametrically on threshold, T . The scales are logarithmic in order to show many decades of FMR.

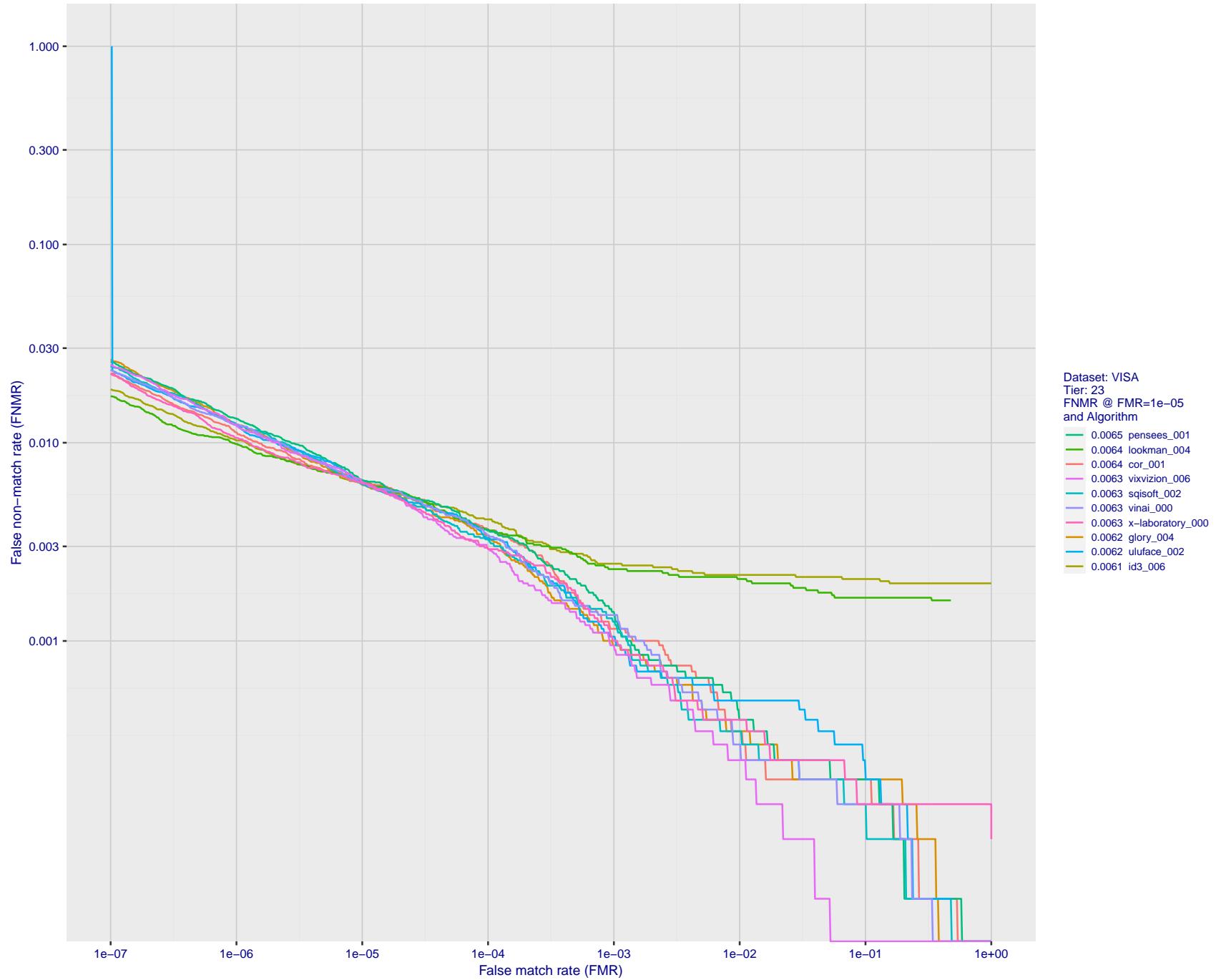


Figure 62: For the visa images, detection error tradeoff (DET) characteristics showing false non-match rate vs. false match rate plotted parametrically on threshold, T . The scales are logarithmic in order to show many decades of FMR.

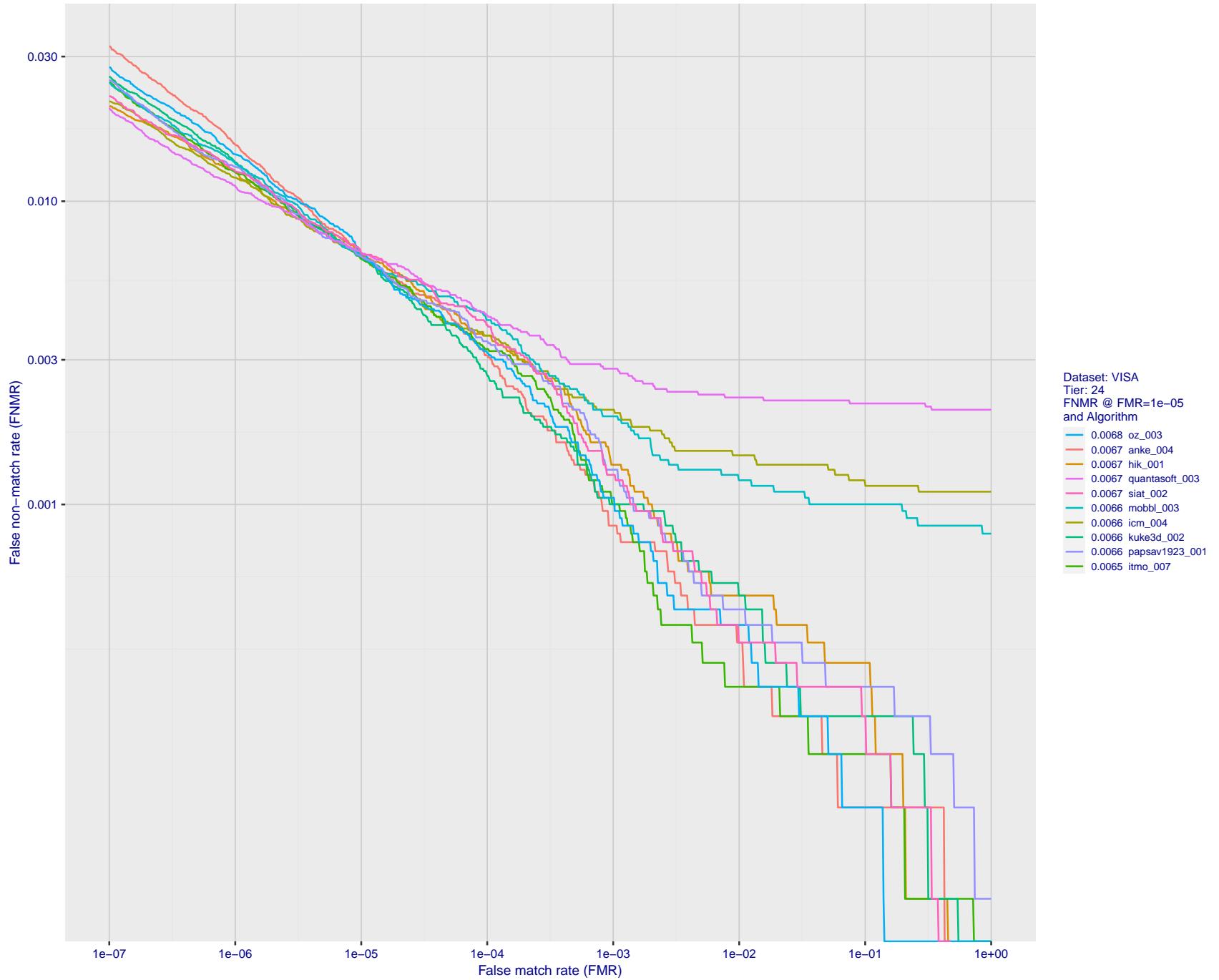


Figure 63: For the visa images, detection error tradeoff (DET) characteristics showing false non-match rate vs. false match rate plotted parametrically on threshold, T . The scales are logarithmic in order to show many decades of FMR.

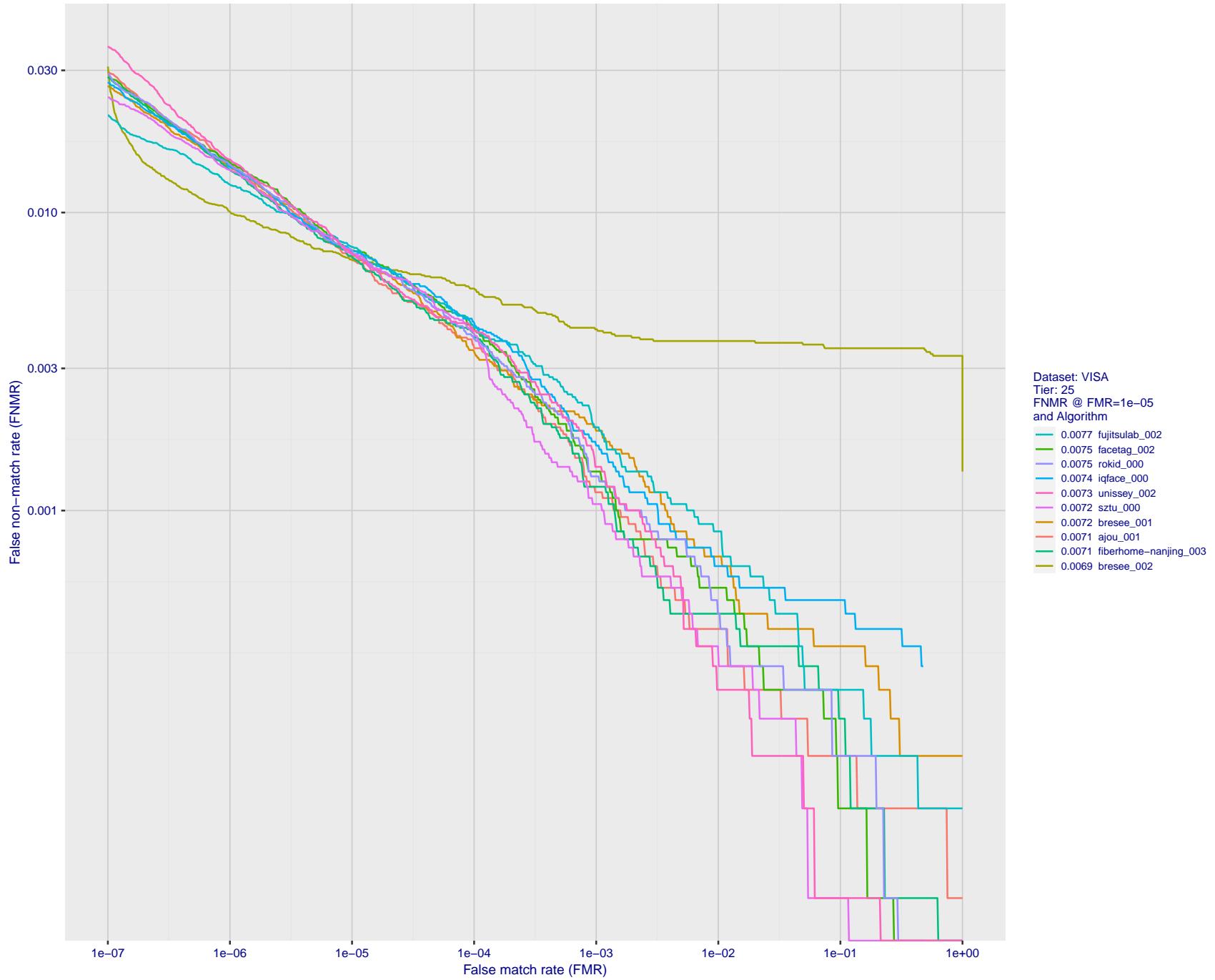


Figure 64: For the visa images, detection error tradeoff (DET) characteristics showing false non-match rate vs. false match rate plotted parametrically on threshold, T . The scales are logarithmic in order to show many decades of FMR.

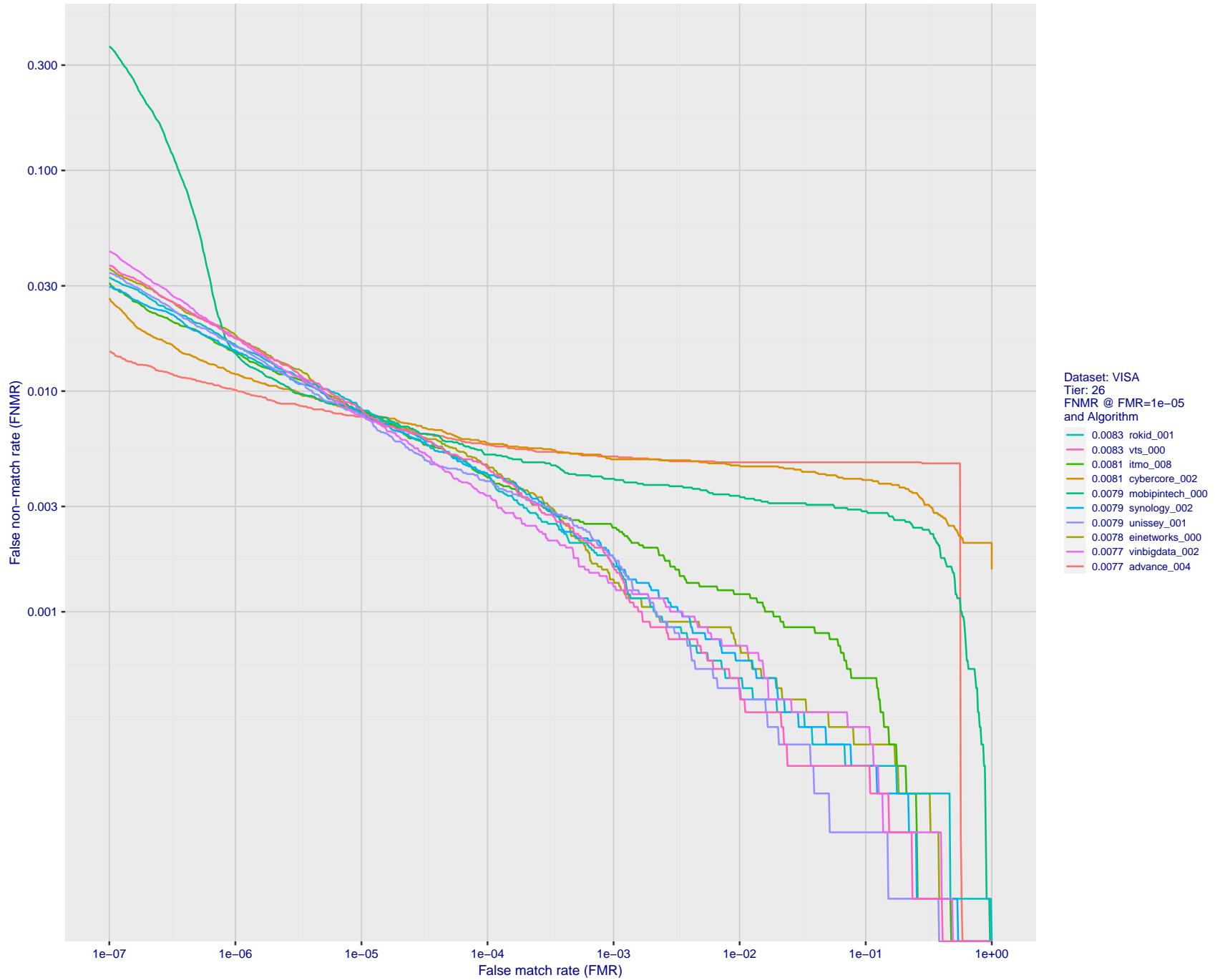


Figure 65: For the visa images, detection error tradeoff (DET) characteristics showing false non-match rate vs. false match rate plotted parametrically on threshold, T . The scales are logarithmic in order to show many decades of FMR.

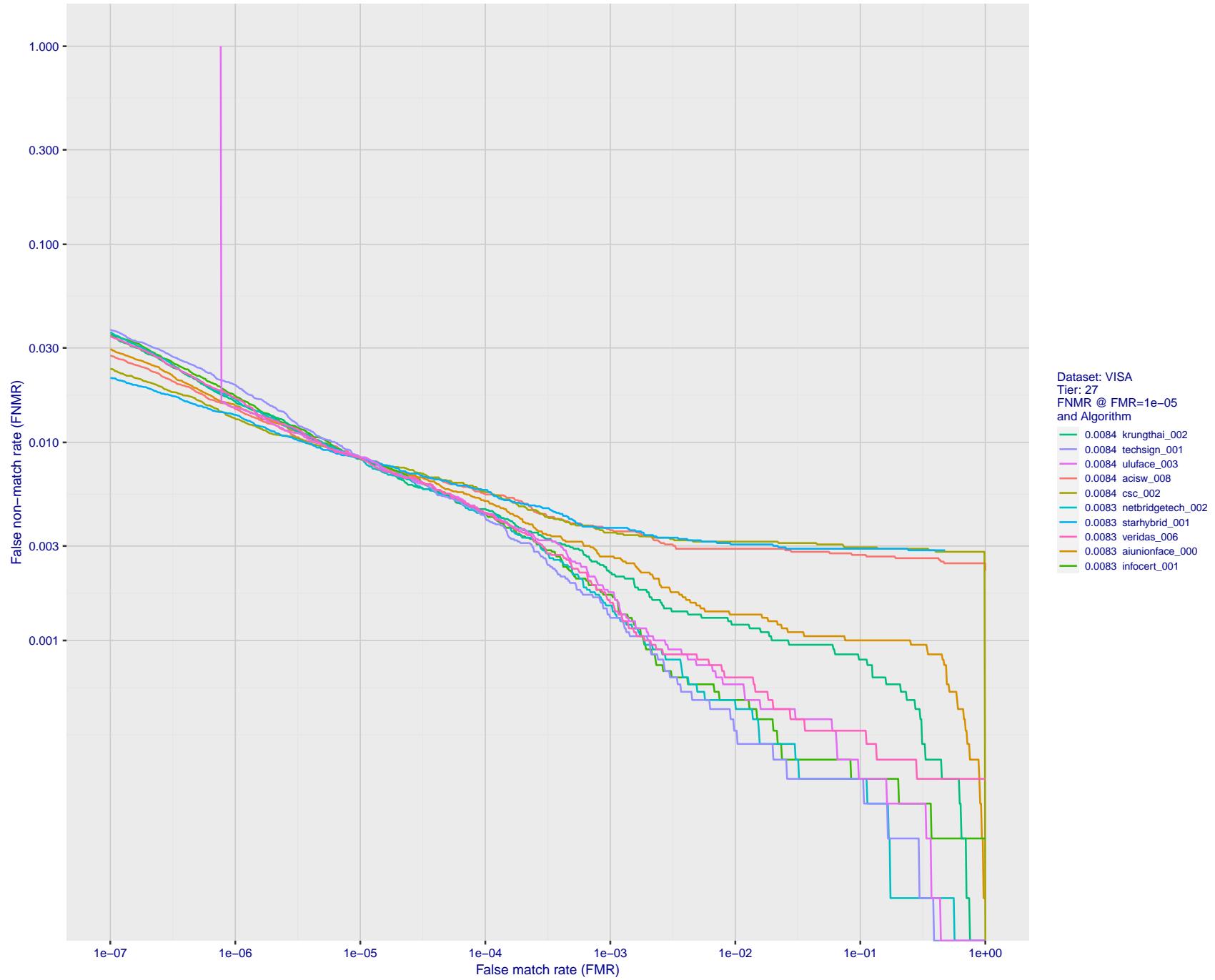


Figure 66: For the visa images, detection error tradeoff (DET) characteristics showing false non-match rate vs. false match rate plotted parametrically on threshold, T . The scales are logarithmic in order to show many decades of FMR.

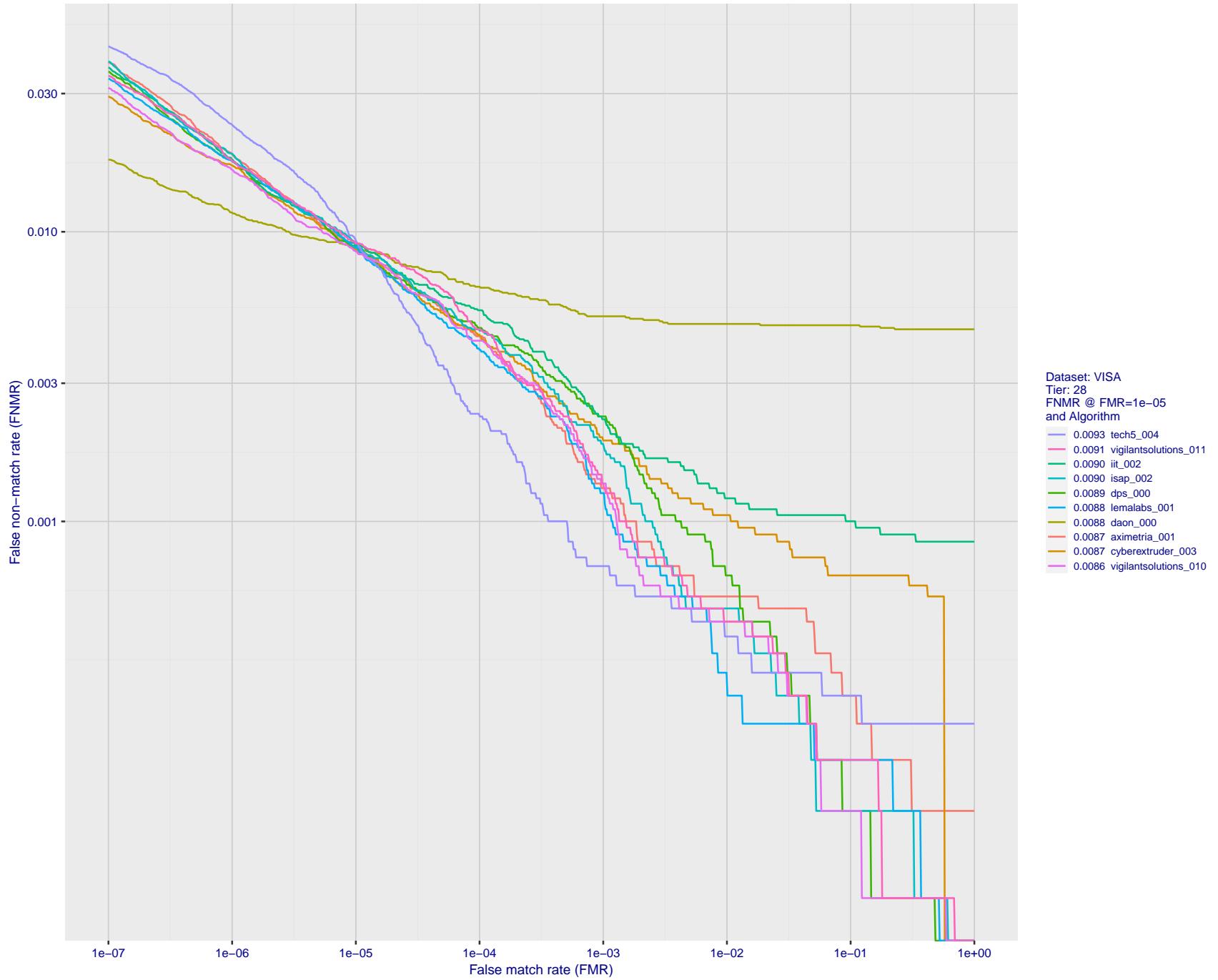


Figure 67: For the visa images, detection error tradeoff (DET) characteristics showing false non-match rate vs. false match rate plotted parametrically on threshold, T . The scales are logarithmic in order to show many decades of FMR.

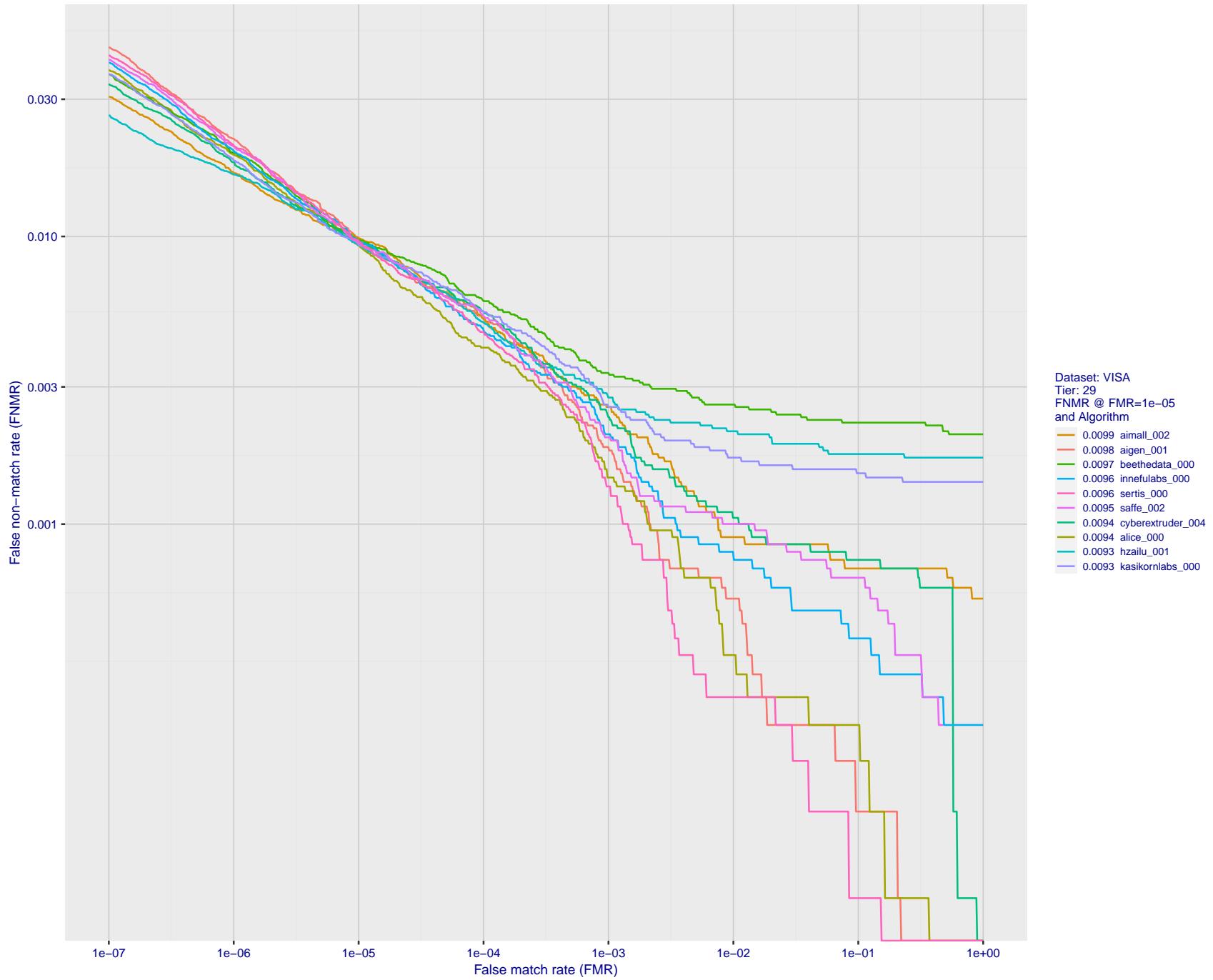


Figure 68: For the visa images, detection error tradeoff (DET) characteristics showing false non-match rate vs. false match rate plotted parametrically on threshold, T . The scales are logarithmic in order to show many decades of FMR.

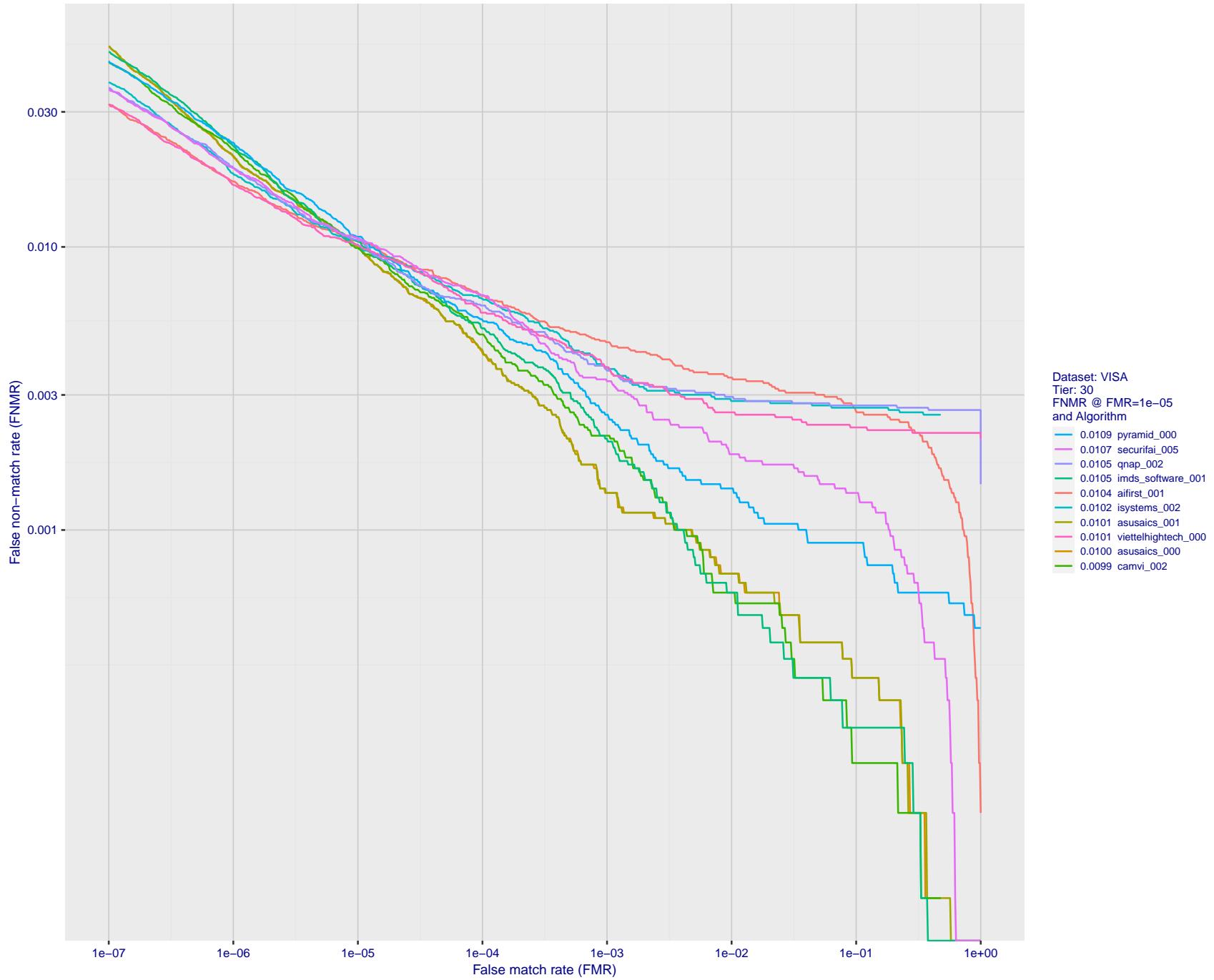


Figure 69: For the visa images, detection error tradeoff (DET) characteristics showing false non-match rate vs. false match rate plotted parametrically on threshold, T . The scales are logarithmic in order to show many decades of FMR.

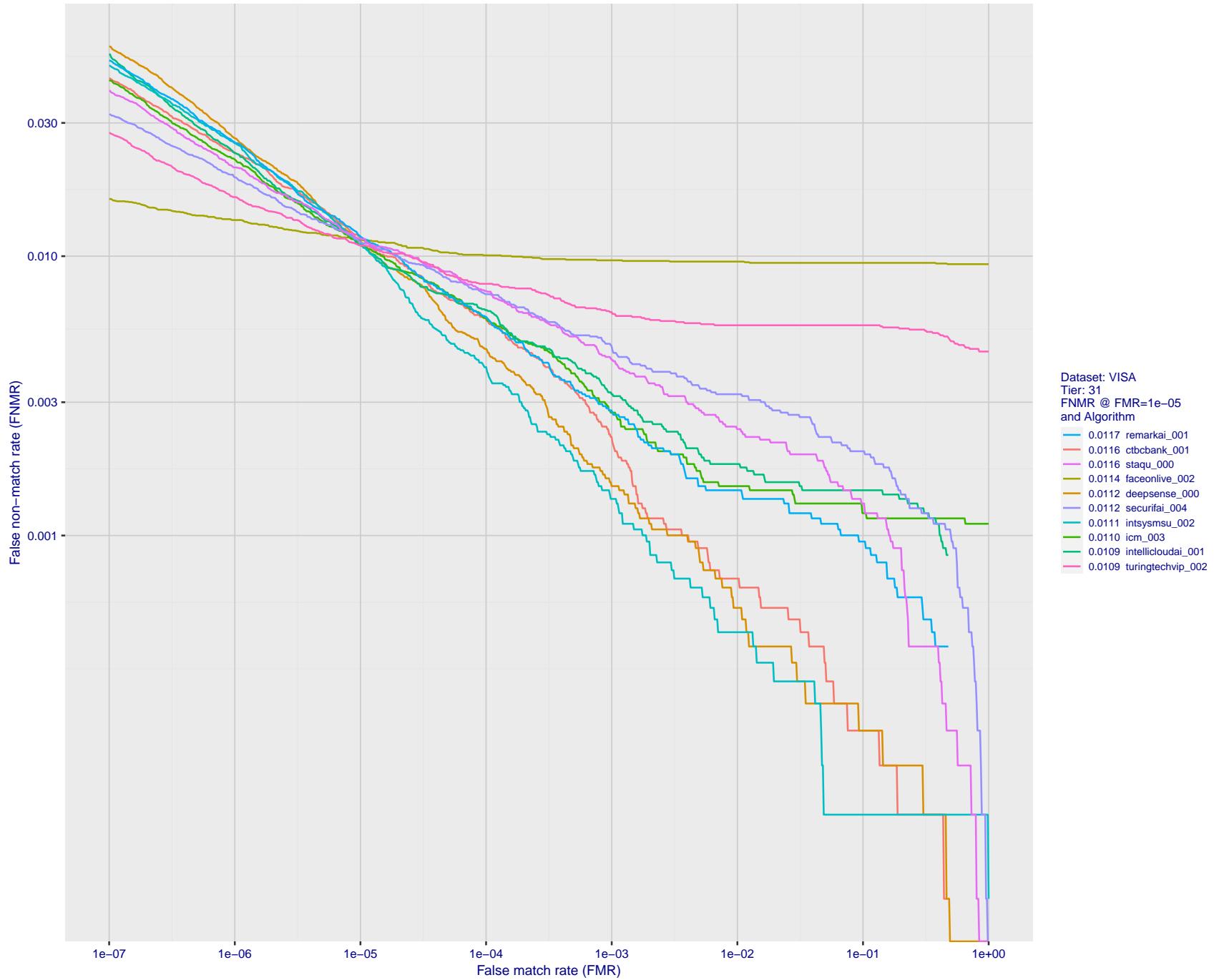


Figure 70: For the visa images, detection error tradeoff (DET) characteristics showing false non-match rate vs. false match rate plotted parametrically on threshold, T . The scales are logarithmic in order to show many decades of FMR.

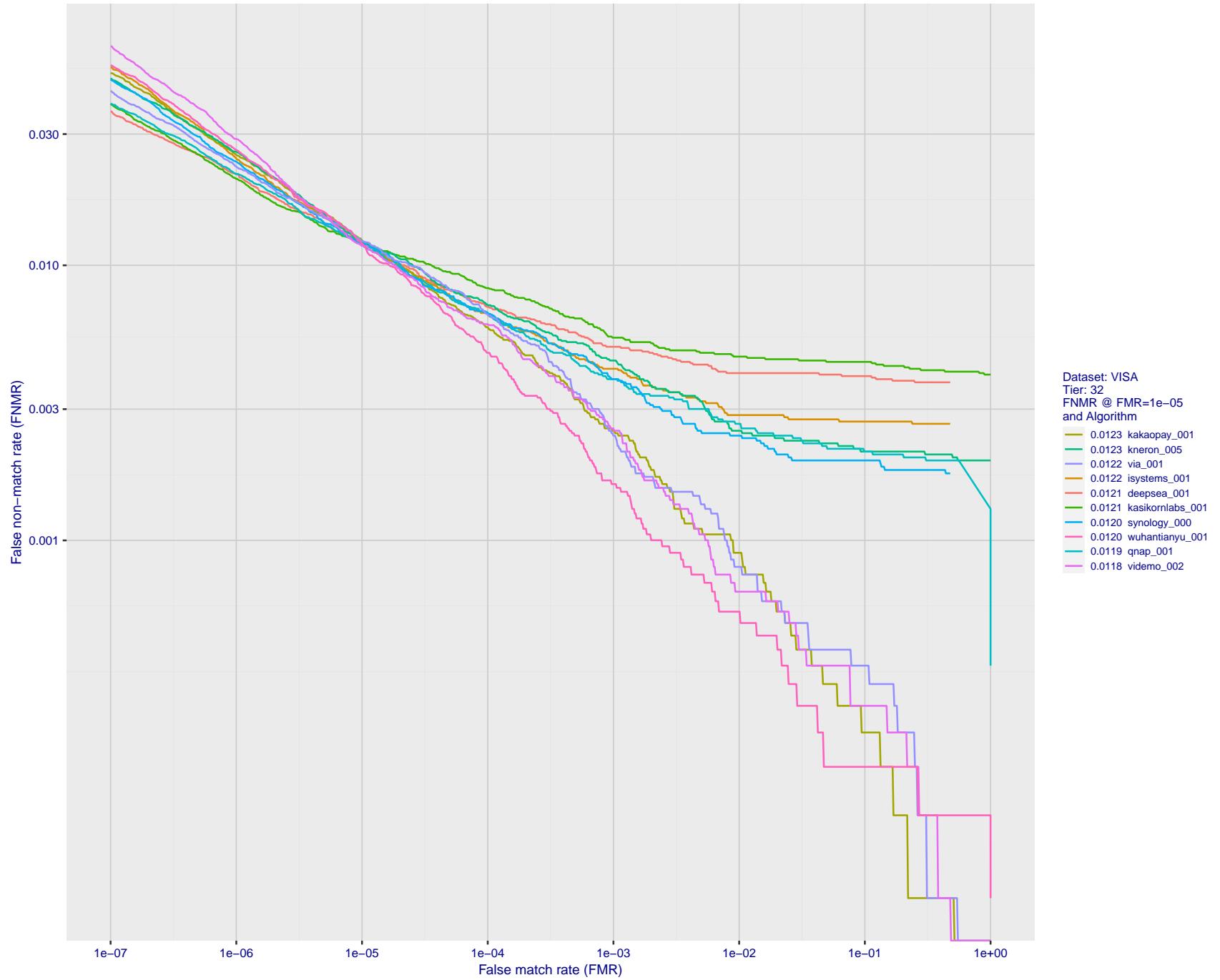


Figure 71: For the visa images, detection error tradeoff (DET) characteristics showing false non-match rate vs. false match rate plotted parametrically on threshold, T . The scales are logarithmic in order to show many decades of FMR.

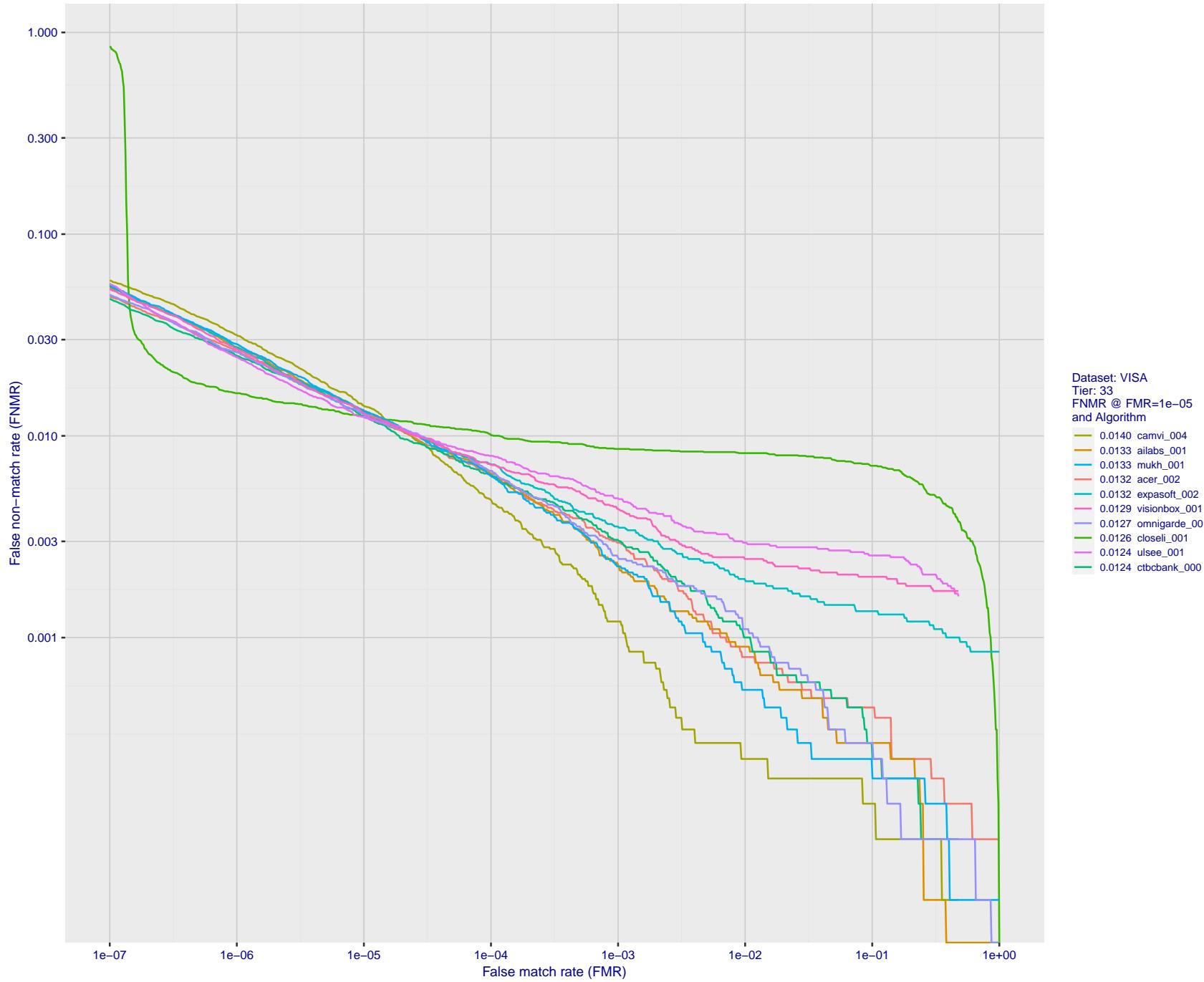


Figure 72: For the visa images, detection error tradeoff (DET) characteristics showing false non-match rate vs. false match rate plotted parametrically on threshold, T . The scales are logarithmic in order to show many decades of FMR.

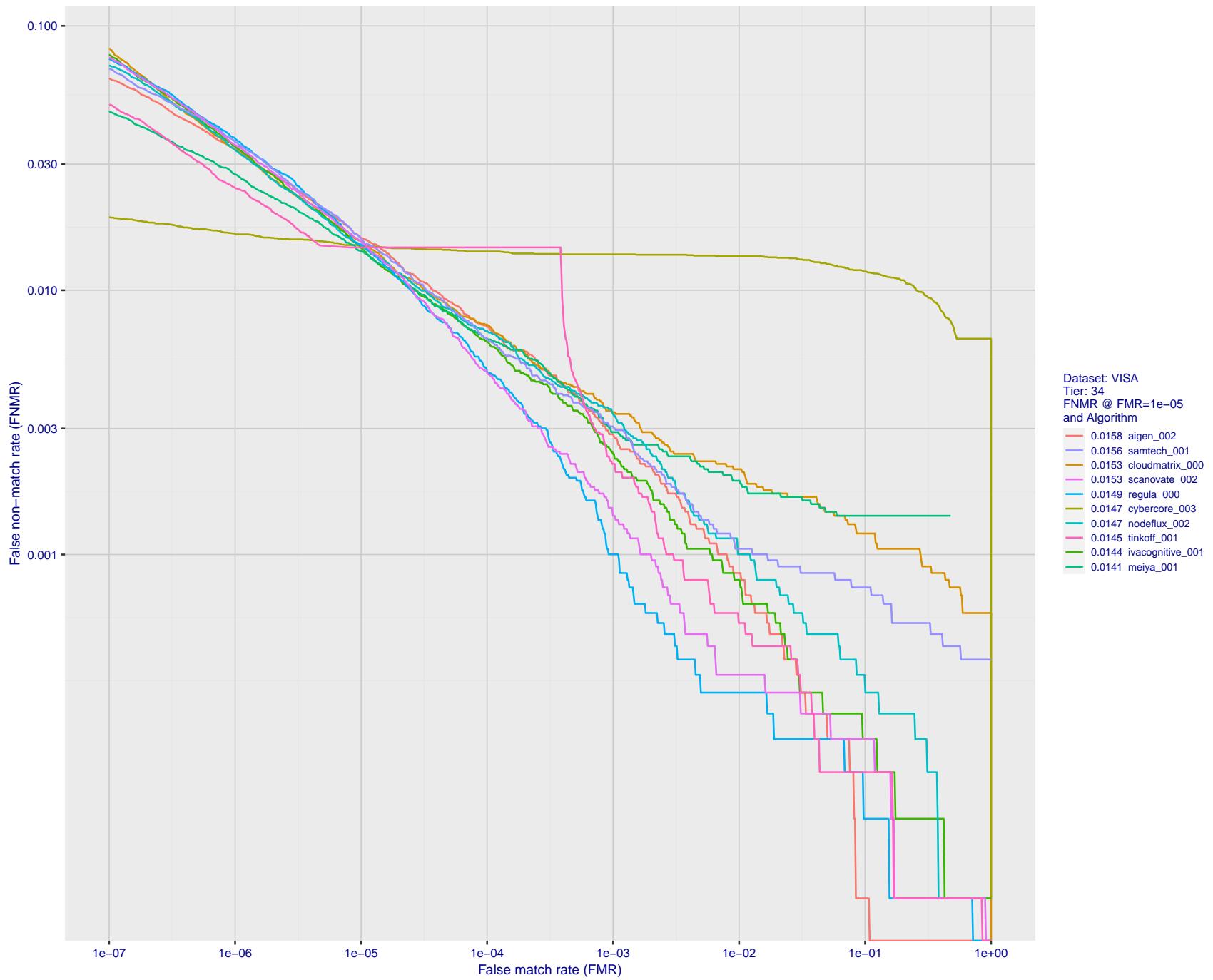


Figure 73: For the visa images, detection error tradeoff (DET) characteristics showing false non-match rate vs. false match rate plotted parametrically on threshold, T . The scales are logarithmic in order to show many decades of FMR.

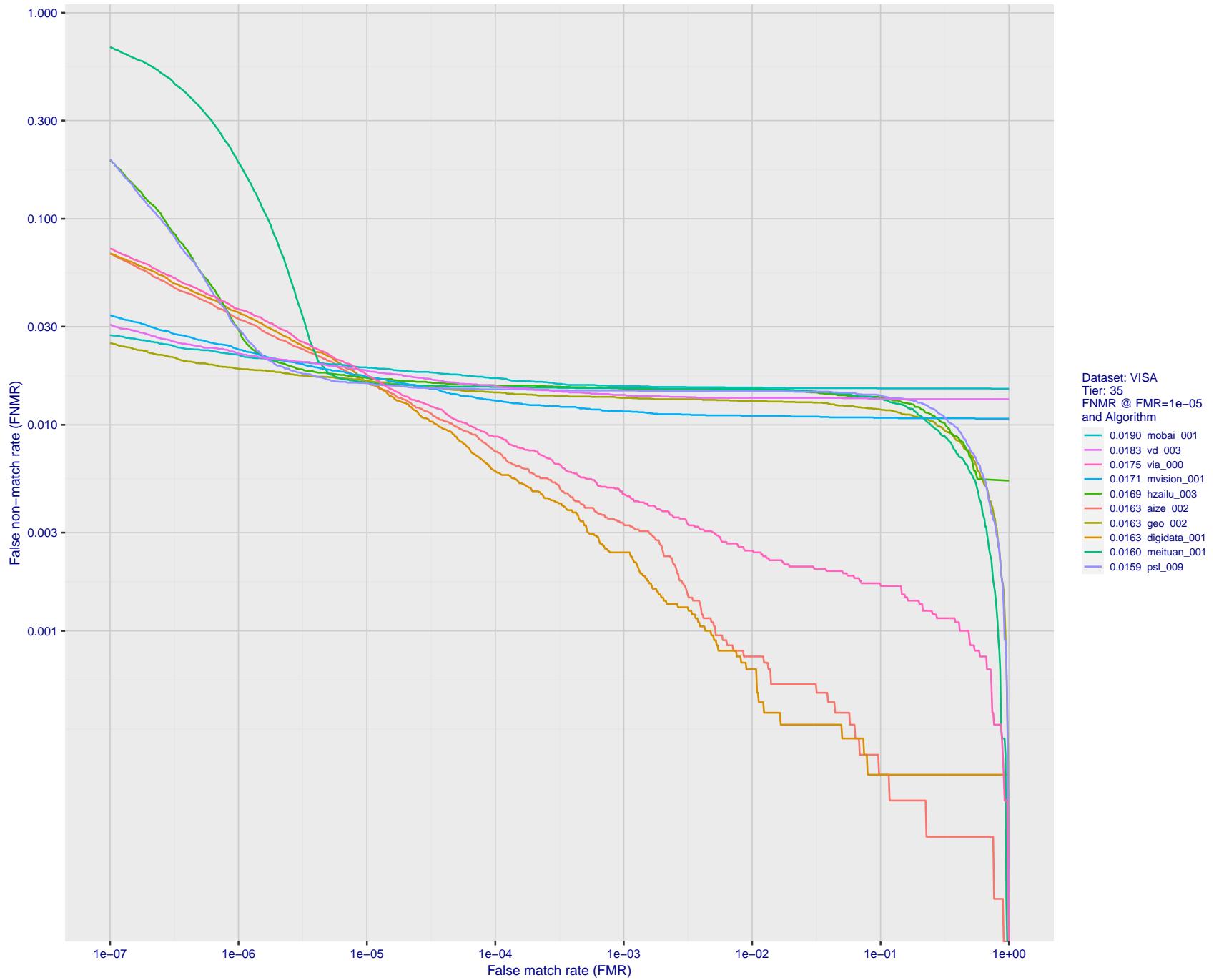


Figure 74: For the visa images, detection error tradeoff (DET) characteristics showing false non-match rate vs. false match rate plotted parametrically on threshold, T . The scales are logarithmic in order to show many decades of FMR.

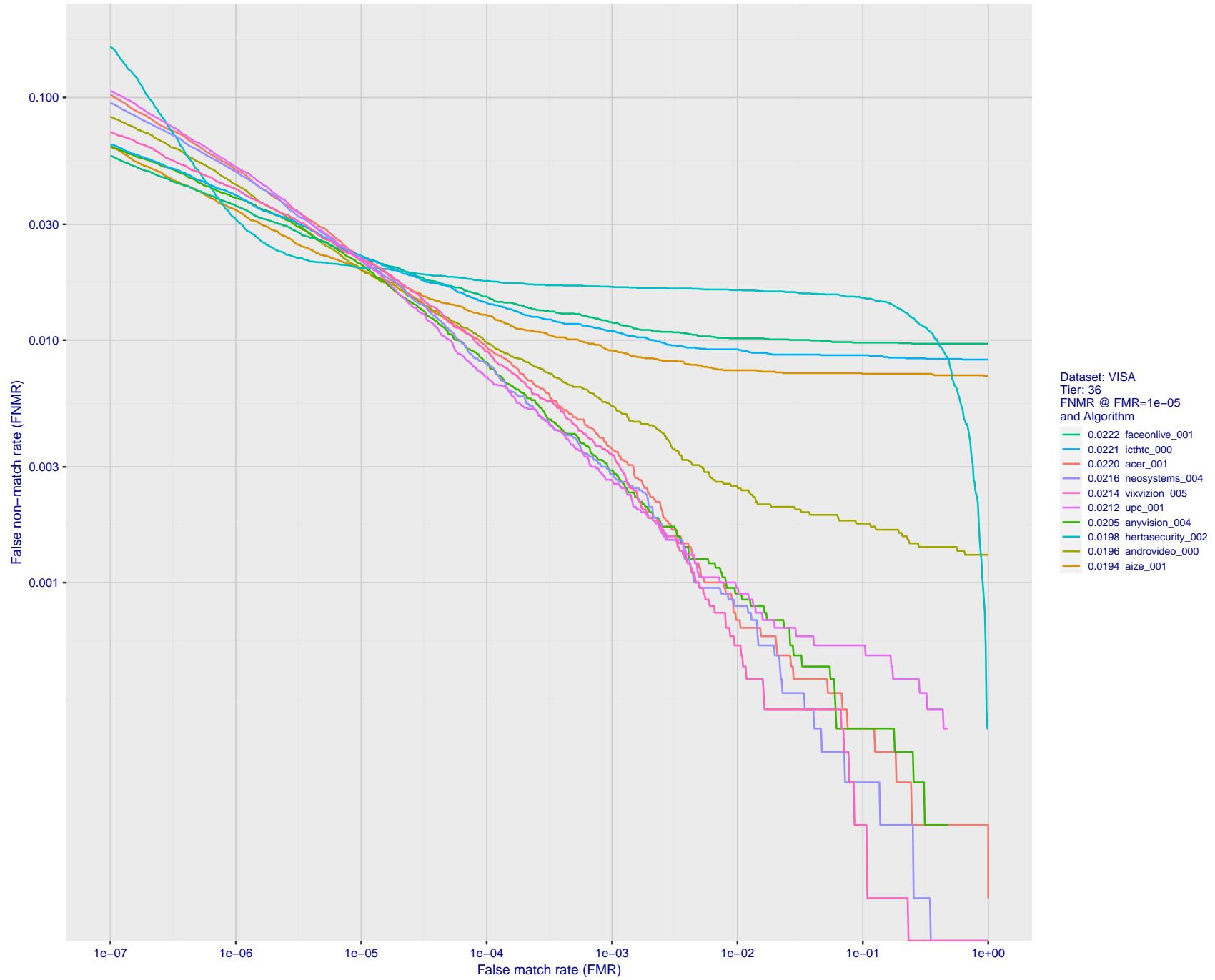


Figure 75: For the visa images, detection error tradeoff (DET) characteristics showing false non-match rate vs. false match rate plotted parametrically on threshold, T . The scales are logarithmic in order to show many decades of FMR.

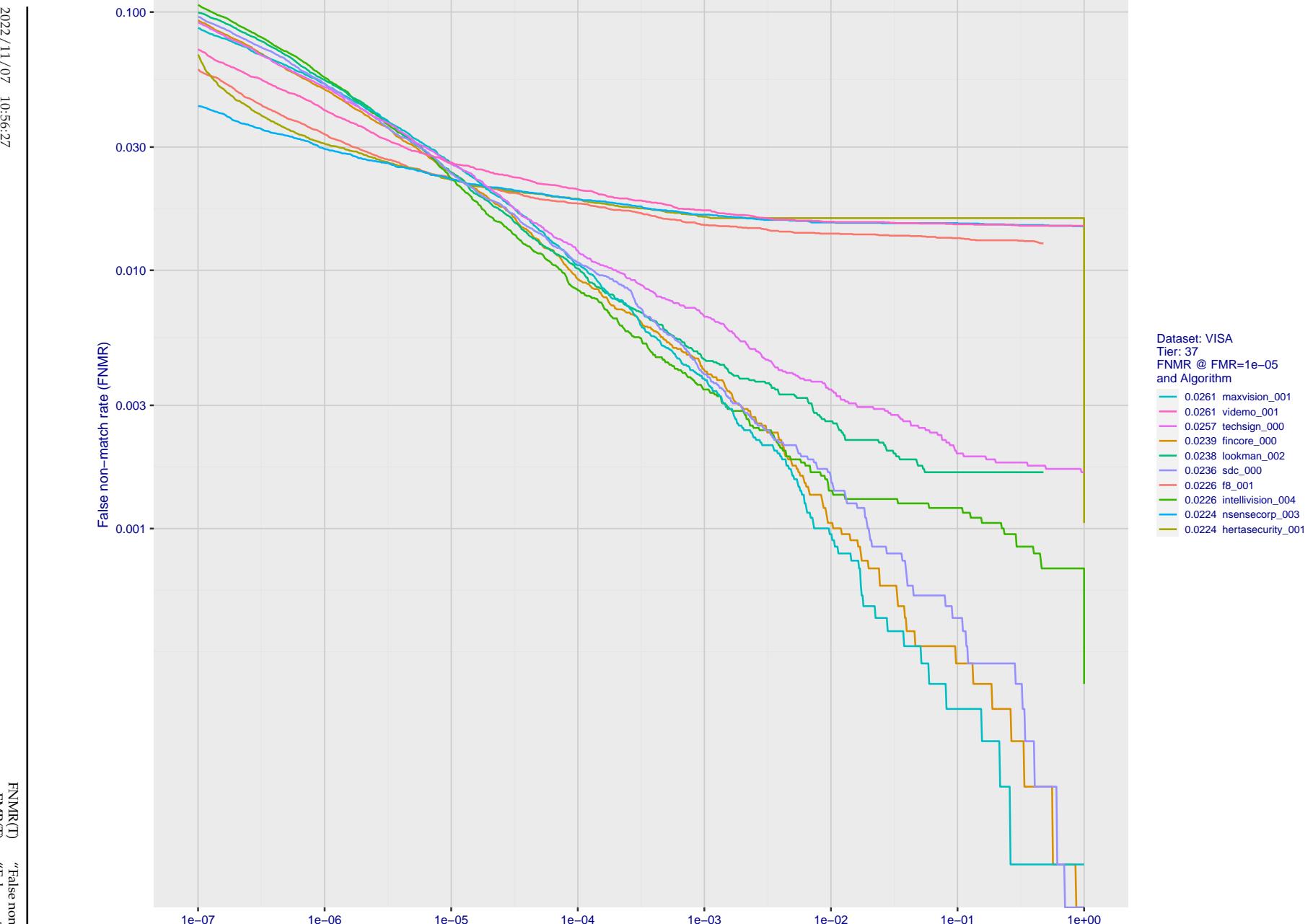


Figure 76: For the visa images, detection error tradeoff (DET) characteristics showing false non-match rate vs. false match rate plotted parametrically on threshold, T . The scales are logarithmic in order to show many decades of FMR.

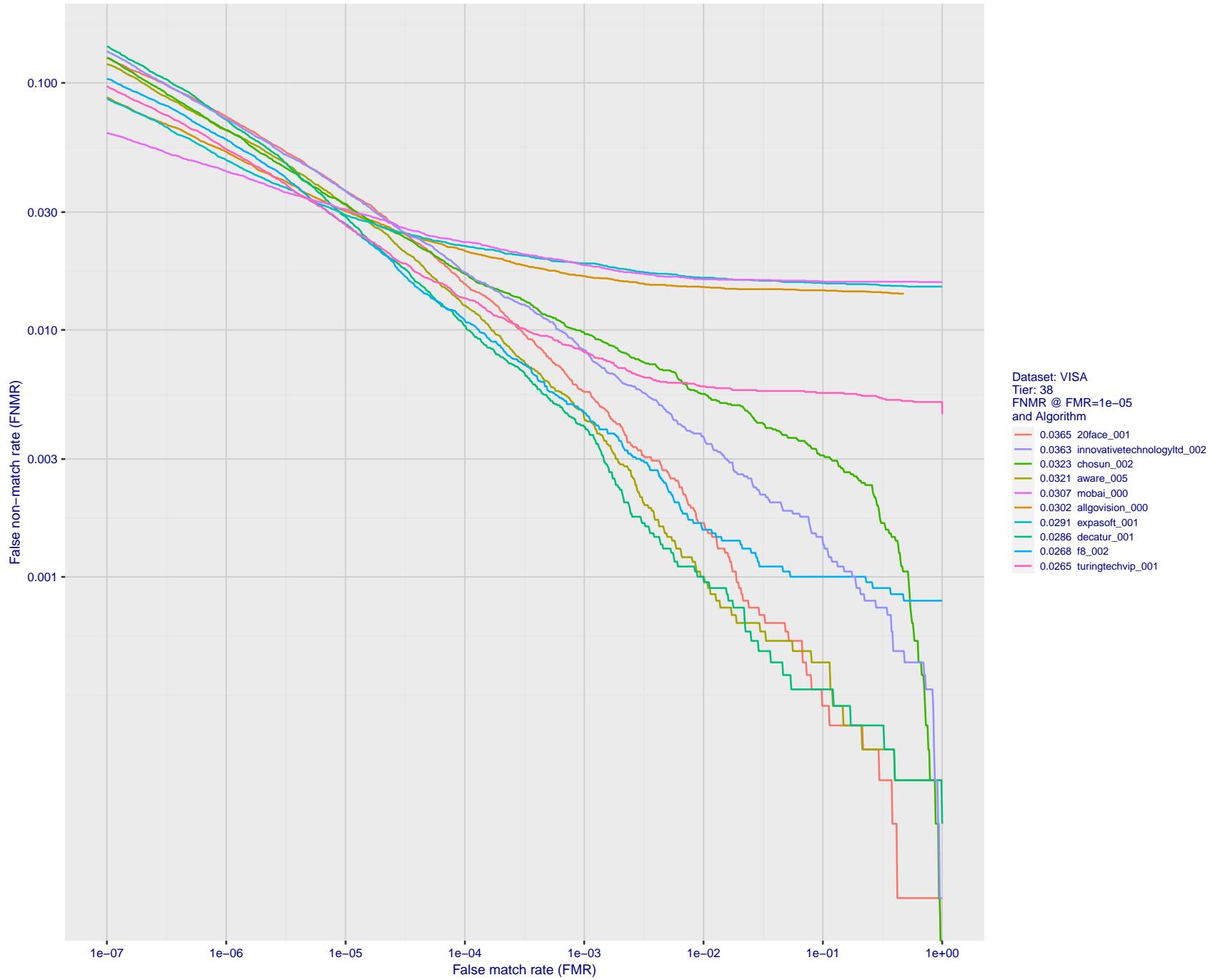


Figure 77: For the visa images, detection error tradeoff (DET) characteristics showing false non-match rate vs. false match rate plotted parametrically on threshold, T . The scales are logarithmic in order to show many decades of FMR.

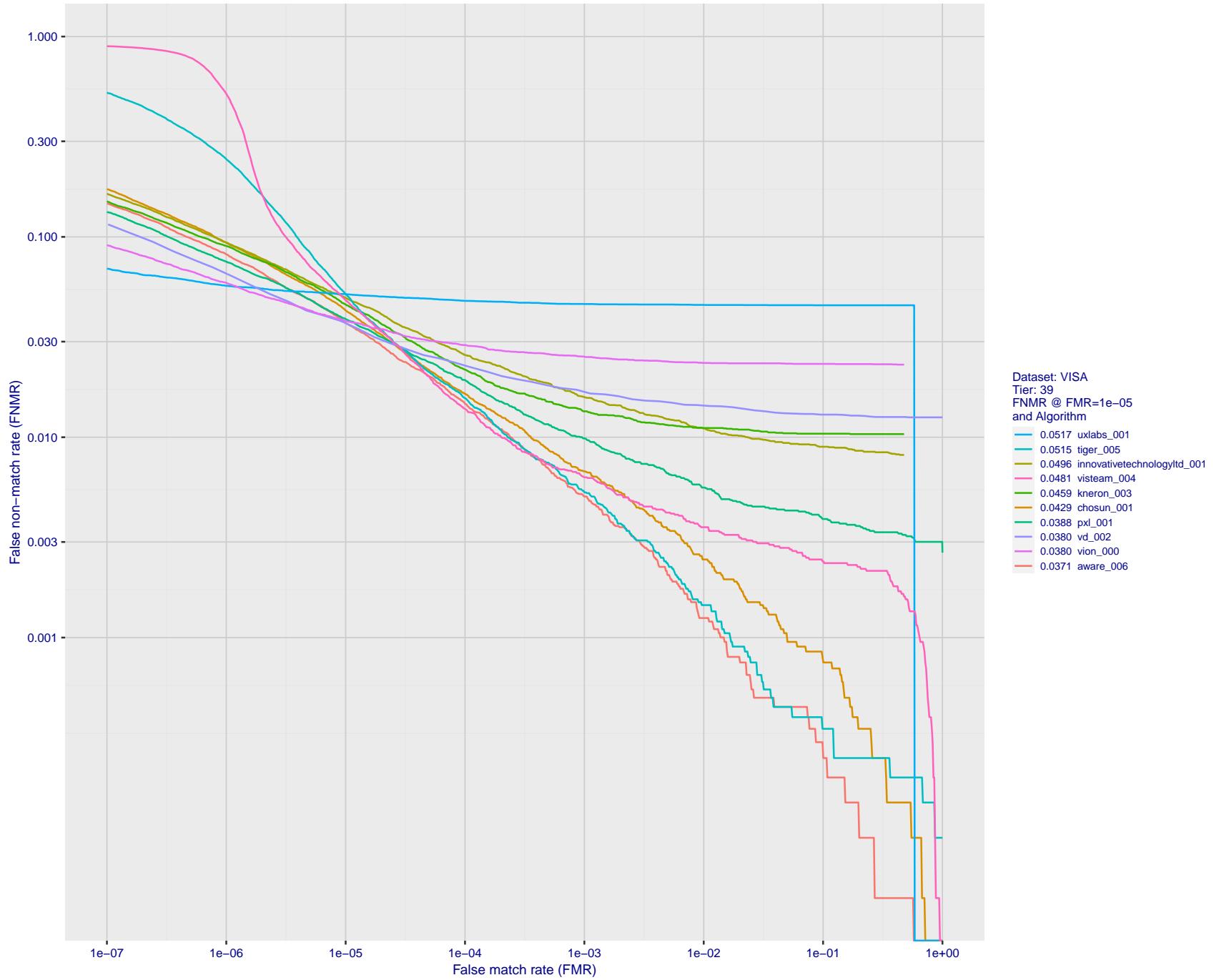


Figure 78: For the visa images, detection error tradeoff (DET) characteristics showing false non-match rate vs. false match rate plotted parametrically on threshold, T . The scales are logarithmic in order to show many decades of FMR.

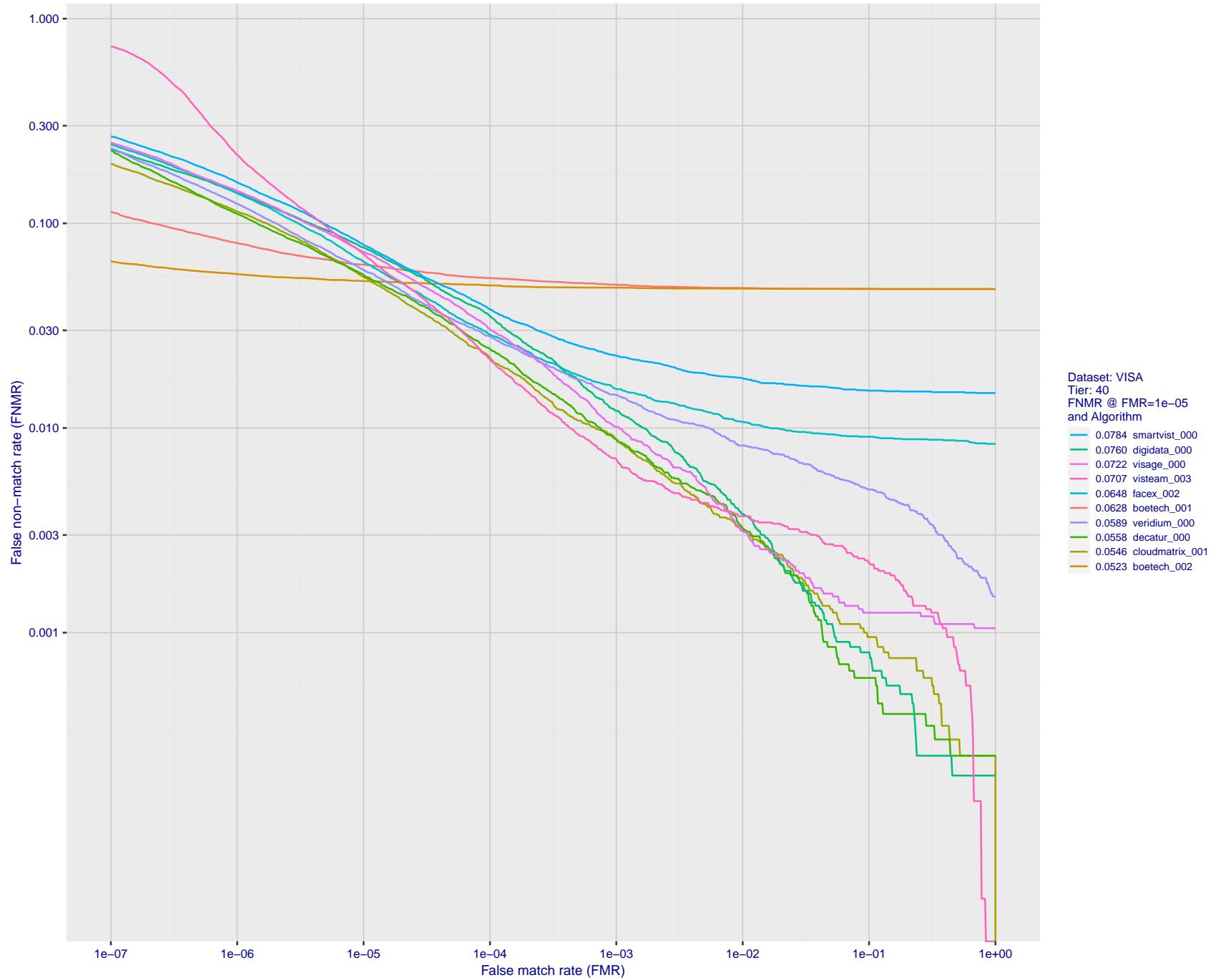


Figure 79: For the visa images, detection error tradeoff (DET) characteristics showing false non-match rate vs. false match rate plotted parametrically on threshold, T . The scales are logarithmic in order to show many decades of FMR.

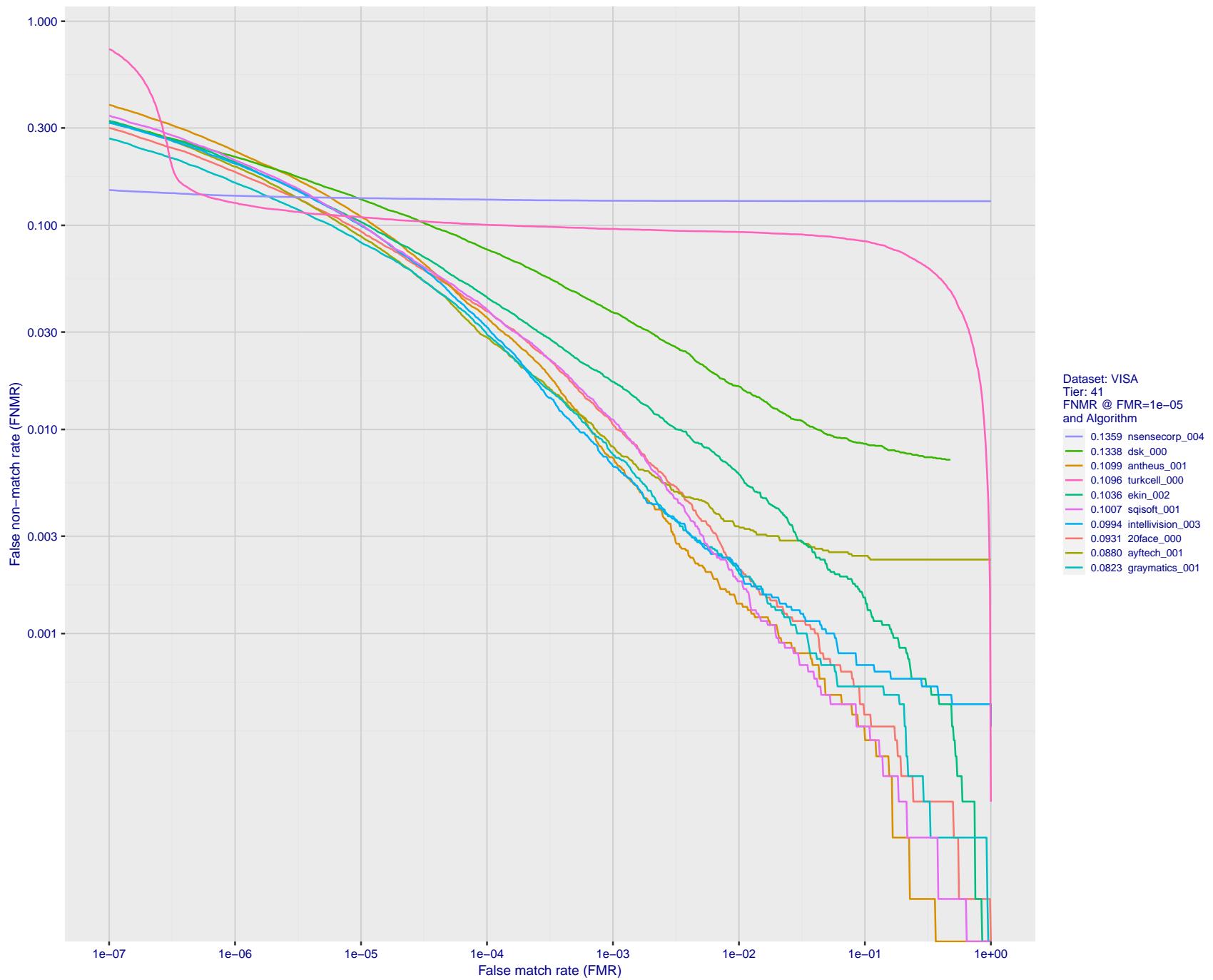


Figure 80: For the visa images, detection error tradeoff (DET) characteristics showing false non-match rate vs. false match rate plotted parametrically on threshold, T . The scales are logarithmic in order to show many decades of FMR.

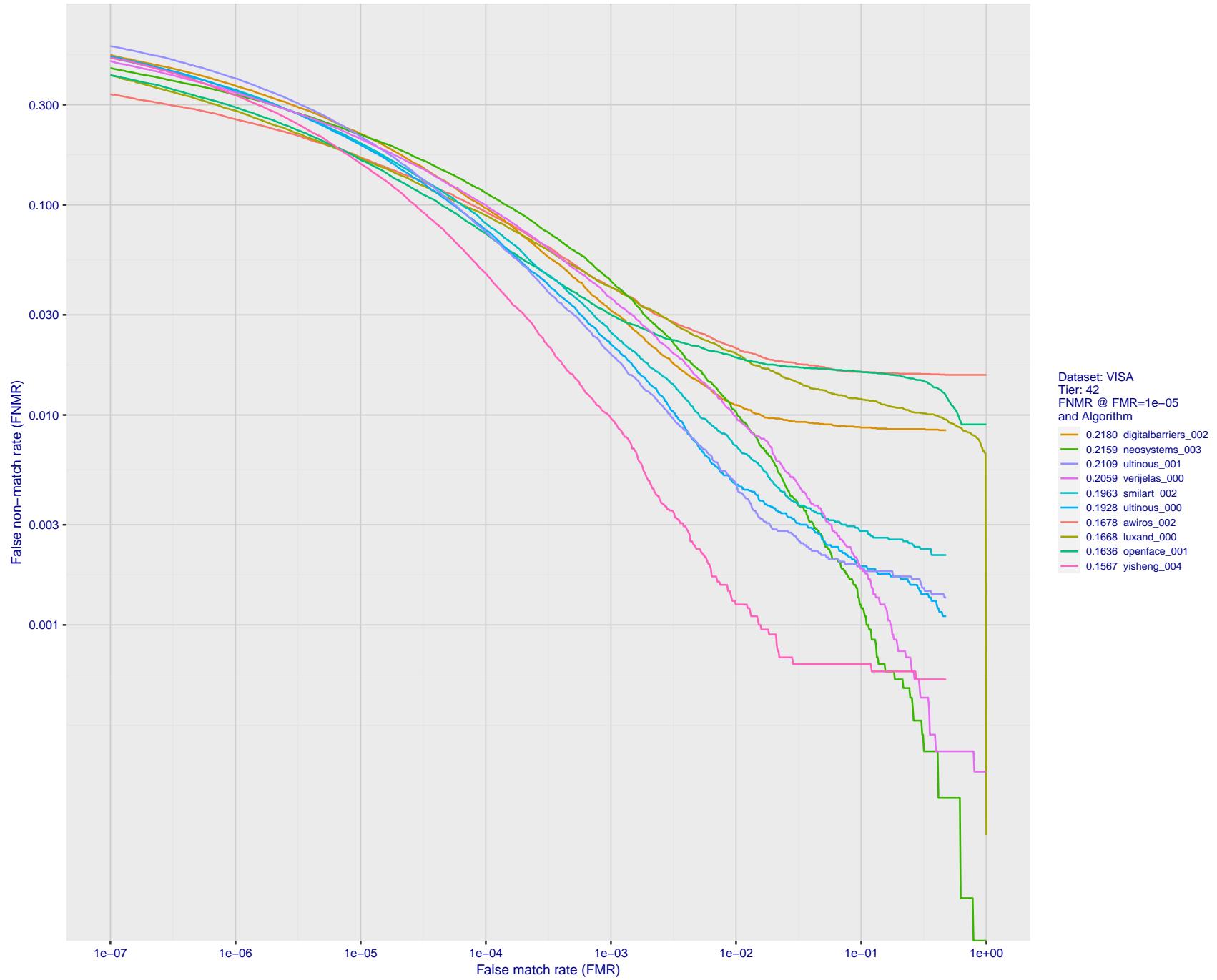


Figure 81: For the visa images, detection error tradeoff (DET) characteristics showing false non-match rate vs. false match rate plotted parametrically on threshold, T . The scales are logarithmic in order to show many decades of FMR.

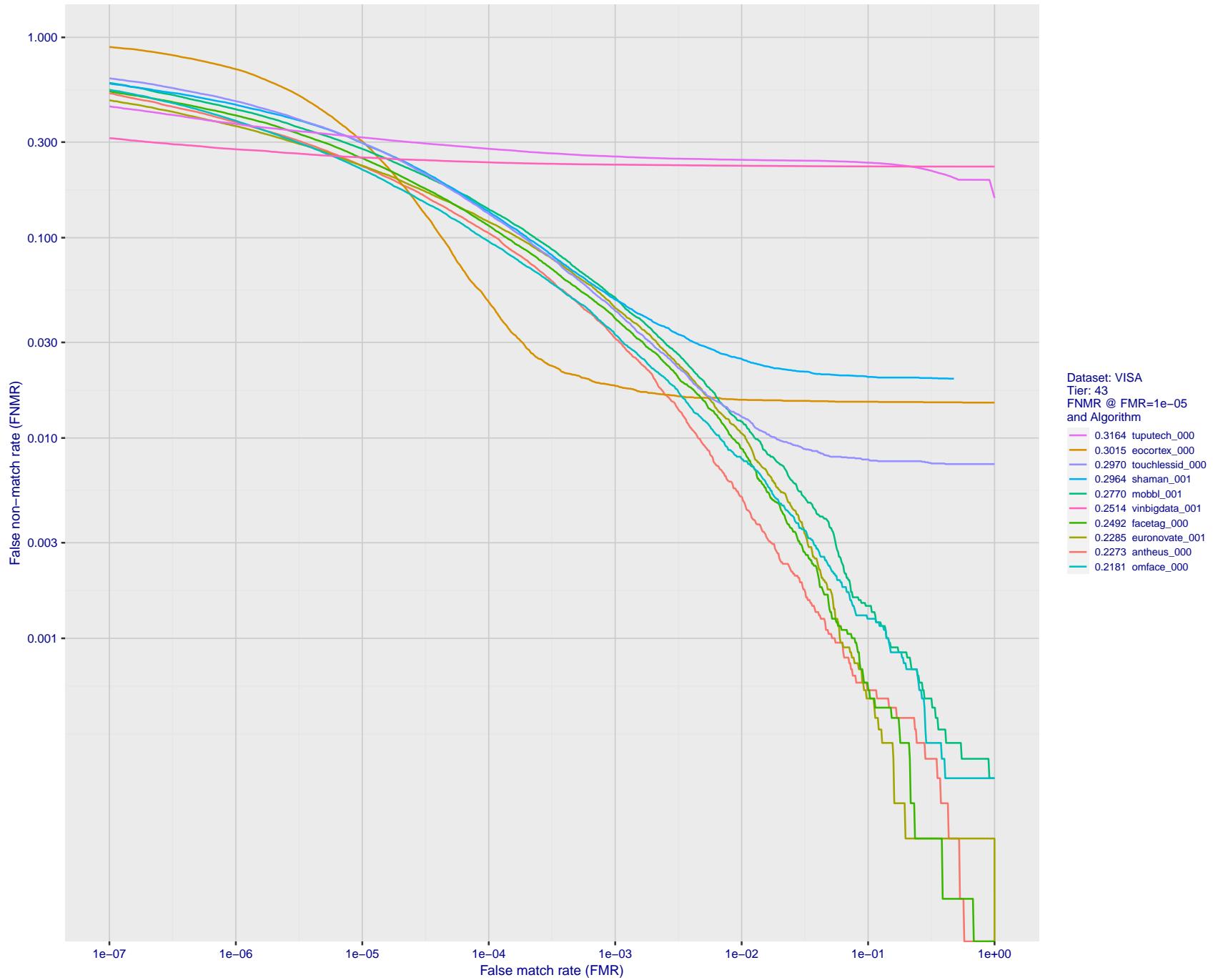


Figure 82: For the visa images, detection error tradeoff (DET) characteristics showing false non-match rate vs. false match rate plotted parametrically on threshold, T . The scales are logarithmic in order to show many decades of FMR.

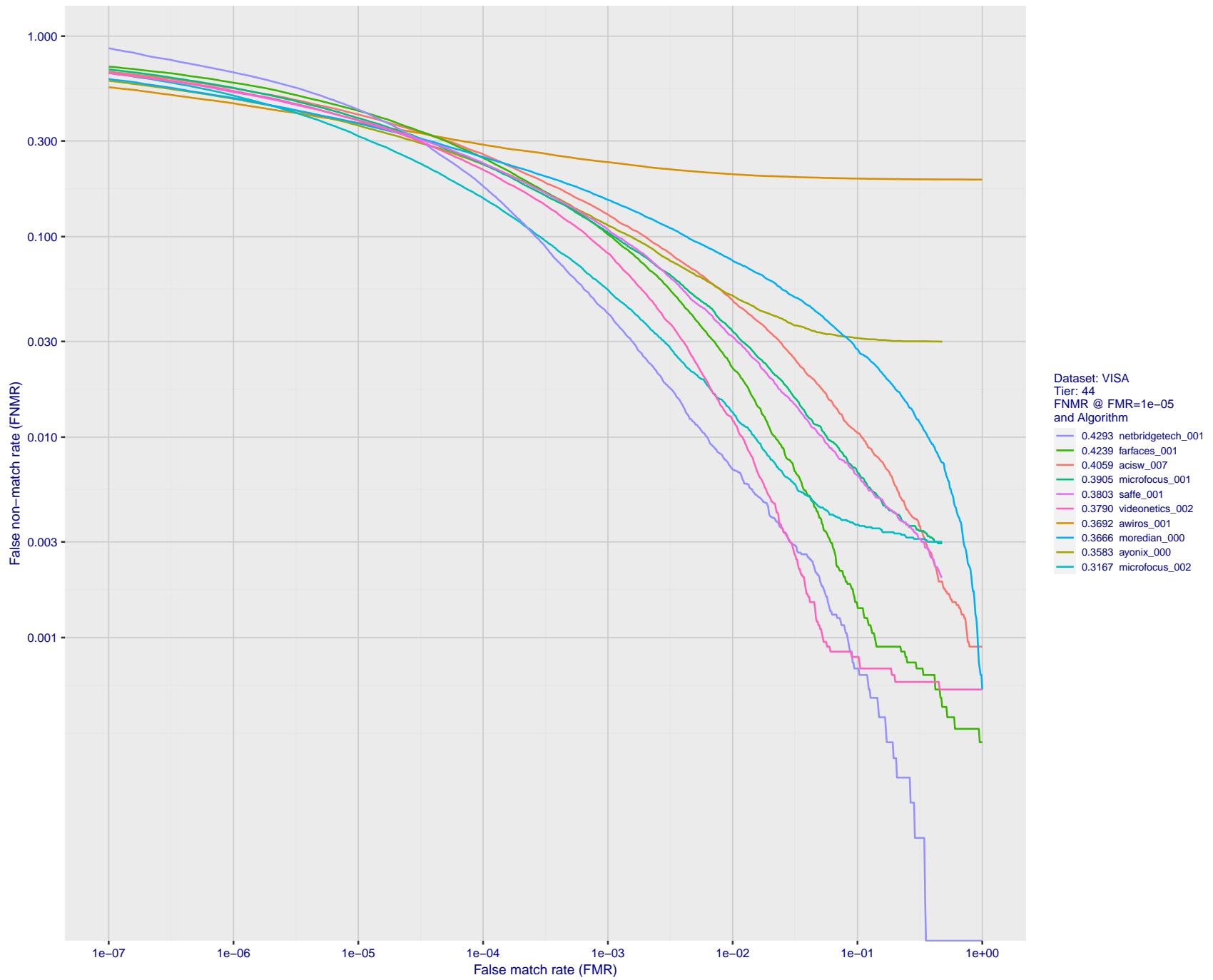


Figure 83: For the visa images, detection error tradeoff (DET) characteristics showing false non-match rate vs. false match rate plotted parametrically on threshold, T . The scales are logarithmic in order to show many decades of FMR.

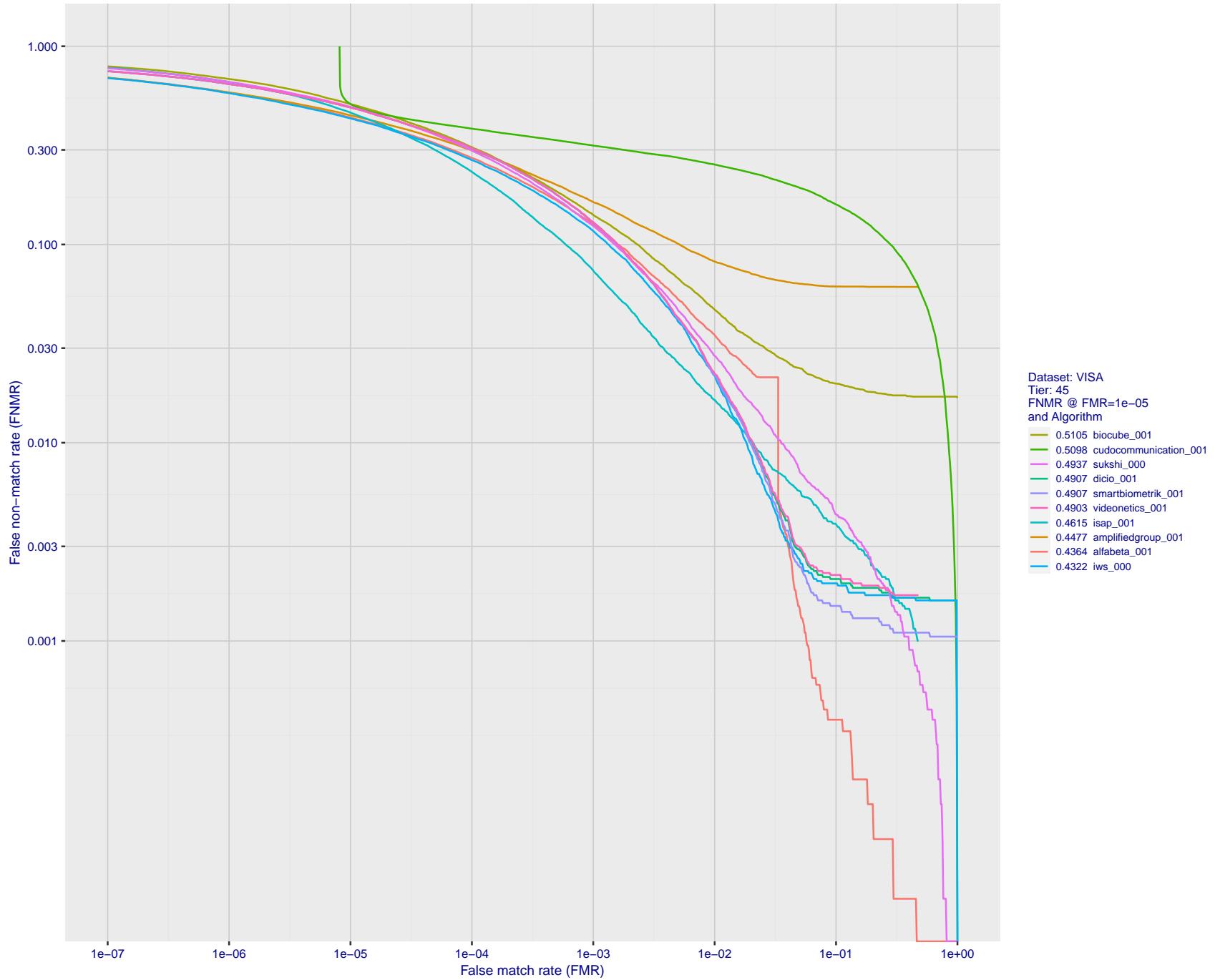


Figure 84: For the visa images, detection error tradeoff (DET) characteristics showing false non-match rate vs. false match rate plotted parametrically on threshold, T . The scales are logarithmic in order to show many decades of FMR.

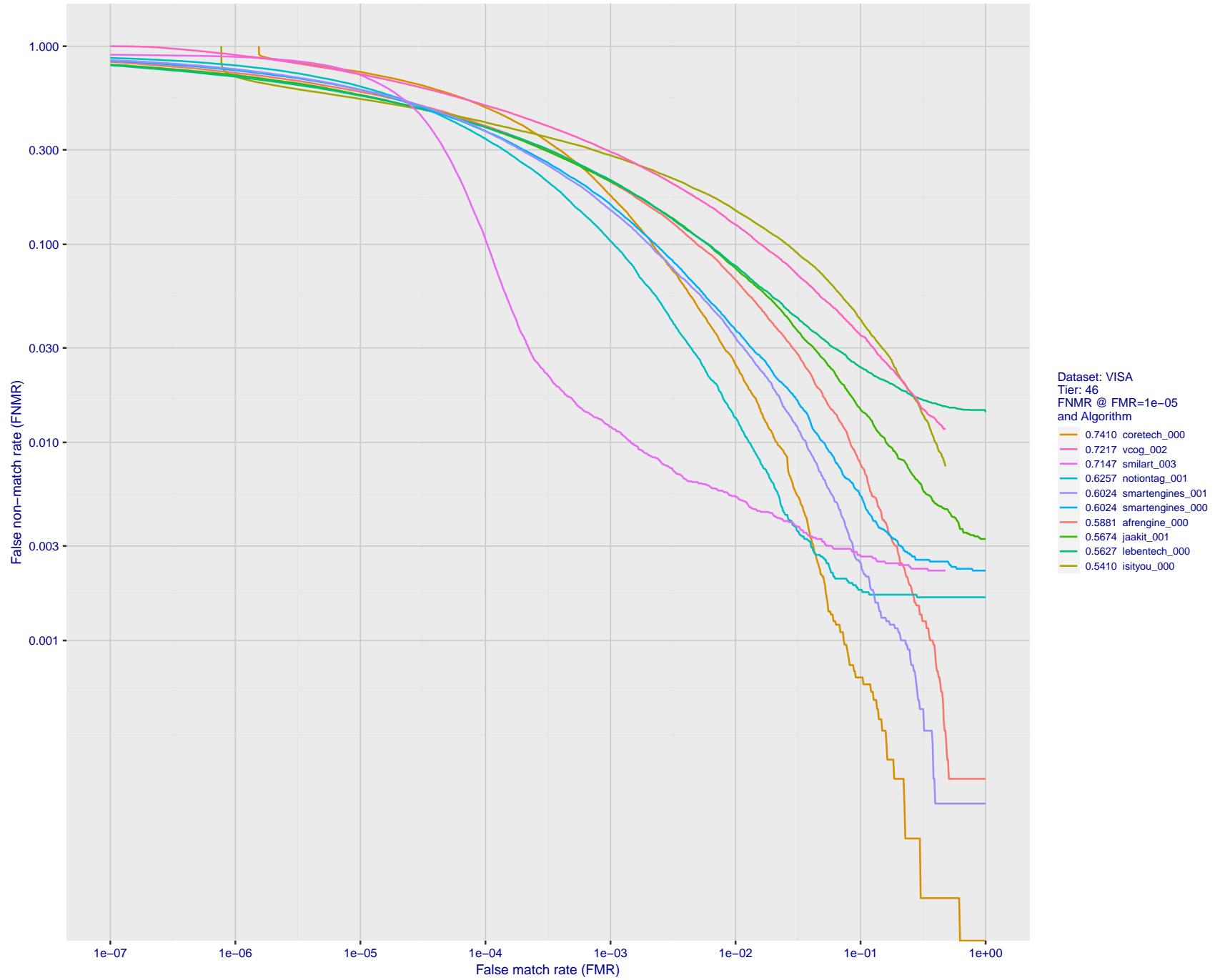


Figure 85: For the visa images, detection error tradeoff (DET) characteristics showing false non-match rate vs. false match rate plotted parametrically on threshold, T . The scales are logarithmic in order to show many decades of FMR.

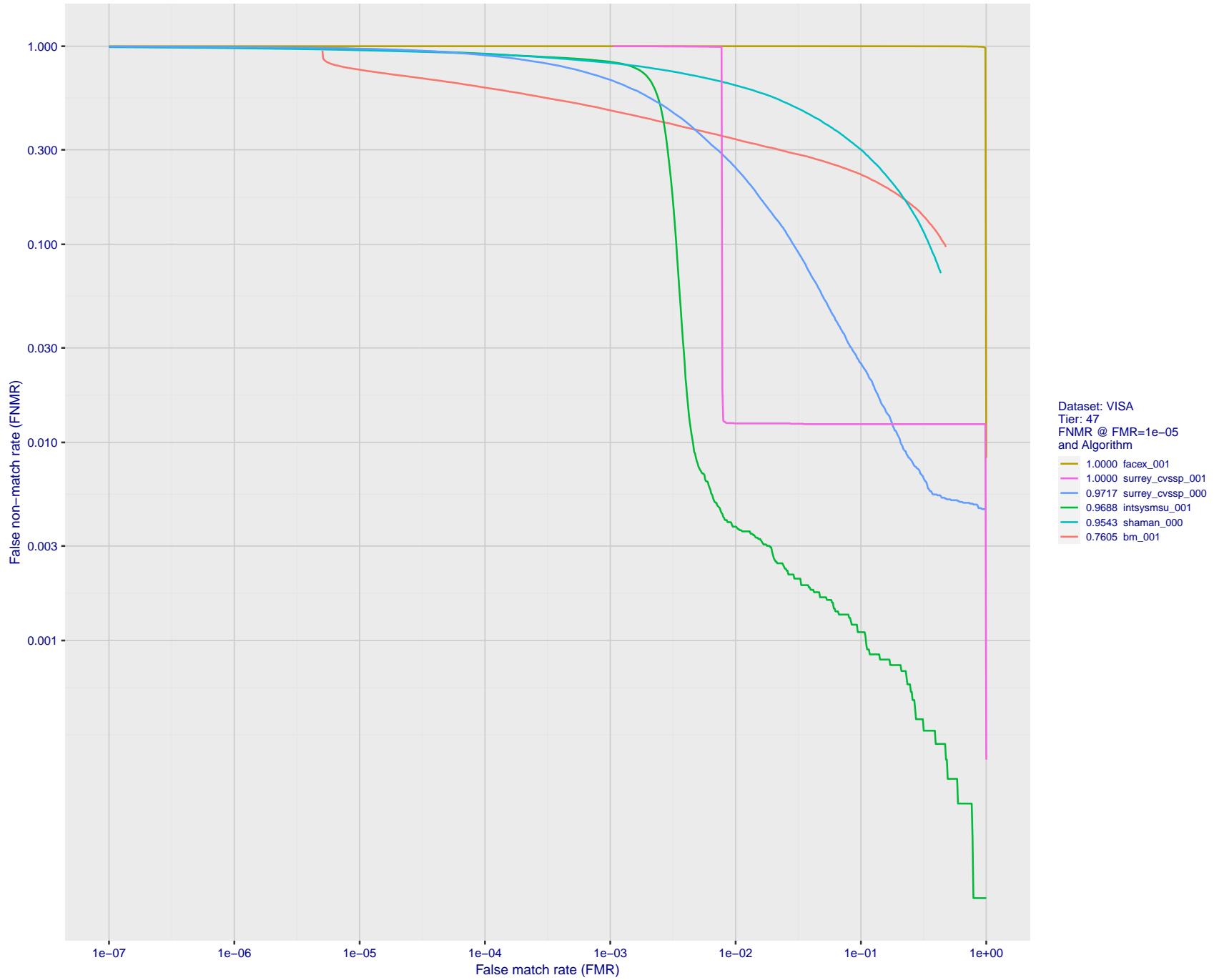


Figure 86: For the visa images, detection error tradeoff (DET) characteristics showing false non-match rate vs. false match rate plotted parametrically on threshold, T . The scales are logarithmic in order to show many decades of FMR.

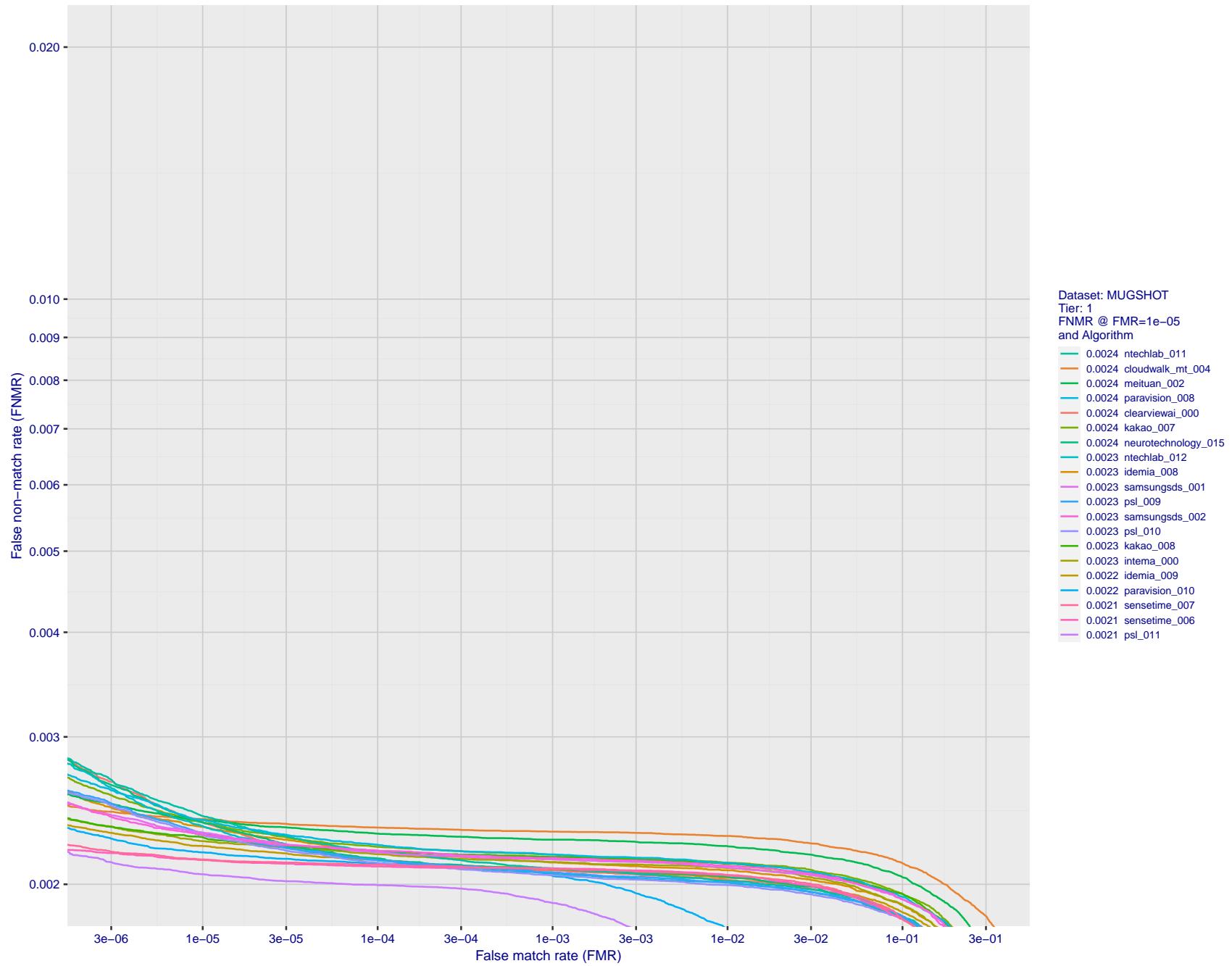


Figure 87: For the mugshot images, detection error tradeoff (DET) characteristics showing false non-match rate vs. false match rate plotted parametrically on threshold, T . The scales are logarithmic in order to show decades of FMR.

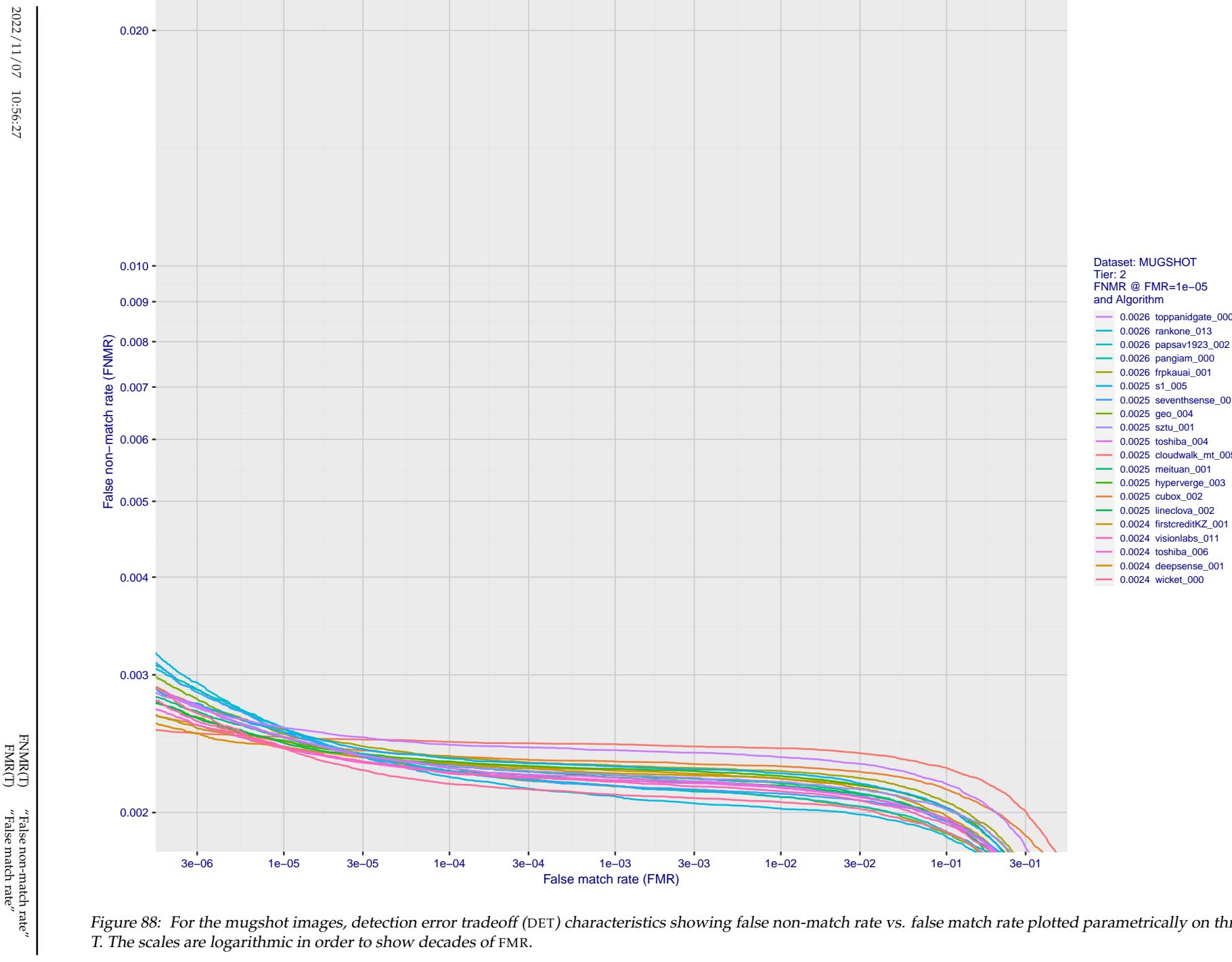
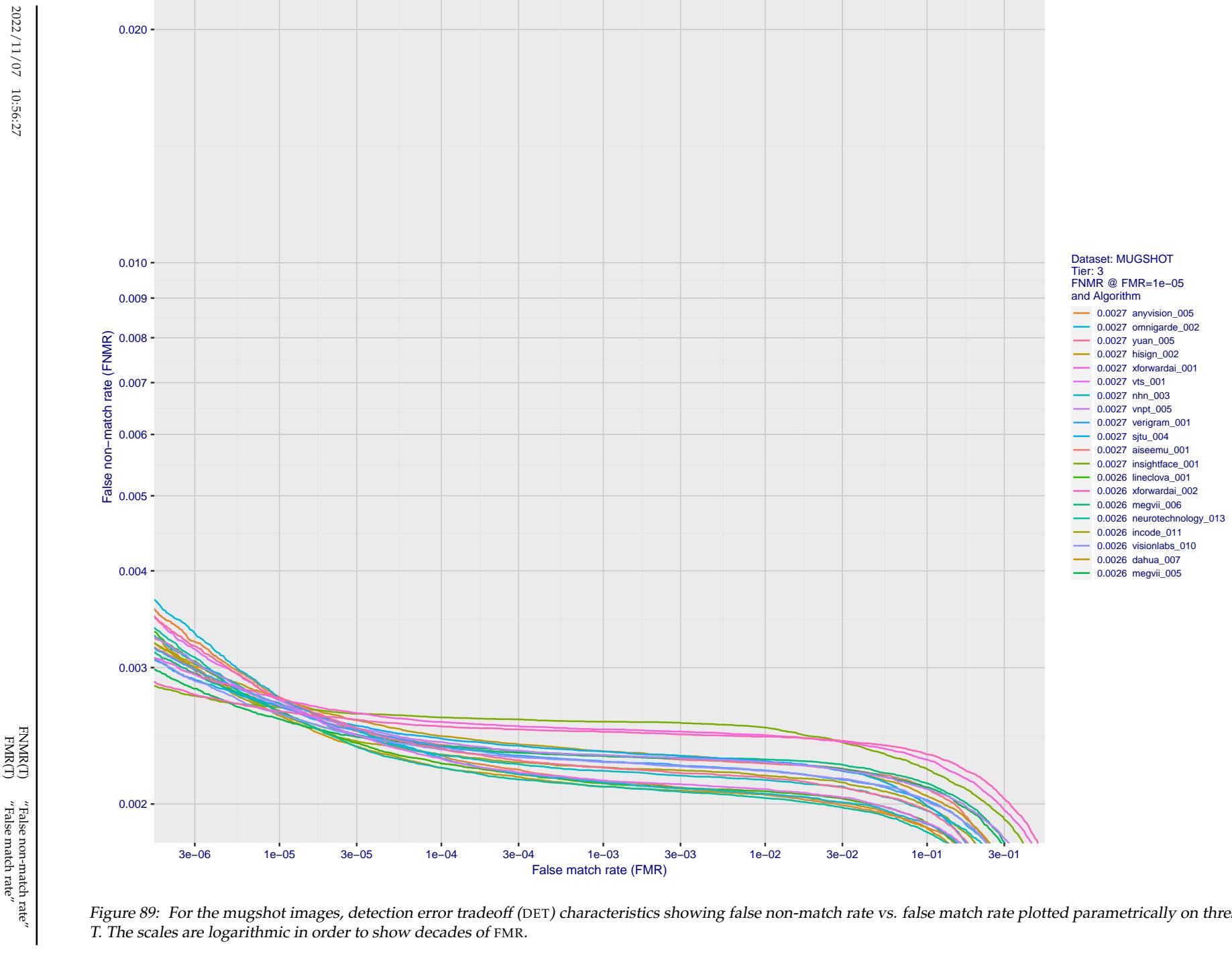


Figure 88: For the mugshot images, detection error tradeoff (DET) characteristics showing false non-match rate vs. false match rate plotted parametrically on threshold, T . The scales are logarithmic in order to show decades of FMR.



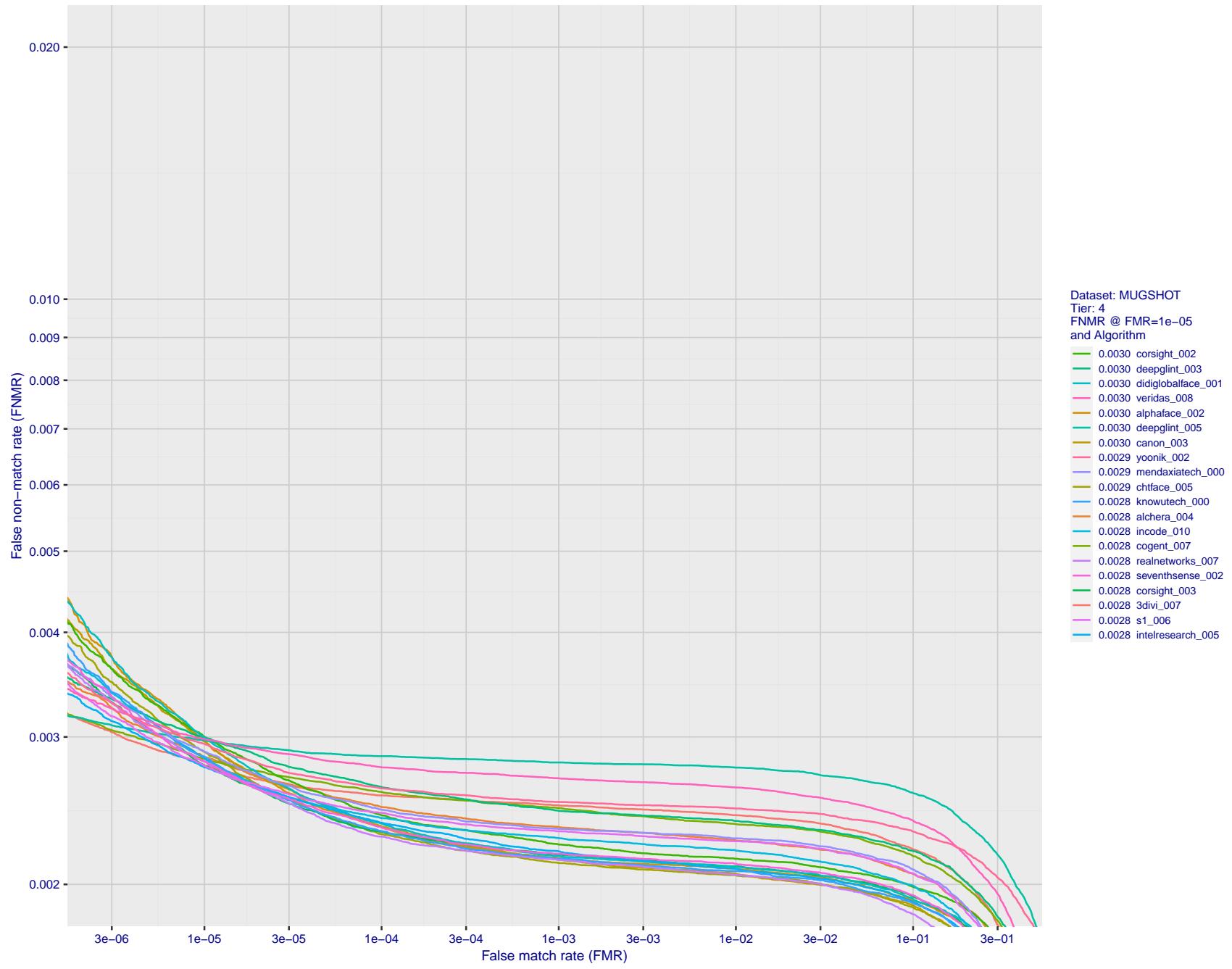


Figure 90: For the mugshot images, detection error tradeoff (DET) characteristics showing false non-match rate vs. false match rate plotted parametrically on threshold, T . The scales are logarithmic in order to show decades of FMR.

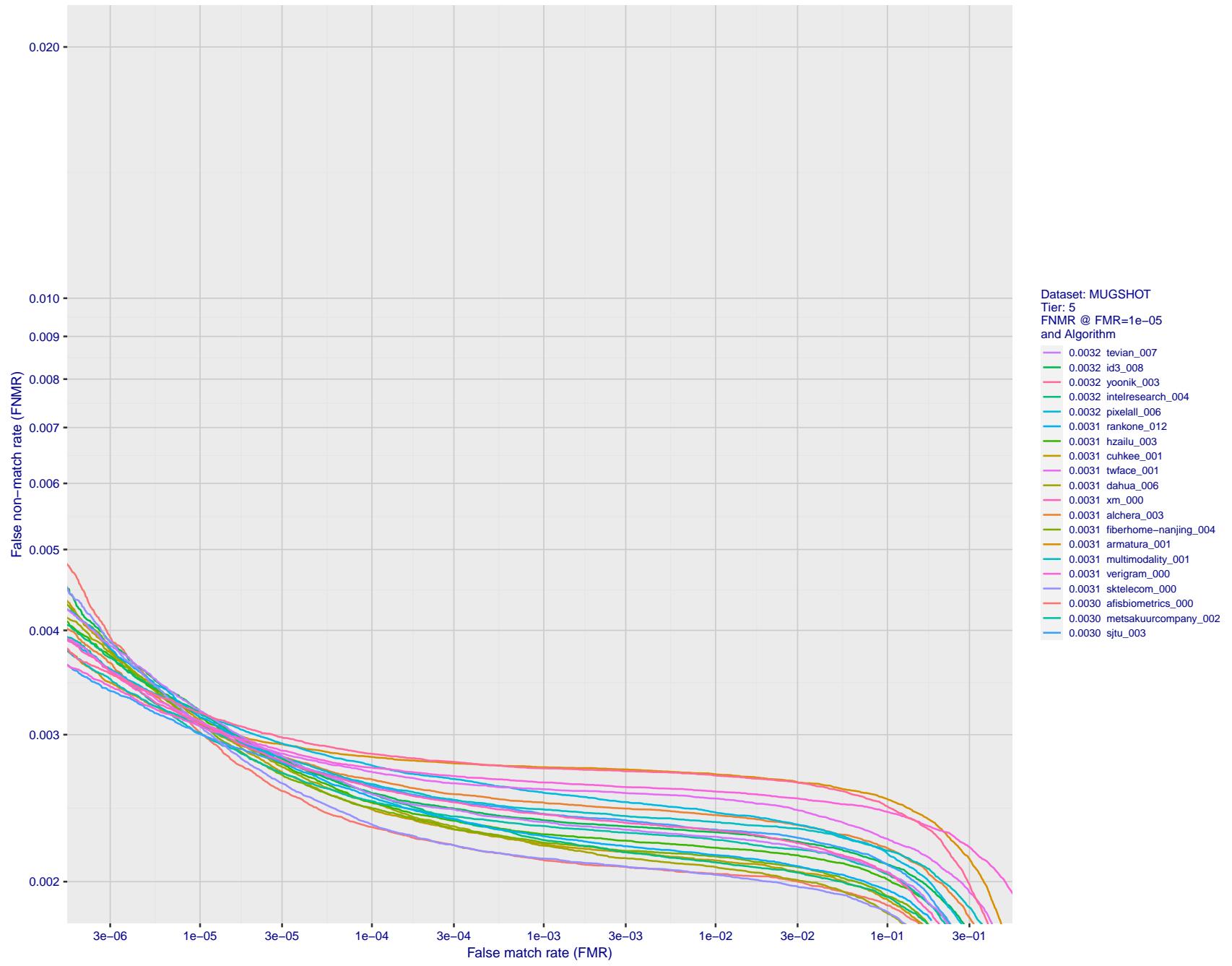


Figure 91: For the mugshot images, detection error tradeoff (DET) characteristics showing false non-match rate vs. false match rate plotted parametrically on threshold, T . The scales are logarithmic in order to show decades of FMR.

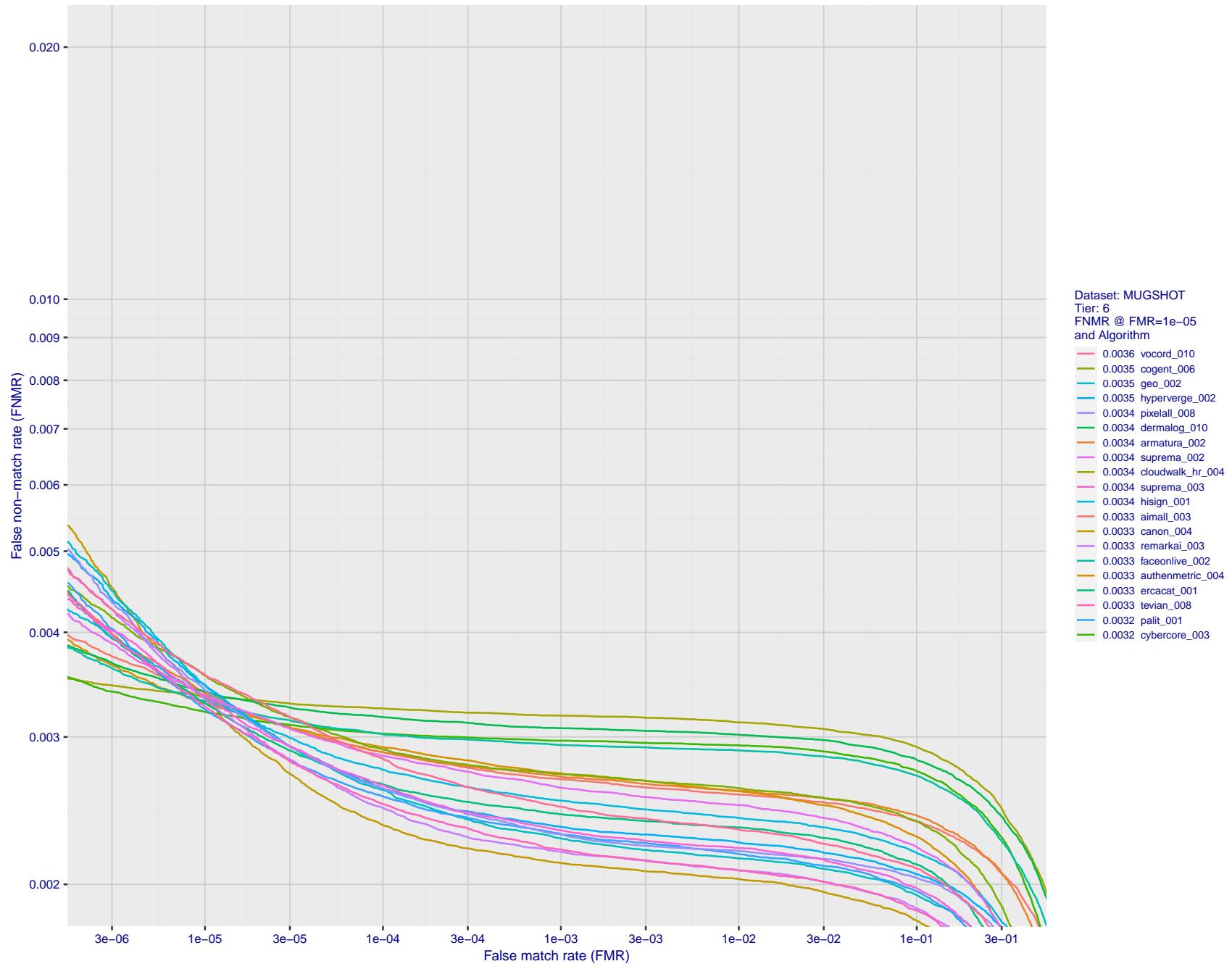


Figure 92: For the mugshot images, detection error tradeoff (DET) characteristics showing false non-match rate vs. false match rate plotted parametrically on threshold, T . The scales are logarithmic in order to show decades of FMR.

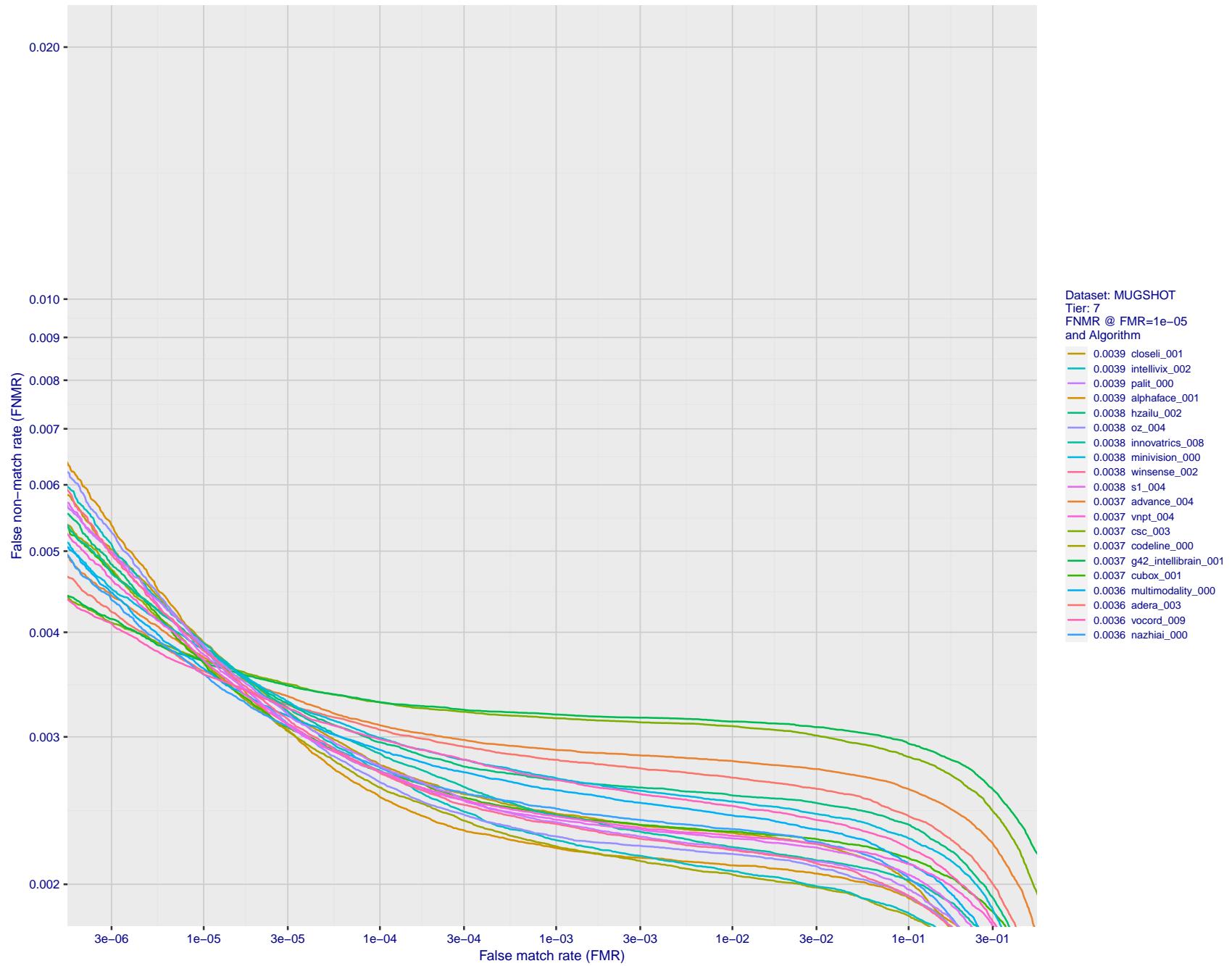


Figure 93: For the mugshot images, detection error tradeoff (DET) characteristics showing false non-match rate vs. false match rate plotted parametrically on threshold, T . The scales are logarithmic in order to show decades of FMR.

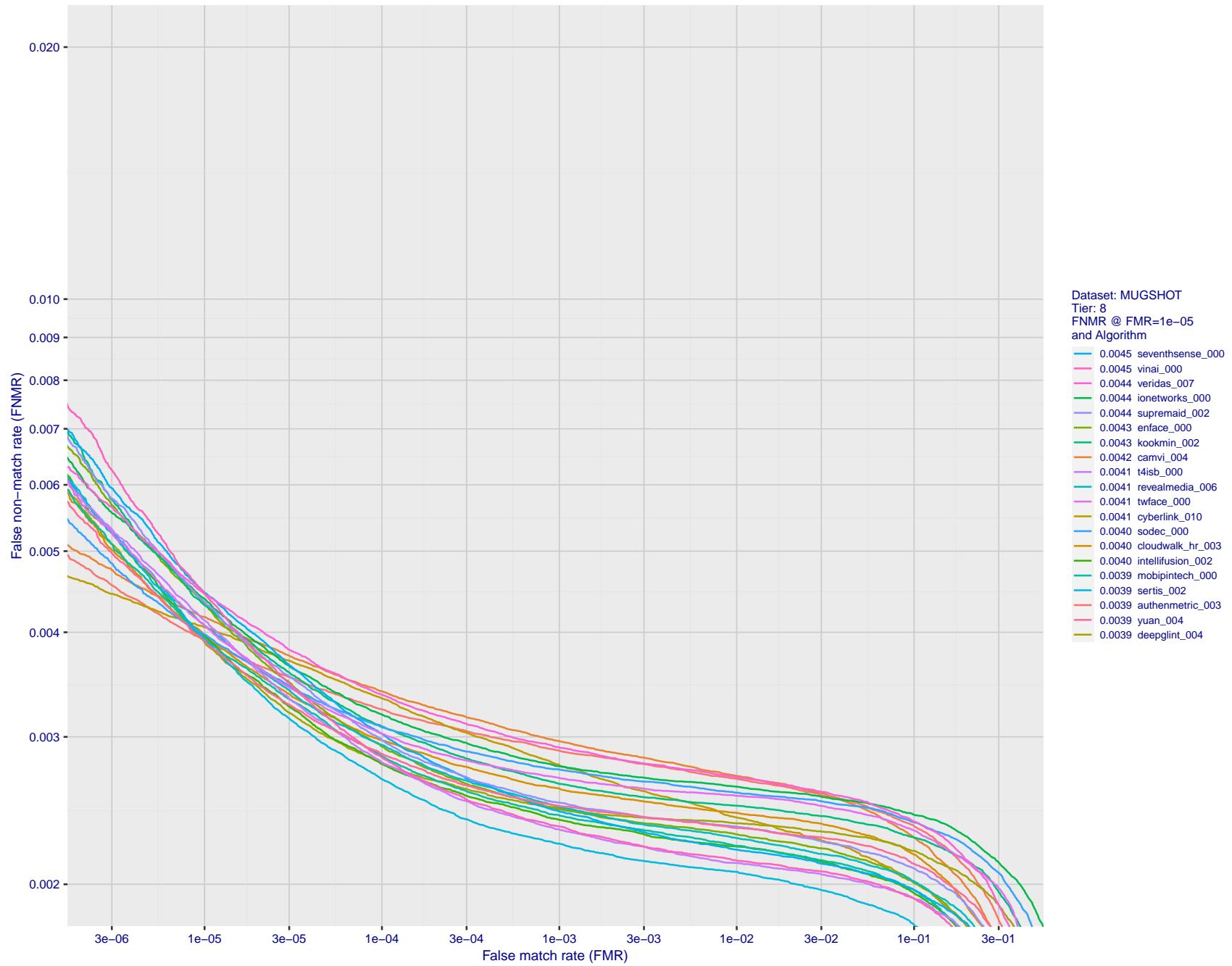


Figure 94: For the mugshot images, detection error tradeoff (DET) characteristics showing false non-match rate vs. false match rate plotted parametrically on threshold, T . The scales are logarithmic in order to show decades of FMR.

2022/11/07 10:56:27

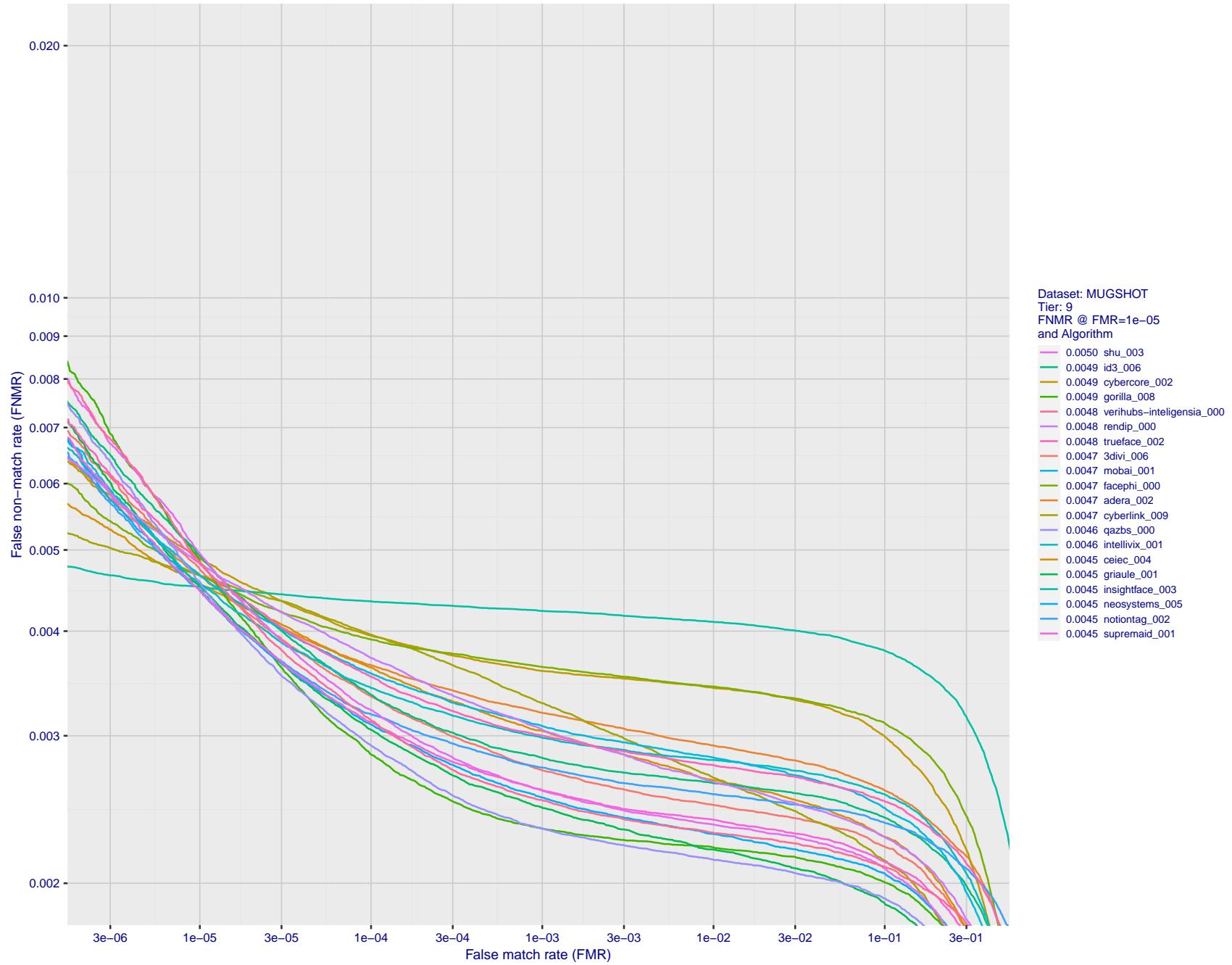


Figure 95: For the mugshot images, detection error tradeoff (DET) characteristics showing false non-match rate vs. false match rate plotted parametrically on threshold, T . The scales are logarithmic in order to show decades of FMR.

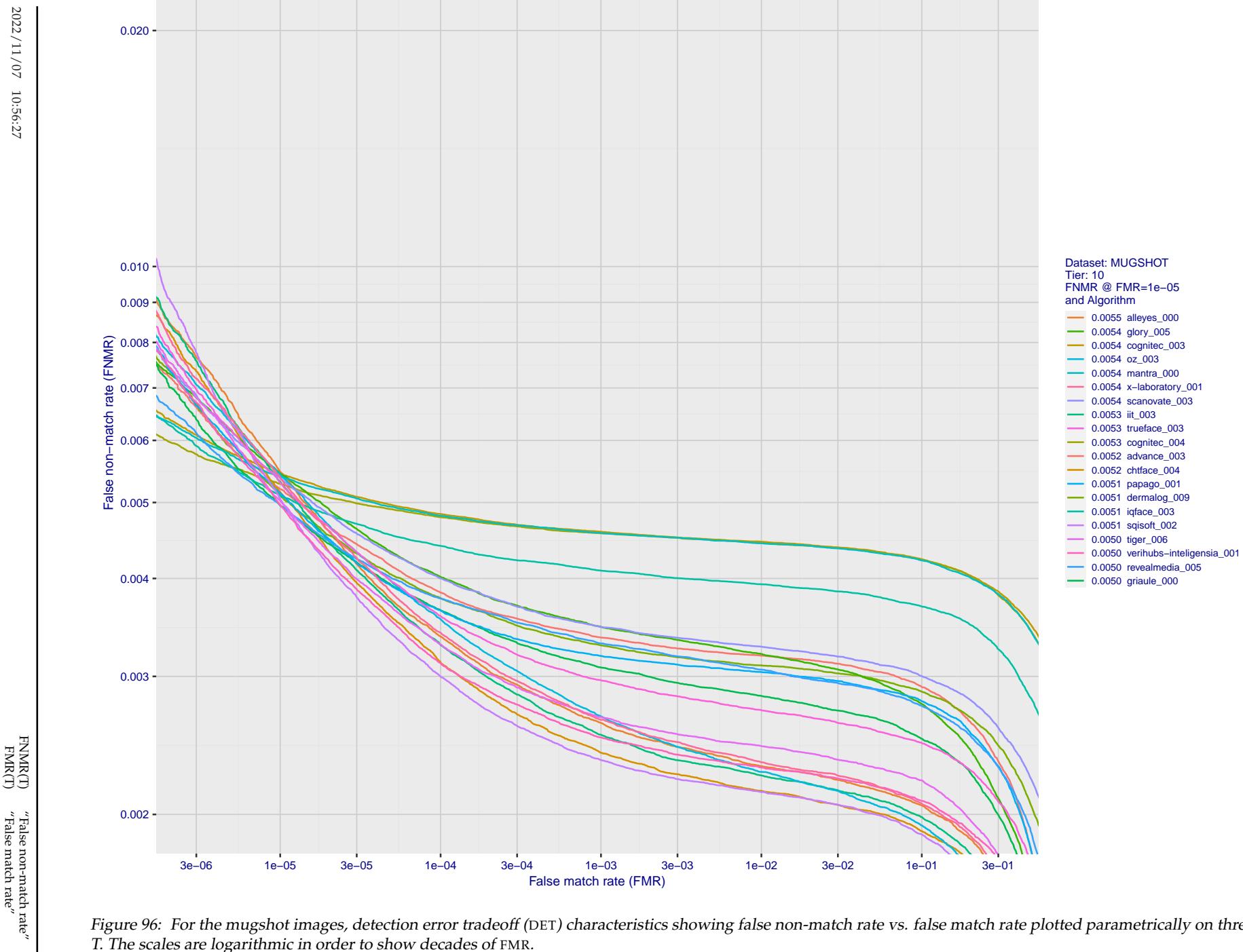


Figure 96: For the mugshot images, detection error tradeoff (DET) characteristics showing false non-match rate vs. false match rate plotted parametrically on threshold, T . The scales are logarithmic in order to show decades of FMR.

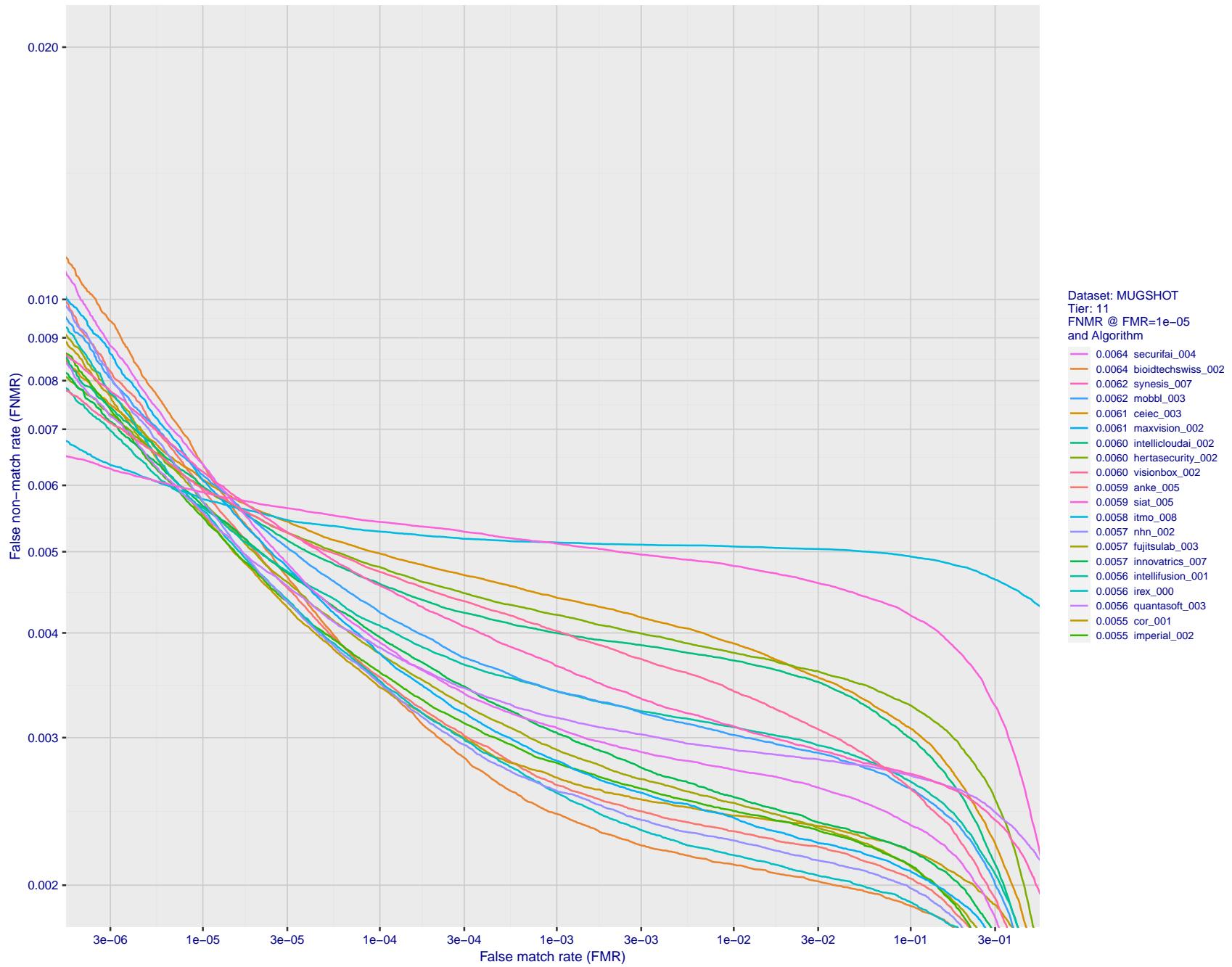


Figure 97: For the mugshot images, detection error tradeoff (DET) characteristics showing false non-match rate vs. false match rate plotted parametrically on threshold, T . The scales are logarithmic in order to show decades of FMR.

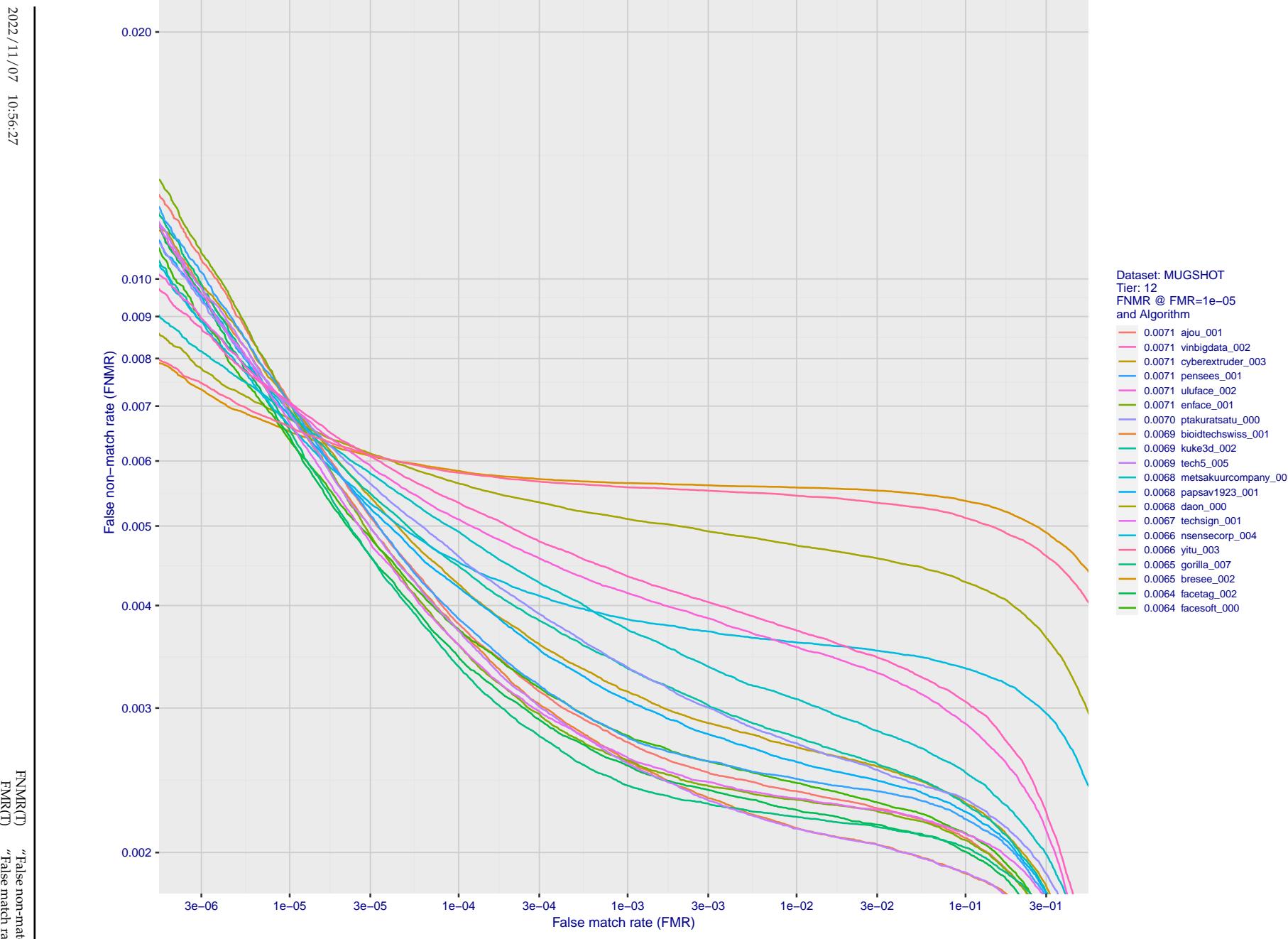


Figure 98: For the mugshot images, detection error tradeoff (DET) characteristics showing false non-match rate vs. false match rate plotted parametrically on threshold, T . The scales are logarithmic in order to show decades of FMR.

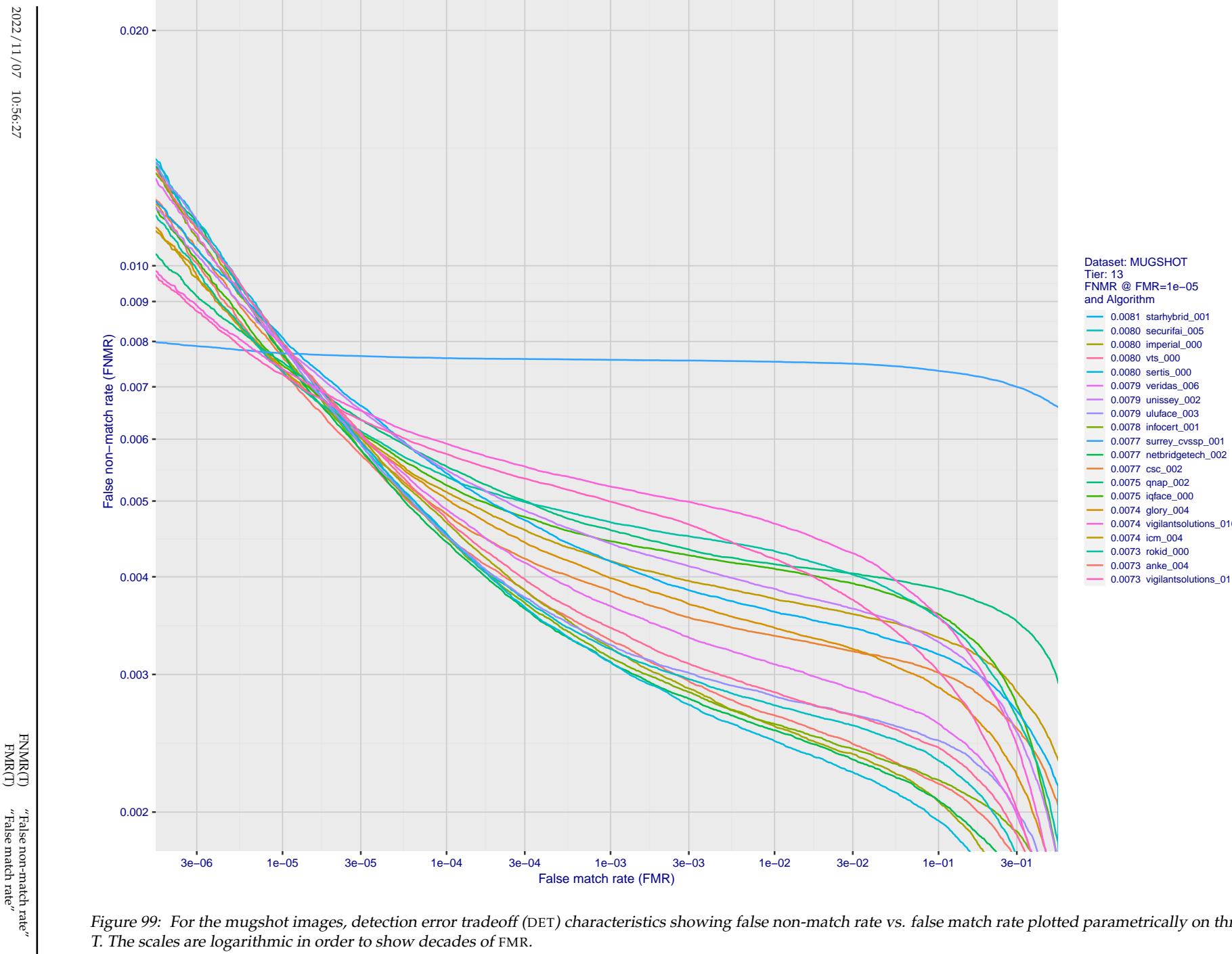


Figure 99: For the mugshot images, detection error tradeoff (DET) characteristics showing false non-match rate vs. false match rate plotted parametrically on threshold, T . The scales are logarithmic in order to show decades of FMR.

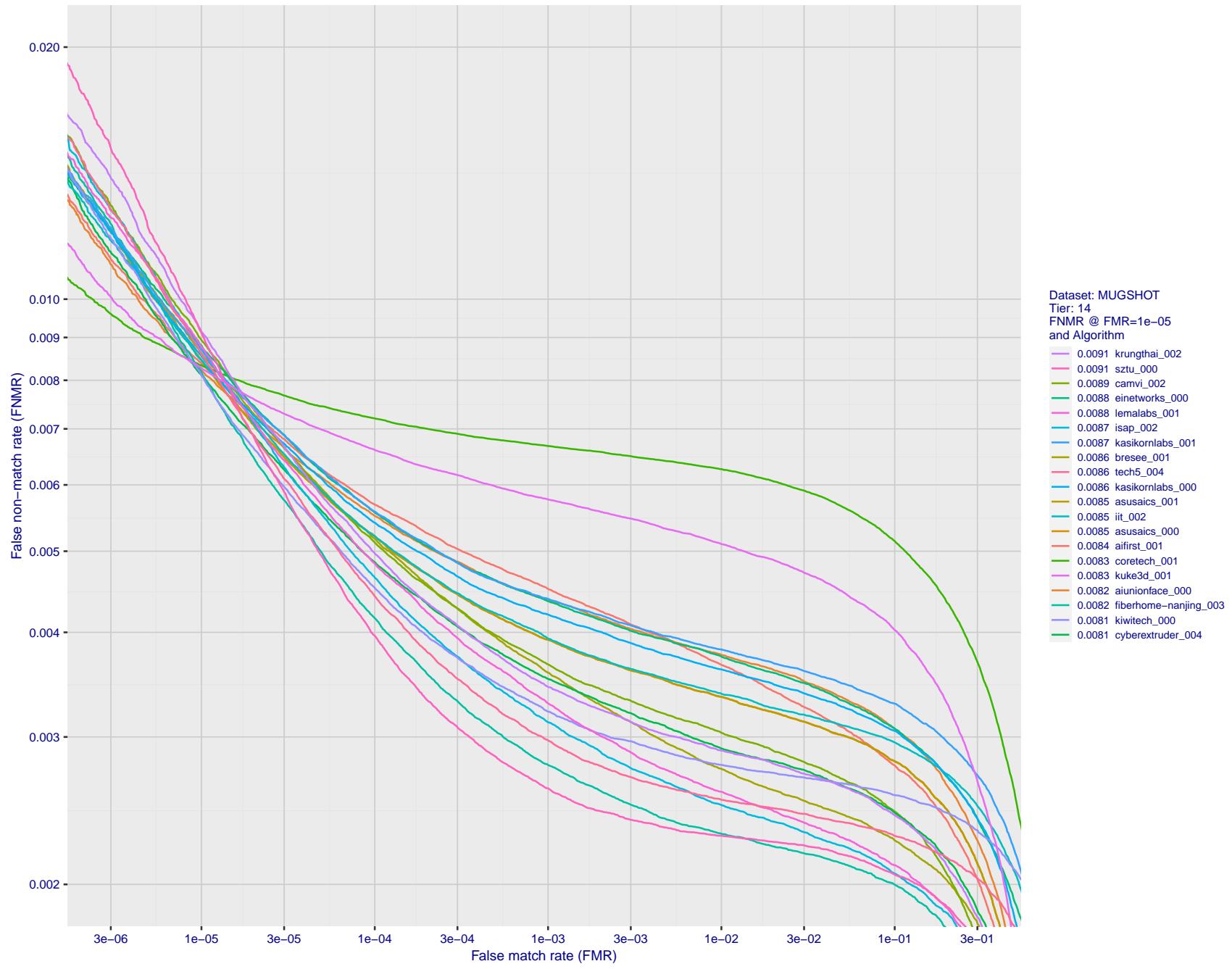


Figure 100: For the mugshot images, detection error tradeoff (DET) characteristics showing false non-match rate vs. false match rate plotted parametrically on threshold, T . The scales are logarithmic in order to show decades of FMR.

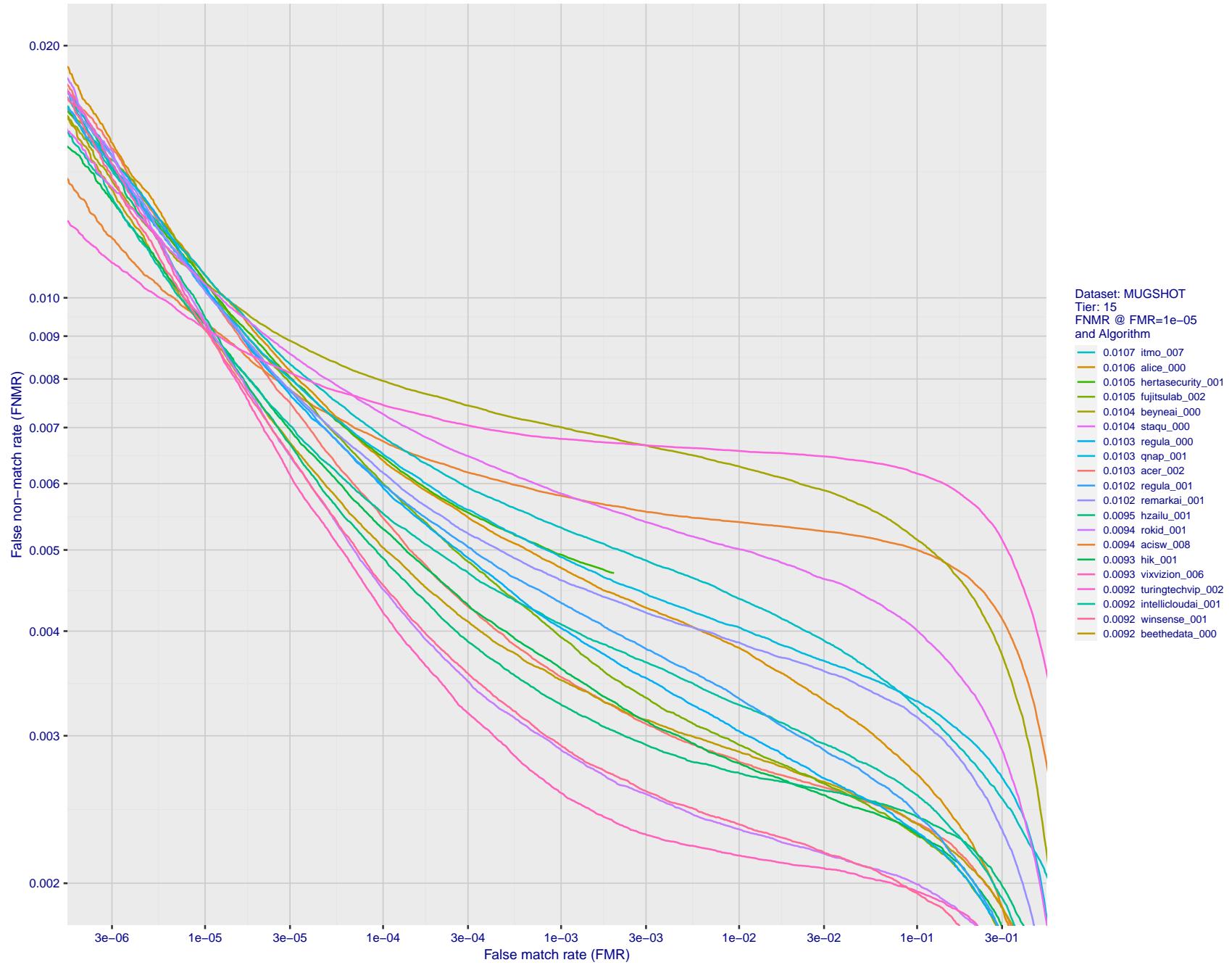


Figure 101: For the mugshot images, detection error tradeoff (DET) characteristics showing false non-match rate vs. false match rate plotted parametrically on threshold, T . The scales are logarithmic in order to show decades of FMR.

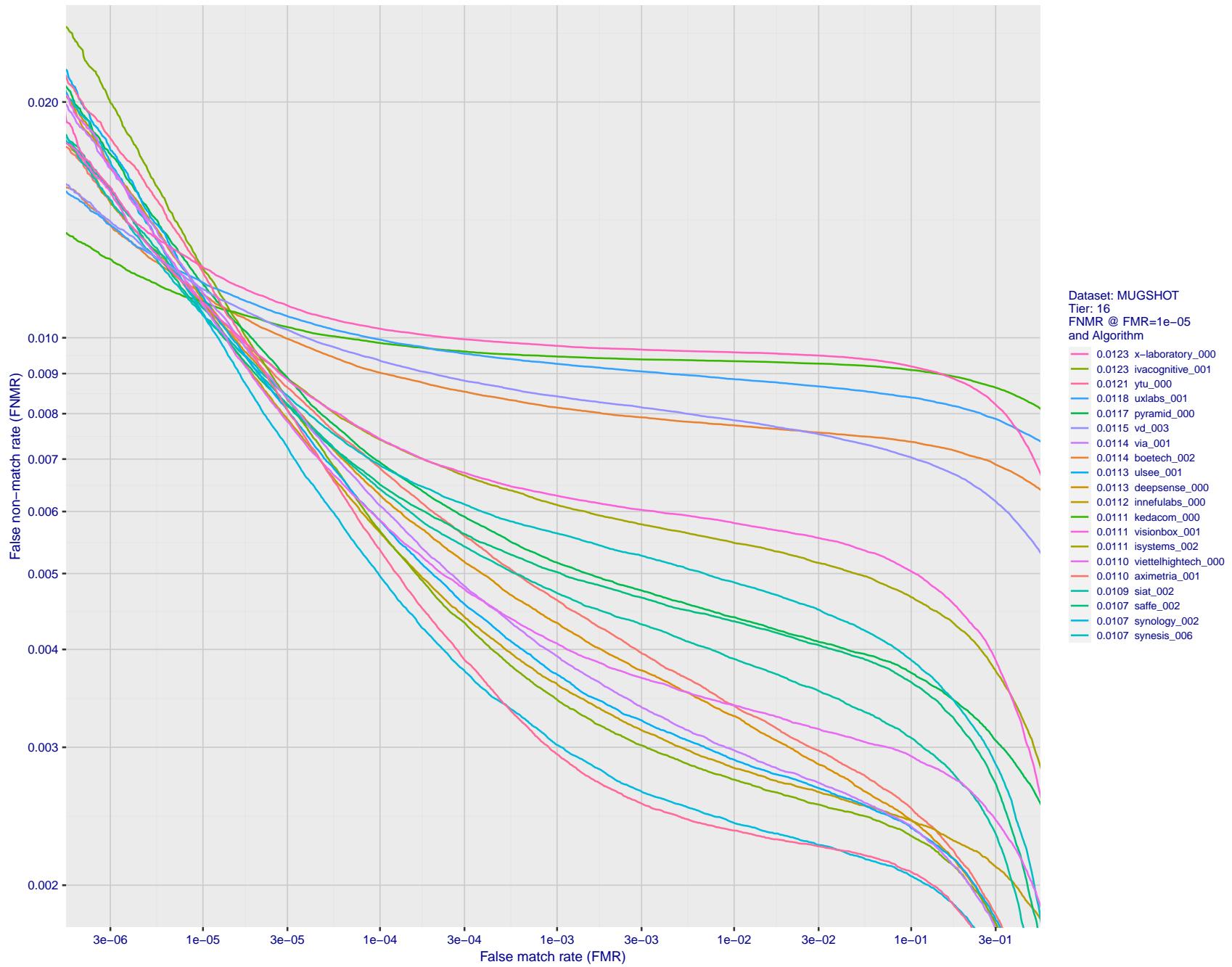


Figure 102: For the mugshot images, detection error tradeoff (DET) characteristics showing false non-match rate vs. false match rate plotted parametrically on threshold, T . The scales are logarithmic in order to show decades of FMR.

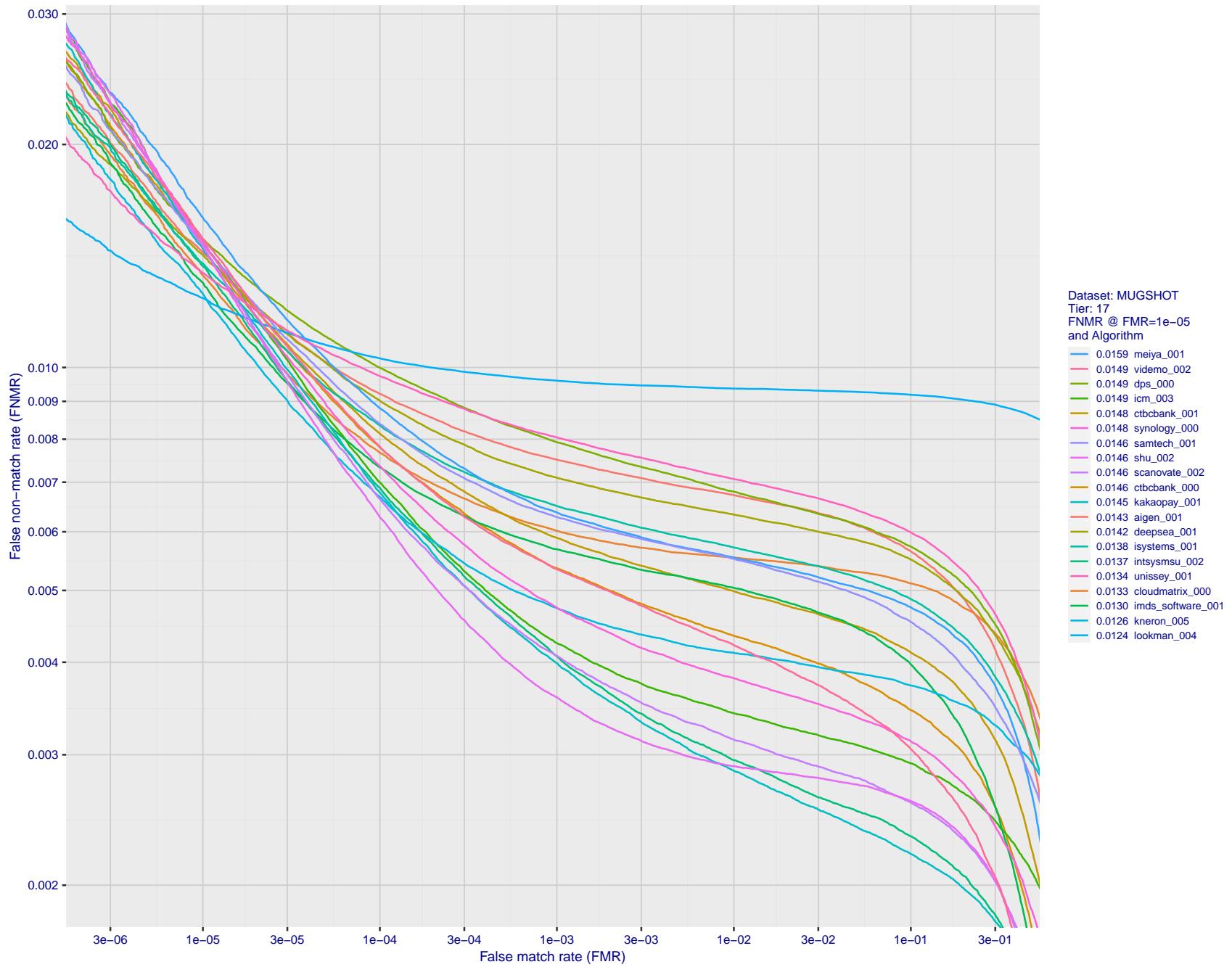


Figure 103: For the mugshot images, detection error tradeoff (DET) characteristics showing false non-match rate vs. false match rate plotted parametrically on threshold, T . The scales are logarithmic in order to show decades of FMR.

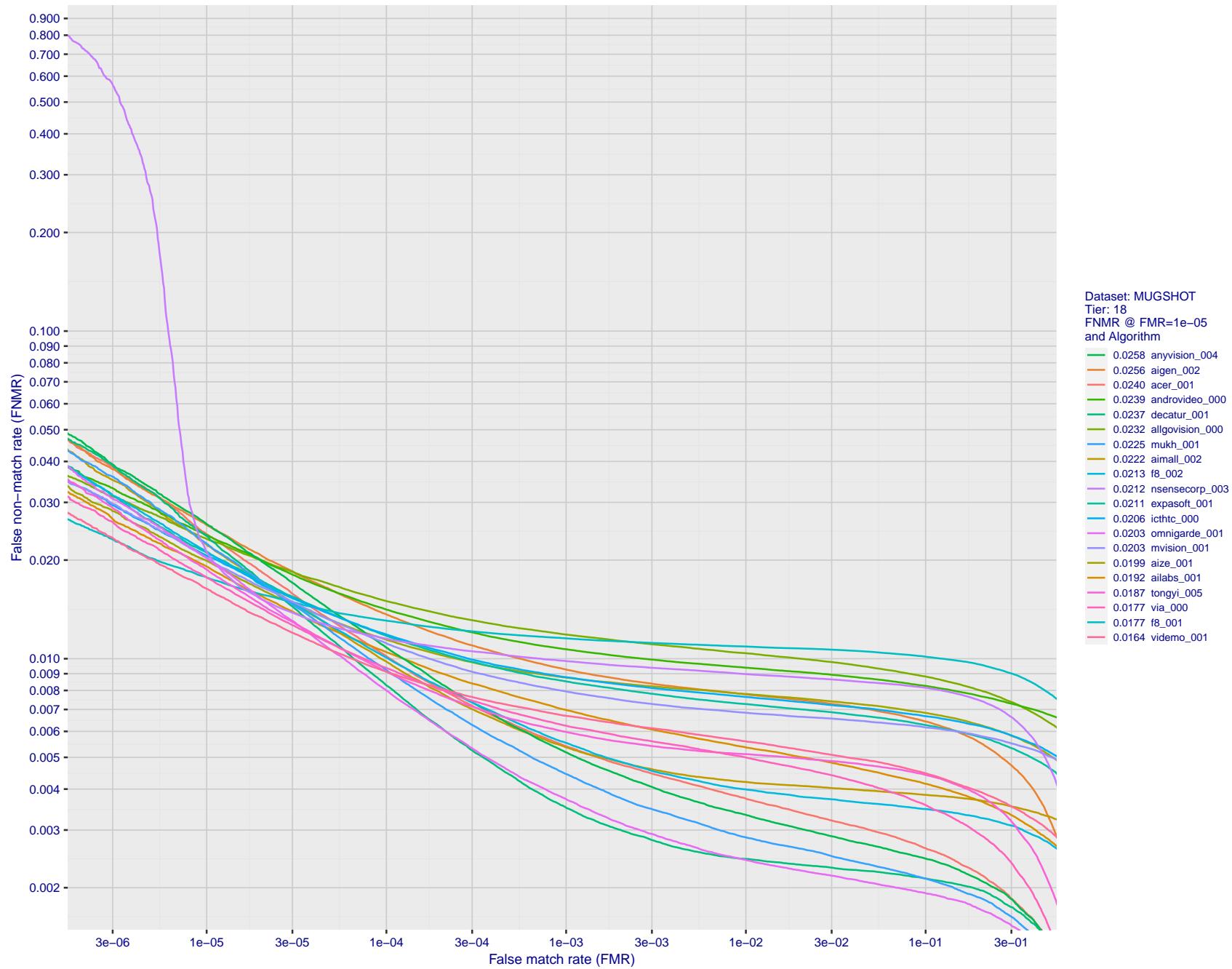


Figure 104: For the mugshot images, detection error tradeoff (DET) characteristics showing false non-match rate vs. false match rate plotted parametrically on threshold, T . The scales are logarithmic in order to show decades of FMR.

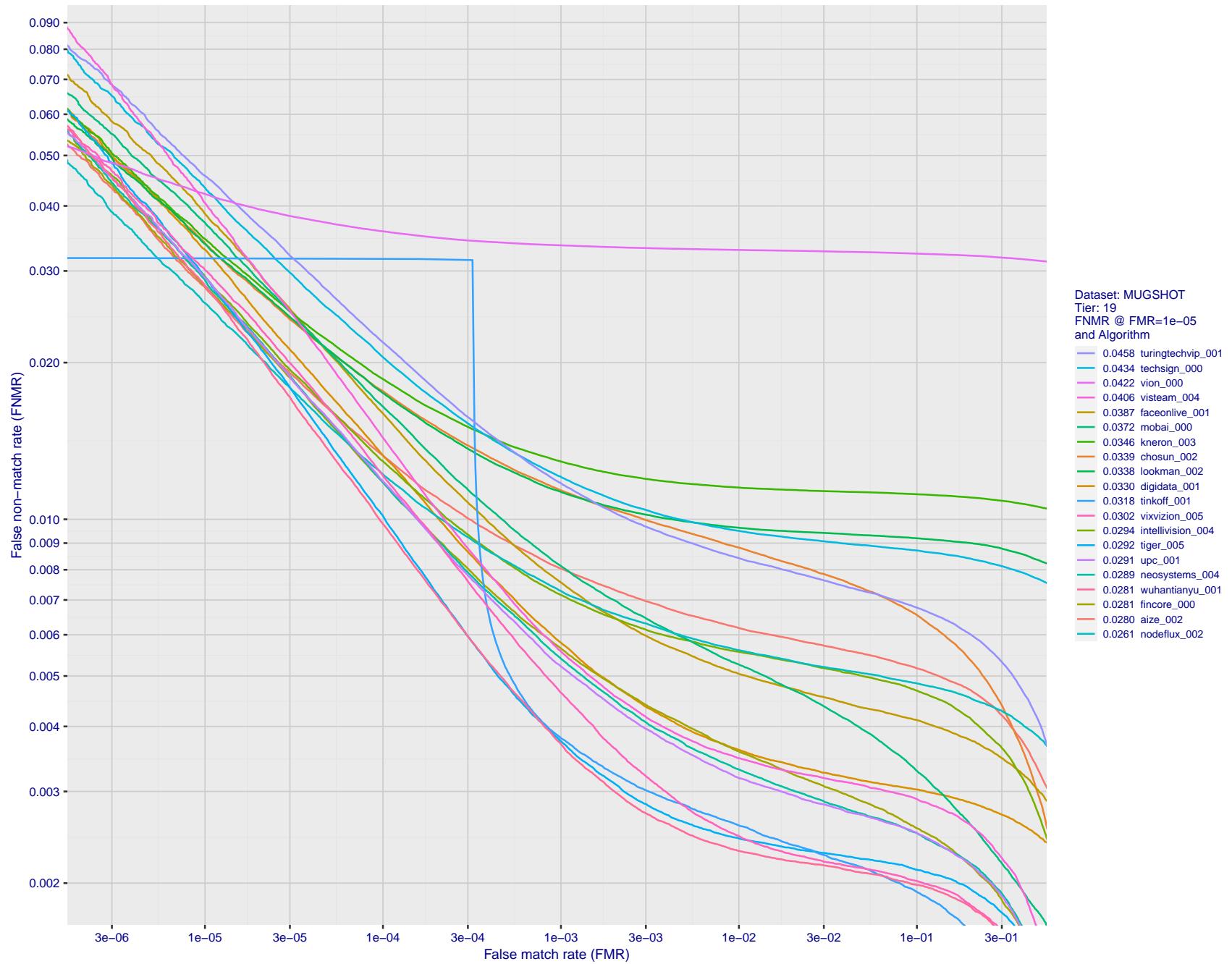


Figure 105: For the mugshot images, detection error tradeoff (DET) characteristics showing false non-match rate vs. false match rate plotted parametrically on threshold, T . The scales are logarithmic in order to show decades of FMR.

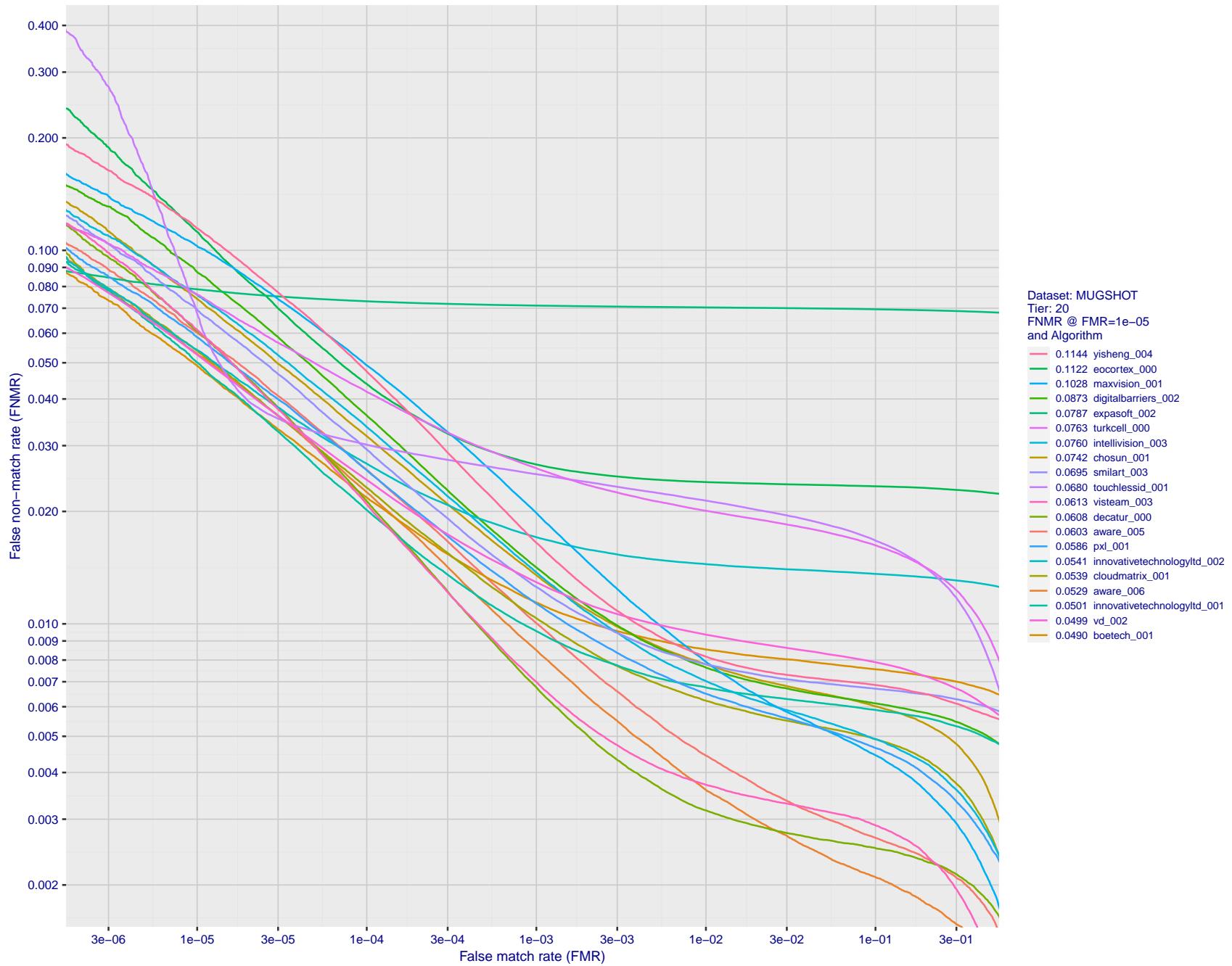


Figure 106: For the mugshot images, detection error tradeoff (DET) characteristics showing false non-match rate vs. false match rate plotted parametrically on threshold, T . The scales are logarithmic in order to show decades of FMR.

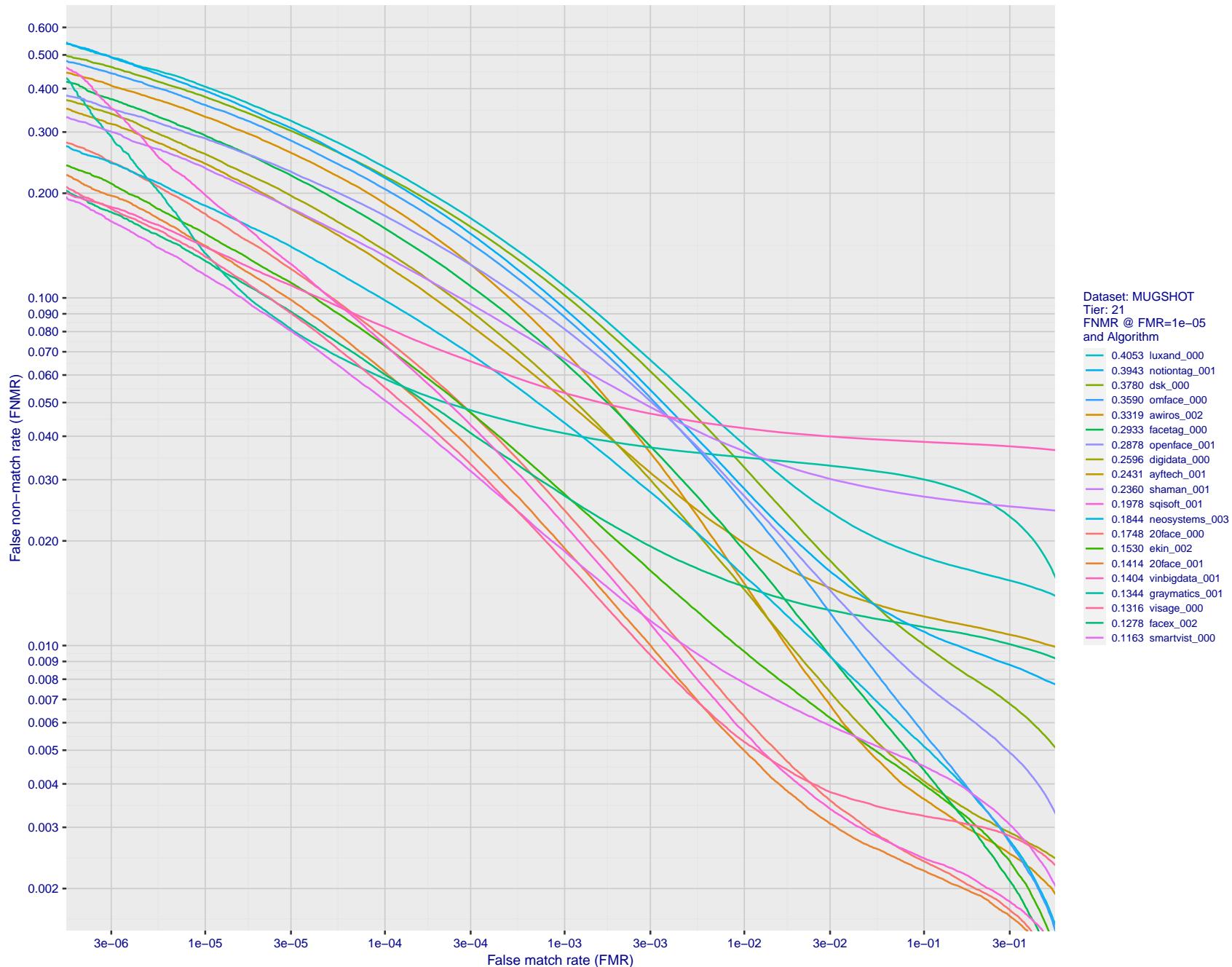


Figure 107: For the mugshot images, detection error tradeoff (DET) characteristics showing false non-match rate vs. false match rate plotted parametrically on threshold, T . The scales are logarithmic in order to show decades of FMR.

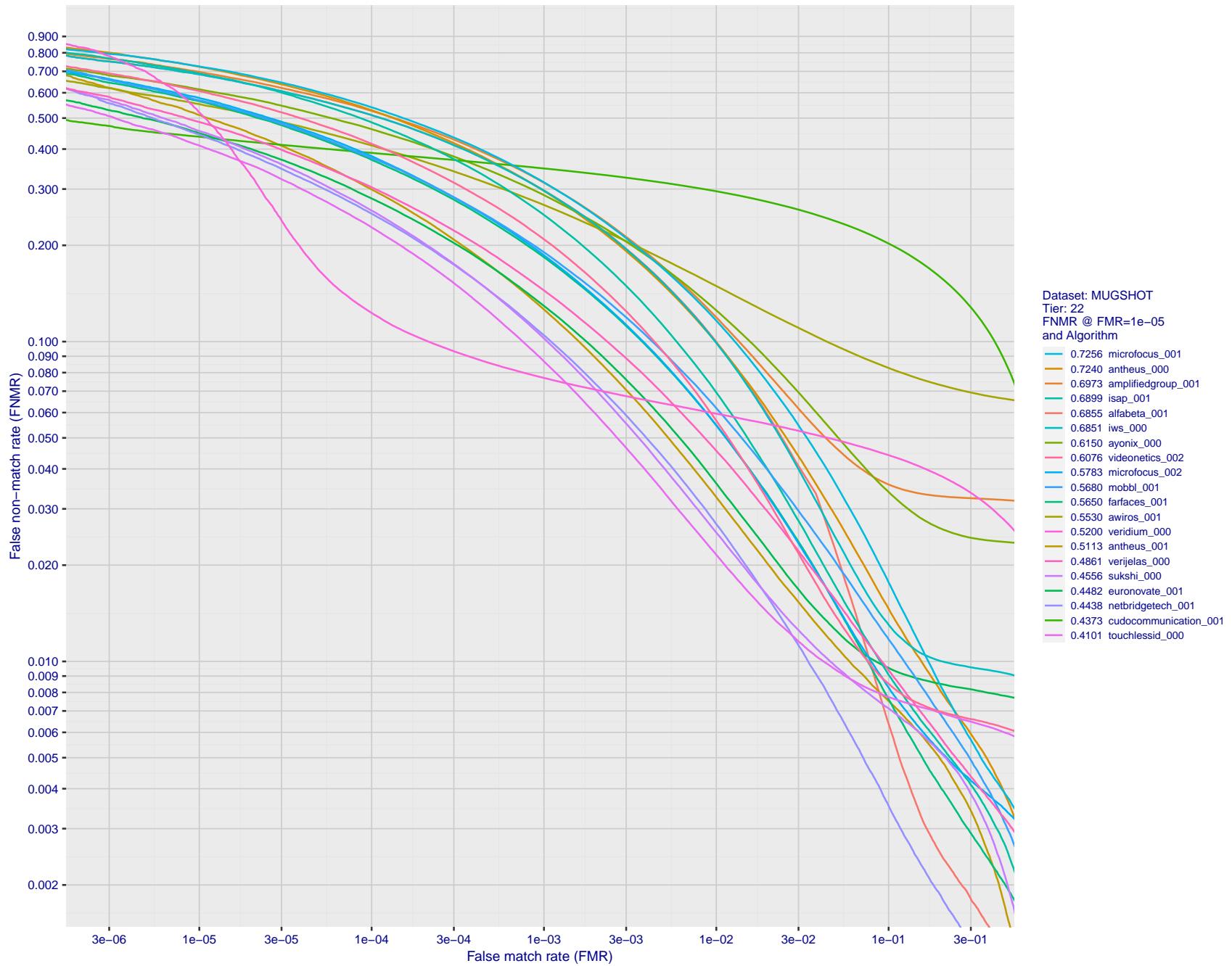


Figure 108: For the mugshot images, detection error tradeoff (DET) characteristics showing false non-match rate vs. false match rate plotted parametrically on threshold, T . The scales are logarithmic in order to show decades of FMR.

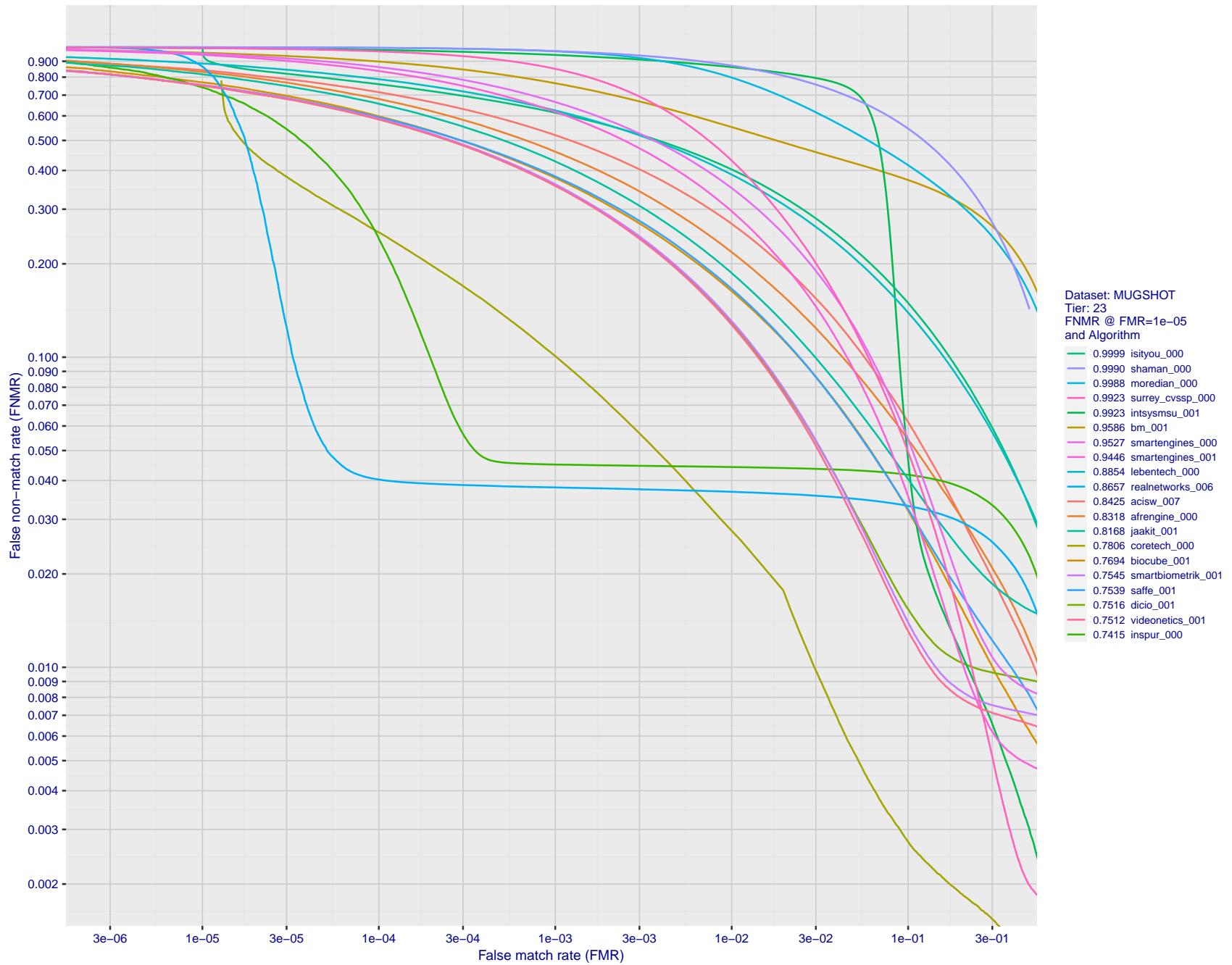


Figure 109: For the mugshot images, detection error tradeoff (DET) characteristics showing false non-match rate vs. false match rate plotted parametrically on threshold, T . The scales are logarithmic in order to show decades of FMR.

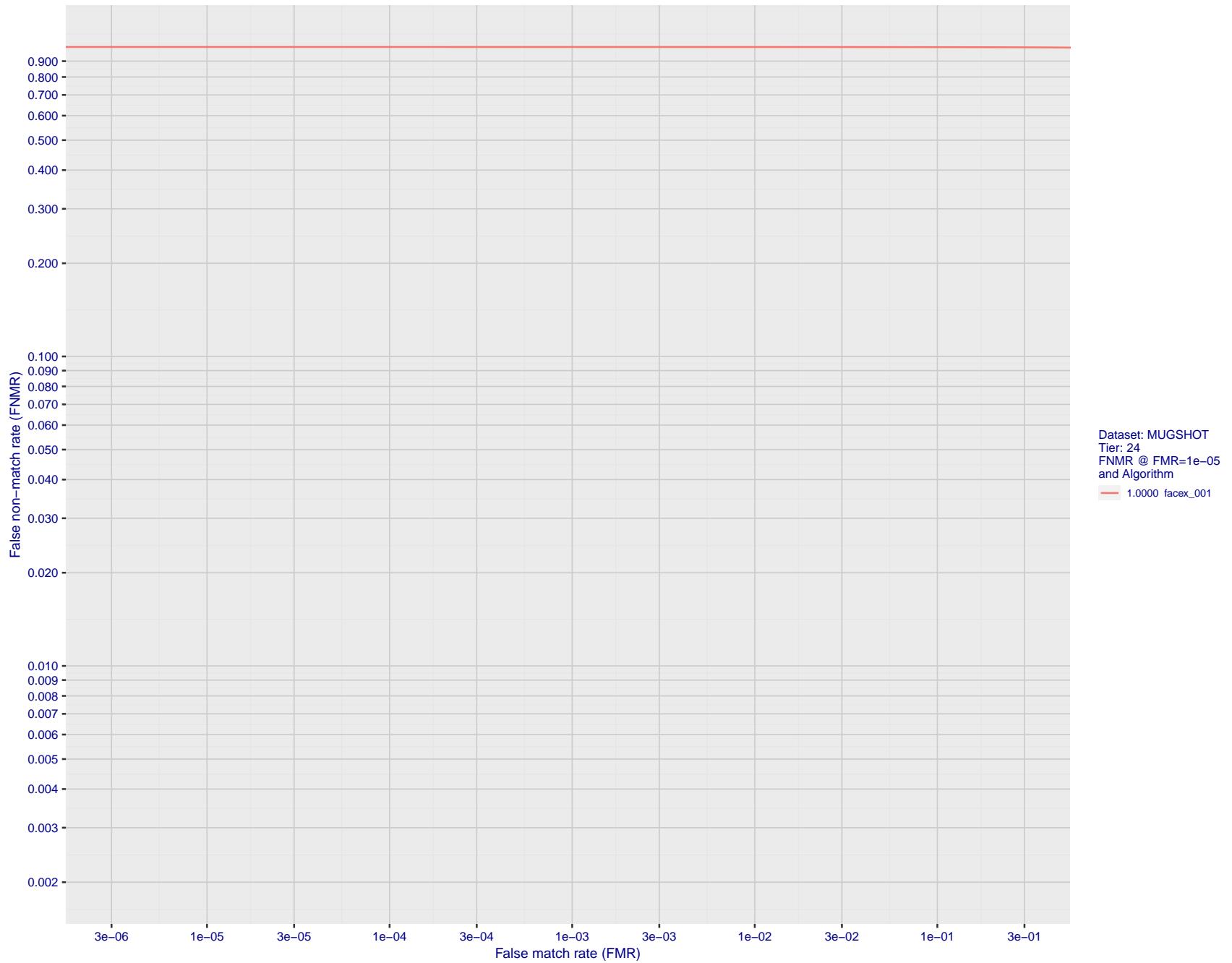


Figure 110: For the mugshot images, detection error tradeoff (DET) characteristics showing false non-match rate vs. false match rate plotted parametrically on threshold, T . The scales are logarithmic in order to show decades of FMR.

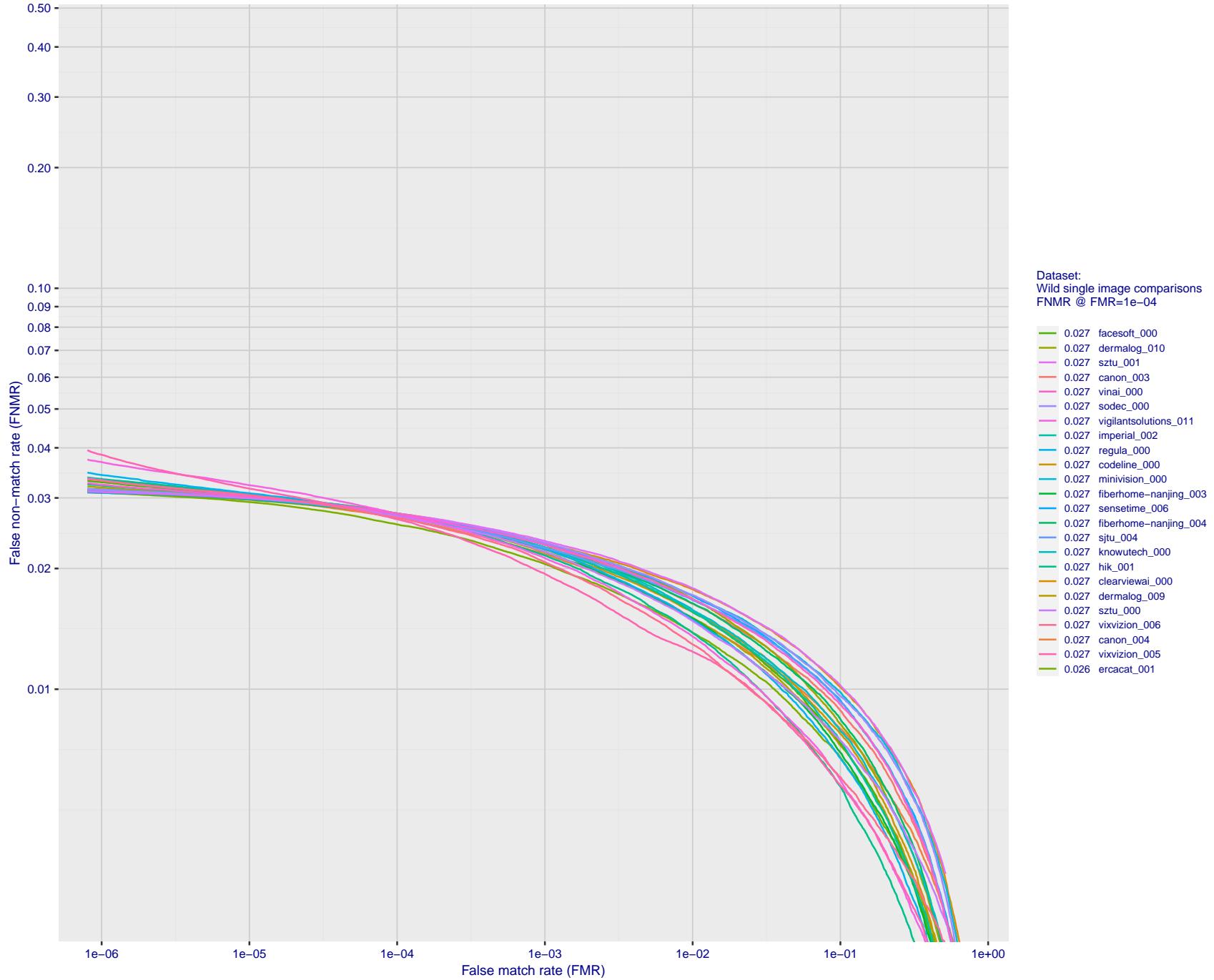


Figure 111: For the 2018 wild image comparisons, detection error tradeoff (DET) characteristics showing false non-match rate vs. false match rate plotted parametrically on threshold, T . The scales are logarithmic in order to show several decades of FMR.

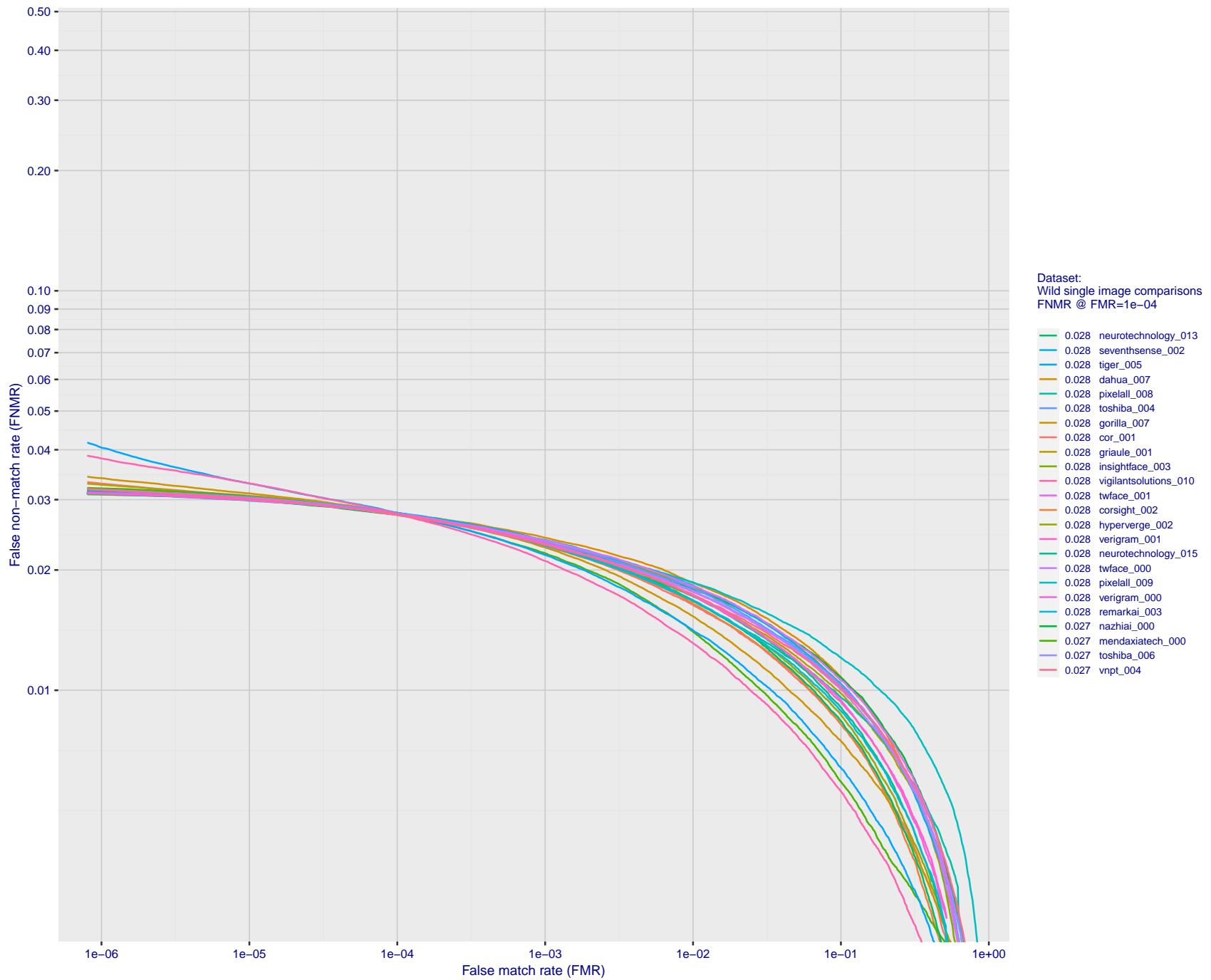


Figure 112: For the 2018 wild image comparisons, detection error tradeoff (DET) characteristics showing false non-match rate vs. false match rate plotted parametrically on threshold, T. The scales are logarithmic in order to show several decades of FMR.

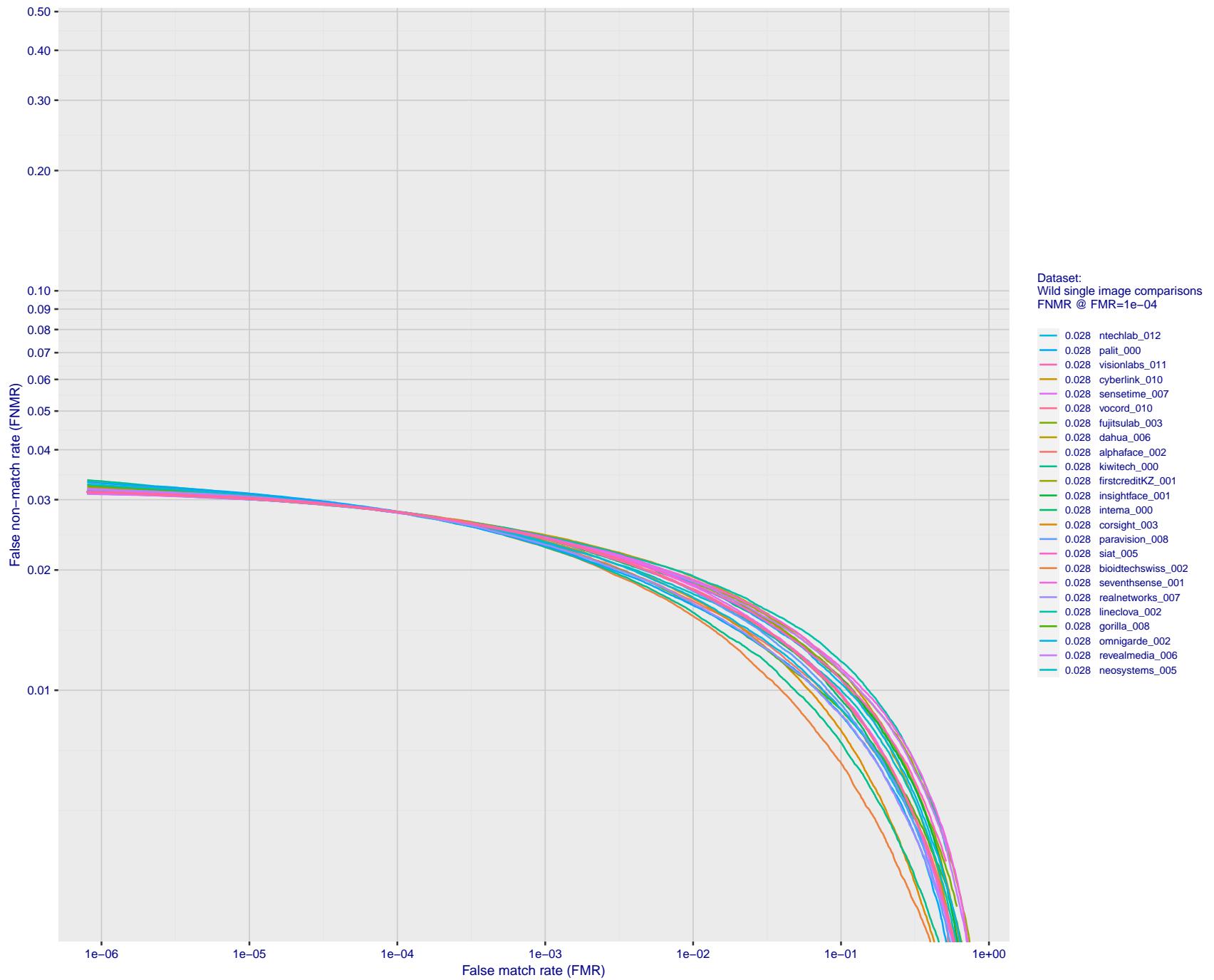


Figure 113: For the 2018 wild image comparisons, detection error tradeoff (DET) characteristics showing false non-match rate vs. false match rate plotted parametrically on threshold, T. The scales are logarithmic in order to show several decades of FMR.

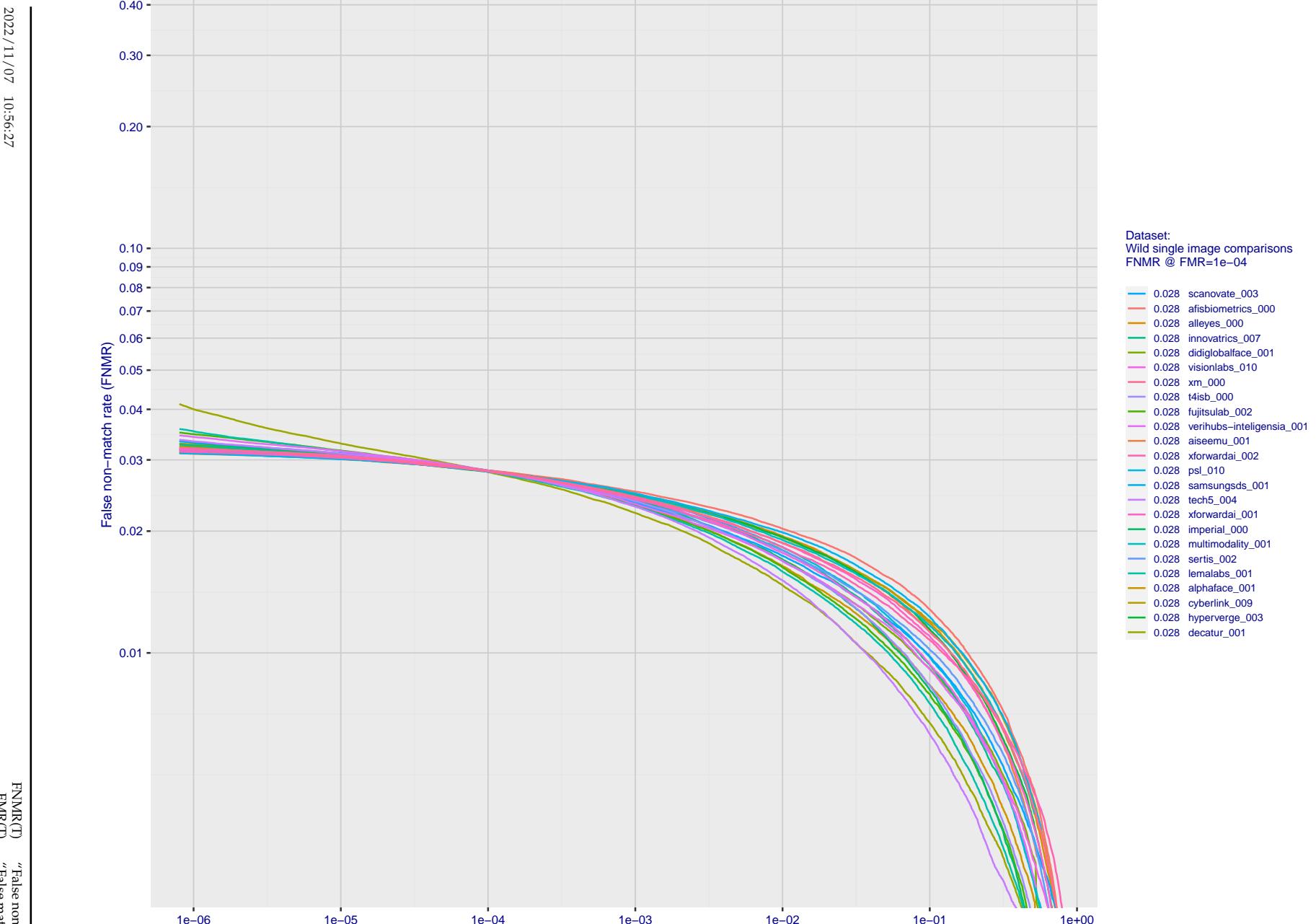


Figure 114: For the 2018 wild image comparisons, detection error tradeoff (DET) characteristics showing false non-match rate vs. false match rate plotted parametrically on threshold, T . The scales are logarithmic in order to show several decades of FMR.

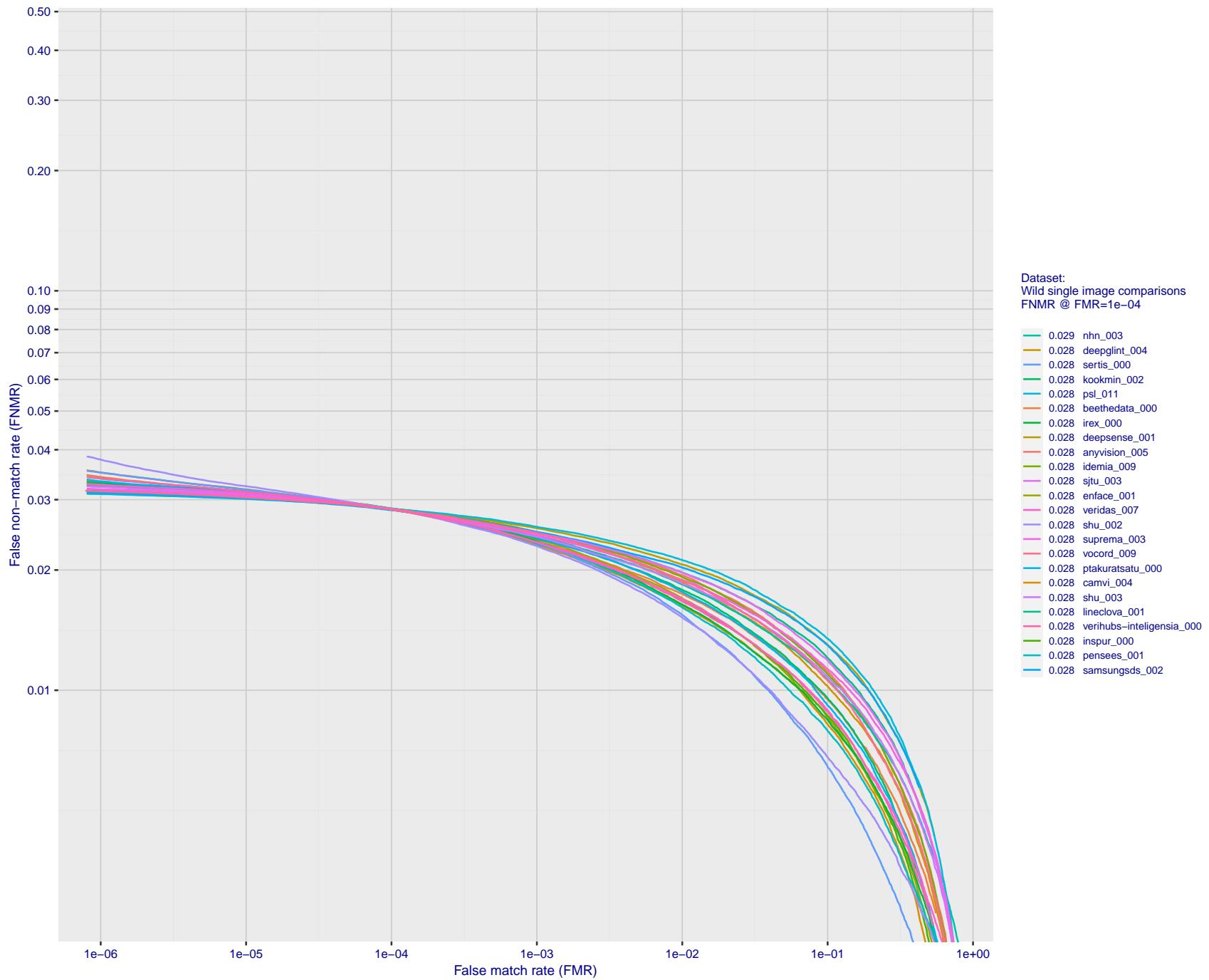


Figure 115: For the 2018 wild image comparisons, detection error tradeoff (DET) characteristics showing false non-match rate vs. false match rate plotted parametrically on threshold, T. The scales are logarithmic in order to show several decades of FMR.

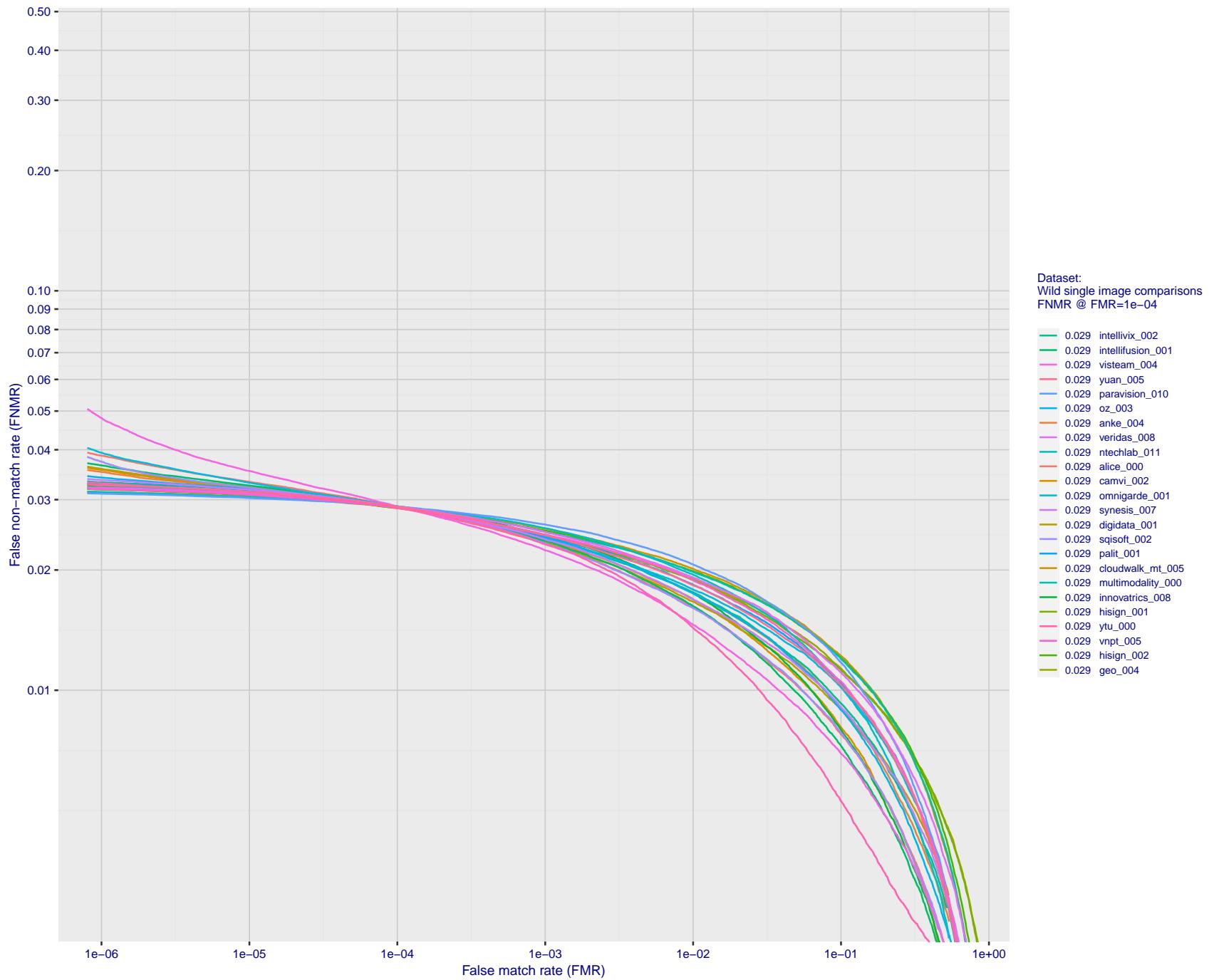


Figure 116: For the 2018 wild image comparisons, detection error tradeoff (DET) characteristics showing false non-match rate vs. false match rate plotted parametrically on threshold, T . The scales are logarithmic in order to show several decades of FMR.

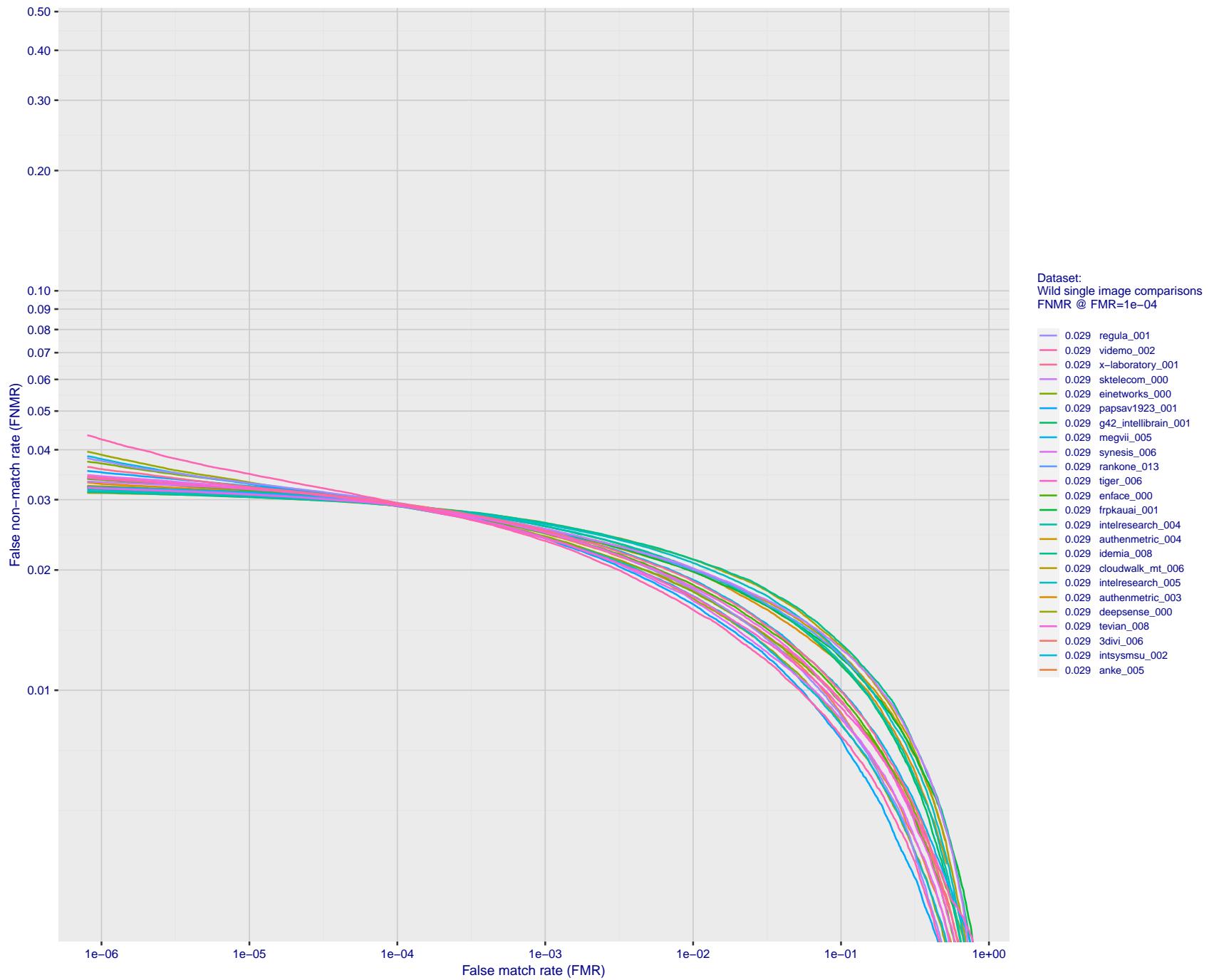


Figure 117: For the 2018 wild image comparisons, detection error tradeoff (DET) characteristics showing false non-match rate vs. false match rate plotted parametrically on threshold, T. The scales are logarithmic in order to show several decades of FMR.

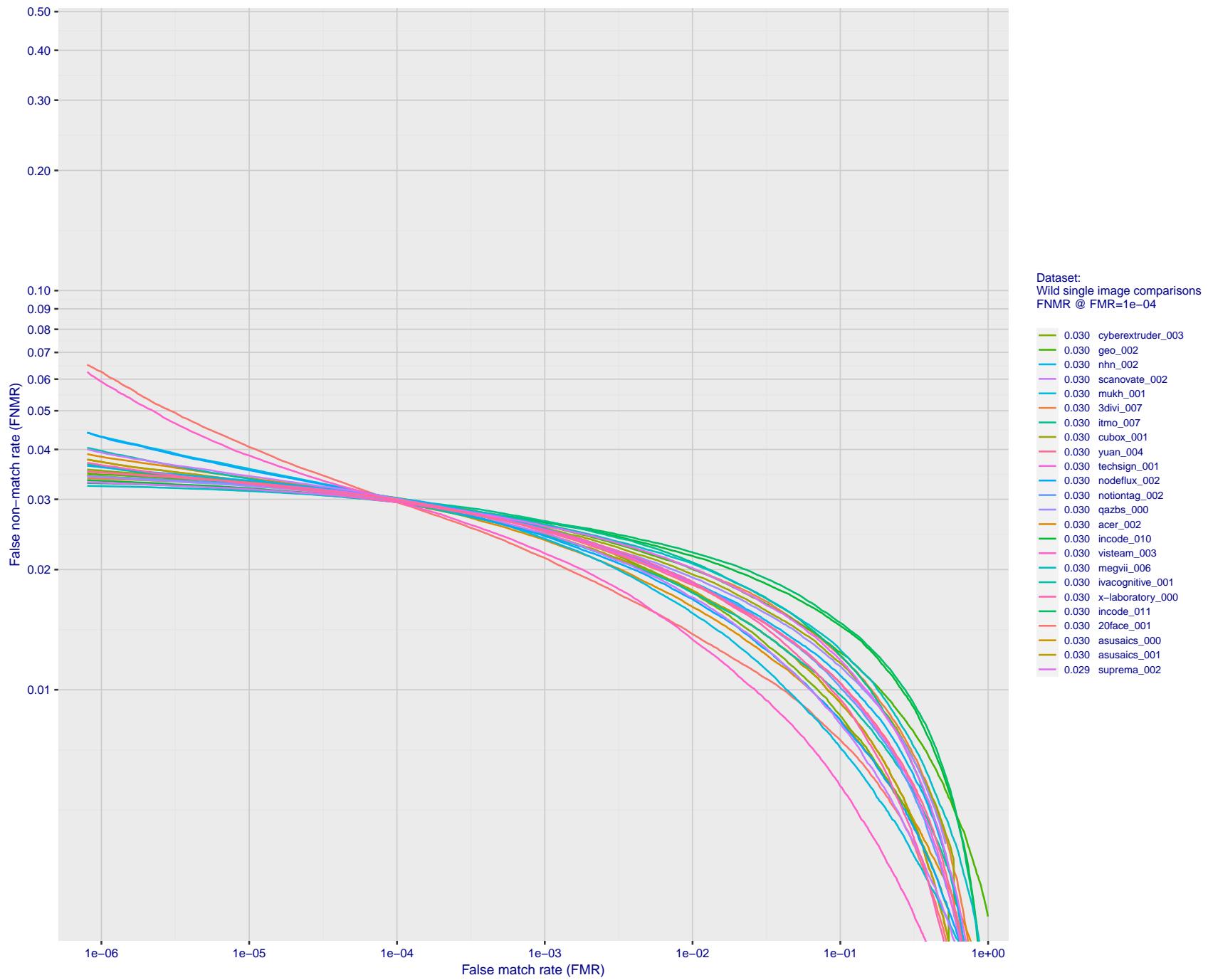


Figure 118: For the 2018 wild image comparisons, detection error tradeoff (DET) characteristics showing false non-match rate vs. false match rate plotted parametrically on threshold, T . The scales are logarithmic in order to show several decades of FMR.

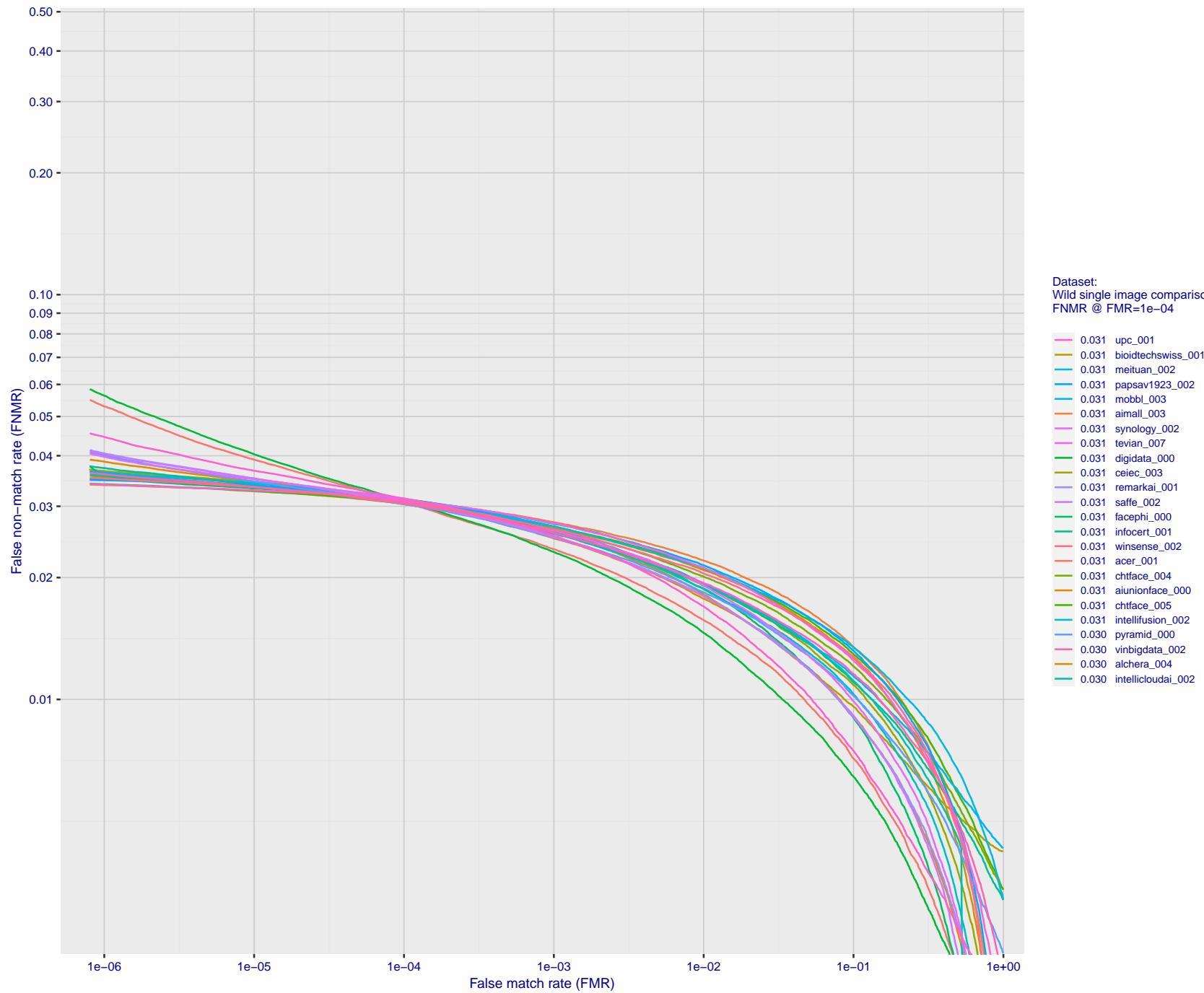


Figure 119: For the 2018 wild image comparisons, detection error tradeoff (DET) characteristics showing false non-match rate vs. false match rate plotted parametrically on threshold, T. The scales are logarithmic in order to show several decades of FMR.

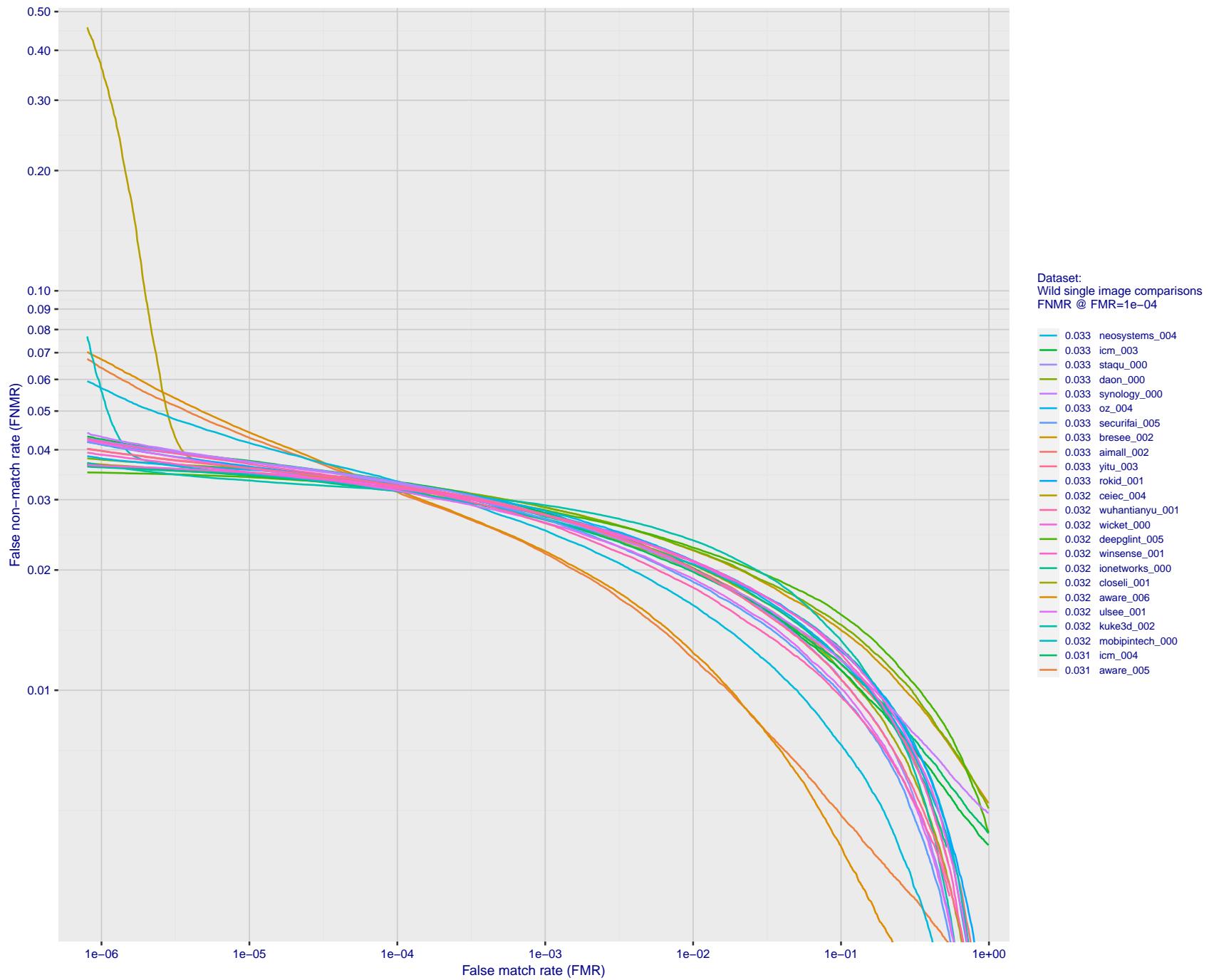


Figure 120: For the 2018 wild image comparisons, detection error tradeoff (DET) characteristics showing false non-match rate vs. false match rate plotted parametrically on threshold, T . The scales are logarithmic in order to show several decades of FMR.

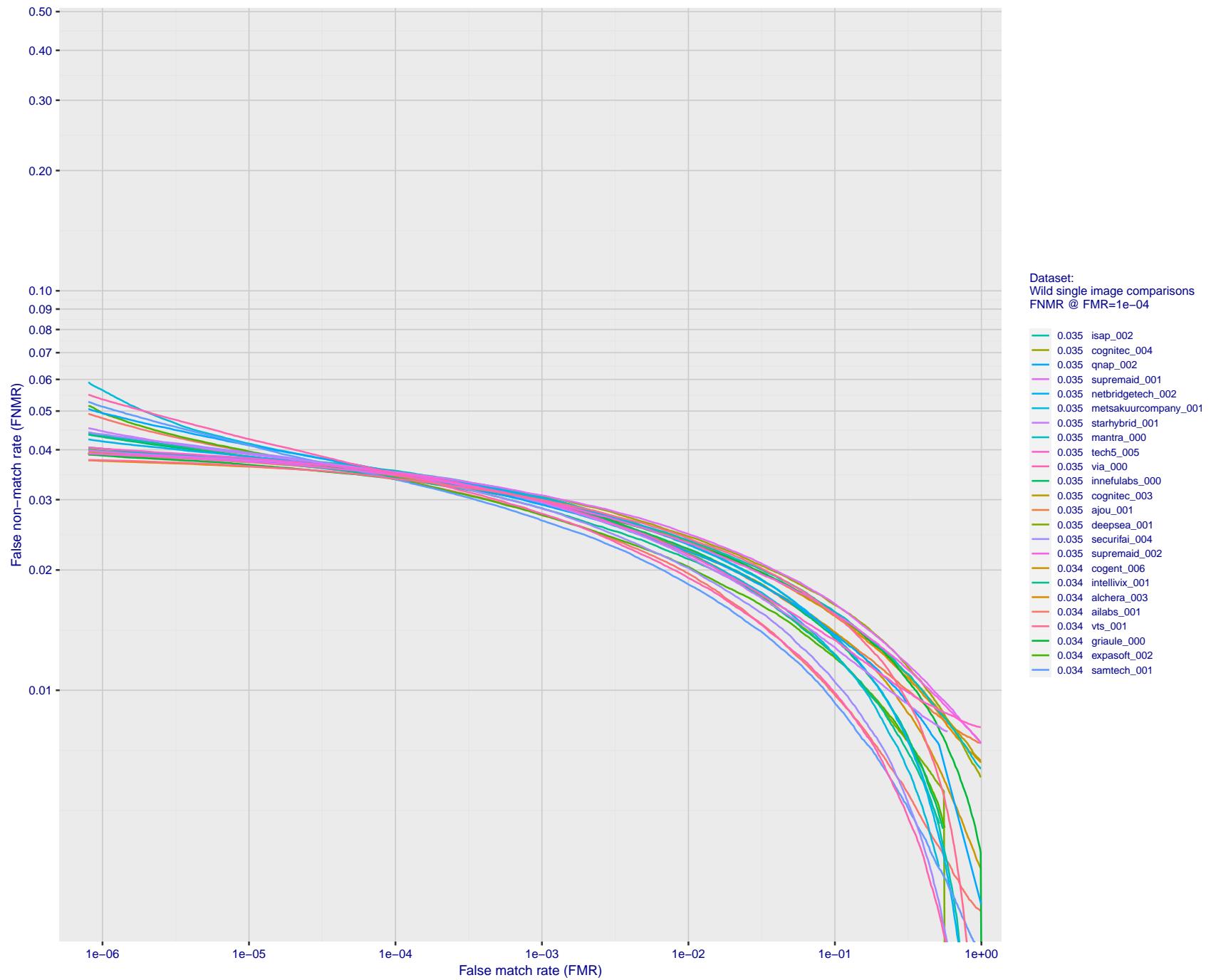


Figure 121: For the 2018 wild image comparisons, detection error tradeoff (DET) characteristics showing false non-match rate vs. false match rate plotted parametrically on threshold, T . The scales are logarithmic in order to show several decades of FMR.

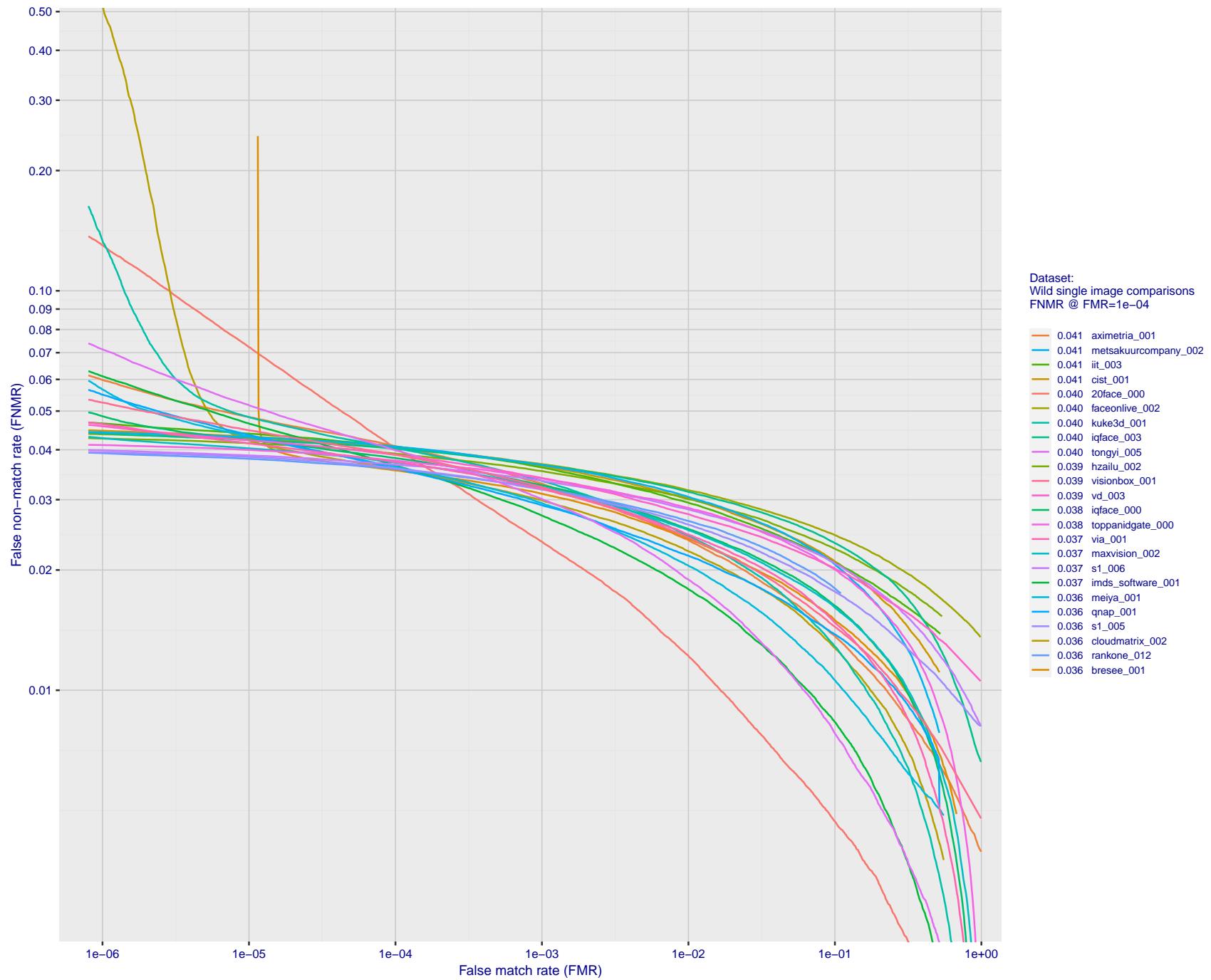


Figure 122: For the 2018 wild image comparisons, detection error tradeoff (DET) characteristics showing false non-match rate vs. false match rate plotted parametrically on threshold, T. The scales are logarithmic in order to show several decades of FMR.

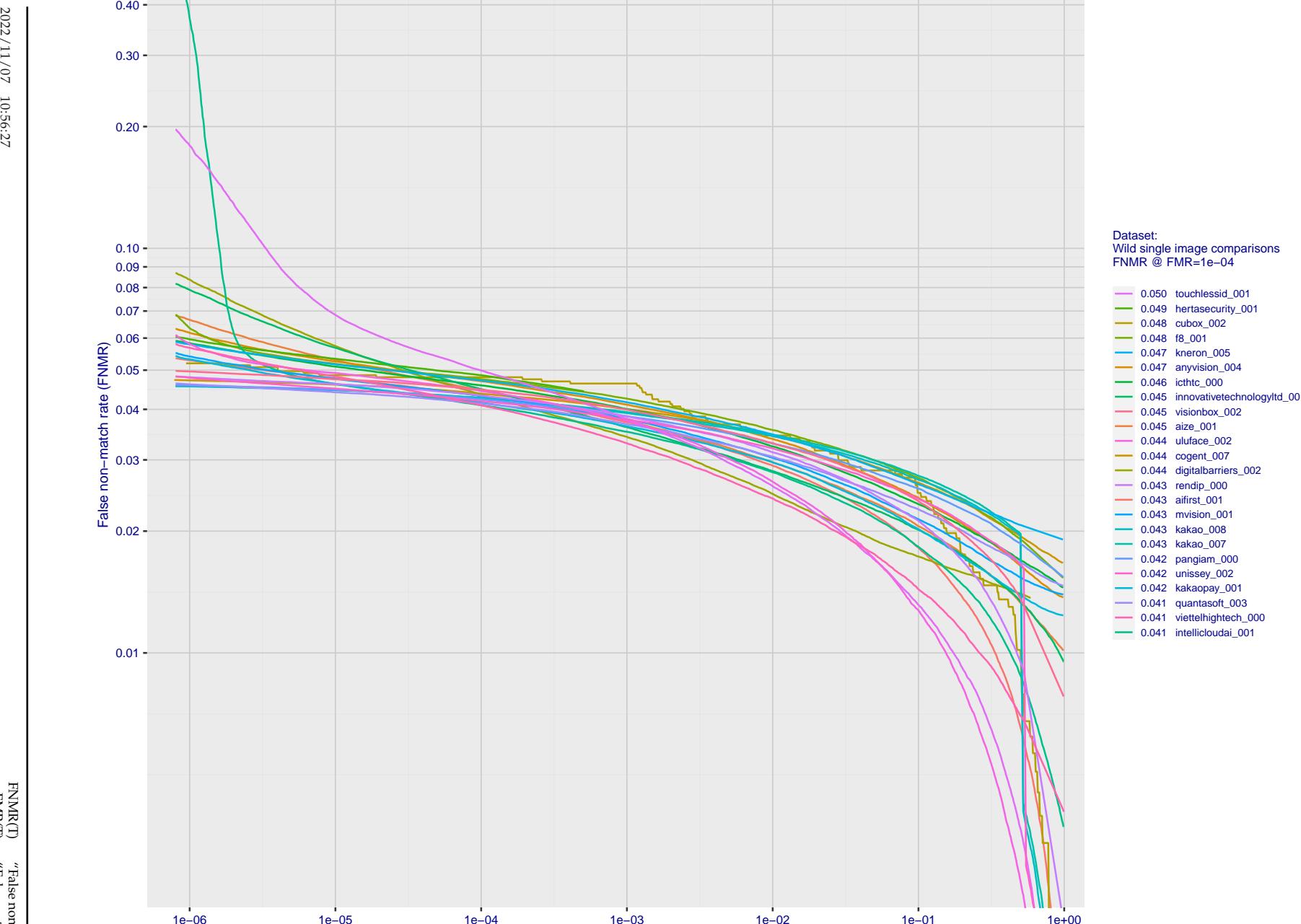


Figure 123: For the 2018 wild image comparisons, detection error tradeoff (DET) characteristics showing false non-match rate vs. false match rate plotted parametrically on threshold, T . The scales are logarithmic in order to show several decades of FMR.

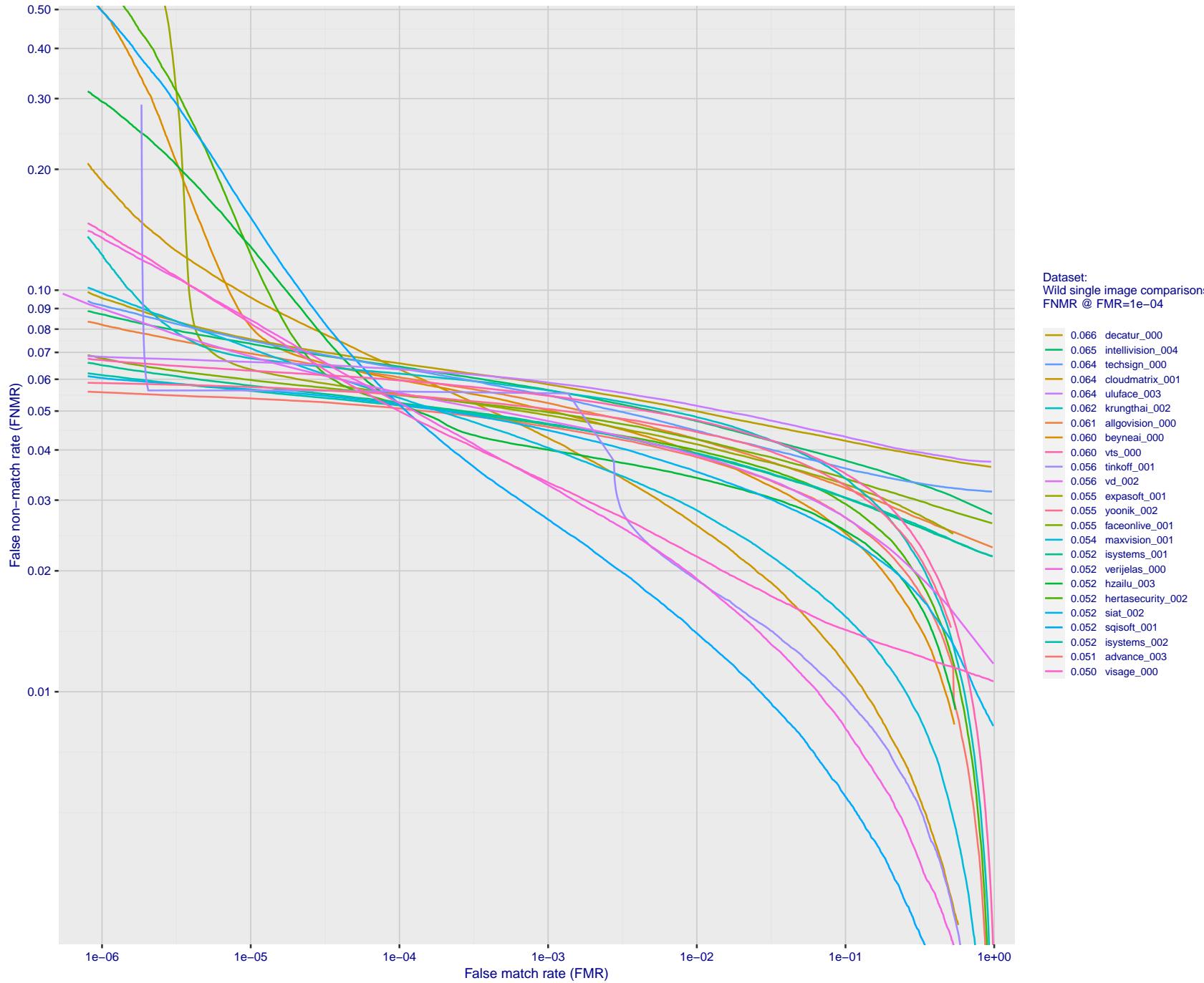


Figure 124: For the 2018 wild image comparisons, detection error tradeoff (DET) characteristics showing false non-match rate vs. false match rate plotted parametrically on threshold, T . The scales are logarithmic in order to show several decades of FMR.

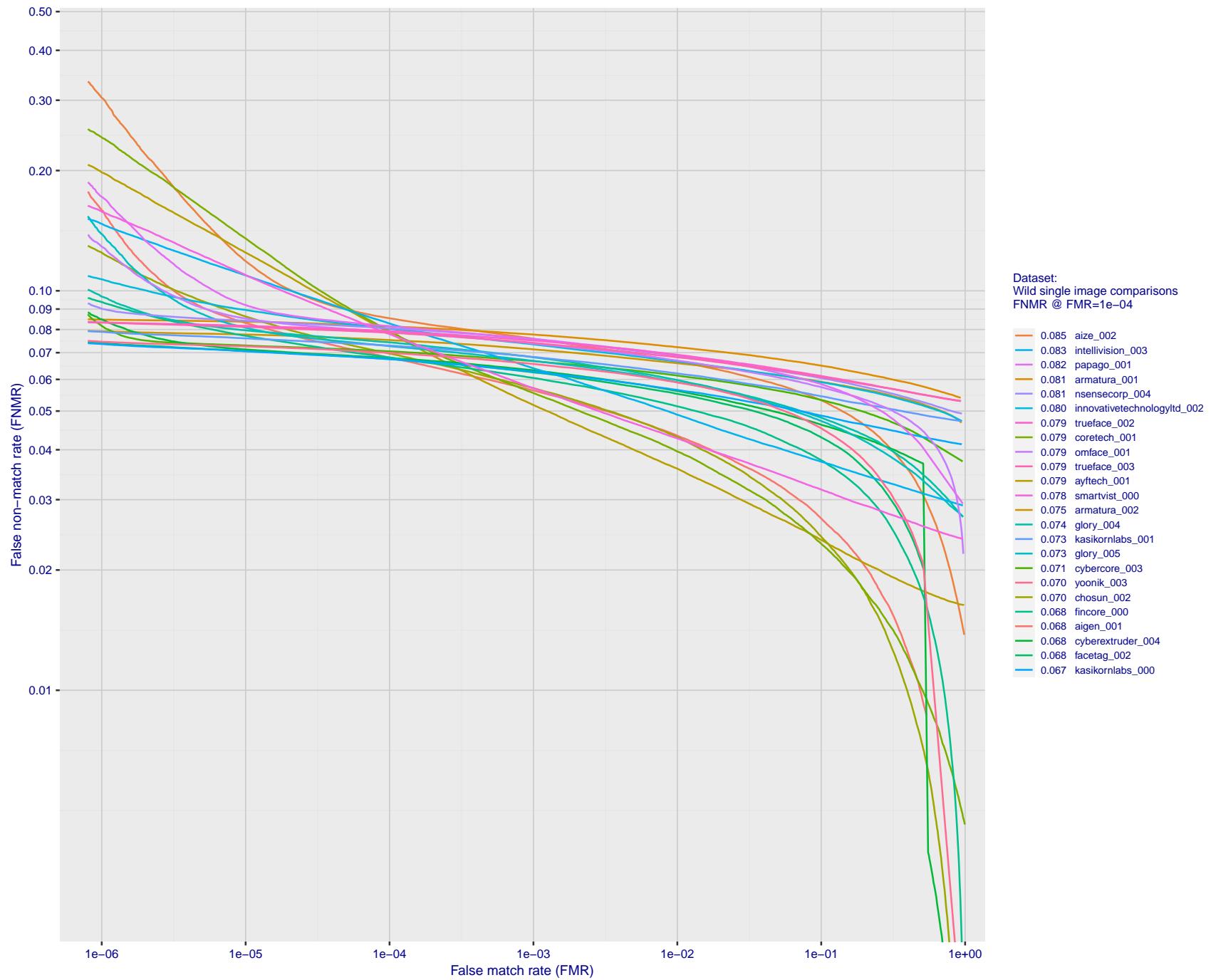


Figure 125: For the 2018 wild image comparisons, detection error tradeoff (DET) characteristics showing false non-match rate vs. false match rate plotted parametrically on threshold, T . The scales are logarithmic in order to show several decades of FMR.

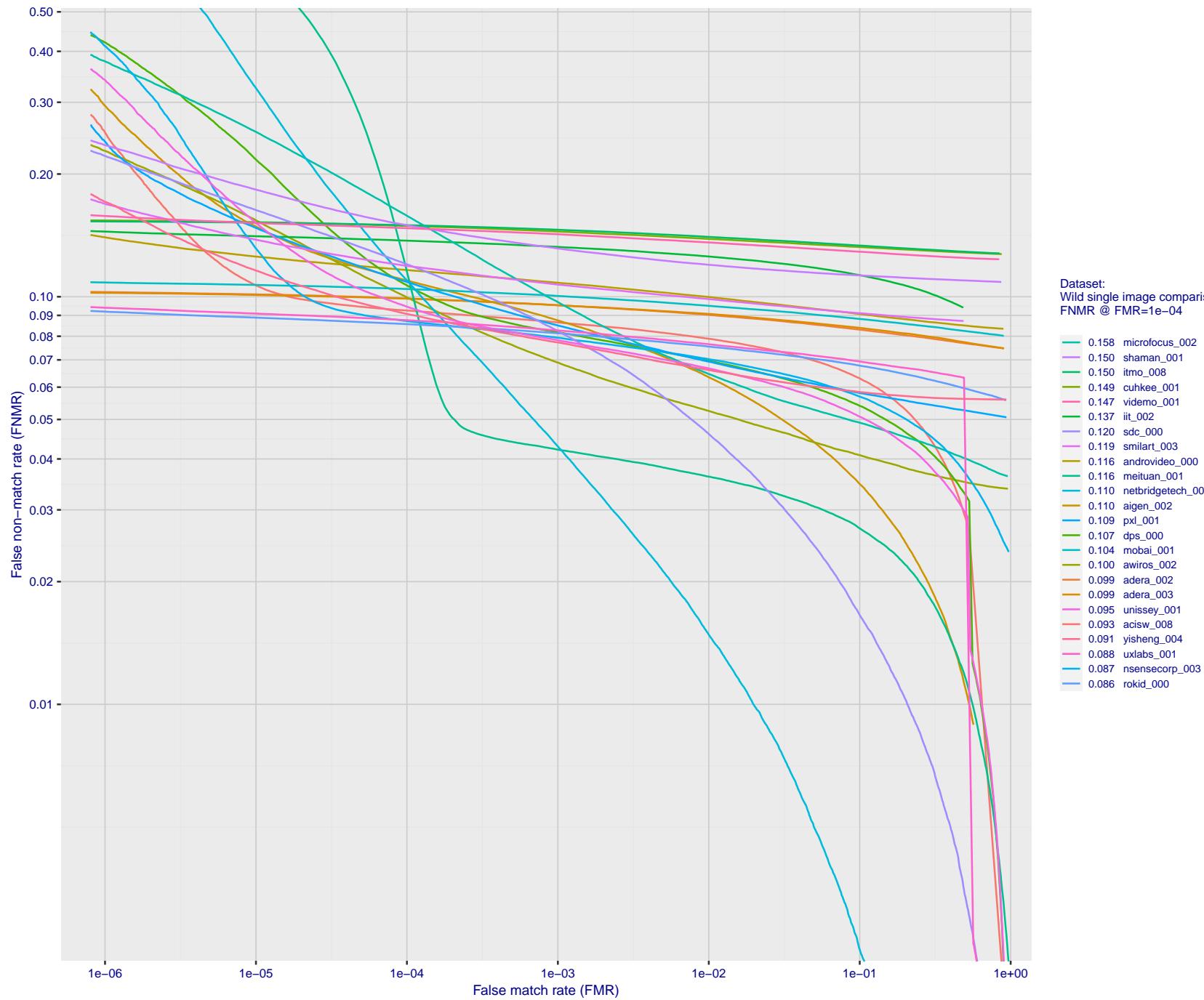


Figure 126: For the 2018 wild image comparisons, detection error tradeoff (DET) characteristics showing false non-match rate vs. false match rate plotted parametrically on threshold, T. The scales are logarithmic in order to show several decades of FMR.

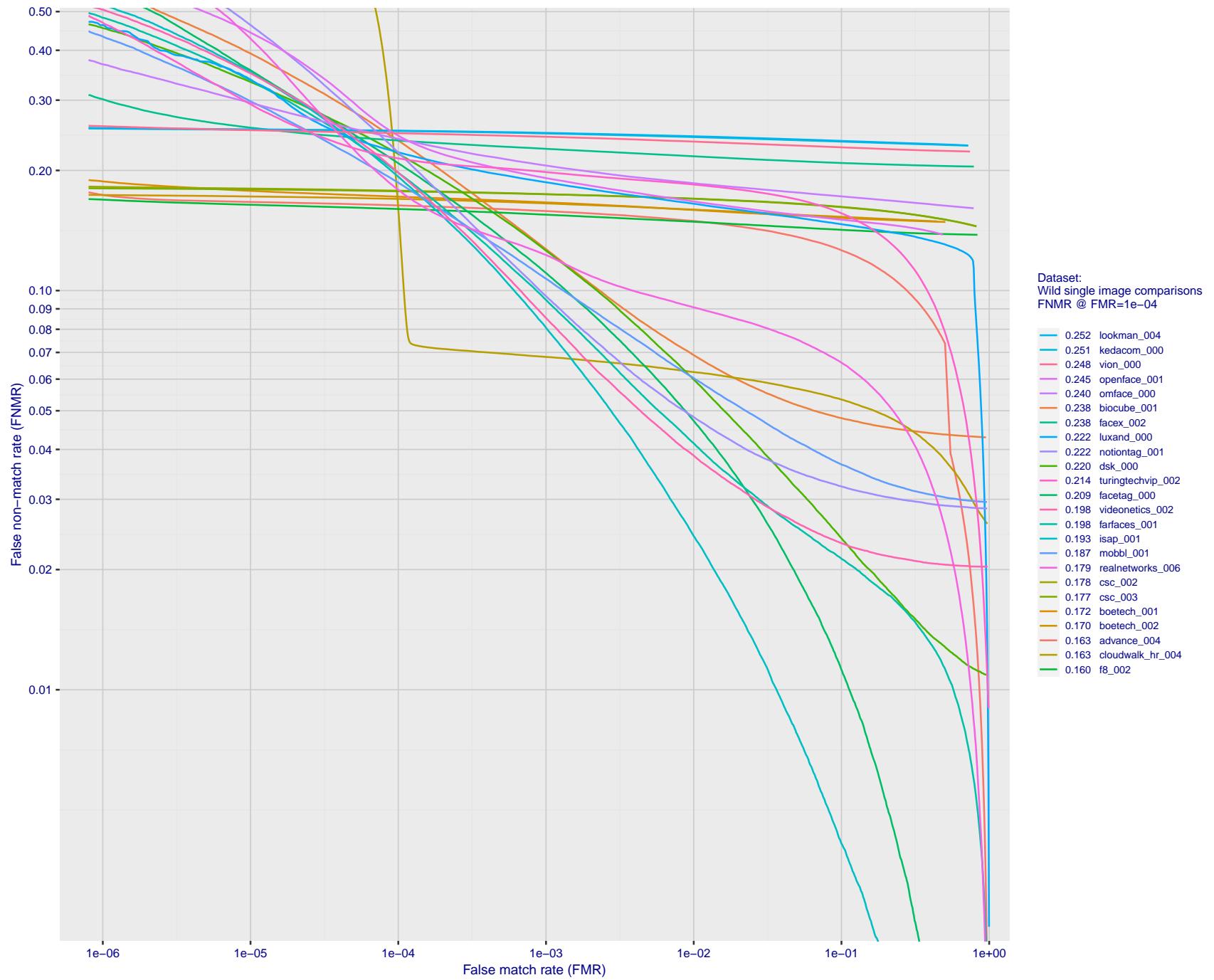


Figure 127: For the 2018 wild image comparisons, detection error tradeoff (DET) characteristics showing false non-match rate vs. false match rate plotted parametrically on threshold, T . The scales are logarithmic in order to show several decades of FMR.

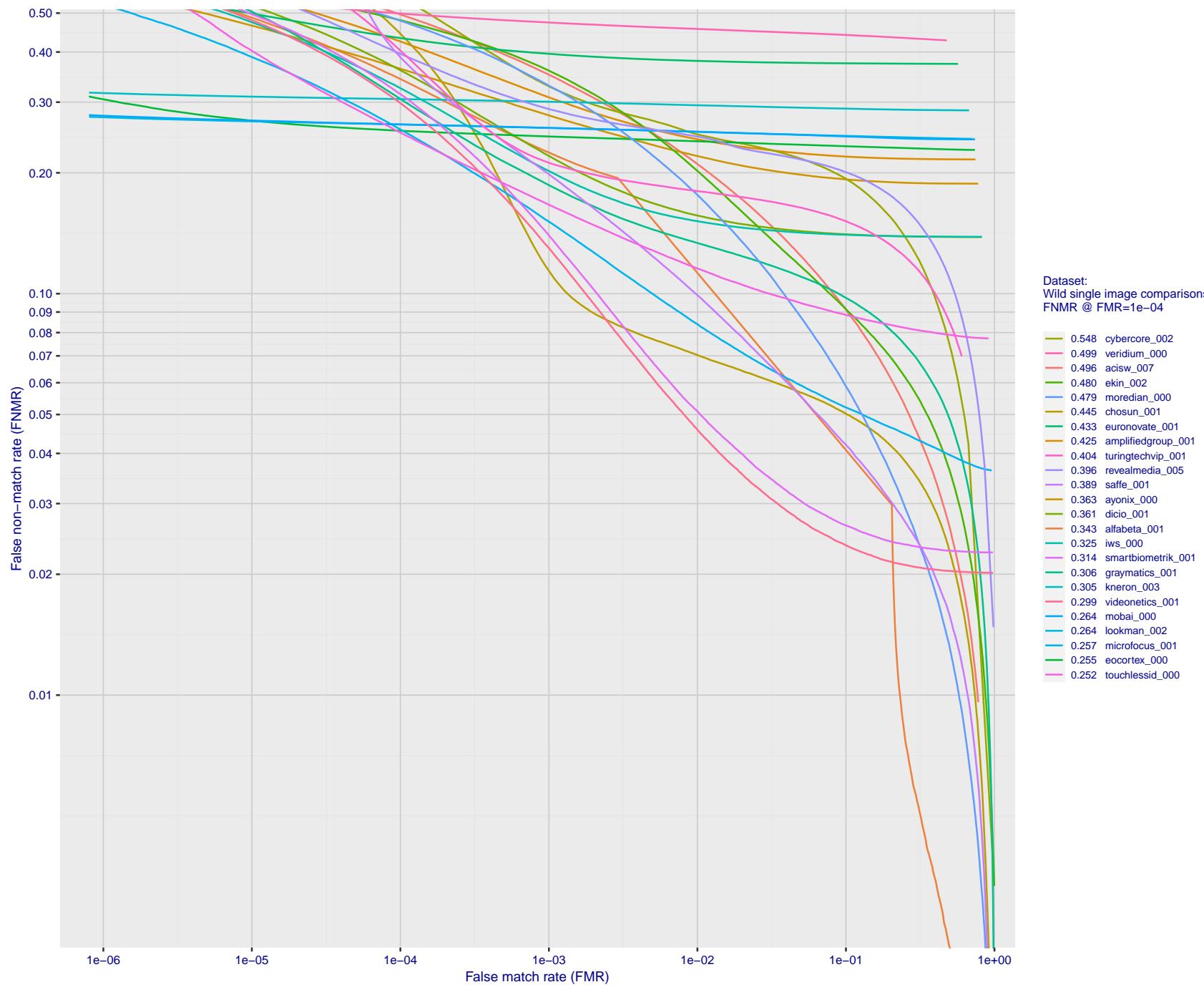


Figure 128: For the 2018 wild image comparisons, detection error tradeoff (DET) characteristics showing false non-match rate vs. false match rate plotted parametrically on threshold, T . The scales are logarithmic in order to show several decades of FMR.

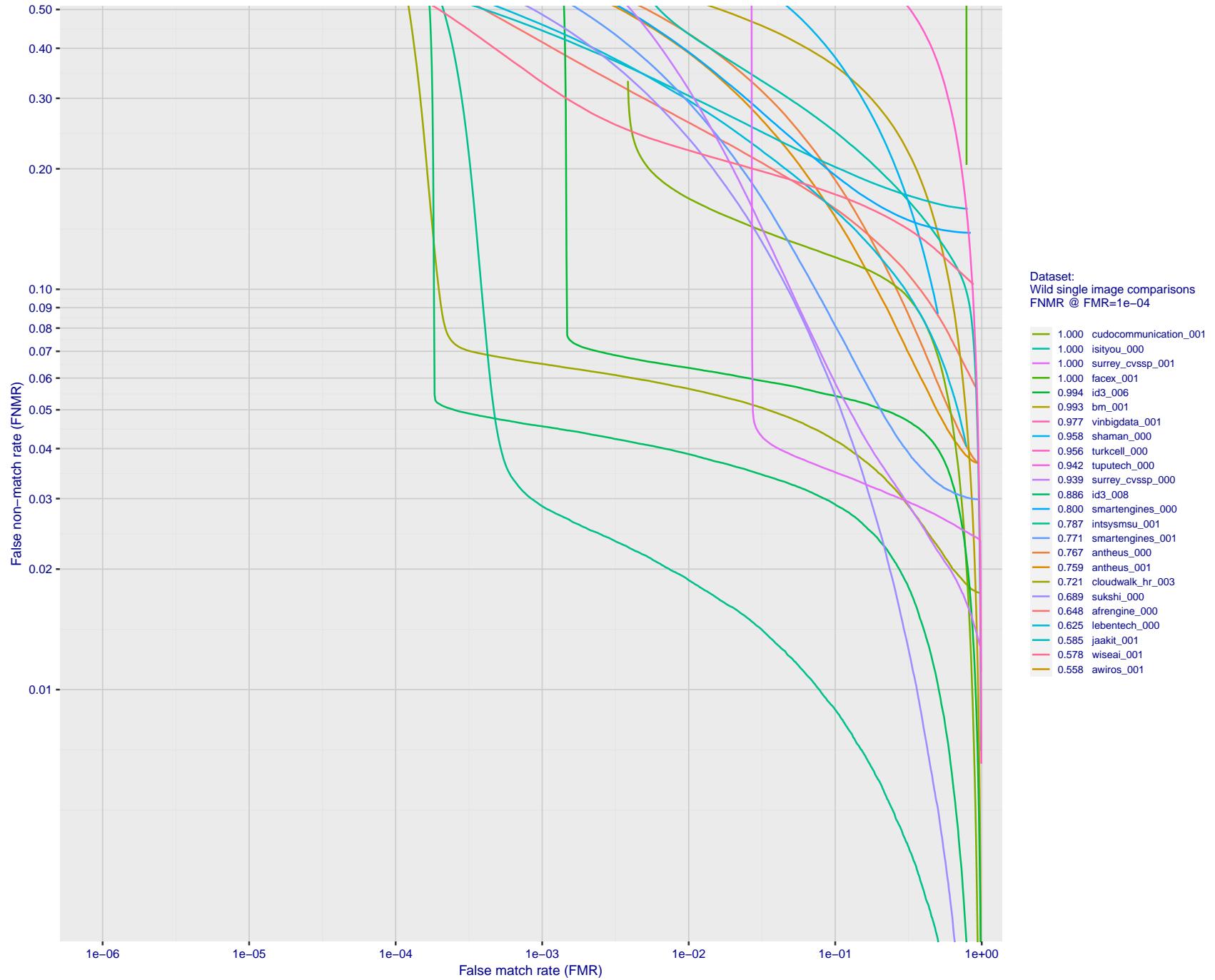


Figure 129: For the 2018 wild image comparisons, detection error tradeoff (DET) characteristics showing false non-match rate vs. false match rate plotted parametrically on threshold, T . The scales are logarithmic in order to show several decades of FMR.

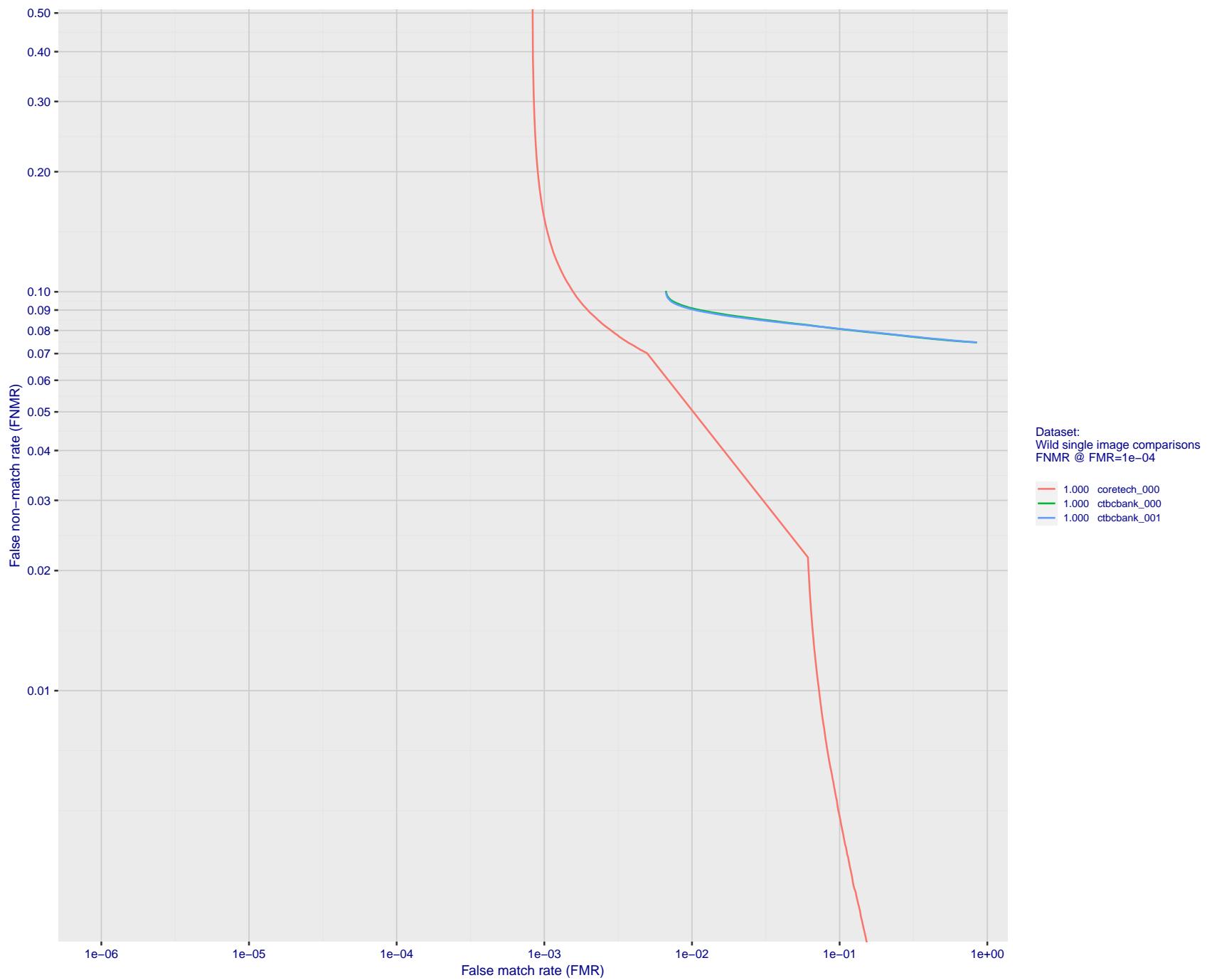


Figure 130: For the 2018 wild image comparisons, detection error tradeoff (DET) characteristics showing false non-match rate vs. false match rate plotted parametrically on threshold, T . The scales are logarithmic in order to show several decades of FMR.



Figure 131: For the mugshot images, FMR for same-sex impostor pairs of images annotated with codes for black female, black male, white female, white male. The threshold is set for each algorithm to give $FMR = 0.001$ for white males which is the demographic that usually gives the lowest FMR. This means the top right box is the same color in all panels. The panels are sorted over multiple pages in order of FMR on black females, which is the demographic that usually gives the highest FMR.

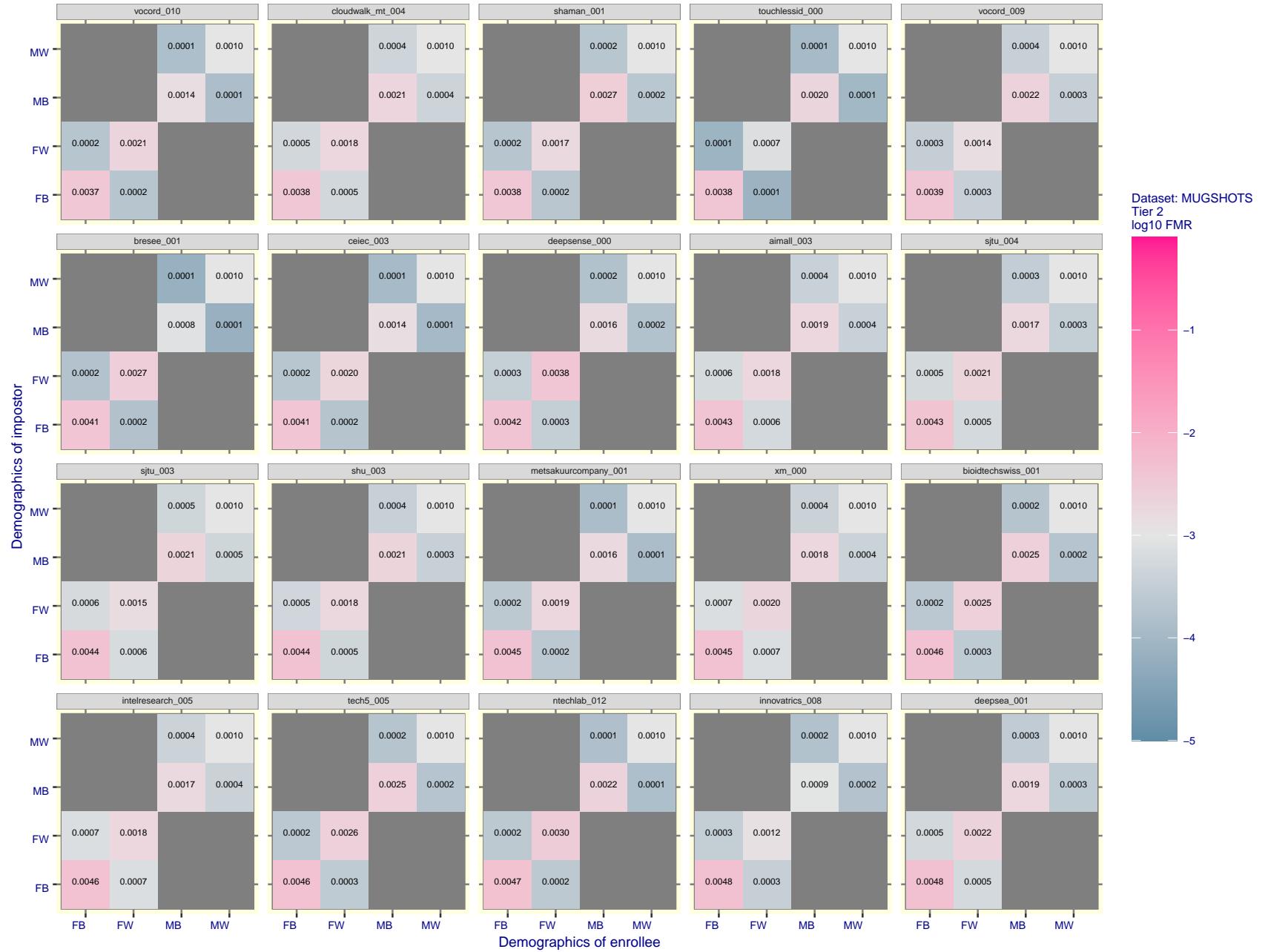


Figure 132: For the mugshot images, FMR for same-sex impostor pairs of images annotated with codes for black female, black male, white female, white male. The threshold is set for each algorithm to give $\text{FMR} = 0.001$ for white males which is the demographic that usually gives the lowest FMR. This means the top right box is the same color in all panels. The panels are sorted over multiple pages in order of FMR on black females, which is the demographic that usually gives the highest FMR.

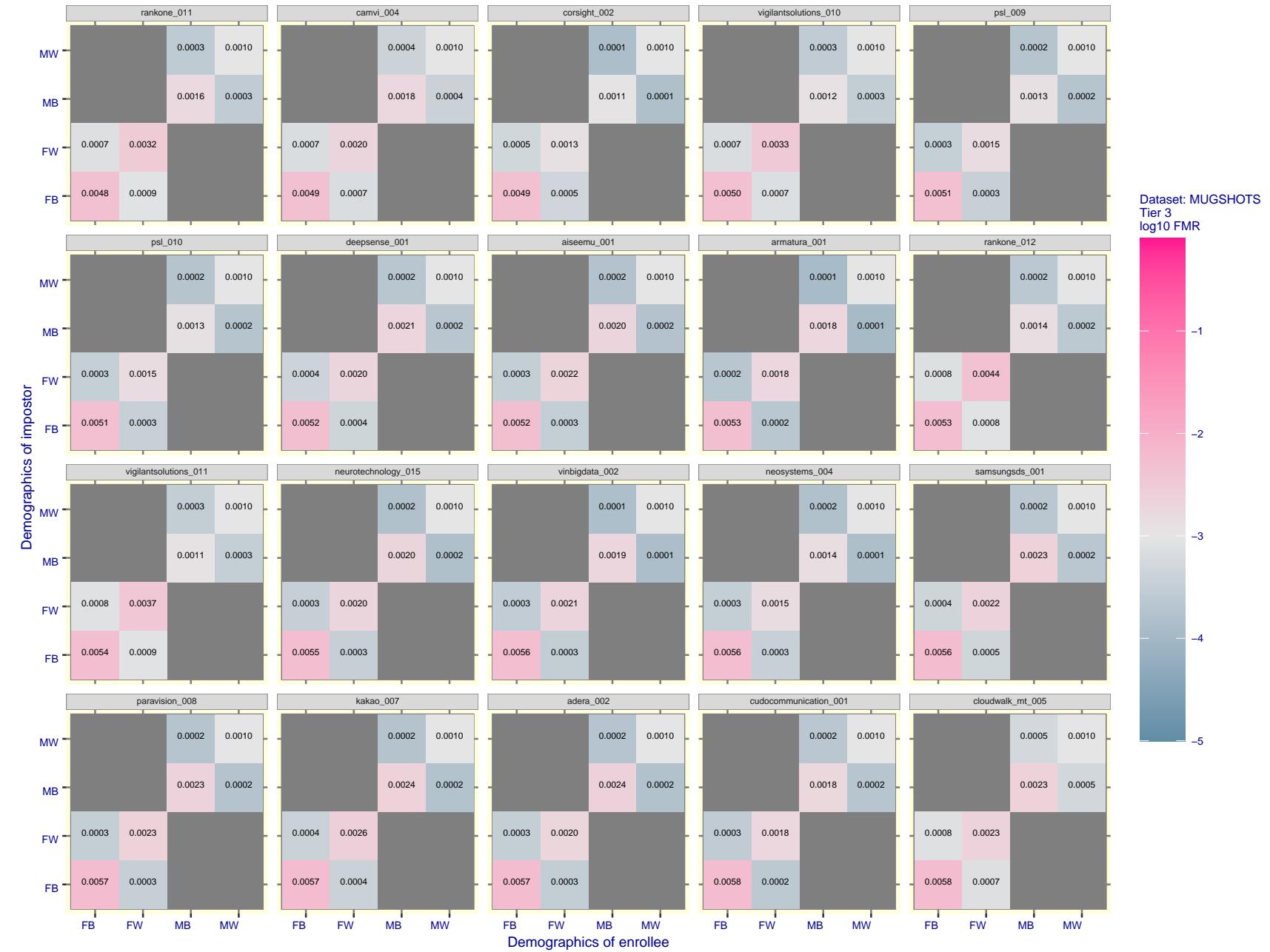


Figure 133: For the mugshot images, FMR for same-sex impostor pairs of images annotated with codes for black female, black male, white female, white male. The threshold is set for each algorithm to give $FMR = 0.001$ for white males which is the demographic that usually gives the lowest FMR. This means the top right box is the same color in all panels. The panels are sorted over multiple pages in order of FMR on black females, which is the demographic that usually gives the highest FMR.

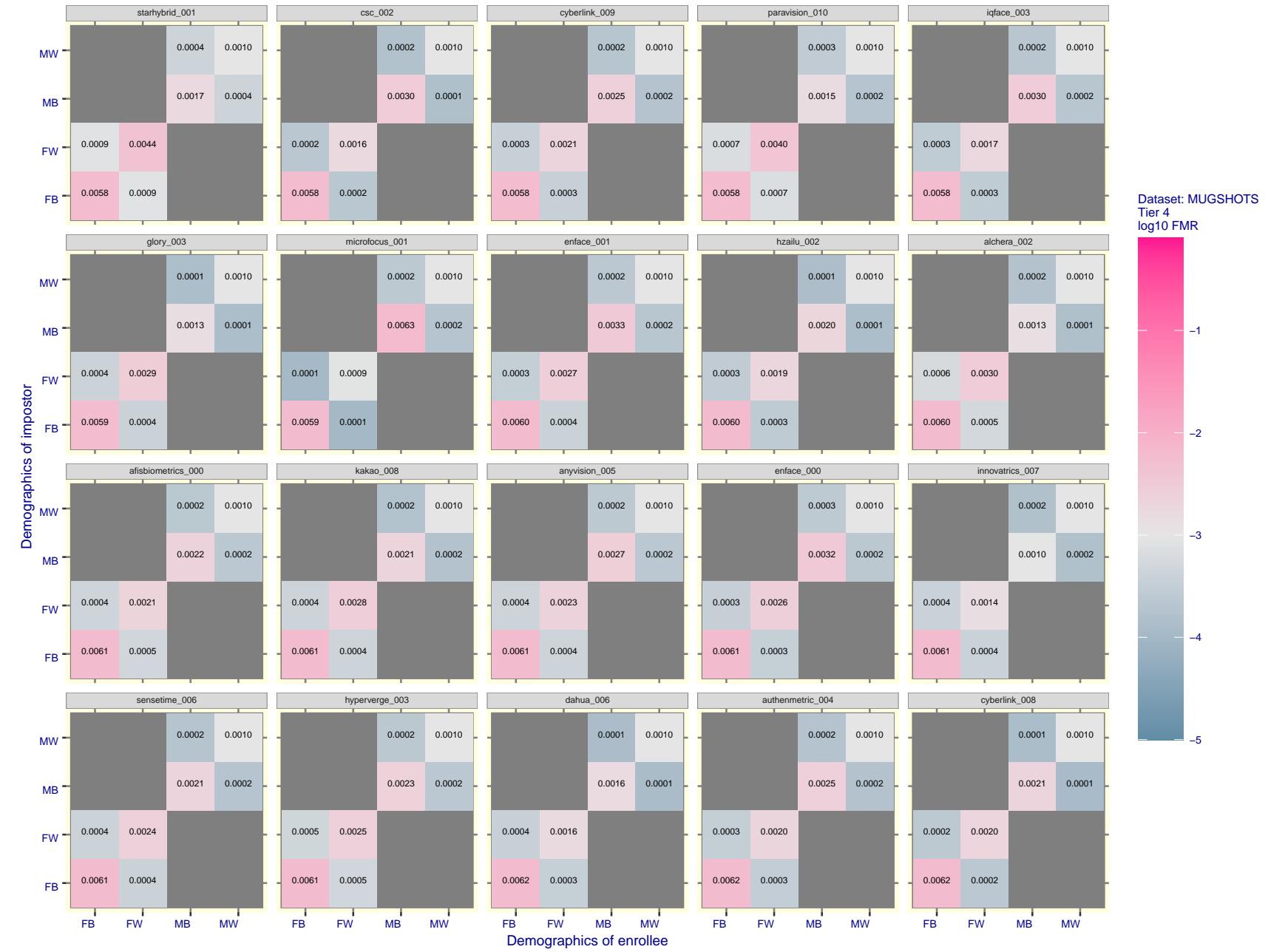


Figure 134: For the mugshot images, FMR for same-sex impostor pairs of images annotated with codes for black female, black male, white female, white male. The threshold is set for each algorithm to give FMR = 0.001 for white males which is the demographic that usually gives the lowest FMR. This means the top right box is the same color in all panels. The panels are sorted over multiple pages in order of FMR on black females, which is the demographic that usually gives the highest FMR.

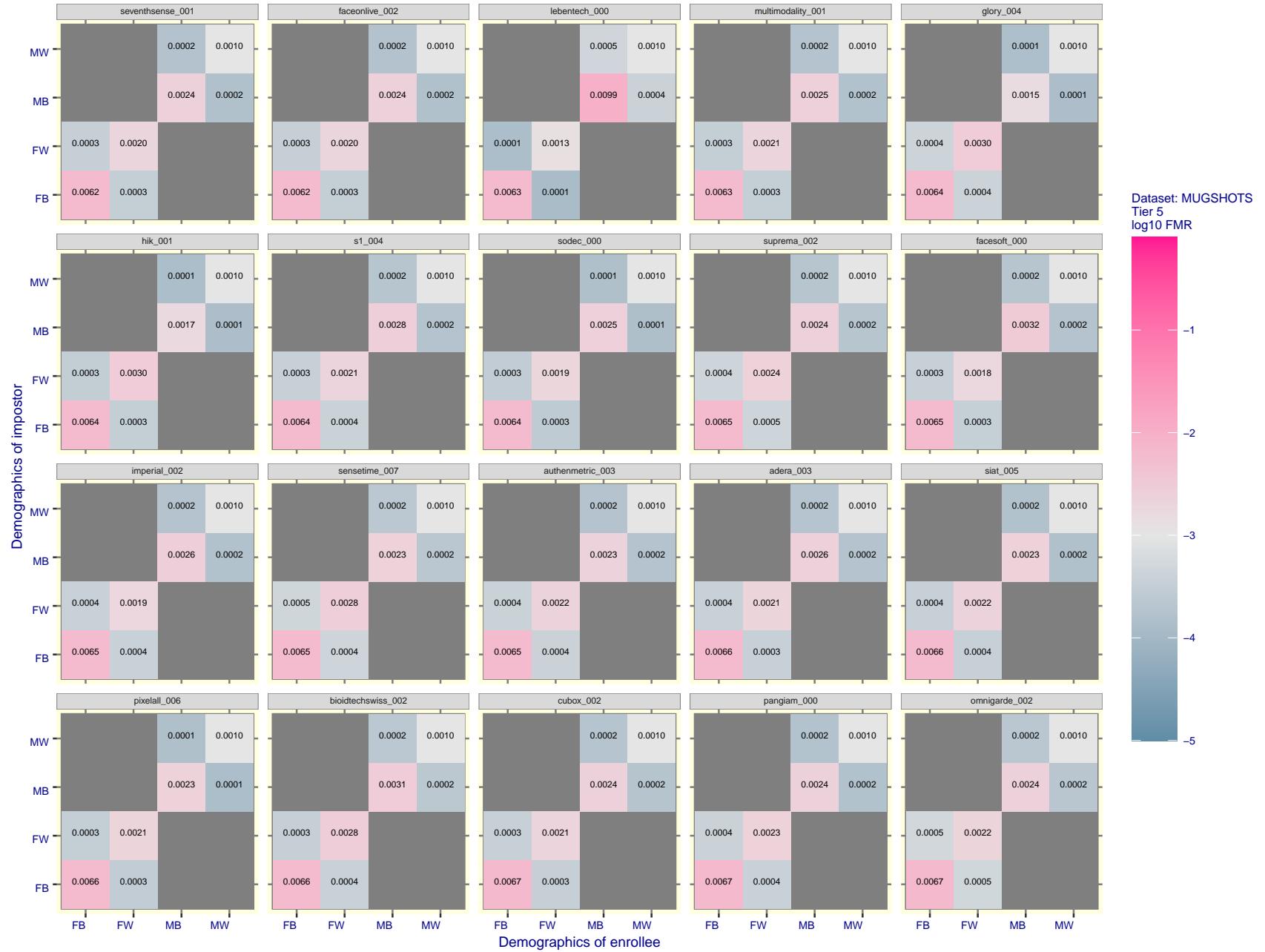


Figure 135: For the mugshot images, FMR for same-sex impostor pairs of images annotated with codes for black female, black male, white female, white male. The threshold is set for each algorithm to give FMR = 0.001 for white males which is the demographic that usually gives the lowest FMR. This means the top right box is the same color in all panels. The panels are sorted over multiple pages in order of FMR on black females, which is the demographic that usually gives the highest FMR.

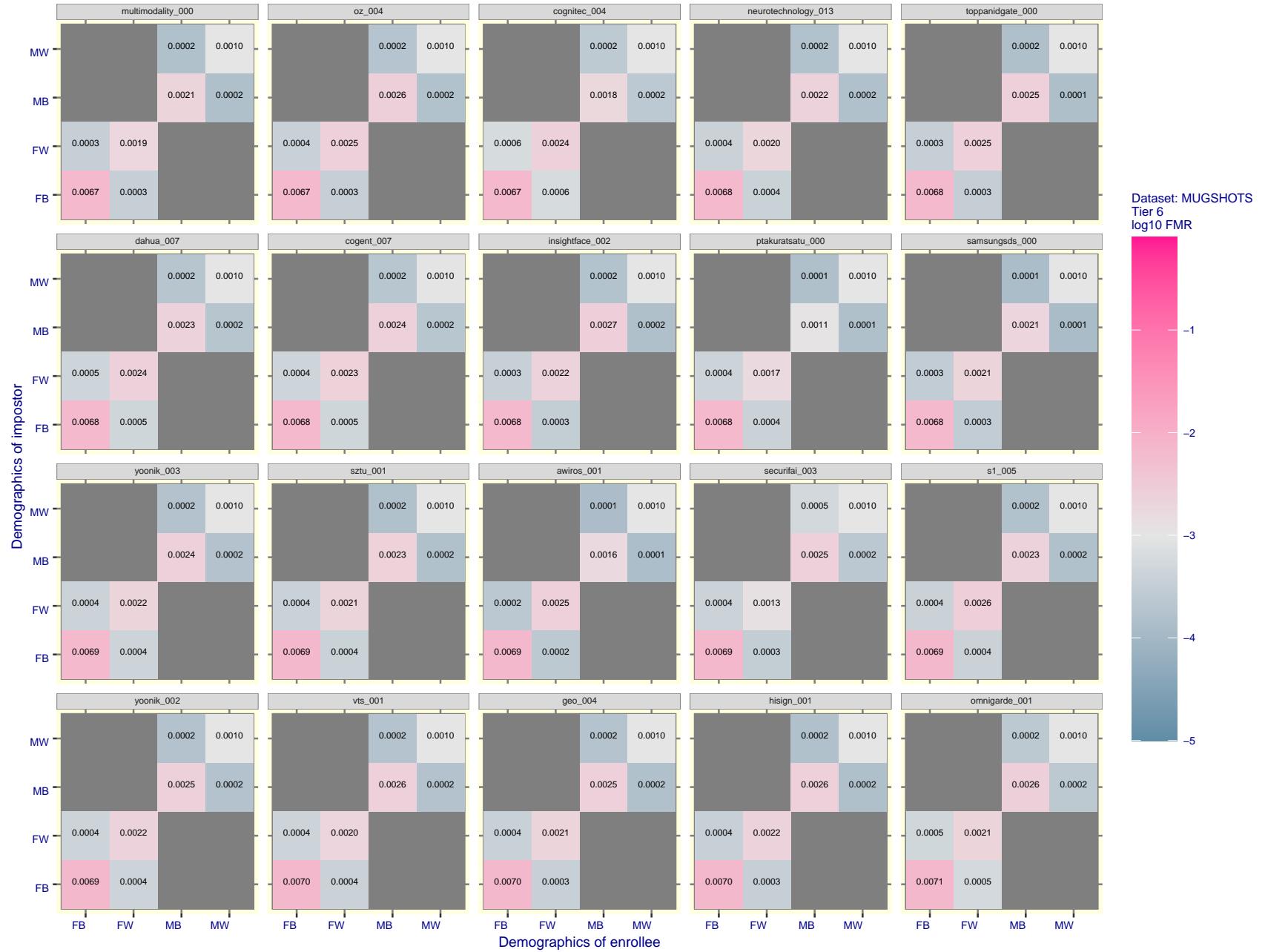


Figure 136: For the mugshot images, FMR for same-sex impostor pairs of images annotated with codes for black female, black male, white female, white male. The threshold is set for each algorithm to give FMR = 0.001 for white males which is the demographic that usually gives the lowest FMR. This means the top right box is the same color in all panels. The panels are sorted over multiple pages in order of FMR on black females, which is the demographic that usually gives the highest FMR.

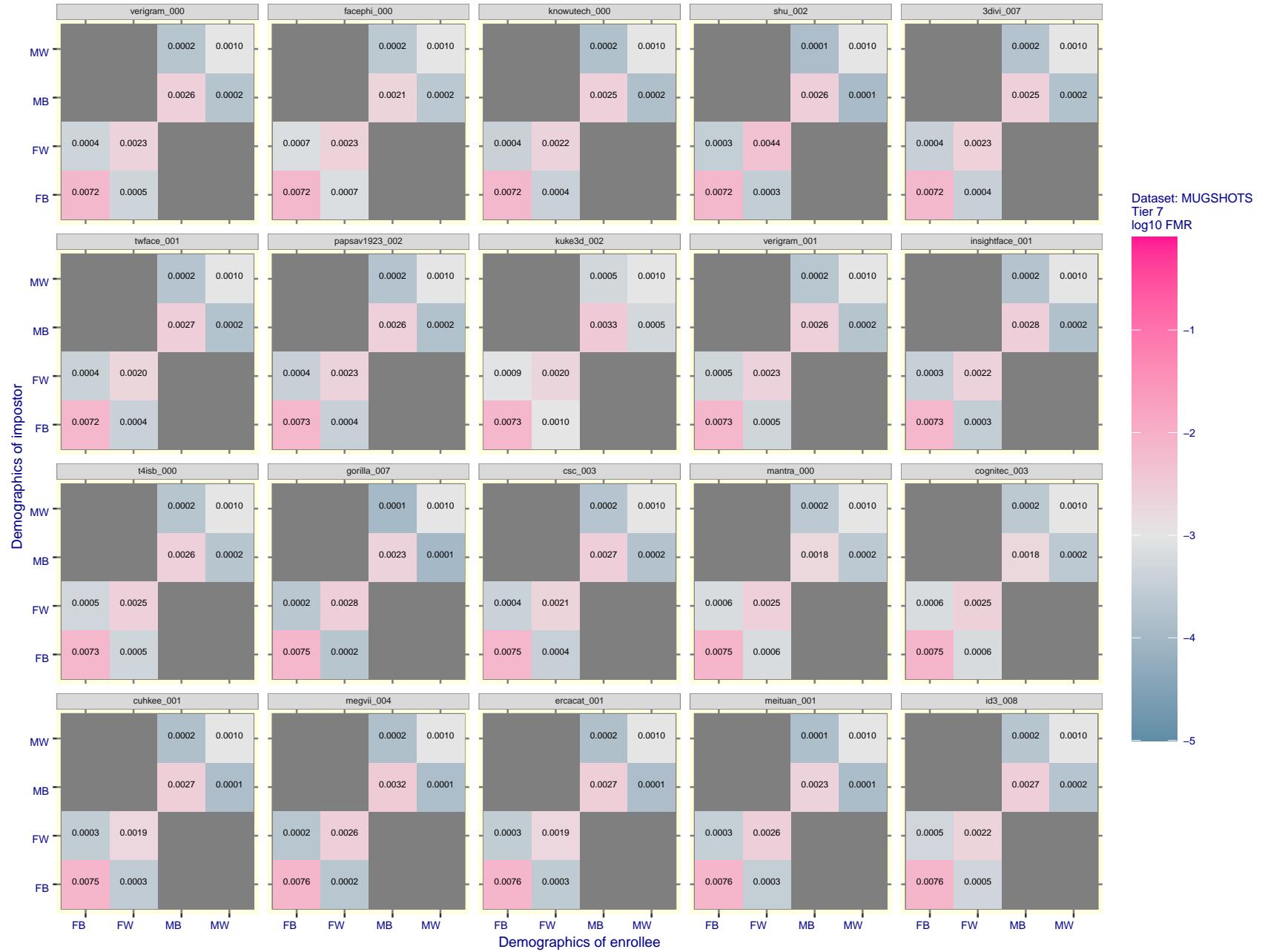


Figure 137: For the mugshot images, FMR for same-sex impostor pairs of images annotated with codes for black female, black male, white female, white male. The threshold is set for each algorithm to give FMR = 0.001 for white males which is the demographic that usually gives the lowest FMR. This means the top right box is the same color in all panels. The panels are sorted over multiple pages in order of FMR on black females, which is the demographic that usually gives the highest FMR.

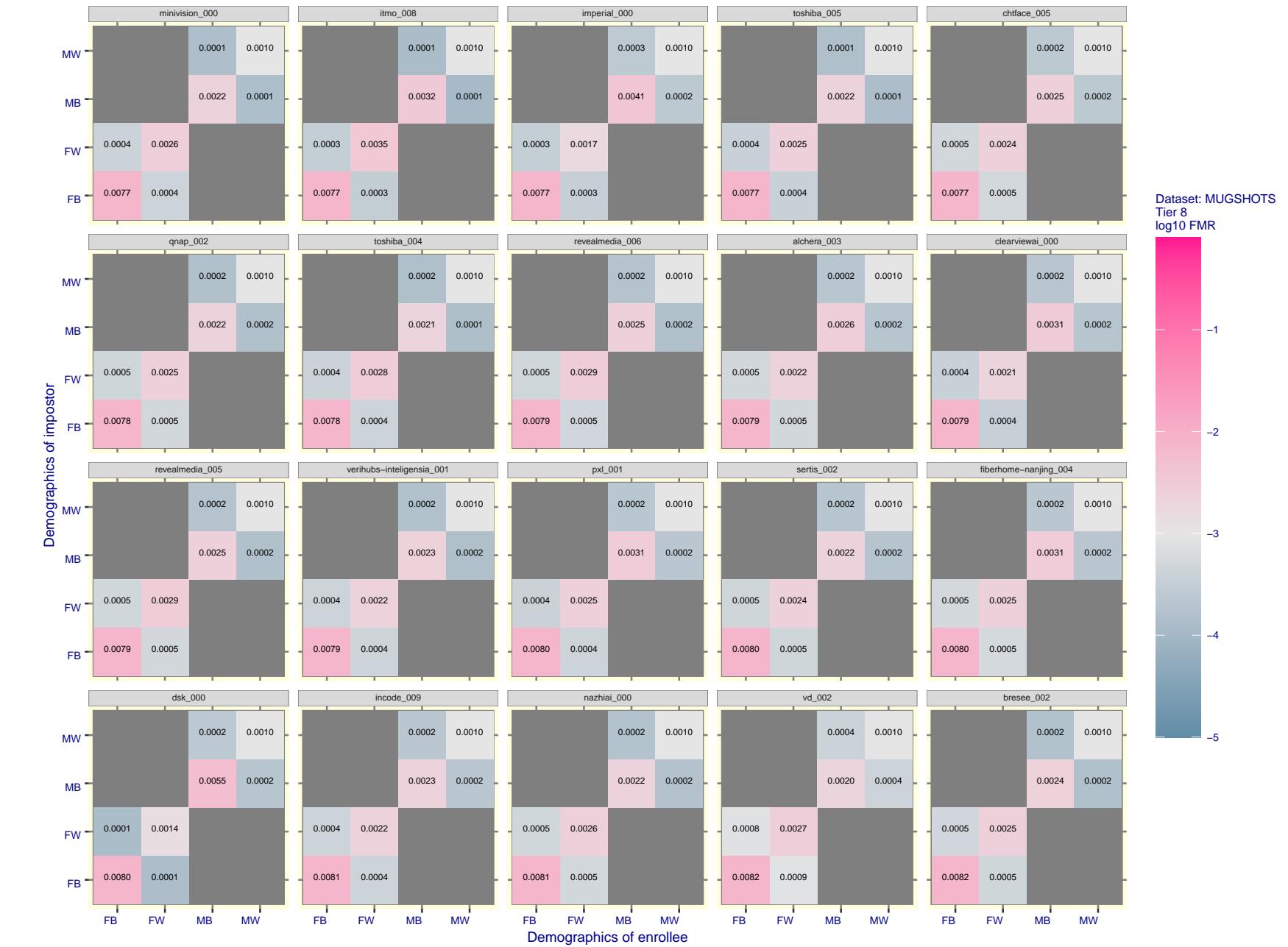


Figure 138: For the mugshot images, FMR for same-sex impostor pairs of images annotated with codes for black female, black male, white female, white male. The threshold is set for each algorithm to give $FMR = 0.001$ for white males which is the demographic that usually gives the lowest FMR. This means the top right box is the same color in all panels. The panels are sorted over multiple pages in order of FMR on black females, which is the demographic that usually gives the highest FMR.

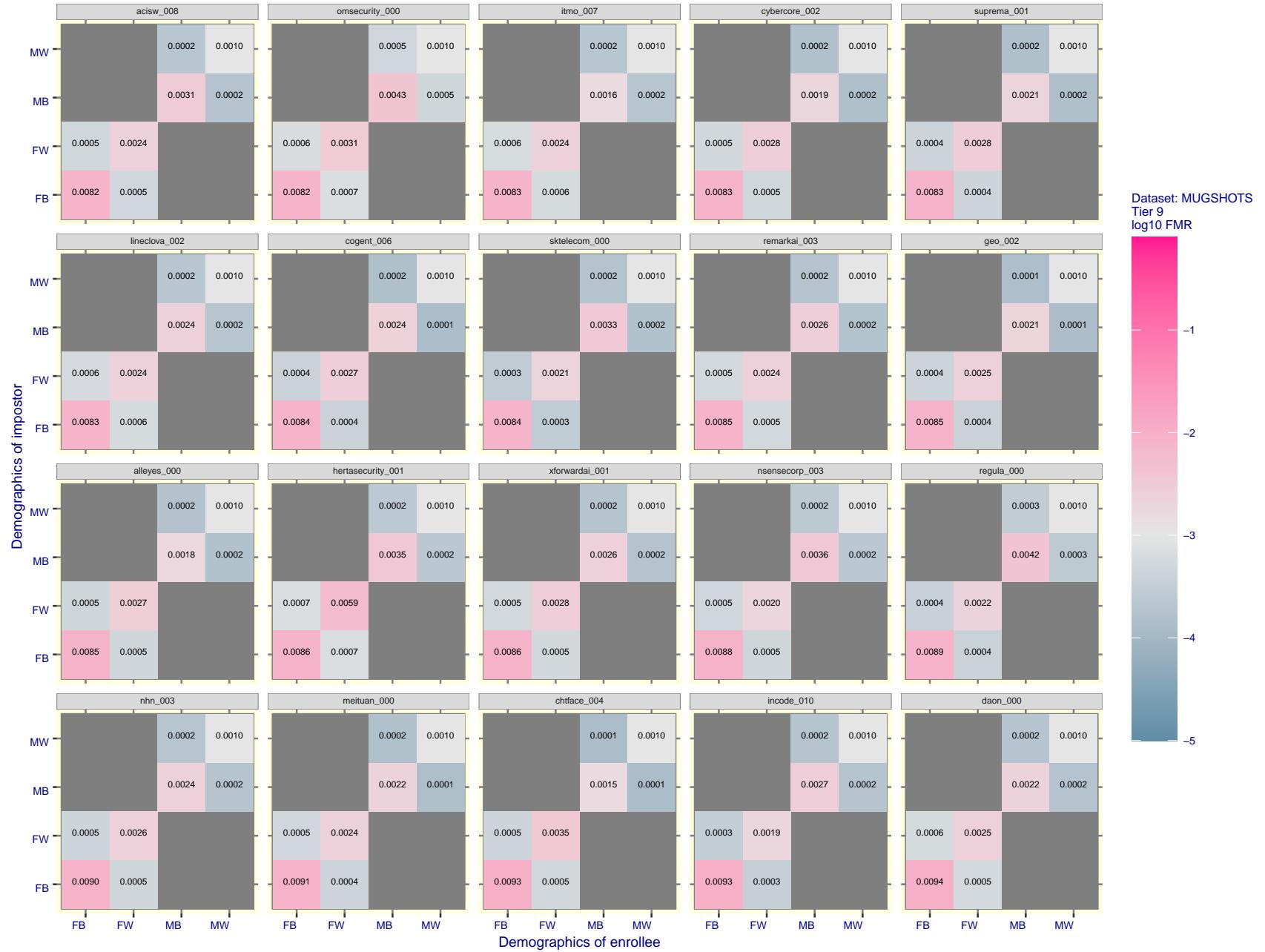


Figure 139: For the mugshot images, FMR for same-sex impostor pairs of images annotated with codes for black female, black male, white female, white male. The threshold is set for each algorithm to give FMR = 0.001 for white males which is the demographic that usually gives the lowest FMR. This means the top right box is the same color in all panels. The panels are sorted over multiple pages in order of FMR on black females, which is the demographic that usually gives the highest FMR.

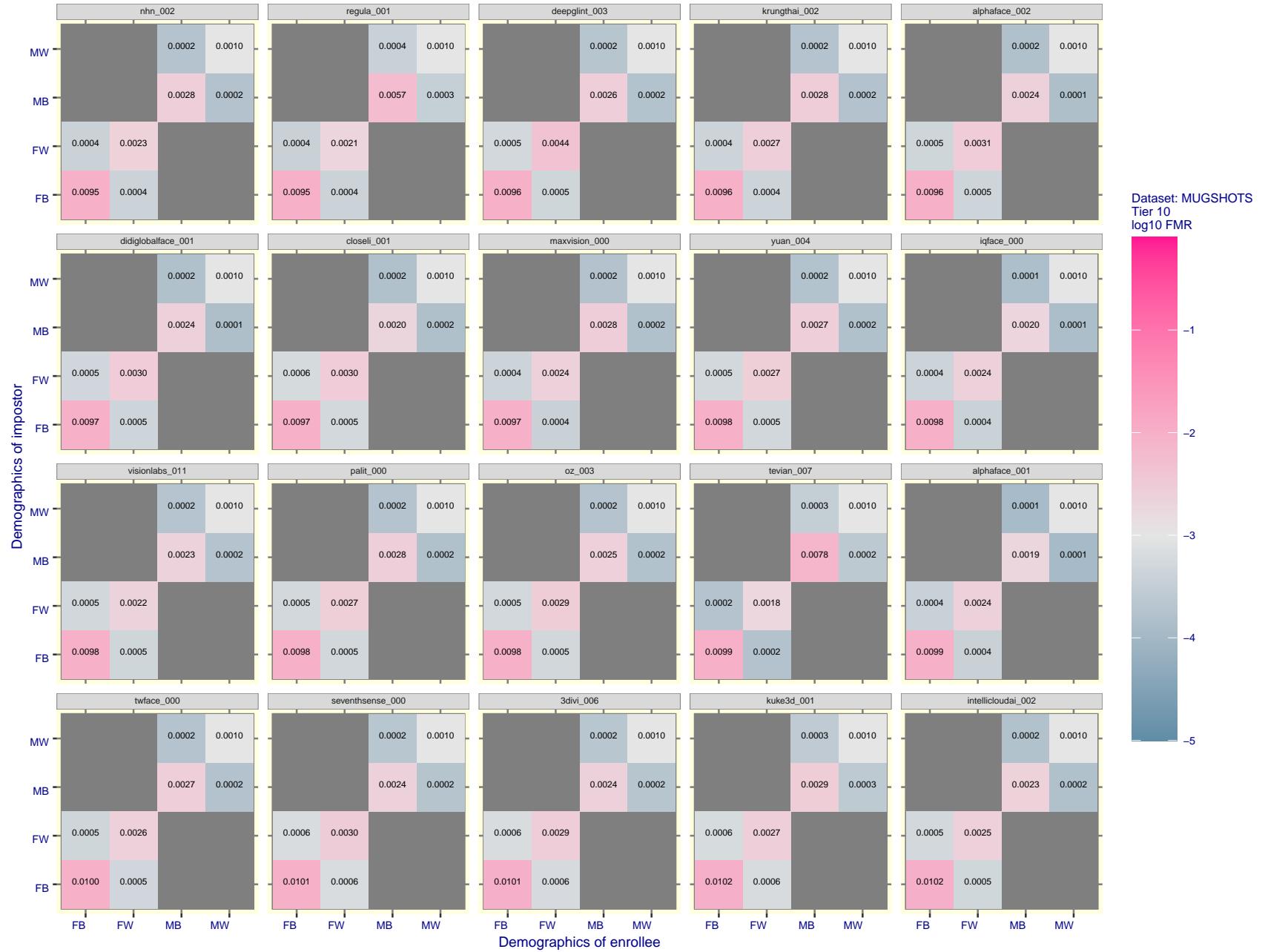


Figure 140: For the mugshot images, FMR for same-sex impostor pairs of images annotated with codes for black female, black male, white female, white male. The threshold is set for each algorithm to give FMR = 0.001 for white males which is the demographic that usually gives the lowest FMR. This means the top right box is the same color in all panels. The panels are sorted over multiple pages in order of FMR on black females, which is the demographic that usually gives the highest FMR.

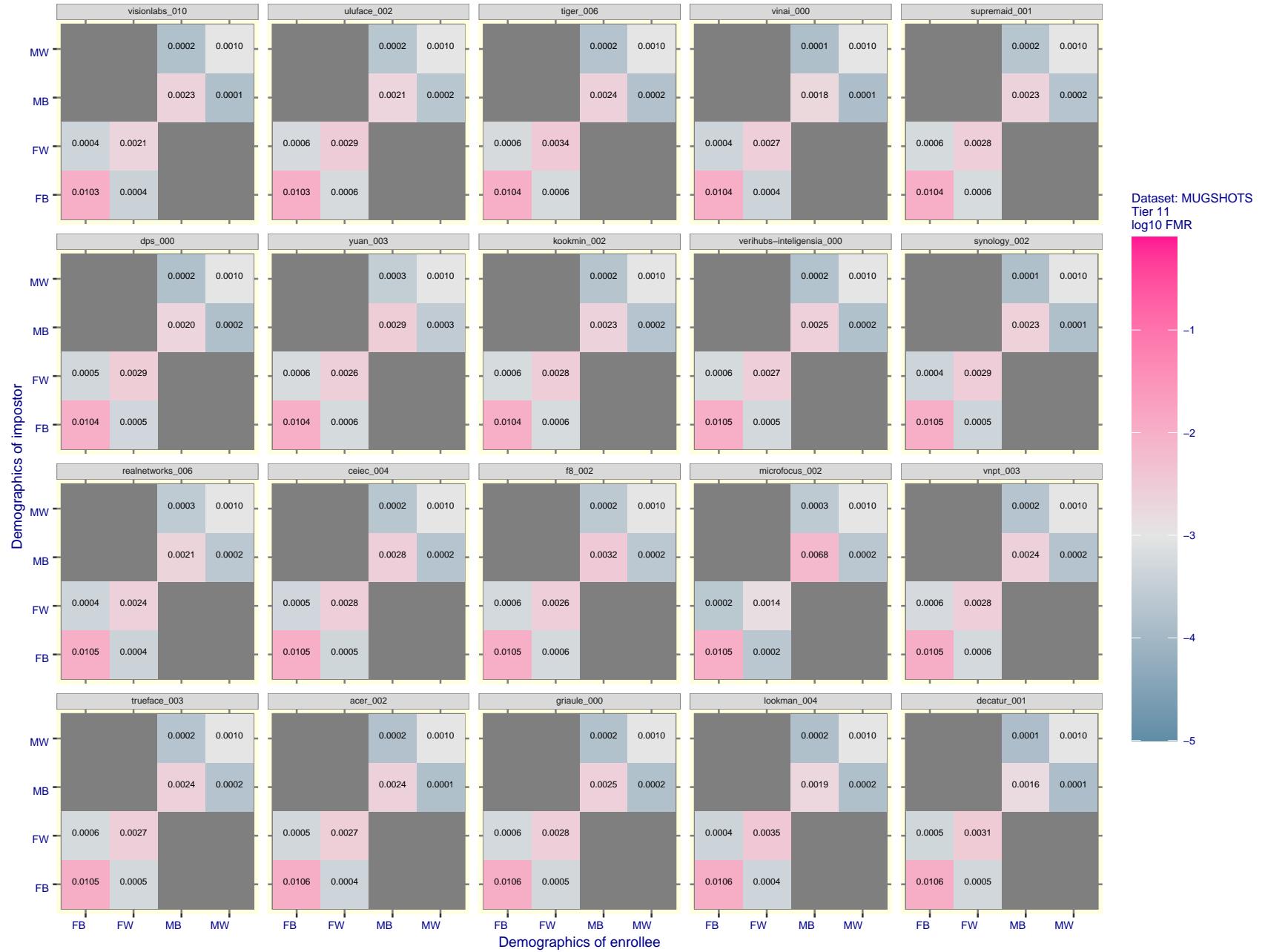


Figure 141: For the mugshot images, FMR for same-sex impostor pairs of images annotated with codes for black female, black male, white female, white male. The threshold is set for each algorithm to give FMR = 0.001 for white males which is the demographic that usually gives the lowest FMR. This means the top right box is the same color in all panels. The panels are sorted over multiple pages in order of FMR on black females, which is the demographic that usually gives the highest FMR.

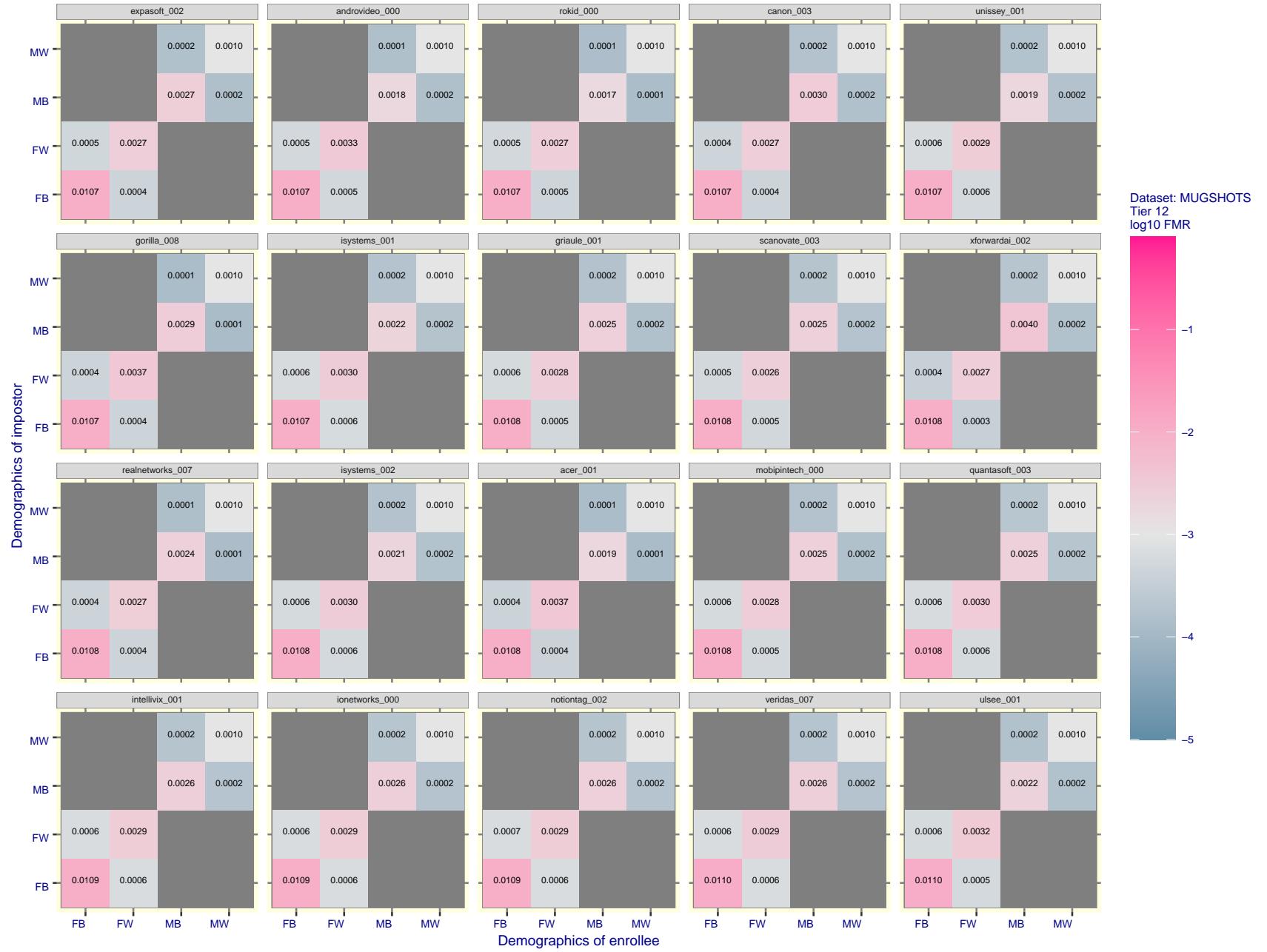


Figure 142: For the mugshot images, FMR for same-sex impostor pairs of images annotated with codes for black female, black male, white female, white male. The threshold is set for each algorithm to give FMR = 0.001 for white males which is the demographic that usually gives the lowest FMR. This means the top right box is the same color in all panels. The panels are sorted over multiple pages in order of FMR on black females, which is the demographic that usually gives the highest FMR.

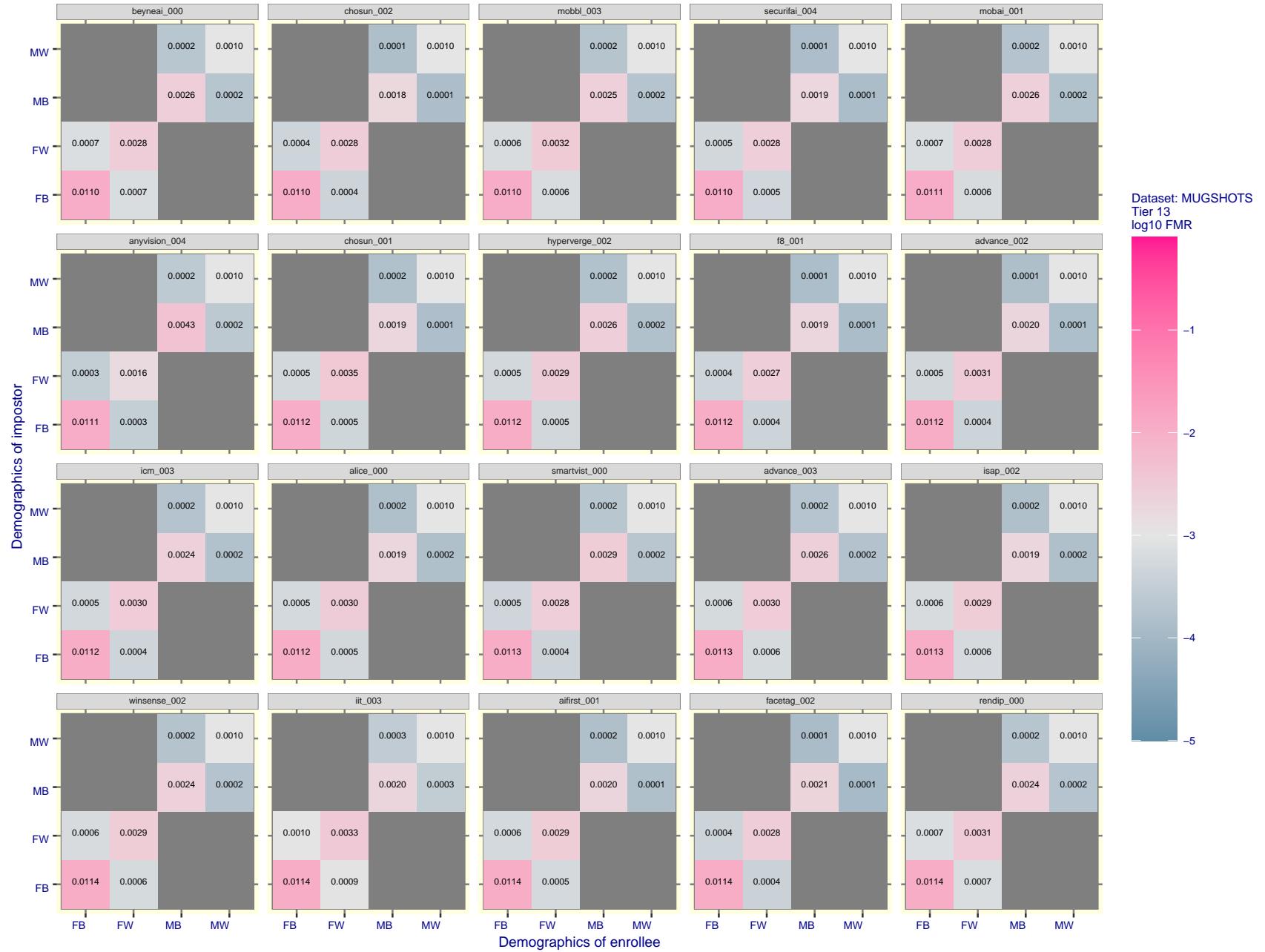


Figure 143: For the mugshot images, FMR for same-sex impostor pairs of images annotated with codes for black female, black male, white female, white male. The threshold is set for each algorithm to give FMR = 0.001 for white males which is the demographic that usually gives the lowest FMR. This means the top right box is the same color in all panels. The panels are sorted over multiple pages in order of FMR on black females, which is the demographic that usually gives the highest FMR.

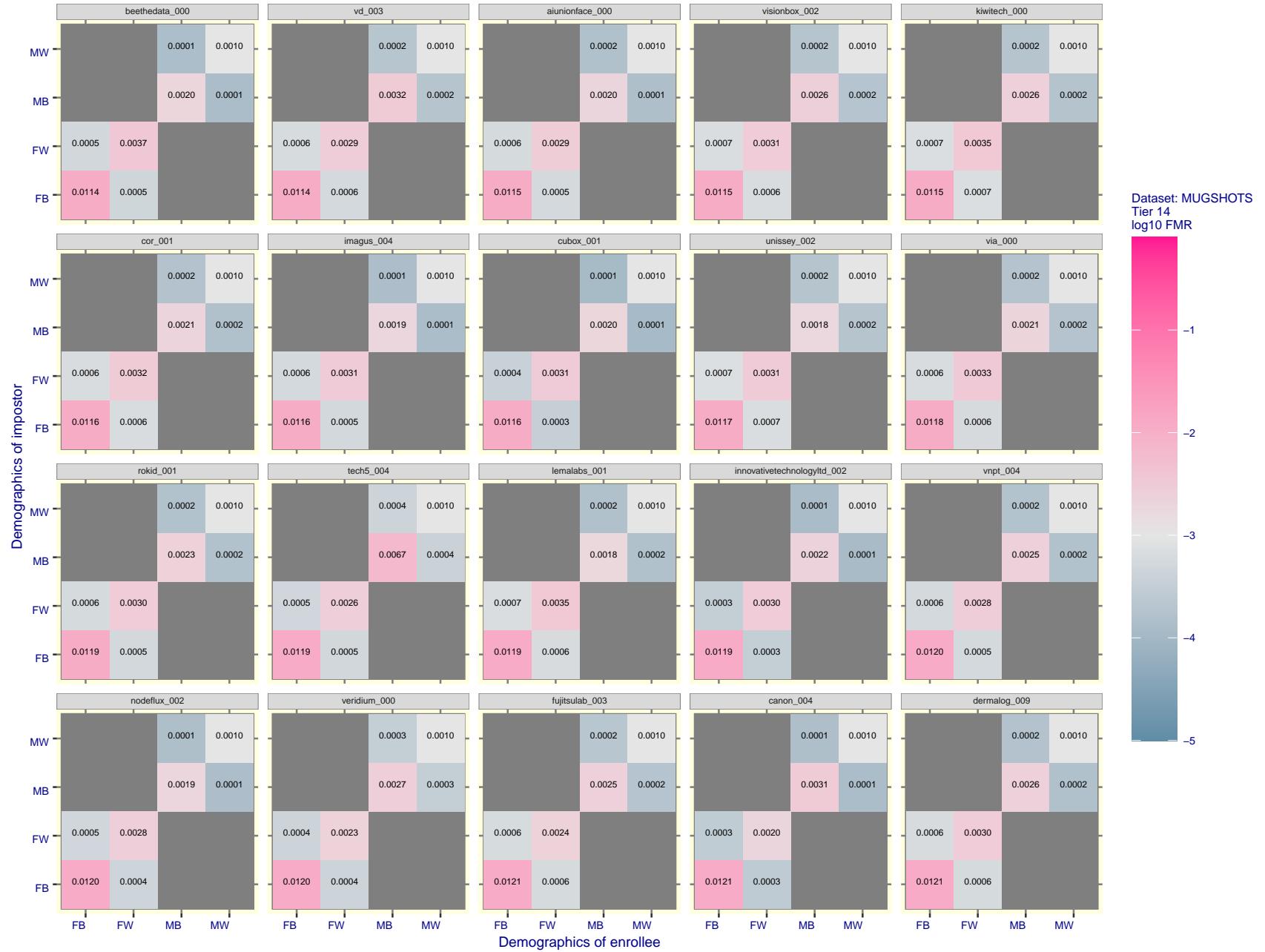
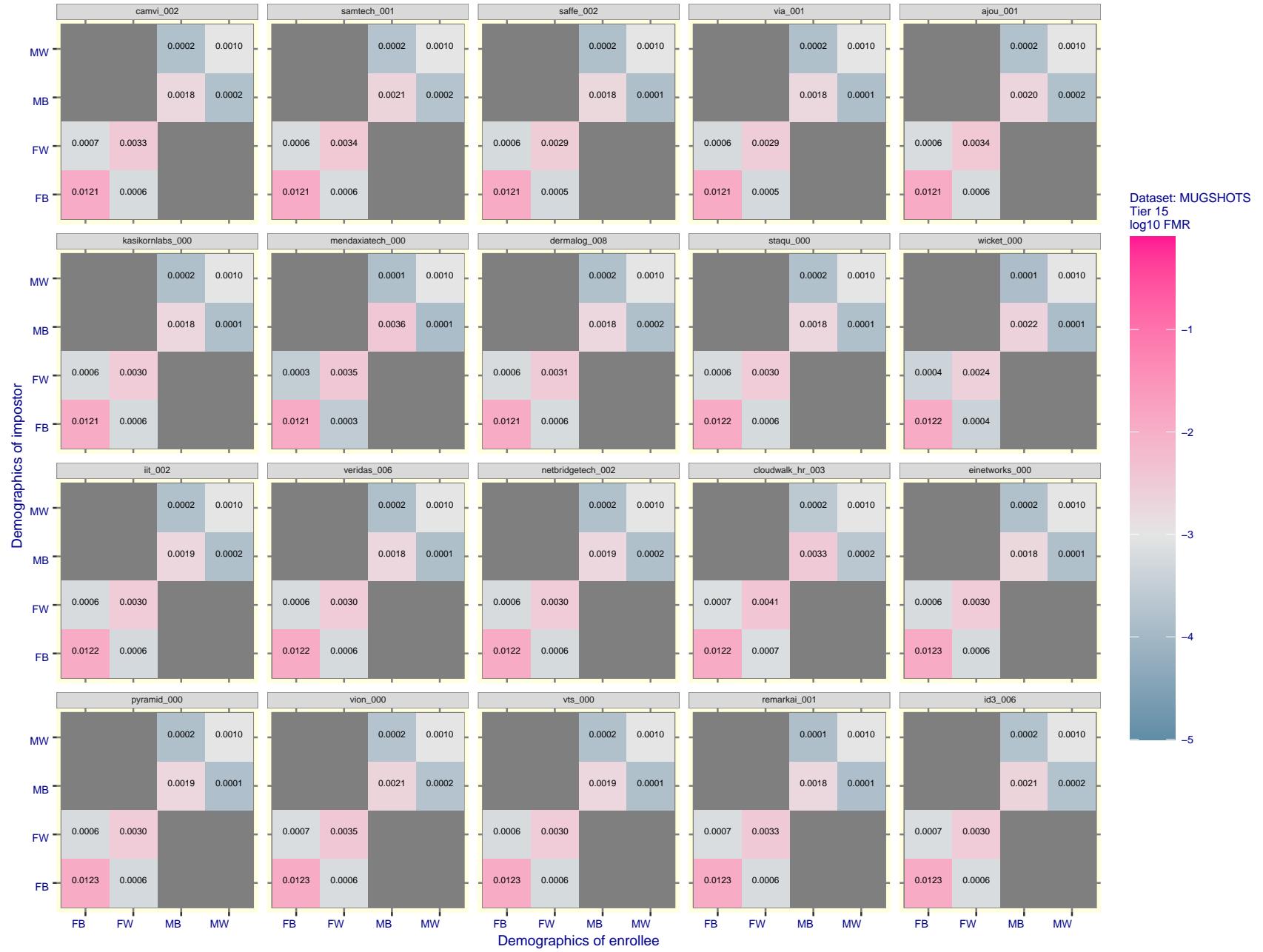


Figure 144: For the mugshot images, FMR for same-sex impostor pairs of images annotated with codes for black female, black male, white female, white male. The threshold is set for each algorithm to give FMR = 0.001 for white males which is the demographic that usually gives the lowest FMR. This means the top right box is the same color in all panels. The panels are sorted over multiple pages in order of FMR on black females, which is the demographic that usually gives the highest FMR.



FRVT - FACE RECOGNITION VENDOR TEST - VERIFICATION

Figure 145: For the mugshot images, FMR for same-sex impostor pairs of images annotated with codes for black female, black male, white female, white male. The threshold is set for each algorithm to give FMR = 0.001 for white males which is the demographic that usually gives the lowest FMR. This means the top right box is the same color in all panels. The panels are sorted over multiple pages in order of FMR on black females, which is the demographic that usually gives the highest FMR.

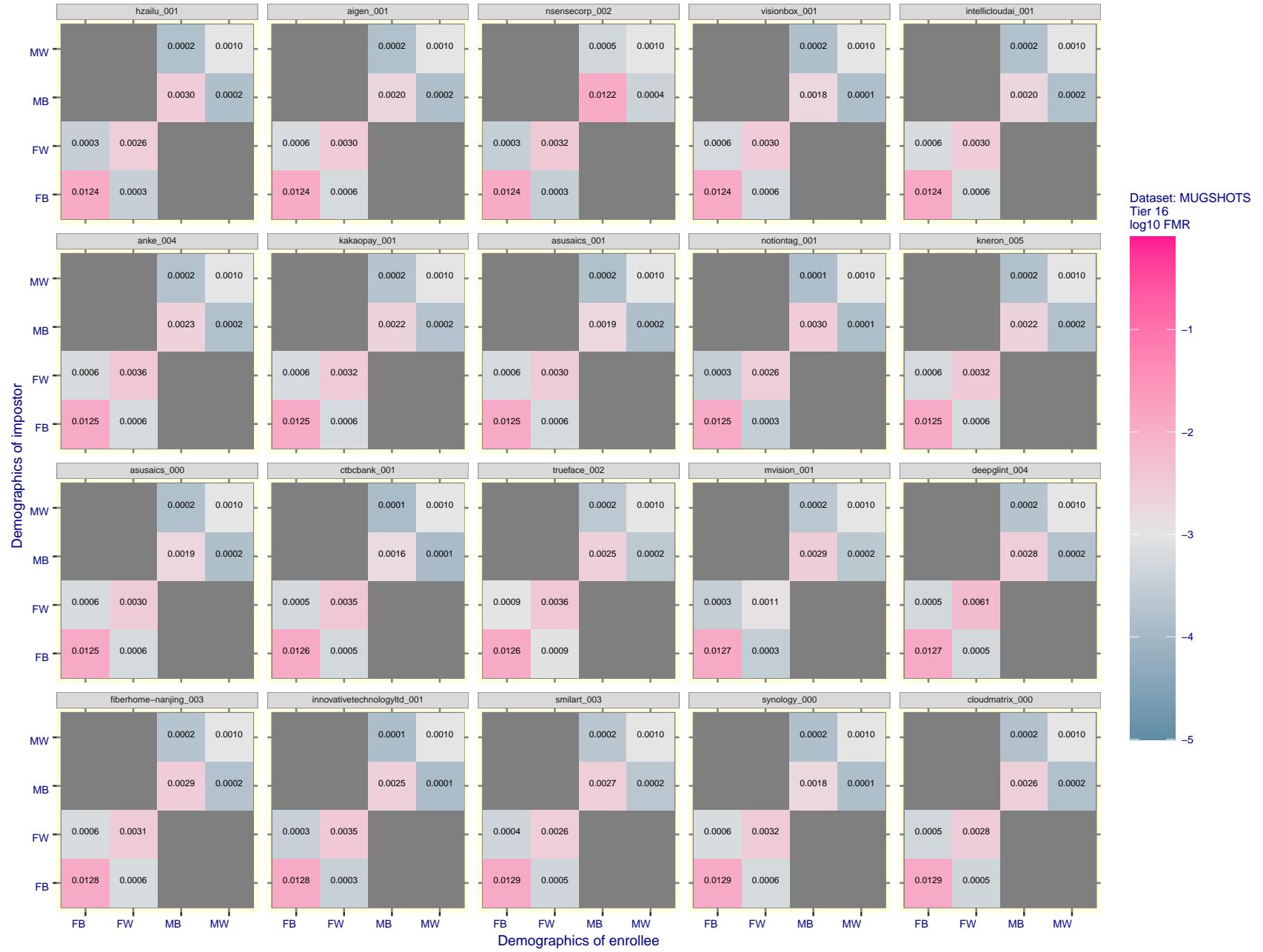


Figure 146: For the mugshot images, FMR for same-sex impostor pairs of images annotated with codes for black female, black male, white female, white male. The threshold is set for each algorithm to give FMR = 0.001 for white males which is the demographic that usually gives the lowest FMR. This means the top right box is the same color in all panels. The panels are sorted over multiple pages in order of FMR on black females, which is the demographic that usually gives the highest FMR.

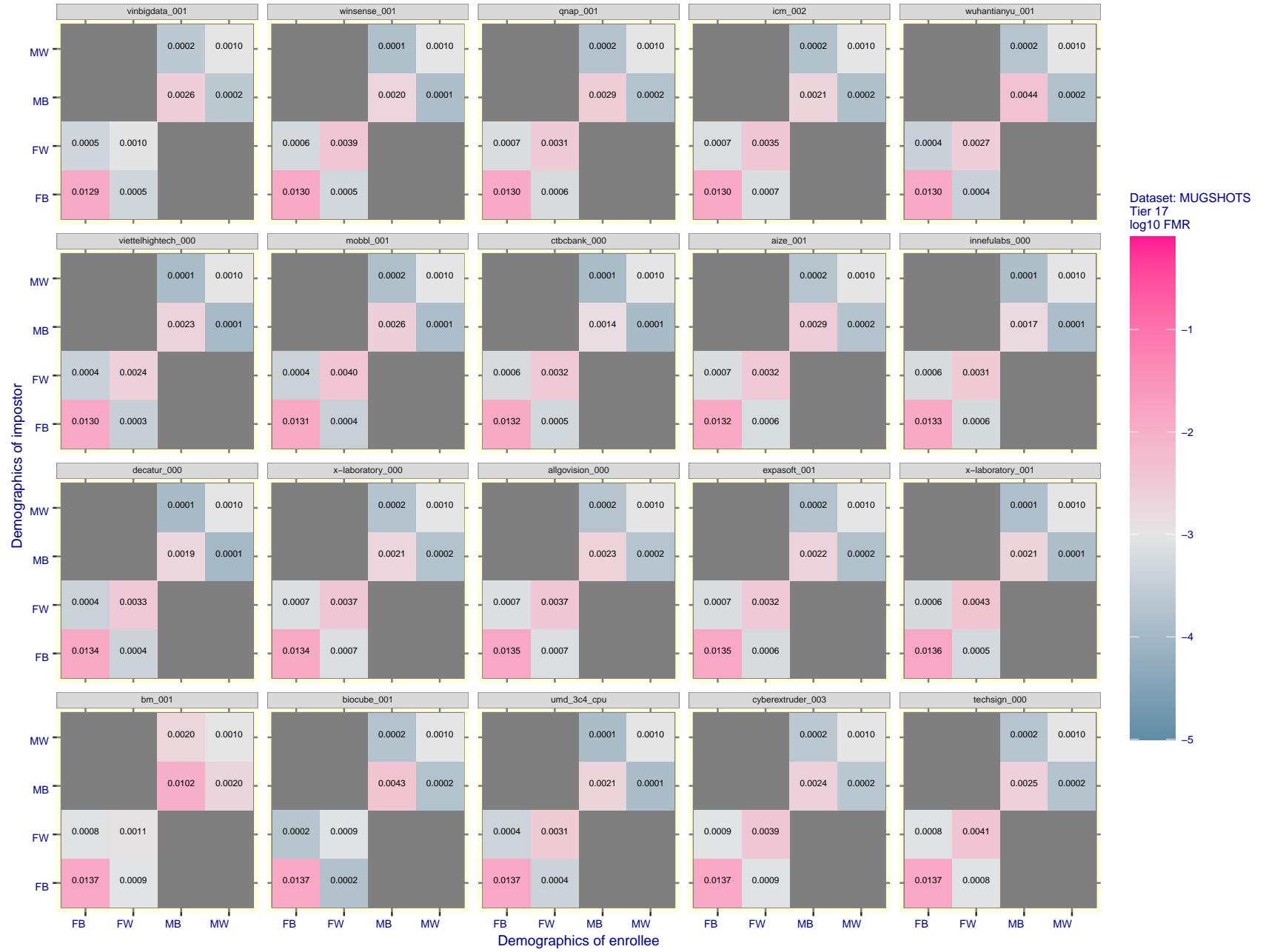


Figure 147: For the mugshot images, FMR for same-sex impostor pairs of images annotated with codes for black female, black male, white female, white male. The threshold is set for each algorithm to give FMR = 0.001 for white males which is the demographic that usually gives the lowest FMR. This means the top right box is the same color in all panels. The panels are sorted over multiple pages in order of FMR on black females, which is the demographic that usually gives the highest FMR.

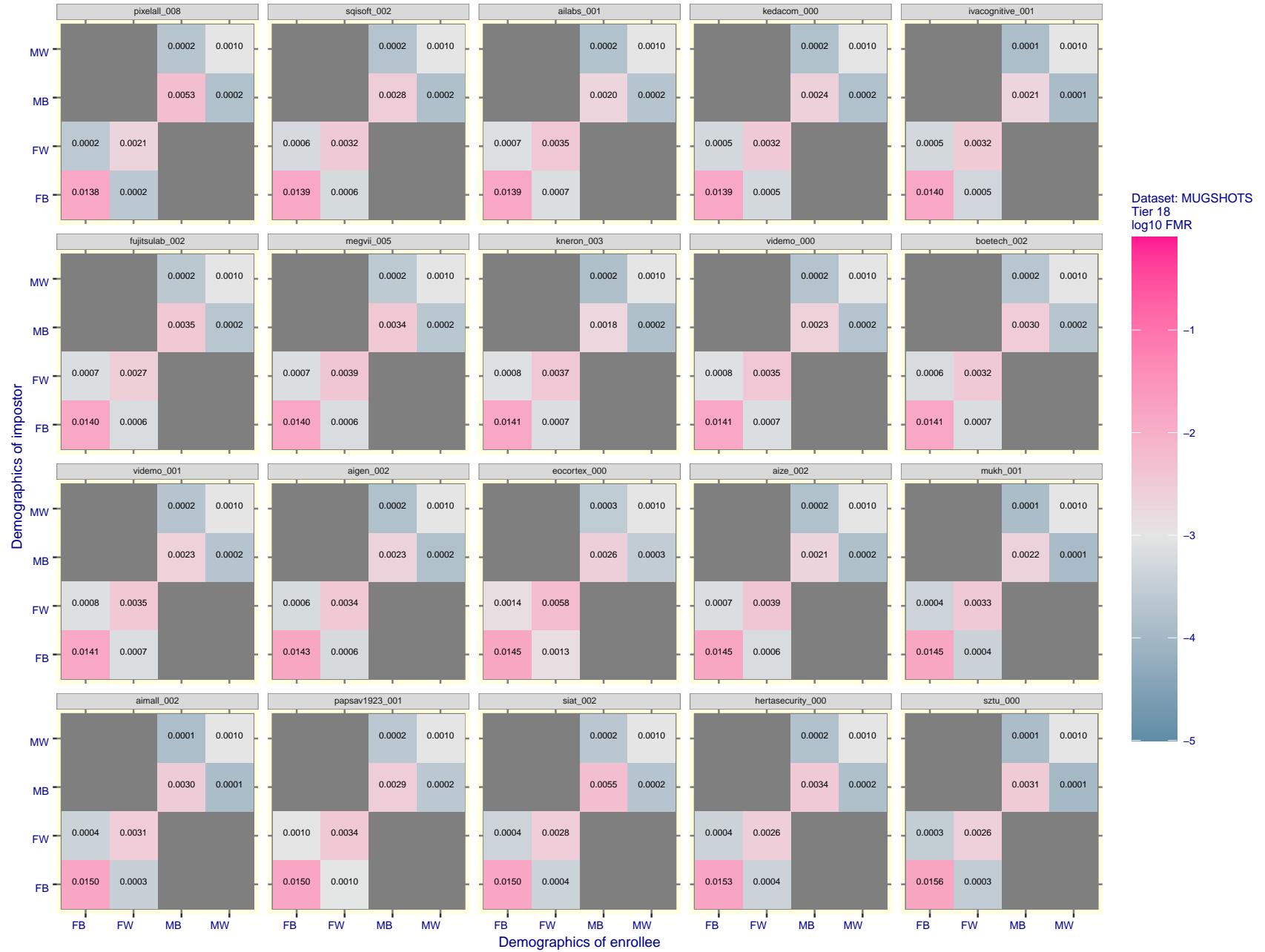


Figure 148: For the mugshot images, FMR for same-sex impostor pairs of images annotated with codes for black female, black male, white female, white male. The threshold is set for each algorithm to give FMR = 0.001 for white males which is the demographic that usually gives the lowest FMR. This means the top right box is the same color in all panels. The panels are sorted over multiple pages in order of FMR on black females, which is the demographic that usually gives the highest FMR.

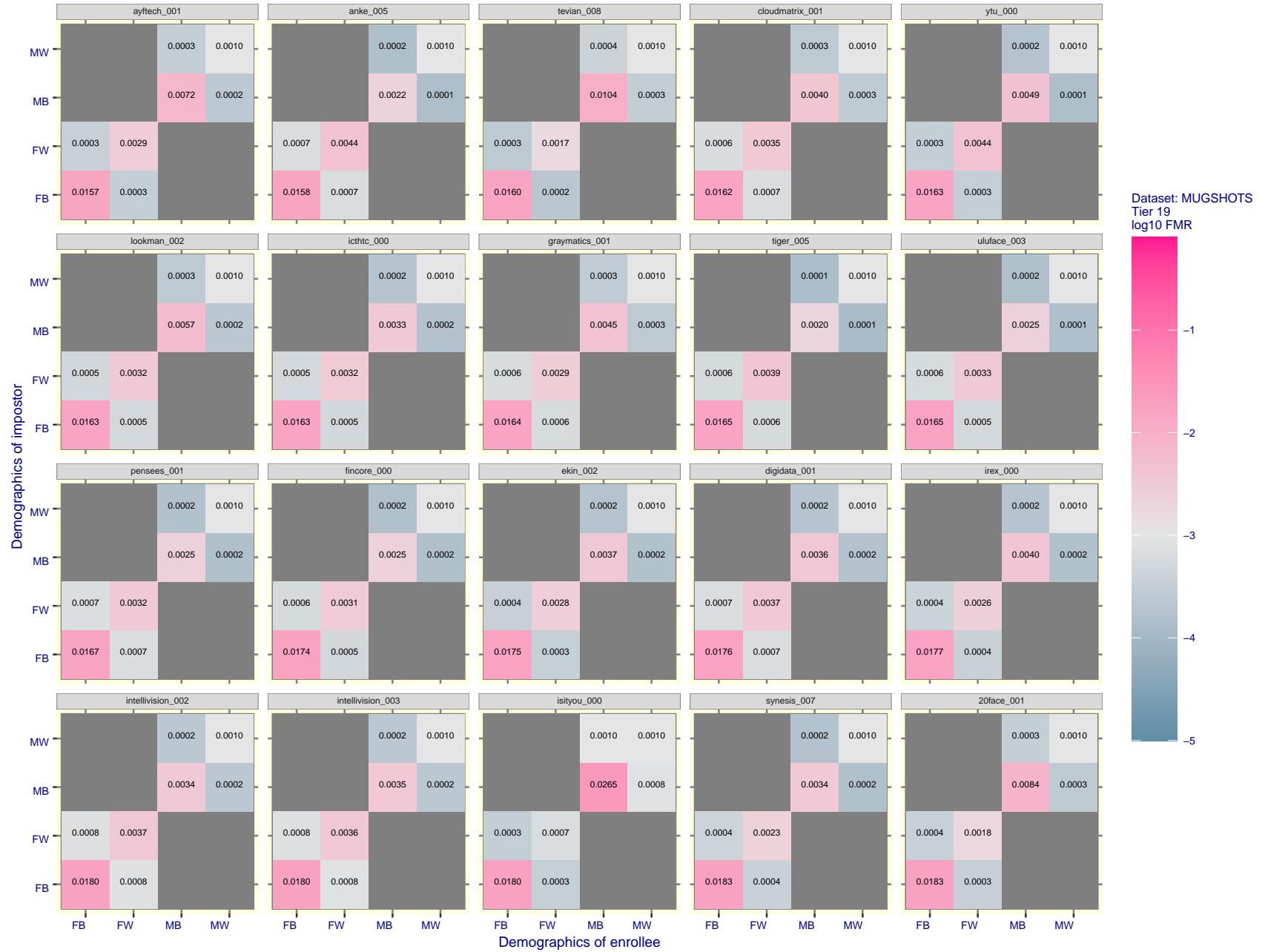


Figure 149: For the mugshot images, FMR for same-sex impostor pairs of images annotated with codes for black female, black male, white female, white male. The threshold is set for each algorithm to give FMR = 0.001 for white males which is the demographic that usually gives the lowest FMR. This means the top right box is the same color in all panels. The panels are sorted over multiple pages in order of FMR on black females, which is the demographic that usually gives the highest FMR.

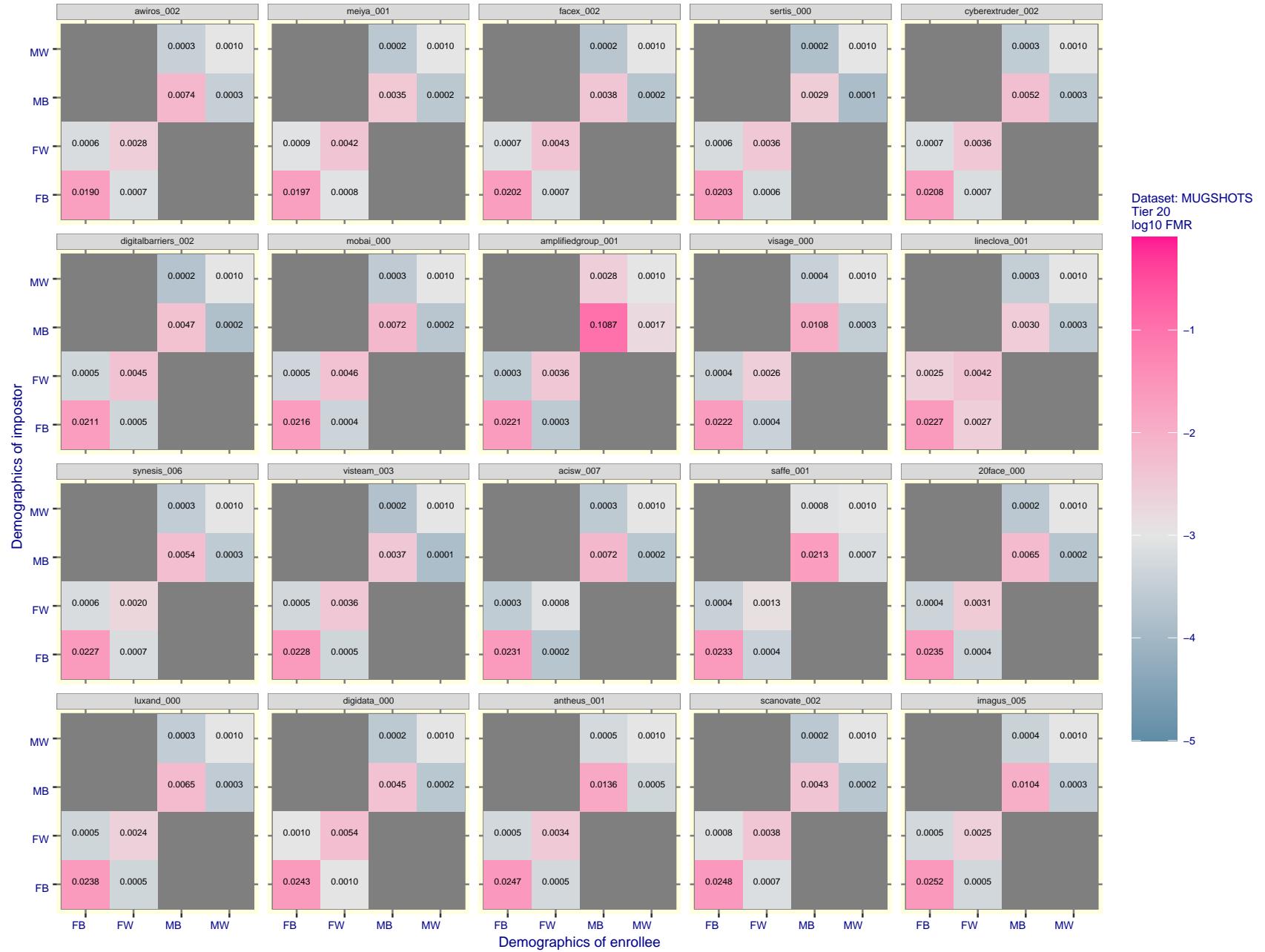


Figure 150: For the mugshot images, FMR for same-sex impostor pairs of images annotated with codes for black female, black male, white female, white male. The threshold is set for each algorithm to give FMR = 0.001 for white males which is the demographic that usually gives the lowest FMR. This means the top right box is the same color in all panels. The panels are sorted over multiple pages in order of FMR on black females, which is the demographic that usually gives the highest FMR.



Figure 151: For the mugshot images, FMR for same-sex impostor pairs of images annotated with codes for black female, black male, white female, white male. The threshold is set for each algorithm to give FMR = 0.001 for white males which is the demographic that usually gives the lowest FMR. This means the top right box is the same color in all panels. The panels are sorted over multiple pages in order of FMR on black females, which is the demographic that usually gives the highest FMR.

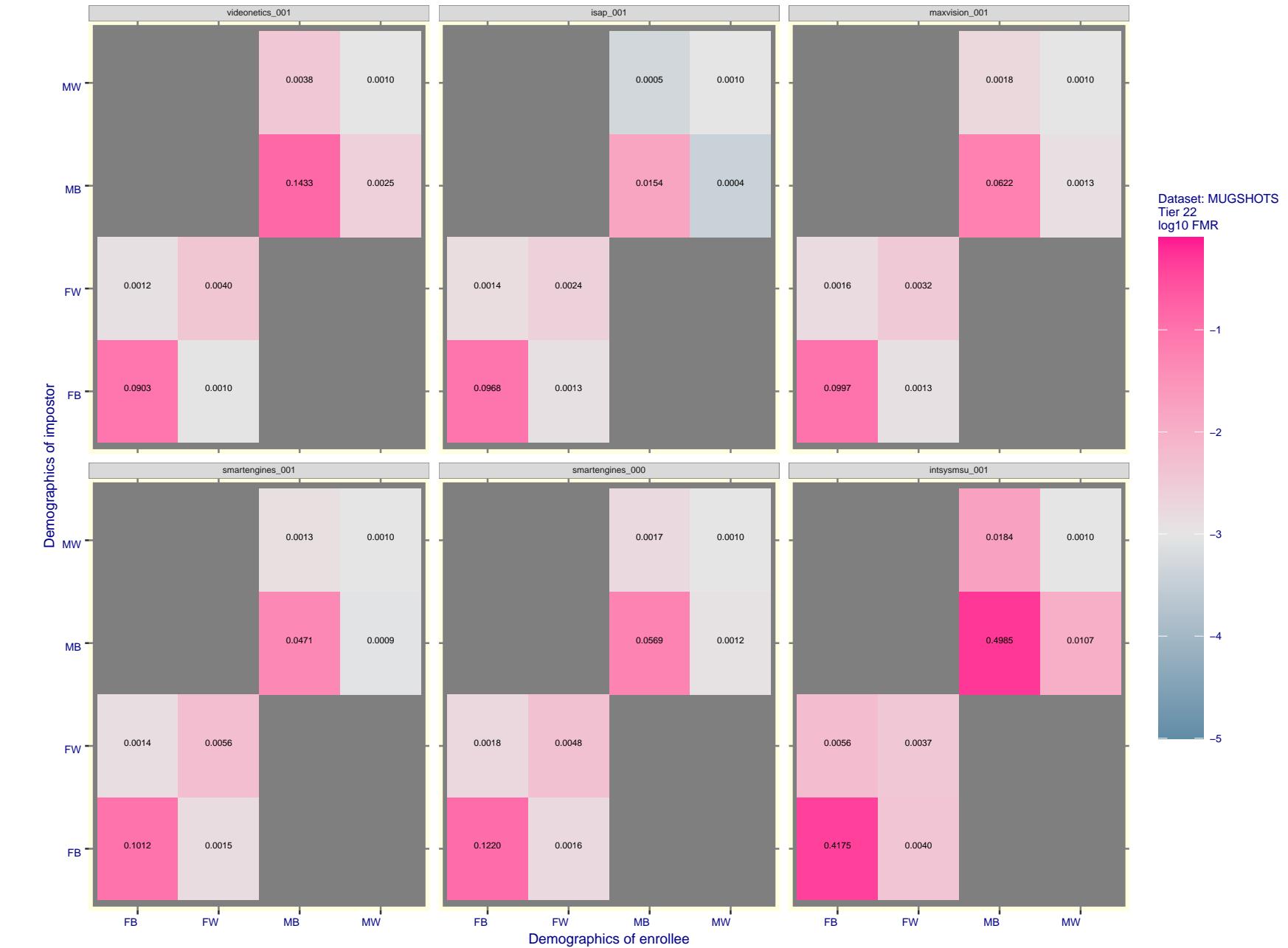


Figure 152: For the mugshot images, FMR for same-sex impostor pairs of images annotated with codes for black female, black male, white female, white male. The threshold is set for each algorithm to give $\text{FMR} = 0.001$ for white males which is the demographic that usually gives the lowest FMR. This means the top right box is the same color in all panels. The panels are sorted over multiple pages in order of FMR on black females, which is the demographic that usually gives the highest FMR.

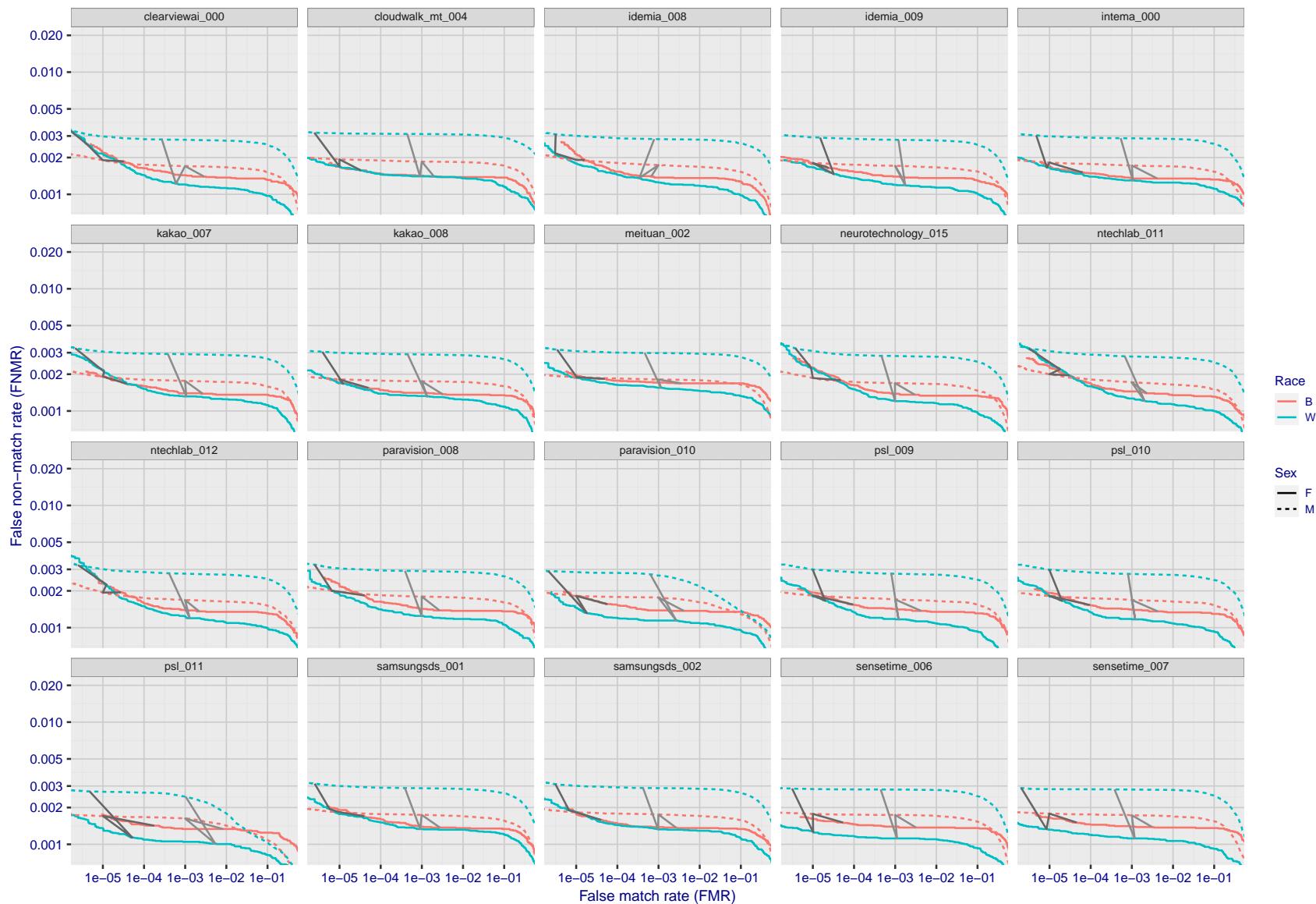


Figure 153: For the mugshot images, error tradeoff characteristics for white females, black females, black males and white males. The Z-shaped grey lines correspond to fixed thresholds, showing both FNMR and FMR vary at one T value. Note: Many of the plots will naively be read as saying women gives worse error rates than men because the solid traces lie above the dotted ones. However, this is misleading and incomplete: The grey lines show the traces reveal horizontal shifts. Thus for the cogent-003 algorithm FNMR for men is higher than for women at a fixed threshold but, at the same time, FMR is higher for women - see Figure 239. As access control systems almost always operate at a fixed threshold, the naive interpretation is incorrect.

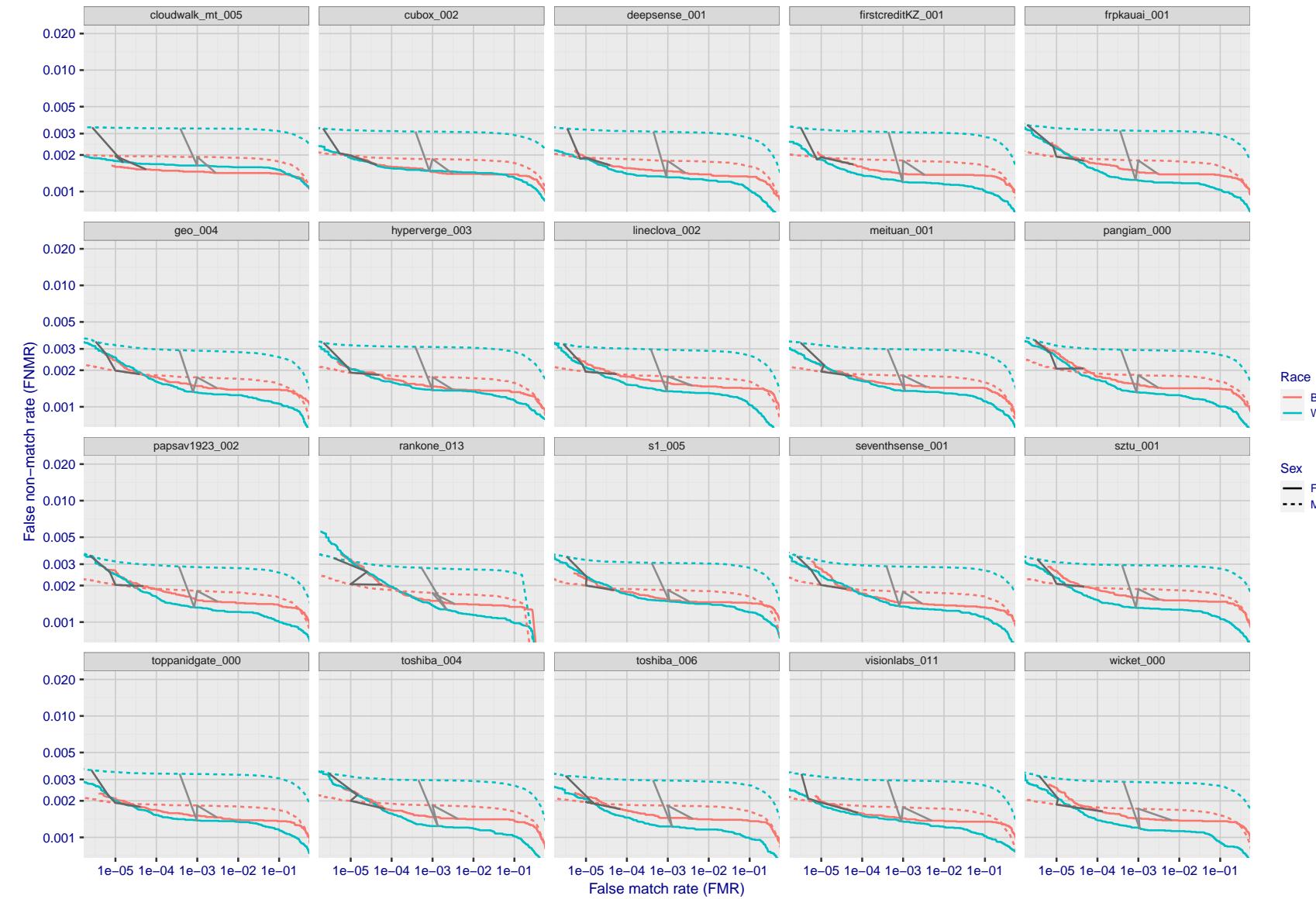


Figure 154: For the mugshot images, error tradeoff characteristics for white females, black females, black males and white males. The Z-shaped grey lines correspond to fixed thresholds, showing both FNMR and FMR vary at one T value. Note: Many of the plots will naively be read as saying women gives worse error rates than men because the solid traces lie above the dotted ones. However, this is misleading and incomplete: The grey lines show the traces reveal horizontal shifts. Thus for the cogent-003 algorithm FNMR for men is higher than for women at a fixed threshold but, at the same time, FMR is higher for women - see Figure 239. As access control systems almost always operate at a fixed threshold, the naive interpretation is incorrect.

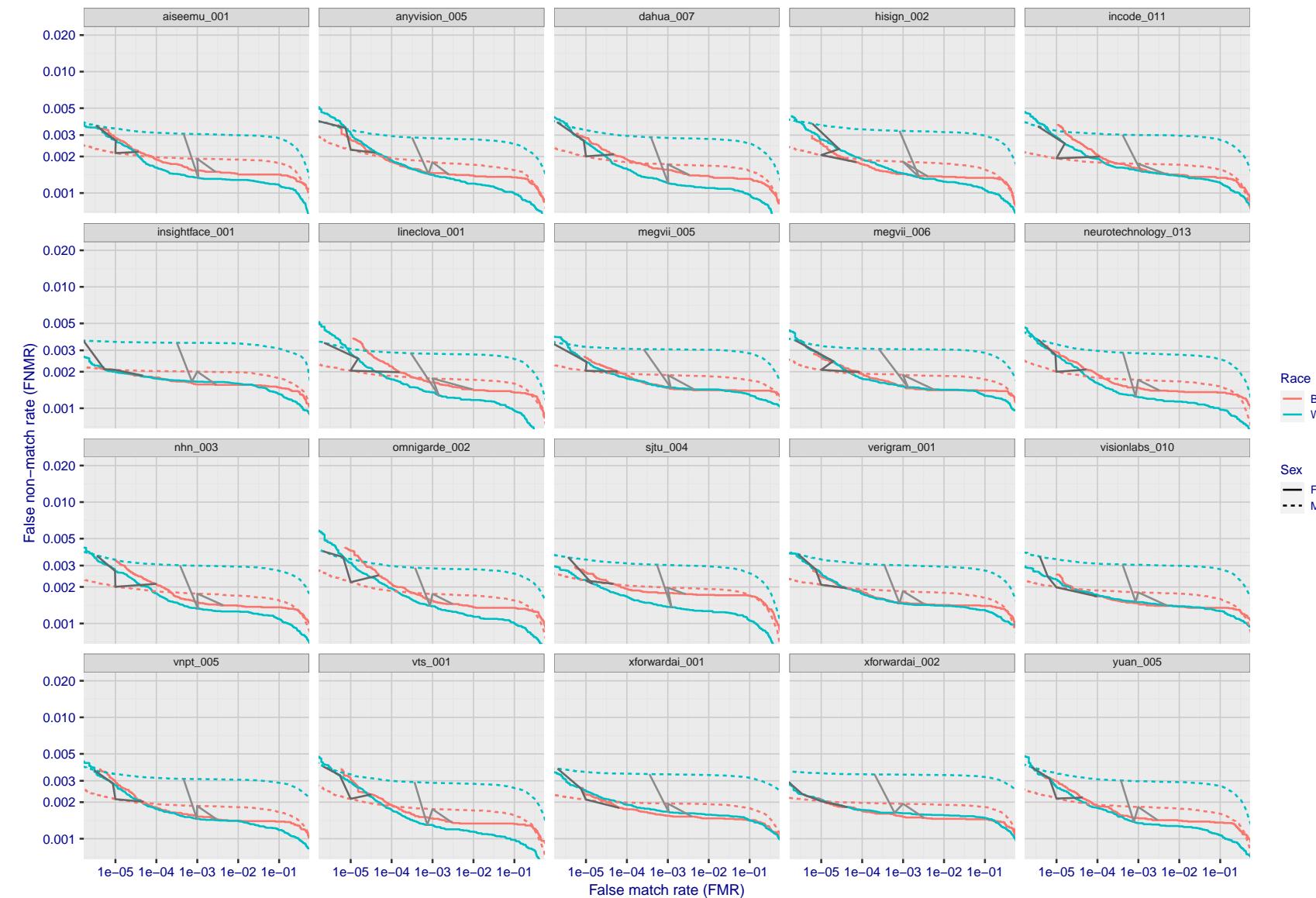


Figure 155: For the mugshot images, error tradeoff characteristics for white females, black females, black males and white males. The Z-shaped grey lines correspond to fixed thresholds, showing both FNMR and FMR vary at one T value. Note: Many of the plots will naively be read as saying women gives worse error rates than men because the solid traces lie above the dotted ones. However, this is misleading and incomplete: The grey lines show the traces reveal horizontal shifts. Thus for the cogent-003 algorithm FNMR for men is higher than for women at a fixed threshold but, at the same time, FMR is higher for women - see Figure 239. As access control systems almost always operate at a fixed threshold, the naive interpretation is incorrect.

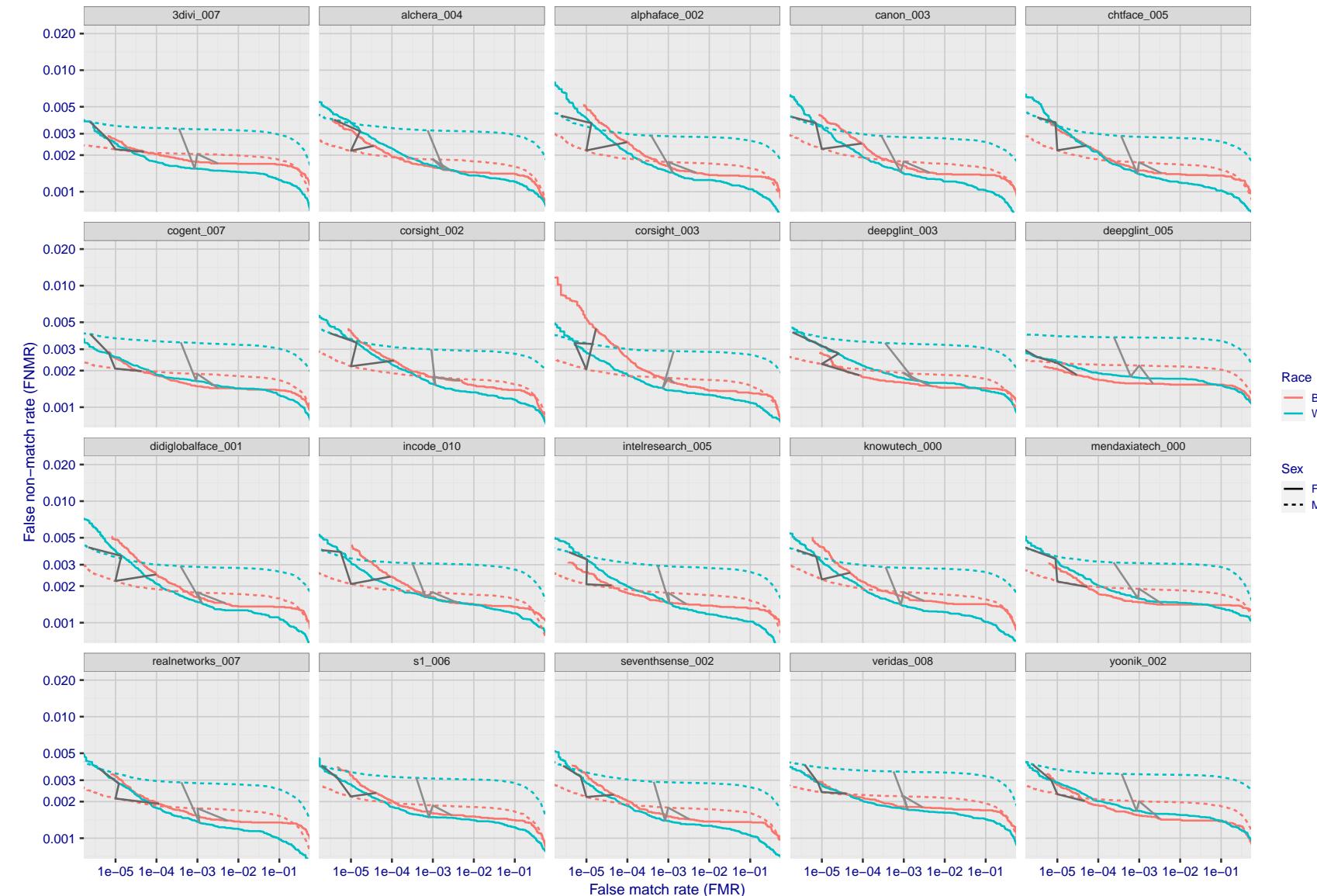


Figure 156: For the mugshot images, error tradeoff characteristics for white females, black females, black males and white males. The Z-shaped grey lines correspond to fixed thresholds, showing both FNMR and FMR vary at one T value. Note: Many of the plots will naively be read as saying women gives worse error rates than men because the solid traces lie above the dotted ones. However, this is misleading and incomplete: The grey lines show the traces reveal horizontal shifts. Thus for the cogent-003 algorithm FNMR for men is higher than for women at a fixed threshold but, at the same time, FMR is higher for women - see Figure 239. As access control systems almost always operate at a fixed threshold, the naive interpretation is incorrect.

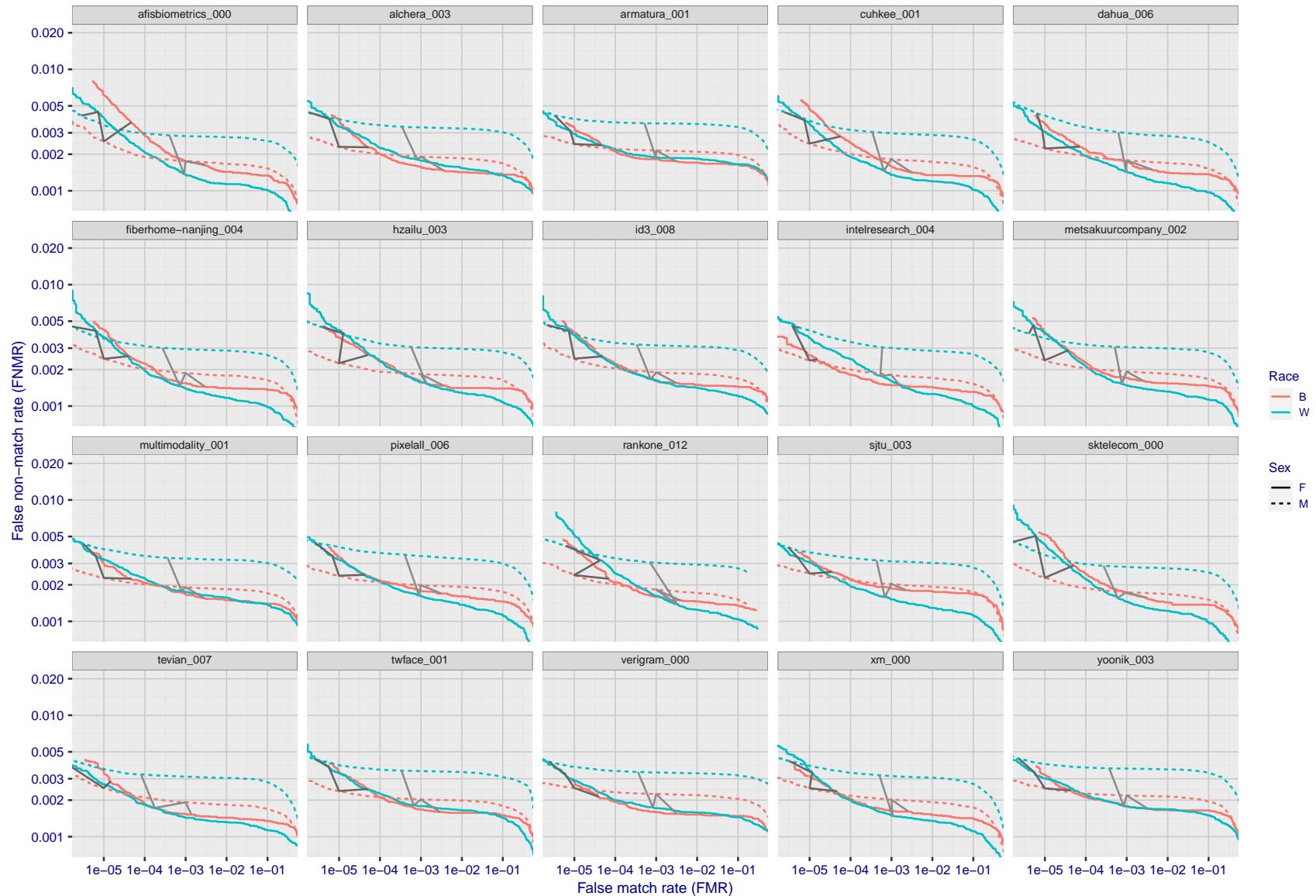


Figure 157: For the mugshot images, error tradeoff characteristics for white females, black females, black males and white males. The Z-shaped grey lines correspond to fixed thresholds, showing both FNMR and FMR vary at one T value. Note: Many of the plots will naively be read as saying women gives worse error rates than men because the solid traces lie above the dotted ones. However, this is misleading and incomplete: The grey lines show the traces reveal horizontal shifts. Thus for the cogent-003 algorithm FNMR for men is higher than for women at a fixed threshold but, at the same time, FMR is higher for women - see Figure 239. As access control systems almost always operate at a fixed threshold, the naive interpretation is incorrect.

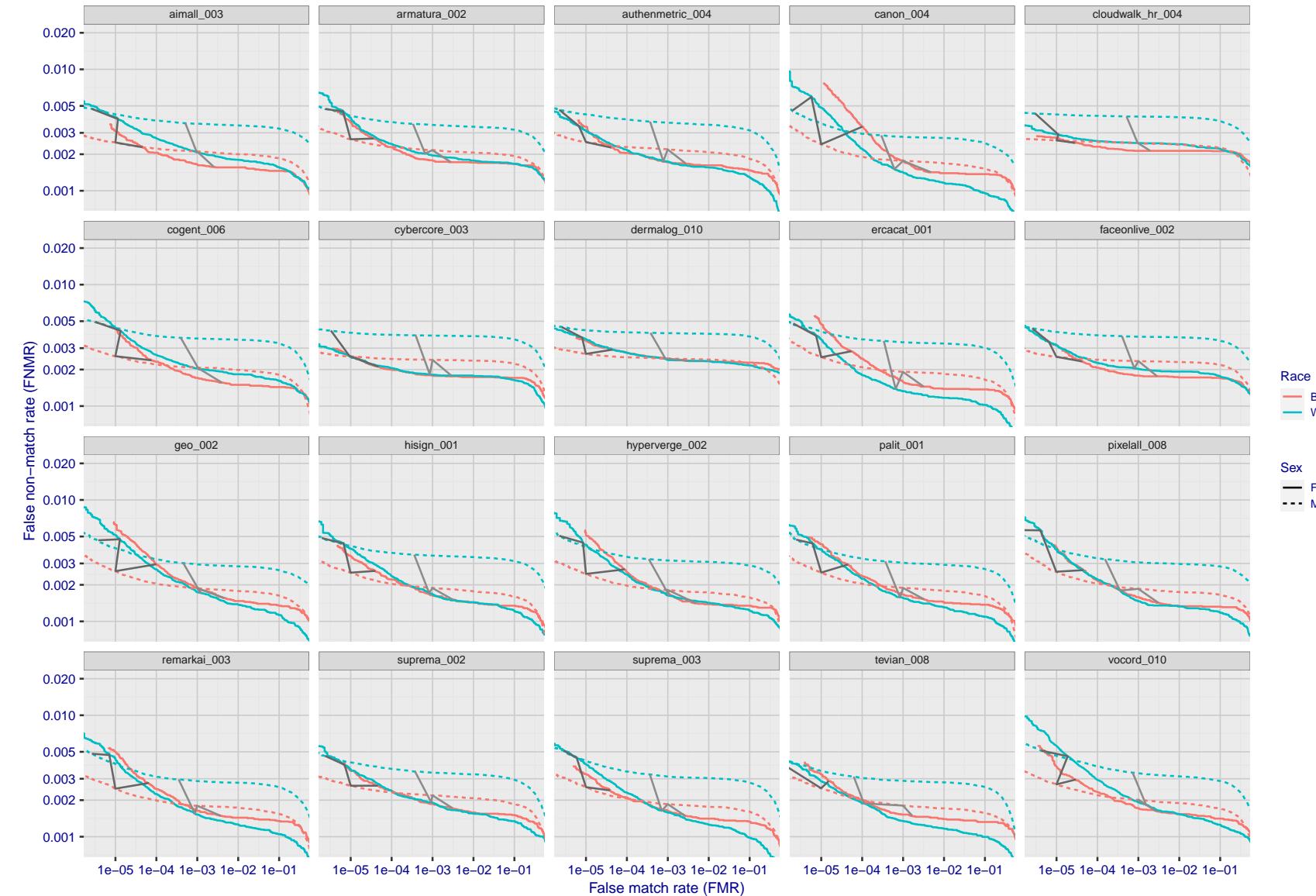


Figure 158: For the mugshot images, error tradeoff characteristics for white females, black females, black males and white males. The Z-shaped grey lines correspond to fixed thresholds, showing both FNMR and FMR vary at one T value. Note: Many of the plots will naively be read as saying women gives worse error rates than men because the solid traces lie above the dotted ones. However, this is misleading and incomplete: The grey lines show the traces reveal horizontal shifts. Thus for the cogent-003 algorithm FNMR for men is higher than for women at a fixed threshold but, at the same time, FMR is higher for women - see Figure 239. As access control systems almost always operate at a fixed threshold, the naive interpretation is incorrect.

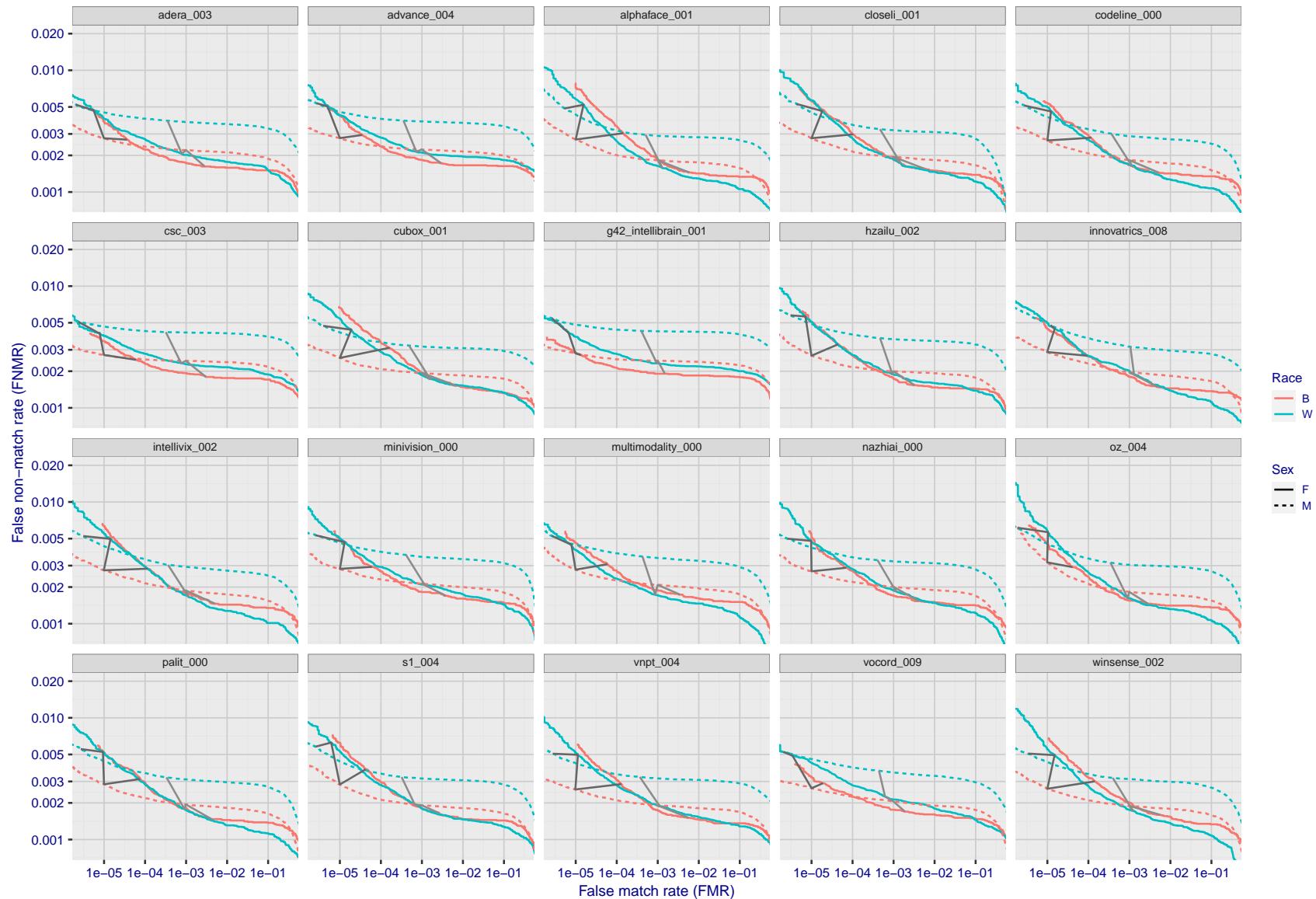


Figure 159: For the mugshot images, error tradeoff characteristics for white females, black females, black males and white males. The Z-shaped grey lines correspond to fixed thresholds, showing both FNMR and FMR vary at one T value. Note: Many of the plots will naively be read as saying women gives worse error rates than men because the solid traces lie above the dotted ones. However, this is misleading and incomplete: The grey lines show the traces reveal horizontal shifts. Thus for the cogent-003 algorithm FNMR for men is higher than for women at a fixed threshold but, at the same time, FMR is higher for women - see Figure 239. As access control systems almost always operate at a fixed threshold, the naive interpretation is incorrect.

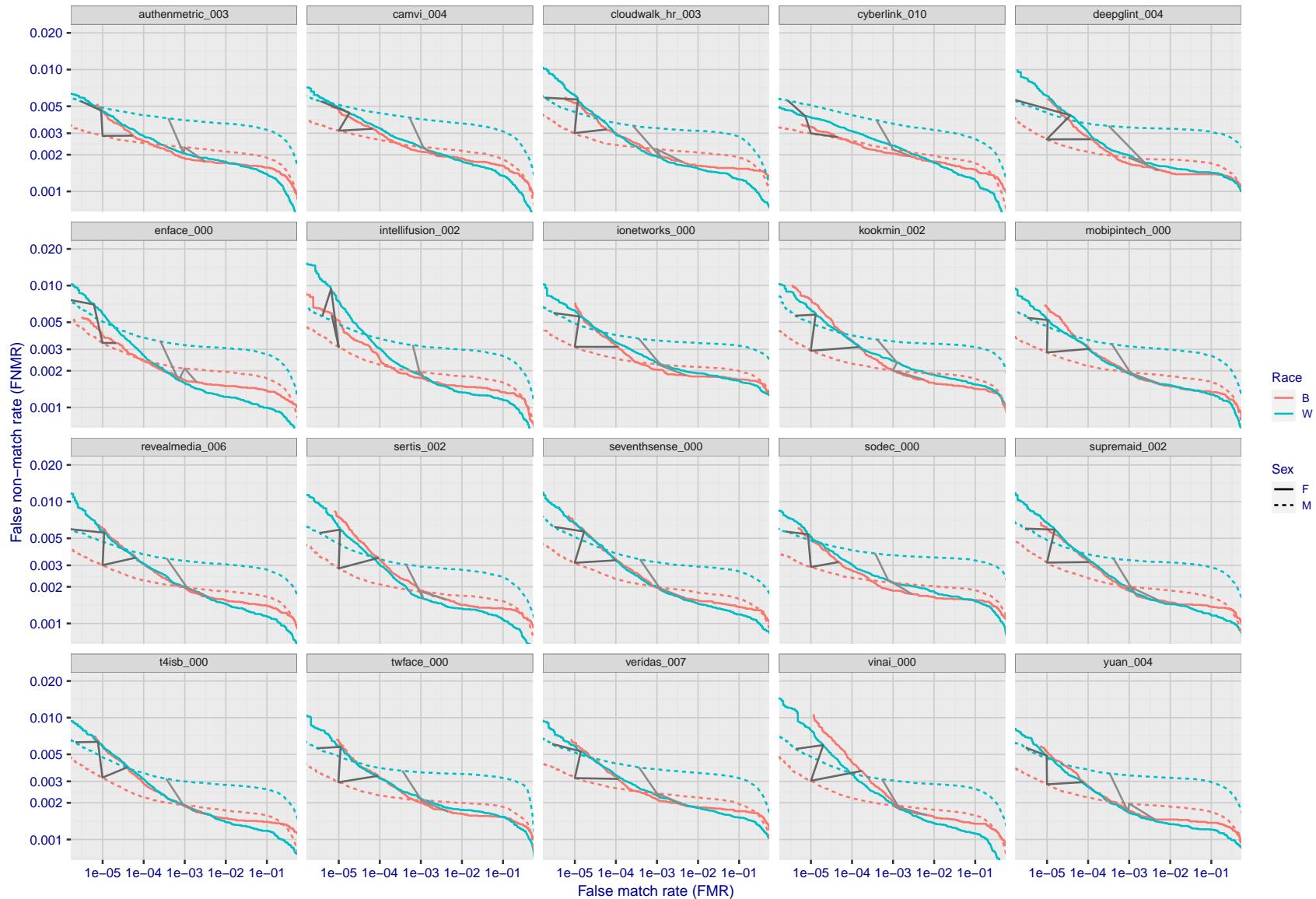


Figure 160: For the mugshot images, error tradeoff characteristics for white females, black females, black males and white males. The Z-shaped grey lines correspond to fixed thresholds, showing both FNMR and FMR vary at one T value. Note: Many of the plots will naively be read as saying women gives worse error rates than men because the solid traces lie above the dotted ones. However, this is misleading and incomplete: The grey lines show the traces reveal horizontal shifts. Thus for the cogent-003 algorithm FNMR for men is higher than for women at a fixed threshold but, at the same time, FMR is higher for women - see Figure 239. As access control systems almost always operate at a fixed threshold, the naive interpretation is incorrect.

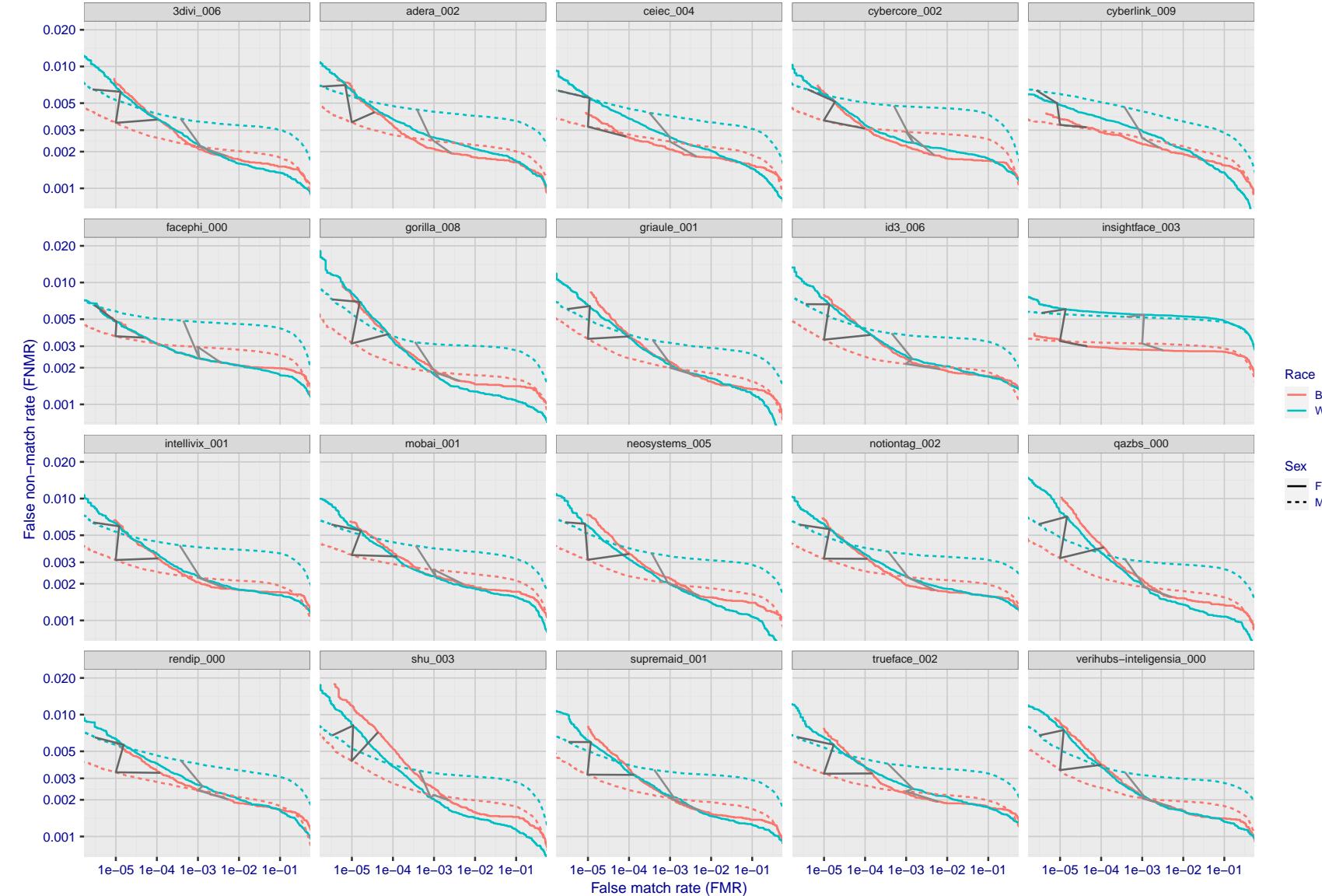


Figure 161: For the mugshot images, error tradeoff characteristics for white females, black females, black males and white males. The Z-shaped grey lines correspond to fixed thresholds, showing both FNMR and FMR vary at one T value. Note: Many of the plots will naively be read as saying women gives worse error rates than men because the solid traces lie above the dotted ones. However, this is misleading and incomplete: The grey lines show the traces reveal horizontal shifts. Thus for the cogent-003 algorithm FNMR for men is higher than for women at a fixed threshold but, at the same time, FMR is higher for women - see Figure 239. As access control systems almost always operate at a fixed threshold, the naive interpretation is incorrect.

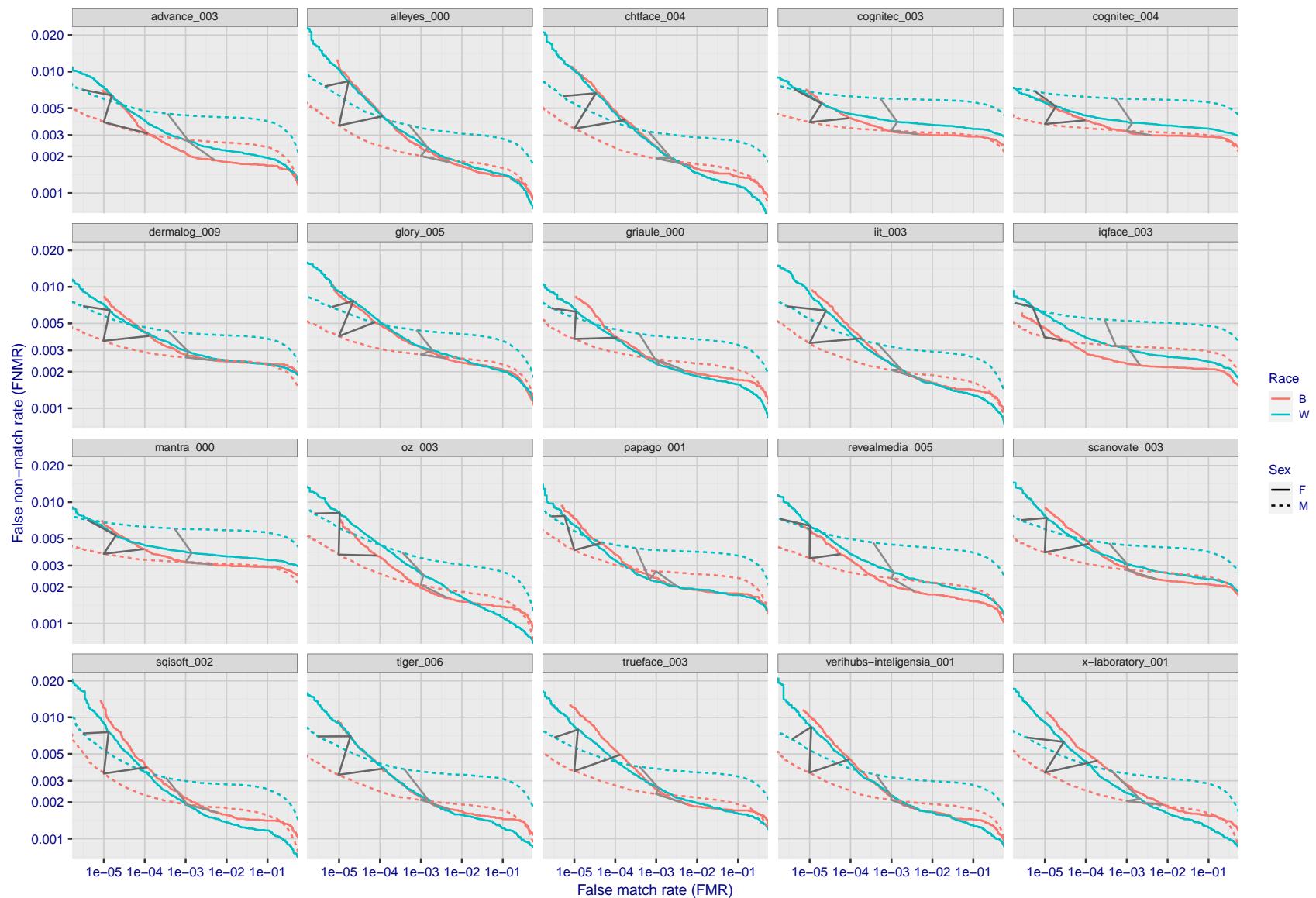


Figure 162: For the mugshot images, error tradeoff characteristics for white females, black females, black males and white males. The Z-shaped grey lines correspond to fixed thresholds, showing both FNMR and FMR vary at one T value. Note: Many of the plots will naively be read as saying women gives worse error rates than men because the solid traces lie above the dotted ones. However, this is misleading and incomplete: The grey lines show the traces reveal horizontal shifts. Thus for the cogent-003 algorithm FNMR for men is higher than for women at a fixed threshold but, at the same time, FMR is higher for women - see Figure 239. As access control systems almost always operate at a fixed threshold, the naive interpretation is incorrect.

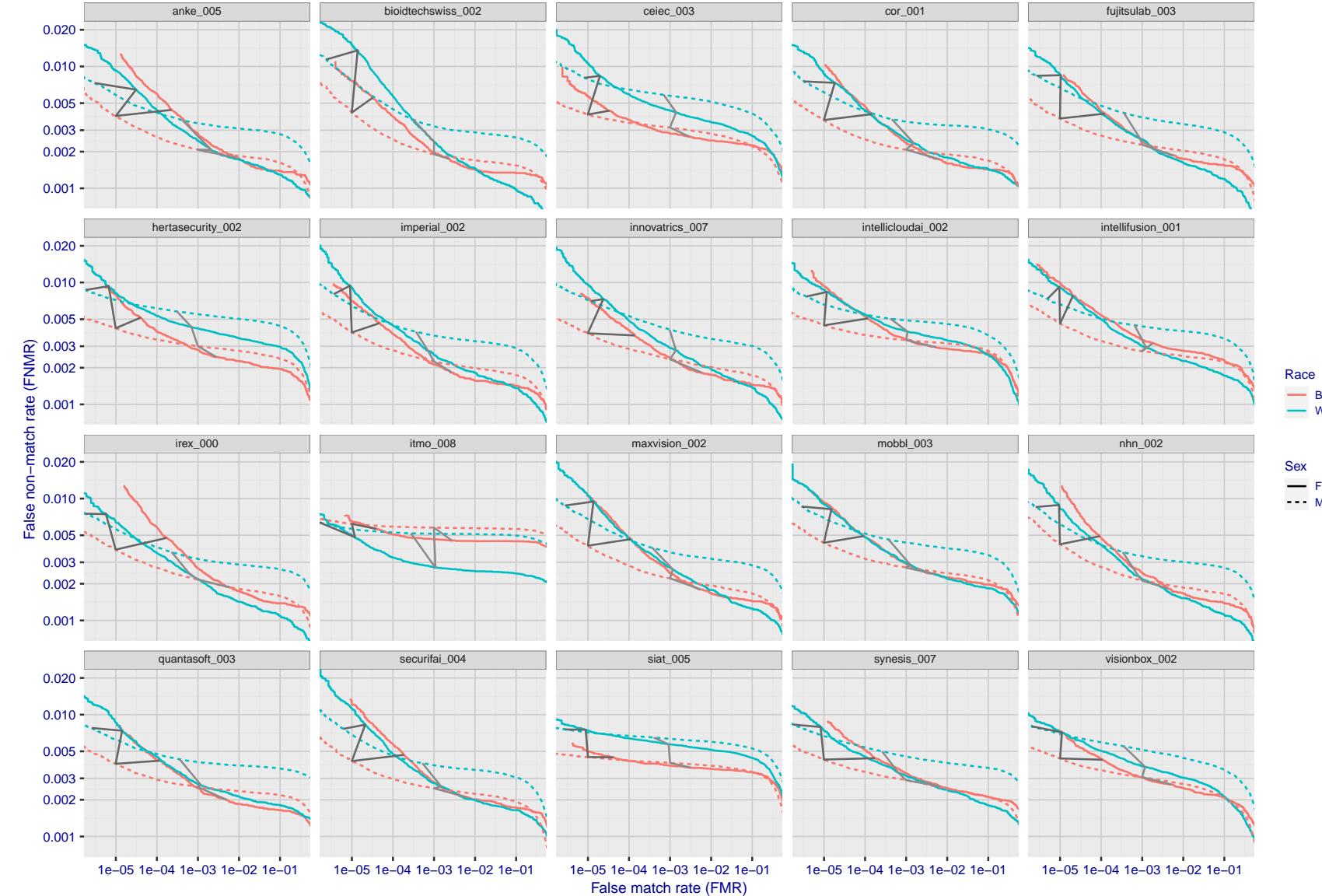


Figure 163: For the mugshot images, error tradeoff characteristics for white females, black females, black males and white males. The Z-shaped grey lines correspond to fixed thresholds, showing both FNMR and FMR vary at one T value. Note: Many of the plots will naively be read as saying women gives worse error rates than men because the solid traces lie above the dotted ones. However, this is misleading and incomplete: The grey lines show the traces reveal horizontal shifts. Thus for the cogent-003 algorithm FNMR for men is higher than for women at a fixed threshold but, at the same time, FMR is higher for women - see Figure 239. As access control systems almost always operate at a fixed threshold, the naive interpretation is incorrect.

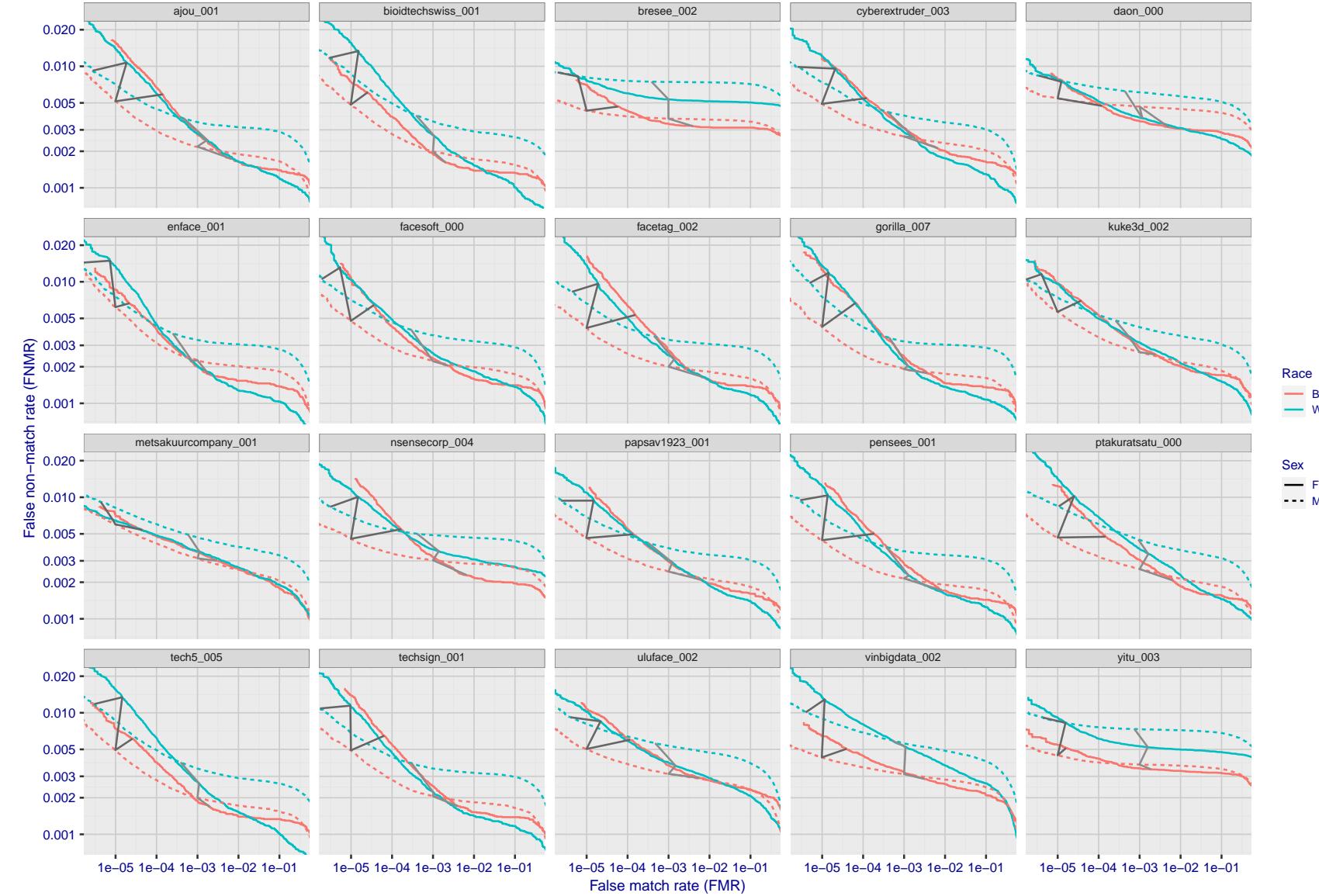


Figure 164: For the mugshot images, error tradeoff characteristics for white females, black females, black males and white males. The Z-shaped grey lines correspond to fixed thresholds, showing both FNMR and FMR vary at one T value. Note: Many of the plots will naively be read as saying women gives worse error rates than men because the solid traces lie above the dotted ones. However, this is misleading and incomplete: The grey lines show the traces reveal horizontal shifts. Thus for the cogent-003 algorithm FNMR for men is higher than for women at a fixed threshold but, at the same time, FMR is higher for women - see Figure 239. As access control systems almost always operate at a fixed threshold, the naive interpretation is incorrect.

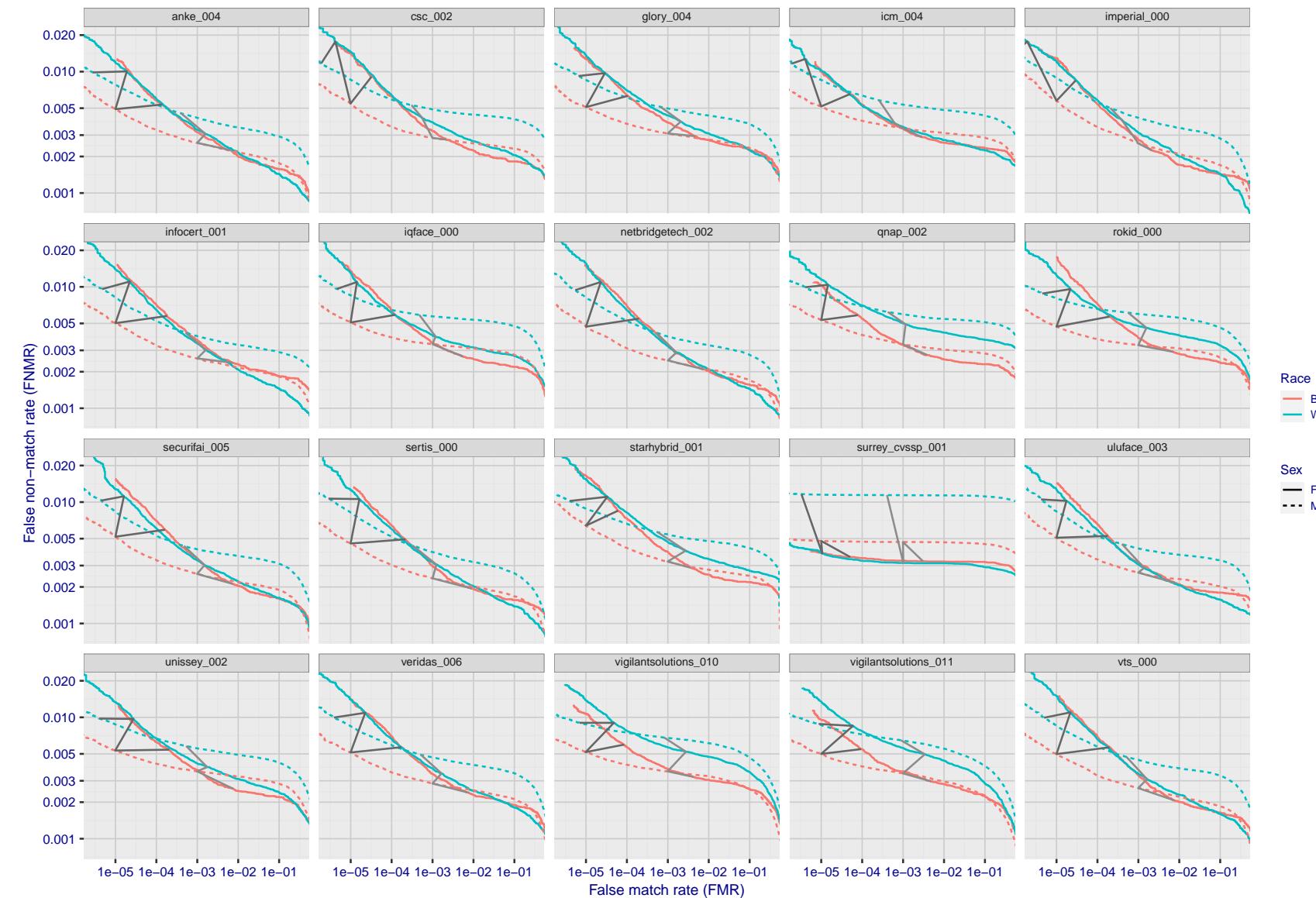


Figure 165: For the mugshot images, error tradeoff characteristics for white females, black females, black males and white males. The Z-shaped grey lines correspond to fixed thresholds, showing both FNMR and FMR vary at one T value. Note: Many of the plots will naively be read as saying women gives worse error rates than men because the solid traces lie above the dotted ones. However, this is misleading and incomplete: The grey lines show the traces reveal horizontal shifts. Thus for the cogent-003 algorithm FNMR for men is higher than for women at a fixed threshold but, at the same time, FMR is higher for women - see Figure 239. As access control systems almost always operate at a fixed threshold, the naive interpretation is incorrect.

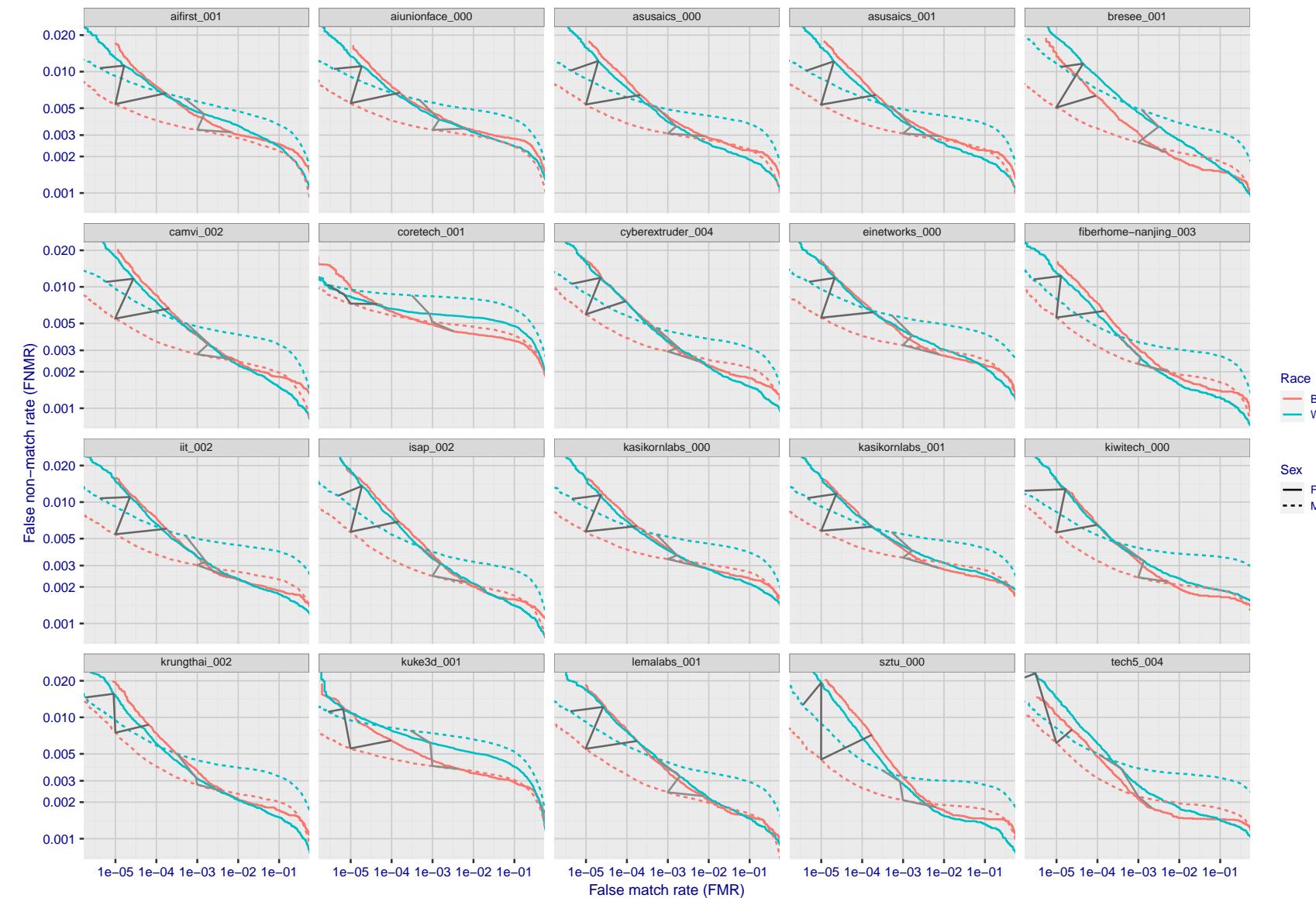


Figure 166: For the mugshot images, error tradeoff characteristics for white females, black females, black males and white males. The Z-shaped grey lines correspond to fixed thresholds, showing both FNMR and FMR vary at one T value. Note: Many of the plots will naively be read as saying women gives worse error rates than men because the solid traces lie above the dotted ones. However, this is misleading and incomplete: The grey lines show the traces reveal horizontal shifts. Thus for the cogent-003 algorithm FNMR for men is higher than for women at a fixed threshold but, at the same time, FMR is higher for women - see Figure 239. As access control systems almost always operate at a fixed threshold, the naive interpretation is incorrect.

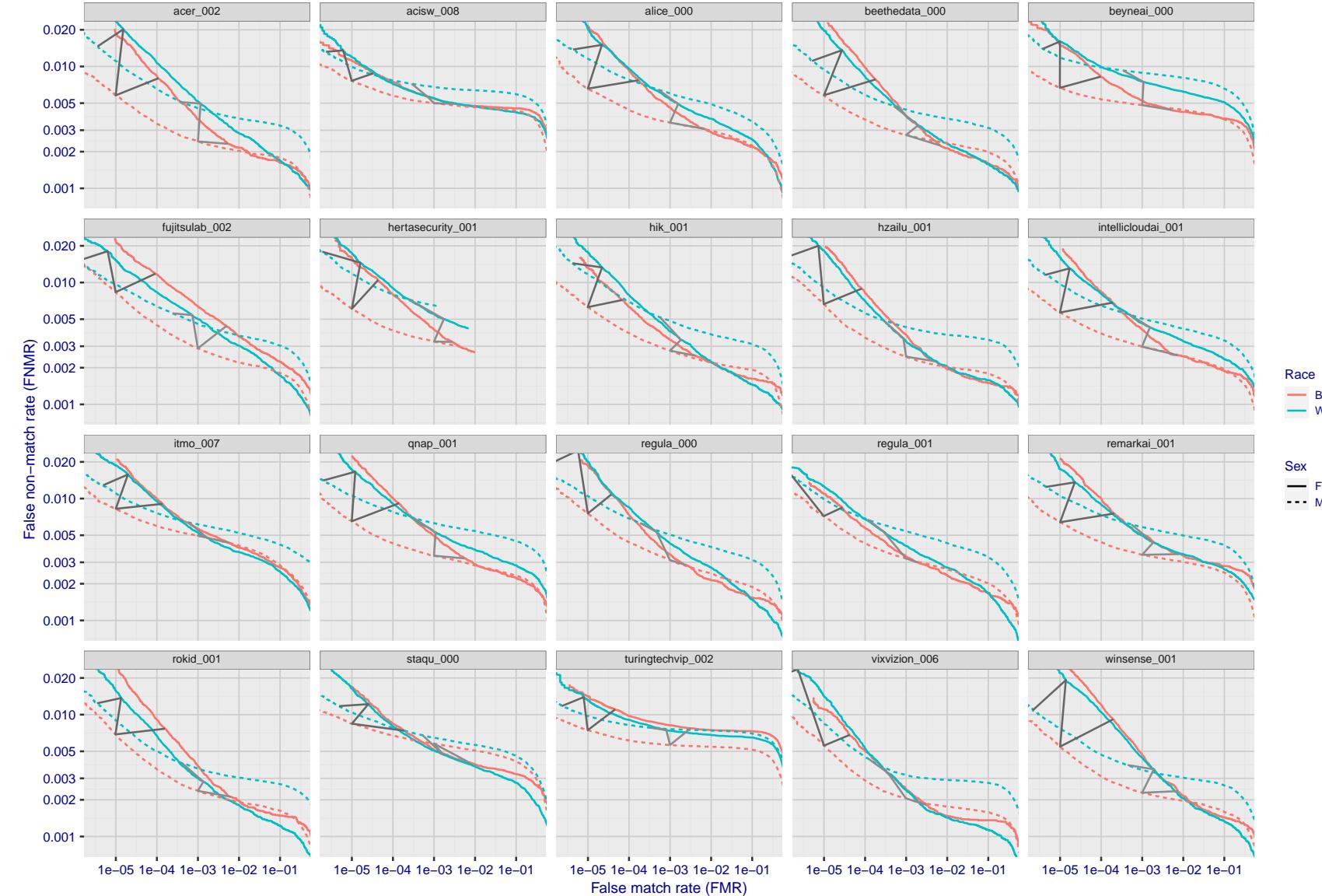


Figure 167: For the mugshot images, error tradeoff characteristics for white females, black females, black males and white males. The Z-shaped grey lines correspond to fixed thresholds, showing both FNMR and FMR vary at one T value. Note: Many of the plots will naively be read as saying women gives worse error rates than men because the solid traces lie above the dotted ones. However, this is misleading and incomplete: The grey lines show the traces reveal horizontal shifts. Thus for the cogent-003 algorithm FNMR for men is higher than for women at a fixed threshold but, at the same time, FMR is higher for women - see Figure 239. As access control systems almost always operate at a fixed threshold, the naive interpretation is incorrect.

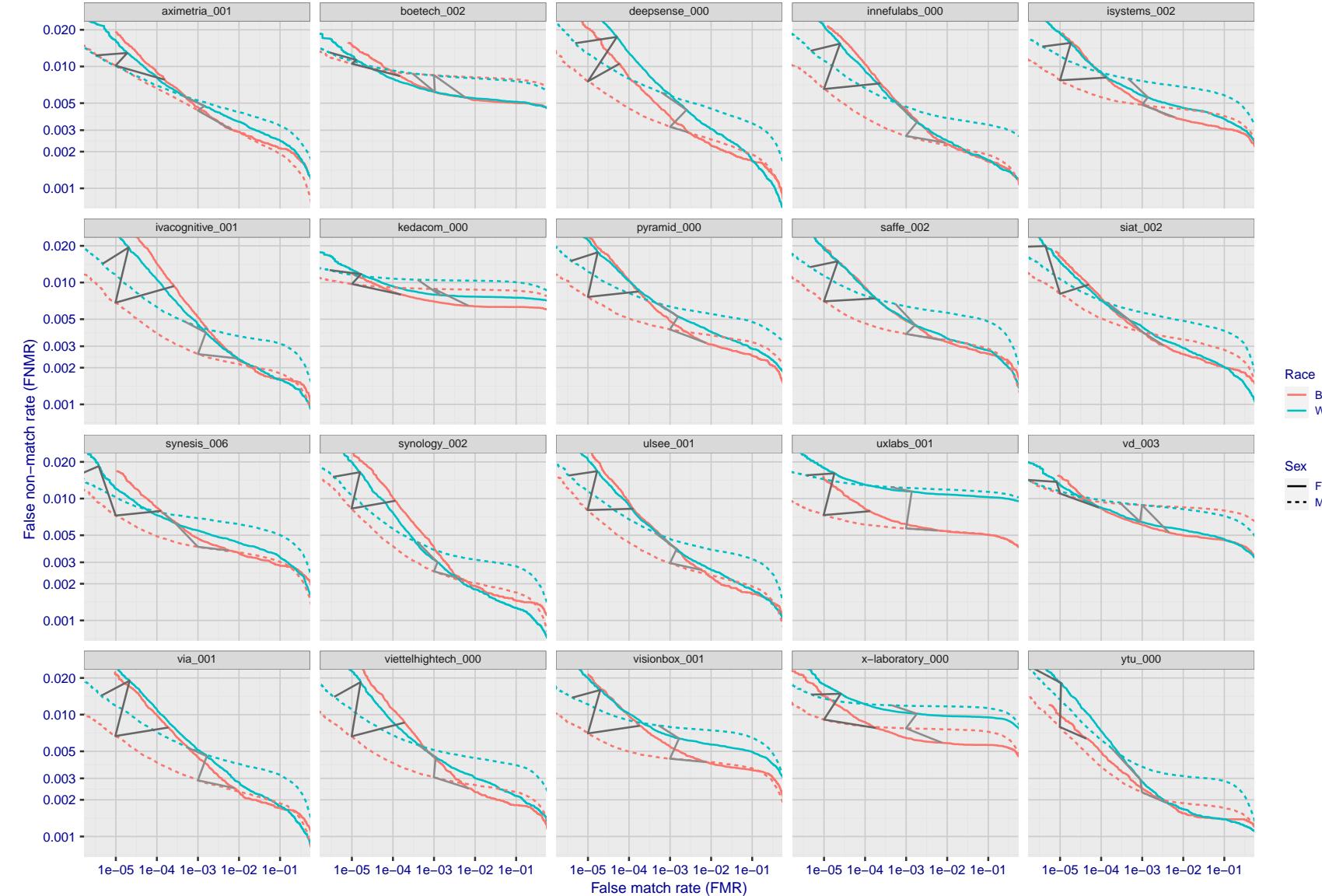


Figure 168: For the mugshot images, error tradeoff characteristics for white females, black females, black males and white males. The Z-shaped grey lines correspond to fixed thresholds, showing both FNMR and FMR vary at one T value. Note: Many of the plots will naively be read as saying women gives worse error rates than men because the solid traces lie above the dotted ones. However, this is misleading and incomplete: The grey lines show the traces reveal horizontal shifts. Thus for the cogent-003 algorithm FNMR for men is higher than for women at a fixed threshold but, at the same time, FMR is higher for women - see Figure 239. As access control systems almost always operate at a fixed threshold, the naive interpretation is incorrect.

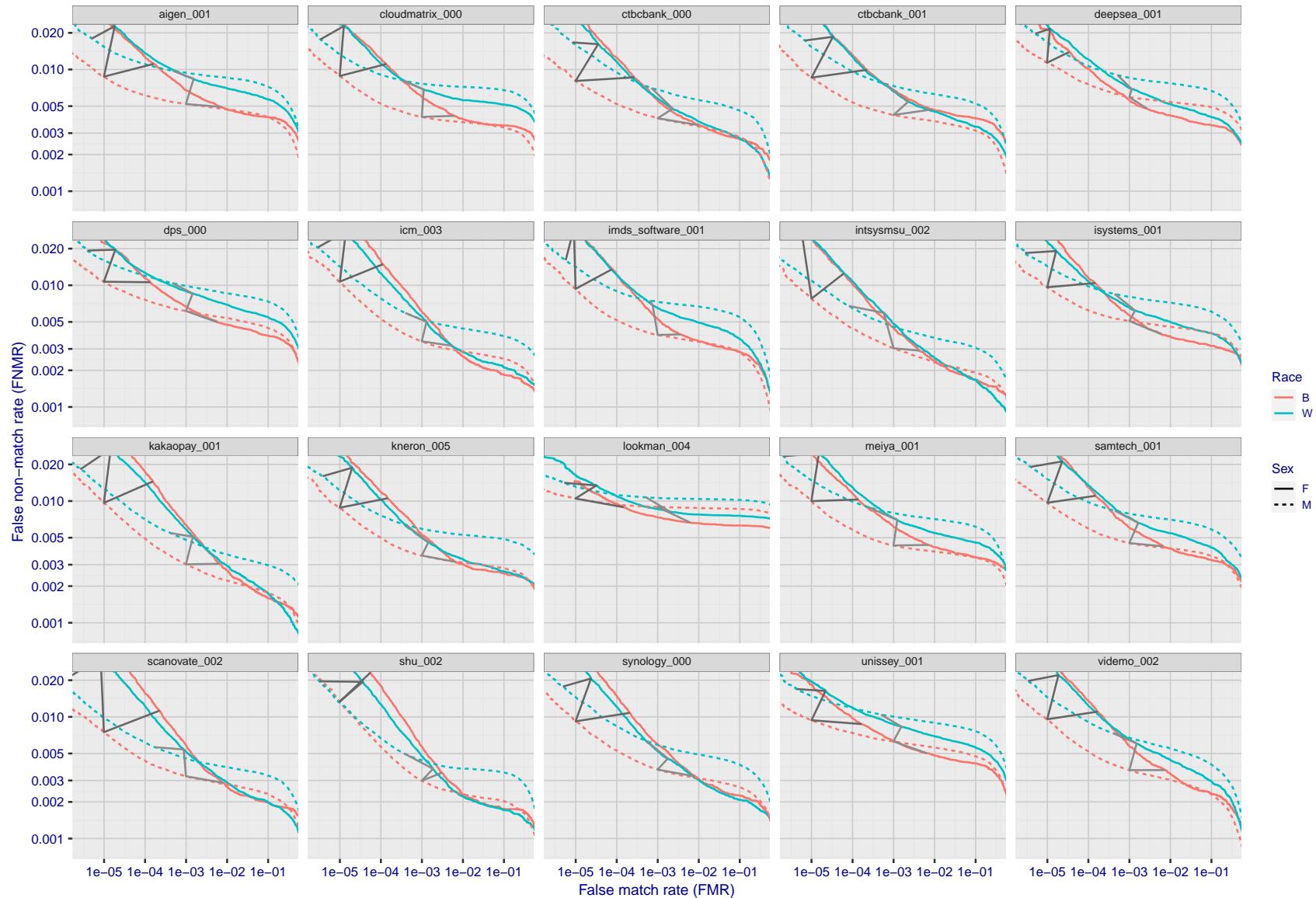


Figure 169: For the mugshot images, error tradeoff characteristics for white females, black females, black males and white males. The Z-shaped grey lines correspond to fixed thresholds, showing both FNMR and FMR vary at one T value. Note: Many of the plots will naively be read as saying women gives worse error rates than men because the solid traces lie above the dotted ones. However, this is misleading and incomplete: The grey lines show the traces reveal horizontal shifts. Thus for the cogent-003 algorithm FNMR for men is higher than for women at a fixed threshold but, at the same time, FMR is higher for women - see Figure 239. As access control systems almost always operate at a fixed threshold, the naive interpretation is incorrect.

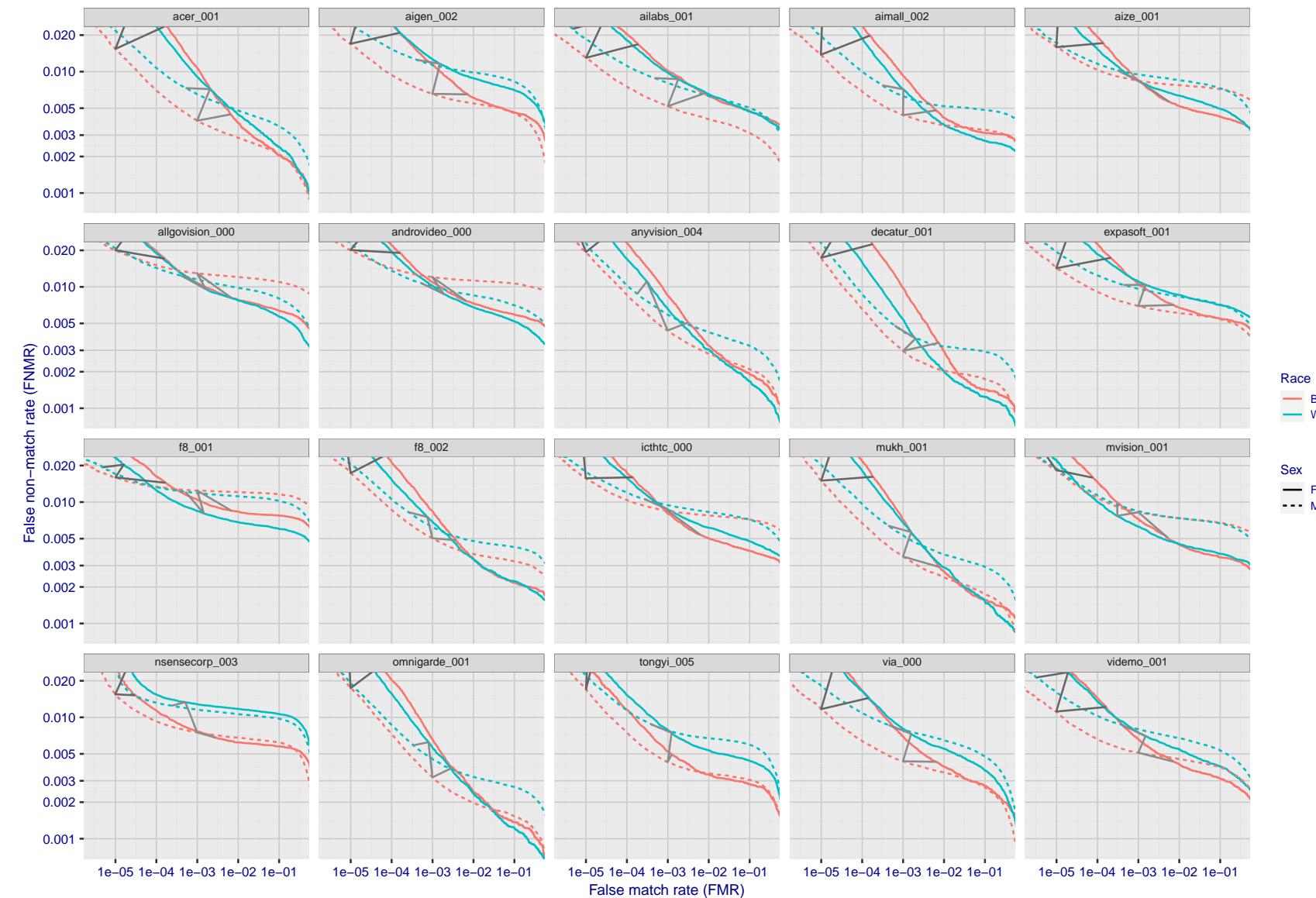


Figure 170: For the mugshot images, error tradeoff characteristics for white females, black females, black males and white males. The Z-shaped grey lines correspond to fixed thresholds, showing both FNMR and FMR vary at one T value. Note: Many of the plots will naively be read as saying women gives worse error rates than men because the solid traces lie above the dotted ones. However, this is misleading and incomplete: The grey lines show the traces reveal horizontal shifts. Thus for the cogent-003 algorithm FNMR for men is higher than for women at a fixed threshold but, at the same time, FMR is higher for women - see Figure 239. As access control systems almost always operate at a fixed threshold, the naive interpretation is incorrect.

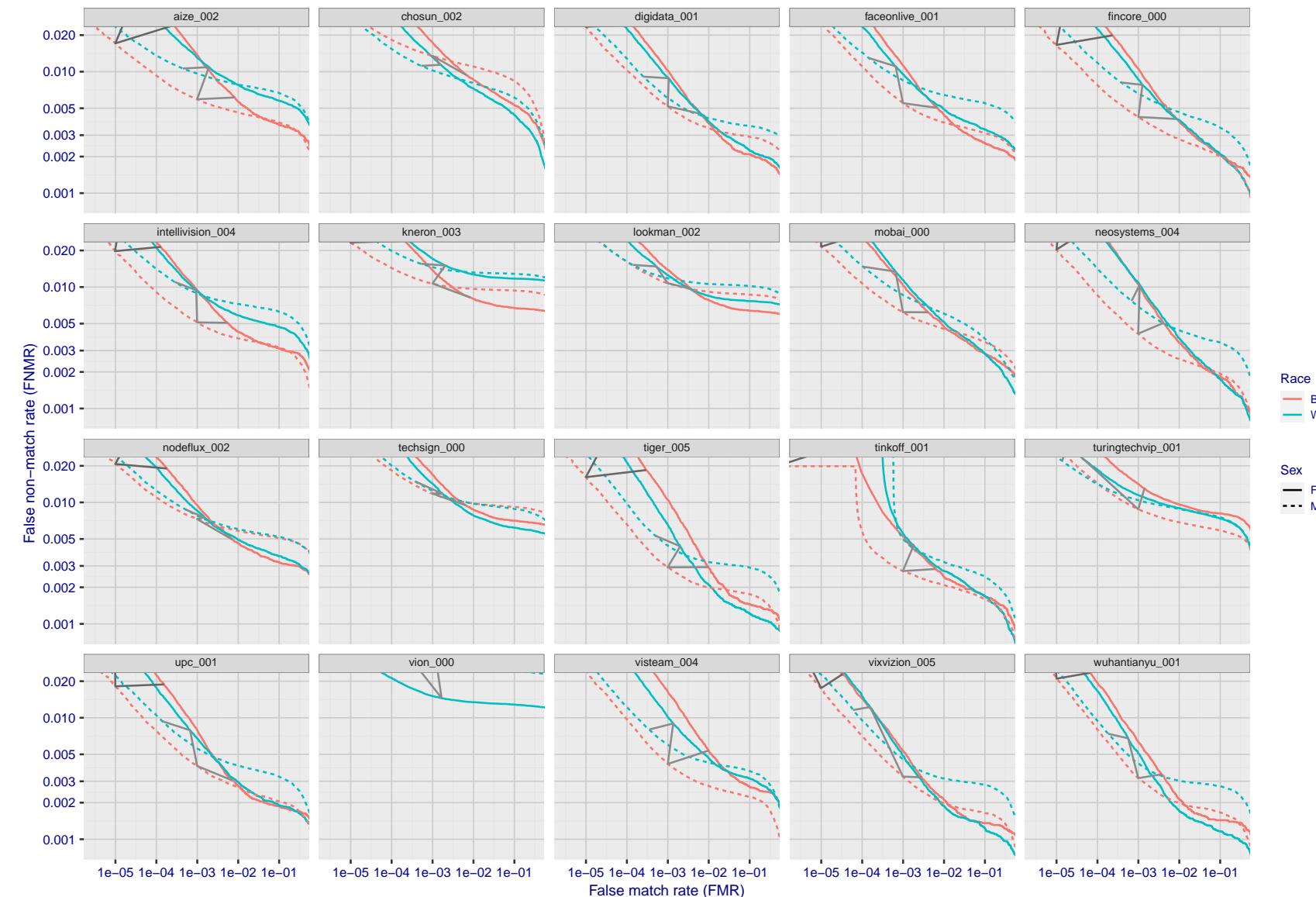


Figure 171: For the mugshot images, error tradeoff characteristics for white females, black females, black males and white males. The Z-shaped grey lines correspond to fixed thresholds, showing both FNMR and FMR vary at one T value. Note: Many of the plots will naively be read as saying women gives worse error rates than men because the solid traces lie above the dotted ones. However, this is misleading and incomplete: The grey lines show the traces reveal horizontal shifts. Thus for the cogent-003 algorithm FNMR for men is higher than for women at a fixed threshold but, at the same time, FMR is higher for women - see Figure 239. As access control systems almost always operate at a fixed threshold, the naive interpretation is incorrect.

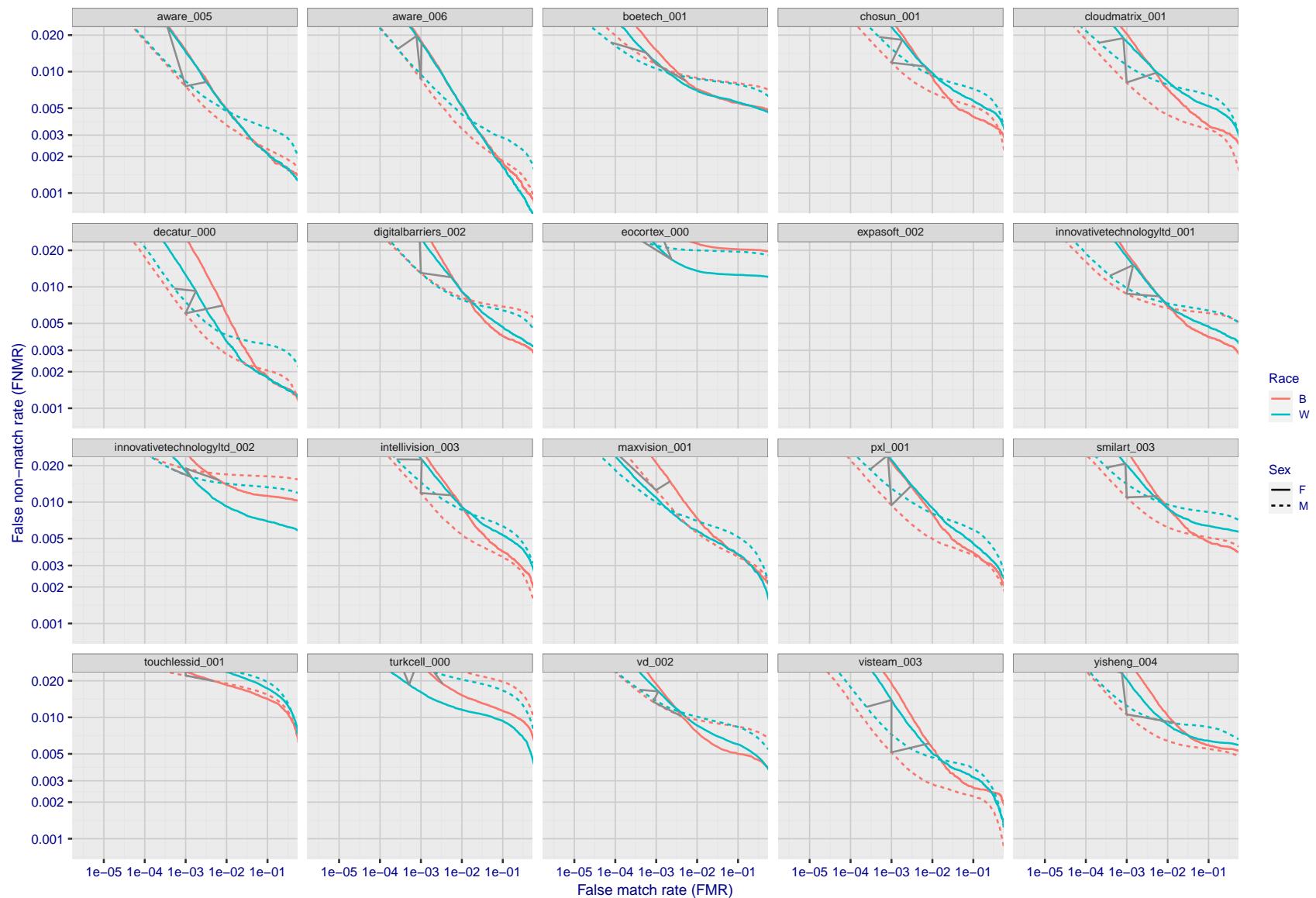


Figure 172: For the mugshot images, error tradeoff characteristics for white females, black females, black males and white males. The Z-shaped grey lines correspond to fixed thresholds, showing both FNMR and FMR vary at one T value. Note: Many of the plots will naively be read as saying women gives worse error rates than men because the solid traces lie above the dotted ones. However, this is misleading and incomplete: The grey lines show the traces reveal horizontal shifts. Thus for the cogent-003 algorithm FNMR for men is higher than for women at a fixed threshold but, at the same time, FMR is higher for women - see Figure 239. As access control systems almost always operate at a fixed threshold, the naive interpretation is incorrect.

2022/11/07 10:56:27

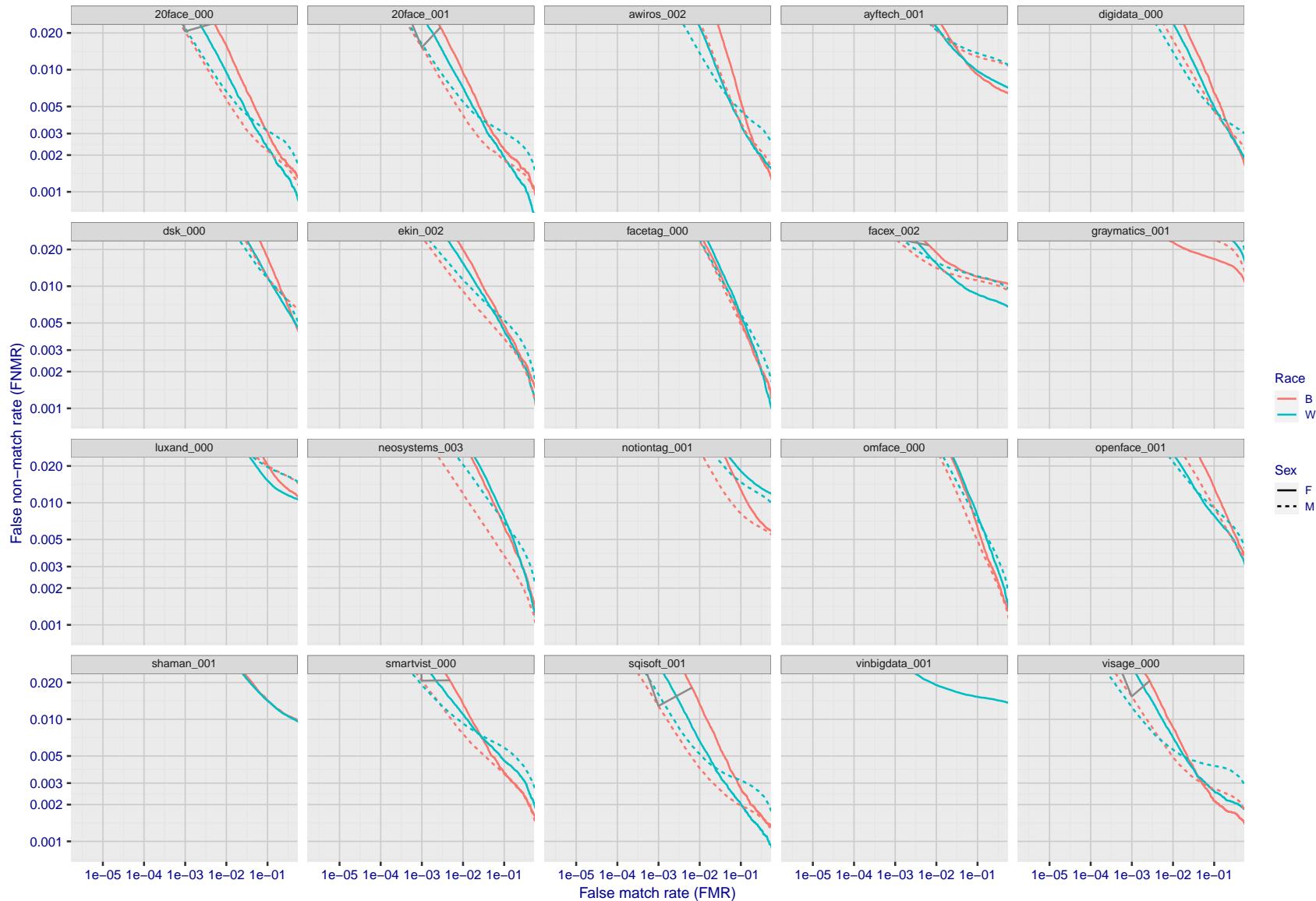


Figure 173: For the mugshot images, error tradeoff characteristics for white females, black females, black males and white males. The Z-shaped grey lines correspond to fixed thresholds, showing both FNMR and FMR vary at one T value. Note: Many of the plots will naively be read as saying women gives worse error rates than men because the solid traces lie above the dotted ones. However, this is misleading and incomplete: The grey lines show the traces reveal horizontal shifts. Thus for the cogent-003 algorithm FNMR for men is higher than for women at a fixed threshold but, at the same time, FMR is higher for women - see Figure 239. As access control systems almost always operate at a fixed threshold, the naive interpretation is incorrect.

FNMR(T)"False non-match rate"
"False match rate"

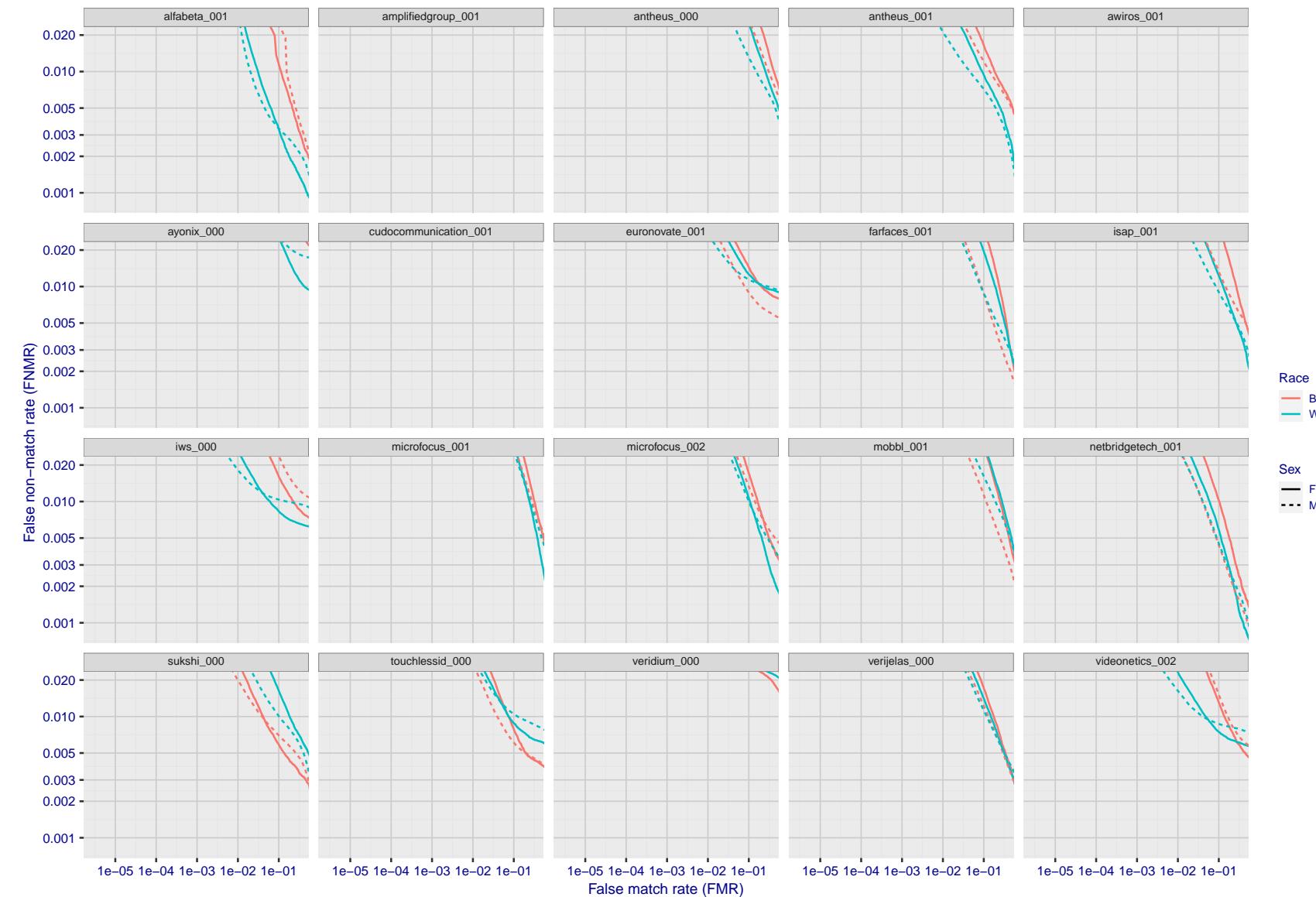


Figure 174: For the mugshot images, error tradeoff characteristics for white females, black females, black males and white males. The Z-shaped grey lines correspond to fixed thresholds, showing both FNMR and FMR vary at one T value. Note: Many of the plots will naively be read as saying women gives worse error rates than men because the solid traces lie above the dotted ones. However, this is misleading and incomplete: The grey lines show the traces reveal horizontal shifts. Thus for the cogent-003 algorithm FNMR for men is higher than for women at a fixed threshold but, at the same time, FMR is higher for women - see Figure 239. As access control systems almost always operate at a fixed threshold, the naive interpretation is incorrect.

2022/11/07 10:56:27

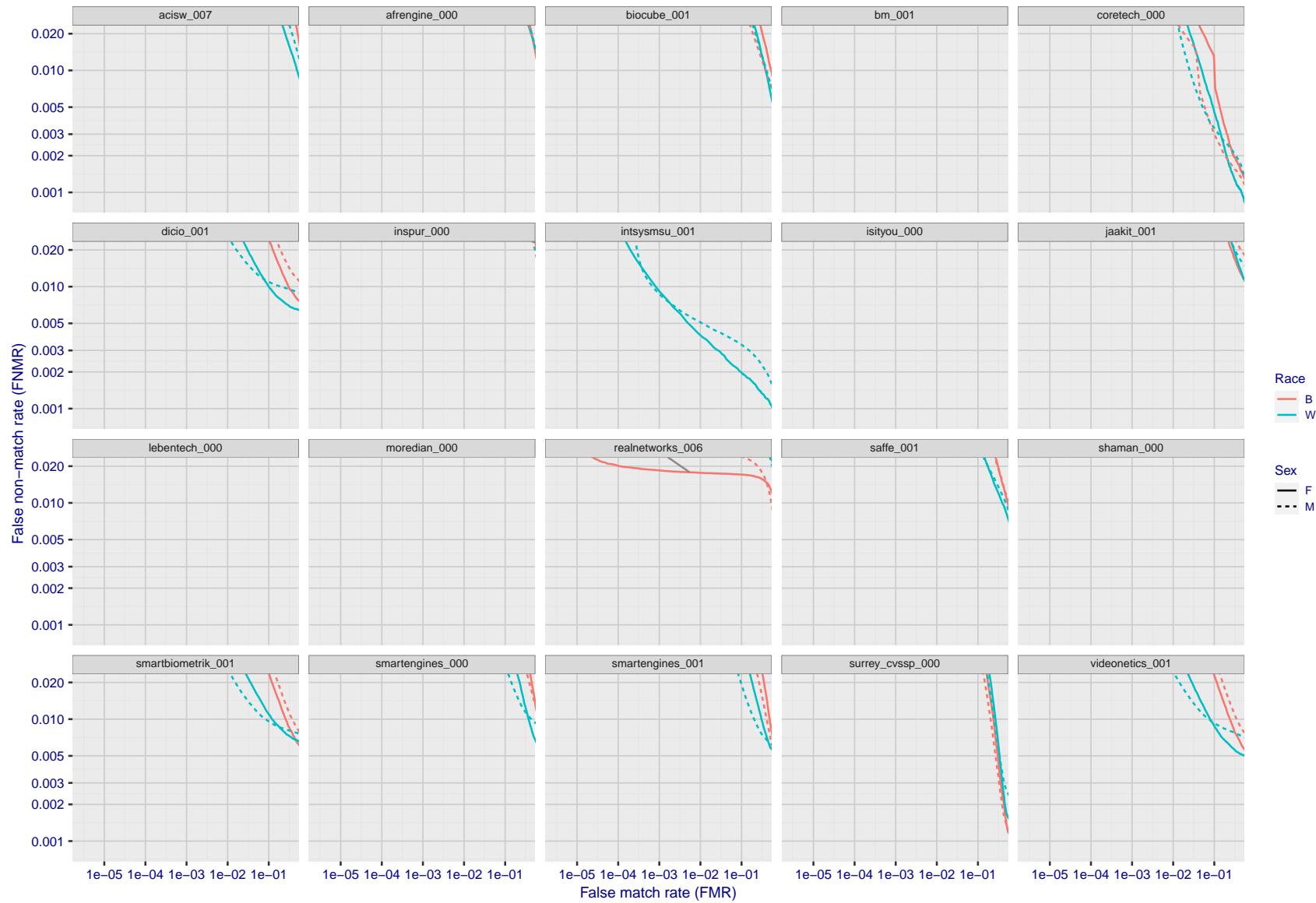


Figure 175: For the mugshot images, error tradeoff characteristics for white females, black females, black males and white males. The Z-shaped grey lines correspond to fixed thresholds, showing both FNMR and FMR vary at one T value. Note: Many of the plots will naively be read as saying women gives worse error rates than men because the solid traces lie above the dotted ones. However, this is misleading and incomplete: The grey lines show the traces reveal horizontal shifts. Thus for the cogent-003 algorithm FNMR for men is higher than for women at a fixed threshold but, at the same time, FMR is higher for women - see Figure 239. As access control systems almost always operate at a fixed threshold, the naive interpretation is incorrect.

FNMR(T)"False non-match rate"
"False match rate"

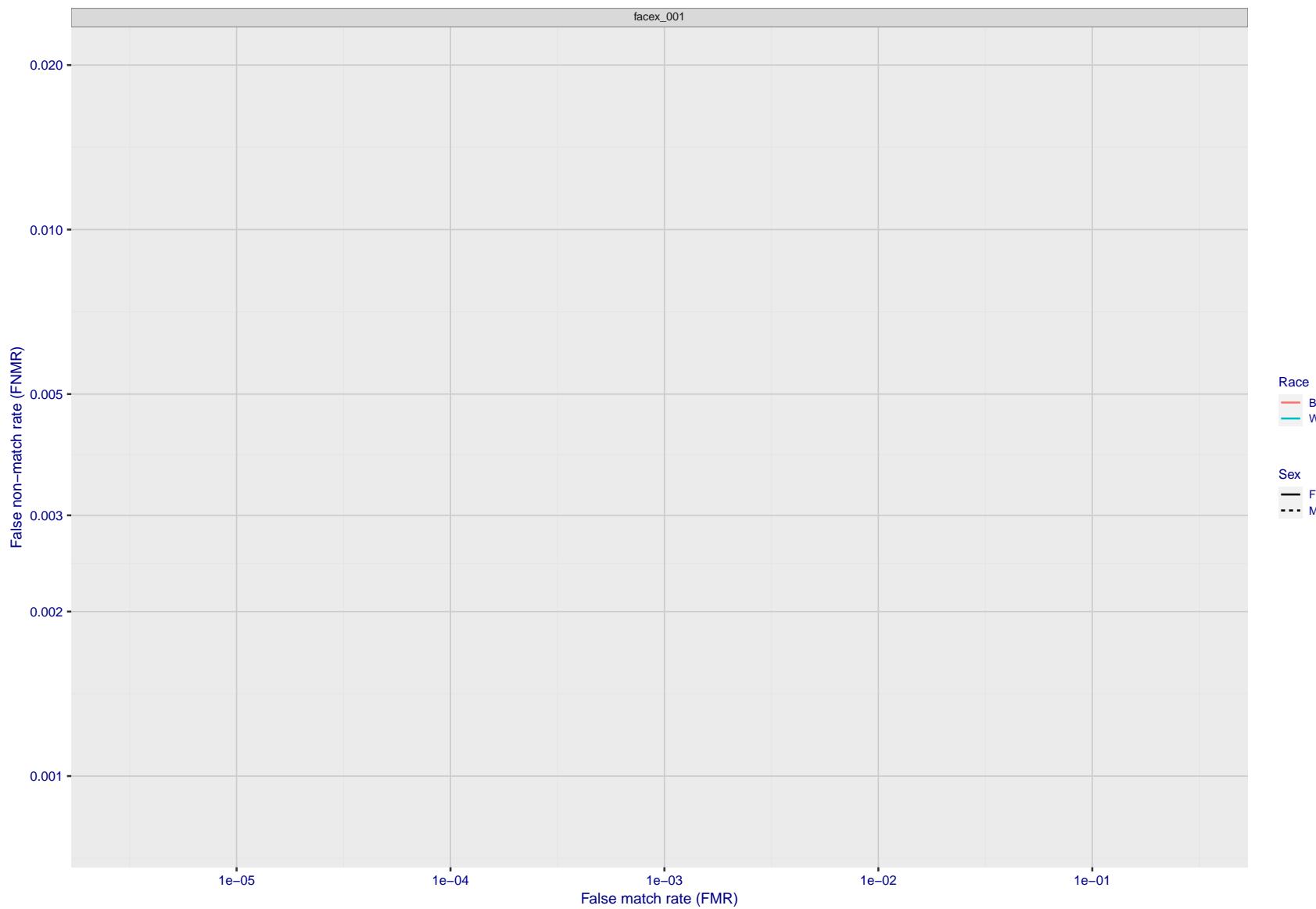


Figure 176: For the mugshot images, error tradeoff characteristics for white females, black females, black males and white males. The Z-shaped grey lines correspond to fixed thresholds, showing both FNMR and FMR vary at one T value. Note: Many of the plots will naively be read as saying women gives worse error rates than men because the solid traces lie above the dotted ones. However, this is misleading and incomplete: The grey lines show the traces reveal horizontal shifts. Thus for the cogent-003 algorithm FNMR for men is higher than for women at a fixed threshold but, at the same time, FMR is higher for women - see Figure 239. As access control systems almost always operate at a fixed threshold, the naive interpretation is incorrect.

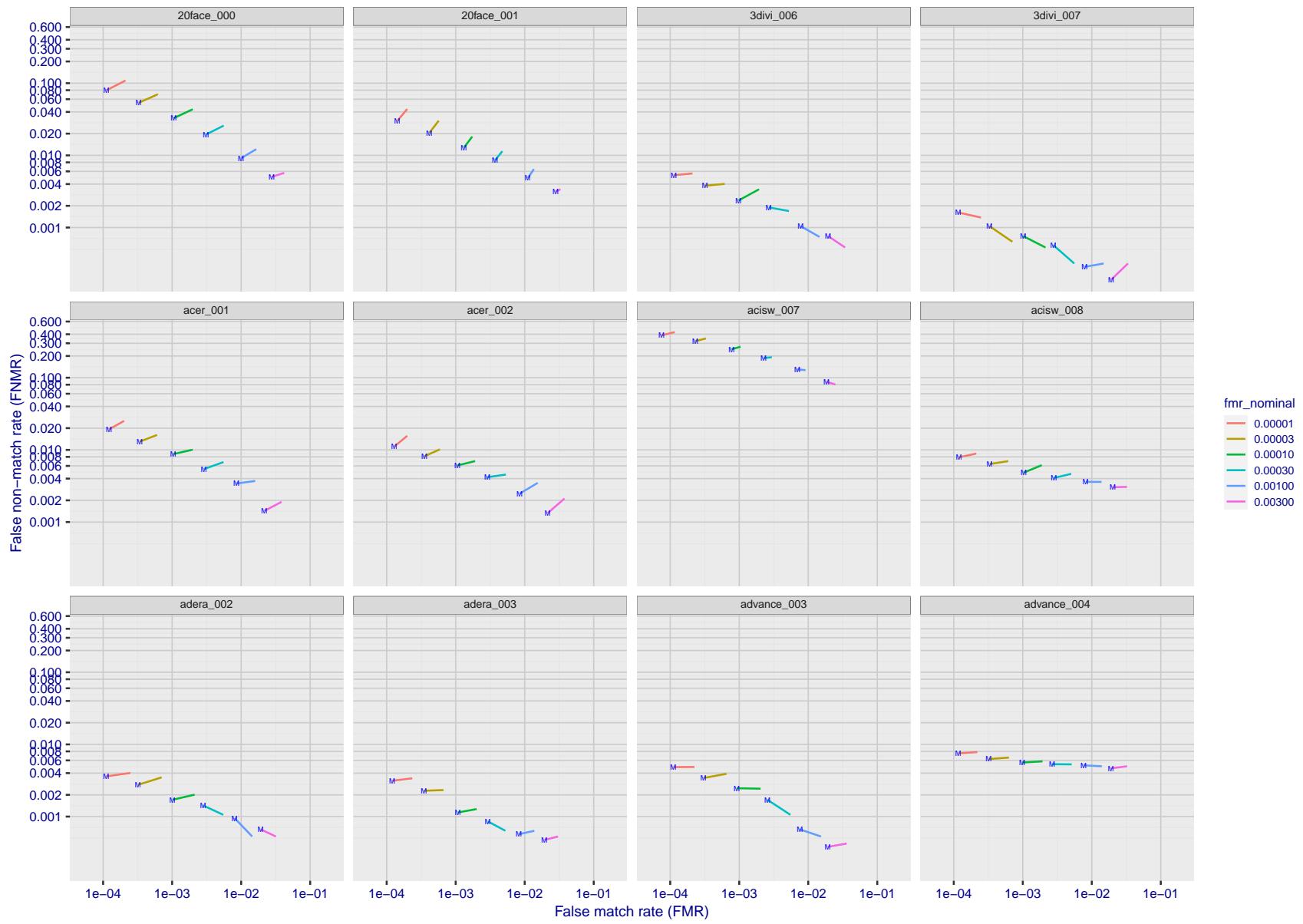


Figure 177: For the visa images, FNMR and FMR at six operating points along the DET characteristic. At each point a line is drawn between $(FMR, FNMR)_{MALE}$ and $(FMR, FNMR)_{FEMALE}$ showing how which sex has lower FMR and/or FNMR. The "M" label denotes male, the other end of the line corresponds to female. The six operating thresholds are selected to give the nominal false match rates given in the legend, and are computed over all impostor pairs regardless of age, sex, and place of birth. The plotted FMR values are broadly an order of magnitude larger than the nominal rates because FMR is computed over demographically-matched impostor pairs i.e individuals of the same sex, from the same geographic region (see section 3.6.1), and the same age group (see section 3.6.2).

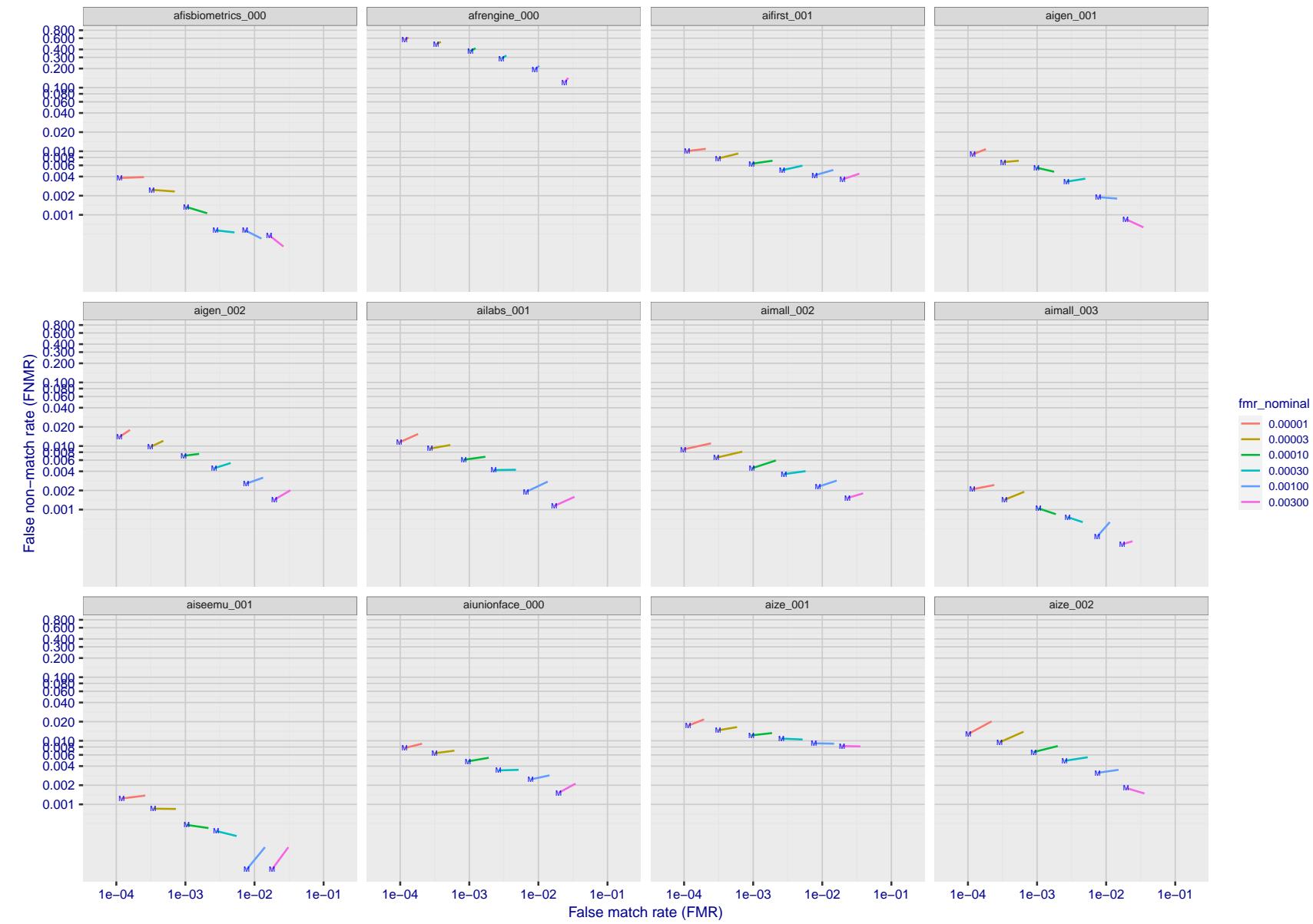


Figure 178: For the visa images, FNMR and FMR at six operating points along the DET characteristic. At each point a line is drawn between $(FMR, FNMR)_{MALE}$ and $(FMR, FNMR)_{FEMALE}$ showing how which sex has lower FMR and/or FNMR. The "M" label denotes male, the other end of the line corresponds to female. The six operating thresholds are selected to give the nominal false match rates given in the legend, and are computed over all impostor pairs regardless of age, sex, and place of birth. The plotted FMR values are broadly an order of magnitude larger than the nominal rates because FMR is computed over demographically-matched impostor pairs i.e individuals of the same sex, from the same geographic region (see section 3.6.1), and the same age group (see section 3.6.2).

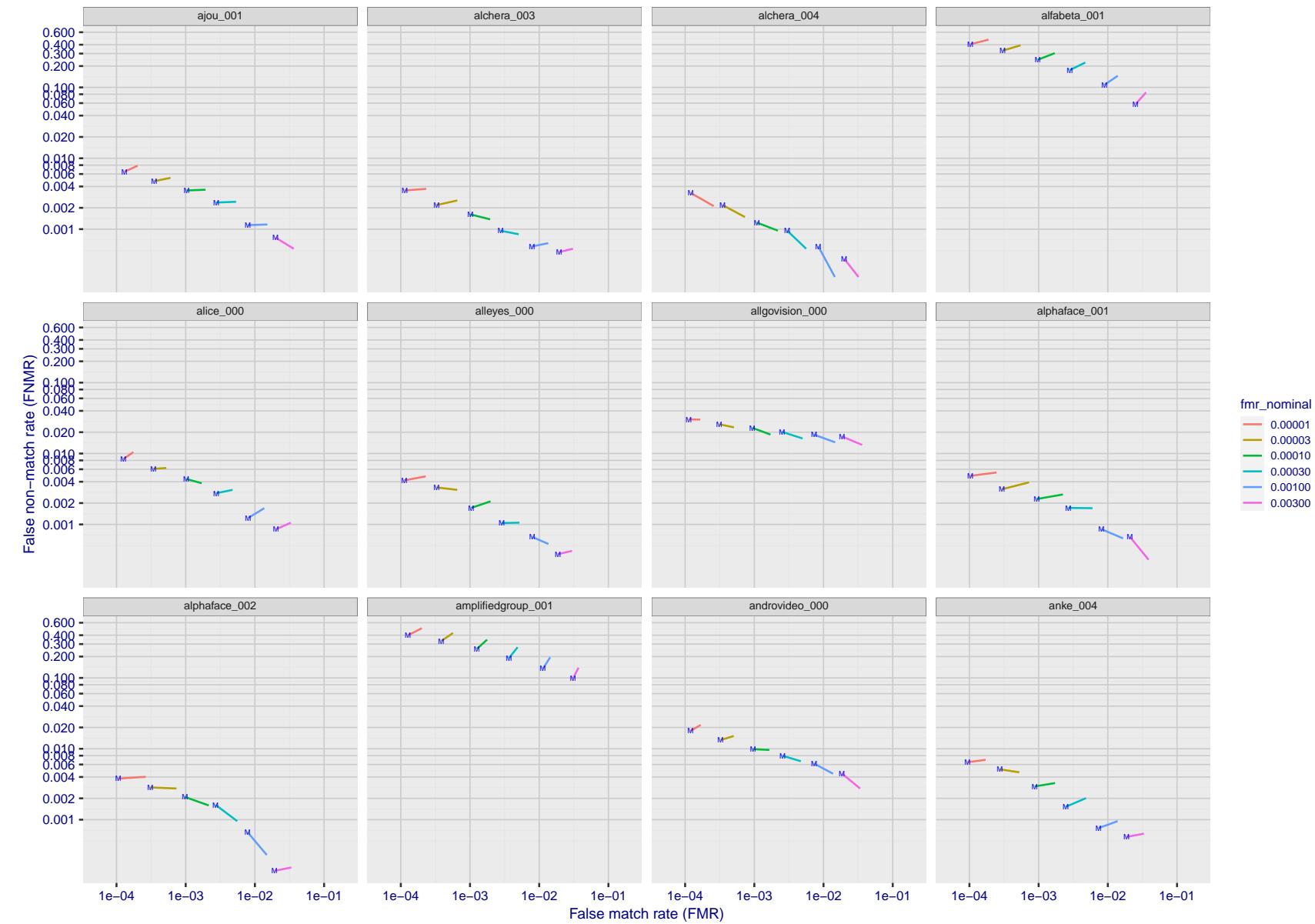


Figure 179: For the visa images, FNMR and FMR at six operating points along the DET characteristic. At each point a line is drawn between $(FMR, FNMR)_{MALE}$ and $(FMR, FNMR)_{FEMALE}$ showing how which sex has lower FMR and/or FNMR. The "M" label denotes male, the other end of the line corresponds to female. The six operating thresholds are selected to give the nominal false match rates given in the legend, and are computed over all impostor pairs regardless of age, sex, and place of birth. The plotted FMR values are broadly an order of magnitude larger than the nominal rates because FMR is computed over demographically-matched impostor pairs i.e individuals of the same sex, from the same geographic region (see section 3.6.1), and the same age group (see section 3.6.2).

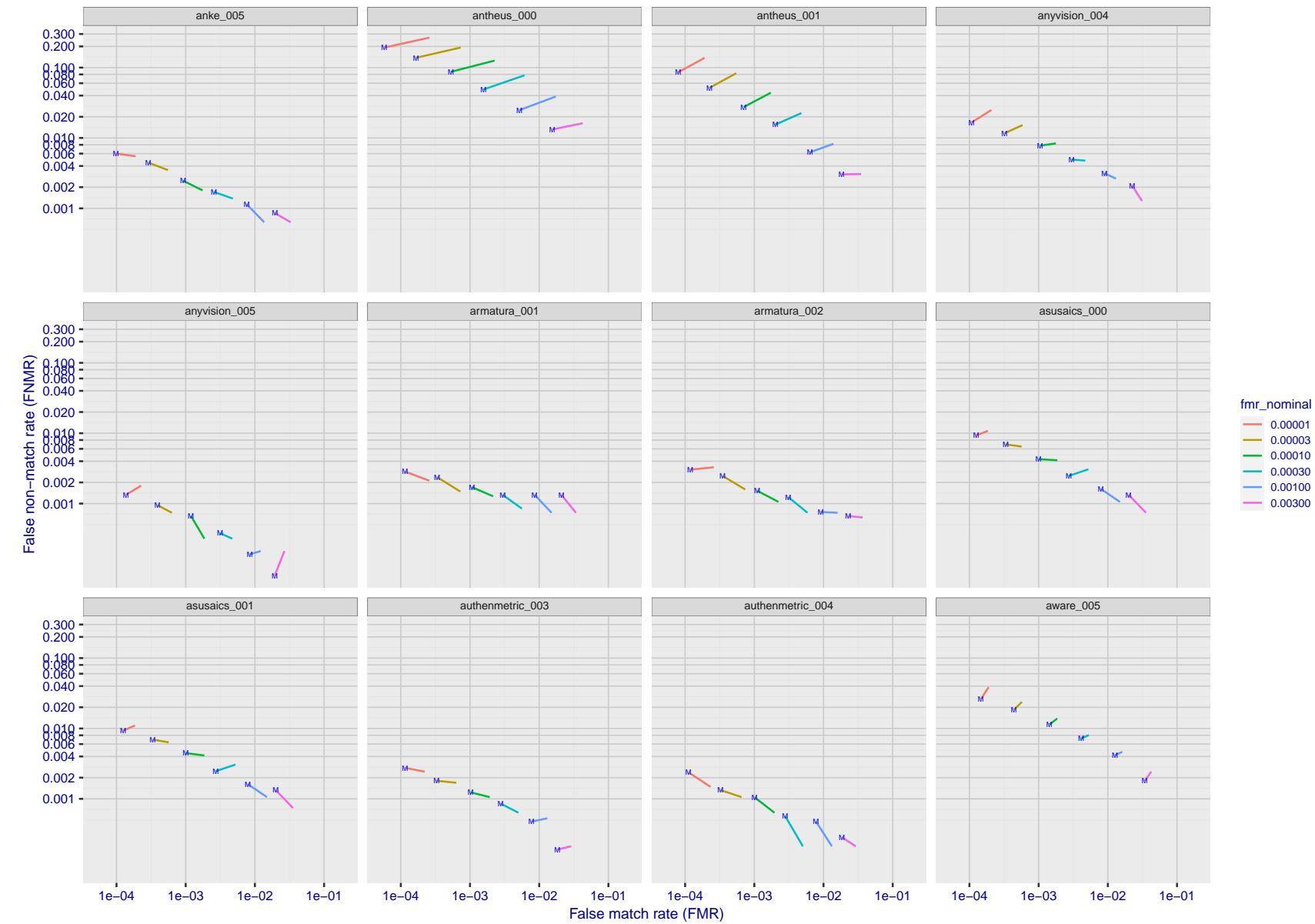


Figure 180: For the visa images, FNMR and FMR at six operating points along the DET characteristic. At each point a line is drawn between $(FMR, FNMR)_{MALE}$ and $(FMR, FNMR)_{FEMALE}$ showing how which sex has lower FMR and/or FNMR. The "M" label denotes male, the other end of the line corresponds to female. The six operating thresholds are selected to give the nominal false match rates given in the legend, and are computed over all impostor pairs regardless of age, sex, and place of birth. The plotted FMR values are broadly an order of magnitude larger than the nominal rates because FMR is computed over demographically-matched impostor pairs i.e individuals of the same sex, from the same geographic region (see section 3.6.1), and the same age group (see section 3.6.2).

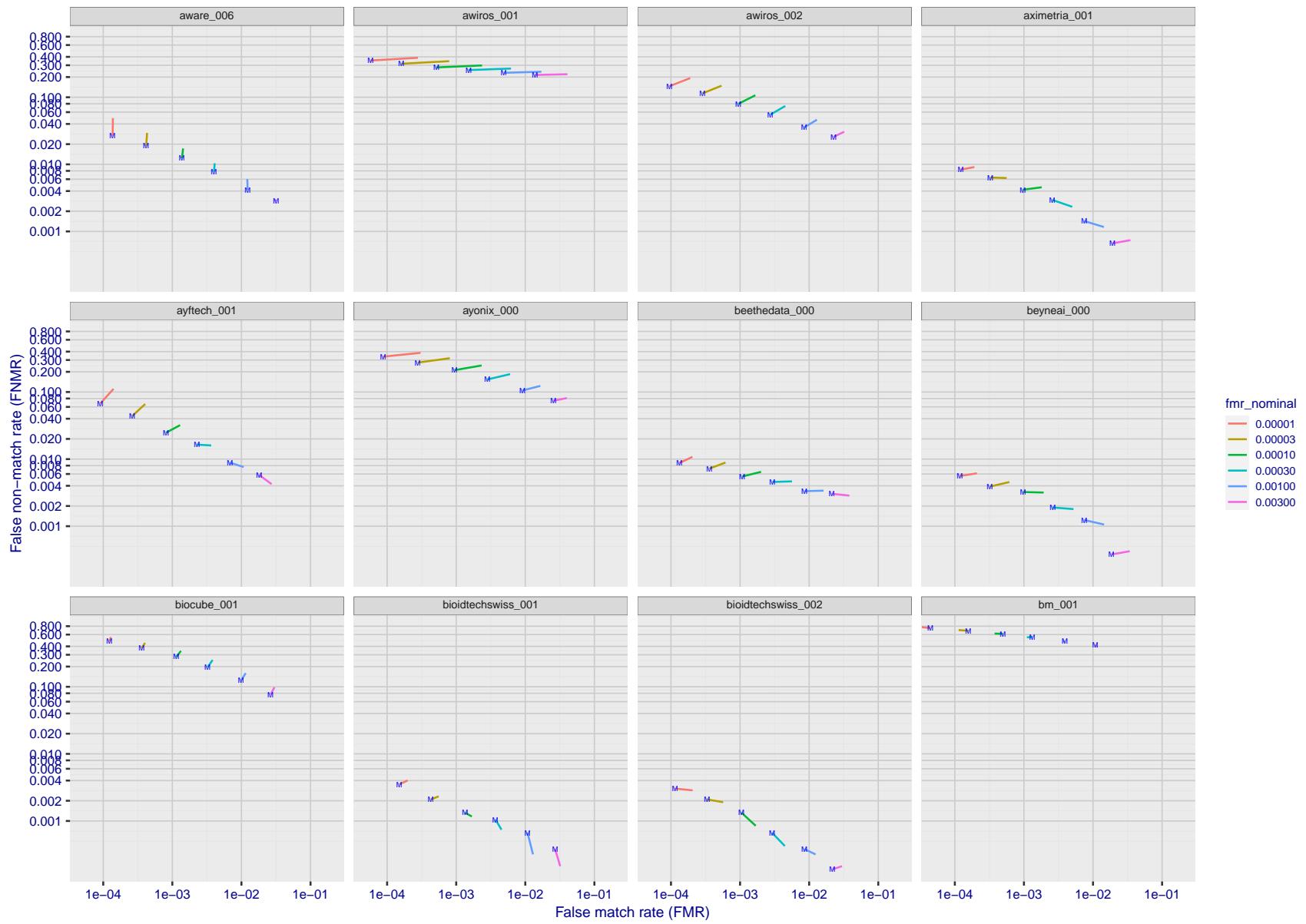


Figure 181: For the visa images, FNMR and FMR at six operating points along the DET characteristic. At each point a line is drawn between $(FMR, FNMR)_{MALE}$ and $(FMR, FNMR)_{FEMALE}$ showing how which sex has lower FMR and/or FNMR. The "M" label denotes male, the other end of the line corresponds to female. The six operating thresholds are selected to give the nominal false match rates given in the legend, and are computed over all impostor pairs regardless of age, sex, and place of birth. The plotted FMR values are broadly an order of magnitude larger than the nominal rates because FMR is computed over demographically-matched impostor pairs i.e individuals of the same sex, from the same geographic region (see section 3.6.1), and the same age group (see section 3.6.2).

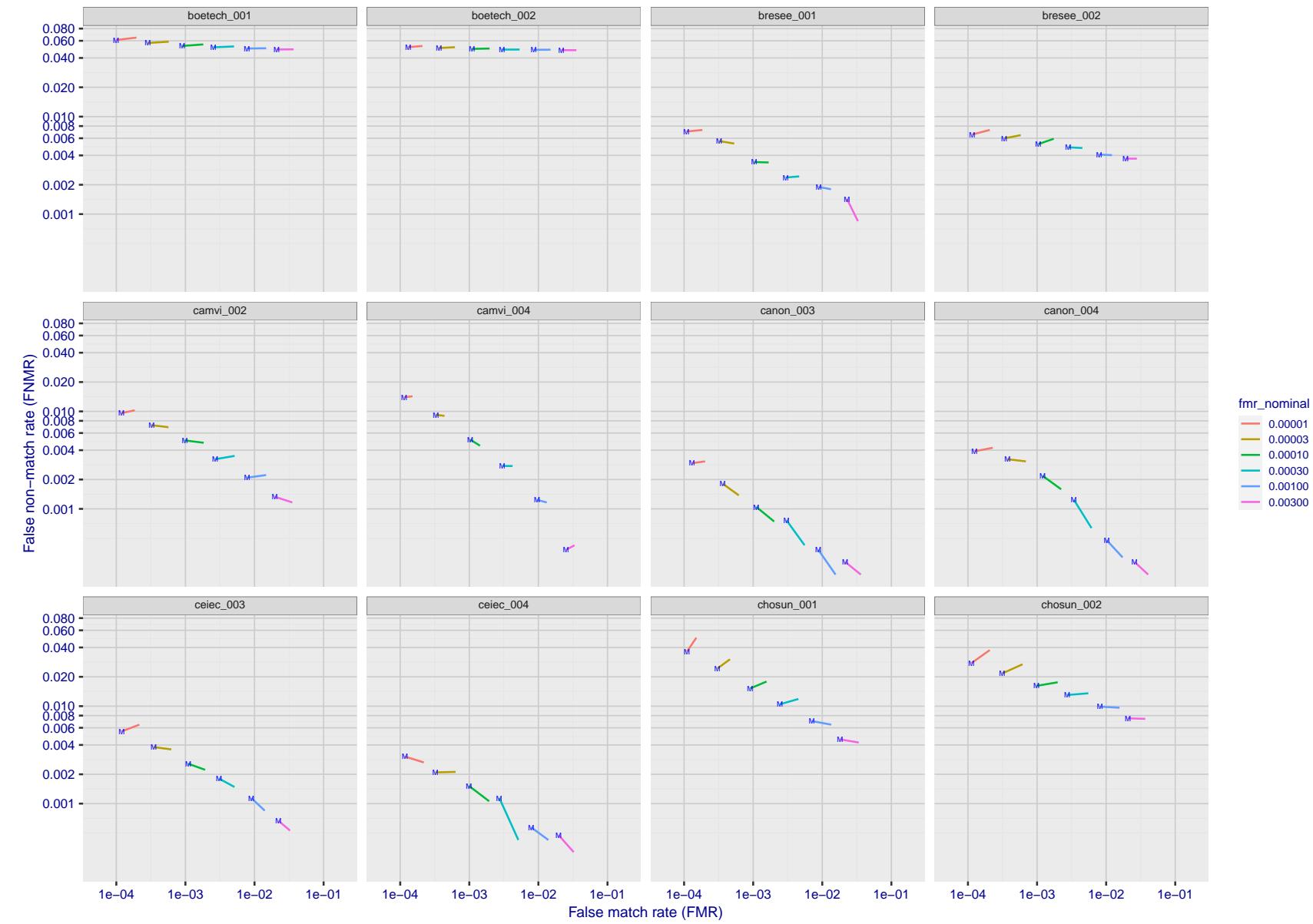


Figure 182: For the visa images, FNMR and FMR at six operating points along the DET characteristic. At each point a line is drawn between $(FMR, FNMR)_{MALE}$ and $(FMR, FNMR)_{FEMALE}$ showing how which sex has lower FMR and/or FNMR. The "M" label denotes male, the other end of the line corresponds to female. The six operating thresholds are selected to give the nominal false match rates given in the legend, and are computed over all impostor pairs regardless of age, sex, and place of birth. The plotted FMR values are broadly an order of magnitude larger than the nominal rates because FMR is computed over demographically-matched impostor pairs i.e individuals of the same sex, from the same geographic region (see section 3.6.1), and the same age group (see section 3.6.2).

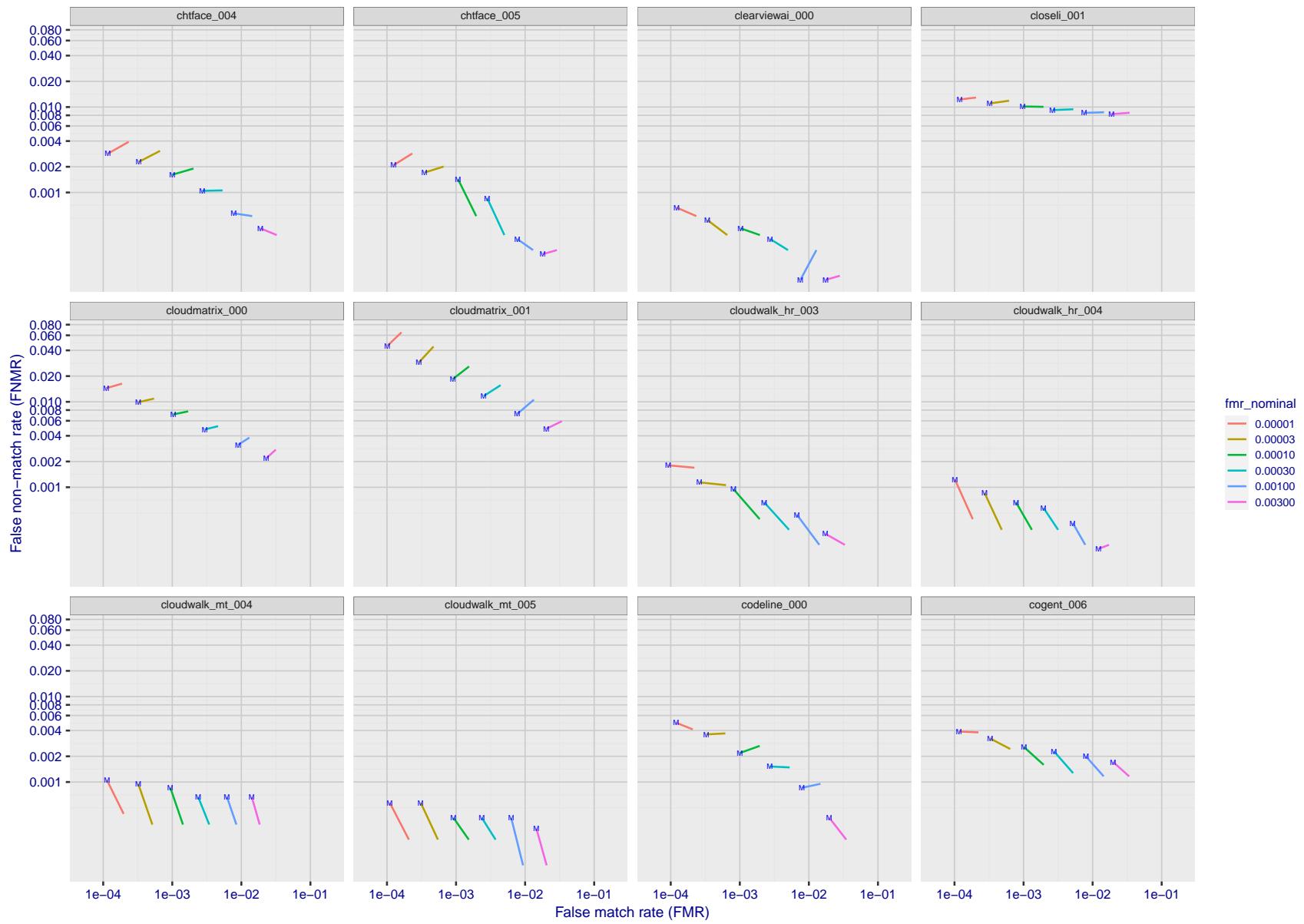


Figure 183: For the visa images, FNMR and FMR at six operating points along the DET characteristic. At each point a line is drawn between $(FMR, FNMR)_{MALE}$ and $(FMR, FNMR)_{FEMALE}$ showing how which sex has lower FMR and/or FNMR. The "M" label denotes male, the other end of the line corresponds to female. The six operating thresholds are selected to give the nominal false match rates given in the legend, and are computed over all impostor pairs regardless of age, sex, and place of birth. The plotted FMR values are broadly an order of magnitude larger than the nominal rates because FMR is computed over demographically-matched impostor pairs i.e individuals of the same sex, from the same geographic region (see section 3.6.1), and the same age group (see section 3.6.2).

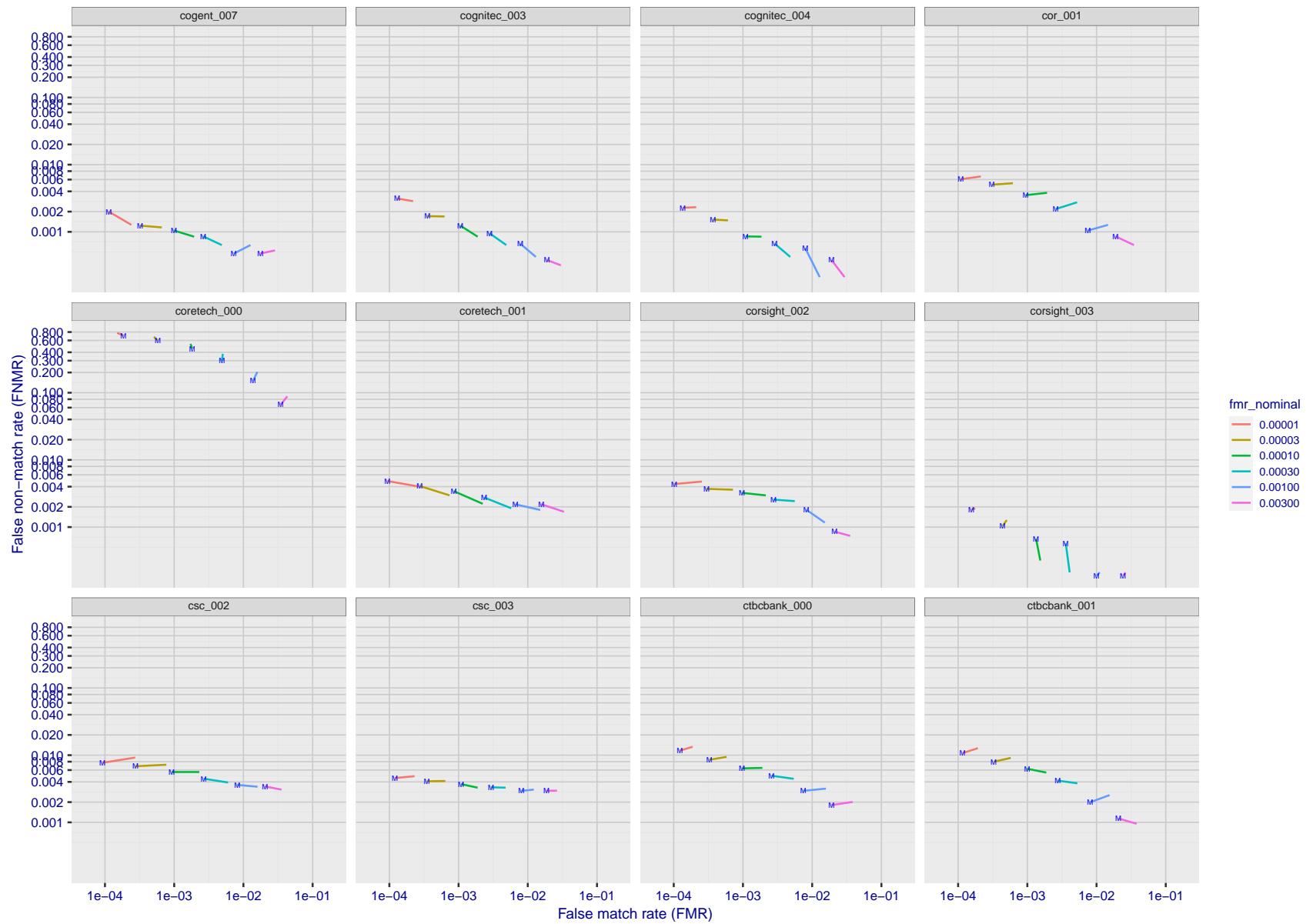


Figure 184: For the visa images, FNMR and FMR at six operating points along the DET characteristic. At each point a line is drawn between $(FMR, FNMR)_{MALE}$ and $(FMR, FNMR)_{FEMALE}$ showing how which sex has lower FMR and/or FNMR. The "M" label denotes male, the other end of the line corresponds to female. The six operating thresholds are selected to give the nominal false match rates given in the legend, and are computed over all impostor pairs regardless of age, sex, and place of birth. The plotted FMR values are broadly an order of magnitude larger than the nominal rates because FMR is computed over demographically-matched impostor pairs i.e individuals of the same sex, from the same geographic region (see section 3.6.1), and the same age group (see section 3.6.2).

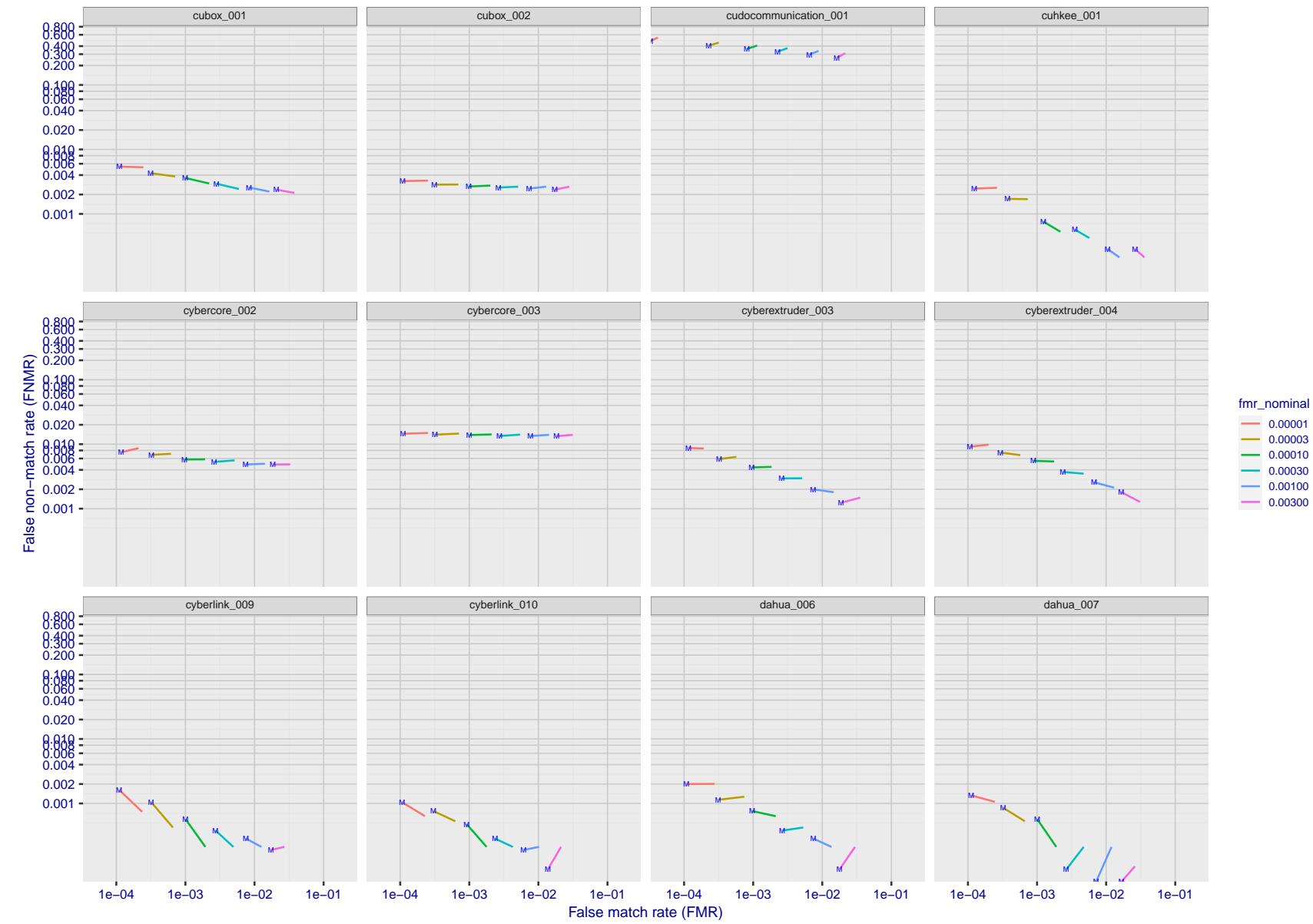


Figure 185: For the visa images, FNMR and FMR at six operating points along the DET characteristic. At each point a line is drawn between $(FMR, FNMR)_{MALE}$ and $(FMR, FNMR)_{FEMALE}$ showing how which sex has lower FMR and/or FNMR. The "M" label denotes male, the other end of the line corresponds to female. The six operating thresholds are selected to give the nominal false match rates given in the legend, and are computed over all impostor pairs regardless of age, sex, and place of birth. The plotted FMR values are broadly an order of magnitude larger than the nominal rates because FMR is computed over demographically-matched impostor pairs i.e individuals of the same sex, from the same geographic region (see section 3.6.1), and the same age group (see section 3.6.2).

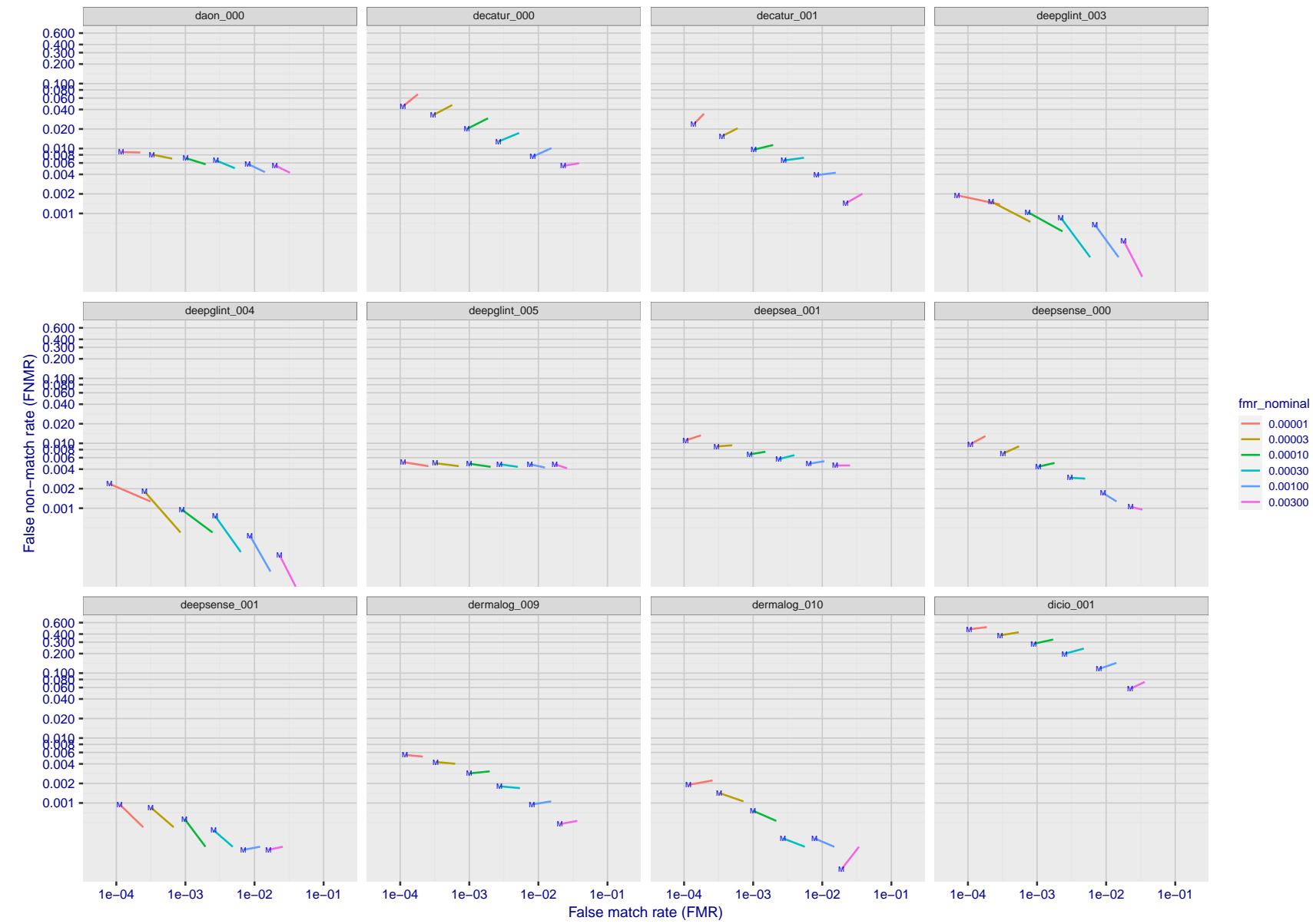


Figure 186: For the visa images, FNMR and FMR at six operating points along the DET characteristic. At each point a line is drawn between $(FMR, FNMR)_{MALE}$ and $(FMR, FNMR)_{FEMALE}$ showing how which sex has lower FMR and/or FNMR. The "M" label denotes male, the other end of the line corresponds to female. The six operating thresholds are selected to give the nominal false match rates given in the legend, and are computed over all impostor pairs regardless of age, sex, and place of birth. The plotted FMR values are broadly an order of magnitude larger than the nominal rates because FMR is computed over demographically-matched impostor pairs i.e individuals of the same sex, from the same geographic region (see section 3.6.1), and the same age group (see section 3.6.2).

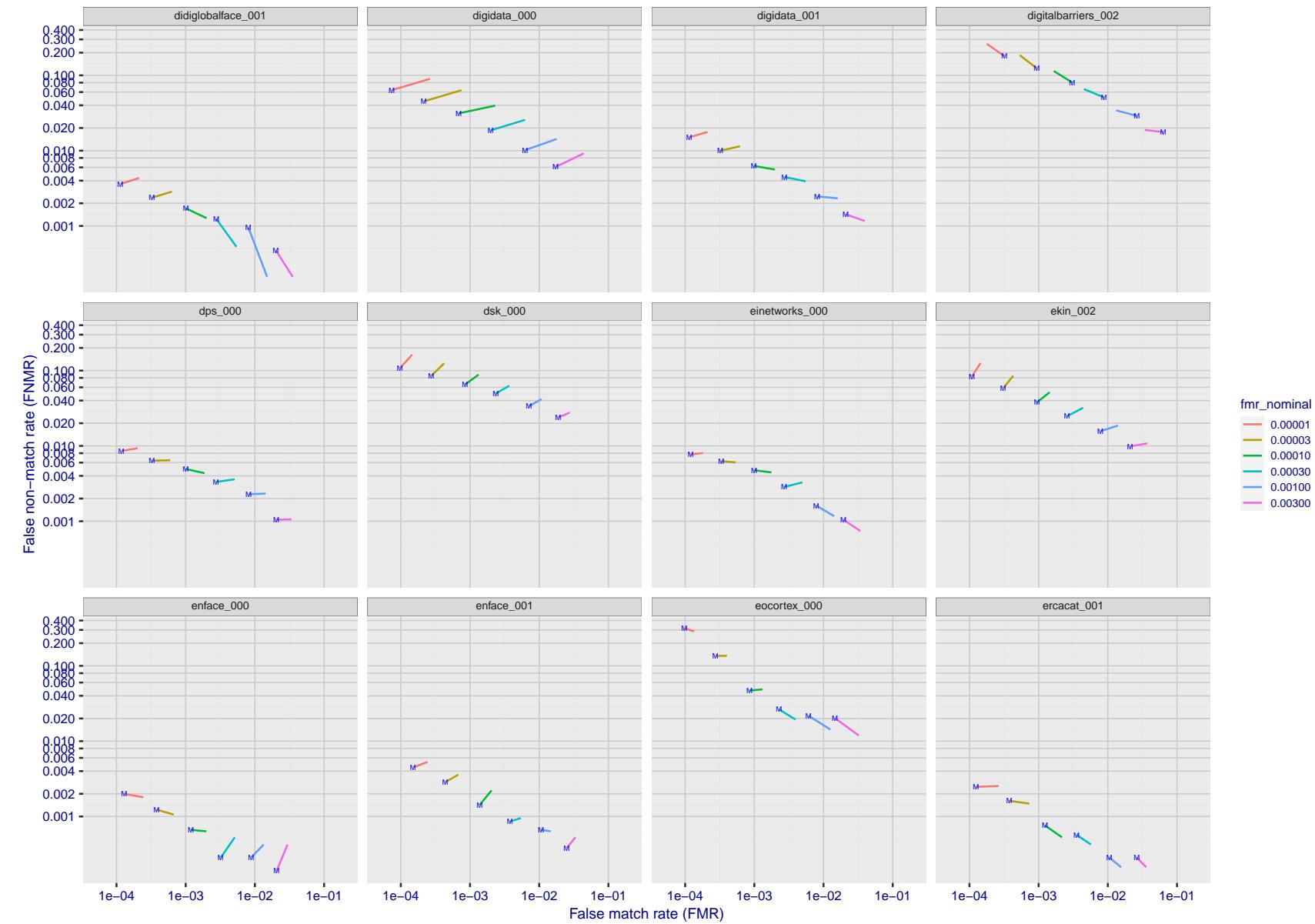


Figure 187: For the visa images, FNMR and FMR at six operating points along the DET characteristic. At each point a line is drawn between $(FMR, FNMR)_{MALE}$ and $(FMR, FNMR)_{FEMALE}$ showing how which sex has lower FMR and/or FNMR. The "M" label denotes male, the other end of the line corresponds to female. The six operating thresholds are selected to give the nominal false match rates given in the legend, and are computed over all impostor pairs regardless of age, sex, and place of birth. The plotted FMR values are broadly an order of magnitude larger than the nominal rates because FMR is computed over demographically-matched impostor pairs i.e individuals of the same sex, from the same geographic region (see section 3.6.1), and the same age group (see section 3.6.2).

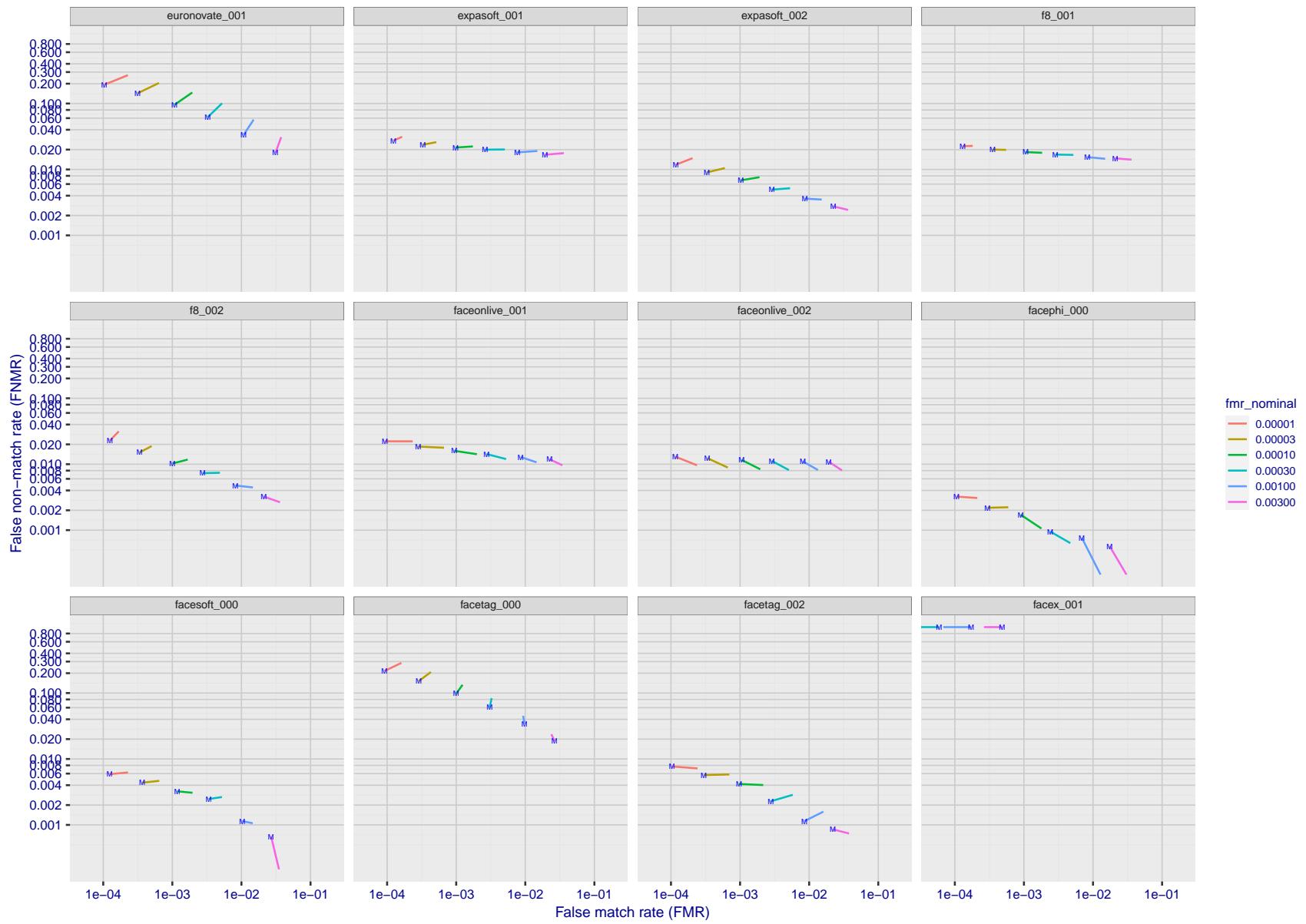


Figure 188: For the visa images, FNMR and FMR at six operating points along the DET characteristic. At each point a line is drawn between $(FMR, FNMR)_{MALE}$ and $(FMR, FNMR)_{FEMALE}$ showing how which sex has lower FMR and/or FNMR. The "M" label denotes male, the other end of the line corresponds to female. The six operating thresholds are selected to give the nominal false match rates given in the legend, and are computed over all impostor pairs regardless of age, sex, and place of birth. The plotted FMR values are broadly an order of magnitude larger than the nominal rates because FMR is computed over demographically-matched impostor pairs i.e individuals of the same sex, from the same geographic region (see section 3.6.1), and the same age group (see section 3.6.2).

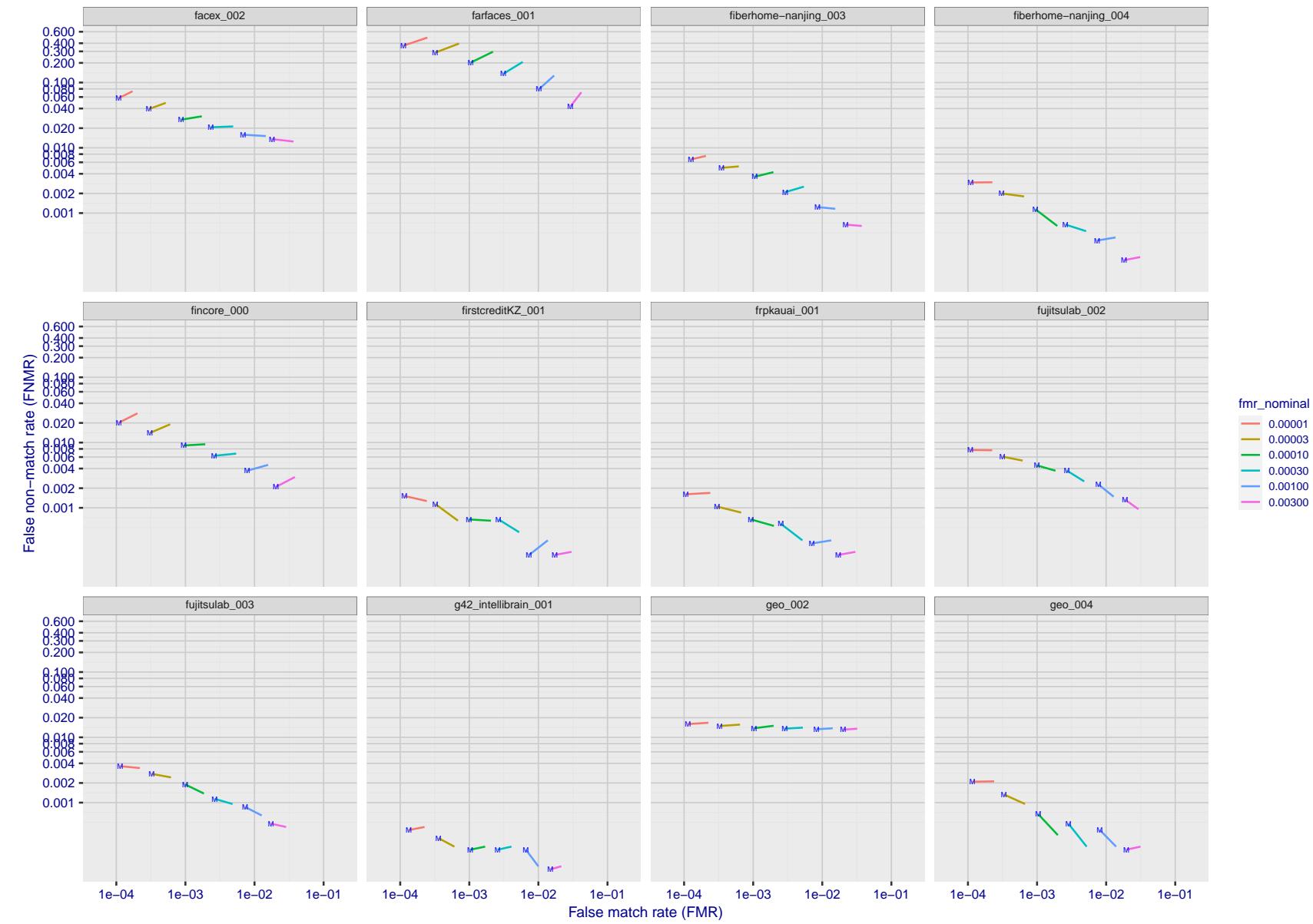


Figure 189: For the visa images, FNMR and FMR at six operating points along the DET characteristic. At each point a line is drawn between $(FMR, FNMR)_{MALE}$ and $(FMR, FNMR)_{FEMALE}$ showing how which sex has lower FMR and/or FNMR. The "M" label denotes male, the other end of the line corresponds to female. The six operating thresholds are selected to give the nominal false match rates given in the legend, and are computed over all impostor pairs regardless of age, sex, and place of birth. The plotted FMR values are broadly an order of magnitude larger than the nominal rates because FMR is computed over demographically-matched impostor pairs i.e individuals of the same sex, from the same geographic region (see section 3.6.1), and the same age group (see section 3.6.2).

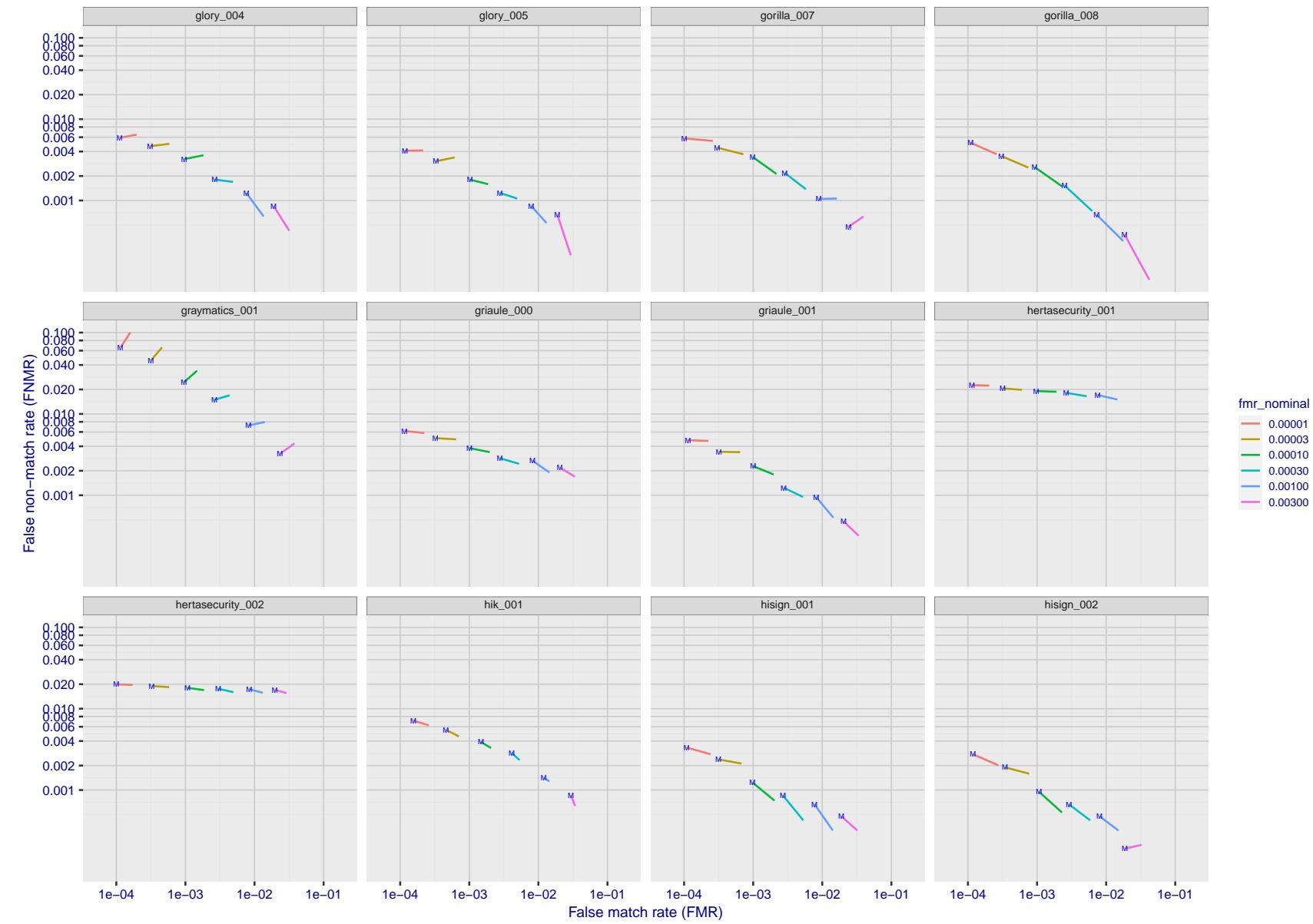


Figure 190: For the visa images, FNMR and FMR at six operating points along the DET characteristic. At each point a line is drawn between $(FMR, FNMR)_{MALE}$ and $(FMR, FNMR)_{FEMALE}$ showing how which sex has lower FMR and/or FNMR. The "M" label denotes male, the other end of the line corresponds to female. The six operating thresholds are selected to give the nominal false match rates given in the legend, and are computed over all impostor pairs regardless of age, sex, and place of birth. The plotted FMR values are broadly an order of magnitude larger than the nominal rates because FMR is computed over demographically-matched impostor pairs i.e individuals of the same sex, from the same geographic region (see section 3.6.1), and the same age group (see section 3.6.2).

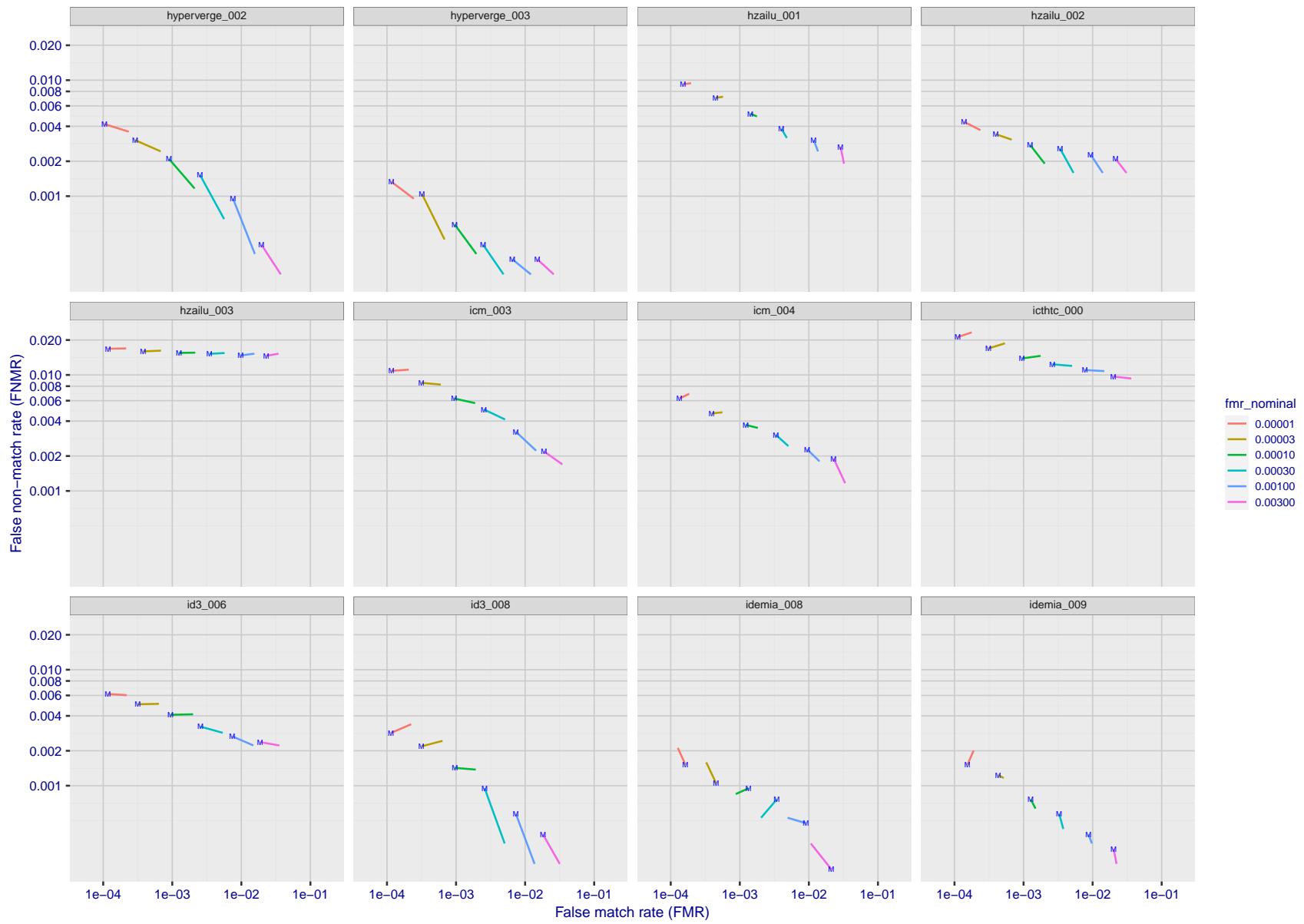


Figure 191: For the visa images, FNMR and FMR at six operating points along the DET characteristic. At each point a line is drawn between $(FMR, FNMR)_{MALE}$ and $(FMR, FNMR)_{FEMALE}$ showing how which sex has lower FMR and/or FNMR. The "M" label denotes male, the other end of the line corresponds to female. The six operating thresholds are selected to give the nominal false match rates given in the legend, and are computed over all impostor pairs regardless of age, sex, and place of birth. The plotted FMR values are broadly an order of magnitude larger than the nominal rates because FMR is computed over demographically-matched impostor pairs i.e individuals of the same sex, from the same geographic region (see section 3.6.1), and the same age group (see section 3.6.2).

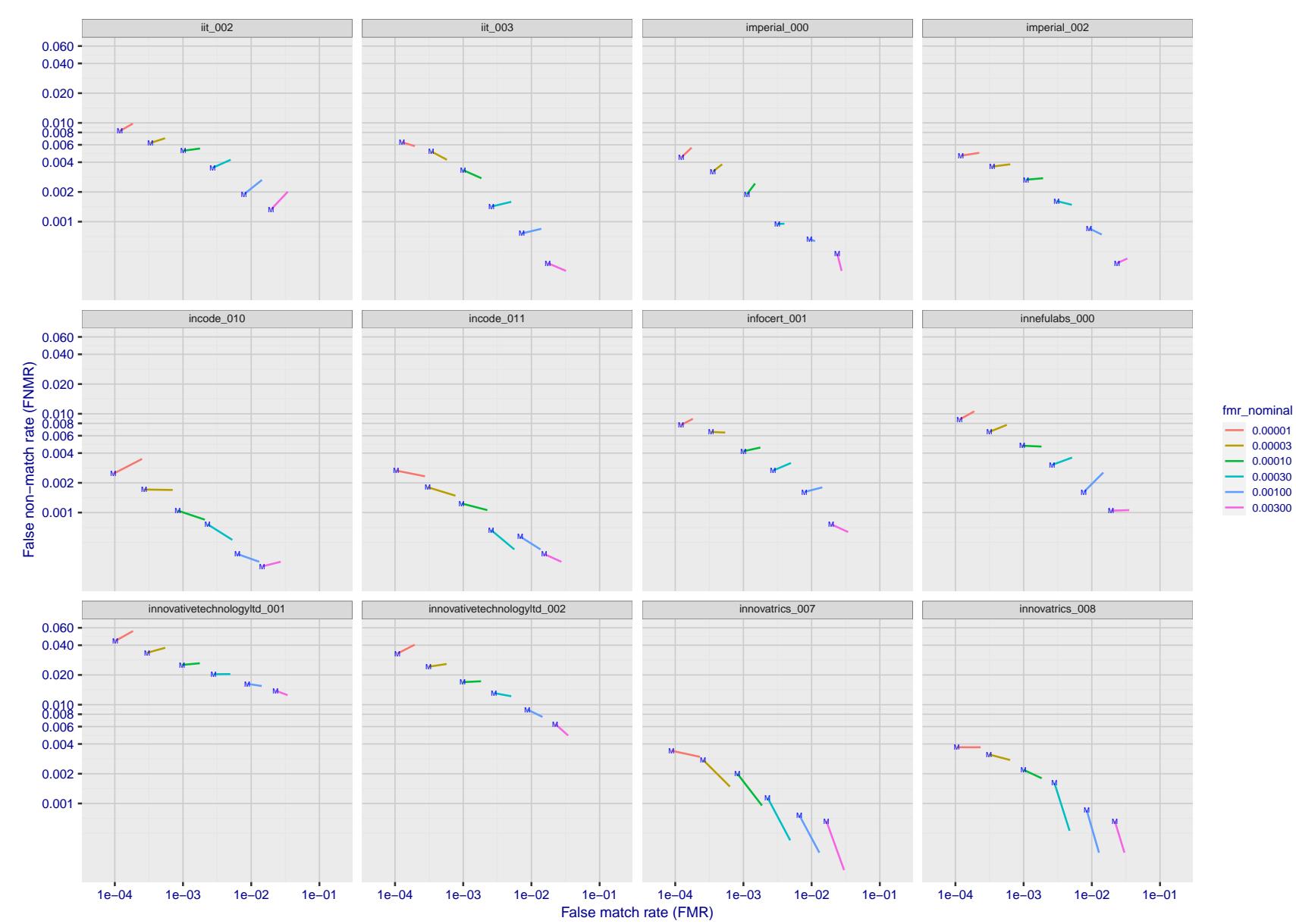


Figure 192: For the visa images, FNMR and FMR at six operating points along the DET characteristic. At each point a line is drawn between $(FMR, FNMR)_{MALE}$ and $(FMR, FNMR)_{FEMALE}$ showing how which sex has lower FMR and/or FNMR. The "M" label denotes male, the other end of the line corresponds to female. The six operating thresholds are selected to give the nominal false match rates given in the legend, and are computed over all impostor pairs regardless of age, sex, and place of birth. The plotted FMR values are broadly an order of magnitude larger than the nominal rates because FMR is computed over demographically-matched impostor pairs i.e individuals of the same sex, from the same geographic region (see section 3.6.1), and the same age group (see section 3.6.2).

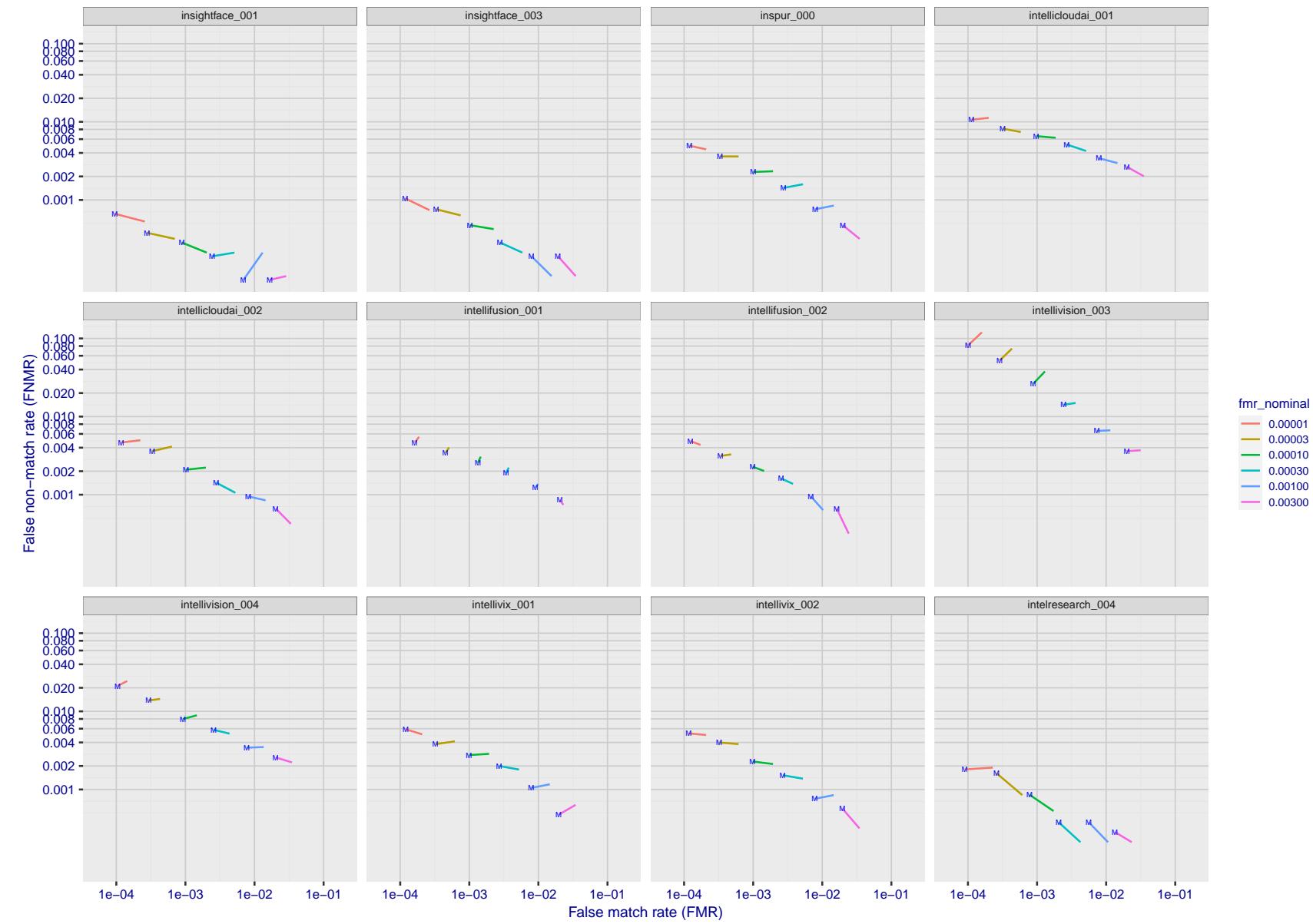


Figure 193: For the visa images, FNMR and FMR at six operating points along the DET characteristic. At each point a line is drawn between $(FMR, FNMR)_{MALE}$ and $(FMR, FNMR)_{FEMALE}$ showing how which sex has lower FMR and/or FNMR. The "M" label denotes male, the other end of the line corresponds to female. The six operating thresholds are selected to give the nominal false match rates given in the legend, and are computed over all impostor pairs regardless of age, sex, and place of birth. The plotted FMR values are broadly an order of magnitude larger than the nominal rates because FMR is computed over demographically-matched impostor pairs i.e individuals of the same sex, from the same geographic region (see section 3.6.1), and the same age group (see section 3.6.2).

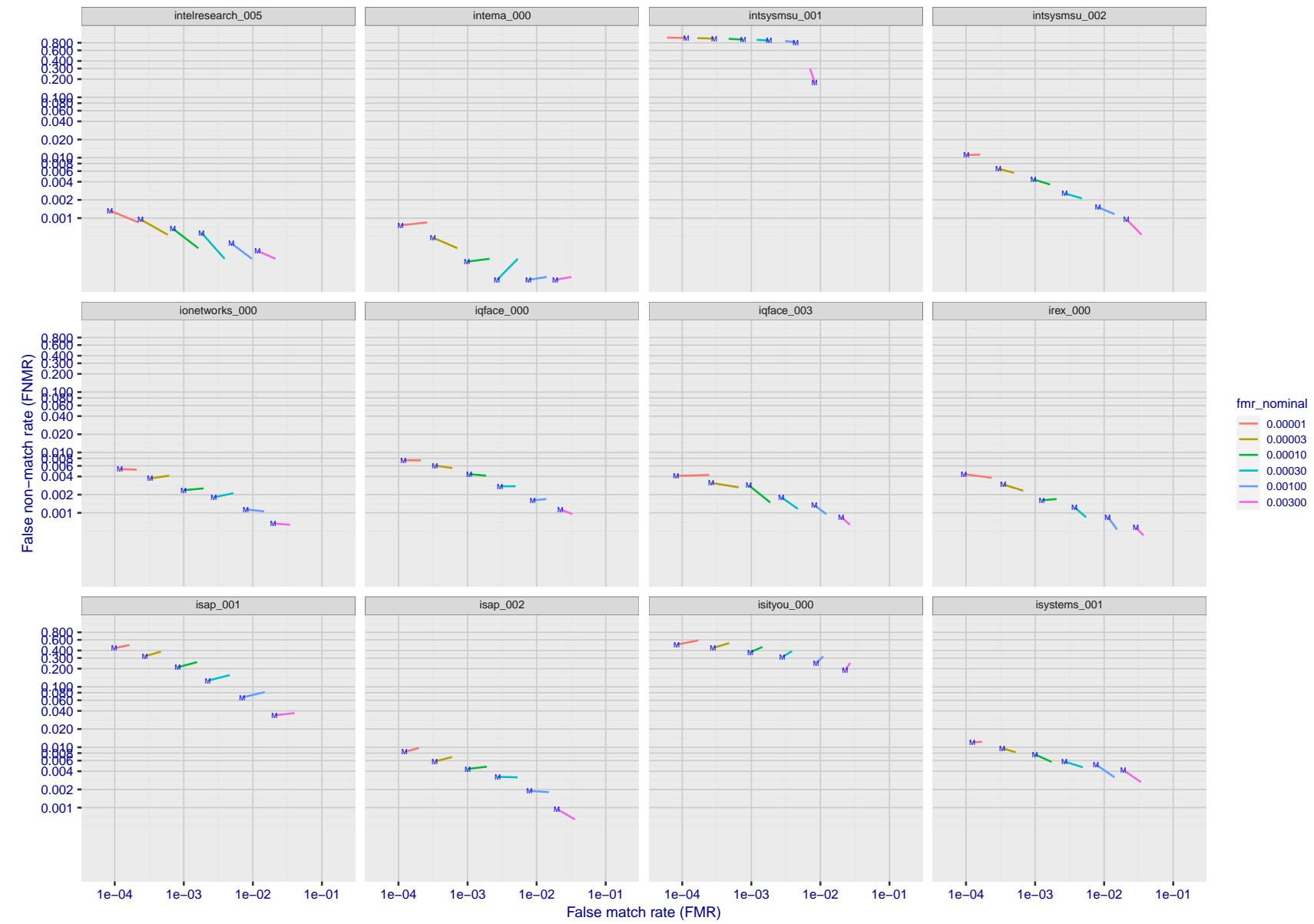


Figure 194: For the visa images, FNMR and FMR at six operating points along the DET characteristic. At each point a line is drawn between $(FMR, FNMR)_{MALE}$ and $(FMR, FNMR)_{FEMALE}$ showing how which sex has lower FMR and/or FNMR. The "M" label denotes male, the other end of the line corresponds to female. The six operating thresholds are selected to give the nominal false match rates given in the legend, and are computed over all impostor pairs regardless of age, sex, and place of birth. The plotted FMR values are broadly an order of magnitude larger than the nominal rates because FMR is computed over demographically-matched impostor pairs i.e individuals of the same sex, from the same geographic region (see section 3.6.1), and the same age group (see section 3.6.2).

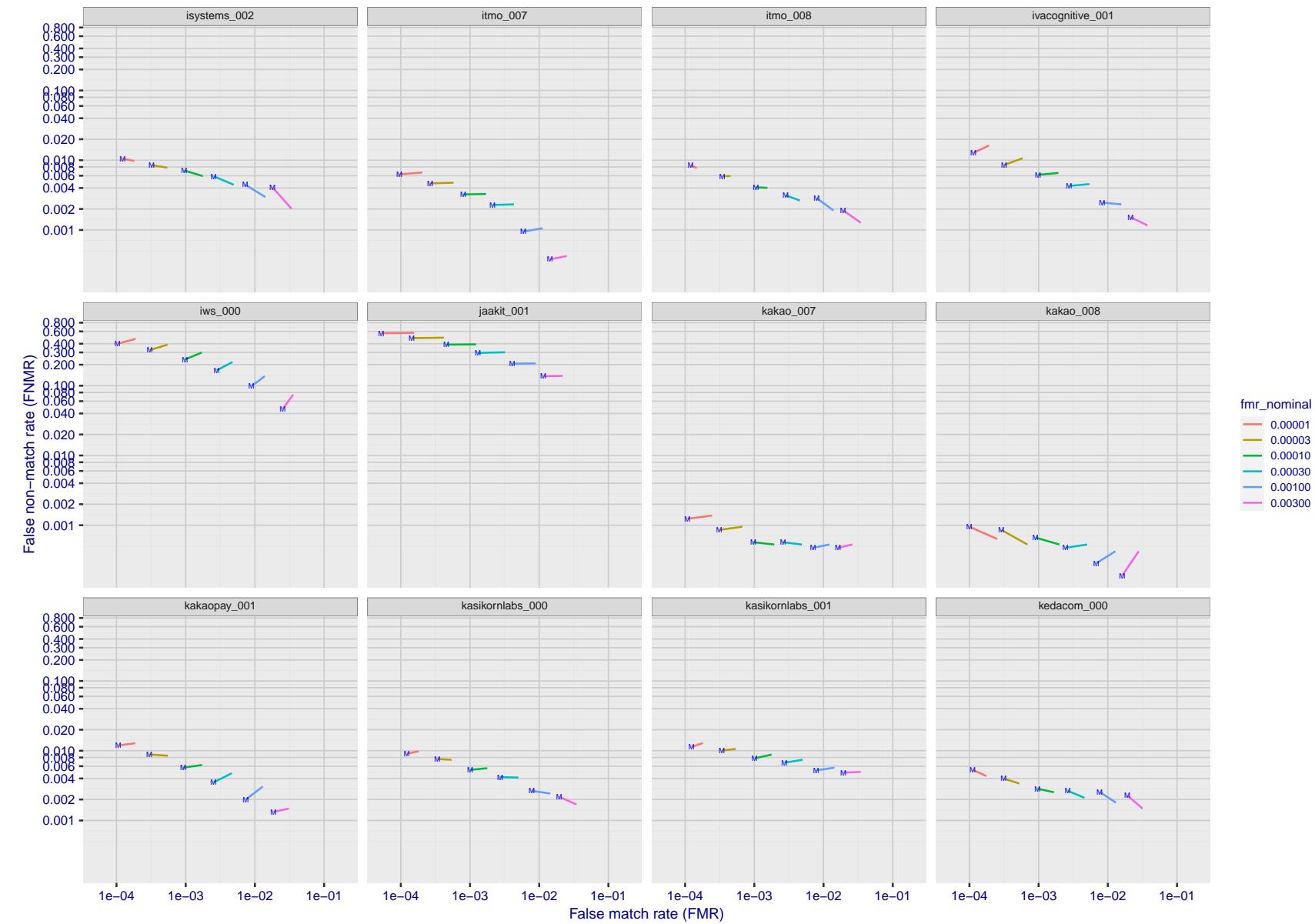


Figure 195: For the visa images, FNMR and FMR at six operating points along the DET characteristic. At each point a line is drawn between $(FMR, FNMR)_{MALE}$ and $(FMR, FNMR)_{FEMALE}$ showing how which sex has lower FMR and/or FNMR. The "M" label denotes male, the other end of the line corresponds to female. The six operating thresholds are selected to give the nominal false match rates given in the legend, and are computed over all impostor pairs regardless of age, sex, and place of birth. The plotted FMR values are broadly an order of magnitude larger than the nominal rates because FMR is computed over demographically-matched impostor pairs i.e individuals of the same sex, from the same geographic region (see section 3.6.1), and the same age group (see section 3.6.2).

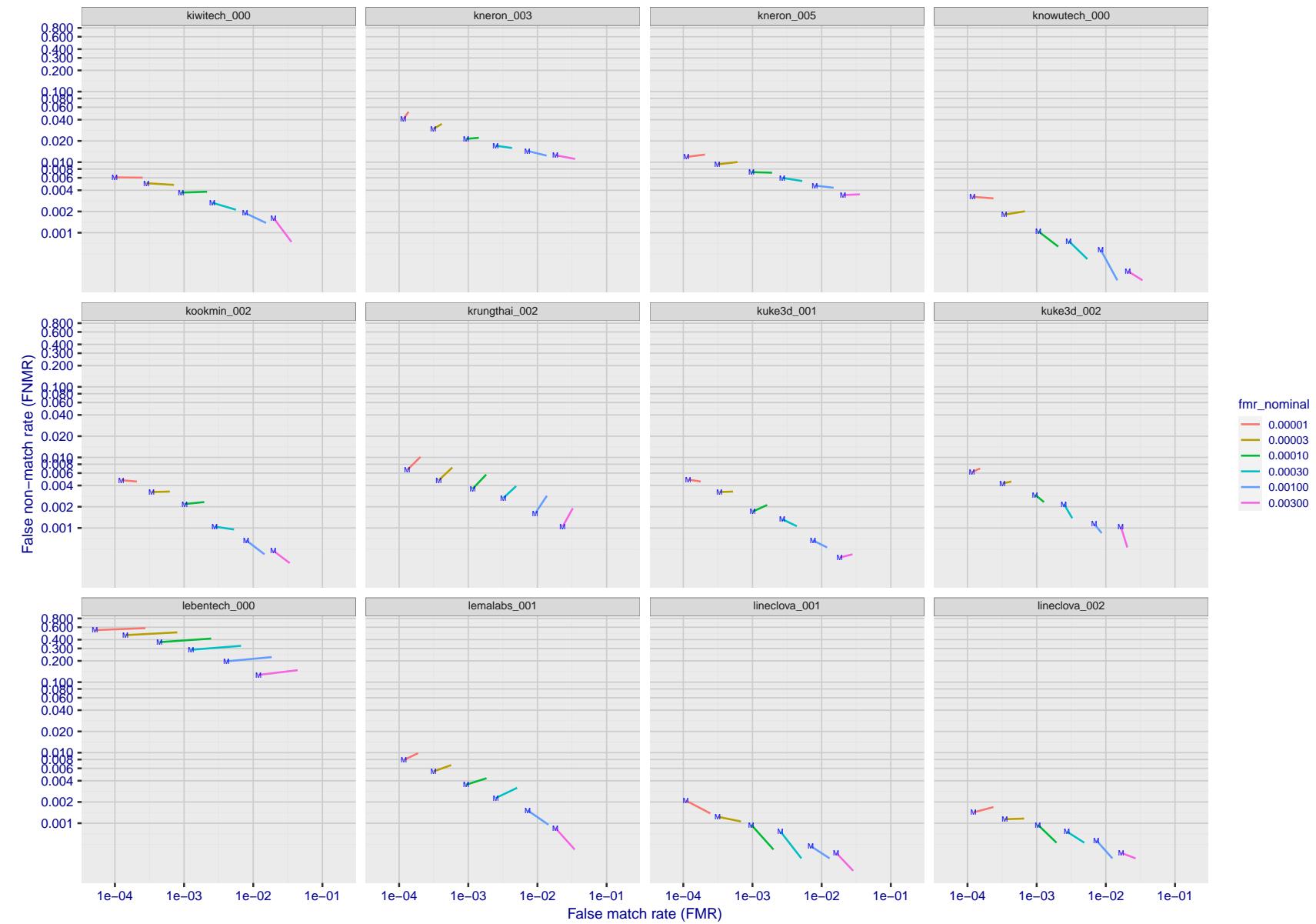


Figure 196: For the visa images, FNMR and FMR at six operating points along the DET characteristic. At each point a line is drawn between $(FMR, FNMR)_{MALE}$ and $(FMR, FNMR)_{FEMALE}$ showing how which sex has lower FMR and/or FNMR. The "M" label denotes male, the other end of the line corresponds to female. The six operating thresholds are selected to give the nominal false match rates given in the legend, and are computed over all impostor pairs regardless of age, sex, and place of birth. The plotted FMR values are broadly an order of magnitude larger than the nominal rates because FMR is computed over demographically-matched impostor pairs i.e individuals of the same sex, from the same geographic region (see section 3.6.1), and the same age group (see section 3.6.2).

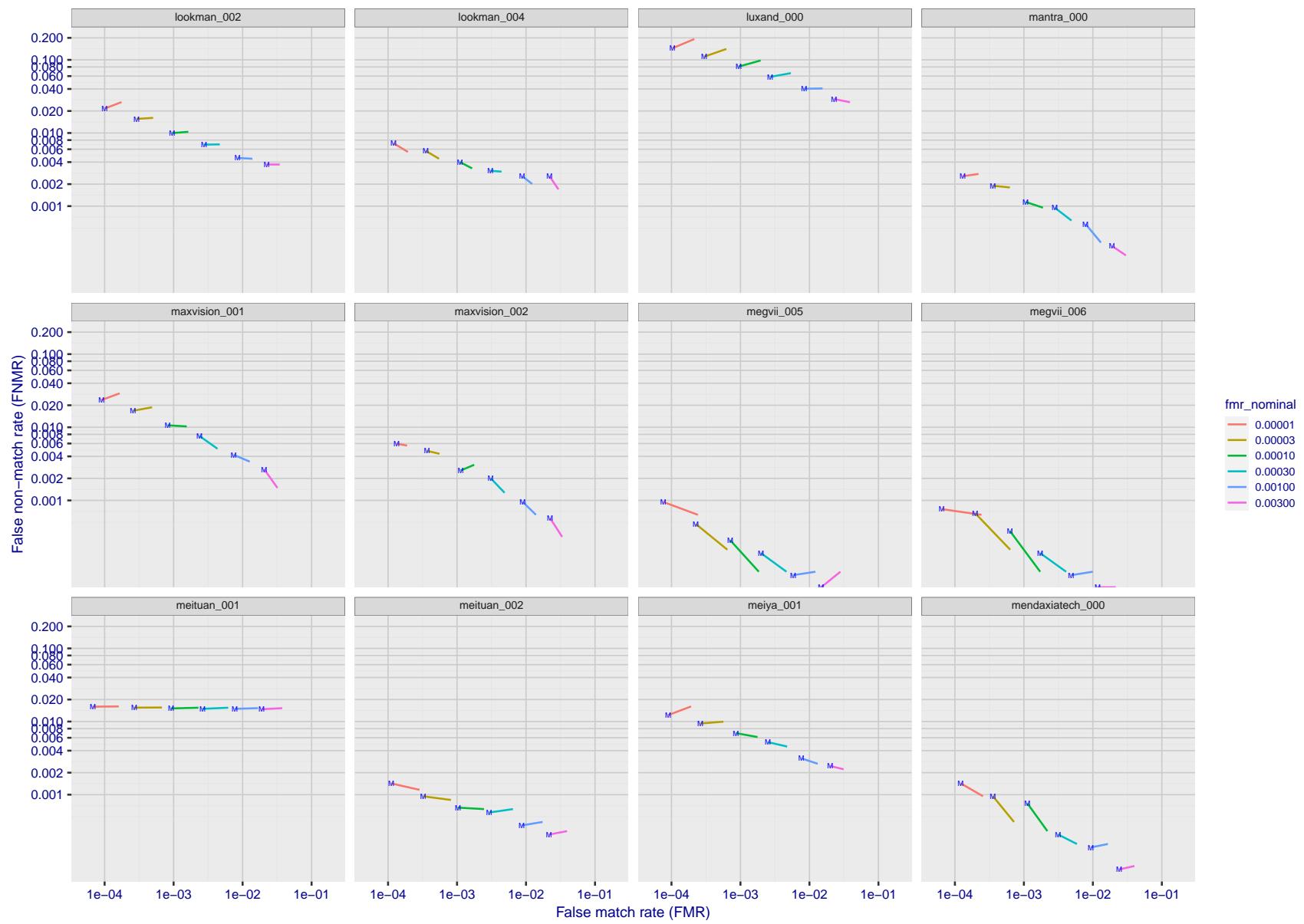


Figure 197: For the visa images, FNMR and FMR at six operating points along the DET characteristic. At each point a line is drawn between $(FMR, FNMR)_{MALE}$ and $(FMR, FNMR)_{FEMALE}$ showing how which sex has lower FMR and/or FNMR. The "M" label denotes male, the other end of the line corresponds to female. The six operating thresholds are selected to give the nominal false match rates given in the legend, and are computed over all impostor pairs regardless of age, sex, and place of birth. The plotted FMR values are broadly an order of magnitude larger than the nominal rates because FMR is computed over demographically-matched impostor pairs i.e individuals of the same sex, from the same geographic region (see section 3.6.1), and the same age group (see section 3.6.2).

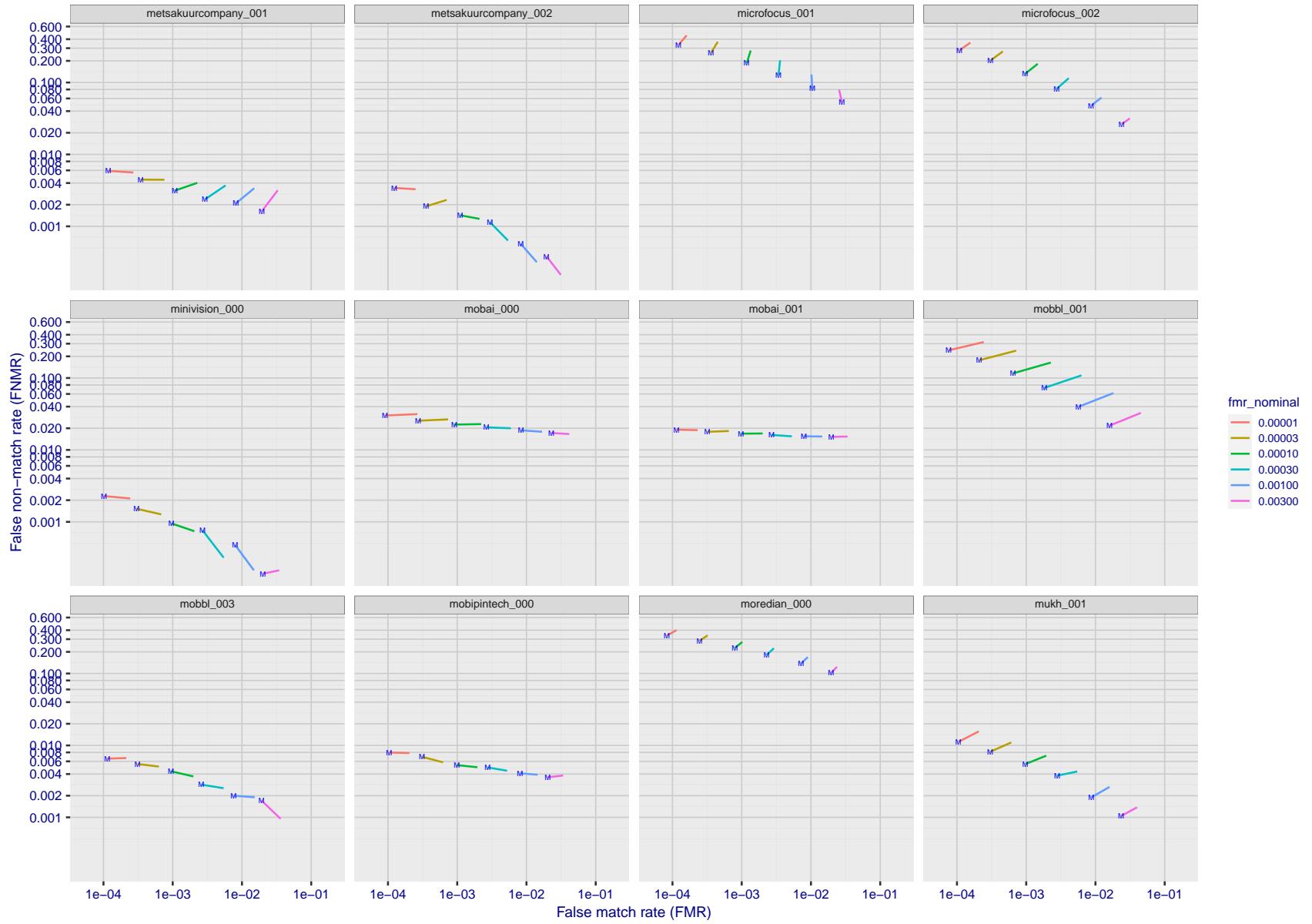


Figure 198: For the visa images, FNMR and FMR at six operating points along the DET characteristic. At each point a line is drawn between $(FMR, FNMR)_{MALE}$ and $(FMR, FNMR)_{FEMALE}$ showing how which sex has lower FMR and/or FNMR. The "M" label denotes male, the other end of the line corresponds to female. The six operating thresholds are selected to give the nominal false match rates given in the legend, and are computed over all impostor pairs regardless of age, sex, and place of birth. The plotted FMR values are broadly an order of magnitude larger than the nominal rates because FMR is computed over demographically-matched impostor pairs i.e individuals of the same sex, from the same geographic region (see section 3.6.1), and the same age group (see section 3.6.2).

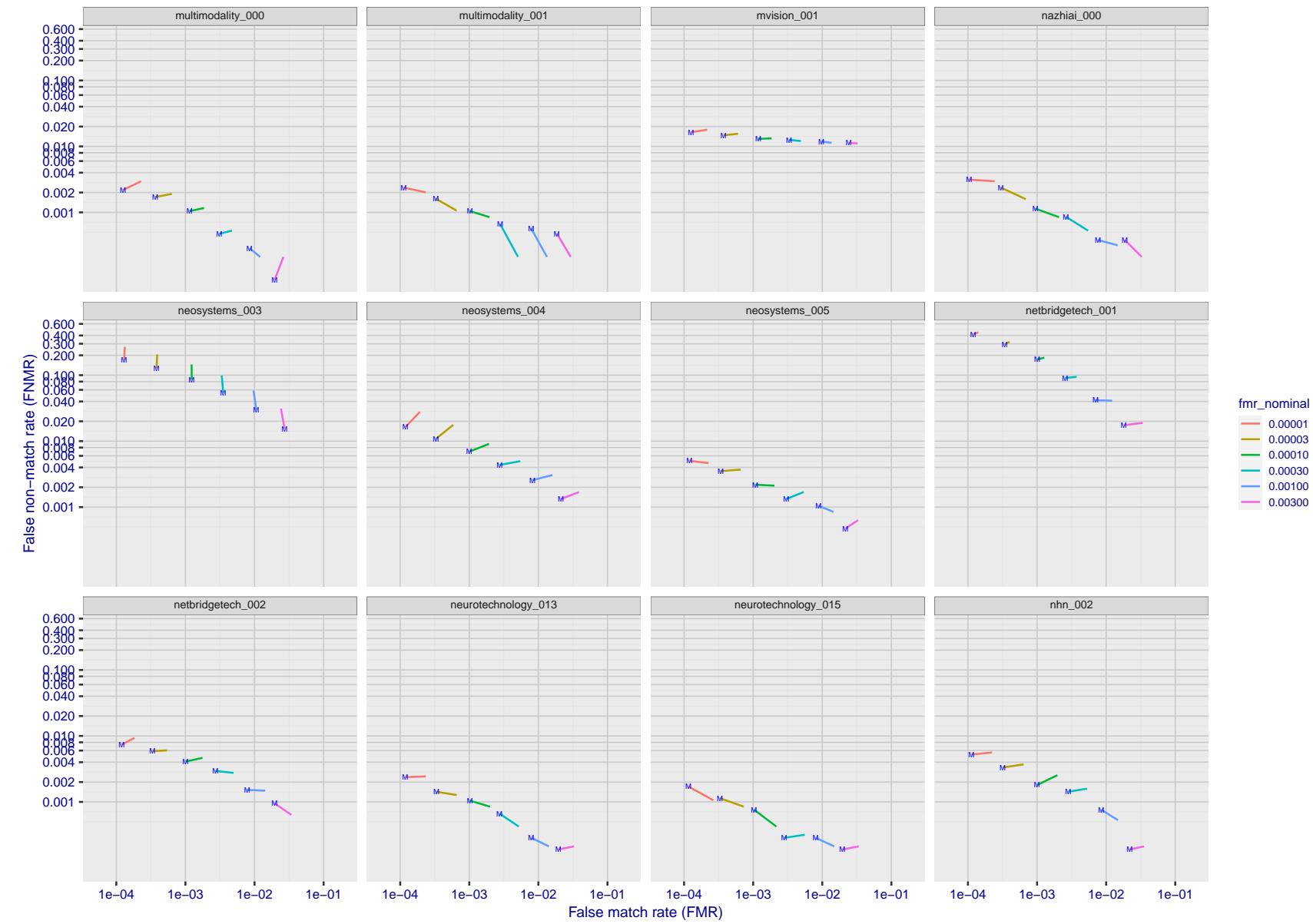


Figure 199: For the visa images, FNMR and FMR at six operating points along the DET characteristic. At each point a line is drawn between $(FMR, FNMR)_{MALE}$ and $(FMR, FNMR)_{FEMALE}$ showing how which sex has lower FMR and/or FNMR. The "M" label denotes male, the other end of the line corresponds to female. The six operating thresholds are selected to give the nominal false match rates given in the legend, and are computed over all impostor pairs regardless of age, sex, and place of birth. The plotted FMR values are broadly an order of magnitude larger than the nominal rates because FMR is computed over demographically-matched impostor pairs i.e individuals of the same sex, from the same geographic region (see section 3.6.1), and the same age group (see section 3.6.2).

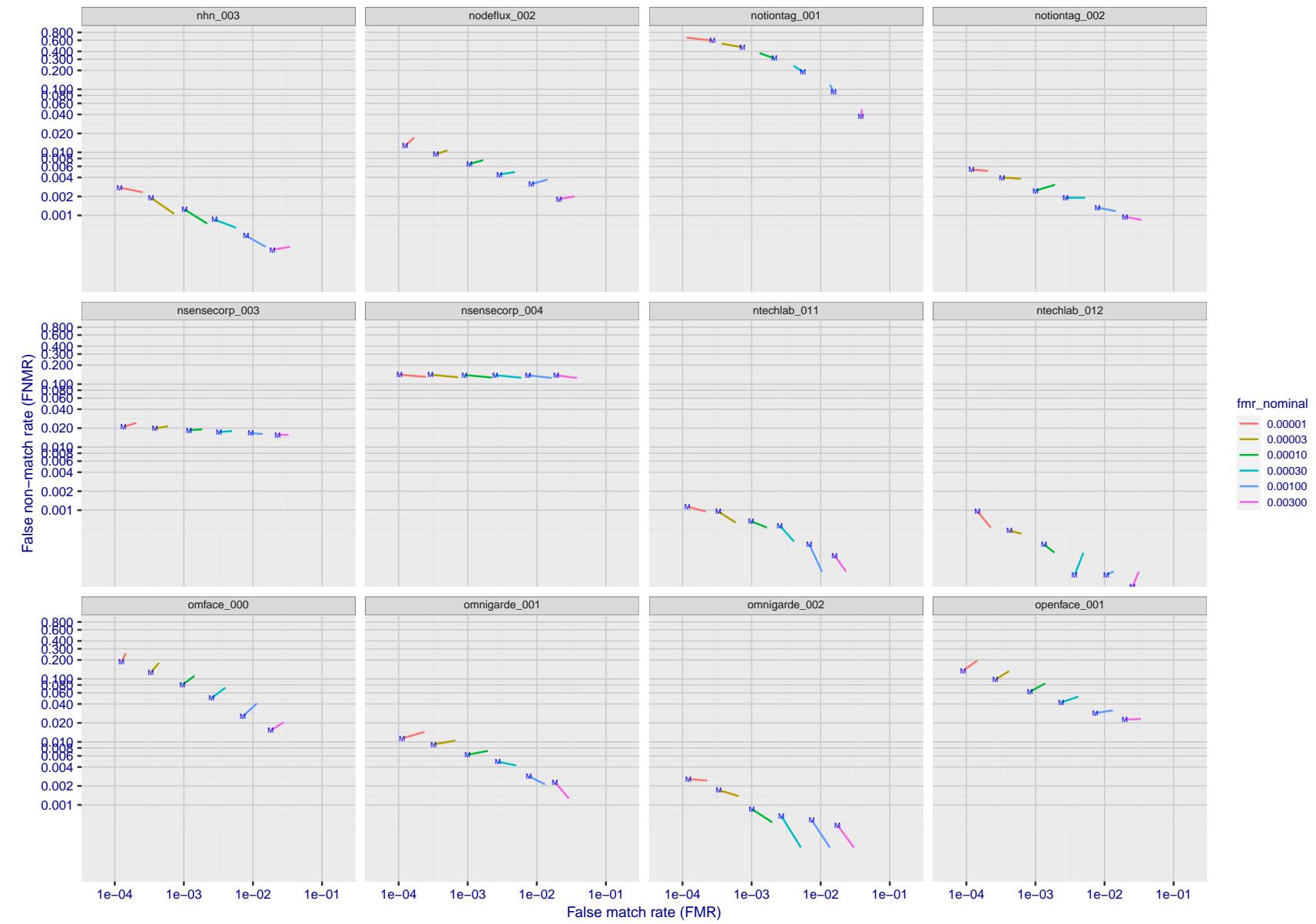


Figure 200: For the visa images, FNMR and FMR at six operating points along the DET characteristic. At each point a line is drawn between $(FMR, FNMR)_{MALE}$ and $(FMR, FNMR)_{FEMALE}$ showing how which sex has lower FMR and/or FNMR. The "M" label denotes male, the other end of the line corresponds to female. The six operating thresholds are selected to give the nominal false match rates given in the legend, and are computed over all impostor pairs regardless of age, sex, and place of birth. The plotted FMR values are broadly an order of magnitude larger than the nominal rates because FMR is computed over demographically-matched impostor pairs i.e individuals of the same sex, from the same geographic region (see section 3.6.1), and the same age group (see section 3.6.2).

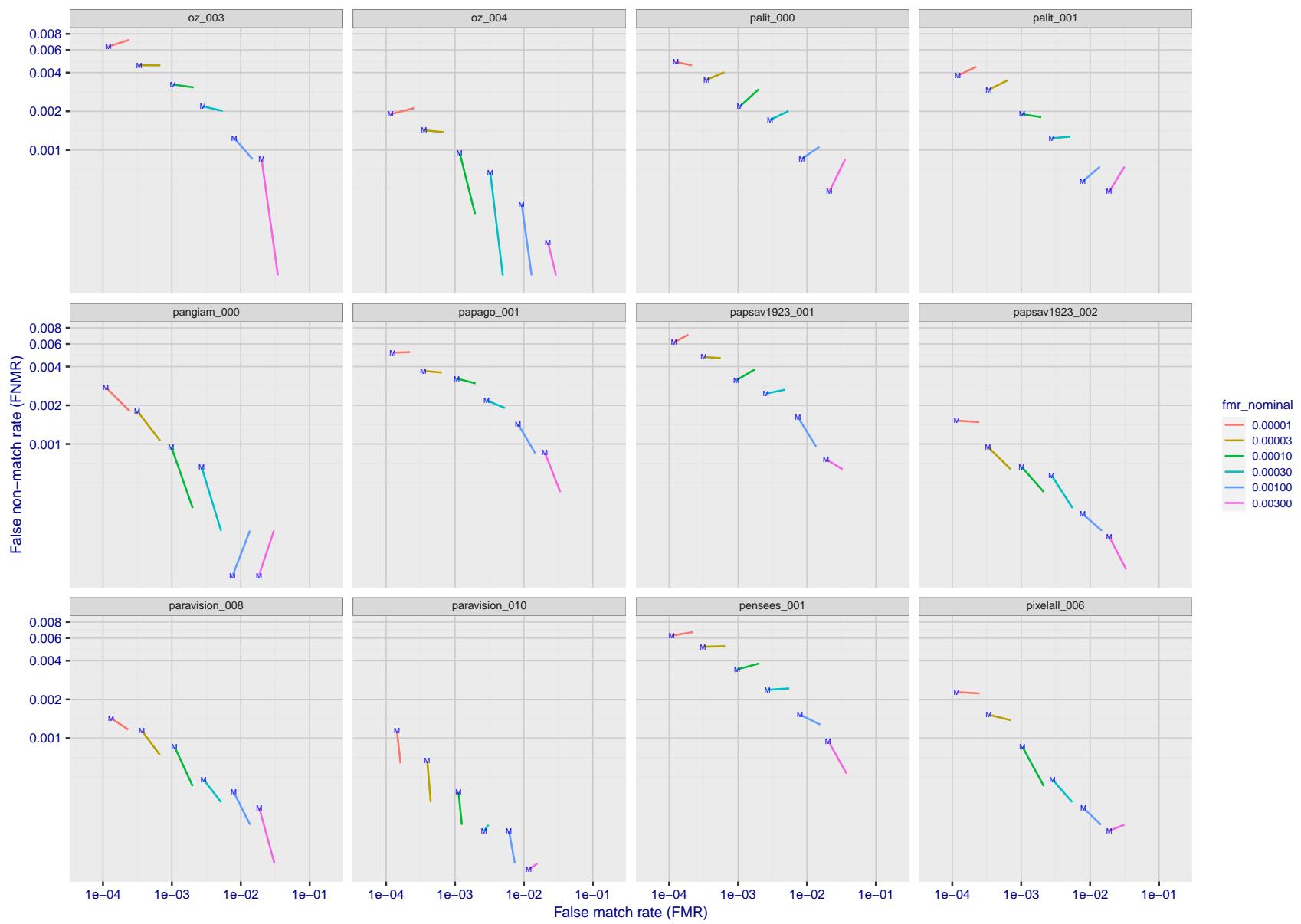


Figure 201: For the visa images, FNMR and FMR at six operating points along the DET characteristic. At each point a line is drawn between $(FMR, FNMR)_{MALE}$ and $(FMR, FNMR)_{FEMALE}$ showing how which sex has lower FMR and/or FNMR. The "M" label denotes male, the other end of the line corresponds to female. The six operating thresholds are selected to give the nominal false match rates given in the legend, and are computed over all impostor pairs regardless of age, sex, and place of birth. The plotted FMR values are broadly an order of magnitude larger than the nominal rates because FMR is computed over demographically-matched impostor pairs i.e individuals of the same sex, from the same geographic region (see section 3.6.1), and the same age group (see section 3.6.2).

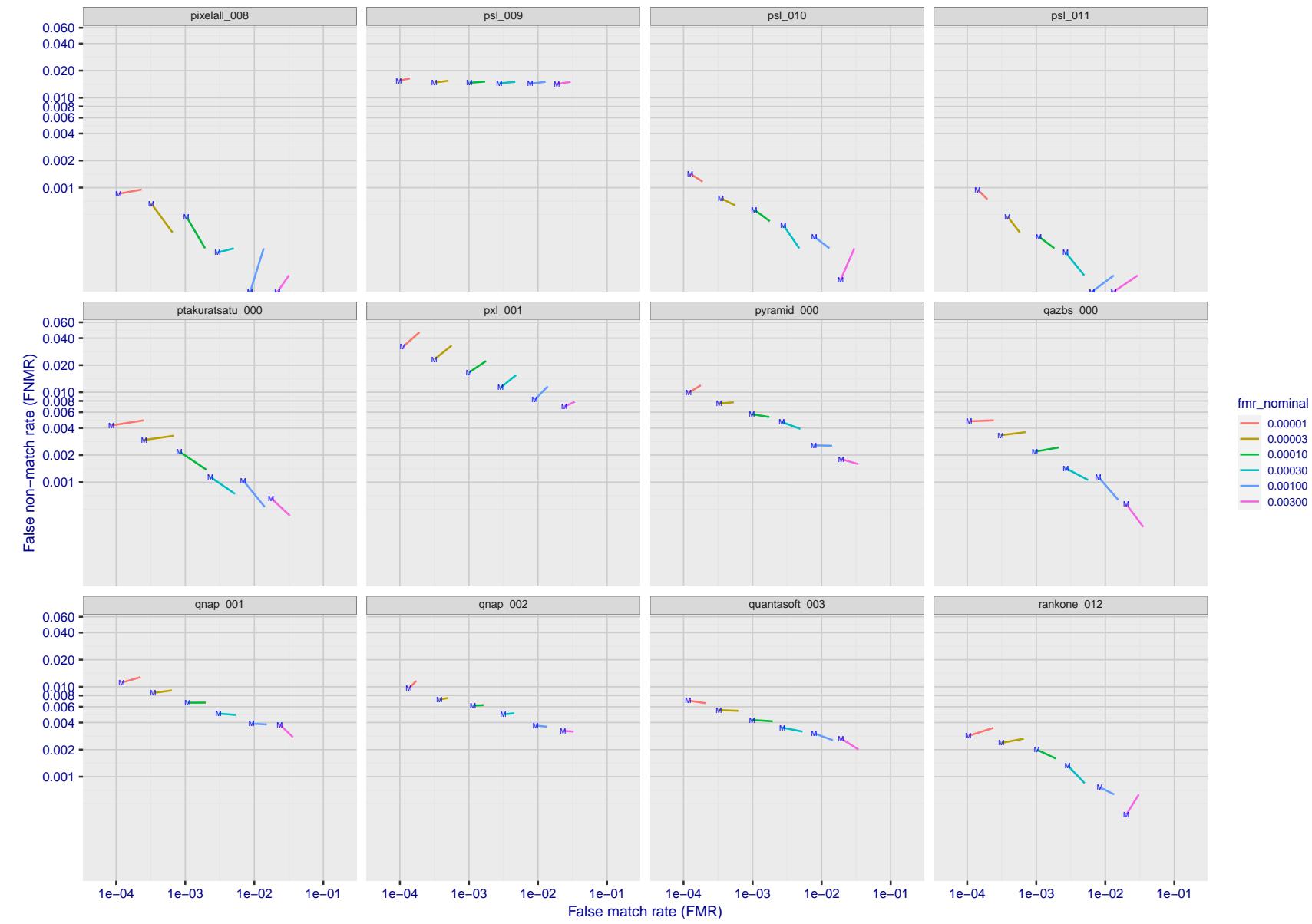


Figure 202: For the visa images, FNMR and FMR at six operating points along the DET characteristic. At each point a line is drawn between $(FMR, FNMR)_{MALE}$ and $(FMR, FNMR)_{FEMALE}$ showing how which sex has lower FMR and/or FNMR. The "M" label denotes male, the other end of the line corresponds to female. The six operating thresholds are selected to give the nominal false match rates given in the legend, and are computed over all impostor pairs regardless of age, sex, and place of birth. The plotted FMR values are broadly an order of magnitude larger than the nominal rates because FMR is computed over demographically-matched impostor pairs i.e individuals of the same sex, from the same geographic region (see section 3.6.1), and the same age group (see section 3.6.2).

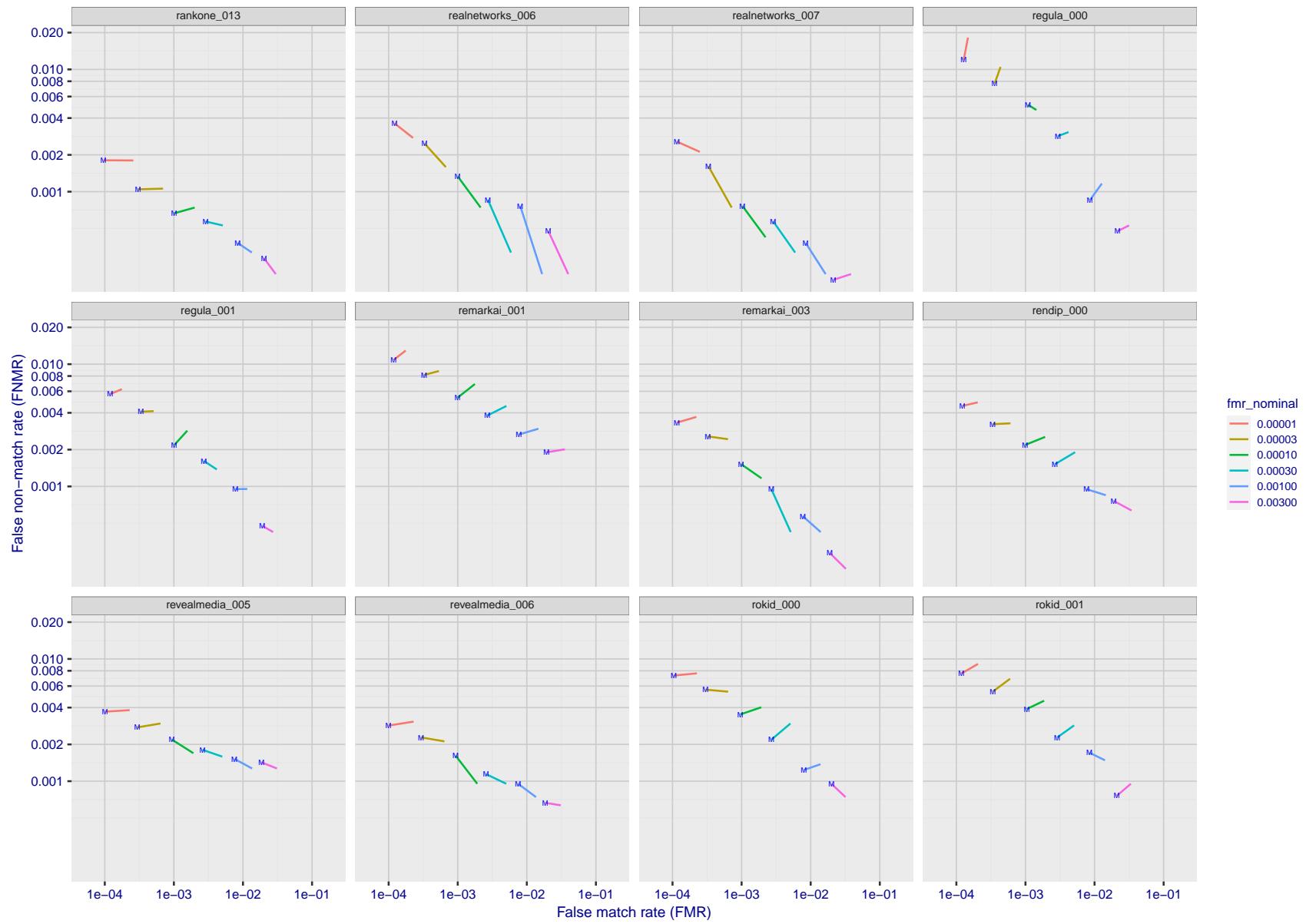


Figure 203: For the visa images, FNMR and FMR at six operating points along the DET characteristic. At each point a line is drawn between $(FMR, FNMR)_{MALE}$ and $(FMR, FNMR)_{FEMALE}$ showing how which sex has lower FMR and/or FNMR. The "M" label denotes male, the other end of the line corresponds to female. The six operating thresholds are selected to give the nominal false match rates given in the legend, and are computed over all impostor pairs regardless of age, sex, and place of birth. The plotted FMR values are broadly an order of magnitude larger than the nominal rates because FMR is computed over demographically-matched impostor pairs i.e individuals of the same sex, from the same geographic region (see section 3.6.1), and the same age group (see section 3.6.2).

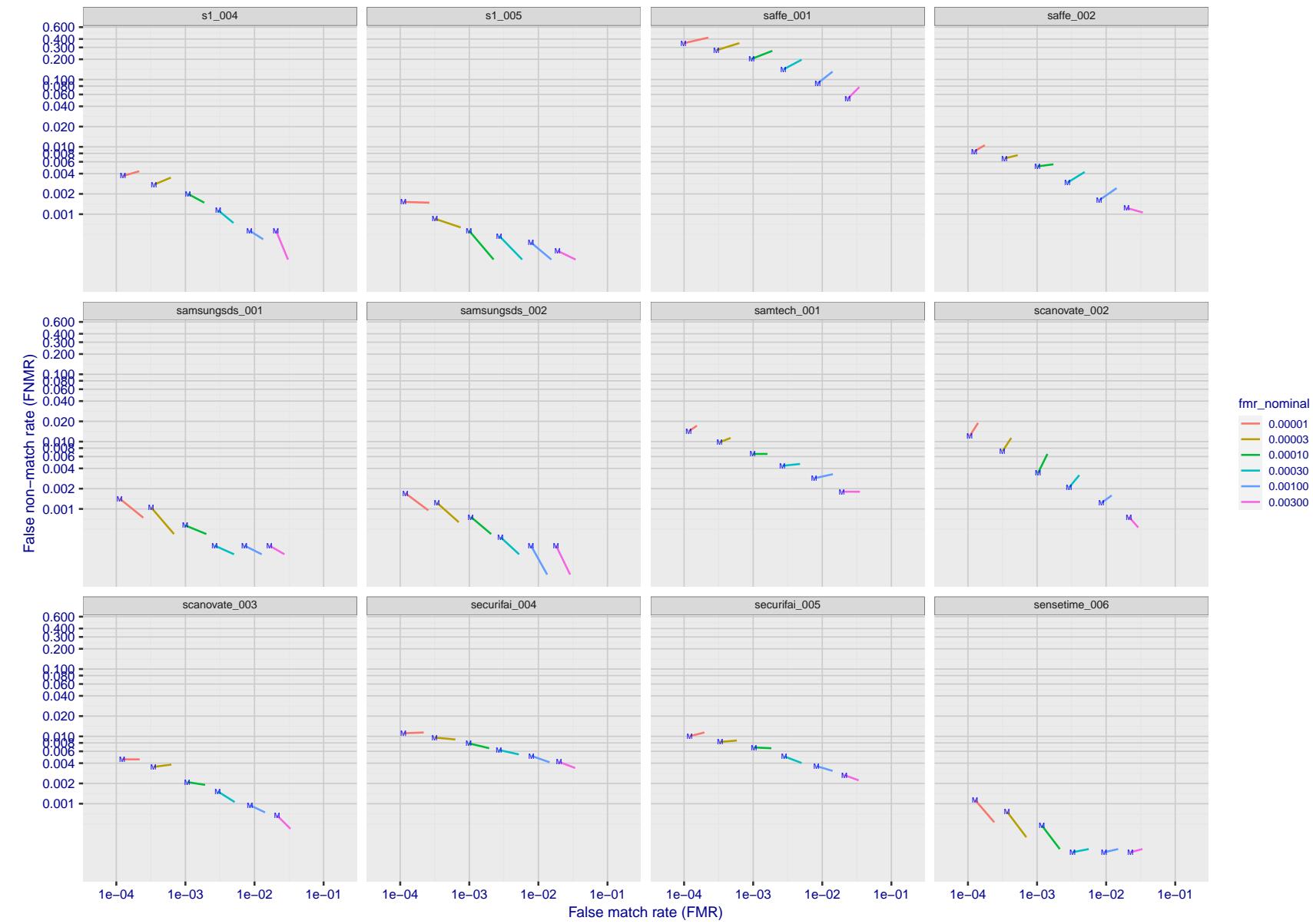


Figure 204: For the visa images, FNMR and FMR at six operating points along the DET characteristic. At each point a line is drawn between $(FMR, FNMR)_{MALE}$ and $(FMR, FNMR)_{FEMALE}$ showing how which sex has lower FMR and/or FNMR. The "M" label denotes male, the other end of the line corresponds to female. The six operating thresholds are selected to give the nominal false match rates given in the legend, and are computed over all impostor pairs regardless of age, sex, and place of birth. The plotted FMR values are broadly an order of magnitude larger than the nominal rates because FMR is computed over demographically-matched impostor pairs i.e individuals of the same sex, from the same geographic region (see section 3.6.1), and the same age group (see section 3.6.2).

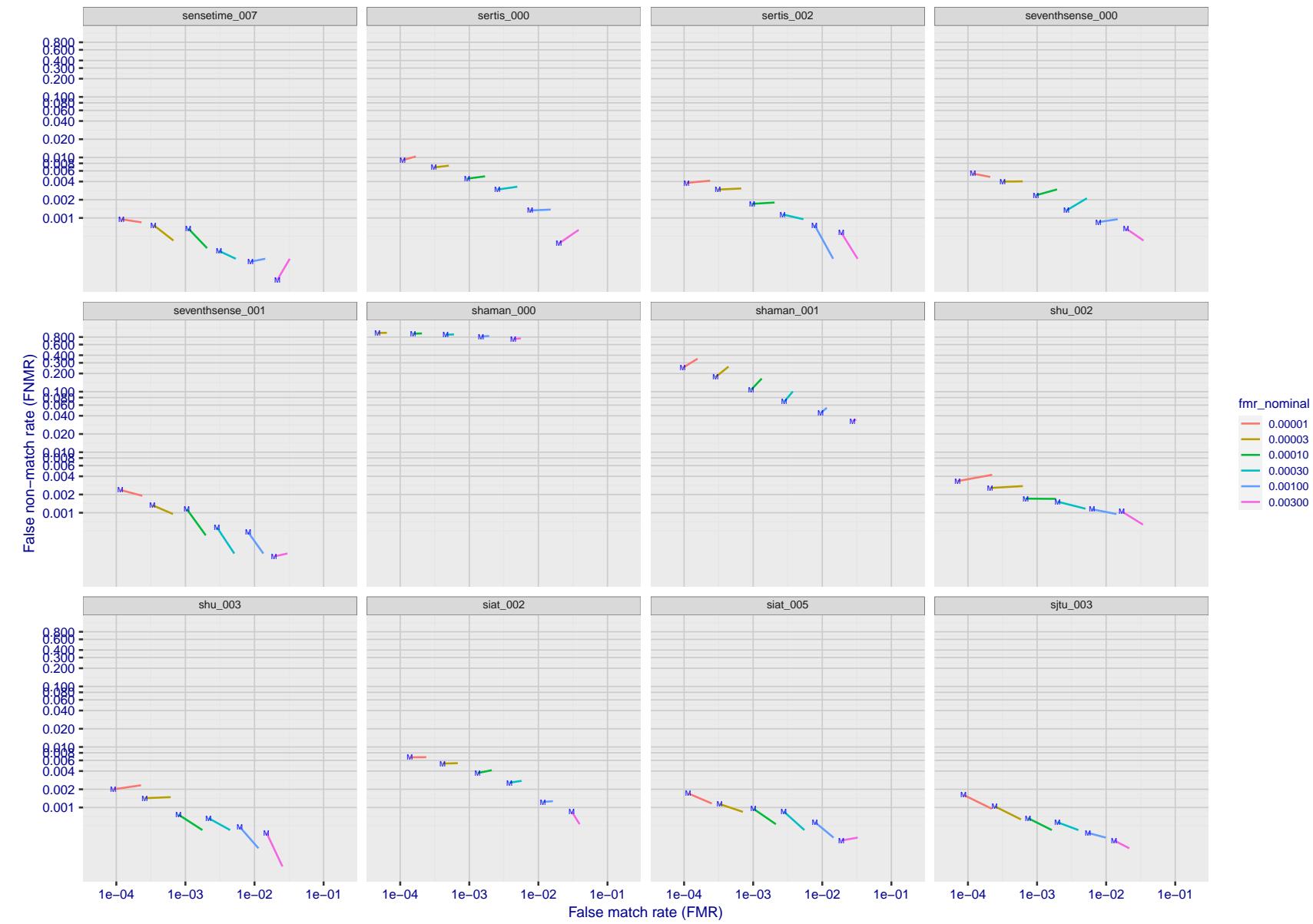


Figure 205: For the visa images, FNMR and FMR at six operating points along the DET characteristic. At each point a line is drawn between $(FMR, FNMR)_{MALE}$ and $(FMR, FNMR)_{FEMALE}$ showing how which sex has lower FMR and/or FNMR. The "M" label denotes male, the other end of the line corresponds to female. The six operating thresholds are selected to give the nominal false match rates given in the legend, and are computed over all impostor pairs regardless of age, sex, and place of birth. The plotted FMR values are broadly an order of magnitude larger than the nominal rates because FMR is computed over demographically-matched impostor pairs i.e individuals of the same sex, from the same geographic region (see section 3.6.1), and the same age group (see section 3.6.2).

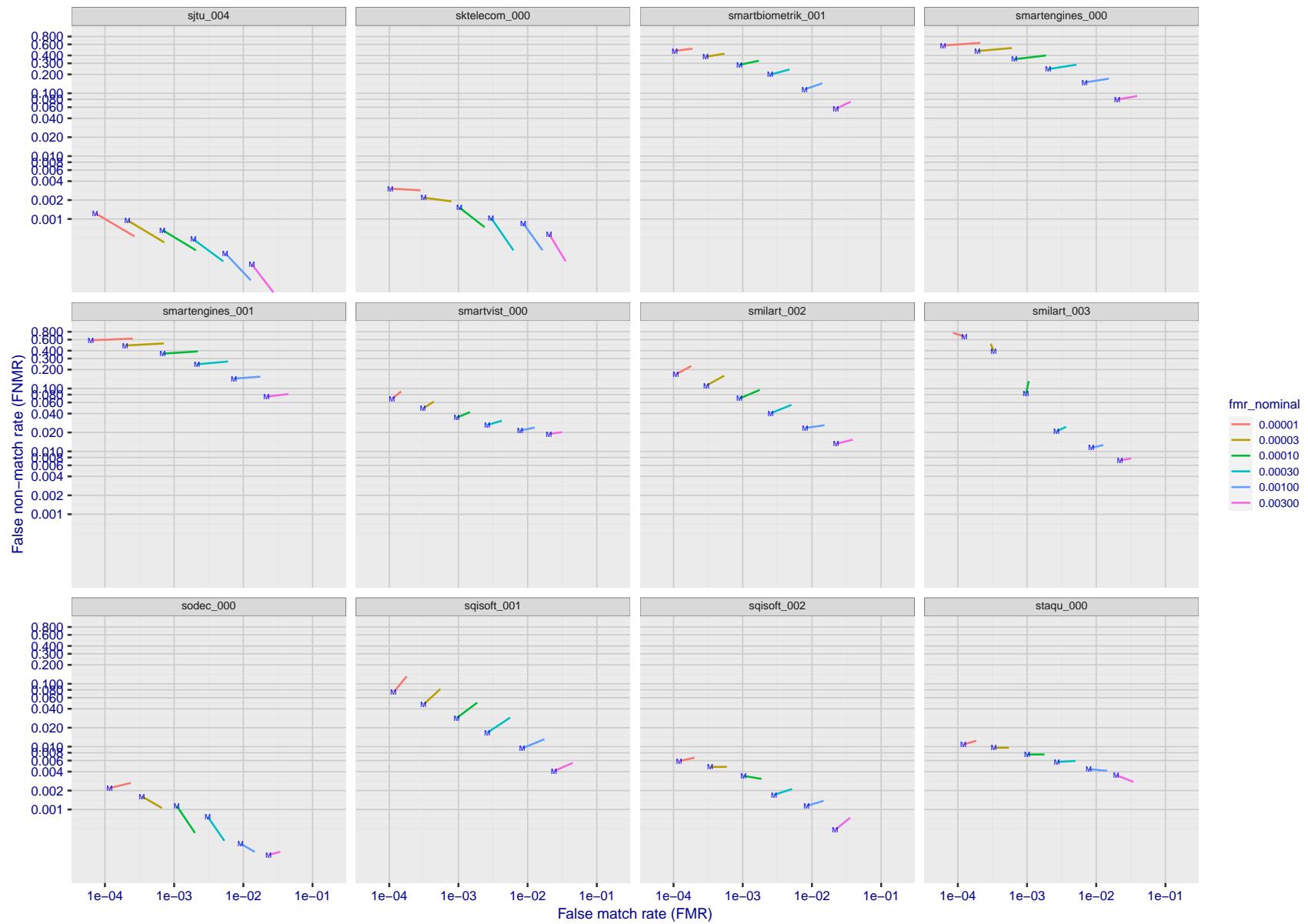


Figure 206: For the visa images, FNMR and FMR at six operating points along the DET characteristic. At each point a line is drawn between $(FMR, FNMR)_{MALE}$ and $(FMR, FNMR)_{FEMALE}$ showing how which sex has lower FMR and/or FNMR. The "M" label denotes male, the other end of the line corresponds to female. The six operating thresholds are selected to give the nominal false match rates given in the legend, and are computed over all impostor pairs regardless of age, sex, and place of birth. The plotted FMR values are broadly an order of magnitude larger than the nominal rates because FMR is computed over demographically-matched impostor pairs i.e individuals of the same sex, from the same geographic region (see section 3.6.1), and the same age group (see section 3.6.2).

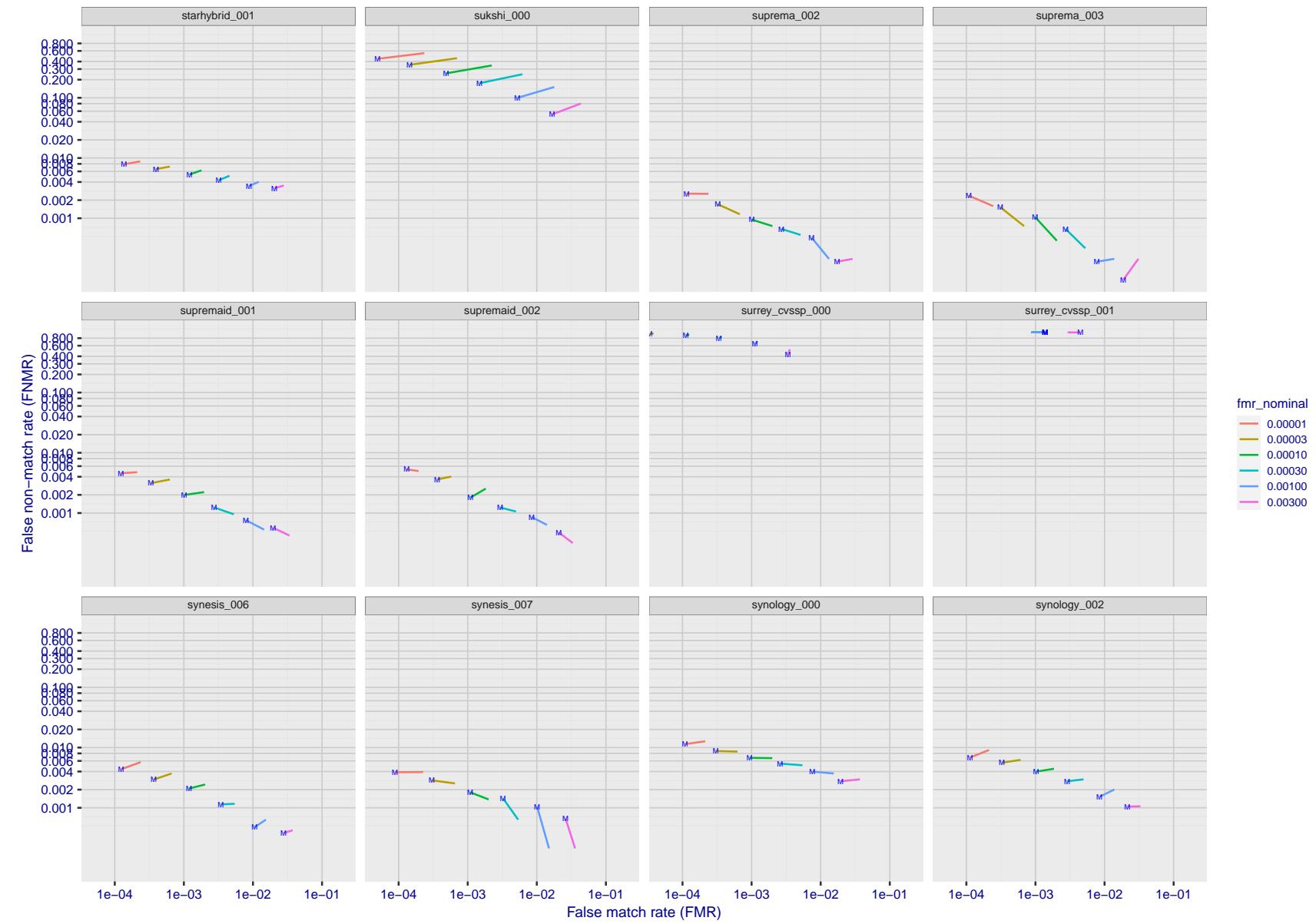


Figure 207: For the visa images, FNMR and FMR at six operating points along the DET characteristic. At each point a line is drawn between $(FMR, FNMR)_{MALE}$ and $(FMR, FNMR)_{FEMALE}$ showing how which sex has lower FMR and/or FNMR. The "M" label denotes male, the other end of the line corresponds to female. The six operating thresholds are selected to give the nominal false match rates given in the legend, and are computed over all impostor pairs regardless of age, sex, and place of birth. The plotted FMR values are broadly an order of magnitude larger than the nominal rates because FMR is computed over demographically-matched impostor pairs i.e individuals of the same sex, from the same geographic region (see section 3.6.1), and the same age group (see section 3.6.2).

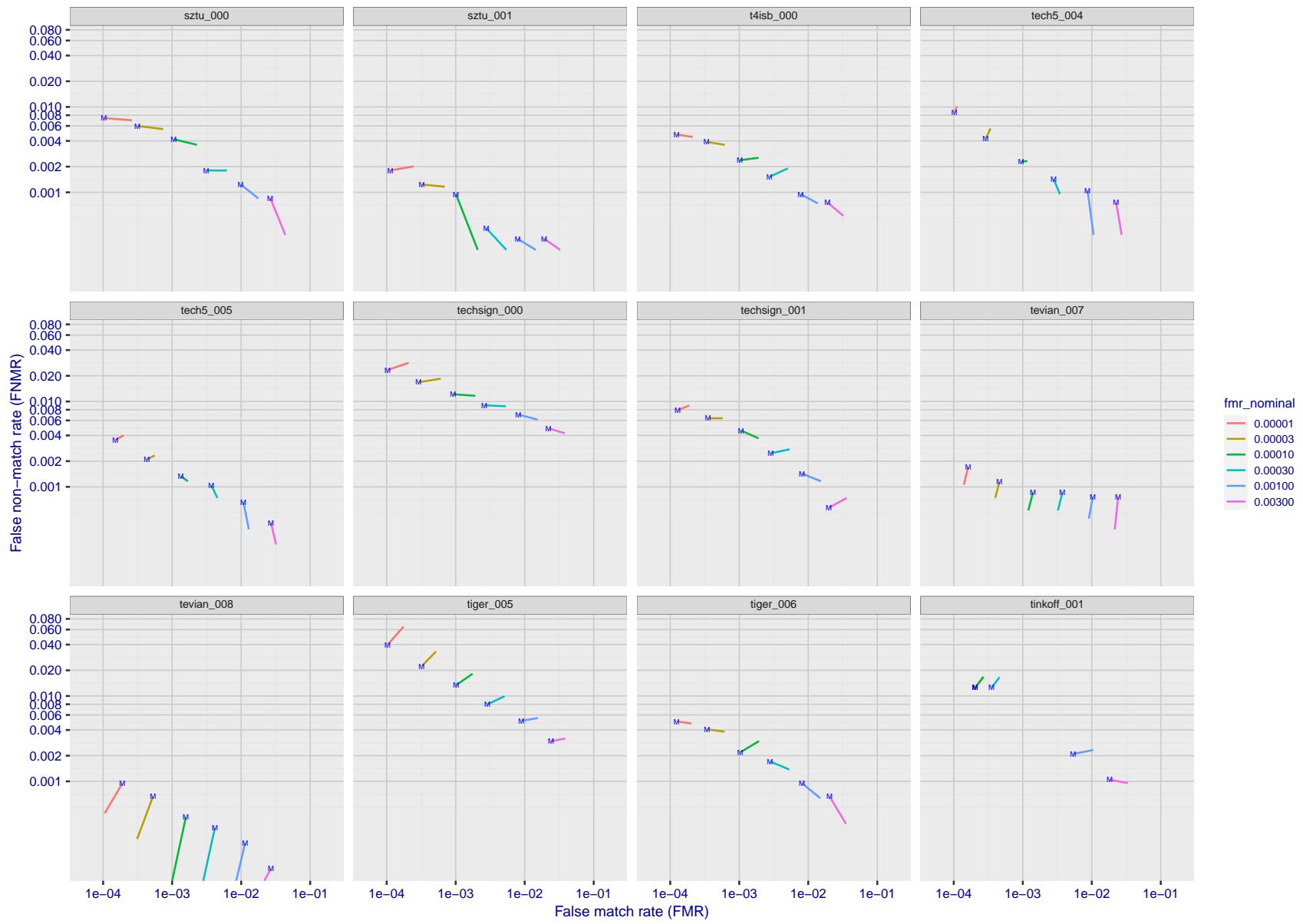


Figure 208: For the visa images, FNMR and FMR at six operating points along the DET characteristic. At each point a line is drawn between $(FMR, FNMR)_{MALE}$ and $(FMR, FNMR)_{FEMALE}$ showing how which sex has lower FMR and/or FNMR. The "M" label denotes male, the other end of the line corresponds to female. The six operating thresholds are selected to give the nominal false match rates given in the legend, and are computed over all impostor pairs regardless of age, sex, and place of birth. The plotted FMR values are broadly an order of magnitude larger than the nominal rates because FMR is computed over demographically-matched impostor pairs i.e individuals of the same sex, from the same geographic region (see section 3.6.1), and the same age group (see section 3.6.2).

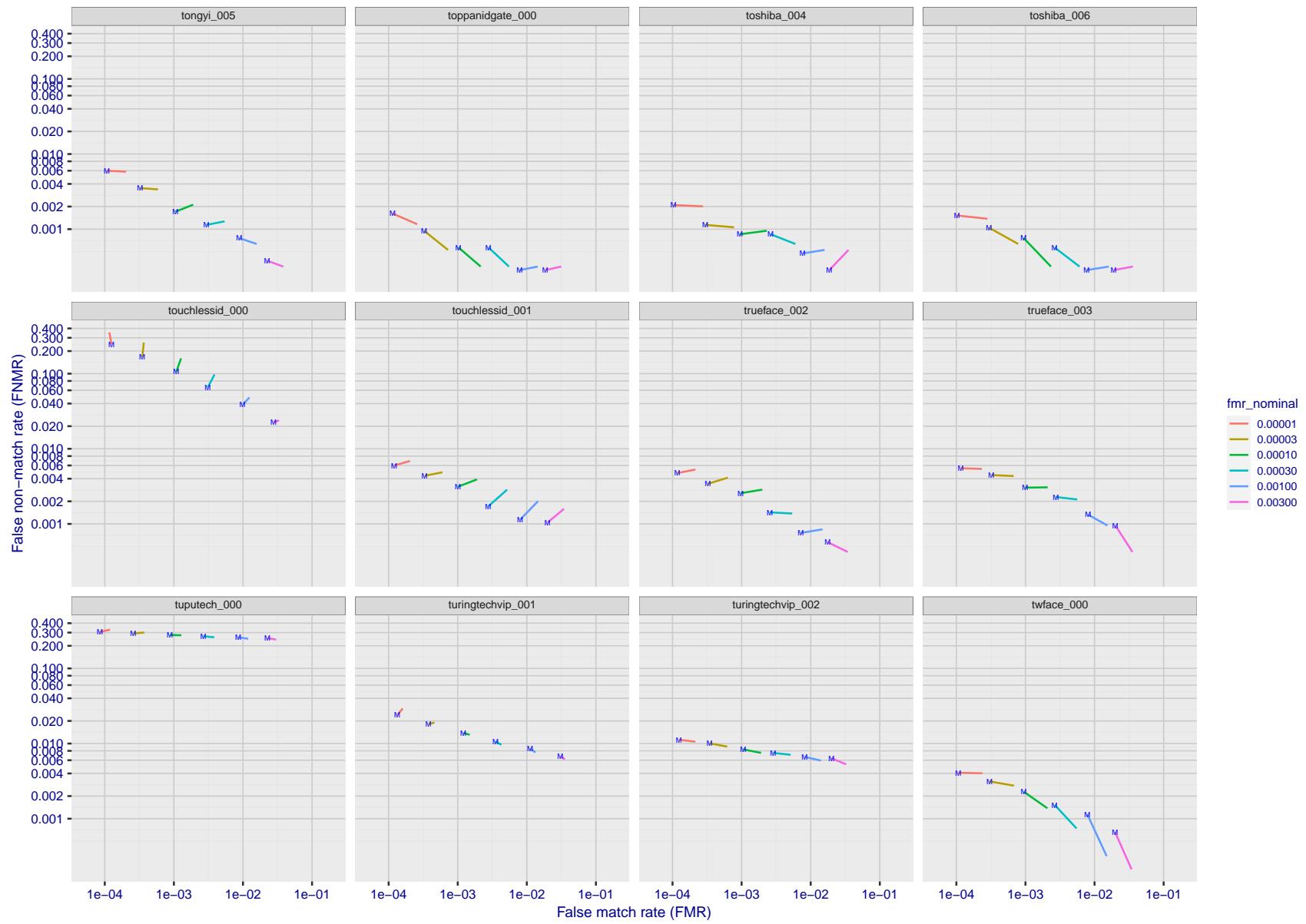


Figure 209: For the visa images, FNMR and FMR at six operating points along the DET characteristic. At each point a line is drawn between $(FMR, FNMR)_{MALE}$ and $(FMR, FNMR)_{FEMALE}$ showing how which sex has lower FMR and/or FNMR. The "M" label denotes male, the other end of the line corresponds to female. The six operating thresholds are selected to give the nominal false match rates given in the legend, and are computed over all impostor pairs regardless of age, sex, and place of birth. The plotted FMR values are broadly an order of magnitude larger than the nominal rates because FMR is computed over demographically-matched impostor pairs i.e individuals of the same sex, from the same geographic region (see section 3.6.1), and the same age group (see section 3.6.2).

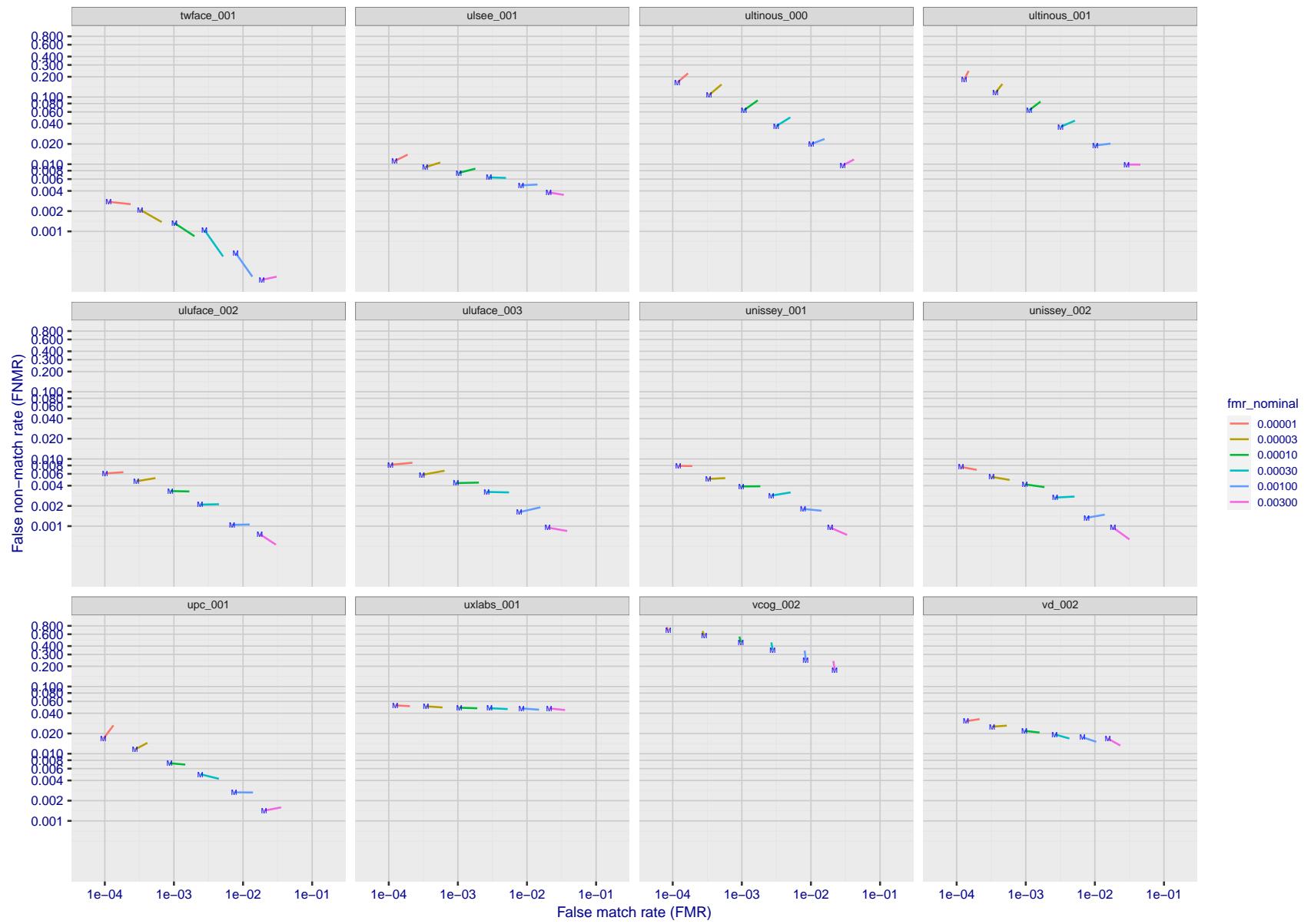


Figure 210: For the visa images, FNMR and FMR at six operating points along the DET characteristic. At each point a line is drawn between $(FMR, FNMR)_{MALE}$ and $(FMR, FNMR)_{FEMALE}$ showing how which sex has lower FMR and/or FNMR. The "M" label denotes male, the other end of the line corresponds to female. The six operating thresholds are selected to give the nominal false match rates given in the legend, and are computed over all impostor pairs regardless of age, sex, and place of birth. The plotted FMR values are broadly an order of magnitude larger than the nominal rates because FMR is computed over demographically-matched impostor pairs i.e individuals of the same sex, from the same geographic region (see section 3.6.1), and the same age group (see section 3.6.2).

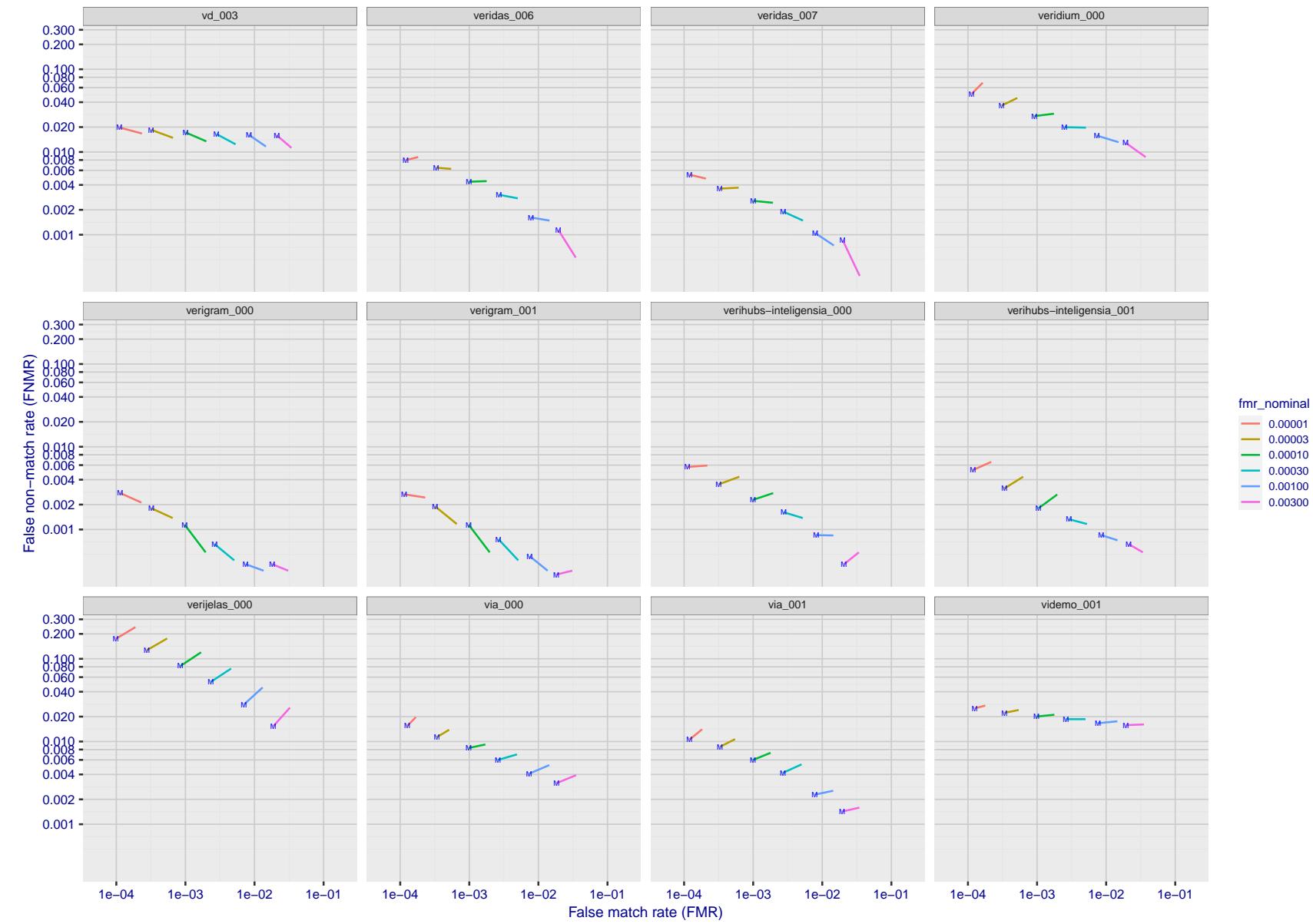


Figure 211: For the visa images, FNMR and FMR at six operating points along the DET characteristic. At each point a line is drawn between $(FMR, FNMR)_{MALE}$ and $(FMR, FNMR)_{FEMALE}$ showing how which sex has lower FMR and/or FNMR. The "M" label denotes male, the other end of the line corresponds to female. The six operating thresholds are selected to give the nominal false match rates given in the legend, and are computed over all impostor pairs regardless of age, sex, and place of birth. The plotted FMR values are broadly an order of magnitude larger than the nominal rates because FMR is computed over demographically-matched impostor pairs i.e individuals of the same sex, from the same geographic region (see section 3.6.1), and the same age group (see section 3.6.2).

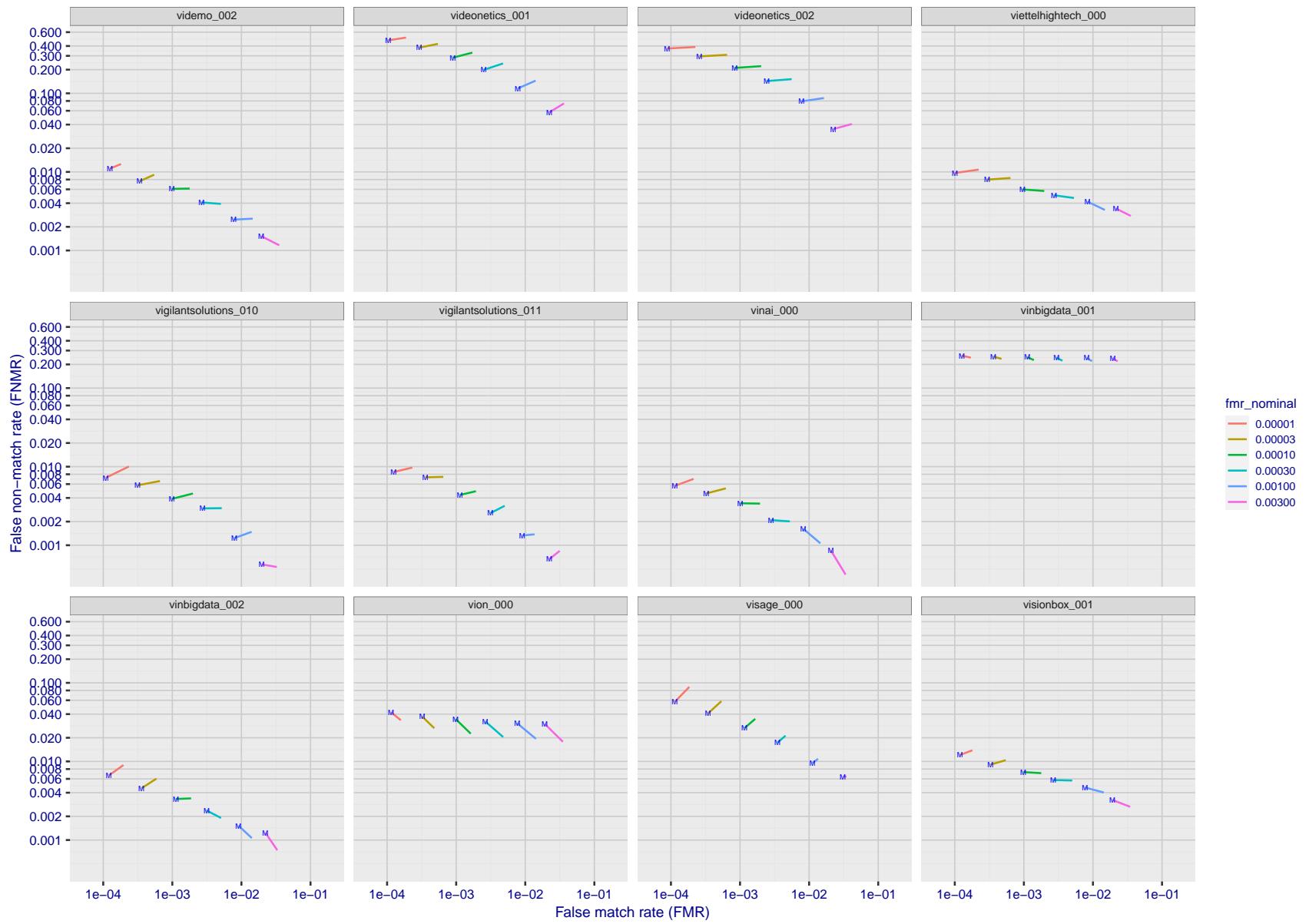


Figure 212: For the visa images, FNMR and FMR at six operating points along the DET characteristic. At each point a line is drawn between $(FMR, FNMR)_{MALE}$ and $(FMR, FNMR)_{FEMALE}$ showing how which sex has lower FMR and/or FNMR. The "M" label denotes male, the other end of the line corresponds to female. The six operating thresholds are selected to give the nominal false match rates given in the legend, and are computed over all impostor pairs regardless of age, sex, and place of birth. The plotted FMR values are broadly an order of magnitude larger than the nominal rates because FMR is computed over demographically-matched impostor pairs i.e individuals of the same sex, from the same geographic region (see section 3.6.1), and the same age group (see section 3.6.2).

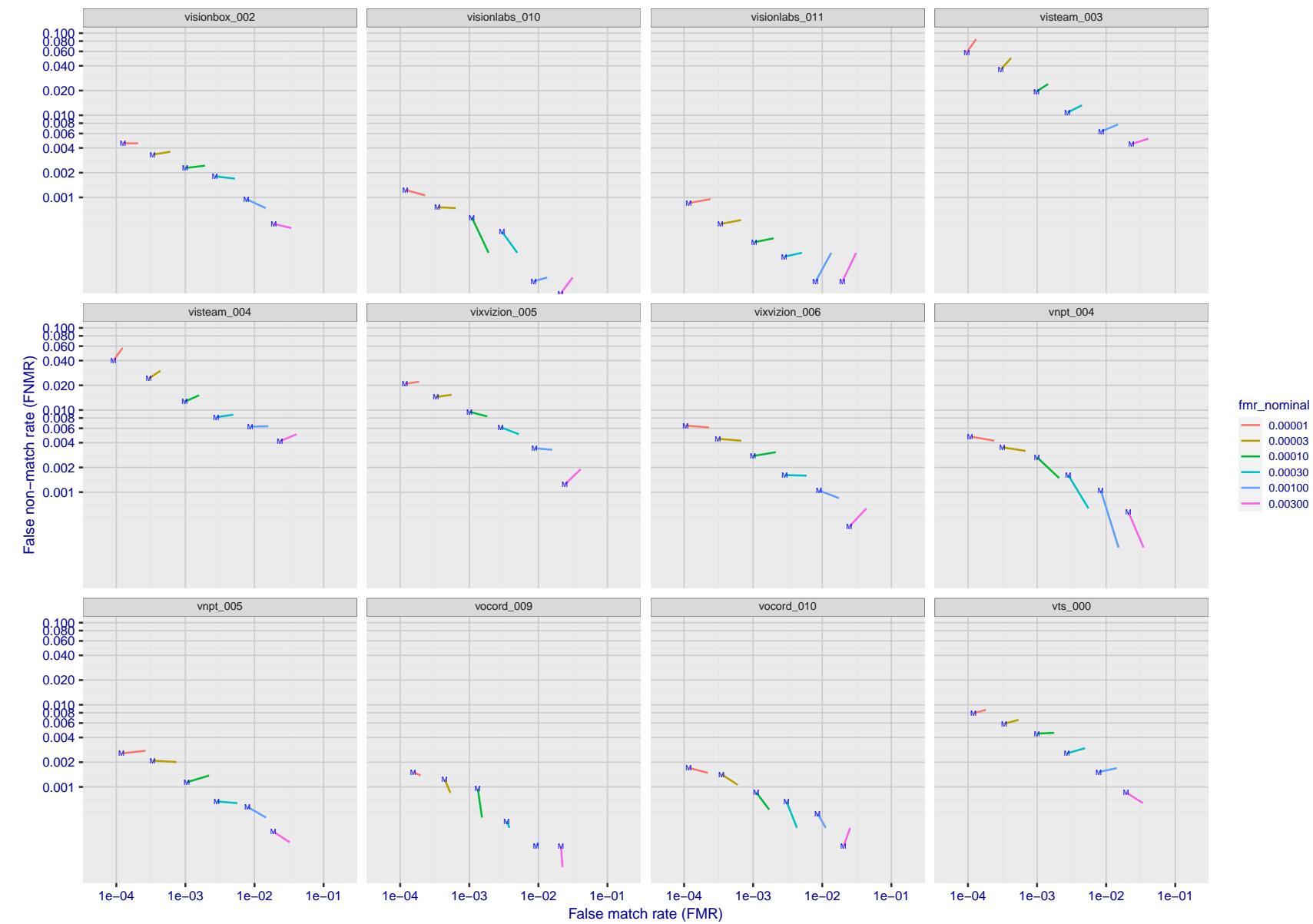


Figure 213: For the visa images, FNMR and FMR at six operating points along the DET characteristic. At each point a line is drawn between $(FMR, FNMR)_{MALE}$ and $(FMR, FNMR)_{FEMALE}$ showing how which sex has lower FMR and/or FNMR. The "M" label denotes male, the other end of the line corresponds to female. The six operating thresholds are selected to give the nominal false match rates given in the legend, and are computed over all impostor pairs regardless of age, sex, and place of birth. The plotted FMR values are broadly an order of magnitude larger than the nominal rates because FMR is computed over demographically-matched impostor pairs i.e individuals of the same sex, from the same geographic region (see section 3.6.1), and the same age group (see section 3.6.2).

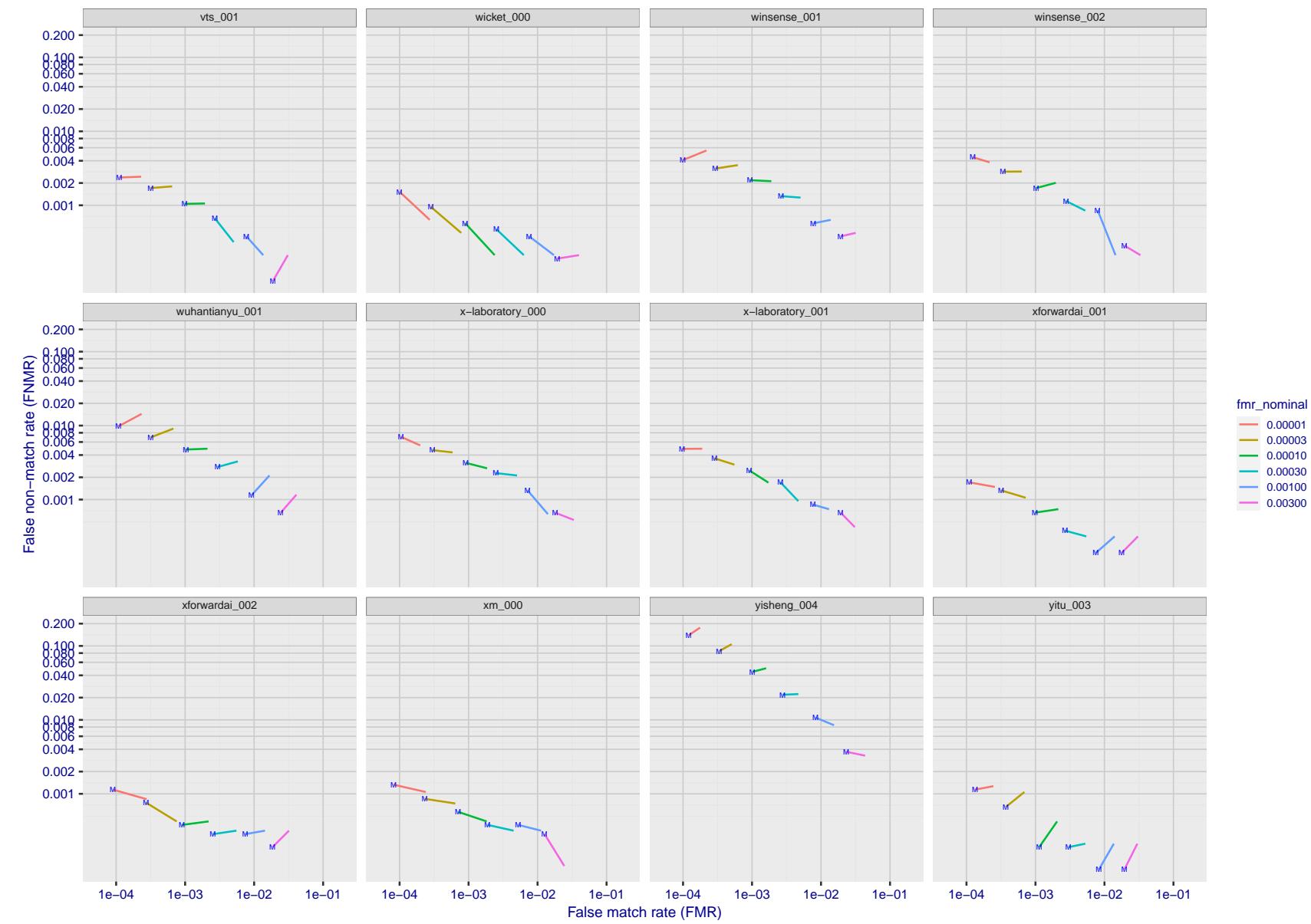


Figure 214: For the visa images, FNMR and FMR at six operating points along the DET characteristic. At each point a line is drawn between $(FMR, FNMR)_{MALE}$ and $(FMR, FNMR)_{FEMALE}$ showing how which sex has lower FMR and/or FNMR. The "M" label denotes male, the other end of the line corresponds to female. The six operating thresholds are selected to give the nominal false match rates given in the legend, and are computed over all impostor pairs regardless of age, sex, and place of birth. The plotted FMR values are broadly an order of magnitude larger than the nominal rates because FMR is computed over demographically-matched impostor pairs i.e individuals of the same sex, from the same geographic region (see section 3.6.1), and the same age group (see section 3.6.2).

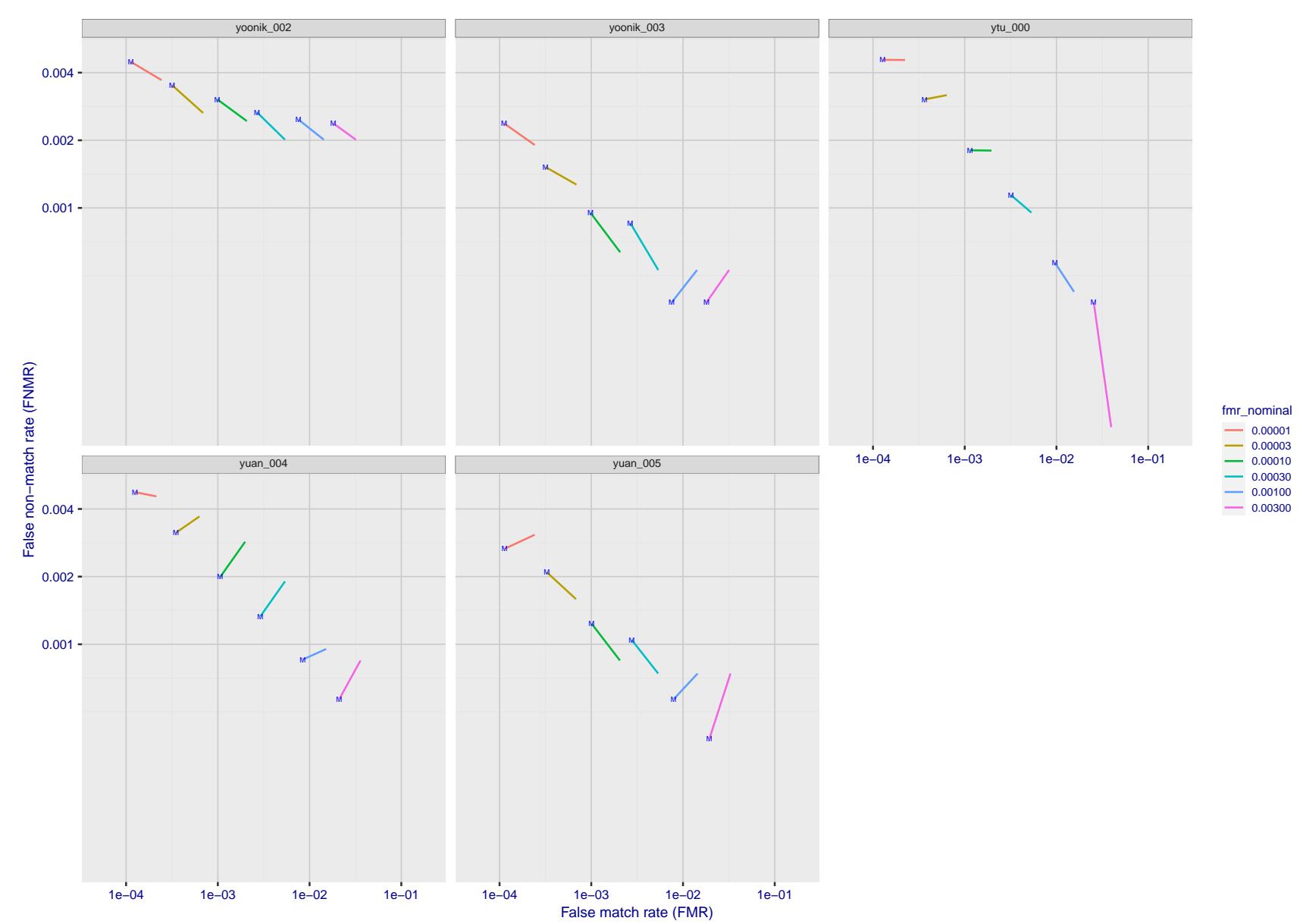


Figure 215: For the visa images, FNMR and FMR at six operating points along the DET characteristic. At each point a line is drawn between $(FMR, FNMR)_{MALE}$ and $(FMR, FNMR)_{FEMALE}$ showing how which sex has lower FMR and/or FNMR. The "M" label denotes male, the other end of the line corresponds to female. The six operating thresholds are selected to give the nominal false match rates given in the legend, and are computed over all impostor pairs regardless of age, sex, and place of birth. The plotted FMR values are broadly an order of magnitude larger than the nominal rates because FMR is computed over demographically-matched impostor pairs i.e individuals of the same sex, from the same geographic region (see section 3.6.1), and the same age group (see section 3.6.2).

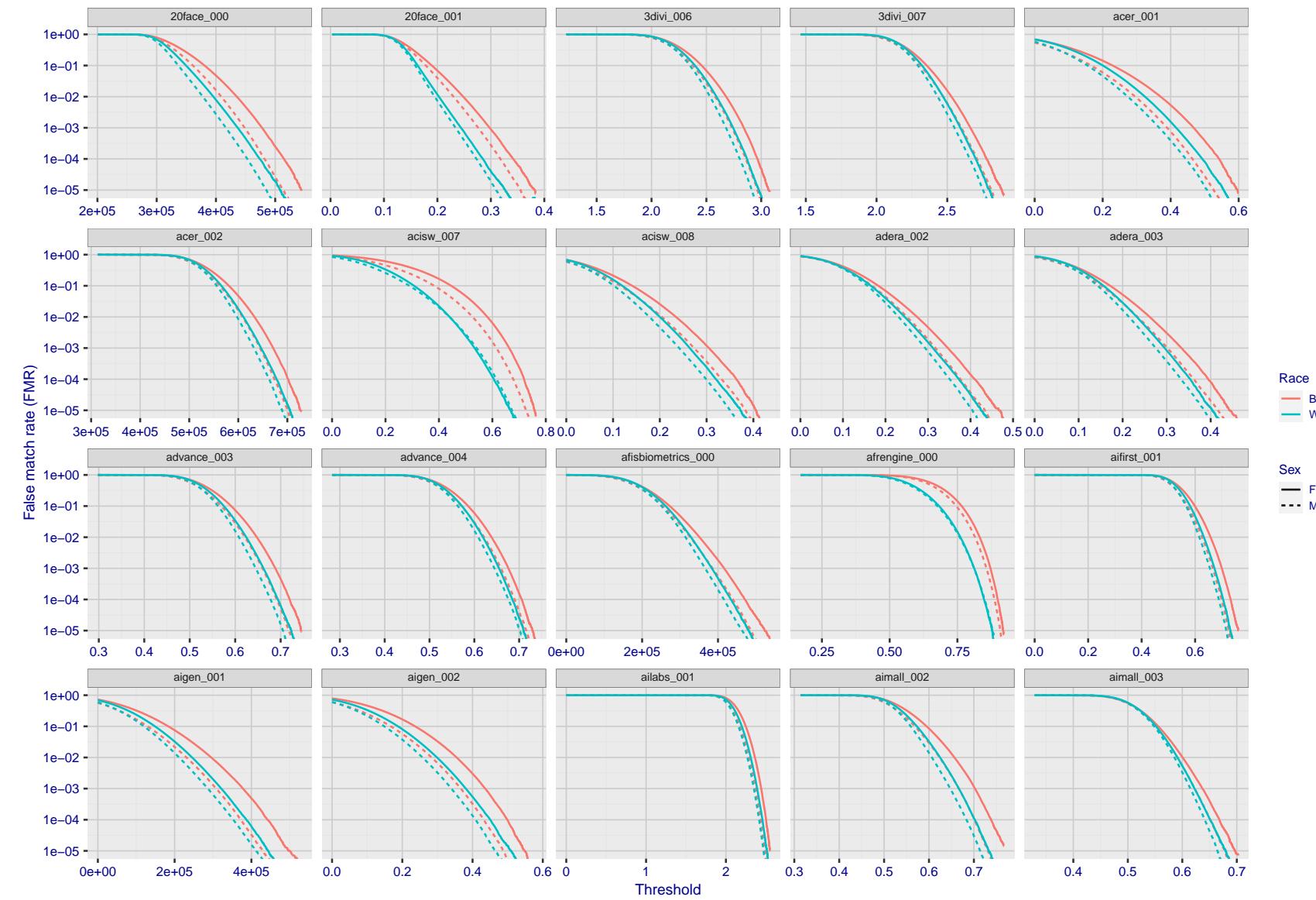


Figure 216: For the mugshot images, the false match calibration curves show false match rate vs. threshold. Separate curves appear for white females, black females, black males and white males.

2022/11/07 10:56:27

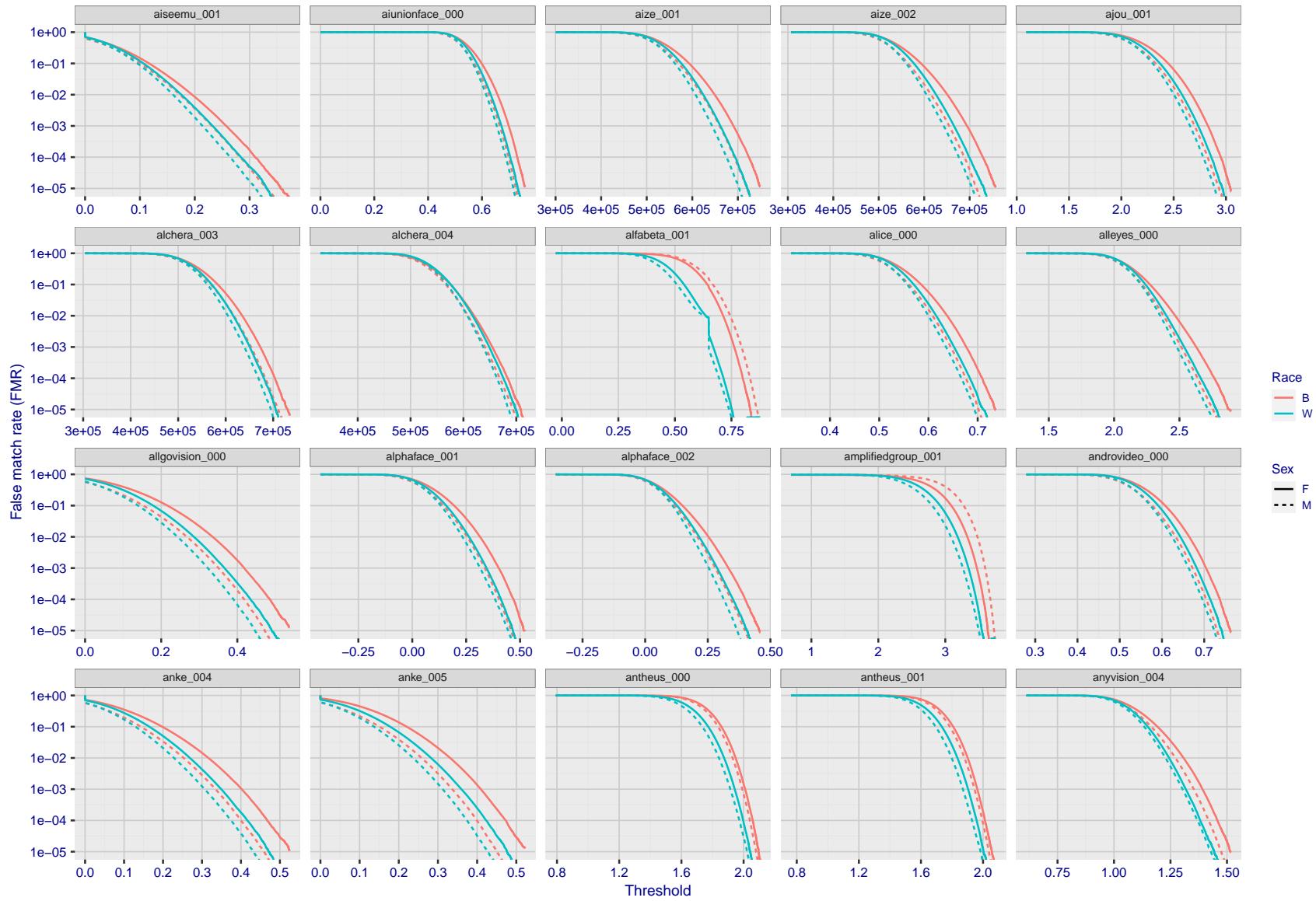


Figure 217: For the mugshot images, the false match calibration curves show false match rate vs. threshold. Separate curves appear for white females, black females, black males and white males.

2022/11/07 10:56:27

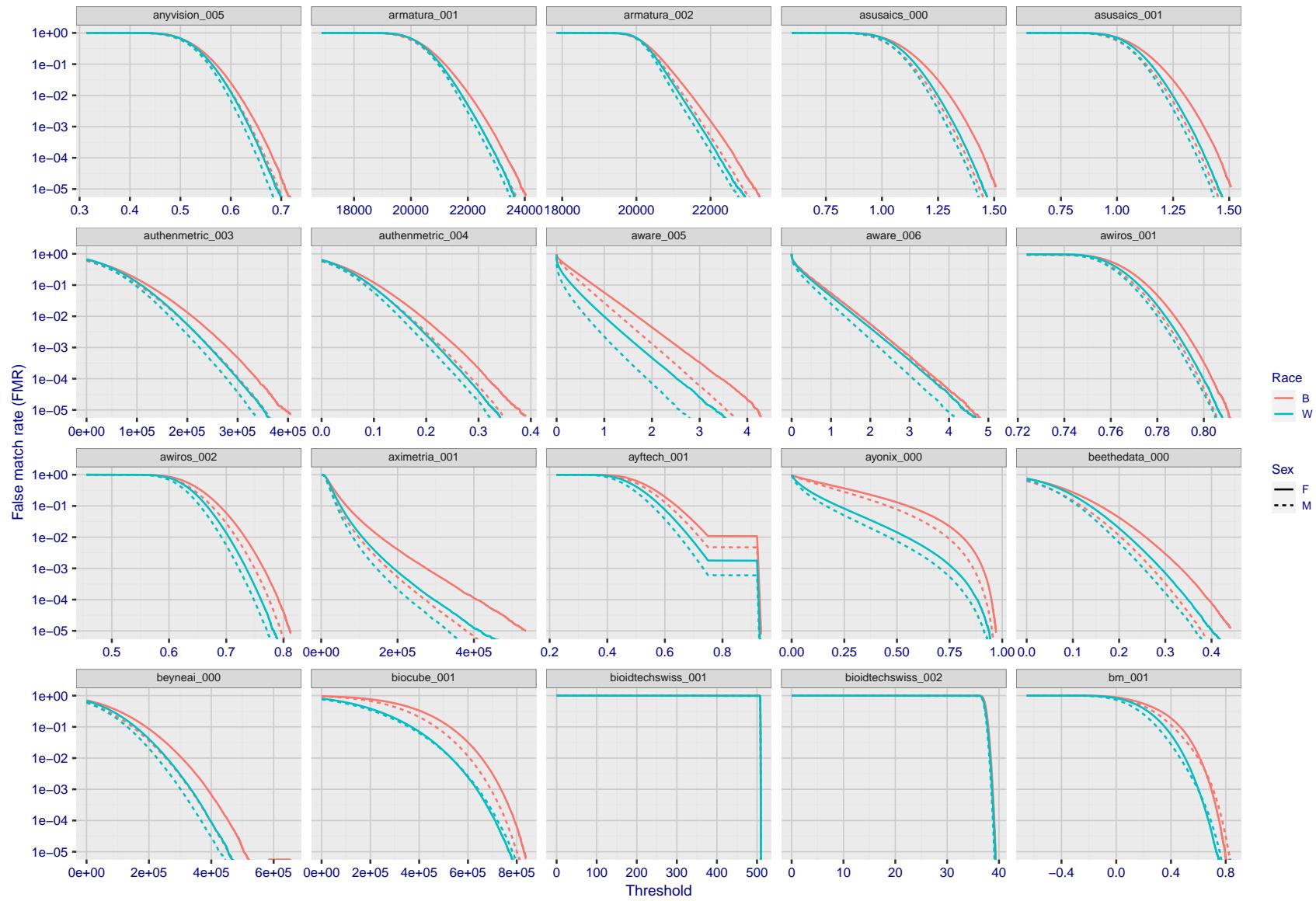


Figure 218: For the mugshot images, the false match calibration curves show false match rate vs. threshold. Separate curves appear for white females, black females, black males and white males.

2022/11/07 10:56:27

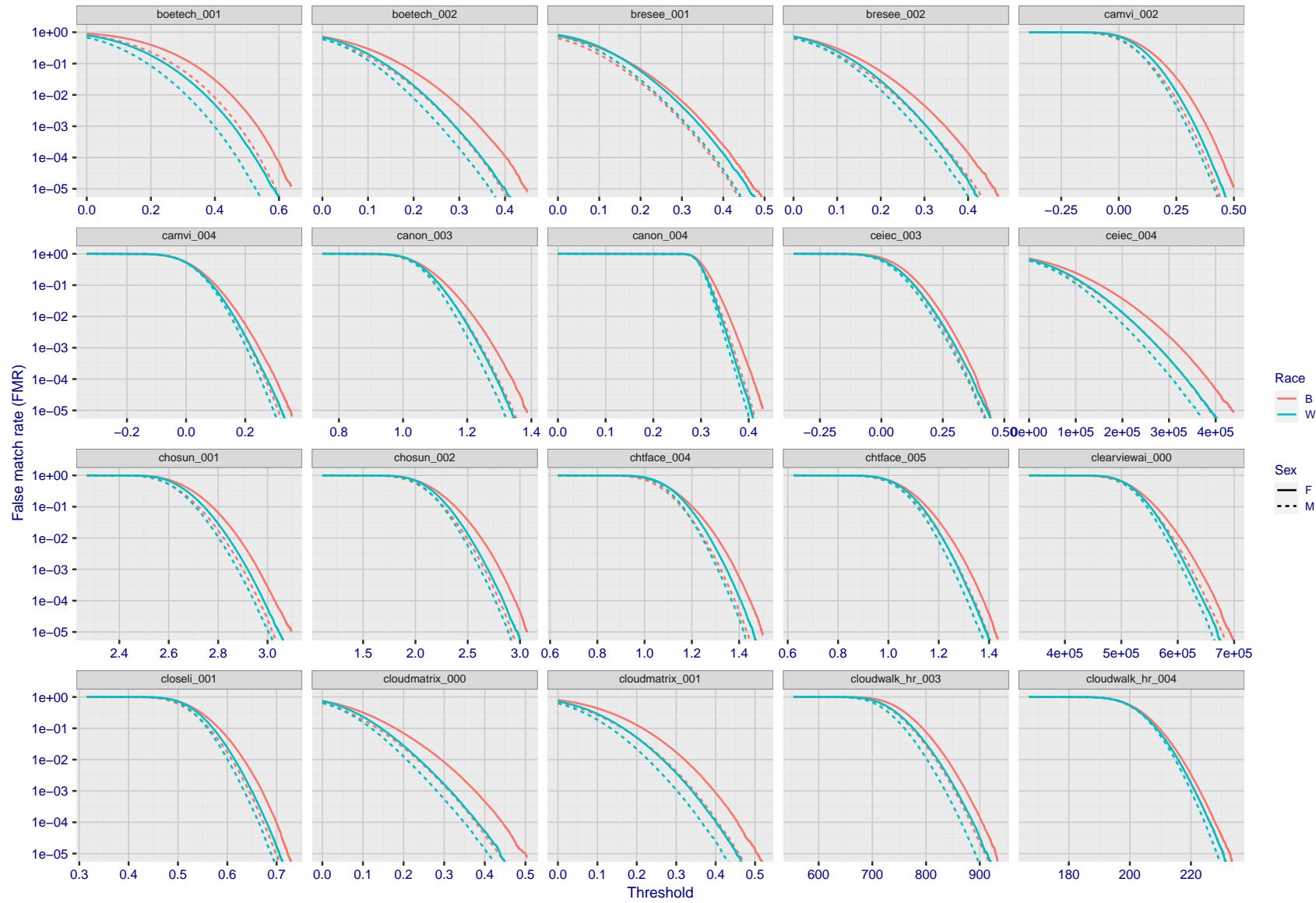


Figure 219: For the mugshot images, the false match calibration curves show false match rate vs. threshold. Separate curves appear for white females, black females, black males and white males.

2022/11/07 10:56:27

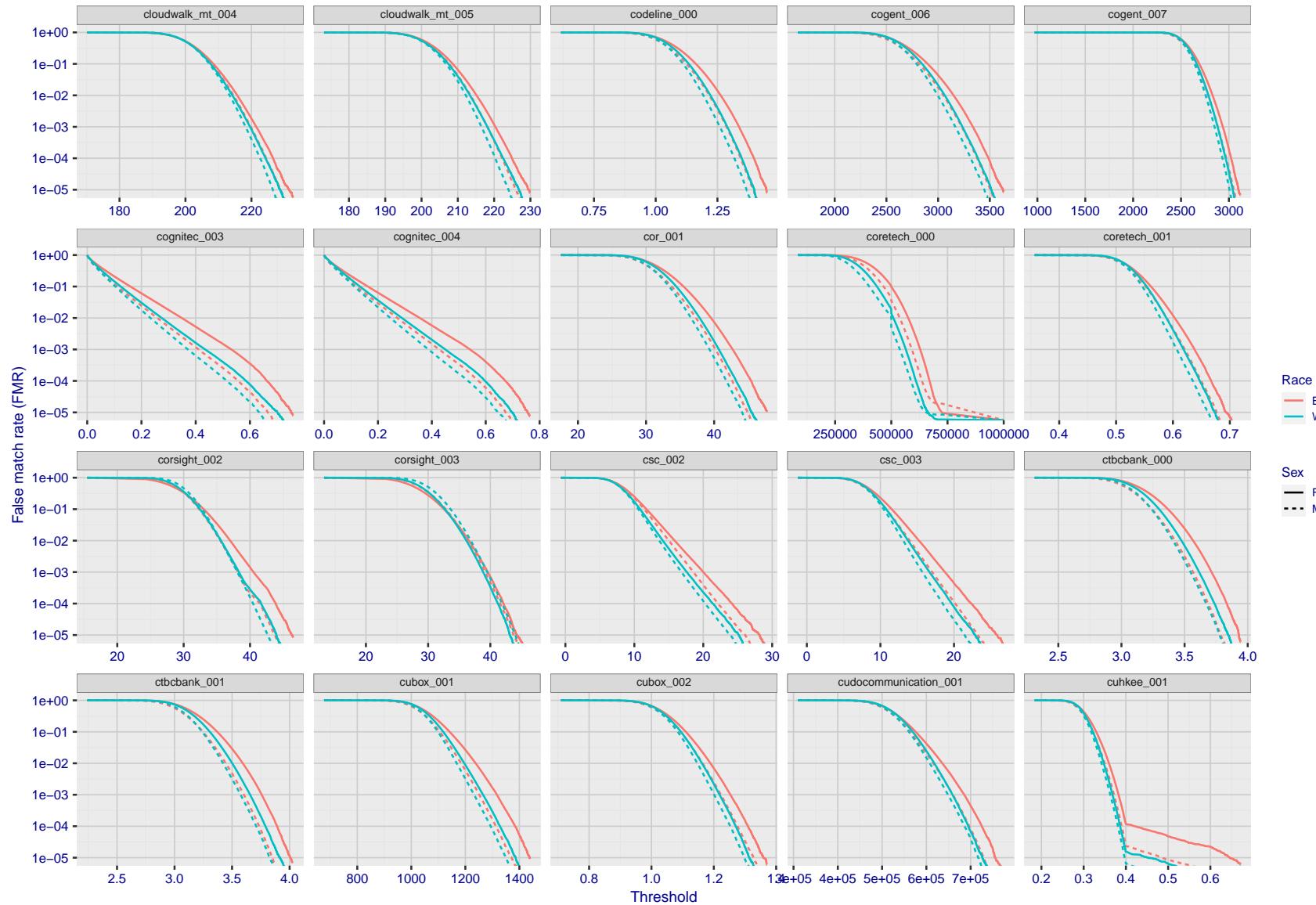


Figure 220: For the mugshot images, the false match calibration curves show false match rate vs. threshold. Separate curves appear for white females, black females, black males and white males.

FNMR(T)
"False non-match rate"
FMR(T)
"False match rate"

2022/11/07 10:56:27

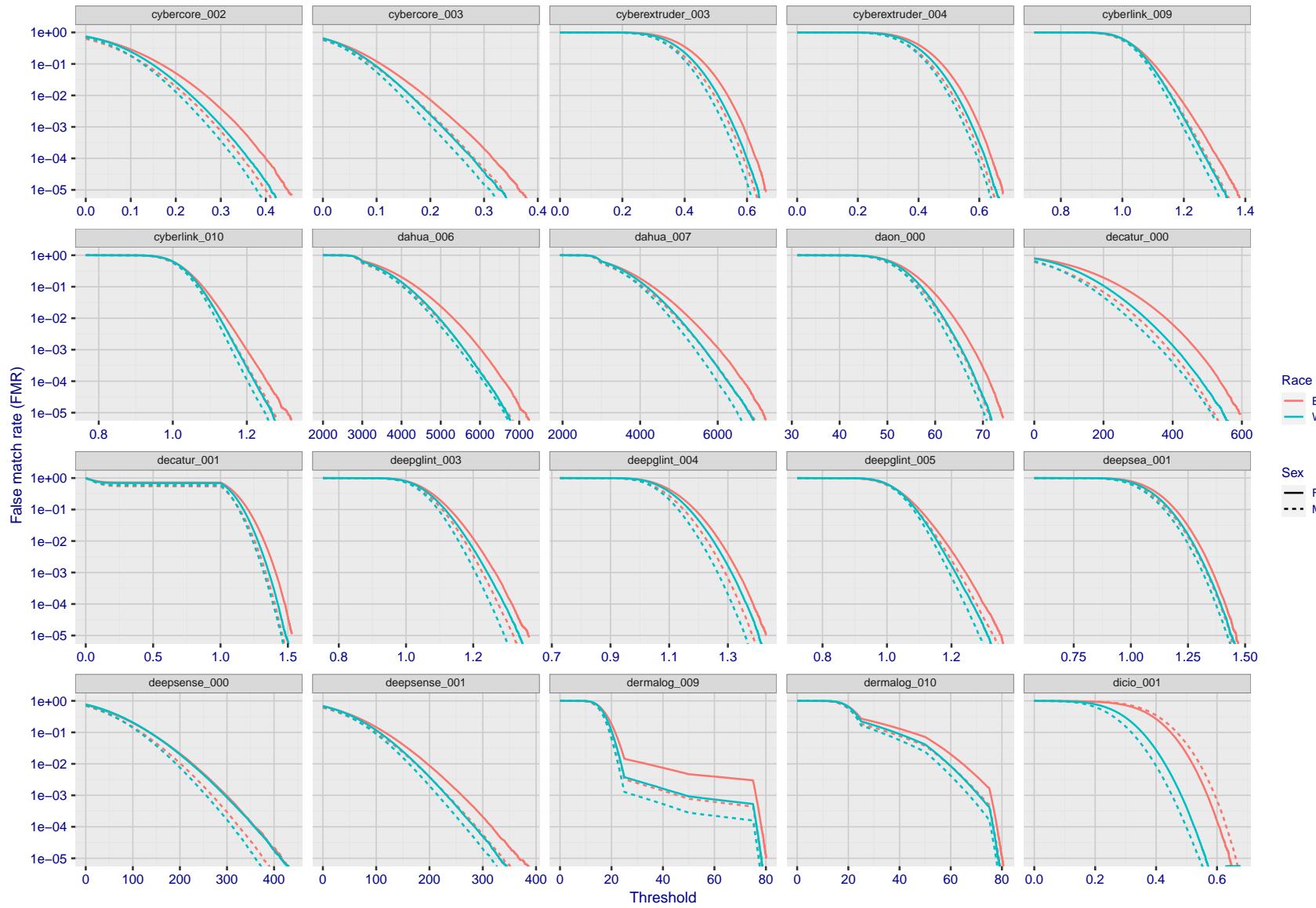


Figure 221: For the mugshot images, the false match calibration curves show false match rate vs. threshold. Separate curves appear for white females, black females, black males and white males.

2022/11/07 10:56:27

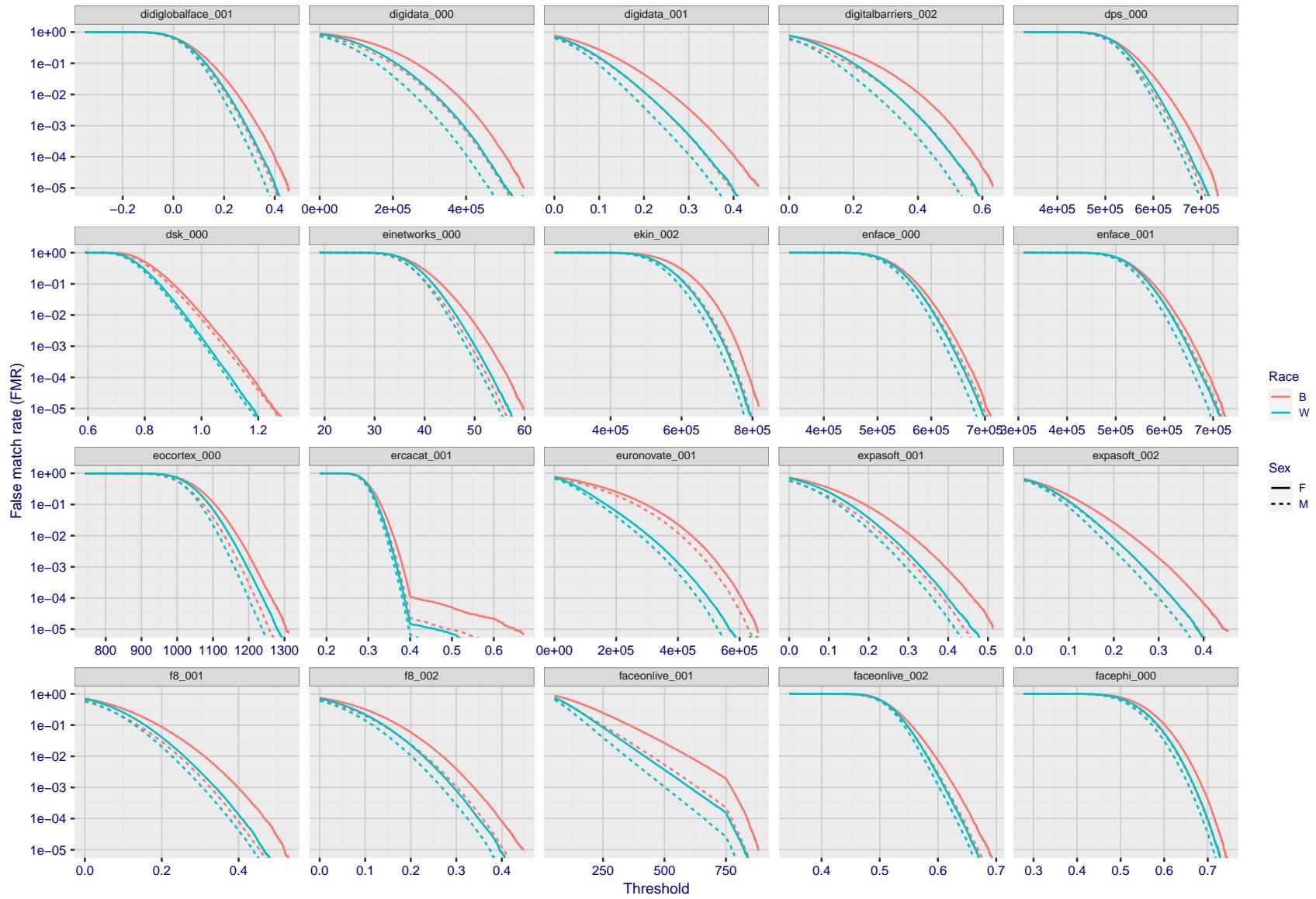


Figure 222: For the mugshot images, the false match calibration curves show false match rate vs. threshold. Separate curves appear for white females, black females, black males and white males.

2022/11/07 10:56:27

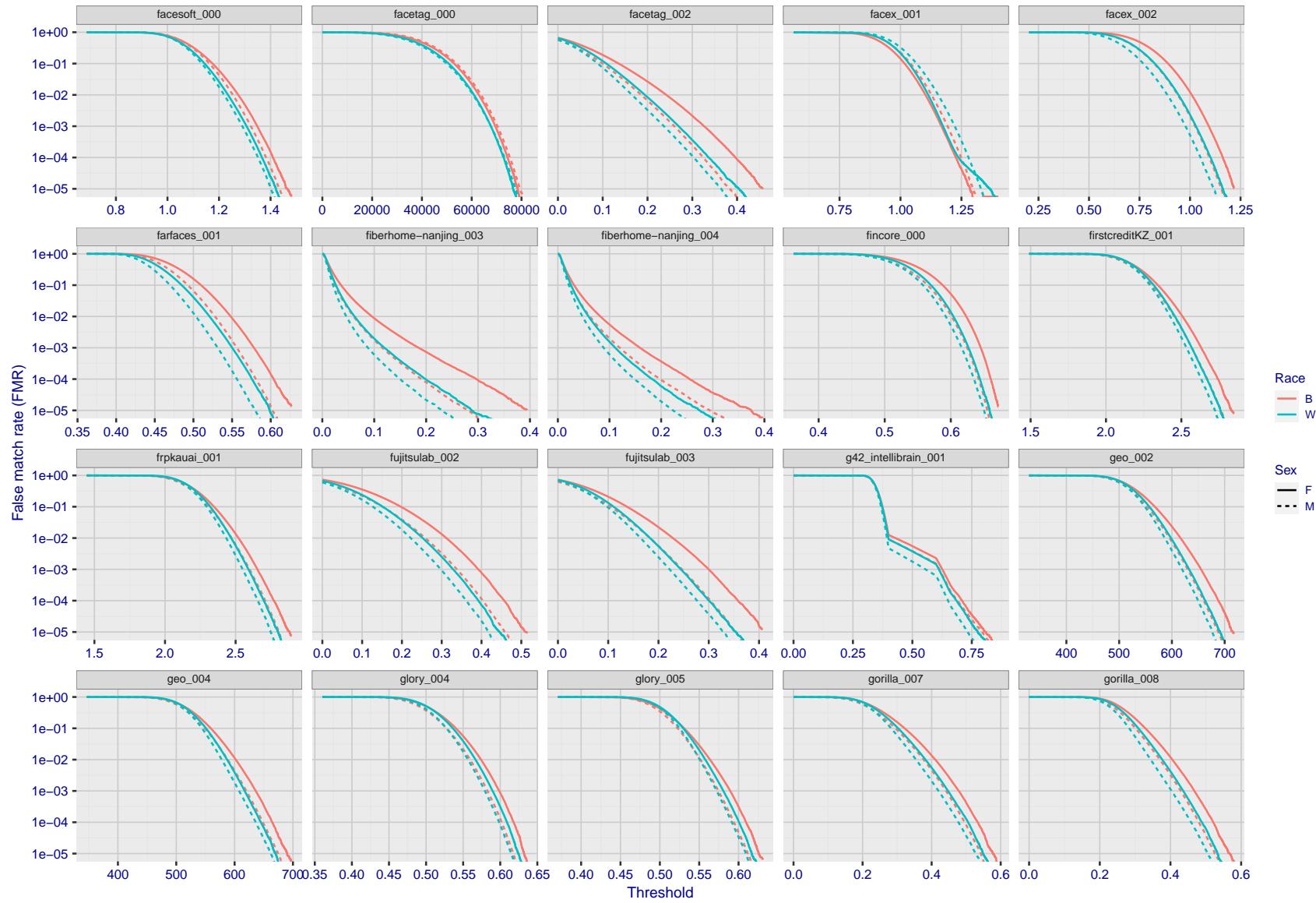


Figure 223: For the mugshot images, the false match calibration curves show false match rate vs. threshold. Separate curves appear for white females, black females, black males and white males.

2022/11/07 10:56:27

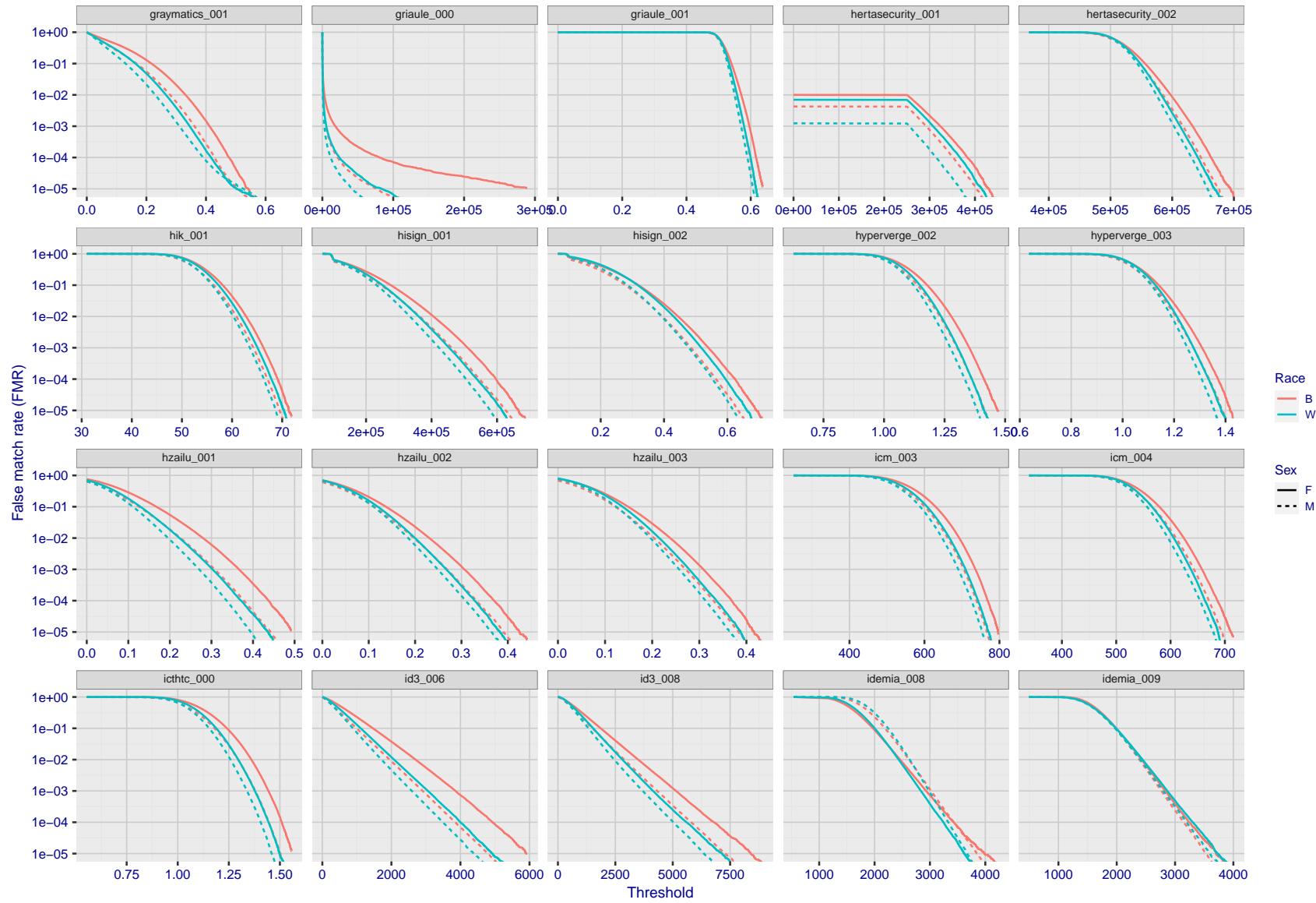


Figure 224: For the mugshot images, the false match calibration curves show false match rate vs. threshold. Separate curves appear for white females, black females, black males and white males.

FNMR(T)
"False non-match rate"
"False match rate"

2022/11/07 10:56:27

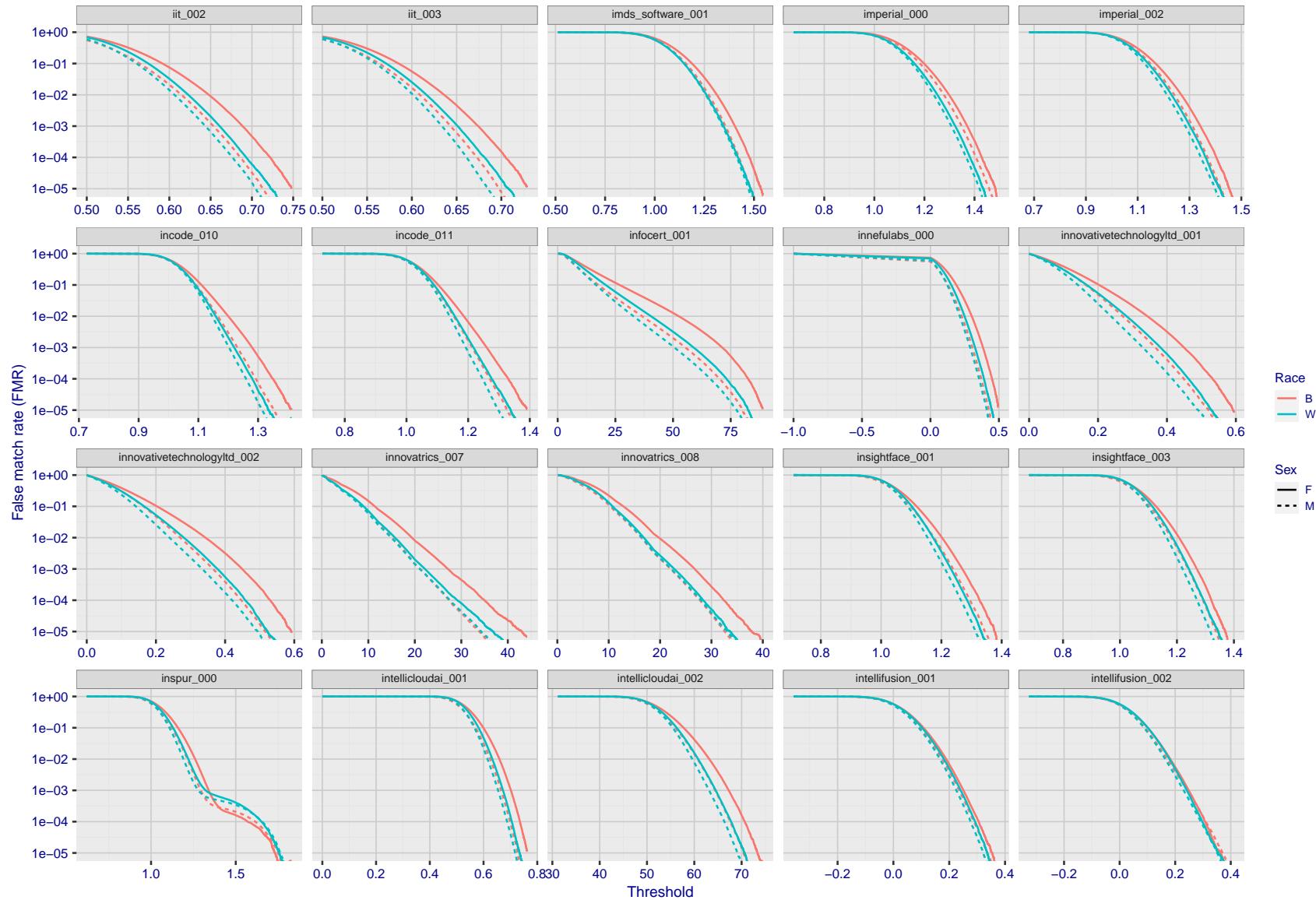


Figure 225: For the mugshot images, the false match calibration curves show false match rate vs. threshold. Separate curves appear for white females, black females, black males and white males.

2022/11/07 10:56:27

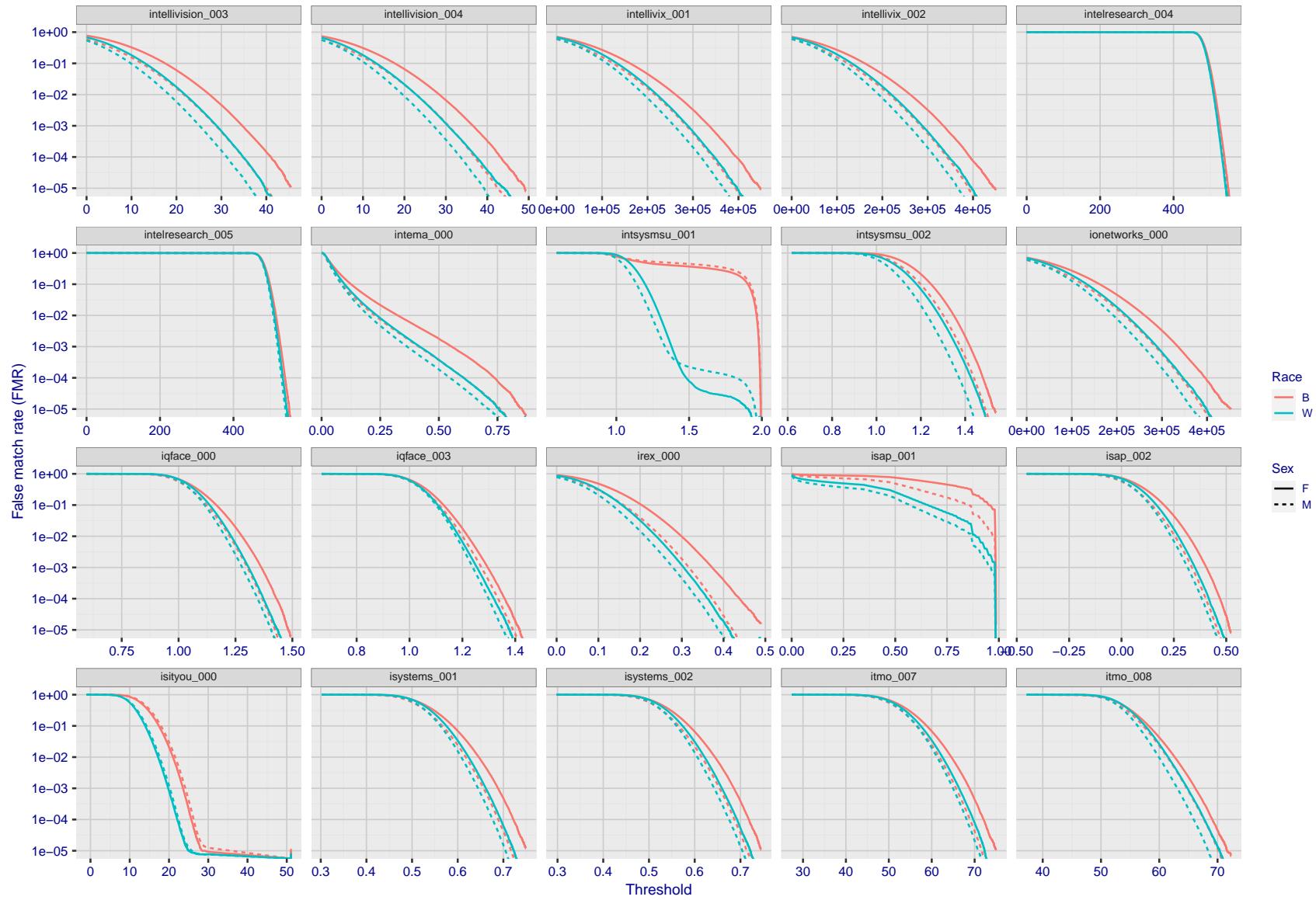


Figure 226: For the mugshot images, the false match calibration curves show false match rate vs. threshold. Separate curves appear for white females, black females, black males and white males.

2022/11/07 10:56:27

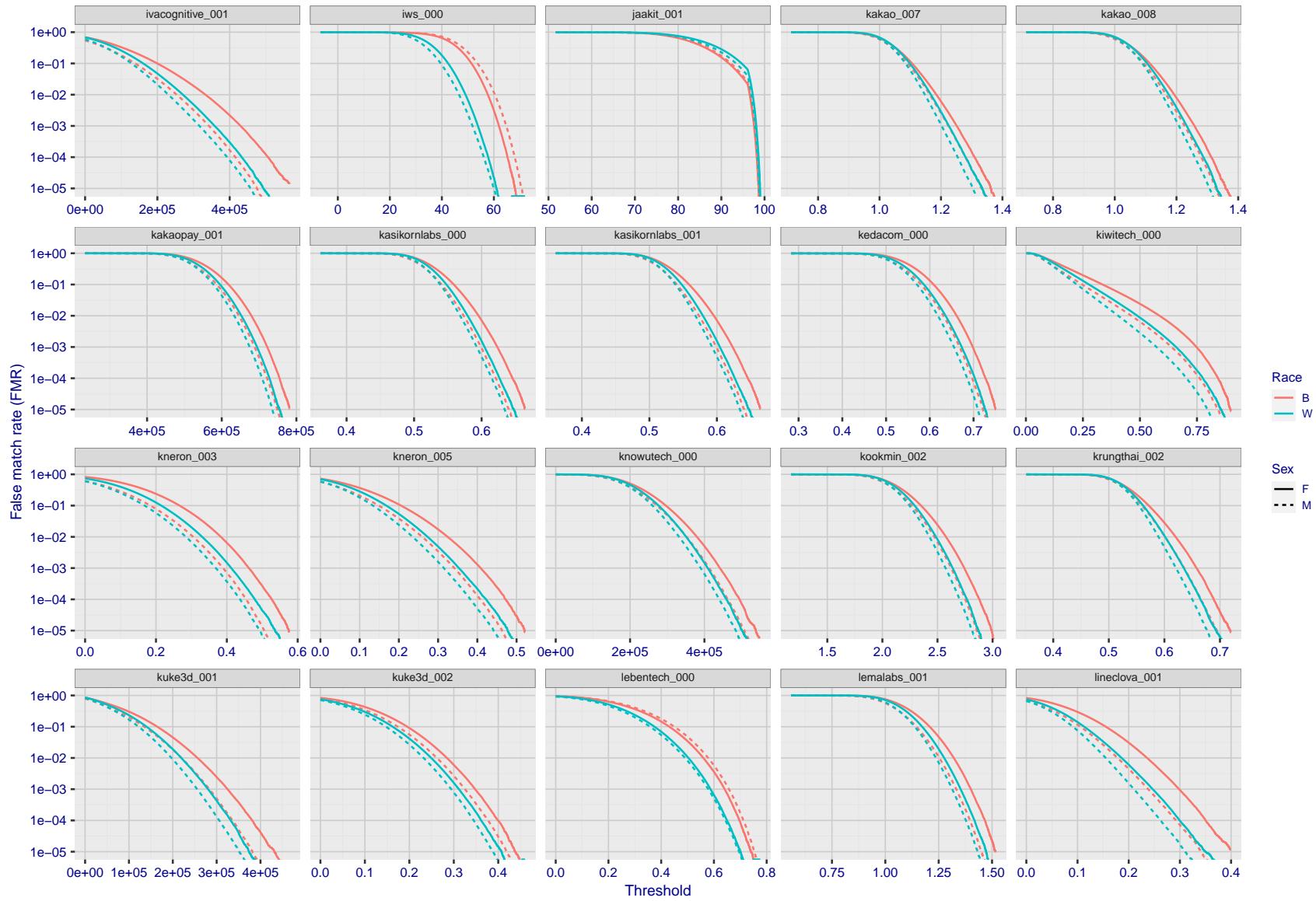


Figure 227: For the mugshot images, the false match calibration curves show false match rate vs. threshold. Separate curves appear for white females, black females, black males and white males.

2022/11/07 10:56:27

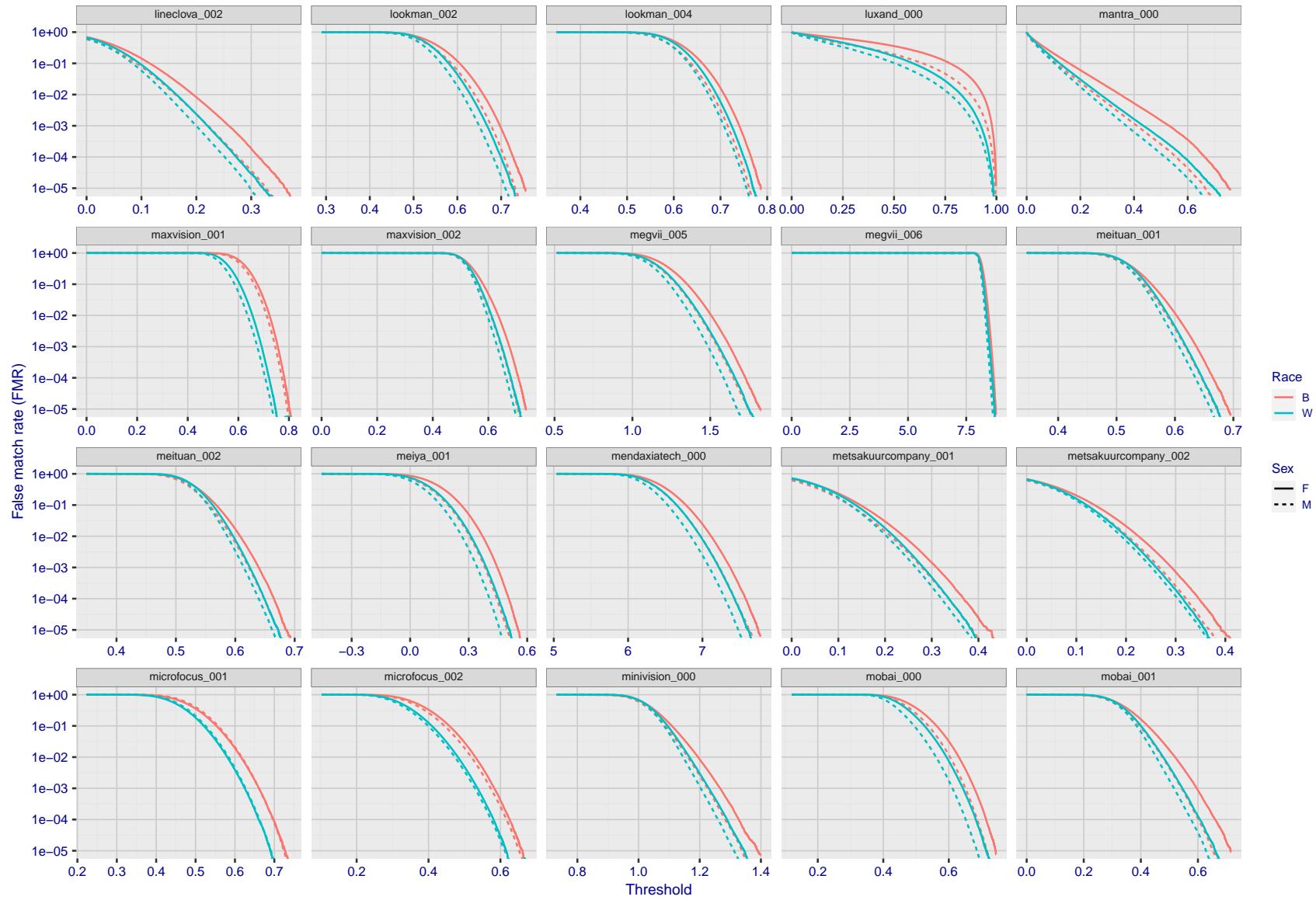


Figure 228: For the mugshot images, the false match calibration curves show false match rate vs. threshold. Separate curves appear for white females, black females, black males and white males.

2022/11/07 10:56:27

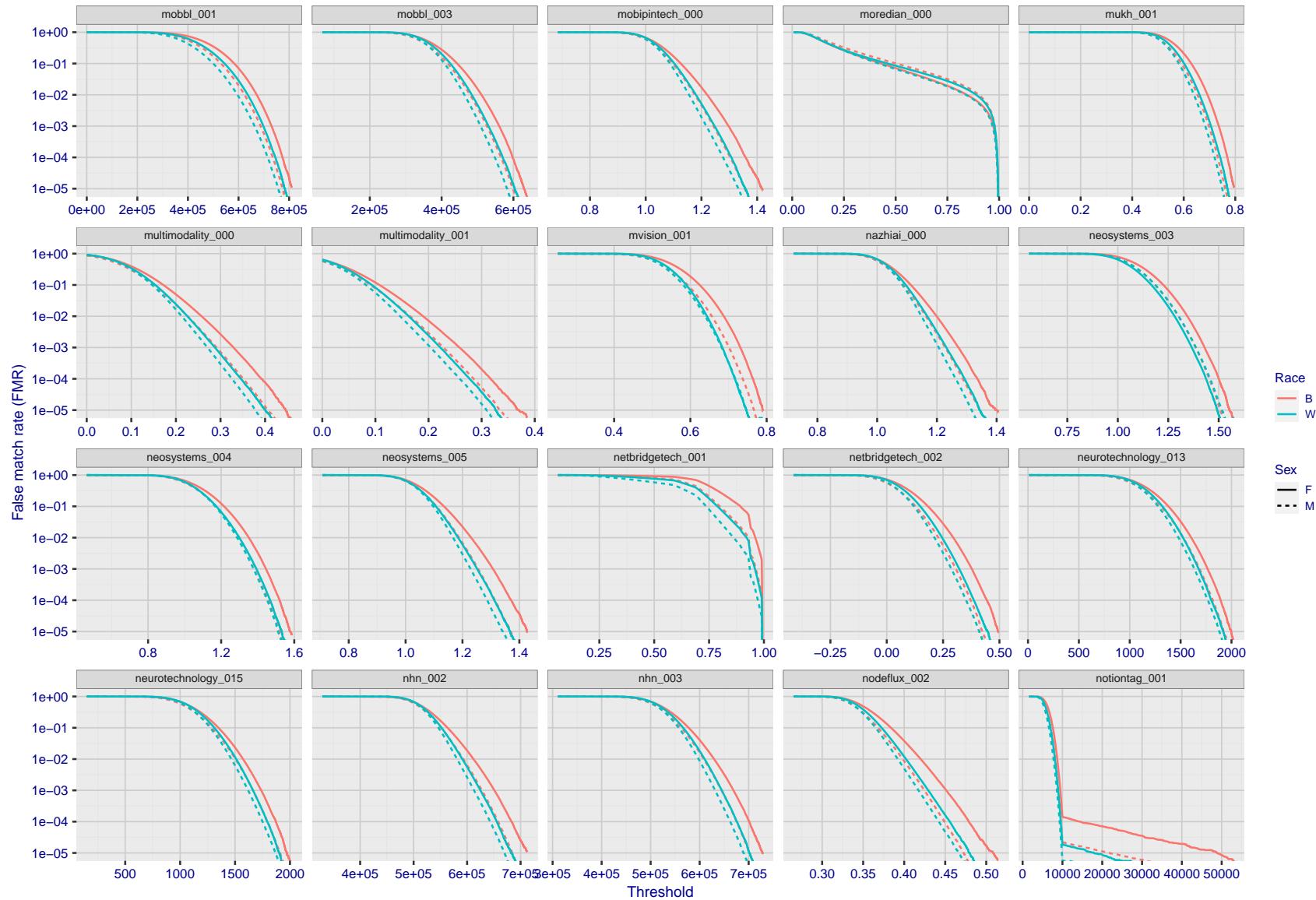


Figure 229: For the mugshot images, the false match calibration curves show false match rate vs. threshold. Separate curves appear for white females, black females, black males and white males.

FNMR(T)
"False non-match rate"
"False match rate"

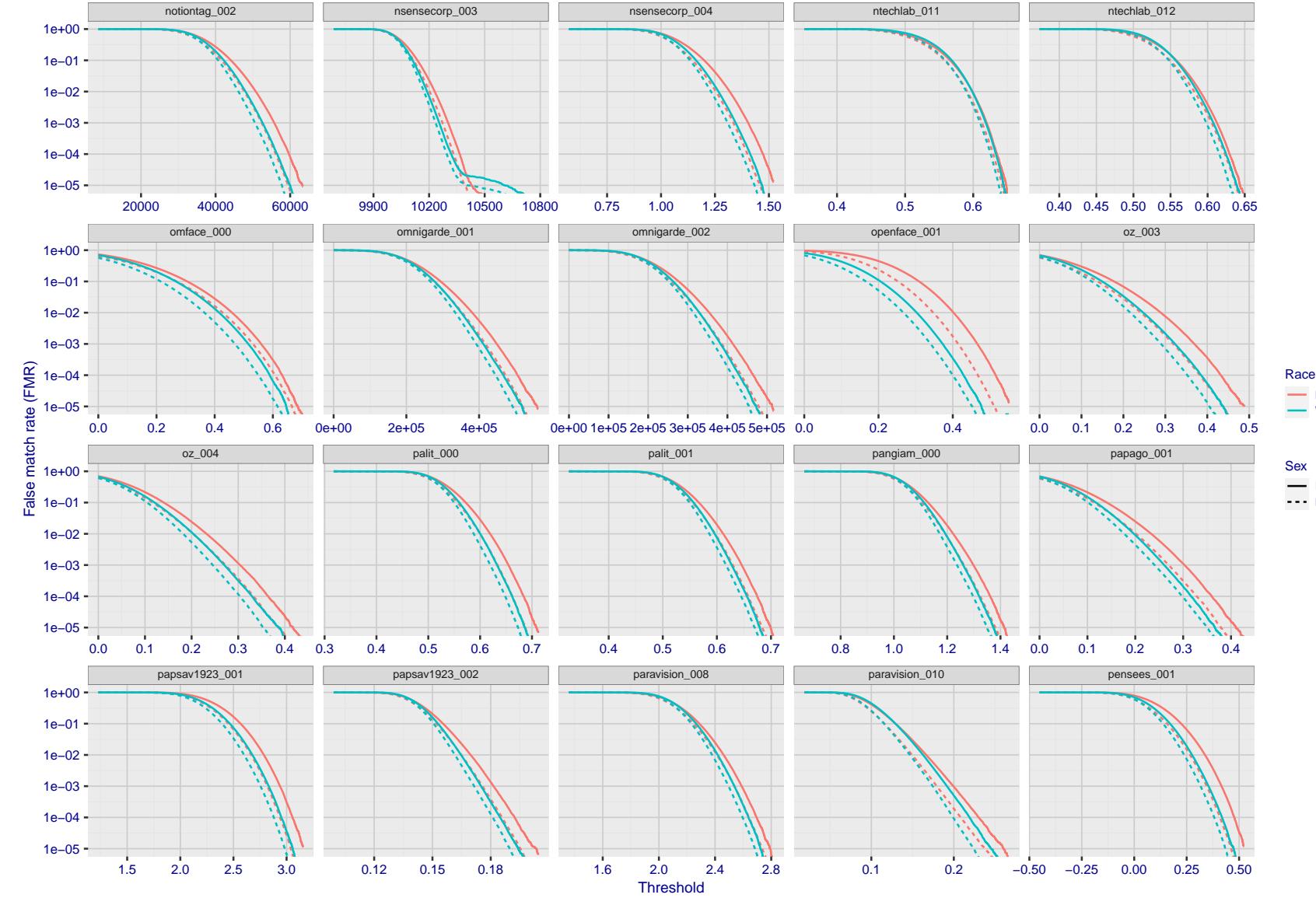


Figure 230: For the mugshot images, the false match calibration curves show false match rate vs. threshold. Separate curves appear for white females, black females, black males and white males.

2022/11/07 10:56:27

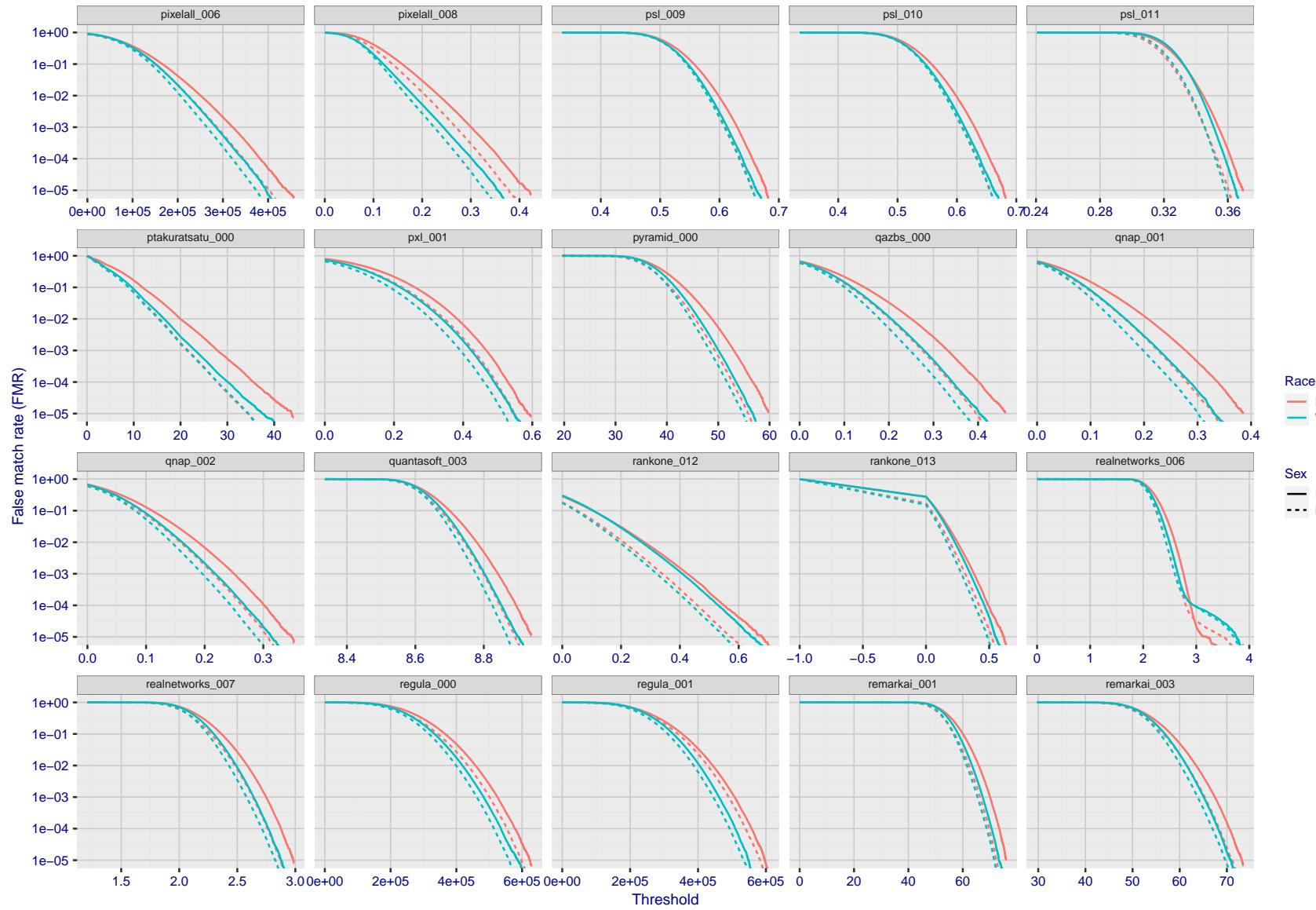


Figure 231: For the mugshot images, the false match calibration curves show false match rate vs. threshold. Separate curves appear for white females, black females, black males and white males.

2022/11/07 10:56:27

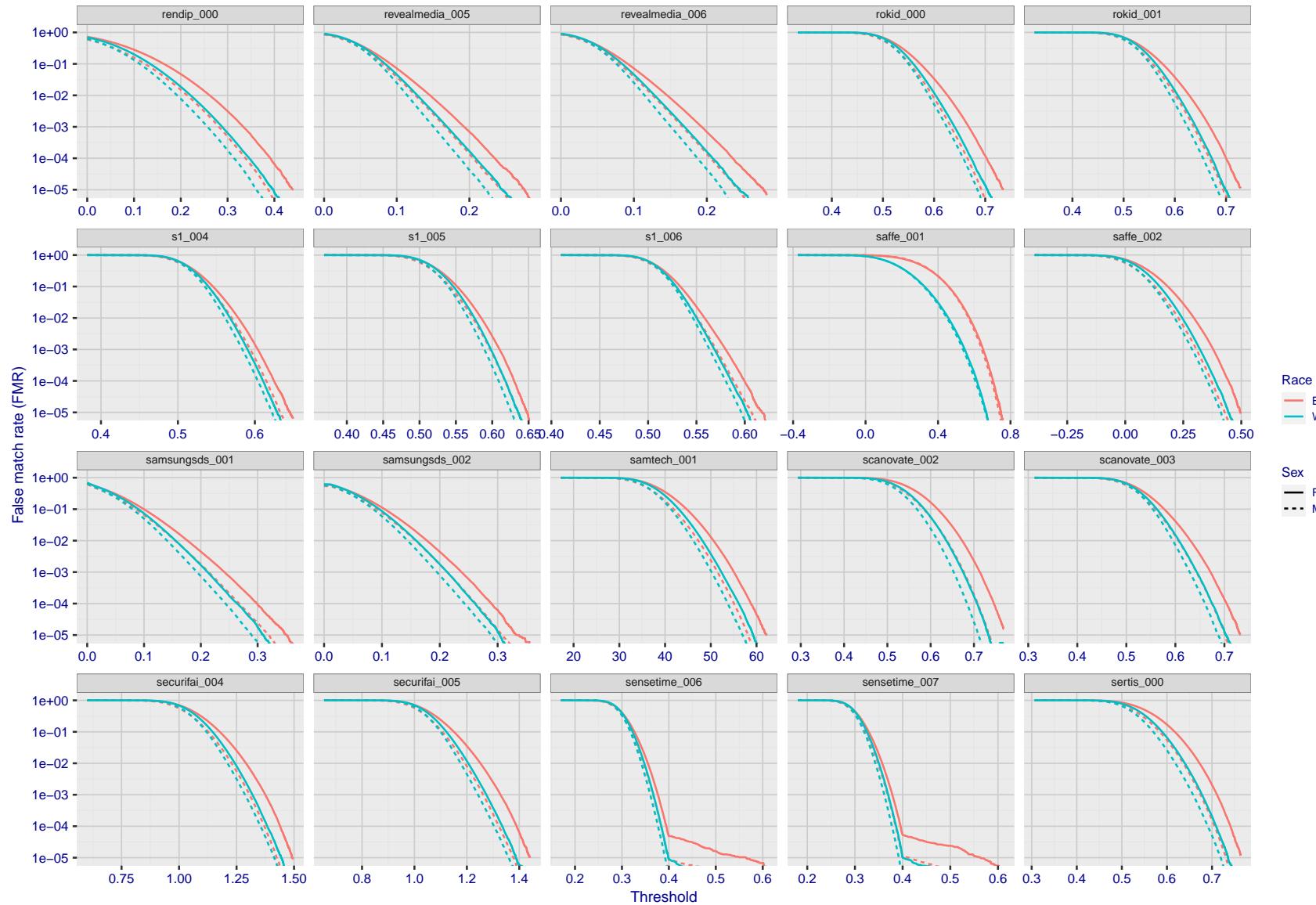


Figure 232: For the mugshot images, the false match calibration curves show false match rate vs. threshold. Separate curves appear for white females, black females, black males and white males.

2022/11/07 10:56:27

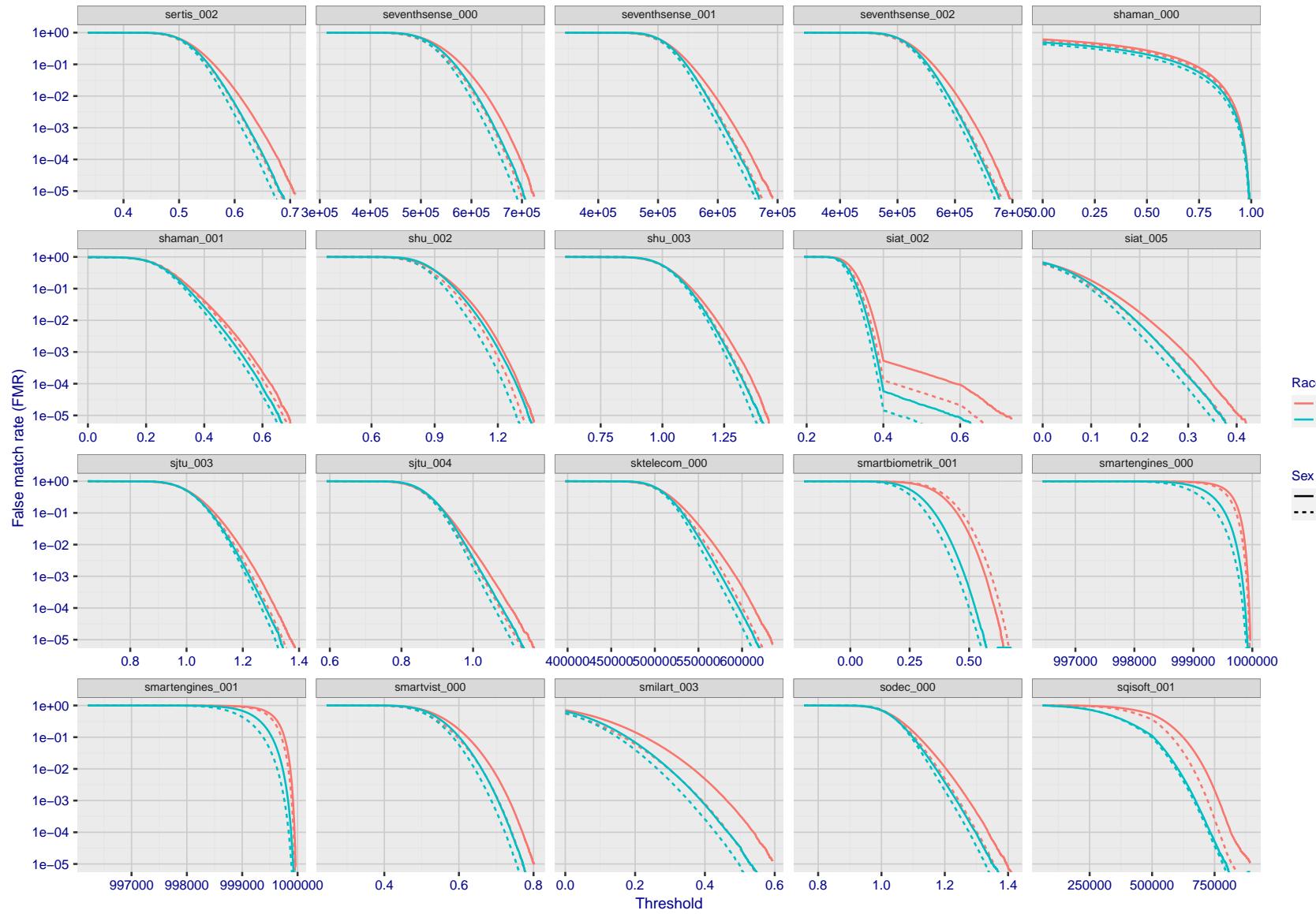


Figure 233: For the mugshot images, the false match calibration curves show false match rate vs. threshold. Separate curves appear for white females, black females, black males and white males.

2022/11/07 10:56:27

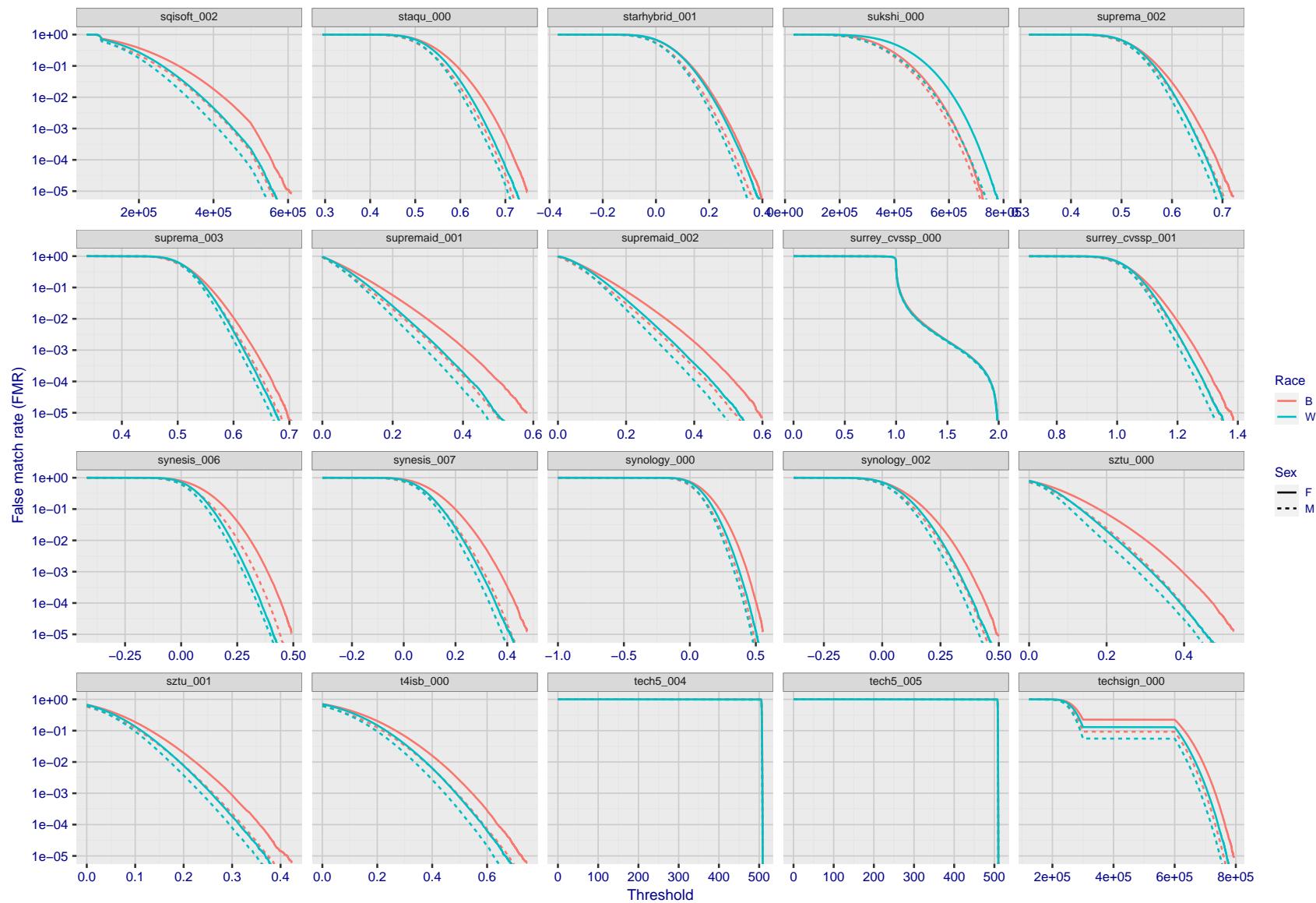


Figure 234: For the mugshot images, the false match calibration curves show false match rate vs. threshold. Separate curves appear for white females, black females, black males and white males.

2022/11/07 10:56:27

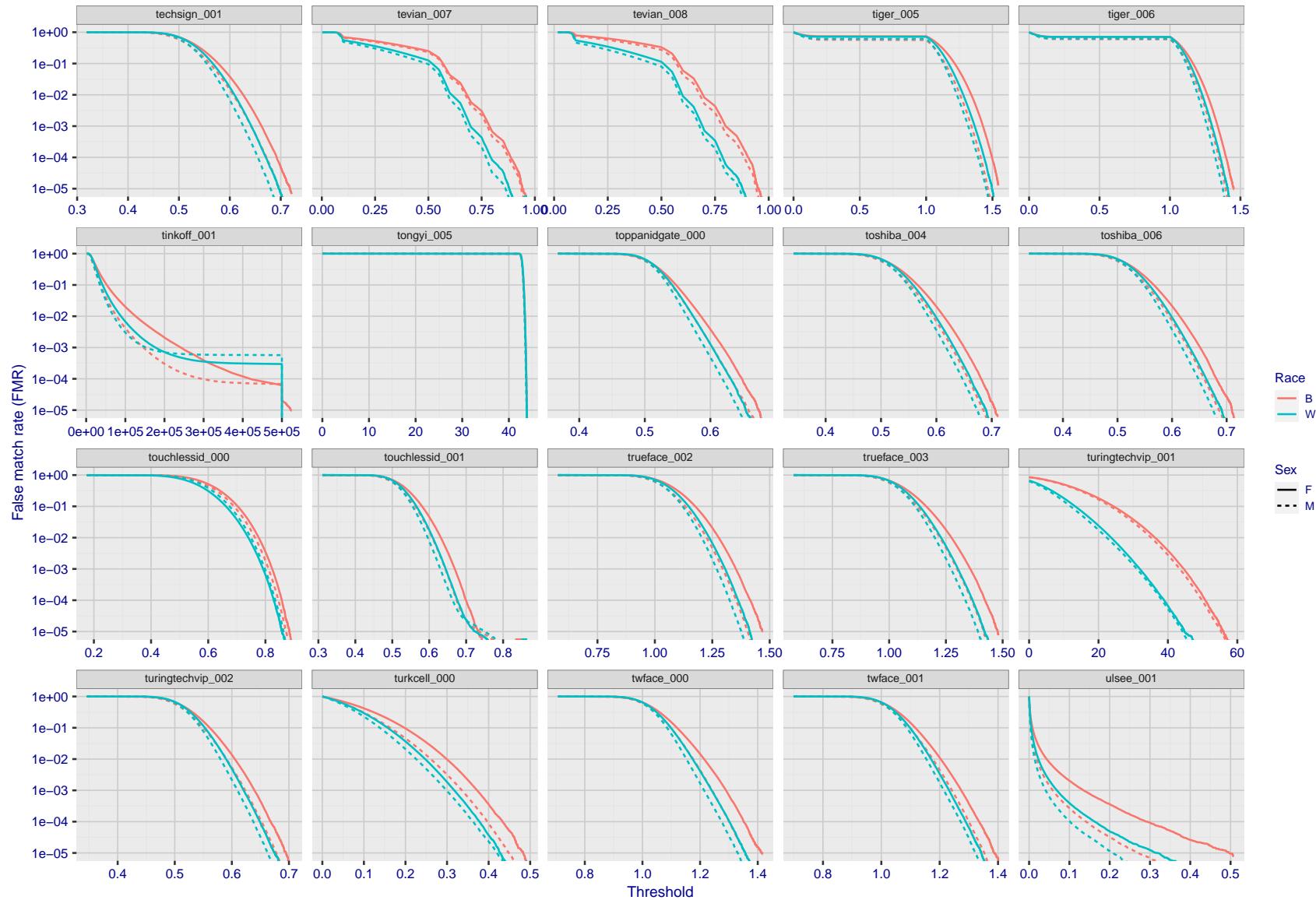


Figure 235: For the mugshot images, the false match calibration curves show false match rate vs. threshold. Separate curves appear for white females, black females, black males and white males.

FNMR(T)
"False non-match rate"
"False match rate"

2022/11/07 10:56:27

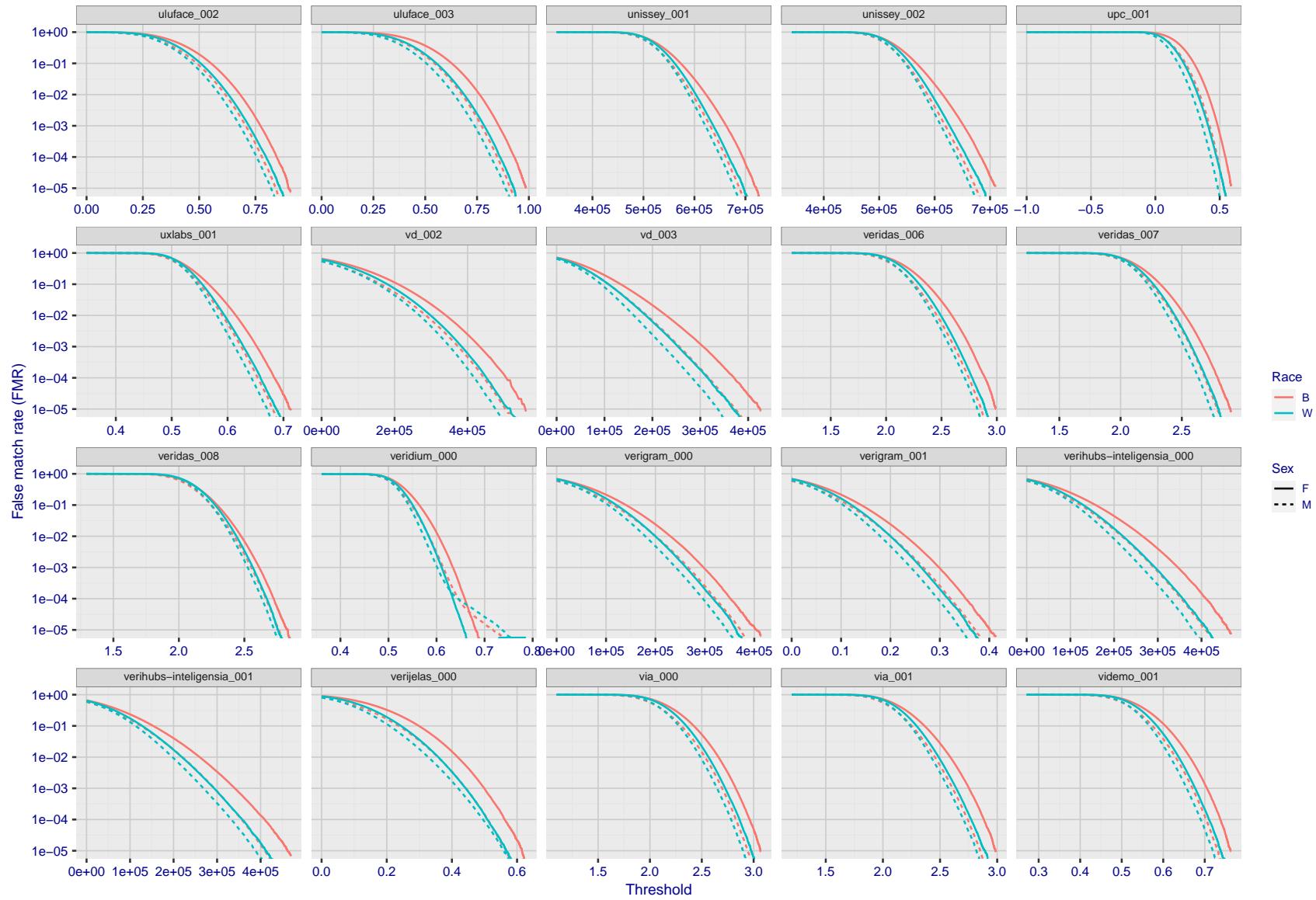


Figure 236: For the mugshot images, the false match calibration curves show false match rate vs. threshold. Separate curves appear for white females, black females, black males and white males.

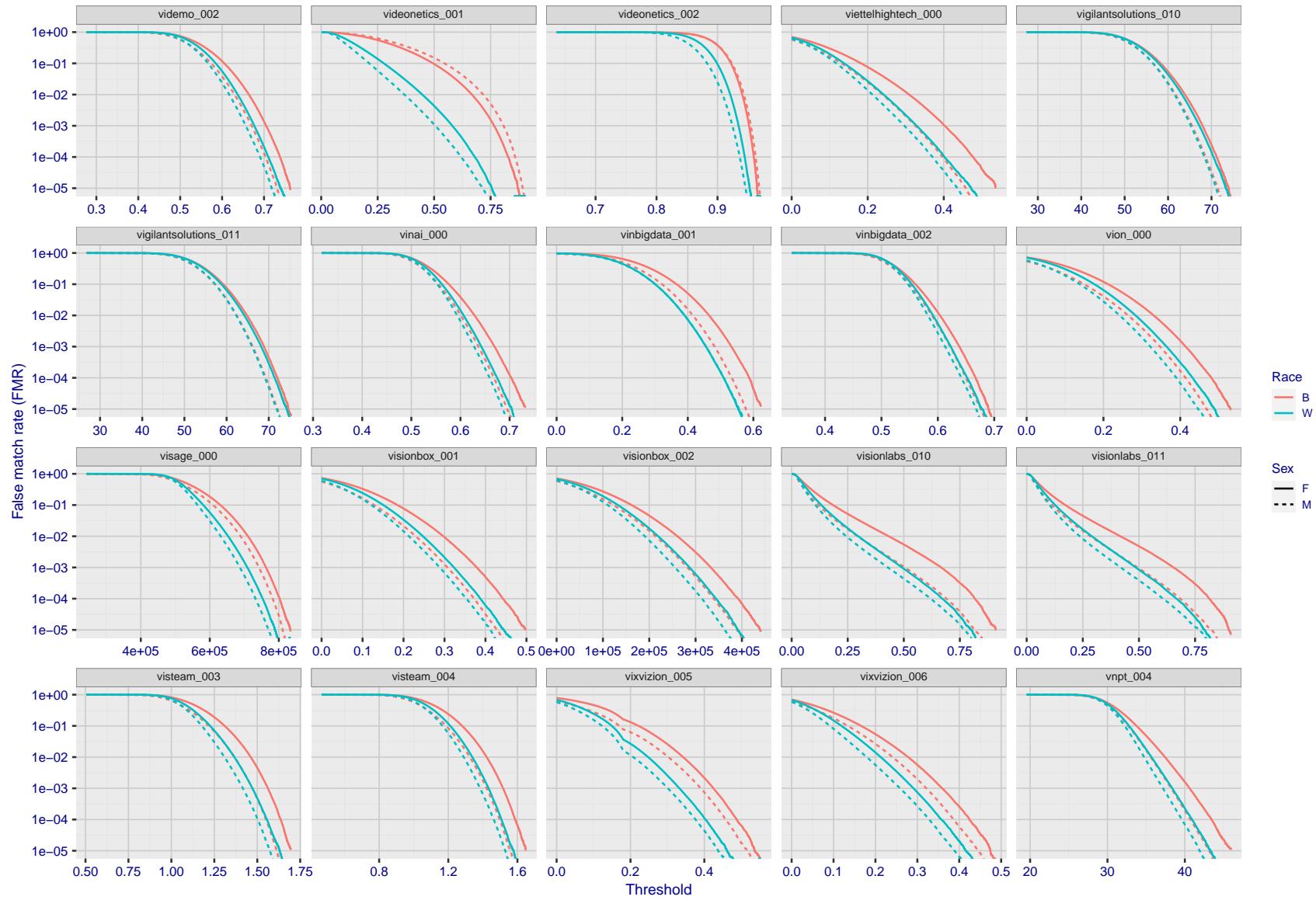


Figure 237: For the mugshot images, the false match calibration curves show false match rate vs. threshold. Separate curves appear for white females, black females, black males and white males.

2022/11/07 10:56:27

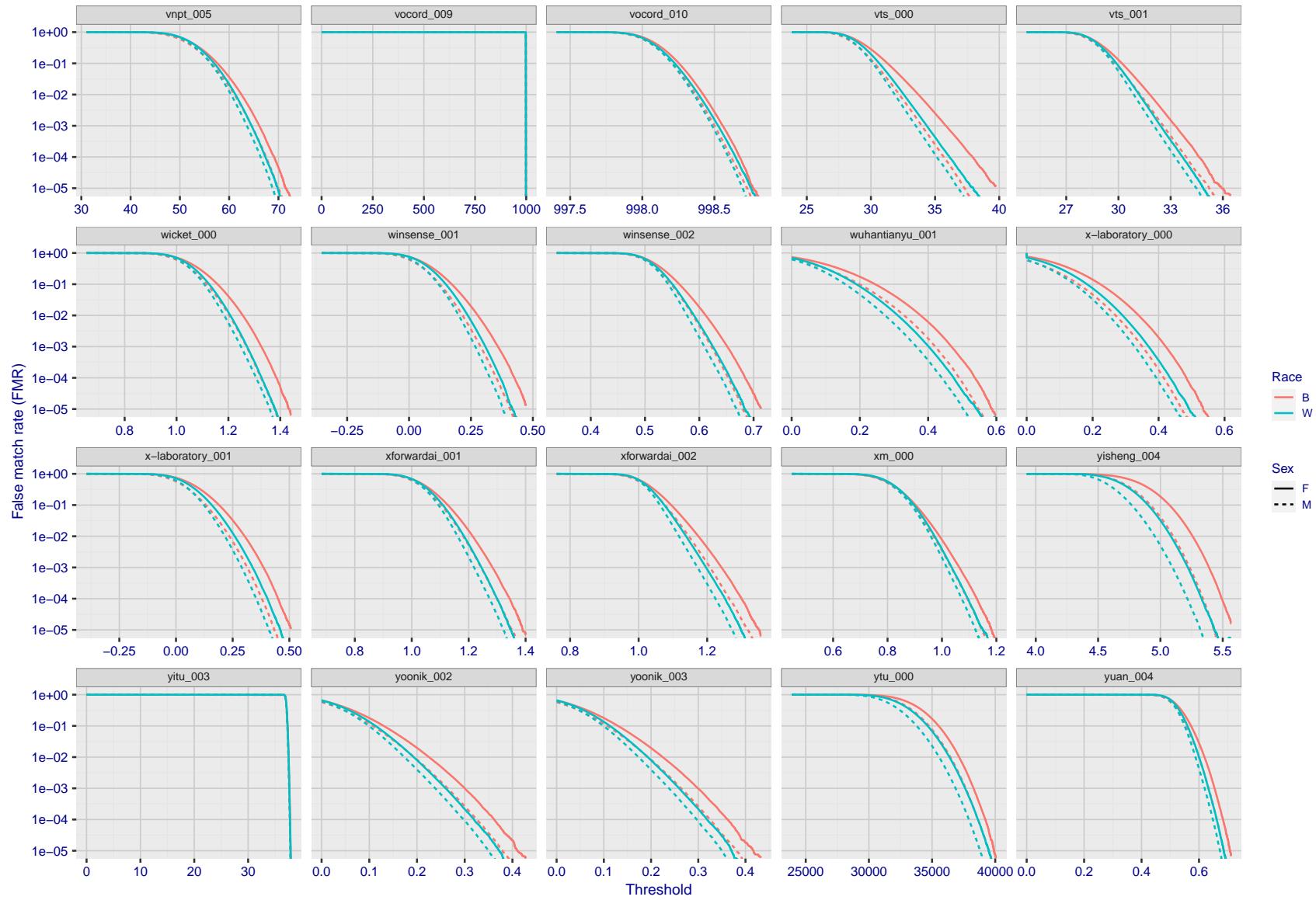


Figure 238: For the mugshot images, the false match calibration curves show false match rate vs. threshold. Separate curves appear for white females, black females, black males and white males.

FNMR(T)

"False non-match rate"

"False match rate"

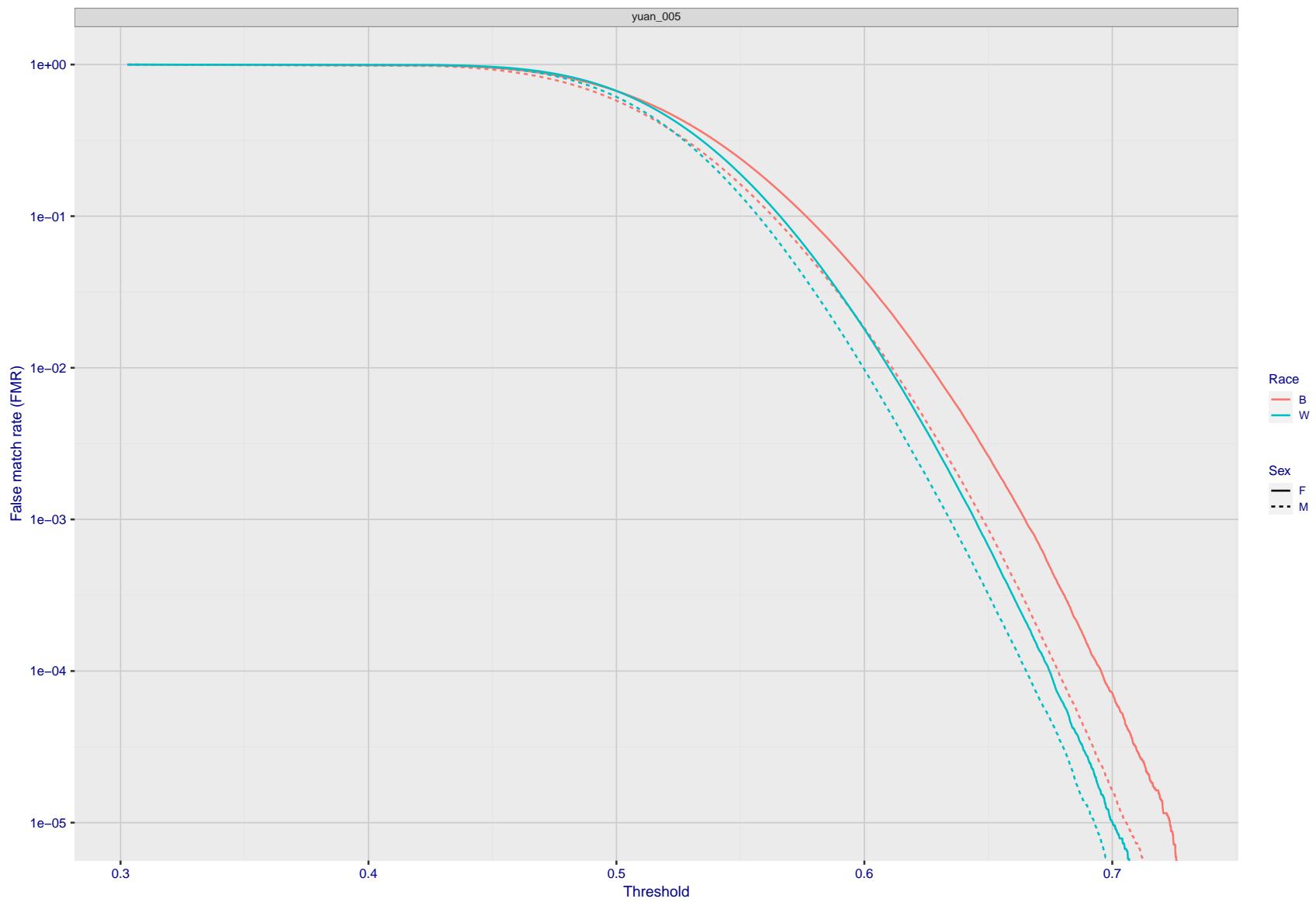


Figure 239: For the mugshot images, the false match calibration curves show false match rate vs. threshold. Separate curves appear for white females, black females, black males and white males.



Figure 240: For the visa images, the false match calibration curves show FMR vs. threshold, T . The blue (lower) curves are for zero-effort impostors (i.e. comparing all images against all). The red (upper) curves are for persons of the same-sex, same-age, and same national-origin. This shows that FMR is underestimated (by a factor of 10 or more) by using a zero-effort impostor calculation to calibrate T . As shown later (sec. 3.6), FMR is higher for demographic-matched impostors.

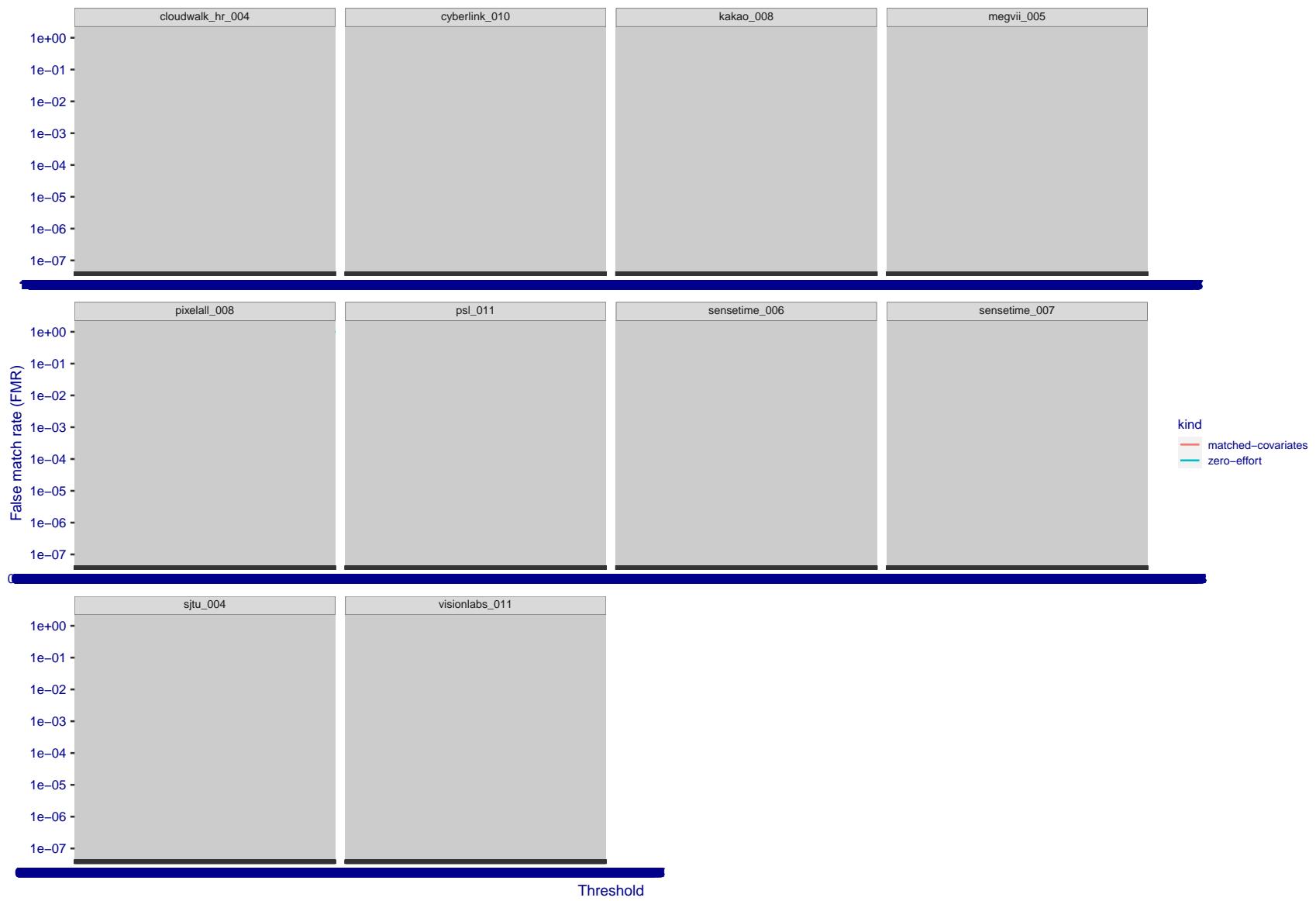


Figure 241: For the visa images, the false match calibration curves show FMR vs. threshold, T . The blue (lower) curves are for zero-effort impostors (i.e. comparing all images against all). The red (upper) curves are for persons of the same-sex, same-age, and same national-origin. This shows that FMR is underestimated (by a factor of 10 or more) by using a zero-effort impostor calculation to calibrate T . As shown later (sec. 3.6), FMR is higher for demographic-matched impostors.

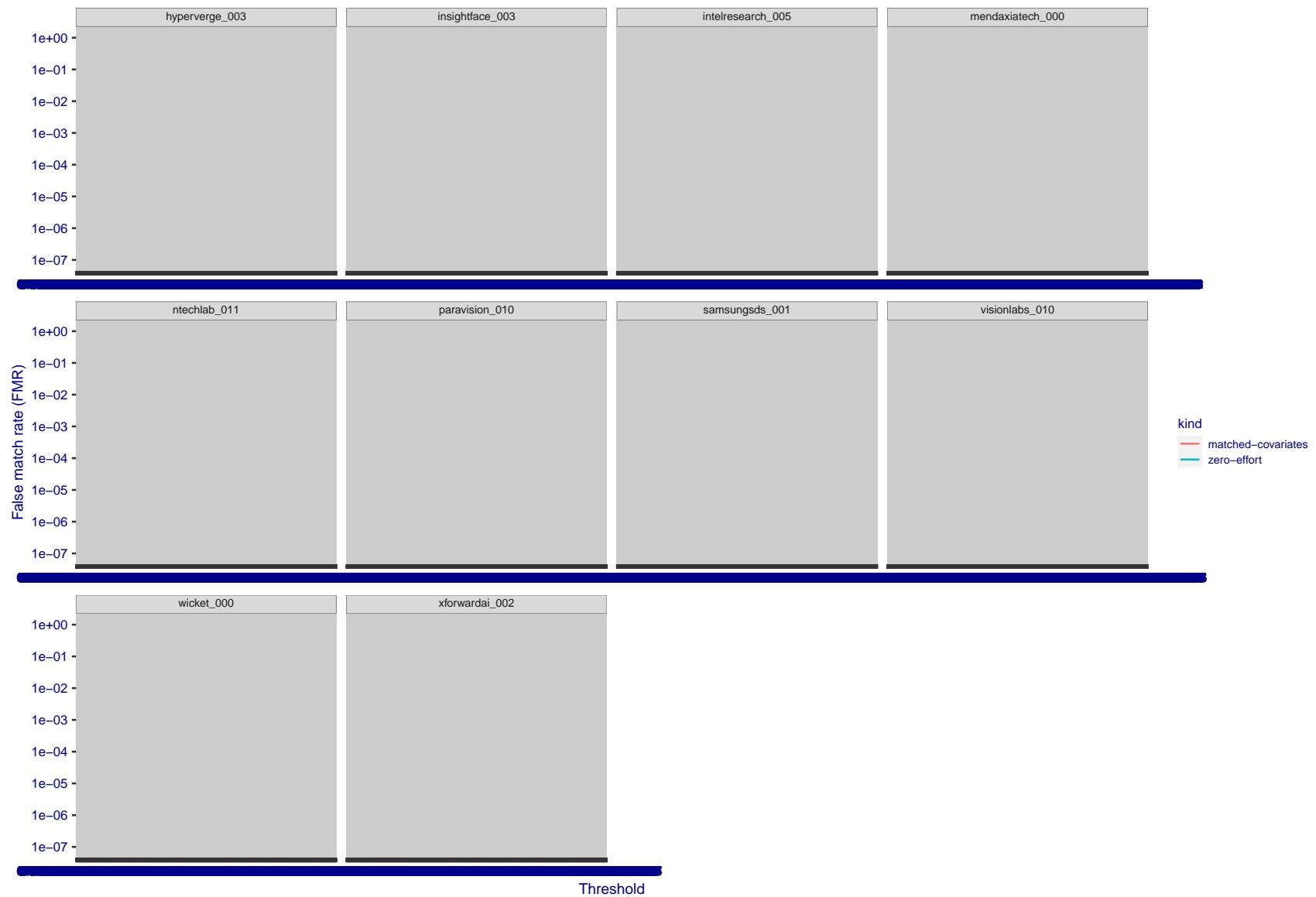


Figure 242: For the visa images, the false match calibration curves show FMR vs. threshold, T . The blue (lower) curves are for zero-effort impostors (i.e. comparing all images against all). The red (upper) curves are for persons of the same-sex, same-age, and same national-origin. This shows that FMR is underestimated (by a factor of 10 or more) by using a zero-effort impostor calculation to calibrate T . As shown later (sec. 3.6), FMR is higher for demographic-matched impostors.

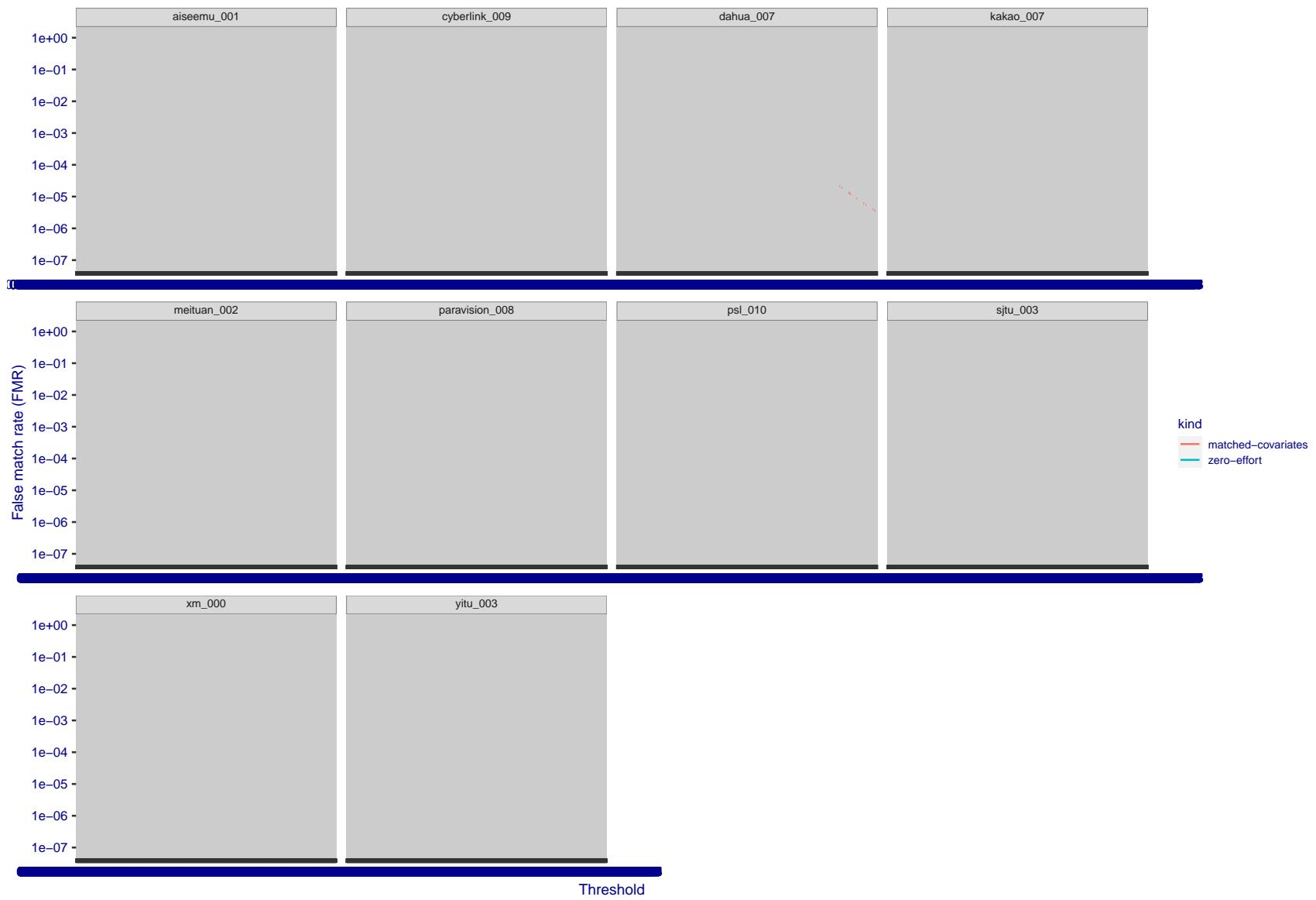


Figure 243: For the visa images, the false match calibration curves show FMR vs. threshold, T . The blue (lower) curves are for zero-effort impostors (i.e. comparing all images against all). The red (upper) curves are for persons of the same-sex, same-age, and same national-origin. This shows that FMR is underestimated (by a factor of 10 or more) by using a zero-effort impostor calculation to calibrate T . As shown later (sec. 3.6), FMR is higher for demographic-matched impostors.

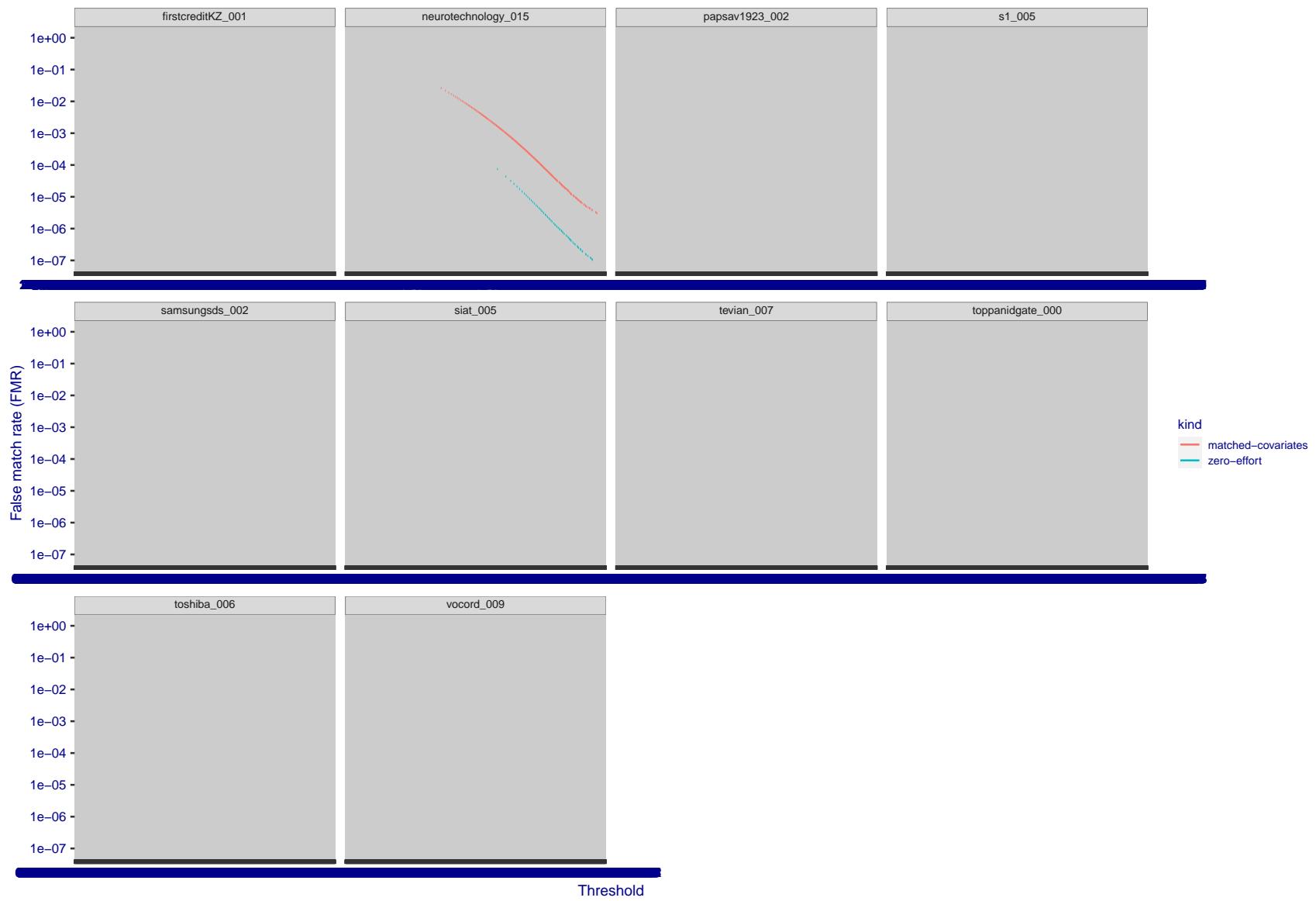


Figure 244: For the visa images, the false match calibration curves show FMR vs. threshold, T . The blue (lower) curves are for zero-effort impostors (i.e. comparing all images against all). The red (upper) curves are for persons of the same-sex, same-age, and same national-origin. This shows that FMR is underestimated (by a factor of 10 or more) by using a zero-effort impostor calculation to calibrate T . As shown later (sec. 3.6), FMR is higher for demographic-matched impostors.

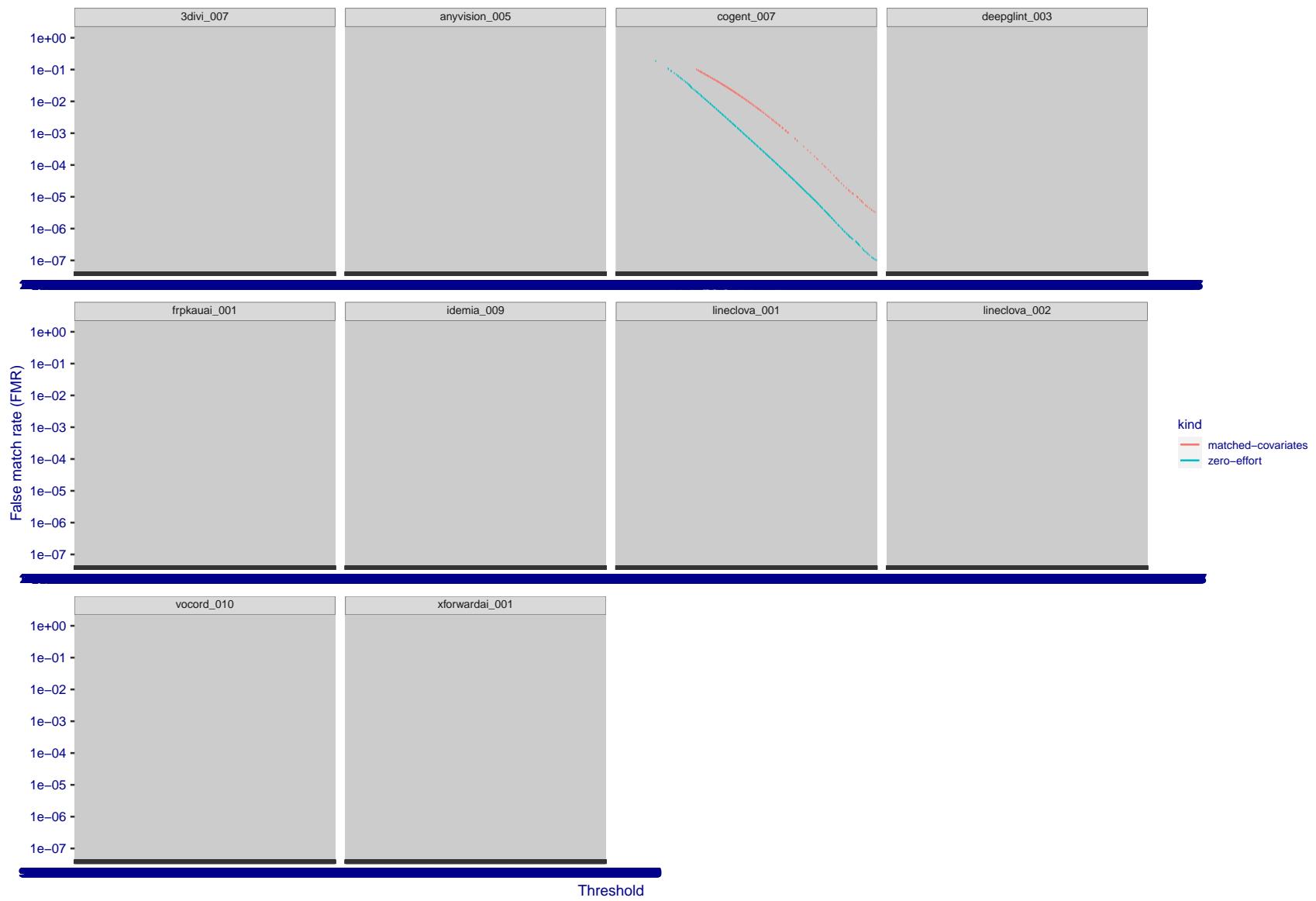


Figure 245: For the visa images, the false match calibration curves show FMR vs. threshold, T . The blue (lower) curves are for zero-effort impostors (i.e. comparing all images against all). The red (upper) curves are for persons of the same-sex, same-age, and same national-origin. This shows that FMR is underestimated (by a factor of 10 or more) by using a zero-effort impostor calculation to calibrate T . As shown later (sec. 3.6), FMR is higher for demographic-matched impostors.

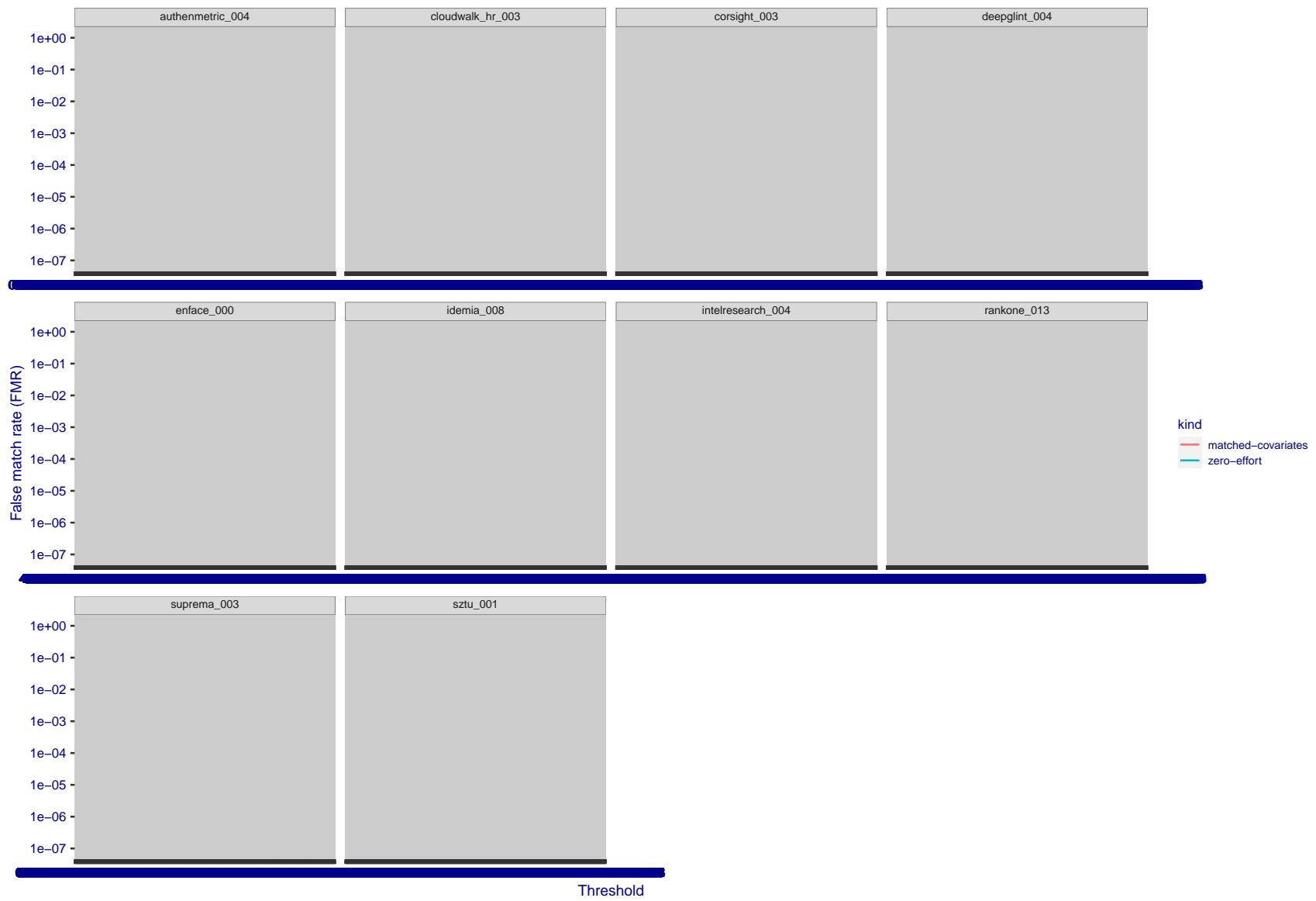


Figure 246: For the visa images, the false match calibration curves show FMR vs. threshold, T . The blue (lower) curves are for zero-effort impostors (i.e. comparing all images against all). The red (upper) curves are for persons of the same-sex, same-age, and same national-origin. This shows that FMR is underestimated (by a factor of 10 or more) by using a zero-effort impostor calculation to calibrate T . As shown later (sec. 3.6), FMR is higher for demographic-matched impostors.

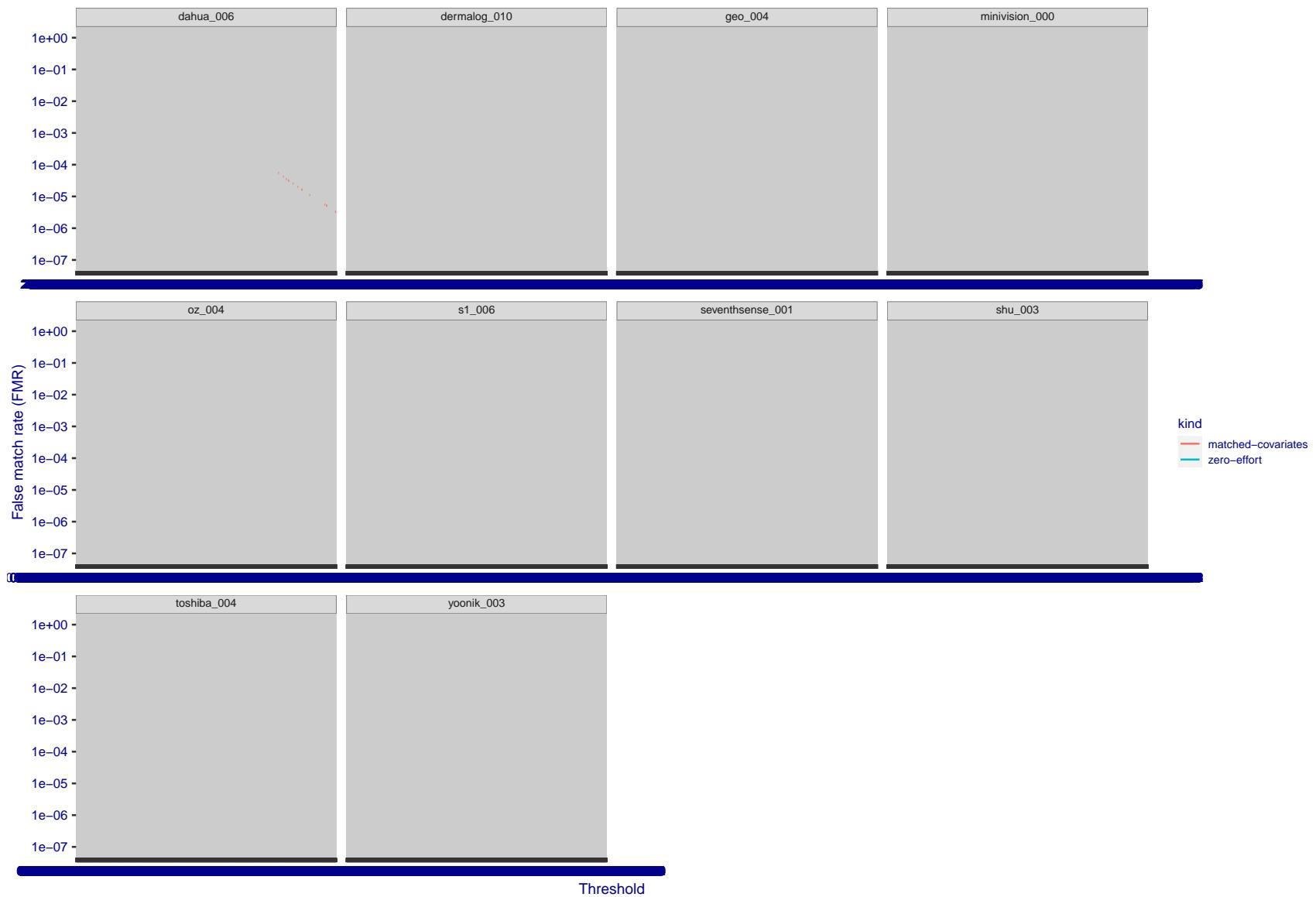


Figure 247: For the visa images, the false match calibration curves show FMR vs. threshold, T . The blue (lower) curves are for zero-effort impostors (i.e. comparing all images against all). The red (upper) curves are for persons of the same-sex, same-age, and same national-origin. This shows that FMR is underestimated (by a factor of 10 or more) by using a zero-effort impostor calculation to calibrate T . As shown later (sec. 3.6), FMR is higher for demographic-matched impostors.

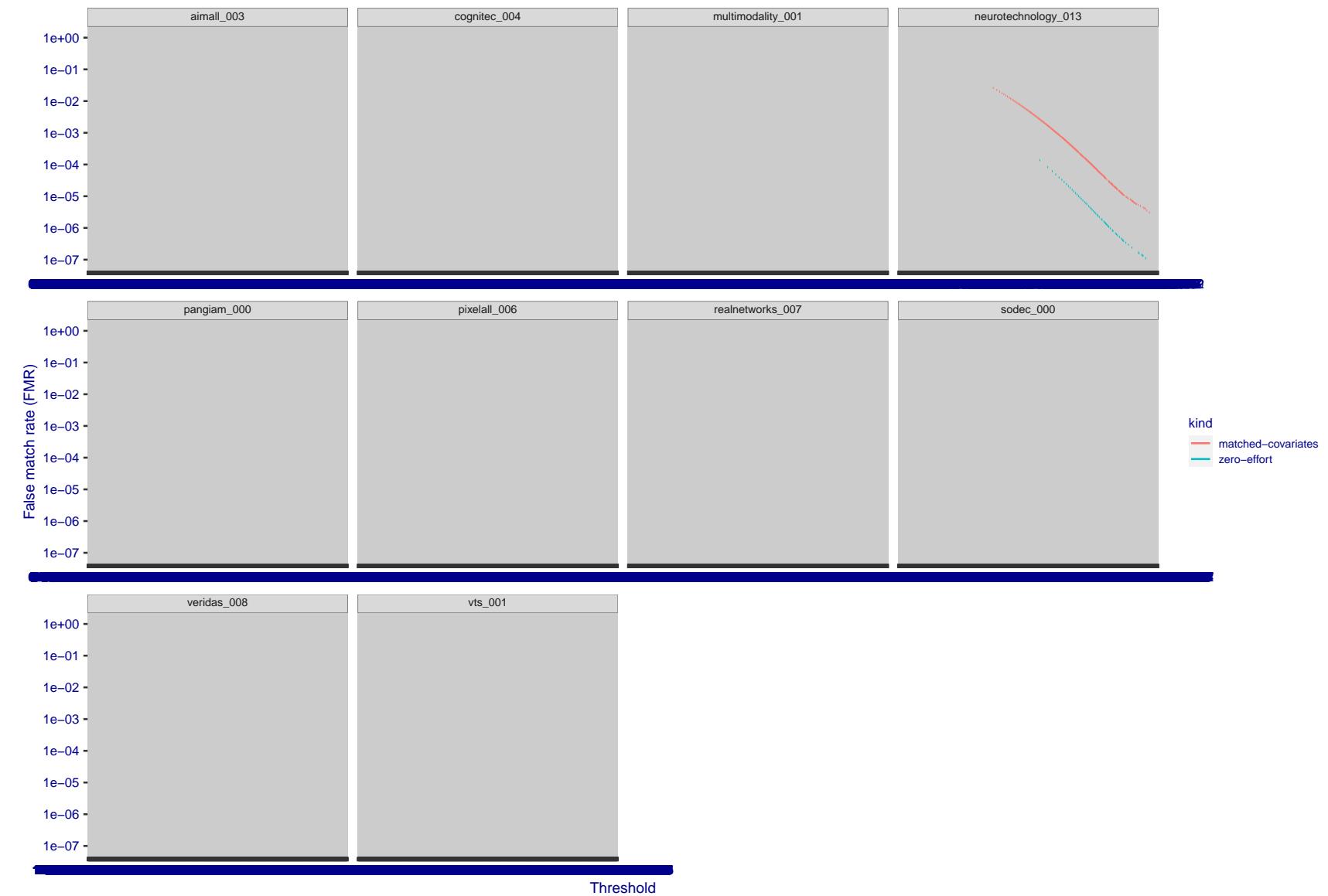


Figure 248: For the visa images, the false match calibration curves show FMR vs. threshold, T . The blue (lower) curves are for zero-effort impostors (i.e. comparing all images against all). The red (upper) curves are for persons of the same-sex, same-age, and same national-origin. This shows that FMR is underestimated (by a factor of 10 or more) by using a zero-effort impostor calculation to calibrate T . As shown later (sec. 3.6), FMR is higher for demographic-matched impostors.

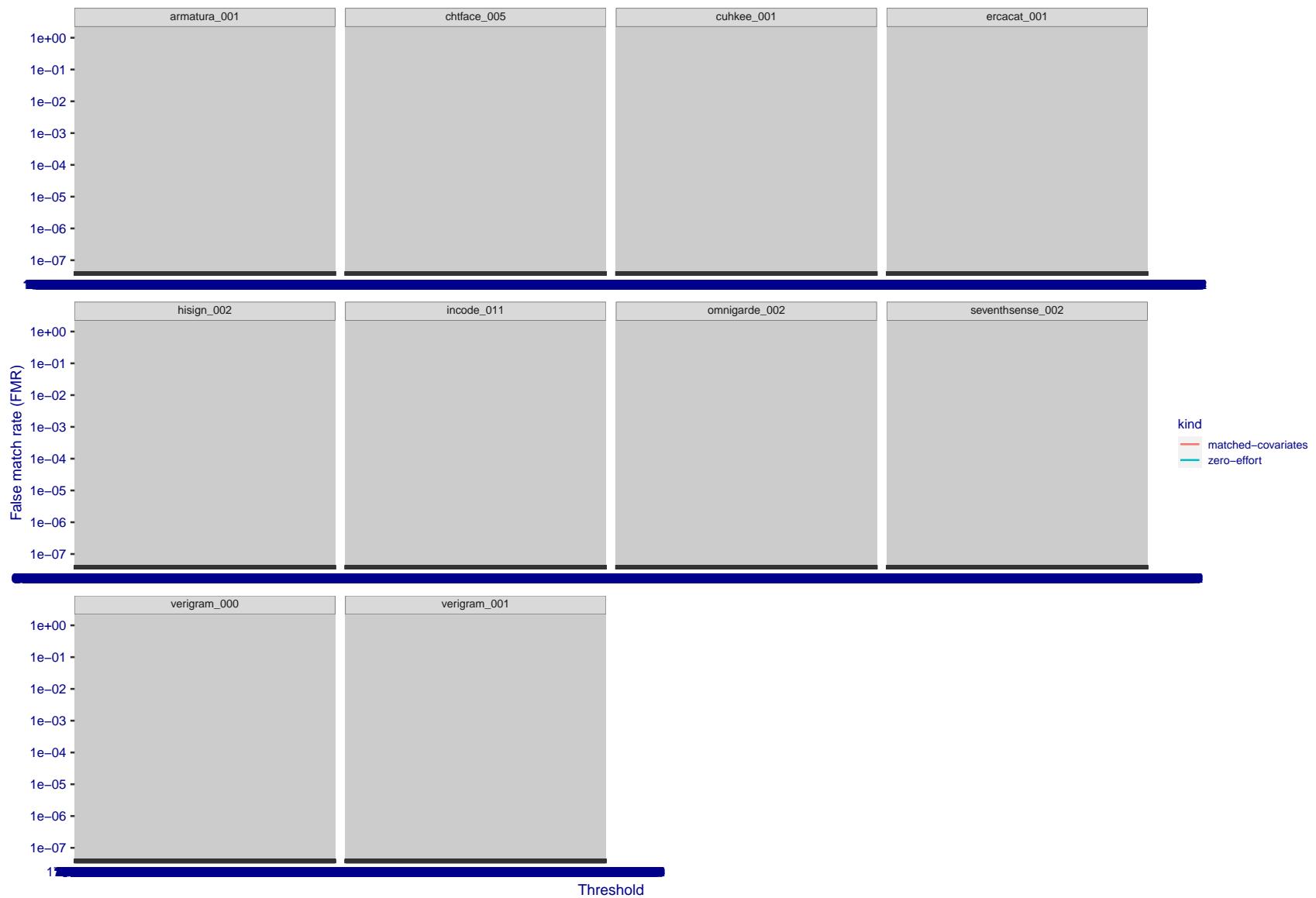


Figure 249: For the visa images, the false match calibration curves show FMR vs. threshold, T . The blue (lower) curves are for zero-effort impostors (i.e. comparing all images against all). The red (upper) curves are for persons of the same-sex, same-age, and same national-origin. This shows that FMR is underestimated (by a factor of 10 or more) by using a zero-effort impostor calculation to calibrate T . As shown later (sec. 3.6), FMR is higher for demographic-matched impostors.

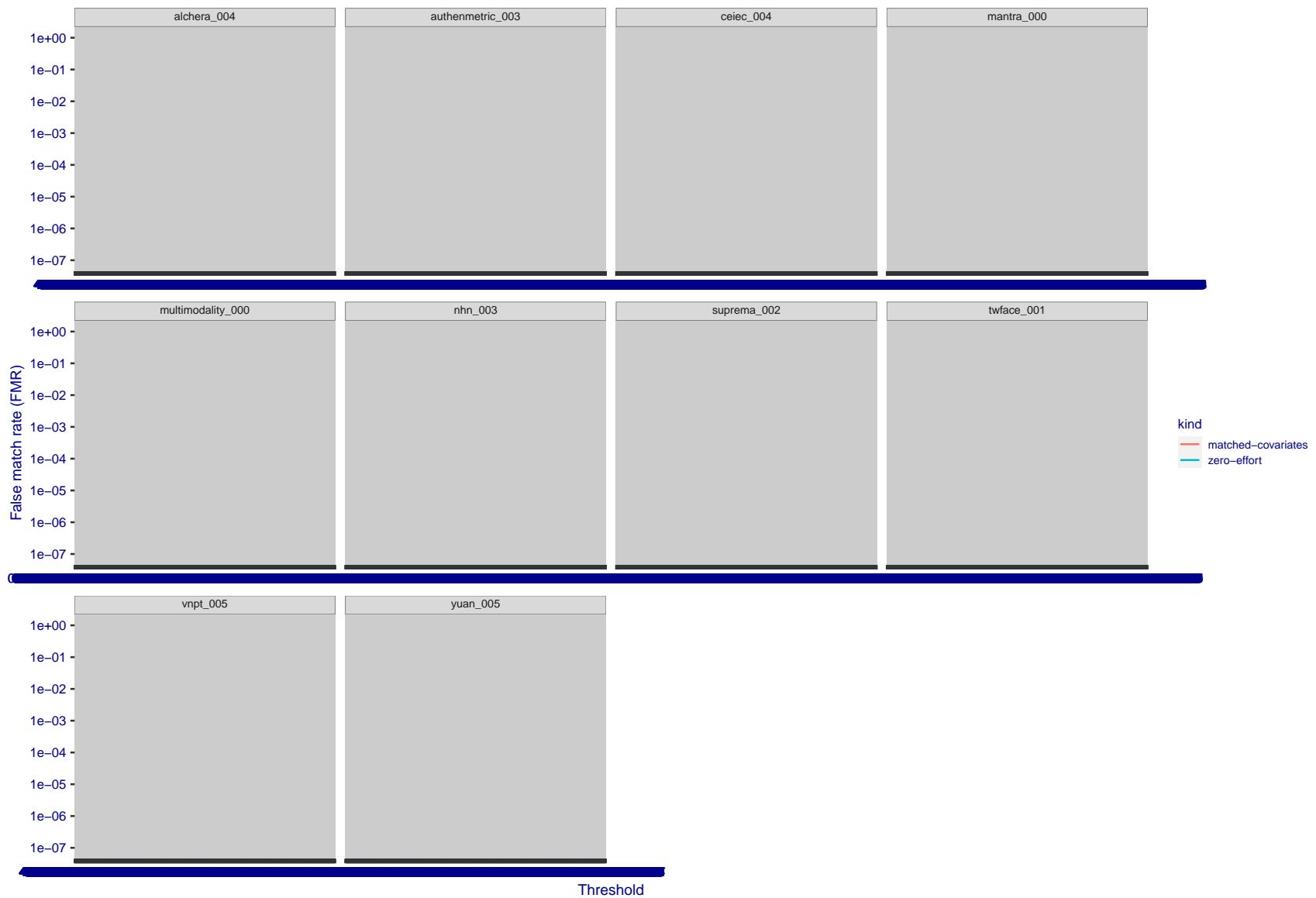


Figure 250: For the visa images, the false match calibration curves show FMR vs. threshold, T . The blue (lower) curves are for zero-effort impostors (i.e. comparing all images against all). The red (upper) curves are for persons of the same-sex, same-age, and same national-origin. This shows that FMR is underestimated (by a factor of 10 or more) by using a zero-effort impostor calculation to calibrate T . As shown later (sec. 3.6), FMR is higher for demographic-matched impostors.

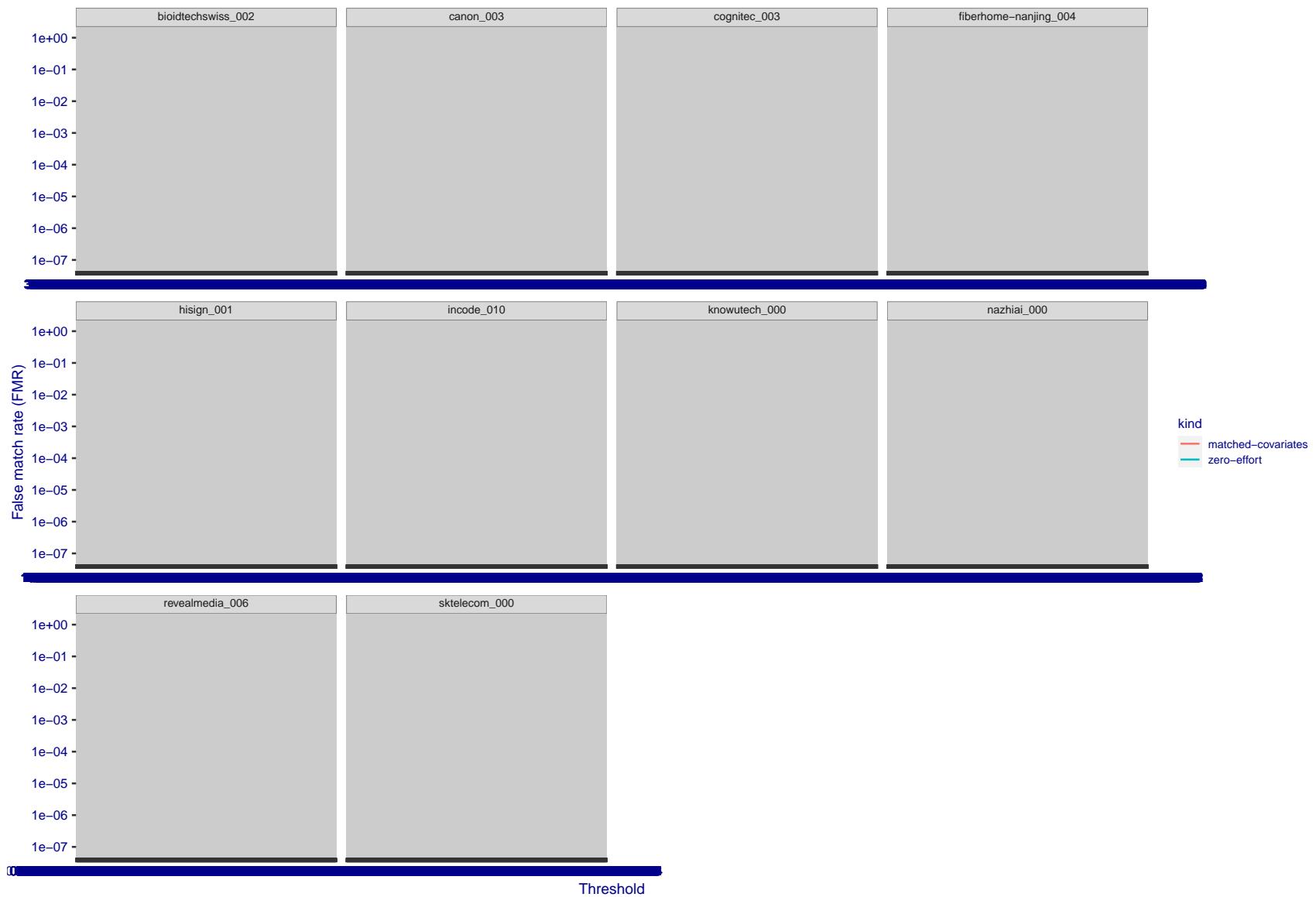


Figure 251: For the visa images, the false match calibration curves show FMR vs. threshold, T . The blue (lower) curves are for zero-effort impostors (i.e. comparing all images against all). The red (upper) curves are for persons of the same-sex, same-age, and same national-origin. This shows that FMR is underestimated (by a factor of 10 or more) by using a zero-effort impostor calculation to calibrate T . As shown later (sec. 3.6), FMR is higher for demographic-matched impostors.

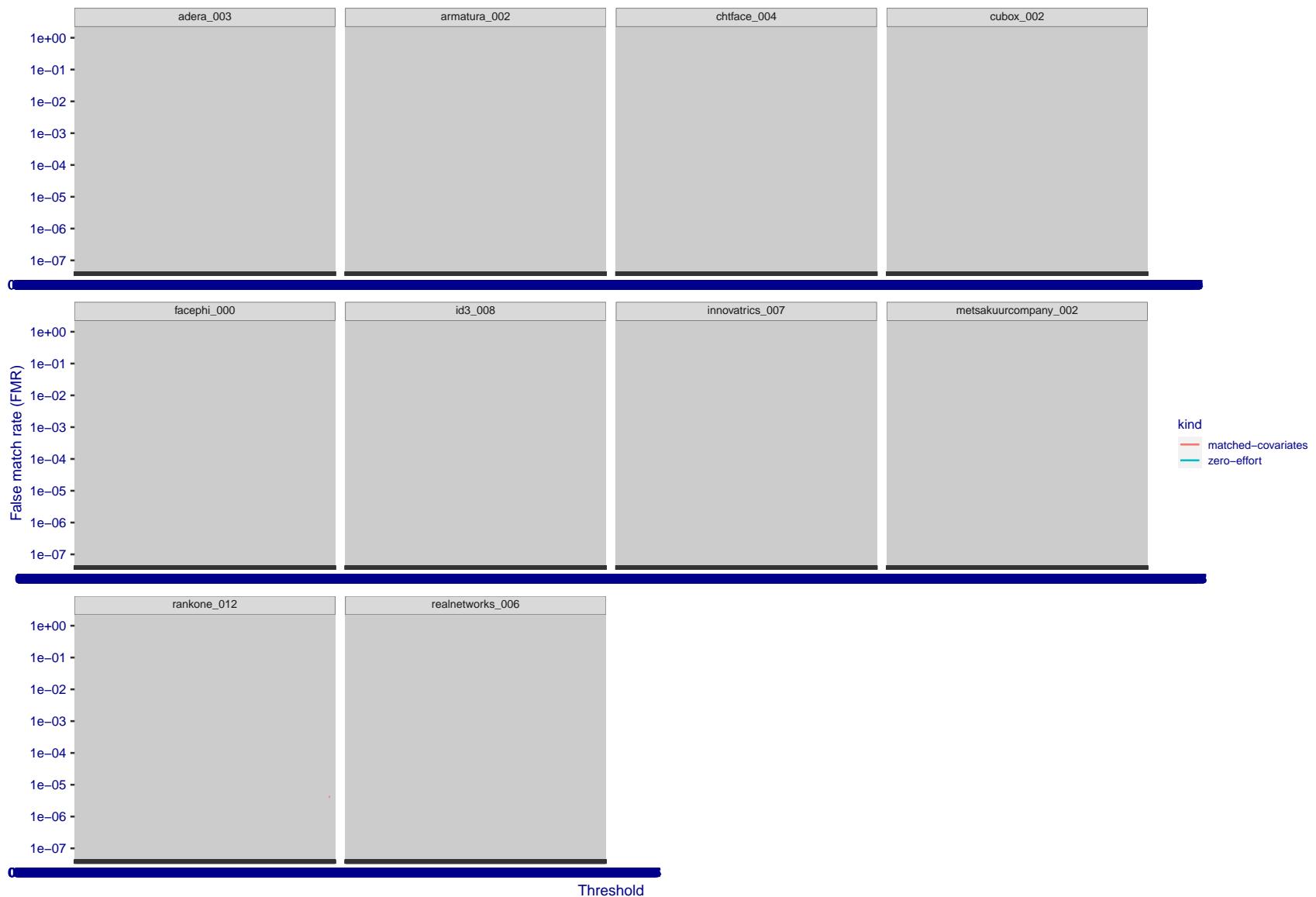


Figure 252: For the visa images, the false match calibration curves show FMR vs. threshold, T . The blue (lower) curves are for zero-effort impostors (i.e. comparing all images against all). The red (upper) curves are for persons of the same-sex, same-age, and same national-origin. This shows that FMR is underestimated (by a factor of 10 or more) by using a zero-effort impostor calculation to calibrate T . As shown later (sec. 3.6), FMR is higher for demographic-matched impostors.

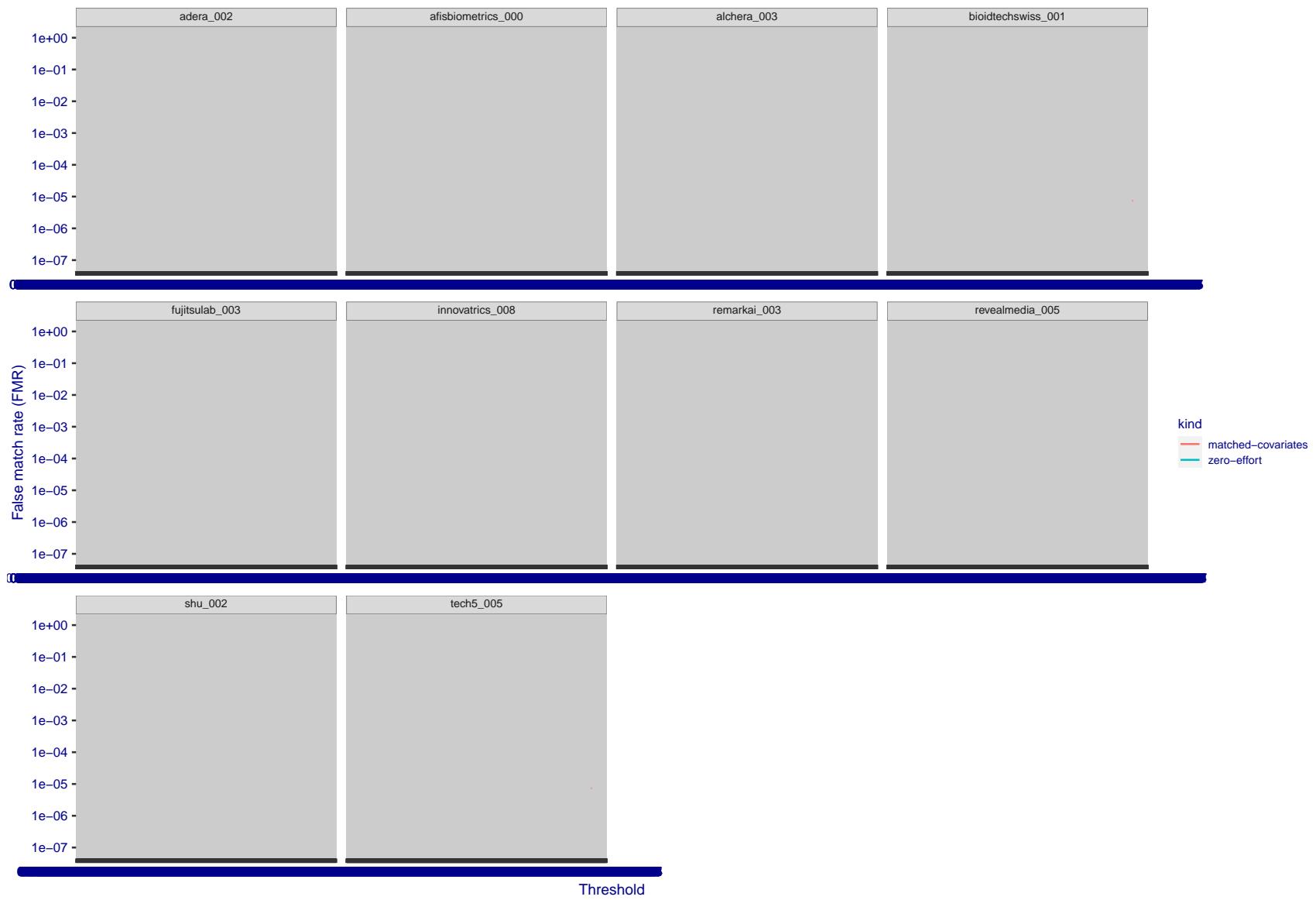


Figure 253: For the visa images, the false match calibration curves show FMR vs. threshold, T . The blue (lower) curves are for zero-effort impostors (i.e. comparing all images against all). The red (upper) curves are for persons of the same-sex, same-age, and same national-origin. This shows that FMR is underestimated (by a factor of 10 or more) by using a zero-effort impostor calculation to calibrate T . As shown later (sec. 3.6), FMR is higher for demographic-matched impostors.

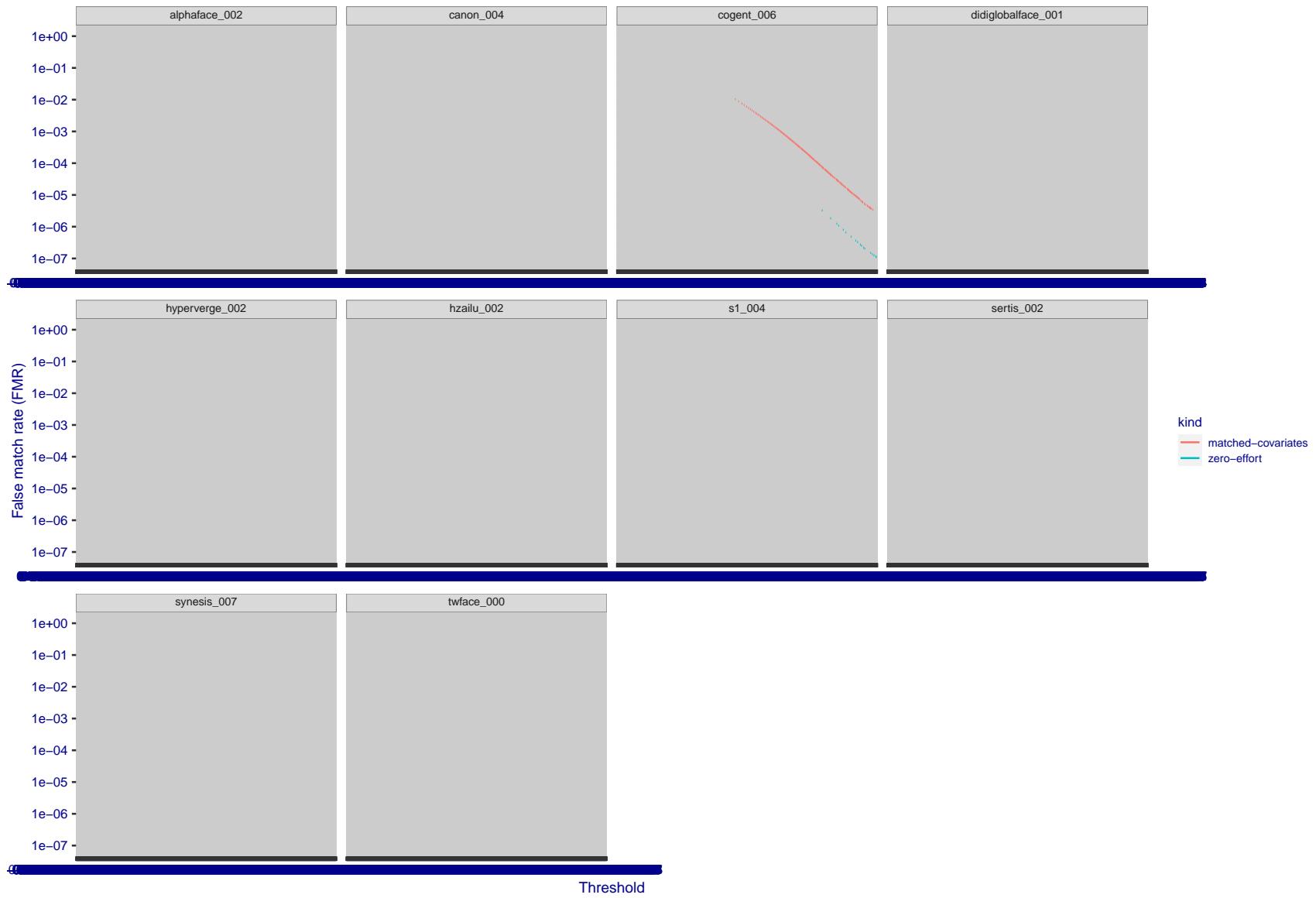


Figure 254: For the visa images, the false match calibration curves show FMR vs. threshold, T . The blue (lower) curves are for zero-effort impostors (i.e. comparing all images against all). The red (upper) curves are for persons of the same-sex, same-age, and same national-origin. This shows that FMR is underestimated (by a factor of 10 or more) by using a zero-effort impostor calculation to calibrate T . As shown later (sec. 3.6), FMR is higher for demographic-matched impostors.

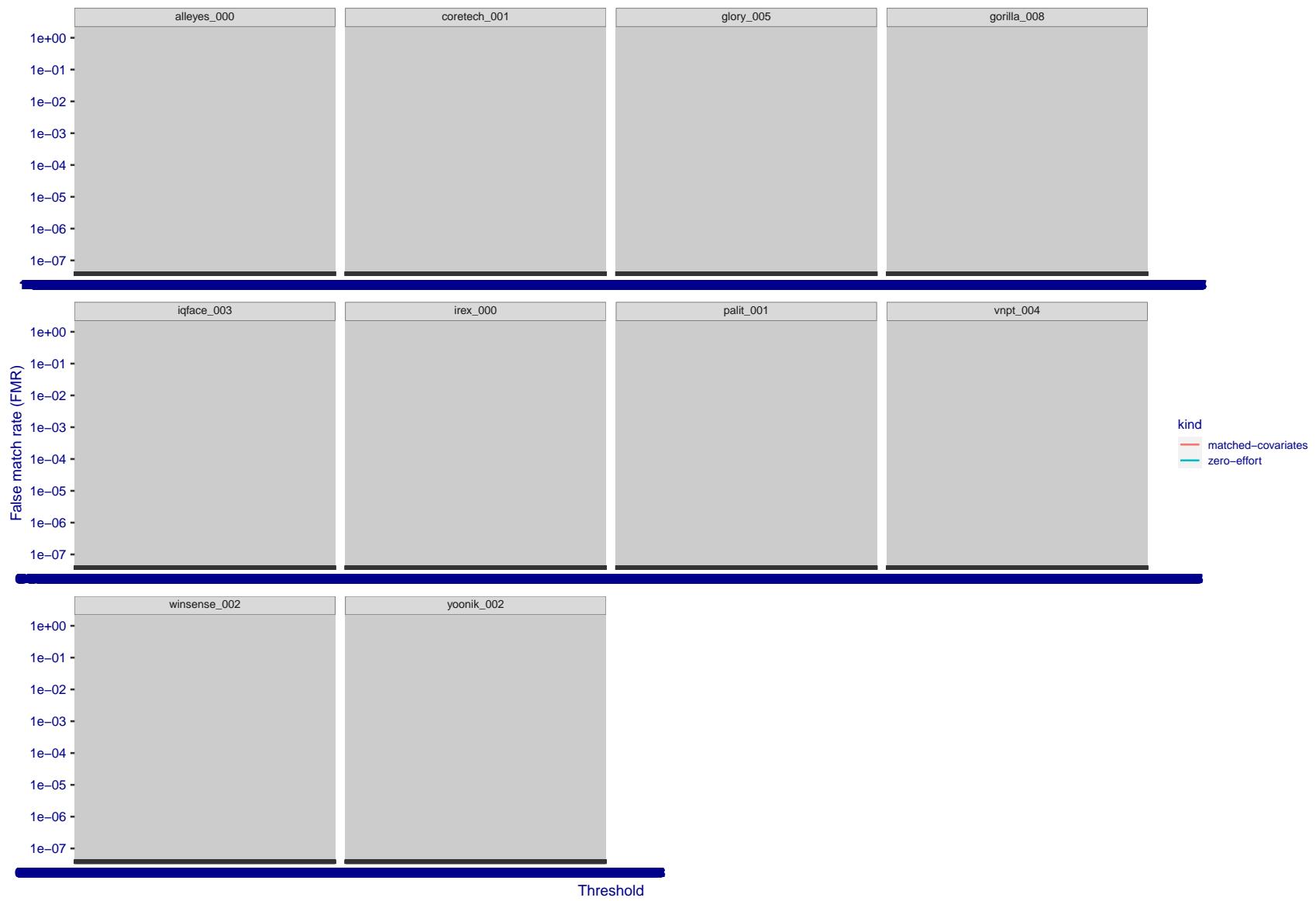


Figure 255: For the visa images, the false match calibration curves show FMR vs. threshold, T . The blue (lower) curves are for zero-effort impostors (i.e. comparing all images against all). The red (upper) curves are for persons of the same-sex, same-age, and same national-origin. This shows that FMR is underestimated (by a factor of 10 or more) by using a zero-effort impostor calculation to calibrate T . As shown later (sec. 3.6), FMR is higher for demographic-matched impostors.

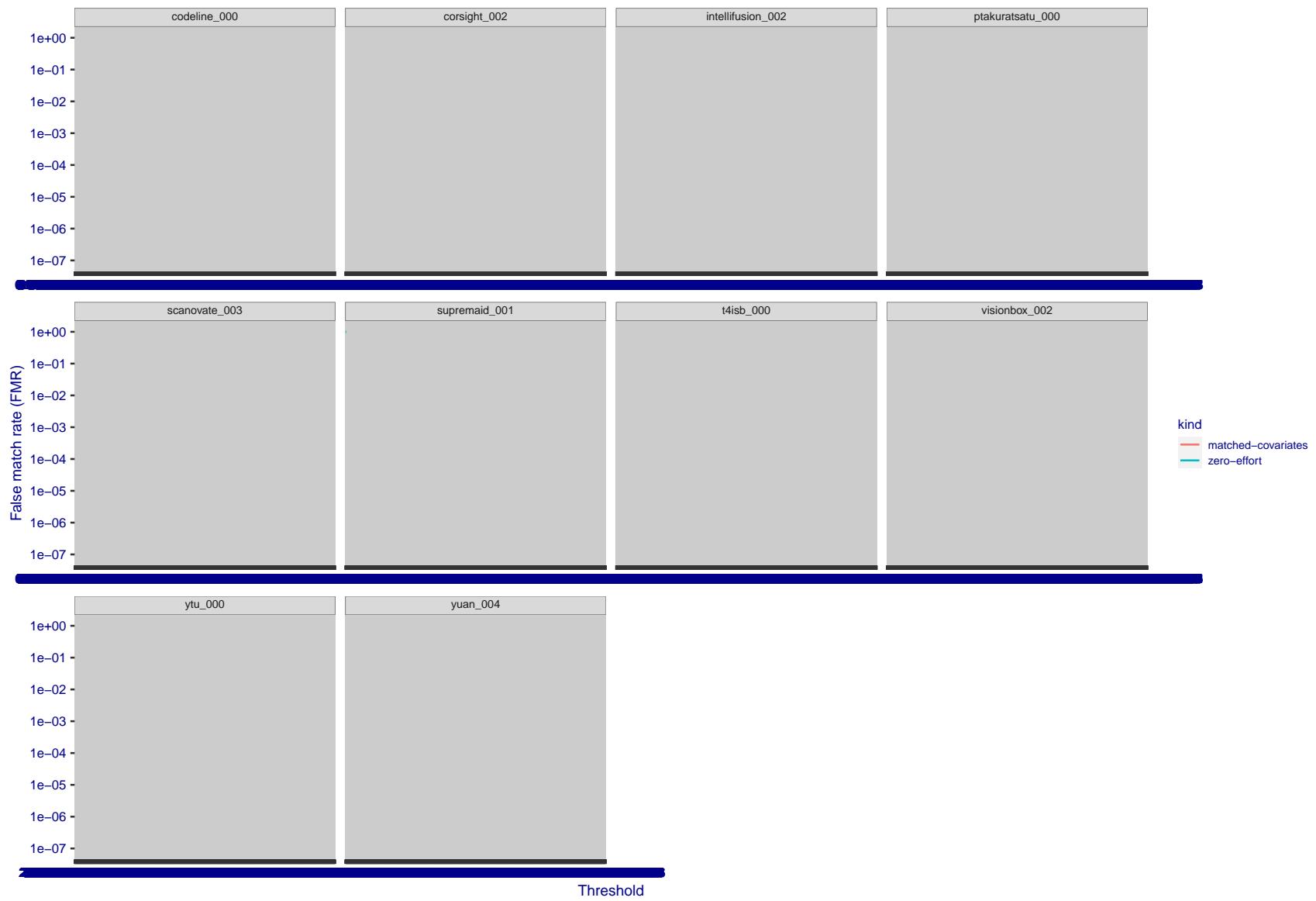


Figure 256: For the visa images, the false match calibration curves show FMR vs. threshold, T . The blue (lower) curves are for zero-effort impostors (i.e. comparing all images against all). The red (upper) curves are for persons of the same-sex, same-age, and same national-origin. This shows that FMR is underestimated (by a factor of 10 or more) by using a zero-effort impostor calculation to calibrate T . As shown later (sec. 3.6), FMR is higher for demographic-matched impostors.

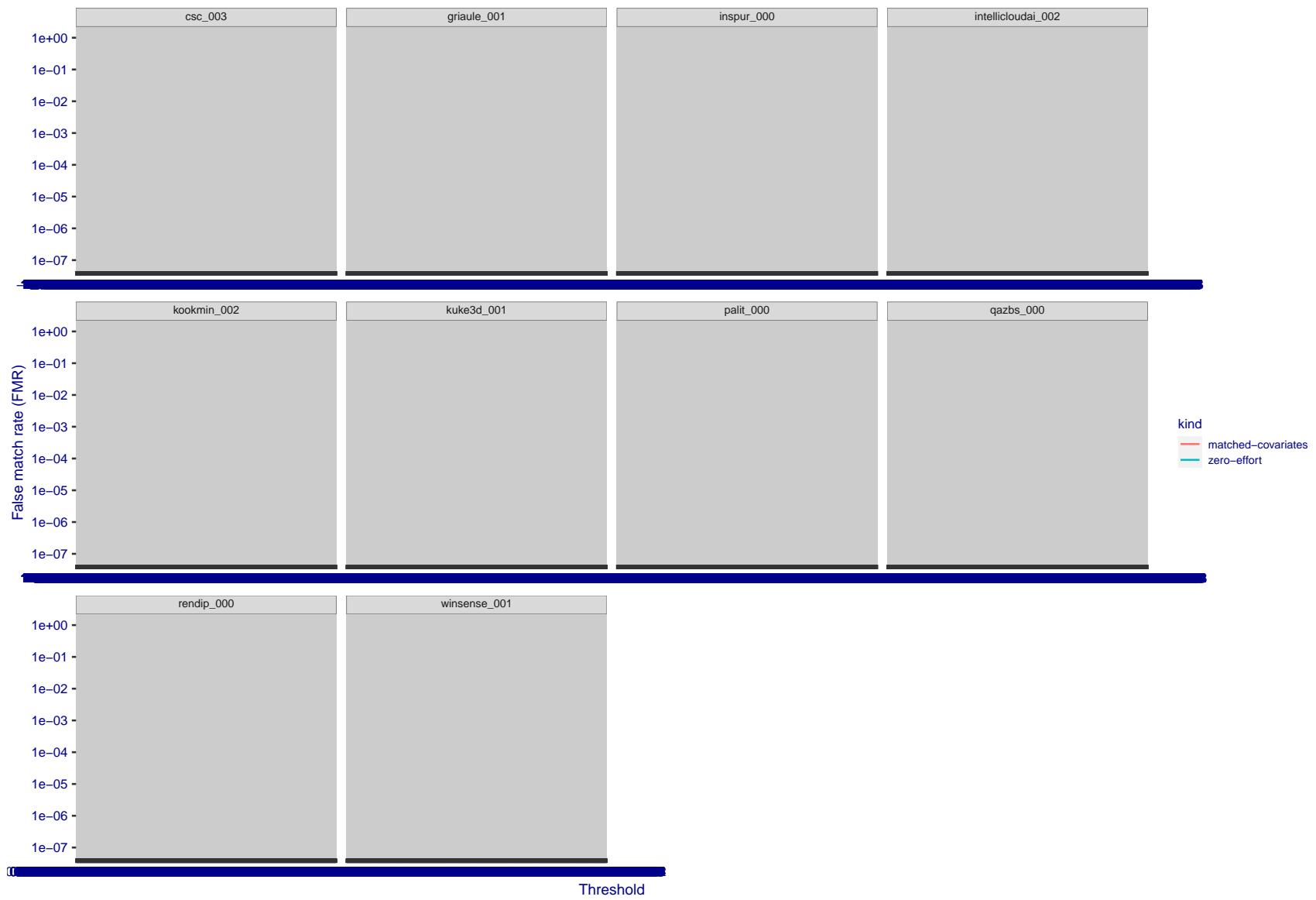


Figure 257: For the visa images, the false match calibration curves show FMR vs. threshold, T . The blue (lower) curves are for zero-effort impostors (i.e. comparing all images against all). The red (upper) curves are for persons of the same-sex, same-age, and same national-origin. This shows that FMR is underestimated (by a factor of 10 or more) by using a zero-effort impostor calculation to calibrate T . As shown later (sec. 3.6), FMR is higher for demographic-matched impostors.

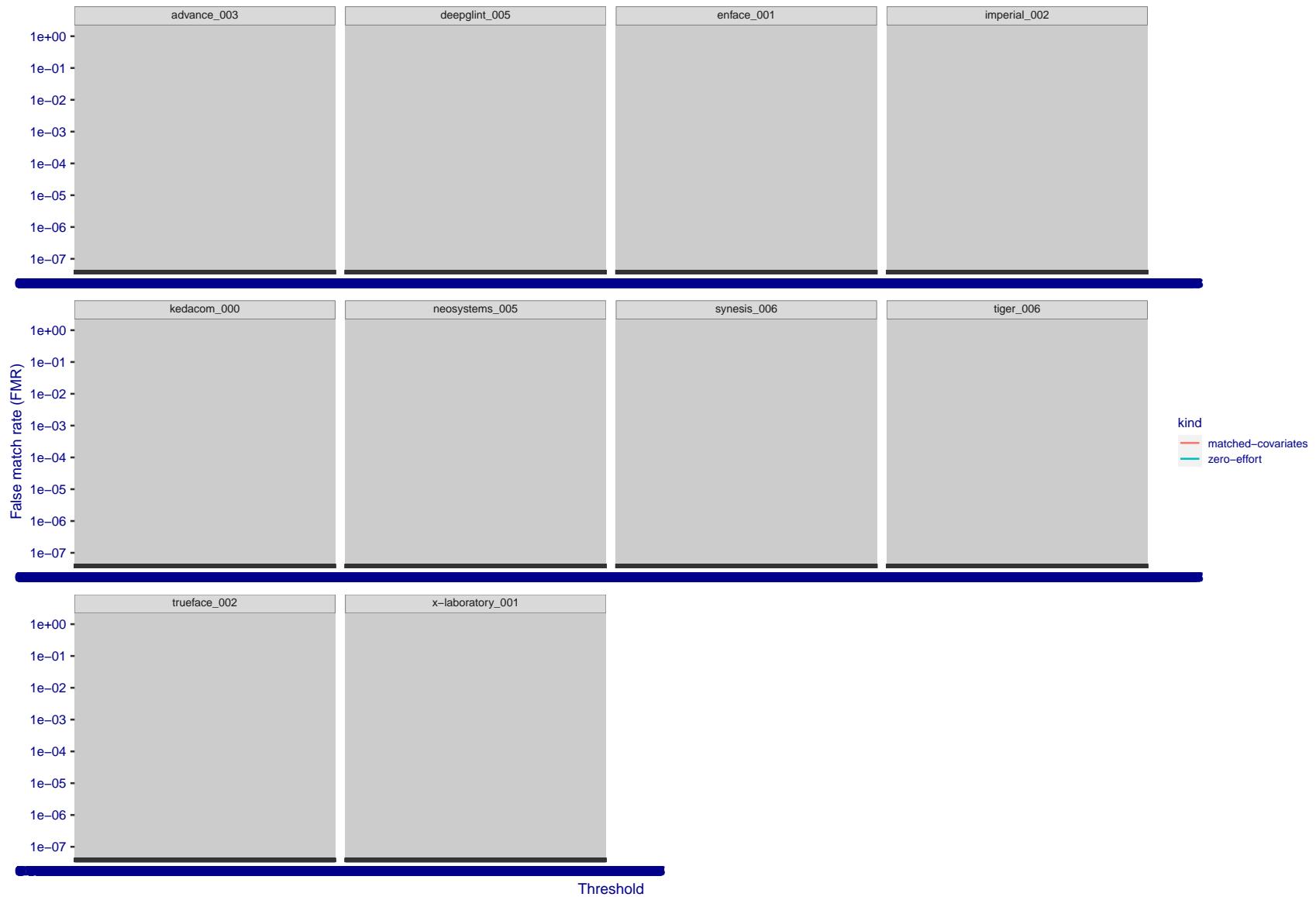


Figure 258: For the visa images, the false match calibration curves show FMR vs. threshold, T . The blue (lower) curves are for zero-effort impostors (i.e. comparing all images against all). The red (upper) curves are for persons of the same-sex, same-age, and same national-origin. This shows that FMR is underestimated (by a factor of 10 or more) by using a zero-effort impostor calculation to calibrate T . As shown later (sec. 3.6), FMR is higher for demographic-matched impostors.

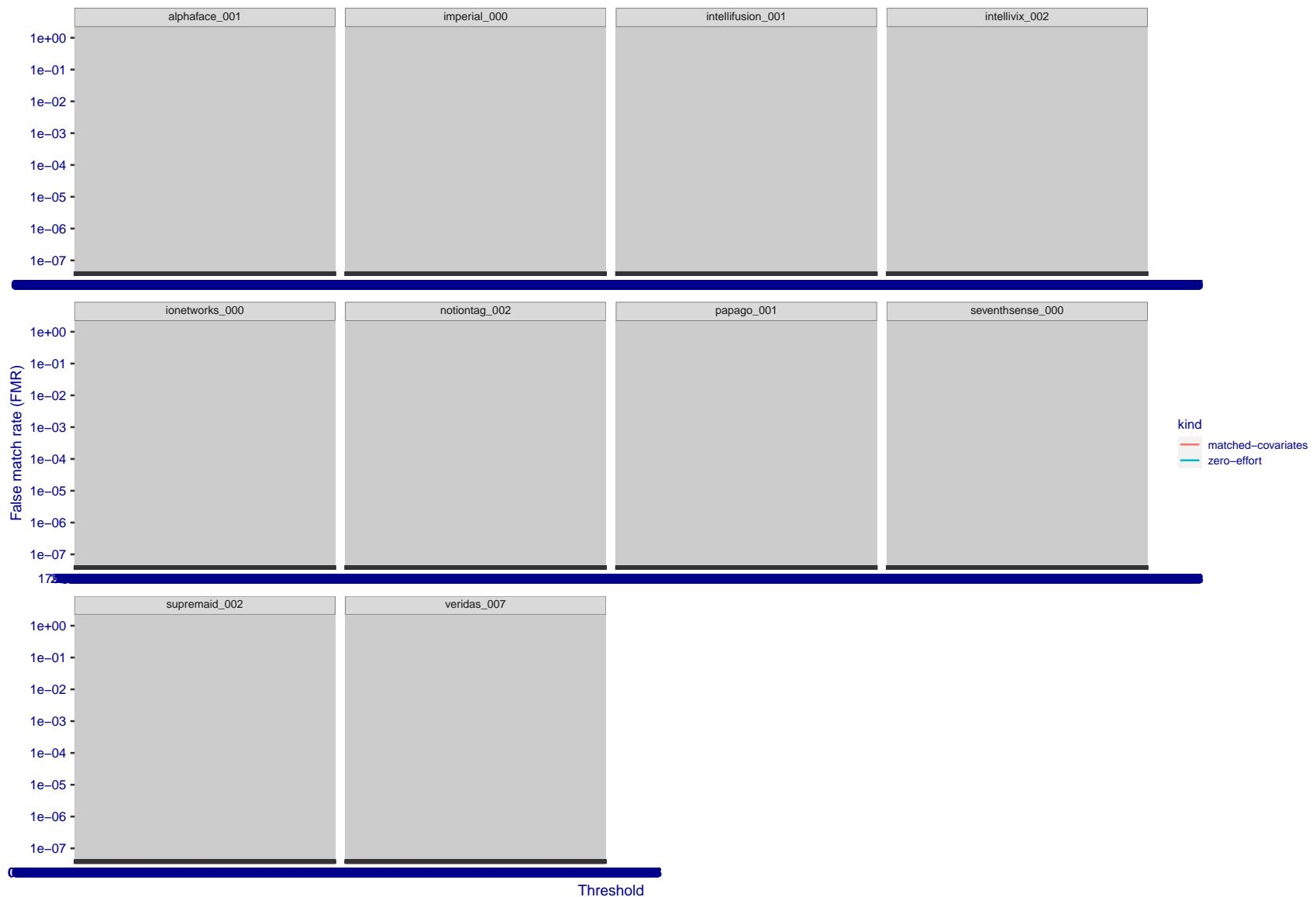


Figure 259: For the visa images, the false match calibration curves show FMR vs. threshold, T . The blue (lower) curves are for zero-effort impostors (i.e. comparing all images against all). The red (upper) curves are for persons of the same-sex, same-age, and same national-origin. This shows that FMR is underestimated (by a factor of 10 or more) by using a zero-effort impostor calculation to calibrate T . As shown later (sec. 3.6), FMR is higher for demographic-matched impostors.

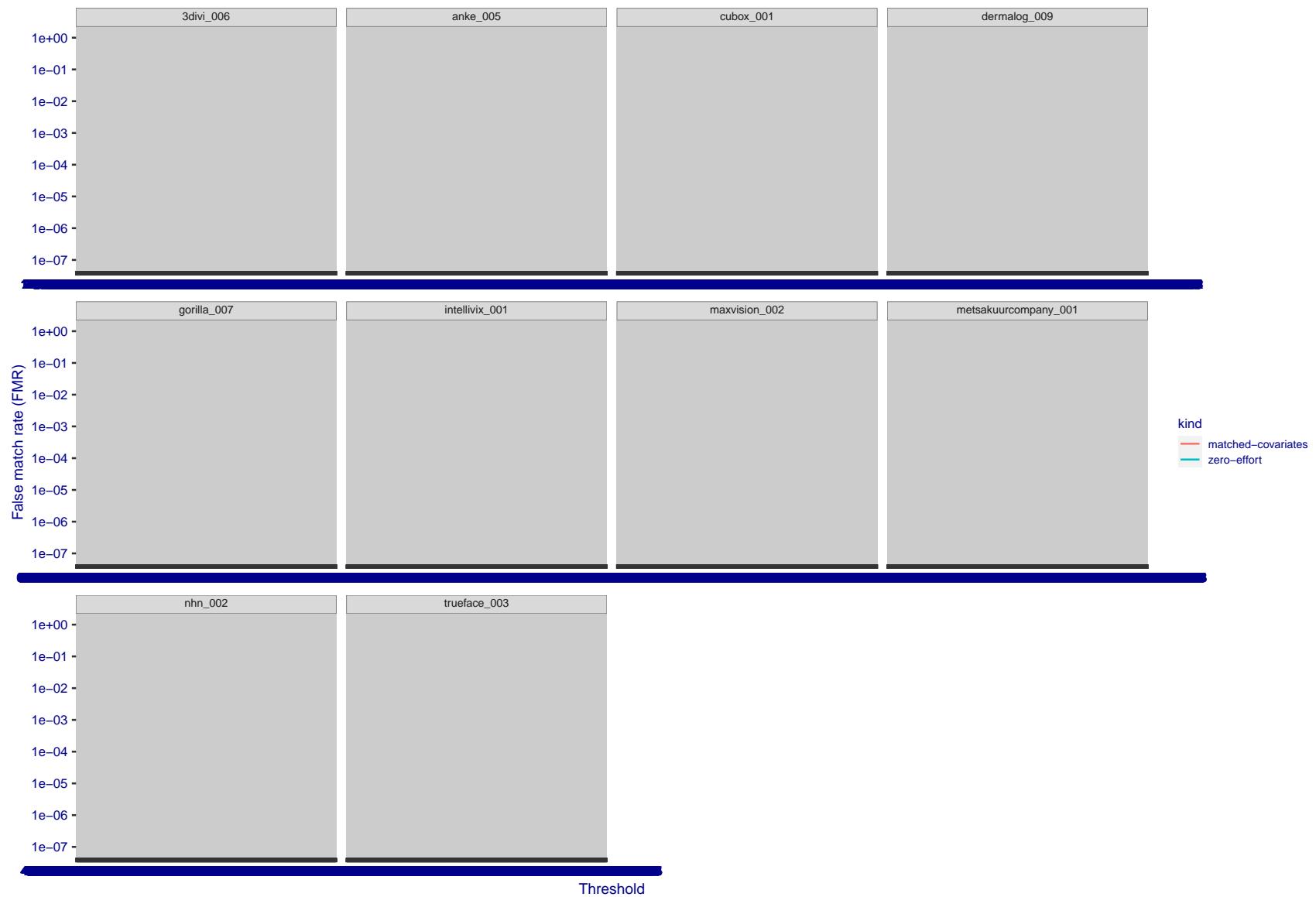


Figure 260: For the visa images, the false match calibration curves show FMR vs. threshold, T . The blue (lower) curves are for zero-effort impostors (i.e. comparing all images against all). The red (upper) curves are for persons of the same-sex, same-age, and same national-origin. This shows that FMR is underestimated (by a factor of 10 or more) by using a zero-effort impostor calculation to calibrate T . As shown later (sec. 3.6), FMR is higher for demographic-matched impostors.

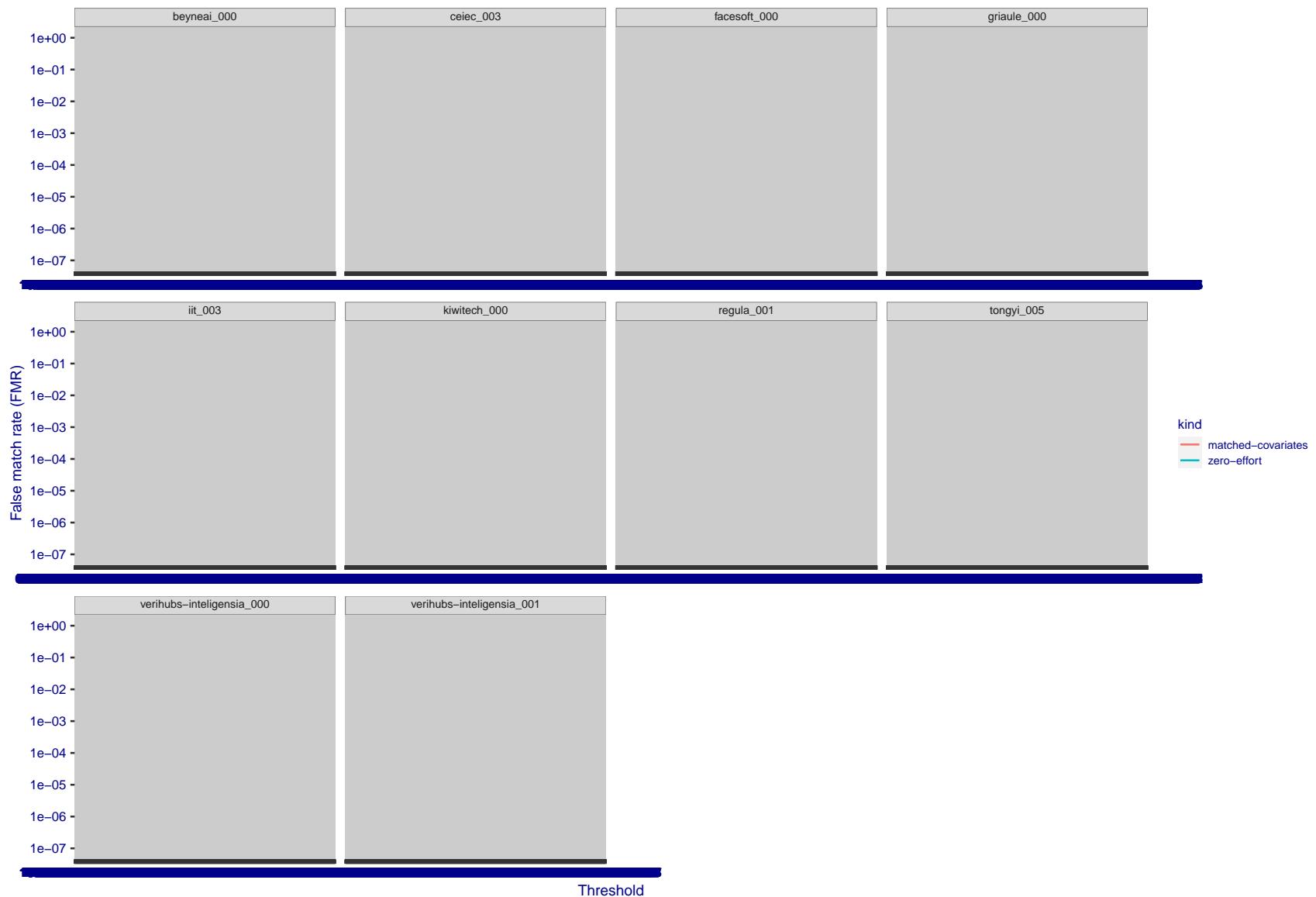


Figure 261: For the visa images, the false match calibration curves show FMR vs. threshold, T . The blue (lower) curves are for zero-effort impostors (i.e. comparing all images against all). The red (upper) curves are for persons of the same-sex, same-age, and same national-origin. This shows that FMR is underestimated (by a factor of 10 or more) by using a zero-effort impostor calculation to calibrate T . As shown later (sec. 3.6), FMR is higher for demographic-matched impostors.

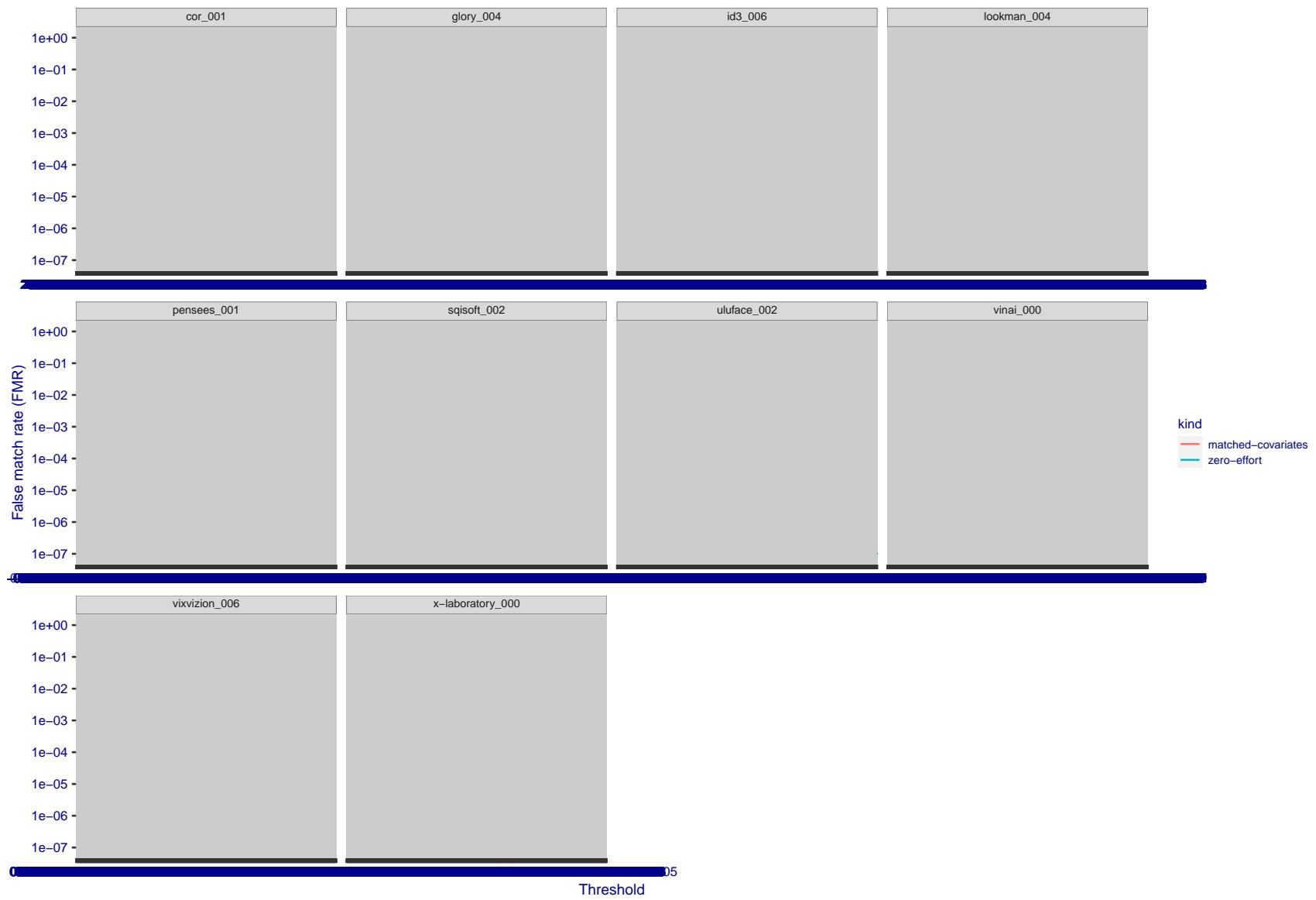


Figure 262: For the visa images, the false match calibration curves show FMR vs. threshold, T . The blue (lower) curves are for zero-effort impostors (i.e. comparing all images against all). The red (upper) curves are for persons of the same-sex, same-age, and same national-origin. This shows that FMR is underestimated (by a factor of 10 or more) by using a zero-effort impostor calculation to calibrate T . As shown later (sec. 3.6), FMR is higher for demographic-matched impostors.

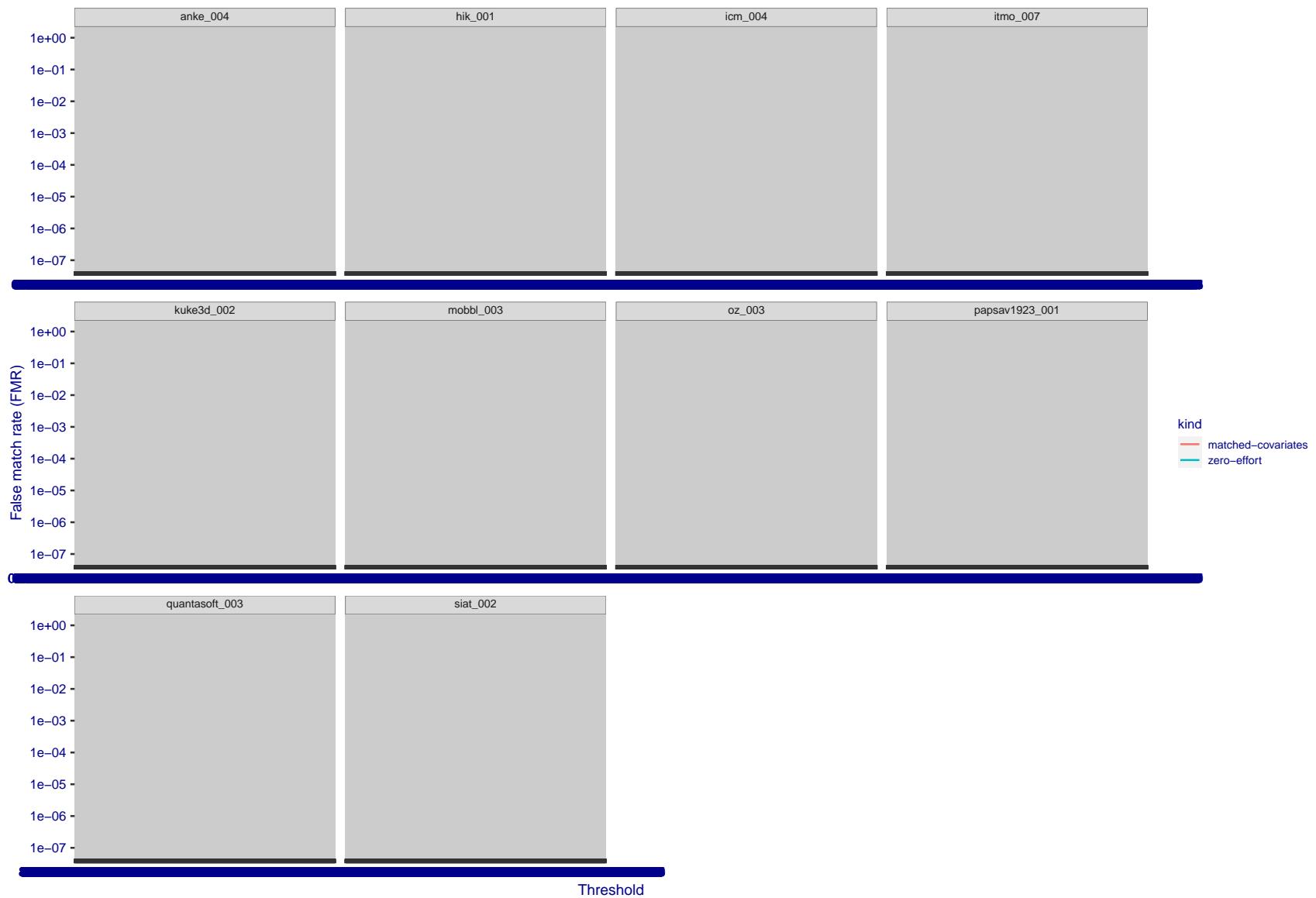


Figure 263: For the visa images, the false match calibration curves show FMR vs. threshold, T . The blue (lower) curves are for zero-effort impostors (i.e. comparing all images against all). The red (upper) curves are for persons of the same-sex, same-age, and same national-origin. This shows that FMR is underestimated (by a factor of 10 or more) by using a zero-effort impostor calculation to calibrate T . As shown later (sec. 3.6), FMR is higher for demographic-matched impostors.

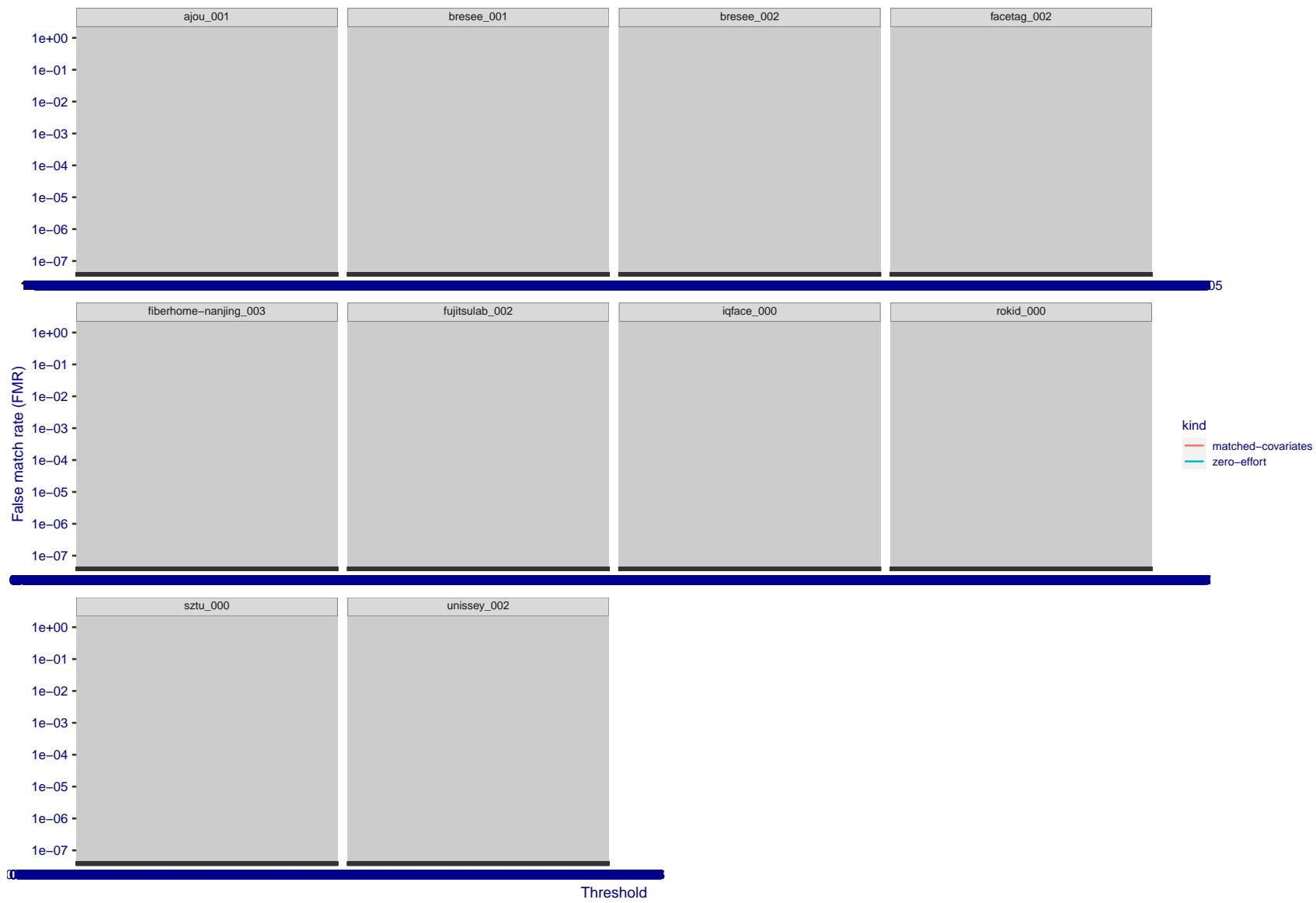


Figure 264: For the visa images, the false match calibration curves show FMR vs. threshold, T . The blue (lower) curves are for zero-effort impostors (i.e. comparing all images against all). The red (upper) curves are for persons of the same-sex, same-age, and same national-origin. This shows that FMR is underestimated (by a factor of 10 or more) by using a zero-effort impostor calculation to calibrate T . As shown later (sec. 3.6), FMR is higher for demographic-matched impostors.

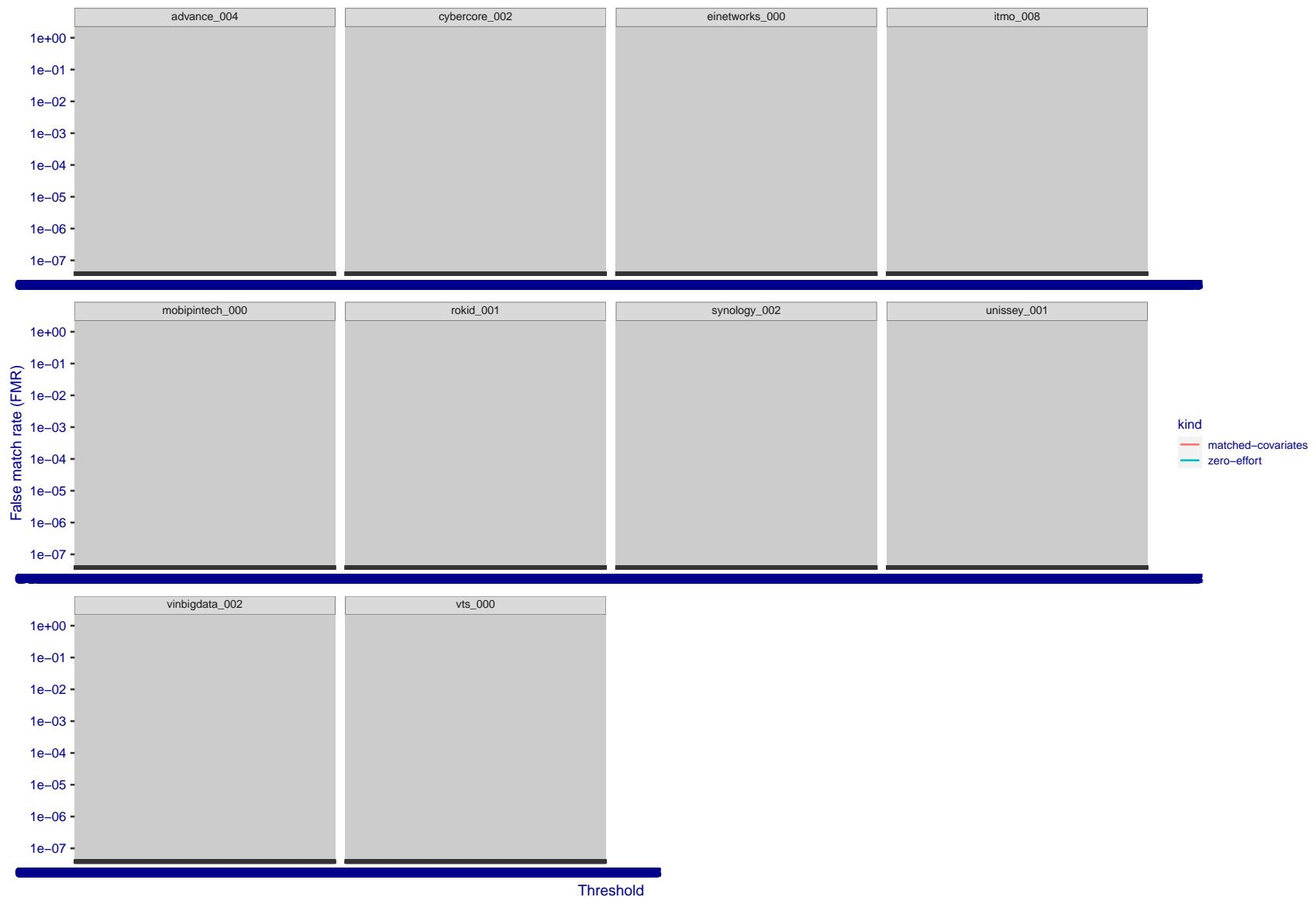


Figure 265: For the visa images, the false match calibration curves show FMR vs. threshold, T . The blue (lower) curves are for zero-effort impostors (i.e. comparing all images against all). The red (upper) curves are for persons of the same-sex, same-age, and same national-origin. This shows that FMR is underestimated (by a factor of 10 or more) by using a zero-effort impostor calculation to calibrate T . As shown later (sec. 3.6), FMR is higher for demographic-matched impostors.

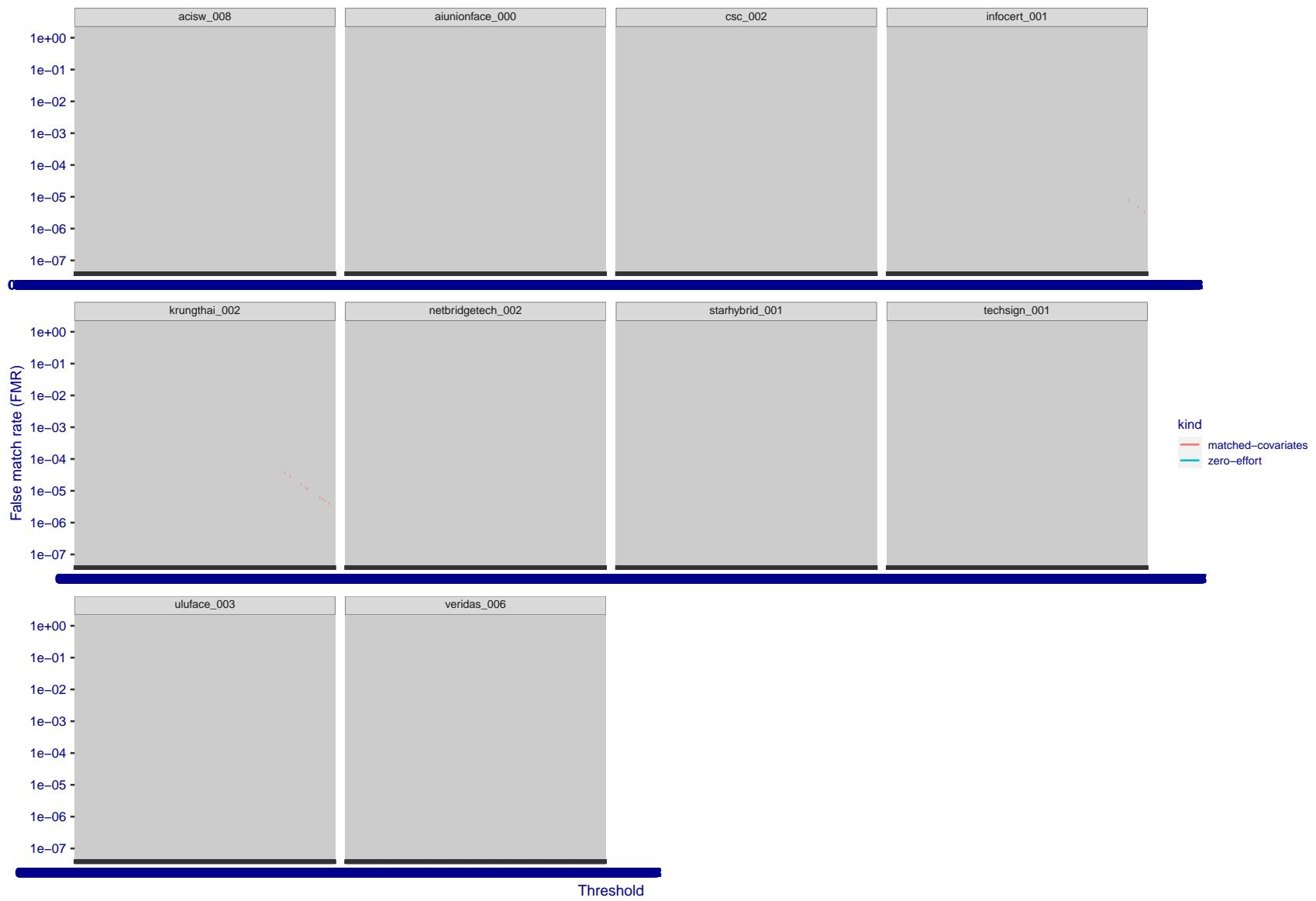


Figure 266: For the visa images, the false match calibration curves show FMR vs. threshold, T . The blue (lower) curves are for zero-effort impostors (i.e. comparing all images against all). The red (upper) curves are for persons of the same-sex, same-age, and same national-origin. This shows that FMR is underestimated (by a factor of 10 or more) by using a zero-effort impostor calculation to calibrate T . As shown later (sec. 3.6), FMR is higher for demographic-matched impostors.

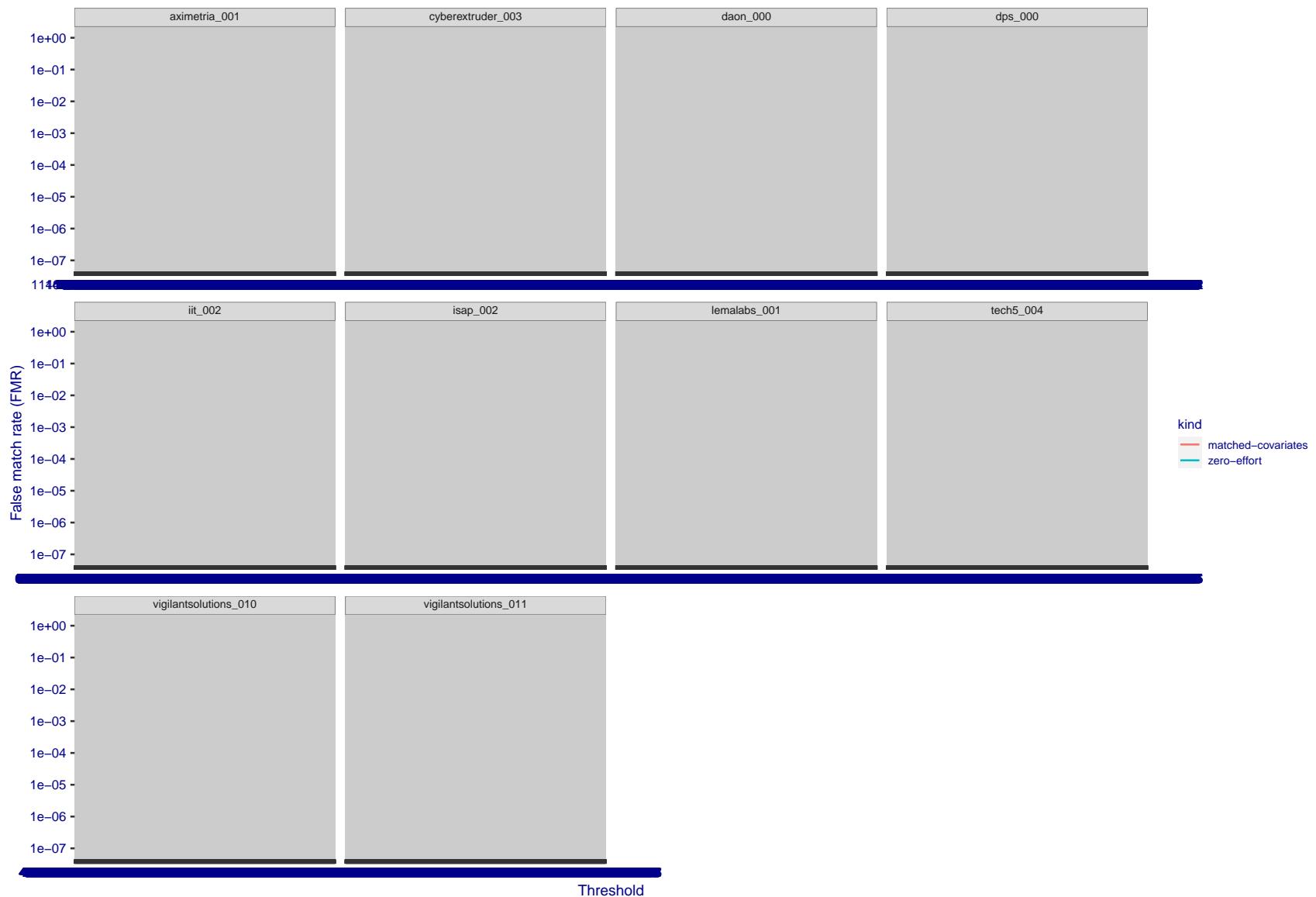


Figure 267: For the visa images, the false match calibration curves show FMR vs. threshold, T . The blue (lower) curves are for zero-effort impostors (i.e. comparing all images against all). The red (upper) curves are for persons of the same-sex, same-age, and same national-origin. This shows that FMR is underestimated (by a factor of 10 or more) by using a zero-effort impostor calculation to calibrate T . As shown later (sec. 3.6), FMR is higher for demographic-matched impostors.

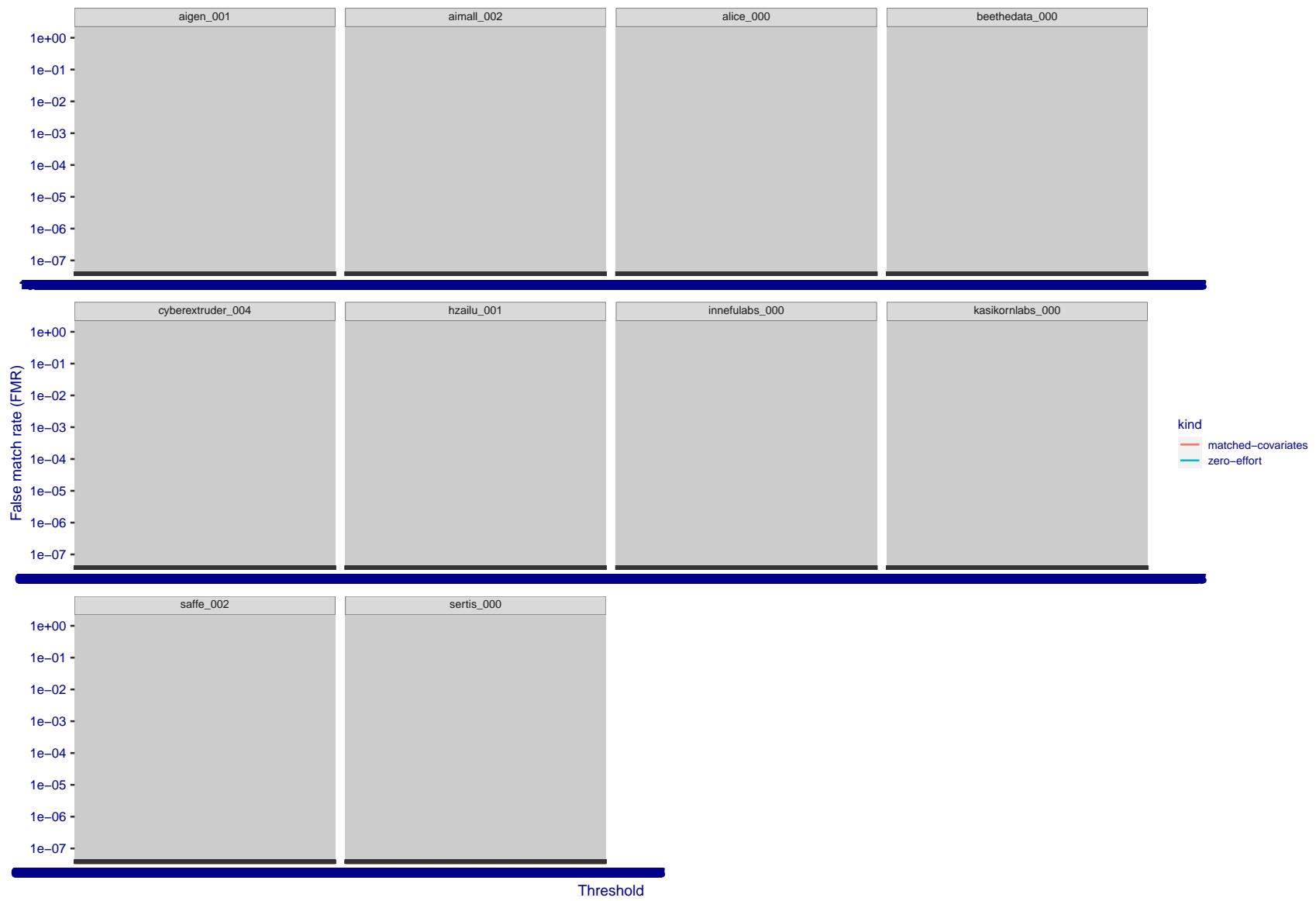


Figure 268: For the visa images, the false match calibration curves show FMR vs. threshold, T . The blue (lower) curves are for zero-effort impostors (i.e. comparing all images against all). The red (upper) curves are for persons of the same-sex, same-age, and same national-origin. This shows that FMR is underestimated (by a factor of 10 or more) by using a zero-effort impostor calculation to calibrate T . As shown later (sec. 3.6), FMR is higher for demographic-matched impostors.

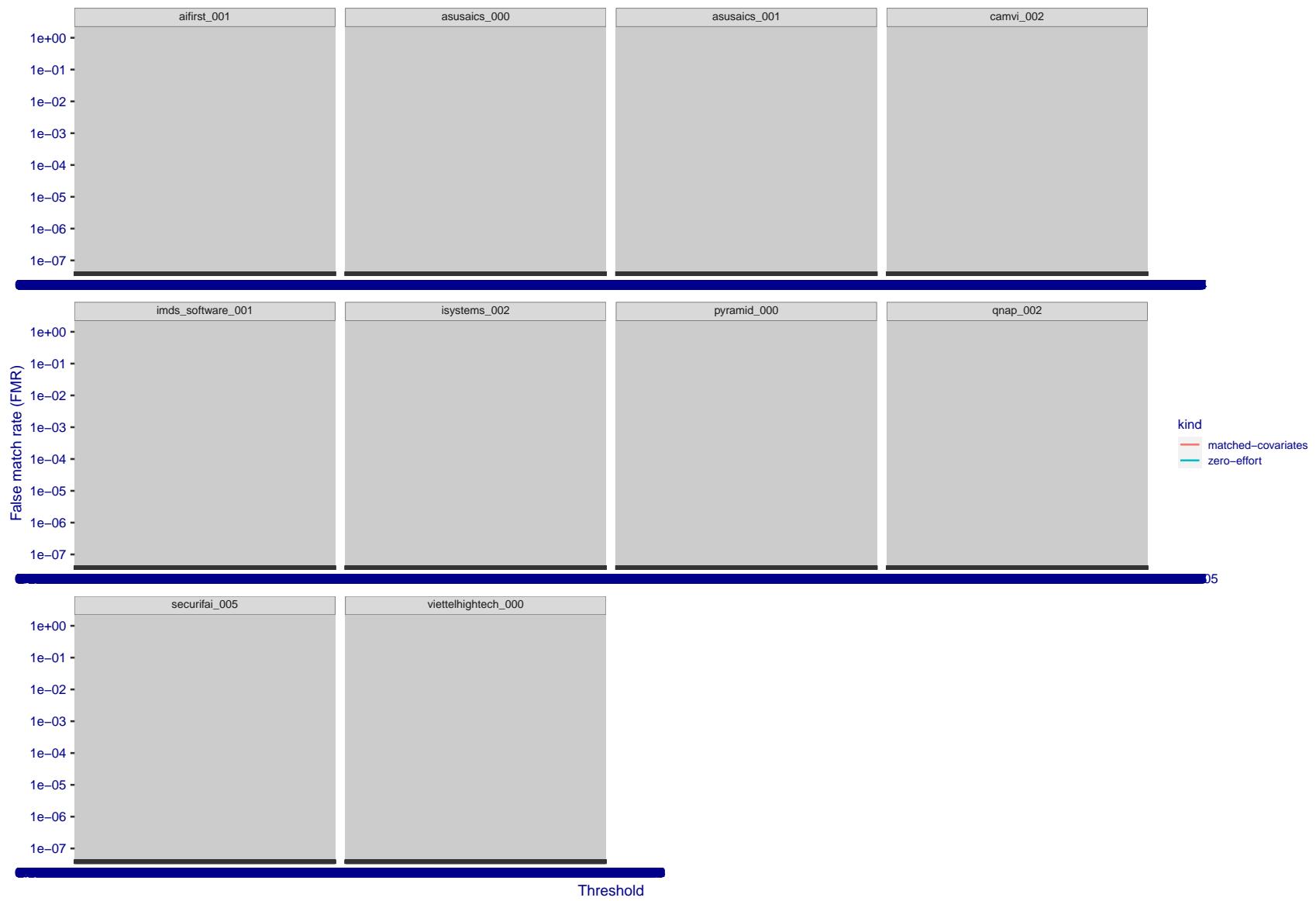


Figure 269: For the visa images, the false match calibration curves show FMR vs. threshold, T . The blue (lower) curves are for zero-effort impostors (i.e. comparing all images against all). The red (upper) curves are for persons of the same-sex, same-age, and same national-origin. This shows that FMR is underestimated (by a factor of 10 or more) by using a zero-effort impostor calculation to calibrate T . As shown later (sec. 3.6), FMR is higher for demographic-matched impostors.

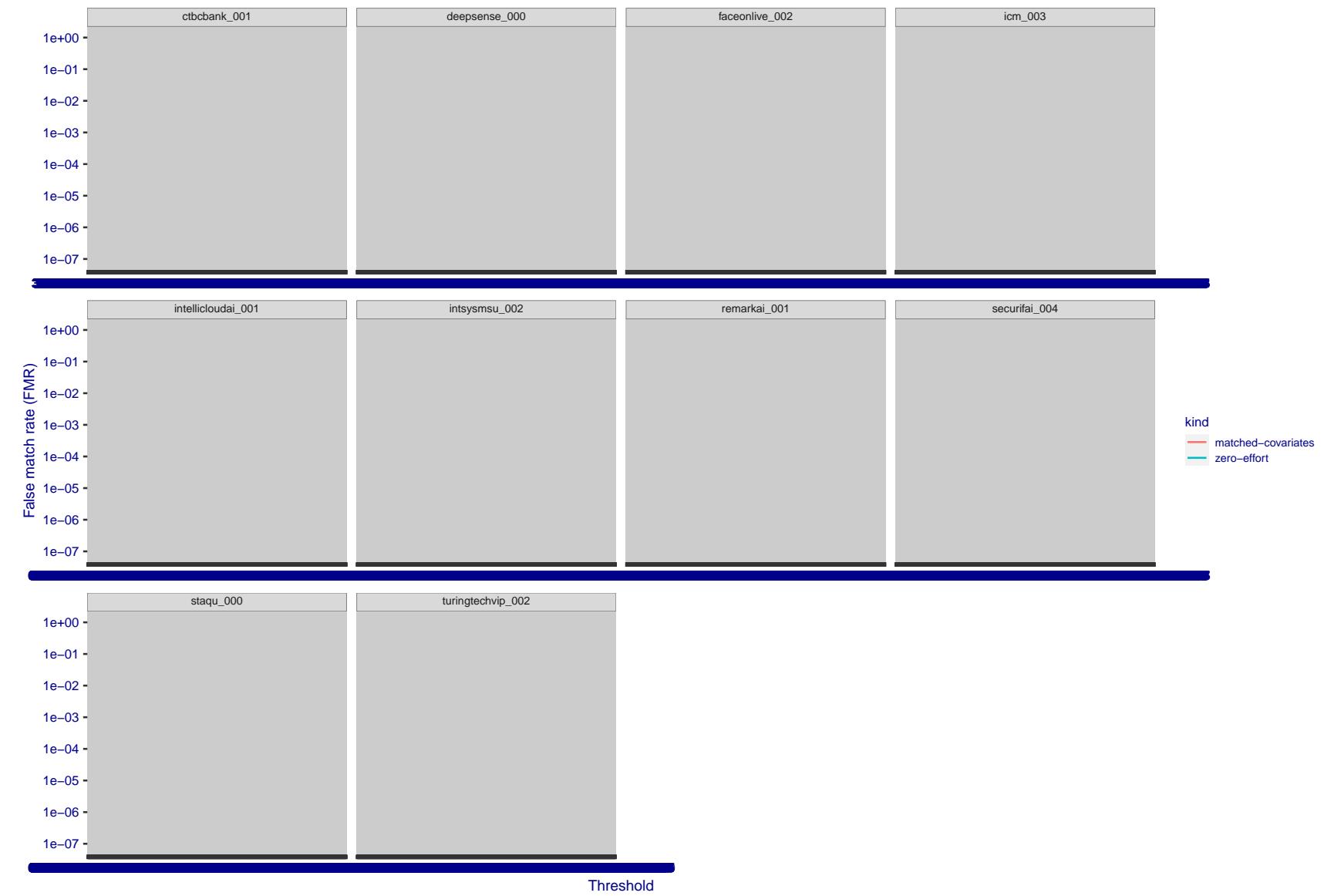


Figure 270: For the visa images, the false match calibration curves show FMR vs. threshold, T . The blue (lower) curves are for zero-effort impostors (i.e. comparing all images against all). The red (upper) curves are for persons of the same-sex, same-age, and same national-origin. This shows that FMR is underestimated (by a factor of 10 or more) by using a zero-effort impostor calculation to calibrate T . As shown later (sec. 3.6), FMR is higher for demographic-matched impostors.

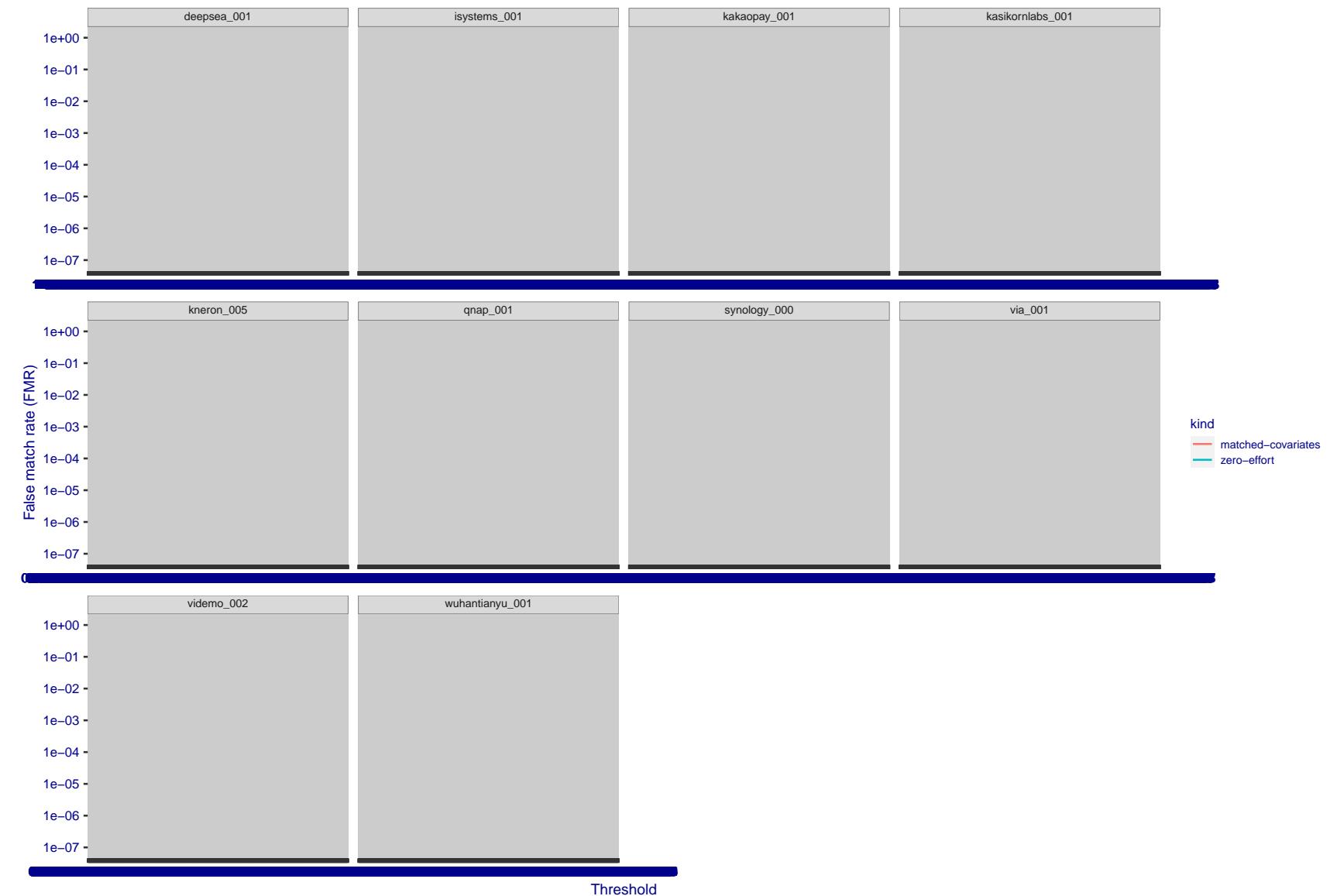


Figure 271: For the visa images, the false match calibration curves show FMR vs. threshold, T . The blue (lower) curves are for zero-effort impostors (i.e. comparing all images against all). The red (upper) curves are for persons of the same-sex, same-age, and same national-origin. This shows that FMR is underestimated (by a factor of 10 or more) by using a zero-effort impostor calculation to calibrate T . As shown later (sec. 3.6), FMR is higher for demographic-matched impostors.

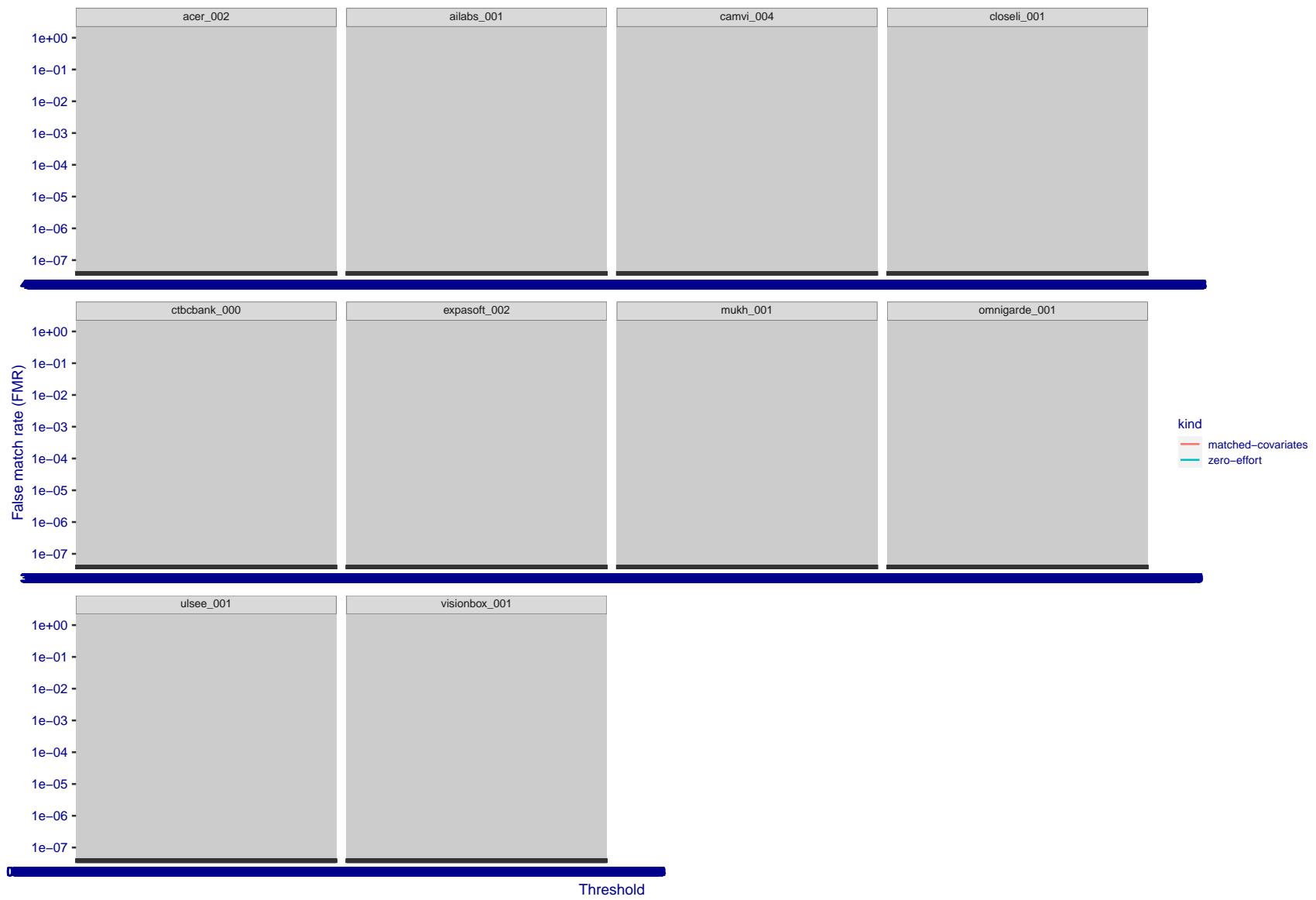


Figure 272: For the visa images, the false match calibration curves show FMR vs. threshold, T . The blue (lower) curves are for zero-effort impostors (i.e. comparing all images against all). The red (upper) curves are for persons of the same-sex, same-age, and same national-origin. This shows that FMR is underestimated (by a factor of 10 or more) by using a zero-effort impostor calculation to calibrate T . As shown later (sec. 3.6), FMR is higher for demographic-matched impostors.

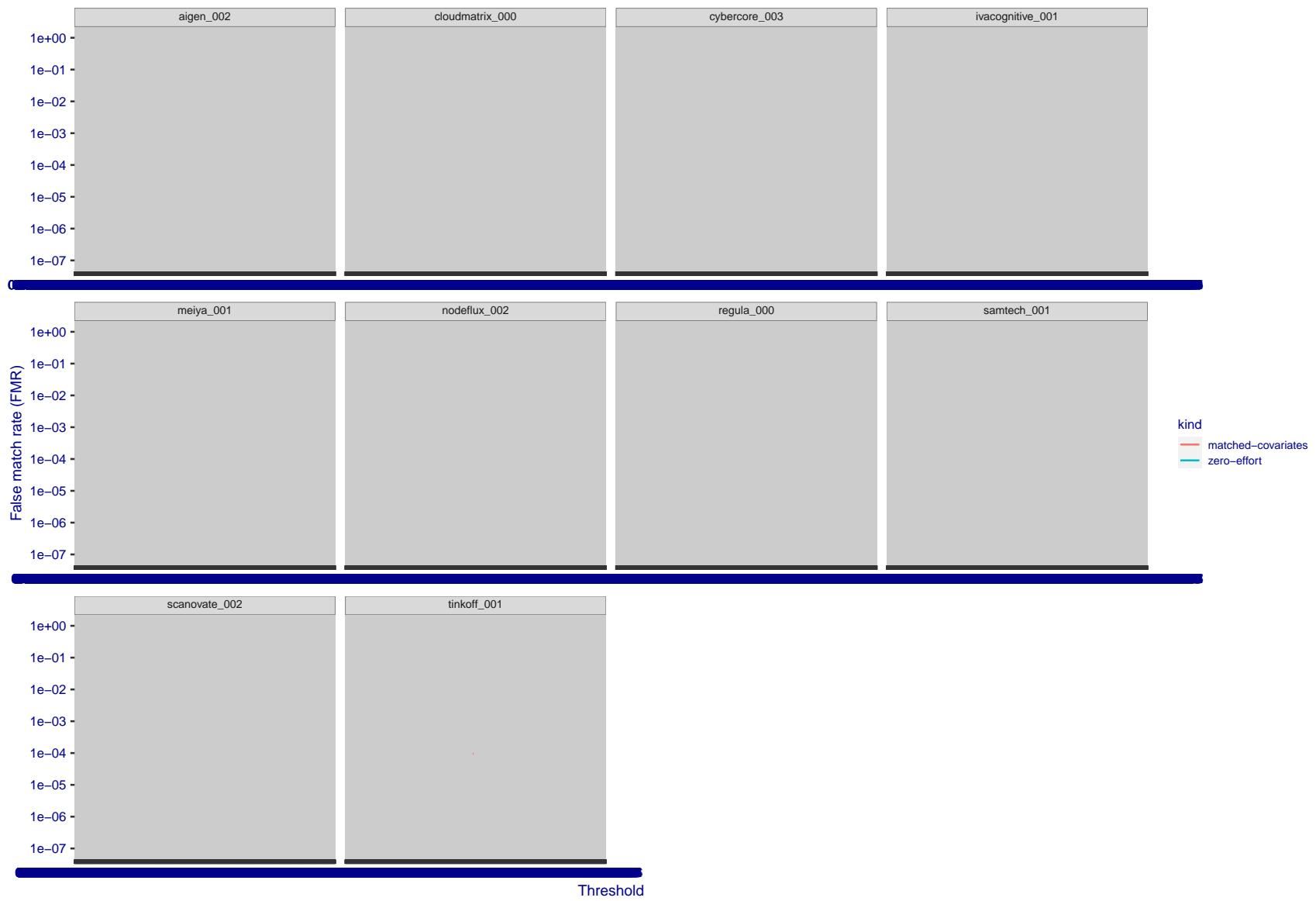


Figure 273: For the visa images, the false match calibration curves show FMR vs. threshold, T . The blue (lower) curves are for zero-effort impostors (i.e. comparing all images against all). The red (upper) curves are for persons of the same-sex, same-age, and same national-origin. This shows that FMR is underestimated (by a factor of 10 or more) by using a zero-effort impostor calculation to calibrate T . As shown later (sec. 3.6), FMR is higher for demographic-matched impostors.

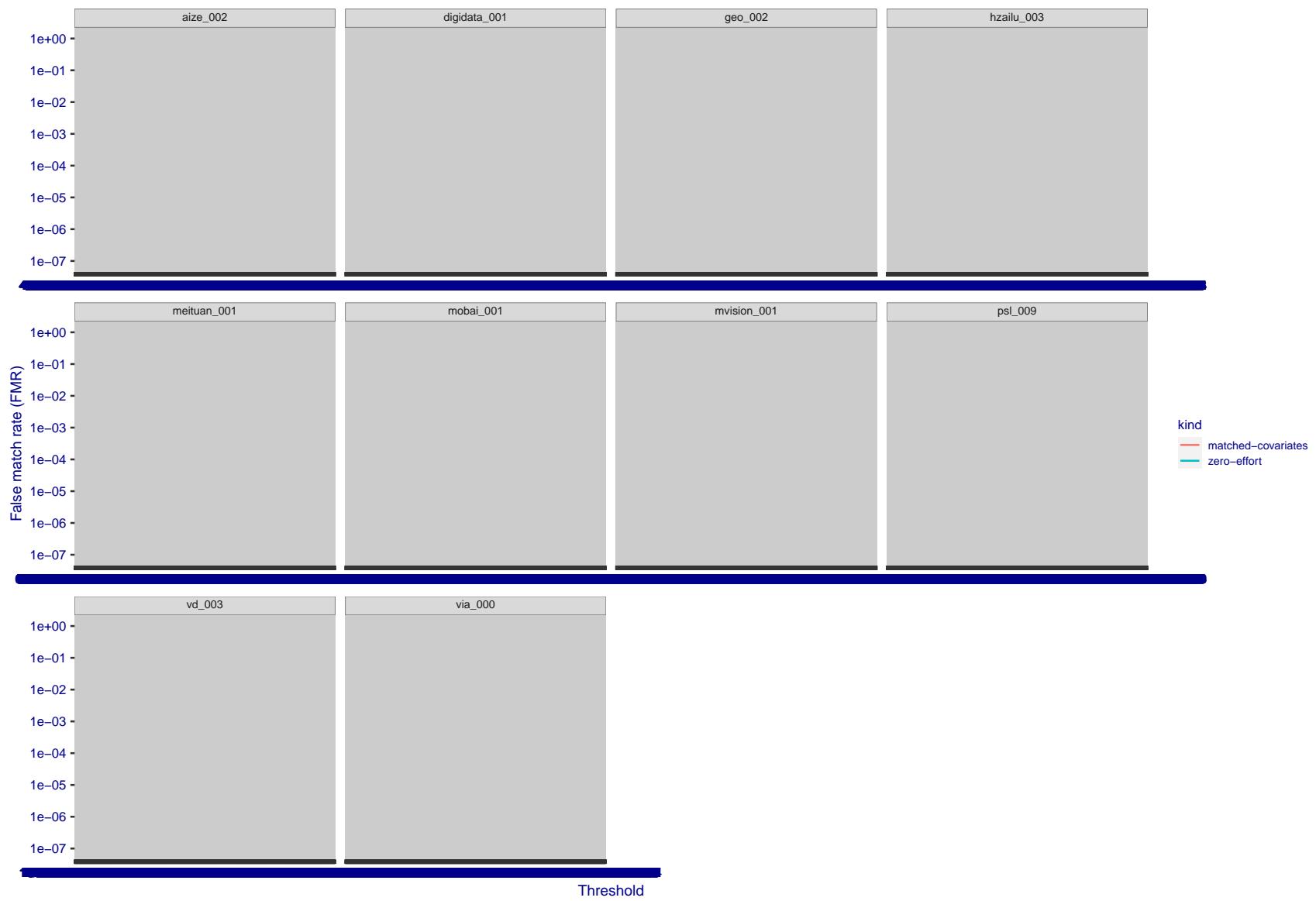


Figure 274: For the visa images, the false match calibration curves show FMR vs. threshold, T . The blue (lower) curves are for zero-effort impostors (i.e. comparing all images against all). The red (upper) curves are for persons of the same-sex, same-age, and same national-origin. This shows that FMR is underestimated (by a factor of 10 or more) by using a zero-effort impostor calculation to calibrate T . As shown later (sec. 3.6), FMR is higher for demographic-matched impostors.

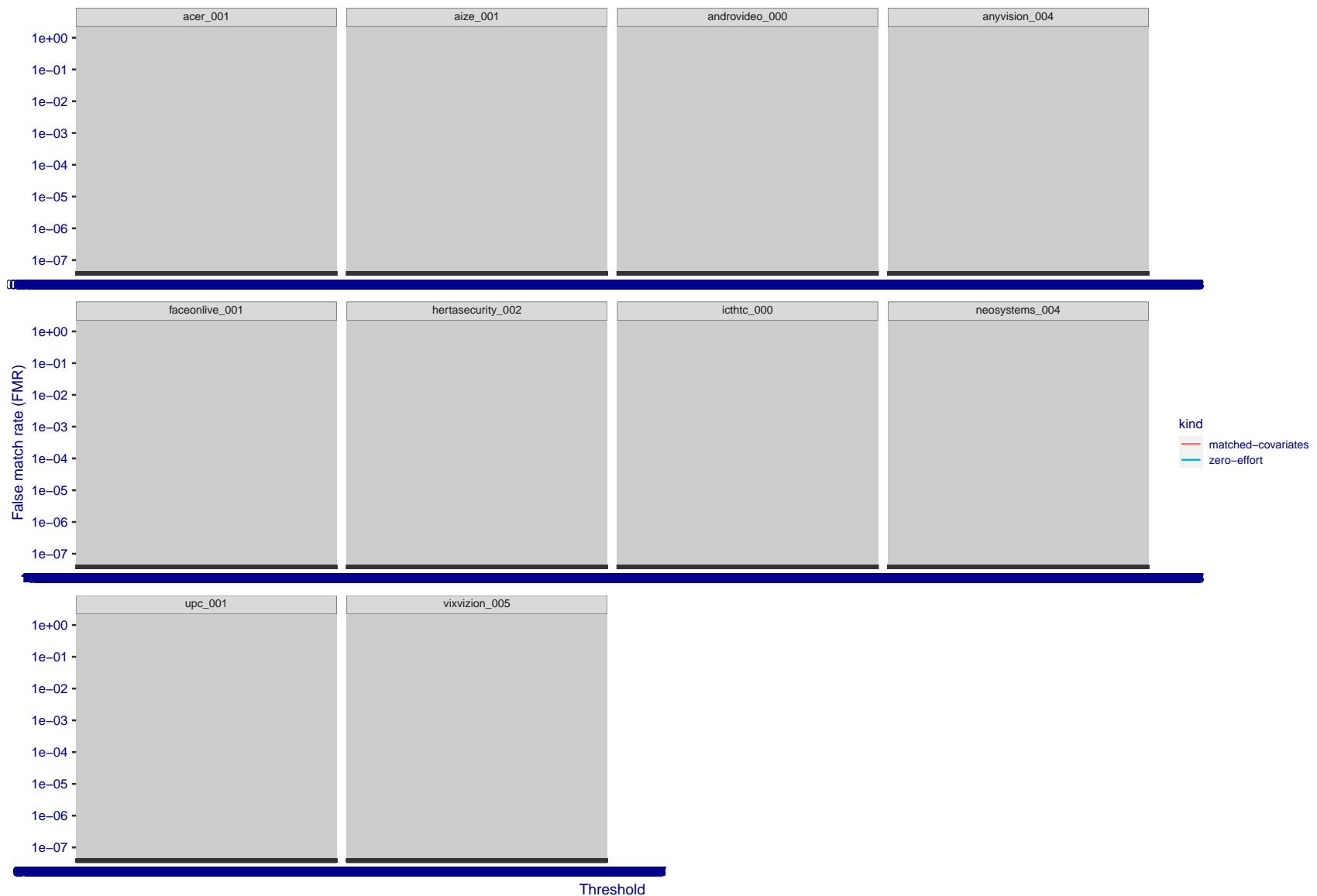


Figure 275: For the visa images, the false match calibration curves show FMR vs. threshold, T . The blue (lower) curves are for zero-effort impostors (i.e. comparing all images against all). The red (upper) curves are for persons of the same-sex, same-age, and same national-origin. This shows that FMR is underestimated (by a factor of 10 or more) by using a zero-effort impostor calculation to calibrate T . As shown later (sec. 3.6), FMR is higher for demographic-matched impostors.

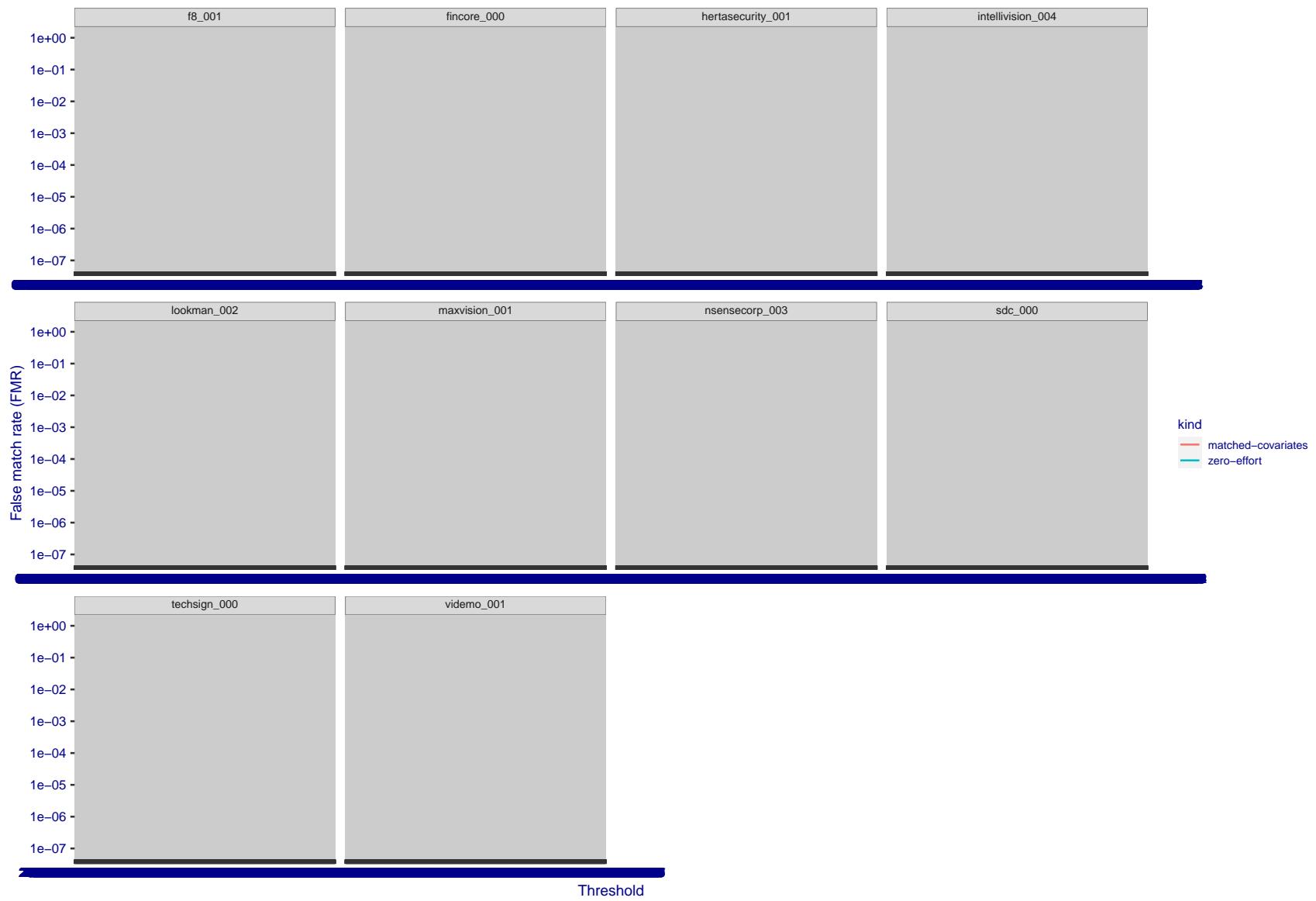


Figure 276: For the visa images, the false match calibration curves show FMR vs. threshold, T . The blue (lower) curves are for zero-effort impostors (i.e. comparing all images against all). The red (upper) curves are for persons of the same-sex, same-age, and same national-origin. This shows that FMR is underestimated (by a factor of 10 or more) by using a zero-effort impostor calculation to calibrate T . As shown later (sec. 3.6), FMR is higher for demographic-matched impostors.

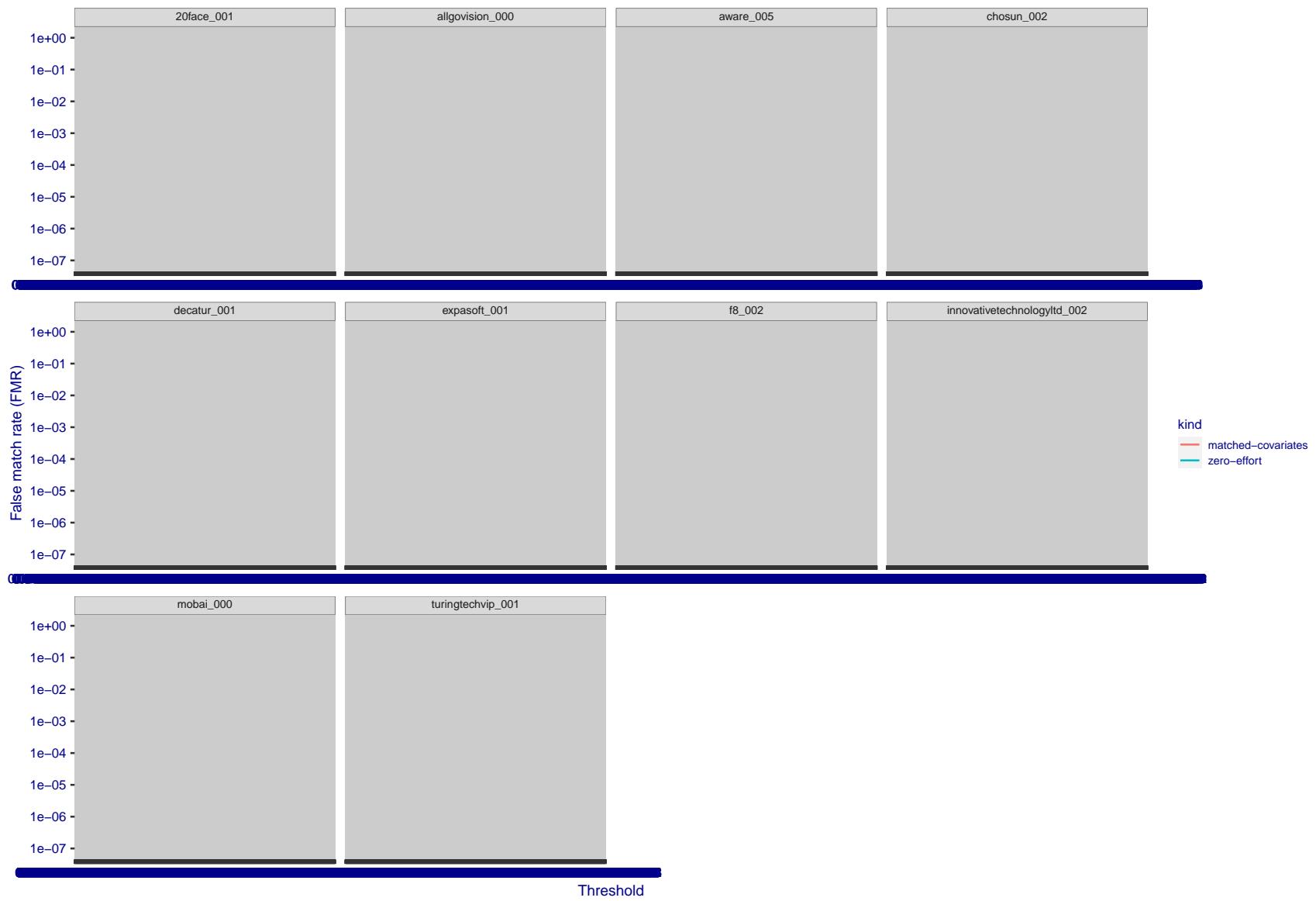


Figure 277: For the visa images, the false match calibration curves show FMR vs. threshold, T . The blue (lower) curves are for zero-effort impostors (i.e. comparing all images against all). The red (upper) curves are for persons of the same-sex, same-age, and same national-origin. This shows that FMR is underestimated (by a factor of 10 or more) by using a zero-effort impostor calculation to calibrate T . As shown later (sec. 3.6), FMR is higher for demographic-matched impostors.

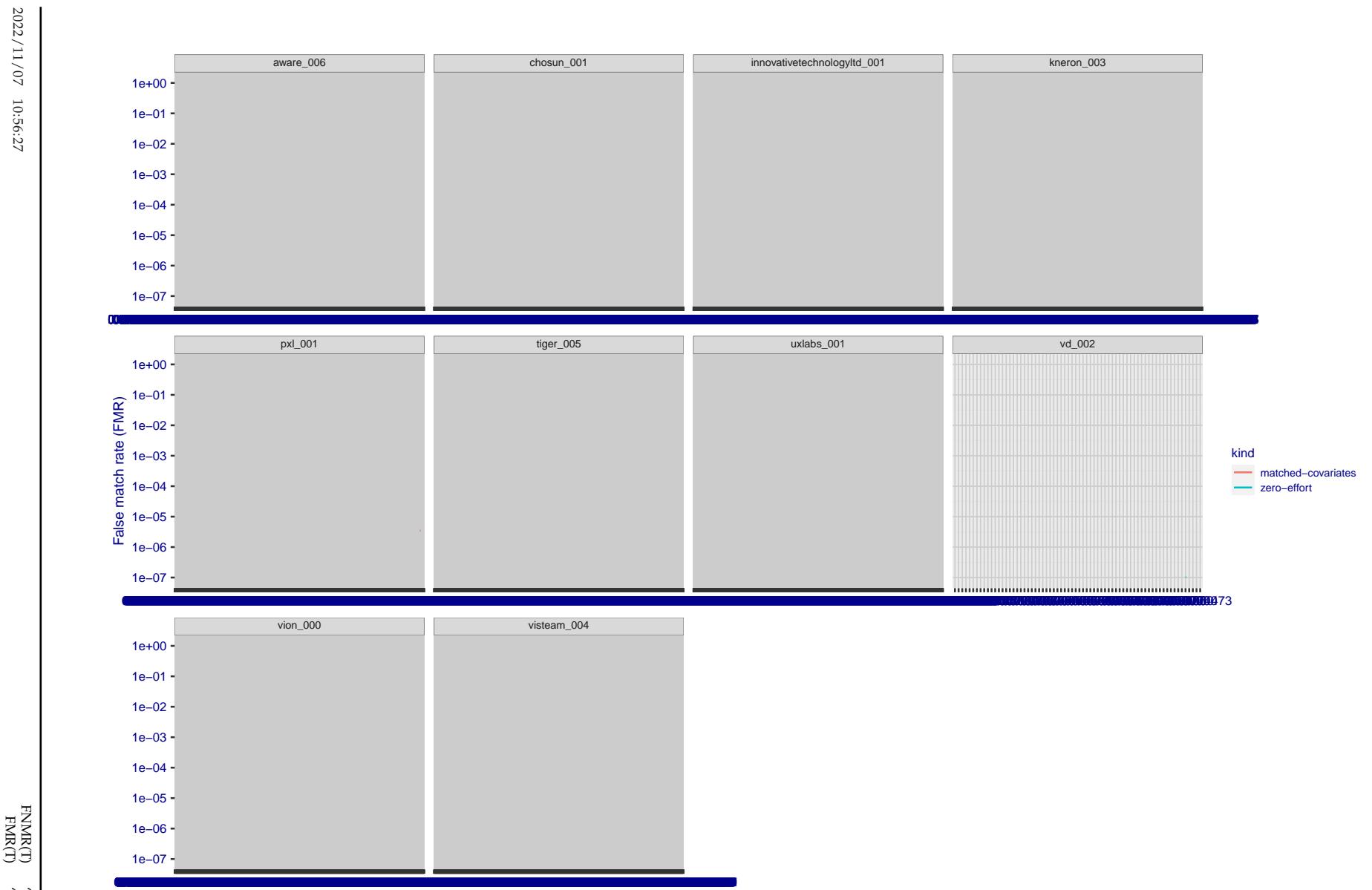


Figure 278: For the visa images, the false match calibration curves show FMR vs. threshold, T . The blue (lower) curves are for zero-effort impostors (i.e. comparing all images against all). The red (upper) curves are for persons of the same-sex, same-age, and same national-origin. This shows that FMR is underestimated (by a factor of 10 or more) by using a zero-effort impostor calculation to calibrate T . As shown later (sec. 3.6), FMR is higher for demographic-matched impostors.

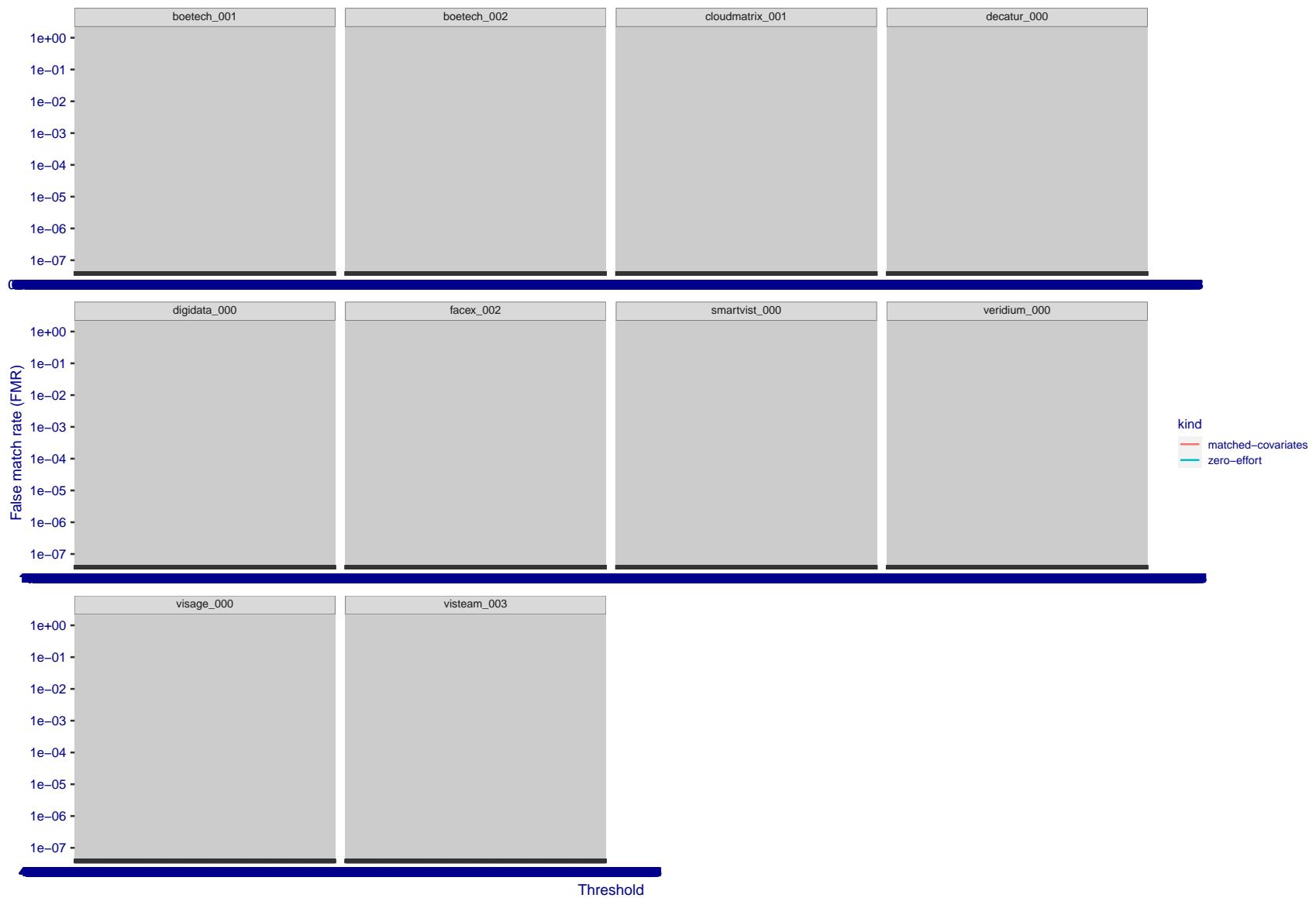


Figure 279: For the visa images, the false match calibration curves show FMR vs. threshold, T . The blue (lower) curves are for zero-effort impostors (i.e. comparing all images against all). The red (upper) curves are for persons of the same-sex, same-age, and same national-origin. This shows that FMR is underestimated (by a factor of 10 or more) by using a zero-effort impostor calculation to calibrate T . As shown later (sec. 3.6), FMR is higher for demographic-matched impostors.

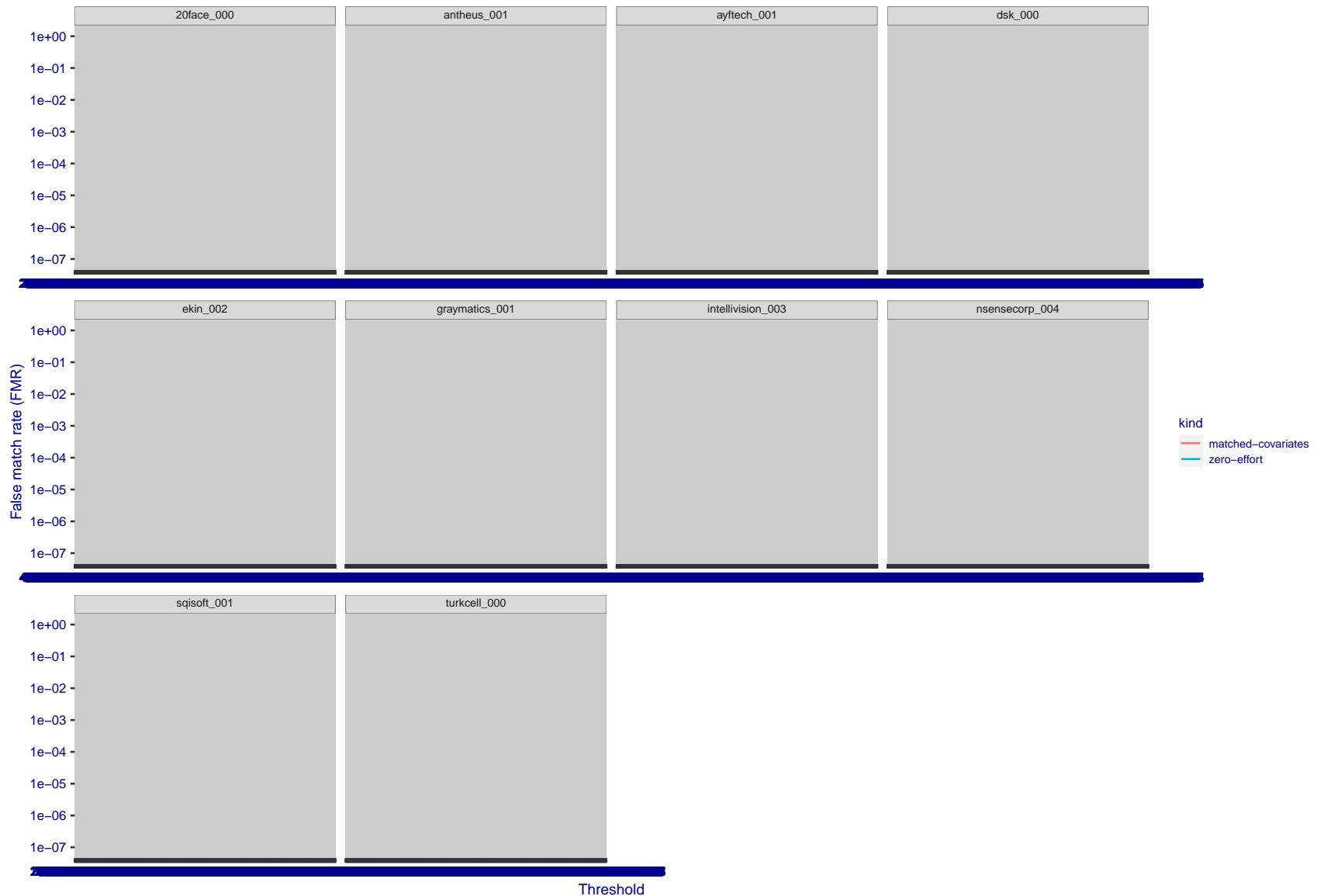


Figure 280: For the visa images, the false match calibration curves show FMR vs. threshold, T . The blue (lower) curves are for zero-effort impostors (i.e. comparing all images against all). The red (upper) curves are for persons of the same-sex, same-age, and same national-origin. This shows that FMR is underestimated (by a factor of 10 or more) by using a zero-effort impostor calculation to calibrate T . As shown later (sec. 3.6), FMR is higher for demographic-matched impostors.

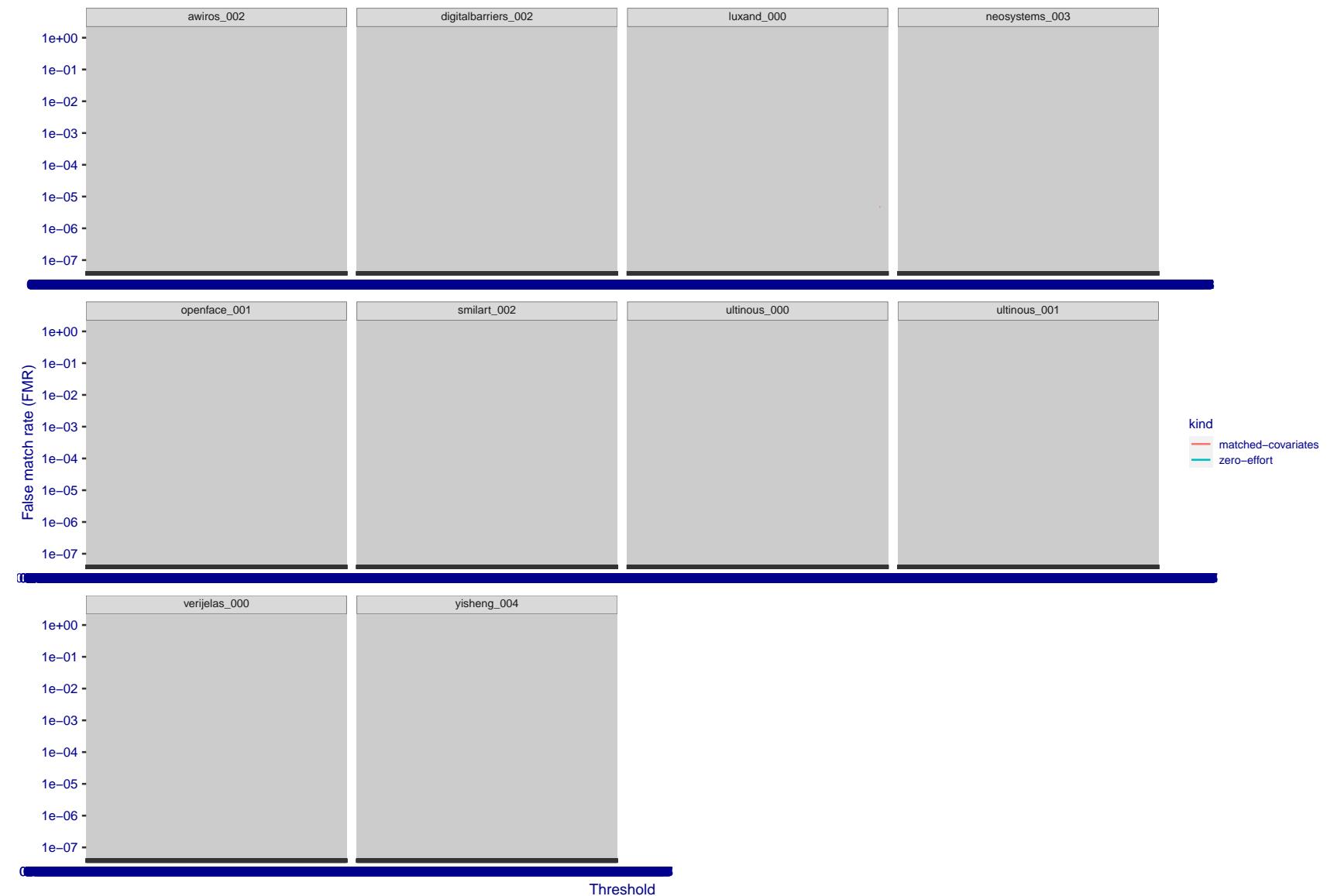


Figure 281: For the visa images, the false match calibration curves show FMR vs. threshold, T . The blue (lower) curves are for zero-effort impostors (i.e. comparing all images against all). The red (upper) curves are for persons of the same-sex, same-age, and same national-origin. This shows that FMR is underestimated (by a factor of 10 or more) by using a zero-effort impostor calculation to calibrate T . As shown later (sec. 3.6), FMR is higher for demographic-matched impostors.

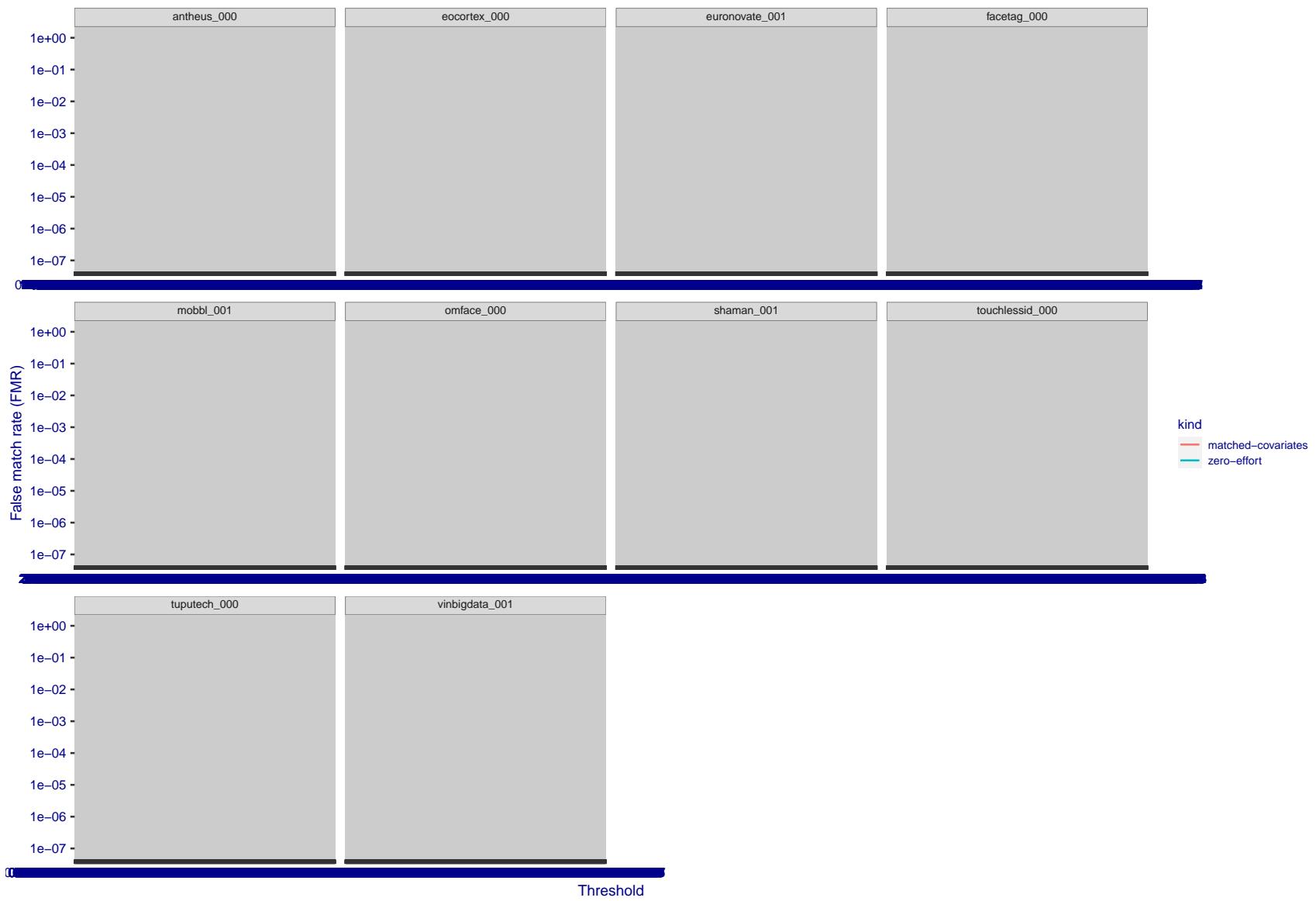


Figure 282: For the visa images, the false match calibration curves show FMR vs. threshold, T . The blue (lower) curves are for zero-effort impostors (i.e. comparing all images against all). The red (upper) curves are for persons of the same-sex, same-age, and same national-origin. This shows that FMR is underestimated (by a factor of 10 or more) by using a zero-effort impostor calculation to calibrate T . As shown later (sec. 3.6), FMR is higher for demographic-matched impostors.

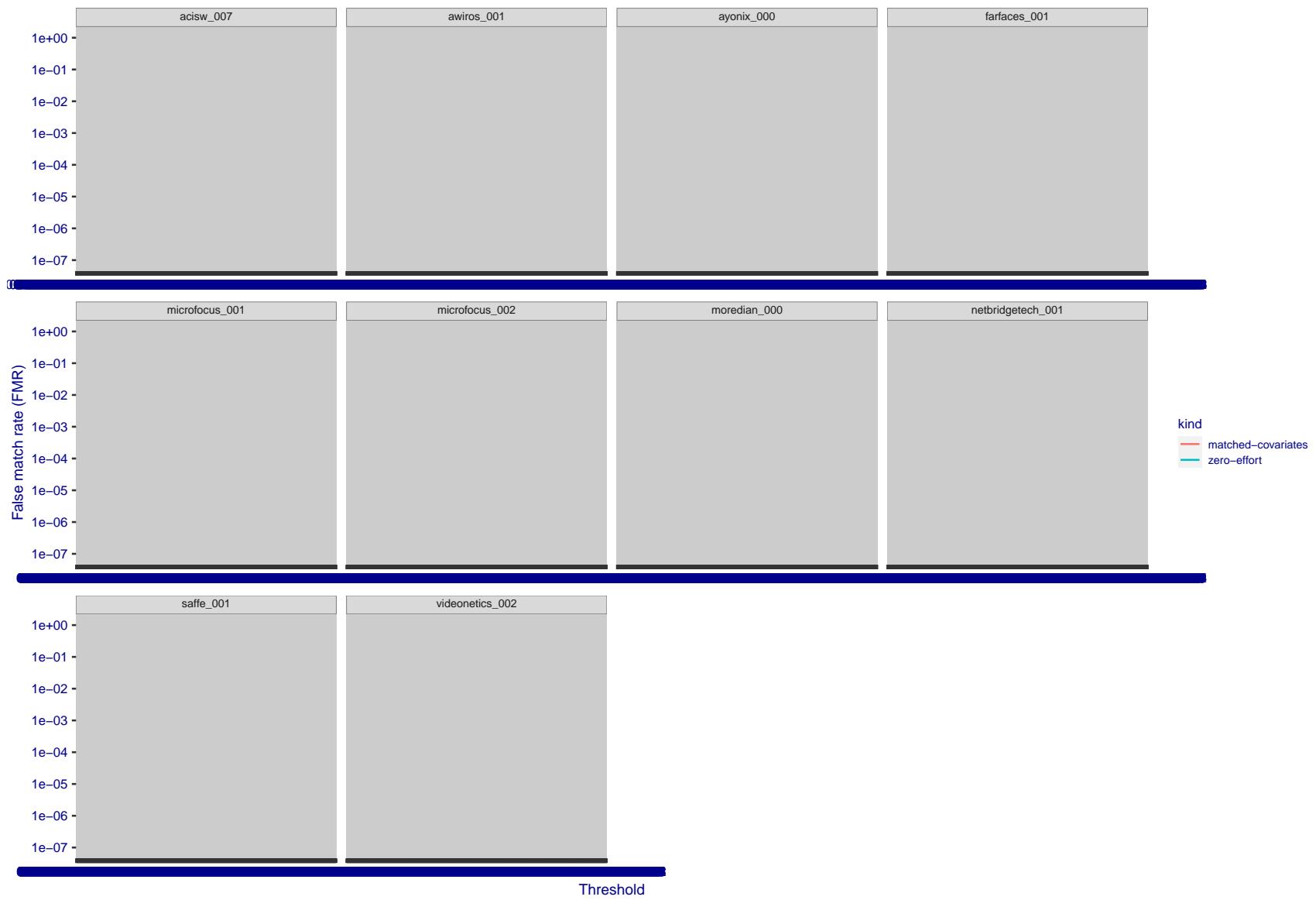


Figure 283: For the visa images, the false match calibration curves show FMR vs. threshold, T . The blue (lower) curves are for zero-effort impostors (i.e. comparing all images against all). The red (upper) curves are for persons of the same-sex, same-age, and same national-origin. This shows that FMR is underestimated (by a factor of 10 or more) by using a zero-effort impostor calculation to calibrate T . As shown later (sec. 3.6), FMR is higher for demographic-matched impostors.

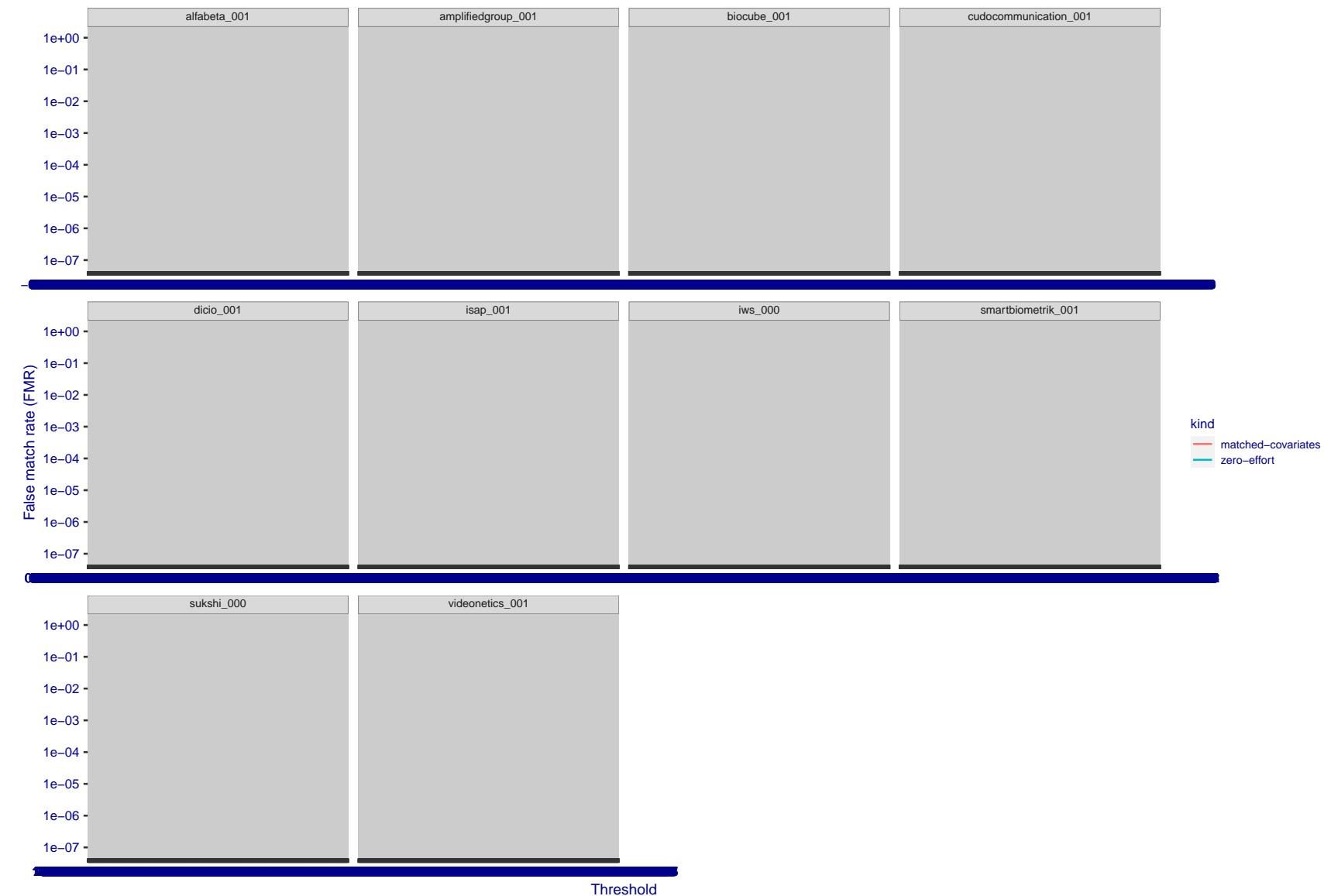


Figure 284: For the visa images, the false match calibration curves show FMR vs. threshold, T . The blue (lower) curves are for zero-effort impostors (i.e. comparing all images against all). The red (upper) curves are for persons of the same-sex, same-age, and same national-origin. This shows that FMR is underestimated (by a factor of 10 or more) by using a zero-effort impostor calculation to calibrate T . As shown later (sec. 3.6), FMR is higher for demographic-matched impostors.

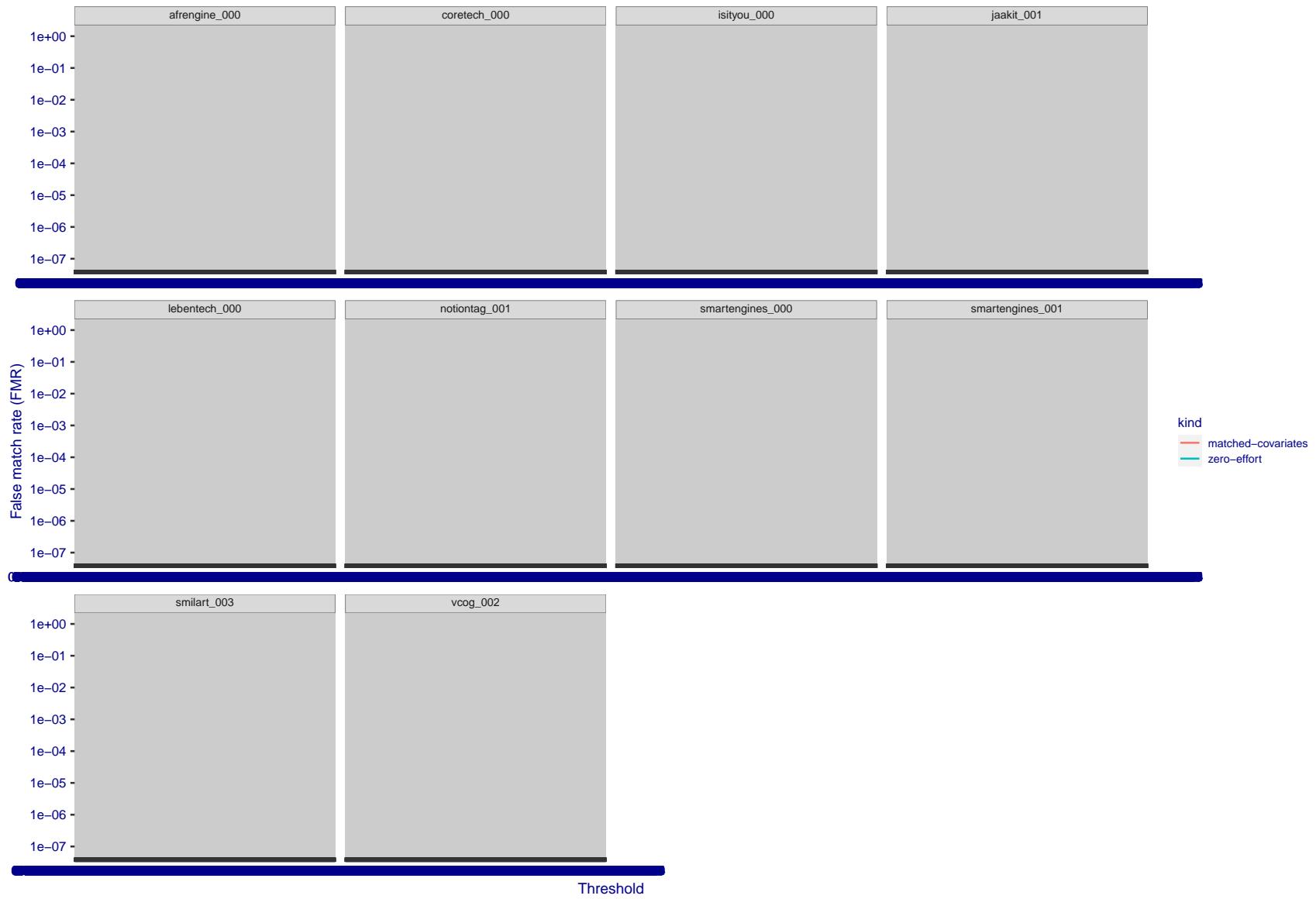


Figure 285: For the visa images, the false match calibration curves show FMR vs. threshold, T . The blue (lower) curves are for zero-effort impostors (i.e. comparing all images against all). The red (upper) curves are for persons of the same-sex, same-age, and same national-origin. This shows that FMR is underestimated (by a factor of 10 or more) by using a zero-effort impostor calculation to calibrate T . As shown later (sec. 3.6), FMR is higher for demographic-matched impostors.

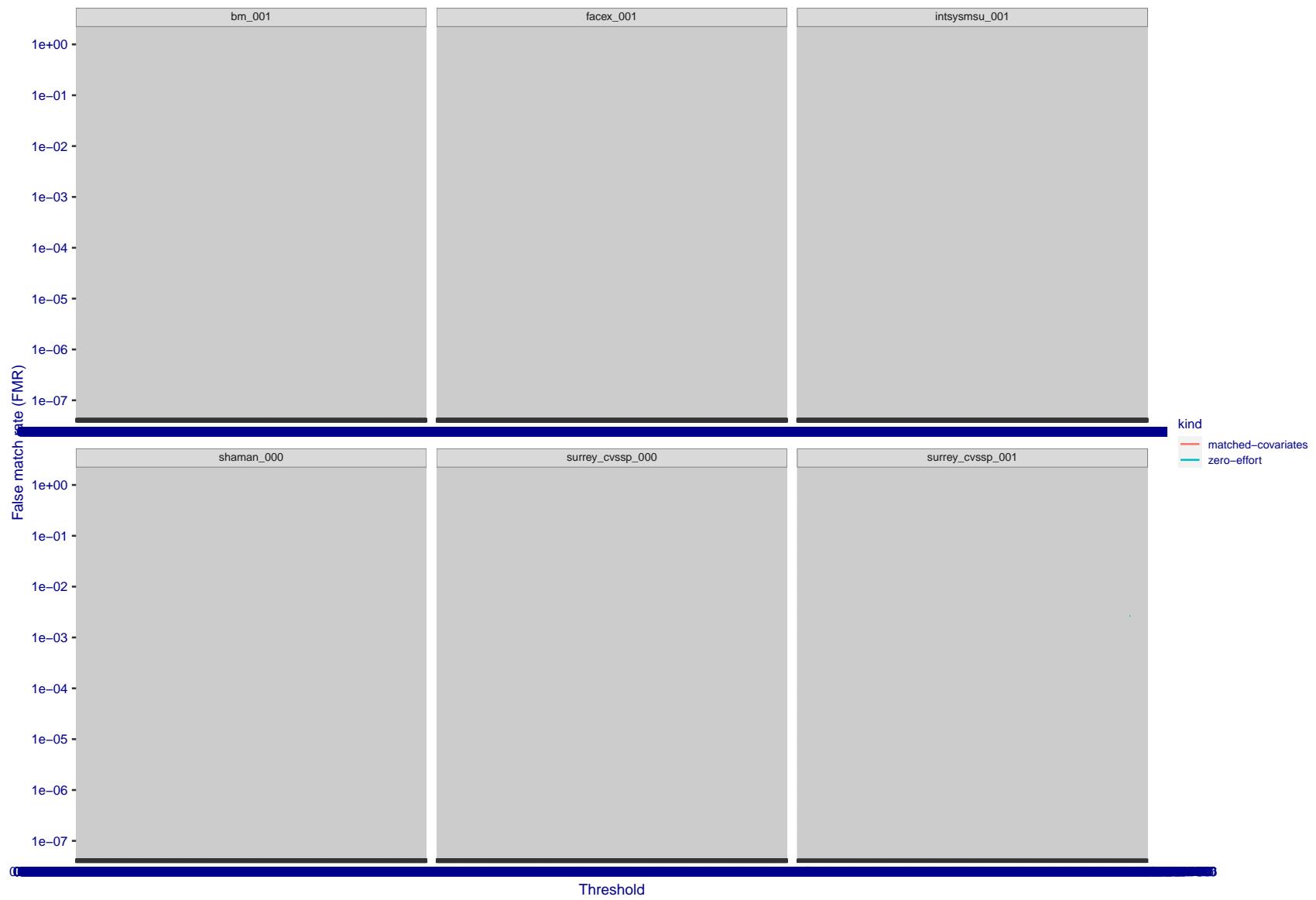


Figure 286: For the visa images, the false match calibration curves show FMR vs. threshold, T . The blue (lower) curves are for zero-effort impostors (i.e. comparing all images against all). The red (upper) curves are for persons of the same-sex, same-age, and same national-origin. This shows that FMR is underestimated (by a factor of 10 or more) by using a zero-effort impostor calculation to calibrate T . As shown later (sec. 3.6), FMR is higher for demographic-matched impostors.



Figure 287: For the visa images, the false match calibration curves show FMR vs. threshold, T . The blue (lower) curves are for zero-effort impostors (i.e. comparing all images against all). The red (upper) curves are for persons of the same-sex, same-age, and same national-origin. This shows that FMR is underestimated (by a factor of 10 or more) by using a zero-effort impostor calculation to calibrate T . As shown later (sec. 3.6), FMR is higher for demographic-matched impostors.

3.5 Genuine distribution stability

3.5.1 Effect of birth place on the genuine distribution

Background: Both skin tone and bone structure vary geographically. Prior studies have reported variations in FNMR and FMR.

Goal: To measure false non-match rate (FNMR) variation with country of birth.

Methods: Thresholds are determined that give $FMR = \{0.001, 0.0001\}$ over the entire impostor set. Then FNMR is measured over 1000 bootstrap replications of the genuine scores. Only those countries with at least 140 individuals are included in the analysis.

Results: Figure 326 shows FNMR by country of birth for the two thresholds.

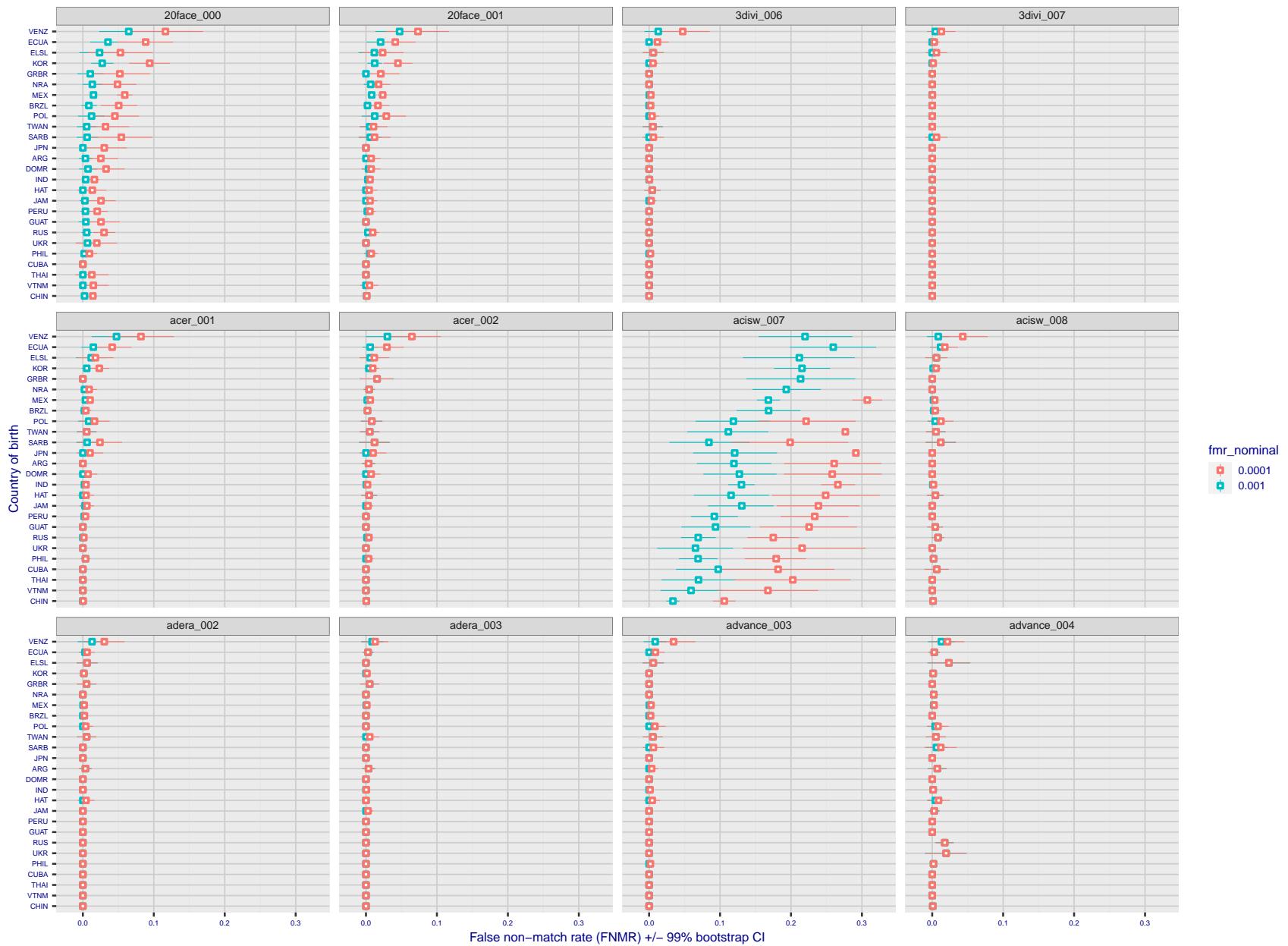


Figure 288: For the visa images, the dots show FNMR by country of birth for two globally set operating thresholds corresponding to $FMR = \{0.001, 0.0001\}$ computed over all on the order of 10^{10} impostor scores. The FMR in each bin will vary also - see subsequent impostor heatmaps in sec. 3.6.1. The figures shows an order of magnitude variation in FNMR across country of birth; these effects are likely due quality variations, then demographics like age and race. The error rates in some cases are zero, and in others the DET is flat so the error rates at the two thresholds are identical. The lines span 1% and 99% of bootstrap replicated FNMR estimates.

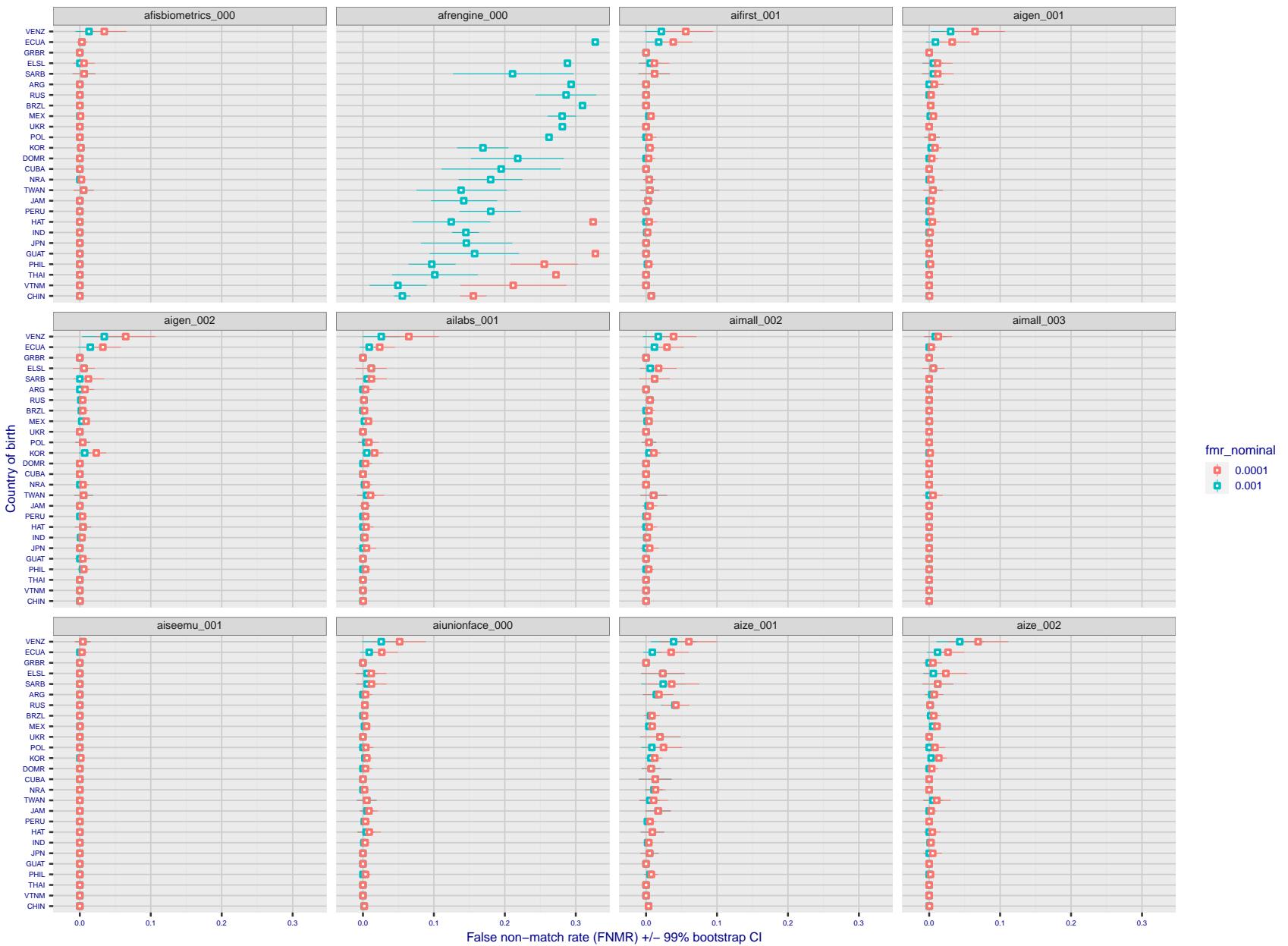


Figure 289: For the visa images, the dots show FNMR by country of birth for two globally set operating thresholds corresponding to $FMR = \{0.001, 0.0001\}$ computed over all on the order of 10^{10} impostor scores. The FMR in each bin will vary also - see subsequent impostor heatmaps in sec. 3.6.1. The figures shows an order of magnitude variation in FNMR across country of birth; these effects are likely due quality variations, then demographics like age and race. The error rates in some cases are zero, and in others the DET is flat so the error rates at the two thresholds are identical. The lines span 1% and 99% of bootstrap replicated FNMR estimates.

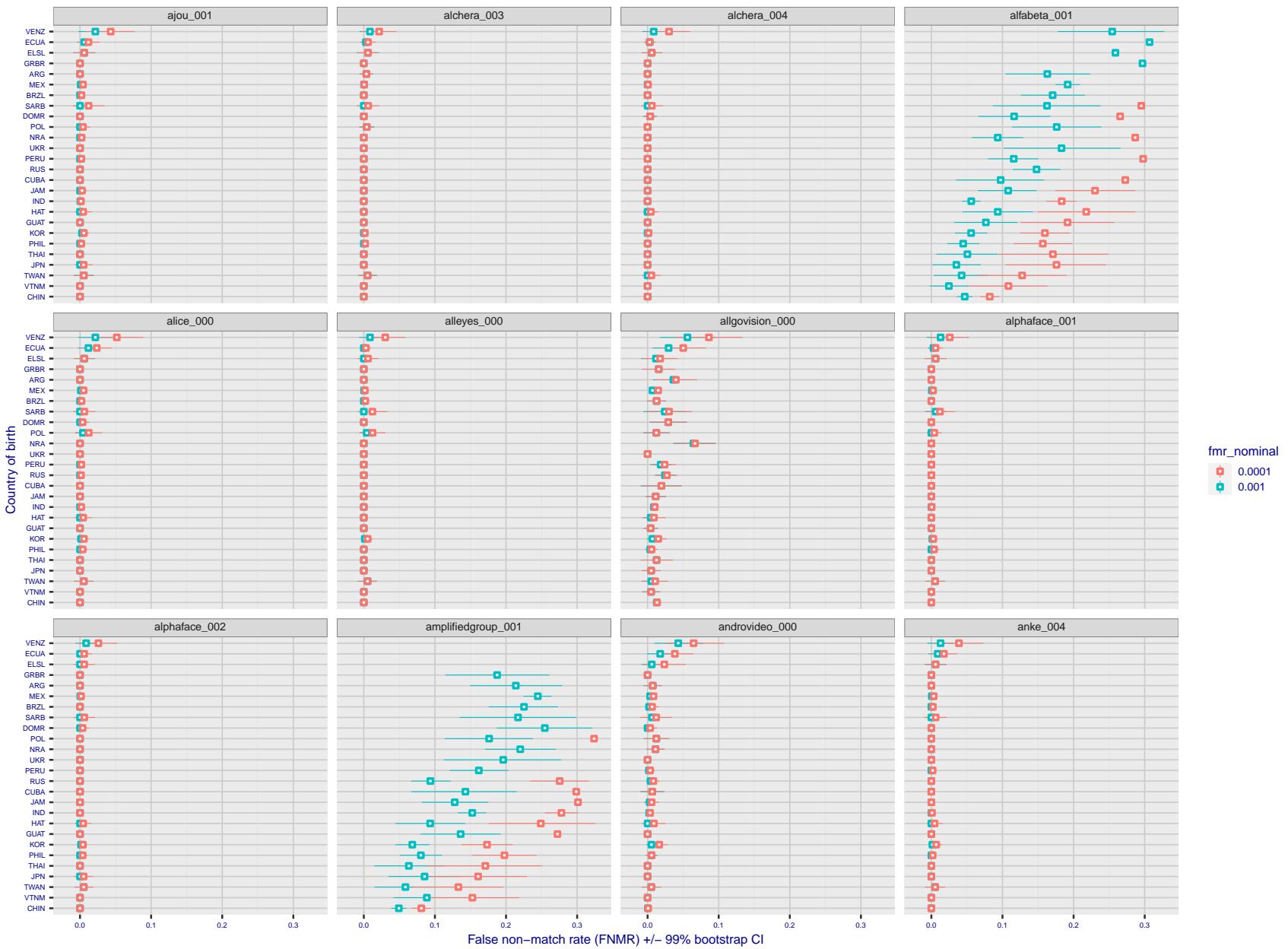


Figure 290: For the visa images, the dots show FNMR by country of birth for two globally set operating thresholds corresponding to $FMR = \{0.001, 0.0001\}$ computed over all on the order of 10^{10} impostor scores. The FMR in each bin will vary also - see subsequent impostor heatmaps in sec. 3.6.1. The figures shows an order of magnitude variation in FNMR across country of birth; these effects are likely due quality variations, then demographics like age and race. The error rates in some cases are zero, and in others the DET is flat so the error rates at the two thresholds are identical. The lines span 1% and 99% of bootstrap replicated FNMR estimates.

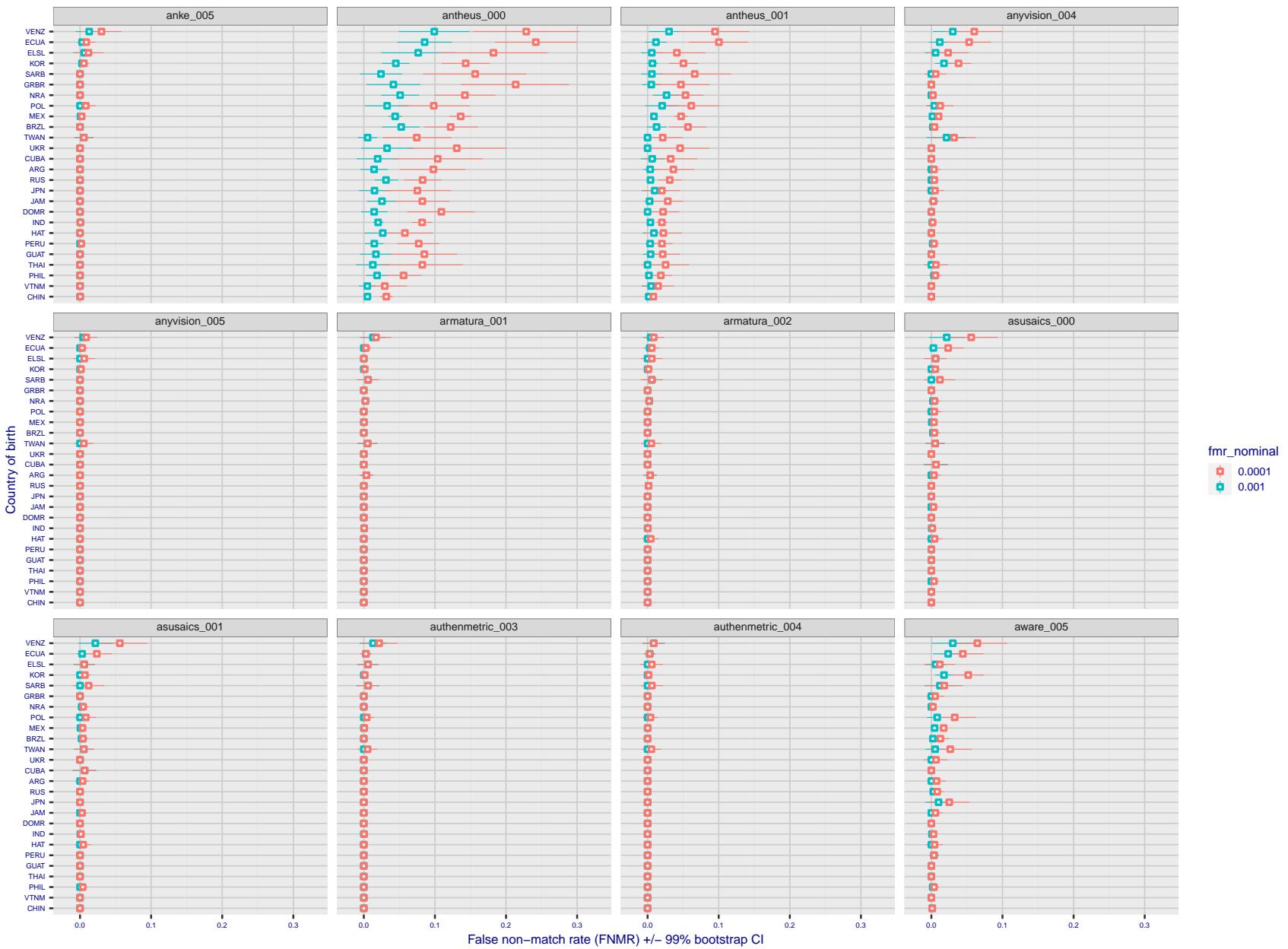


Figure 291: For the visa images, the dots show FNMR by country of birth for two globally set operating thresholds corresponding to $FMR = \{0.001, 0.0001\}$ computed over all on the order of 10^{10} impostor scores. The FMR in each bin will vary also - see subsequent impostor heatmaps in sec. 3.6.1. The figures shows an order of magnitude variation in FNMR across country of birth; these effects are likely due quality variations, then demographics like age and race. The error rates in some cases are zero, and in others the DET is flat so the error rates at the two thresholds are identical. The lines span 1% and 99% of bootstrap replicated FNMR estimates.

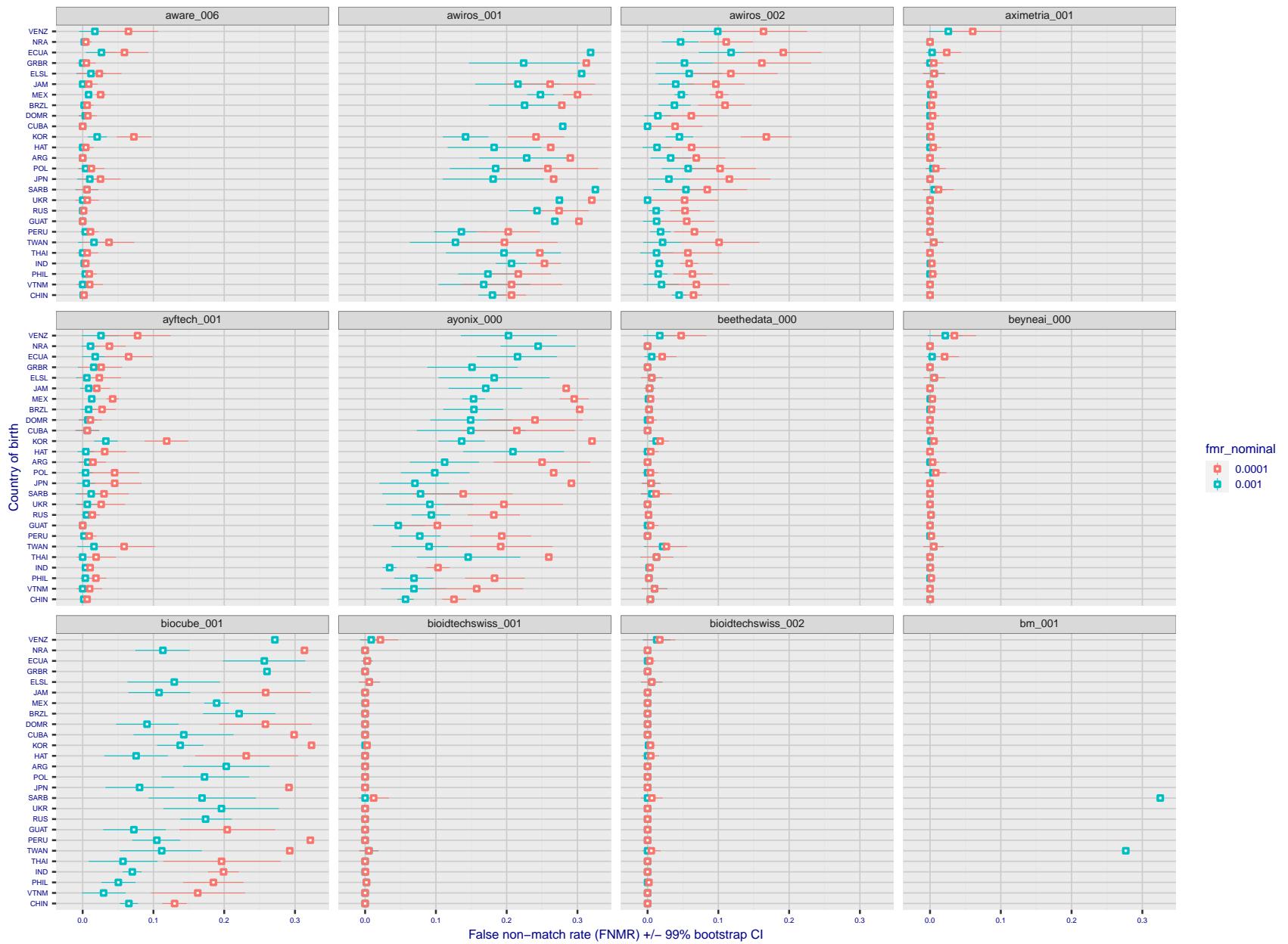


Figure 292: For the visa images, the dots show FNMR by country of birth for two globally set operating thresholds corresponding to $FMR = \{0.001, 0.0001\}$ computed over all on the order of 10^{10} impostor scores. The FMR in each bin will vary also - see subsequent impostor heatmaps in sec. 3.6.1. The figures shows an order of magnitude variation in FNMR across country of birth; these effects are likely due quality variations, then demographics like age and race. The error rates in some cases are zero, and in others the DET is flat so the error rates at the two thresholds are identical. The lines span 1% and 99% of bootstrap replicated FNMR estimates.

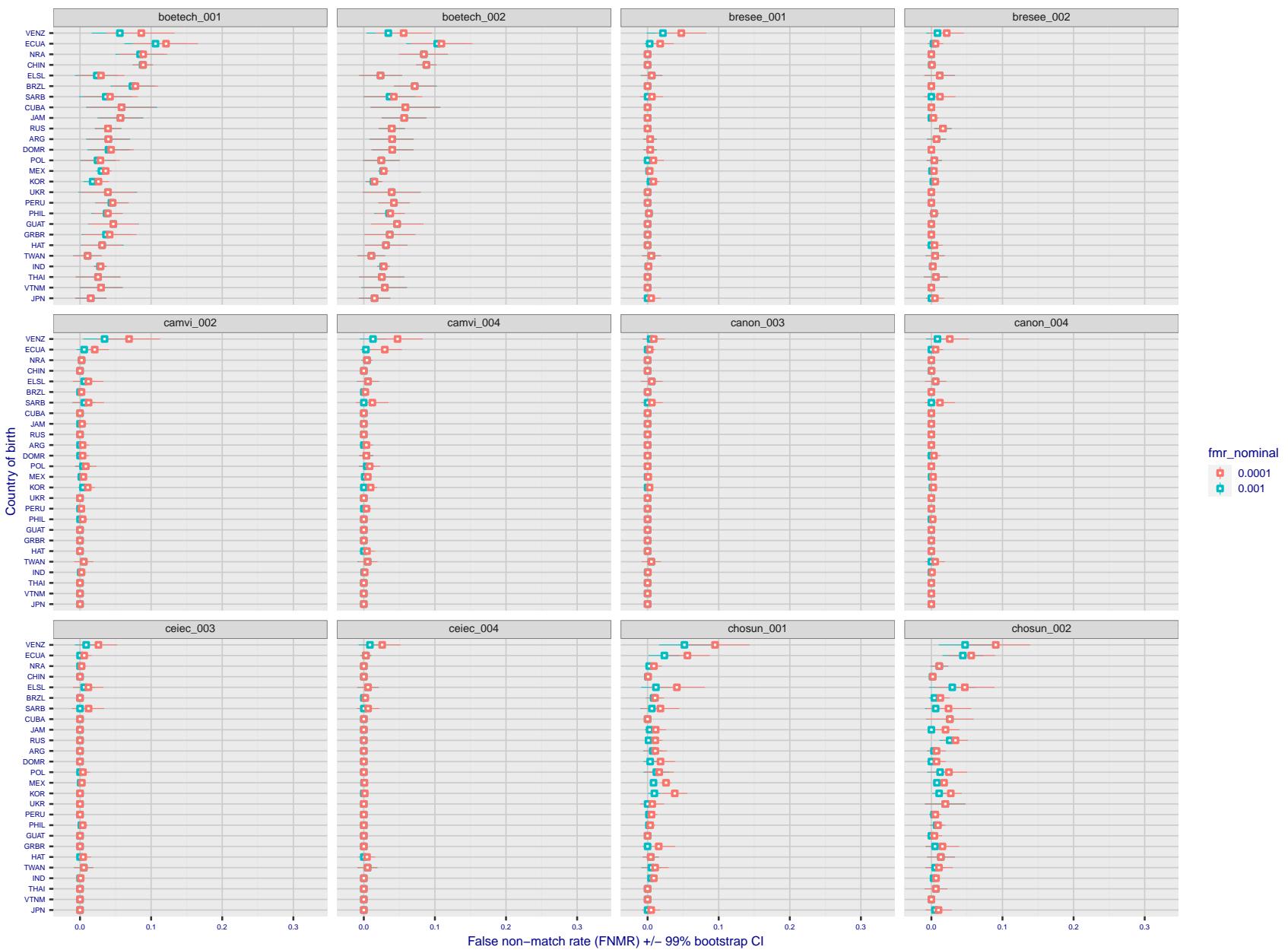


Figure 293: For the visa images, the dots show FNMR by country of birth for two globally set operating thresholds corresponding to $FMR = \{0.001, 0.0001\}$ computed over all on the order of 10^{10} impostor scores. The FMR in each bin will vary also - see subsequent impostor heatmaps in sec. 3.6.1. The figures shows an order of magnitude variation in FNMR across country of birth; these effects are likely due quality variations, then demographics like age and race. The error rates in some cases are zero, and in others the DET is flat so the error rates at the two thresholds are identical. The lines span 1% and 99% of bootstrap replicated FNMR estimates.

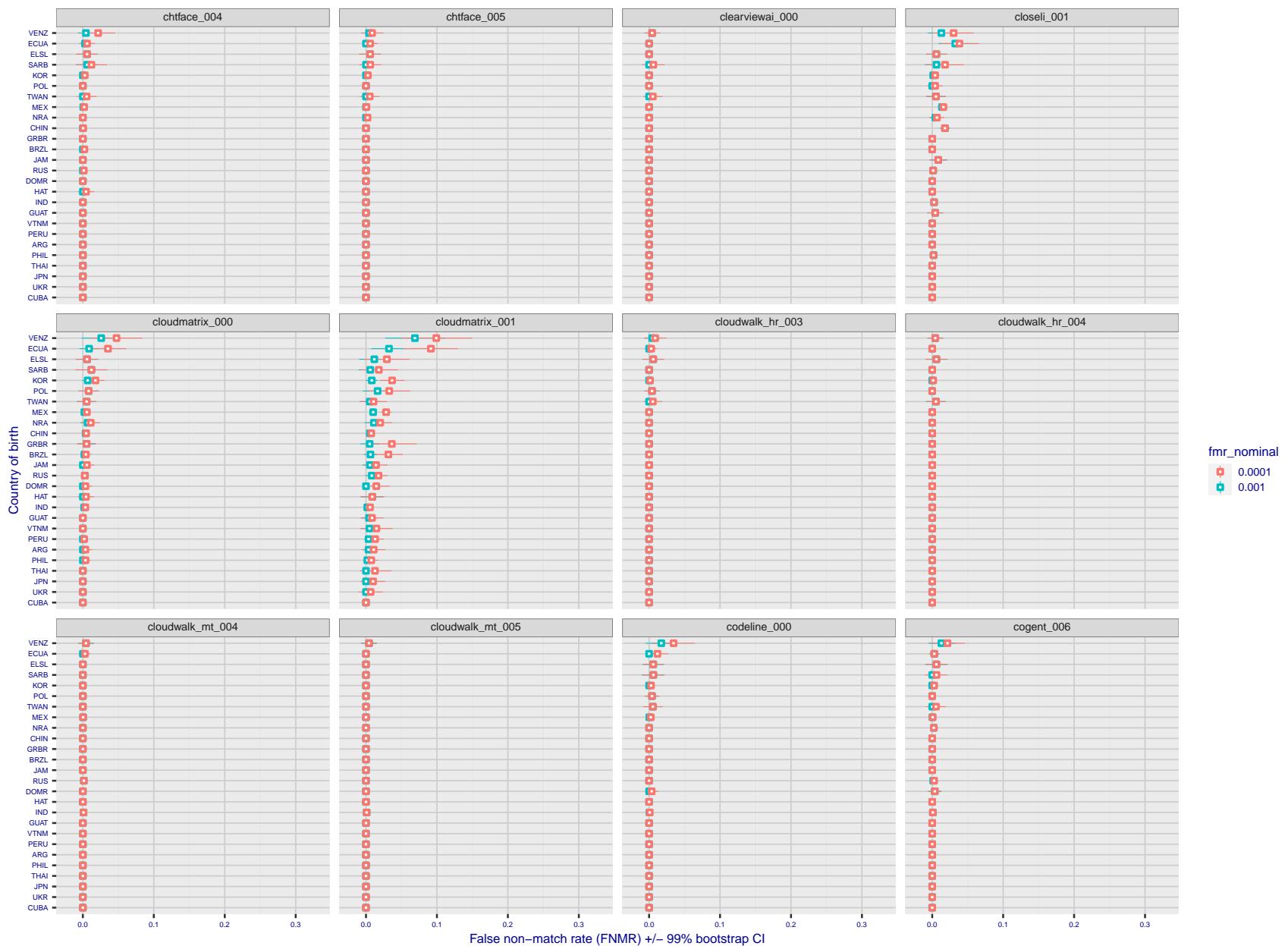


Figure 294: For the visa images, the dots show FNMR by country of birth for two globally set operating thresholds corresponding to $FMR = \{0.001, 0.0001\}$ computed over all on the order of 10^{10} impostor scores. The FMR in each bin will vary also - see subsequent impostor heatmaps in sec. 3.6.1. The figures shows an order of magnitude variation in FNMR across country of birth; these effects are likely due quality variations, then demographics like age and race. The error rates in some cases are zero, and in others the DET is flat so the error rates at the two thresholds are identical. The lines span 1% and 99% of bootstrap replicated FNMR estimates.

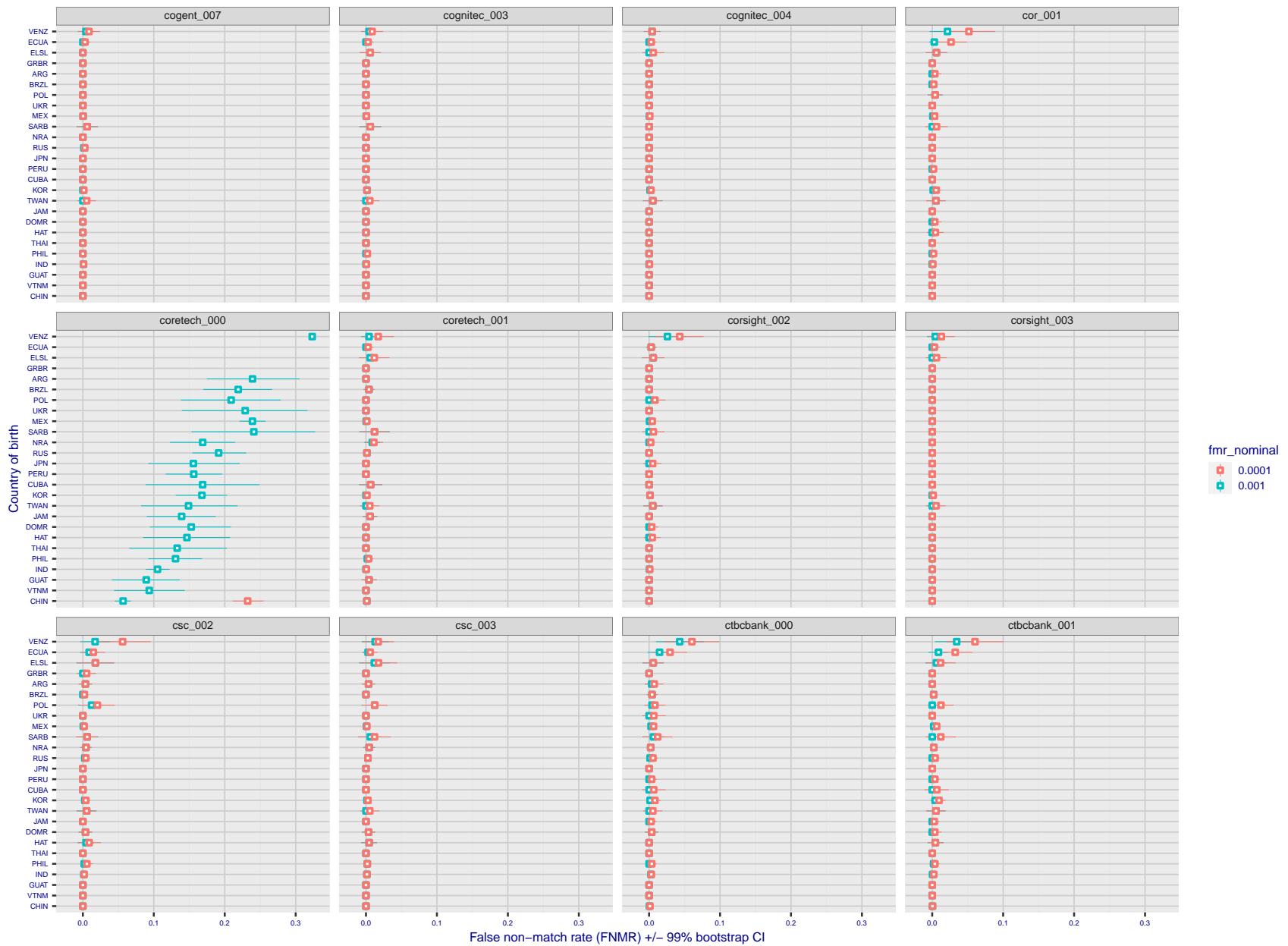


Figure 295: For the visa images, the dots show FNMR by country of birth for two globally set operating thresholds corresponding to $FMR = \{0.001, 0.0001\}$ computed over all on the order of 10^{10} impostor scores. The FMR in each bin will vary also - see subsequent impostor heatmaps in sec. 3.6.1. The figures shows an order of magnitude variation in FNMR across country of birth; these effects are likely due quality variations, then demographics like age and race. The error rates in some cases are zero, and in others the DET is flat so the error rates at the two thresholds are identical. The lines span 1% and 99% of bootstrap replicated FNMR estimates.

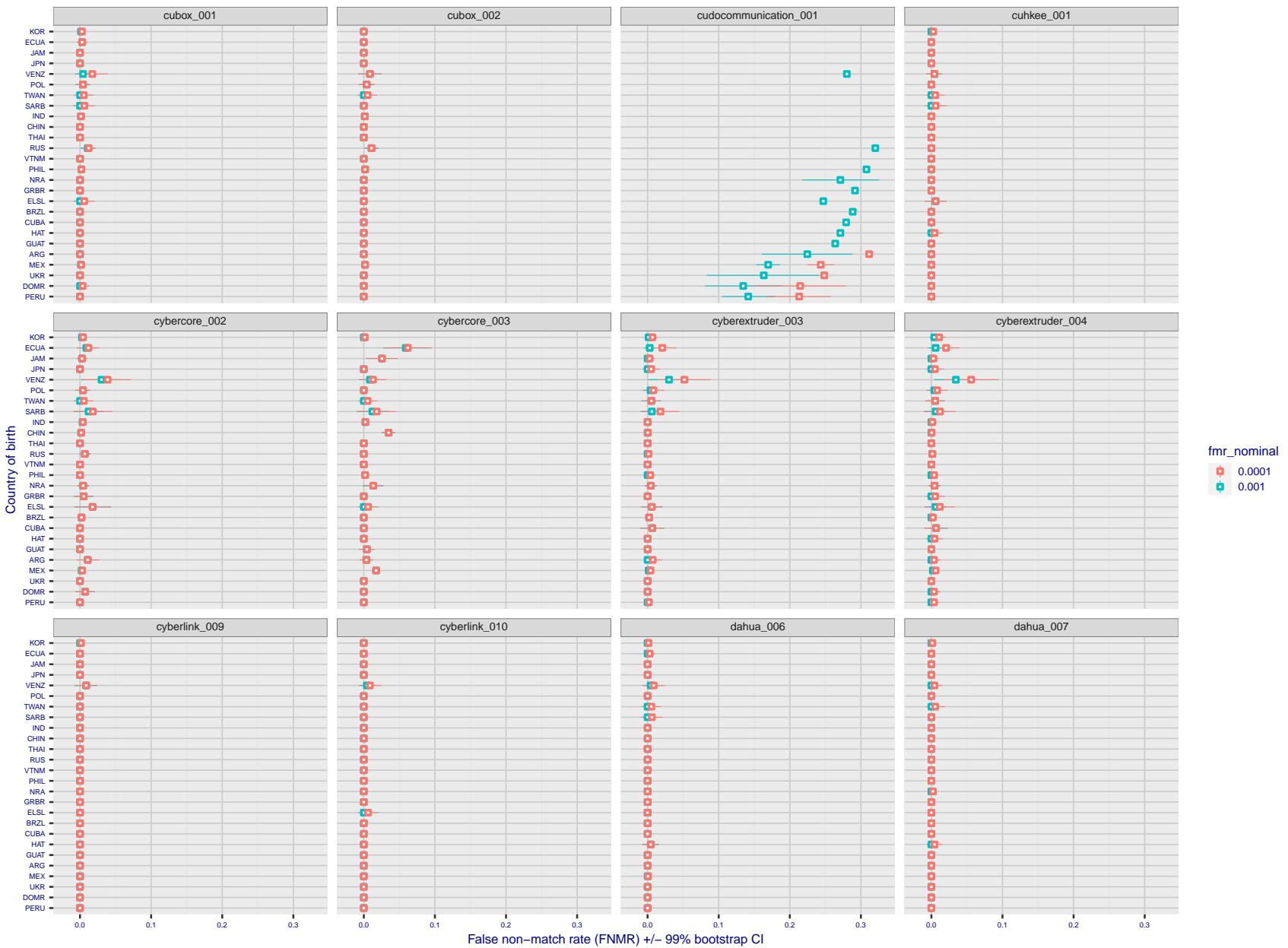


Figure 296: For the visa images, the dots show FNMR by country of birth for two globally set operating thresholds corresponding to $FMR = \{0.001, 0.0001\}$ computed over all on the order of 10^{10} impostor scores. The FMR in each bin will vary also - see subsequent impostor heatmaps in sec. 3.6.1. The figures shows an order of magnitude variation in FNMR across country of birth; these effects are likely due quality variations, then demographics like age and race. The error rates in some cases are zero, and in others the DET is flat so the error rates at the two thresholds are identical. The lines span 1% and 99% of bootstrap replicated FNMR estimates.

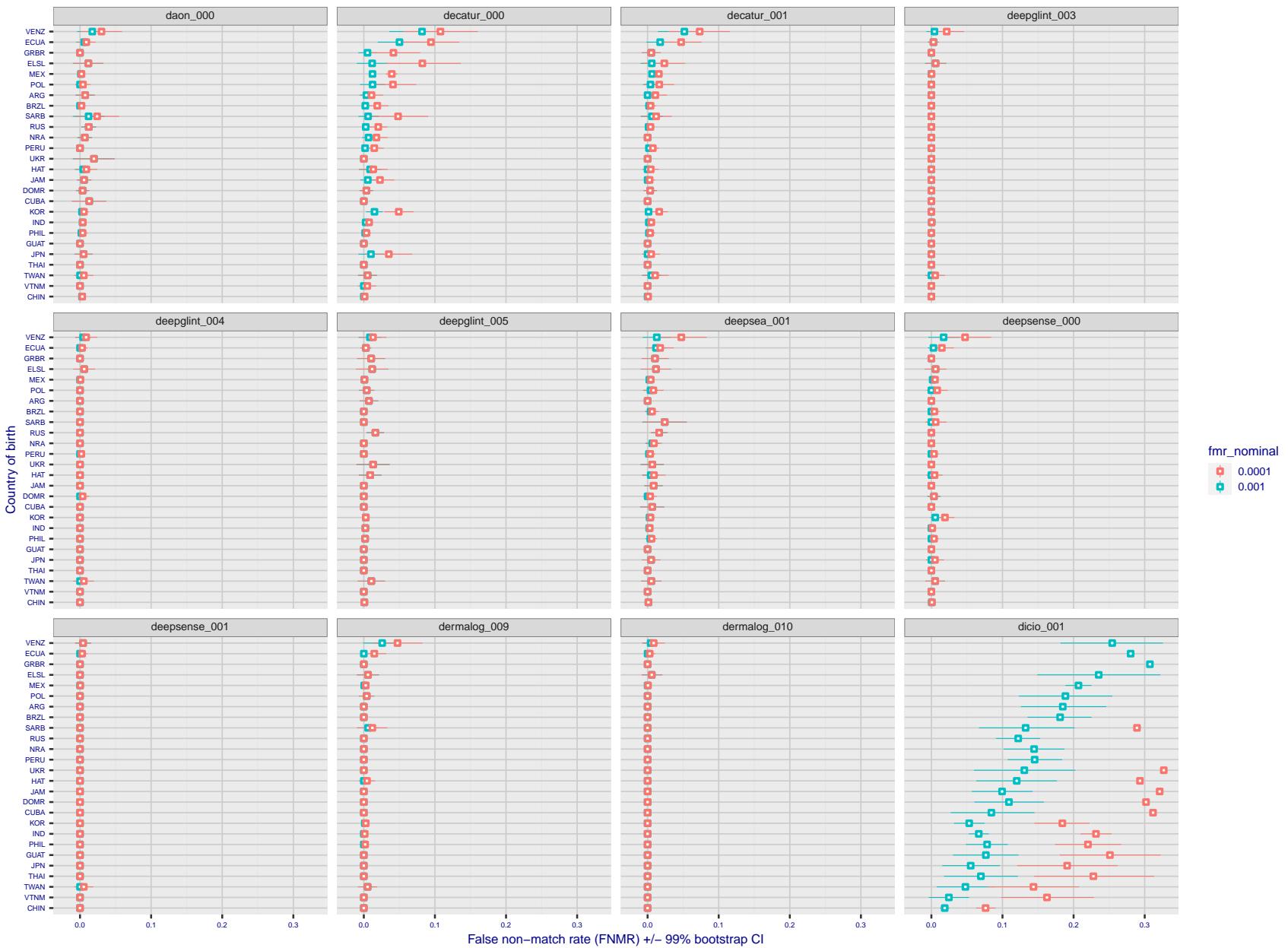


Figure 297: For the visa images, the dots show FNMR by country of birth for two globally set operating thresholds corresponding to $FMR = \{0.001, 0.0001\}$ computed over all on the order of 10^{10} impostor scores. The FMR in each bin will vary also - see subsequent impostor heatmaps in sec. 3.6.1. The figures shows an order of magnitude variation in FNMR across country of birth; these effects are likely due quality variations, then demographics like age and race. The error rates in some cases are zero, and in others the DET is flat so the error rates at the two thresholds are identical. The lines span 1% and 99% of bootstrap replicated FNMR estimates.

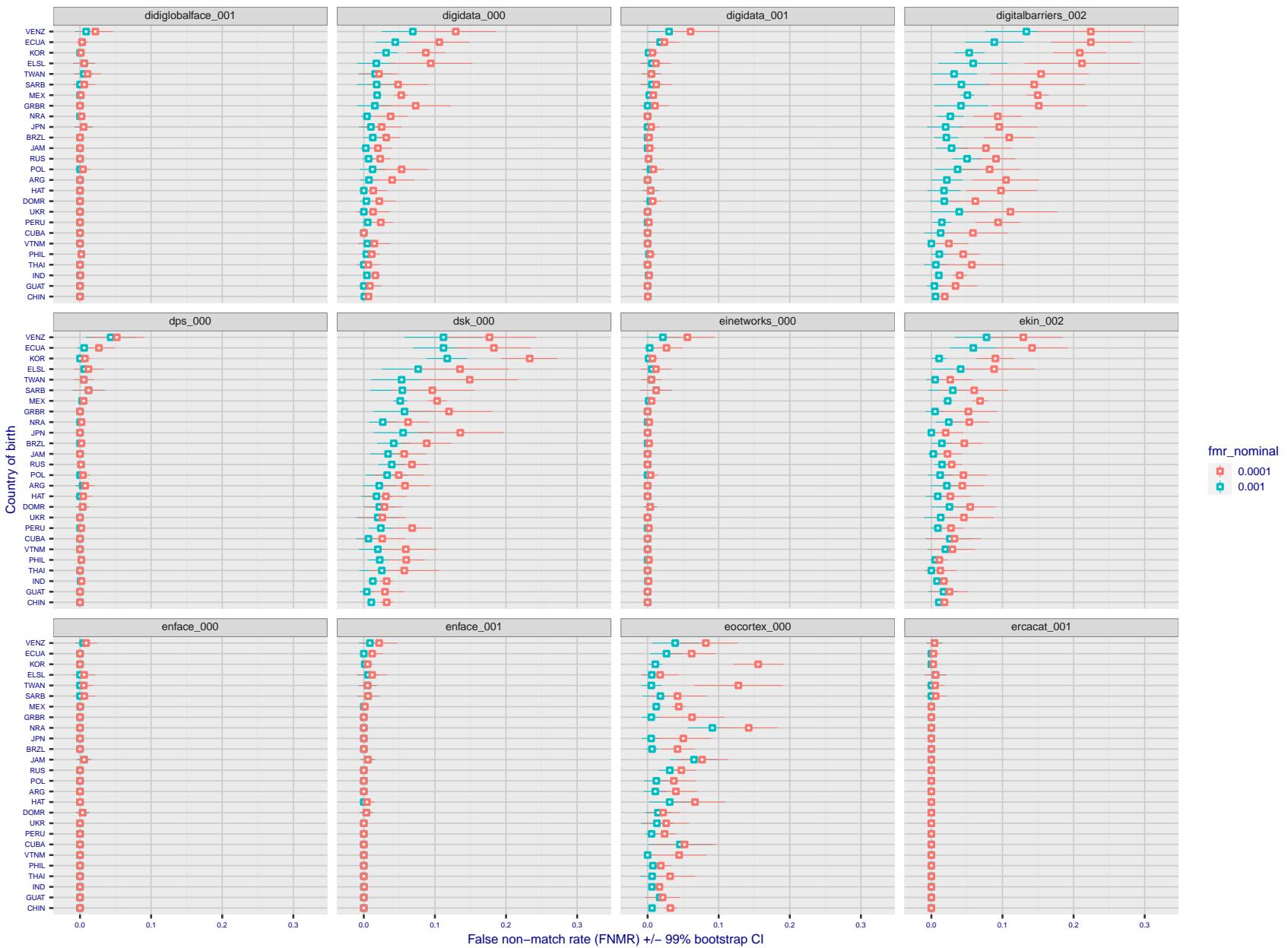


Figure 298: For the visa images, the dots show FNMR by country of birth for two globally set operating thresholds corresponding to $FMR = \{0.001, 0.0001\}$ computed over all on the order of 10^{10} impostor scores. The FMR in each bin will vary also - see subsequent impostor heatmaps in sec. 3.6.1. The figures shows an order of magnitude variation in FNMR across country of birth; these effects are likely due quality variations, then demographics like age and race. The error rates in some cases are zero, and in others the DET is flat so the error rates at the two thresholds are identical. The lines span 1% and 99% of bootstrap replicated FNMR estimates.

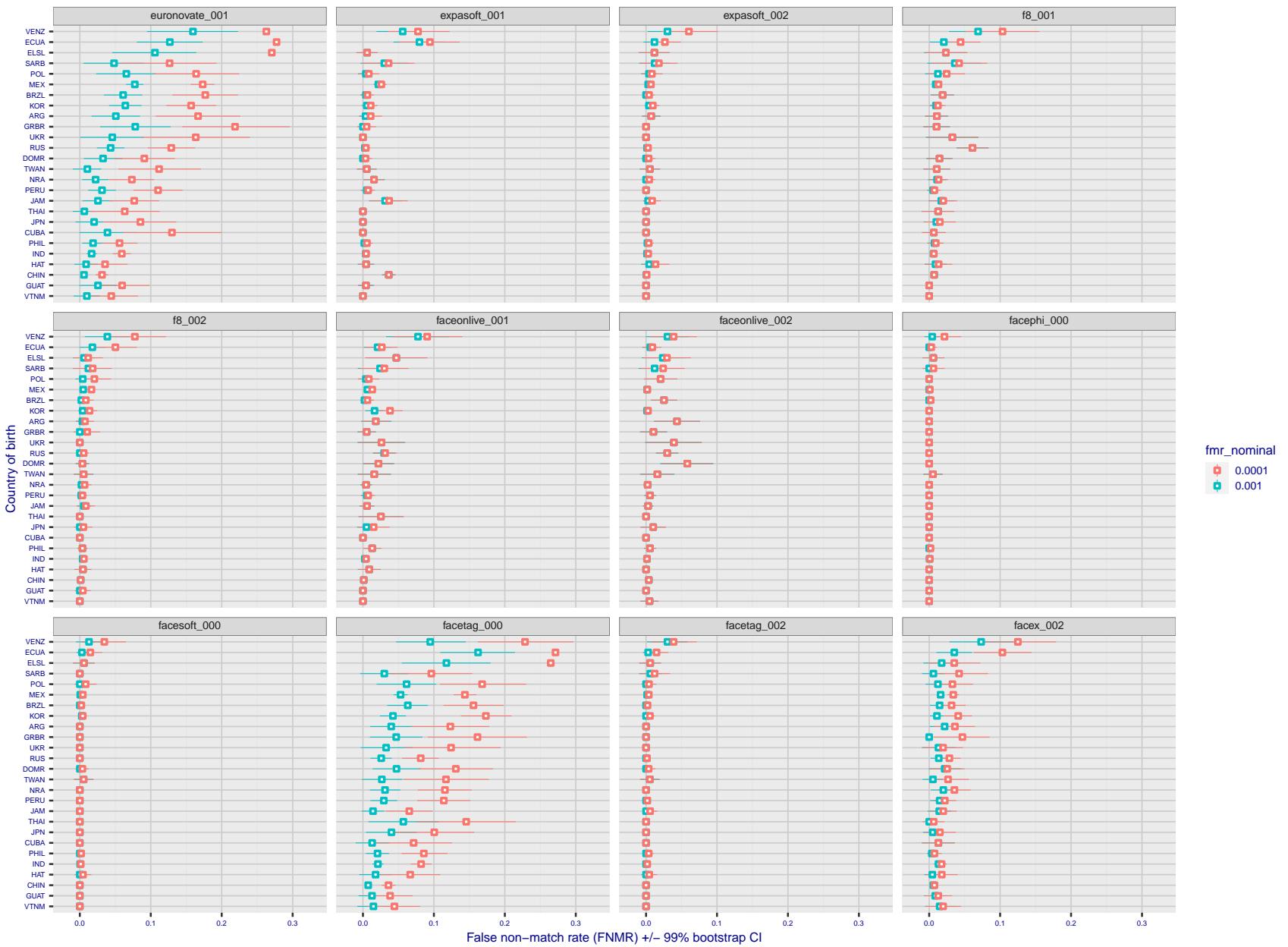


Figure 299: For the visa images, the dots show FNMR by country of birth for two globally set operating thresholds corresponding to $FMR = \{0.001, 0.0001\}$ computed over all on the order of 10^{10} impostor scores. The FMR in each bin will vary also - see subsequent impostor heatmaps in sec. 3.6.1. The figures shows an order of magnitude variation in FNMR across country of birth; these effects are likely due quality variations, then demographics like age and race. The error rates in some cases are zero, and in others the DET is flat so the error rates at the two thresholds are identical. The lines span 1% and 99% of bootstrap replicated FNMR estimates.

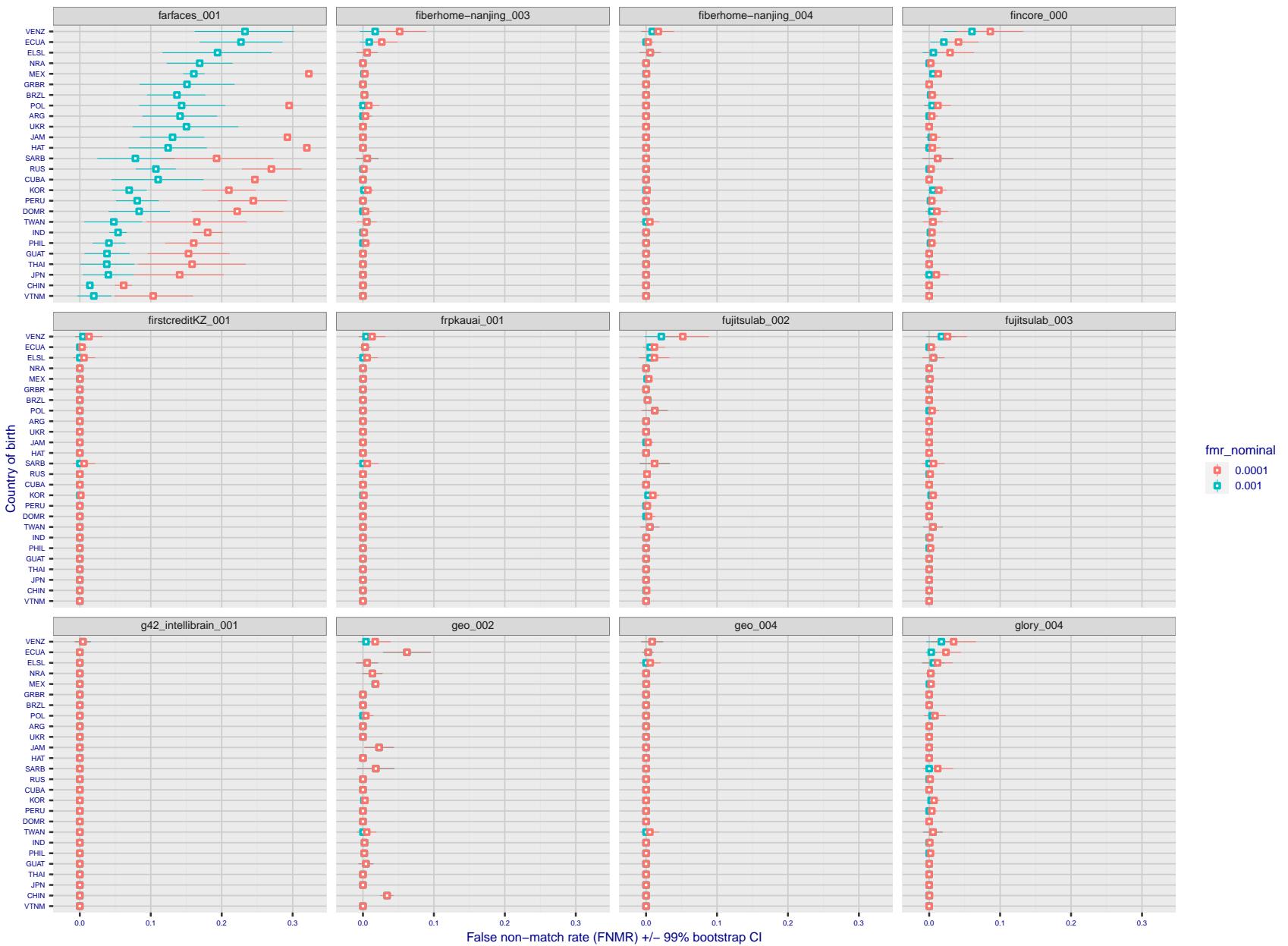


Figure 300: For the visa images, the dots show FNMR by country of birth for two globally set operating thresholds corresponding to $FMR = \{0.001, 0.0001\}$ computed over all on the order of 10^{10} impostor scores. The FMR in each bin will vary also - see subsequent impostor heatmaps in sec. 3.6.1. The figures shows an order of magnitude variation in FNMR across country of birth; these effects are likely due quality variations, then demographics like age and race. The error rates in some cases are zero, and in others the DET is flat so the error rates at the two thresholds are identical. The lines span 1% and 99% of bootstrap replicated FNMR estimates.

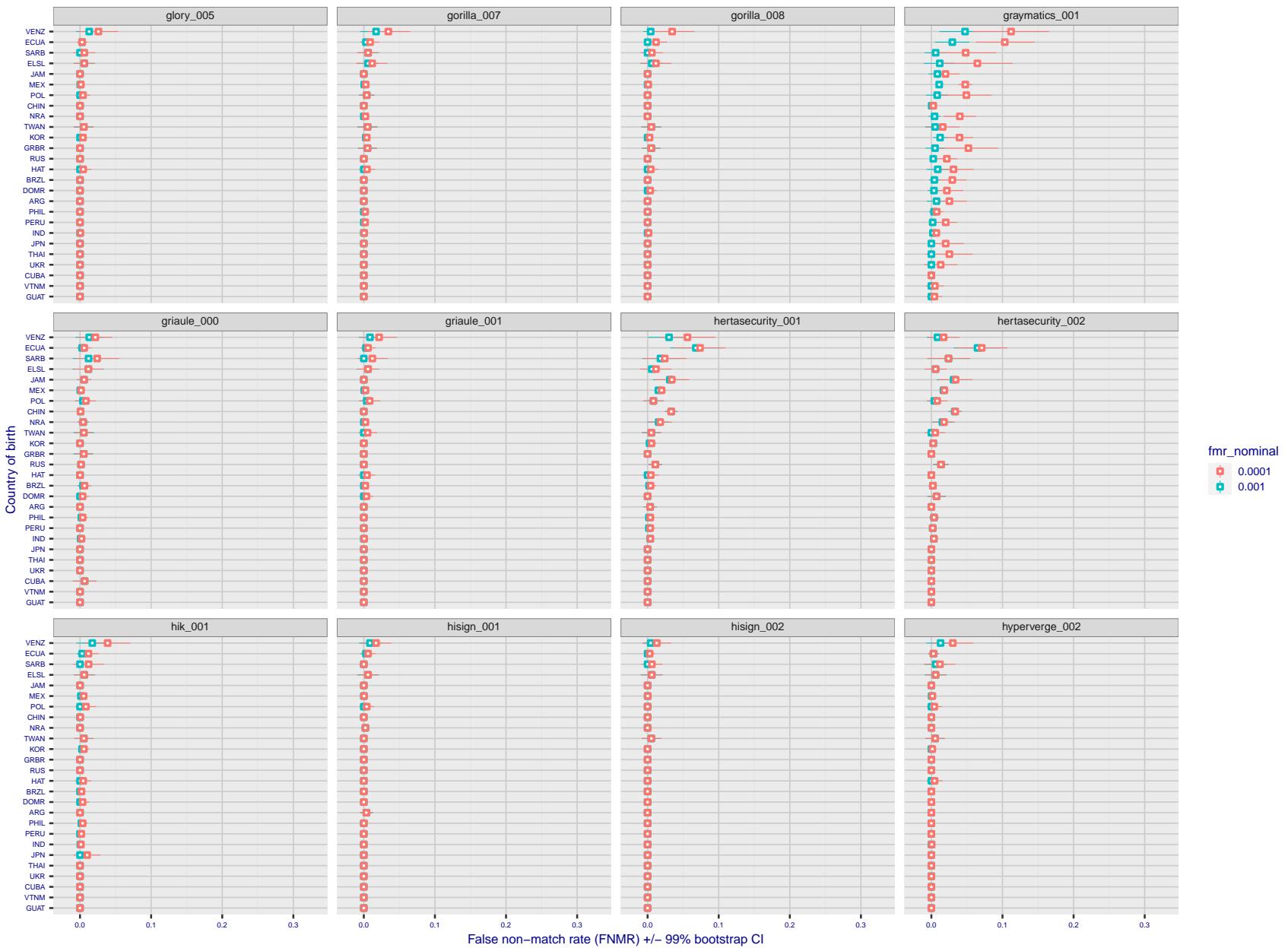


Figure 301: For the visa images, the dots show FNMR by country of birth for two globally set operating thresholds corresponding to $FMR = \{0.001, 0.0001\}$ computed over all on the order of 10^{10} impostor scores. The FMR in each bin will vary also - see subsequent impostor heatmaps in sec. 3.6.1. The figures shows an order of magnitude variation in FNMR across country of birth; these effects are likely due quality variations, then demographics like age and race. The error rates in some cases are zero, and in others the DET is flat so the error rates at the two thresholds are identical. The lines span 1% and 99% of bootstrap replicated FNMR estimates.

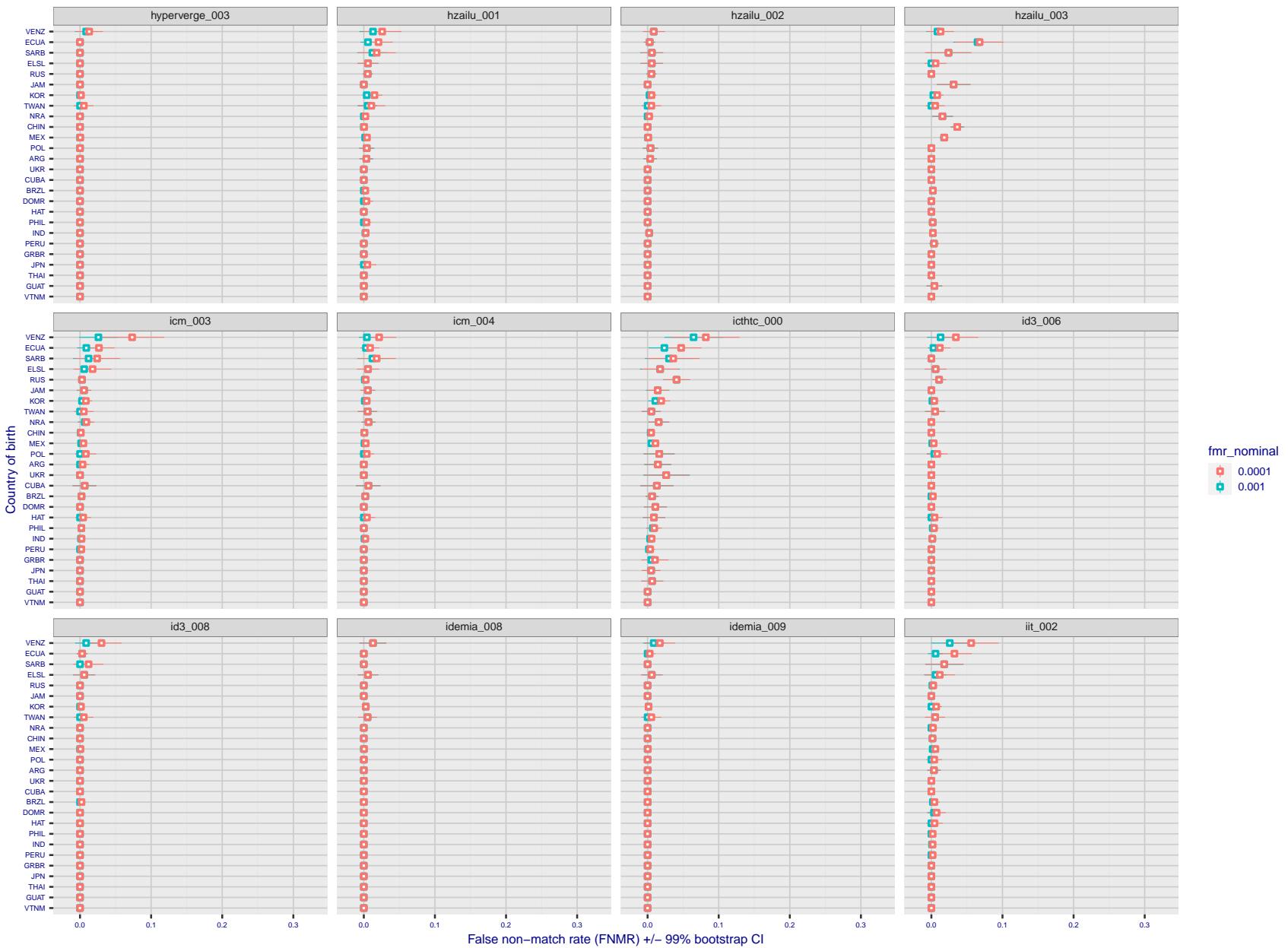


Figure 302: For the visa images, the dots show FNMR by country of birth for two globally set operating thresholds corresponding to $FMR = \{0.001, 0.0001\}$ computed over all on the order of 10^{10} impostor scores. The FMR in each bin will vary also - see subsequent impostor heatmaps in sec. 3.6.1. The figures shows an order of magnitude variation in FNMR across country of birth; these effects are likely due quality variations, then demographics like age and race. The error rates in some cases are zero, and in others the DET is flat so the error rates at the two thresholds are identical. The lines span 1% and 99% of bootstrap replicated FNMR estimates.

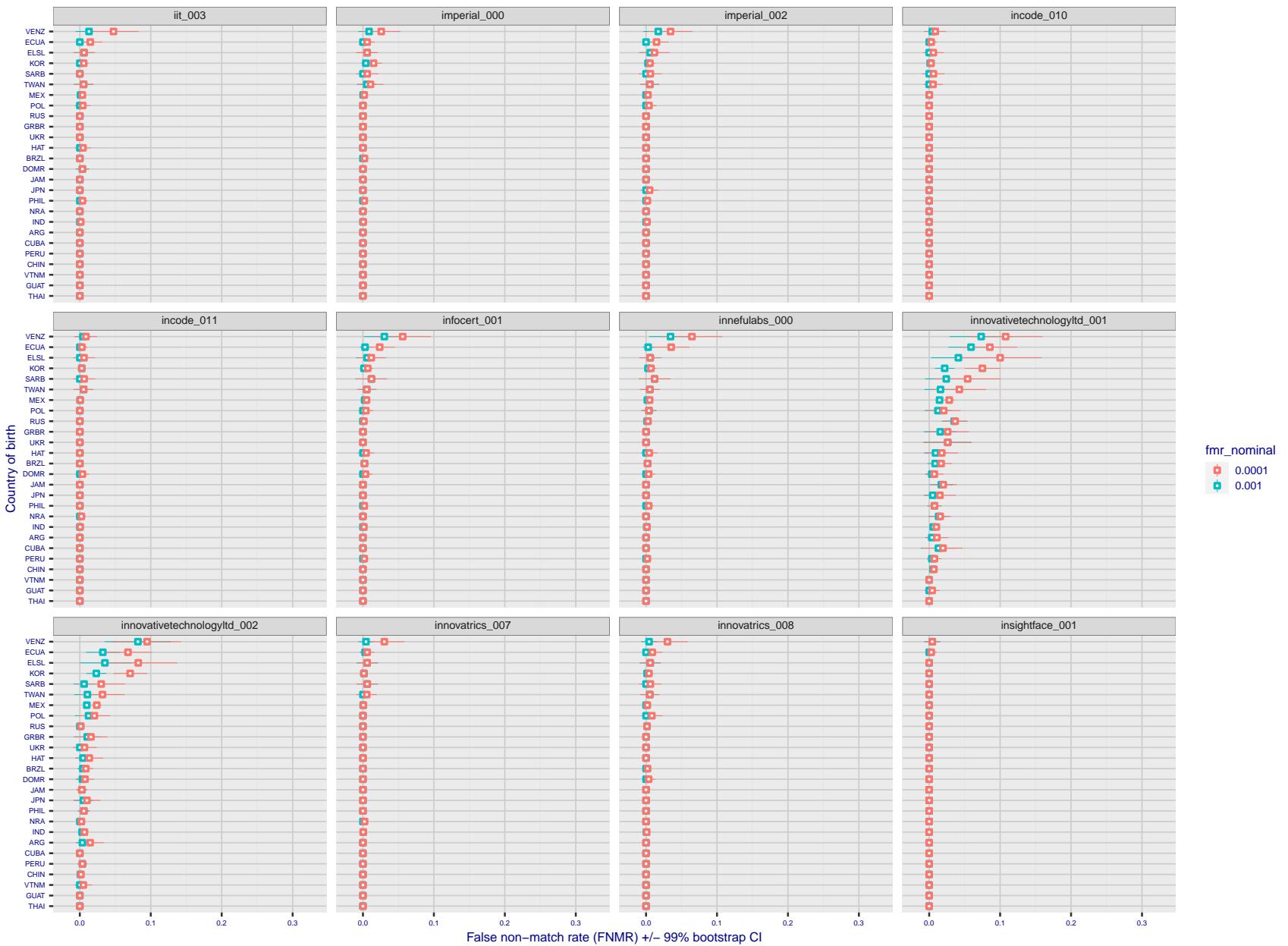


Figure 303: For the visa images, the dots show FNMR by country of birth for two globally set operating thresholds corresponding to $FMR = \{0.001, 0.0001\}$ computed over all on the order of 10^{10} impostor scores. The FMR in each bin will vary also - see subsequent impostor heatmaps in sec. 3.6.1. The figures shows an order of magnitude variation in FNMR across country of birth; these effects are likely due quality variations, then demographics like age and race. The error rates in some cases are zero, and in others the DET is flat so the error rates at the two thresholds are identical. The lines span 1% and 99% of bootstrap replicated FNMR estimates.

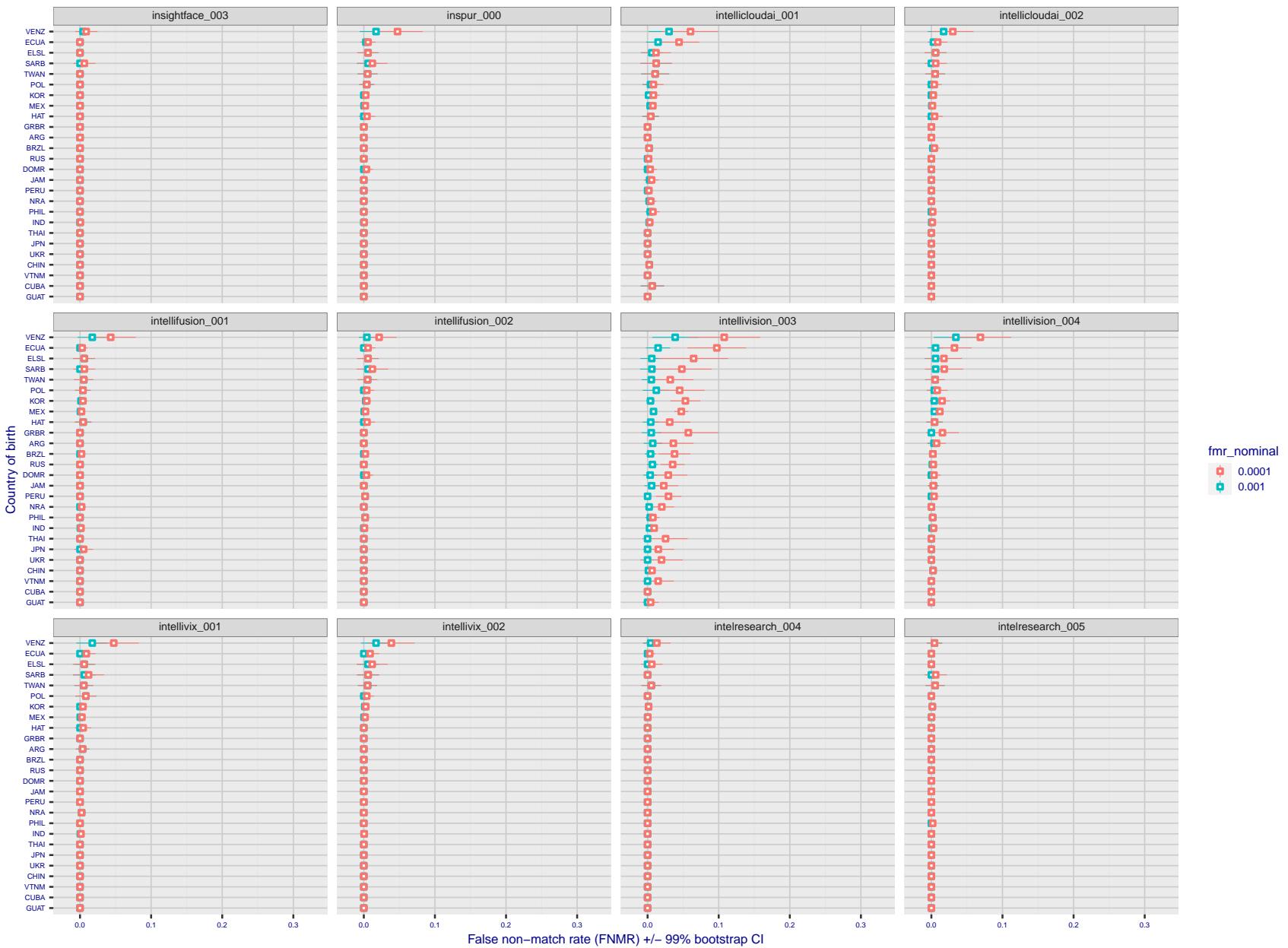


Figure 304: For the visa images, the dots show FNMR by country of birth for two globally set operating thresholds corresponding to $FMR = \{0.001, 0.0001\}$ computed over all on the order of 10^{10} impostor scores. The FMR in each bin will vary also - see subsequent impostor heatmaps in sec. 3.6.1. The figures shows an order of magnitude variation in FNMR across country of birth; these effects are likely due quality variations, then demographics like age and race. The error rates in some cases are zero, and in others the DET is flat so the error rates at the two thresholds are identical. The lines span 1% and 99% of bootstrap replicated FNMR estimates.

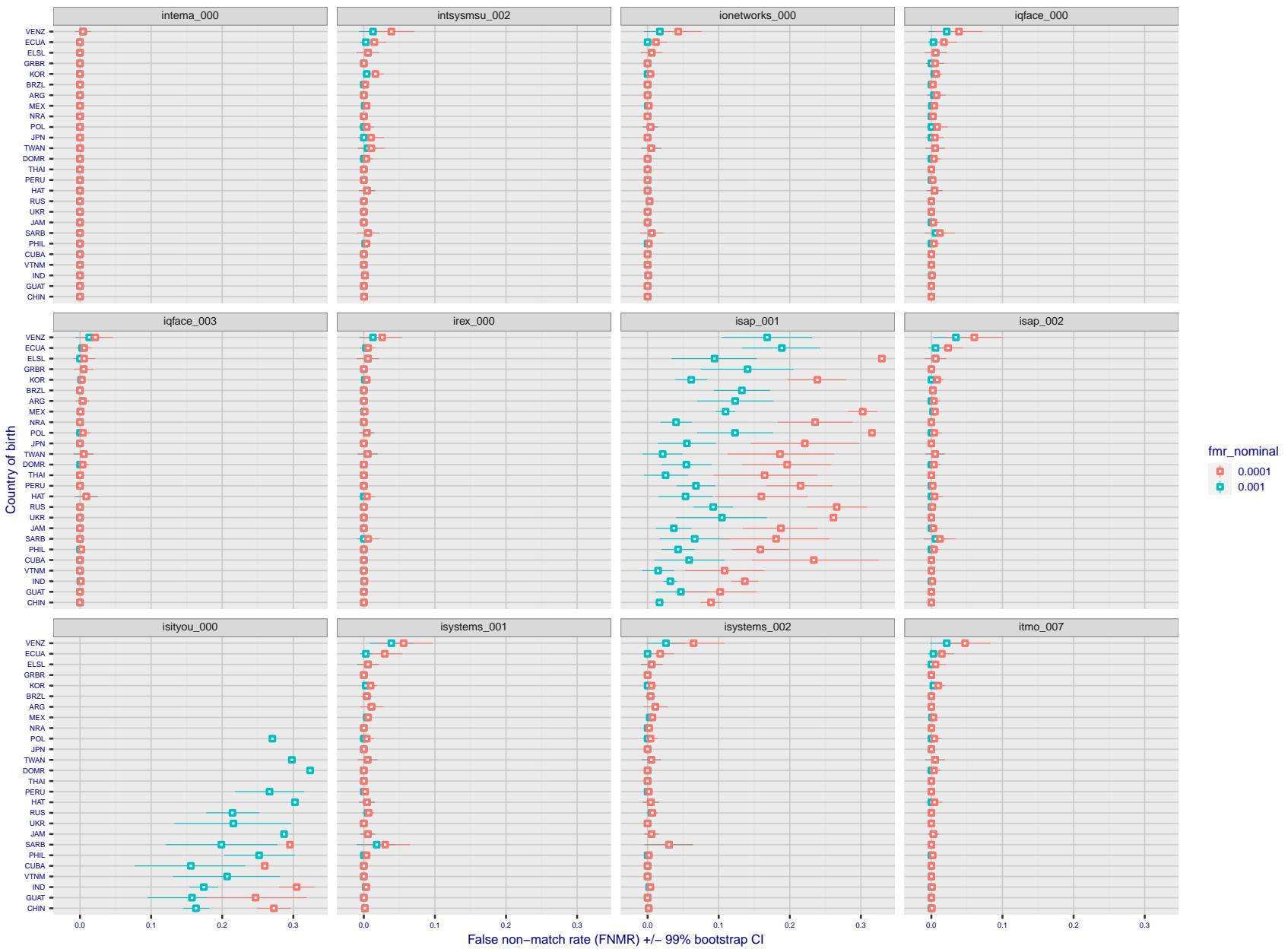


Figure 305: For the visa images, the dots show FNMR by country of birth for two globally set operating thresholds corresponding to $FMR = \{0.001, 0.0001\}$ computed over all on the order of 10^{10} impostor scores. The FMR in each bin will vary also - see subsequent impostor heatmaps in sec. 3.6.1. The figures shows an order of magnitude variation in FNMR across country of birth; these effects are likely due quality variations, then demographics like age and race. The error rates in some cases are zero, and in others the DET is flat so the error rates at the two thresholds are identical. The lines span 1% and 99% of bootstrap replicated FNMR estimates.

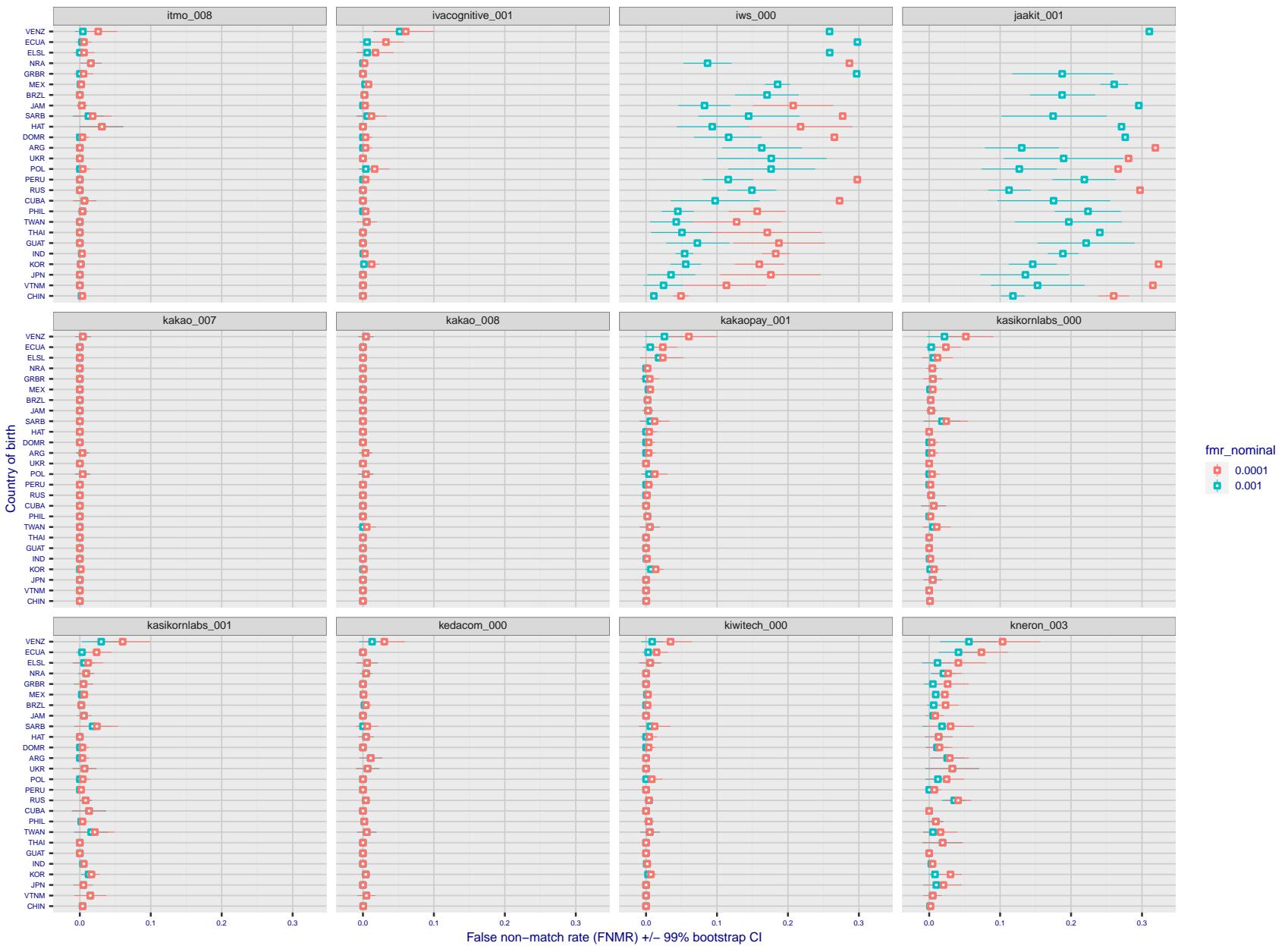


Figure 306: For the visa images, the dots show FNMR by country of birth for two globally set operating thresholds corresponding to $FMR = \{0.001, 0.0001\}$ computed over all on the order of 10^{10} impostor scores. The FMR in each bin will vary also - see subsequent impostor heatmaps in sec. 3.6.1. The figures shows an order of magnitude variation in FNMR across country of birth; these effects are likely due quality variations, then demographics like age and race. The error rates in some cases are zero, and in others the DET is flat so the error rates at the two thresholds are identical. The lines span 1% and 99% of bootstrap replicated FNMR estimates.

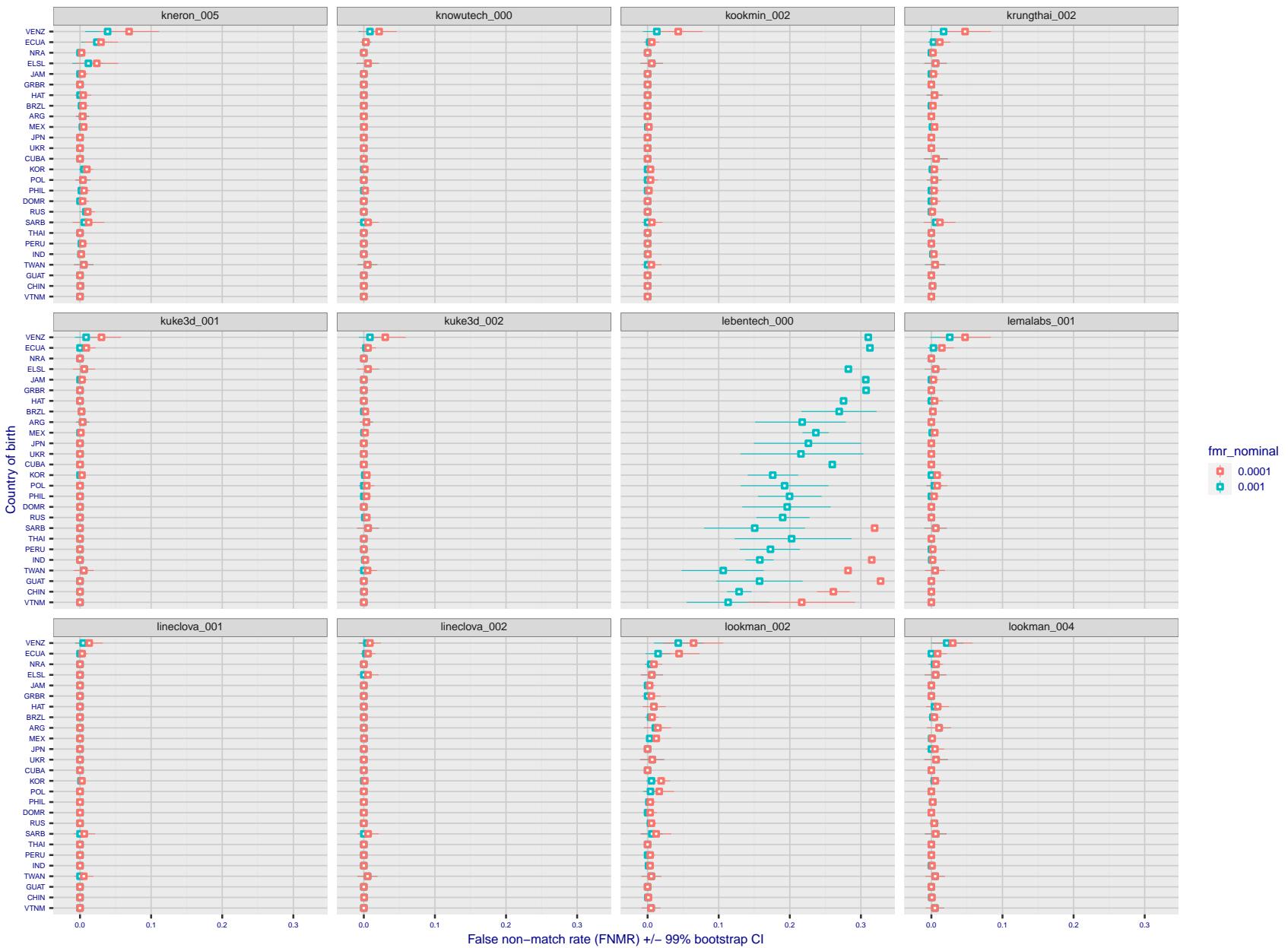


Figure 307: For the visa images, the dots show FNMR by country of birth for two globally set operating thresholds corresponding to $FMR = \{0.001, 0.0001\}$ computed over all on the order of 10^{10} impostor scores. The FMR in each bin will vary also - see subsequent impostor heatmaps in sec. 3.6.1. The figures shows an order of magnitude variation in FNMR across country of birth; these effects are likely due quality variations, then demographics like age and race. The error rates in some cases are zero, and in others the DET is flat so the error rates at the two thresholds are identical. The lines span 1% and 99% of bootstrap replicated FNMR estimates.

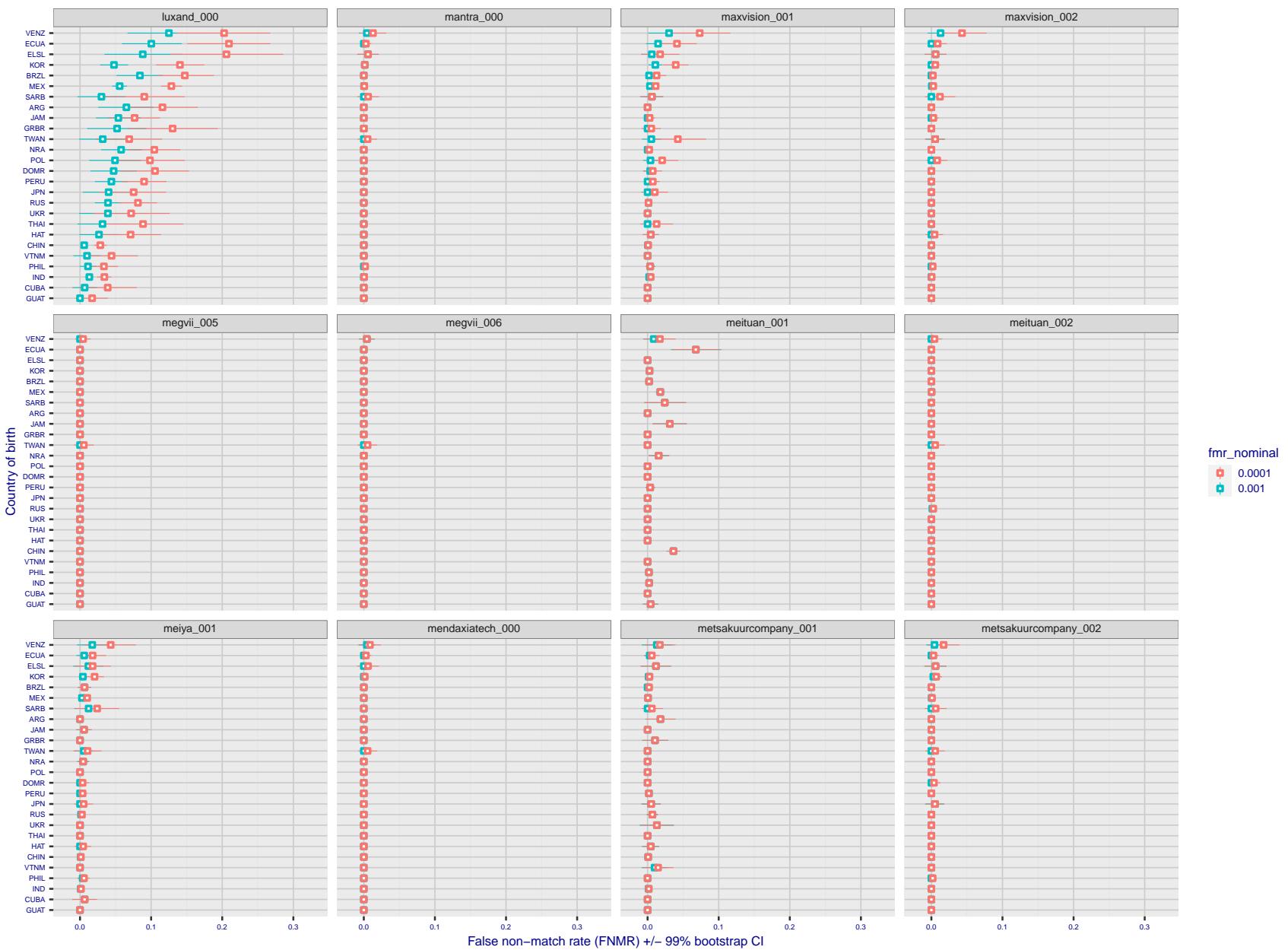


Figure 308: For the visa images, the dots show FNMR by country of birth for two globally set operating thresholds corresponding to $FMR = \{0.001, 0.0001\}$ computed over all on the order of 10^{10} impostor scores. The FMR in each bin will vary also - see subsequent impostor heatmaps in sec. 3.6.1. The figures shows an order of magnitude variation in FNMR across country of birth; these effects are likely due quality variations, then demographics like age and race. The error rates in some cases are zero, and in others the DET is flat so the error rates at the two thresholds are identical. The lines span 1% and 99% of bootstrap replicated FNMR estimates.

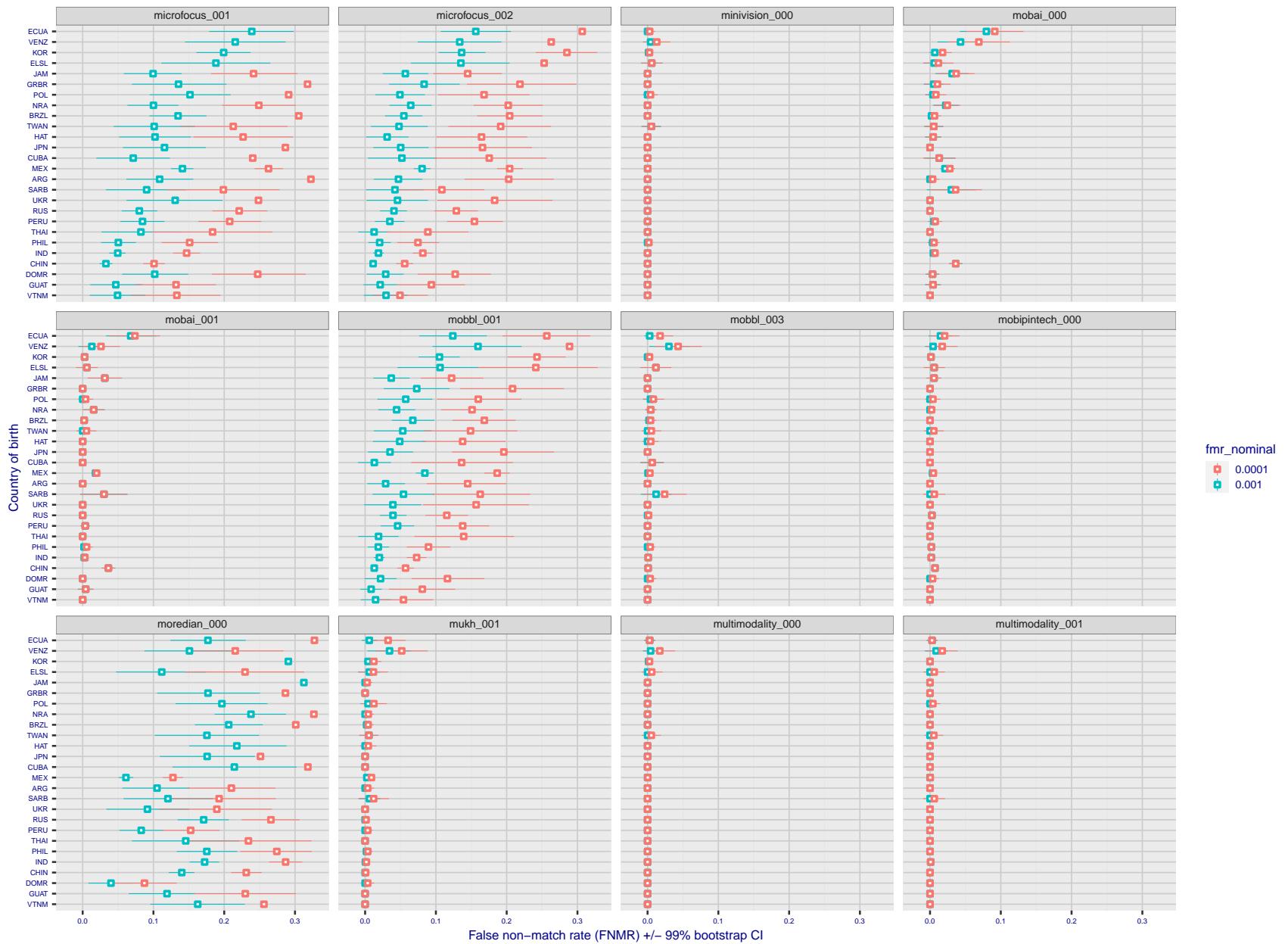


Figure 309: For the visa images, the dots show FNMR by country of birth for two globally set operating thresholds corresponding to $FMR = \{0.001, 0.0001\}$ computed over all on the order of 10^{10} impostor scores. The FMR in each bin will vary also - see subsequent impostor heatmaps in sec. 3.6.1. The figures shows an order of magnitude variation in FNMR across country of birth; these effects are likely due quality variations, then demographics like age and race. The error rates in some cases are zero, and in others the DET is flat so the error rates at the two thresholds are identical. The lines span 1% and 99% of bootstrap replicated FNMR estimates.

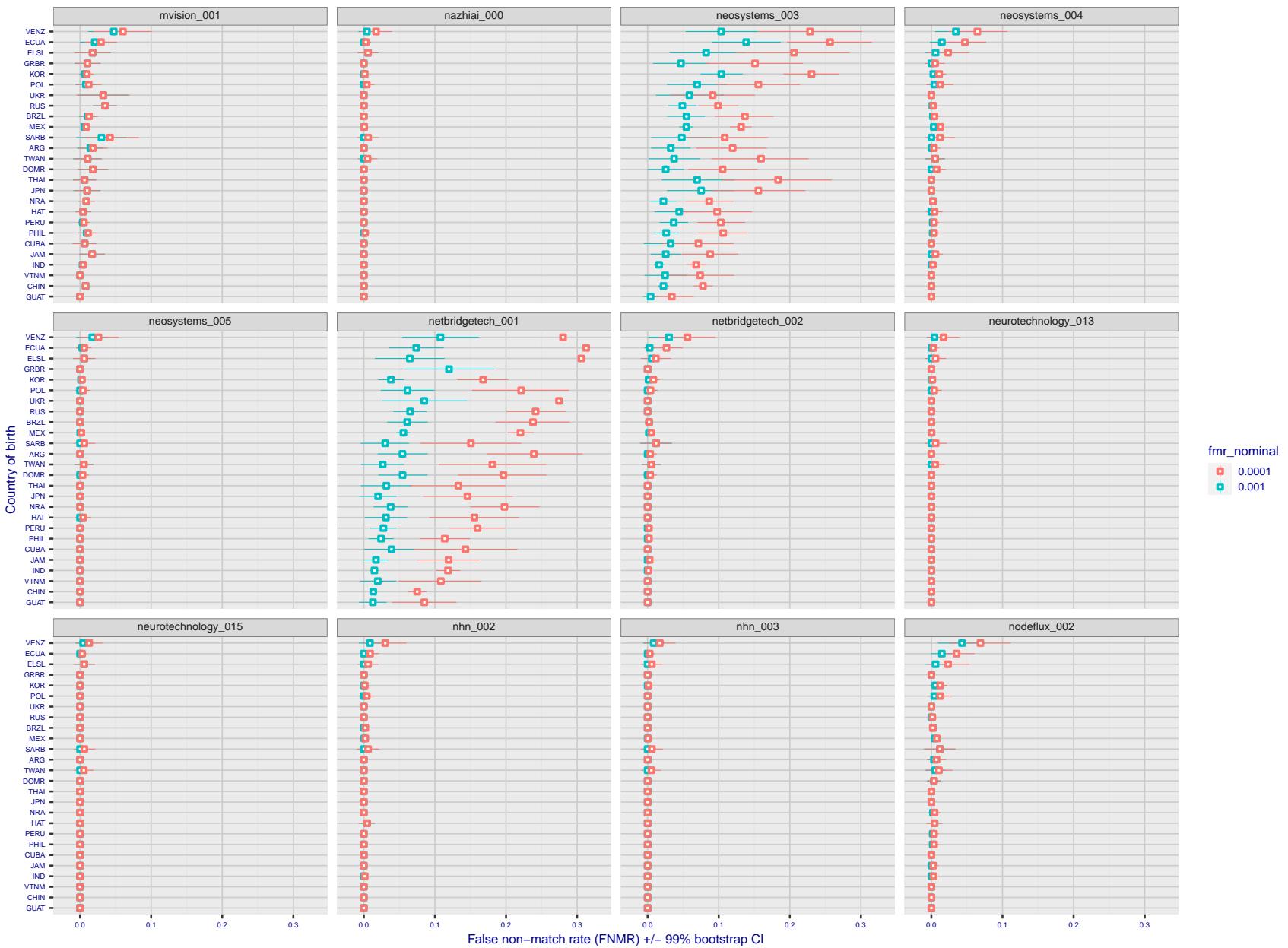


Figure 310: For the visa images, the dots show FNMR by country of birth for two globally set operating thresholds corresponding to $FMR = \{0.001, 0.0001\}$ computed over all on the order of 10^{10} impostor scores. The FMR in each bin will vary also - see subsequent impostor heatmaps in sec. 3.6.1. The figures shows an order of magnitude variation in FNMR across country of birth; these effects are likely due quality variations, then demographics like age and race. The error rates in some cases are zero, and in others the DET is flat so the error rates at the two thresholds are identical. The lines span 1% and 99% of bootstrap replicated FNMR estimates.

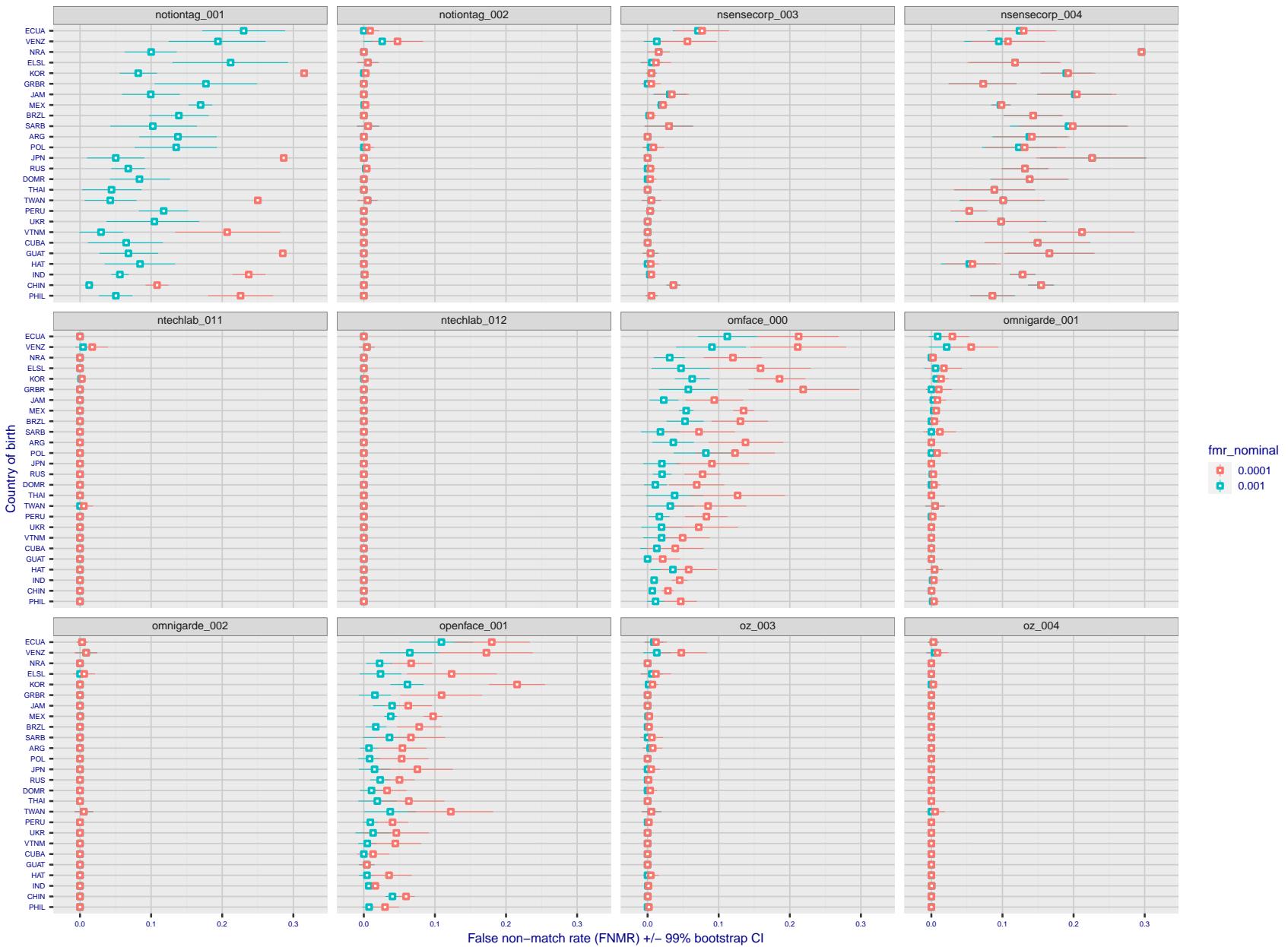


Figure 311: For the visa images, the dots show FNMR by country of birth for two globally set operating thresholds corresponding to $FMR = \{0.001, 0.0001\}$ computed over all on the order of 10^{10} impostor scores. The FMR in each bin will vary also - see subsequent impostor heatmaps in sec. 3.6.1. The figures shows an order of magnitude variation in FNMR across country of birth; these effects are likely due quality variations, then demographics like age and race. The error rates in some cases are zero, and in others the DET is flat so the error rates at the two thresholds are identical. The lines span 1% and 99% of bootstrap replicated FNMR estimates.

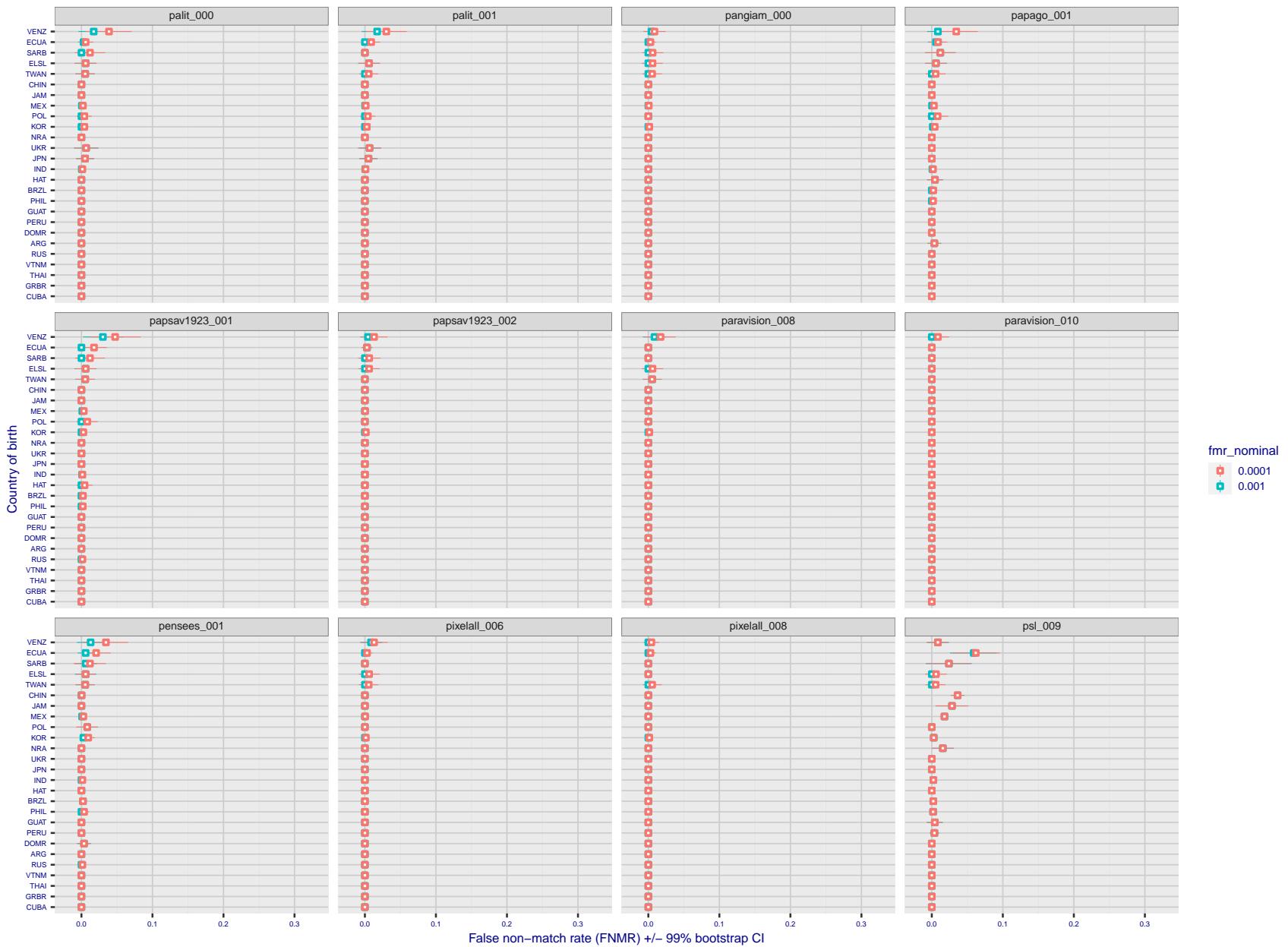


Figure 312: For the visa images, the dots show FNMR by country of birth for two globally set operating thresholds corresponding to $FMR = \{0.001, 0.0001\}$ computed over all on the order of 10^{10} impostor scores. The FMR in each bin will vary also - see subsequent impostor heatmaps in sec. 3.6.1. The figures shows an order of magnitude variation in FNMR across country of birth; these effects are likely due quality variations, then demographics like age and race. The error rates in some cases are zero, and in others the DET is flat so the error rates at the two thresholds are identical. The lines span 1% and 99% of bootstrap replicated FNMR estimates.

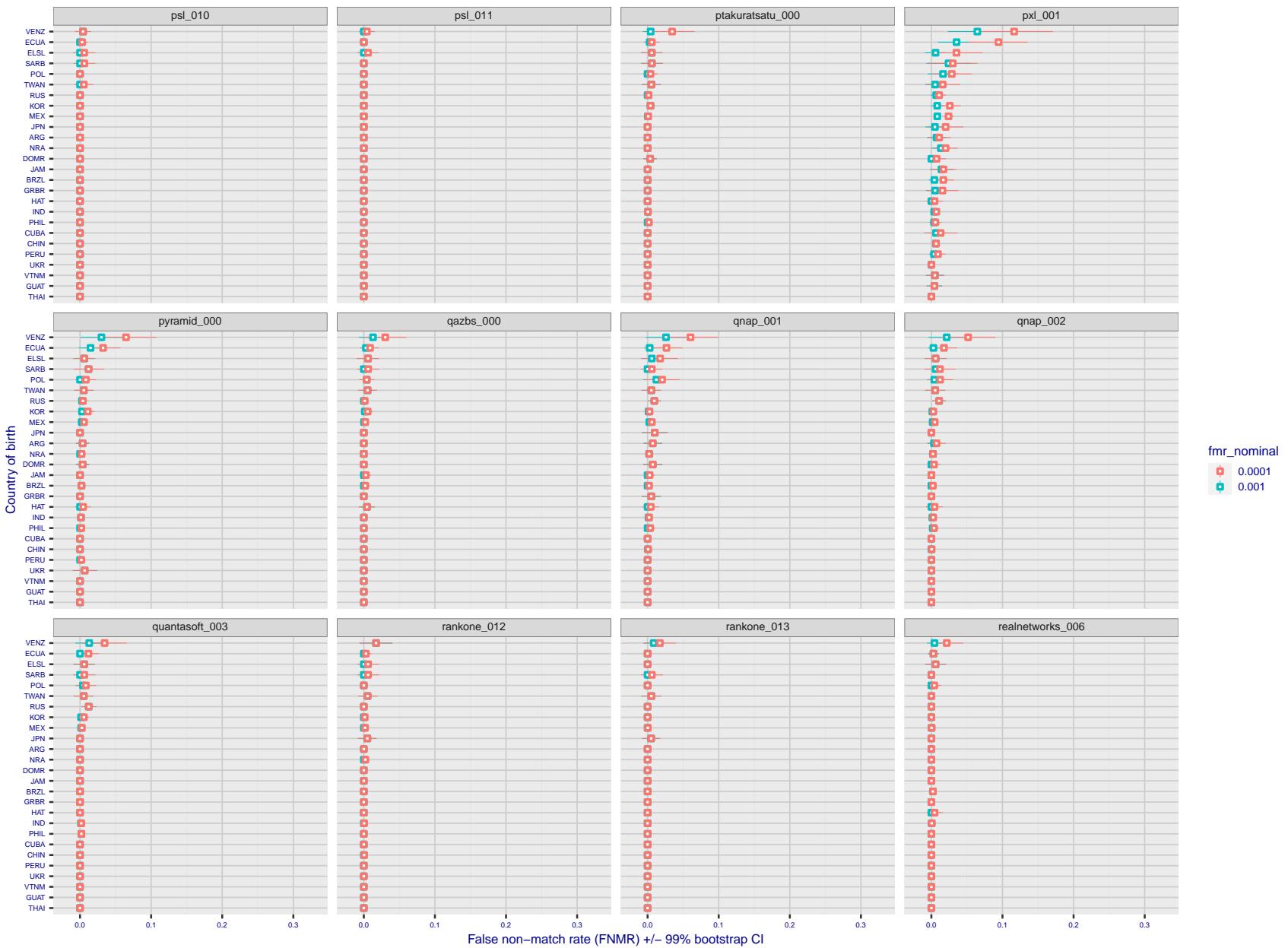


Figure 313: For the visa images, the dots show FNMR by country of birth for two globally set operating thresholds corresponding to $FMR = \{0.001, 0.0001\}$ computed over all on the order of 10^{10} impostor scores. The FMR in each bin will vary also - see subsequent impostor heatmaps in sec. 3.6.1. The figures shows an order of magnitude variation in FNMR across country of birth; these effects are likely due quality variations, then demographics like age and race. The error rates in some cases are zero, and in others the DET is flat so the error rates at the two thresholds are identical. The lines span 1% and 99% of bootstrap replicated FNMR estimates.

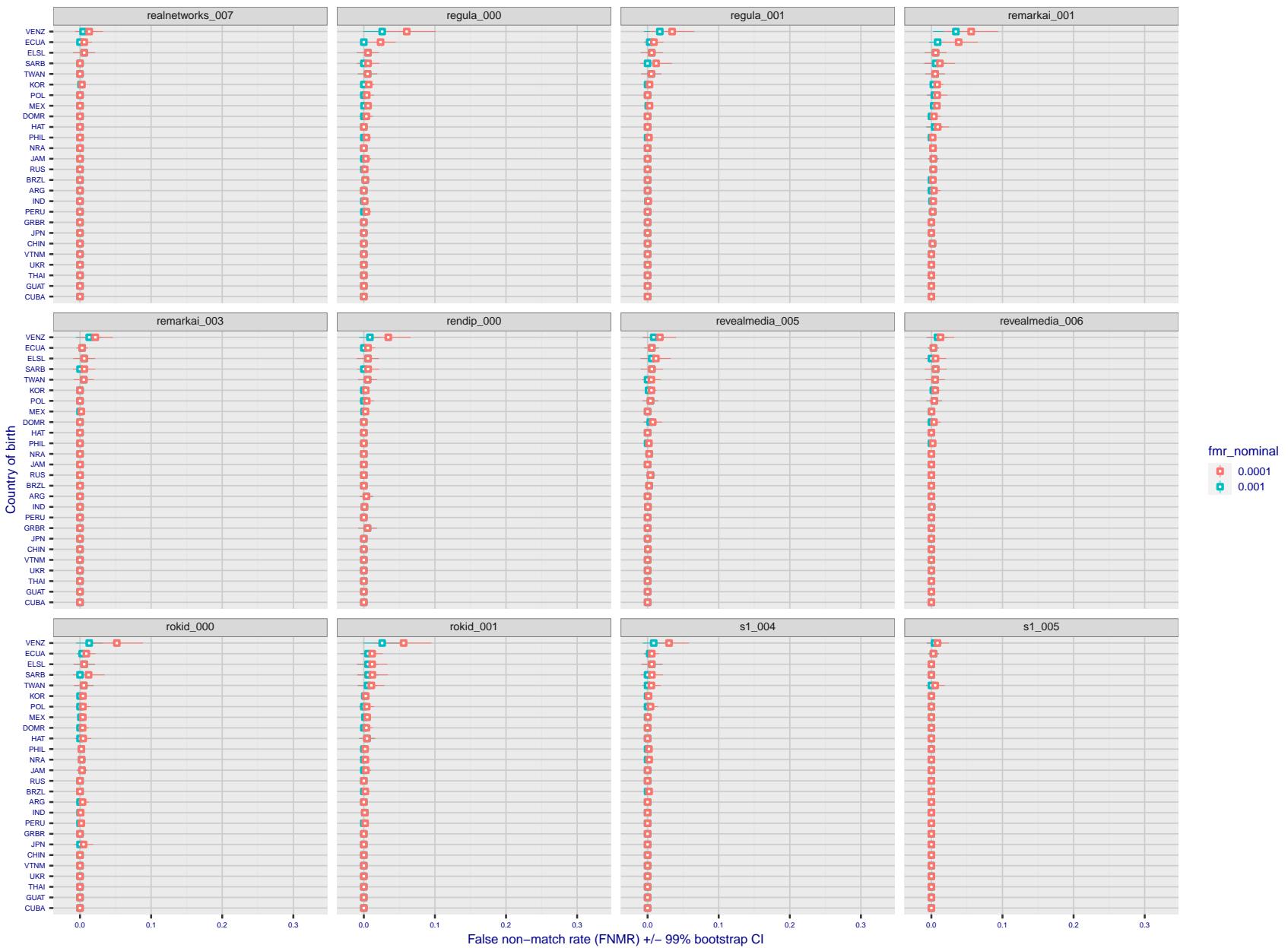


Figure 314: For the visa images, the dots show FNMR by country of birth for two globally set operating thresholds corresponding to $FMR = \{0.001, 0.0001\}$ computed over all on the order of 10^{10} impostor scores. The FMR in each bin will vary also - see subsequent impostor heatmaps in sec. 3.6.1. The figures shows an order of magnitude variation in FNMR across country of birth; these effects are likely due quality variations, then demographics like age and race. The error rates in some cases are zero, and in others the DET is flat so the error rates at the two thresholds are identical. The lines span 1% and 99% of bootstrap replicated FNMR estimates.

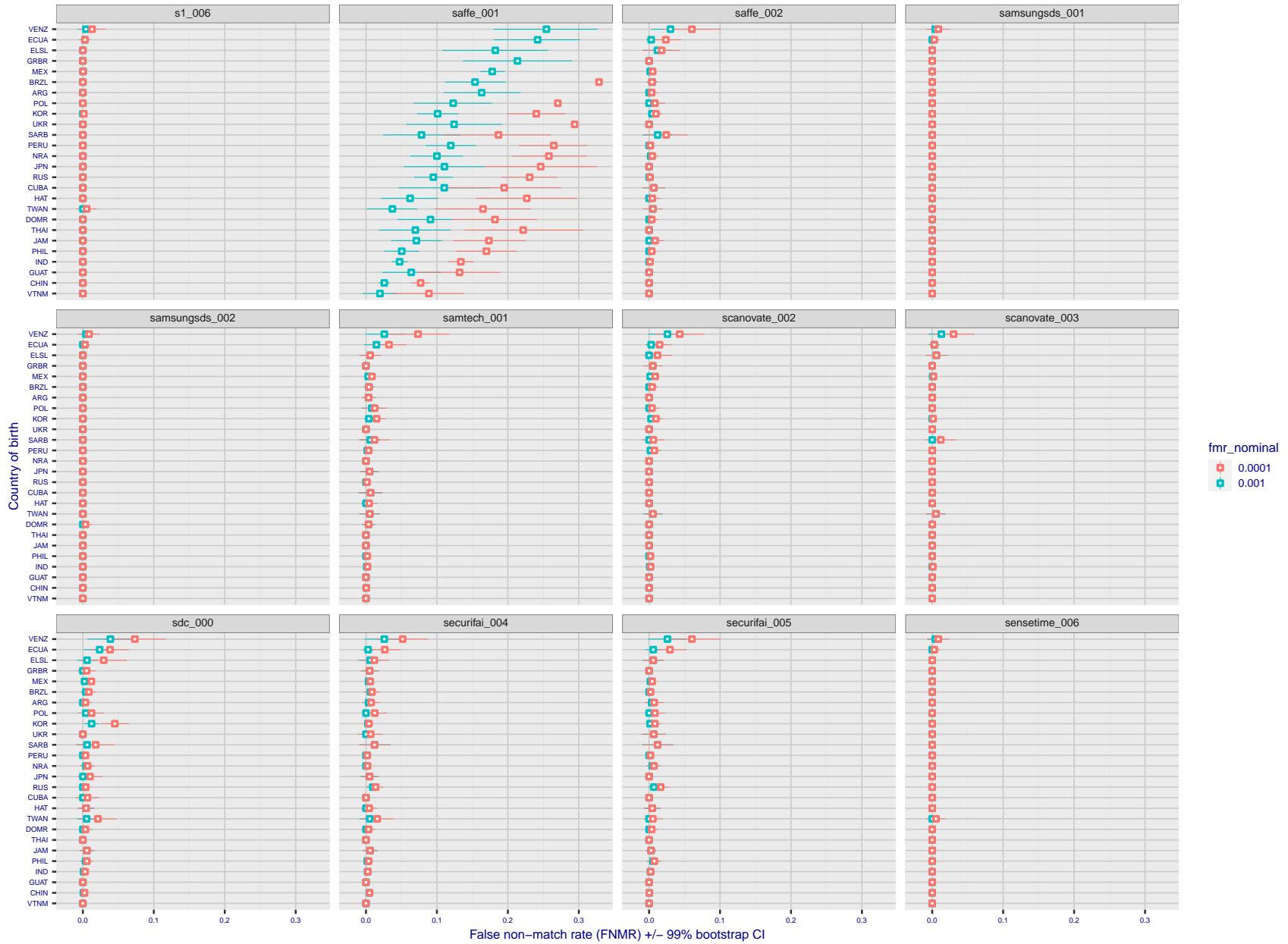


Figure 315: For the visa images, the dots show FNMR by country of birth for two globally set operating thresholds corresponding to $FMR = \{0.001, 0.0001\}$ computed over all on the order of 10^{10} impostor scores. The FMR in each bin will vary also - see subsequent impostor heatmaps in sec. 3.6.1. The figures shows an order of magnitude variation in FNMR across country of birth; these effects are likely due quality variations, then demographics like age and race. The error rates in some cases are zero, and in others the DET is flat so the error rates at the two thresholds are identical. The lines span 1% and 99% of bootstrap replicated FNMR estimates.

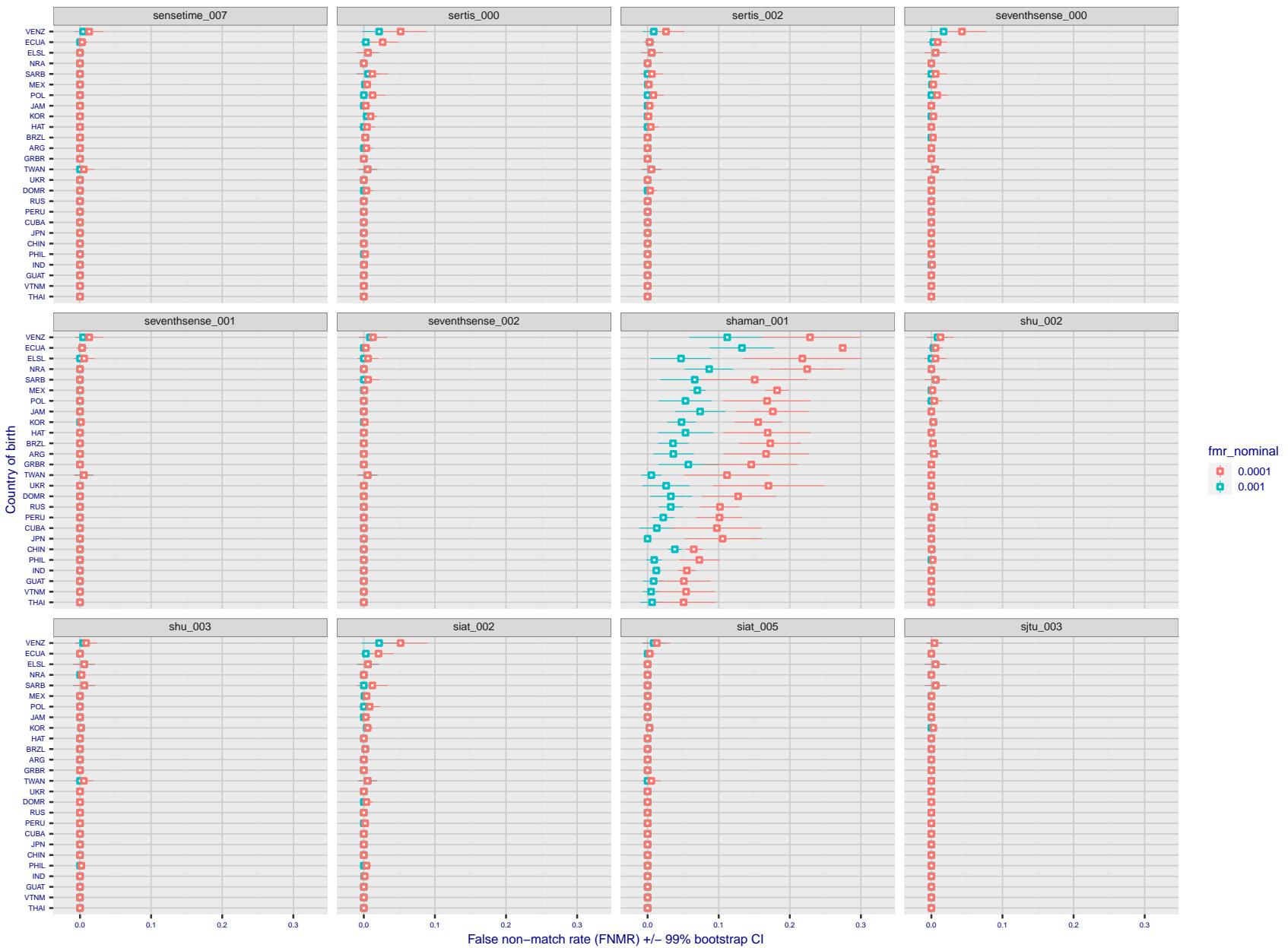


Figure 316: For the visa images, the dots show FNMR by country of birth for two globally set operating thresholds corresponding to $FMR = \{0.001, 0.0001\}$ computed over all on the order of 10^{10} impostor scores. The FMR in each bin will vary also - see subsequent impostor heatmaps in sec. 3.6.1. The figures shows an order of magnitude variation in FNMR across country of birth; these effects are likely due quality variations, then demographics like age and race. The error rates in some cases are zero, and in others the DET is flat so the error rates at the two thresholds are identical. The lines span 1% and 99% of bootstrap replicated FNMR estimates.

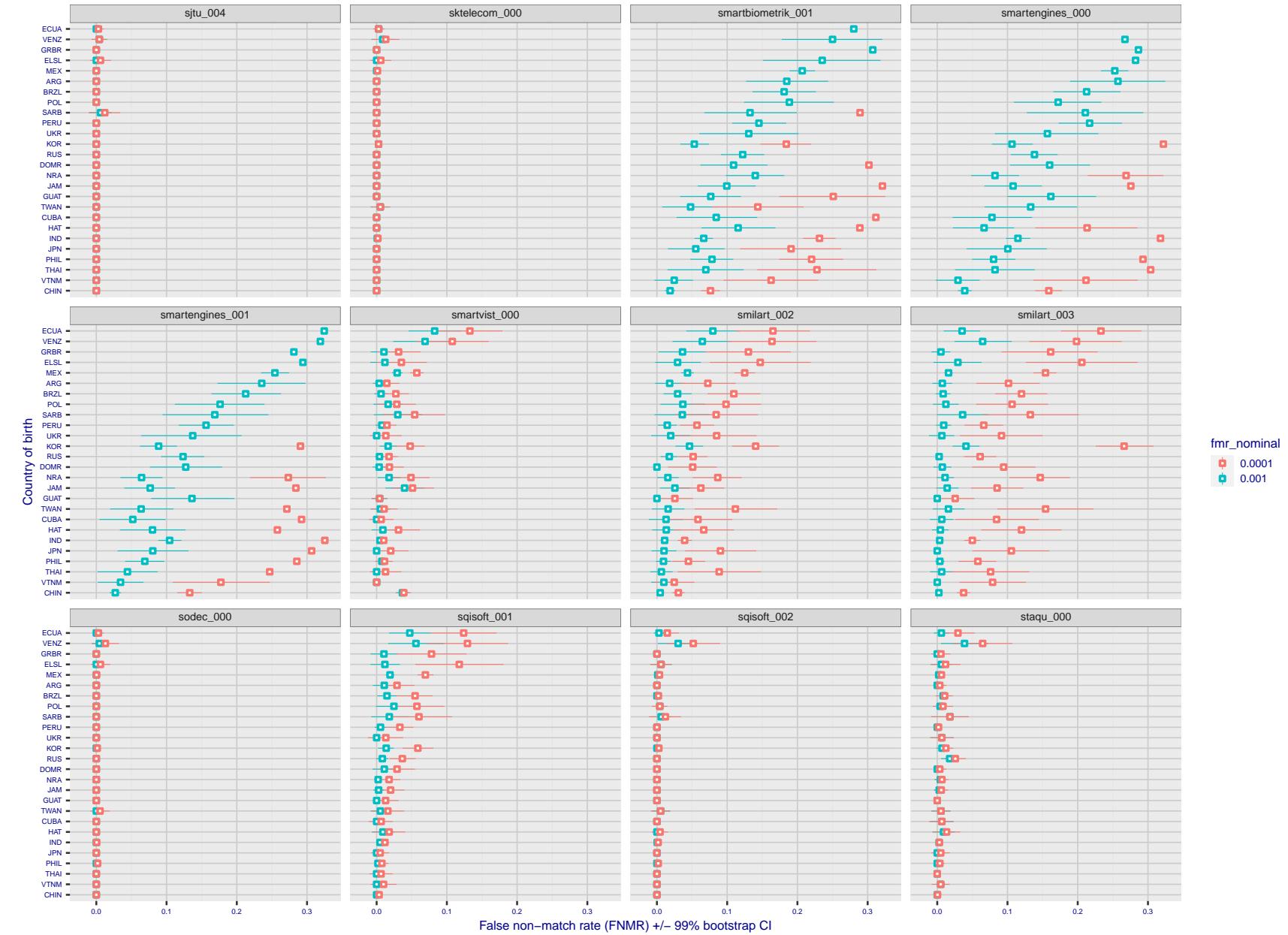


Figure 317: For the visa images, the dots show FNMR by country of birth for two globally set operating thresholds corresponding to $FMR = \{0.001, 0.0001\}$ computed over all on the order of 10^{10} impostor scores. The FMR in each bin will vary also - see subsequent impostor heatmaps in sec. 3.6.1. The figures shows an order of magnitude variation in FNMR across country of birth; these effects are likely due quality variations, then demographics like age and race. The error rates in some cases are zero, and in others the DET is flat so the error rates at the two thresholds are identical. The lines span 1% and 99% of bootstrap replicated FNMR estimates.

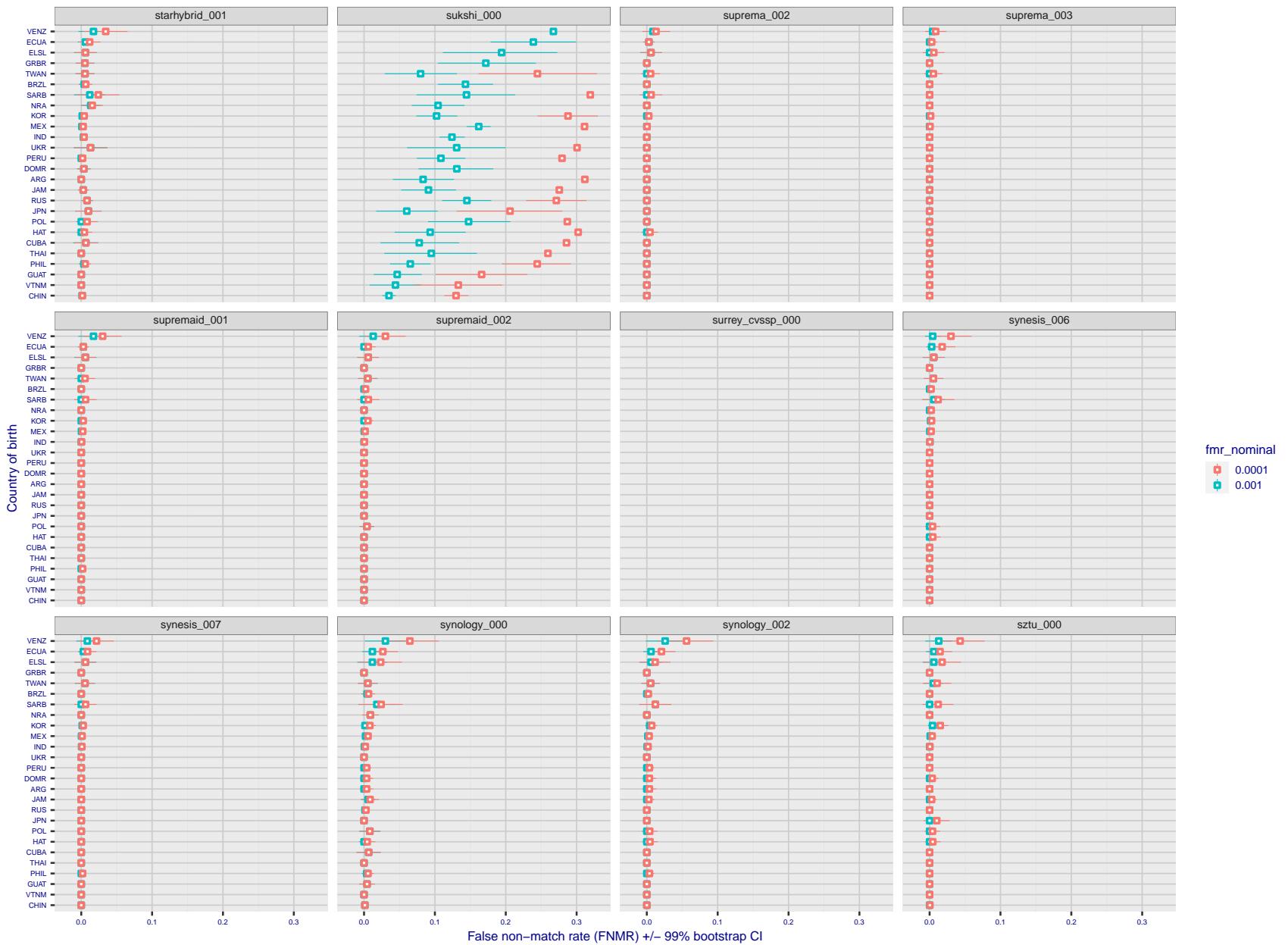


Figure 318: For the visa images, the dots show FNMR by country of birth for two globally set operating thresholds corresponding to $FMR = \{0.001, 0.0001\}$ computed over all on the order of 10^{10} impostor scores. The FMR in each bin will vary also - see subsequent impostor heatmaps in sec. 3.6.1. The figures shows an order of magnitude variation in FNMR across country of birth; these effects are likely due quality variations, then demographics like age and race. The error rates in some cases are zero, and in others the DET is flat so the error rates at the two thresholds are identical. The lines span 1% and 99% of bootstrap replicated FNMR estimates.

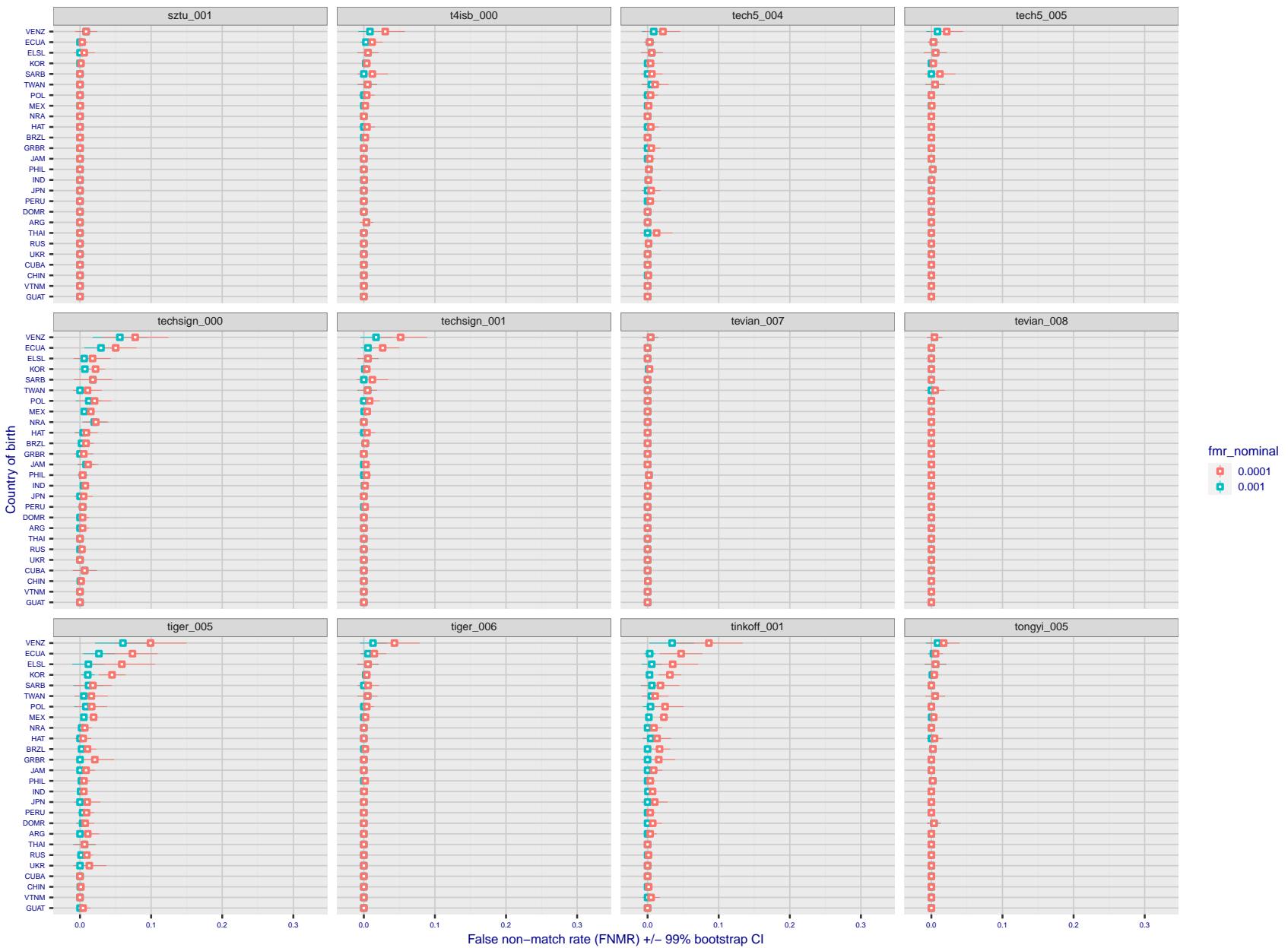


Figure 319: For the visa images, the dots show FNMR by country of birth for two globally set operating thresholds corresponding to $FMR = \{0.001, 0.0001\}$ computed over all on the order of 10^{10} impostor scores. The FMR in each bin will vary also - see subsequent impostor heatmaps in sec. 3.6.1. The figures shows an order of magnitude variation in FNMR across country of birth; these effects are likely due quality variations, then demographics like age and race. The error rates in some cases are zero, and in others the DET is flat so the error rates at the two thresholds are identical. The lines span 1% and 99% of bootstrap replicated FNMR estimates.

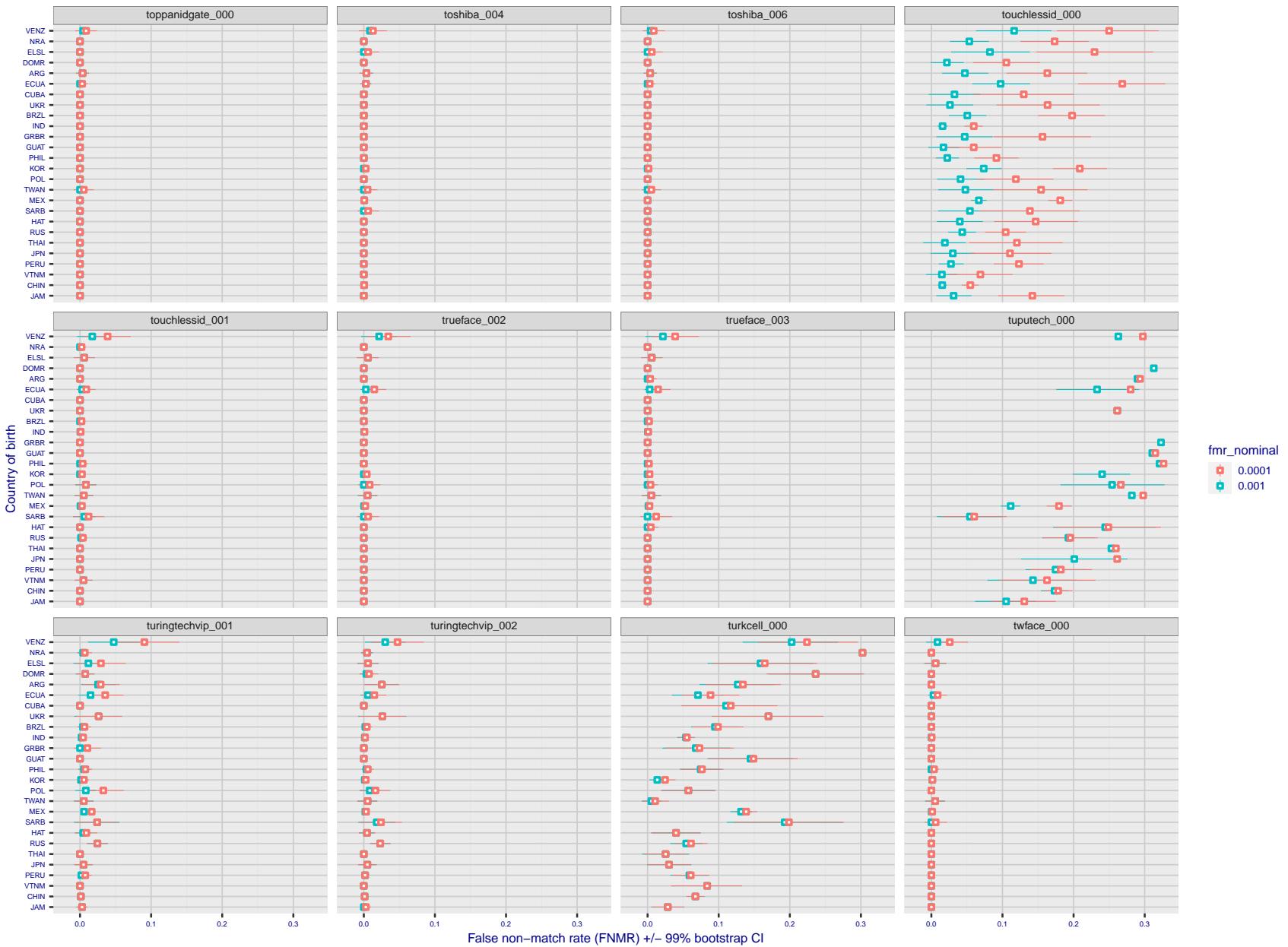


Figure 320: For the visa images, the dots show FNMR by country of birth for two globally set operating thresholds corresponding to $FMR = \{0.001, 0.0001\}$ computed over all on the order of 10^{10} impostor scores. The FMR in each bin will vary also - see subsequent impostor heatmaps in sec. 3.6.1. The figures shows an order of magnitude variation in FNMR across country of birth; these effects are likely due quality variations, then demographics like age and race. The error rates in some cases are zero, and in others the DET is flat so the error rates at the two thresholds are identical. The lines span 1% and 99% of bootstrap replicated FNMR estimates.

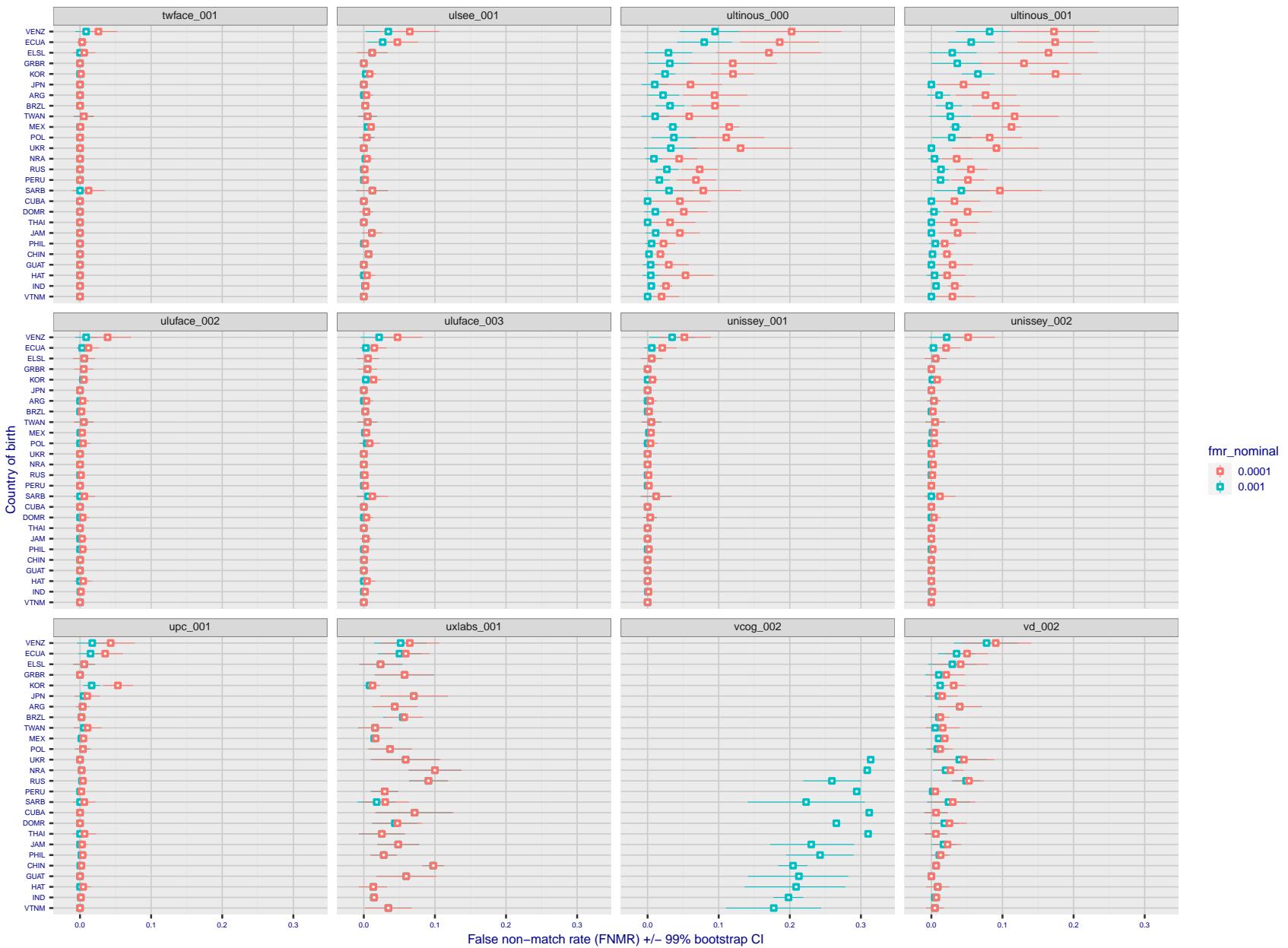


Figure 321: For the visa images, the dots show FNMR by country of birth for two globally set operating thresholds corresponding to $FMR = \{0.001, 0.0001\}$ computed over all on the order of 10^{10} impostor scores. The FMR in each bin will vary also - see subsequent impostor heatmaps in sec. 3.6.1. The figures shows an order of magnitude variation in FNMR across country of birth; these effects are likely due quality variations, then demographics like age and race. The error rates in some cases are zero, and in others the DET is flat so the error rates at the two thresholds are identical. The lines span 1% and 99% of bootstrap replicated FNMR estimates.

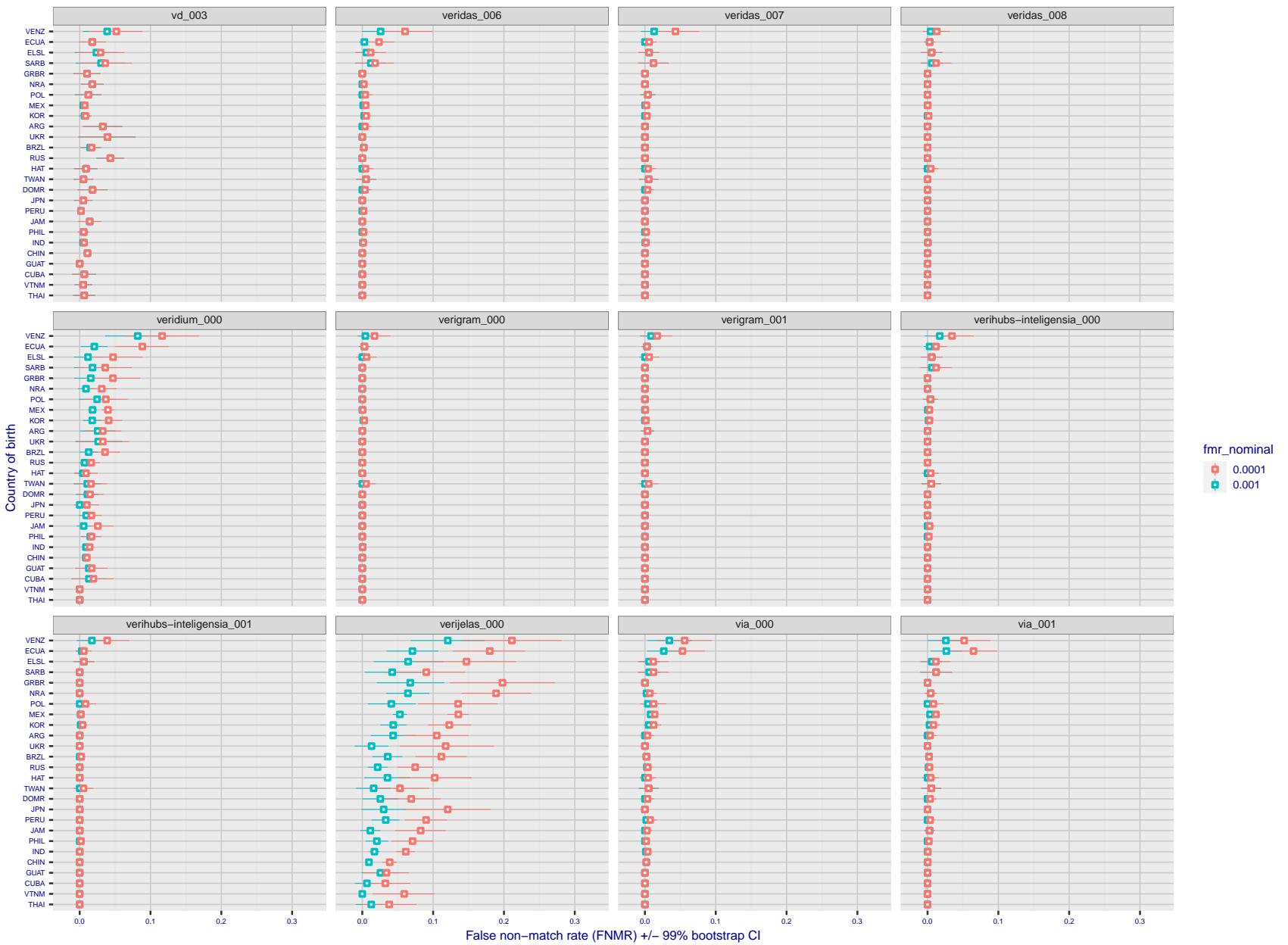


Figure 322: For the visa images, the dots show FNMR by country of birth for two globally set operating thresholds corresponding to $FMR = \{0.001, 0.0001\}$ computed over all on the order of 10^{10} impostor scores. The FMR in each bin will vary also - see subsequent impostor heatmaps in sec. 3.6.1. The figures shows an order of magnitude variation in FNMR across country of birth; these effects are likely due quality variations, then demographics like age and race. The error rates in some cases are zero, and in others the DET is flat so the error rates at the two thresholds are identical. The lines span 1% and 99% of bootstrap replicated FNMR estimates.

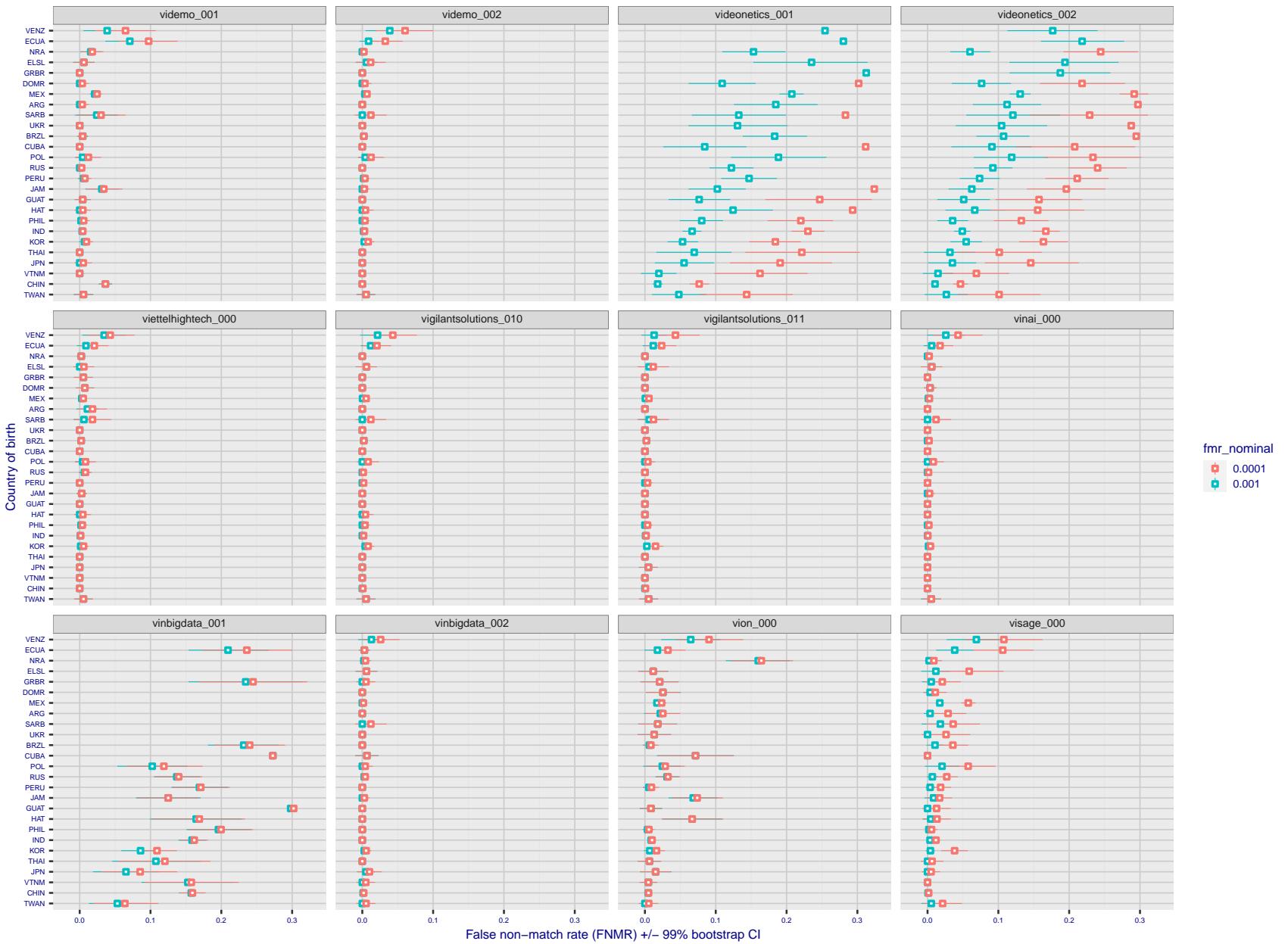


Figure 323: For the visa images, the dots show FNMR by country of birth for two globally set operating thresholds corresponding to $FMR = \{0.001, 0.0001\}$ computed over all on the order of 10^{10} impostor scores. The FMR in each bin will vary also - see subsequent impostor heatmaps in sec. 3.6.1. The figures shows an order of magnitude variation in FNMR across country of birth; these effects are likely due quality variations, then demographics like age and race. The error rates in some cases are zero, and in others the DET is flat so the error rates at the two thresholds are identical. The lines span 1% and 99% of bootstrap replicated FNMR estimates.

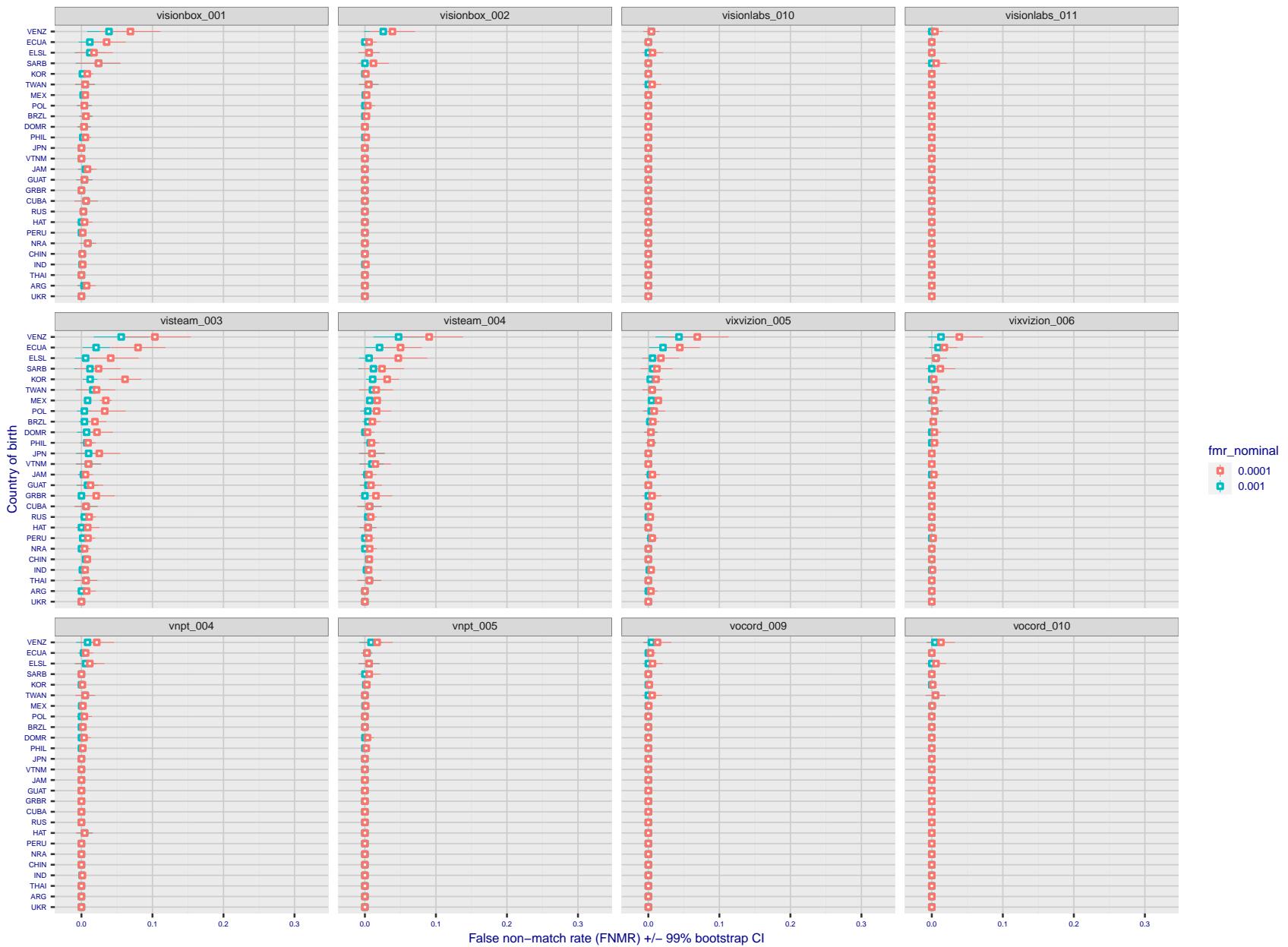


Figure 324: For the visa images, the dots show FNMR by country of birth for two globally set operating thresholds corresponding to $FMR = \{0.001, 0.0001\}$ computed over all on the order of 10^{10} impostor scores. The FMR in each bin will vary also - see subsequent impostor heatmaps in sec. 3.6.1. The figures shows an order of magnitude variation in FNMR across country of birth; these effects are likely due quality variations, then demographics like age and race. The error rates in some cases are zero, and in others the DET is flat so the error rates at the two thresholds are identical. The lines span 1% and 99% of bootstrap replicated FNMR estimates.

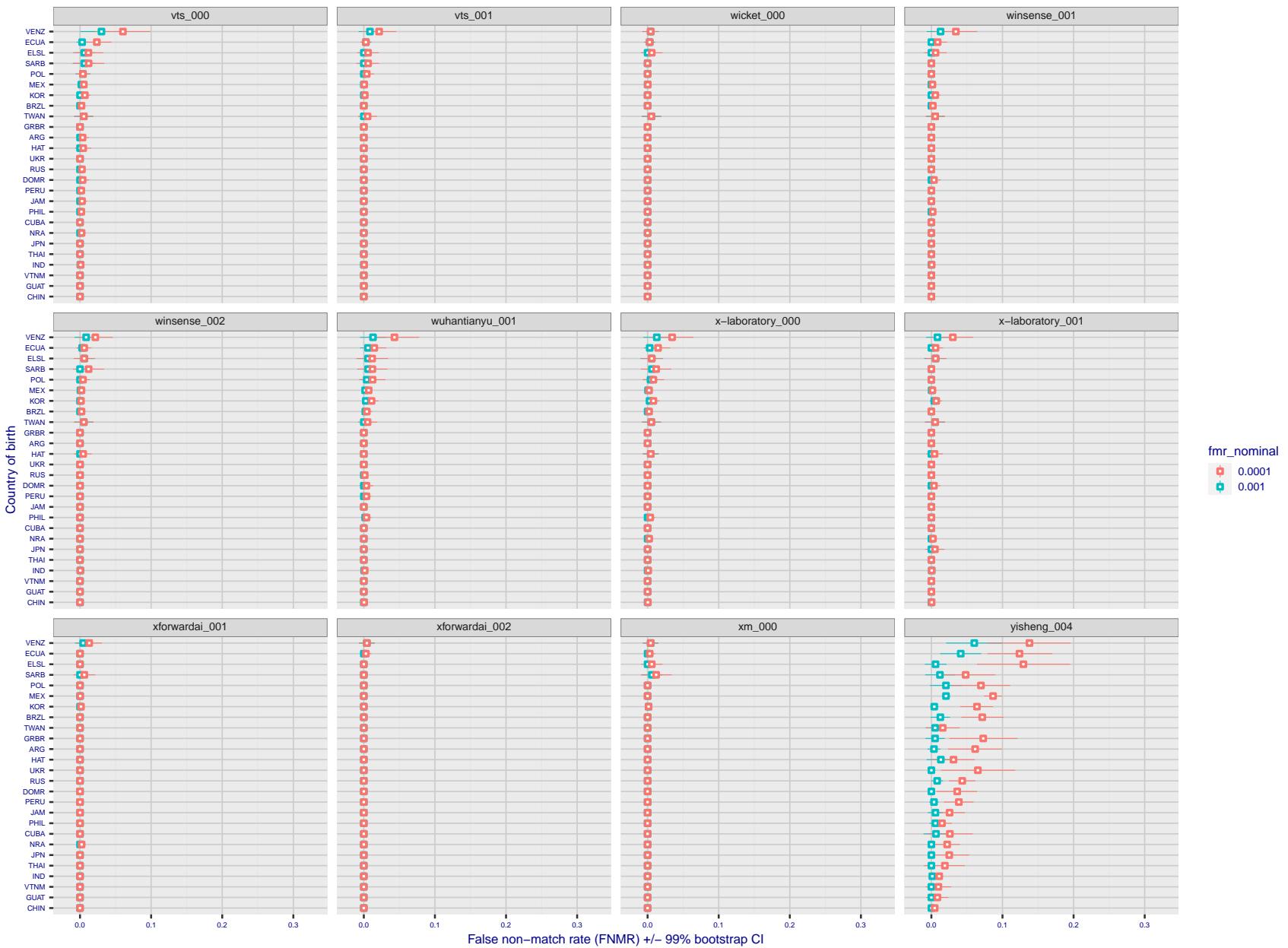


Figure 325: For the visa images, the dots show FNMR by country of birth for two globally set operating thresholds corresponding to $FMR = \{0.001, 0.0001\}$ computed over all on the order of 10^{10} impostor scores. The FMR in each bin will vary also - see subsequent impostor heatmaps in sec. 3.6.1. The figures shows an order of magnitude variation in FNMR across country of birth; these effects are likely due quality variations, then demographics like age and race. The error rates in some cases are zero, and in others the DET is flat so the error rates at the two thresholds are identical. The lines span 1% and 99% of bootstrap replicated FNMR estimates.

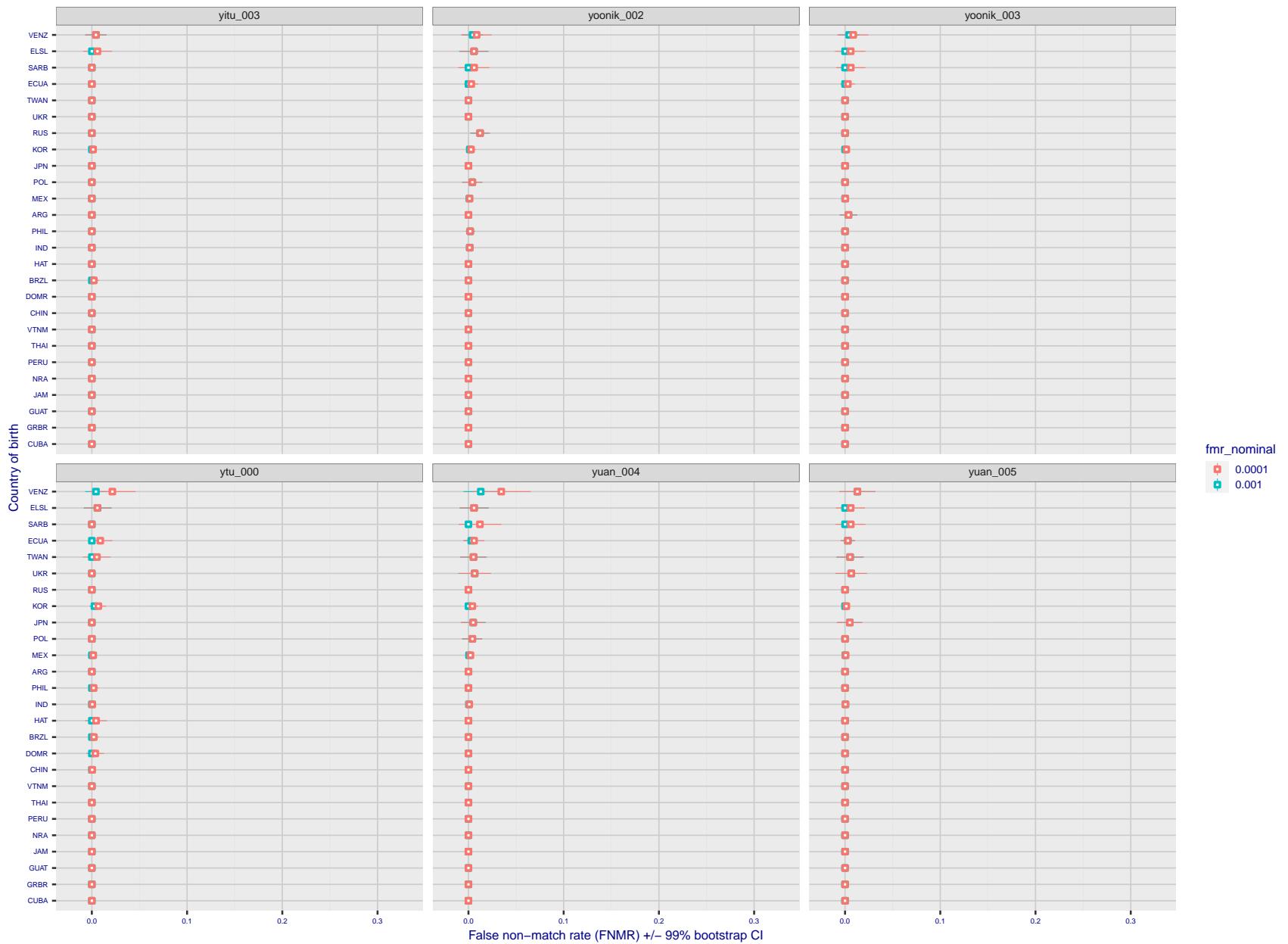


Figure 326: For the visa images, the dots show FNMR by country of birth for two globally set operating thresholds corresponding to $FMR = \{0.001, 0.0001\}$ computed over all on the order of 10^{10} impostor scores. The FMR in each bin will vary also - see subsequent impostor heatmaps in sec. 3.6.1. The figures shows an order of magnitude variation in FNMR across country of birth; these effects are likely due quality variations, then demographics like age and race. The error rates in some cases are zero, and in others the DET is flat so the error rates at the two thresholds are identical. The lines span 1% and 99% of bootstrap replicated FNMR estimates.

Caveats: The results may not relate to subject-specific properties. Instead they could reflect image-specific quality differences, which could occur due to collection protocol or software processing variations.

3.5.2 Effect of ageing

Background: Faces change appearance throughout life. This change gradually reduces similarity of a new image to an earlier image. Face recognition algorithms give reduced similarity scores and more frequent false rejections.

Goal: To quantify false non-match rates (FNMR) as a function of elapsed time in an adult population.

Methods: Using the mugshot images, a threshold is set to give FMR = 0.00001 over the entire impostor set. Then FNMR is measured over 1000 bootstrap replications of the genuine scores.

Results: For the visa images, Figure 355 shows how false non-match rates for genuine users, as a function of age group.

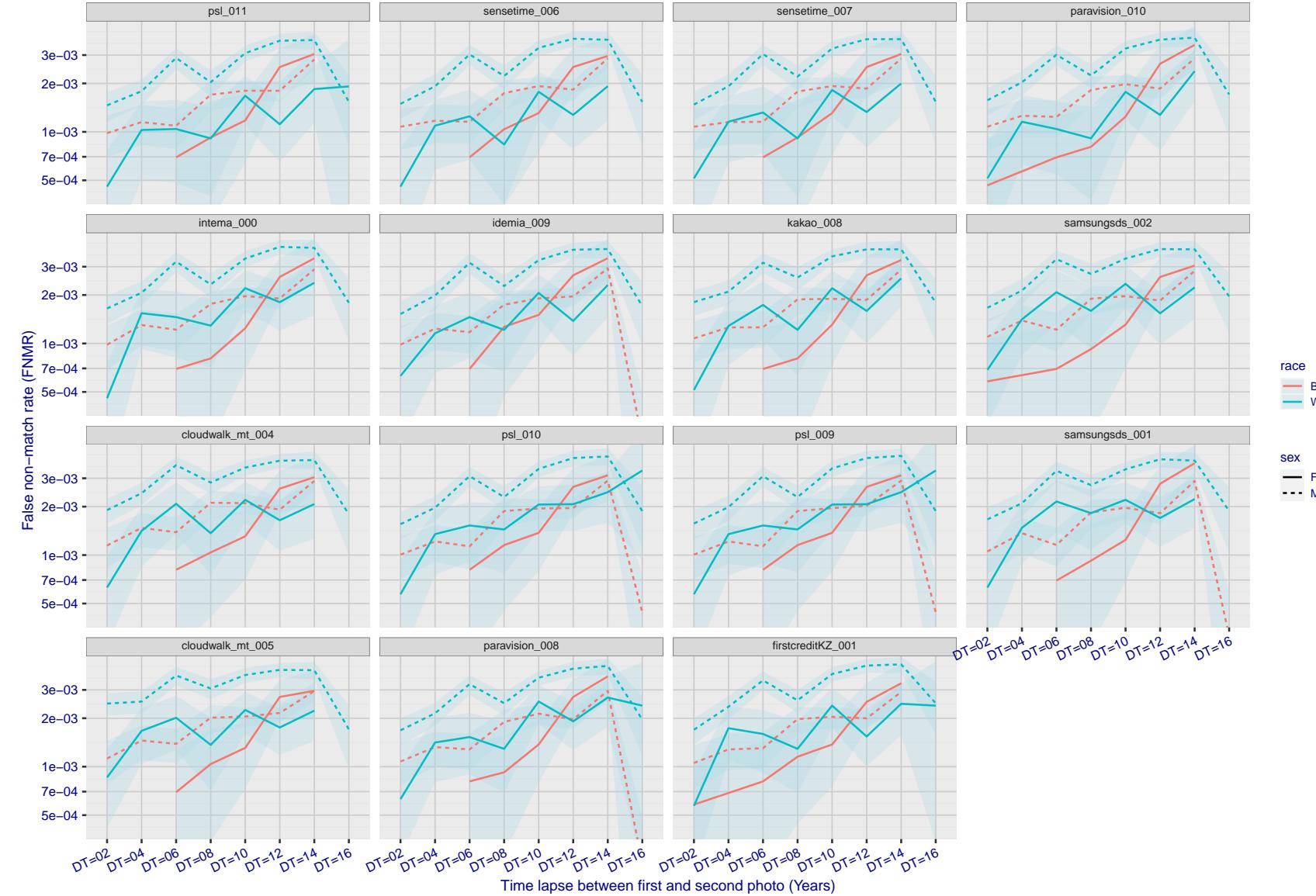


Figure 327: For the mugshot images, FNMR as a function of elapsed time between initial enrollment and second verification images. The panels appear most accurate first, and vertical scale changes on each page. The four traces correspond to images annotated with codes for black female, black male, white female, white male. The threshold is fixed for each algorithm to give FMR = 0.00001 over all (10^8) impostor comparisons. For short time-lapses, the most accurate algorithms give very few errors (FNMR < 0.001) so that the uncertainty estimates are high.

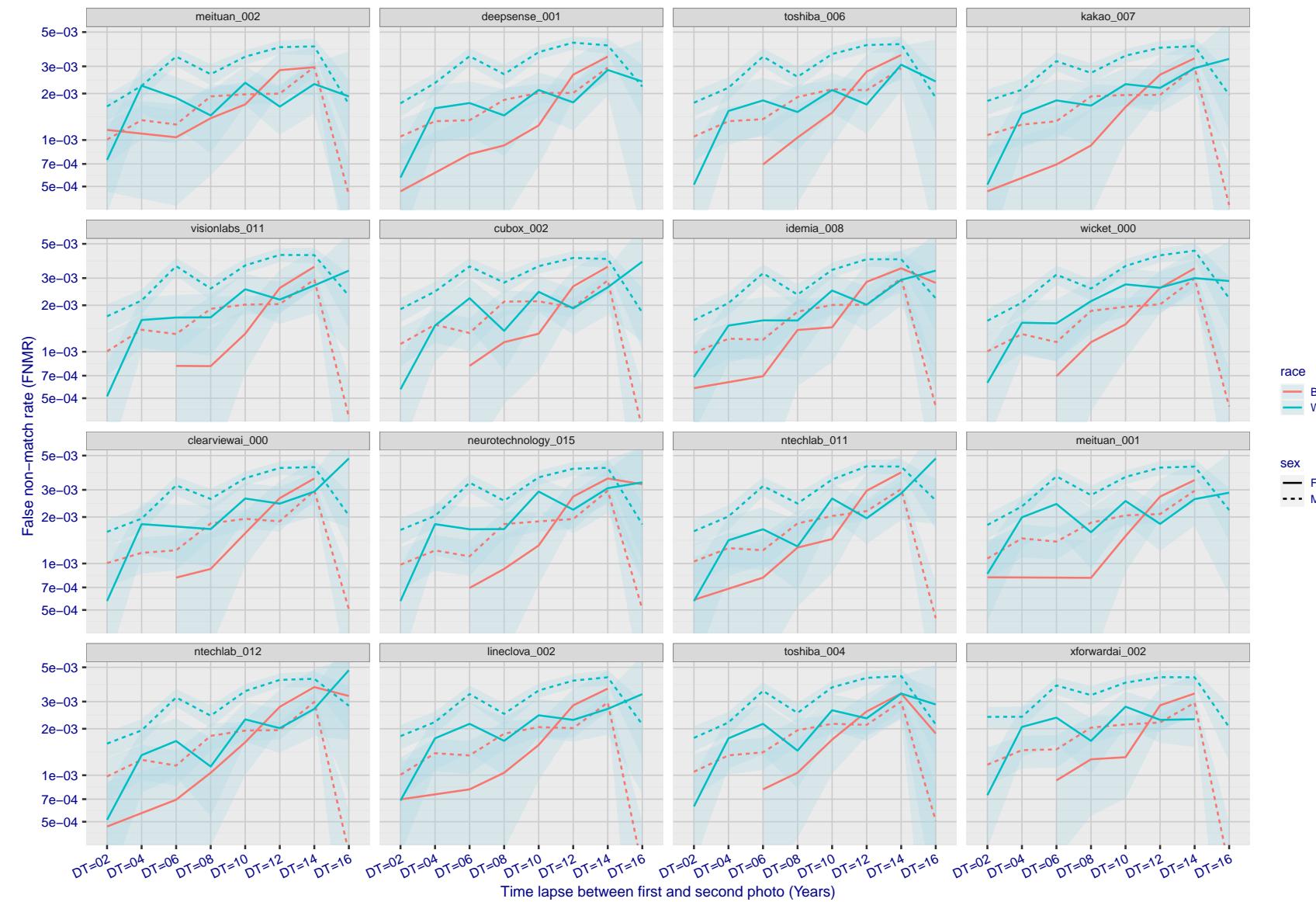


Figure 328: For the mugshot images, FNMR as a function of elapsed time between initial enrollment and second verification images. The panels appear most accurate first, and vertical scale changes on each page. The four traces correspond to images annotated with codes for black female, black male, white female, white male. The threshold is fixed for each algorithm to give FMR = 0.00001 over all (10^8) impostor comparisons. For short time-lapses, the most accurate algorithms give very few errors (FNMR < 0.001) so that the uncertainty estimates are high.

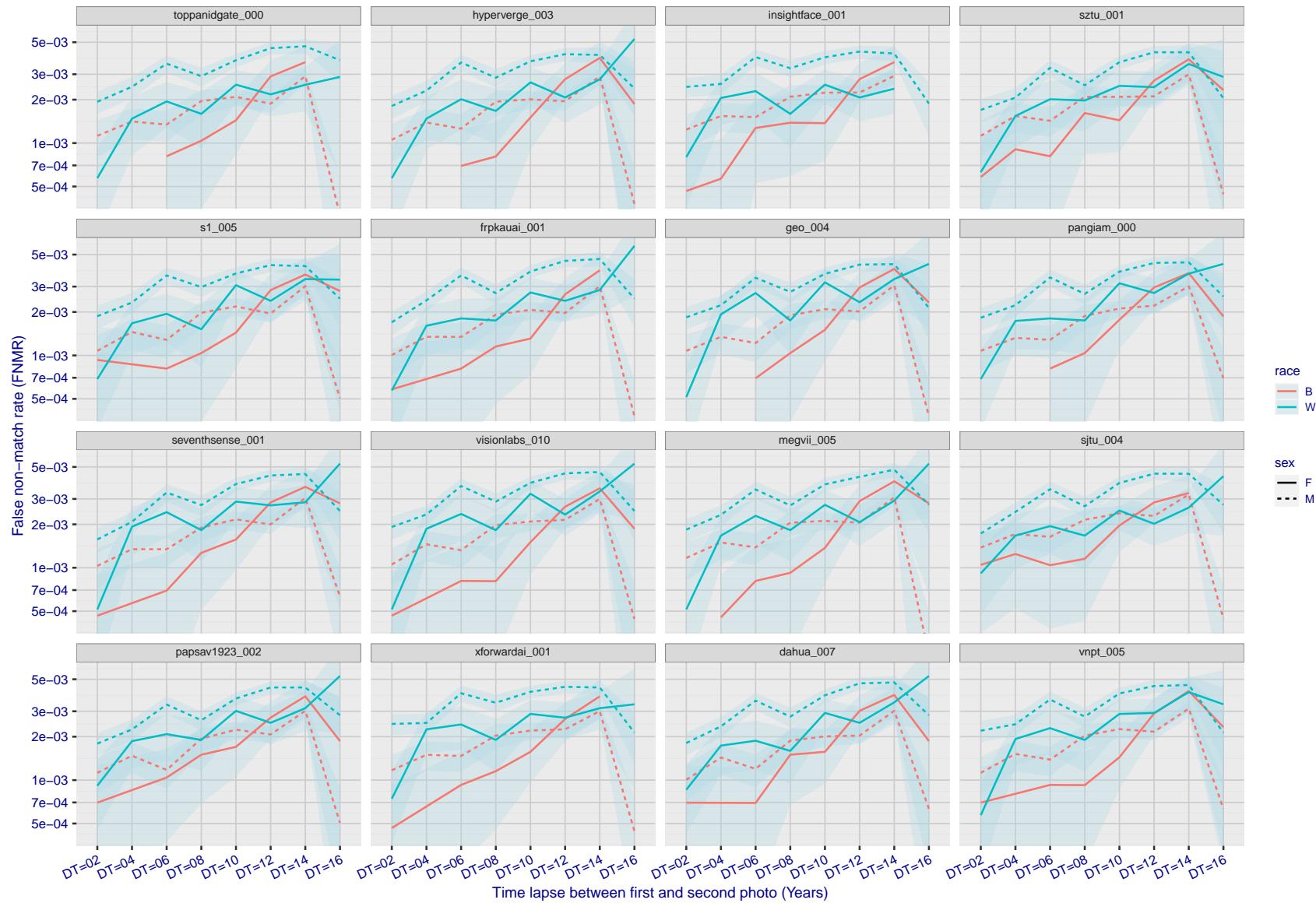


Figure 329: For the mugshot images, FNMR as a function of elapsed time between initial enrollment and second verification images. The panels appear most accurate first, and vertical scale changes on each page. The four traces correspond to images annotated with codes for black female, black male, white female, white male. The threshold is fixed for each algorithm to give FMR = 0.00001 over all (10^8) impostor comparisons. For short time-lapses, the most accurate algorithms give very few errors (FNMR < 0.001) so that the uncertainty estimates are high.

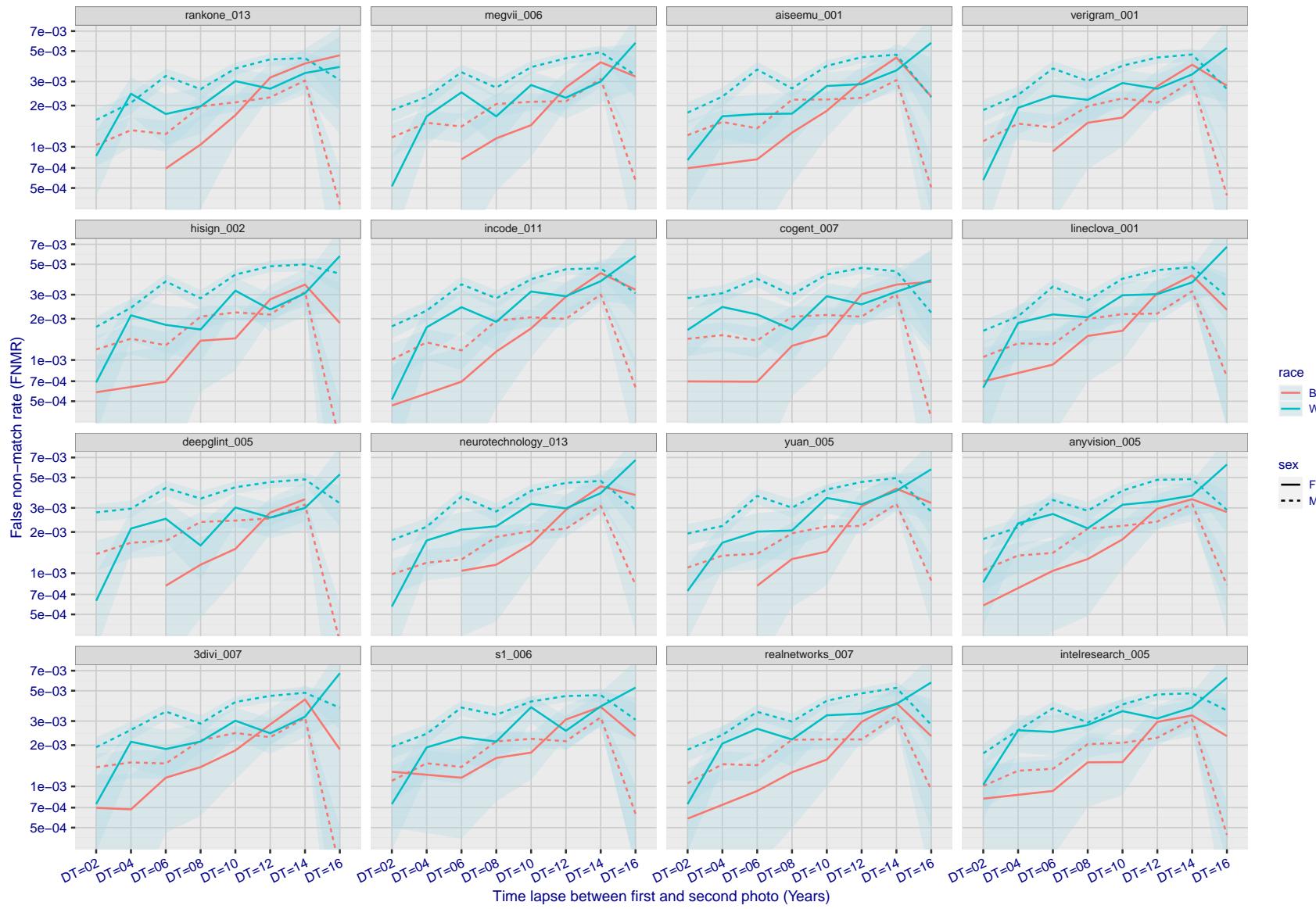


Figure 330: For the mugshot images, FNMR as a function of elapsed time between initial enrollment and second verification images. The panels appear most accurate first, and vertical scale changes on each page. The four traces correspond to images annotated with codes for black female, black male, white female, white male. The threshold is fixed for each algorithm to give FMR = 0.00001 over all (10^8) impostor comparisons. For short time-lapses, the most accurate algorithms give very few errors (FNMR < 0.001) so that the uncertainty estimates are high.

2022/11/07 10:56:27

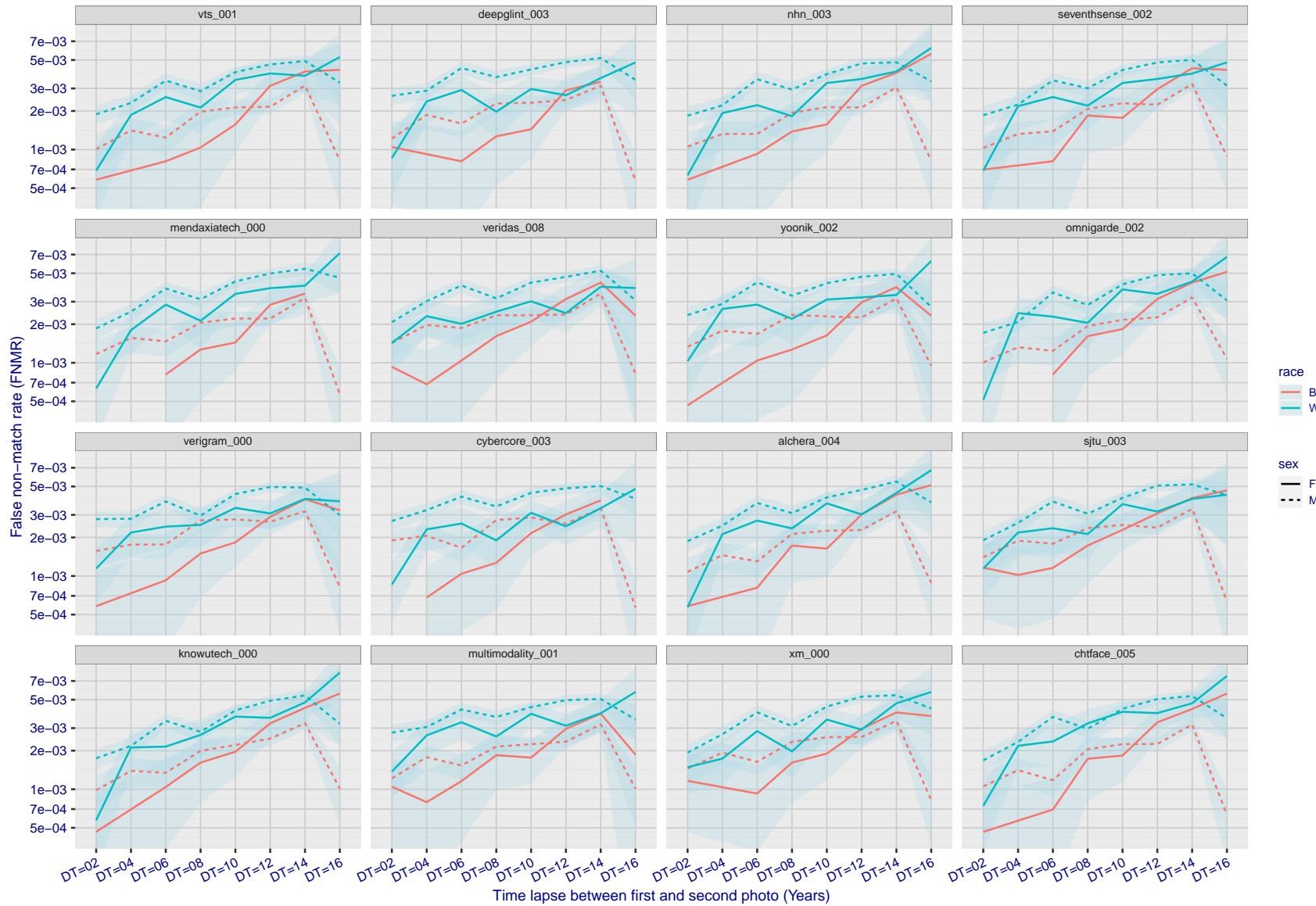


Figure 331: For the mugshot images, FNMR as a function of elapsed time between initial enrollment and second verification images. The panels appear most accurate first, and vertical scale changes on each page. The four traces correspond to images annotated with codes for black female, black male, white female, white male. The threshold is fixed for each algorithm to give FMR = 0.00001 over all (10^8) impostor comparisons. For short time-lapses, the most accurate algorithms give very few errors (FNMR < 0.001) so that the uncertainty estimates are high.

FNMR(T)
FMR(T)
"False match rate"

2022/11/07 10:56:27

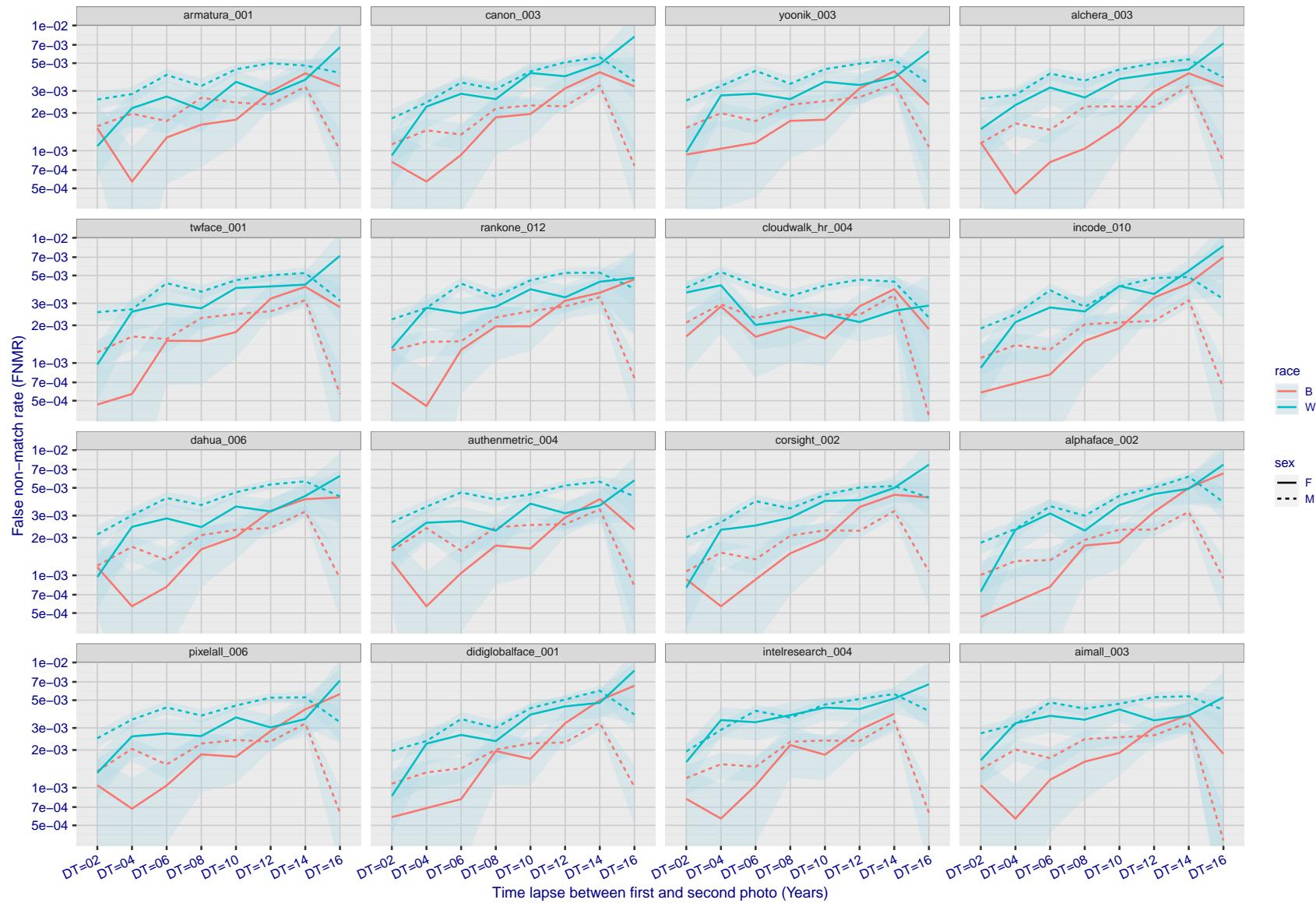


Figure 332: For the mugshot images, FNMR as a function of elapsed time between initial enrollment and second verification images. The panels appear most accurate first, and vertical scale changes on each page. The four traces correspond to images annotated with codes for black female, black male, white female, white male. The threshold is fixed for each algorithm to give FMR = 0.00001 over all (10^8) impostor comparisons. For short time-lapses, the most accurate algorithms give very few errors (FNMR < 0.001) so that the uncertainty estimates are high.

FNMR(T)
FMR(T)
"False match rate"

2022/11/07 10:56:27

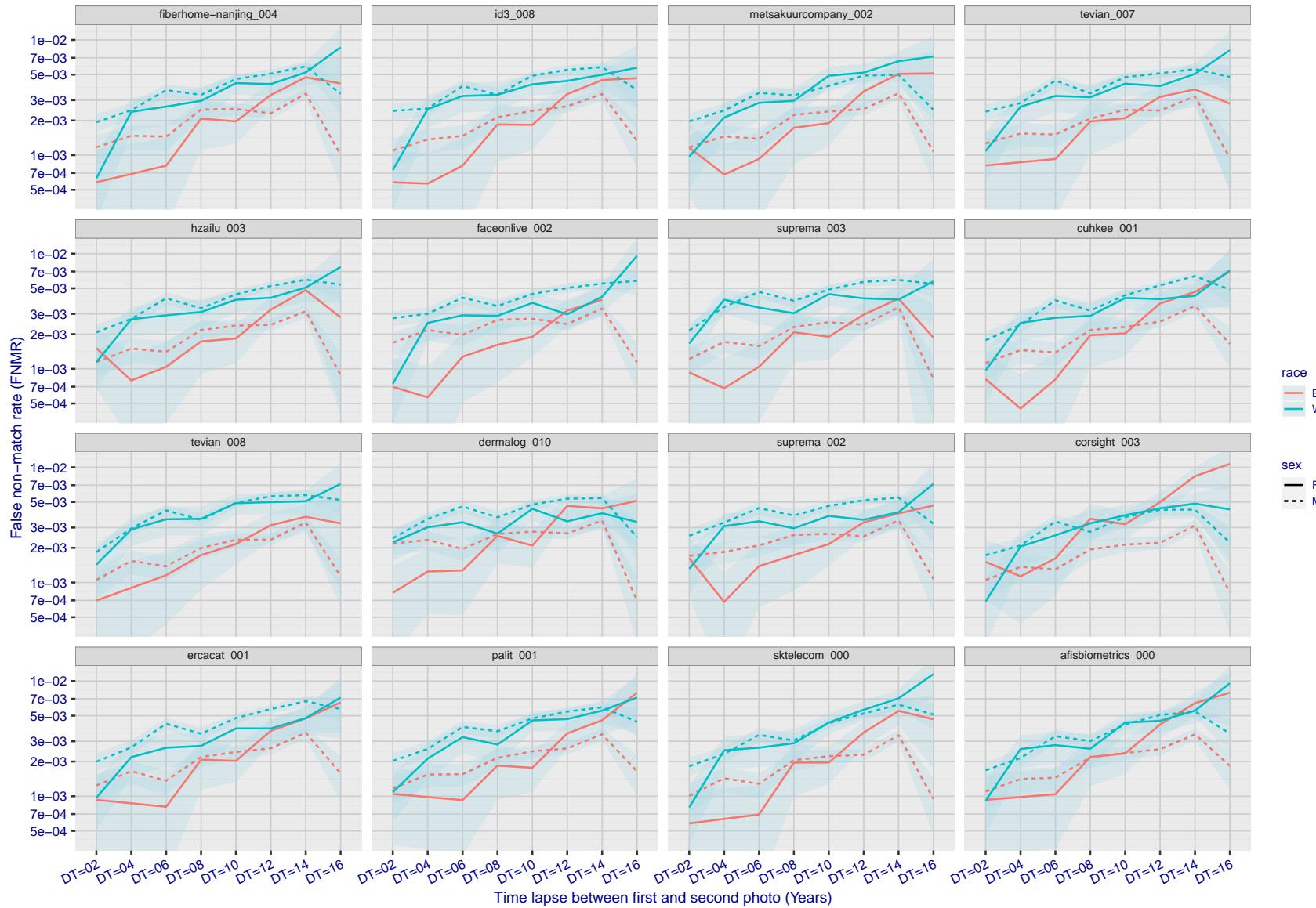


Figure 333: For the mugshot images, FNMR as a function of elapsed time between initial enrollment and second verification images. The panels appear most accurate first, and vertical scale changes on each page. The four traces correspond to images annotated with codes for black female, black male, white female, white male. The threshold is fixed for each algorithm to give FMR = 0.00001 over all (10^8) impostor comparisons. For short time-lapses, the most accurate algorithms give very few errors (FNMR < 0.001) so that the uncertainty estimates are high.

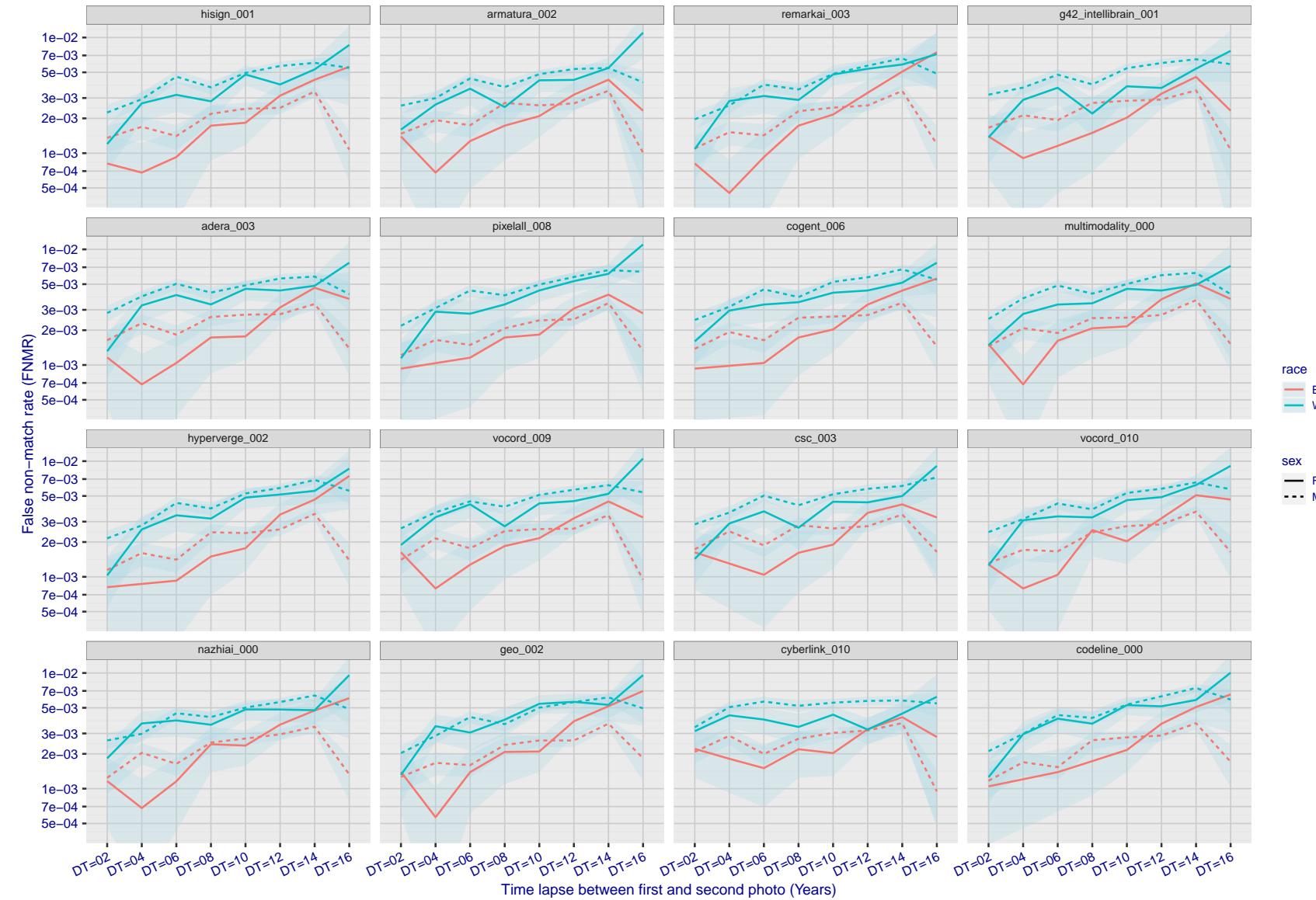


Figure 334: For the mugshot images, FNMR as a function of elapsed time between initial enrollment and second verification images. The panels appear most accurate first, and vertical scale changes on each page. The four traces correspond to images annotated with codes for black female, black male, white female, white male. The threshold is fixed for each algorithm to give $FMR = 0.00001$ over all (10^8) impostor comparisons. For short time-lapses, the most accurate algorithms give very few errors ($FNMR < 0.001$) so that the uncertainty estimates are high.

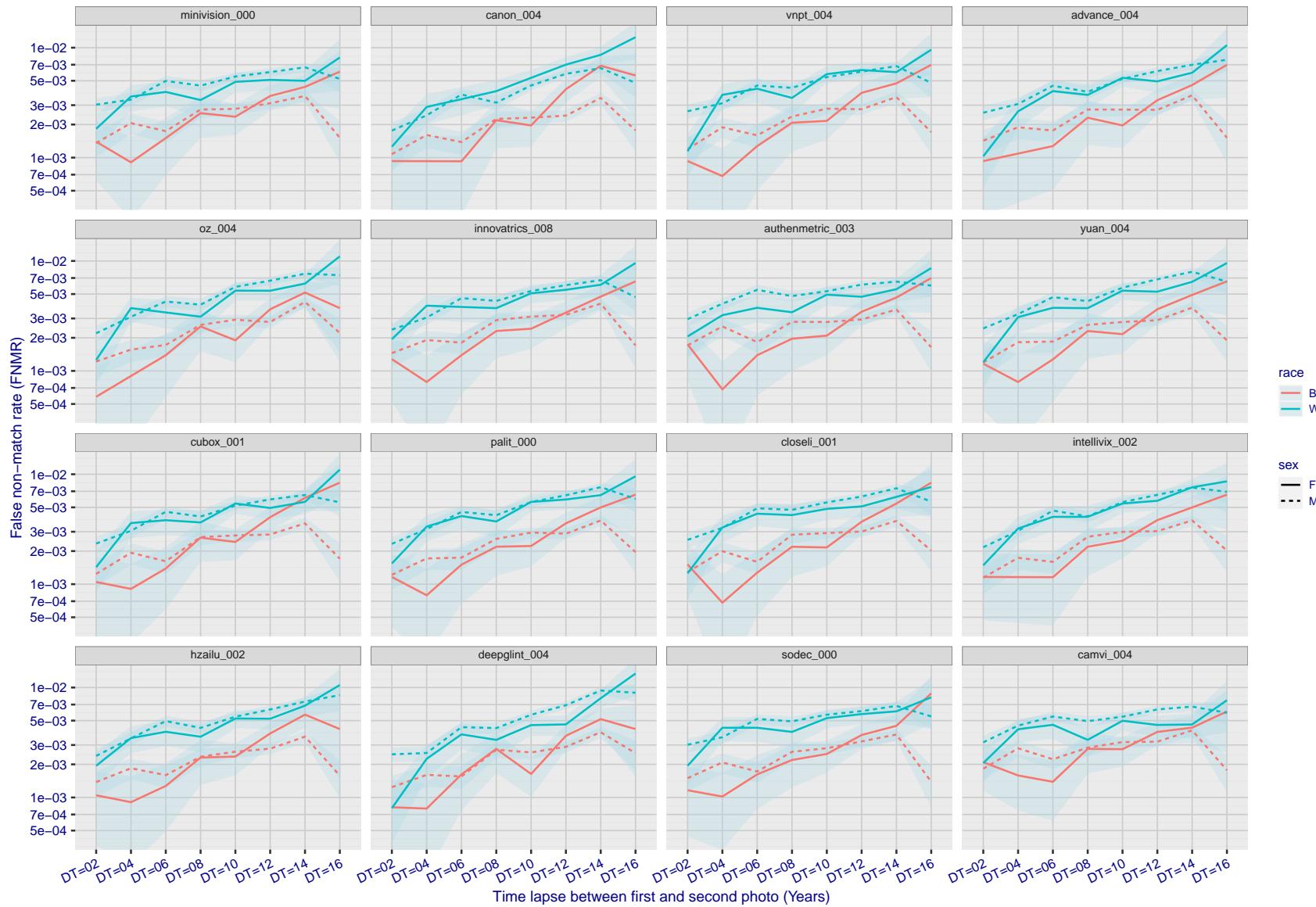


Figure 335: For the mugshot images, FNMR as a function of elapsed time between initial enrollment and second verification images. The panels appear most accurate first, and vertical scale changes on each page. The four traces correspond to images annotated with codes for black female, black male, white female, white male. The threshold is fixed for each algorithm to give FMR = 0.00001 over all (10^8) impostor comparisons. For short time-lapses, the most accurate algorithms give very few errors (FNMR < 0.001) so that the uncertainty estimates are high.

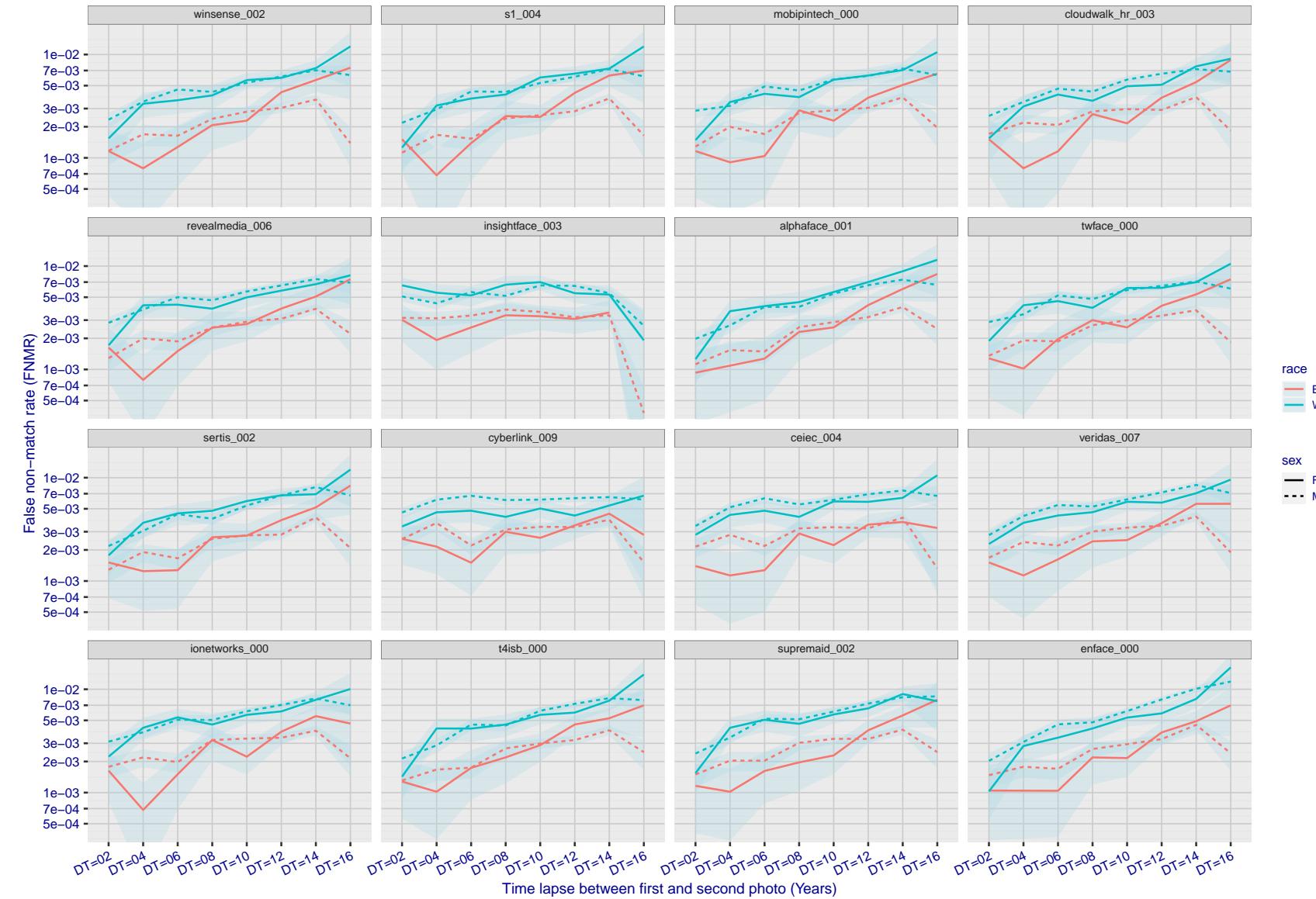


Figure 336: For the mugshot images, FNMR as a function of elapsed time between initial enrollment and second verification images. The panels appear most accurate first, and vertical scale changes on each page. The four traces correspond to images annotated with codes for black female, black male, white female, white male. The threshold is fixed for each algorithm to give $FMR = 0.00001$ over all (10^8) impostor comparisons. For short time-lapses, the most accurate algorithms give very few errors ($FNMR < 0.001$) so that the uncertainty estimates are high.

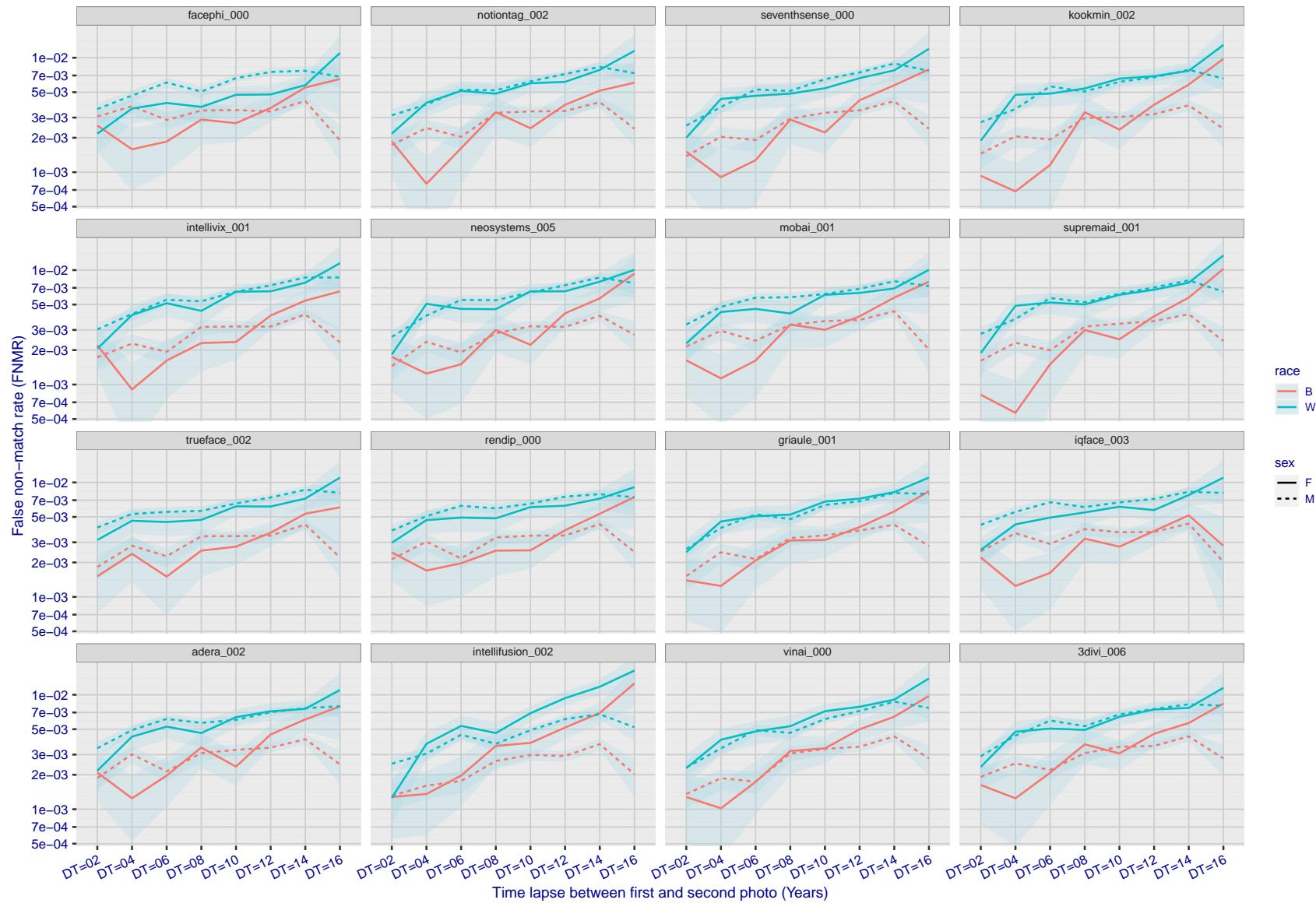


Figure 337: For the mugshot images, FNMR as a function of elapsed time between initial enrollment and second verification images. The panels appear most accurate first, and vertical scale changes on each page. The four traces correspond to images annotated with codes for black female, black male, white female, white male. The threshold is fixed for each algorithm to give FMR = 0.00001 over all (10^8) impostor comparisons. For short time-lapses, the most accurate algorithms give very few errors (FNMR < 0.001) so that the uncertainty estimates are high.

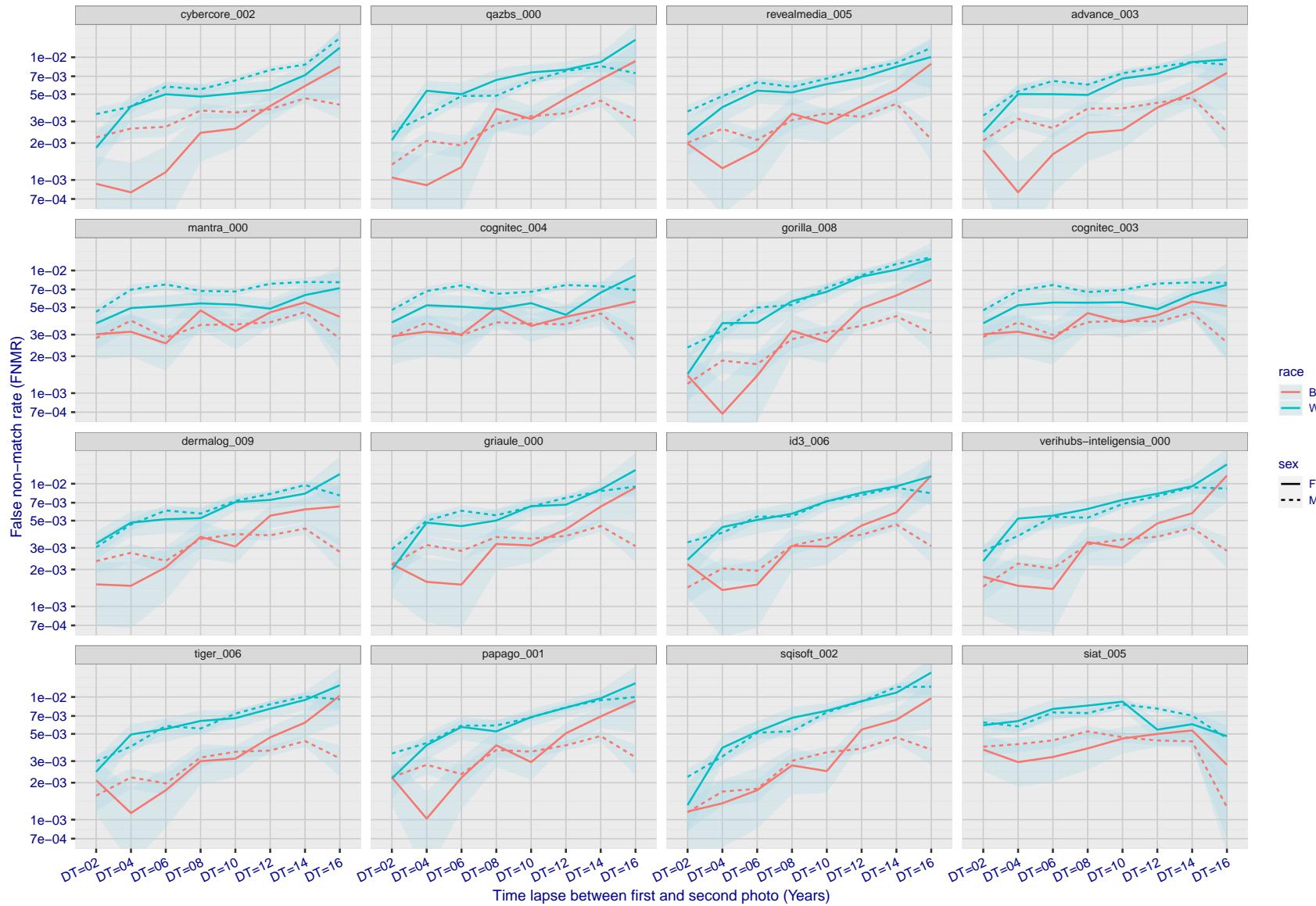


Figure 338: For the mugshot images, FNMR as a function of elapsed time between initial enrollment and second verification images. The panels appear most accurate first, and vertical scale changes on each page. The four traces correspond to images annotated with codes for black female, black male, white female, white male. The threshold is fixed for each algorithm to give $FMR = 0.00001$ over all (10^8) impostor comparisons. For short time-lapses, the most accurate algorithms give very few errors ($FNMR < 0.001$) so that the uncertainty estimates are high.

2022/11/07 10:56:27

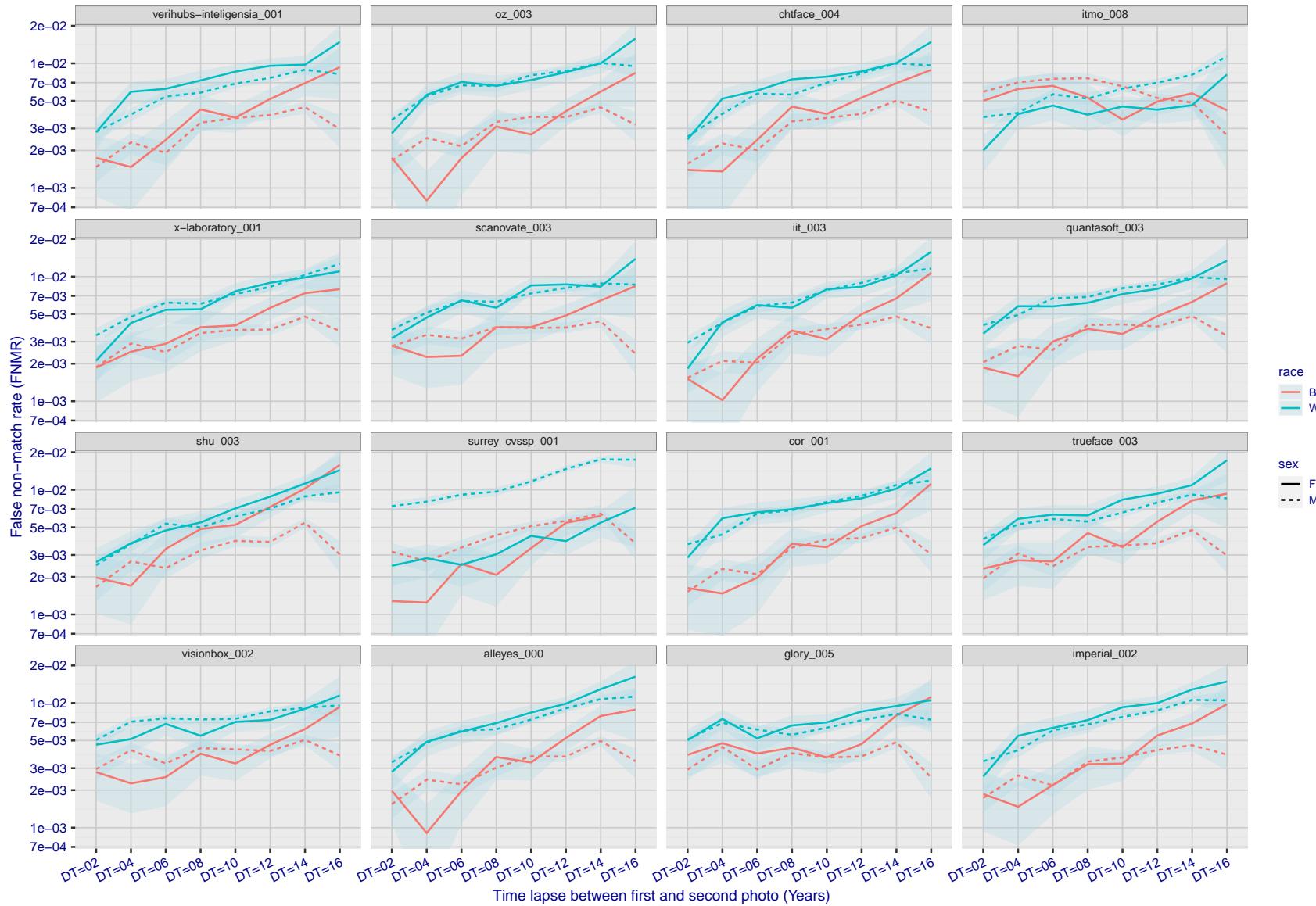


Figure 339: For the mugshot images, FNMR as a function of elapsed time between initial enrollment and second verification images. The panels appear most accurate first, and vertical scale changes on each page. The four traces correspond to images annotated with codes for black female, black male, white female, white male. The threshold is fixed for each algorithm to give $FMR = 0.00001$ over all (10^8) impostor comparisons. For short time-lapses, the most accurate algorithms give very few errors ($FNMR < 0.001$) so that the uncertainty estimates are high.

FNMR(T)
FMR(T)
"False non-match rate"
"False match rate"

2022/11/07 10:56:27

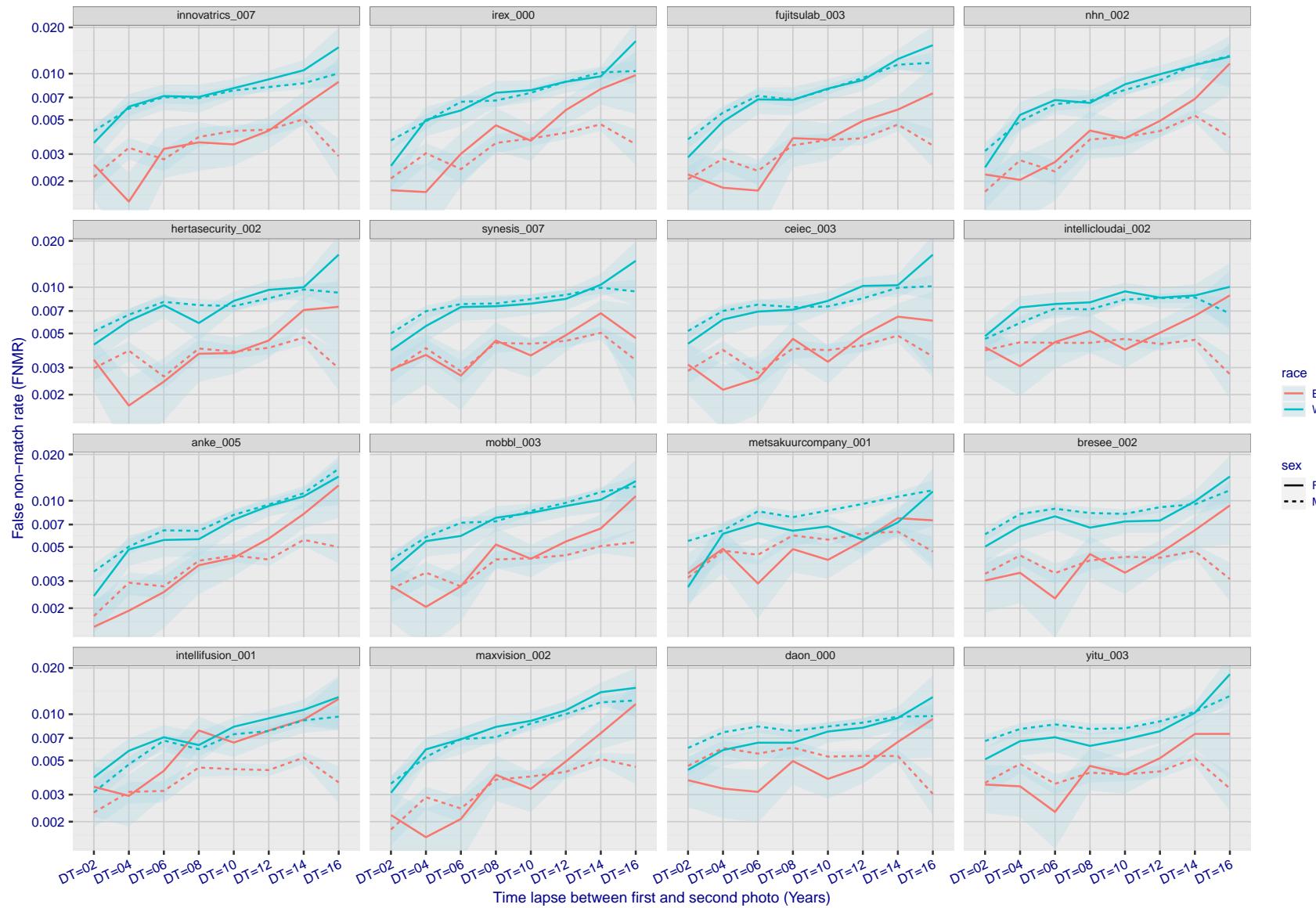


Figure 340: For the mugshot images, FNMR as a function of elapsed time between initial enrollment and second verification images. The panels appear most accurate first, and vertical scale changes on each page. The four traces correspond to images annotated with codes for black female, black male, white female, white male. The threshold is fixed for each algorithm to give FMR = 0.00001 over all (10^8) impostor comparisons. For short time-lapses, the most accurate algorithms give very few errors (FNMR < 0.001) so that the uncertainty estimates are high.

FNMR(T)
FMR(T)
"False non-match rate"
"False match rate"

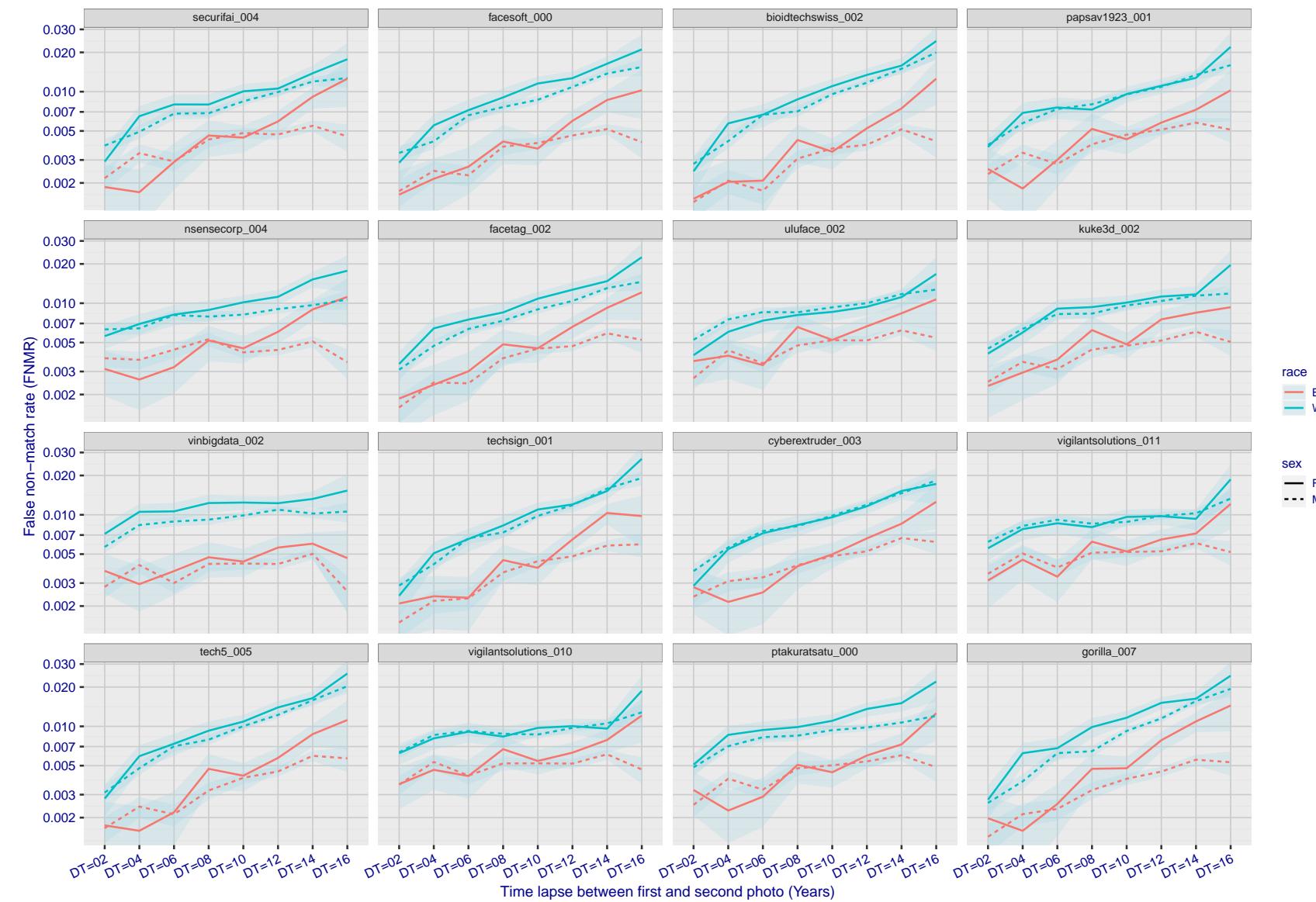


Figure 341: For the mugshot images, FNMR as a function of elapsed time between initial enrollment and second verification images. The panels appear most accurate first, and vertical scale changes on each page. The four traces correspond to images annotated with codes for black female, black male, white female, white male. The threshold is fixed for each algorithm to give FMR = 0.00001 over all (10^8) impostor comparisons. For short time-lapses, the most accurate algorithms give very few errors (FNMR < 0.001) so that the uncertainty estimates are high.

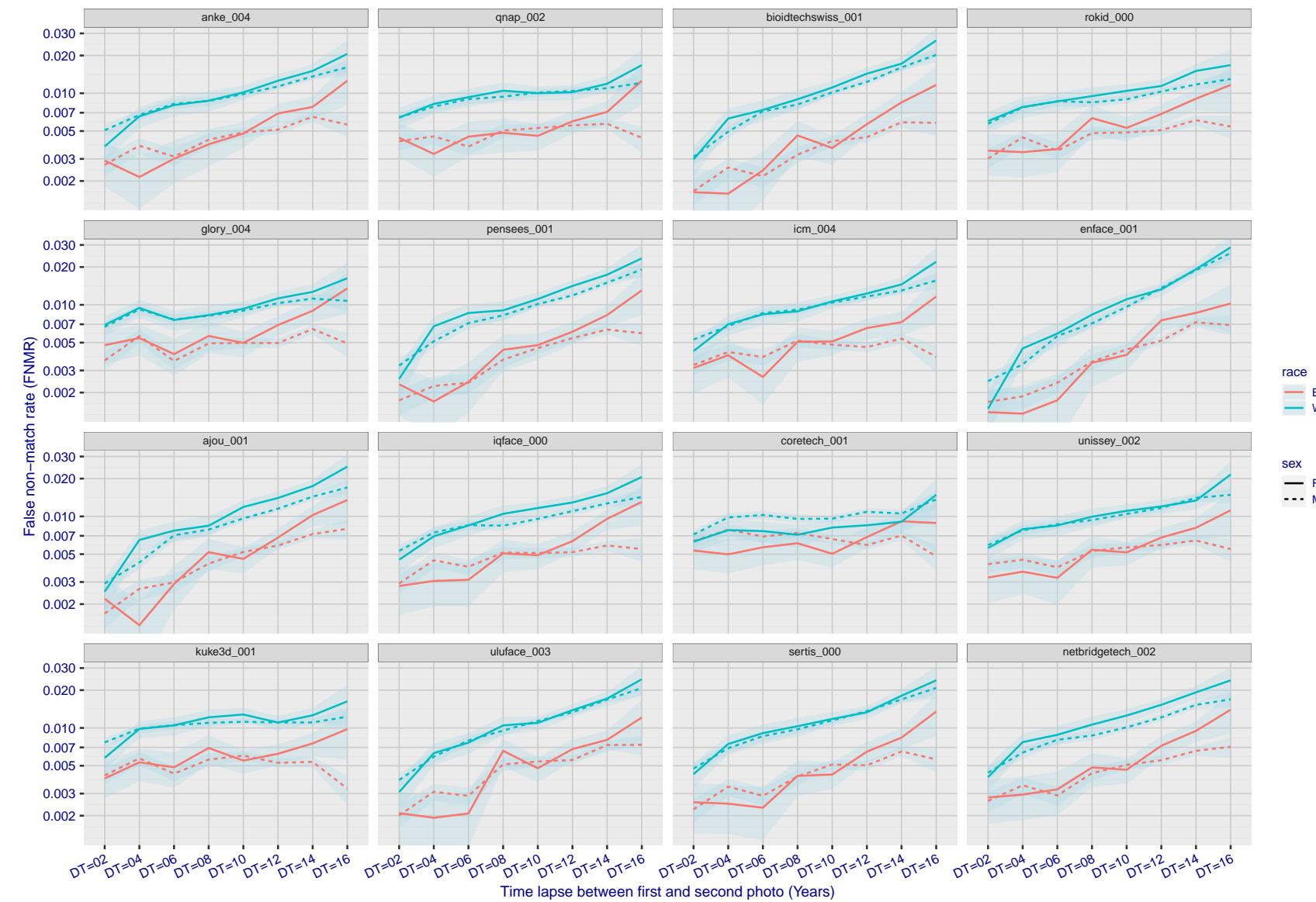


Figure 342: For the mugshot images, FNMR as a function of elapsed time between initial enrollment and second verification images. The panels appear most accurate first, and vertical scale changes on each page. The four traces correspond to images annotated with codes for black female, black male, white female, white male. The threshold is fixed for each algorithm to give FMR = 0.00001 over all (10^8) impostor comparisons. For short time-lapses, the most accurate algorithms give very few errors (FNMR < 0.001) so that the uncertainty estimates are high.

2022/11/07 10:56:27

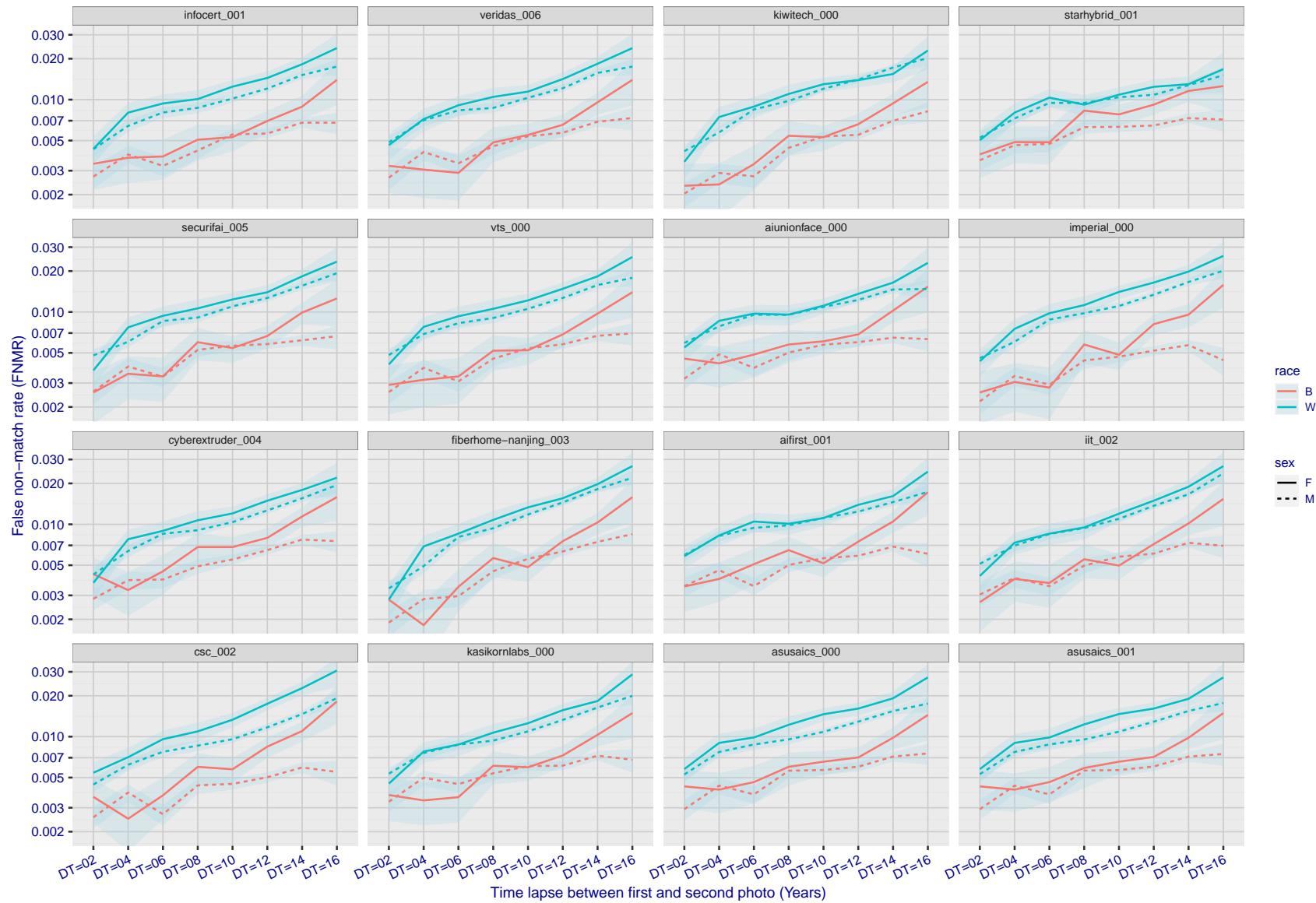


Figure 343: For the mugshot images, FNMR as a function of elapsed time between initial enrollment and second verification images. The panels appear most accurate first, and vertical scale changes on each page. The four traces correspond to images annotated with codes for black female, black male, white female, white male. The threshold is fixed for each algorithm to give FMR = 0.00001 over all (10^8) impostor comparisons. For short time-lapses, the most accurate algorithms give very few errors (FNMR < 0.001) so that the uncertainty estimates are high.

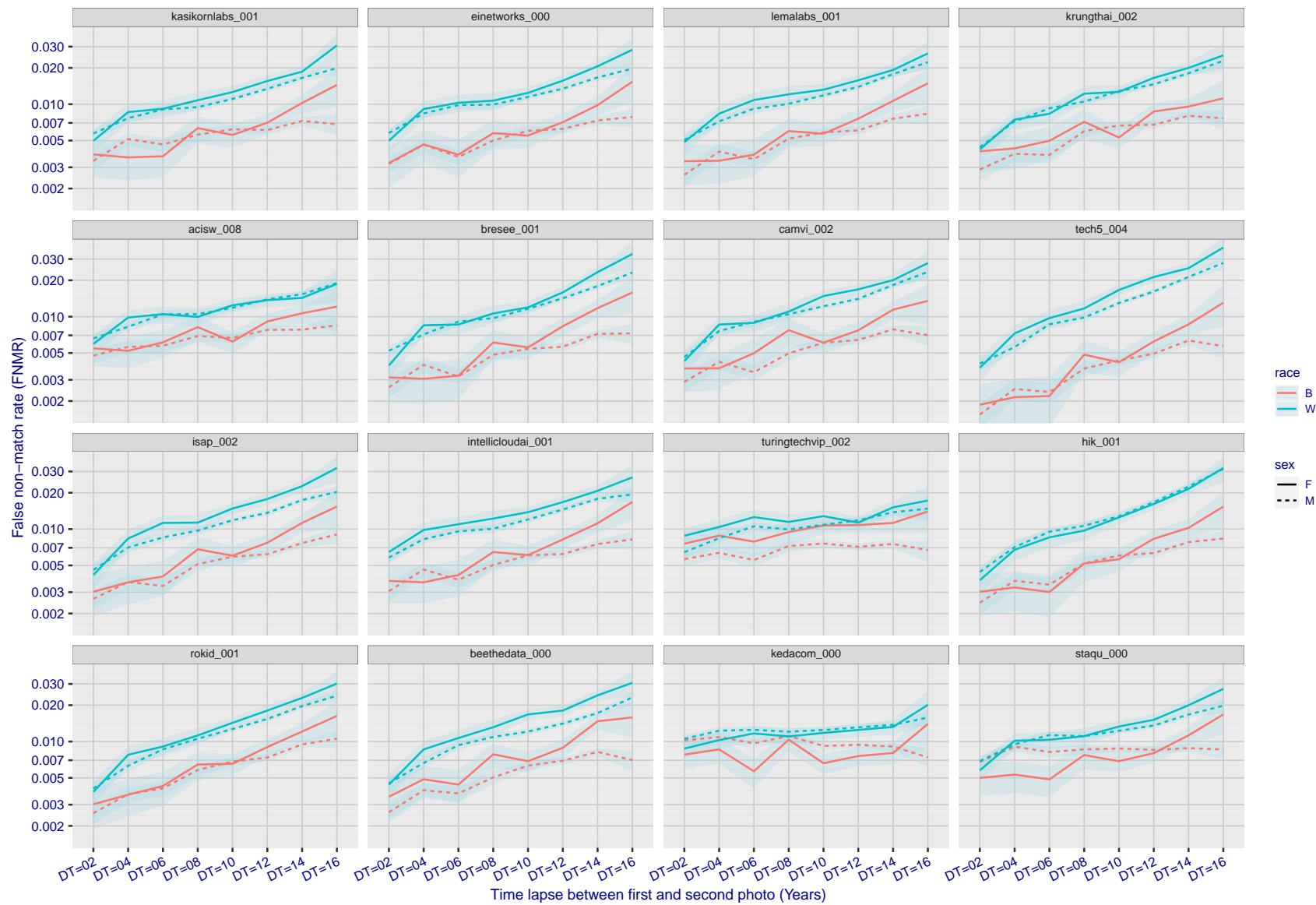


Figure 344: For the mugshot images, FNMR as a function of elapsed time between initial enrollment and second verification images. The panels appear most accurate first, and vertical scale changes on each page. The four traces correspond to images annotated with codes for black female, black male, white female, white male. The threshold is fixed for each algorithm to give FMR = 0.00001 over all (10^8) impostor comparisons. For short time-lapses, the most accurate algorithms give very few errors (FNMR < 0.001) so that the uncertainty estimates are high.

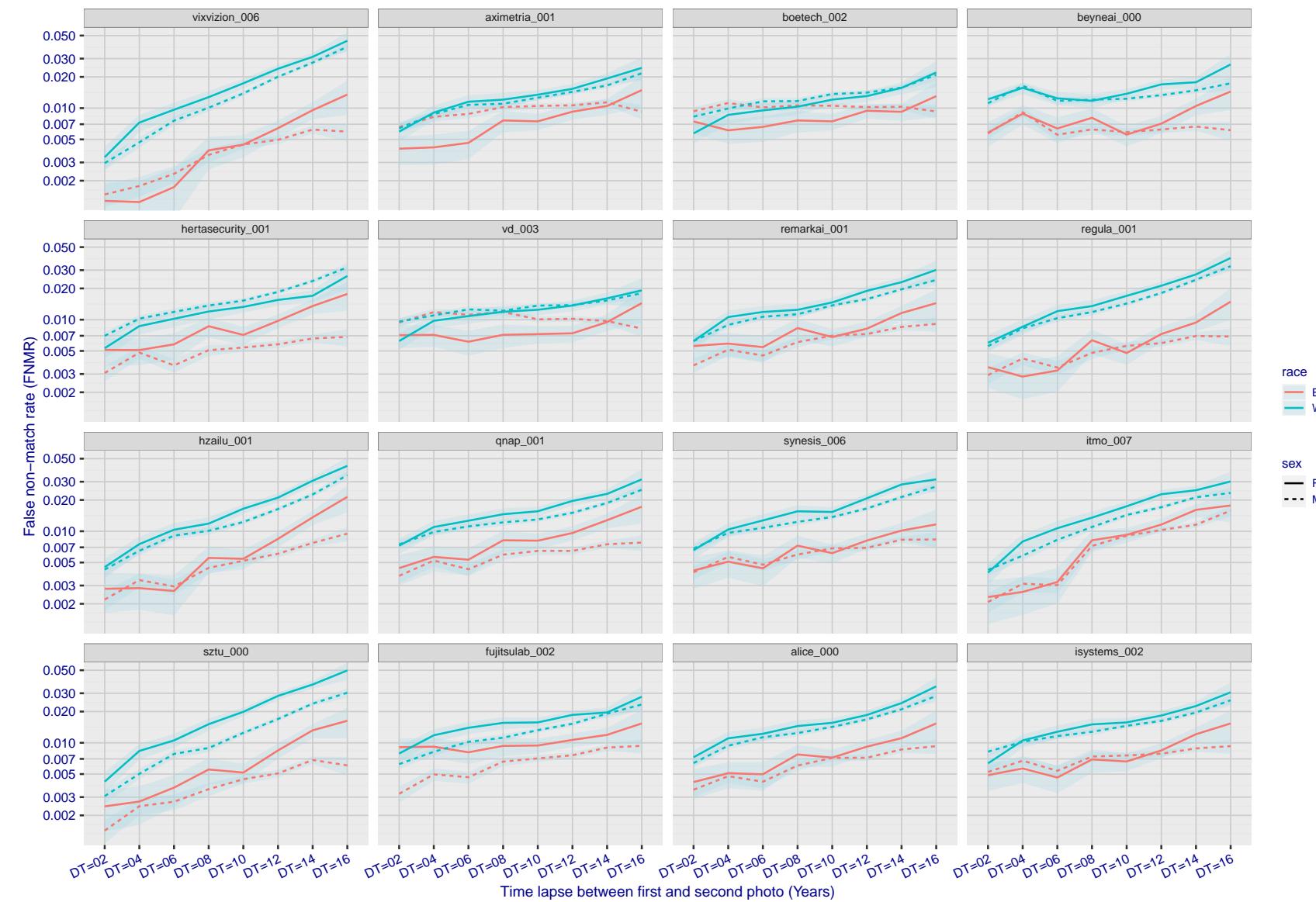


Figure 345: For the mugshot images, FNMR as a function of elapsed time between initial enrollment and second verification images. The panels appear most accurate first, and vertical scale changes on each page. The four traces correspond to images annotated with codes for black female, black male, white female, white male. The threshold is fixed for each algorithm to give FMR = 0.00001 over all (10^8) impostor comparisons. For short time-lapses, the most accurate algorithms give very few errors (FNMR < 0.001) so that the uncertainty estimates are high.

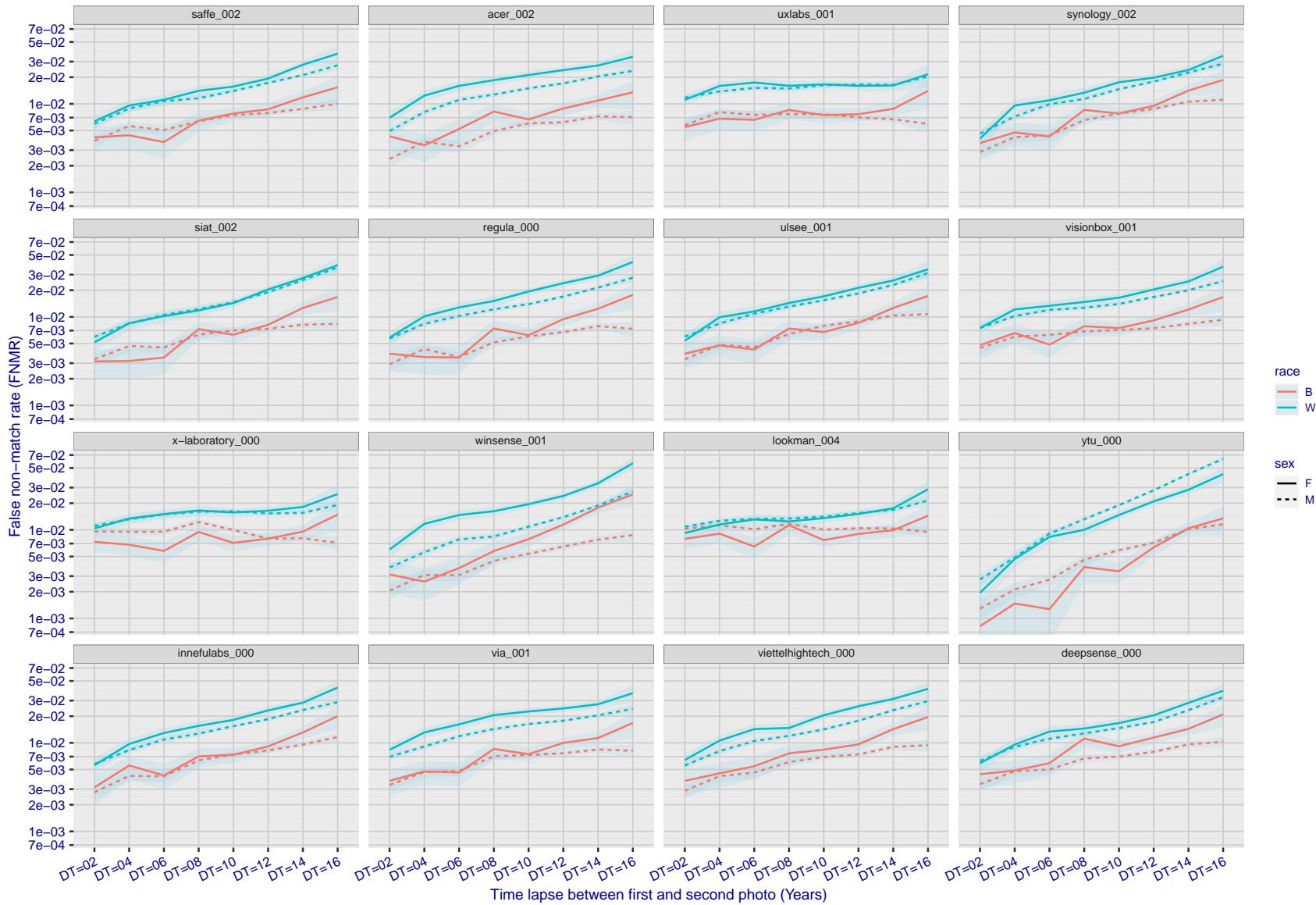


Figure 346: For the mugshot images, FNMR as a function of elapsed time between initial enrollment and second verification images. The panels appear most accurate first, and vertical scale changes on each page. The four traces correspond to images annotated with codes for black female, black male, white female, white male. The threshold is fixed for each algorithm to give $FMR = 0.00001$ over all (10^8) impostor comparisons. For short time-lapses, the most accurate algorithms give very few errors ($FNMR < 0.001$) so that the uncertainty estimates are high.

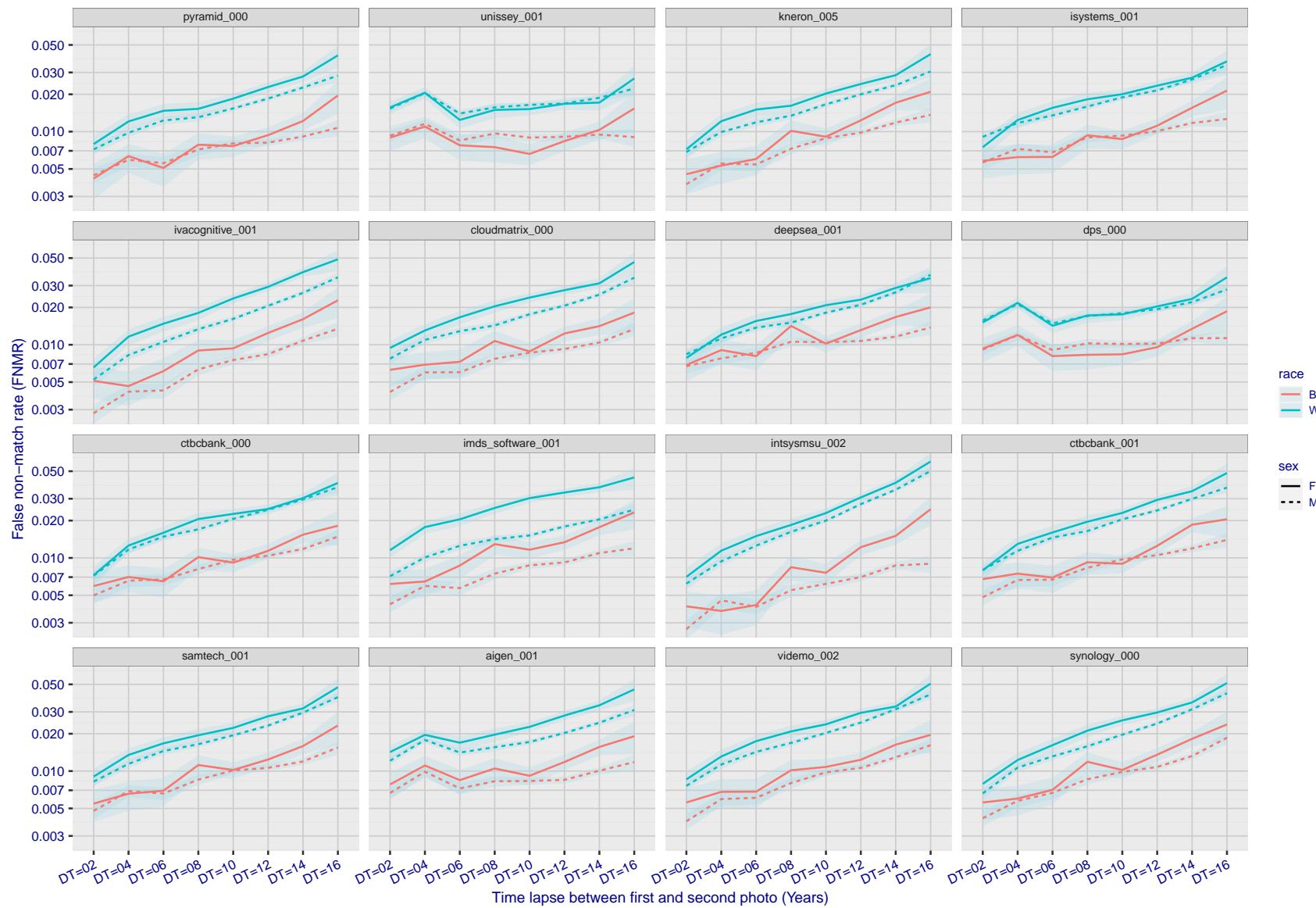


Figure 347: For the mugshot images, FNMR as a function of elapsed time between initial enrollment and second verification images. The panels appear most accurate first, and vertical scale changes on each page. The four traces correspond to images annotated with codes for black female, black male, white female, white male. The threshold is fixed for each algorithm to give FMR = 0.00001 over all (10^8) impostor comparisons. For short time-lapses, the most accurate algorithms give very few errors (FNMR < 0.001) so that the uncertainty estimates are high.

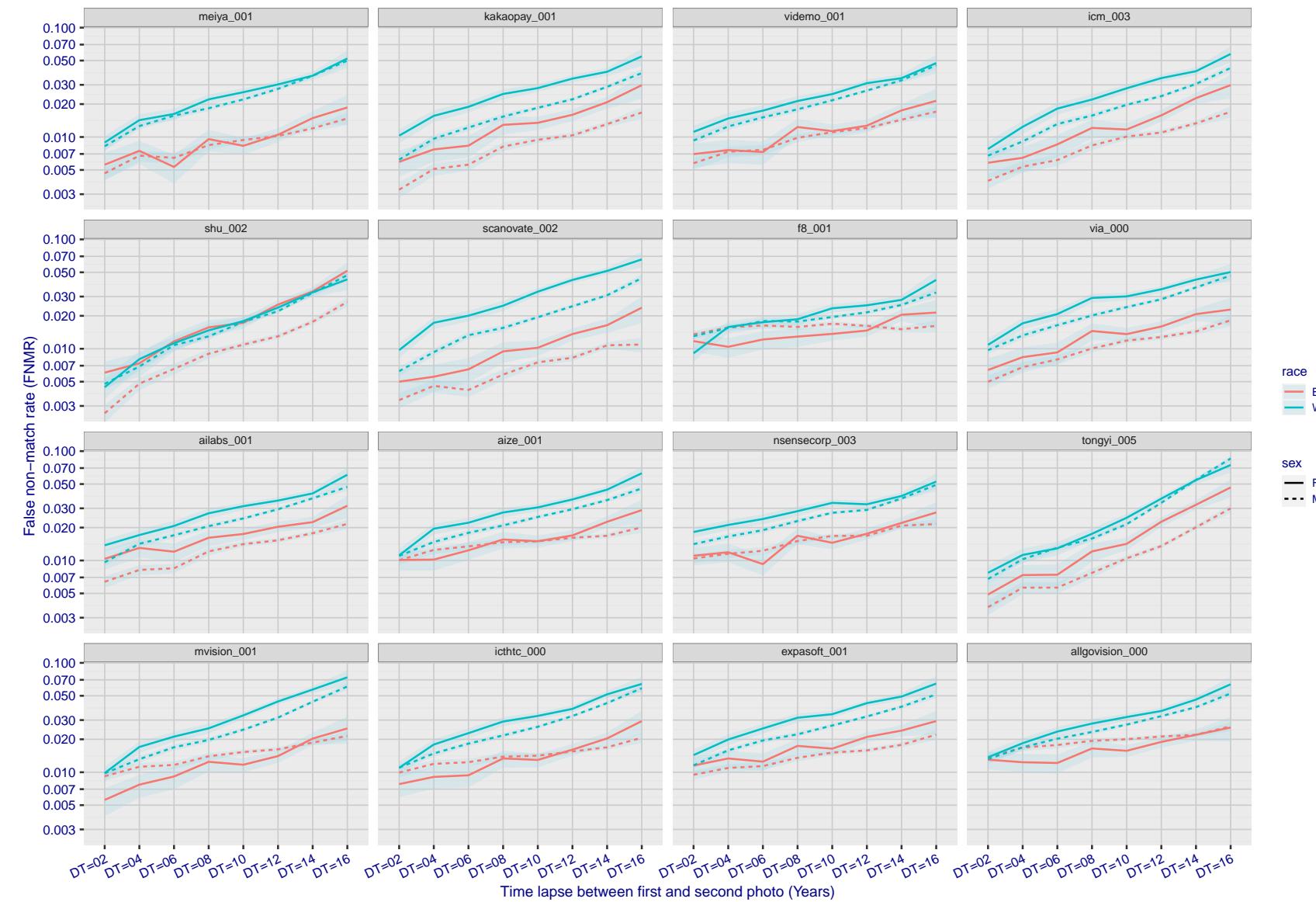


Figure 348: For the mugshot images, FNMR as a function of elapsed time between initial enrollment and second verification images. The panels appear most accurate first, and vertical scale changes on each page. The four traces correspond to images annotated with codes for black female, black male, white female, white male. The threshold is fixed for each algorithm to give FMR = 0.00001 over all (10^8) impostor comparisons. For short time-lapses, the most accurate algorithms give very few errors (FNMR < 0.001) so that the uncertainty estimates are high.

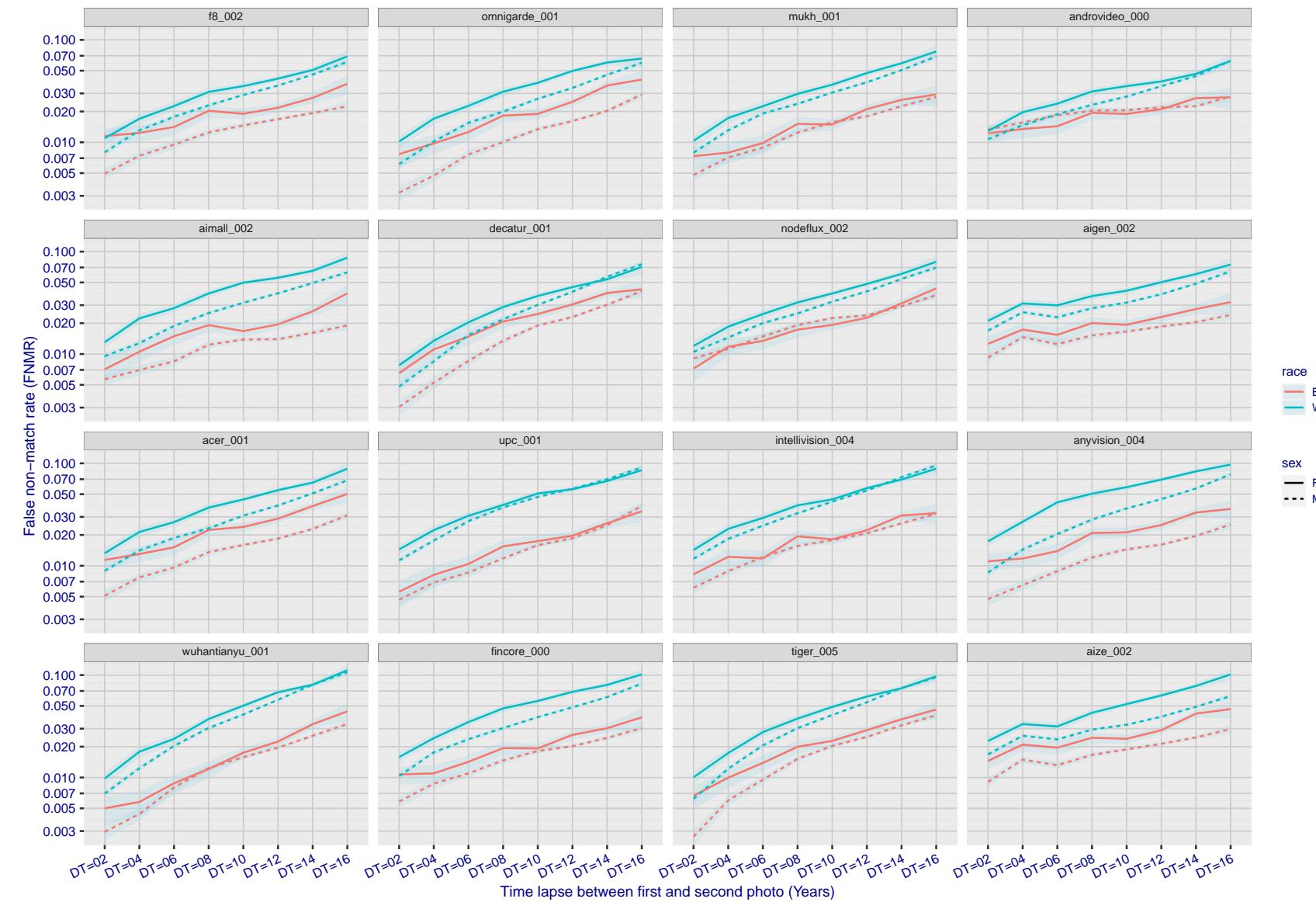


Figure 349: For the mugshot images, FNMR as a function of elapsed time between initial enrollment and second verification images. The panels appear most accurate first, and vertical scale changes on each page. The four traces correspond to images annotated with codes for black female, black male, white female, white male. The threshold is fixed for each algorithm to give $FMR = 0.00001$ over all (10^8) impostor comparisons. For short time-lapses, the most accurate algorithms give very few errors ($FNMR < 0.001$) so that the uncertainty estimates are high.

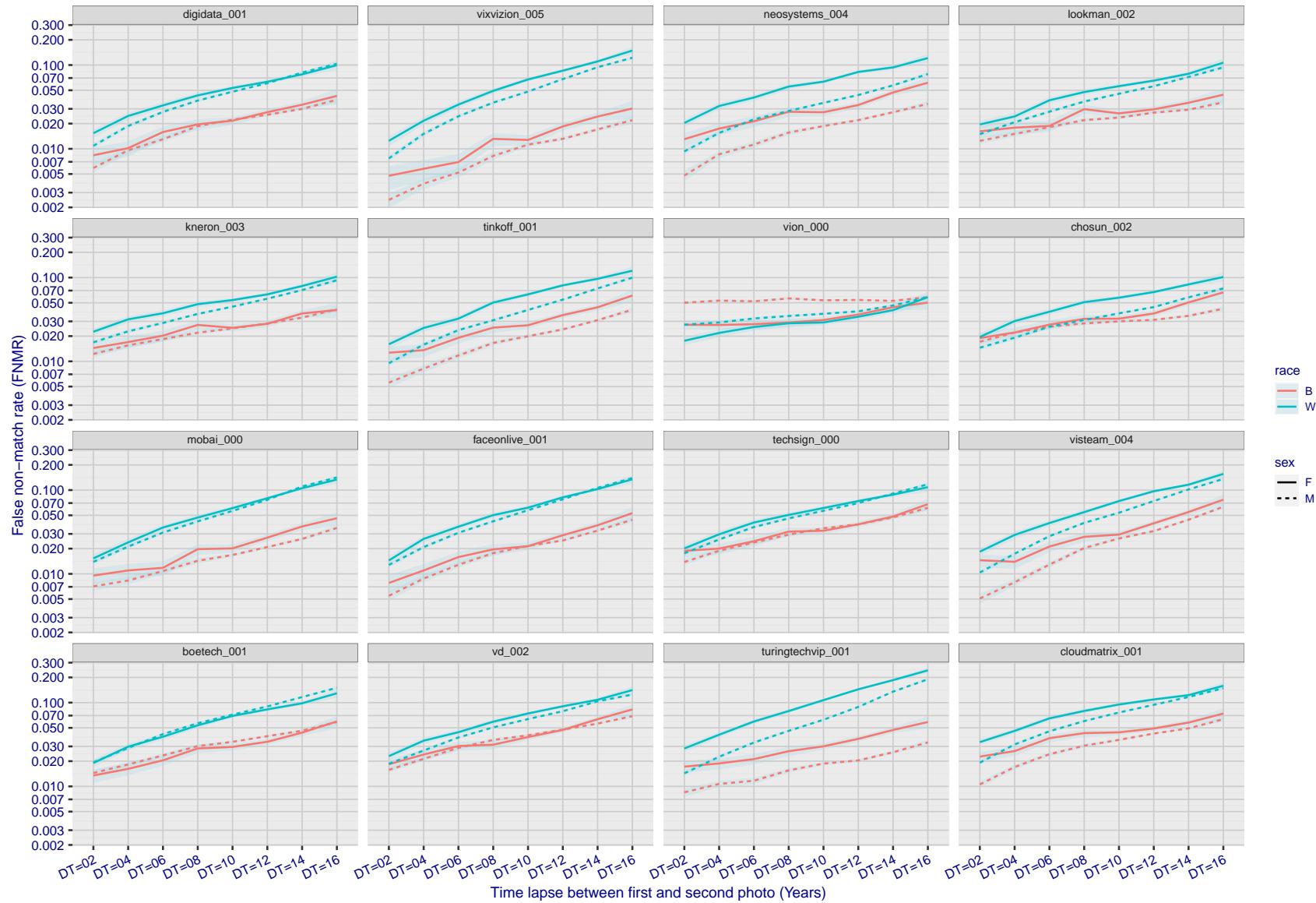


Figure 350: For the mugshot images, FNMR as a function of elapsed time between initial enrollment and second verification images. The panels appear most accurate first, and vertical scale changes on each page. The four traces correspond to images annotated with codes for black female, black male, white female, white male. The threshold is fixed for each algorithm to give FMR = 0.00001 over all (10^8) impostor comparisons. For short time-lapses, the most accurate algorithms give very few errors (FNMR < 0.001) so that the uncertainty estimates are high.

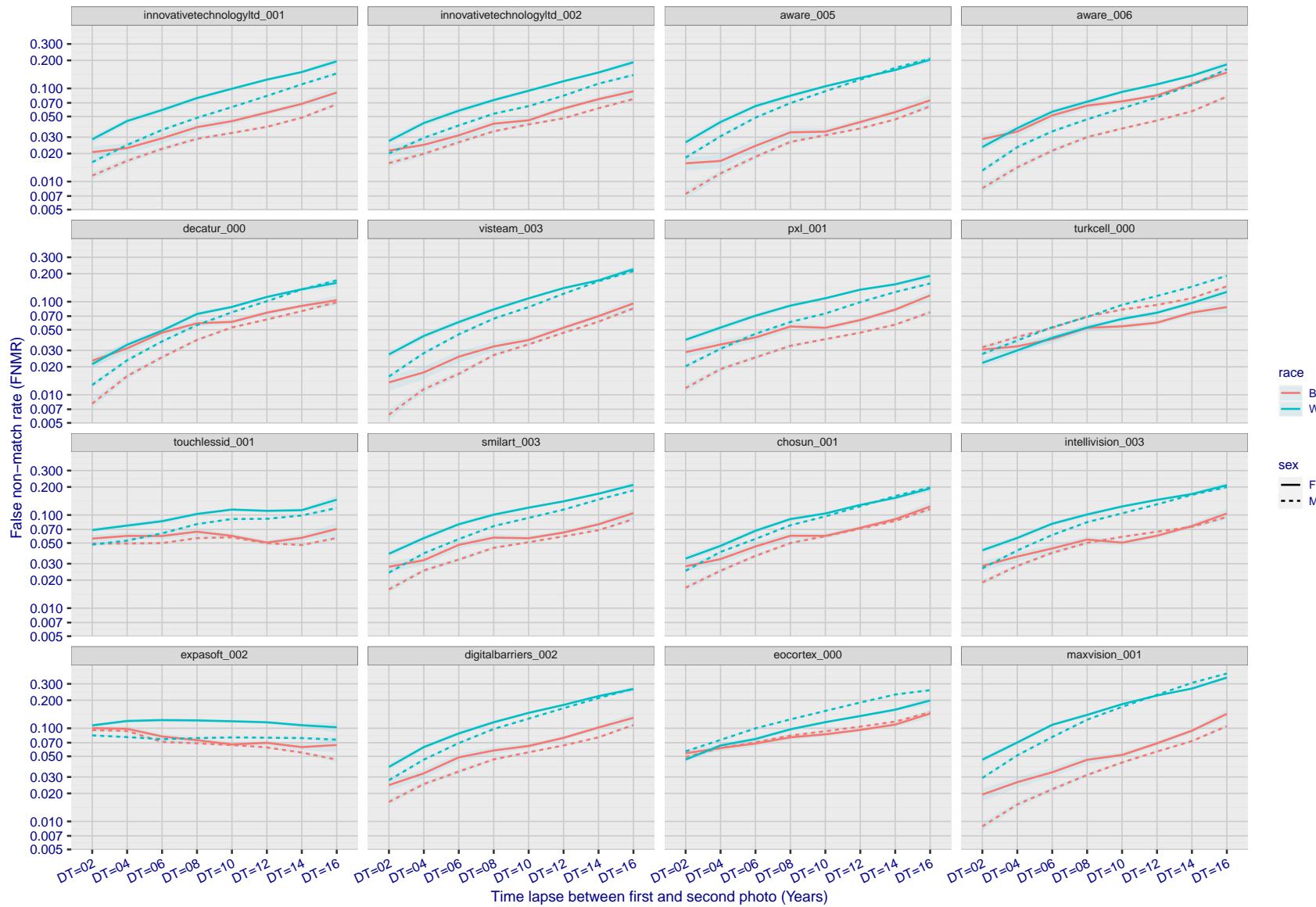


Figure 351: For the mugshot images, FNMR as a function of elapsed time between initial enrollment and second verification images. The panels appear most accurate first, and vertical scale changes on each page. The four traces correspond to images annotated with codes for black female, black male, white female, white male. The threshold is fixed for each algorithm to give FMR = 0.00001 over all (10^8) impostor comparisons. For short time-lapses, the most accurate algorithms give very few errors (FNMR < 0.001) so that the uncertainty estimates are high.

2022/11/07 10:56:27

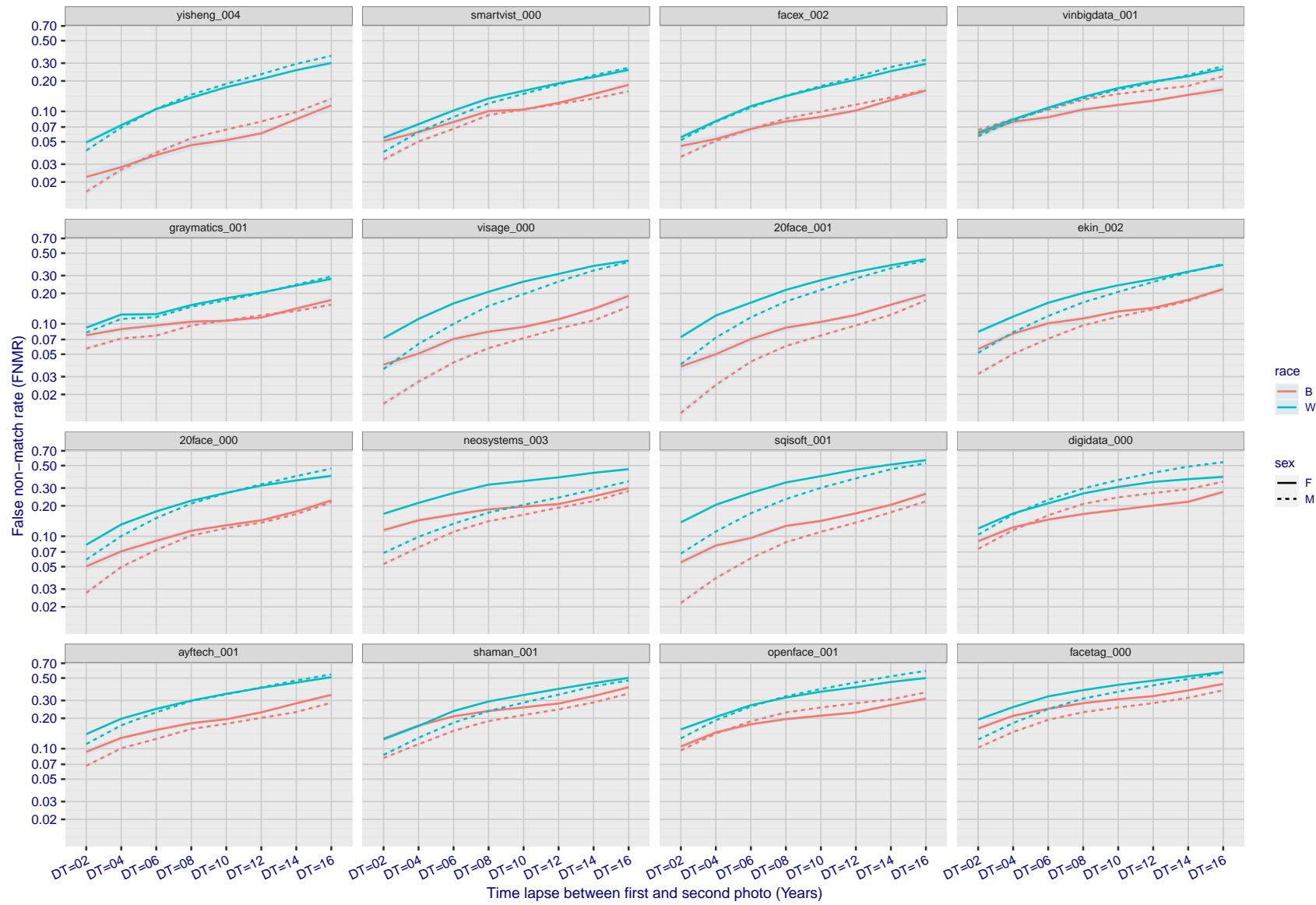


Figure 352: For the mugshot images, FNMR as a function of elapsed time between initial enrollment and second verification images. The panels appear most accurate first, and vertical scale changes on each page. The four traces correspond to images annotated with codes for black female, black male, white female, white male. The threshold is fixed for each algorithm to give FMR = 0.00001 over all (10^8) impostor comparisons. For short time-lapses, the most accurate algorithms give very few errors (FNMR < 0.001) so that the uncertainty estimates are high.

FNMR(T)
FMR(T)
"False non-match rate"
"False match rate"

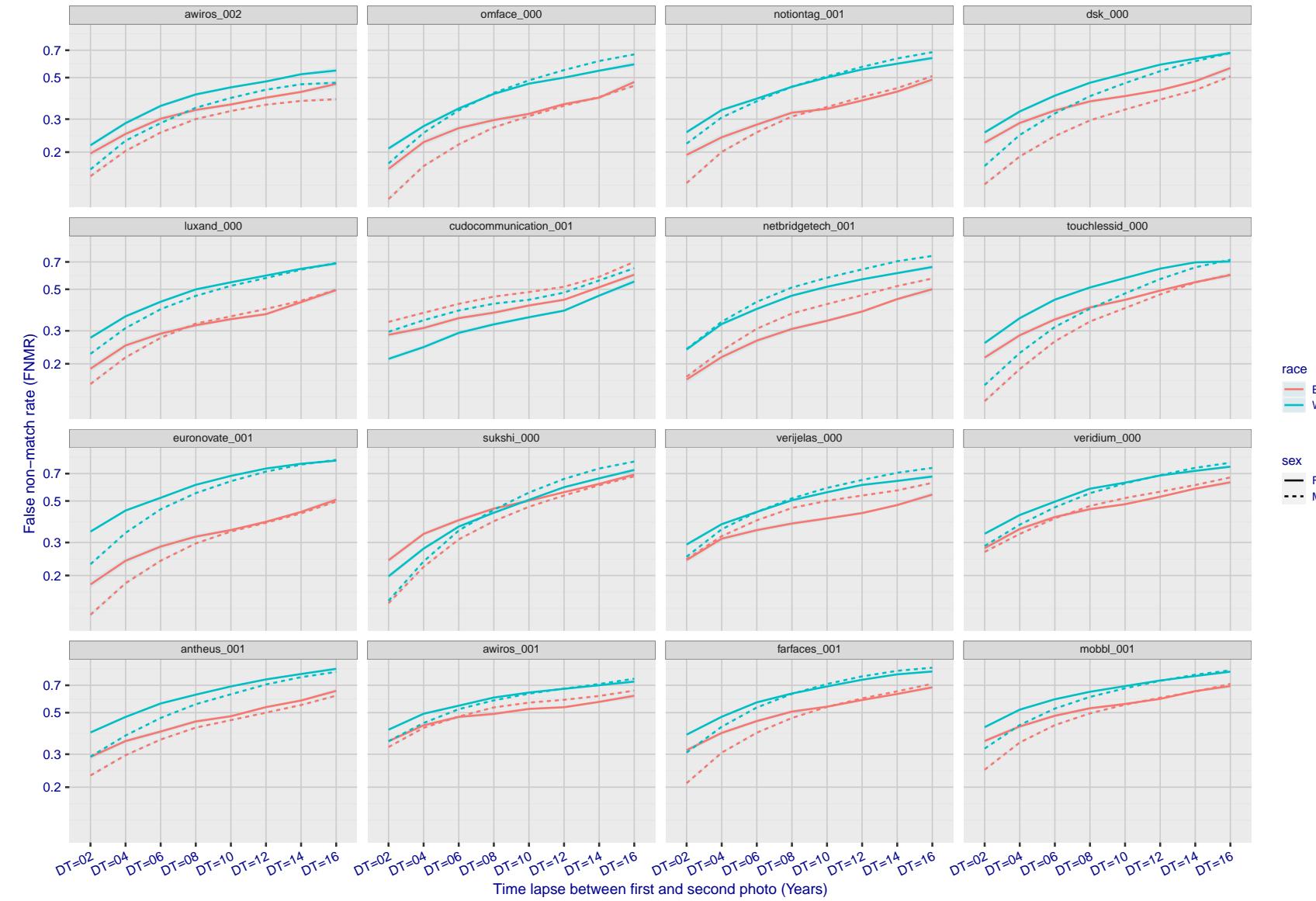


Figure 353: For the mugshot images, FNMR as a function of elapsed time between initial enrollment and second verification images. The panels appear most accurate first, and vertical scale changes on each page. The four traces correspond to images annotated with codes for black female, black male, white female, white male. The threshold is fixed for each algorithm to give FMR = 0.00001 over all (10^8) impostor comparisons. For short time-lapses, the most accurate algorithms give very few errors (FNMR < 0.001) so that the uncertainty estimates are high.

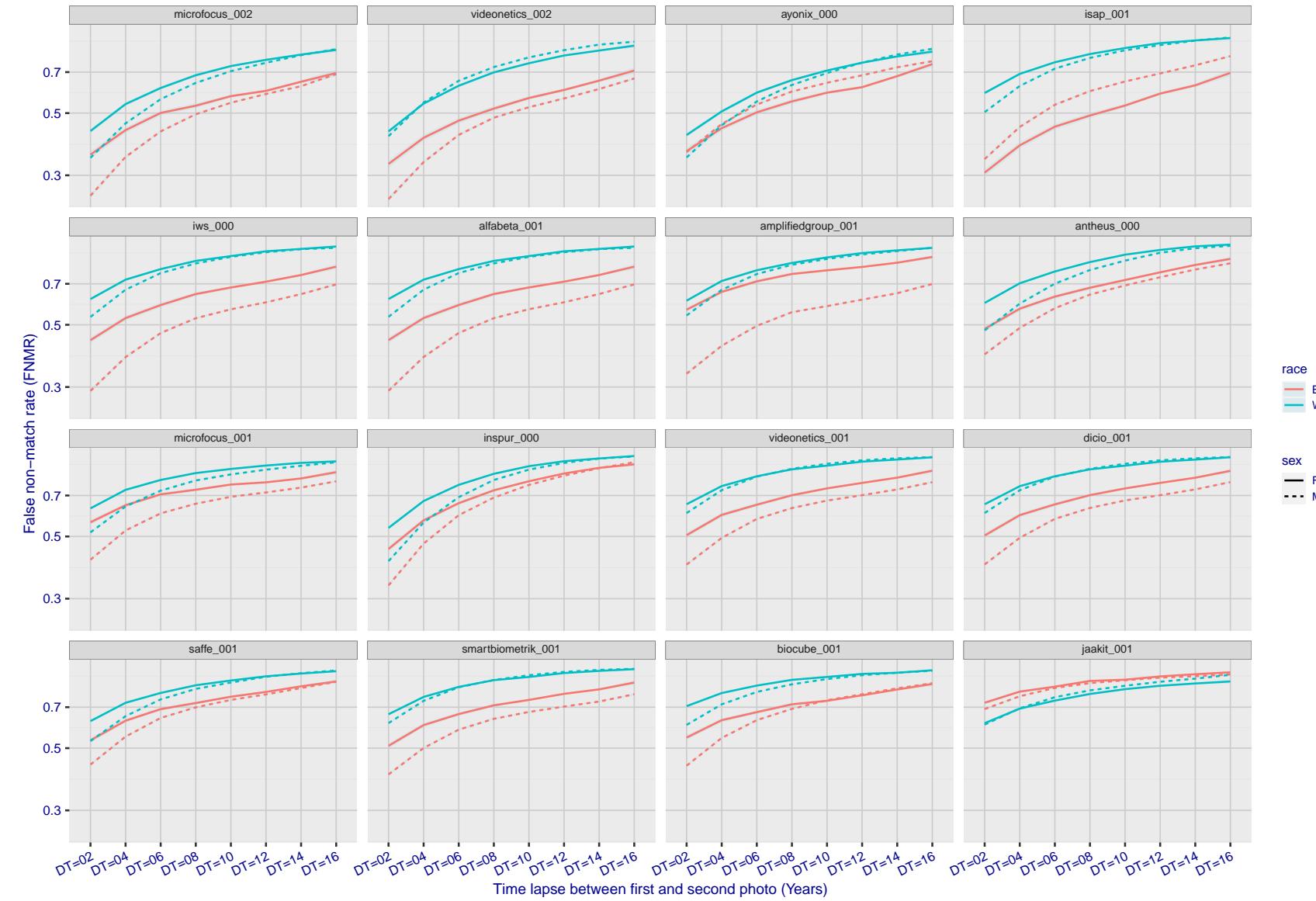


Figure 354: For the mugshot images, FNMR as a function of elapsed time between initial enrollment and second verification images. The panels appear most accurate first, and vertical scale changes on each page. The four traces correspond to images annotated with codes for black female, black male, white female, white male. The threshold is fixed for each algorithm to give $FMR = 0.00001$ over all (10^8) impostor comparisons. For short time-lapses, the most accurate algorithms give very few errors ($FNMR < 0.001$) so that the uncertainty estimates are high.

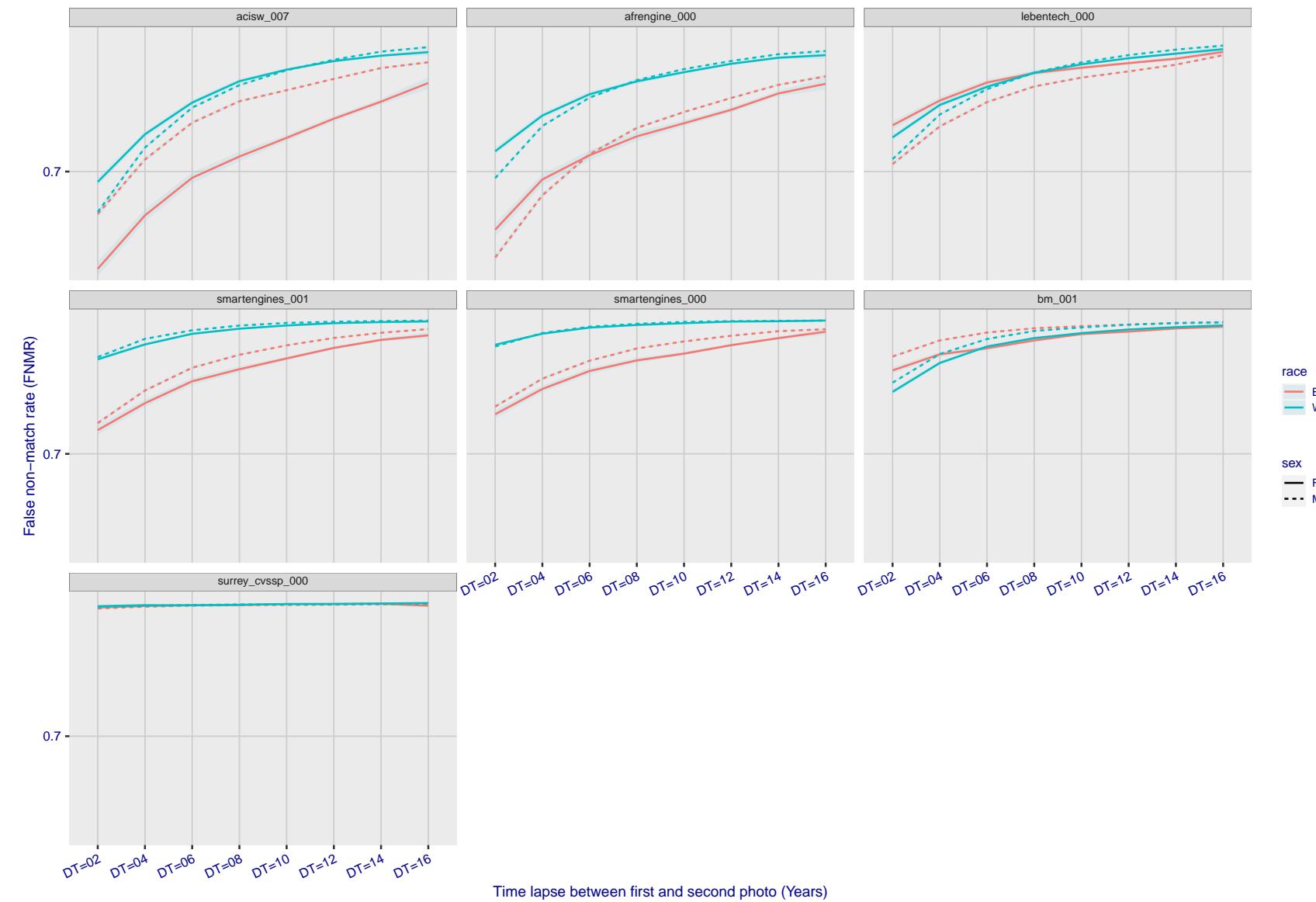


Figure 355: For the mugshot images, FNMR as a function of elapsed time between initial enrollment and second verification images. The panels appear most accurate first, and vertical scale changes on each page. The four traces correspond to images annotated with codes for black female, black male, white female, white male. The threshold is fixed for each algorithm to give $FMR = 0.00001$ over all (10^8) impostor comparisons. For short time-lapses, the most accurate algorithms give very few errors ($FNMR < 0.001$) so that the uncertainty estimates are high.

3.5.3 Effect of age on genuine subjects

Background: Faces change appearance throughout life. Face recognition algorithms have previously been reported to give better accuracy on older individuals (See NIST IR 8009).

Goal: To quantify false non-match rates (FNMR) as a function of age, without an ageing component.

Methods: Using the visa images, which span fewer than five years, thresholds are determined that give FMR = 0.001 and 0.0001 over the entire impostor set. Then FNMR is measured over 1000 bootstrap replications of the genuine scores.

Results: For the visa images, Figure 394 shows how false non-match rates for genuine users, as a function of age group.

The notable aspects are:

- ▷ Younger subjects give considerably higher FNMR. This is likely due to rapid growth and change in facial appearance.
- ▷ FNMR trends down throughout life. The last bin, AGE > 72, contains fewer than 140 mated pairs, and may be affected by small sample size.

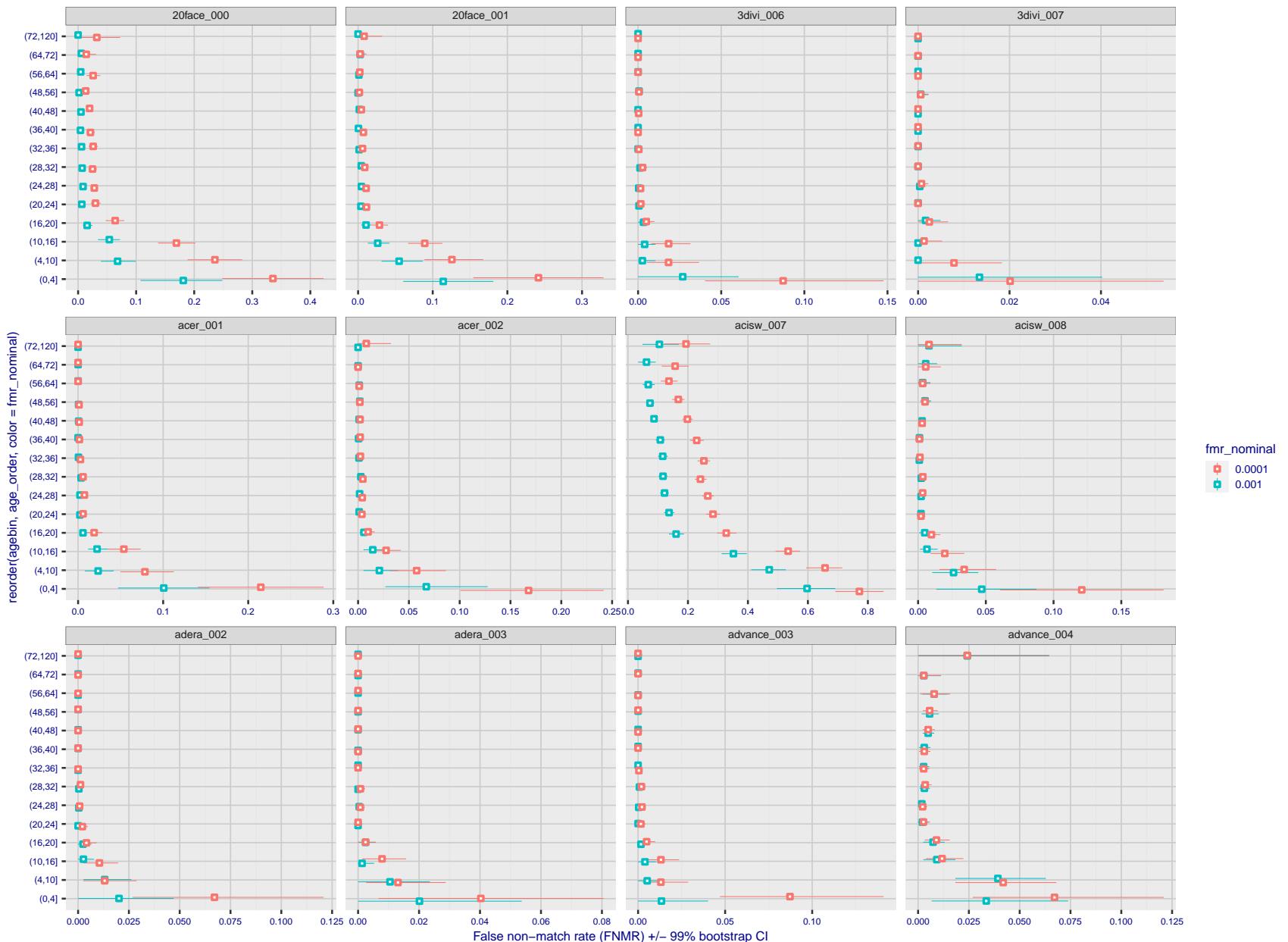


Figure 356: For the visa images, the dots show FNMR by age group for two operating thresholds corresponding to $FMR = \{0.001, 0.0001\}$ computed over all on the order of 10^{10} impostor scores. The FMR in each bin will vary also - see subsequent impostor heatmaps in sec. 3.6.2. Given a pair of face images taken at different times, we assign the comparison to the bin that is the arithmetic average of the subject's ages. This plot shows only the effect of age, not ageing. The number of comparisons in each bin is generally in the thousands, however the first and last bins are computed over 149 and 124 respectively. The error rates in some (adult) cases are zero, and in others the DET is flat so the error rates at the two thresholds are identical. The lines span 1% and 99% of bootstrap replicated FNMR estimates.

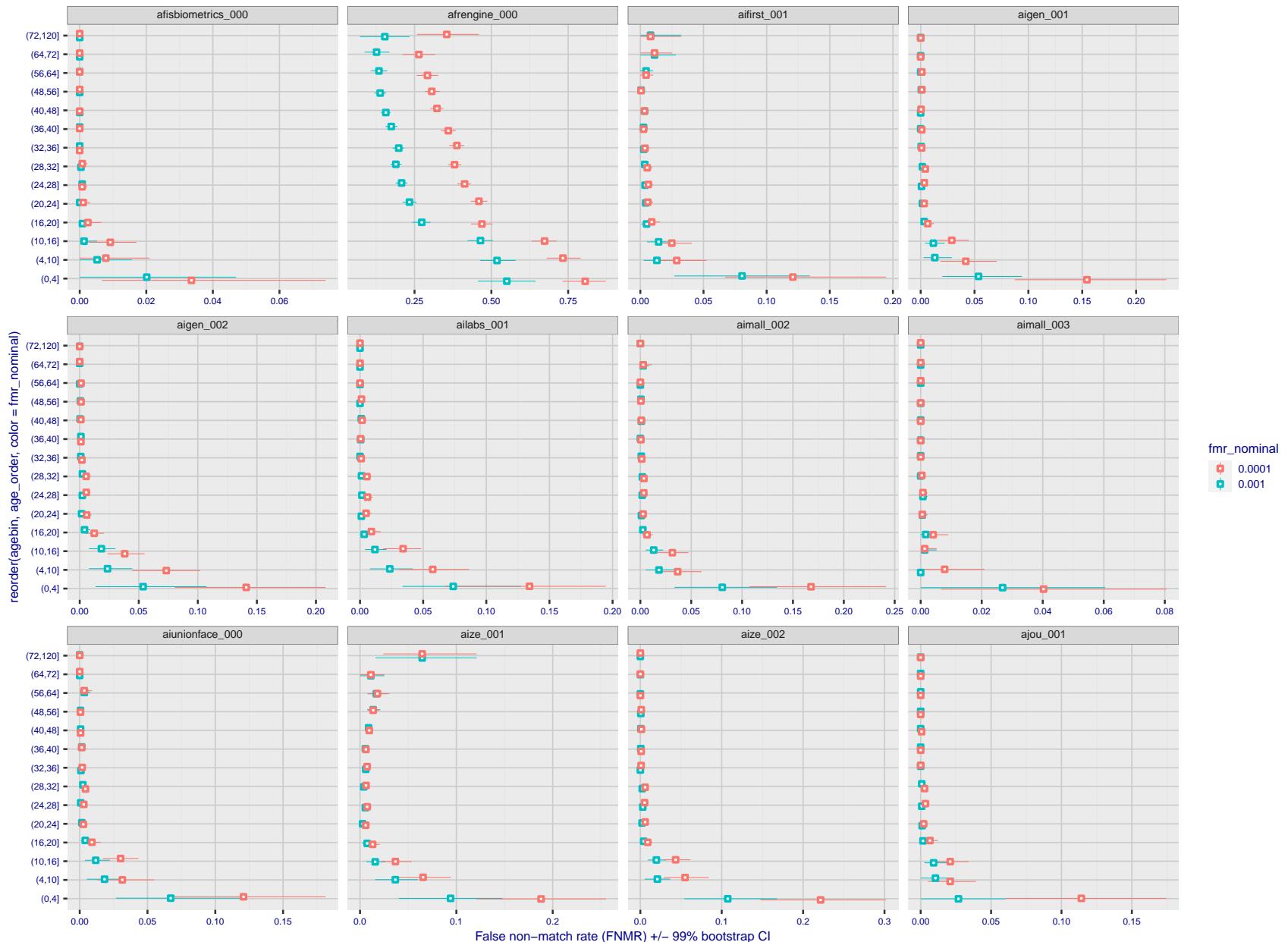


Figure 357: For the visa images, the dots show FNMR by age group for two operating thresholds corresponding to $FMR = \{0.001, 0.0001\}$ computed over all on the order of 10^{10} impostor scores. The FMR in each bin will vary also - see subsequent impostor heatmaps in sec. 3.6.2. Given a pair of face images taken at different times, we assign the comparison to the bin that is the arithmetic average of the subject's ages. This plot shows only the effect of age, not ageing. The number of comparisons in each bin is generally in the thousands, however the first and last bins are computed over 149 and 124 respectively. The error rates in some (adult) cases are zero, and in others the DET is flat so the error rates at the two thresholds are identical. The lines span 1% and 99% of bootstrap replicated FNMR estimates.

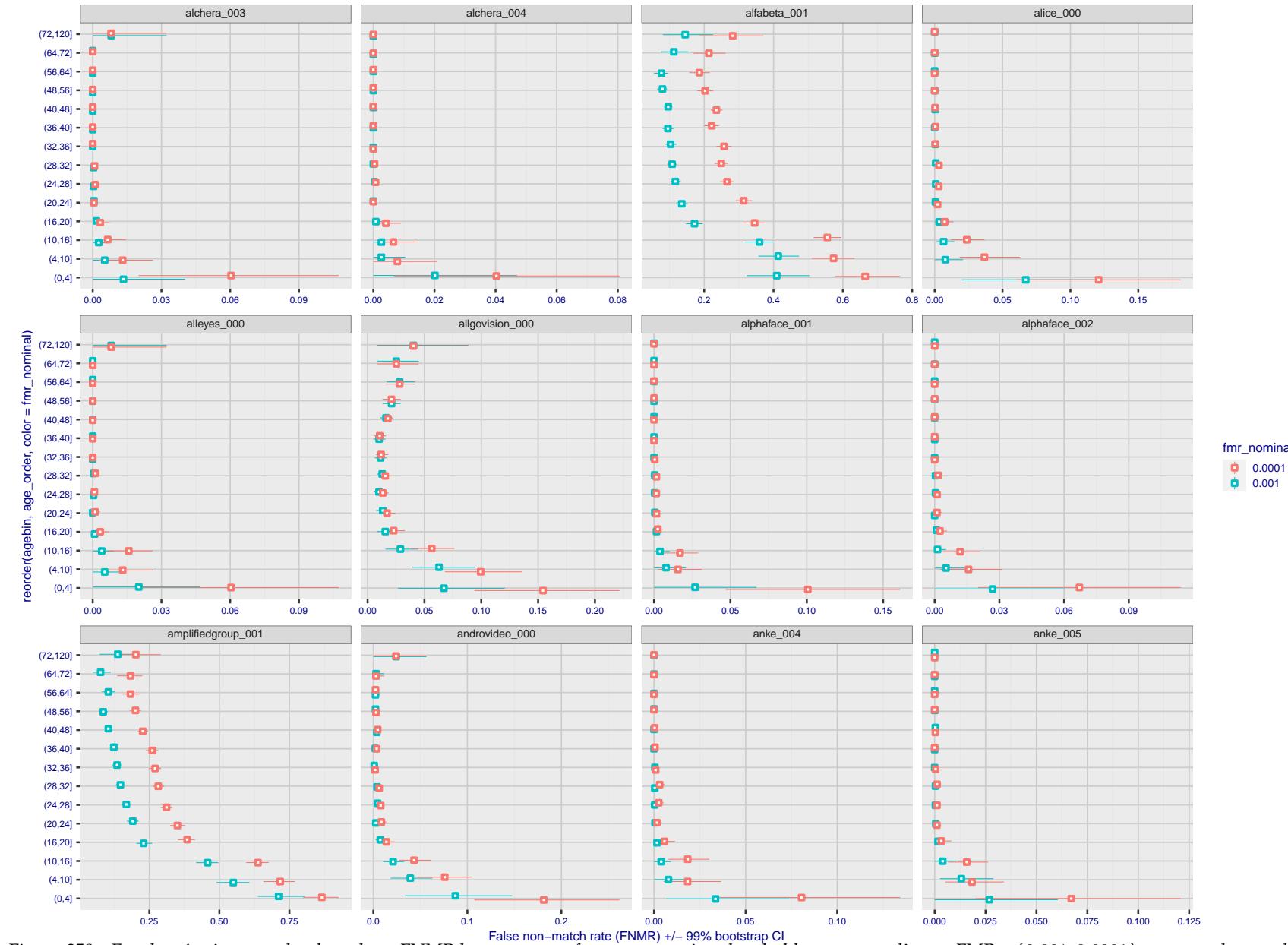


Figure 358: For the visa images, the dots show FNMR by age group for two operating thresholds corresponding to $FMR = \{0.001, 0.0001\}$ computed over all on the order of 10^{10} impostor scores. The FMR in each bin will vary also - see subsequent impostor heatmaps in sec. 3.6.2. Given a pair of face images taken at different times, we assign the comparison to the bin that is the arithmetic average of the subject's ages. This plot shows only the effect of age, not ageing. The number of comparisons in each bin is generally in the thousands, however the first and last bins are computed over 149 and 124 respectively. The error rates in some (adult) cases are zero, and in others the DET is flat so the error rates at the two thresholds are identical. The lines span 1% and 99% of bootstrap replicated FNMR estimates.



Figure 359: For the visa images, the dots show FNMR by age group for two operating thresholds corresponding to $FMR = \{0.001, 0.0001\}$ computed over all on the order of 10^{10} impostor scores. The FMR in each bin will vary also - see subsequent impostor heatmaps in sec. 3.6.2. Given a pair of face images taken at different times, we assign the comparison to the bin that is the arithmetic average of the subject's ages. This plot shows only the effect of age, not ageing. The number of comparisons in each bin is generally in the thousands, however the first and last bins are computed over 149 and 124 respectively. The error rates in some (adult) cases are zero, and in others the DET is flat so the error rates at the two thresholds are identical. The lines span 1% and 99% of bootstrap replicated FNMR estimates.

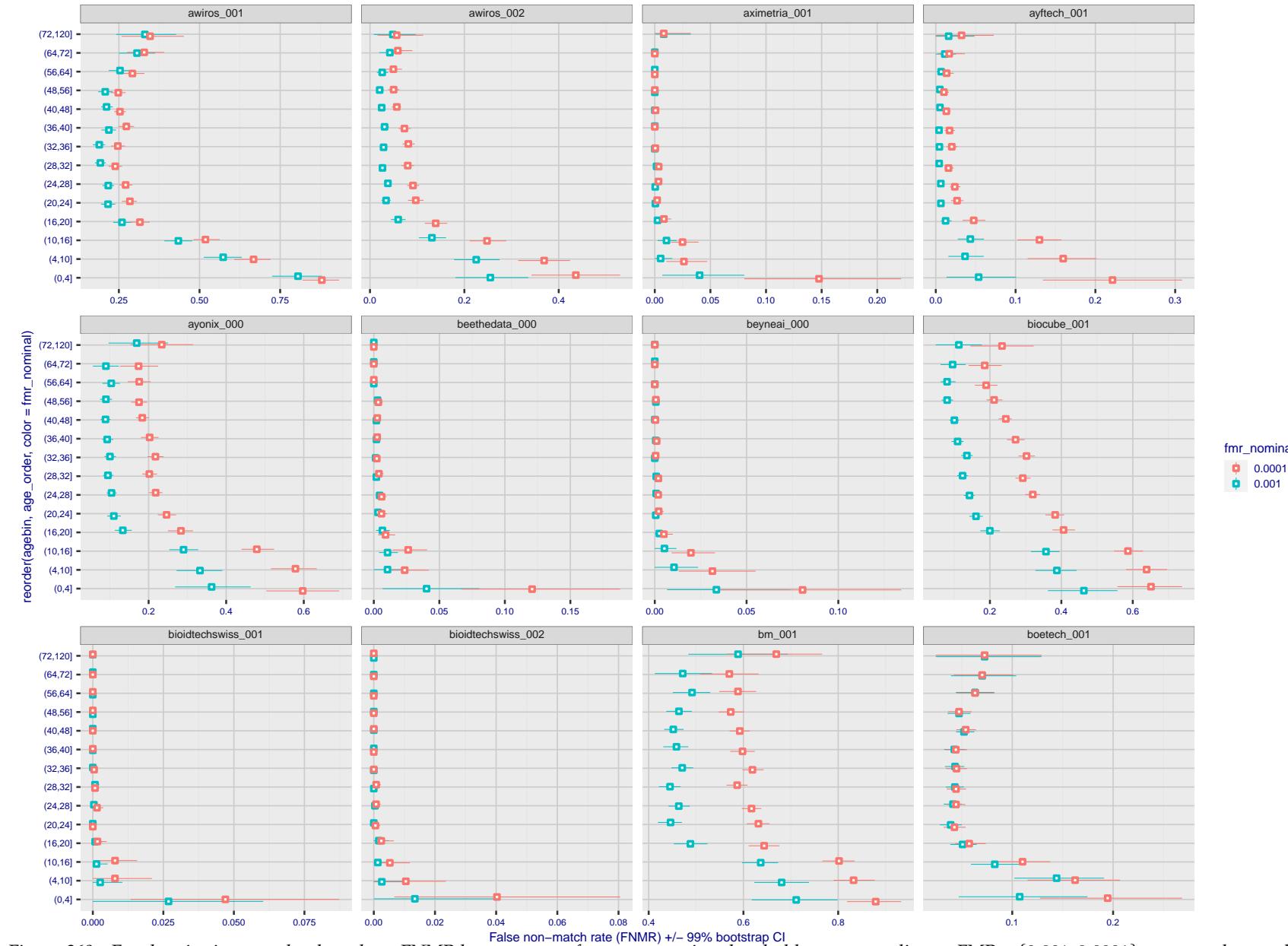


Figure 360: For the visa images, the dots show FNMR by age group for two operating thresholds corresponding to $FMR = \{0.001, 0.0001\}$ computed over all on the order of 10^{10} impostor scores. The FMR in each bin will vary also - see subsequent impostor heatmaps in sec. 3.6.2. Given a pair of face images taken at different times, we assign the comparison to the bin that is the arithmetic average of the subject's ages. This plot shows only the effect of age, not ageing. The number of comparisons in each bin is generally in the thousands, however the first and last bins are computed over 149 and 124 respectively. The error rates in some (adult) cases are zero, and in others the DET is flat so the error rates at the two thresholds are identical. The lines span 1% and 99% of bootstrap replicated FNMR estimates.



Figure 361: For the visa images, the dots show FNMR by age group for two operating thresholds corresponding to $FMR = \{0.001, 0.0001\}$ computed over all on the order of 10^{10} impostor scores. The FMR in each bin will vary also - see subsequent impostor heatmaps in sec. 3.6.2. Given a pair of face images taken at different times, we assign the comparison to the bin that is the arithmetic average of the subject's ages. This plot shows only the effect of age, not ageing. The number of comparisons in each bin is generally in the thousands, however the first and last bins are computed over 149 and 124 respectively. The error rates in some (adult) cases are zero, and in others the DET is flat so the error rates at the two thresholds are identical. The lines span 1% and 99% of bootstrap replicated FNMR estimates.

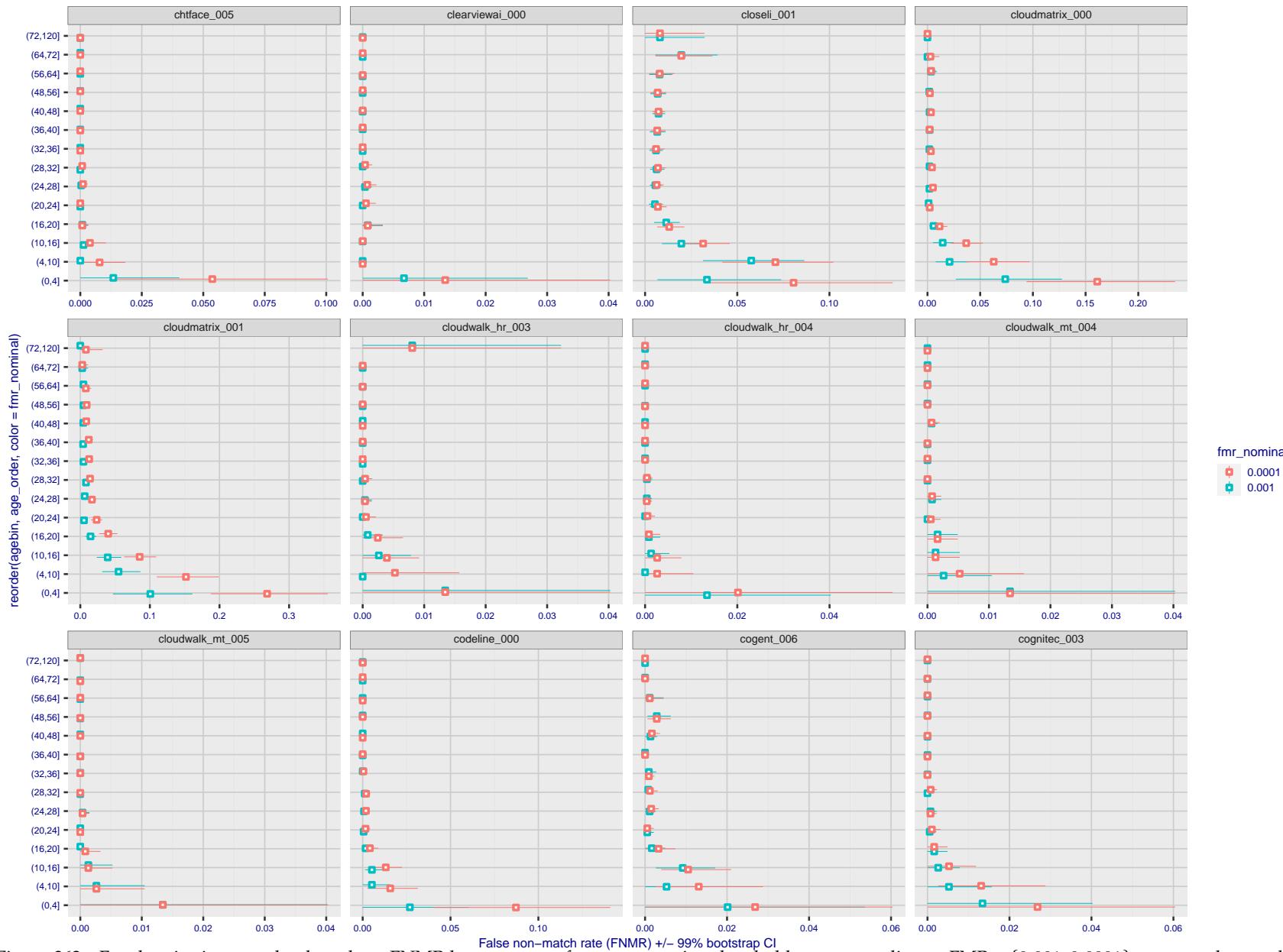


Figure 362: For the visa images, the dots show FNMR by age group for two operating thresholds corresponding to $FMR = \{0.001, 0.0001\}$ computed over all on the order of 10^{10} impostor scores. The FMR in each bin will vary also - see subsequent impostor heatmaps in sec. 3.6.2. Given a pair of face images taken at different times, we assign the comparison to the bin that is the arithmetic average of the subject's ages. This plot shows only the effect of age, not ageing. The number of comparisons in each bin is generally in the thousands, however the first and last bins are computed over 149 and 124 respectively. The error rates in some (adult) cases are zero, and in others the DET is flat so the error rates at the two thresholds are identical. The lines span 1% and 99% of bootstrap replicated FNMR estimates.

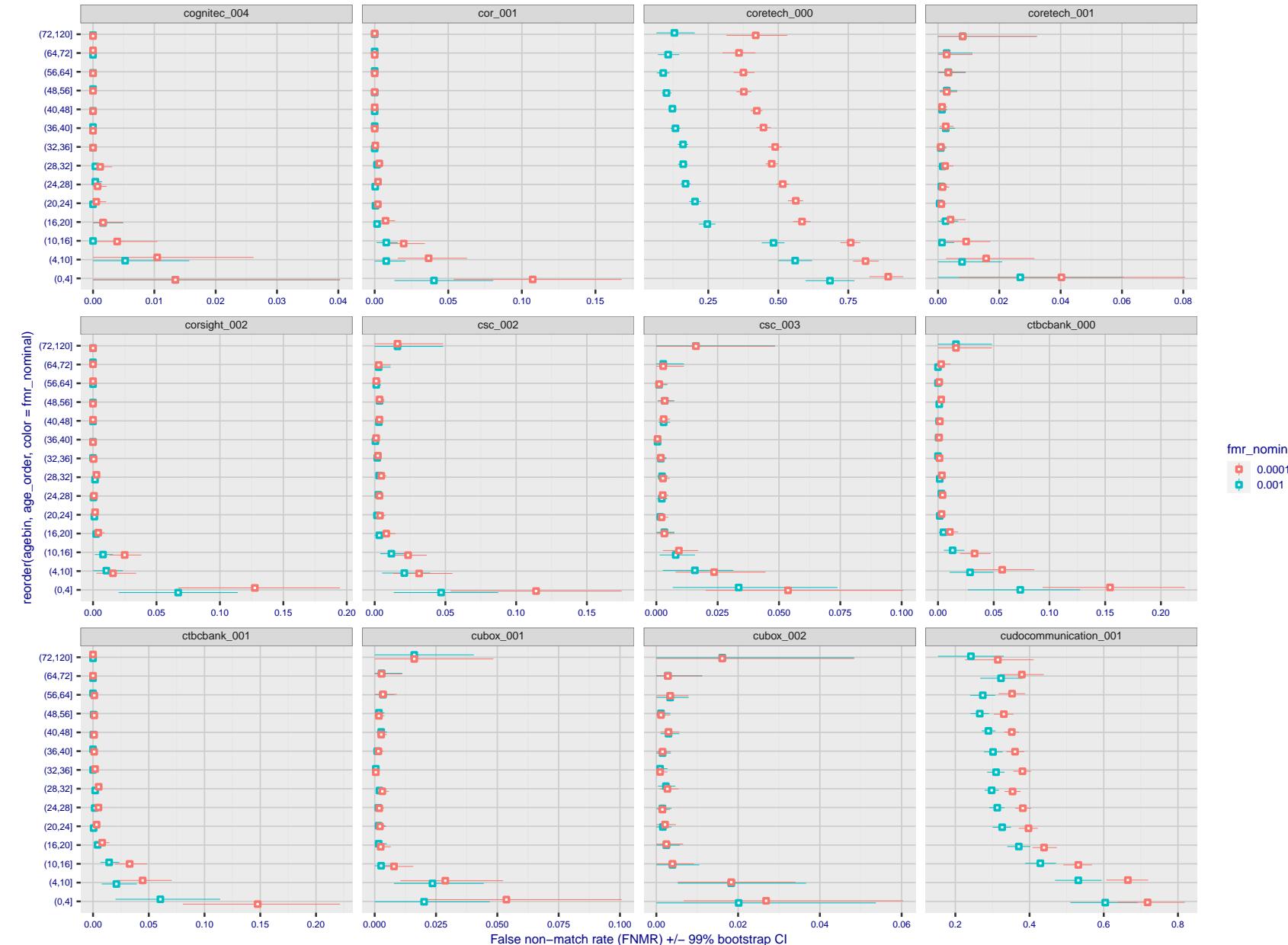


Figure 363: For the visa images, the dots show FNMR by age group for two operating thresholds corresponding to $FMR = \{0.001, 0.0001\}$ computed over all on the order of 10^{10} impostor scores. The FMR in each bin will vary also - see subsequent impostor heatmaps in sec. 3.6.2. Given a pair of face images taken at different times, we assign the comparison to the bin that is the arithmetic average of the subject's ages. This plot shows only the effect of age, not ageing. The number of comparisons in each bin is generally in the thousands, however the first and last bins are computed over 149 and 124 respectively. The error rates in some (adult) cases are zero, and in others the DET is flat so the error rates at the two thresholds are identical. The lines span 1% and 99% of bootstrap replicated FNMR estimates.



Figure 364: For the visa images, the dots show FNMR by age group for two operating thresholds corresponding to $FMR = \{0.001, 0.0001\}$ computed over all on the order of 10^{10} impostor scores. The FMR in each bin will vary also - see subsequent impostor heatmaps in sec. 3.6.2. Given a pair of face images taken at different times, we assign the comparison to the bin that is the arithmetic average of the subject's ages. This plot shows only the effect of age, not ageing. The number of comparisons in each bin is generally in the thousands, however the first and last bins are computed over 149 and 124 respectively. The error rates in some (adult) cases are zero, and in others the DET is flat so the error rates at the two thresholds are identical. The lines span 1% and 99% of bootstrap replicated FNMR estimates.



Figure 365: For the visa images, the dots show FNMR by age group for two operating thresholds corresponding to $FMR = \{0.001, 0.0001\}$ computed over all on the order of 10^{10} impostor scores. The FMR in each bin will vary also - see subsequent impostor heatmaps in sec. 3.6.2. Given a pair of face images taken at different times, we assign the comparison to the bin that is the arithmetic average of the subject's ages. This plot shows only the effect of age, not ageing. The number of comparisons in each bin is generally in the thousands, however the first and last bins are computed over 149 and 124 respectively. The error rates in some (adult) cases are zero, and in others the DET is flat so the error rates at the two thresholds are identical. The lines span 1% and 99% of bootstrap replicated FNMR estimates.

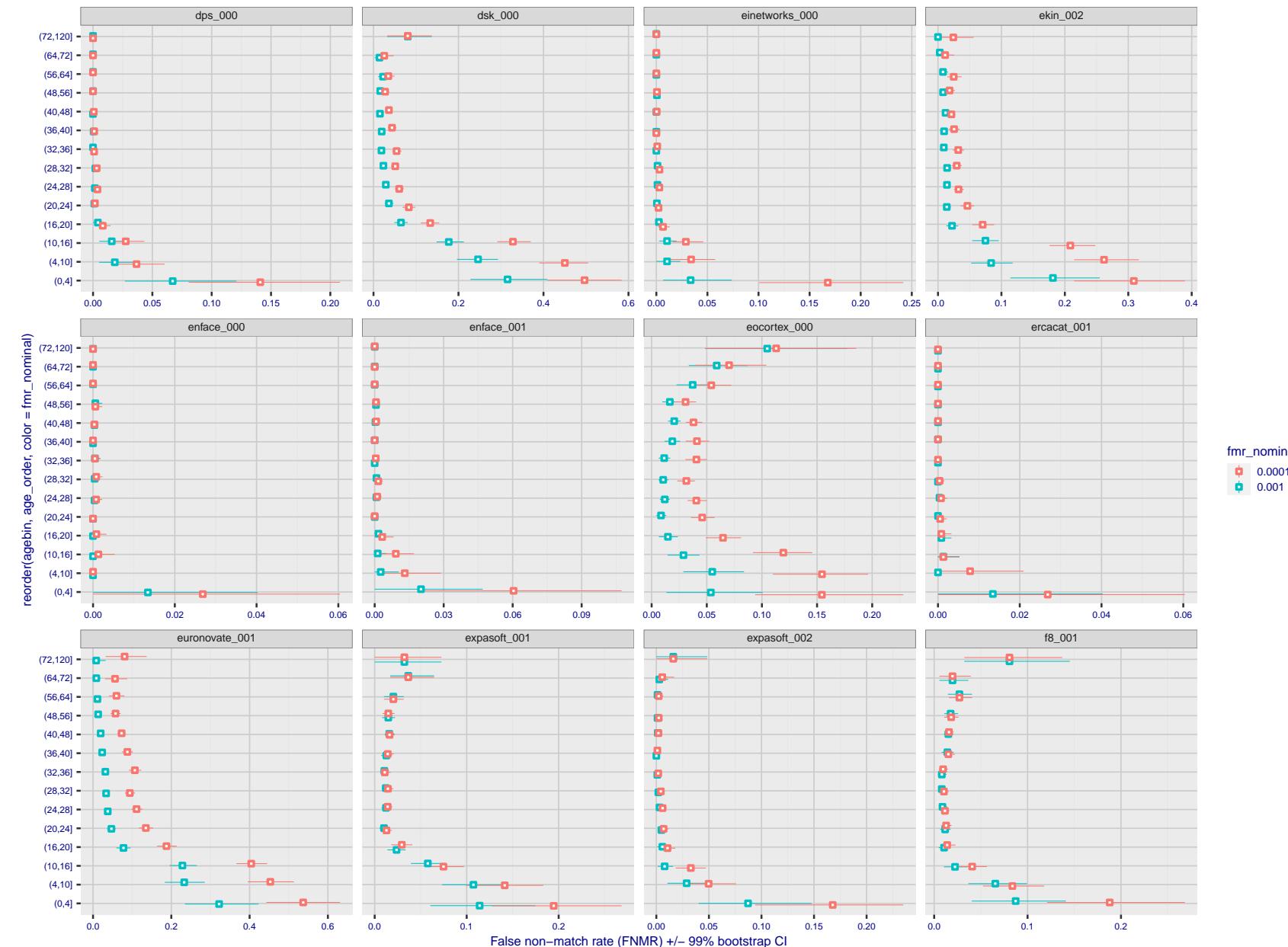


Figure 366: For the visa images, the dots show FNMR by age group for two operating thresholds corresponding to $FMR = \{0.001, 0.0001\}$ computed over all on the order of 10^{10} impostor scores. The FMR in each bin will vary also - see subsequent impostor heatmaps in sec. 3.6.2. Given a pair of face images taken at different times, we assign the comparison to the bin that is the arithmetic average of the subject's ages. This plot shows only the effect of age, not ageing. The number of comparisons in each bin is generally in the thousands, however the first and last bins are computed over 149 and 124 respectively. The error rates in some (adult) cases are zero, and in others the DET is flat so the error rates at the two thresholds are identical. The lines span 1% and 99% of bootstrap replicated FNMR estimates.

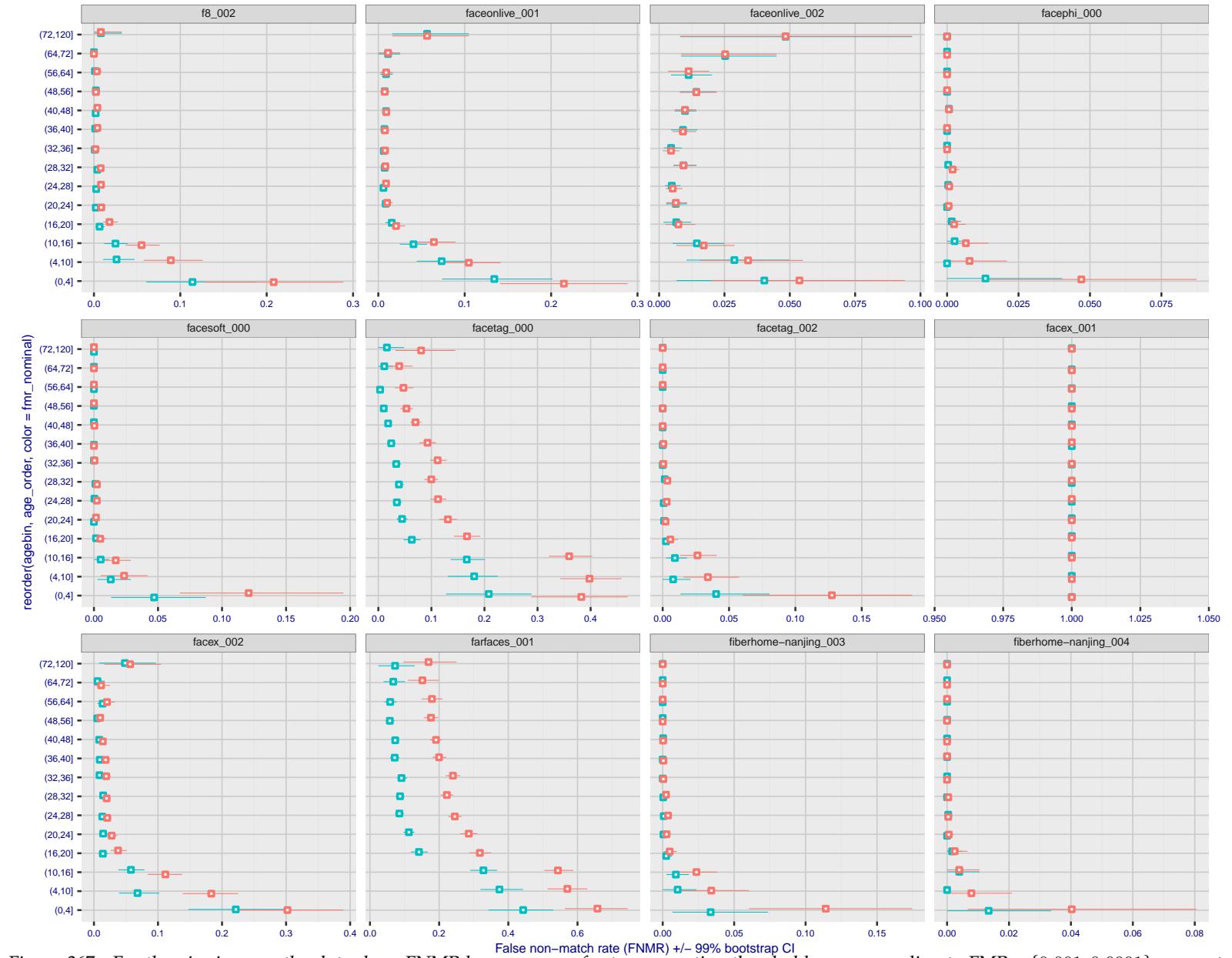


Figure 367: For the visa images, the dots show FNMR by age group for two operating thresholds corresponding to $FMR = \{0.001, 0.0001\}$ computed over all on the order of 10^{10} impostor scores. The FMR in each bin will vary also - see subsequent impostor heatmaps in sec. 3.6.2. Given a pair of face images taken at different times, we assign the comparison to the bin that is the arithmetic average of the subject's ages. This plot shows only the effect of age, not ageing. The number of comparisons in each bin is generally in the thousands, however the first and last bins are computed over 149 and 124 respectively. The error rates in some (adult) cases are zero, and in others the DET is flat so the error rates at the two thresholds are identical. The lines span 1% and 99% of bootstrap replicated FNMR estimates.



Figure 368: For the visa images, the dots show FNMR by age group for two operating thresholds corresponding to $FMR = \{0.001, 0.0001\}$ computed over all on the order of 10^{10} impostor scores. The FMR in each bin will vary also - see subsequent impostor heatmaps in sec. 3.6.2. Given a pair of face images taken at different times, we assign the comparison to the bin that is the arithmetic average of the subject's ages. This plot shows only the effect of age, not ageing. The number of comparisons in each bin is generally in the thousands, however the first and last bins are computed over 149 and 124 respectively. The error rates in some (adult) cases are zero, and in others the DET is flat so the error rates at the two thresholds are identical. The lines span 1% and 99% of bootstrap replicated FNMR estimates.

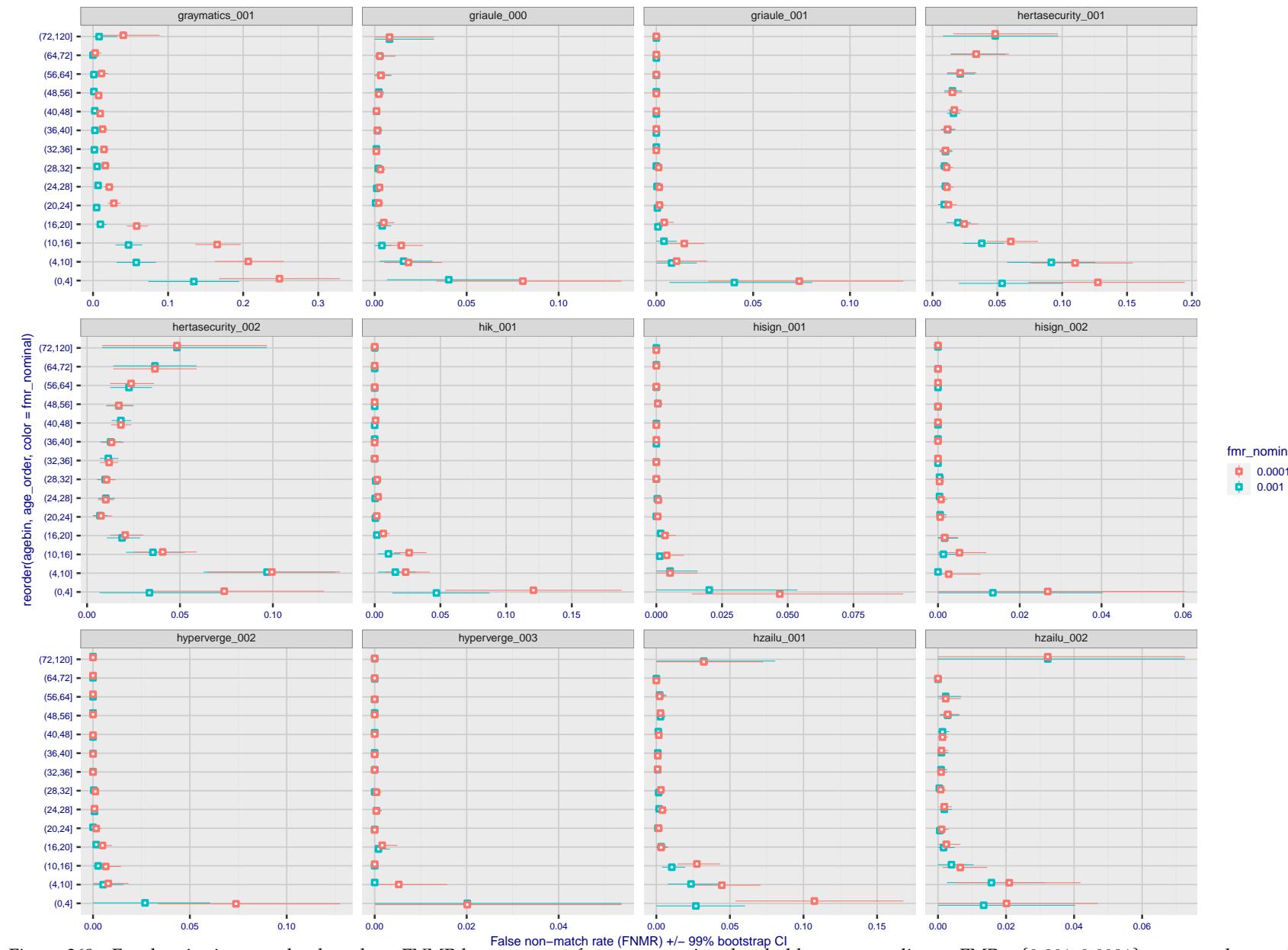


Figure 369: For the visa images, the dots show FNMR by age group for two operating thresholds corresponding to $FMR = \{0.001, 0.0001\}$ computed over all on the order of 10^{10} impostor scores. The FMR in each bin will vary also - see subsequent impostor heatmaps in sec. 3.6.2. Given a pair of face images taken at different times, we assign the comparison to the bin that is the arithmetic average of the subject's ages. This plot shows only the effect of age, not ageing. The number of comparisons in each bin is generally in the thousands, however the first and last bins are computed over 149 and 124 respectively. The error rates in some (adult) cases are zero, and in others the DET is flat so the error rates at the two thresholds are identical. The lines span 1% and 99% of bootstrap replicated FNMR estimates.

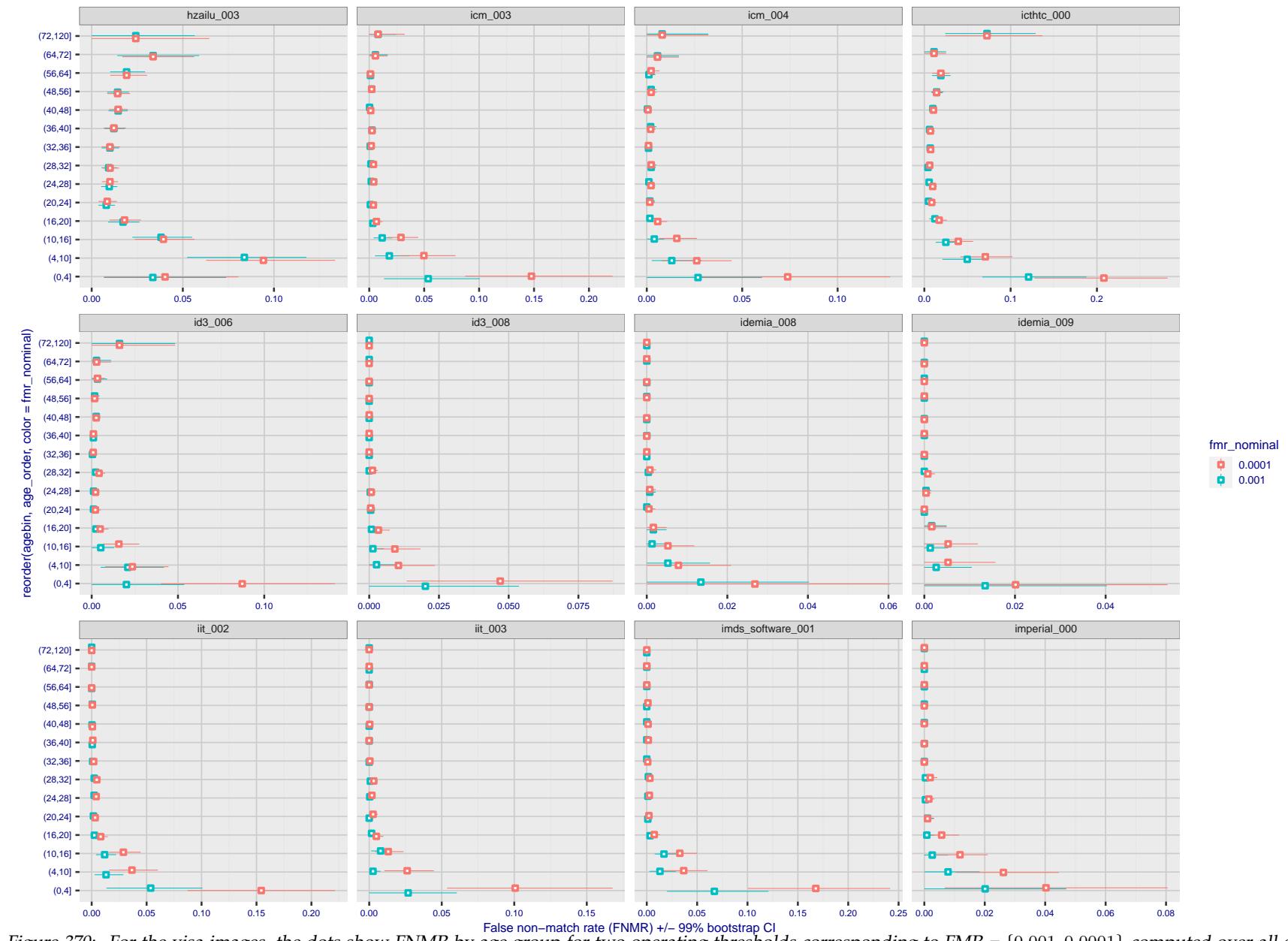


Figure 370: For the visa images, the dots show FNMR by age group for two operating thresholds corresponding to $FMR = \{0.001, 0.0001\}$ computed over all on the order of 10^{10} impostor scores. The FMR in each bin will vary also - see subsequent impostor heatmaps in sec. 3.6.2. Given a pair of face images taken at different times, we assign the comparison to the bin that is the arithmetic average of the subject's ages. This plot shows only the effect of age, not ageing. The number of comparisons in each bin is generally in the thousands, however the first and last bins are computed over 149 and 124 respectively. The error rates in some (adult) cases are zero, and in others the DET is flat so the error rates at the two thresholds are identical. The lines span 1% and 99% of bootstrap replicated FNMR estimates.

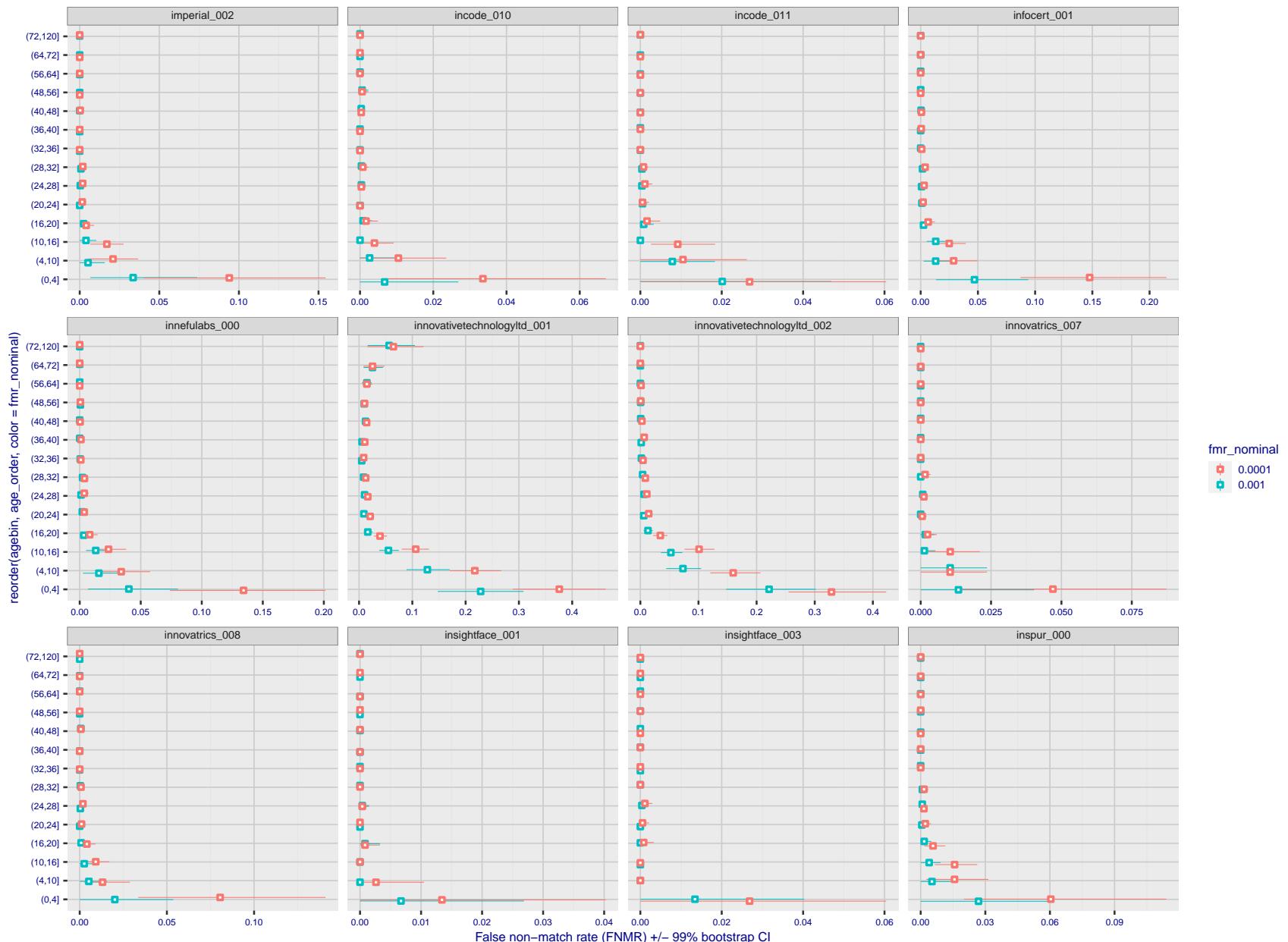


Figure 371: For the visa images, the dots show FNMR by age group for two operating thresholds corresponding to $FMR = \{0.001, 0.0001\}$ computed over all on the order of 10^{10} impostor scores. The FMR in each bin will vary also - see subsequent impostor heatmaps in sec. 3.6.2. Given a pair of face images taken at different times, we assign the comparison to the bin that is the arithmetic average of the subject's ages. This plot shows only the effect of age, not ageing. The number of comparisons in each bin is generally in the thousands, however the first and last bins are computed over 149 and 124 respectively. The error rates in some (adult) cases are zero, and in others the DET is flat so the error rates at the two thresholds are identical. The lines span 1% and 99% of bootstrap replicated FNMR estimates.

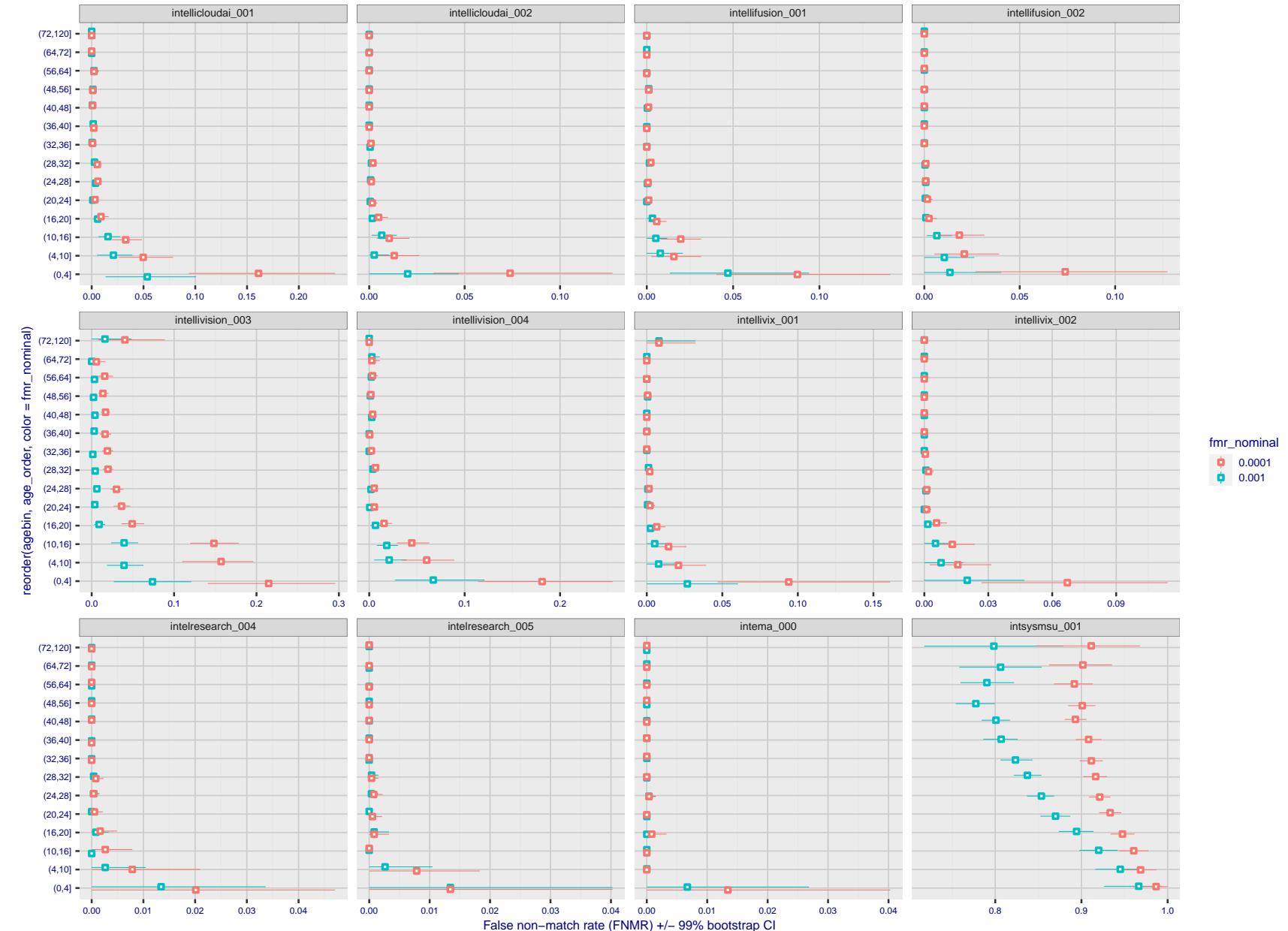


Figure 372: For the visa images, the dots show FNMR by age group for two operating thresholds corresponding to $FMR = \{0.001, 0.0001\}$ computed over all on the order of 10^{10} impostor scores. The FMR in each bin will vary also - see subsequent impostor heatmaps in sec. 3.6.2. Given a pair of face images taken at different times, we assign the comparison to the bin that is the arithmetic average of the subject's ages. This plot shows only the effect of age, not ageing. The number of comparisons in each bin is generally in the thousands, however the first and last bins are computed over 149 and 124 respectively. The error rates in some (adult) cases are zero, and in others the DET is flat so the error rates at the two thresholds are identical. The lines span 1% and 99% of bootstrap replicated FNMR estimates.

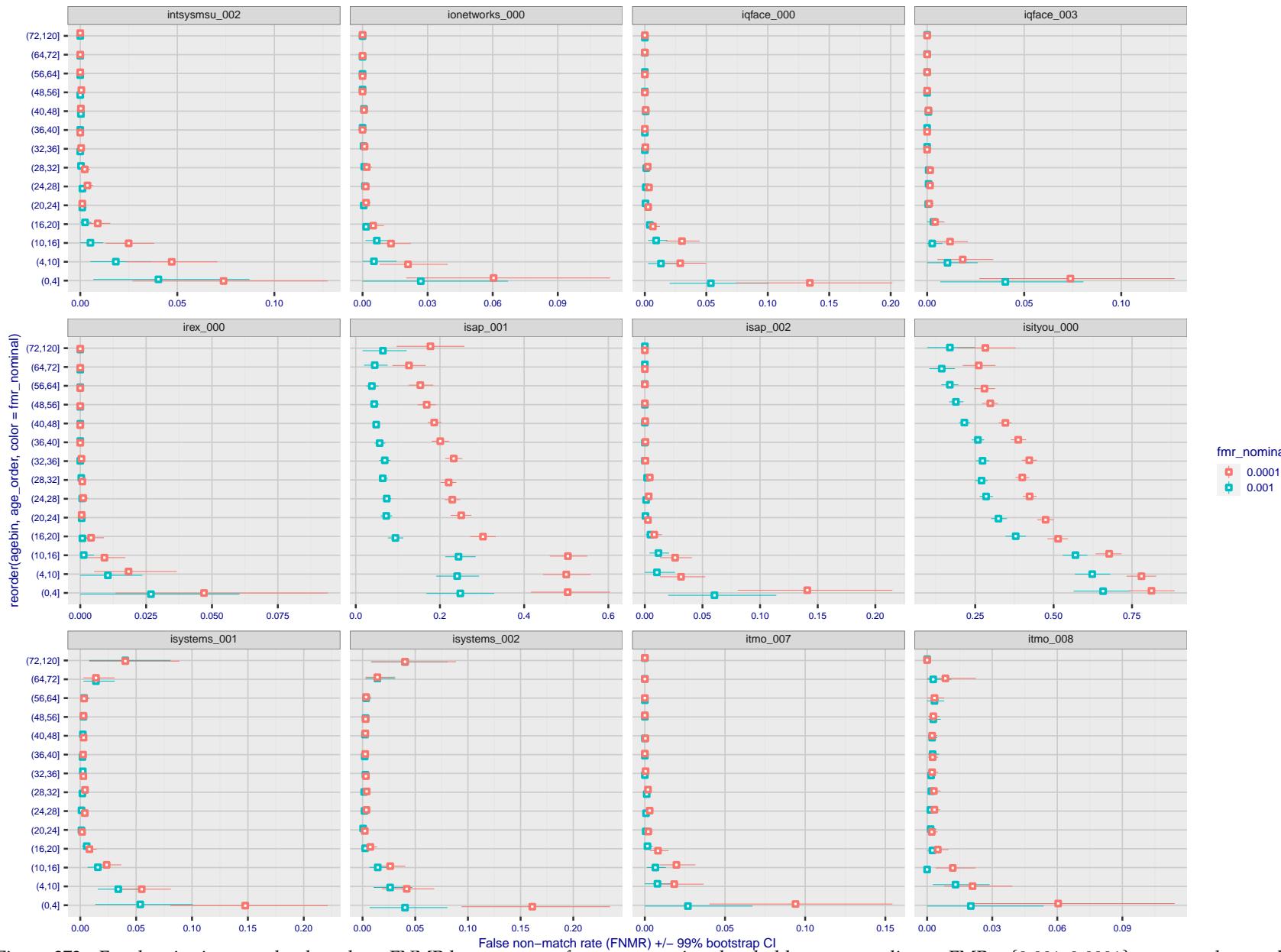


Figure 373: For the visa images, the dots show FNMR by age group for two operating thresholds corresponding to $FMR = \{0.001, 0.0001\}$ computed over all on the order of 10^{10} impostor scores. The FMR in each bin will vary also - see subsequent impostor heatmaps in sec. 3.6.2. Given a pair of face images taken at different times, we assign the comparison to the bin that is the arithmetic average of the subject's ages. This plot shows only the effect of age, not ageing. The number of comparisons in each bin is generally in the thousands, however the first and last bins are computed over 149 and 124 respectively. The error rates in some (adult) cases are zero, and in others the DET is flat so the error rates at the two thresholds are identical. The lines span 1% and 99% of bootstrap replicated FNMR estimates.

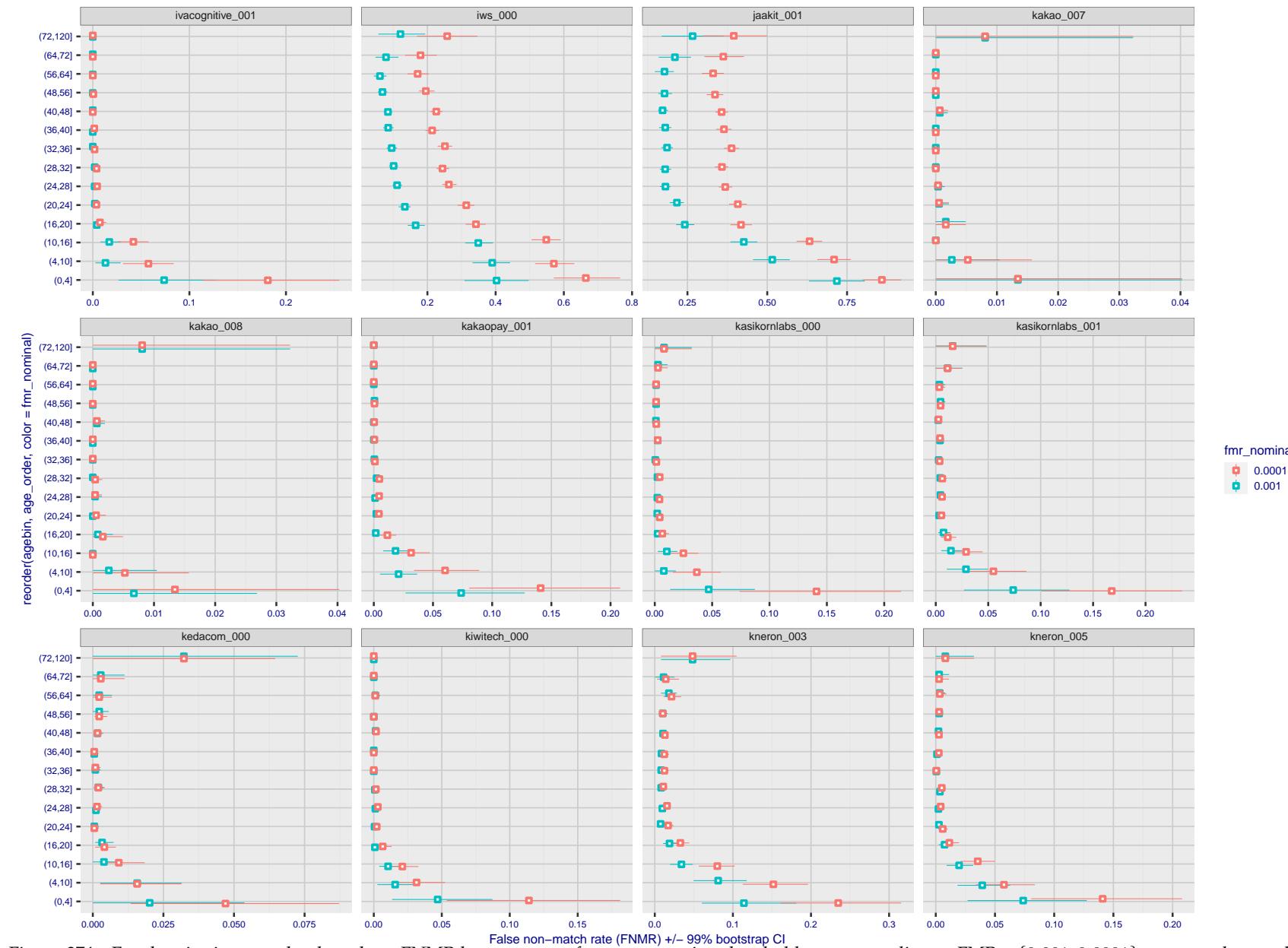


Figure 374: For the visa images, the dots show FNMR by age group for two operating thresholds corresponding to $FMR = \{0.001, 0.0001\}$ computed over all on the order of 10^{10} impostor scores. The FMR in each bin will vary also - see subsequent impostor heatmaps in sec. 3.6.2. Given a pair of face images taken at different times, we assign the comparison to the bin that is the arithmetic average of the subject's ages. This plot shows only the effect of age, not ageing. The number of comparisons in each bin is generally in the thousands, however the first and last bins are computed over 149 and 124 respectively. The error rates in some (adult) cases are zero, and in others the DET is flat so the error rates at the two thresholds are identical. The lines span 1% and 99% of bootstrap replicated FNMR estimates.



Figure 375: For the visa images, the dots show FNMR by age group for two operating thresholds corresponding to $FMR = \{0.001, 0.0001\}$ computed over all on the order of 10^{10} impostor scores. The FMR in each bin will vary also - see subsequent impostor heatmaps in sec. 3.6.2. Given a pair of face images taken at different times, we assign the comparison to the bin that is the arithmetic average of the subject's ages. This plot shows only the effect of age, not ageing. The number of comparisons in each bin is generally in the thousands, however the first and last bins are computed over 149 and 124 respectively. The error rates in some (adult) cases are zero, and in others the DET is flat so the error rates at the two thresholds are identical. The lines span 1% and 99% of bootstrap replicated FNMR estimates.

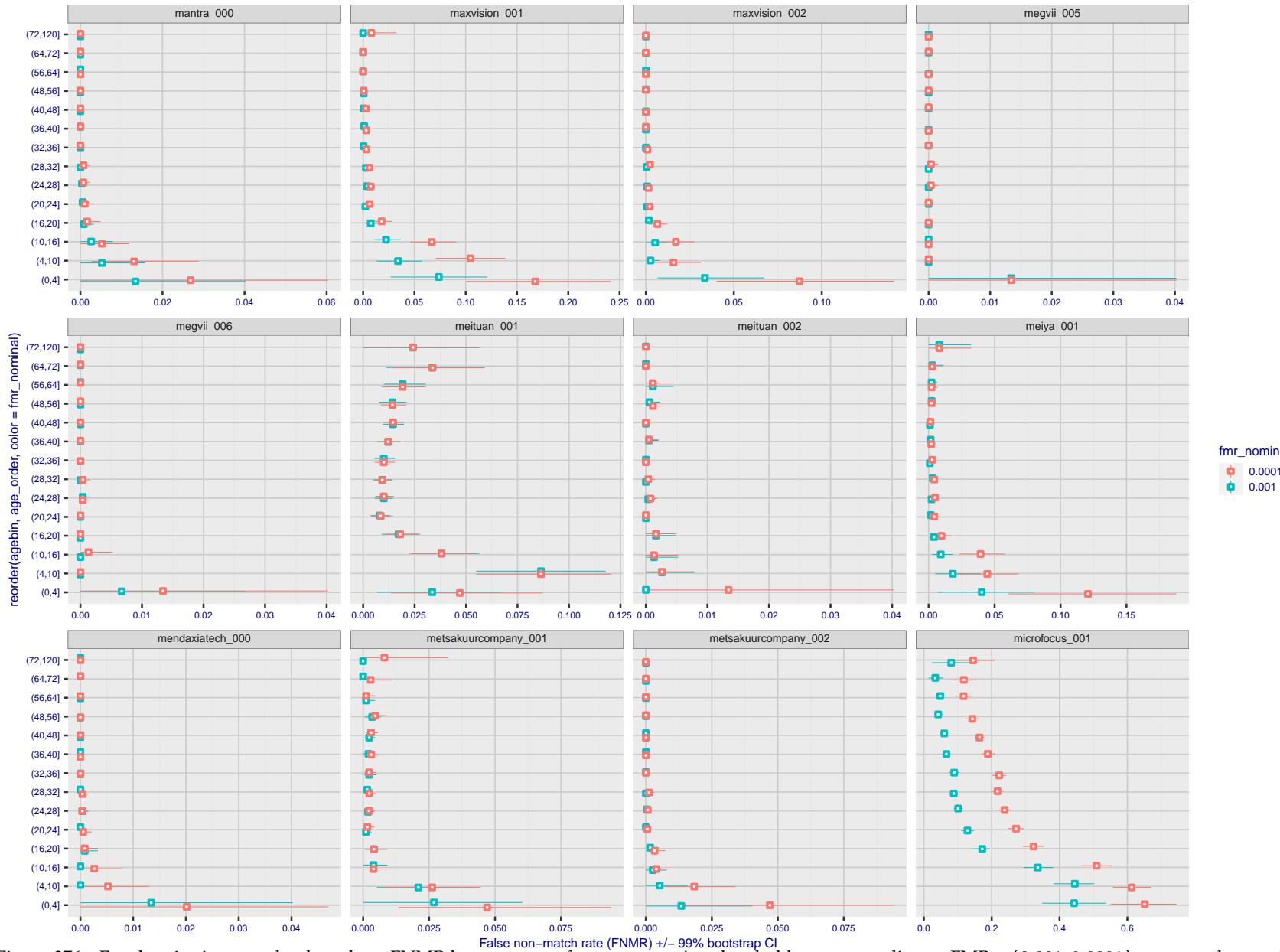


Figure 376: For the visa images, the dots show FNMR by age group for two operating thresholds corresponding to $FMR = \{0.001, 0.0001\}$ computed over all on the order of 10^{10} impostor scores. The FMR in each bin will vary also - see subsequent impostor heatmaps in sec. 3.6.2. Given a pair of face images taken at different times, we assign the comparison to the bin that is the arithmetic average of the subject's ages. This plot shows only the effect of age, not ageing. The number of comparisons in each bin is generally in the thousands, however the first and last bins are computed over 149 and 124 respectively. The error rates in some (adult) cases are zero, and in others the DET is flat so the error rates at the two thresholds are identical. The lines span 1% and 99% of bootstrap replicated FNMR estimates.

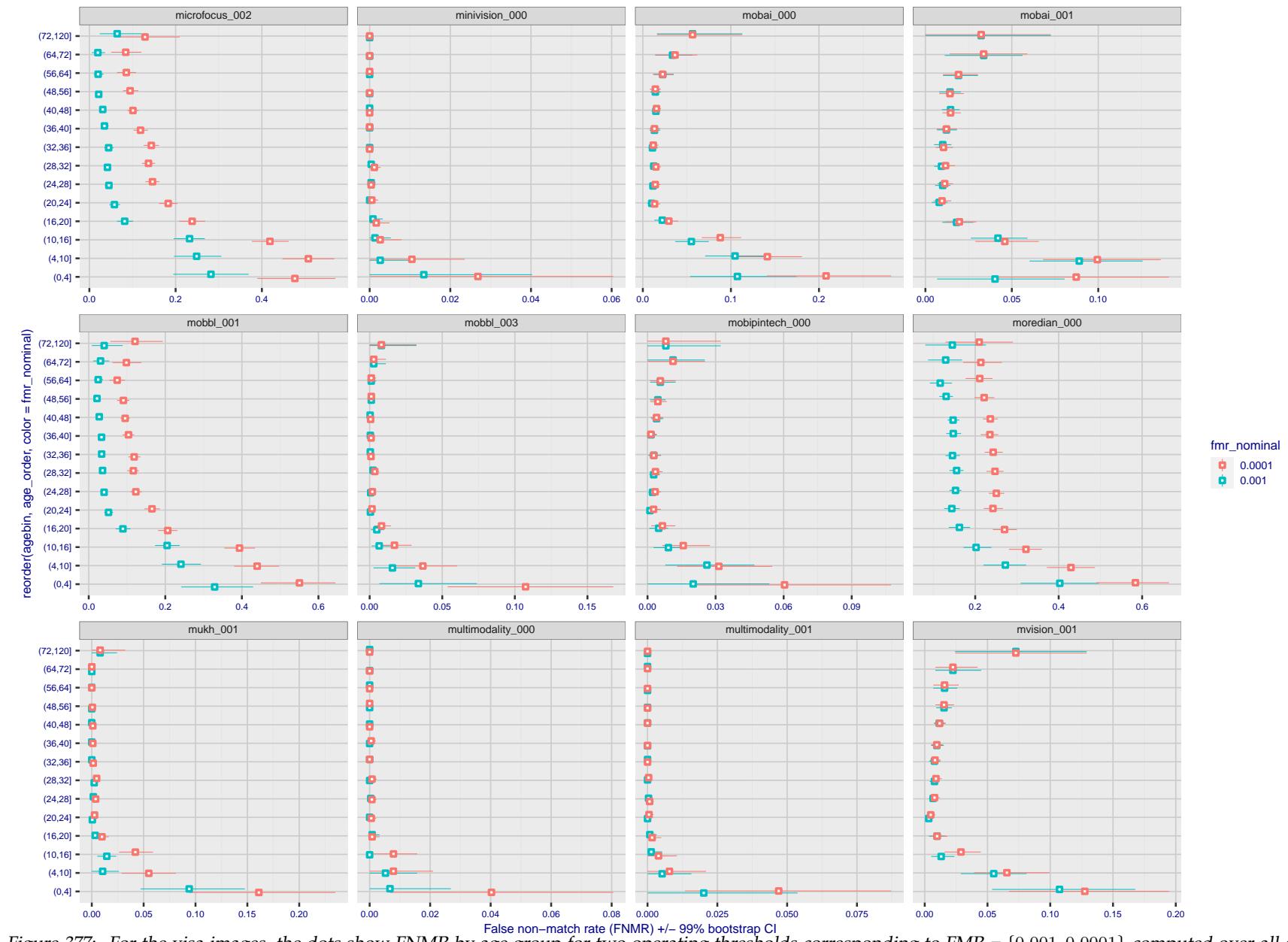


Figure 377: For the visa images, the dots show FNMR by age group for two operating thresholds corresponding to $FMR = \{0.001, 0.0001\}$ computed over all on the order of 10^{10} impostor scores. The FMR in each bin will vary also - see subsequent impostor heatmaps in sec. 3.6.2. Given a pair of face images taken at different times, we assign the comparison to the bin that is the arithmetic average of the subject's ages. This plot shows only the effect of age, not ageing. The number of comparisons in each bin is generally in the thousands, however the first and last bins are computed over 149 and 124 respectively. The error rates in some (adult) cases are zero, and in others the DET is flat so the error rates at the two thresholds are identical. The lines span 1% and 99% of bootstrap replicated FNMR estimates.

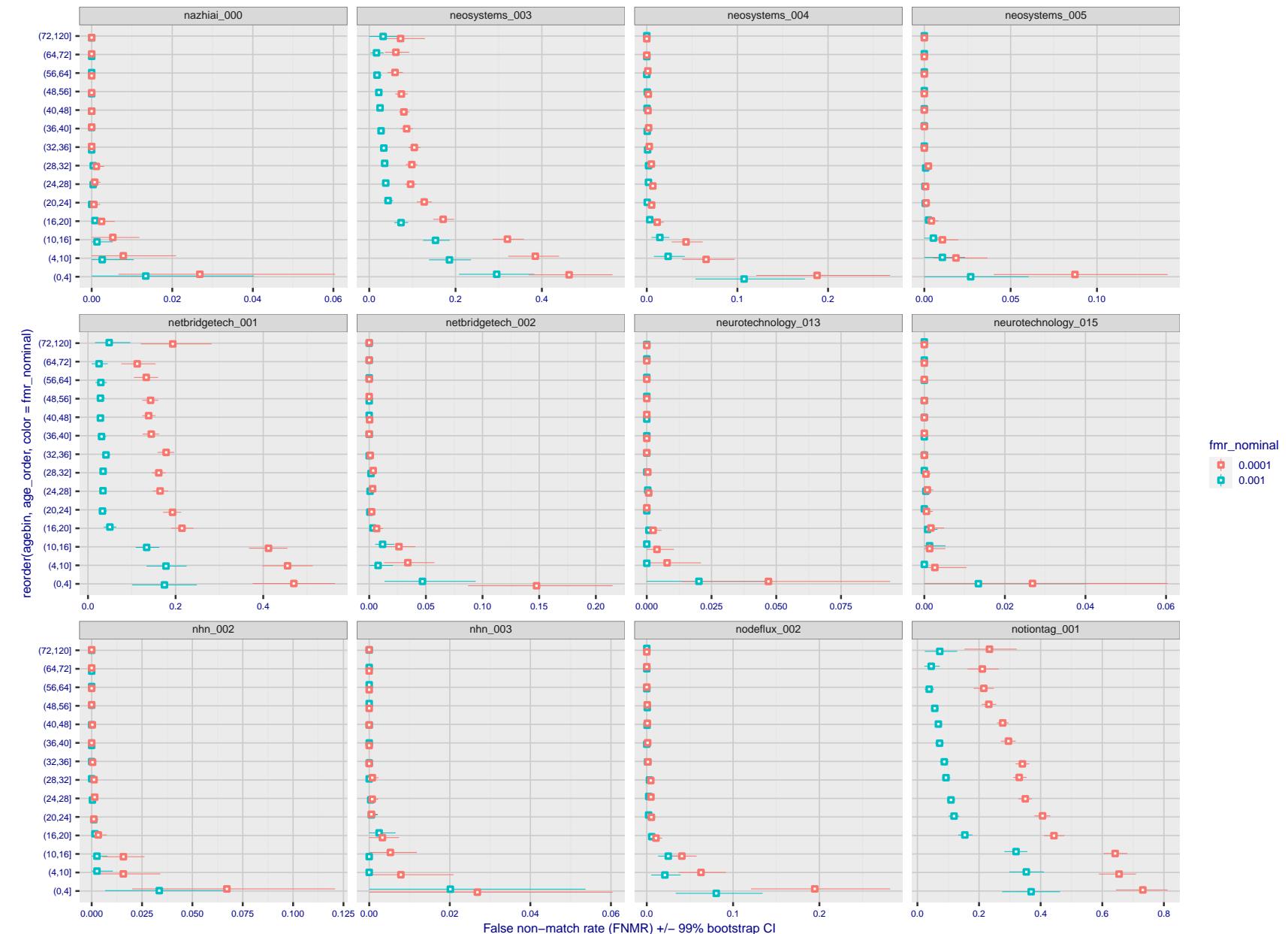


Figure 378: For the visa images, the dots show FNMR by age group for two operating thresholds corresponding to $FMR = \{0.001, 0.0001\}$ computed over all on the order of 10^{10} impostor scores. The FMR in each bin will vary also - see subsequent impostor heatmaps in sec. 3.6.2. Given a pair of face images taken at different times, we assign the comparison to the bin that is the arithmetic average of the subject's ages. This plot shows only the effect of age, not ageing. The number of comparisons in each bin is generally in the thousands, however the first and last bins are computed over 149 and 124 respectively. The error rates in some (adult) cases are zero, and in others the DET is flat so the error rates at the two thresholds are identical. The lines span 1% and 99% of bootstrap replicated FNMR estimates.

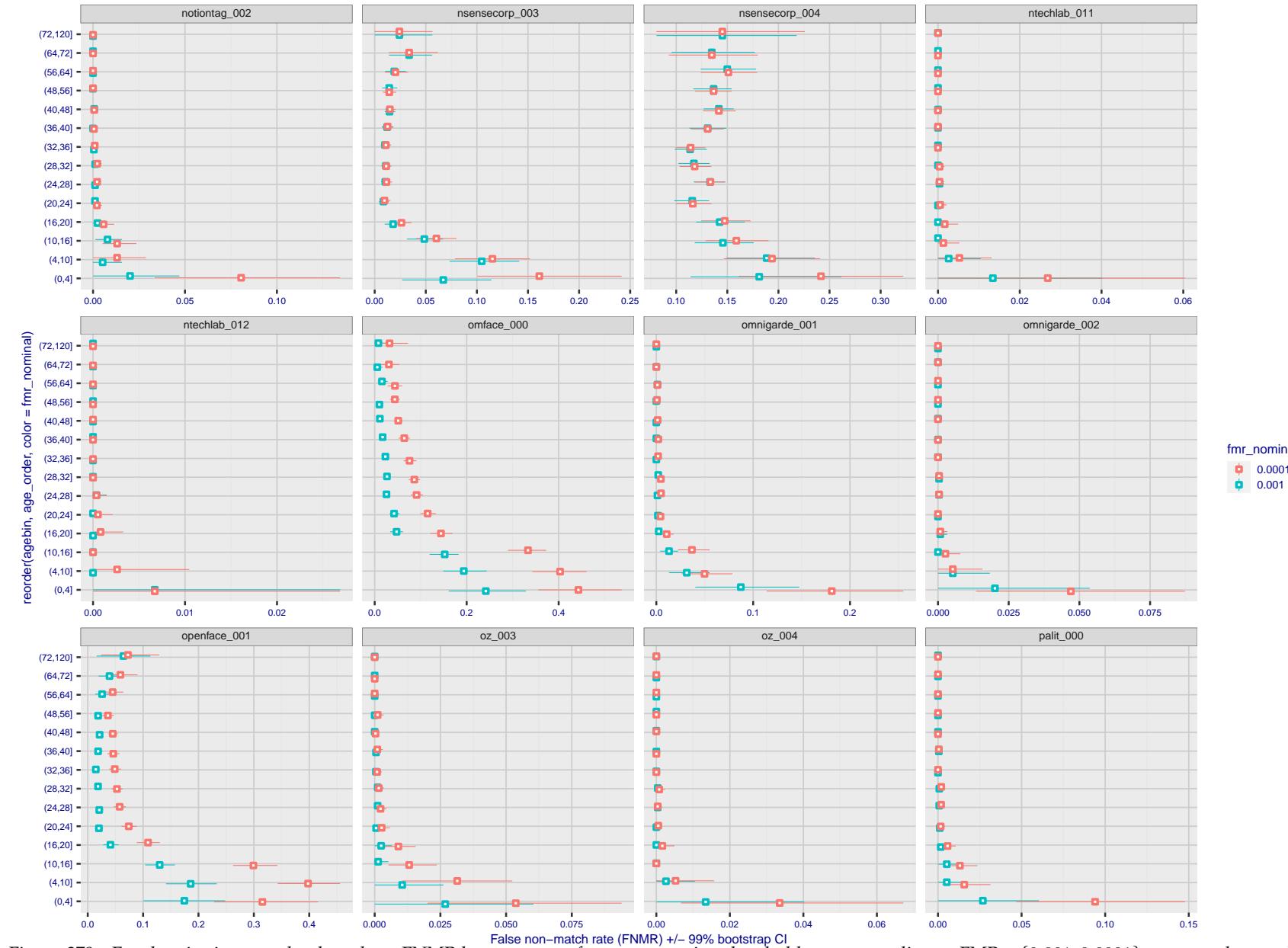


Figure 379: For the visa images, the dots show FNMR by age group for two operating thresholds corresponding to $FMR = \{0.001, 0.0001\}$ computed over all on the order of 10^{10} impostor scores. The FMR in each bin will vary also - see subsequent impostor heatmaps in sec. 3.6.2. Given a pair of face images taken at different times, we assign the comparison to the bin that is the arithmetic average of the subject's ages. This plot shows only the effect of age, not ageing. The number of comparisons in each bin is generally in the thousands, however the first and last bins are computed over 149 and 124 respectively. The error rates in some (adult) cases are zero, and in others the DET is flat so the error rates at the two thresholds are identical. The lines span 1% and 99% of bootstrap replicated FNMR estimates.



Figure 380: For the visa images, the dots show FNMR by age group for two operating thresholds corresponding to $FMR = \{0.001, 0.0001\}$ computed over all on the order of 10^{10} impostor scores. The FMR in each bin will vary also - see subsequent impostor heatmaps in sec. 3.6.2. Given a pair of face images taken at different times, we assign the comparison to the bin that is the arithmetic average of the subject's ages. This plot shows only the effect of age, not ageing. The number of comparisons in each bin is generally in the thousands, however the first and last bins are computed over 149 and 124 respectively. The error rates in some (adult) cases are zero, and in others the DET is flat so the error rates at the two thresholds are identical. The lines span 1% and 99% of bootstrap replicated FNMR estimates.



Figure 381: For the visa images, the dots show FNMR by age group for two operating thresholds corresponding to $FMR = \{0.001, 0.0001\}$ computed over all on the order of 10^{10} impostor scores. The FMR in each bin will vary also - see subsequent impostor heatmaps in sec. 3.6.2. Given a pair of face images taken at different times, we assign the comparison to the bin that is the arithmetic average of the subject's ages. This plot shows only the effect of age, not ageing. The number of comparisons in each bin is generally in the thousands, however the first and last bins are computed over 149 and 124 respectively. The error rates in some (adult) cases are zero, and in others the DET is flat so the error rates at the two thresholds are identical. The lines span 1% and 99% of bootstrap replicated FNMR estimates.



Figure 382: For the visa images, the dots show FNMR by age group for two operating thresholds corresponding to $FMR = \{0.001, 0.0001\}$ computed over all on the order of 10^{10} impostor scores. The FMR in each bin will vary also - see subsequent impostor heatmaps in sec. 3.6.2. Given a pair of face images taken at different times, we assign the comparison to the bin that is the arithmetic average of the subject's ages. This plot shows only the effect of age, not ageing. The number of comparisons in each bin is generally in the thousands, however the first and last bins are computed over 149 and 124 respectively. The error rates in some (adult) cases are zero, and in others the DET is flat so the error rates at the two thresholds are identical. The lines span 1% and 99% of bootstrap replicated FNMR estimates.

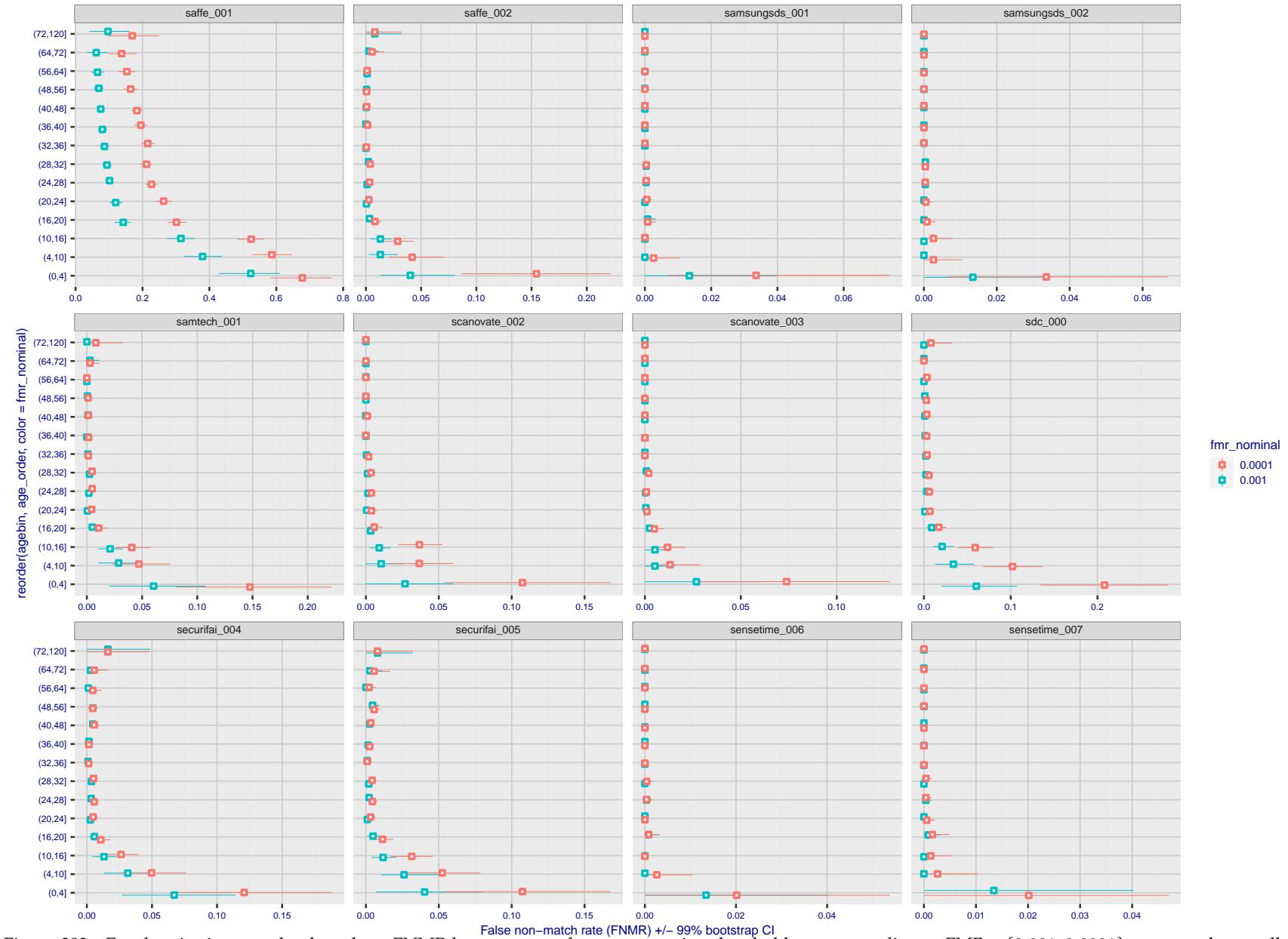


Figure 383: For the visa images, the dots show FNMR by age group for two operating thresholds corresponding to $FMR = \{0.001, 0.0001\}$ computed over all on the order of 10^{10} impostor scores. The FMR in each bin will vary also - see subsequent impostor heatmaps in sec. 3.6.2. Given a pair of face images taken at different times, we assign the comparison to the bin that is the arithmetic average of the subject's ages. This plot shows only the effect of age, not ageing. The number of comparisons in each bin is generally in the thousands, however the first and last bins are computed over 149 and 124 respectively. The error rates in some (adult) cases are zero, and in others the DET is flat so the error rates at the two thresholds are identical. The lines span 1% and 99% of bootstrap replicated FNMR estimates.

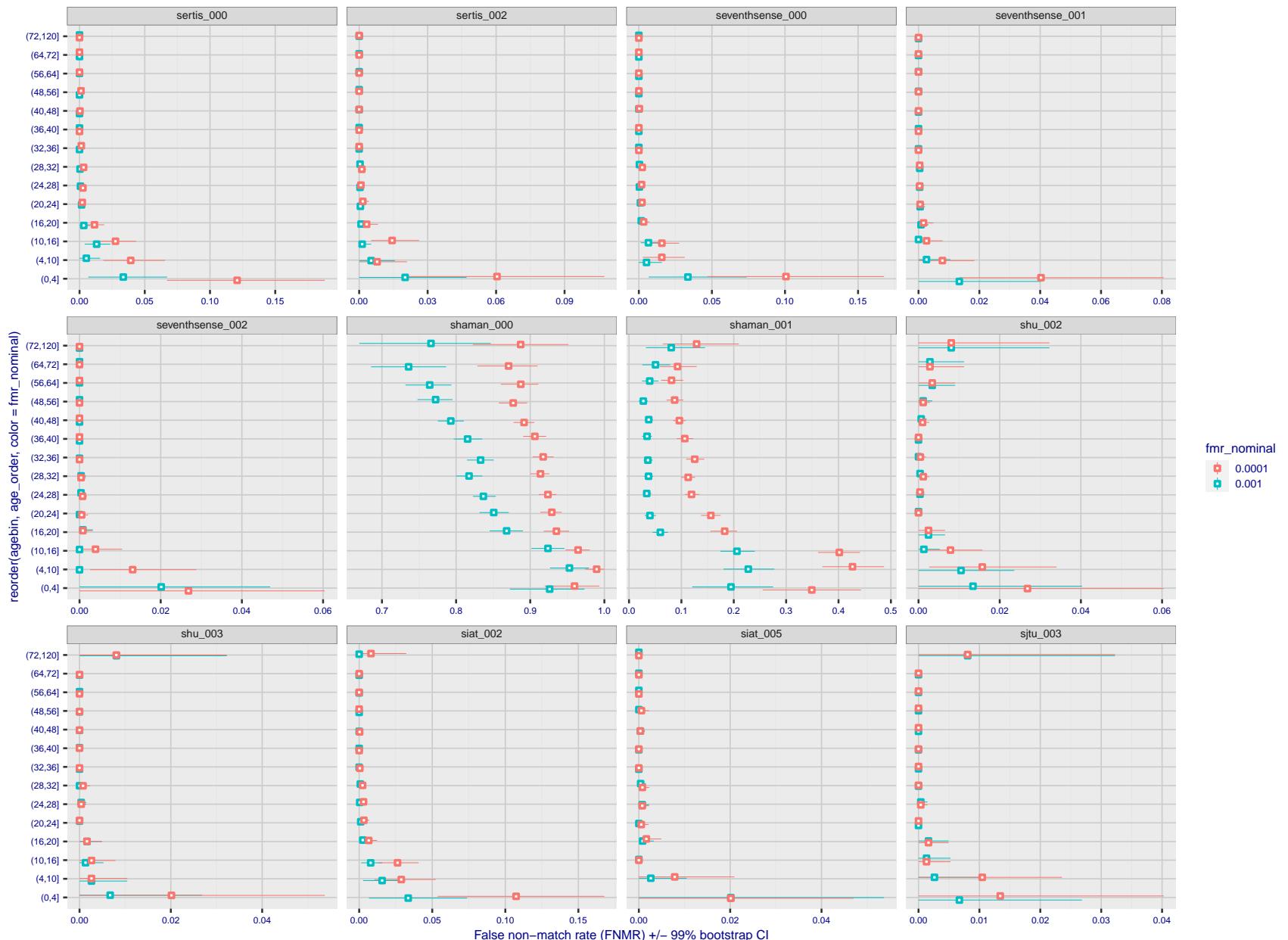


Figure 384: For the visa images, the dots show FNMR by age group for two operating thresholds corresponding to $FMR = \{0.001, 0.0001\}$ computed over all on the order of 10^{10} impostor scores. The FMR in each bin will vary also - see subsequent impostor heatmaps in sec. 3.6.2. Given a pair of face images taken at different times, we assign the comparison to the bin that is the arithmetic average of the subject's ages. This plot shows only the effect of age, not ageing. The number of comparisons in each bin is generally in the thousands, however the first and last bins are computed over 149 and 124 respectively. The error rates in some (adult) cases are zero, and in others the DET is flat so the error rates at the two thresholds are identical. The lines span 1% and 99% of bootstrap replicated FNMR estimates.

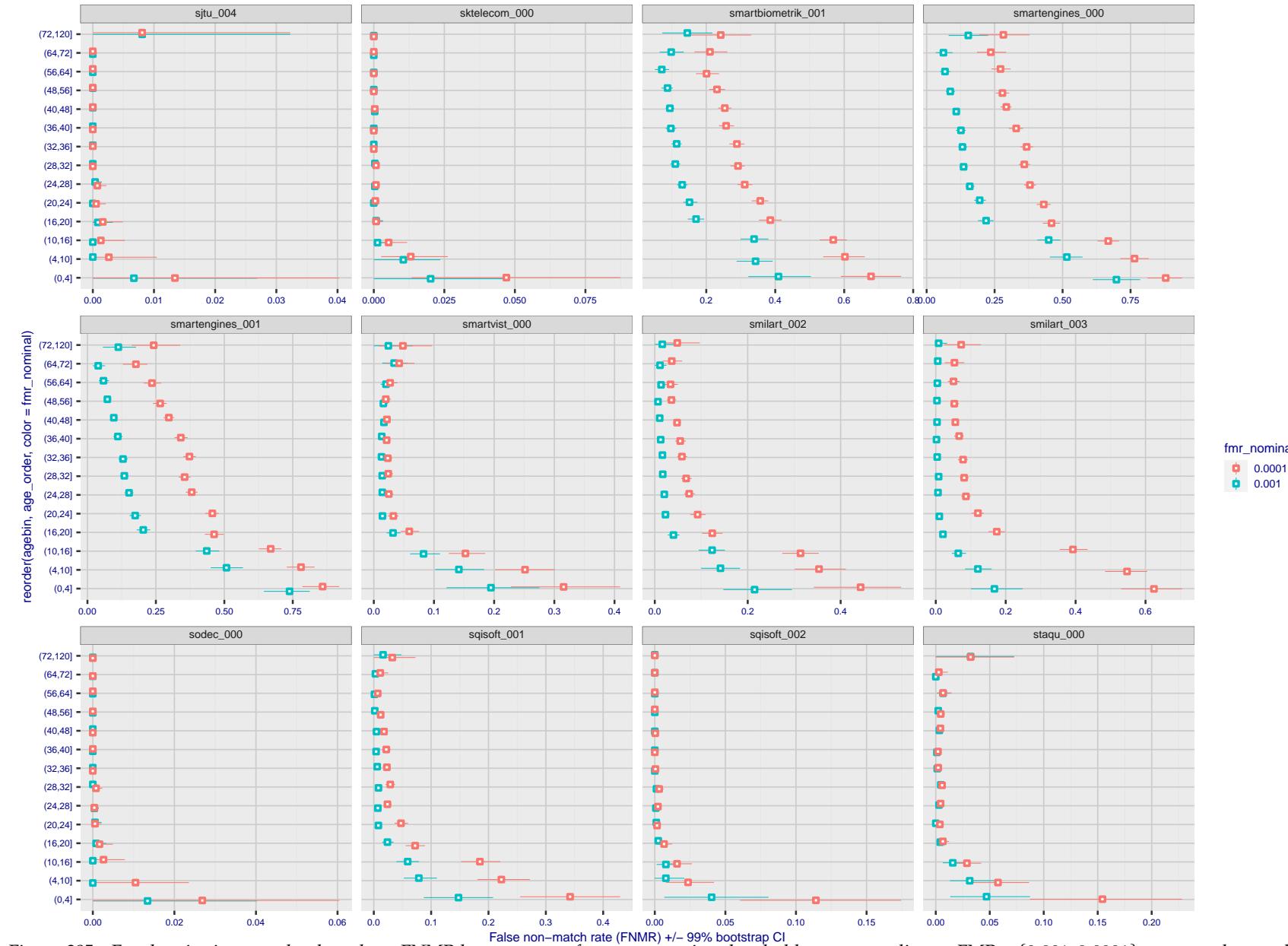


Figure 385: For the visa images, the dots show FNMR by age group for two operating thresholds corresponding to $FMR = \{0.001, 0.0001\}$ computed over all on the order of 10^{10} impostor scores. The FMR in each bin will vary also - see subsequent impostor heatmaps in sec. 3.6.2. Given a pair of face images taken at different times, we assign the comparison to the bin that is the arithmetic average of the subject's ages. This plot shows only the effect of age, not ageing. The number of comparisons in each bin is generally in the thousands, however the first and last bins are computed over 149 and 124 respectively. The error rates in some (adult) cases are zero, and in others the DET is flat so the error rates at the two thresholds are identical. The lines span 1% and 99% of bootstrap replicated FNMR estimates.

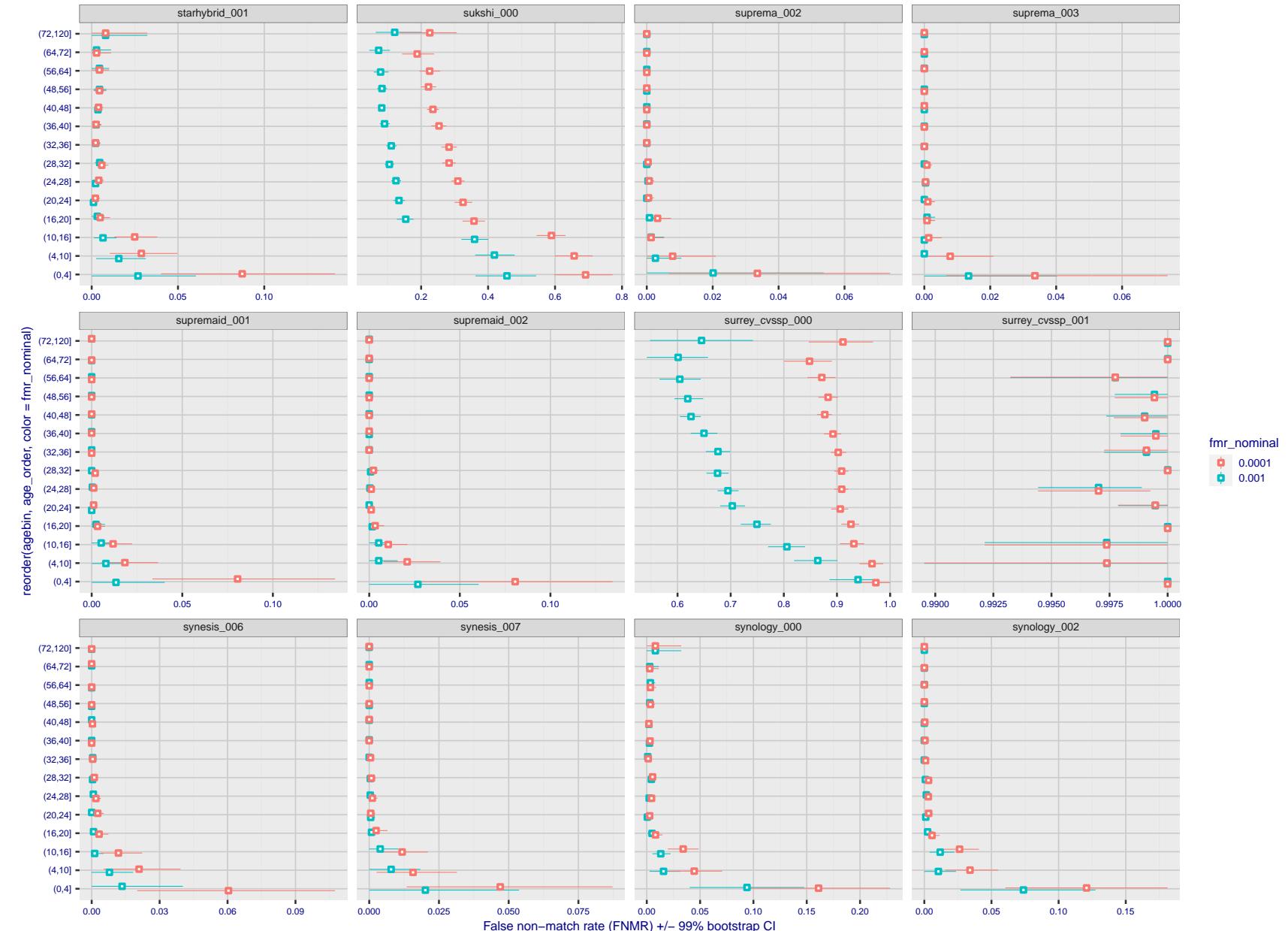


Figure 386: For the visa images, the dots show FNMR by age group for two operating thresholds corresponding to $FMR = \{0.001, 0.0001\}$ computed over all on the order of 10^{10} impostor scores. The FMR in each bin will vary also - see subsequent impostor heatmaps in sec. 3.6.2. Given a pair of face images taken at different times, we assign the comparison to the bin that is the arithmetic average of the subject's ages. This plot shows only the effect of age, not ageing. The number of comparisons in each bin is generally in the thousands, however the first and last bins are computed over 149 and 124 respectively. The error rates in some (adult) cases are zero, and in others the DET is flat so the error rates at the two thresholds are identical. The lines span 1% and 99% of bootstrap replicated FNMR estimates.



Figure 387: For the visa images, the dots show FNMR by age group for two operating thresholds corresponding to $FMR = \{0.001, 0.0001\}$ computed over all on the order of 10^{10} impostor scores. The FMR in each bin will vary also - see subsequent impostor heatmaps in sec. 3.6.2. Given a pair of face images taken at different times, we assign the comparison to the bin that is the arithmetic average of the subject's ages. This plot shows only the effect of age, not ageing. The number of comparisons in each bin is generally in the thousands, however the first and last bins are computed over 149 and 124 respectively. The error rates in some (adult) cases are zero, and in others the DET is flat so the error rates at the two thresholds are identical. The lines span 1% and 99% of bootstrap replicated FNMR estimates.



Figure 388: For the visa images, the dots show FNMR by age group for two operating thresholds corresponding to $FMR = \{0.001, 0.0001\}$ computed over all on the order of 10^{10} impostor scores. The FMR in each bin will vary also - see subsequent impostor heatmaps in sec. 3.6.2. Given a pair of face images taken at different times, we assign the comparison to the bin that is the arithmetic average of the subject's ages. This plot shows only the effect of age, not ageing. The number of comparisons in each bin is generally in the thousands, however the first and last bins are computed over 149 and 124 respectively. The error rates in some (adult) cases are zero, and in others the DET is flat so the error rates at the two thresholds are identical. The lines span 1% and 99% of bootstrap replicated FNMR estimates.

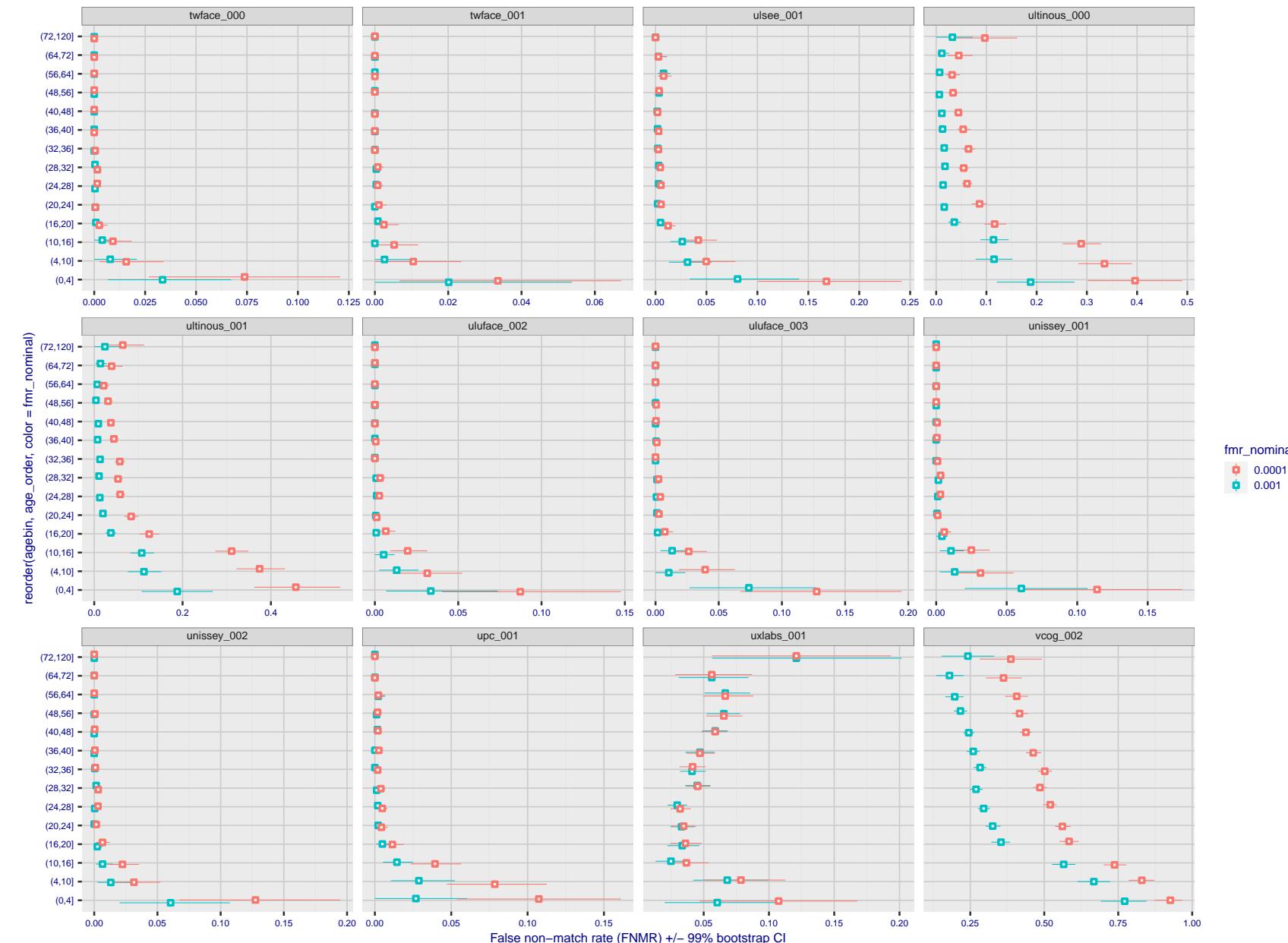


Figure 389: For the visa images, the dots show FNMR by age group for two operating thresholds corresponding to $FMR = \{0.001, 0.0001\}$ computed over all on the order of 10^{10} impostor scores. The FMR in each bin will vary also - see subsequent impostor heatmaps in sec. 3.6.2. Given a pair of face images taken at different times, we assign the comparison to the bin that is the arithmetic average of the subject's ages. This plot shows only the effect of age, not ageing. The number of comparisons in each bin is generally in the thousands, however the first and last bins are computed over 149 and 124 respectively. The error rates in some (adult) cases are zero, and in others the DET is flat so the error rates at the two thresholds are identical. The lines span 1% and 99% of bootstrap replicated FNMR estimates.

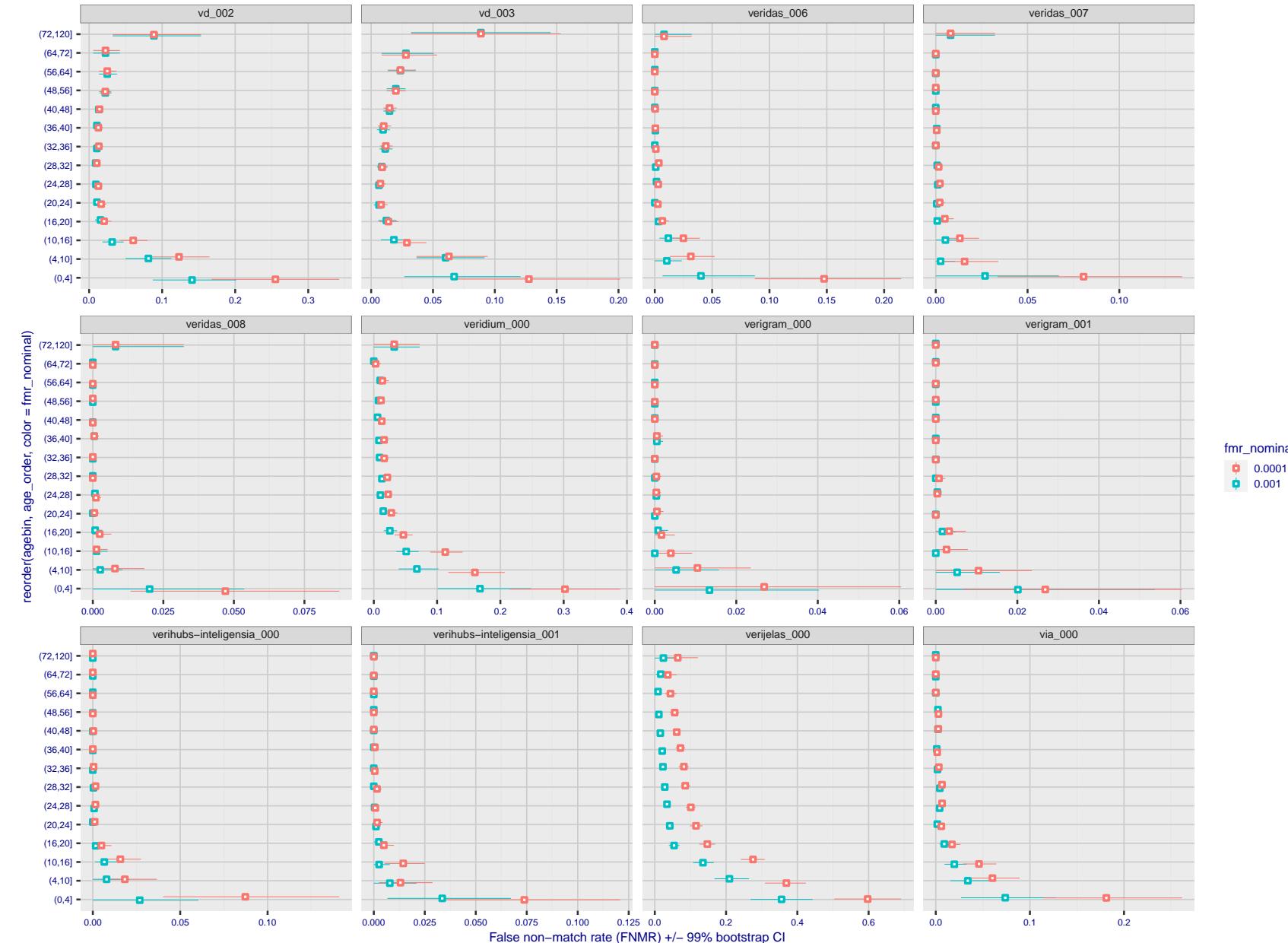


Figure 390: For the visa images, the dots show FNMR by age group for two operating thresholds corresponding to $FMR = \{0.001, 0.0001\}$ computed over all on the order of 10^{10} impostor scores. The FMR in each bin will vary also - see subsequent impostor heatmaps in sec. 3.6.2. Given a pair of face images taken at different times, we assign the comparison to the bin that is the arithmetic average of the subject's ages. This plot shows only the effect of age, not ageing. The number of comparisons in each bin is generally in the thousands, however the first and last bins are computed over 149 and 124 respectively. The error rates in some (adult) cases are zero, and in others the DET is flat so the error rates at the two thresholds are identical. The lines span 1% and 99% of bootstrap replicated FNMR estimates.

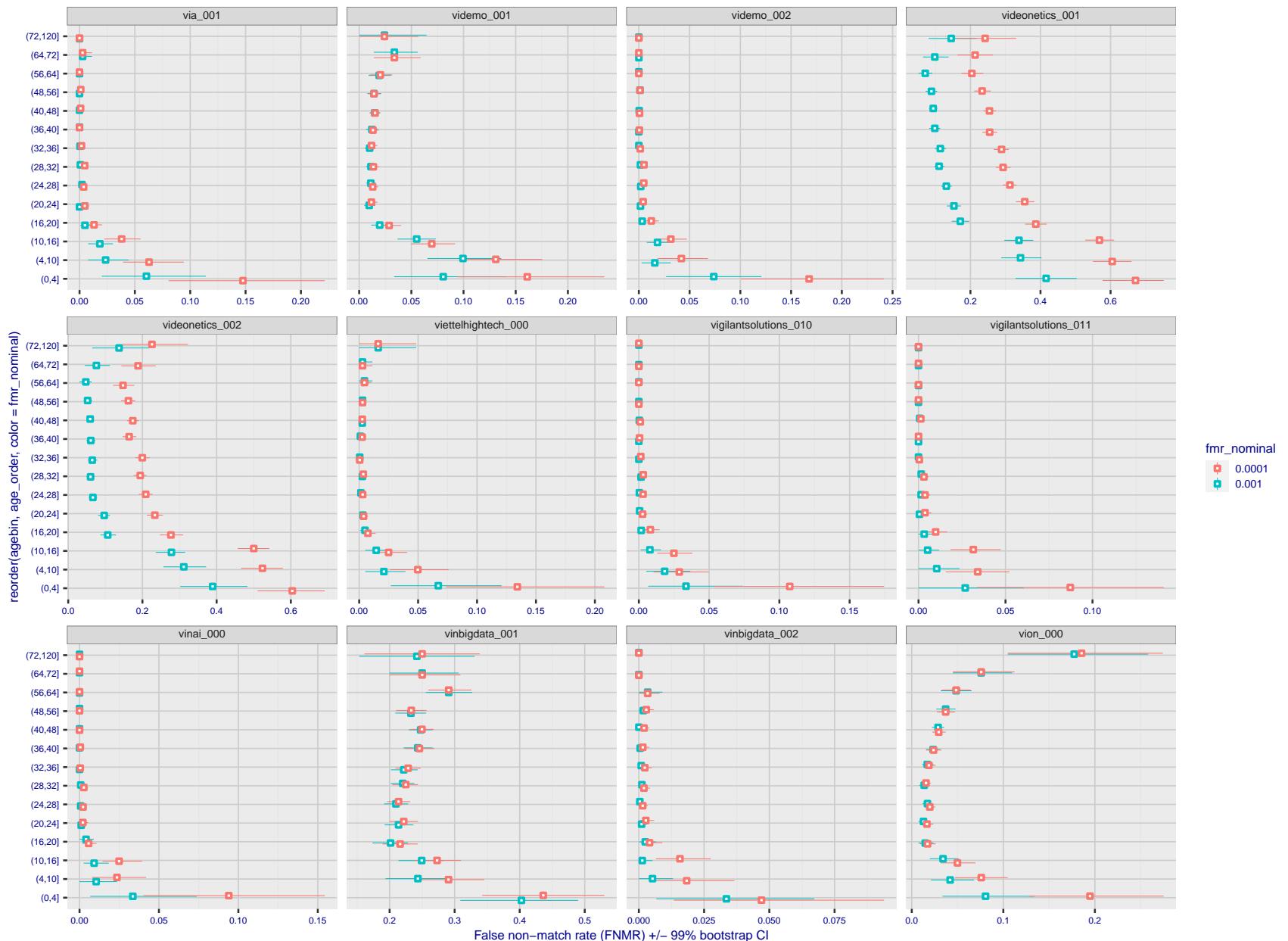


Figure 391: For the visa images, the dots show FNMR by age group for two operating thresholds corresponding to $FMR = \{0.001, 0.0001\}$ computed over all on the order of 10^{10} impostor scores. The FMR in each bin will vary also - see subsequent impostor heatmaps in sec. 3.6.2. Given a pair of face images taken at different times, we assign the comparison to the bin that is the arithmetic average of the subject's ages. This plot shows only the effect of age, not ageing. The number of comparisons in each bin is generally in the thousands, however the first and last bins are computed over 149 and 124 respectively. The error rates in some (adult) cases are zero, and in others the DET is flat so the error rates at the two thresholds are identical. The lines span 1% and 99% of bootstrap replicated FNMR estimates.



Figure 392: For the visa images, the dots show FNMR by age group for two operating thresholds corresponding to $FMR = \{0.001, 0.0001\}$ computed over all on the order of 10^{10} impostor scores. The FMR in each bin will vary also - see subsequent impostor heatmaps in sec. 3.6.2. Given a pair of face images taken at different times, we assign the comparison to the bin that is the arithmetic average of the subject's ages. This plot shows only the effect of age, not ageing. The number of comparisons in each bin is generally in the thousands, however the first and last bins are computed over 149 and 124 respectively. The error rates in some (adult) cases are zero, and in others the DET is flat so the error rates at the two thresholds are identical. The lines span 1% and 99% of bootstrap replicated FNMR estimates.

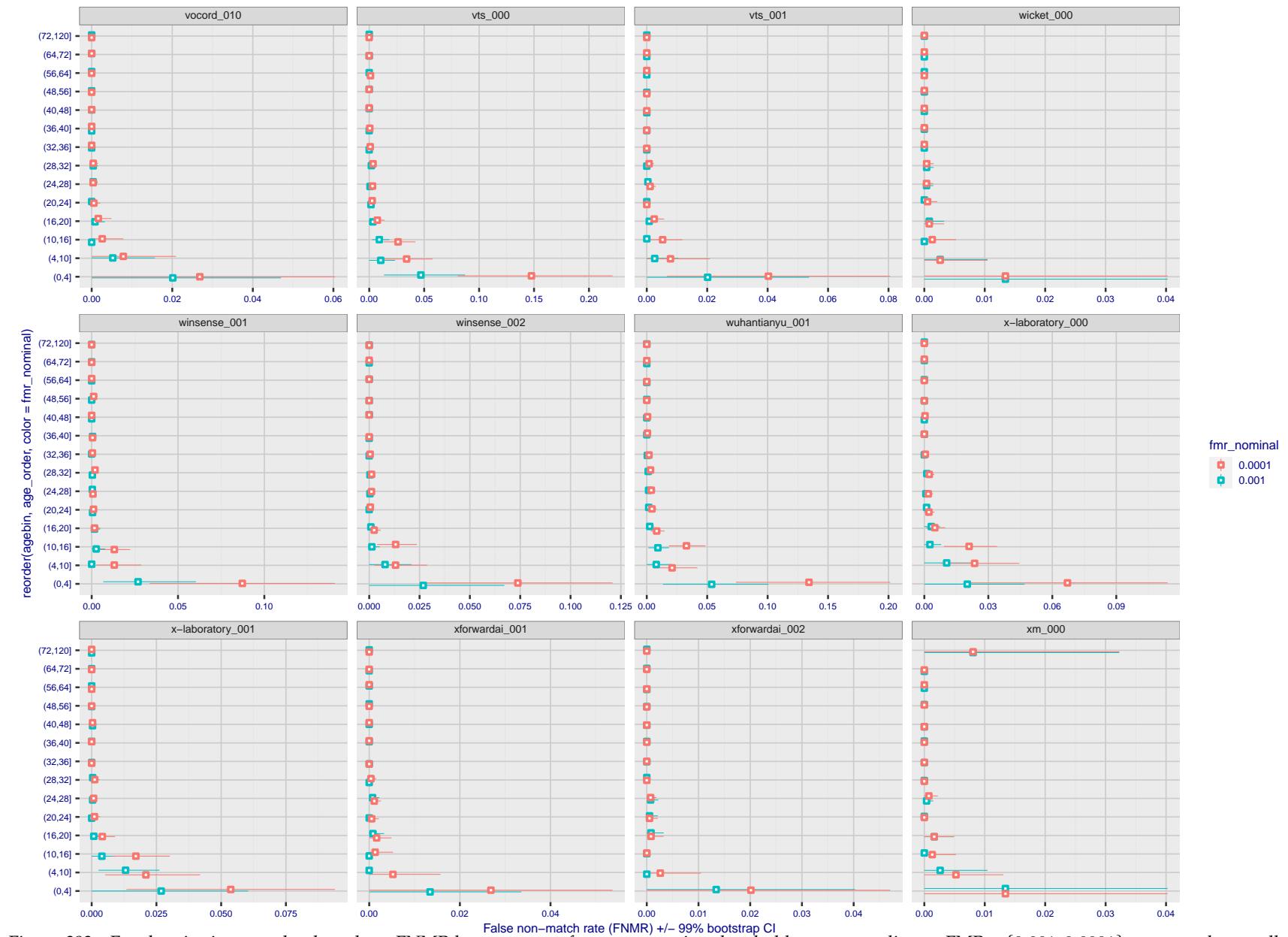
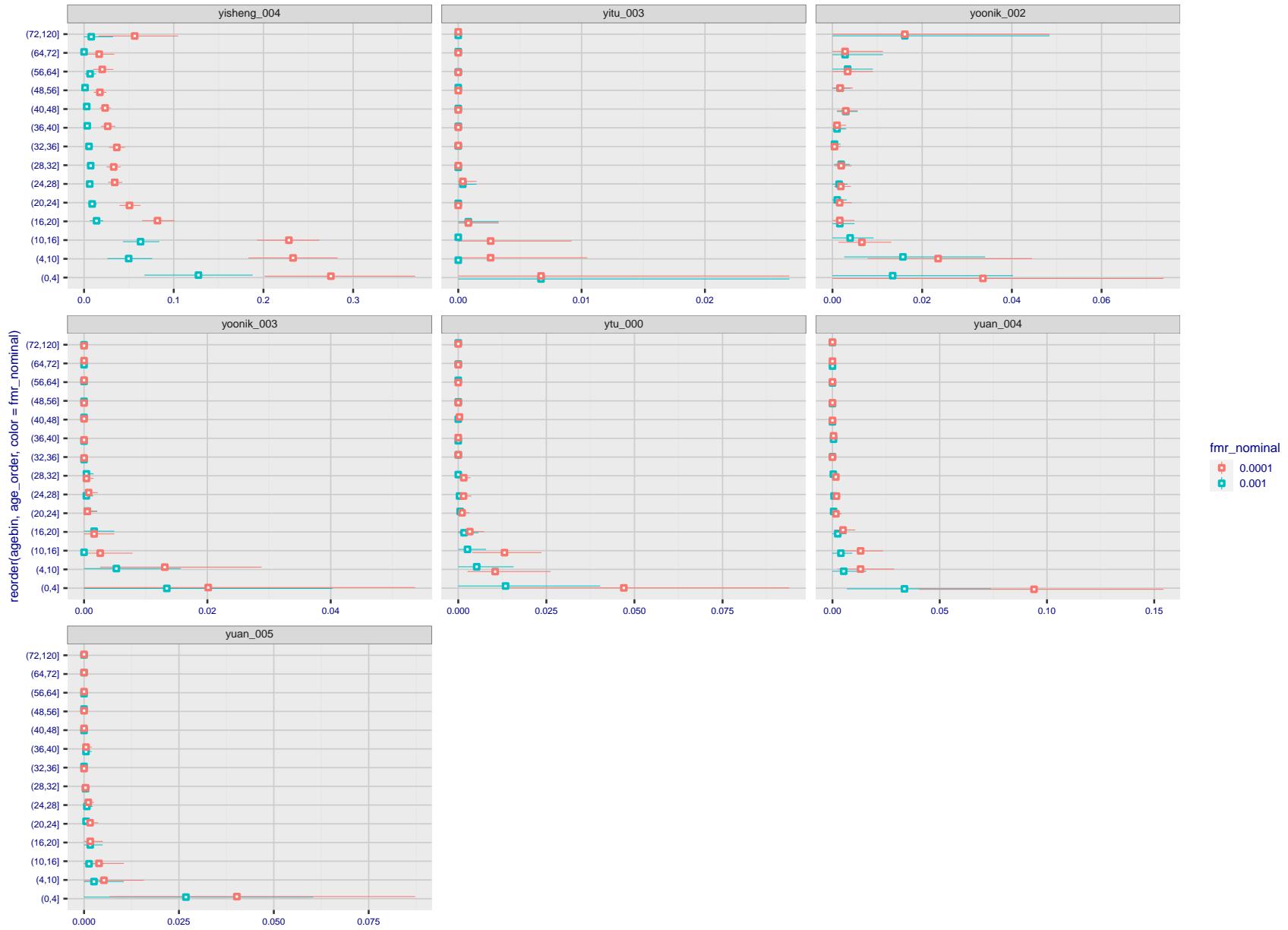


Figure 393: For the visa images, the dots show FNMR by age group for two operating thresholds corresponding to $FMR = \{0.001, 0.0001\}$ computed over all on the order of 10^{10} impostor scores. The FMR in each bin will vary also - see subsequent impostor heatmaps in sec. 3.6.2. Given a pair of face images taken at different times, we assign the comparison to the bin that is the arithmetic average of the subject's ages. This plot shows only the effect of age, not ageing. The number of comparisons in each bin is generally in the thousands, however the first and last bins are computed over 149 and 124 respectively. The error rates in some (adult) cases are zero, and in others the DET is flat so the error rates at the two thresholds are identical. The lines span 1% and 99% of bootstrap replicated FNMR estimates.



False non-match rate (FNMR) +/- 99% bootstrap CI

Figure 394: For the visa images, the dots show FNMR by age group for two operating thresholds corresponding to $FMR = \{0.001, 0.0001\}$ computed over all on the order of 10^{10} impostor scores. The FMR in each bin will vary also - see subsequent impostor heatmaps in sec. 3.6.2. Given a pair of face images taken at different times, we assign the comparison to the bin that is the arithmetic average of the subject's ages. This plot shows only the effect of age, not ageing. The number of comparisons in each bin is generally in the thousands, however the first and last bins are computed over 149 and 124 respectively. The error rates in some (adult) cases are zero, and in others the DET is flat so the error rates at the two thresholds are identical. The lines span 1% and 99% of bootstrap replicated FNMR estimates.

Caveats: None.

3.6 Impostor distribution stability

3.6.1 Effect of birth place on the impostor distribution

Background: Facial appearance varies geographically, both in terms of skin tone, cranio-facial structure and size. This section addresses whether false match rates vary intra- and inter-regionally.

Goals:

- ▷ To show the effect of birth region of the impostor and enrollee on false match rates.
- ▷ To determine whether some algorithms give better impostor distribution stability.

Methods:

- ▷ For the visa images, NIST defined 10 regions: Sub-Saharan Africa, South Asia, Polynesia, North Africa, Middle East, Europe, East Asia, Central and South America, Central Asia, and the Caribbean.
- ▷ For the visa images, NIST mapped each country of birth to a region. There is some arbitrariness to this. For example, Egypt could reasonably be assigned to the Middle East instead of North Africa. An alternative methodology could, for example, assign the Philippines to *both* Polynesia and East Asia.
- ▷ FMR is computed for cases where all face images of impostors born in region r_2 are compared with enrolled face images of persons born in region r_1 .

$$\text{FMR}(r_1, r_2, T) = \frac{\sum_{i=1}^{N_{r_1, r_2}} H(s_i - T)}{N_{r_1, r_2}} \quad (5)$$

where the same threshold, T , is used in all cells, and H is the unit step function. The threshold is set to give $\text{FMR}(T) = 0.001$ over the entire set of visa image impostor comparisons.

- ▷ This analysis is then repeated by country-pair, but only for those country pairs where both have at least 1000 images available. The countries¹ appear in the axes of graphs that follow.
- ▷ The mean number of impostor scores in any cross-region bin is 33 million. The smallest number of impostor scores in any bin is 135000, for Central Asia - North Africa. While these counts are large enough to support reasonable significance, the number of individual faces is much smaller, on the order of $N^{0.5}$.
- ▷ The numbers of impostor scores in any cross-country bin is shown in Figure 395.

Results: Subsequent figures show heatmaps that use color to represent the base-10 logarithm of the false match rate. Red colors indicate high (bad) false match rates. Dark colors indicate benign false match rates. There are two series of graphs corresponding to aggregated geographical regions, and to countries. The notable observations are:

- ▷ The on-diagonal elements correspond to within-region impostors. FMR is generally above the nominal value of $\text{FMR} = 0.001$. Particularly there is usually higher FMR in, Sub-Saharan Africa, South Asia, and the Caribbean. Europe and Central Asia, on the other hand, usually give FMR closer to the nominal value.
- ▷ The off-diagonal elements correspond to across-region impostors. The highest FMR is produced between the Caribbean and Sub-Saharan Africa.
- ▷ Algorithms vary.

¹These are Argentina, Australia, Brazil, Chile, China, Costa Rica, Cuba, Czech Republic, Dominican Republic, Ecuador, Egypt, El Salvador, Germany, Ghana, Great Britain, Greece, Guatemala, Haiti, Hong Kong, Honduras, Indonesia, India, Israel, Jamaica, Japan, Kenya, Korea, Lebanon, Mexico, Malaysia, Nepal, Nigeria, Peru, Philippines, Pakistan, Poland, Romania, Russia, South Africa, Saudi Arabia, Thailand, Trinidad, Turkey, Taiwan, Ukraine, Venezuela, and Vietnam.

- ▷ We computed the same quantities for a global FMR = 0.0001. The effects are similar.

Caveats:

- ▷ The effects of variable impostor rates on one-to-many identification systems may well differ from what's implied by these one-to-one verification results. Two reasons for this are a) the enrollment galleries are usually imbalanced across countries of birth, age and sex; b) one-to-many identification algorithms often implement techniques aimed at stabilizing the impostor distribution. Further research is necessary.
- ▷ In principle, the effects seen in this subsection could be due to differences in the image capture process. We consider this unlikely since the effects are maintained across geography - e.g. Caribbean vs. Africa, or Japan vs. China.

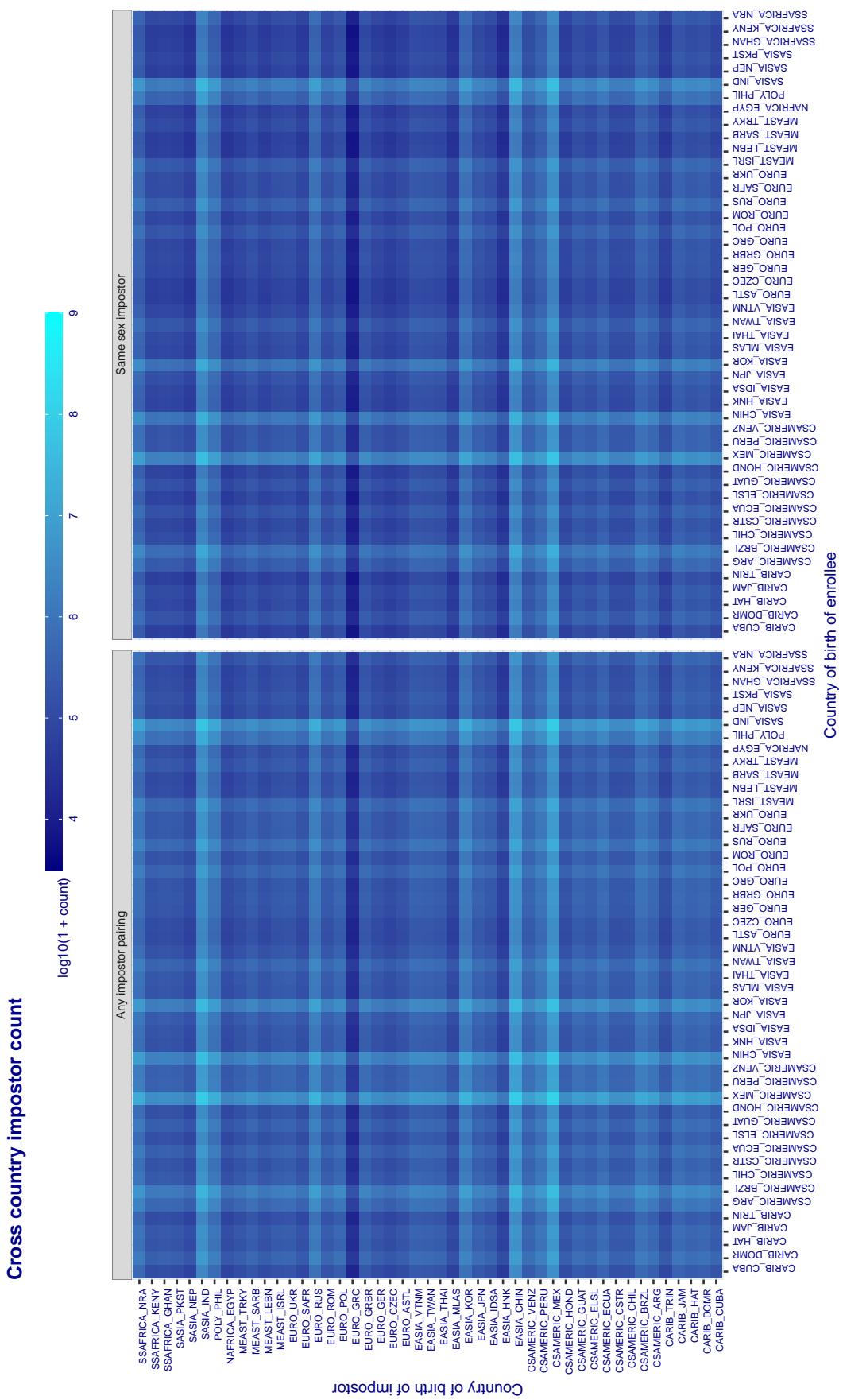


Figure 395: For visa images, the heatmap shows the count of impostor comparisons of faces from different individuals who were born in the given country pair. The FMR heatmaps themselves appear in the 1:1 report cards, for example, [this one](#).

3.6.2 Effect of age on impostors

Background: This section shows the effect of age on the impostor distribution. The ideal behaviour is that the age of the enrollee and the impostor would not affect impostor scores. This would support FMR stability over sub-populations.

Goals:

- ▷ To show the effect of relative ages of the impostor and enrollee on false match rates.
- ▷ To determine whether some algorithms have better impostor distribution stability.

Methods:

- ▷ Define 14 age group bins, spanning 0 to over 100 years old.
- ▷ Compute FMR over all impostor comparisons for which the subjects in the enrollee and impostor images have ages in two bins.
- ▷ Compute FMR over all impostor comparisons for which the subjects are additionally of the same sex, and born in the same geographic region.

Results:

The notable aspects are:

- ▷ Diagonal dominance: Impostors are more likely to be matched against their same age group.
- ▷ Same sex and same region impostors are more successful. On the diagonal, an impostor is more likely to succeed by posing as someone of the same sex. If $\Delta \log_{10} \text{FMR} = 0.2$, then same-sex same-region FMR exceeds the all-pairs FMR by factor of $10^{0.2} = 1.6$.
- ▷ Young children impostors give elevated FMR against young children. Older adult impostor give elevated FMR against older adults. These effects are quite large, for example if $\Delta \log_{10} \text{FMR} = 1.0$ larger than a 32 year old, then these groups have higher FMR by a factor of $10^1 = 10$. This would imply an FMR above 0.01 for a nominal (global) FMR = 0.001.
- ▷ Algorithms vary.
- ▷ We computed the same quantities for a global FMR = 0.0001. The effects are similar.

Note the calculations in this section include impostors paired across all countries of birth.

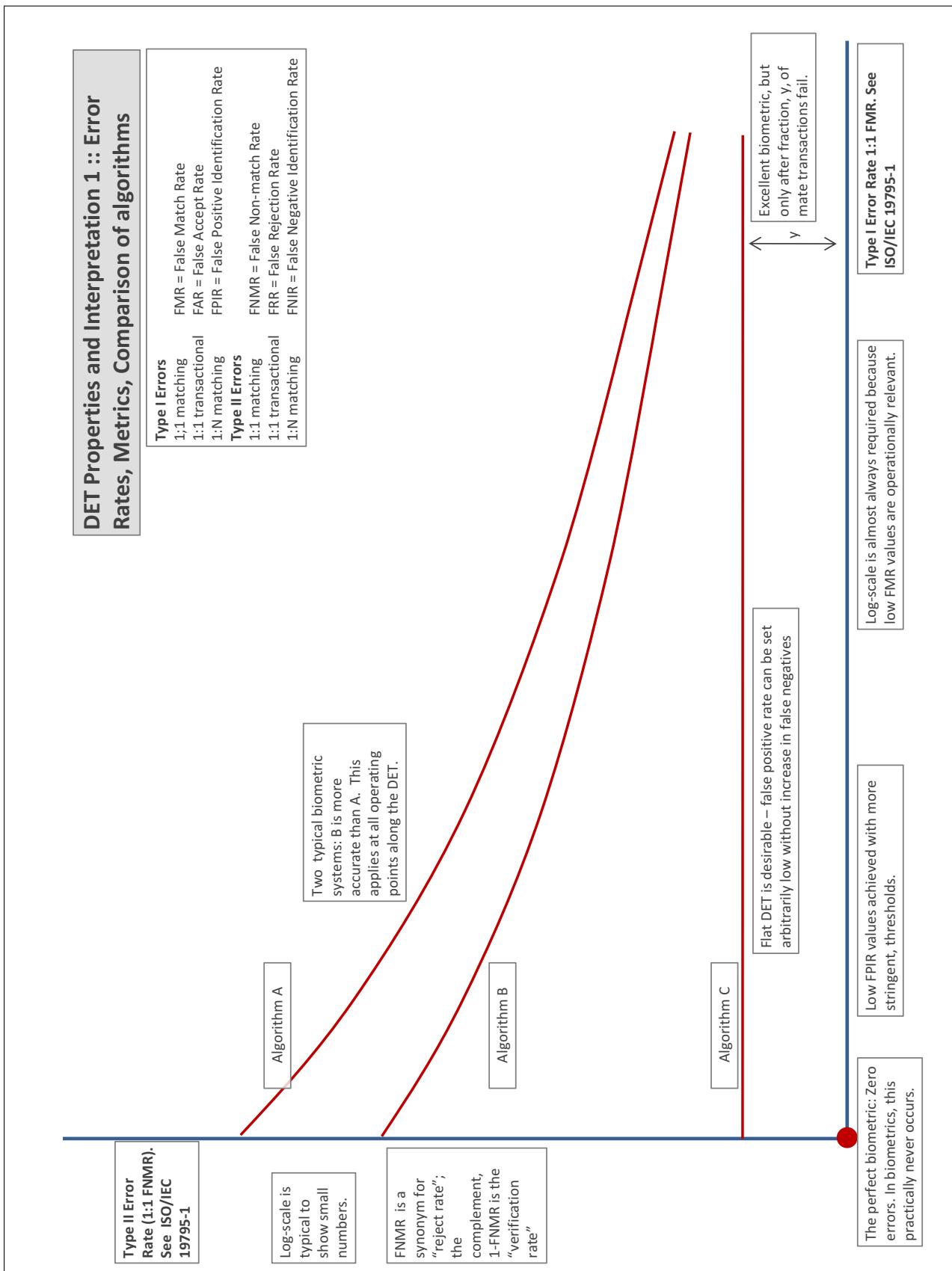
Accuracy Terms + Definitions

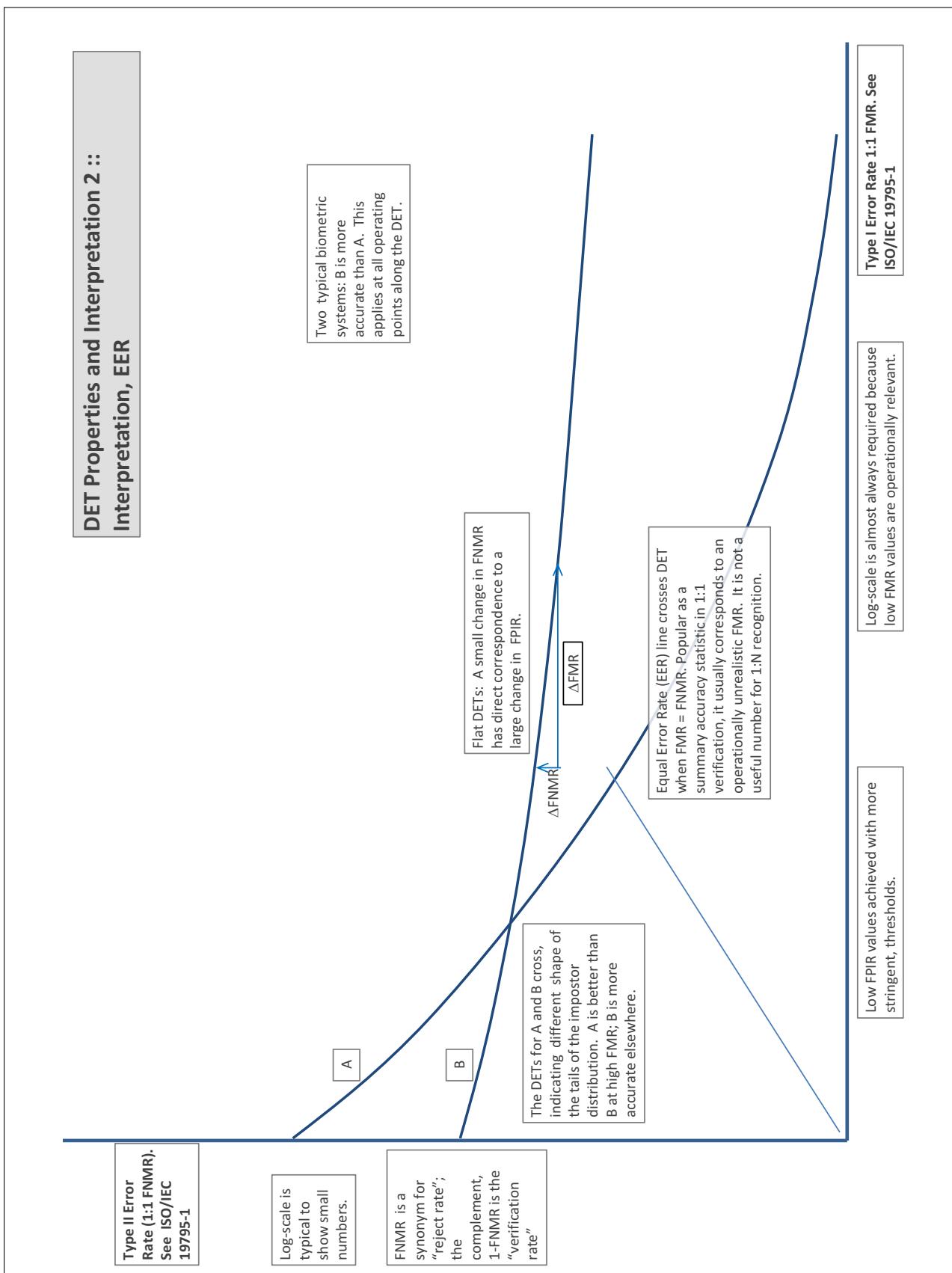
In biometrics, Type II errors occur when two samples of one person do not match – this is called a **false negative**. Correspondingly, Type I errors occur when samples from two persons do match – this is called a **false positive**. Matches are declared by a biometric system when the native comparison score from the recognition algorithm meets some **threshold**. Comparison scores can be either **similarity scores**, in which case higher values indicate that the samples are more likely to come from the same person, or **dissimilarity scores**, in which case higher values indicate different people. Similarity scores are traditionally computed by **fingerprint** and **face** recognition algorithms, while dissimilarities are used in **iris recognition**. In some cases, the dissimilarity score is a distance; this applies only when **metric** properties are obeyed. In any case, scores can be either **mate** scores, coming from a comparison of one person's samples, or **nonmate** scores, coming from comparison of different persons' samples. The words **genuine** or **authentic** are synonyms for mate, and the word **impostor** is used as a synonym for nonmatch. The words mate and nonmatch are traditionally used in identification applications (such as law enforcement search, or background checks) while genuine and impostor are used in verification applications (such as access control).

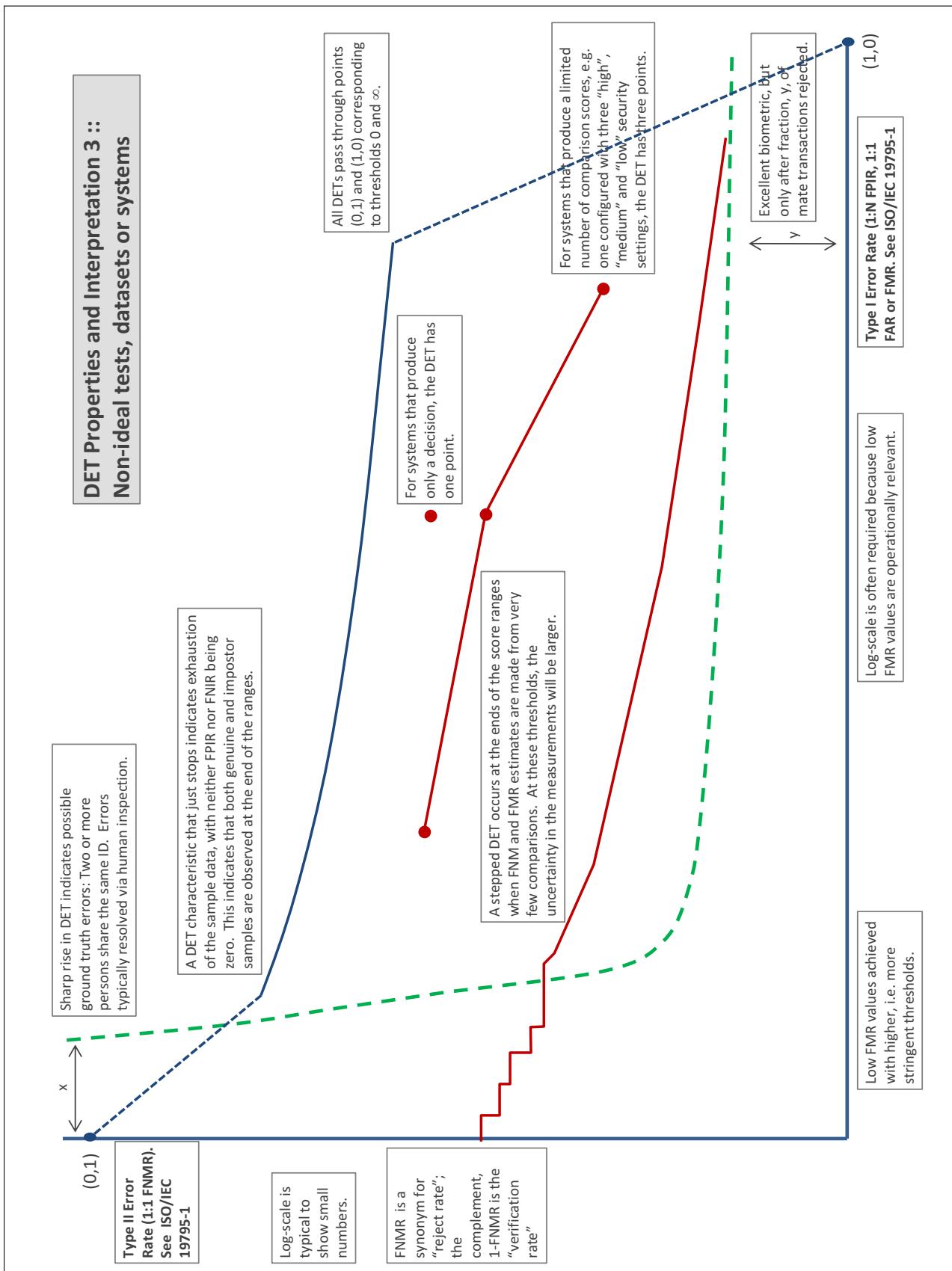
A **error tradeoff** characteristic represents the tradeoff between Type II and Type I classification errors. For verification this plots false non-match rate (FNMR) vs. false match rate (FMR) parametrically with T.

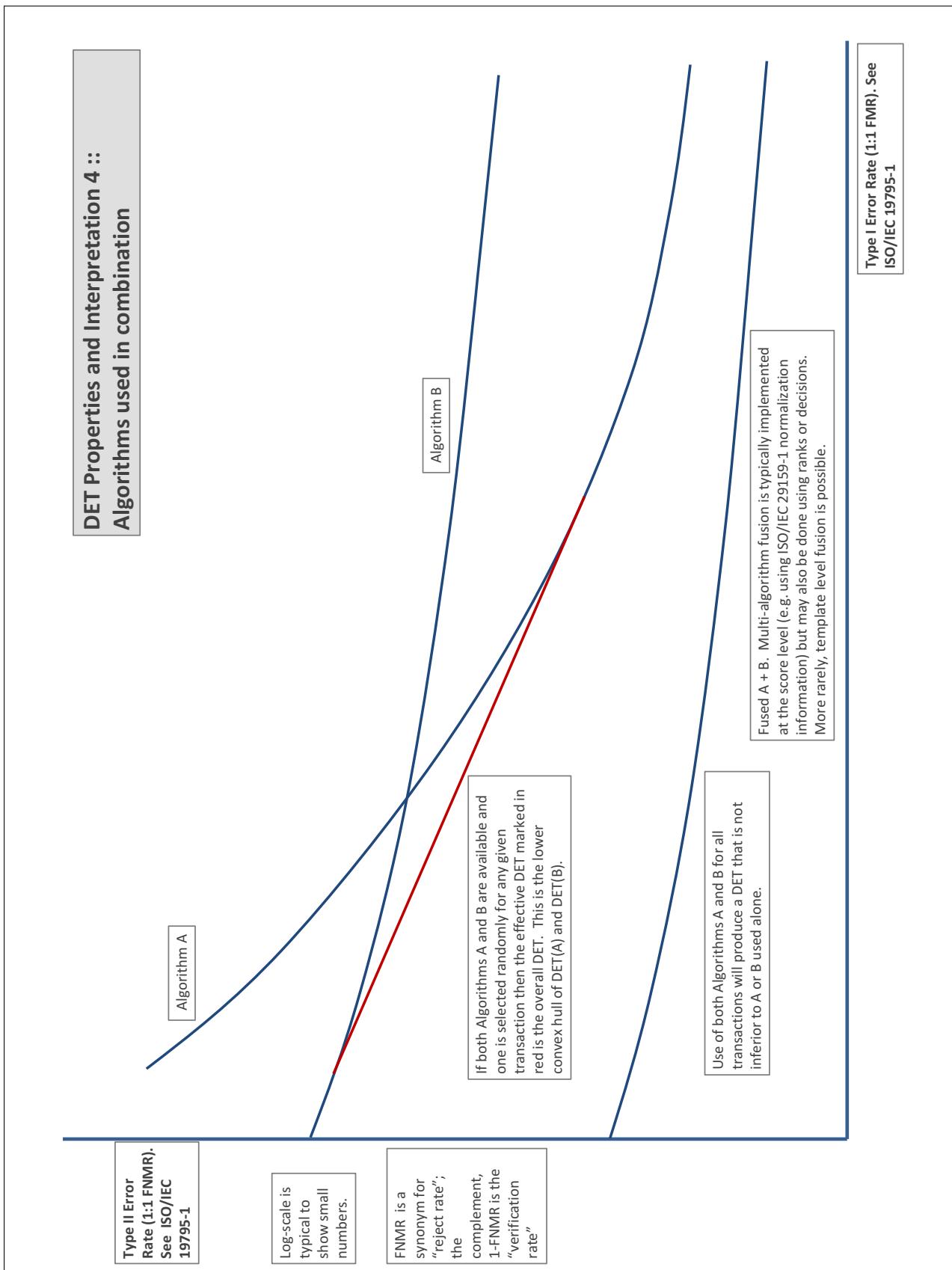
The error tradeoff plots are often called **detection error tradeoff (DET)** characteristics or **receiver operating characteristic (ROC)**. These serve the same function but differ, for example, in plotting the complement of an error rate (e.g., $TMR = 1 - FNMR$) and in transforming the axes most commonly using logarithms, to show multiple decades of FMR. More rarely, the function might be the inverse Gaussian function.

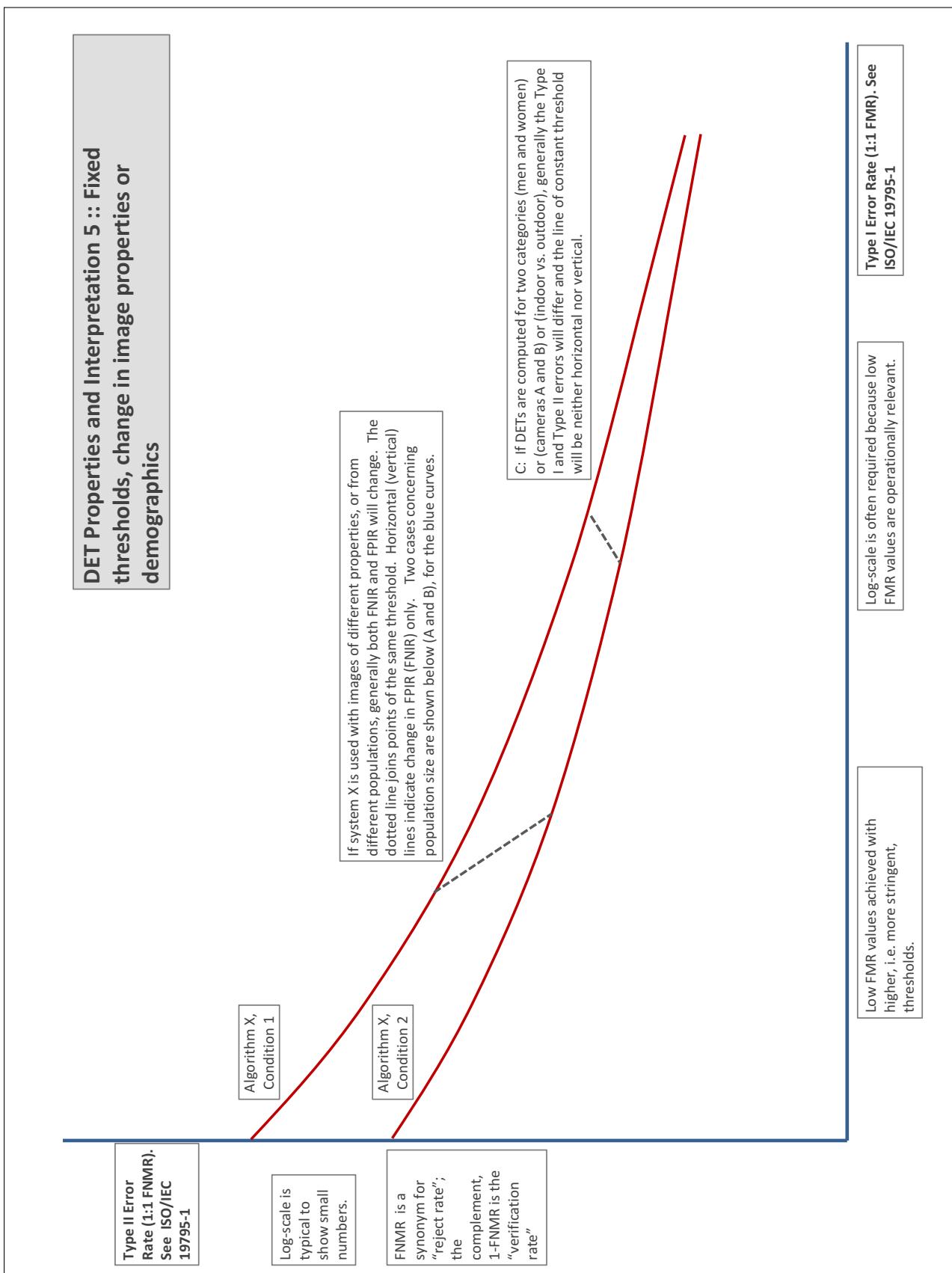
More detail and generality is provided in formal biometrics testing standards, see the various parts of [ISO/IEC 19795 Biometrics Testing and Reporting](#). More terms, including and beyond those to do with accuracy, see [ISO/IEC 2382-37 Information technology -- Vocabulary -- Part 37: Harmonized biometric vocabulary](#)











References

- [1] P. Jonathon Phillips, Amy N. Yates, Ying Hu, Carina A. Hahn, Eilidh Noyes, Kelsey Jackson, Jacqueline G. Cavazos, Géraldine Jeckeln, Rajeev Ranjan, Swami Sankaranarayanan, Jun-Cheng Chen, Carlos D. Castillo, Rama Chellappa, David White, and Alice J. O'Toole. Face recognition accuracy of forensic examiners, superrecognizers, and face recognition algorithms. *Proceedings of the National Academy of Sciences*, 115(24):6171–6176, 2018.